

S. 1176 1 CUB - H02912 - 3 - P024428




AJR

American
Journal of
Roentgenology



3

July 1976



Searle's Pho/Trax CT scanner is the newest and most technically advanced instrument of its type available today. But even more important is the fact that Pho/Trax is designed to retain its state-of-the-art status for years to come.

Pho/Trax takes just 5 seconds to travel around a patient's head or torso in a smooth, continuous 360° sweep. Because of this rapid scanning capability, Pho/Trax potentially eliminates blurred exposures due to patient motion; allows breath-holding even with the severely ill and facilitates infant studies.

Pho/Trax has a 23.5" aperture, which means you can perform torso scans on all but the most obese patients. Evaluation of certain structures in the brain, orbits and abdominal organs may require angled or off-axis views. To help you obtain optimum images in these instances, the Pho/Trax gantry can be tilted in both directions over a 30° range.

VARIABLE SLICE THICKNESS

In scanning small structures such as the optic nerve, a narrower slice thickness can often aid accurate diagnosis. With Pho/Trax, the operator can choose any slice thickness from 3mm to 12mm in 1mm increments. A unique beam-shaping technique controls the x-ray fan, keeping it very close to the slice thickness selected.

VARIABLE SCAN SPEED

For most images, a 5 second scan speed is highly desirable; at this speed, radiation exposure is at a new low while resolution is of a very high order. In circumstances where patient motion is not a problem, and where an exceptional degree of clarity is needed, Pho/Trax lets you select a 10 or 20 second scan speed.

FIELD OF VIEW OPTIMIZATION

Advanced computer technology enables Pho/Trax to use a very high number of picture elements (or "pixels") on the 256 x 256 matrix regardless of the actual size of the area of interest. This is not a simple magnification or "zoom" process, but an algorithmic function which uses 100% of the raw data and does not degrade resolution in any way.

A VARIETY OF IMAGING MODES

Reconstruction time with Pho/Trax is 40 seconds for head and torso scans. There is also a 20-second preview mode which allows the operator to evaluate each scan, with subsequent batch image processing after the study is completed. Typically, 6 12mm brain slices can be reconstructed in 4 minutes, while the next patient is being positioned.

Pho/Trax was developed with the dedication to technical superiority that made Searle the recognized leader for in-vivo and in-vitro radionuclide applications. And as with all Searle instrumentation, Pho/Trax is backed by the industry's largest service organization dedicated to medical imaging devices.

For more information, including sample studies, write Searle CT Systems or call our toll-free 800 number.

CALL 800-323-0221 TOLL-FREE

SEARLE

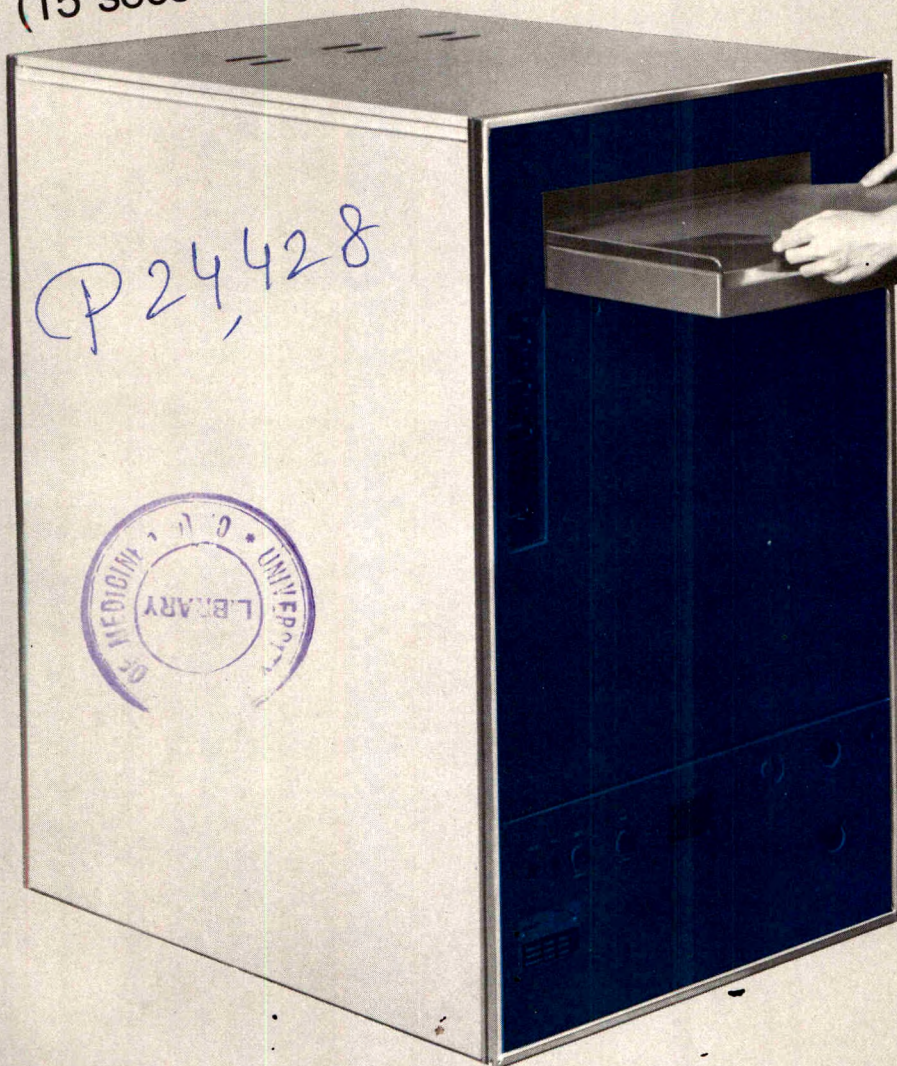
Searle CT Systems
Division of Searle Radiographics, Inc.
4233 North United Parkway
Schiller Park, IL 60176

Designed with the future in mind
New Pho/Trax™ CT scanner

Announcing
the new cold water supply
X-ray film processor.

PAKO 17X-90

engineered to process 240
RP films (14x17) per hour
(15 second feed time)



The 17X-90 can handle the most demanding work load of hospital and clinic with

speed:

240 RP films (14x17) per hour
15 second feed time

quality:

radiographs are free of streaks, patterns, and artifacts . . . our 30 plus years of experience in design and manufacture assure quality

processing from a quality processor:
one year full factory warranty

versatile:

accepts any major brand RP films and chemistries . . . sizes from 5x7 to 17 inches wide by any length

economy:

cold water installation (no mixing valve or hot water) low water consumption — 1/2 gpm with built in auto shut off valve

price:

U.S. User Price \$7495 (FOB Minneapolis)

For further information contact Pako distributor in your community or us directly.

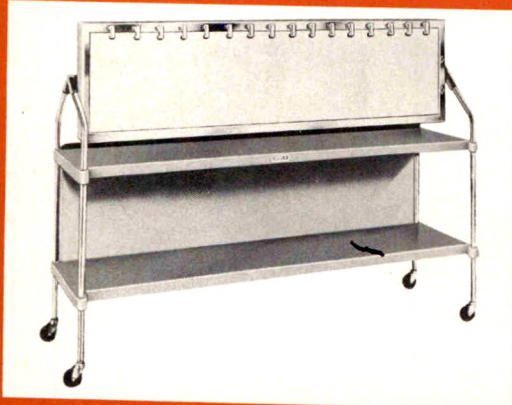
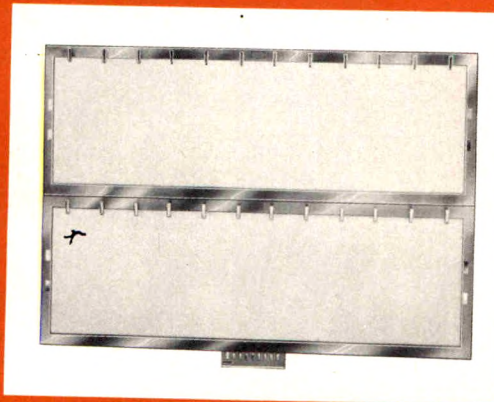
PAKO

PAKO CORPORATION

6300 Olson Memorial Highway
Minneapolis, Minnesota 55440

Wolf X-Ray

"the illuminator people!"



Singles ■ Panels ■ Mobiles ■
 Angle Vision ■ Explosion-
 Proof ■ Hi-Intensity ■ Spine ■
 Intensi-Spot ■ Fluorescent ■
 Medical ■ Incandescent ■
 Enameled ■ Stainless Steel ■
 Plastic ■ Wall Hanging ■
 Recessed ■ Desk Models ■
 Multiple ■ Specials ■
 Circline ■ Dental.

Whatever your illuminator need, we've got it! Over 235 different sizes and styles, designed for wall installation, desk, or mobile use.

All Wolf illuminators feature a choice of our highly efficient "Roller Clip," or our exclusive "Magic Grip" film retainer that's built right into the frame for positive grip tension. Low voltage leakage is another Wolf feature. And our "Instant Start Lighting" eliminates annoying light delay and flicker... gives you full illumination at the flip of the switch.

The next time you're in need of an illuminator... any kind... think of Wolf. Contact your local Wolf X-Ray Dealer for information.

When you think accessories, think Wolf.

Wolf X-Ray

Division of IPCO Hospital Supply Corporation
 182-20 Liberty Ave., Jamaica, New York 11412

AMERICAN JOURNAL OF ROENTGENOLOGY

EDITOR MELVIN M. FIGLEY

ASSISTANT EDITOR ROSALIND H. TROUPIN

ASSOCIATE EDITORS LUTHER W. BRADY
KENNETH L. KRABbenhOFT
E. FREDERICK LANG
RUSSELL H. MORGAN

EDITOR
EMERITUS TRAIAN LEUCUTIA

INCLUDING DIAGNOSTIC RADIOLOGY, RADIATION ONCOLOGY, NUCLEAR
MEDICINE, ULTRASONOGRAPHY AND RELATED BASIC SCIENCES

CONSULTING EDITORIAL BOARD

KENT ELLIS
E. ROBERT HEITZMAN
DONALD L. KING
JOHN A. KIRKPATRICK, JR.
EUGENE C. KLATTE

JOHN G. MCAFEE
THOMAS H. NEWTON
ROBERT G. PARKER
STEWART R. REUTER
WILLIAM B. SEAMAN

ROBERT J. SHALEK
JOHN STORER
MICHEL M. TER-POGOSSIAN
JOSEPH P. WHALEN
DAVID M. WITTEN

EDITORIAL STAFF: M. J. LEONARD, K. A. MURRAY, M. B. WIECKOWICZ



OFFICIAL JOURNAL
AMERICAN ROENTGEN RAY SOCIETY
AMERICAN RADIUM SOCIETY



The American Journal of Roentgenology is issued monthly by Charles C Thomas, Publisher, 301-327 East Lawrence Ave., Springfield, Illinois 62717. Correspondence regarding subscriptions, advertisements and other business should be addressed to the Publisher. Annual subscription prices: United States and U. S. Possessions \$30.00, Pan America, Canada and others \$35.00. Printed by the George Banta Co., Menasha, Wisconsin. Copyright © 1976 by American Roentgen Ray Society. Second-class postage paid at Springfield, Illinois and at additional mailing offices. Printed in U.S.A.

Guidelines for Authors

The *American Journal of Roentgenology* publishes original and timely contributions to the advancement of radiologic diagnosis and treatment. Although the content is predominantly clinical in origin, laboratory investigations are accepted when their relevance to clinical practice is demonstrable. Contributions are reviewed by two outside consultants and are accepted on condition that they are submitted only to this Journal and that they will not be reprinted or translated without consent of the Editor. Statements within an article are the responsibility of the authors and not the Journal or its publisher.

Address all manuscripts and correspondence to the Editor, Dr. Melvin M. Figley, 403 Pacific National Bank Building, 4545 15th Avenue N.E., Seattle, Washington 98105.

Manuscript Form

Manuscripts should be typed double-spaced throughout, including references, tables, and footnotes. Tables, footnotes, and figure legends should be on separate sheets, and a separate title page should be provided. In addition to the original typewritten copy, a duplicate copy complete with figures, tables, and references is required.

Figures should be submitted as 5" x 7" glossy prints, untrimmed and unmounted. Identifying information (author name, figure number, and indication of the top of the figure) should be attached to the back of each figure with a gummed label. Line illustrations and graphs should be drawn in black ink on white background. Labels on all figures should be of professional quality and sufficiently large to be easily read when reduced in size.

References should be cited in the text by number (e.g., [3, 4]). The bibliography should be arranged in the numerical order that references are cited in the text and typed double-spaced throughout. Data for each reference should be arranged according to the uniform style on bibliographic citations adopted by many biomedical journals. Abbreviations for titles of medical periodicals should conform to those published in *Index Medicus*. Examples:

1. Miller RE, Chernish SM, Skulas J, Rosenak BD, Rodda BE: Hypotonic roentgenography with glucagon. *Am J Roentgenol* 121:264-274, 1974
2. Boijesen E: Superior mesenteric angiography, in *Angiography*, edited by Abrams H, Boston, Little, Brown, 1971, pp 1091-1119

Organization

Title page. Titles should be brief and specific. Include full names and addresses of all authors and acknowledgment of grant support when appropriate.

Abstract. A description of the purpose, methods, results, and conclusions of the study is required. It should be informative to a reader who has not read the text of the article.

Key indexing words. Five to 10 words or short phrases should be supplied to enable cross-indexing of the article.

Introduction. Clearly state the purpose of the investigation including necessary background facts.

Materials and methods. Describe the protocol clearly so that an experienced worker can understand what was done. Use standard abbreviations as presented in the *Council of Biology Editors Style Manual*, 3d edition.

Results. Present results in logical sequence.

Discussion. Interpret the results to lend meaning and importance to the observations. If hypotheses and speculation are included, they must be labeled as such. When results differ from those of previous investigators, an attempt should be made to explain the discrepancy.

References. Only include those references which provide adequate background and present fairly any opposing evidence and concepts. Accuracy of reference data is the responsibility of the author.

Legends. Legends should be brief but should provide sufficient description to interpret the figure.

Special Communications

Case Reports. Concise case reports are accepted if they present unusual experiences that are medically important and educational. Clarity and brevity are essential.

Technical notes. Brief descriptions of new techniques or significant modifications of older ones which are directly applicable to clinical practice will be accepted.

Letters to the Editor. Letters should be limited to between 250 and 500 words. Criticism of published articles should be objective and constructive. Letters may also discuss matters of general interest to radiologists.

Proofs and Reprints

Galley proofs will be sent for correction of errors. The corrected proof, copy-edited manuscript, and the reprint order should be returned directly to the Editor. If the author fails to return proof by the date specified, it may be necessary to publish without the author's approval.



Excellent visualization in intravenous pyelogram 18 hours after administration of 2½ oz. X-PREP Liquid for preradiographic bowel cleansing. (In the files of the Medical Department of The Purdue Frederick Company.)

To prep the bowel for intravenous pyelography

X-PREP[®] Liquid

(standardized extract of senna fruit)

One step • One dose • One bottle

□ X-PREP Liquid is designed specifically for preradiographic bowel cleansing — without enemas, suppositories or overhydration.

□ A single 2½ oz. oral dose is usually all that is required. No residual oil droplets (such as may occur with castor oil).

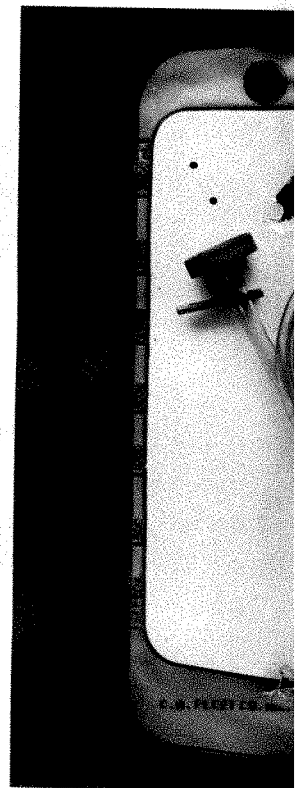
□ Pleasant taste meets with high patient acceptance. Ease of administration is appreciated by the patient and nursing staff.

**Gray Pharmaceutical Co., Affiliate
The Purdue Frederick Company**

© COPYRIGHT 1975, GRAY PHARMACEUTICAL CO./NORWALK, CONN. 06856 A7901 160875

From start to finish, Fleet systematizes

For cleaner colons, clearer x-rays, and fewer retakes.



For preparation,
Fleet Barium Enema
Prep Kits assure
thorough, reliable
colon cleansing by
utilizing a combination
of diet, hydration, and
evacuation.

- Available in two convenient forms with suppository or enema as final step.
- Offering an effective and balanced method of prepping.
- Meeting all criteria for colon preparation as recommended by the American College of Radiology Ad Hoc Committee on Detection of Cancer of the Colon.
- With easy-to-follow instructions.
- With 3 convenient time schedules to fit better into your schedule and your patient's routine.

For the examination,
Fleet Barbag offers
greater visibility because it contains
Ultrasperse® with a
combination of barium
sulfate USP (98%) and
selected suspending
and dispersing agents
(2%) for "instantized"
mixability.

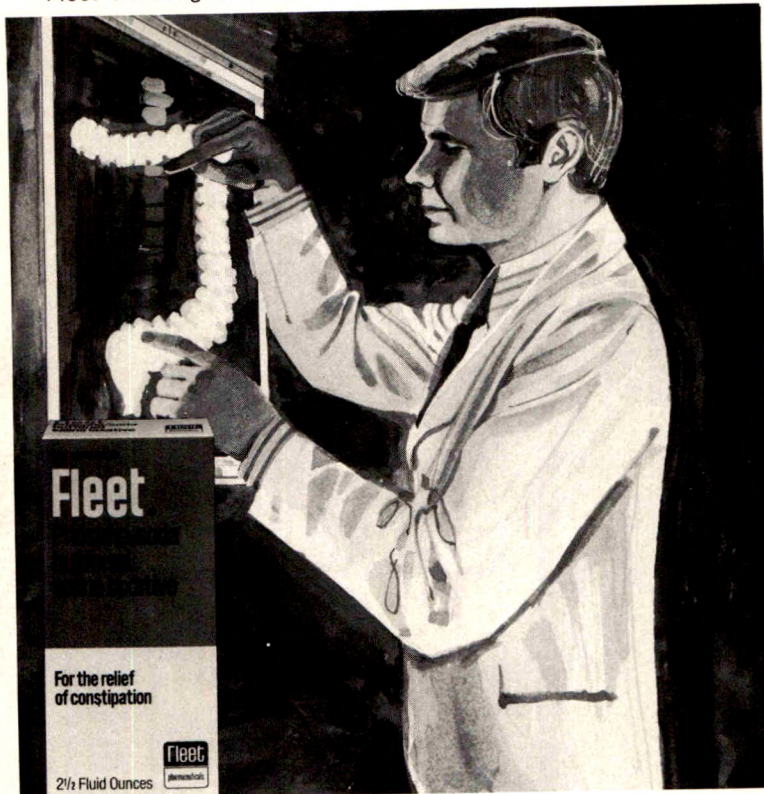
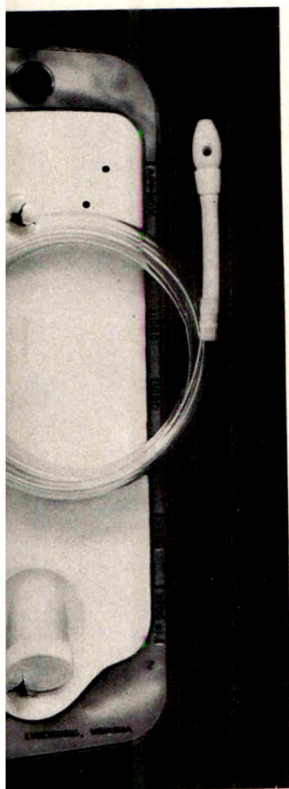
- With excellent suspension stability—up to 2 hours.
- With rapid, free-flow emptying.

barium enema exams...

C. B. Fleet presents a unique three-part system of products that can help you give quality

barium enema exams. It includes Fleet® Barium Enema Prep Kits for colon preparation, Fleet® Barobag for the actual

barium enema examination, and Fleet® Phospho-Soda for aftercare.



- Leakproof with screw closures for convenience.
- With angled spout (45°) for easier filling and handling.
- Available with either 12 or 16 oz. Ultrasperse® (barium sulfate USP).
- Also available with retention catheter.

For aftercare,

Fleet Phospho-Soda is gentle and most effective for cleansing the colon of barium and for preventing fecal impaction.

- Works in an hour or overnight, according to dosage, for convenience and flexibility in scheduling.
- Usually produces soft, formed stool with no unusual side effects.
- Promotes natural peristalsis to assure thorough action.

- Buffered for gentleness.
- Easy-to-take.
- Safe for use by patients of all ages, as indicated.

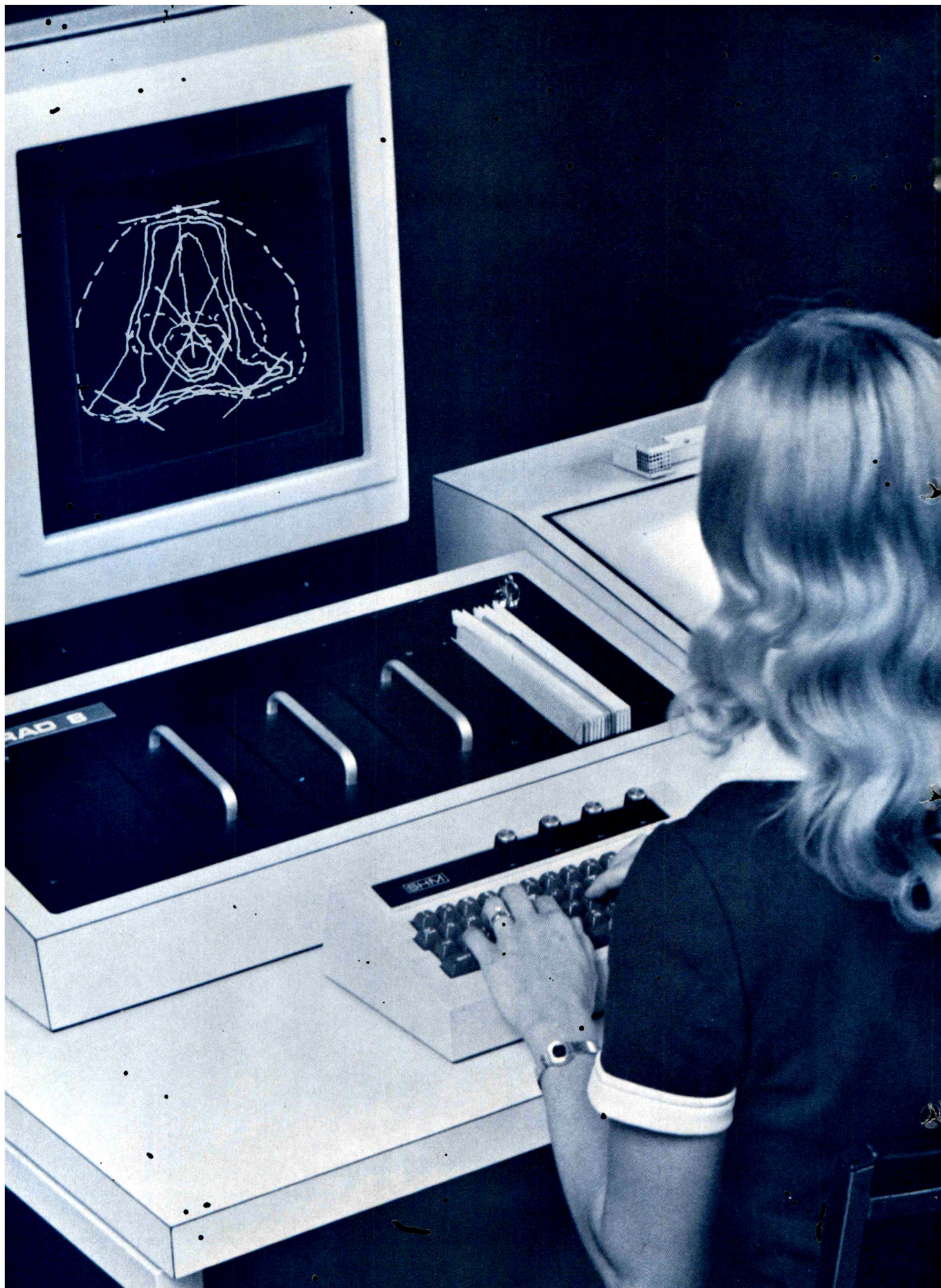
In the final note to *Detection of Colon Lesions* by the American College of Radiology Ad Hoc Committee on Detection of Cancer of the Colon, R. E. Miller states: "Almost every recommendation made is part of urging *quality control* by the radiologist in all aspects of his colon examination."

Fleet's new system of products will answer almost every need you'll encounter in barium enema examinations—from start to finish.

In barium enema exams, quality controls results. And Fleet controls quality.

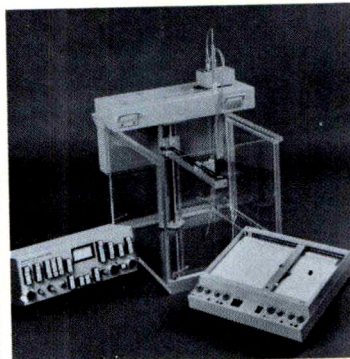
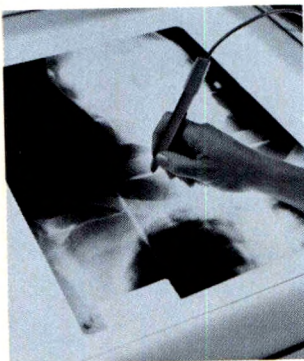


C. B. FLEET CO., INC.
Lynchburg, Va. 24505



RAD 8: IT BREAKS THE TIME BARRIER.

Time is the biggest barrier to detailed therapy planning. Time required for calculations that optimize the treatment plan, correct for tissue density, adjust for deviations from the central axis. □ The Rad 8 therapy planning system breaks the time barrier. Performing in seconds calculations that take 15 to 20 minutes manually. Producing detailed treatment plans two to three times faster than any other system. □ Rad 8 saves time in entering plan values. They can be traced directly from x-ray images with an acoustic pen, or they can be typed in by the operator using simple interactive English. It saves time in plan interpretation, displaying a graphic map of treatment landmarks that can be instantly varied for heterogeneity corrections, off-axis treatment, changes in patient condition and tumor response. And Rad 8 saves time in record keeping. It gathers plan and treatment information on high capacity floppy discs, the fastest and most convenient storage media. □ All the time you save can be devoted to more thorough planning and more precise treatment. Which means more efficient equipment utilization and improved patient care. □ SHM Nuclear Corp., 570 Del Rey, Sunnyvale, CA 94086 (408) 245-3136

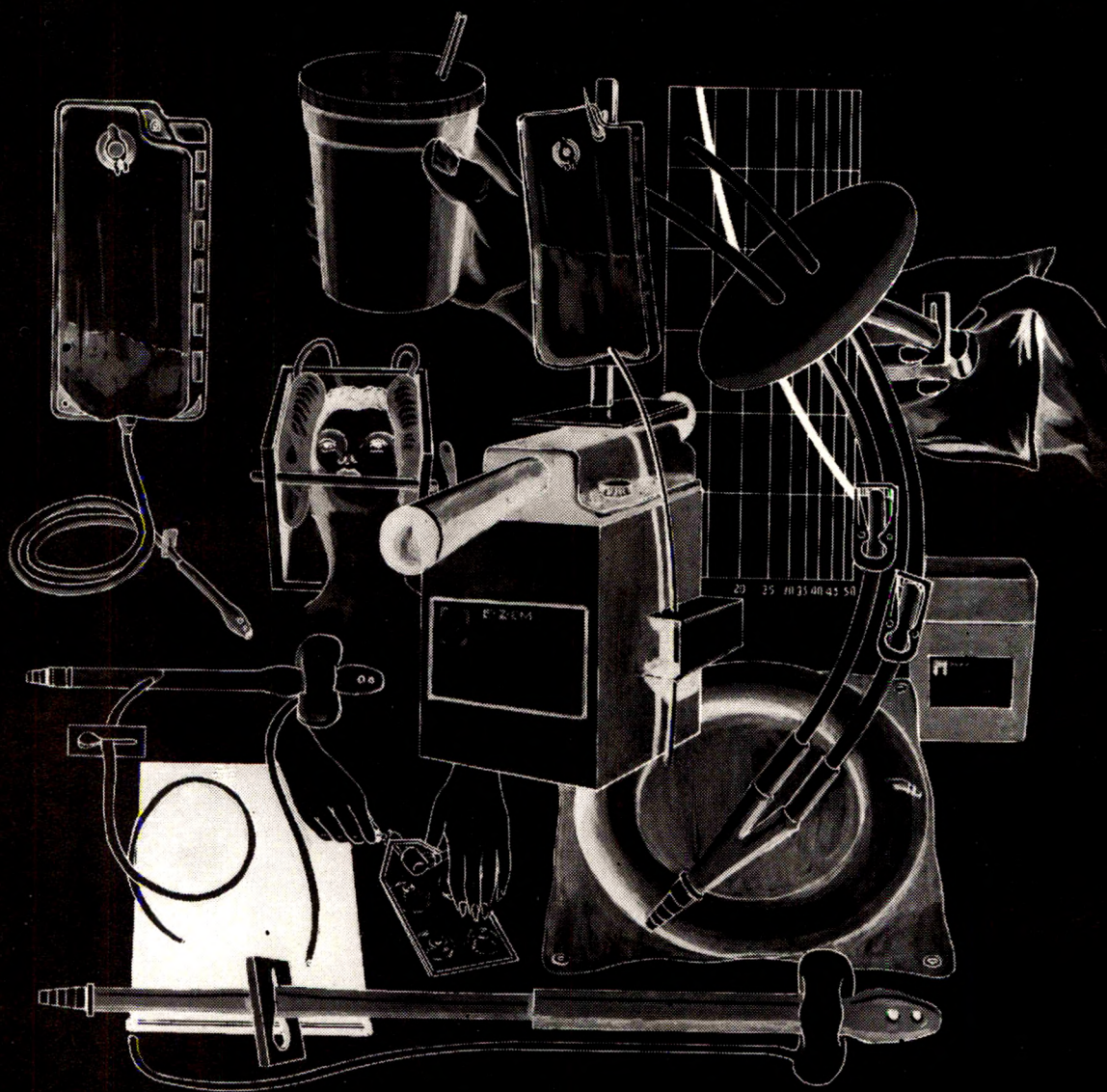


The Rad 8 console includes a modern plasma display, floppy disc storage, acoustic pen data entry system. Rad 8 is supported by the profession's most extensive software library. SHM is a total therapy company, offering linear accelerators, isodose plotters and other therapy equipment.

SHM Nuclear Corporation

Barium, Barium Systems, and Ancillary Products

...formulated and designed to meet the realistic
needs of the Modern Radiology Department



System of your choice

111 SWALM STREET

Westbury, N.Y. 11590 (516) 333-8230

International Affiliates: E-Z-EM Rooster B. V., Infirmieriestraat 6-8, Rotterdam 16, Netherlands

AGFA-GEVAERT

Mamoray RP-3

10X faster than conventional non screen films...up to 33% faster than the popular "low dose" system!

Mamoray RP-3...another new generation film from Agfa-Gevaert, the world's leader in sophisticated imaging technology.

Mamoray RP-3 features:

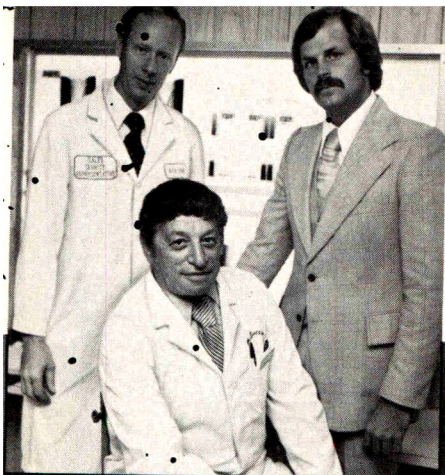
- An exposure speed less than 1/10 that of non screen techniques; up to 1/3 faster than other low dose systems currently in use, and...with a remarkable increase in contrast in all low density areas.
- Fine grain for optimum visualization of minute calcifications.
- A high contrast level that enhances clarity in diagnosing low density areas.

These, and other important features, make Mamoray RP-3 the ultimate film for all fine detail techniques: non screen, single and double screen.

If you're still utilizing older mammographic film techniques it's time that you looked at Mamoray RP-3. Contact your local Low X-Ray representative today. He'll gladly discuss these, and other Mamoray RP-3 features with you.

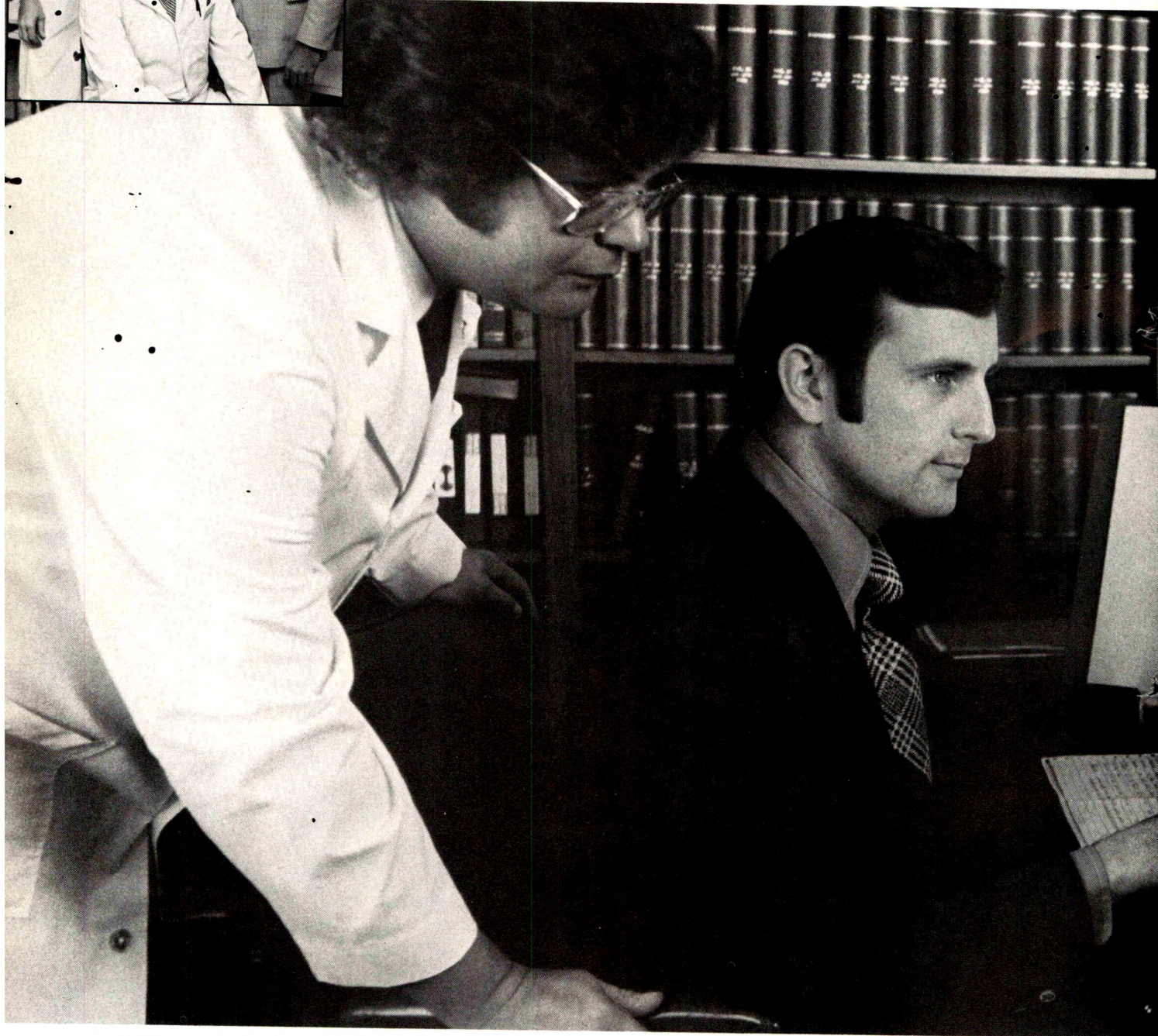


Division of IPCO Hospital Supply Corporation
1025 Westchester Avenue
White Plains, New York 10604



DuPont helped cut more than 20%

Buck Shaw (left), Du Pont Sales and Service Representative;
Joseph Galluccio, M.D. (seated), Director of Radiology;
Bob Pryor (right), Du Pont Senior Technical Representative.



In his responsibility as Administrative Assistant for the Radiology Department at Mercy Hospital, John Harlin's chief objective is reducing costs while maintaining high-quality patient care.

To help him realize this objective, Du Pont instituted a comprehensive Quality Control Program designed to deliver the best possible radiograph at the lowest possible cost per exam.

This Program consisted of services and

resources tailor-made for Mercy and aimed at eliminating many of the processing/imaging variables that can adversely affect radiographic quality.

To quantify the value of these quality control efforts, Du Pont conducted a Cost Control Program, which analyzed departmental expenses and income to determine if cost reduction objectives had been realized.

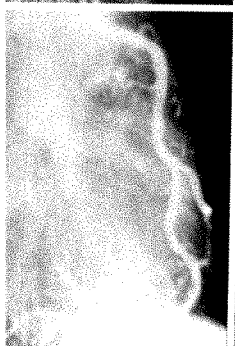
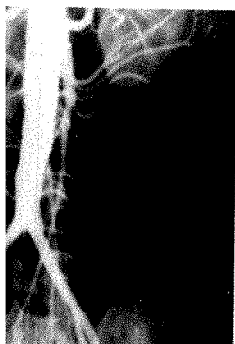
It's all part of Du Pont's commitment: personal involvement and quality in everything we do and sell to provide reduced operating costs and better patient care.



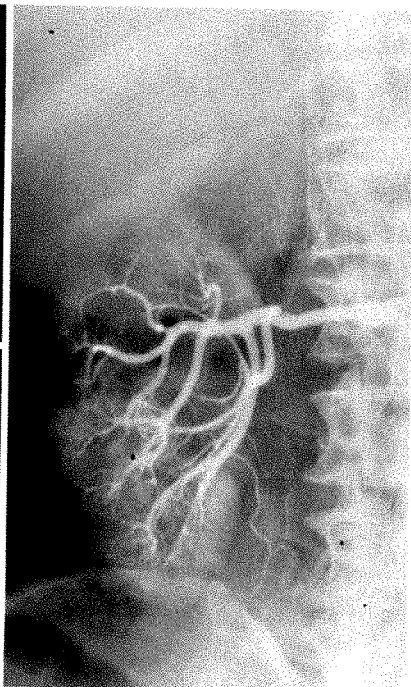
DEC 11 1994 MAY 14 1995

the reason is clear™

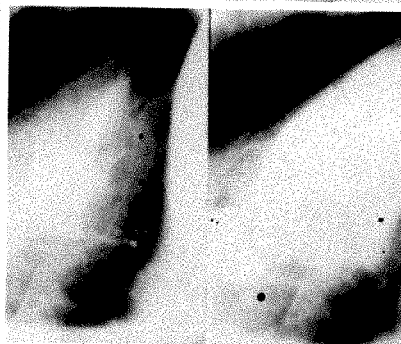
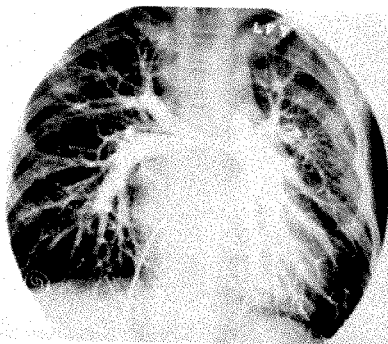
- Excellent image quality
- Rapid visualization of renal pelvis, ureters, and bladder... maximal opacification of renal passages may begin as early as 5 minutes after injection
- 8 indications*



raphy
ve coronary
graphy



• Selective renal arteriography



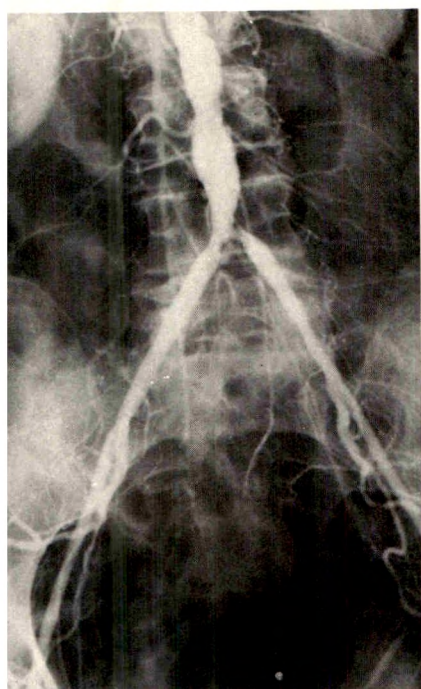
Pediatric angiocardiology
Left ventriculography performed
following coronary arteriography



Selective visceral
arteriography

Renografin®-76

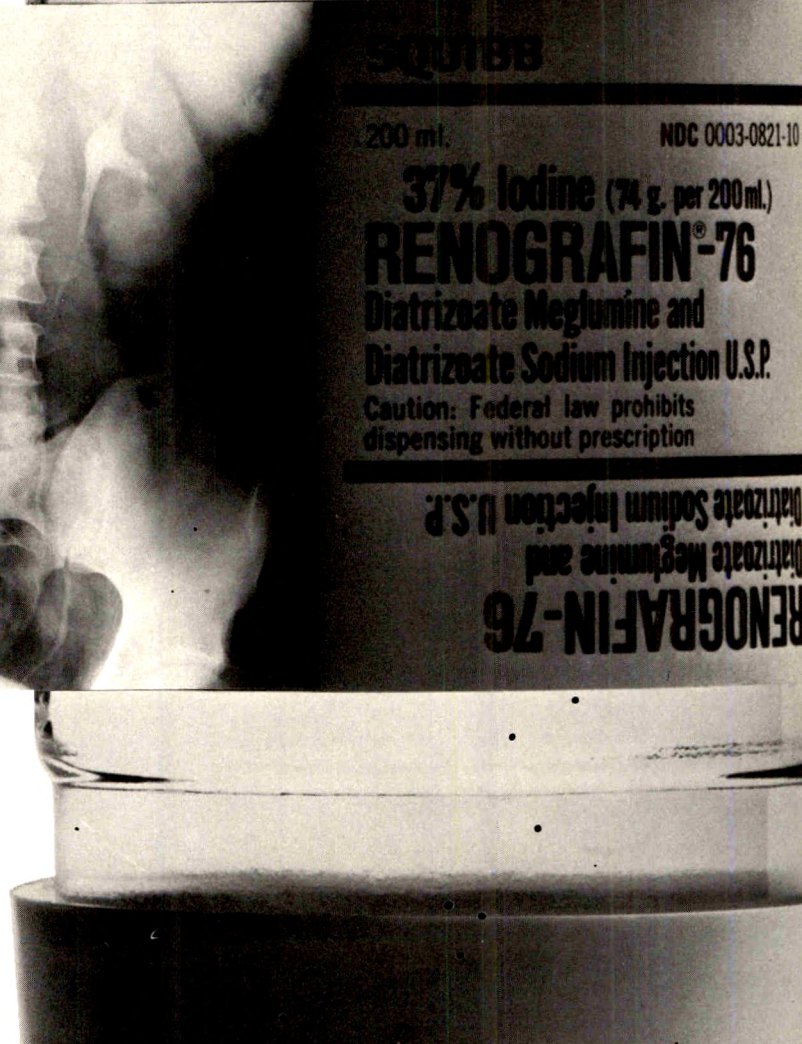
Diatrizoate Meglumine and
Diatrizoate Sodium Injection U.S.P.



Peripheral arteriography



Excretion urography



*For dosage and administration recommendations, see package insert.

Please see following page for brief summary.

RENOGRAFIN-76

Diatrizoate Meglumine and Diatrizoate Sodium Injection U.S.P.

Renografin-76 (Diatrizoate Meglumine and Diatrizoate Sodium Injection U.S.P.) is supplied as a sterile, aqueous solution providing 66% diatrizoate meglumine and 10% diatrizoate sodium with 0.32% sodium citrate as a buffer and 0.04% edetate disodium as a sequestering agent. The solution contains approximately 37% (370 mg./ml.) bound iodine and approximately 4.48 mg. (0.19 mEq.) sodium per ml.

CONTRAINDICATIONS: In patients with a hypersensitivity to salts of diatrizoic acid. Urography contraindicated in patients with anuria.

WARNINGS: A definite risk exists with the use of contrast agents in excretion urography in patients with multiple myeloma. There has been anuria with progressive uremia, renal failure and death. This risk of the procedure in these patients is not a contraindication; however, partial dehydration in preparation for study is not recommended since it may predispose for precipitation of myeloma protein in renal tubules. No therapy, including dialysis, has been successful in reversing this effect. Myeloma should be considered in persons over 40 before undertaking urographic procedures.

In cases of known or suspected pheochromocytoma, if the physician feels that the possible benefits outweigh the considered risks, radiopaque materials should be administered with extreme caution; however, an absolute minimum of material should be injected, and the blood pressure should be assessed throughout the procedure, and measures for treating a hypertensive crisis should be available.

Contrast media may promote sickling in homozygous individuals when injected I.V. or intra-arterially. Although a history of sensitivity to iodine per se or to other contrast media is not an absolute contraindication, administration of diatrizoate requires extreme caution in such cases. Perform thyroid function tests prior to administration of Renografin-76 (Diatrizoate Meglumine and Diatrizoate Sodium Injection U.S.P.) since iodine-containing contrast agents may alter the test results.

Weigh the inherent risks against necessity for performing *angiocardiology* in cyanotic infants and patients with chronic pulmonary emphysema. In *pediatric angiocardiology*, a dose of 10 to 20 ml. may be particularly hazardous in infants weighing less than 7 kg.; this risk is probably significantly increased if these infants have preexisting right heart "strain," right heart failure, and effectively decreased or obliterated pulmonary vascular beds. Perform *urography* with extreme caution in persons with severe concomitant hepatic and renal disease. Perform *selective coronary arteriography* only in selected patients and those in whom expected benefits outweigh the procedural risk. Perform *selective visceral arteriography* with extreme caution in presence of severe generalized atherosclerosis, specifically with plaques or aneurysms at level of iliac or femoral arteries.

Usage in Pregnancy: Use Renografin-76 (Diatrizoate Meglumine and Diatrizoate Sodium Injection U.S.P.) in pregnant patients only when the physician deems its use essential to the welfare of the patient since safe use during pregnancy has not been established.

PRECAUTIONS: Diagnostic procedures involving use of contrast agents should be performed under the direction of personnel with prerequisite training and a thorough knowledge of the particular procedure. Appropriate facilities should be available for coping with situations which may arise as a result of the procedure and for emergency treatment of severe reactions to the contrast agent itself; competent personnel and emergency facilities should be available for at least 30 to 60 minutes after I.V. administration since delayed reactions have been known to occur. These severe life-threatening reactions suggest hypersensitivity to the contrast agent. A personal or family history of asthma or allergy or a history of a previous reaction to a contrast agent warrants special attention and may predict more accurately than pre-testing the likelihood of a reaction although not the type nor severity of the reaction in the individual. The value of any pretest is questionable. The pretest most performed is the slow I.V. injection of 0.5 to 1.0 ml. of the preparation prior to injection of the full dose; however, the absence of a reaction to the test dose does not preclude the possibility of reaction to the full diagnostic dose. Should the test dose produce an untoward response, the necessity for continuing the examination should be re-evaluated. If deemed essential, examination should proceed with all possible caution. In rare instances, reaction to the test dose may be extremely severe; therefore, close observation and facilities for emergency treatment are indicated.

Renal toxicity has been reported in a few patients with liver dysfunction who were given oral cholecystographic agents followed by urographic agents; therefore, if known or suspected hepatic or biliary disorder exists, administration of Renografin-76 (Diatrizoate Meglumine and Diatrizoate Sodium Injection U.S.P.) should be postponed following the ingestion of cholecystographic agents. Consider the functional ability of the kidneys before injecting the contrast agent. Use cautiously in severely debilitated patients and in those with marked hypertension. Bear in mind the possibility of thrombosis when using percutaneous techniques. Since contrast agents may interfere with some chemical determinations made on urine specimens, collect urine before or two or more days after administration of the contrast agent.

In *excretion urography*, adequate visualization may be difficult or impossible in uremic patients or others with severely impaired renal function (see Contraindications). In *aortography* repeated intra-aortic injections may be hazardous; this also applies to *pediatric angiocardiology* particularly in infants weighing less than 7 kg. (see Warnings). In *peripheral arteriography*, hypotension or moderate decreases in blood pressure seem to occur frequently with intra-arterial (brachial) injections; this is transient and usually requires no treatment. Monitor blood pressure during the immediate 10 minutes after injection. It is recommended that *selective coronary arteriography* not be performed for about 4 weeks after diagnosis of myocardial infarction; mandatory prerequisites to this procedure are experienced personnel, ECG monitoring apparatus, and adequate facilities for immediate resuscitation and cardioversion.

ADVERSE REACTIONS: Nausea, vomiting, flushing, or a generalized feeling of warmth are the reactions seen most frequently with intravascular injection. Symptoms which may occur are chills, fever, sweating, headache, dizziness, pallor, weakness, severe retching and choking, wheezing, a rise or fall in blood pressure, facial or conjunctival petechiae, urticaria, pruritus, rash, and other eruptions, edema, cramps, tremors, itching, sneezing, lacrimation, etc. Antihistaminic agents may be of benefit; rarely, such reactions may be severe enough to require discontinuation of dosage. There have been a few reports of a burning or stinging sensation or numbness, of venospasm or venous pain, and of partial collapse of the injected vein. Neutropenia or thrombophlebitis may occur. Severe reactions which may require emergency measures (see Precautions) are a possibility and include cardiovascular reaction characterized by peripheral vasodilatation with hypotension and reflex tachycardia, dyspnea, agitation, confusion, and cyanosis progressing to unconsciousness. An allergic-like reaction ranging from rhinitis or angioneurotic edema to laryngeal or bronchial spasm or anaphylactoid shock may occur. Temporary renal shutdown or other nephropathy may occur.

Adverse reactions as a consequence of *excretion urography* include cardiac arrest, ventricular fibrillation, anaphylaxis with severe asthmatic reaction, and flushing due to generalized vasodilatation. Risks of *aortography* procedures include injury to aorta and neighboring organs, pleural puncture, renal damage (including infarction and acute tubular necrosis with oliguria and anuria), accidental selective filling of right renal artery during translumbar procedure in presence of preexistent renal disease, retroperitoneal hemorrhage from translumbar approach, spinal cord injury and pathology associated with syndrome of transverse myelitis, generalized petechiae, and death following hypotension, arrhythmia, and anaphylactoid reactions. In *pediatric angiocardiology*, arrhythmia and death have occurred. During *peripheral arteriography*, hemorrhage from puncture site, thrombosis of the vessel, and brachial plexus palsy (following axillary artery injection) have occurred. During *selective coronary arteriography* and *selective coronary arteriography with left ventriculography*, transient ECG changes (most patients); transient arrhythmias (infrequent); ventricular fibrillation (from manipulation of catheter or administration of medium); hypotension; chest pain; myocardial infarction; transient elevation of creatinine phosphokinase (occurred in about 30% of patients tested); fatalities have been reported; hemorrhage, thrombosis, pseudoaneurysms at puncture site, dislodgment of arteriosclerotic plaques, dissection of coronary vessels, and transient sinus arrest have occurred due to the procedure. Adverse reactions in *selective renal arteriography* include nausea, vomiting, hypotension, hypertension, and post-arteriographic transient elevations in BUN, serum creatinine and glucose. Complications of *selective visceral arteriography* include hematomas, thrombosis, pseudoaneurysms at injection site, dislodgment of arteriosclerotic plaques; other reactions may include urticaria, hypotension, hypertension, and insignificant changes in renal function and liver chemistry tests.

For full prescribing information, consult package insert.

HOW SUPPLIED: Available in 20 ml. and 50 ml. single-dose vials and in 100 ml. and 200 ml. single-dose bottles.

SQUIBB HOSPITAL DIVISION

E. R. Squibb & Sons, Inc.

the reason
is clear™



You are entering a remarkable era of diagnostic advancement. Instead of being limited to a single imaging method, you will take advantage of many techniques, choosing them to meet your specific diagnostic criteria and the condition of your patient.

Searle is helping shape this era of advancement. Over the past decade, guided by your needs, we have developed sophisticated nuclear imaging instruments to a high degree of performance. Now, the knowledge gained during that time is being applied to the creation of instrumentation in the fields of ultrasound and CT scanning.

What Searle developed yesterday in nuclear imaging, the medical community relies on today. And today we are planning significant advances in ultrasonic, CT, and nuclear imaging. Tomorrow is in view.

IMAGING:

The Living Art



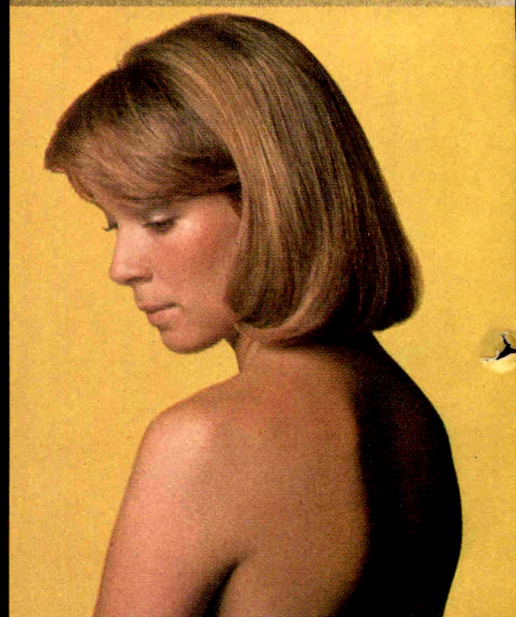
SEARLE

Searle Radiographics Inc.

Introducing Kodak Min-R products
for mammography.

Increased speed...
reduced exposure.

In breast x-ray examinations,
consider the speed,
consider the patient exposure,
consider the technic flexibility.



Two new Kodak products represent an important advance in early breast cancer detection: Kodak Min-R film and Kodak Min-R screen.

Compared with any other Kodak film/screen combination for mammography, Min-R products provide the fastest speed, with equal or better image sharpness.



characteristics of Min-R screen and film, minute structural detail is imaged sharply. Excellent low-density contrast in the film emulsion enhances the imaging of detail (calcifications and fibrous structures), particularly in the thick areas of the breast which are inherently low in subject contrast.

Increased speed of Min-R products permits added technic

flexibility. Options include: use of shorter exposure times to minimize motion unsharpness, use of smaller focal spots or longer focus-film distances for improved image geometry. Through careful selection of technic, use of Kodak Min-R screen and film can also lengthen tube life.

Your Kodak Technical Sales Representative can give

you details on Kodak Min-R products. Or if you prefer, ask your medical x-ray products dealer for more information. Or write: Eastman Kodak Company, Department 740-B, Rochester, New York 14650.



A commitment to quality

WHAT'S NOW SQUIBB?

On the current nuclear medicine scene



MINITEC® (Technetium 99m) Generator

The Technetium 99m Generator using fission product molybdenum to produce technetium 99m. MINITEC is unlike any generator you've ever used—made small to make sense.

Designed for easy handling

- MINITEC has its own handle for easy lifting, easy carrying and reduced hand exposure
- Weighs only 24½ lbs., less than 5" in diameter, under 8½" high

Designed for easy elution

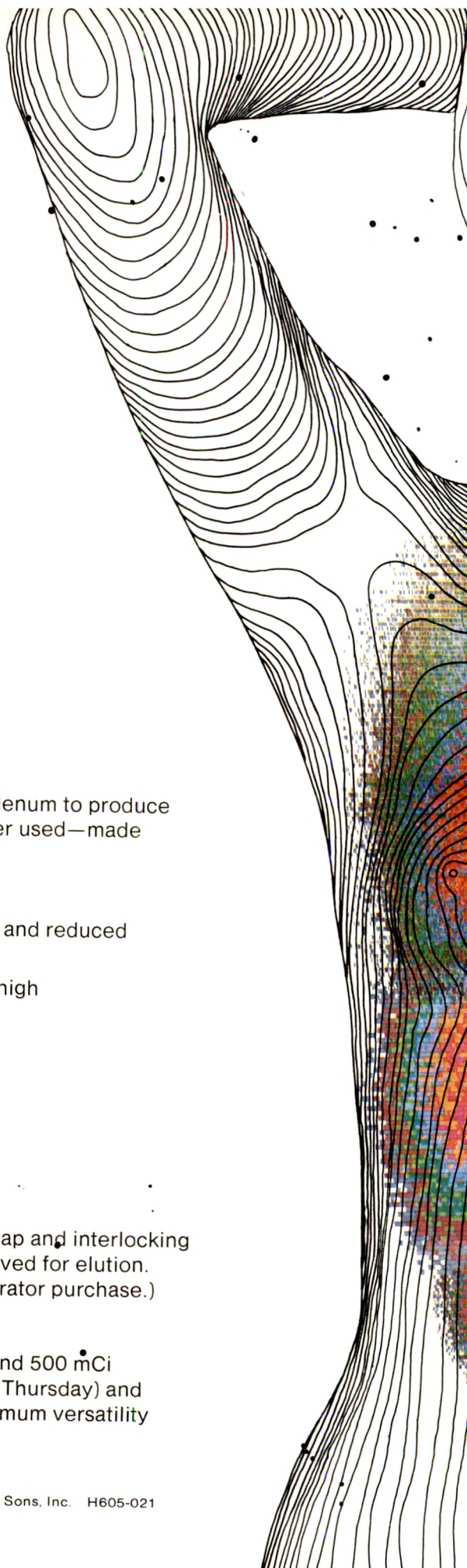
- Sets up in seconds
- Elutes in only 3 minutes after eluent vial has emptied

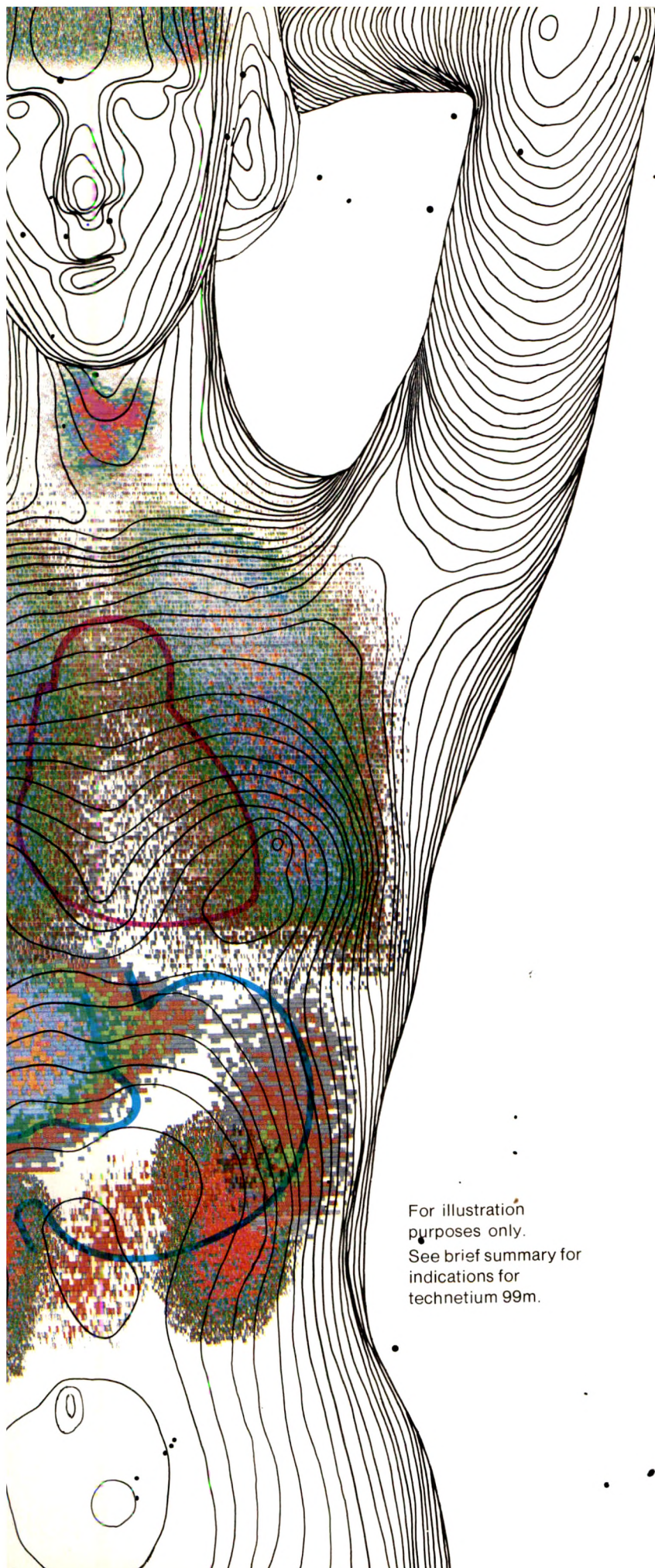
Designed for safety

- No exposed tubing when eluting
- 1½" lead surrounds the MINITEC column
- 1½" of extra lead protection from MAXI-SHIELD™. Base, cap and interlocking half rings easily assembled on site . . . only the cap is removed for elution. (You get MAXI-SHIELD free with your first MINITEC Generator purchase.)

Designed for convenience

- MINITEC Generator is available in 50, 100, 200, 300, 400 and 500 mCi potencies. Delivery on Monday AM (precalibrated through Thursday) and Wednesday (precalibrated through Monday) provides maximum versatility to satisfy technetium requirements of your lab's work load.





For illustration purposes only. See brief summary for indications for technetium 99m.

Minitec[®] (Technetium 99m) Generator

Minitec[®] (Technetium 99m) Generator provides a means of obtaining a sterile, non-pyrogenic supply of technetium 99m (^{99m}Tc) as sodium pertechnetate ^{99m}Tc.

Indications: Sodium pertechnetate ^{99m}Tc is indicated for brain imaging, thyroid imaging, salivary gland imaging, blood pool imaging, and placenta localization.

Contraindications: At present, there are no known contraindications to the use of sodium pertechnetate ^{99m}Tc.

Warnings: Radiopharmaceuticals should be used only by physicians who are qualified by specific training in the safe use and safe handling of radionuclides, produced by nuclear reactor or cyclotron, and whose experience and training have been approved by the appropriate federal or state agency authorized to license the use of radionuclides.

This radiopharmaceutical should not be administered to women who are pregnant or who may become pregnant or during lactation unless the information to be obtained outweighs the possible potential risks from the radiation exposure involved. Ideally, examinations using radiopharmaceuticals, especially those elective in nature, of a woman of childbearing capability should be performed during the first few (approximately 10) days following the onset of menses.

Since radioactive pertechnetate is secreted in milk during lactation, formula-feedings should be substituted for breast-feedings.

Important: Since material obtained from the generator may be intended for intravenous administration, aseptic technique must be strictly observed in all handling. Only the eluent provided should be used to elute the generator. Do not administer material eluted from the generator if there is any evidence of foreign matter.

Precautions: As in the use of any other radioactive material, care should be taken to insure minimum radiation exposure to the patient consistent with proper patient management and to insure minimum radiation exposure to occupational workers.

At the time of administration, the solution should be crystal clear.

Adverse Reactions: At present, adverse reactions have not been reported following the use of sodium pertechnetate ^{99m}Tc.

For complete prescribing information, consult package insert.

How Supplied: Minitec (Technetium 99m) Generator is available in potencies of 50, 100, 200, 300, 400, and 500 mCi. Supplied with the generator are vials of eluent containing 5 ml. of a sterile, non-pyrogenic solution of 0.9% sodium chloride in water for injection. Also supplied is suitable equipment for eluting, collecting, and assaying the technetium 99m.

Medotopes[®]



SQUIBB HOSPITAL DIVISION

E. R. Squibb & Sons, Inc.
Princeton, N.J. 08540





A new series of x-ray generators featuring simple push-button programming: Siemens Organomatic.

- **Convenience** is the idea behind these generators. Any one of 49 preset programs may be selected simply by the turn of the knob and the push of a button.

For ease of identification, push-buttons are organ related. The proper kV, mAs, mA, focus, screen and tube can be selected with only one button. The need to consult reference tables for desired settings is eliminated. Moreover, through automation, the chances of error and the need for time consuming repeats are substantially reduced.

Selection. Available as a single-phase 600 mA generator (model 502) or a three-phase 500 mA generator (model 506), the Organomatic may be customized to meet specific user needs. All automatic programs can be preset during installation to accommodate any desired combination of kV and mAs settings.

Ease of Service. Solid state circuitry guarantees performance reliability. Circuit board and swing-out rack assembly assures accessibility and ease of maintenance.

The Organomatic also features an exclusive automatic fault locator/indicator to pinpoint service requirements.

Options. A variety of add-on system features make the Organomatic fully adaptable to specific needs. Among them:

- Automatic exposure timer for correct patient size compensation.
- Planigraphy programming (28 additional programs).
- Fluoroscopy with automatic brightness control.
- Indirect exposure technique with 100 mm cut film camera.
- Override module for free kV and mAs selection.

Investigate the Siemens Organomatic and ask about convenient lease financing arrangements. For detailed information, contact your Siemens representative, or you may write to: Siemens Corporation, Medical Systems Division, 186 Wood Avenue South, Iselin, N.J. 08830 (201) 494-1000

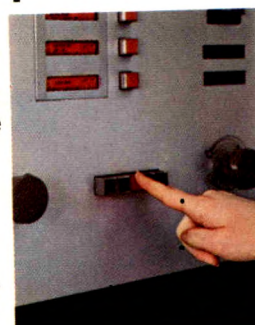
In Canada: Siemens Canada Limited, P.O. Box 7300, Pointe Claire 730-P.Q.



1 Body region selector.



2 Organ selector buttons.

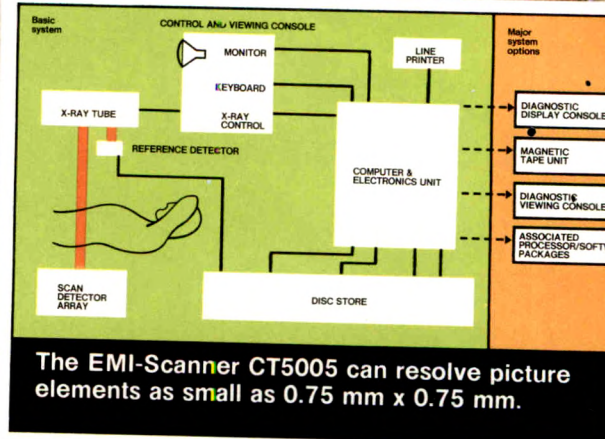
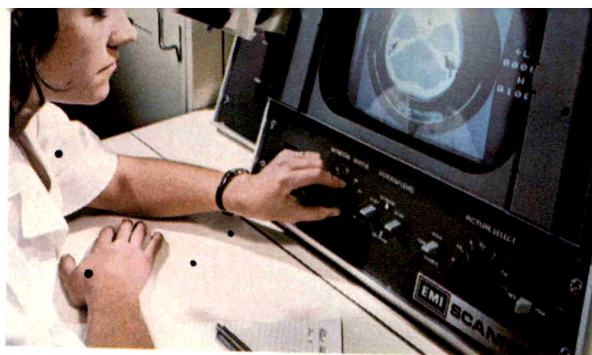
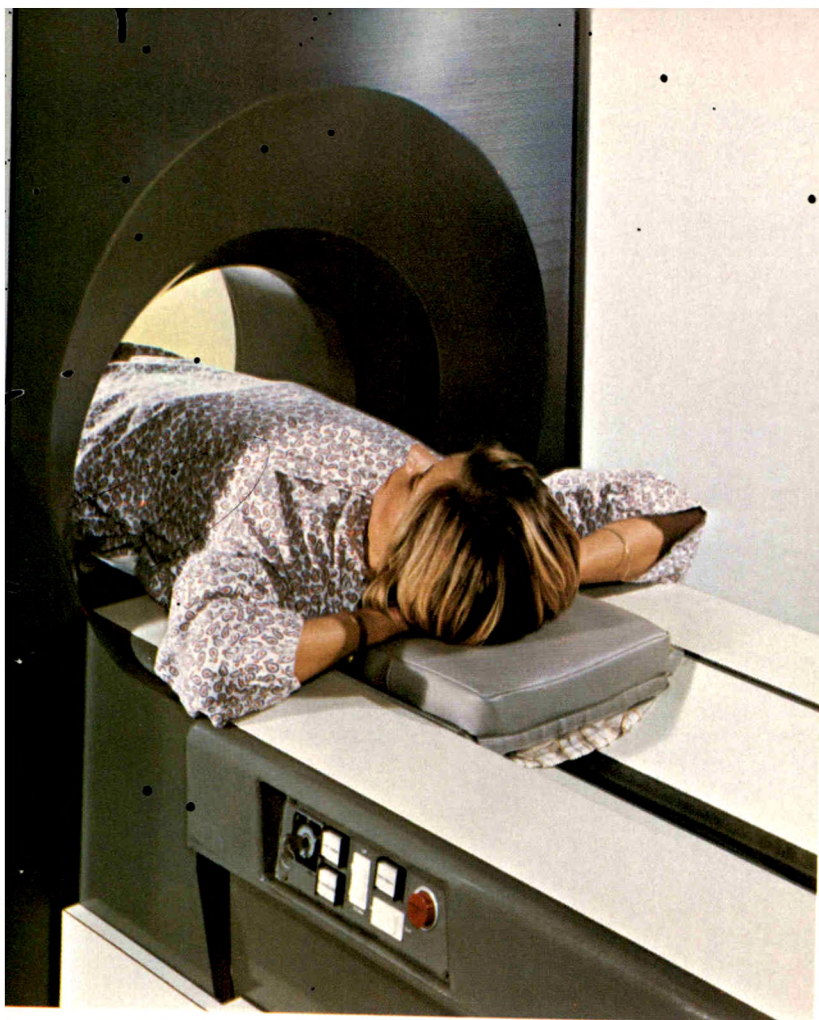


3 Patient thickness compensation.

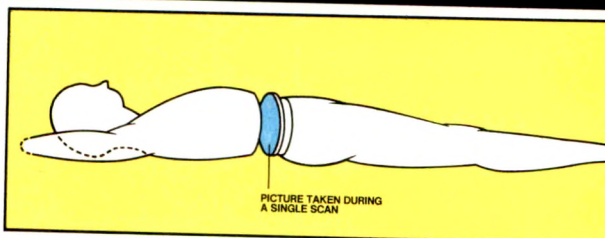


4 Exposure release.

SIEMENS



The EMI-Scanner CT5005 can resolve picture elements as small as 0.75 mm x 0.75 mm.



6-216

The EMI CT5005 head and body scanner provides

CT Scans, cranium to calcaneus

Like its companion system—the EMI CT1010 Neuro C.T. Scanner—our new EMI-Scanner CT5005 Advanced General Diagnostic C.T. System is based on fully proven technology that has established EMI as the unrivaled world leader in computerized tomographic scanning. This new head and body scanning system combines the capability for exceptional resolution, definition and accuracy in the pictures produced, a very fast scanning cycle, unusually powerful computing capability and other advanced features that con-



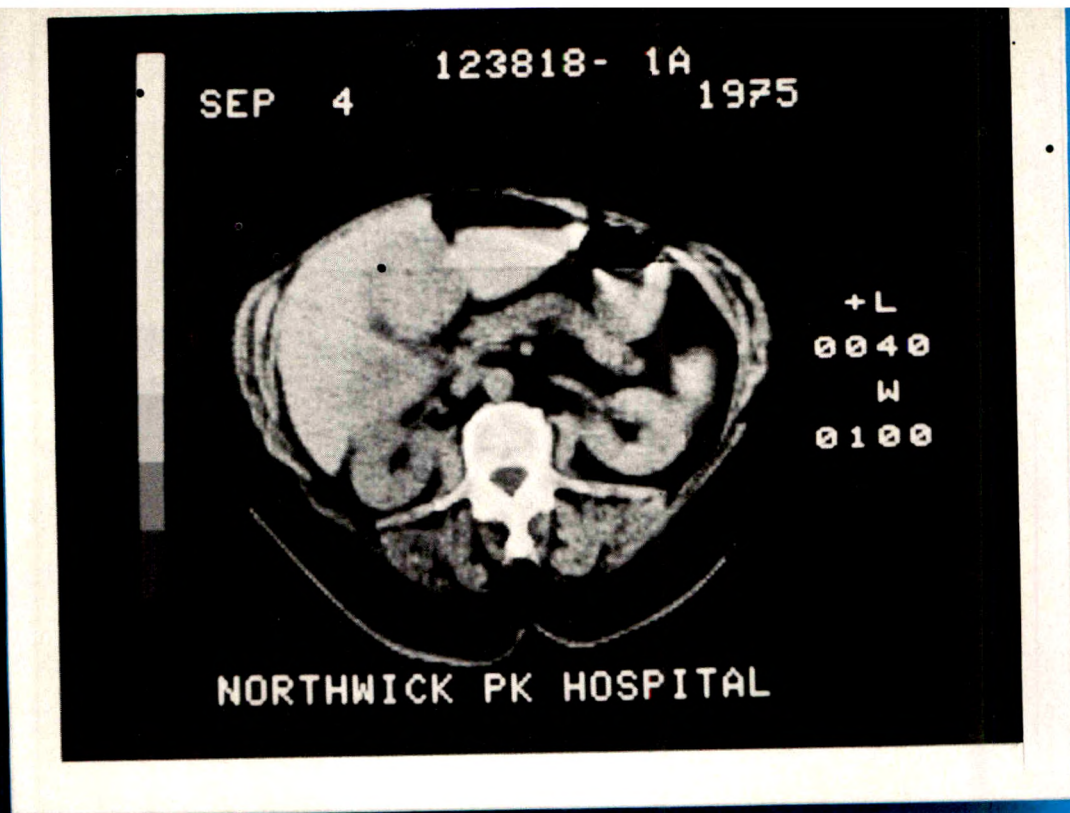
**First in CT
system
engineering**

EMI MEDICAL INC

tribute to ease-of-operation and efficient patient handling. The CT5005 General Diagnostic System

can be tailored by selection of the appropriate choice of peripherals and software packages to meet specific clinical needs. Obviously, for the radiologist and referring physician alike, the quality of the scan picture itself is the final proof of any CT system's performance. The EMI-Scanner System has met this test in hundreds of institutions. It is the world's only fully proven scanner system. For information, call us or write.

3605 Woodhead Drive, Northbrook, Illinois 60062 Telephone: (312) 504-0000



Scan taken through the 1st lumbar vertebra. Note the liver, spleen, kidneys, aorta, superior mesenteric artery, stomach, pancreas, inferior vena cava, and right renal vein.

6-217

Superior diagnostic information in every EMI-SCAN:

A bright window at L1

The picture you see above is a reproduction of an EMI-SCAN. The EMI-Scanner CT5005 Advanced General Diagnostic C.T. System (cranium and body scanner) results in pictures composed of more than 300,000 X-ray readings. The CT5005 differentiates between tissue densities that can vary by as little as one unit in 2000. In addition to resolving picture elements 0.75 mm x 0.75 mm in area, the EMI-Scanner CT5005 high-resolution option provides a special clinician's Diagnostic Viewing Console that enables any section

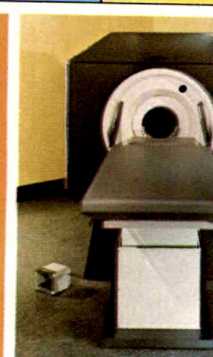
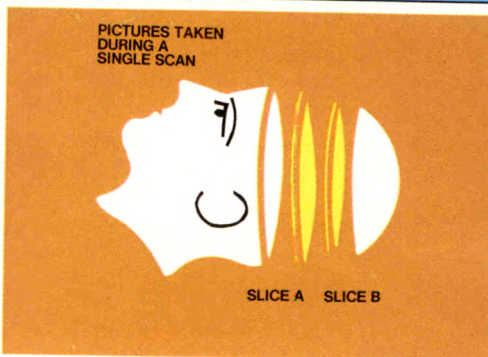
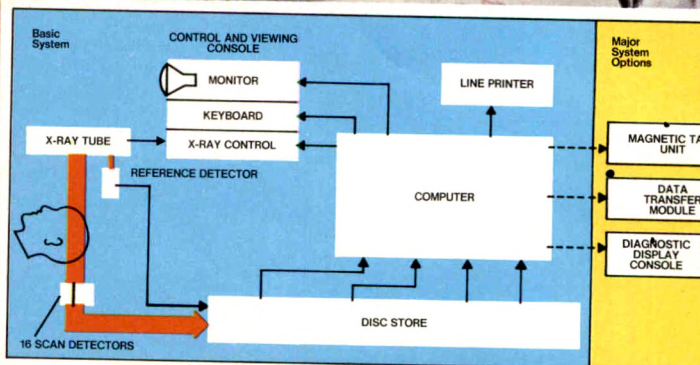
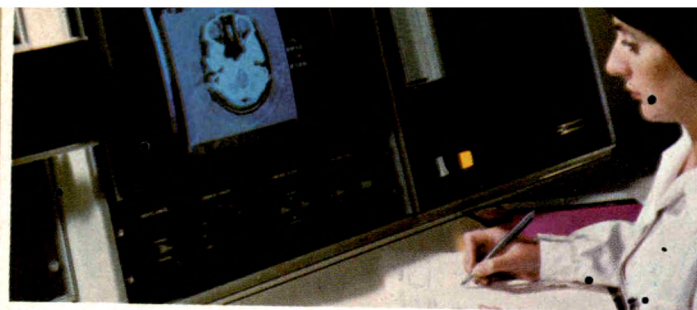


**First in CT
imaging,
worldwide**

EMI MEDICAL INC

of the total scan picture to be enlarged four times. This special viewing facility may be operated completely independently of the in-use status of the main installation—either at the scanner site or a remote location. Additional diagnostic display and data processing options are provided to meet specific clinical needs. The EMI-Scanner is unexcelled in accuracy, resolution, and clinical versatility. It is unrivaled in clinical acceptance and use, worldwide. There is no brighter diagnostic window. For more information, call us or write.

3605 Woodhead Drive, Northbrook, Illinois 60062 Telephone: (312) 564-2000



6-215

An unmatched performance record makes the EMI-Scanner

The fully proven CT system

EMI Medical now offers two computerized tomographic systems based on thoroughly proven EMI technology. For scanning both the head and body, there is the EMI-Scanner CT5005 Advanced General Diagnostic C.T. System. In recognition of the specialized requirements of neuroradiological studies, EMI Medical also offers the EMI-Scanner CT1010 Advanced Neuro C.T. System, designed specifically for institutions whose neurological and neurosurgical case-loads warrant a computerized tomographic system

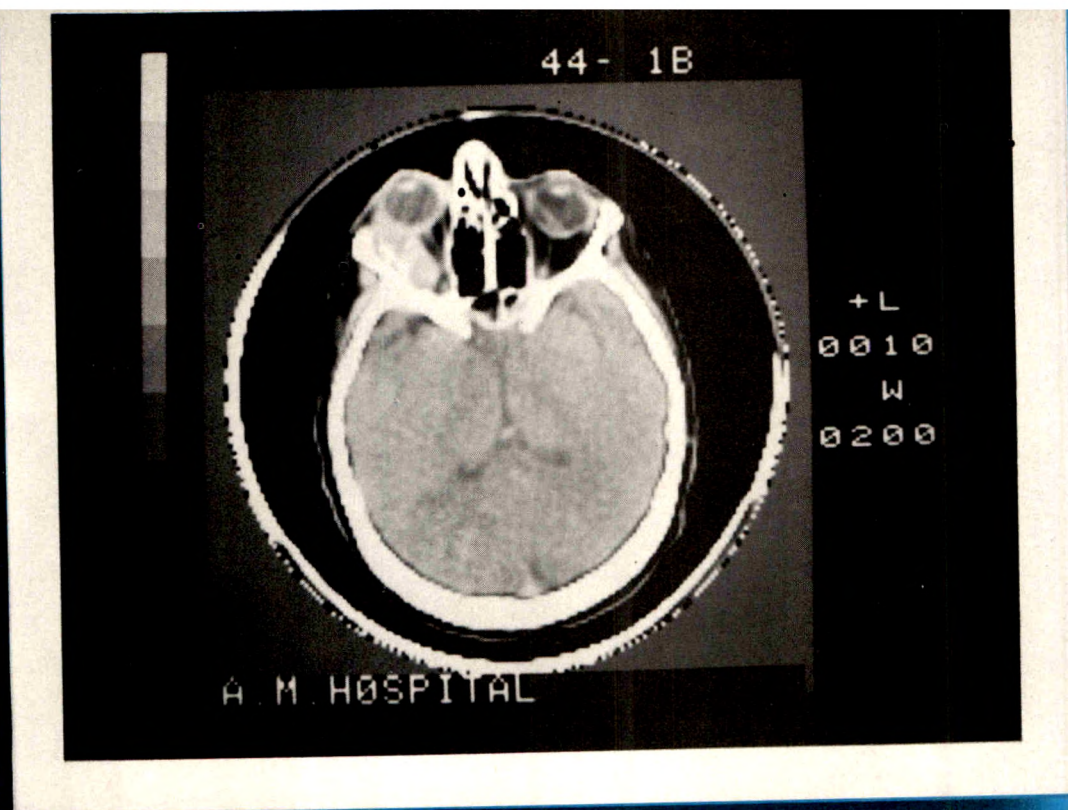


**First in CT
system
engineering**

EMI MEDICAL INC

dedicated solely to scanning of the head and upper spinal column. The CT1010 allows high patient throughput and increased clinical flexibility within a significantly more economical system. Obviously, the final test of any CT system is the quantity and quality of the diagnostic information it provides. The EMI-Scanner has met this test in actual diagnostic use in hundreds of institutions. It is the world's only fully proven CT scanner system. For more information on the CT1010 Neuro C.T. System, call us or write.

3605 Woodhead Drive, Northbrook, Illinois 60062 Telephone: (312) 564-2000



Reproduction of an EMI-SCAN of a young male patient with a 12 month history of increasing proptosis and limitation of lateral ocular movements. The scan demonstrates a mass in the lateral section of the left orbit with early calcification visible within the mass. Note the detail visible in the orbital regions.

6-219

Superior diagnostic information in every EMI-SCAN:

The optimal orbital view

The EMI CT1010 Advanced Neuro C.T. System is designed for exclusive use in scanning the head and upper spinal column. The CT1010 provides capability for both standard (180°) and wide (240°) scan angles, the latter being particularly useful in examining patients who may be subject to involuntary head movement. Likewise, standard and high-accuracy scanning speeds are offered. In the high-accuracy mode, the sensitivity of the system is increased by 2½ times. Still greater resolution can be achieved by selecting any section of



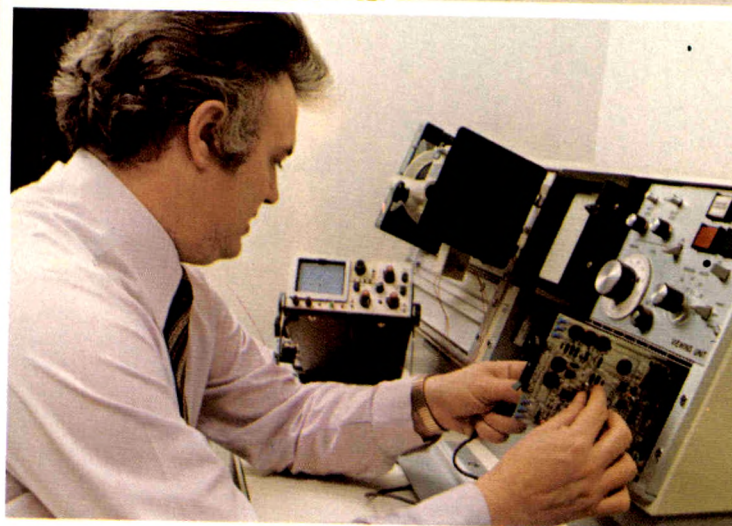
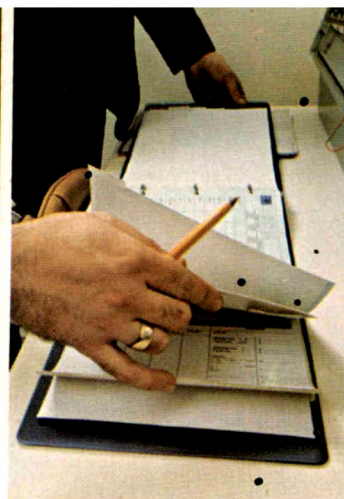
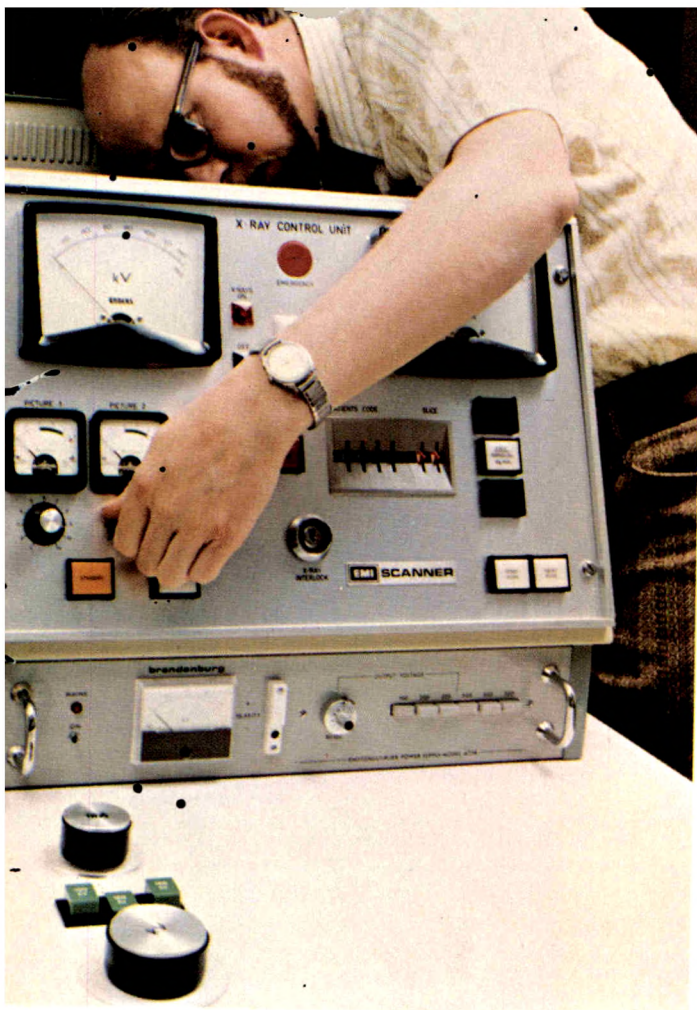
**First in CT
imaging,
worldwide**

EMI MEDICAL INC

a scan to be enlarged four times for whole-screen display. An optional clinician's Diagnostic Display

Console adds to system flexibility by allowing the viewing of existing results independently of the in-use status of the main scanner installation. For institutions whose case-load warrants a C.T. system dedicated solely to neuroradiological use, the CT1010 allows high patient throughput and increased clinical flexibility within a significantly more economical system. For more information, call us or write.

3605 Woodhead Drive, Northbrook, Illinois 60062 Telephone: (312) 564-2000



6-214

Universal acceptance of the EMI-Scanner means we have

A service engineer almost everywhere

The EMI-Scanner System has been installed in hundreds of institutions across the United States and Canada; an unrivaled record of acceptance which EMI Medical has matched with an expansive network of locally-based service engineers. The world's largest corps of trained and experienced CT service engineers are on-the-job to meet both routine and emergency maintenance needs of our client institutions. At our headquarters, EMI Medical maintains a working facility for analyzing all aspects of system performance.



**First in CT
maintenance
services**

EMI MEDICAL INC

Inventories of key replacement parts are maintained at our headquarters, regional offices, and nationwide parts depots. Both the EMI-Scanner CT 1010 Advanced Neuro C.T. System and the EMI-Scanner CT 5005 Advanced General Diagnostic C.T. System are warranted for 12 months. Extended coverage is available through EMI Medical Service Contracts. Our service team is the most experienced in the world in preventing scanner system "downtime." For more information, call us or write.

3605 Woodhead Drive, Northbrook, Illinois 60062 Telephone: (312) 564-2000

The Challenge of Computed Tomography

It is a gentle irony that this issue of the *American Journal of Roentgenology* commemorating the bicentennial anniversary of the American revolution is devoted to computed tomography, a British development. We pay honor to Godfrey N. Hounsfield and his superb innovation, observing that it enhances the kinship of two peoples "separated by a common language" by benefiting both. Indeed, while the export success of the EMI scanner undoubtedly has aided the British balance of payments, the great majority of these devices are now used in the United States to the great advantage of our patients. But the British challenge in this field has not remained unanswered. There are now at least eight U.S. companies either producing or developing CT equipment, some of which have specifications exceeding those of existing units.

While we have all seen the images produced by CT, it is perhaps worthwhile to recall its fundamental aspects. As in most radiologic procedures, the variable forming the CT image is the difference in x-ray attenuation properties of various tissues. In CT, a series of profiles of x-ray attenuations are obtained at different angles from the object examined. By the application of a computer-applied algorithm, they yield a cross-sectional image of the x-ray attenuation coefficients. This image reflects anatomical structures and often pathologic alterations heretofore invisible by conventional radiologic techniques. The success of CT stems from three factors: (1) utilization of a narrow beam of x-rays and a highly collimated detector(s) to provide a signal which is nearly free of scattered radiation; (2) the property of CT detectors, be they scintillation counters or gas-filled, to be significantly more free of noise than conventional screen-film combinations; and (3) reconstruction of a cross-sectional image unencumbered by superimposed activity. Anatomic structures often can be identified by CT although only negligible differences in attenuation coefficients exist, provided these structures are separated by interfaces of different attenuation properties. In the abdomen, for instance, the liver and pancreas can be distinguished from other structures because of low attenuation lipid-containing interfaces.

The introduction of CT in radiology has been revolutionary, producing socioeconomic reverberations in areas remote from its primary medical site of action. The acceptance of CT by the radiologic community has been immediate, unreserved, and overwhelming, even without well documented proof of its clinical usefulness. This enthusiasm is easily understandable in light of the obvious potential of CT, not only in diagnostic radiology but also in radiation therapy and, as emission CT, in nuclear medicine. While the benefits of CT for brain imaging were rapidly documented, radiologists have also enthusiastically assumed the extrapolation of CT to the rest of the body. This confidence in CT has been completely justified. Body scans reveal with astonishing clarity details of morphology previously seen only at necropsy or in anatomic atlases.

Yet this enthusiasm has some disquieting aspects. Usually prudent radiologists who in the past have de-

manded a thorough evaluation of x-ray equipment before purchase are buying costly CT units which exist only in the form of untested engineering prototypes. At no other time in the history of radiology have we been willing to purchase on faith such costly equipment. In some instances the existence and performance of units offered for sale are substantiated only by a series of specifications provided by companies with little or no previous experience in the manufacture of radiologic equipment.

The overwhelming response of the radiologic community has not remained unnoticed by industry. The EMI company, which in the early days hoped optimistically for the sale of a few CT units, has expanded its manufacturing capabilities to tens of units per month. In only 4 years, more than a dozen other companies have rapidly turned their interests to this field. The number of U.S. companies developing and manufacturing CT equipment now exceeds those producing conventional radiologic equipment. These companies span a broad spectrum of enterprising individuals, industrial giants, companies previously in marginally related fields such as nuclear medicine or radiation therapy planning systems, and even pharmaceutical companies. Some of them, beginning early in 1975, declared themselves ready to write orders for CT devices during the December 1975 meeting of the Radiological Society of North America. Others were willing to accept orders and financial deposits for units which had not yet produced any images and which sometimes existed only in the minds of their engineers. These actions of industry were the natural response to a buying frenzy by the radiologic community.

Although exact financial figures are difficult to obtain, some educated guesses can be made regarding the magnitude of the CT market. It is probable that by now more than 600 CT units have been sold (not installed) in the world, for a total sum of over \$250 million. It is also probable that the annual U.S. market for CT units, in the absence of any controlling mechanism, represents over \$250 million. This figure is approximately 50% of the total U.S. market for radiologic equipment.

Completely aside from the clinical benefits, the financial gains from this modality are as inspiring from the physician's standpoint as they are for industry. In some instances, installed CT devices have been completely paid for in 1 year. Situations are developing in which nonradiologic physicians are installing CT devices in their offices. In radiology departments of all sizes, liberal funds are being diverted to CT equipment after relatively cursory evaluation of over-all departmental needs.

Health planning agencies, reeling under the formidable impact of CT (more than 20 requests in the state of Missouri alone), are having to make costly decisions utilizing scant clinical criteria, while being subject to enormous, and justified, professional pressure.* Under these circumstances, it is understandable that some health planning agencies

* By the time this editorial is published, some of these criteria may be available through clinical experience and through work of various committees of the American College of Radiology.

have decided to impose a moratorium on the purchase of CT devices. It behooves them, however, to develop suitable criteria to allow the growth of this technique.

The very high cost of CT equipment, which obviously at some point will be borne by the patient, has sharpened the focus of concern regarding cost/benefit ratio in the delivery of health care. It has shown thoughtful physicians the example of a very costly, widely demanded (both by physicians and patients) medical procedure whose clinical value awaits complete assessment.

Another intriguing aspect of CT is the extraordinary awareness of this technique by the lay population. Never since the discovery of x-rays has a radiologic procedure been so widely reported and discussed by the media. A number of television programs have been devoted to this field; major national magazines have covered the subject thoroughly; local newspapers, which have never published an x-ray picture, are now showing sections of the brain and pictures of pancreatic malignancies.

As this CT publicity reaches the current crop of medical students, young scholars who, in the past, never would have thought of visiting an angiographic suite or a nuclear medicine facility are flocking to see the CT device. In some cases this early interest may be translated into a radiologic career.

A fundamental impact of CT in radiology is to emphasize the importance of physico-mathematical sciences in this medical discipline. There is little doubt that well before CT,

radiology provided the most fertile ground for the interaction of physicians with physicists and mathematicians. The formidable impact of CT clearly enhances the strength of this relationship, particularly in the fields of mathematics and computer technology, where the activities of these scientists (to their great satisfaction) have found an immediate and widely recognized clinical application. Never before have radiologists in such numbers pondered the significance of terms such as algorithm, Fourier transforms, convolution, and microprocessing. For the first time in diagnostic radiology, CT provides a technique whereby computer manipulation and electronic data storage are clearly superior to film. The development of CT has been so rapid that radiological education is struggling to keep pace. Crash courses have been held, and at least five post-graduate courses are scheduled in 1976.

This bicentennial issue is devoted to a peaceful revolution, a revolution in radiology to be sure, but one of enormous significance and promise to all of medicine. We salute Godfrey Hounsfield and the EMI company for their magnificent achievement and look forward to the challenge of this new era in medicine and radiology which they have pioneered.

Michel M. Ter-Pogossian
Mallinckrodt Institute of Radiology
St. Louis, Missouri 63110

The journal gratefully acknowledges the very special efforts of the following authors who produced the magnificent invited papers for this issue in commemoration of the nation's bicentennial anniversary. And to Michel Ter-Pogossian special thanks are due for initial concept, inspiration, and guidance.

Godfrey N. Hounsfield

Ralph J. Alfidi, William J. MacIntyre, John R. Haaga

Patrick F. Sheedy, II, David H. Stephens, Robert R. Hattery, John R. Muhm, Glen W. Hartman

Robert J. Stanley, Stuart S. Sagel, Robert G. Levitt

Raymond Gramiak, Robert C. Waag

Hillier L. Baker, Jr.

Kenneth R. Davis, Juan M. Taveras, Glenn H. Roberson, Robert H. Ackerman

Torgny Greitz

James H. Christie, Hirofumi Mori, Raymundo T. Go, Steven H. Cornell, Rolf L. Schapiro

Gwynn L. Jelden, Edward S. Chernak, Antonio Rodriguez-Antunez,
John R. Haaga, Paul S. Lavik, Ranjit S. Dhaliwal

Lee E. Cloe

Ronald G. Evens, R. Gilbert Jost

Picture Quality of Computed Tomography

G. N. HOUNSFIELD¹

Some limitations that impair the picture quality of computed tomography are presented. Picture grain is analyzed in detail and its relationship to different matrix sizes is demonstrated. The choices of matrix size for viewing various parts of the body are defined, and the need for higher resolution in the future is debated. Comparison is made between two scanning systems: the moving fan beam with rotation and the simple rotating fan beam. Possible artifacts in the picture caused by drift and delay in detector response are discussed.

Computed tomography has for some 4 years been used extensively for diagnosing lesions within the head; the technique is now being extended for diagnosis within the body using faster, higher resolution machines.

This system has been operative long enough for most of its capabilities to be appreciated: soft tissue has been rendered visible; the pictures are presented in tomographic form; and a quantitative measurement can be obtained of the x-ray absorption values of the various organs.

The quality of the pictures currently obtained is amply demonstrated in figures 1 and 2. On the whole, the organs appear well defined in outline and tone. However, some imperfections are apparent. It is the purpose of this article to examine some of the major defects in CT pictures, state their causes in simple mathematical terms, and indicate which of these are fundamental to the principles under which the CT system operates. It is important to understand the limitations which govern picture quality before assessing whether the system can be further improved.

Some of the terms used are defined below:

Picture matrix. The picture is made up of a series of absorption values appearing as a grid of equally spaced squares, the number of squares in the vertical and horizontal lines being the matrix size (e.g., 320×320).

Spatial resolution. This term defines the clarity of the picture and is determined by the matrix size. It could also be defined as the spatial distance between the squares of the matrix.

Picture accuracy. This is the accuracy to which the absorption value of each picture square can be calculated.

Sensitivity. Sensitivity is a measure of the contrast of the picture (i.e., the width of the range of absorption values or window of values) which reproduces the tones between black and white displayed on the picture.

Limitations Governing Picture Quality

Picture Grain

A major defect that may be apparent on the picture is "picture grain"; this is particularly noticeable in figure 1. While the picture is clear, the clarity of metastasis of the liver (top left) is impaired by a mottled appearance. On the

other hand, the kidney in the same picture stands out above the picture grain and appears well defined.

What is the cause of the picture grain? Can anything be done to counteract it? These are important questions since the indistinctness of an image caused by picture grain is a major hindrance to accurate diagnosis.

Basically, picture grain is caused by an insufficiency of photons arriving in the detectors after penetrating the body, and this limits the accuracy to which each picture point can be calculated within the matrix. This random variation of the amplitude of the matrix points is the picture grain, which can be expressed in terms of amplitude and coarseness (fig. 3).

Picture Spatial Resolution

So far, only the *inaccuracy* of the value of each picture point (grain) has been discussed. Improving picture *resolution* (gaining clarity) may be more important when variations in the shape of certain organs need to be detected. This obviously involves increasing the number of picture points (i.e., increasing matrix size), which in turn requires scanning with a narrower beam and taking more readings across the body. Unfortunately, the more the matrix size is increased, the greater the grain amplitude of the picture, since the restricted amount of information must now be shared among a greater number of picture points.

The relationship can be expressed as follows: $(\text{inaccuracy})^2 \propto (\text{resolution})^3$ or, in looser terms, $(\text{grain})^2 \propto (\text{matrix size})^3$. Practically speaking, if the matrix size is

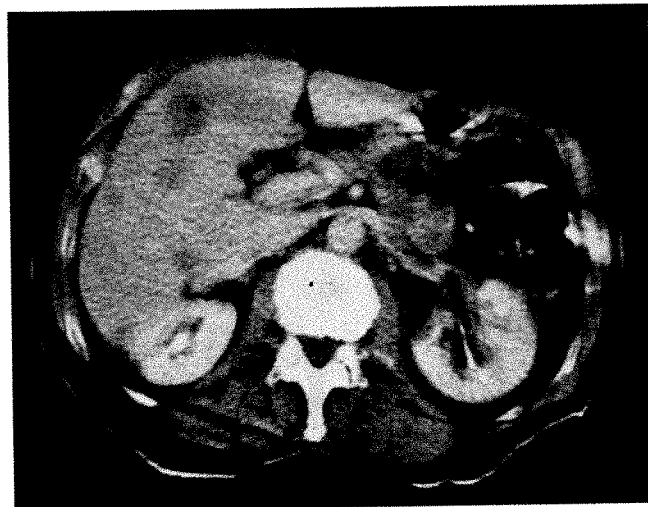


Fig. 1.—Section of abdomen taken through liver and kidneys showing metastasis of liver (top left). Kidney appears much clearer than liver metastasis, which has been impaired by picture grain, due to small variations of tissue density.

Received March 30, 1976.

¹ Central Research Laboratories, EMI Limited, Shoenberg House, Trevor Road, Hayes, Middlesex, UB3 1HH, England.

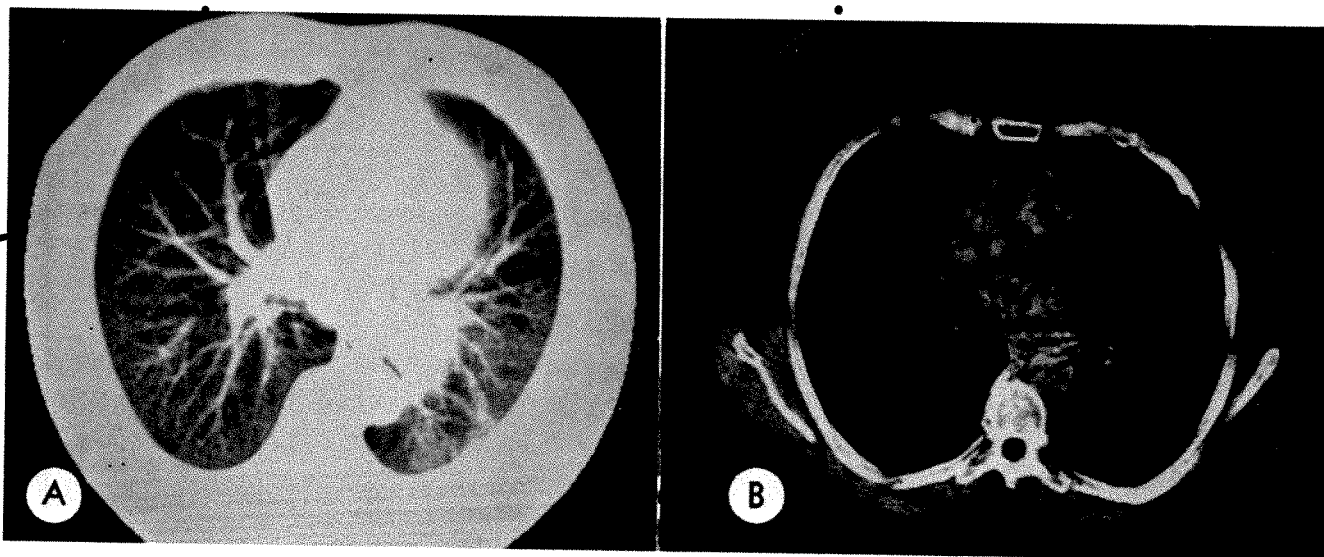


Fig. 2.—A, Section through lungs and heart. Window height adjusted to display lung tissue. B, Section approximately 3 cm higher on different patient. Window height adjusted to differentiate fat and tissue of heart. Picture grain of both these pictures considerably improved by reduced absorption of lungs.

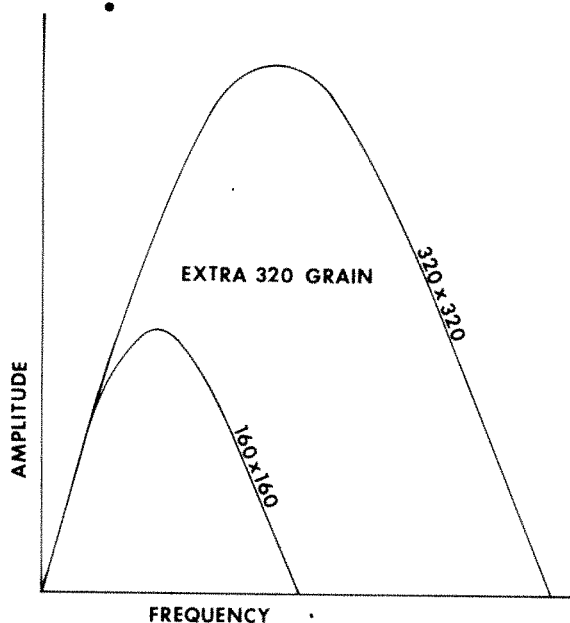


Fig. 3.—Plot of frequency spectrum of x-ray photon noise after modification by algorithm for application to picture matrix. Peak amplitude occurs at frequency well below maximum frequency applied to matrix. This lower frequency accounts for coarseness of grain compared to finer detail seen in pictures of certain organs (e.g., kidney, fig. 1), where clarity is result of sum of higher, nonrandom frequencies. The 320×320 curve peaks at twice the frequency, so that a greater amplitude is expected as well as finer grain by factor of two.

doubled from 160×160 picture points to 320×320 , the grain will increase in amplitude by a factor of 2.8. However, as indicated in figure 3, the additional grain will be of a finer nature (cf. figs 4A and 4C).

In the strict sense, increasing the matrix size should not be considered as a trade-off between accuracy and resolution, as can be understood if the process is seen in reverse. If accuracy were to be improved by intentionally blurring

the picture, it is obvious that extra information is not added. All that happens is that spatial information is removed in the interest of making the picture more intelligible to the eye (which has a limited tone range easily saturated by the presence of excessive grain on the picture).

The presence of grain must be accepted as fundamental to any CT system. Current machines have reached a level of detector efficiency such that grain has been reduced to a level close to the theoretical limit; thus there is little room for improvement unless x-ray dosage to the patient is increased.

Patient Dosage

For normal examinations, the dose is usually limited to about 3 R. This is the incident intensity of radiation to the skin and applies to both the head and body. If the slices are taken such that the radiation does not overlap, then the dose to the skin will be the same for one slice as for a series of slices. If dosage exceeds 3 R, the benefits of the examination to the patient must obviously be taken into account.

Picture grain varies according to the relationship $1/\sqrt{\text{dosage}}$. Thus with increased dose, picture grain improves. Figure 4B has been taken using four times the x-ray dose used for figure 4A. Consequently, the grain is only half as apparent.

There are obvious factors influencing the amount of x-rays penetrating the patient's body, such as body width and its mean absorption. These, too, will naturally influence the grain of the picture.

Choice of Matrix Size

The differential absorption of the specific organs to be viewed is of fundamental importance in the choice of an appropriate matrix size, since it may be advantageous to show them at the maximum spatial resolution obtainable without impairment by grain. For example, when very accurate readings are required on rather large objects (e.g.,

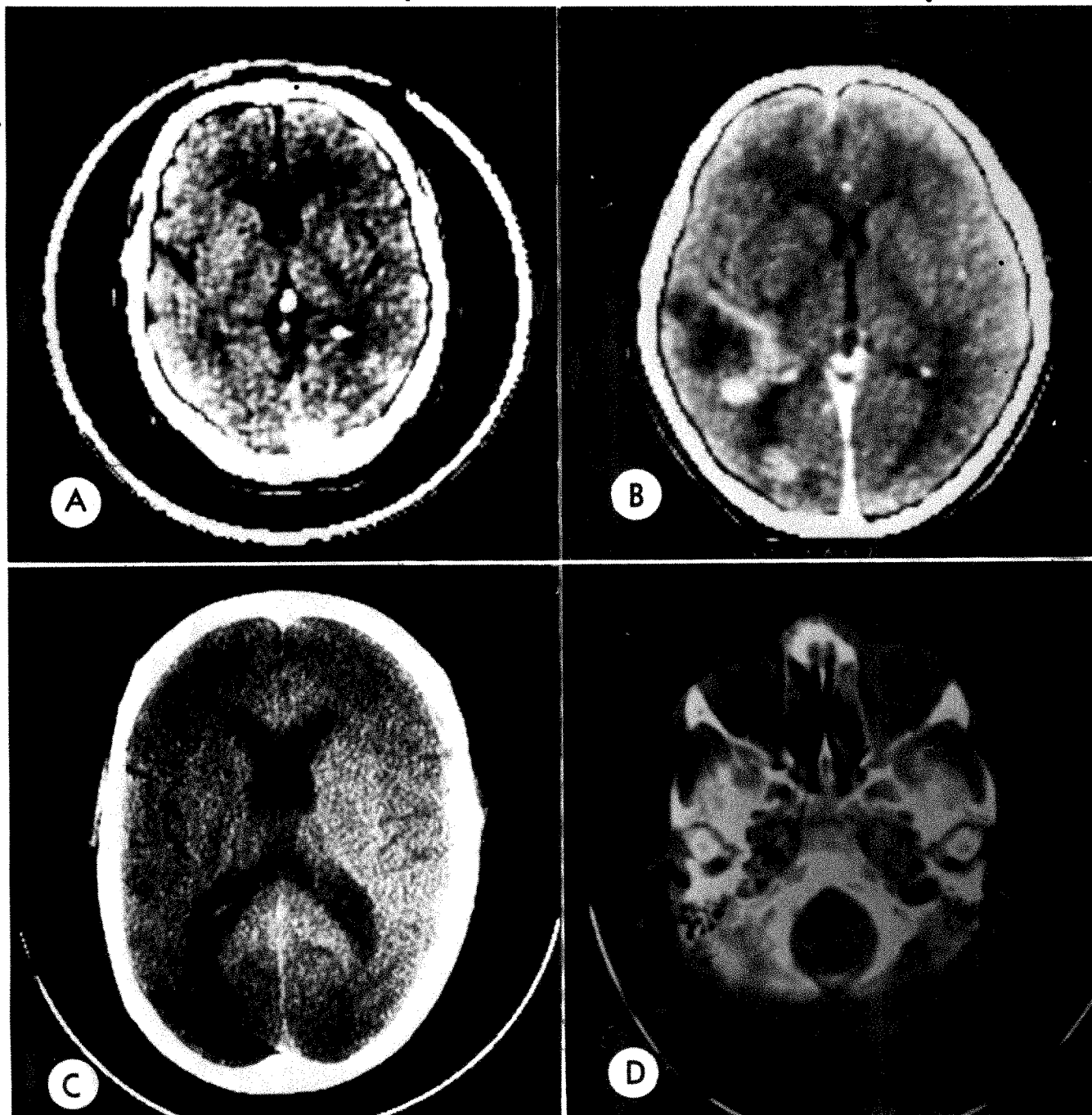


Fig. 4.—Comparison of grain structure and effect of dose on grain. Reduced grain of 160×160 matrix enables use of more sensitive ranges so that grey and white matter can be viewed which cannot be seen on 320×320 matrix. A, Head taken at dose of approximately 3 R viewed on 160×160 matrix. High sensitivity, window width 30 EMI units. B, Head with lesion taken at dose of approximately 12 R viewed on 160×160 matrix. High sensitivity, window width 25 EMI units. C, Head viewed on 320×320 matrix, dose approximately 12 R. Medium sensitivity, window width 75 EMI units. D, Head taken through eyes, viewed on 320×320 matrix (window width 200 EMI units). At this sensitivity, picture grain not a serious problem; even finer matrix could be used.

scanning for brain tumor or liver metastasis), a coarse matrix is desirable to reduce grain to a minimum. This is illustrated in figure 5 where a picture of a liver is displayed at varying matrix sizes and reduced window widths. The lower matrix sizes show the structure within the liver very clearly. On the other hand, when shape is of paramount importance (e.g., in scanning the vertebrae), a very fine matrix could well be used.

Processing very fine matrices involves at present a lengthy computer operation. This problem is partially overcome by processing only a small area of the picture and magnifying it on a matrix of conventional size. For this reason, in this article matrix size is frequently translated in terms of spatial picture point resolution, assuming that a 320×320 picture has a spatial resolution of 1 mm between picture points.

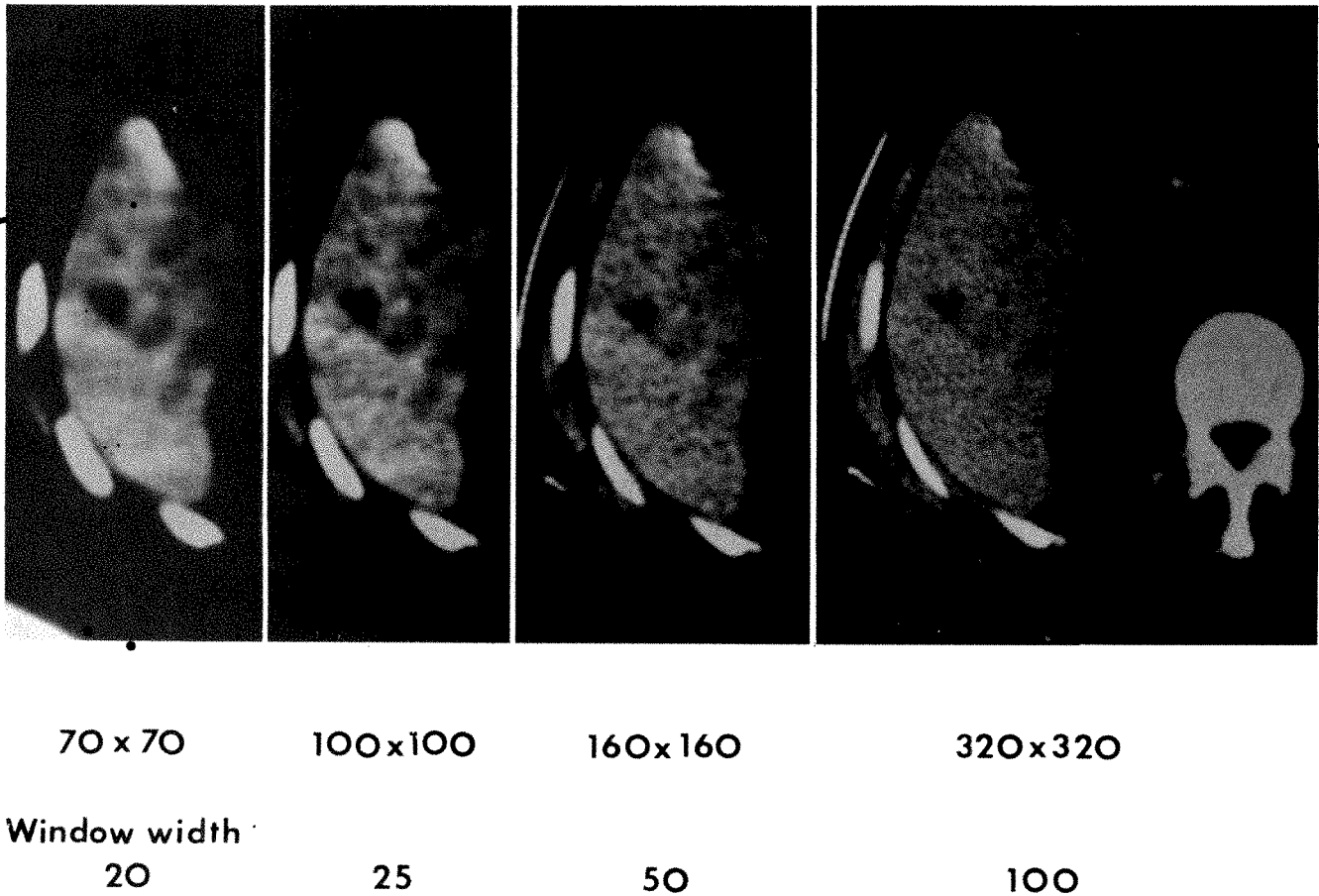


Fig. 5.—Variation of matrix size and window width for optimal viewing of metastasis of liver. The 100×100 matrix more readily emphasizes small variations within liver.

Figure 6 demonstrates the relationship between picture resolution (matrix size) and grain for optimal viewing of various parts of the body.

Abdomen

In scanning the abdomen where fat and tissue are well differentiated, a resolution of 1 mm (320×320 matrix) is adequate (as can be seen in fig. 1.). However, if finer detail is desired, the matrix size could well be increased, perhaps almost doubled, before the tone range of the picture would be seriously impaired by increased grain. The resolution would then be 0.5 mm, and the image could be displayed using the picture magnification technique as previously described. At the other end of the scale, the spine, owing to its high absorption, could be displayed in fine detail at a higher resolution without serious grain interference (fig. 6).

Head

A head scan usually requires discrimination between minute tissue differences for the purpose of tumor location; consequently grain must be reduced to a minimum. Twenty times as many x-rays penetrate the head as do the abdomen, but the resultant reduction of grain is still insufficient for fine discrimination. It is therefore preferable to use a low resolu-

tion 160×160 matrix rather than a 320×320. This is illustrated in figures 4B and 4C where on a 160×160 matrix grey and white matter are clearly distinguished, but on a 320×320 matrix they are not. (To take advantage of the reduced grain, figure 4B has been displayed at three times the sensitivity.)

However, if one is looking at the bone of the head or at the middle ear, the matrix may be increased to 320×320 (1 mm resolution) as in figure 4D and could be taken as high as 0.25 mm before the picture would be seriously affected by grain.

Scanning the inner ear and the eye would benefit from matrices 320×320 or a little larger.

Heart

Heart scans, where the x-rays also penetrate the lungs, benefit from the low mean absorption path caused by the presence of air in the lungs. The presence of fat in certain parts of the heart can be clearly seen on a 320×320 matrix.

If the effects of heart motion can be satisfactorily reduced either by synchronization or by much higher machine speed, conditions for scanning the heart would be similar to those for the head. Since slight differences between tissue and blood would have to be detectable, a low resolution of

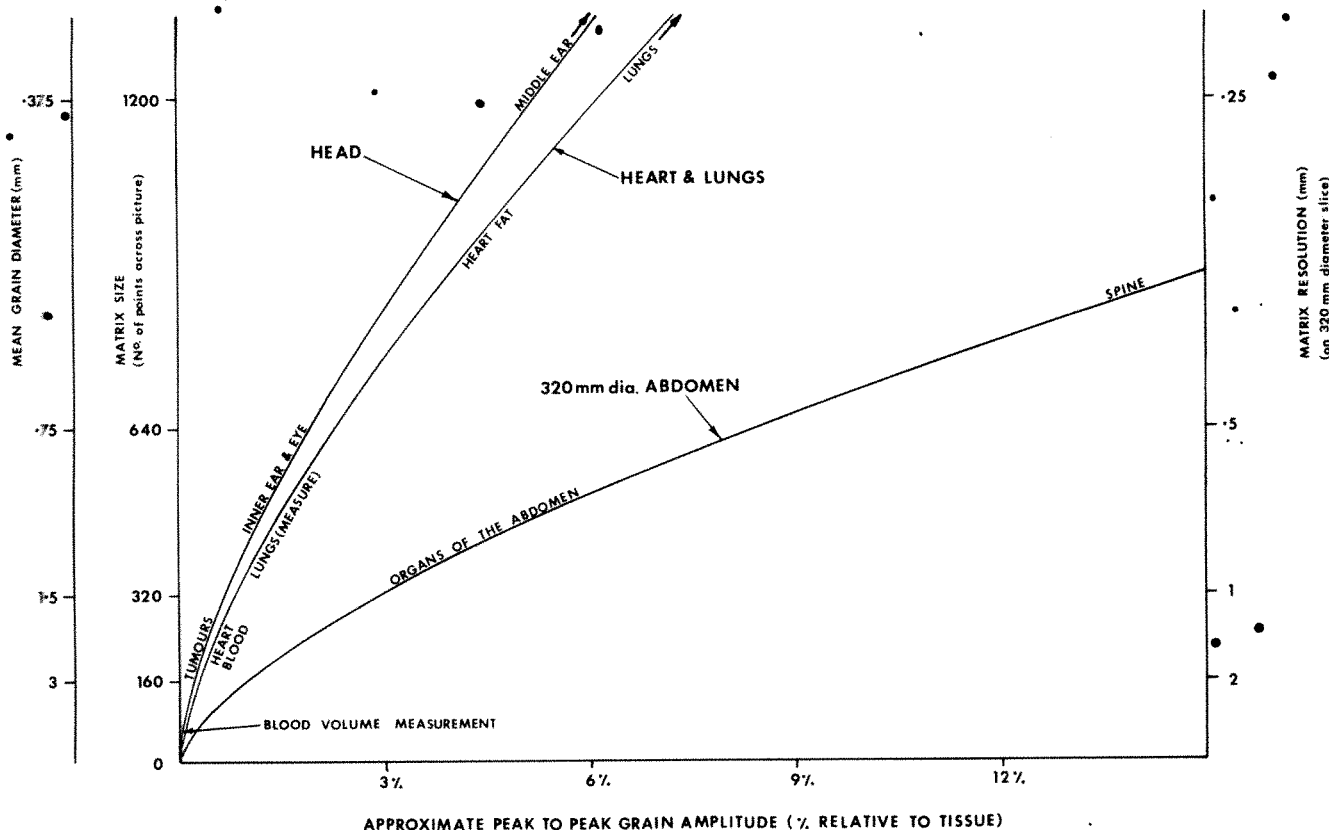


Fig. 6.—Relationship between picture resolution (matrix size) and picture grain amplitude.

between 160×160 and 320×320 would be preferable.

Lungs

Figure 24 shows the lungs on a 320×320 matrix. Although this matrix has produced a clear picture at 1 mm resolution, it should be possible to take an even clearer picture at 0.25 mm spatial resolution which would be reasonably grain free. The high absorption differential between air and lung tissue makes this possible. However, if the lung tissue must be measured quantitatively, it would be more practical to use the lower resolution matrix.

Implications of Maximizing Resolution

Is there anything to be gained diagnostically by increasing resolution to its highest possible limit? At present CT is performing very well at low and intermediate resolution. It is successful mainly because it is a highly efficient method of isolating similar soft tissue organs which would normally be superimposed in conventional x-ray pictures or which, because of their similarity, would be virtually indistinguishable even if x-ray film were sensitive enough to detect them. In these areas, CT has no competitor in the x-ray field. As seen in figure 6, most of its uses require a resolution of between 160×160 and 640×640 .

If resolution were to be increased to its maximum, the picture grain would accordingly increase and the uses of CT would have to be limited, in general, to the examination of

contrast media and bone. It would then be competing with conventional x-ray techniques.

In this situation, CT has the advantage of greater detector efficiency than conventional x-ray film methods: it would compete very favorably, producing pictures of either higher resolution or greater sensitivity. The system's ability to position objects three dimensionally and to measure their absorption values would remain an added bonus.

However, these advantages may well turn out to be of only moderate diagnostic value. Moreover, a high resolution machine would be very complicated and costly under present technology, and it would be difficult to justify these costs unless there were a spectacular breakthrough in machine design, to simplify construction.

Scanning Systems and Their Artifacts

Picture grain caused by x-ray photons is unavoidable in any x-ray scanning technique. Whatever system is used, the nature of the grain cannot be improved beyond the extent demonstrated above. A picture may also be deteriorated by artifacts caused by the machine, depending on the scanning system adopted. It is possible to imagine many different scanning techniques which would operate satisfactorily, but the following two are probably the best known. A discussion of their respective merits and the artifacts peculiar to each follows.

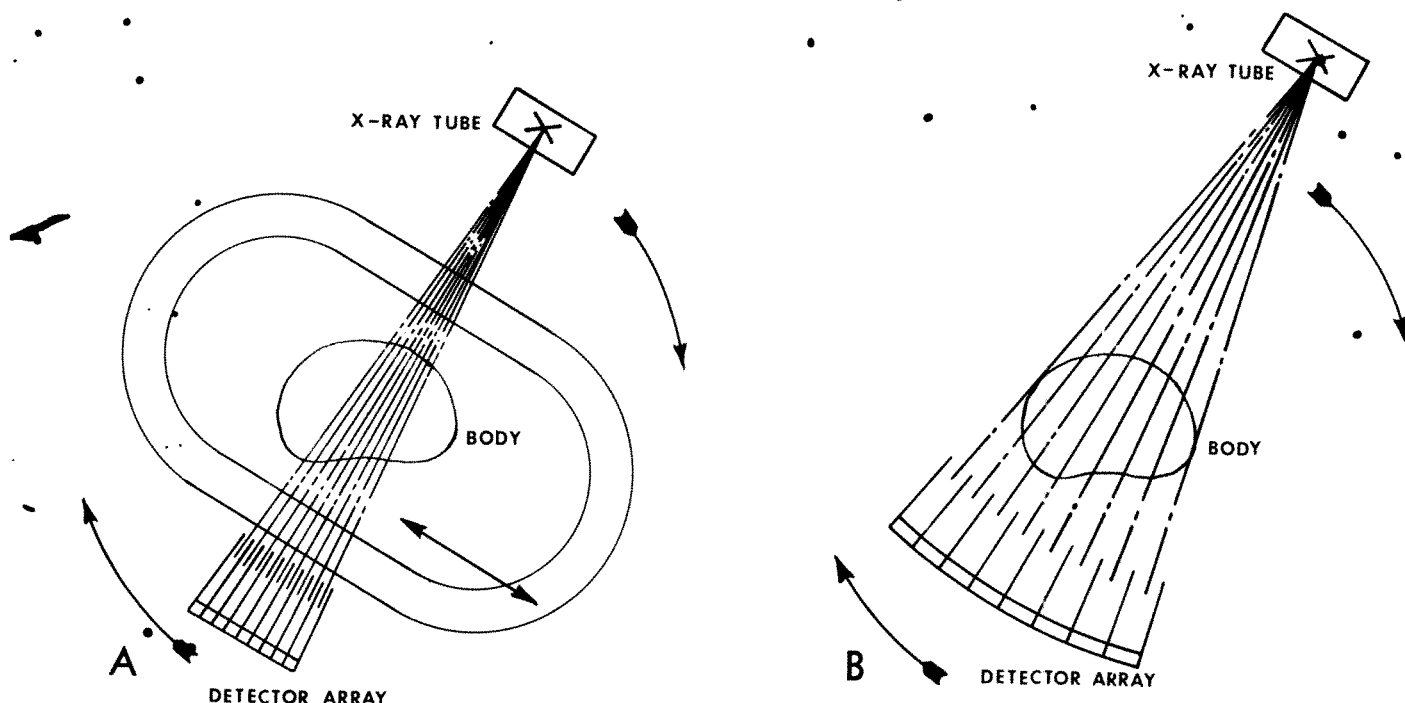


Fig. 7.—A, Moving fan beam with rotation system. Fan beam produced from x-ray tube falls on array of detectors and scans backward and forward linearly across patient. At end of each scanning stroke, angle of scanning traverse changed by amount equal to that of angle of fan beam. In this rotational method, all possible angles of scan across entire body will have been recorded after 180° rotation. B, Rotating fan beam system. X-ray tube produces fan beam as wide as largest patient to be scanned. This falls on wide array of 300 detectors. To obtain picture, assembly rotated around patient 360° .

Description of Systems

Moving fan beam with rotation. In this system, the fan beam scans across as well as rotates around the patient (fig. 7A). One advantage of this system is its flexibility. Both the length of the scanning stroke taken across the patient and the spatial interval between readings along each stroke can be changed. The scale of the picture can therefore be varied, magnifying small areas if desired.

The detectors can be calibrated outside the body at the end of each stroke, and their electronic stability is not a serious problem. However, owing to mechanical limitations, the maximum speed at which the system can operate is about 10 sec per picture.

Rotating fan beam. This method uses a wider fan beam and has a rotational motion around the body only (fig. 7B). The advantage of this system is that it can operate faster than the one previously described since the fan beam, being wider, can take three times as many readings in a given time. In addition, no time is lost at the end of the stroke in reversing the direction of the traverse (as in system 1).

However, many more expensive detectors are required, and these have to be fixed in pitch to fit the largest patient. Since the detector spacing and beam width are fixed, it is difficult to vary the resolution of the machine. Many detectors could be redundant when small patients are scanned. The system is therefore less flexible for viewing small areas. Maintaining electronic stability and calibration of the detectors are major problems and may be a possible cause of artifacts (see below).

Artifacts

In both machines the detectors take readings over a wide range of values, and here technology is stretched to the limit. Any imperfections in the detectors may cause artifacts which take different forms according to the particular scanning system used. The main problem areas are drift of detector sensitivity and delay in detector response.

Drift of detector sensitivity. In the moving fan beam system, the picture is affected very little by mismatch of detector gain within the bank of detectors. During each stroke, the detectors scan across the whole body, so that detector error is spread across the entire picture and does not concentrate in any one place. The only effect is a change in overall picture intensity which can easily be calibrated out.

In contrast, the rotating fan beam geometry by no means spreads the detector errors evenly across the picture (fig. 8). Certain areas (particularly at the center of the body) are seen exclusively by specific detectors or groups of detectors. It is therefore necessary to match the gain of these detectors extremely accurately if concentric circles are to be prevented. A mismatch of one part in 5,000 could cause the circles to appear, resulting in a spot at the center.

In pictures of the abdomen, with favorable detector calibration these artifacts may tend to merge into the picture grain. But in the case of the most sensitive pictures of the head, it remains to be seen to what extent these artifacts can be eliminated by machine design.

Delay in detector response. The detectors have to take readings over a very wide range of values. When large

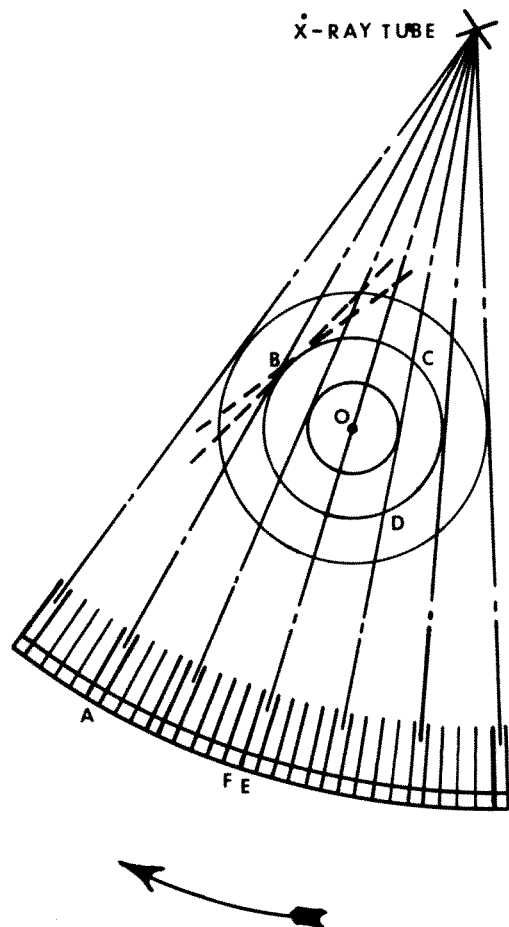


Fig. 8.—Geometry of rotating fan beam. As x-ray beam associated with each detector rotates around body, it passes through material of body lying in circle tangential to beam; thus detector sees mostly material lying close to this circle. For example, detector A will be associated chiefly with material lying close to circle BCD. Worst condition is at center O, which is seen only by detector E and its neighbor F, bright spot would occur at center. Similarly, any variation between other detectors would cause concentric circles unless matched exceedingly accurately.

changes occur, such as at the edges of bone, small delays in detector response (lag) can cause artifacts which show up in different ways on the two systems.

Figure 9 illustrates the artifacts on the pictures of the two systems when two dense bones are scanned. In the case of the moving fan beam system, the error is evenly dispersed around the object, whereas for the rotating fan beam, it takes the form of a concentrated tail which could result in a more objectionable artifact of higher intensity.

One is left with the impression that neither system is the final word in CT scanning technique and that, in the future, systems will be devised which incorporate the benefits of both.

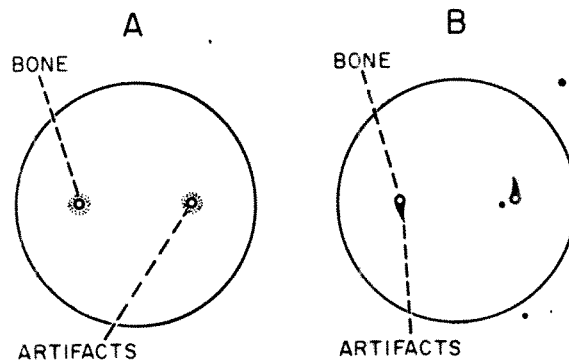


Fig. 9.—Comparison of artifacts produced by very small amounts of detector lag in moving fan beam with rotation (A) and rotating fan beam (B) systems.

Conclusions

In the field of differentiation of soft tissue by x-ray and of viewing the shape of soft tissue organs, CT has no rival. However, its performance is limited by the extent to which photon noise can be tolerated in the picture. This limitation is fundamental to the system, and the clarity and accuracy of the picture are not expected to improve spectacularly in the future.

On the other hand, for viewing objects of greater differential absorption than soft tissue, the machine could be stretched considerably further in resolution and could improve on the performance of conventional x-ray machines. At present it is difficult to say whether the added diagnostic value would warrant the greater complexity of the machine, but it is to be hoped that simpler techniques may eventually be found.

Many different systems for scanning the patient are likely to evolve in the future, and some of these may be faster. Each will have its own advantages and disadvantages, and only time and further experimentation will tell which technique will survive.

ACKNOWLEDGMENTS

I wish to thank the directors of EMI Limited for permission to publish this article. I also wish to acknowledge the research team at EMI, particularly C. A. G. Le-May and S. R. Bates.

SELECTED REFERENCES

1. Ambrose J: Computerised transverse axial scanning (tomography). II. Clinical application. *Br J Radiol* 46:1023-1047, 1973
2. Ambrose J: Computerised x-ray scanning of the brain. *J Neurosurg* 40:679-695, 1974
3. Brooks RA, Di Chiro RA: Theory of image reconstruction in computed tomography. *Radiology* 117:561-572, 1975
4. Cho ZH, Chan JK, Hall EL, Kruger RP, McCaughey DG: A comparative study of 3-D image reconstruction algorithms with reference to number of projections and noise filtering, in *Transactions of Nuclear Science*, IEEE Catalog no. NS-22 (1), 1975, pp. 344-358
5. Hounsfield GN: Computerised transverse axial scanning (tomography). I. Description of system. *Br J Radiol* 46:1016-1022, 1973

The Effects of Biological Motion on CT Resolution

RALPH J. ALFIDI,¹ WILLIAM J. MAC INTYRE,² AND JOHN R. HAAGA¹

A variety of periodic and aperiodic physiologic motions affect the quality of CT images. This study was initiated to estimate what an optimal scan period should be in the design of CT units. Ultrashort scan periods were experimentally simulated in the heart and liver to approximate the parameters of future technology.

Introduction

Voluntary and involuntary muscular motion, peristaltic motion, respiratory motion, and cardiovascular motion all contribute to the degradation of in vivo and in vitro CT imaging. Each motion produces image degradation, and the results can be additive. Each motion constitutes a plateau which must be surmounted to improve CT resolution. It is obvious that a frontal assault on cardiovascular motion would require extremely short imaging times and would not be possible until a "fourth generation" of CT scanners became available (fig. 1).

Materials and Methods

This work was performed on an Ohio Nuclear Delta body scanner and an EMI head scanner. The Ohio Nuclear scanner required 160 sec to complete a "40 cm scan" which was used throughout this study. The EMI head unit with the 160² matrix modification required 4 min and 55 sec to complete a cycle.

In Vivo Motion

Anesthetized mongrel dogs were scanned in the Ohio Nuclear Delta scanner before and after sacrifice to study the effects of biological motion in an in vivo preparation. Following sacrifice, the animals were scanned completely motionless simulating zero scan time. An endotracheal tube with cuff had been placed and insufflated prior to sacrifice. Using a 2,000 ml syringe, the animals were "respired" at 300–600 ml volumes depending upon size. These experiments were carried out at respiration frequencies of 16, 15, 11, six, and two per minute. It was also possible to simulate one or two "breaths" of variable duration as could occur in the simulation of 20 sec and 5 sec scanning machines. Studies were also made of one-half of a respiratory cycle such as would occur in a displacement of 2½ sec in a "5 sec scan" (fig. 2).

Considerable discussion has focused on the possibility of CT heart imaging. It has been postulated that areas of akinetic and diskinetic myocardium could be shown if extremely short scan times were available [1]. With this possibility in mind, a dog was sacrificed and scans were obtained through the heart at zero heart rate and zero respirations before and after the injection of contrast material into a vein of the foreleg.

In Vitro Motion

Plastic spheres were used in in vitro simulations so that results could be expressed quantitatively. This procedure was performed using solid nylon spheres, nylon spheres with a central air cavity, and nylon spheres scanned in the same field with a balloon in-

sufflated to simulate peristaltic motion artifacts. The spheres were 1, ½, and ¼ inch in diameter. They were suspended in a water bath and reciprocated in the Z axis of the CT plane using a respiratory motion simulator (figs. 3A and 3B). A special cam was constructed which made it possible to closely simulate human respiration (fig. 3C). The throw of the cam was 2 cm. The machine could be made to simulate respiratory motion from 28 cycles/min to ½ cycle in 2½ min. In this manner, virtually all CT units available today could be simulated (figs. 4 and 5).

Peristaltic motion of gas was simulated by placing a Foley catheter in the field with the plastic spheres held static and insufflating the balloon at variable volumes and frequency (fig. 5). Motion of gas as a result of respiration was shown in plastic spheres containing a central air cavity. When the gas-plastic interface was cycled through the image plane, similar artifacts to those of peristalsis were seen (figs. 7).

Results

In the "biological preparations," visual evidence of image degradation was convincing (fig. 2). However, it could not be expressed quantitatively.

It can be seen from the simulated ultrashort heart scan that there is no appreciable difference in density between the myocardium and the blood pool (fig. 8A). Contrast material will be necessary to define the internal structures

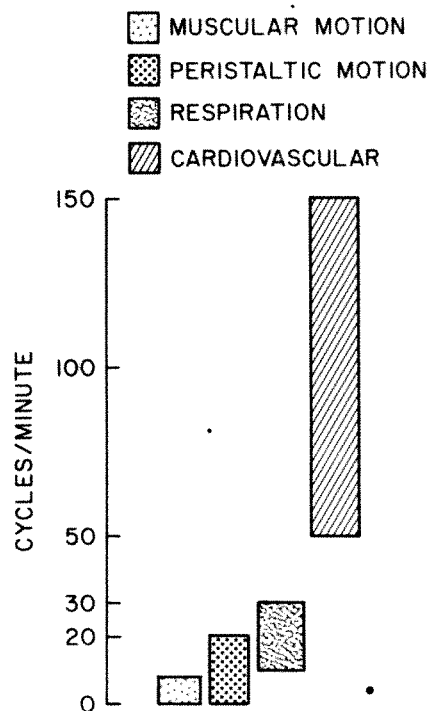


Fig. 1.—Approximate frequencies of periodic and aperiodic physiological motions.

Received March 1, 1976.

¹ Department of Radiology, Cleveland Clinic Foundation, 9500 Euclid Avenue, Cleveland, Ohio 44106.

² Department of Radiation Therapy and Nuclear Medicine, Cleveland Clinic Foundation, Cleveland, Ohio 44106.

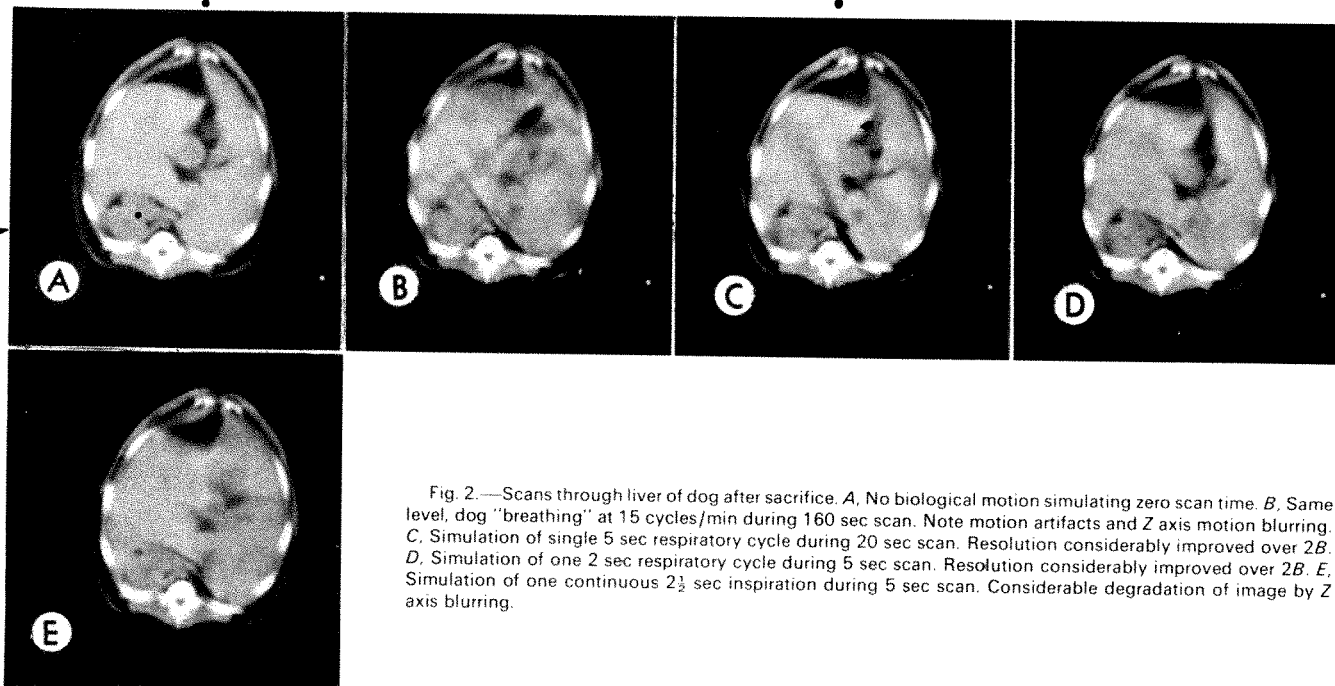


Fig. 2.—Scans through liver of dog after sacrifice. *A*, No biological motion simulating zero scan time. *B*, Same level, dog "breathing" at 15 cycles/min during 160 sec scan. Note motion artifacts and Z axis motion blurring. *C*, Simulation of single 5 sec respiratory cycle during 20 sec scan. Resolution considerably improved over *2B*. *D*, Simulation of one 2 sec respiratory cycle during 5 sec scan. Resolution considerably improved over *2B*. *E*, Simulation of one continuous $2\frac{1}{2}$ sec inspiration during 5 sec scan. Considerable degradation of image by Z axis blurring.

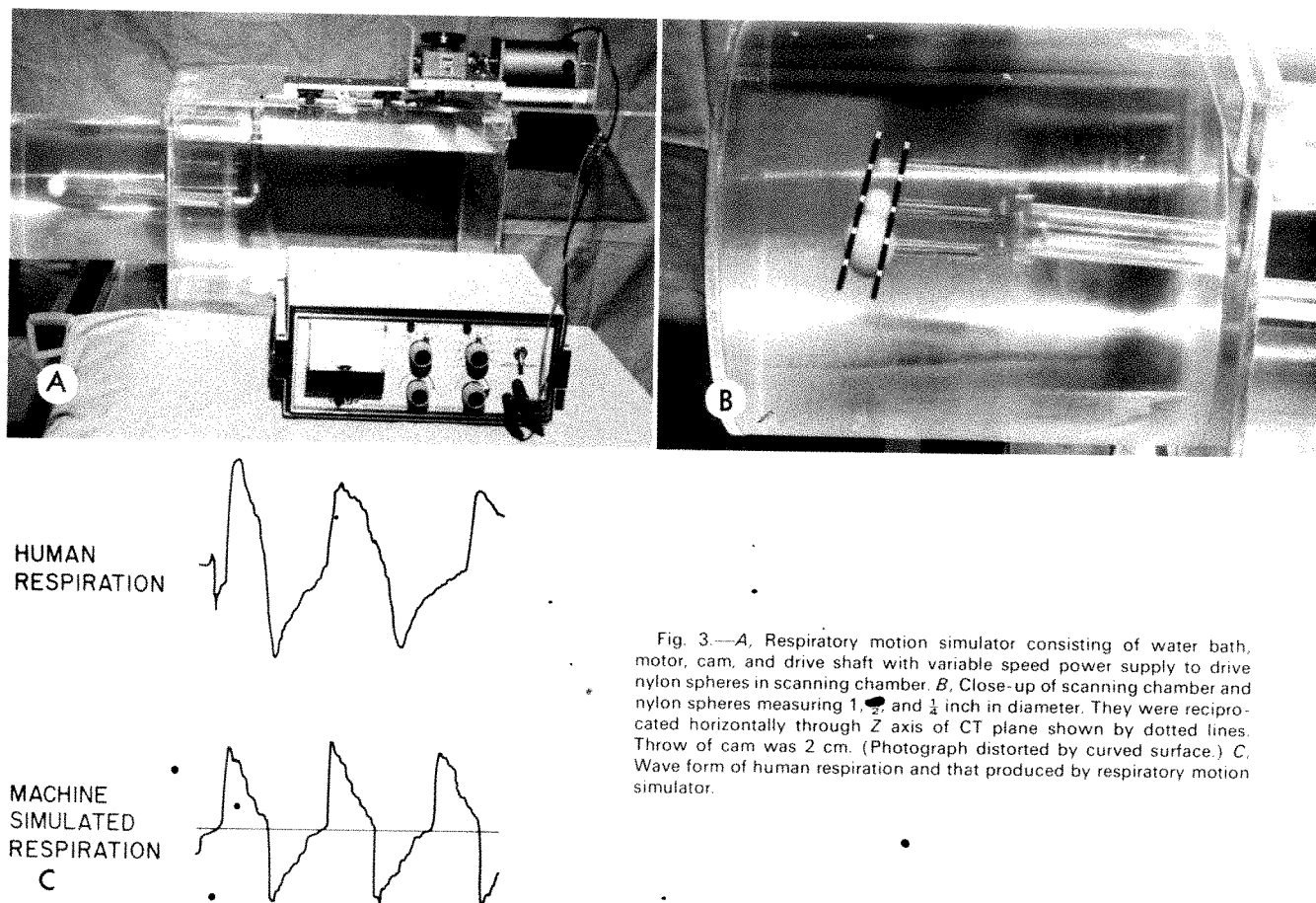


Fig. 3.—*A*, Respiratory motion simulator consisting of water bath, motor, cam, and drive shaft with variable speed power supply to drive nylon spheres in scanning chamber. *B*, Close-up of scanning chamber and nylon spheres measuring 1, $\frac{1}{2}$, and $\frac{1}{4}$ inch in diameter. They were reciprocated horizontally through Z axis of CT plane shown by dotted lines. Throw of cam was 2 cm. (Photograph distorted by curved surface.) *C*, Wave form of human respiration and that produced by respiratory motion simulator.

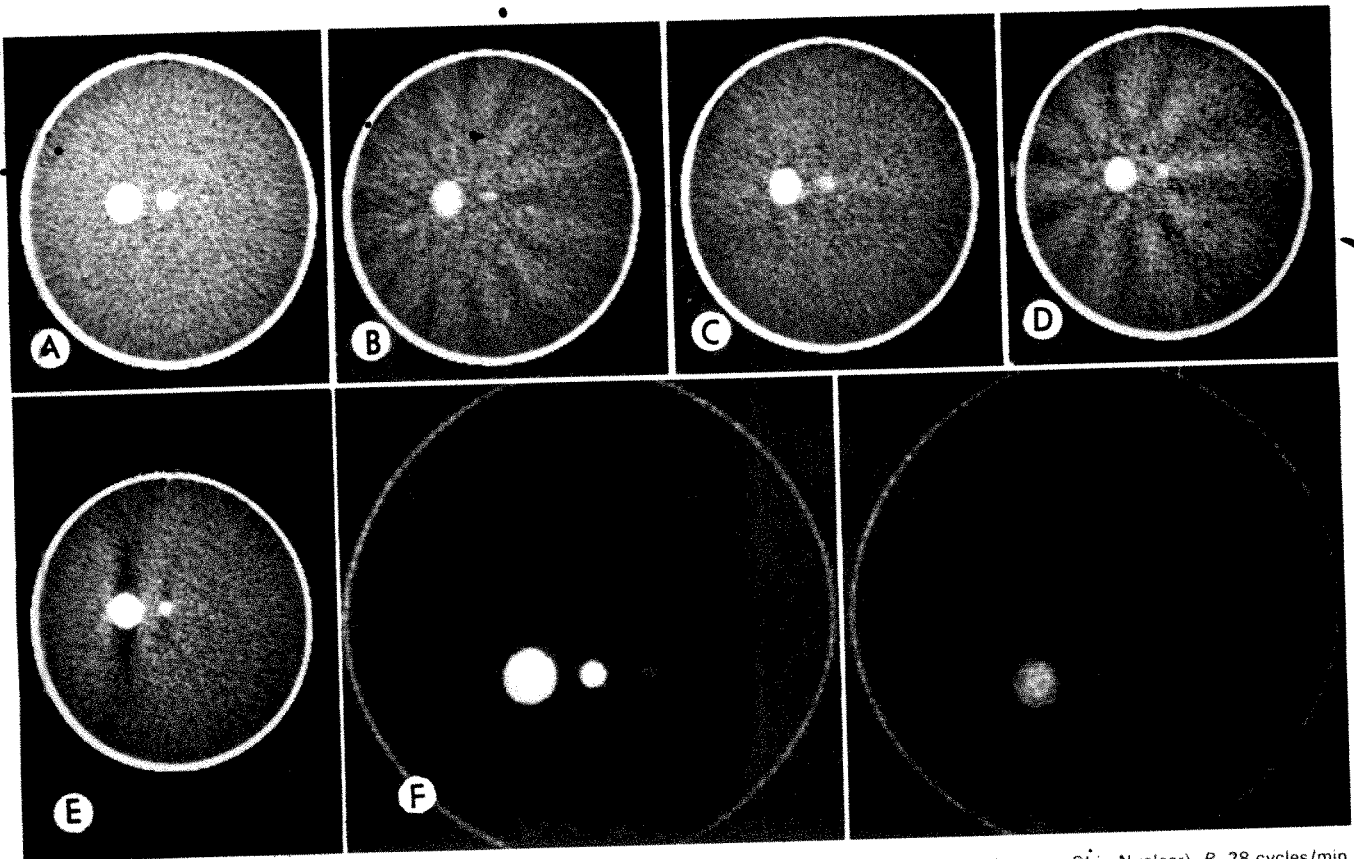


Fig. 4.—Scans of nylon spheres as “seen by CT.” A, Zero motion. Smallest nylon sphere barely perceptible (Delta scan, Ohio Nuclear). B, 28 cycles/min. Larger spheres have decreased in attenuation coefficient and size. Multiple resonance artifacts seen. Smallest sphere no longer perceptible. C, 11 cycles/min. Resonance artifacts not present but spatial and contrast resolution decreased as in B. D, 2 cycles/min; similar findings. E, Simulation of one 5 sec respiration in 20 sec scan period. Spatial and contrast resolution decreased. F, zero motion (EMI head scanner). G, 16 cycles/min (EMI head scanner). Note degradation of spatial and contrast resolution.

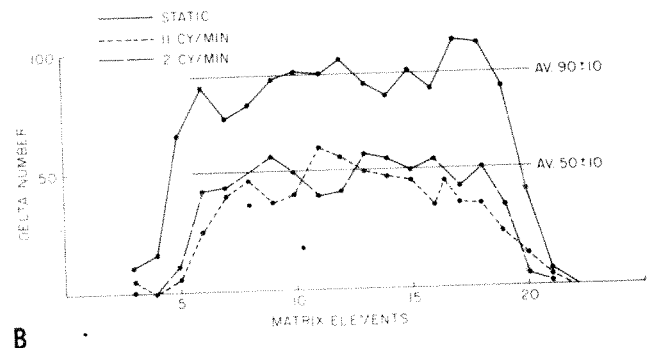
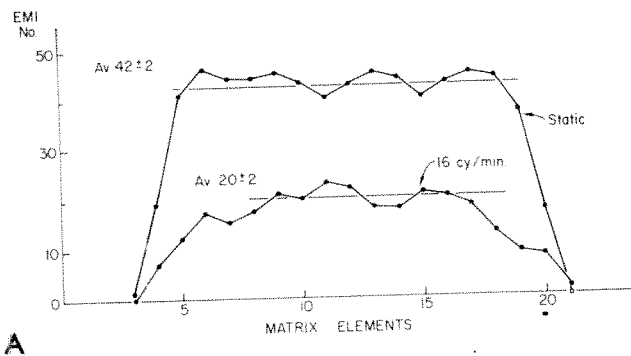


Fig. 5.—A, Cross section of μ numbers of EMI scan (figs. 4F and 4G). Loss of contrast and spatial resolution demonstrated quantitatively. B, Cross section of μ numbers from Ohio Nuclear unit (figs. 4A, 4C, and 4D). Similar loss of spatial and contrast resolution.

of the heart as well as to “stain” areas of perfused myocardium (fig. 8B).

Analysis of data from the nylon spheres scanned static and in motion revealed that motion causes degradation of both contrast and spatial resolution and introduces artifacts affecting the entire field of the CT image.

The loss of contrast can be assessed quantitatively by comparing the profiles of μ numbers drawn through the central axis of the 2.5 cm spheres scanned at rest and during

transit of the sphere in and out of the field of view of the detectors at various frequencies. Such profiles recorded at rest and at 16 cycles/min by the EMI scanner (figs. 4F and 4G) are shown in figure 5A. Similar profiles of the spheres recorded by the Ohio Nuclear Delta scanner at rest and at frequencies of 11 cycles/min and 2 cycles/min (figs. 4C and 4D) are shown in figure 5B.

In the EMI scans, the average EMI number dropped from 42 to 20, and in Delta scans the contrast dropped from 90

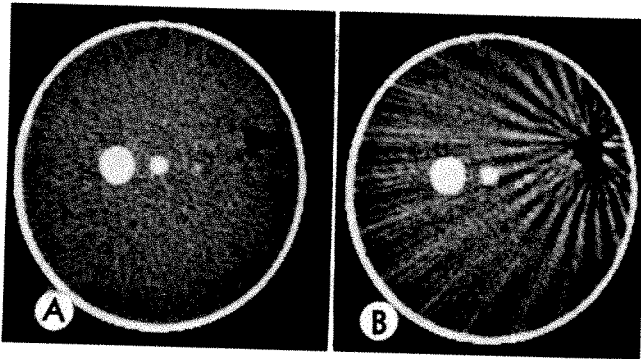


Fig. 6.—Peristaltic motion experiment. *A*, Nylon spheres scanned static in same field with Foley catheter balloon placed in field at 2:00 and seen as black circular object. *B*, Nylon spheres static but Foley balloon insufflated six times per minute, 5 cm³ volume, simulating peristaltic artifacts.

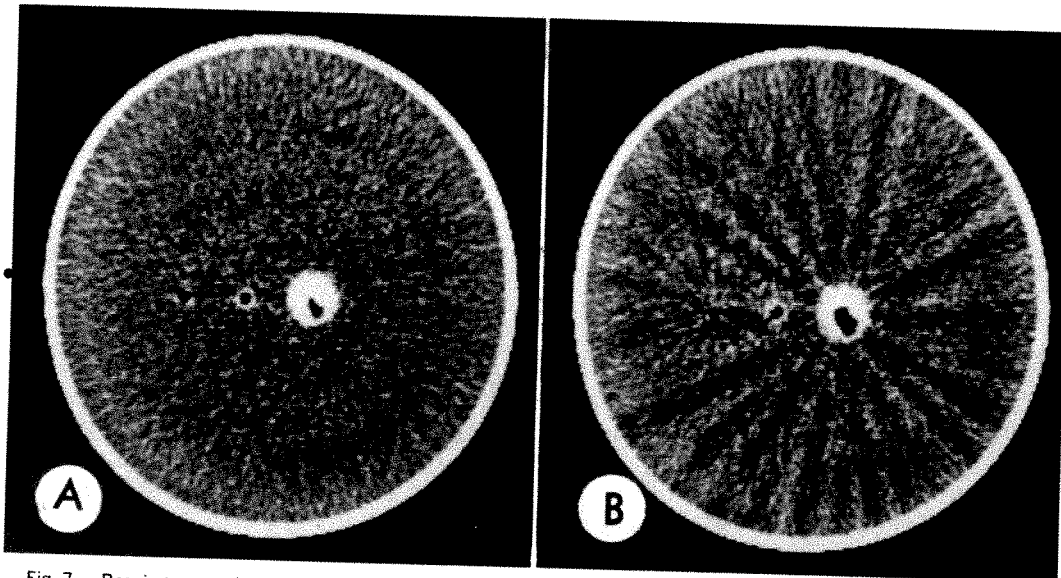


Fig. 7.—Respiratory motion artifacts. *A*, Three nylon spheres with central air cavity scanned static. *B*, Same nylon spheres reciprocated on respiratory motion simulator at 16 cycles/min. Artifacts similar to simulated peristaltic artifacts. Also note that artifacts in both 5*B* and 6*B* affect entire image.

to 50 Delta numbers. Both of these values are reasonably consistent with the concept of the spheres being out of the field of view of the detectors for approximately half of the total scan time. In addition, the diameters are reduced and the borders of the sphere edges become more indistinct.

At the low motion frequency of five, two or one displacement of the sphere per scan (fig. 4*D*), a periodic perturbation was observed through the whole field which did not affect the quantitative values of contrast appreciably. While such periodicity was not normally noted at the displacement frequencies of 6, 11, or 16 cycles/min, at higher frequencies a resonance phenomenon may occur at some subharmonic of the apparent frequency (fig. 4*B*, 28 cycles/min).

Motion Artifacts

Motion artifacts arise from any object in motion in the field. The most objectionable are those caused by either low attenuation (air) or high attenuation (bone or metal) objects that are in motion in the field (figs. 6 and 7). Any motion of either of these will result in stellate or linear artifacts and can originate from muscular, respiratory, or

peristaltic motion. Depending on the length of the scan, the period of the motion, and the attenuation coefficients of objects in the scan, these artifacts become apparent. Motion of objects of intermediate attenuation coefficient also produces artifacts, as evident in the nylon-water motion experiments (figs. 4*B*, 4*D*, and 4*E*). Although in vitro measurements show no change in density of objects superimposed by stellate artifacts, perceptibility is greatly decreased (fig. 6). The smallest sphere is not perceptible even though it is static.

Discussion

When all biological motion is analyzed by CT, three categories of motion become apparent: (1) rotational and off-axis shift; (2) contractile-expansile motion; and (3) Z axis motion blurring. All can produce degradation of contrast and spatial resolution, and all produce attendant stellate or linear artifacts in the CT image.

Rotational Off-Axis Shift

Off-axis and rotational shifts are those motions caused by voluntary or involuntary muscular motion. These represent

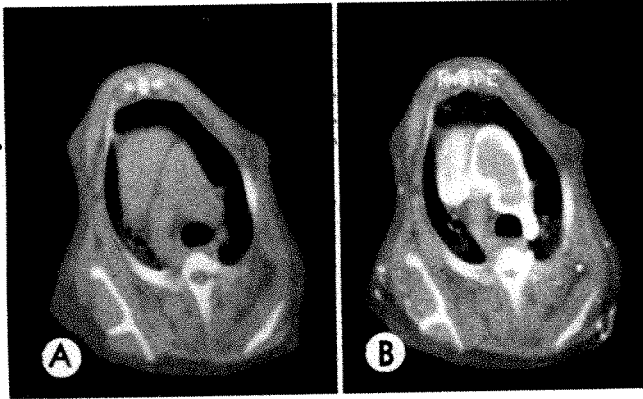


Fig. 8.—A, Scan of canine heart and lungs after sacrifice. Low attenuation structure running from 1:00 to 7:00 is fat in atrioventricular groove. Note lack of difference in attenuation coefficients between myocardium and blood pool. B, Scan at same level after 100 ml of intravenous contrast material injected. Contrast medium outlines vena cava, clot in right atrium, right ventricle, and paravertebral and muscular veins.

the majority of artifacts witnessed in the CNS scans. Such artifacts are also evident in body scans if the patient is unable to hold his body still throughout the duration of the scan. The resultant artifacts are aperiodic and can be enumerated in the scan if the motion is significant.

Contractile and Expansile Motion

This category of motion is characterized either by peristalsis or by contractions and expansions of the cardiovascular system. Cardiovascular motion does not presently cause significant or discernible artifacts in present CT scans. However, spatial and contrast resolution are greatly degraded when scanning the heart at normal frequencies.

Peristaltic motion produces artifacts which are linear or stellate depending upon the number of events occurring in the scan cycle.

Z Axis Motion Blurring

Z axis motion blurring is similar to respiratory motion in

which the object passes from the plane of the image into the plane either above or below during respiration. This motion causes considerable degradation of the image by loss of both contrast and spatial resolution.

All of the above described motions contribute to degradation of the image and in most cases are additive. The obvious solution is to decrease scan time as has been done in conventional radiography.

The present state of the art (fastest prototype available is 4.8 sec) is concerned with the possible and not the ideal. As technology advances, each of the motion plateaus (muscular, peristaltic, respiratory, and cardiovascular) will have to be surmounted if artifact and image degradation are to be eliminated.

Based on results obtained from this study, the shorter the scan time, the better the spatial and contrast resolution provided that noise and other factors remain the same. For present-day technical considerations, scan periods of 2 sec or less would appear to be desirable to eliminate the combination of muscular, respiratory, and peristaltic artifacts. Whether units can be developed with a short enough scan time to "stop" cardiovascular motion remains to be determined.

If ultrashort scan times (less than 50 msec) become available, the detection of akinetic and diskietic myocardium should be possible. It is conceivable that visualization of atrial myxomas, obstructive cardiomyopathy, and CT volumetry could also be accomplished.

ACKNOWLEDGMENTS

We thank Mr. Joseph Bortnick and the Department of Biomedical Engineering of the Cleveland Clinic Foundation who assisted in making this study possible:

REFERENCE

1. Wood EH: Paper presented at the workshop on Reconstruction Tomography in Diagnostic Radiology and Nuclear Medicine, San Juan, Puerto Rico, April 1975

Picture Processing in Computed Tomography

MATS BERGSTRÖM¹ AND ROGER SUNDMAN¹

Using the EMI scanner system computer, picture processing of various kinds can be performed. Computer programs enabling analysis of regions of interest, subtraction, smoothing, and reconstruction in three dimensions have been designed; they are easy enough to be handled by the regular staff. The potential of the methods is illustrated.

Computed tomography is characterized by a very high sensitivity, enabling determination of attenuation differences of about 0.5% and a geometric resolution of about 3 mm. The main factors which limit resolution and sensitivity are noise and artifacts. Noise in the picture is predominantly caused by photon noise (i.e., statistical fluctuation in a limited number of photons). It can only be decreased by increasing the number of photons, which means a higher dose to the patient. The most severe artifacts are usually caused by patient movements during scanning.

Whether a suspected lesion will show up in a picture depends on several factors: attenuation factor of lesion compared to background; size and shape of lesion; homogeneity of lesion and background; and noise and artifacts in the picture. In some instances the eye is not well adapted to detect differences, especially where a large region of slightly different attenuation is overlapped with noise. To gain more information from the pictures, computer pro-

grams have been developed for the EMI scanner system.

Method

Regions of Interest

By calculating mean value, standard deviation, and number of elements in regions of interest, differences in attenuation can be tested statistically. With a normal distribution of the noise, a difference is significant if it exceeds three times the noise divided by the square root of the number of elements. In EMI pictures, noise is approximately 3 units.

Calculation of regions of interest of rectangular and elliptic shape for a whole series of pictures can be done automatically using the EMI scanner system computer. As in the following programs, the pictures to be processed are originally on a storage tape, and an RDOS disc is inserted into the disc drive. A transfer program is called for on the teletype, and transfer from tape to disc is performed when the file numbers of the desired pictures are given to the teletype. When call is made for the program calculating regions of interest, a set of questions is typed by the teletype. Specification of the coordinates of the center of the region, shape, height, width, and angle for a number of regions, as well as number of pictures to be calculated are given on the teletype.

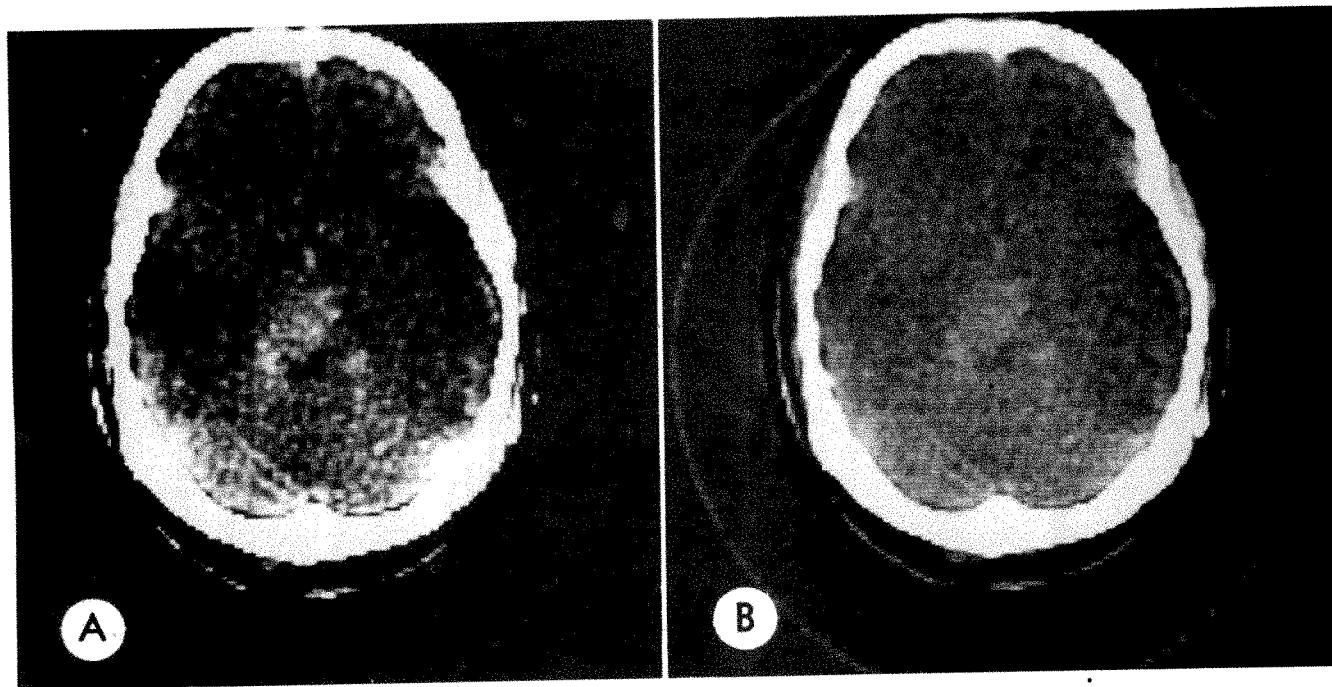


Fig. 1.—Head scan with two different window settings on viewing unit. A, Window 30, level 16.5; B, window 100, level 16.5.

Received February 27, 1976.

This work was supported by a grant from the Swedish Cancer Society.

¹ Department of Neuroradiology, Karolinska Sjukhuset, S-104 01 Stockholm, Sweden.

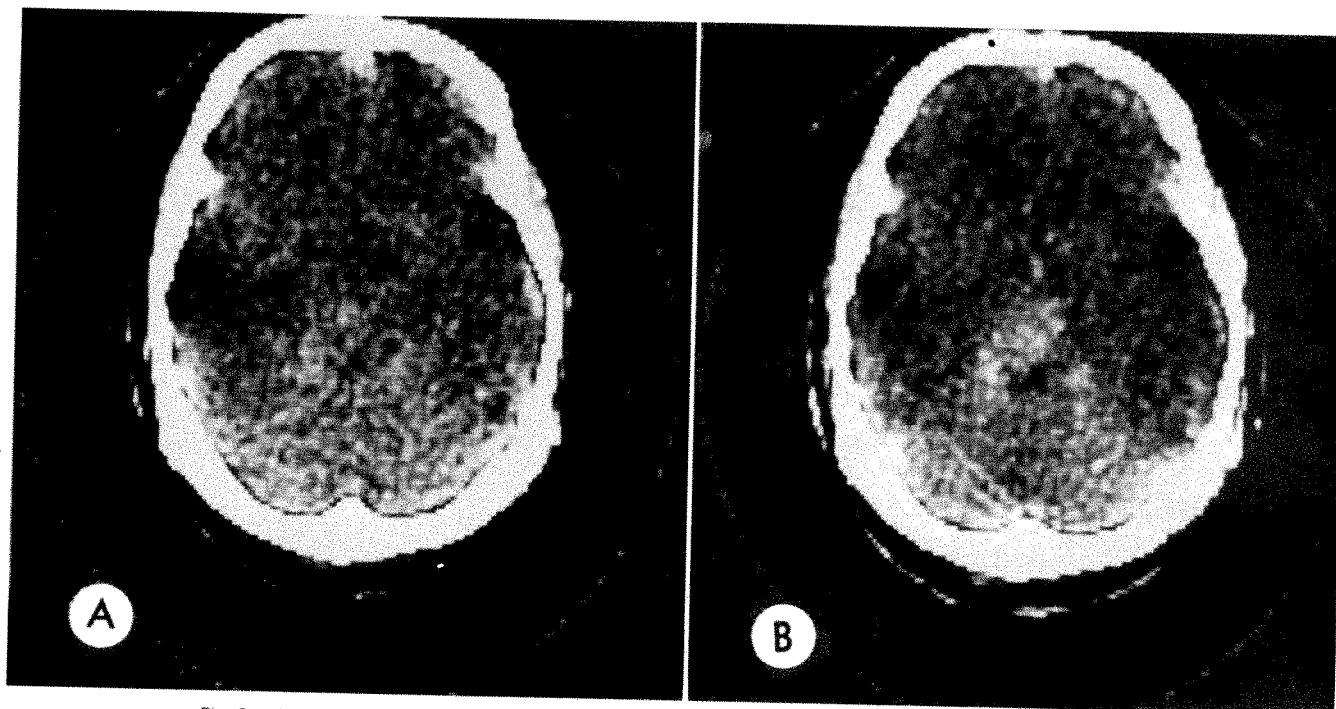


Fig. 2.—Same patient before (A) and after (B) injection of contrast material. Uptake in central glioma shown.

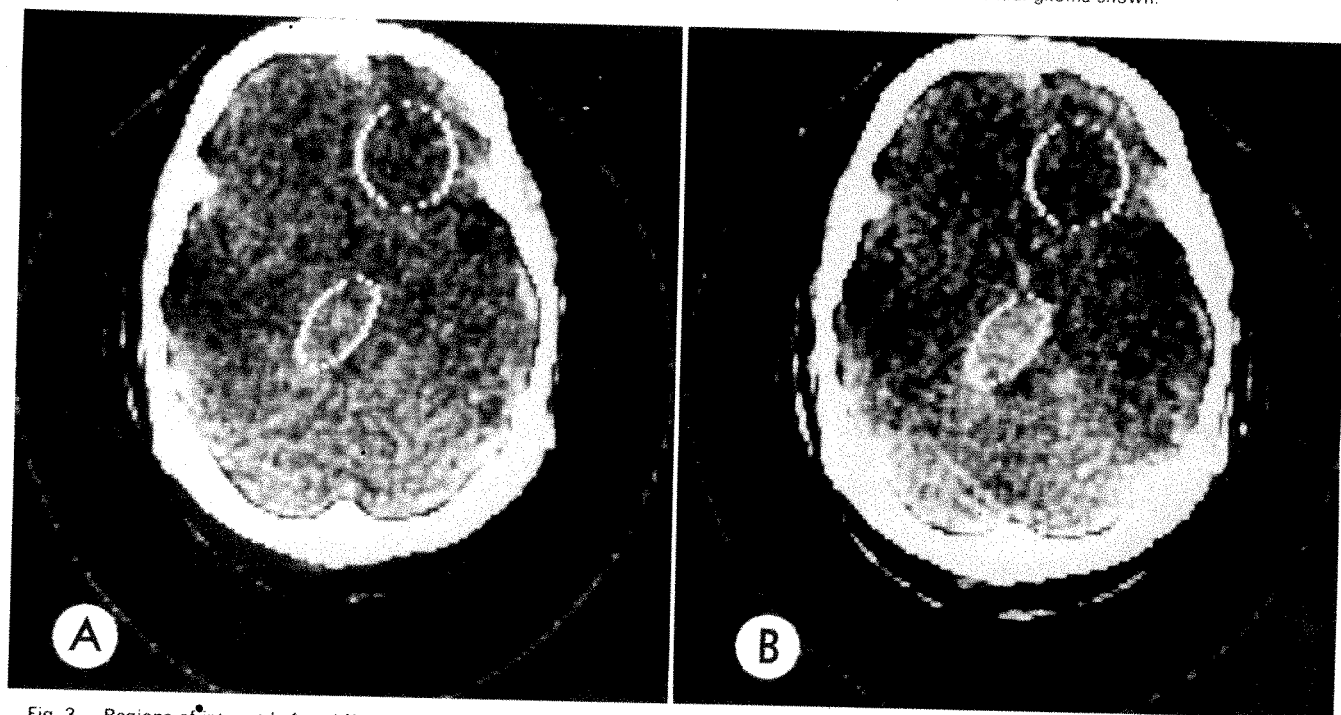


Fig. 3.—Regions of interest before (A) and after (B) injection of contrast material. Upper circle (region 1) represents normal brain tissue; central ellipse (region 2) represents lesion.

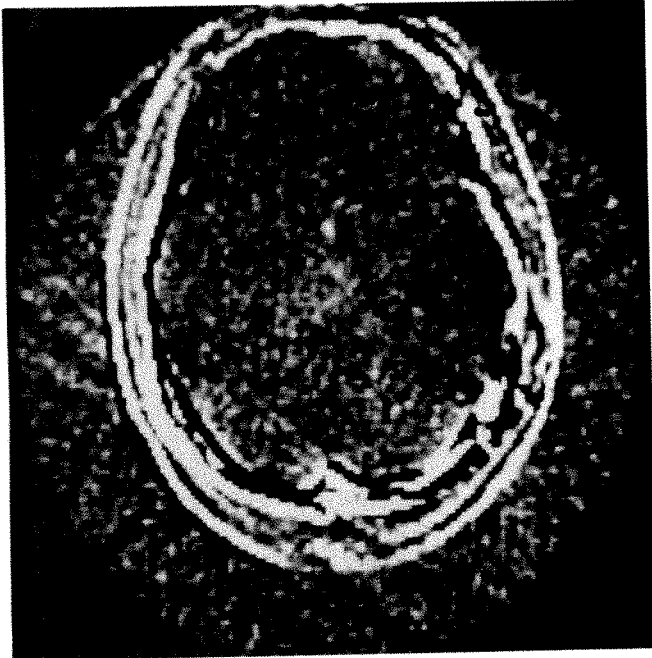


Fig. 4.—Subtraction of pictures (figs. 2B and 2A) obtained after and before injection of contrast material.

After a few seconds the teletype prints picture identification, mean value, standard deviation, number of elements, and transposition of the head for each region and each patient. The regions calculated are positioned with regard to the skull and thus corrected for transposition of the patient in the plane of the picture between each picture. The regions are outlined in the pictures to enable inspection, transferred back to tape, and subsequently viewed. (So far we do not have direct access to the viewing unit from the RDOS system.)

Subtraction

Such factors as uptake of iodine in a tumor and changes due to treatment may be difficult to interpret by mere inspection. In some instances better visualization is obtained by having the computer subtract pictures taken at different occasions element by element. This is done by simply typing the file numbers of the pictures to be subtracted after a call has been made to the subtraction program. The subtracted picture may then be displayed on the ordinary display unit or further processed. However, it must be realized that noise in the subtracted picture is about 40% higher than in the unsubtracted picture. Due to the impaired signal-to-noise ratio, too great expectations should not be attached to the subtraction technique.

Smoothing

Noise in the picture can be reduced by setting a wide window on the display unit. However, at the same time the possibility for the eye to detect small differences in attenuation is lessened (fig. 1). After digital smoothing of the fine structures, a narrow window can be used instead, thereby enabling recognition of large regions with slight

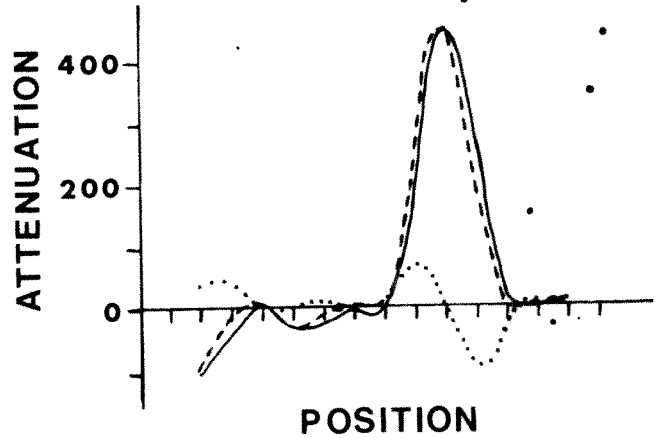


Fig. 5.—Attenuation profiles across bone shown in fig. 4. Solid line, taken from fig. 2A; dashed line, taken from fig. 2B; dotted line, difference of attenuation profiles. Slight shift in position of bone causes large error in subtracted profile.



Fig. 6.—Smoothing of subtraction picture shown in Fig. 4 using 9×9 convolution matrix.

difference in attenuation. The smoothing is performed by convoluting the picture with a quadratic matrix with 5×5 , 7×7 , 9×9 , 11×11 , or 17×17 elements. Each element in the matrix is formed according to the formula $A_{ij} = B_i \times B_j$, where $i=1, \dots, n$, $j=1, \dots, n$. The coefficients B_i ($i=1, \dots, n$) are taken from Savitsky and Golay [1], and n is the number of rows in the convolution matrix. After a call for the smoothing program, the size of the convolution matrix is specified, whereupon smoothing is performed.

Reconstruction in Three Dimensions

Data obtained from several adjacent slices through the head can be used to reconstruct any cut in three dimen-

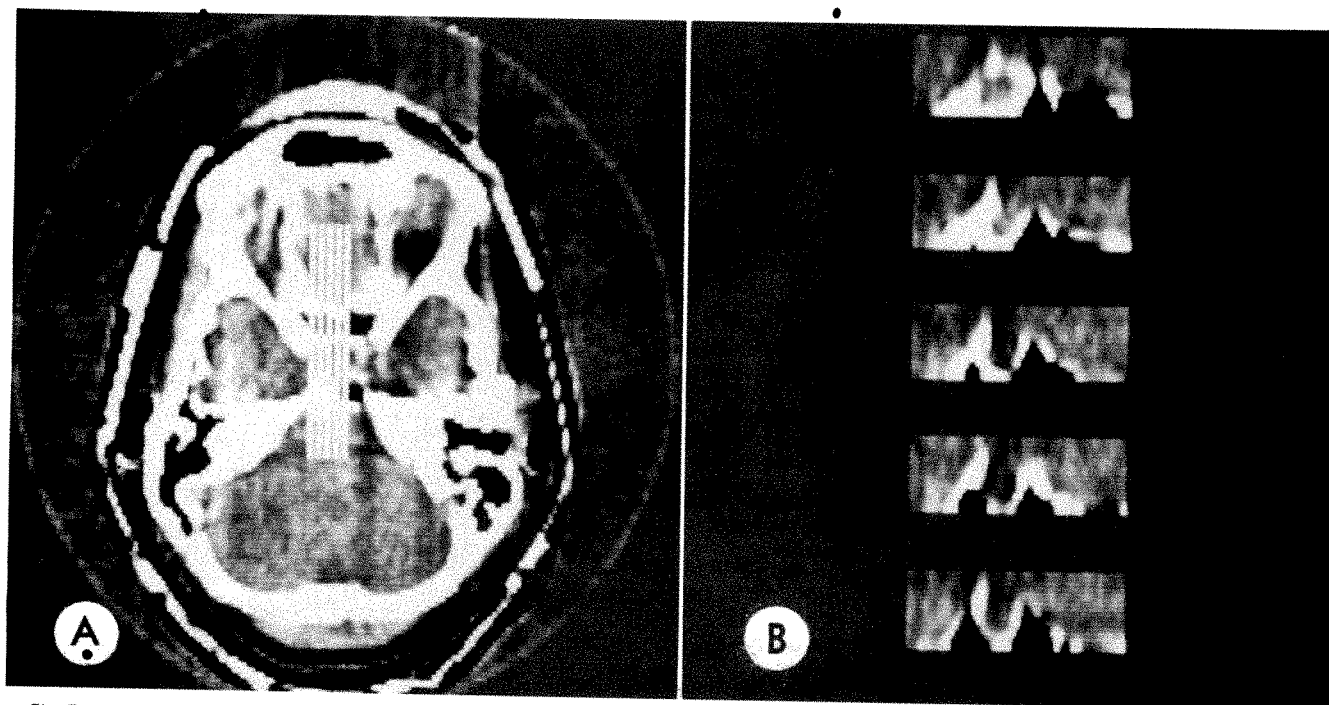


Fig. 7.—A, Tomographic picture with lines indicating where cuts for lateral reconstructions are made. B, Lateral reconstructions through sella region.

sions [2]. However, by just storing slices obtained with 1.3 cm or 0.8 cm collimator upon each other, the geometric resolution in the vertical direction is much less than in the horizontal. This could be improved by using a much smaller collimator, 1 or 2 mm. However, there would then be a significant increase in noise. To overcome this problem, partly overlapping cuts can be taken by successively moving the collimator 1 or 2 mm [3]. The lower noise level is gained at the expense of a higher dose to the patient, four times higher when successively moving a 0.8 cm collimator 2 mm. Successively moving a wide collimator has the same smoothing effect as a moving average.

To restore the actual distribution of attenuation coefficients in the vertical direction, a deconvolution could be applied, but since for practical reasons the number of cuts is usually limited to about eight, the deconvolution might introduce "overswings" in the transition between bone and tissue. Therefore we have chosen not to deconvolute.

A call is made for the reconstruction program. After specifying lateral or frontal projection, location and size of the area to be reconstructed, and number of slices, the computer chooses five evenly distributed cuts through the area and puts the reconstructed cuts in a picture for further processing or viewing. The positions of the cuts are also indicated in another picture. Computer time is about 1 min.

Results and Discussion

Figure 2 shows pictures of the same section before and after injection of contrast material (Isopaque Cerebral). Applying the program for regions of interest (fig. 3) shows that region 1 increased in attenuation with 0.5 EMI units

($\sigma/\sqrt{n}=0.2$) and region 2 with 4.5 EMI units ($\sigma/\sqrt{n}=0.2$). Thus there is a very significant increase of attenuation in the suspected central region.

By subtracting the two pictures shown in figure 2, the uptake of contrast material can be visualized (fig. 4). The central region of increased attenuation is faintly observed, though the noise level is increased. The impression from looking at the bone of the skull is that a marked transpositioning of the head has occurred. This is mainly imaginary, as can be seen from figure 5 where attenuation profiles of the two pictures are plotted. Due to the great gradient close to bone, even a very small transpositioning will cause wide regions where overlapping seems inaccurate.

Figure 6 is obtained by smoothing the picture shown in figure 4 with a 9×9 matrix. The central region of increased attenuation is better identified due to reduction of noise. Narrow structures are significantly widened, as can be seen from the bone edge, and care must be taken to note such effects when analyzing smoothed pictures.

Figure 7 shows lateral reconstructions through the sella region. An 0.8 cm collimator successively moving 2 mm and making eight slices was used. The left picture indicates where the cuts are made. The upper reconstruction is to the patient's left, and posterior is to the right in the reconstruction. The sella turcica is easily identified in the pictures.

Conclusions

Once all attenuation coefficients of the 160×160 matrix are stored on magnetic tape, further processing of the EMI pictures can easily be made with the EMI scanner system computer. This can be achieved by every user with some

initial help in designing the computer programs. The programmer has to have access to a magnetic disc and an RDOS disc operation system (delivered by Data General). Programming can be done in FORTRAN. The clue to processing the pictures is a knowledge of how the information is stored on the magnetic tape. This is now specified in a technical bulletin from EMI [4].

Once the programs have been designed, picture processing can be handled by the regular staff. (In our department it is done by the radiographers.)

The potential of a few of the most obvious methods for picture processing has been described. We are convinced that these methods may be further developed in many ways.

REFERENCES

1. Savitzky A, Golay M: Smoothing and differentiation of data by simplified least squares procedures. *Anal Chem* 36:1627-1639, 1964
2. Peters TM: Enhanced display of three-dimensional data from computerized x-ray tomograms. *Comput Biol Med* 5:49-52, 1975
3. Glenn WV, Taveras JM, Johnston RJ, Morton PW, Dwyer SJ: Clinical feasibility of reconstructing coronal, sagittal and thin transverse sections from overlapped 8.0 mm CT scans. Paper presented at the workshop on Reconstruction Tomography in Diagnostic Radiology and Nuclear Medicine, San Juan, Puerto Rico, 1975
4. EMI Limited, X-ray Systems Division: *Breakdown of Word Structure*, Technical Bulletin no. 8. Hayes, Middlesex, EMI Limited, 1976

P24,428

Computed Tomography of the Body: Initial Clinical Trial with the EMI Prototype

PATRICK F. SHEEDY, II,¹ DAVID H. STEPHENS, ROBERT R. HATTERY,
JOHN R. MUHM, AND GLEN W. HARTMAN

A review of the first 400 cases examined on one of three prototype EMI body scanners is presented. During the initial evaluation phases, it became obvious that computed tomography of the body has tremendous potential in the evaluation of various organs and disease states. The technique has been most useful in evaluating patients with known or suspected abdominal neoplasm, particularly lesions of liver, pancreas, retroperitoneum, and kidney. Too few cases have been studied to realistically quantitate its impact on the total field of medical diagnostic imaging.

Introduction

The introduction and use of equipment designed to produce reconstructed images of the brain has profoundly altered the radiologic approach to diagnosis of diseases affecting the central nervous system. For the first time the parenchyma of the brain can be evaluated rather than only adjacent tissues such as bone, blood vessels, and fluid-filled spaces. This experience has underscored the potential application of this technique to other body parts. Several reports on experiences with in vitro and in vivo scanning have been reported recently [1-10]. Three manufacturers already have provided equipment (ACTA, Delta, EMI) that can be used to conveniently examine any part of the body; many other manufacturers (Artronix, Philips, General Electric, Varian, Syntex, American Science and Engineering, and Picker) have scanning units in various stages of development and investigation. The availability of these units introduces a bewildering variety of factors that must be considered in evaluating both the technique itself and the various scanning units. Specifications such as speed of scan, image processing time, matrix size, resolution, number and types of detectors, scanning type (fan beam, scan, or fan scan), thickness of slice, recording techniques, and display of absorption values all must be considered in the overall evaluation of CT [11].

This review presents the clinical experience gained in the first 400 patients scanned at the Mayo Clinic with the investigational prototype of the EMI body scanning unit.

Materials and Methods

CT Scanning Equipment

In October 1975, one of three engineering prototypes of the EMI body scanning unit was installed at the Mayo Clinic. The unit is composed of a scanning gantry, patient table, computer, and viewing unit.

The scanning gantry consists of an x-ray source that produces a highly collimated, fan-shaped x-ray beam mounted opposite an array of 30 NaI crystalline detectors. The x-ray source and detectors rotate around the patient at 10° increments for a total of

180°, with a linear transverse scan occurring at each of the 18 rotational points. A single scan, completed in 20 sec, produces one tomographic slice. The information obtained during each scan is processed by a 64 K Data General Eclipse Computer, and the reconstructed image is presented on a television monitor for viewing and photographic recording. Each tomographic section produced is formed by a series of picture elements representing the absorption coefficient of a volume of tissue 1×1×13 mm for the 13 inch scanning circle. (A 10 inch scanning circle is also available. This produces a picture element representing a volume of tissue 0.75×0.75×13 mm.)

The 80,000 individual picture elements are assembled and displayed in the form of a circular matrix with a diameter of 320 picture elements. Even though each picture element is displayed in two dimensions as an area 1×1 mm, the absorption coefficient depicted actually represents that of a volume of tissue 13 mm deep. The reconstructed image can be recorded on film and can be manipulated on the display console to permit a selective display of any particular absorption value from the wide spectrum of values obtained during a scan. Manipulation of images with the present prototype viewing unit is rather cumbersome. However, the planned addition of an improved display unit will greatly facilitate viewing and manipulation of the reconstructed images.

Currently we use a Shackman camera and Polaroid film for permanent recording. All scans are placed on magnetic tape and are retrievable.

Patients and Methods

More than 400 patients with a wide variety of clinical problems were examined during the first 4 months of use of this scanning unit (table 1). Almost all patients had, or were highly suspect of having, a mass lesion. Special emphasis was placed on patients who were likely to have a diagnosis confirmed by a surgical procedure or who had a relatively definite diagnosis established by another reliable diagnostic modality. However, early experience revealed that the CT technique provided diagnostic information so convincing that, when correlated with other clinical data, nonoperative management of some patients was decided on. This was particularly true when the CT scan revealed no abnormality.

No attempt was made to exclude from study any clinical problem or possibility of a mass lesion in any organ or location. Thus there would be no failure to recognize a potential application.

Currently all requests for CT examination are reviewed carefully and approved by one of us. Before the examination, a single anteroposterior recumbent roentgenographic view is taken of the area of the body (except head and extremities) to be scanned. The roentgenogram is made with a lead-Plexiglas grid placed on the chest or abdomen of the patient. Appropriate marks are then made on the patient's skin to ensure that the cross-sectional images are made through the anatomic area of interest. Generally, eight, 10, or 12 scans are needed to cover a particular area of interest. The examination is carefully planned in advance, and a decision is made regarding location and number of slices, whether to administer con-

Received March 26, 1976.

¹ All authors: Mayo Clinic and Mayo Foundation, Rochester, Minnesota 55901. Address reprint requests to P. F. Sheedy.

TABLE 1
Anatomic Areas Scanned

Anatomic Area	No. Cases
Abdomen:	
General.....	23
Liver.....	38
Pancreas.....	77
Retroperitoneum.....	44
Kidney.....	27
Adrenal.....	5
Spleen.....	1
Prostate.....	3
Pelvis and genitalia.....	6
Total.....	224
Chest:	
Lung.....	29
Mediastinum.....	14
Total.....	43
Head.....	83
Orbits.....	14
Other:	
Spinal cord.....	17
Thyroid.....	7
Extremities.....	7
Unsatisfactory.....	5
Total.....	36
Grand total.....	400

trast material intravenously or orally, and whether to use a position other than the supine one. The images are not viewed until after all have been processed and the patient has left the department. If additional views or scanning after contrast injection or ingestion is needed, this is carried out on another day. This method allows from eight to 10 examinations each day, but it is not ideal. On-line processing and viewing should lead to an increased flexibility in technique, and we shall use this approach when the planned addition of another computer to the system permits a faster scan processing time, while preserving a reasonable patient handling time.

All examinations, except those of the head and extremities, are made while the patient is holding his breath. Most patients can do this for the duration of the 20 sec scan. Respiratory motion results in artifacts that seriously degrade image quality. McCullough et al. [11] have shown that it is the motion of air rather than its presence which creates undesirable artifacts.

The reconstructed images of the body are displayed on the console so that the right side of the patient's body is on the observer's left, as is the custom with routine radiography. This orientation has certain advantages because it simplifies comparison with other imaging methods in the body (routine radiography, excretory urography, angiography, ultrasonography) which are displayed with the same orientation. This orientation differs from that of the ACTA and Delta scanner display and from the EMI head scan display. Nevertheless, this depiction, which conforms to the traditional one in radiology, is most appropriate. The scans in the present review are so oriented.

Results

The distribution of patients and organs scanned (table 1) suggests areas in which CT body scanning has greatest

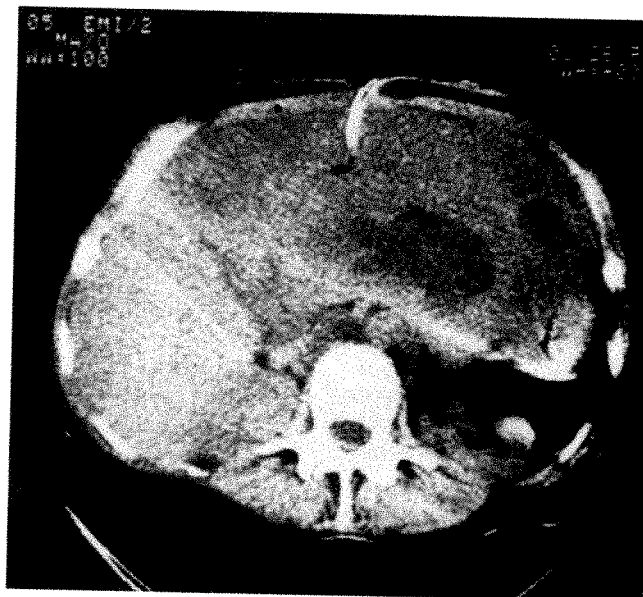


Fig. 1.—CT scan of 68-year-old woman who had previous resection of large leiomyosarcoma of pancreas containing malignant pseudocyst. Huge low density mass occupies two-thirds of abdomen. Note one large area and several small areas of even lower density within mass, indicating multiple cysts. Diagnosis was massive recurrence of leiomyosarcoma of pancreas, with multiple pseudocysts within mass. Mass extensively invaded and abutted multiple intraabdominal organs.

potential. Three basic factors should be considered in regard to any disease, and CT has value in each: (1) initial detection of disease, (2) determination of extent of a known disease, and (3) determination of type of disease.

Abdomen

Most examinations were directed at an evaluation of intraabdominal disease processes, primarily neoplasms. Liver, pancreas, retroperitoneum, and the genitourinary tract were the most commonly studied regions. Although many large intraabdominal masses are obvious clinically, it is important to determine the origin and extent of the lesion and the nature of the process—whether diffuse or focal. Frequently, large masses impinge on many abdominal organs (fig. 1). Such information has significant implication when the patient is being evaluated for possible surgery.

Liver. The liver was the organ of primary interest in 38 patients studied. The normal liver appears slightly more dense than other intraabdominal organs, is homogeneous in density, and is variable in size and configuration. Indications for liver scans included primary malignant tumor, metastatic disease, inflammatory disease, and evaluation of the jaundiced patient.

Tumors in the liver, whether benign or malignant, are generally less dense than the normal liver parenchyma (fig. 2); intravenously administered contrast medium, although increasing the density of both the normal and abnormal tissue, tends to accentuate this density difference (fig. 3). An exception was seen in a patient with highly vascular metastatic lesions. The lesions initially were less dense than parenchyma but had the same density as liver

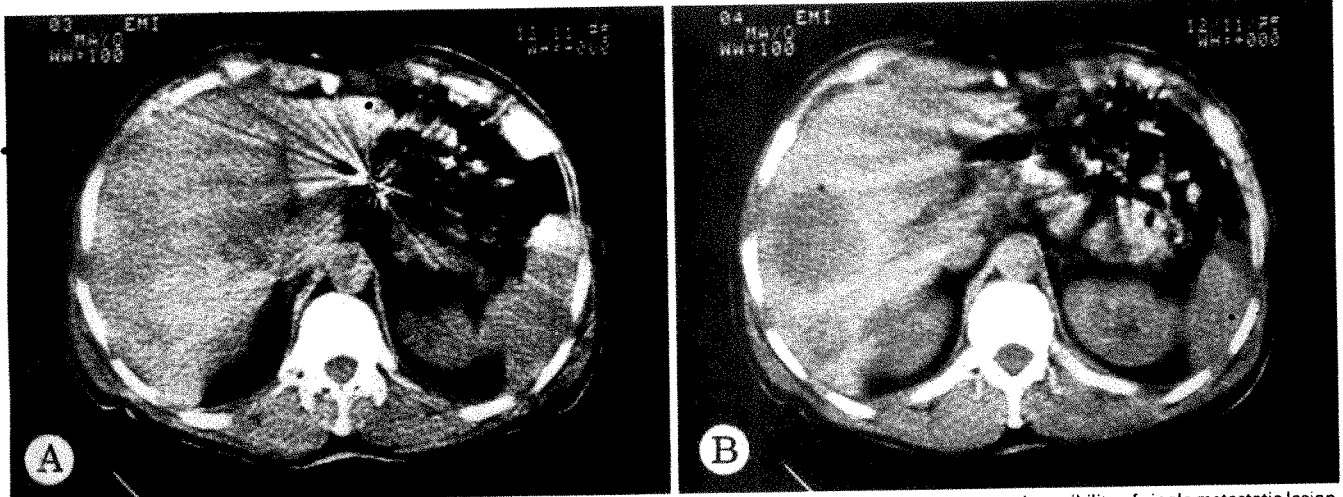


Fig. 2.—CT scans of 48-year-old man 7 months after resection of gastric leiomyosarcoma. Liver nuclear scan suggested possibility of single metastatic lesion. A, Faint, low density mass in medial portion of right lobe of liver, partially obscured by streaking artifact due to motion of metallic surgical clip. B, One large and one small low density metastasis in posterior portion of right lobe of liver. Grade 2 metastatic leiomyosarcoma confirmed by liver biopsy.

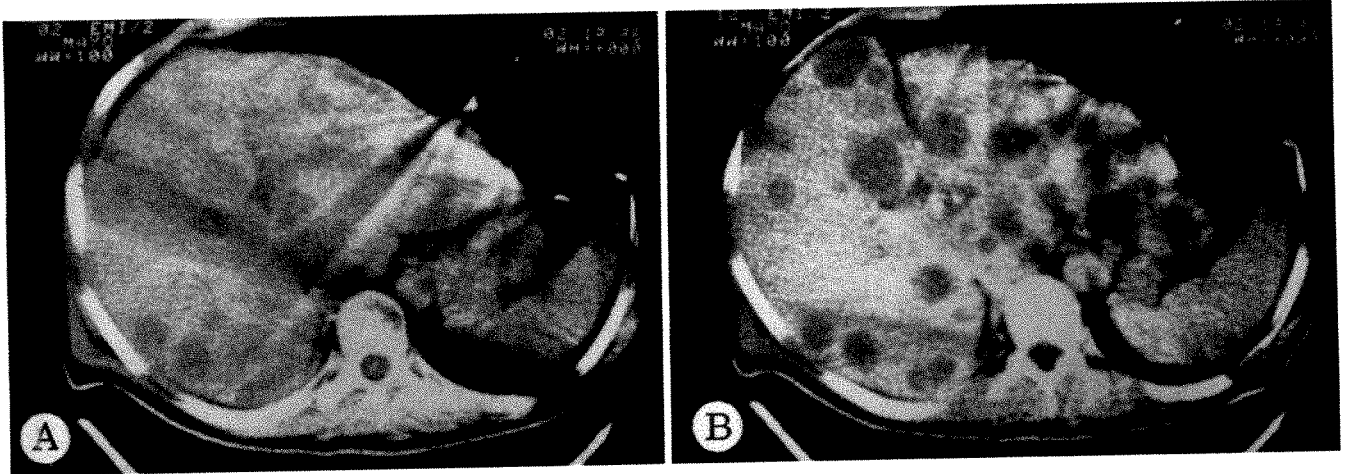


Fig. 3.—CT scans of 51-year-old man with loss of weight, back pain, and large supraclavicular lymph node. Biopsy of node revealed mucous adenocarcinoma. Hepatic metastases shown before (A) and after (B) contrast material given intravenously.

tissue after contrast material had been administered intravenously [6].

Initially some difficulty was experienced in distinguishing metastatic lesions from a dilated intrahepatic biliary duct. However, experience revealed that dilated ducts tended to be more sharply circumscribed and less dense than metastatic lesions. Moreover, a branching ductal pattern could be detected especially in the region of the porta hepatis when the ducts were dilated. Dilated ducts were seen as round filling defects in the right lobe and as horizontally oriented defects in the left lobe, as would be expected from the general orientation of the ducts in these lobes (fig. 4). Also, dilated ducts were more centrally located and of more uniform size than the metastatic lesions. Several liver masses differed only slightly in density from normal parenchyma, and only careful scrutiny of the scan permitted their detection (fig. 5). CT allows the detection of smaller and deeper lesions than does the nuclear scan. Several CT scans done to evaluate a solitary mass

seen on the nuclear scan resulted in a diagnosis of multiple lesions indicating metastasis, subsequently confirmed by biopsy (fig. 6). However, one huge hepatoma that was obvious on a nuclear scan because of the complete absence of nuclide uptake was not appreciated on the CT scan. This lesion occupied almost the entire right lobe of the liver, with virtually no normal tissue remaining, and there was no interface of normal and abnormal density in the right lobe. The normal left lobe appeared less dense than the hepatoma (fig. 7). Several instances of focal nodular hyperplasia of the liver have been discovered. Such hyperplasia differs in density only minimally from the normal liver, but frequently it alters the normal contour of the affected portion of the liver (fig. 8).

Hepatic abscesses are less dense than the liver and are less sharply margined than neoplastic lesions (fig. 9). Other benign lesions have features sufficiently unique to permit a reasonably specific diagnosis (fig. 10).

The superior margin of the liver is difficult to evaluate

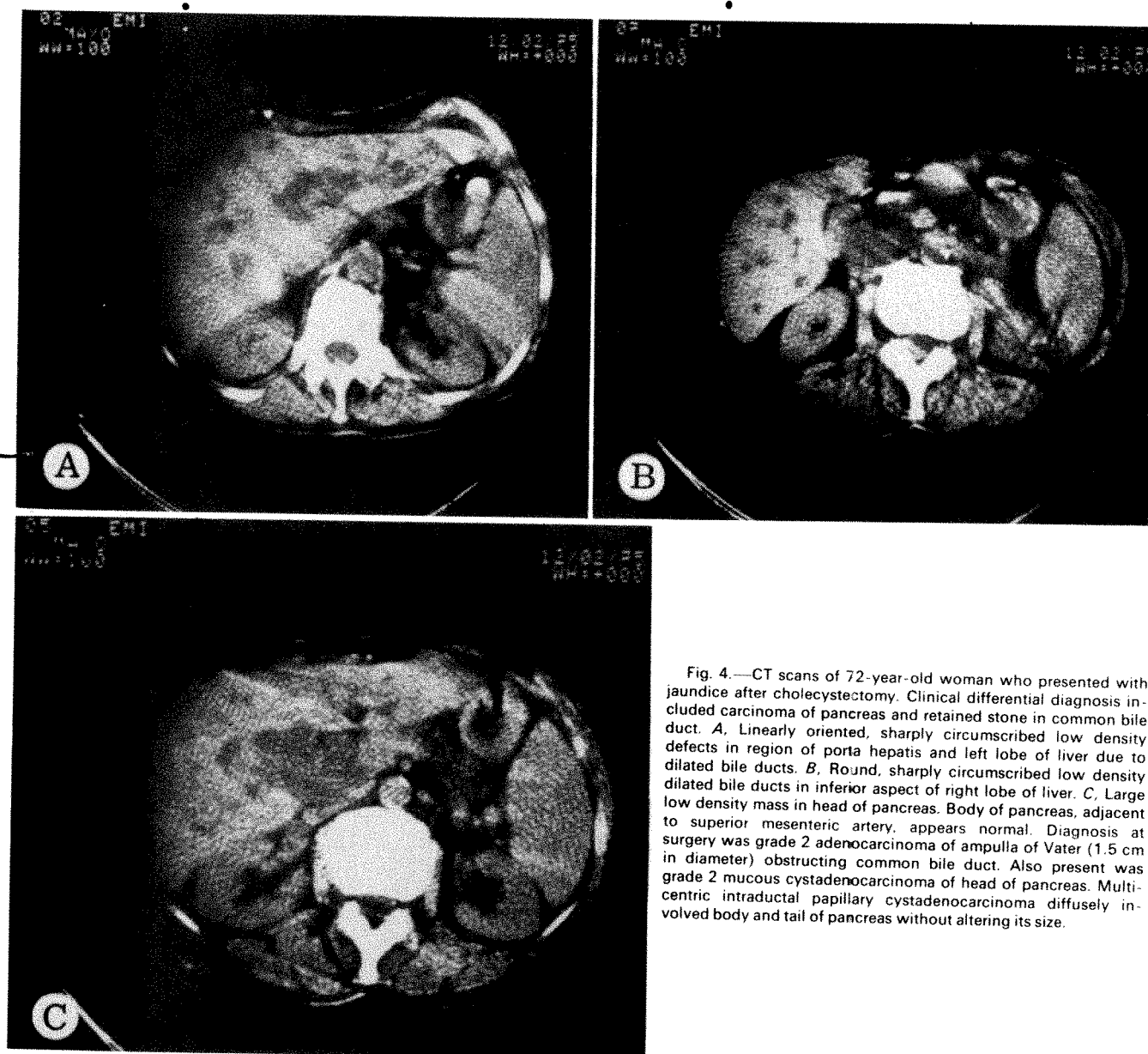


Fig. 4.—CT scans of 72-year-old woman who presented with jaundice after cholecystectomy. Clinical differential diagnosis included carcinoma of pancreas and retained stone in common bile duct. A, Linearly oriented, sharply circumscribed low density defects in region of porta hepatis and left lobe of liver due to dilated bile ducts. B, Round, sharply circumscribed low density dilated bile ducts in inferior aspect of right lobe of liver. C, Large low density mass in head of pancreas. Body of pancreas, adjacent to superior mesenteric artery, appears normal. Diagnosis at surgery was grade 2 adenocarcinoma of ampulla of Vater (1.5 cm in diameter) obstructing common bile duct. Also present was grade 2 mucous cystadenocarcinoma of head of pancreas. Multicentric intraductal papillary cystadenocarcinoma diffusely involved body and tail of pancreas without altering its size.

because it often is obscured by a peculiar linear artifact. It is thought that cardiac motion at the lung-abdomen interface causes this disconcerting streaklike artifact.

The gallbladder usually can be seen on CT scans of the liver. The discovery of a distended gallbladder often serves as a secondary sign of biliary obstruction from a neoplasm in the bile ducts or the pancreas. Occasionally an unsuspected gallstone is detected, but we anticipate no particular future for CT of the gallbladder, except, perhaps, in the evaluation of the nonvisualized gallbladder.

Pancreas. The prospects of an accurate, noninvasive diagnostic examination to evaluate the pancreas is exciting, and preliminary results in 77 patients are encouraging. As expected, most patients referred for CT of the pancreas either had suspected pancreatic lesions or had evidence of metastatic carcinoma of unknown origin.

Perhaps more than for any other organ, the normal

anatomy of the pancreas must be appreciated in order to correctly interpret abnormal pancreatic scans. The pancreas, or a portion of it, can be identified on most scans because it is separated from other organs by fat planes. The pancreas is oriented in the abdomen either horizontally or obliquely. If the pancreas is oriented horizontally, the entire organ can be seen on one or more of the 13-mm-thick slices (fig. 11). However, if the pancreas is oriented obliquely, only a portion will be depicted on any one slice. Thus the highest cut shows the tail, the middle cut shows the body, and the lowest cut shows the head and uncinate process (fig. 12).

Recognition of the pancreas can also be aided by its relationship to other organs. The tail is near the hilum of the spleen and extends anteriorly, ventral to the upper pole of the left kidney, where the body passes over the vertebral body and aorta and immediately in front of the superior

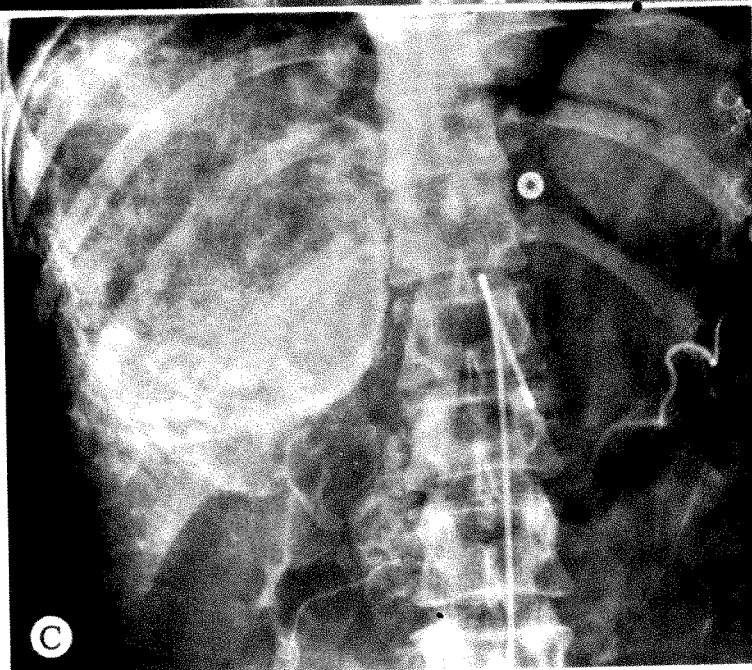
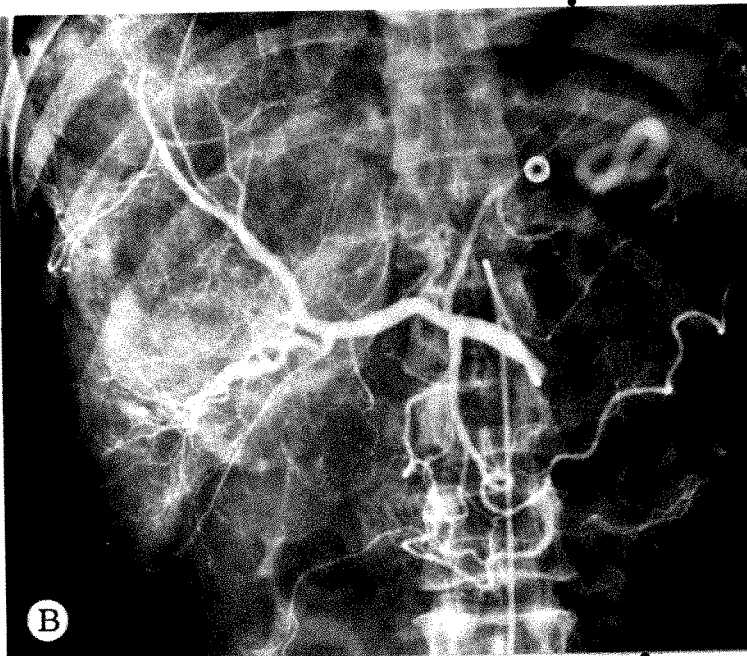
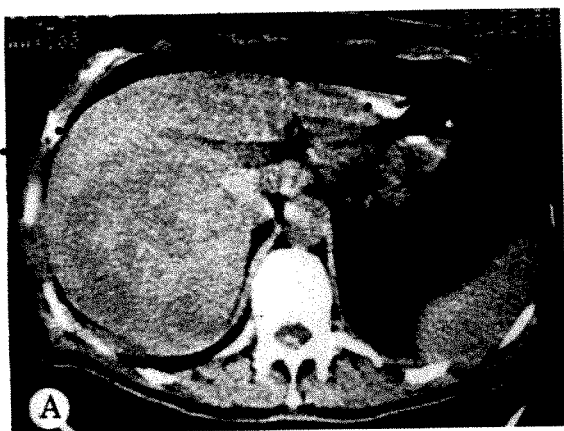


Fig. 5.—62-year-old man 5 years after resection of carcinoma of midrectum. Nuclear scan of liver demonstrated diffuse abnormality in right lobe. *A*, CT scan showing large round lesion of diminished density occupying practically entire right lobe of liver. Some inhomogeneity of density present within mass. *B*, Hepatic angiogram, arterial phase, showing stretching and displacement of right hepatic artery branches to upper portion of right lobe, with tumor vascularity in periphery of large solitary lesion. *C*, Hepatic arteriogram, venous phase, showing dense stain in periphery of lesion. Right hepatic lobectomy revealed solitary metastatic grade 2 adenocarcinoma consistent with rectal primary lesion.

mesenteric artery. It then turns slightly dorsally, with the pancreatic head located just in front of the inferior vena cava. In this region, the head lies in the loop formed by the second and third portions of the duodenum and is often inseparable from the bowel by virtue of density alone.

Knowledge of the relationship of the pancreas to the superior mesenteric artery is helpful because the superior mesenteric artery arises from the aorta at the superior border of the body of the pancreas, passes inferiorly behind the pancreas, and then passes in front of the third portion of the duodenum. Thus on the scans, the body of the pancreas lies ventral to the superior mesenteric artery, but a similarly shaped structure that lies dorsal to the superior mesenteric

artery is the third portion of the duodenum. These relationships of the pancreas to other structures are critical because a difference in density between the pancreas and the adjacent organs is often not detectable. Thus identification of the pancreas depends on recognition of its contour and configuration and not on a unique or specific pancreatic density.

In fact, sometimes the entire pancreas is difficult to identify on a scan, and often the margin of the organ must be estimated as it lies in relation to the second portion of the duodenum and the posterior portion of the stomach. The introduction of dilute water-soluble contrast medium has helped differentiate these two portions of the bowel from

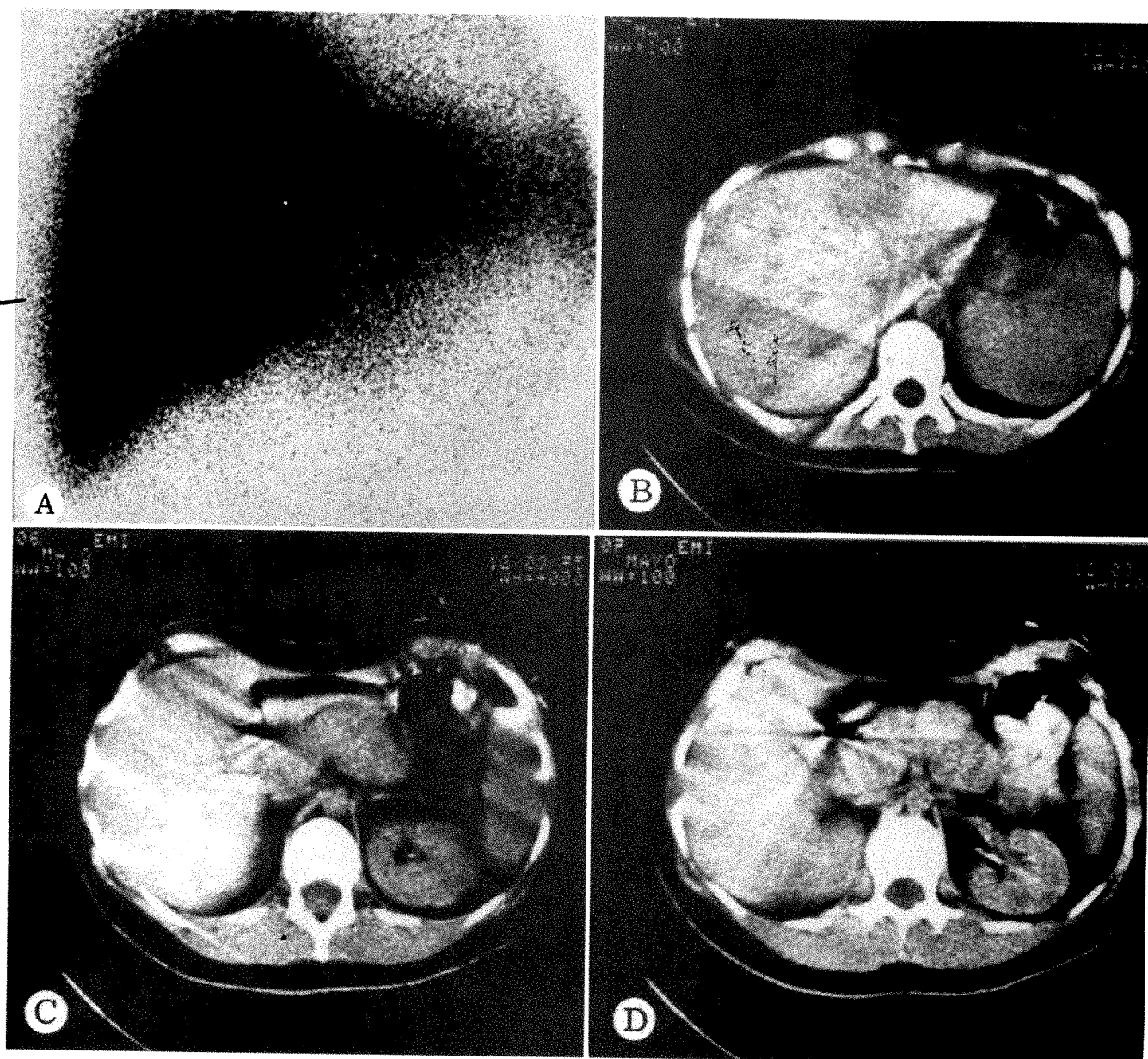


Fig. 6.—30-year-old woman found to have mass (4 cm in diameter) in anterior portion of liver at laparoscopy for tubal ligation. *A*, Nuclear scan showing area of diminished uptake at junction of right and left lobes of liver anteriorly. *B*, CT scan showing low-density mass (4 cm in diameter) in anterior portion of liver and several small lesions (some 1 cm in diameter) scattered throughout right lobe, indicating multiple metastatic lesions. *C*, CT scan demonstrating diffuse pancreatic enlargement due to neoplasm. *D*, Lobular mass at inferior aspect of pancreas raising possibility of nodal involvement. Large nonfunctioning malignant islet-cell tumor of pancreas found at operation as well as one large nodule and multiple smaller metastatic nodules on surface and within parenchyma of liver. Several enlarged lymph nodes present at inferior aspect of pancreatic mass.

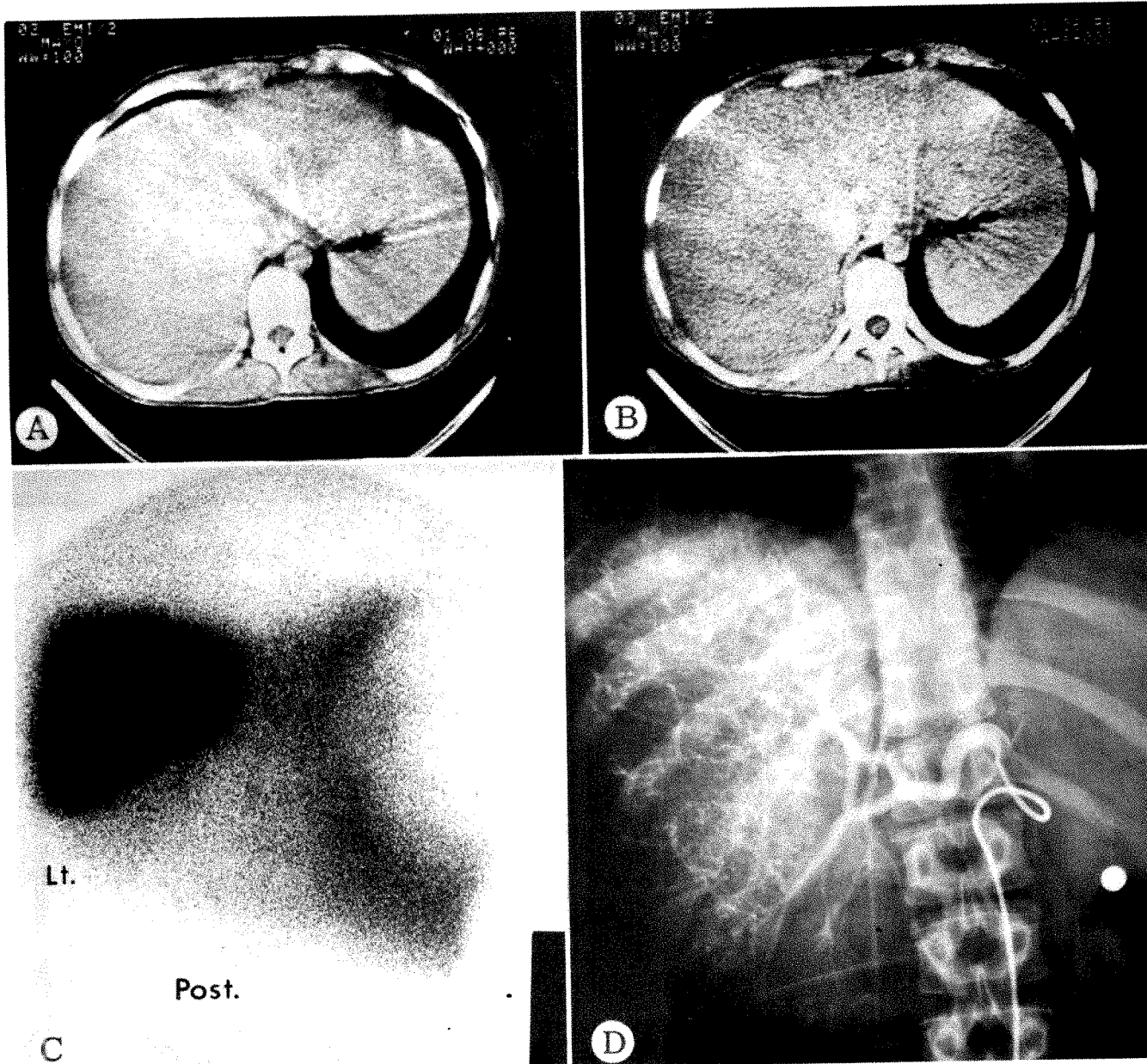
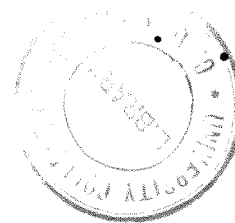


Fig. 7.—18-year-old man with right flank pain. Liver function tests abnormal; nuclear scan revealed huge mass occupying posterior superior aspect of right lobe. *A and B*, CT scans showing hepatomegaly with right lobe slightly more dense than anterior portion of left lobe. *C*, Nuclear scan showing huge defect in posterior portion of right lobe. *D*, Hepatic arteriogram, arterial phase, showing huge vascular lesion with appearance of hepatoma occupying practically entire right lobe. Hepatoma removed at right hepatic lobectomy. Only thin rim of normal hepatic tissue at periphery of specimen.

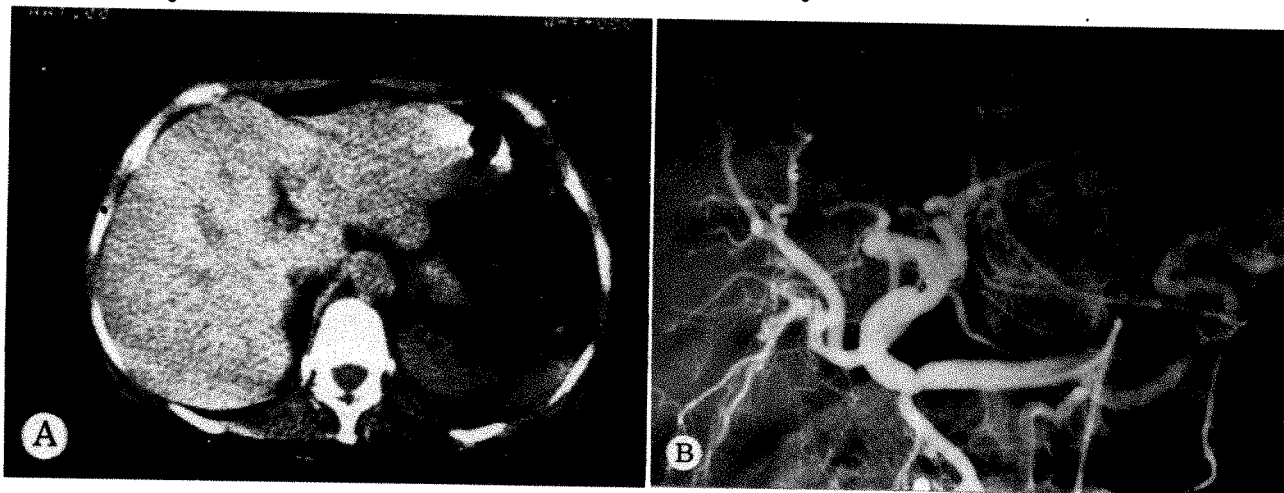


Fig. 8.—49-year-old woman with tumor of left lobe of liver discovered at bilateral salpingo-oophorectomy and hysterectomy. **A**, CT scan showing lobulated mass in left lobe of liver of slightly diminished density compared to adjacent normal parenchyma. Several low density areas in region of porta hepatis within normal limits. **B**, Hepatic arteriogram showing mass lesion in left lobe of liver with tumor vascularity. Focal nodular hyperplasia of left lobe of liver discovered at operation.

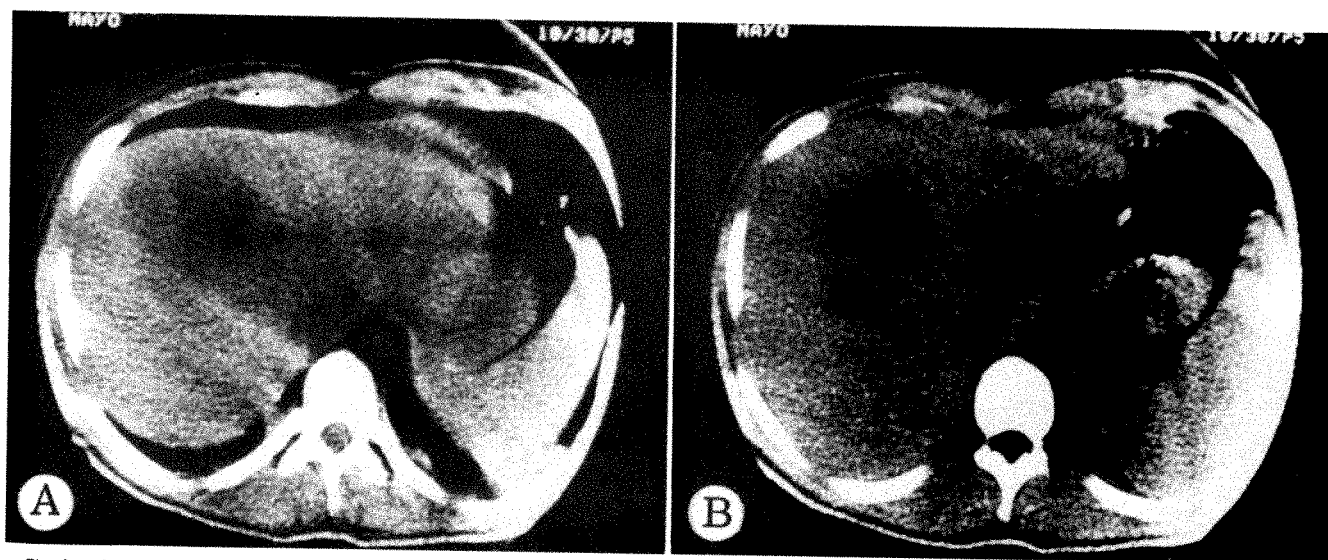
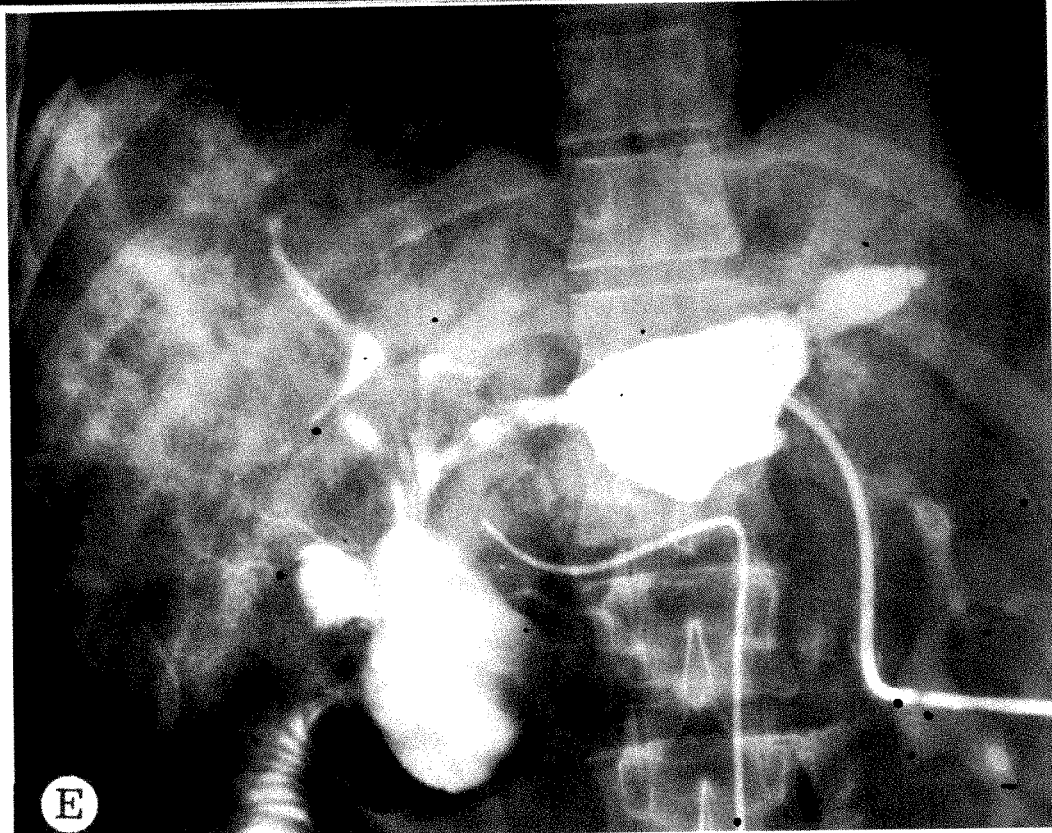
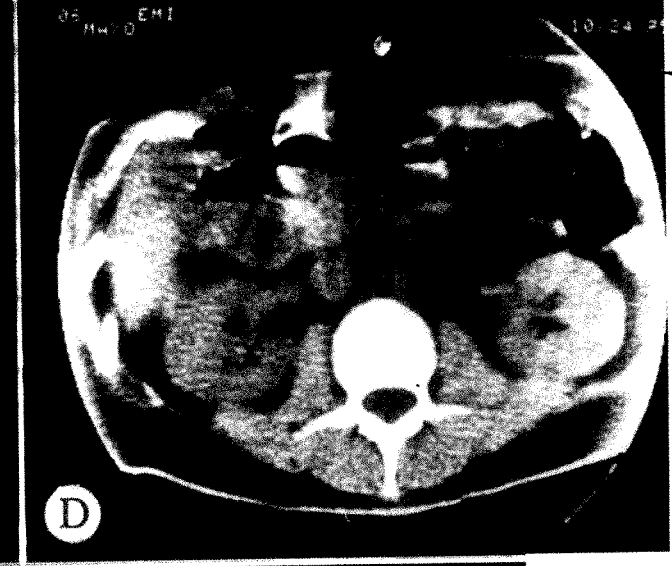
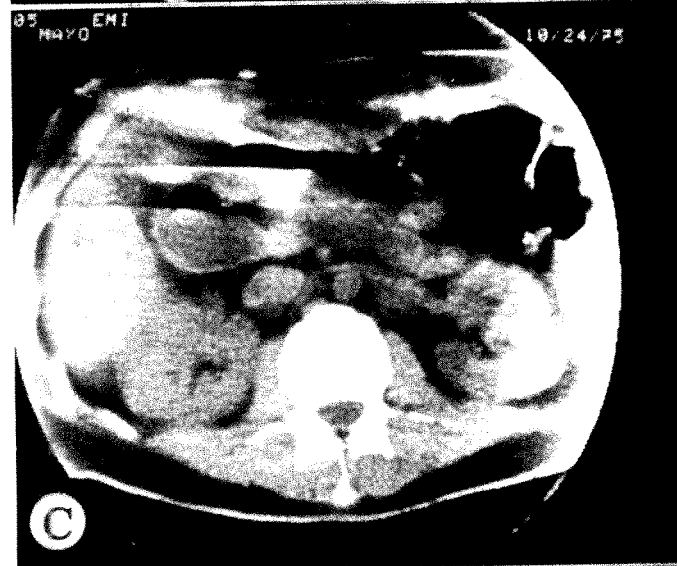
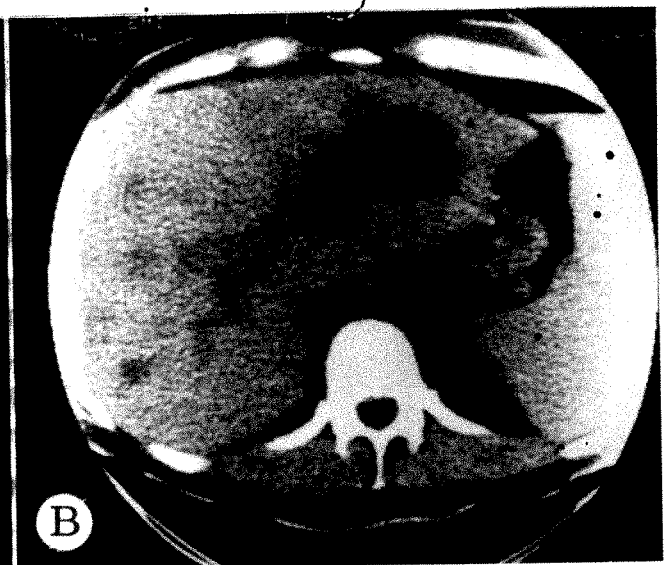
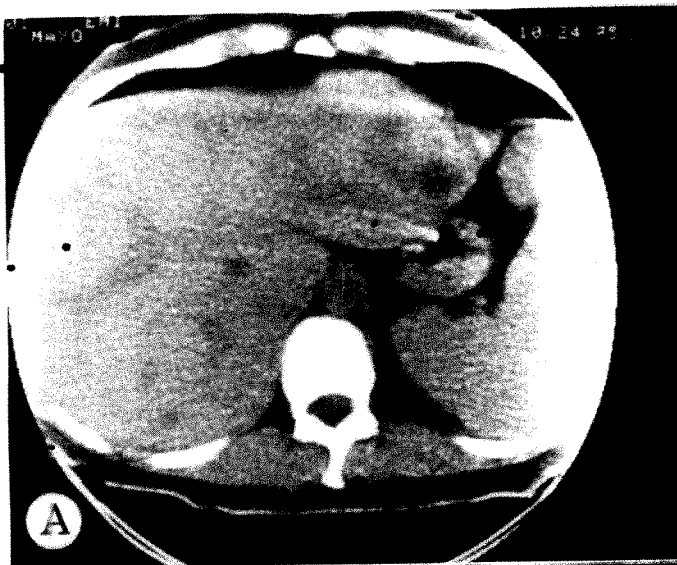


Fig. 9.—21-year-old man with recurrent fever, large area of low uptake on technetium liver scan, and increased uptake on gallium scan. **A and B**, CT scans showing large low density lesion with indistinct margins in right lobe of liver. Hepatic abscess drained at operation.

Fig. 10.—30-year-old man with history of choledochocystojejunostomy for large choledochal cyst. Large area of diminished activity in left lobe on technetium scan associated with questionable increased activity on gallium scan. **A**, CT scan showing multiple, sharply circumscribed low density areas in both right and left lobes, with suggestion of branching quality to two of defects in right lobe. **B**, Large sharply circumscribed area of low density in left lobe appearing to communicate with dilated ducts in region of porta hepatis. **C and D**, Medial to right lobe of liver and anterior to upper pole of right kidney and inferior vena cava is sharply circumscribed round lesion containing air-fluid level. Cystic dilatation of intrahepatic bile ducts with one large ductal cyst in left lobe discovered at operation. Choledochal cyst still present, and choledochocystojejunostomy functioned normally; considered variant of Caroli's disease. **E**, Postoperative cholangiogram at time of hepatic arteriography. Contrast material injected through tube placed in left lobe of liver demonstrated large left hepatic ductal cyst and choledochal cyst.



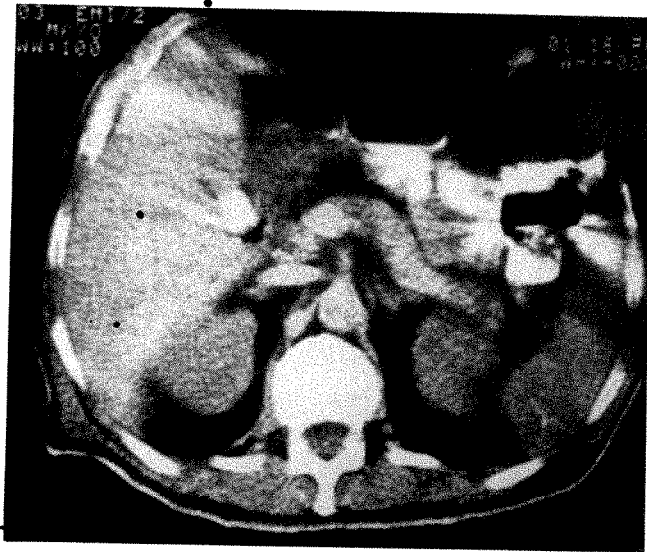


Fig. 11.—CT scan of 61-year-old man with suspected carcinoma of tail of pancreas. Horizontally oriented pancreas is seen in its entirety and is of normal size and configuration.

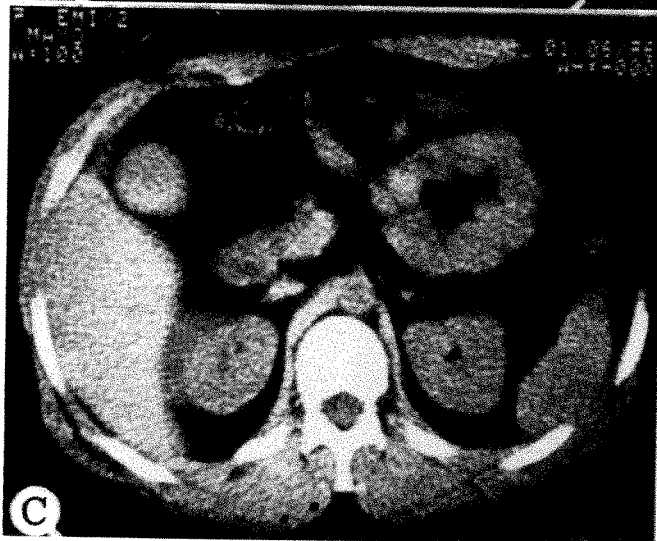
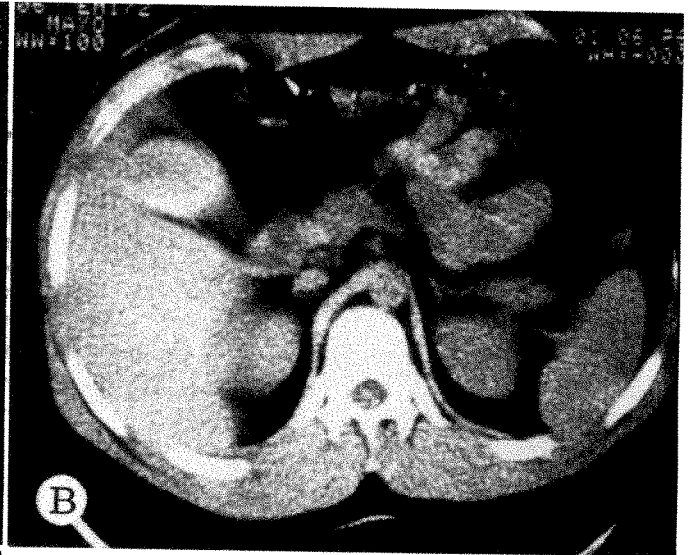
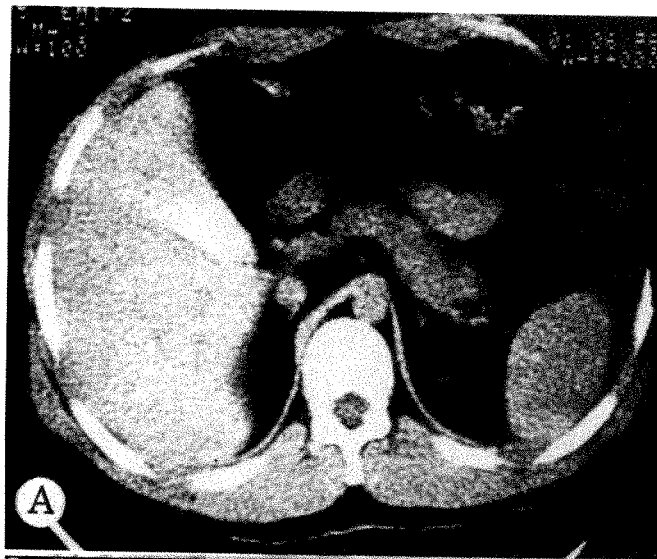


Fig. 12.—CT scans of 19-year-old man with history suggestive of pancreatitis. *A*, Highest tomographic cut includes tail and superior portion of body of pancreas. *B*, Middle cut includes body and superior portion of head of pancreas. *C*, Lowest cut is through head and uncinate process of pancreas. Second portion of duodenum located just lateral to head of pancreas and anterior to inferior vena cava.

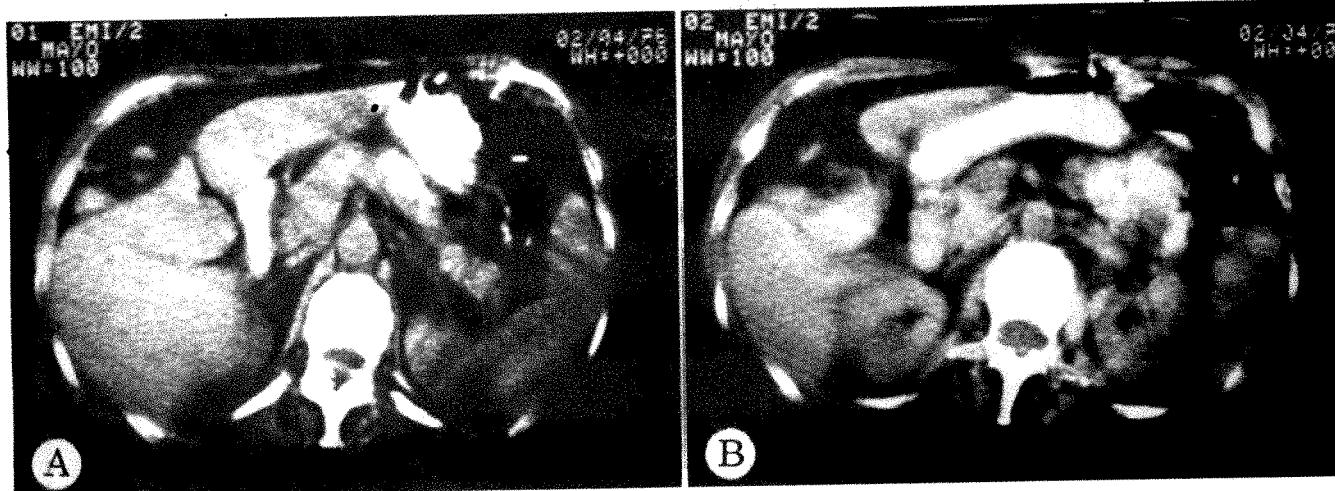


Fig. 13.—CT scans after ingestion of dilute water-soluble contrast material in 55-year-old woman with bilateral thrombophlebitis examined for possible malignancy. *A*, Contrast material in midportion of stomach and second portion of duodenum clearly separates duodenum from head of pancreas. *B*, Contrast material in body and antrum of stomach clearly separates posterior portion of stomach from anterior portion of normal head of pancreas.

Fig. 14.—CT scan of 45-year-old man with large carcinoma of pancreas found during recent operation; scan performed to define limits of tumor before institution of radiation therapy. Presence of massive ascites obscured margins of intraabdominal organs; pancreatic mass not identifiable



the pancreas (fig. 13). The difficulty in identifying the complete margin of the pancreas is especially evident in the examination of very thin or debilitated patients, because the fat planes are thin and organs of similar density are not clearly separated by fat. Also, ascites obscures the margin of intraabdominal organs, and this is particularly so in the case of the pancreas (fig. 14). Apparently, there is an advantage in examining the slightly obese patient because the abdominal fat planes are generous and clearly separate adjacent intraabdominal organs of similar density.

Unfortunately, carcinoma of the pancreas does not differ significantly in density from the normal pancreas. Thus detection depends on recognition of an alteration in the size or morphologic contour of the gland (fig. 15) and on secondary signs such as a pseudocyst lying proximal to an

obstructing carcinoma (fig. 16.)

Some carcinomas were well circumscribed and seen as discrete, well defined masses, whereas others were more diffuse with no clear-cut margins. In the latter circumstance, the addition of dilute contrast medium orally helped differentiate the stomach and duodenum, which frequently adhere to the pancreatic neoplasm and actually constitute a portion of the mass lesion (fig. 17).

Whether small intrapancreatic lesions or diffuse pancreatic lesions can be detected is not clear. The chances of finding such lesions seem remote because the lesions do not differ sufficiently in density from normal pancreas. However, the presence of a small lesion in certain locations can be inferred from secondary signs such as pancreatic and biliary ductal dilatation or distended gallbladder (fig. 18).

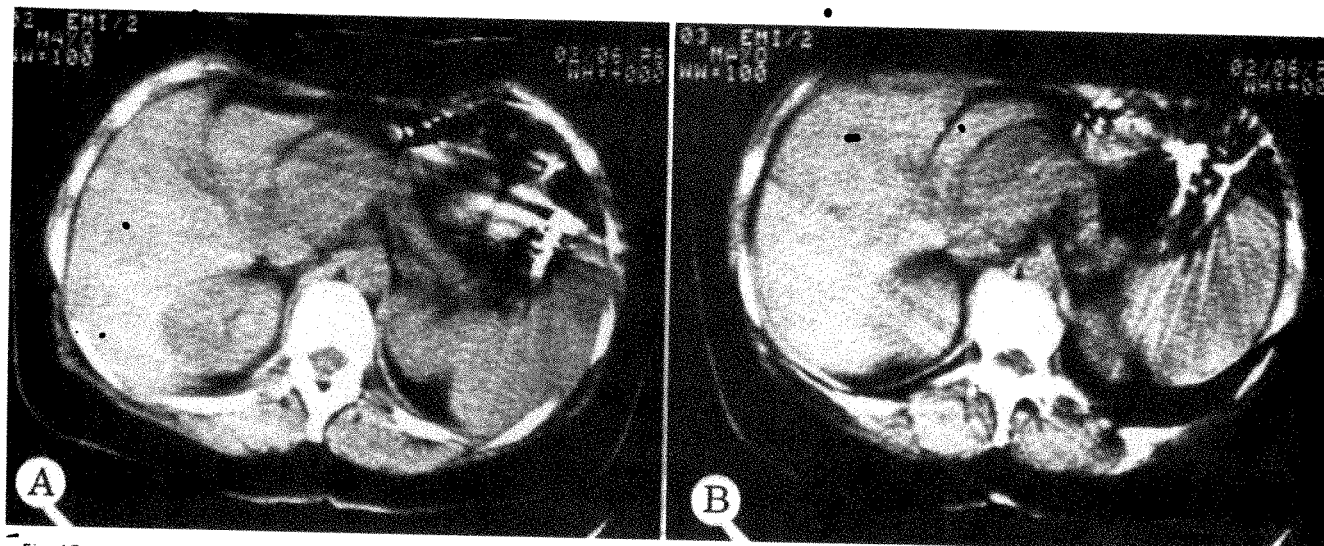


Fig. 15.—CT scans of 49-year-old woman with 5 month history of abdominal pain and weight loss. A, Large mass in head of pancreas; tail normal size. B, In addition to pancreatic mass, several low density metastatic lesions present in anterior portion of right lobe of liver. Large carcinoma of head and body of pancreas confirmed at surgery, and multiple hepatic metastatic lesions 1 and 2 cm in diameter found. (Mass also clearly outlined at time of gray-scale ultrasound examination.)

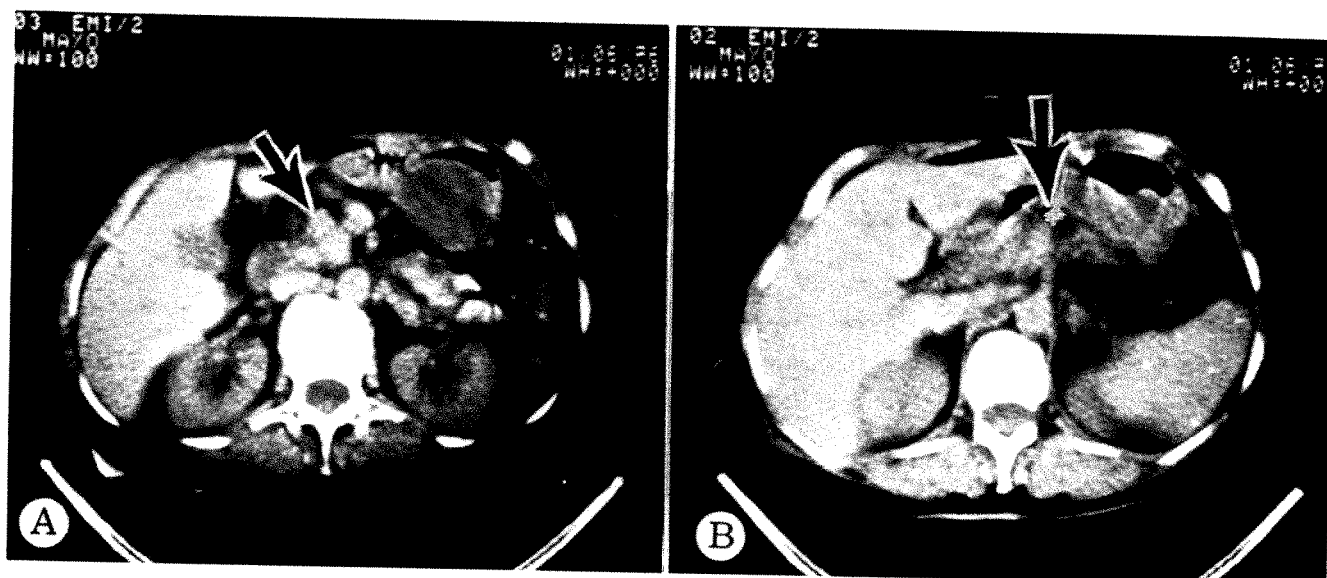


Fig. 16.—CT scans of 69-year-old woman with weight loss and abdominal pain. B-scan ultrasound showed possible lesion in head of pancreas. A, Irregular lobulated mass (arrow) posterior to stomach and medial to second portion of duodenum. B, Stomach displaced anteriorly by large ill-defined mass in body of pancreas containing lucent area suggesting pseudocyst (arrow). At operation, lobulated carcinoma in head of pancreas found associated with pseudocyst in midportion of body of pancreas.

Experience with pancreatitis is limited, and the CT results are not definite. Pseudocysts are identifiable. Occasionally the pancreas is diffusely enlarged, but this is a subjective impression because the size of a pancreas varies considerably among patients. Also, inflammatory reaction tends to obscure the margin of the pancreas, making the evaluation of size difficult.

Even though CT scanning represents a significant advance in the ability to detect pancreatic disease, some limitations still remain, particularly in evaluating small subclinical lesions. The possibility of selectively altering the density of the pancreas or a tumor in the pancreas to make it more de-

tectable with this method is attractive.

Retroperitoneum. The retroperitoneal space is an area that is difficult to evaluate with routine radiographic techniques. Abnormal lymph nodes can be demonstrated with lymphangiography, but often large lesions are undetectable by any means. CT scans appear to be one of the best examinations to detect retroperitoneal disease and to determine its extent. Retroperitoneal lymphoma has presented as a discrete mass of slightly decreased density in comparison with other organs (fig. 19), and has been seen as a diffuse infiltrating mass that obliterates tissue planes and obscures contiguous organs (fig. 20). Lymphoma can be differenti-

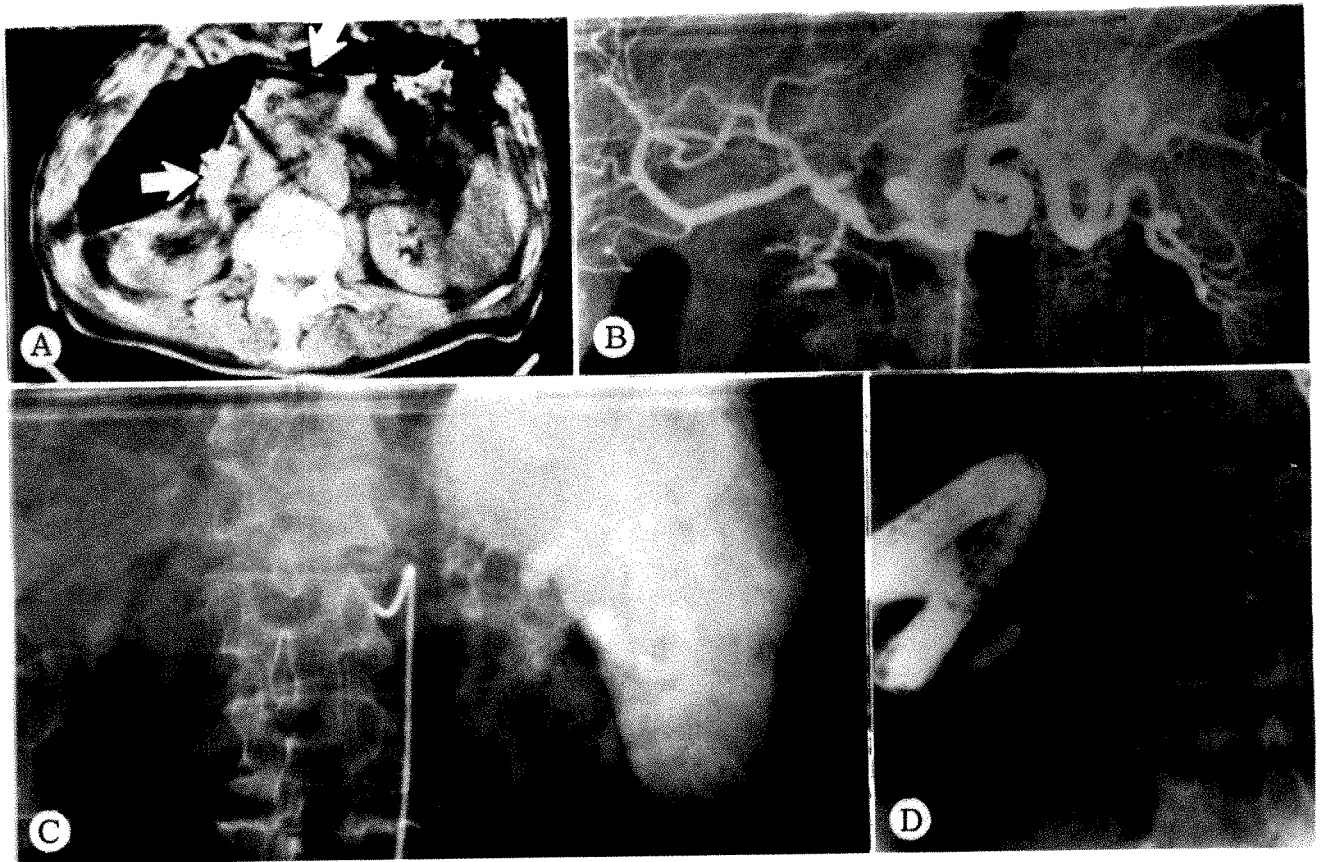


Fig. 17.—75-year-old man with weight loss and epigastric pain had evidence of esophageal varices and hypersplenism. A, CT scan showing large, diffuse, ill-defined mass obscuring tissue planes located in region of head of pancreas, medial to second portion of duodenum (*arrow*) and posterior to antrum of stomach (*arrow*). B, Celiac angiogram, arterial phase, showing evidence of carcinoma of pancreas involving origin of celiac axis, proximal portion of hepatic artery, and gastroduodenal artery. C, Celiac angiogram, venous phase, showing obstructed splenic vein. Epiploic veins are enlarged, serving as collateral channels of venous drainage, and spleen is enlarged. D, Endoscopic retrograde cholangiopancreatogram. Main pancreatic duct obstructed. Unresectable carcinoma of pancreas found at operation.

ated from other mass lesions because of its diffuseness and because it arises in the retroperitoneum rather than from a specific organ. In several cases, lymphoma was discovered when scanning the pancreas or the kidney, especially in patients presenting with ureteral obstruction (fig. 21).

Metastatic lymphadenopathy, often from primary lesions in the genitalia, is clearly outlined (fig. 22). This condition, too, has frequently been discovered during the scanning of patients who had partial ureteral obstruction detected by excretory urography (fig. 23).

Equally important, though less spectacular, is the identification of an entirely normal retroperitoneal space (fig. 24). All clinicians are familiar with the problem of the patient who has unremitting back pain and negative workup and in whom a retroperitoneal lesion is suspected. The exoneration of the retroperitoneal space as the site of a lesion is a significant step in diagnostic ability.

Kidney and Genitourinary Tract. The kidneys are particularly well demonstrated on abdominal CT scans because they are surrounded by perinephric fat which demarcates the outer margin of the renal cortex, and they contain renal

sinus fat which outlines the inner margin of the renal parenchyma. Renal masses are detectable because they alter the contour of the kidney, project beyond the renal margin, or differ in density from normal parenchyma. Renal cell carcinomas are usually less dense and of less uniform density than normal parenchyma. However, the presence of calcification, necrosis, and hemorrhage within some tumors can substantially increase the range of densities found in such a tumor. The density of vascular tumors usually increases after the intravenous injection of contrast material (fig. 25). Carcinomas are particularly obvious when they distort the renal contour or manifest secondary signs, such as local invasion into the perinephric space. In one case, a notable secondary finding was that of considerable enlargement of the inferior vena cava because of the huge arteriovenous shunt within the tumor (fig. 26).

Benign simple renal cysts tend to be more round and circumscribed than tumors. Also, the density of a cyst is more uniform than that of a tumor and does not change after intravenous injection of contrast material (fig. 27).

The density of any mass, cyst or tumor, depends on whether all or a part is included in the volume of a given

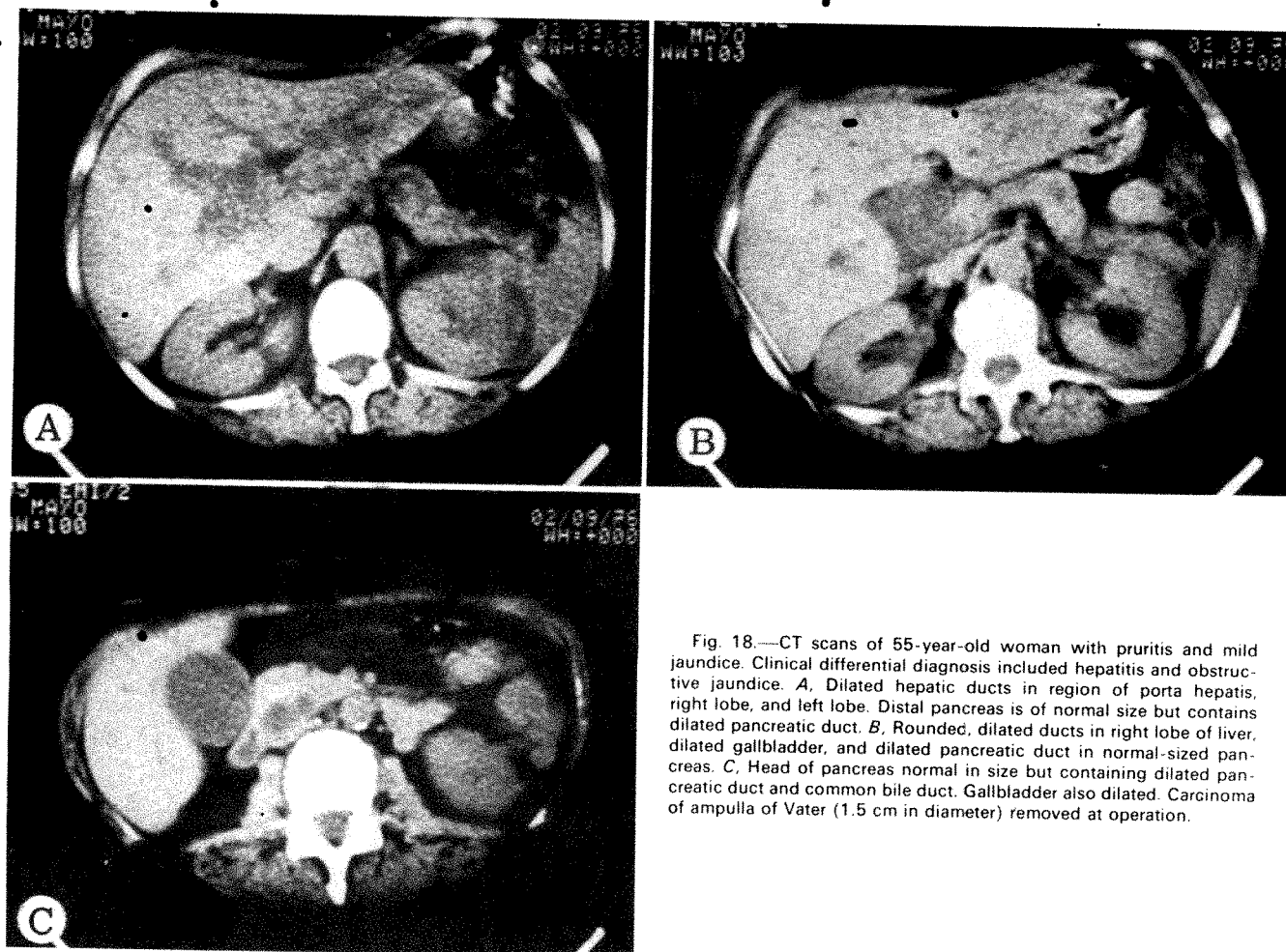
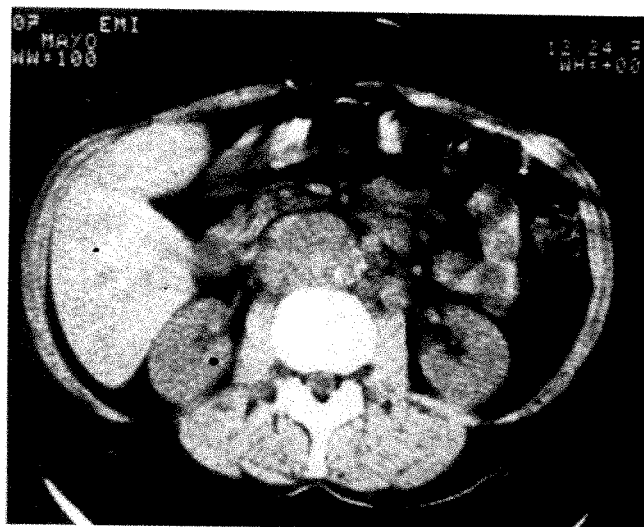


Fig. 18.—CT scans of 55-year-old woman with pruritis and mild jaundice. Clinical differential diagnosis included hepatitis and obstructive jaundice. *A*, Dilated hepatic ducts in region of porta hepatis, right lobe, and left lobe. Distal pancreas is of normal size but contains dilated pancreatic duct. *B*, Rounded, dilated ducts in right lobe of liver, dilated gallbladder, and dilated pancreatic duct in normal-sized pancreas. *C*, Head of pancreas normal in size but containing dilated pancreatic duct and common bile duct. Gallbladder also dilated. Carcinoma of ampulla of Vater (1.5 cm in diameter) removed at operation.

Fig. 19.—CT scan of 54-year-old woman with 6 month history of leg and back pain and no objective findings except for elevated erythrocyte sedimentation rate. Patient allergic to iodized contrast material. Large circumscribed mass in right side of abdomen adjacent to aorta and anterior to upper pole of right kidney. Slightly diminished density in central portion of mass. At operation, diffuse, poorly differentiated lymphoma present behind and below head and body of pancreas.



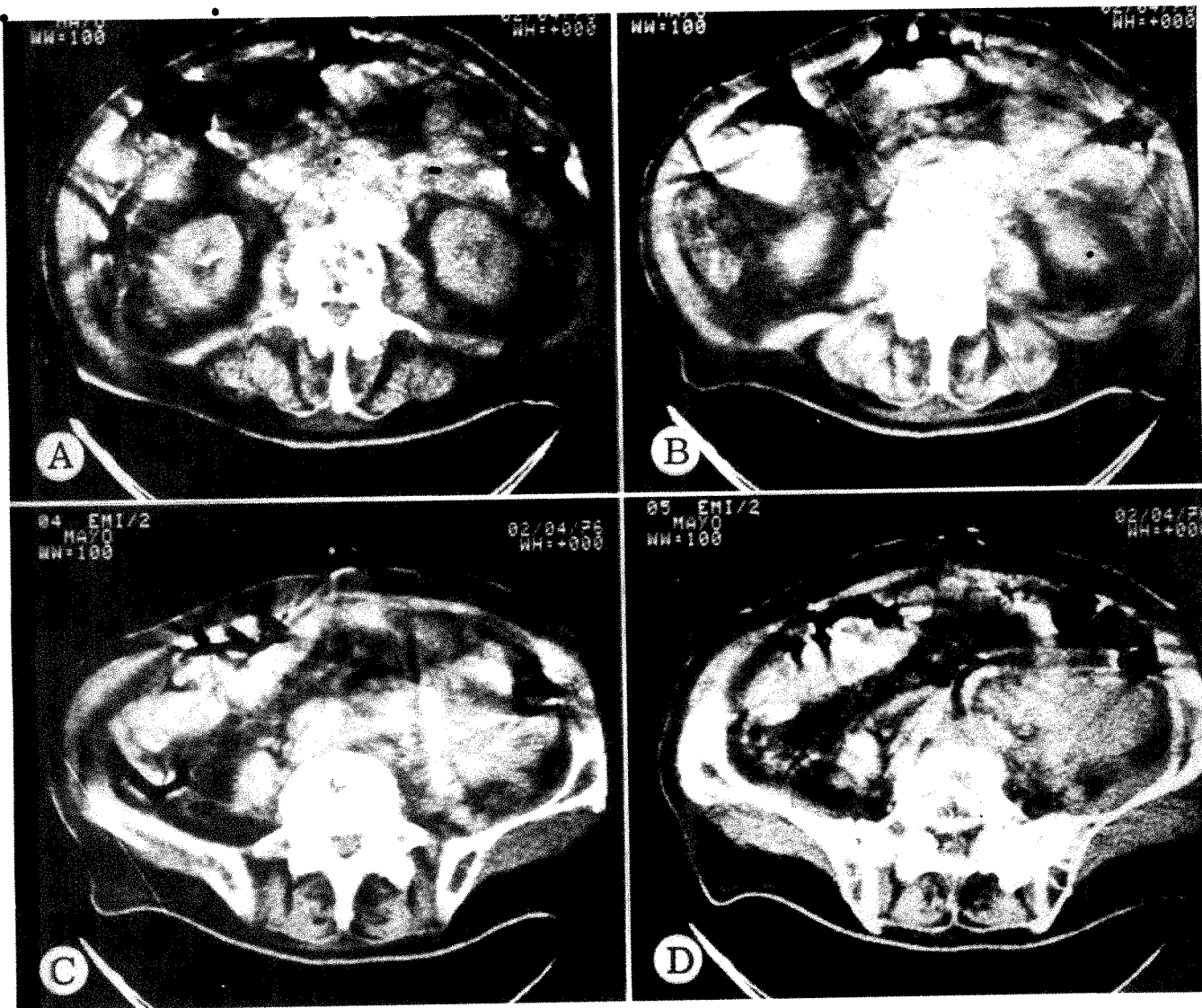


Fig. 20.—CT scans of 91-year-old man with severe, unrelenting back pain and tenderness over L4 vertebral body. Clinical suspicion was epidural abscess. Poorly circumscribed infiltrating mass seen adjacent to lower abdominal aorta (A and B) appearing to infiltrate or be adherent to several loops of bowel (C and D). At operation, malignant lymphoma extended from left kidney down over aorta and adjacent to left iliac artery. Portions of mass infiltrated mesocolon.

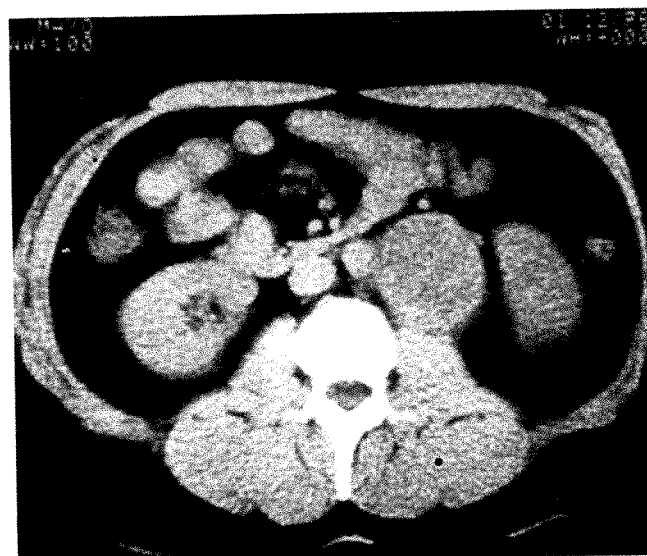


Fig. 21.—CT scan of 63-year-old man with abdominal pain suggestive of carcinoma of pancreas. Retrograde pancreaticogram and angiogram were negative. Excretory urogram revealed pyelocaliectasis on right. Hydronephrosis of right kidney was associated with small mass of slightly diminished density between kidneys and aorta. Retroperitoneal lymphoma causing obstruction of midright ureter found at operation.

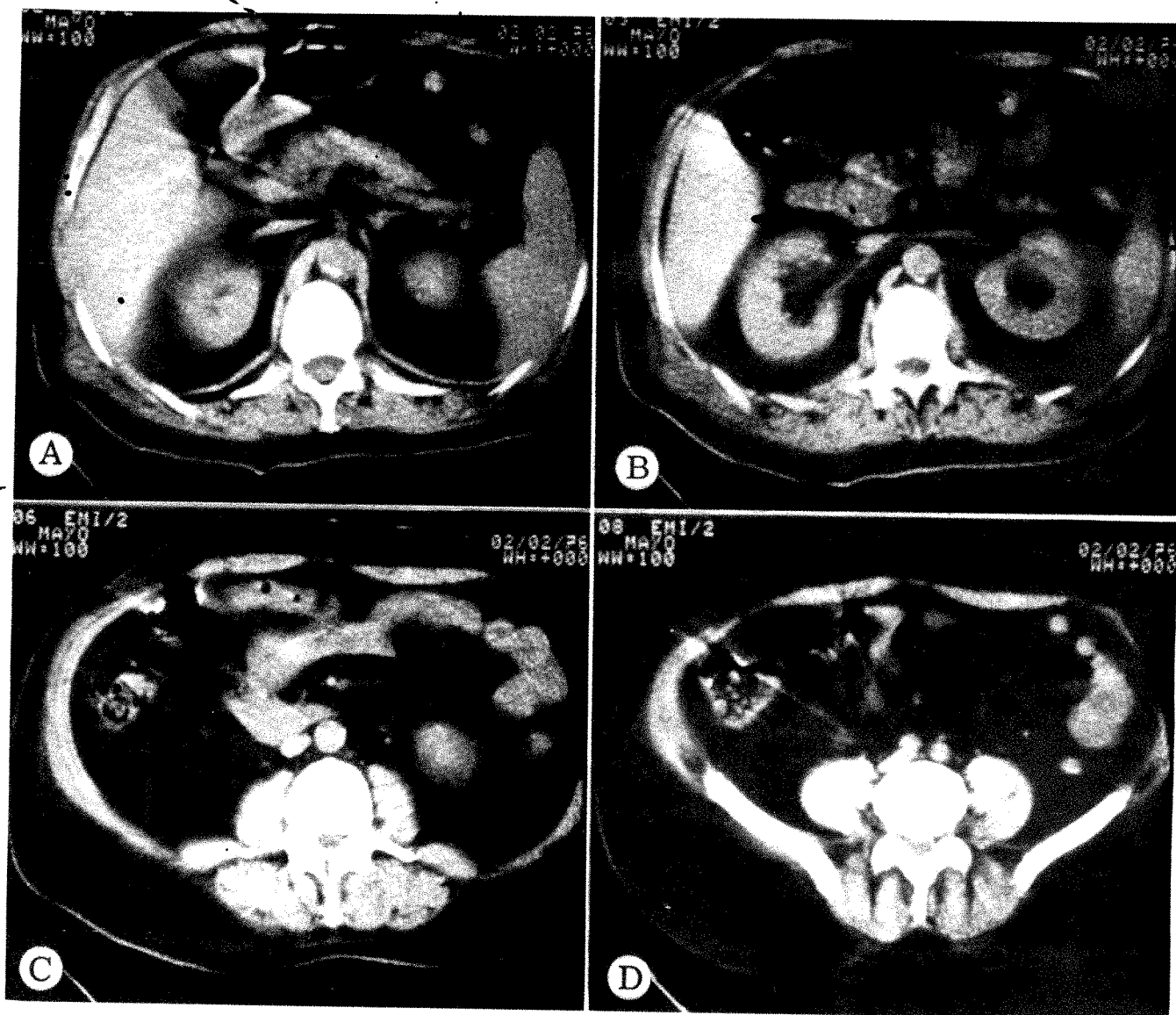


Fig. 22.—CT scan of 32-year-old man with slight lateral displacement of left kidney and ureter on excretory urogram. Tomographic slice through portion of sharply circumscribed mass lesion in left retroperitoneal space showed slight low density within mass suggesting necrosis. Operation revealed mass of metastatic teratocarcinoma from testicle.

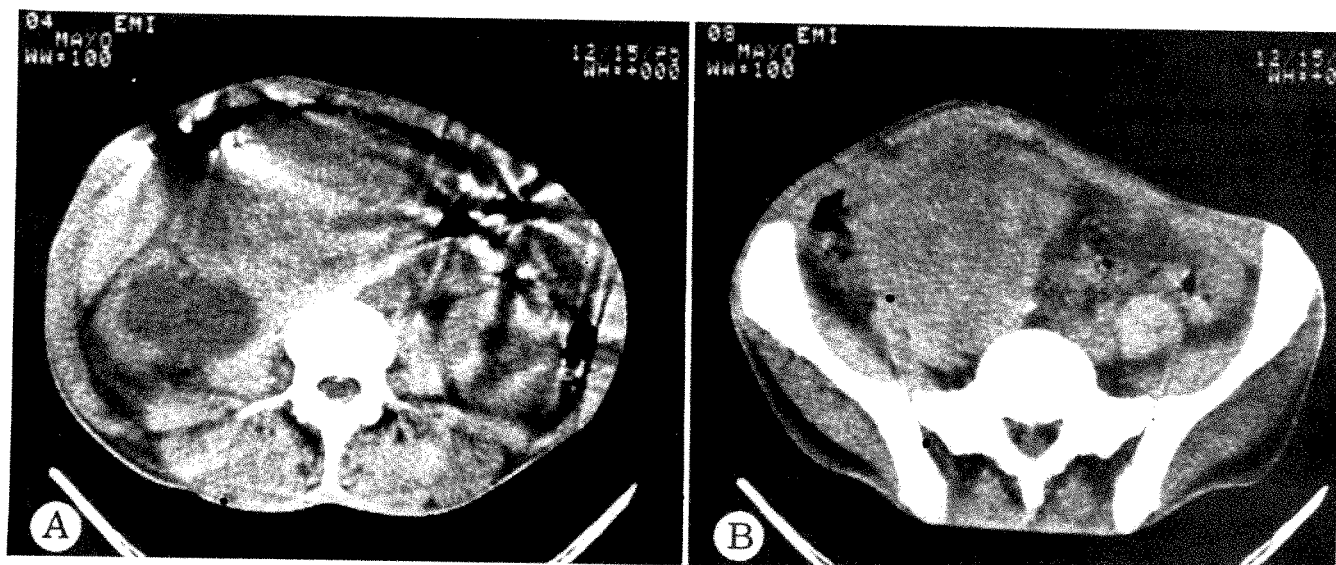


Fig. 23.—CT scans of 39-year-old man presenting with palpable mass in right lower abdomen after recent orchiectomy for seminoma. Right kidney non-functioning at the time of excretory urography. A, Hydronephrosis of right kidney associated with large mass occupying two-thirds of abdomen anterior to right kidney. B, Scan through pelvis showing portion of lower extent of gigantic abdominal mass obstructing right ureter and bulging anterior abdominal wall. Metastatic seminoma confirmed by biopsy.

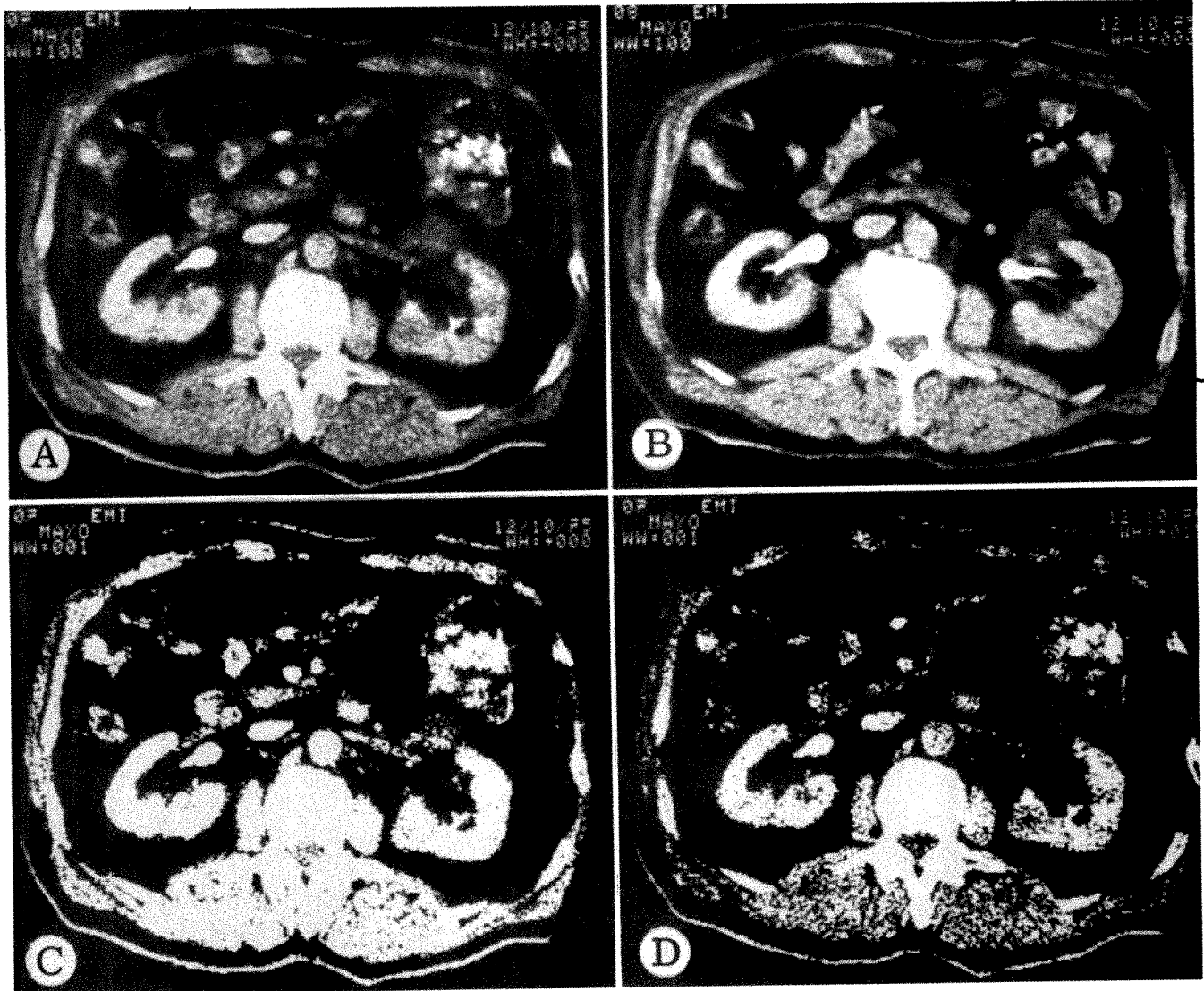


Fig. 24.—CT scans of 59-year-old man with nephrotic syndrome and blood smear findings consistent with retroperitoneal lymphoma. A–D. Selected tomographic cuts through retroperitoneal space from level of pancreas to midpelvis. Abundant fat planes clearly demonstrate normality of patient's retroperitoneal space.

picture element [12]. At present, small lesions cannot be confidently differentiated because differences in density among cyst, tumor, and normal parenchyma may be slight and difficult to display. The current prototype display unit does not lend itself to a convenient and accurate determination of the absolute density that seems necessary to make the critical distinction between cyst and tumor on the basis of density alone.

CT is useful in evaluation of obstructive uropathy, and often the cause can be precisely shown (fig. 28). Although experience in children is limited, the evaluation of flank masses in such patients holds great promise (fig. 29).

The bladder and prostate have had limited study. Both can be imaged, and information unobtainable by other radiographic methods can be gained (fig. 30). However, whether small bladder tumors can be detected or whether a distinction can be made between benign prostatic hypertrophy and carcinoma of the prostate gland is not known.

Adrenal Gland. A normal adrenal gland occasionally can be seen, especially on the left (fig. 31). Both primary and secondary adrenal tumors have been seen and correctly diagnosed with CT. The adrenal lesions have been fairly circumscribed masses, distinct from the kidney and other retroperitoneal organs. One rather large mass in the right adrenal gland, which had been overlooked on an angiogram and on abdominal exploration 14 months before the CT scan, was seen as a large posterior hepatic filling defect on a radionuclide scan (fig. 32). However, on the CT scan the difference in density between the adrenal gland mass and the liver was obvious, and a definite cleft was seen between the mass and the posterior aspect of the liver.

Chest

The chest was examined in 43 patients. The scans were usually done on patients who had obvious lesions on chest

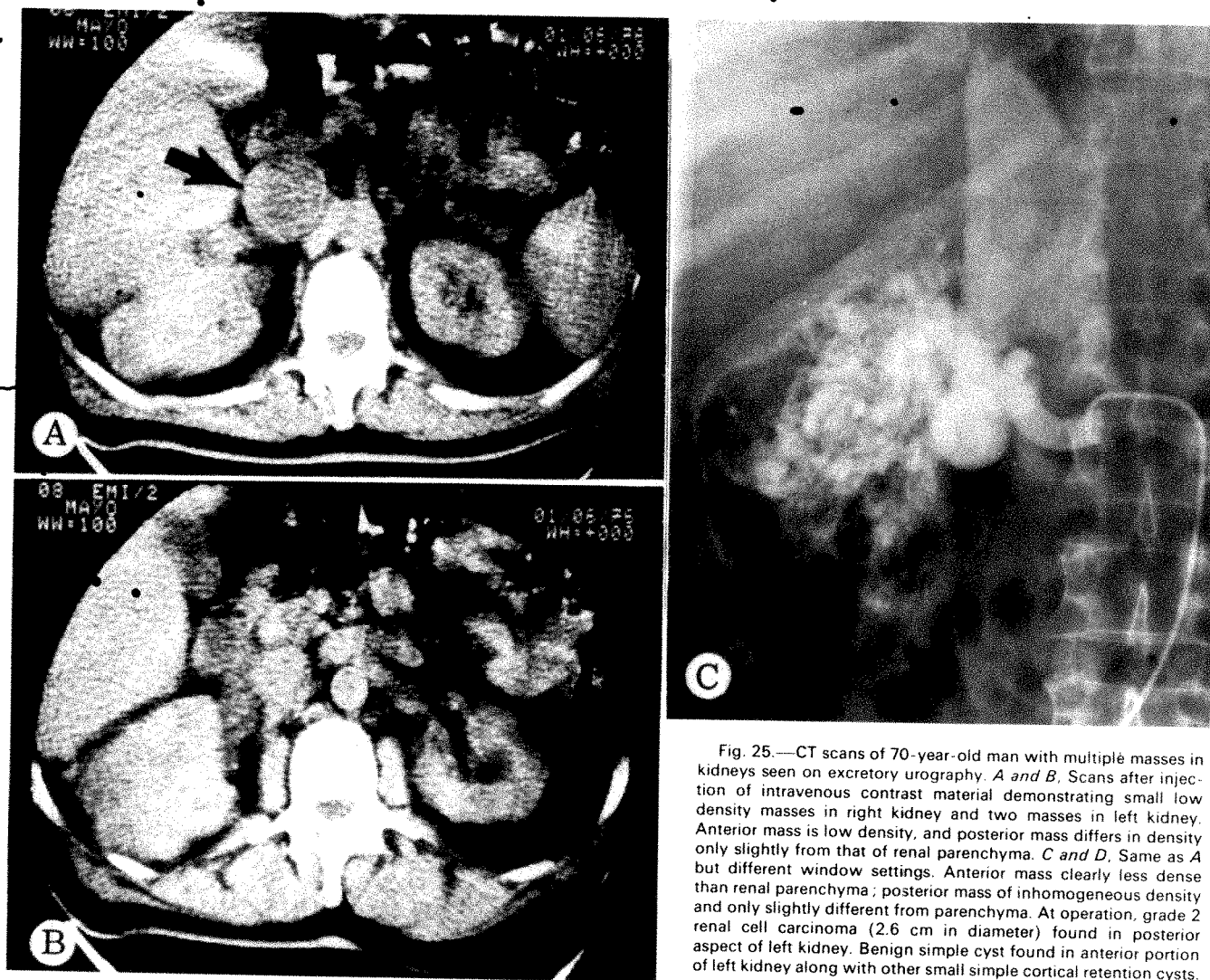


Fig. 25.—CT scans of 70-year-old man with multiple masses in kidneys seen on excretory urography. *A and B*, Scans after injection of intravenous contrast material demonstrating small low density masses in right kidney and two masses in left kidney. Anterior mass is low density, and posterior mass differs in density only slightly from that of renal parenchyma. *C and D*, Same as *A* but different window settings. Anterior mass clearly less dense than renal parenchyma; posterior mass of inhomogeneous density and only slightly different from parenchyma. At operation, grade 2 renal cell carcinoma (2.6 cm in diameter) found in posterior aspect of left kidney. Benign simple cyst found in anterior portion of left kidney along with other small simple cortical retention cysts.

roentgenograms in an effort to evaluate the lesion from a different perspective and to determine the extent of the disease.

Examining a lesion from the cross-sectional perspective has obvious advantages but may not be a necessary part of the evaluation of a pulmonary mass. However, in several of these cases an area of higher density was surrounded by an infiltrate of lower density, with the smaller central lesion representing the neoplasm [5].

The evaluation of pleural disease is attractive because the extent of involvement of the pleura can be seen in a circumferential fashion (fig. 33). Also, lesions of the chest wall, which may be obvious on the chest roentgenogram, can have significant extension outside the chest wall which can be appreciated more fully on the CT scan (fig. 34). In several cases, chest scans were performed to evaluate nodules seen on a chest roentgenogram. Additional nodules, undetected on the chest film, were discovered in the lung parenchyma (fig. 35). This discovery suggests the possible use of CT in the preoperative evaluation of patients with suspected solitary metastasis before

the contemplation of lung resection. Additionally, one patient was seen who had sputum positive for large cell carcinoma in whom no lesion was identifiable on the chest roentgenogram. The CT scan revealed an obscure, small lesion that subsequently could be studied by means of routine tomography (fig. 36). More experience in the evaluation of patients who have positive sputum and negative chest films is necessary.

The mediastinum is difficult to assess because the density of masses in this region is not much different from that of the normal structures. The administration of intravenous contrast agents is helpful in distinguishing the aorta from mediastinal mass lesions. A mass that was not identifiable on a routine chest roentgenogram has yet to be discovered.

Head and Orbit

A total of 83 head scans were performed on the body scanner. The scanner proved to be versatile enough to be used for both head and body scanning. In addition, the higher resolution on the 320×320 matrix and the versatility of positioning that was possible (coronal sections) without

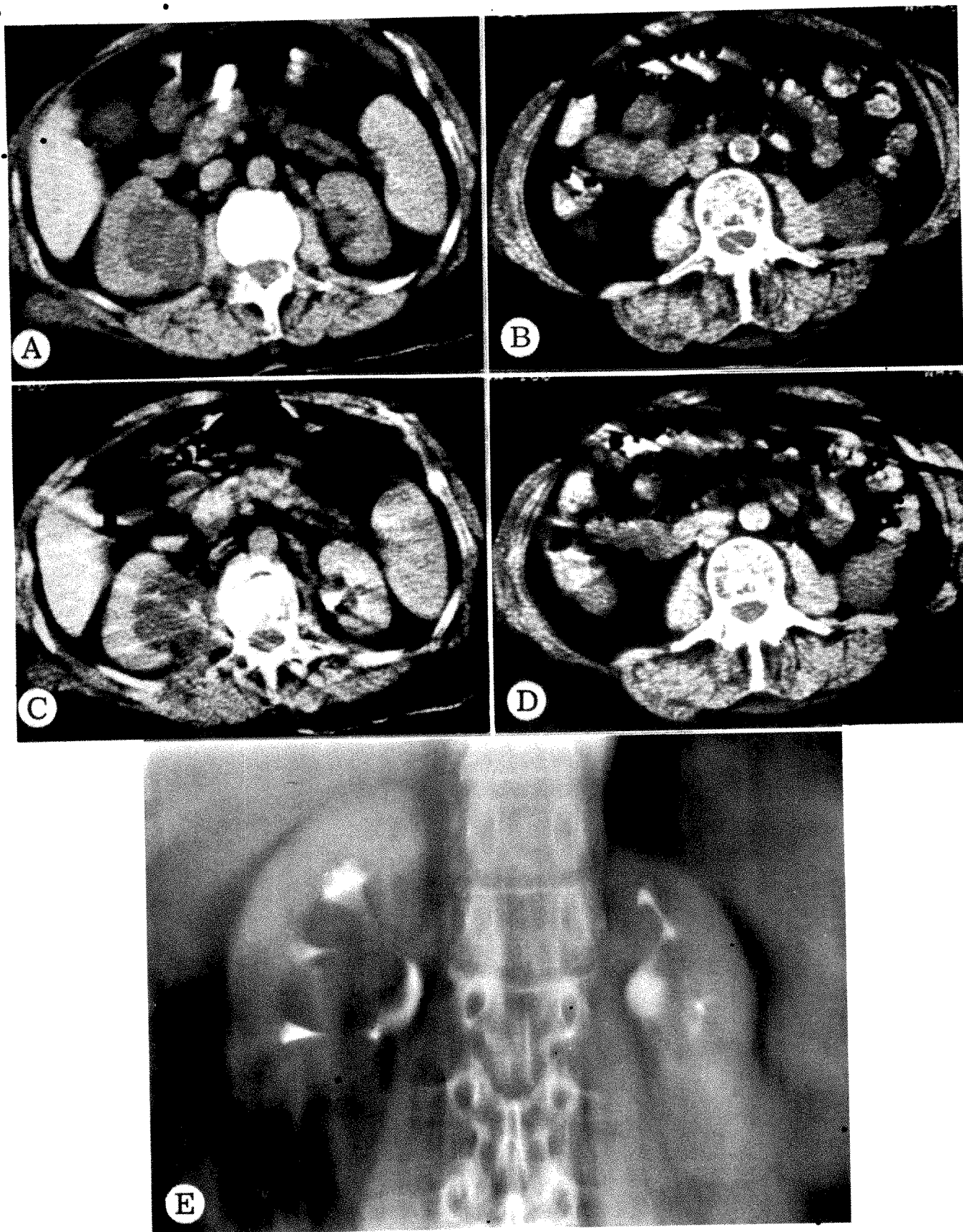


Fig. 26.—59-year-old man with known large right renal mass. *A*, CT scan showing portion of mass in upper right kidney. Rounded mass anterior to upper pole of right kidney is enlarged inferior vena cava (*arrow*). *B*, Lower tomographic section showing large renal mass distorting configuration of kidney and containing some areas of low density peripherally. *C*, Selective right renal arteriogram, arterial phase, showing huge vascular tumor in right kidney with tremendous arteriovenous shunt opacifying dilated inferior vena cava. Diagnosis was large, highly vascular renal cell carcinoma.

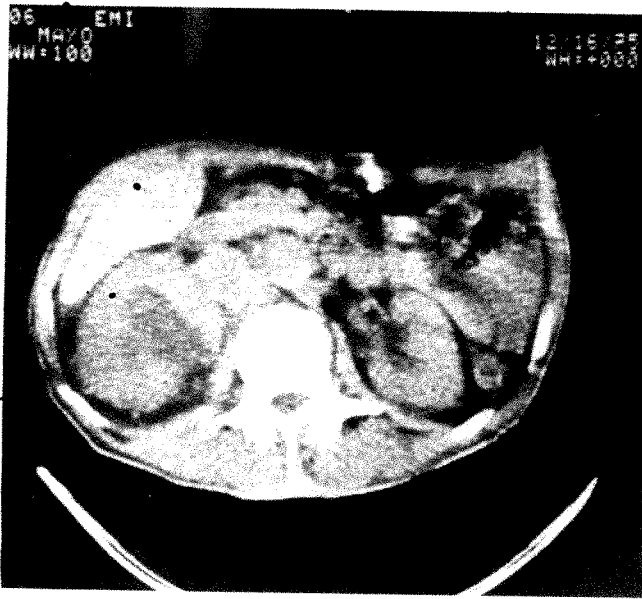


Fig. 27.—72-year-old woman with evidence of metastatic carcinoma to brain. Excretory urogram revealed 5 cm mass in lower pole of left kidney and large parapelvic mass on right. *A*, CT scan showing sharply circumscribed low density mass in central portion of right kidney. *B*, Section through low density mass in lower pole of left kidney. *C*, Injected contrast material in collecting system causes streaklike artifacts but no change in density of centrally located renal mass. *D*, No change in density of mass in lower pole of left kidney after injection of contrast material. *E*, Excretory urogram showing right parapelvic mass and left lower pole mass. Diagnosis was bilateral renal cysts.

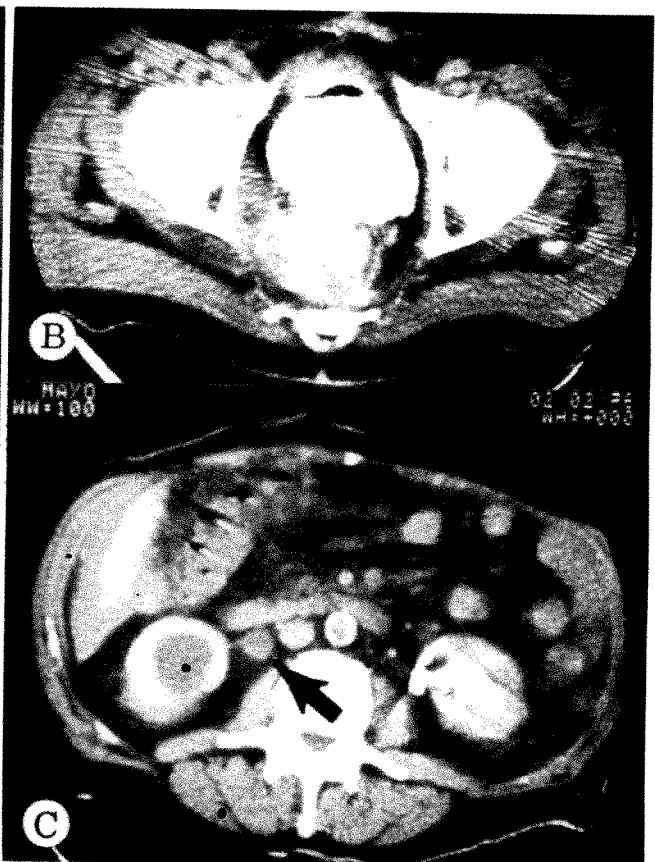
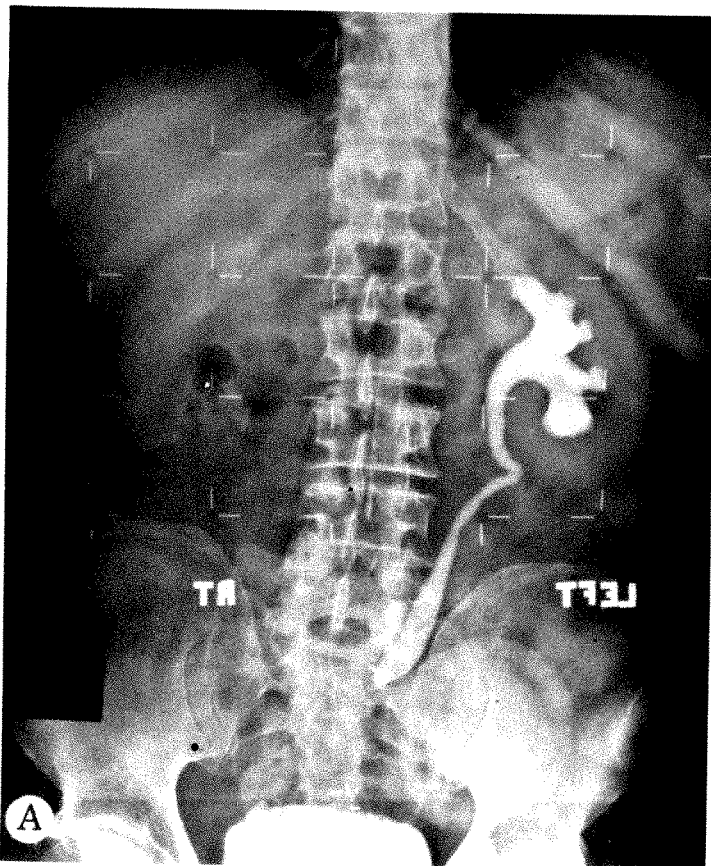


Fig. 28.—75-year-old man with previous resection of carcinoma of rectosigmoid. *A*, Excretory urogram (delayed film) showing nonfunctioning right kidney with faint nephrogram. Obstruction of left ureter at level of upper sacrum, with pyelocaliectasis and ureterectasis. (Note grid used for localization of levels of cuts.) *B*, Tomographic cut through level of pelvis showing large, dense mass due to recurrent metastatic carcinoma of colon posterior to bladder obstructing right ureter completely and left ureter partially. *C*, Tomographic section through lower pole of right kidney showing hydronephrosis and dilatation of right ureter located between inferior vena cava and lower pole of kidney (arrow). Note small amount of ascitic fluid lateral to tip of right lobe of liver.

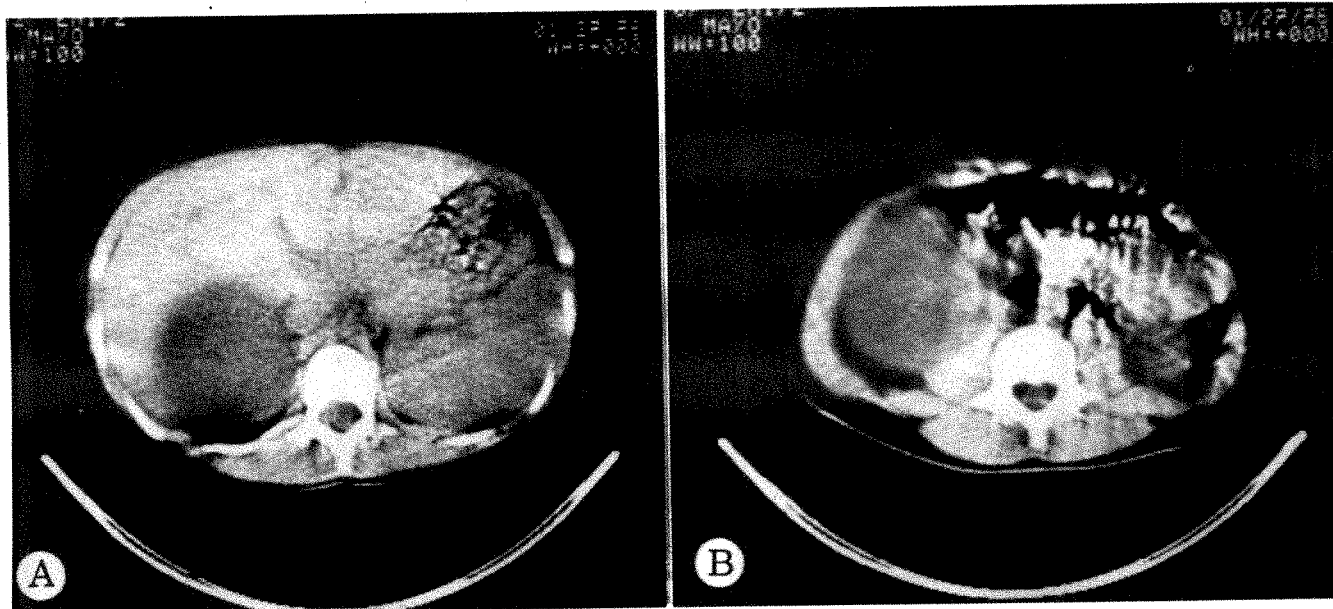


Fig. 29.—CT scans of 5-year-old boy with palpable right flank mass. A, Large, sharply circumscribed low density mass in area of right kidney posterior to liver. (Absence of substantial intraabdominal fat makes identification of intraabdominal organs difficult in children.) B, Scan through lower portion of large right flank mass showing homogeneity of density within mass. No renal tissue on right identifiable on scans. Hydronephrosis with complete destruction of right kidney secondary to congenital ureteropelvic junction obstruction found at operation.

the need for the water bag offered some distinct advantages.

The highest quality head scans are obtained using a slow scan (70 sec) rather than the fast scan used for other areas of the body. While the patient is exposed to greater amounts of radiation, the scan has less noise and seemingly greater resolution. Because of the increased radiation dosage, the slow scan is performed only on selected patients. The indications include suspected brain-stem lesions, pituitary tumors, and lesions in the cerebellopontine angle. This method has made it possible to detect lesions that could not be seen on the conventional head CT scan with water bag and the 160×160 matrix (figs. 37 and 38).

The greater resolution and the faster scan time produce orbital images of remarkable diagnostic clarity (figs. 39–41). Consequently, the body scanner is used to evaluate most patients who have suspected orbital tumors. The ability to position the patient's head so that coronal sections can be obtained is important in evaluation of pituitary tumors, particularly those with suprasellar extension (fig. 42). Also, because the patient's head can be placed deep in the scanner, the extent of nasopharyngeal tumors can be appreciated. This information assists in planning for radiation therapy (fig. 43).

Extremities

The bones, tissue planes, and muscle bundles in the extremities are clearly depicted on CT scans, and it is possible to assess the extent of the local invasion of soft tissue tumors as well as the extent of soft tissue invasion by bone tumors. Present experience is too limited to determine whether such information will have realistic diagnostic and therapeutic implications.

Miscellaneous Organs

Scans of other organs have been obtained, but the limited number does not permit meaningful appraisal. They are listed below.

Spinal Cord. A total of 17 patients have been specifically studied for possible spinal cord lesions, but there is serious doubt whether the cord is reliably imaged. The noise levels present in the bony spinal canal on the fast scan tend to obscure the discrete margins of the cord itself.

Aorta, Heart, and Vascular Structures. The aorta is clearly seen on practically all chest and abdomen scans, and the diagnosis of atheromatous calcification and aneurysm can be made. Occasionally an abdominal mass suspected of having its origin elsewhere is found to be an abdominal aortic aneurysm (fig. 44). However, the CT technique, basically a transversely oriented examination, seems to be limited in the study of longitudinally oriented structures such as the aorta, especially in comparison to ultrasound. The heart can be seen on chest scans and the configuration of the chambers estimated, but cardiac motion precludes obtaining an image with discrete margins. Blood vessels such as the celiac axis, the superior mesenteric artery and its branches, the renal vascular pedicles, the splenic artery and vein, and the great vessels in the mediastinum are often seen, but we have not specifically studied them nor have we depicted any specific lesion involving them.

Pelvis and Gynecologic Masses. While our experience is limited, we believe that there will be an increasing demand for CT scanning of the pelvis, especially in evaluating gynecologic malignancy.

Thyroid and Parathyroid Glands. Several thyroid glands

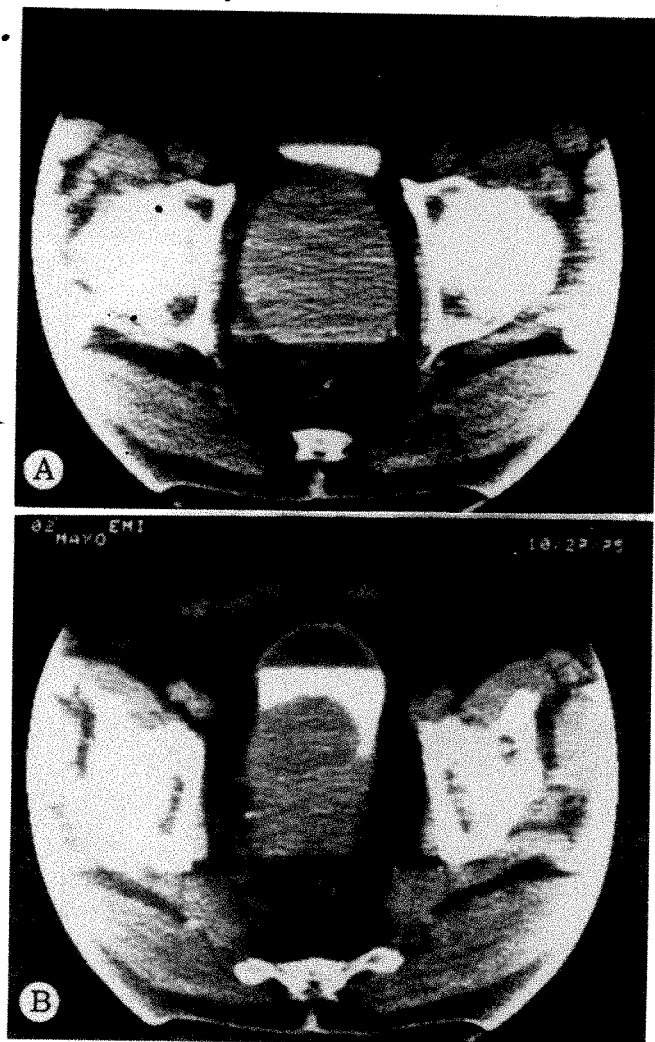


Fig. 30.—CT scans of 70-year-old man with symptoms of enlarged prostate. A, Scan through pelvis showing marked enlargement of prostate gland between rectum and bladder. B, Enlarged prostate gland indenting and deforming posterior aspect of bladder. Note fluid level representing interface between urine and contrast material in bladder. Bladder wall distinct from urine in bladder and from fat in lower pelvis.

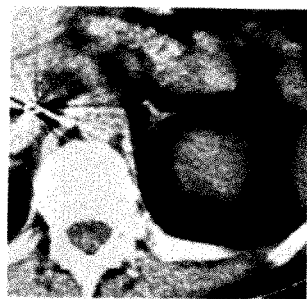


Fig. 31.—CT scan of 55-year-old man with suspected carcinoma of pancreas. Pancreas normal, but triangular normal left adrenal gland found anterior to upper pole of left kidney.

have been studied, and masses in the thyroid have been identified. However, at present, CT scanning offers no advantage over palpation, nuclide scan, and ultrasound. The possibility of detecting abnormalities in the parathyroid gland and localizing parathyroid tumors or hyperplasia is appealing. However, no evidence exists that the parathyroid gland differs significantly in density from the thyroid

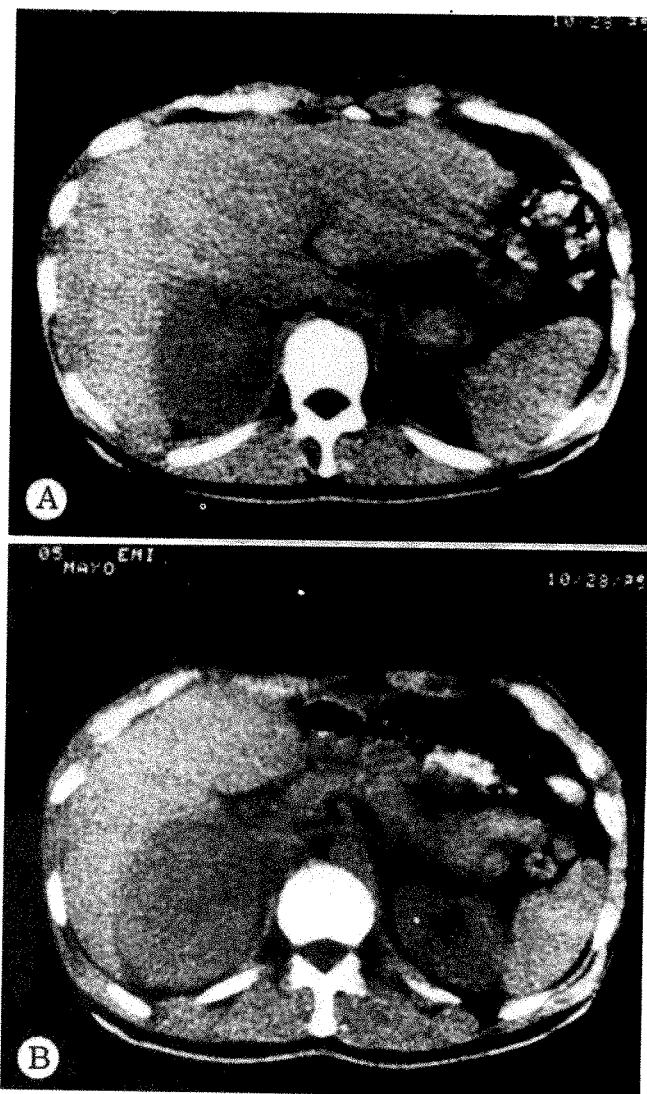


Fig. 32.—CT scans of 43-year-old man presenting with chronic relapsing febrile illness. Nuclear scan of liver showed large filling defect in posterior aspect, suggesting tumor or hepatic abscess. (Exploratory laparotomy and angiogram, performed 14 months before CT scans, were negative.) A and B, Two sections through lower portion of liver showing large, sharply circumscribed low density mass lesion posterior to right lobe. At operation, adrenal corticocarcinoma resected; regional lymphadenopathy present anterior to lower pole of large mass.

gland or from other soft tissue structures in the neck. Neither does it have any particularly distinguishing morphologic characteristics. The possibility of selectively altering the density of the parathyroid glands to make them more detectable on CT should be investigated.

Discussion

Experience in the first 400 cases using the CT body scanning unit is encumbered by the fact that in a given patient two separate types of investigations are being conducted simultaneously. The first and most important is the expeditious diagnostic evaluation of a sick person, and the second is the careful evaluation of a new and as yet unproved diagnostic technique. There is no doubt that in

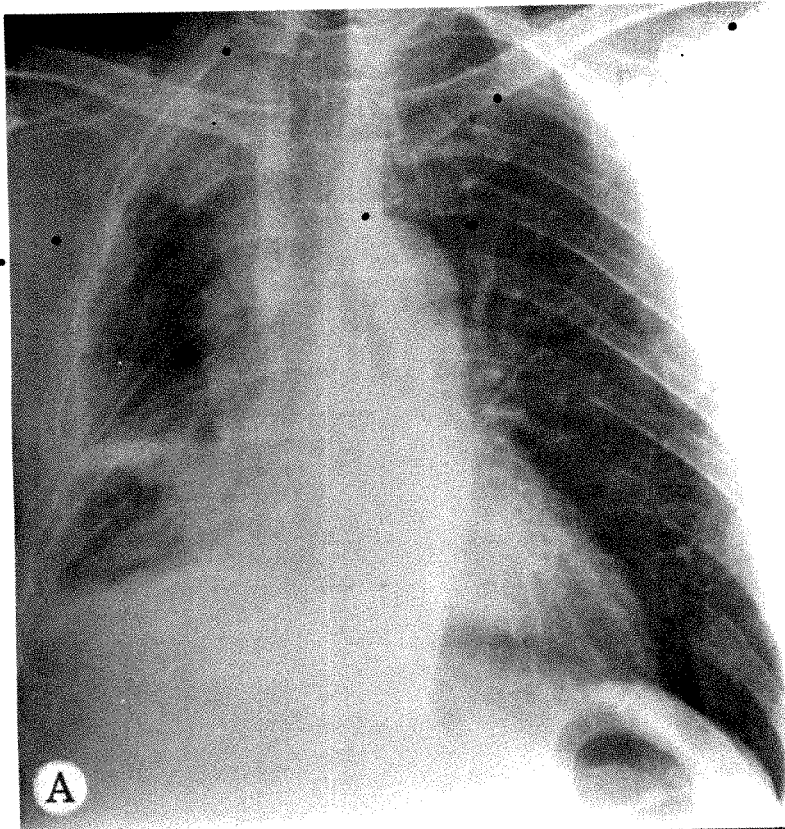
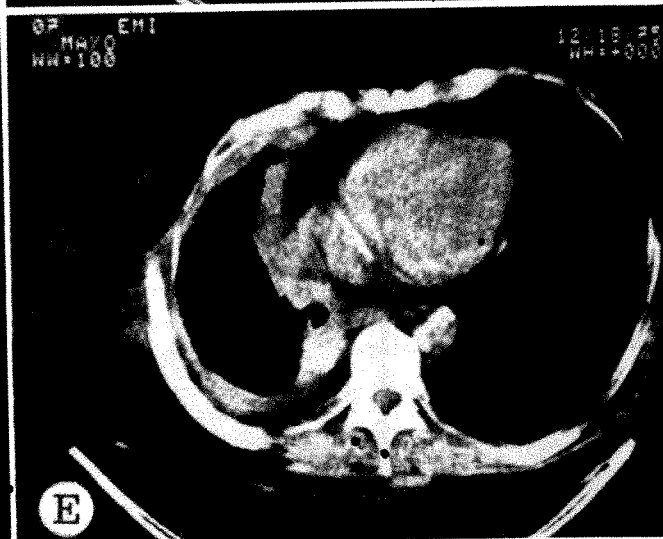
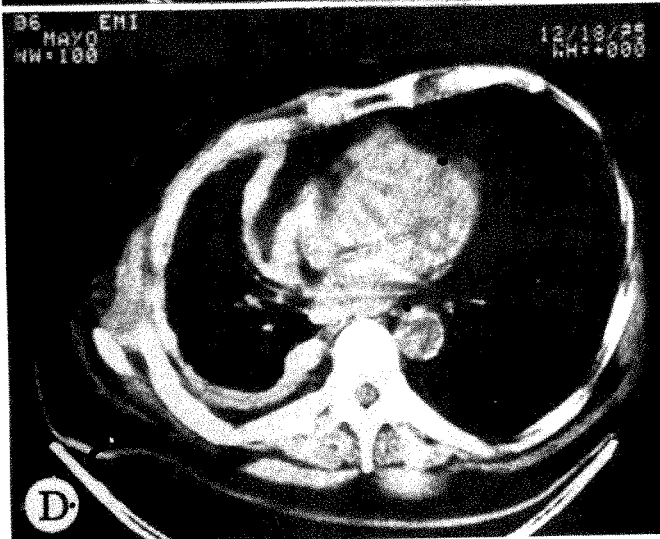
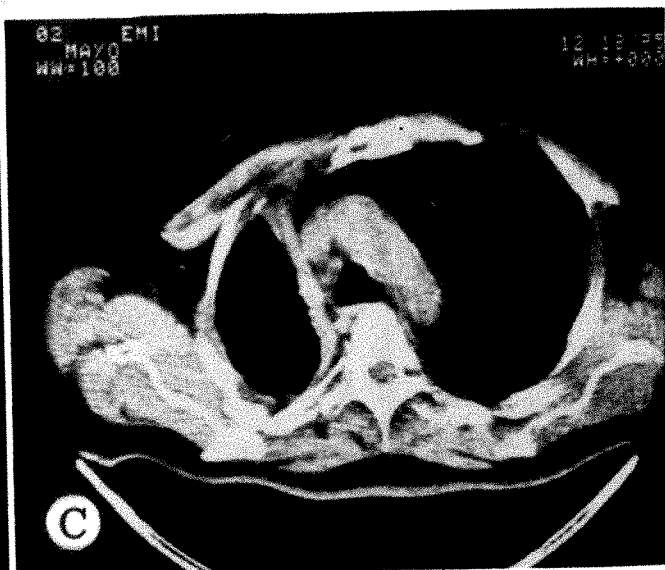
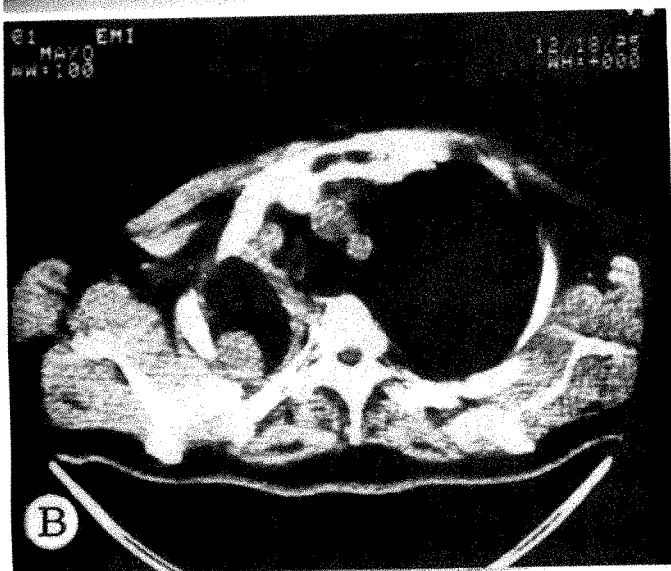


Fig. 33.—55-year-old man with decortication of right lung 3 years earlier because of recurrent pleural effusion. *A*, Chest film showing decreased volume of right lung with slight shift of mediastinum to right, mass in apex of right lung, and thickened pleura in periphery of hemithorax. *B*, Tomographic section through apex of right lung showing rind of pleural thickening associated with rounded mass posteriorly. (Innominate artery and left carotid artery seen in cross section anterior to vertebral body.) *C*, Scan at lower level showing large rind of thickened pleura completely encircling right lung. Note arch of aorta anterior to vertebral body. *D* and *E*, Cuts at lower level just below right hilum showing extensive thickened pleural rind to better advantage. Biopsy confirmed progressive entrapment of right lung due to pleural thickening associated with growth of mesothelioma.



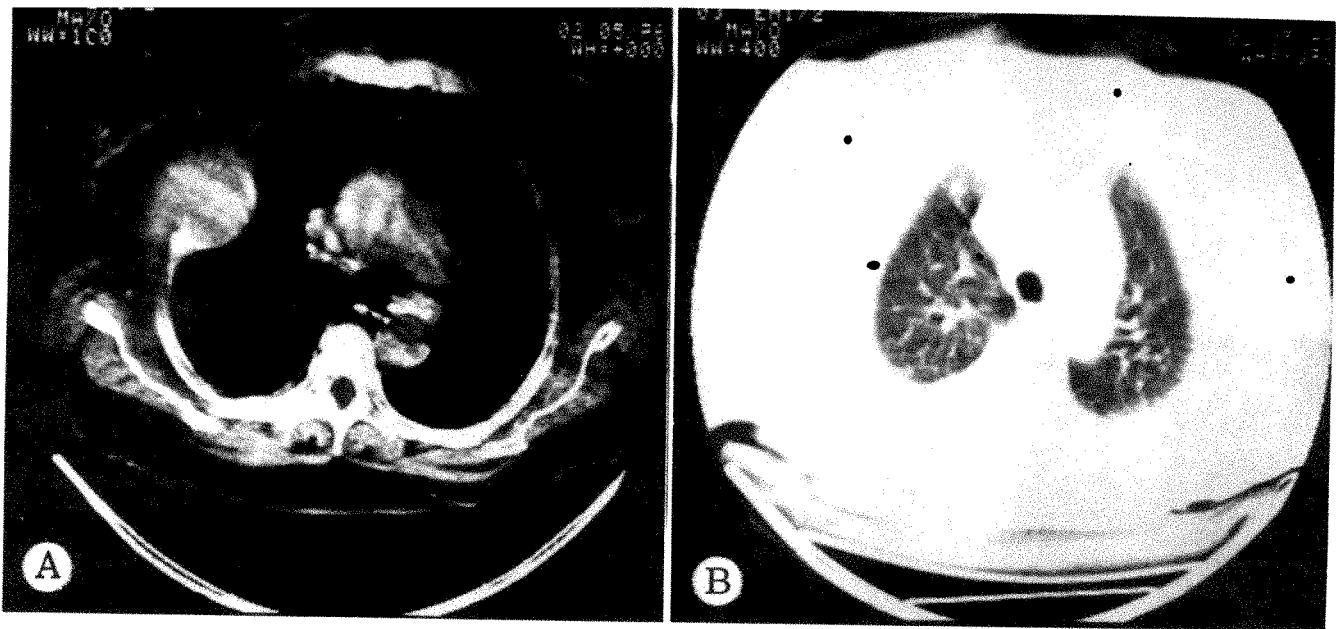


Fig. 34.—CT scans of 79-year-old woman who had subtotal thyroidectomy 3 years earlier for papillary adenocarcinoma. Destructive lesion had recently developed in right third rib and in right side of pelvis. *A*, Tomographic section through chest revealing large destructive lesion in rib on right. Large portion of mass projects into chest and tumor extends considerably into chest wall. *B*, Lung parenchyma revealed after adjusting window height and width. Note tiny nodule in apex of right lung anteriorly which was not appreciated on chest film.

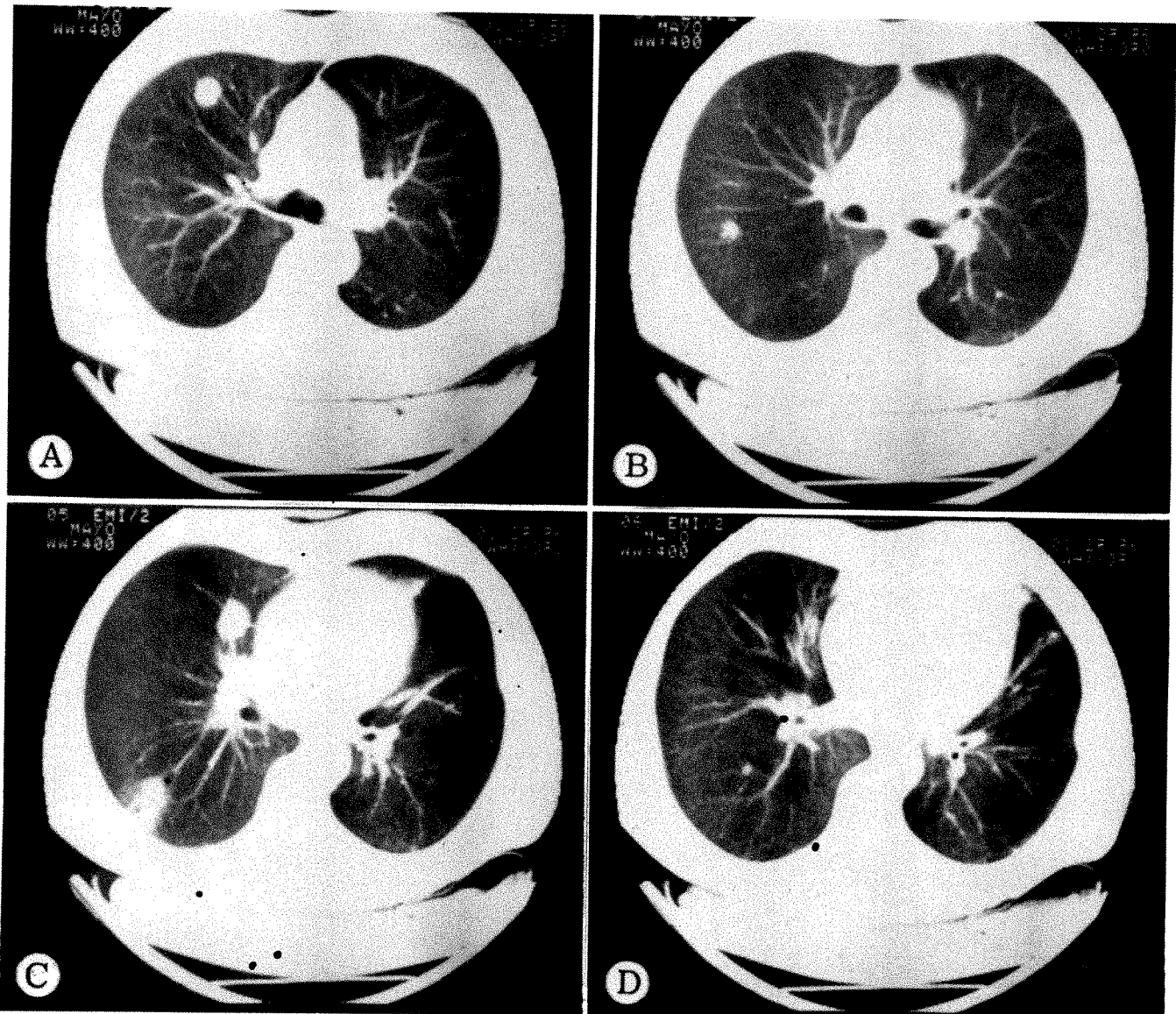


Fig. 35.—CT scans of 60-year-old man with two (possibly three) lung nodules on routine chest film and no known primary tumor. *A–D*, Multiple tomographic sections through lungs revealing multiple pulmonary nodules, some not seen on chest film. Biopsy showed nodules (1–3 cm) to be grades 2 and 3 metastatic adenocarcinoma (still of unknown primary origin).

Fig. 36.—CT scan of 72-year-old man who had left upper lobectomy for large cell carcinoma. Postoperatively, sputum remained positive for large cell carcinoma. Bronchoscopic examination was normal, but bronchial brushings from right side revealed tumor cells. No lesion seen on chest film. Scan at level of right hilum revealed tiny irregular lesion in posterior medial aspect of right lung immediately behind hilum. (In retrospect, slight thickening of pleura present on scan just posterolateral to small nodule.) Lesion then evaluated with routine tomography. At operation, metastatic large cell carcinoma found in location indicated on CT scan. Metastatic implants present in pleura posteriorly.

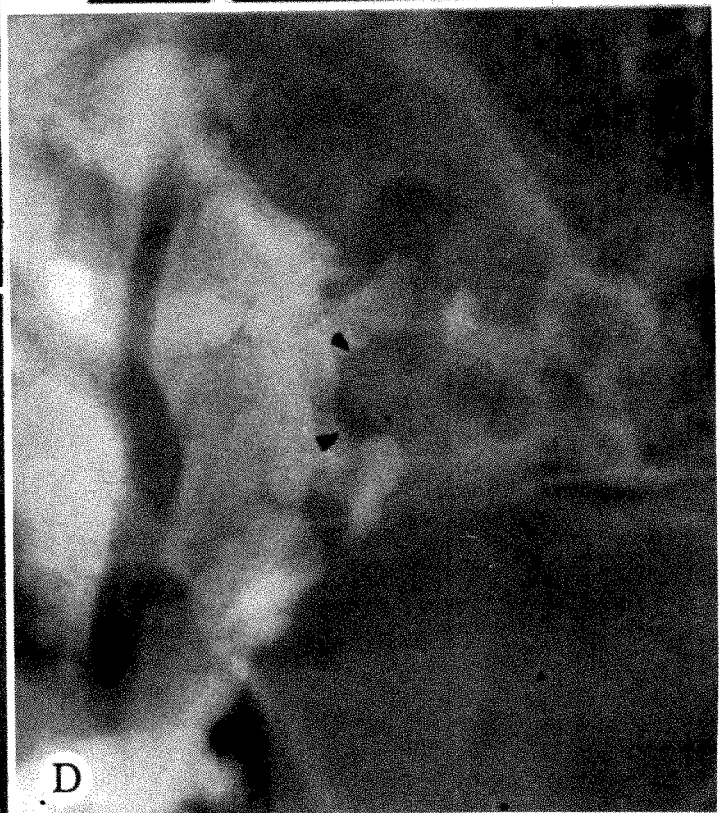
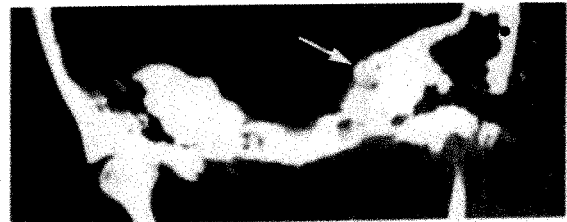
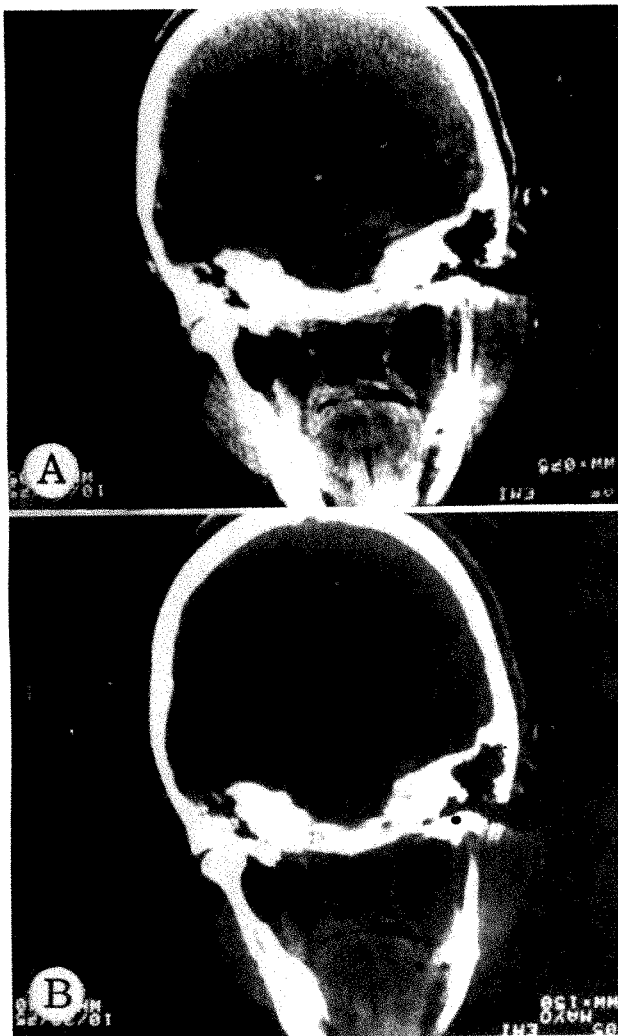
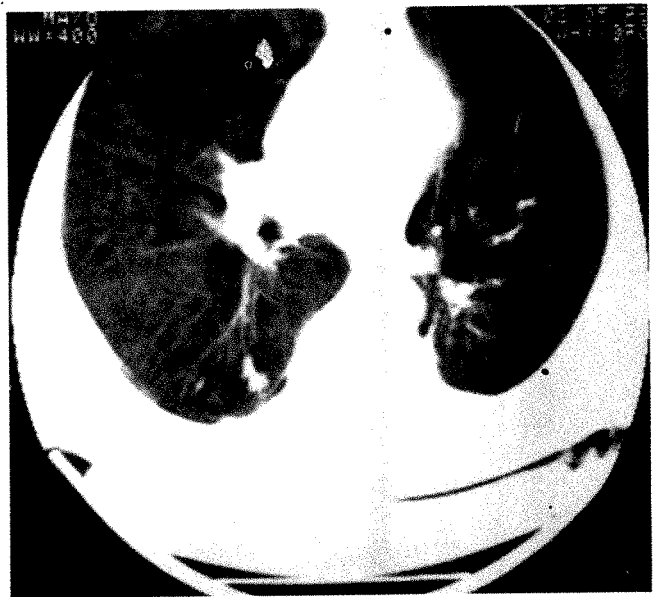


Fig. 37.—60-year-old woman with suspected lesion in left cerebellopontine angle. Routine CT head scan negative. Body scanner used to compare results with routine head scanner (160×160 matrix) and to obtain coronal section tomograms. *A and B*, Coronal sections through region of petrous bones, with window width and height altered to eliminate low density structures. *C*, Enlarged view of *B* revealing tiny tumor (arrow) projecting from left internal auditory canal. *D*, Pantopaque myelogram showing small filling defect caused by tumor projecting from left internal auditory canal. 8 mm acoustic neuroma removed at operation.

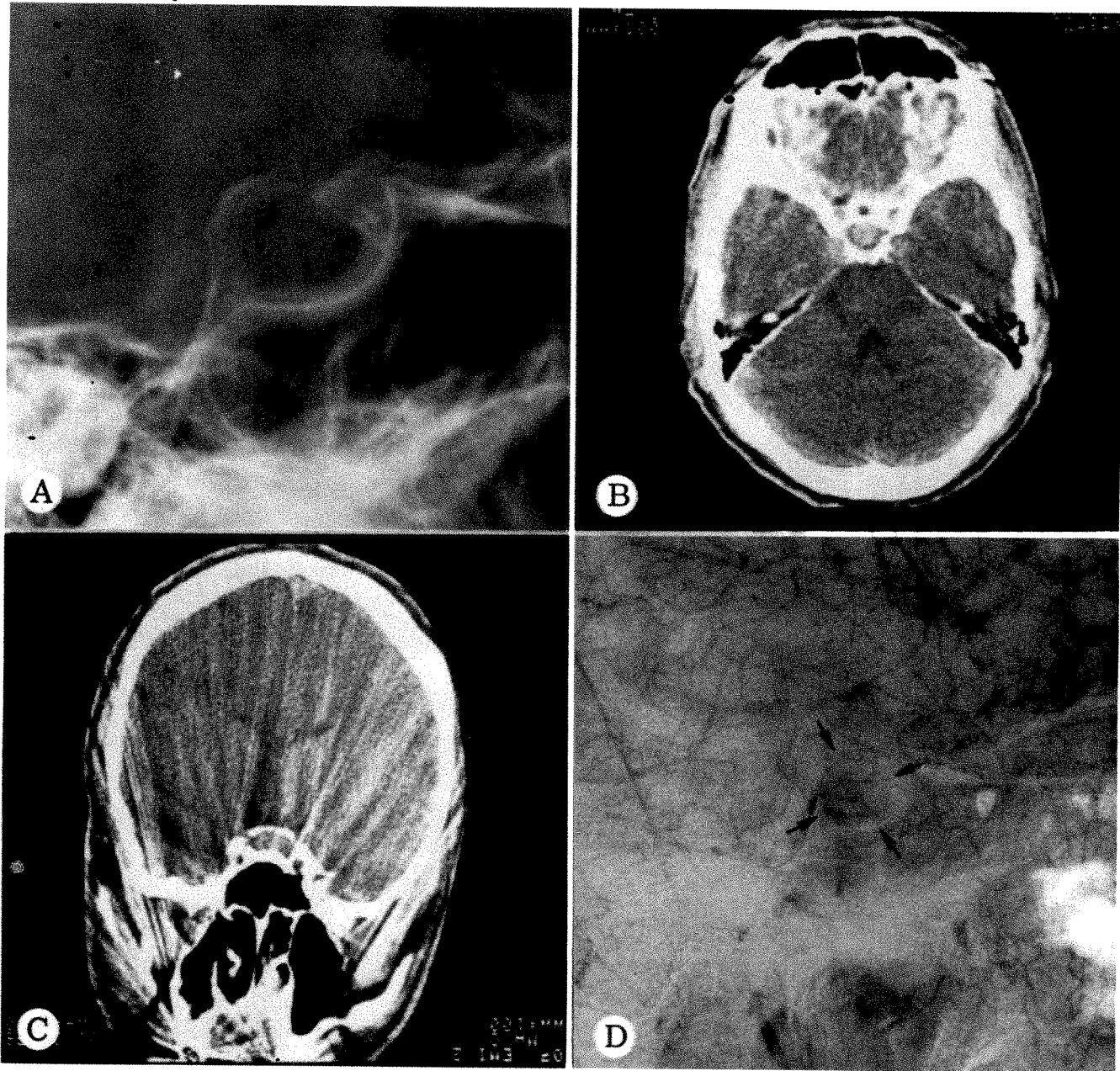


Fig. 38.—34-year-old man with possible acromegaly. *A*, Localized radiograph showing slight asymmetry of sella. (Tomograms showed sella slightly larger on left.) *B*, CT scan through sella in horizontal projection after injection of contrast material. Small intrasellar tumor clearly defined. Siphon of both carotid arteries seen lateral to sella. *C*, CT scan in coronal projection through sella, including dorsum of sella and both anterior clinoids, showing no evidence of suprasellar extension of tumor. *D*, Angiogram, parenchymal phase. Stain present in small intrasellar tumor (arrows), with no definite suprasellar extension. At surgery, small intrasellar chromophobe adenoma with minimal suprasellar extension removed.

many cases CT has helped solve diagnostic problems and beneficially affected the management of patients. However, it is difficult to quantitate this in relation to what might have happened had CT information not been available.

As previously mentioned, the ability of CT to initially detect a disease process, to determine its extent, and to define the exact nature of the disorder will have to be considered in relation to any particular pathologic process. Also, at this stage, there are interpretive problems similar to those found in all fields of radiology. Improvement in diagnostic ability comes with experience and with the develop-

ment of an appreciation of the normal and pathologic variations discovered on these unfamiliar cross-sectional images. This is evidenced by the fact that each newly discovered case of an abnormality now frequently seems to be unique, which leads to a somewhat anecdotal approach to initial evaluations. However, we are in the process of accumulating more quantitative data regarding various organs and diseases.

Experience gained in these 400 cases indicates that CT of the body has its greatest value in evaluating an abdominal mass, either suspected or known, and that the liver,

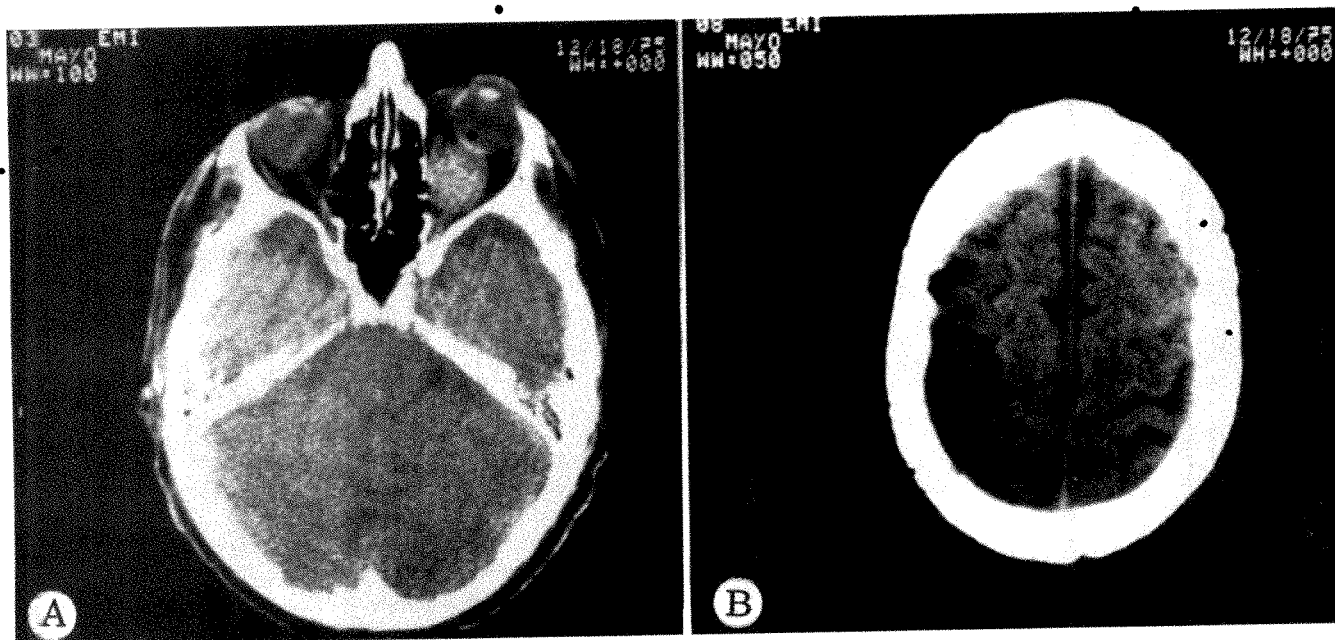


Fig. 39.—CT scans of 49-year-old man with right proptosis and extraocular muscle weakness. A, Orbital mass in posterior right orbit causing significant proptosis. B, Highest cut showing gyri and sulci more clearly than possible with 160×160 matrix. Benign hemangioma in right orbit found at operation.

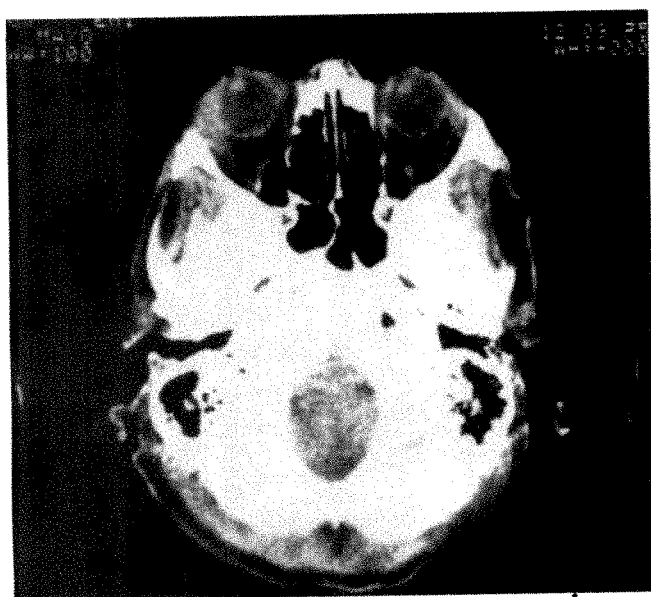


Fig. 40.—CT scan of 74-year-old man with slight proptosis on left. Small high density mass located lateral to left globe. Patient has not yet had surgery, but tumor probably in lacrimal gland.



Fig. 41.—CT scan (enlarged view of coronal section) of patient with proptosis due to recurrent squamous cell carcinoma in superior portion of left orbit. Note inferior displacement of globe (arrow) and dense infiltrating tumor.

pancreas, and retroperitoneal spaces are the most rewarding target regions. This is partly because conventional methods can be lacking in sensitivity and specificity or frequently entail risk and morbidity.

CT of the kidney must be evaluated separately because effective and accurate methods with low morbidity exist to detect and differentiate renal disease, especially renal masses. The same reasoning applies to CT of the chest, since the chest roentgenogram is a sensitive tool in detection.

CT of the head, however, is a proved technique, and our experience with head scanning using the body scanner has produced even better images. This is particularly encouraging because it tends to forecast additional improvements in body scanning techniques.

Because the CT scanner is located in our outpatient facility, we have had no experience in examination of patients in acute trauma. We anticipate the creation of a scanning capacity in one of our hospital facilities and expect it to be useful in evaluating the traumatized patient.

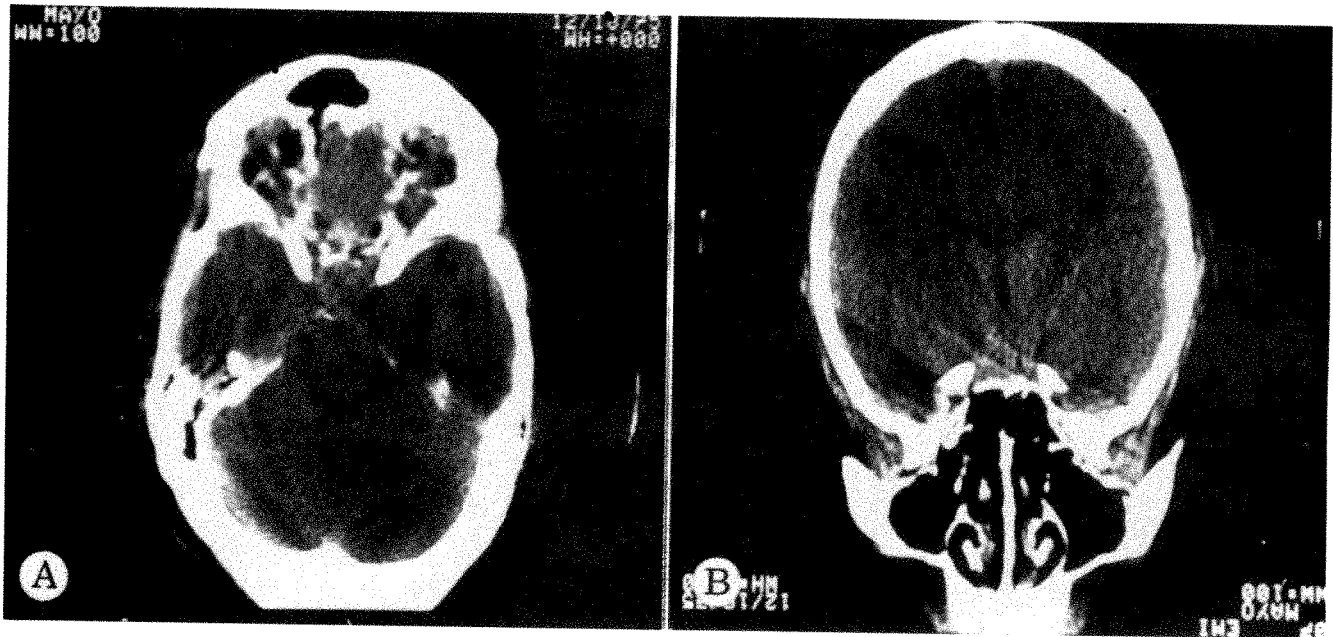


Fig. 42.—CT scans of patient with large pituitary tumor. *A*, Horizontal section through sella. *B*, Coronal section showing suprasellar extension of pituitary tumor.

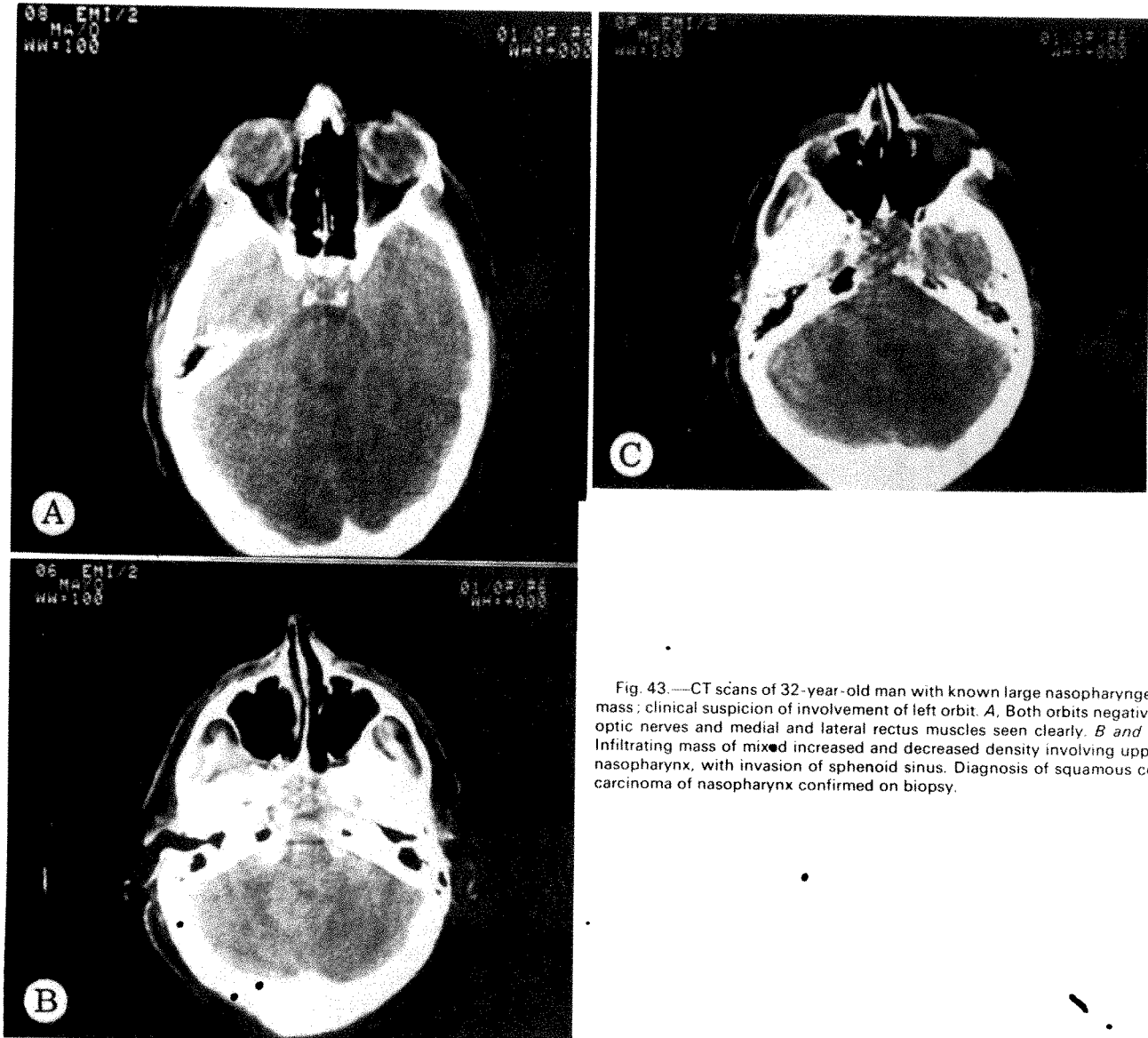


Fig. 43.—CT scans of 32-year-old man with known large nasopharyngeal mass; clinical suspicion of involvement of left orbit. *A*, Both orbits negative; optic nerves and medial and lateral rectus muscles seen clearly. *B* and *C*, Infiltrating mass of mixed increased and decreased density involving upper nasopharynx, with invasion of sphenoid sinus. Diagnosis of squamous cell carcinoma of nasopharynx confirmed on biopsy.

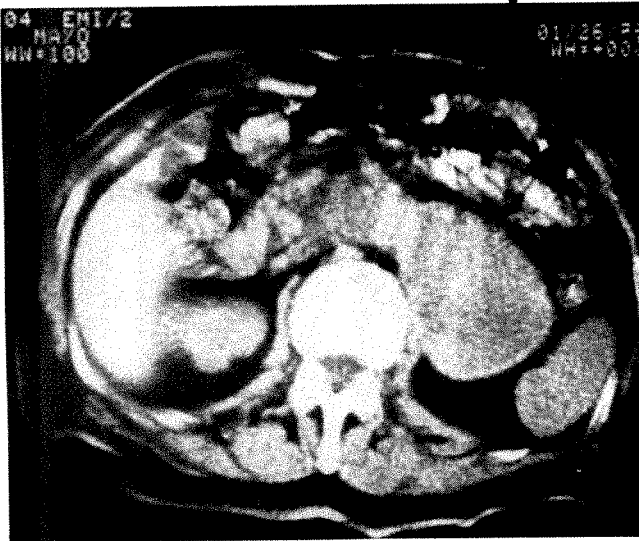


Fig. 44.—CT scan of 81-year-old man with hematuria. Excretory urogram showed 10 cm mass projected over upper pole of left kidney (thought possibly due to adrenal tumor). Enlarged, sharply circumscribed mass in left parasagittal region likely arises from abdominal aorta which is not clearly outlined. Angiogram confirmed large secular aneurysm of abdominal aorta.

We doubt that CT will be useful in the diagnosis of diseases involving the stomach, duodenum, small intestine, or colon. One exception would be a large lesion that presented with a significant abdominal mass.

Diffuse parenchymal disease, such as cirrhosis of the liver, Wilson's disease, or hemochromatosis, has not been studied with CT, but there may be some value in such a study when the ability to obtain precise and absolute attenuation coefficients has been achieved. The same holds true for the evaluation of diseases involving the bone, such as osteoporosis and osteomalacia.

CT produces information about both the morphology and the absorption coefficients of organs. Density difference permits visualization of lesions within organs, but the contour or shape of the organ has an equally important (and often greater) role in the detection of a lesion. This is particularly so in the pancreas. Future technological developments may make it possible to assign a specific range of absolute numbers to an organ or a lesion. Presently, however, there is considerable overlap in the density ranges found in adjacent organs. To accomplish this density differential, substances could be developed to permit selective alteration of the density of an organ or lesion. Intravenously administered contrast material has helped in this regard because it can accentuate differences in density, but it also can diminish these differences. This nonselective total body opacification is helpful but is perhaps only the first step in the direction of density alteration possibilities. Ingestion of dilute water-soluble contrast material is helpful in opacifying bowel loops that cause annoying densities adjacent to organs of interest. Although helpful in identifying bowel loops, this contrast medium tends to stimulate peristalsis that produces artifact due to motion of bowel content [11].

In this regard, we believe that the speed of scan is important and that scanning should be done during respiratory suspension. However, cardiac motion and peristalsis in the bowel create motion of air that causes artifacts. To obviate these problems, scans would have to be made in a much shorter time than 20 sec or even 5 sec.

We are in the process of comparing CT with other diagnostic modalities including ultrasound, nuclear medicine, and angiography. It is possible that no single examination will prove best, some modalities having advantages over others in relation to a particular organ or disease. It is doubtful that any particular diagnostic technique will become obsolete because of the introduction of CT, but the pattern of use and the indication for many examinations may change. Increased experience and careful scrutiny of comparative studies should provide the information that will enable correct decisions regarding future use of this exciting new diagnostic technique. CT may become primarily a screening procedure or it may be reserved for definitive analysis of particular disease states. Its role, more likely, will be somewhere between these two extremes.

REFERENCES

- Schellinger D, Di Chiro G, Axelbaum SP, Twigg HL, Ledley RS: Early clinical experience with the ACTA scanner. *Radiology* 114:257-261, 1975
- Alfidi RJ, Haaga J, Meaney TF, MacIntyre WJ, Gonzalez L, Tarar R, Zelch MG, Boller M, Cook SA, Jelden G: Computed tomography of the thorax and abdomen: a preliminary report. *Radiology* 117:257-264, 1975
- Sagel SS, Stanley RJ, Evens RG: Early clinical experience with motionless whole body computerized tomography. *Radiology*. In press, 1976
- Stephens DH, Hattery RR, Sheedy PF II: Computed tomography of the abdomen: early experience with the EMI body scanner. *Radiology*. In press, 1976
- Muhm JR, Brown LR, Rosenow EC III: Early experience with computerized tomography of the chest using the EMI CT 5000 body scanner. Submitted for publication
- Stephens DH, Sheedy PF II, Hattery RR, Hartman GW: Initial clinical experience with computerized tomography of the body. *Radiol Clin North Am*. In press, 1976
- Philips RL, Stephens DH: Computed tomography of liver specimens. *Radiology* 115:43-46, 1975
- Pickering RS, Hattery RR, Hartman GW, Holley KE: Computed tomography of the excised kidney. *Radiology* 113:643-647, 1974
- Alfidi RJ, MacIntyre WJ, Meaney TF, Chernak ES, Janicki P, Tarar R, Levin H: Experimental studies to determine application of CAT scanning to the human body. *Am J Roentgenol* 124:199-207, 1975
- Twigg HL, Axelbaum SP, Schellinger D: Computerized body tomography with the ACTA scanner. *JAMA* 234:314-317, 1975
- McCullough EC, Baker HL Jr, Hattery RR, Sheedy PF II, Stephens DH, Payne JT, Gedgaudas E: Performance evaluation and quality assurance of computed tomography (CT) scanners with illustrations from the EMI and ACTA and Delta scanners. *Radiology*. In press, 1976
- Hattery RR, Williamson B Jr, Hartman GW: Urinary tract tomography. *Radiol Clin North Am*. In press, 1976

Computed Tomography of the Body: Early Trends in Application and Accuracy of the Method

ROBERT J. STANLEY,¹ STUART S. SAGEL, AND ROBERT G. LEVITT

• Early experience with extracranial CT has shown this diagnostic method to be highly accurate in evaluating the liver, pancreas, kidneys, retroperitoneum, and pelvis. The diagnosis of neoplasm, inflammatory changes, and normal morphologic variants is possible. Initial data indicate that this modality may assume a primary role in the evaluation of the liver, pancreas, and retroperitoneum (e.g., the differentiation of medical from surgical jaundice and the distinction of solid from cystic lesions). In the thorax, the results appear far less dramatic. CT scans rarely surpass the diagnostic accuracy of conventional radiologic studies.

Initial results indicate a need for studies comparing CT with radionuclide examinations, ultrasonography, and other conventional radiographic procedures as well as for evaluating its use in radiation therapy planning and follow-up.

Introduction

The usefulness of computed tomography (CT) in the evaluation of the brain is well established [1-3]. This is reflected in major changes in patterns of utilization of other diagnostic radiological examinations [4, 5]. Fewer pneumoencephalograms and radionuclide brain scans are being performed, and the percentage of negative cerebral arteriograms has been sharply reduced. Stated simply, the impact of computed tomography has been overwhelming in neurologic diagnosis.

This major innovation in imaging has been applied more recently to the evaluation of the remainder of the body. Several whole body scanners have been in use for 1 or more years [6, 7]. Since October 1975, the Mallinckrodt Institute of Radiology has been evaluating the whole body scanner designed by EMI Limited, the originator of computed tomography [8].

Over 350 patients have been evaluated in the first 4½ months of use. This report describes the early trends related to applicability and accuracy of this diagnostic method through detailed analysis of the first 275 cases. No attempt will be made to provide an exhaustive review of all of the studies capable of being performed with the whole body scanner. This report will concentrate on those clinical problems in which the EMI body scanner appears to provide the most useful diagnostic information.

Materials and Methods

Instrumentation

The physical and functional characteristics of the EMI body scanner have been described [9]. In summary, the scanner consists of an x-ray tube and a reference detector mounted opposite an array of 30 sodium iodide crystal detectors on an oval frame. The

beam of x-rays linearly traverses the patient to be scanned, recording thousands of discrete measurements of attenuation per sweep. The scanning frame indexes 10° and the process is repeated in the opposite direction. Eighteen separate traverses encompass 180° in a total scanning time of 18 sec. This short scanning time permits motionless images of the body in areas affected by respiration in 89% of the patients studied, resulting in far greater spatial resolution of discrete anatomic structures than heretofore possible.

Computers reconstruct the image by means of a convolution algorithm (filtered back-projection method) [10]. The image, displayed on a cathode ray tube, is viewed as if from below with the patient's right side on the viewer's left, comparable to conventional radiographic studies [9]. The various radiodensities are displayed as shades of gray ranging from black to white. A numerical printout can be obtained. However, the 320×320 matrix results in an unwieldy-size to the printout reconstruction and is generally not used for clinical purposes. Two additional cathode ray tube monitors display the image for recording with Shackman (Polaroid film) and Hasselblad (Kodak Linagraph Shellburst) cameras.

Method

At the Mallinckrodt Institute, CT of the body has not been used as a screening test. Patients are selected who have either a well defined clinical problem or a known disease process. Prior to scanning, the patient's clinical history, physical findings, and laboratory tests are reviewed. Pertinent conventional radiologic studies are evaluated. After placing a tape containing lead markers spaced 2 cm apart on the patient's skin, a scout radiograph of the patient's chest, abdomen, or pelvis is taken. Based on the topography determined by the scout film, the appropriate areas are scanned.

Each study is viewed immediately after processing, and a decision is made regarding completeness of the examination or the need for additional scans with or without contrast medium. The length of an examination varies from 15 min for a few selected scan levels to 1½ hr for extensive abdominal scans before and after contrast medium. Water-soluble iodinated contrast agents are injected intravenously in certain selected cases.

Results

Table 1 divides the cases by anatomic areas studied. The majority of studies performed were of the abdomen (table 2). The results of CT scans of the liver, pancreas, kidneys, extraperitoneal space, pelvic organs, and chest are separately tabulated. In the proven cases, the overall diagnostic accuracy has been high. The interpretation of the CT scans in the various organs and anatomic areas will be considered separately in the following sections.

Liver (tables 3 and 4)

The CT diagnosis of normal is given when the liver contour is normal in size and shape, the attenuation coefficients are uniform throughout and in the range of 25-35 EMI

¹Received March 23, 1976.

All authors: Mallinckrodt Institute of Radiology, Washington University School of Medicine, 510 South Kingshighway, St. Louis, Missouri 63110. Address reprint requests to R. J. Stanley.

TABLE 1
Distribution of Cases by Anatomic Area

Area	No.
Brain	15
Head and neck	12
Chest	36
Abdomen	168
Pelvis	27
Extremities	6
Subtotal	264
Normal volunteers and research experiments	11
Total	275

Note.—First 275 examinations.

TABLE 2
Primary Organ or Area Studied within Abdomen

Organ or Area	No.
Liver	41
Pancreas	32
Liver and pancreas	47
Spleen	8
Renal	35
Retroperitoneum	22
Miscellaneous*	9

Note.—168 cases. Cases appear more than once in this table since in more than 10% two or more organs were of equal interest.

* Peritoneal cavity, gallbladder, stomach, colon, duodenum.

TABLE 3
Accuracy of Interpretation of CT Scans of Liver

CT Diagnosis	No. Cases	Accuracy		
		Correct*	Incorrect	Unconfirmed†
Normal	33	8	1	24
Solid space-occupying lesions†	17	11	1	5
Dilated bile ducts	22	17	0	5
Abscess	4	4	0	0
Fatty infiltration	2	2	0	0
Occult gallstones	3	2	0	1
Simple hepatic cysts	2	1	0	1
Intrahepatic hematoma	1	1	0	0
Total	84	46	2	36

* Histologic or operative confirmation.

† Primary or metastatic.

TABLE 4
Correlation of CT and Radionuclide Liver Scan Findings

CT Finding	Radionuclide Finding		
	Space-occupying Lesion	Inhomogeneous	Enlarged Porta
Norm	2*	5	2†
Solid tumor	10	0	0
Abscess	3‡	0	0
Dilated ducts	0	6	3
Cyst	1	0	0

* CT correct in one case, radionuclide in one.

† No confirmation.

‡ A finding of space-occupying lesion is consistent with abscess.

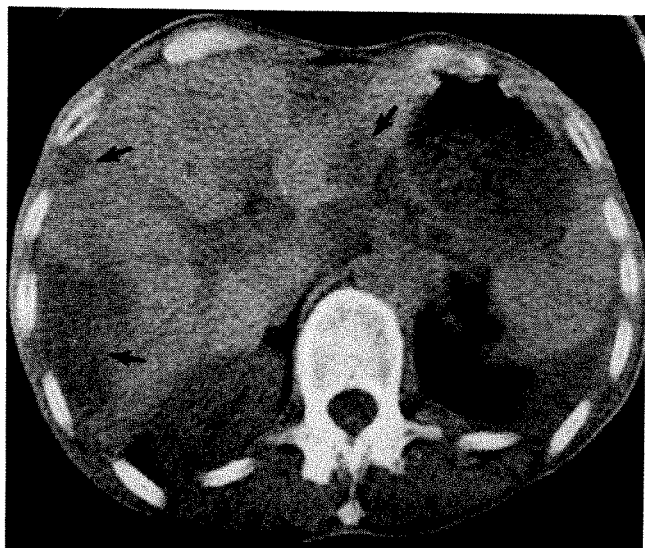


Fig. 1.—48-year-old man with weight loss and upper abdominal pain; 2 years postresection of carcinoma of colon. CT scan showing multiple areas with attenuation coefficients slightly lower than normal liver (arrows), consistent with metastases. Percutaneous needle biopsy disclosed adenocarcinoma.

units, and peripheral bile ducts are not visible. Nondilated central portions of the biliary tree can be seen in some normal patients. Without the use of contrast media, arteriovenous structures within the normal liver are not visible. The normal gallbladder appears as a well defined oval area of water density or slightly higher (10–15 EMI units) at the level of the porta hepatis.

Tumors within the liver are defined as more or less sharply margined areas of lower density, in the range of 5–10 EMI units below the normal hepatic parenchyma but always higher than the density of hepatic cysts or dilated bile ducts (figs. 1–3). Primary and metastatic tumors of the liver have been diagnosed by CT in 17 cases, and 11 are biopsy proven. Liver abscess (fig. 4) can mimic primary or metastatic tumor but is usually distinguishable by the clinical history.

Intravenous iodinated contrast agents have improved the definition of the single or multiple areas of low density within the liver by raising the attenuation coefficients of the surrounding hepatic parenchyma in approximately one-half of the cases in which contrast was used (table 5). On one occasion, a central necrotic filling defect was recog-

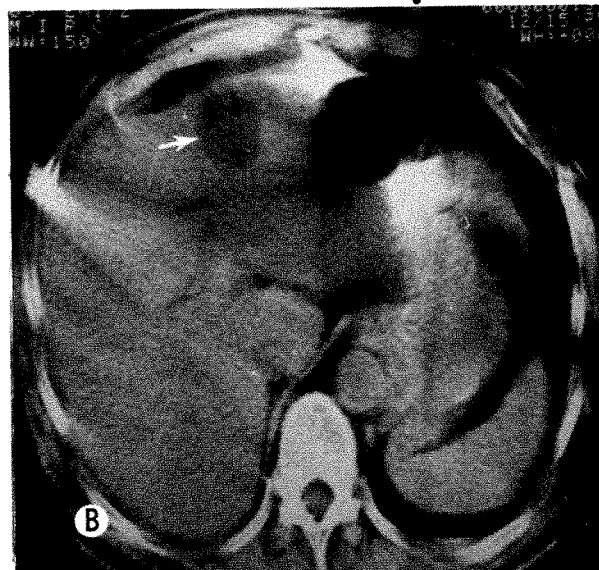
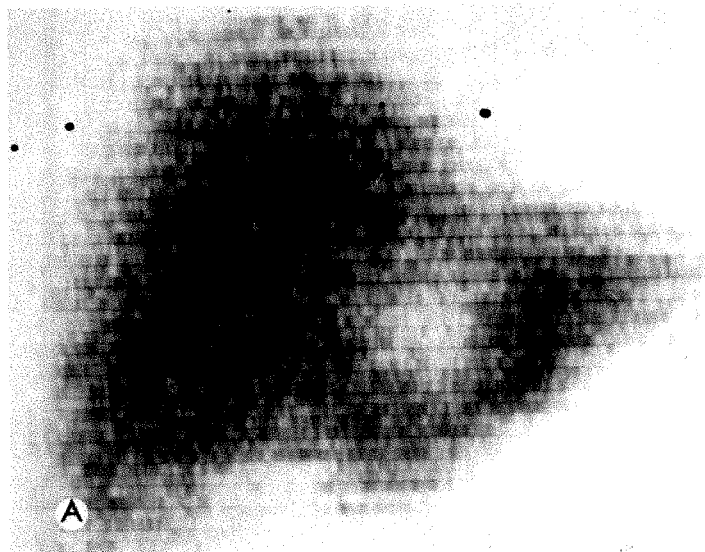


Fig. 2.—59-year-old man with renal mass. *A*, Radionuclide liver scan showing large filling defect in left lobe consistent with metastasis. *B*, CT scan showing single 3 cm sharply demarcated lesion in anterior aspect of left lobe (arrow). *C*, Measure mode with narrow window setting. Attenuation equivalent of filling defect is 3 EMI units, equal to water density. Findings diagnostic of cyst rather than metastases. Surgery disclosed benign hepatic cyst without metastases in liver and renal cell carcinoma.

nized only after the use of a contrast agent. In three cases, however, the use of a contrast agent hindered the evaluation by causing the "holes" to blend into the normal hepatic parenchyma, resulting in a homogeneous appearing liver.

In an attempt to differentiate medical from surgical jaundice, 27 jaundiced patients were scanned. High levels of accuracy were achieved. In 17 jaundiced patients who were found to have dilated bile ducts by CT scan, obstruction by tumor or stone was operatively proven (fig. 5). Five cases with dilated bile ducts remain unconfirmed. Of the remaining five patients whose bile ducts were not visibly dilated, hepatocellular disease rather than obstruction was confirmed to be the cause of the jaundice in three (figs. 6 and 7). Two cases remain unconfirmed.

Biliary tree dilatation and metastatic disease occurred together in five patients. Four had primary cancers of the pancreas and one had a primary cancer of the liver metastatic within the liver. In three the liver metastases were initially overlooked due to their resemblance to dilated ducts on end. In retrospect, the metastatic tumors in some cases could be differentiated from the dilated bile ducts by their greater size compared to the diameters of the contiguous bile ducts. In some instances, careful attention to the attenuation coefficients of the metastatic tumors revealed that they had a higher EMI number than the bile ducts. Increasing experience with such cases has already reduced this error.

Not enough cases have been studied by both radionuclide and CT scans to warrant a valid comparison. Table 4 presents in a limited way some of the differences in findings and interpretations between abnormal radio-

nuclide scans and the associated CT scans. A close correlation exists between radionuclide and CT scans when the radionuclide diagnosis is "space-occupying lesion(s)." However, CT can differentiate solid lesions, fluid filled cysts (fig. 2), and normal anatomic variants (fig. 8) among these space-occupying lesions. Benign hepatic cysts have been seen in four patients.

CT can distinguish dilated bile ducts from other hepatocellular or diffusely infiltrative diseases which produce "inhomogeneous" radionuclide scans. However, various hepatocellular and diffusely infiltrating diseases, such as sarcoidosis or amyloidosis, could be present in a liver appearing normal by CT scan. At present only diffuse fatty infiltration (fig. 6) and hemachromatosis [6] have been recognized on a CT scan by unusually low and abnormally high attenuation coefficients, respectively.

Pancreas (table 6)

The normal pancreas by CT scan has a uniform density

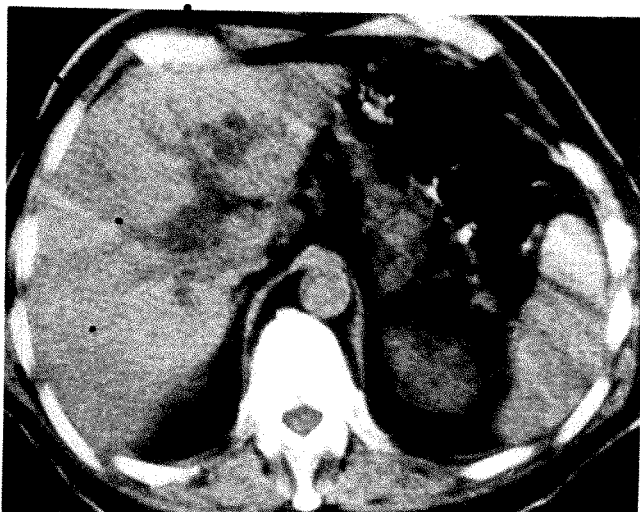


Fig. 3.—CT scan of 76-year-old man with jaundice showing dilated intrahepatic bile ducts as linear branching structures of low density radiating from porta hepatis. Mass within pancreatic head seen on lower level cuts. Surgery disclosed obstructing carcinoma of head of pancreas.

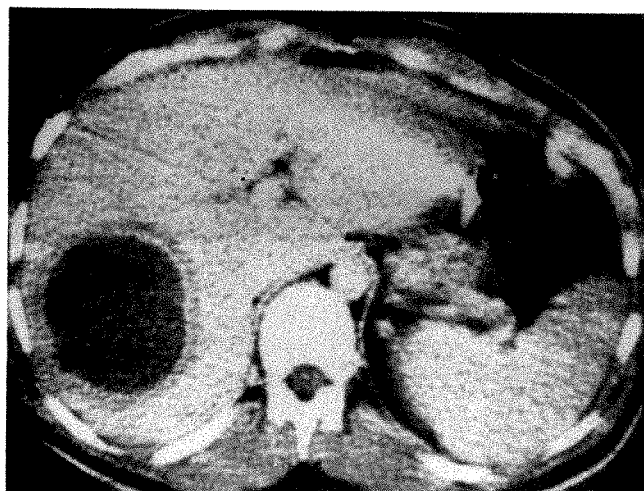


Fig. 4.—29-year-old man (recently returned from El Salvador) with fever, chills, and right upper quadrant pain. CT scan after intravenous administration of 75 ml of Conray 400 showing discrete filling defect 8 cm in diameter in right lobe of liver demarcated against enhanced normal liver parenchyma. Note thin intermediate zone of radiodensity surrounding filling defect, probably due to edema. At operation, amebic abscess was drained.

throughout which is slightly lower than that of the liver. It is necessary to identify the superior mesenteric artery and the fat plane anterior to it in order to be sure that the pancreas (anterior to both these structures) is being viewed rather than the third and fourth portions of the duodenum which lie posterior to this artery. A guide for judging the normalcy of the gland size has been described [11], relating the thickness of the gland to the diameter of the adjacent vertebral body. In that study, the normal body and tail varied from one-third to two-thirds the diameter, while the normal head could be as large as two-thirds to one times the diameter. The size of the normal pancreas in our experience bore a similar relationship. A gradual change in the

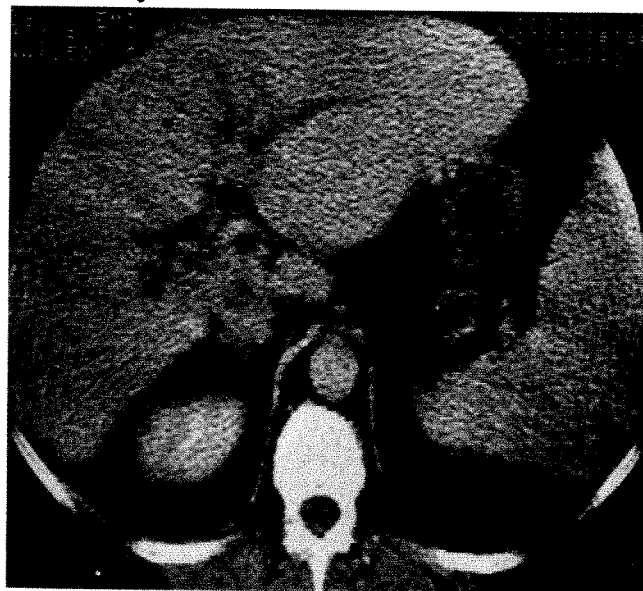


Fig. 5.—55-year-old man with malaise and pruritis; bilirubin=2.6 mg/100 ml. CT scan showing mild dilatation of intrahepatic biliary tree. Lower level scans failed to disclose dilated gallbladder, stone in distal common duct, or mass in pancreatic head, suggesting obstructing lesion proximally in biliary tract. Subsequent transhepatic cholangiography demonstrated obstruction at junction of common hepatic ducts. Surgical exploration disclosed cholangiocarcinoma.

TABLE 5

Value of Intravenous Contrast Medium

Anatomic area	Diagnostic	Improved Definition	No Improvement	Hindered
Liver	0	10	5	3
Pancreas	0	3	7	0
Kidney	1	4	4	0
Retroperitoneum	0	3	0	0
Spleen	0	1	1	0
Aorta	0	0	1	0
Inferior vena cava	0	1	0	0
Total	1	22	18	3

Note.—Data represent 25% of 168 abdominal cases.

anteroposterior thickness of the pancreas was seen in the normal gland when moving from the tail to the head rather than abrupt increases. When applying the guide for size, consideration had to be given to the gland as a whole. A cancer of the head of the pancreas, causing the thickness of the head to be equal to the diameter of the vertebral body (within normal limits?), could be suspected if the body and tail were uniformly one-third the diameter.

Pancreatic tumors have presented as gross focal alterations in the size and shape of the gland when diagnosed by CT scanning. Several tumors were inhomogeneous and appeared to contain cystic or necrotic areas of lower x-ray density (fig. 9). The use of intravenous iodinated contrast agents failed to have a definitive effect on the diagnosis of these tumors but in some cases helped to define their in-

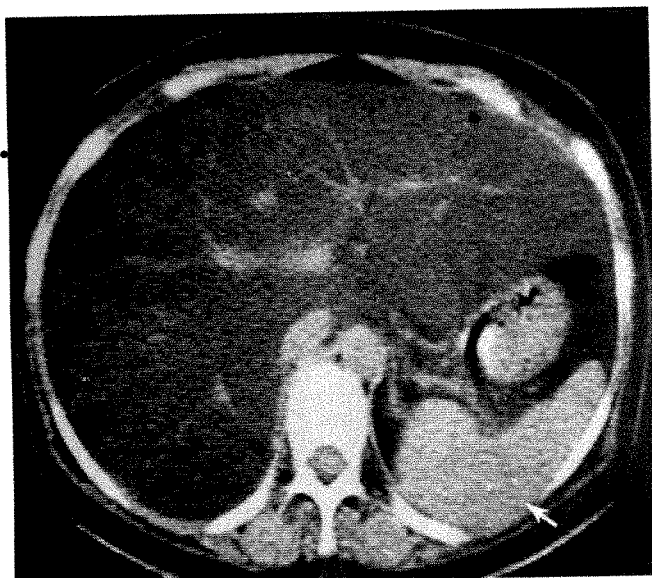


Fig. 6.—39-year-old woman with jaundice 4 years post jejunoileal bypass for obesity; bilirubin=5.3 mg/100 ml, alkaline phosphatase=980 U. CT scan showing striking difference in density between liver (4 EMI units) and spleen (arrow; 32 EMI units). No dilated bile ducts present within liver although vascular structures within liver clearly demonstrated. Findings diagnostic of diffuse fatty infiltration of liver.

TABLE 6

Accuracy of Interpretation of CT Scans of Pancreas

CT Diagnosis	No. Cases	Accuracy		
		Correct	Incorrect	Unconfirmed
Normal	31	5	3	23
Tumor	20	16	2	2
Pancreatitis*	7	2	0	5
Pseudocyst	4	4	0	0
Mass†	10	1	1	8
Miscellaneous	3	3	0	0
Total	75	31	6	38

* Acute or chronic.

† Enlargement of portion of gland; not otherwise specified.

homogeneous composition (table 5). A false positive diagnosis of tumor in the tail of the pancreas was made when there was insufficient effort to separate contiguous loops of bowel from the tail (fig. 10). Subsequently, in patients in whom a mass lesion of the pancreatic tail was suspected but not definitively separated from adjacent structures, the examination has been repeated either in the prone position or after oral administration of a dilute solution of radiopaque water soluble bowel contrast media. Utilizing such techniques, water-filled bowel simulating a mass has become readily separable from the pancreas either by movement anteriorly or through opacification.

Loss of part or all of the normal fat plane posterior to the pancreas due to invasion by tumor was seen in 11 confirmed cases. This sign was never an isolated finding but was

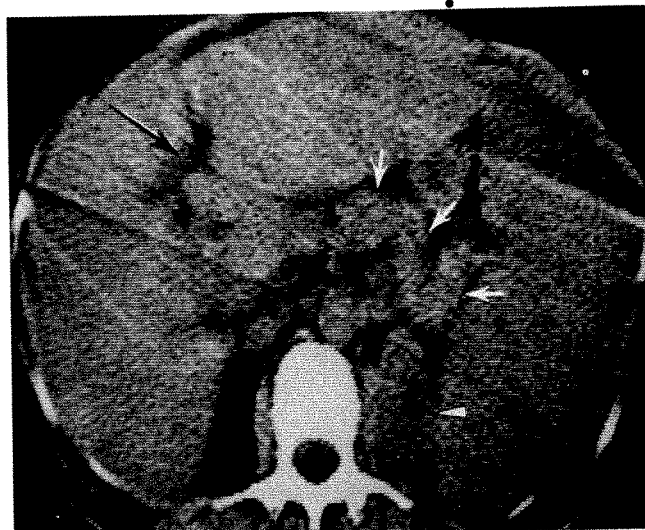


Fig. 7.—42-year-old woman with pruritis and jaundice and known systemic sarcoidosis. CT scan showing marked hepatosplenomegaly with compression of pancreas (white arrows) and kidney (white arrowhead). Some fat visible near porta hepatis (black arrow) but no evidence of dilated intrahepatic bile ducts. Percutaneous liver biopsy disclosed no caseating granulomas.

TABLE 7

Accuracy of Interpretation of CT Scans of Kidney

CT Diagnosis	No. Cases	Accuracy		
		Correct	Incorrect	Unconfirmed
Tumor	6	6	0	0
Cyst(s)	20	4	0	16
Polycystic renal disease	2	2	0	0
Obstruction	1	1	0	0
Abscess	1	0	1	0
Normal perinephric fat	1	0	0	1
Normal variant	1	1	0	0
Atrophic pyelonephritis	2	1	0	1
Acute inflammatory process	1	1	0	0
Infarctions in a transplant kidney	1	1	0	0
Total	36	17	1	18

associated with a mass in all cases. Lower density in the body and tail, presumed to be related to obstructive edema, was seen in five cancers of the head. Marked atrophy of the body and tail was found associated with one large tumor in the head and proximal body.

Sixteen cancers of the pancreas diagnosed by CT scan were operatively confirmed. In seven cases where bulky masses were present, upper gastrointestinal barium contrast examination failed to suggest abnormality either prospectively or retrospectively. Too few of the cases were evaluated with ultrasound to allow a valid comparison of these two diagnostic methods. Fifteen cancers of the head of the pancreas were associated with obstructive dilatation

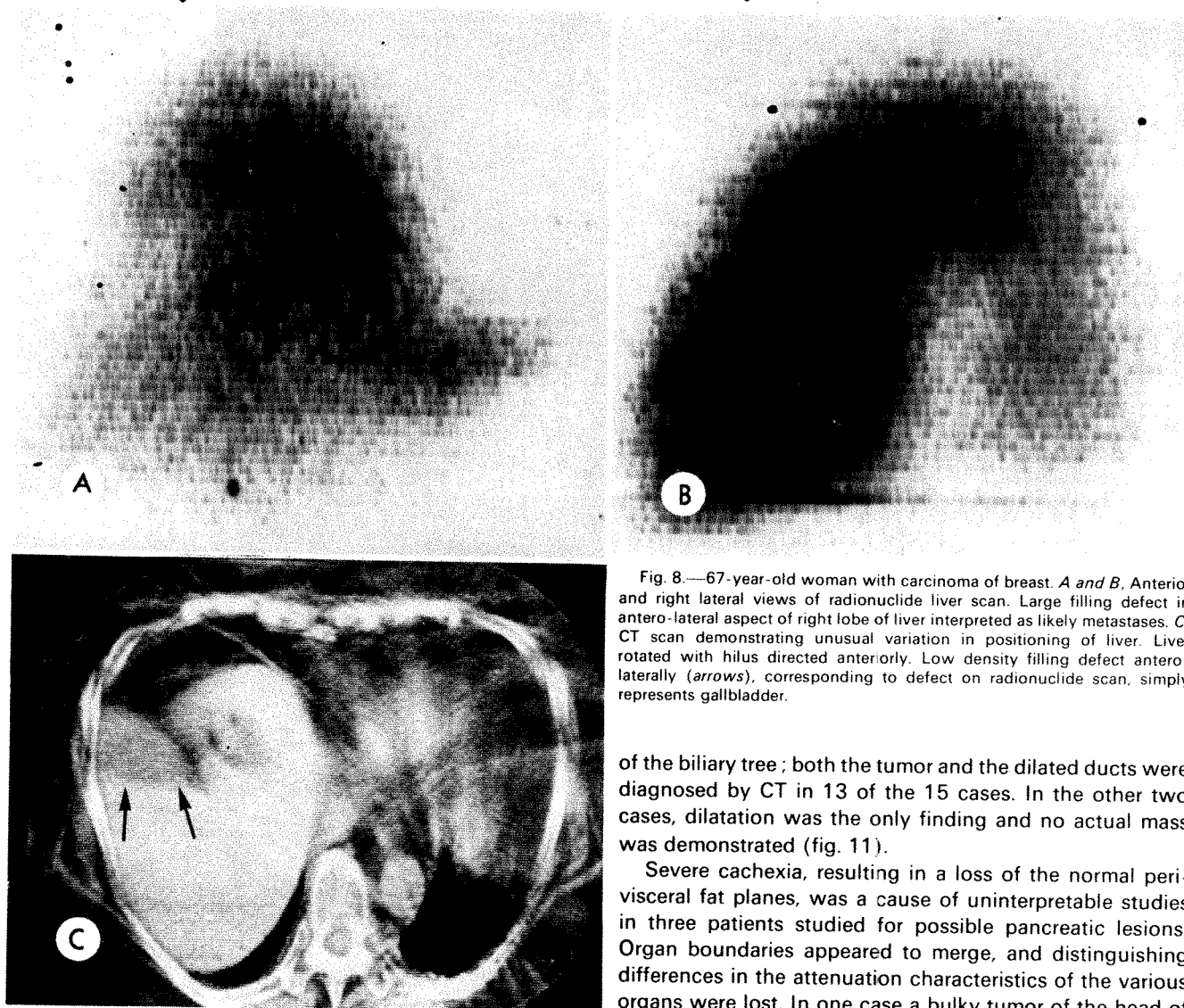


Fig. 8.—67-year-old woman with carcinoma of breast. *A and B*, Anterior and right lateral views of radionuclide liver scan. Large filling defect in antero-lateral aspect of right lobe of liver interpreted as likely metastases. *C*, CT scan demonstrating unusual variation in positioning of liver. Liver rotated with hilus directed anteriorly. Low density filling defect antero-laterally (*arrows*), corresponding to defect on radionuclide scan, simply represents gallbladder.

of the biliary tree; both the tumor and the dilated ducts were diagnosed by CT in 13 of the 15 cases. In the other two cases, dilatation was the only finding and no actual mass was demonstrated (fig. 11).

Severe cachexia, resulting in a loss of the normal perivisceral fat planes, was a cause of uninterpretable studies in three patients studied for possible pancreatic lesions. Organ boundaries appeared to merge, and distinguishing differences in the attenuation characteristics of the various organs were lost. In one case a bulky tumor of the head of the pancreas was missed, but metastatic spread to the liver could still be distinguished.

Severe acute pancreatitis presented as uniform enlargement of the entire gland in two cases (fig. 12). In each case the pancreas had lower than normal attenuation coefficients, presumed to be related to edema and/or necrosis. Calcification within the pancreas was commonly seen in cases with a history of chronic pancreatitis; small atrophic glands were also encountered.

Pseudocyst of the pancreas was correctly diagnosed in all four cases. The pseudocysts have been sharply margined round or oval masses of uniformly low density (5–10 EMI units) (fig. 13).

In ten patients a smooth, gradual focal enlargement of the pancreas was encountered. Most of these patients manifested signs and symptoms of a mild, acute, or subacute pancreatitis at the time of the scan. No alteration of the normal adjacent tissue plane was seen, and the enlarged area was of a homogeneous density equal to the rest of the gland. One case was subsequently proven to be a carcinoma. In another case, the mass proved to be hyperplastic

TABLE 8

Accuracy of Interpretation of CT Scans of Extraperitoneal Space

CT Diagnosis	No. Cases	Accuracy		
		Correct	Incorrect	Unconfirmed
Normal	7	1	0	6
Tumor	14	11	0	3
Osteomyelitis	1	1	0	0
Abscess	1	0	0	1
Mass in rectus sheath*	1	1	0	0
Total	24	14	0	10

* Clinical diagnosis, intraabdominal mass. CT localized a solid mass to area of rectus sheath; was a desmoid reaction.



Fig. 9.—62-year-old man with abdominal pain and weight loss; normal upper gastrointestinal series and normal bilirubin. CT scan showing large mass in pancreatic head (arrows), inhomogeneous with large areas of low absorption (22 EMI units). Small tail of pancreas seen separated by fat from splenic vein (white arrowhead). Surgery disclosed mucin-producing adenocarcinoma of pancreas.



Fig. 10.—46-year-old man with midepigastic pain and 30 pound weight loss; ultrasonography suggested mass in tail of pancreas. CT scan interpreted as demonstrating enlargement of tail of pancreas (arrows) consistent with neoplasm. Surgical exploration disclosed normal pancreas. In retrospect, the "mass" undoubtedly represented bowel loops immediately contiguous to pancreas simulating mass lesion.

TABLE 9
Accuracy of Interpretation of CT Scans of Pelvis

CT Diagnosis	No. Cases	Accuracy		
		Correct	Incorrect	Unconfirmed
Normal	7	2	0	5
Tumor:				
Localized	7	4	0	3
Extensive	4	4	0	0
Lymphocele	2	2	0	0
Aneurysms of femoral artery	1	1	0	0
Total	21	13	0	8

lymph nodes surrounding a normal pancreatic head. The majority of unconfirmed cases in this category suggests that this finding usually was associated with a benign clinical course.

Kidney (table 7)

The kidneys can be defined exceptionally well by CT scans because of the presence of abundant perinephric fat in all but the thinnest patients. Without contrast enhancement, normal renal parenchyma has an attenuation equivalent of 20–30 EMI units. After contrast, the value can rise to 40–60 EMI units in the parenchyma and substantially higher in the collecting system. The area of the renal calyces and pelvis is a low density area due to the contiguous renal sinus fat. After intravenous contrast has increased the density of the collecting system, the characteristic shape of

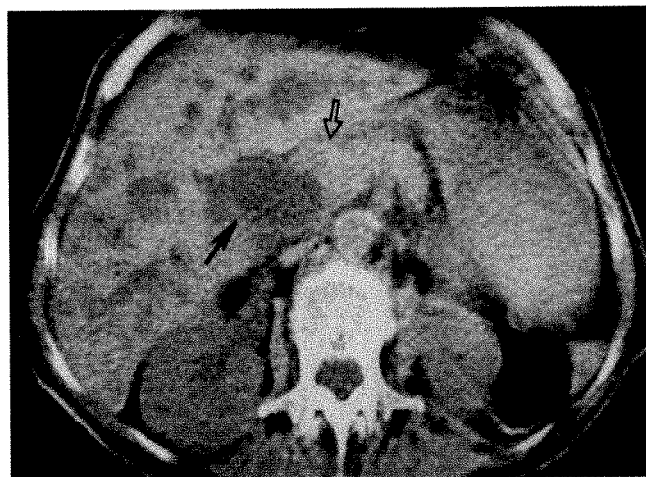


Fig. 11.—CT scan of 53-year-old woman with jaundice showing marked dilatation of common bile duct (closed arrow) and multiple dilated intrahepatic bile ducts (low density areas). No definite mass within pancreatic head (open arrow) identified. Surgery disclosed adenocarcinoma of pancreatic head as cause of obstructive jaundice.

the calyces and pelvis is sharply defined. The contour of the normal renal cortex is smooth and rounded. A break in the round or oval outline occurs at the hilus where the vascular pedicle is directed anteromedially towards the inferior vena cava and aorta.

Solid renal masses are easily distinguishable from benign renal cysts by CT scanning. The renal neoplasms studied altered the contour of the involved kidney and had an attenuation value approximately equal to the normal renal parenchyma (fig. 14). After contrast, the tumors enhanced slightly but far less than the surrounding normal renal tissue. The six cases diagnosed as tumors by CT were all operatively proven.

Two unusual cases were encountered. A large histiocytic

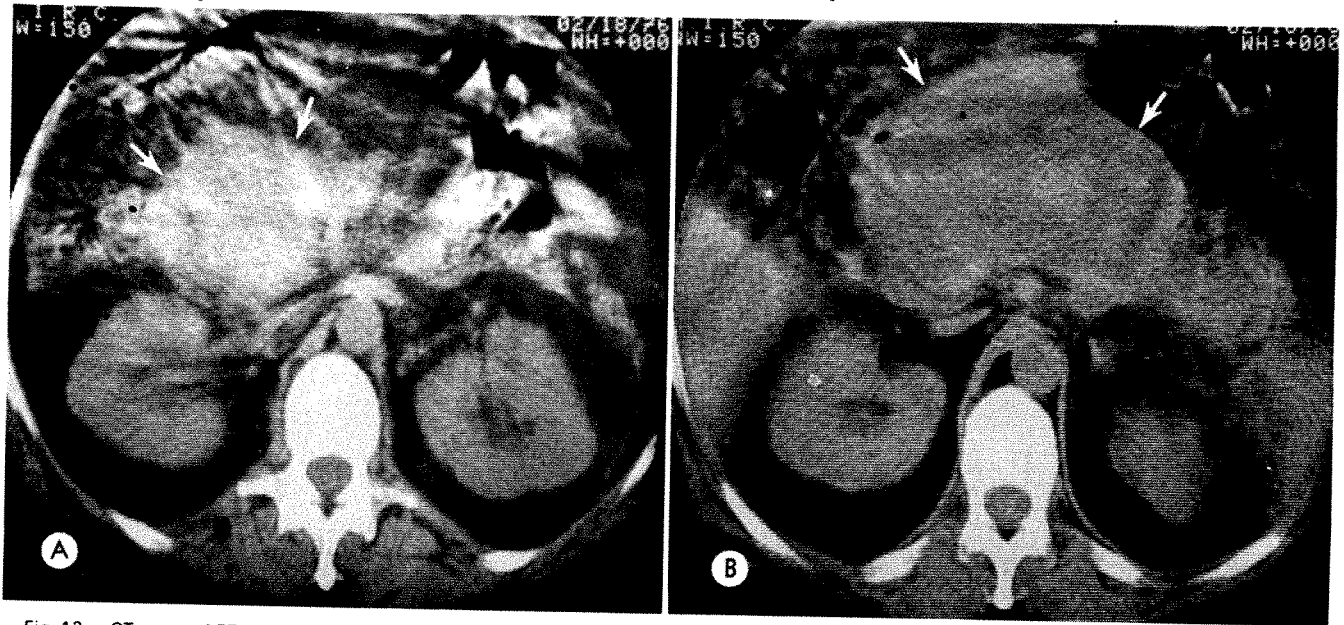


Fig. 12.—CT scans of 57-year-old man with severe upper abdominal pain, mild hypotension, and markedly elevated serum amylase. A, Massive enlargement of pancreatic head (arrows); B, similar enlargement of pancreatic body (arrows). Marked enlargement of tail seen on higher level scans. Postmortem examination disclosed severe acute hemorrhagic pancreatitis.

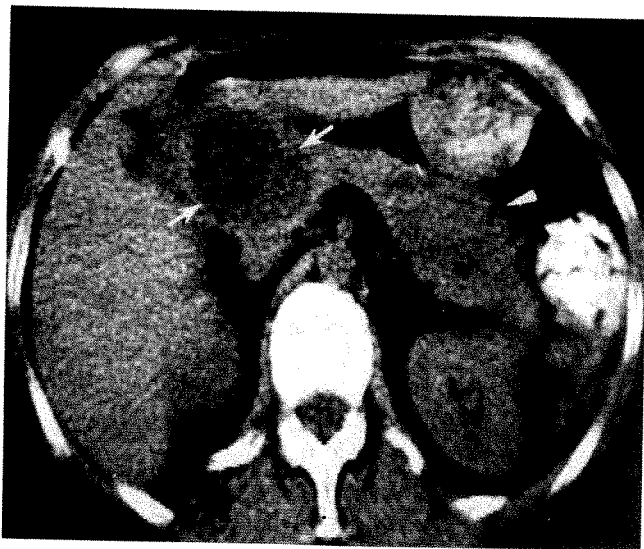


Fig. 13.—40-year-old woman with unexplained upper abdominal pain for 2 years; conventional radiographic studies normal and endoscopic retrograde pancreaticocholangiography unsuccessful. CT scan showing 6 cm low density (15 EMI units) pseudocyst within head of pancreas (arrows) with another pseudocyst of equal size within the tail (arrowhead). Second pseudocyst more clearly defined on a more cephalad scan and confirmed at surgery.

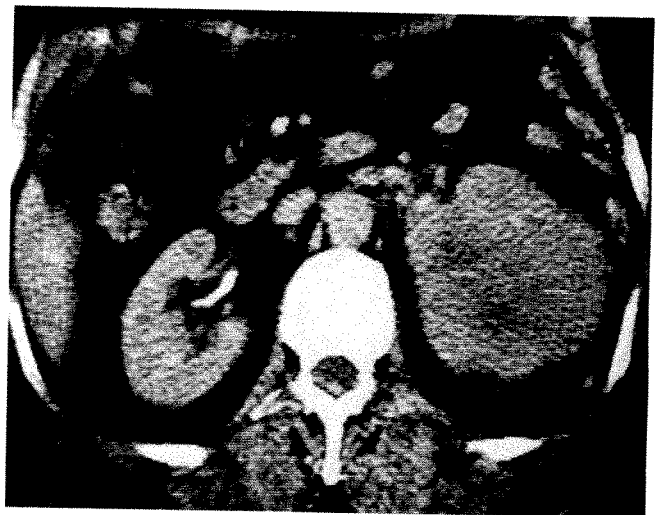


Fig. 14.—70-year-old man with hematuria; urography demonstrated large left renal mass. CT scan performed 3 hr after urogram showing large irregularly margined mass in left kidney similar in absorption density to normal right kidney (38 and 46 EMI units). Since normal renal parenchyma is 30–34 EMI units, some enhancement of tumor has occurred, although not as much as normal renal parenchyma. Surgery disclosed large renal cell carcinoma extending into perirenal fat.

lymphoma, incorrectly thought to be renal in origin from the results of urography and arteriography, was shown by CT scan to lie anterior to the kidney and separated from it by a distinct tissue plane (fig. 15). Multiple angiomyolipomas, presenting as bilateral renal masses and diagnosed as malignant tumors by angiography, were shown to contain discrete rounded zones of fat by CT scans (fig. 16).

Renal cysts are sharply margined round or oval struc-

tures on CT scans. Their attenuation equivalent is 5–10 EMI units (fig. 17). Cysts smaller than 1 cm can be identified, especially when projecting well beyond the cortex. Incidental renal cysts were common findings in patients being scanned for other reasons, some of whom had “normal” intravenous pyelograms. Four of the 20 renal masses diagnosed as cysts by CT are confirmed. No further evaluation has been made on the remaining 16.

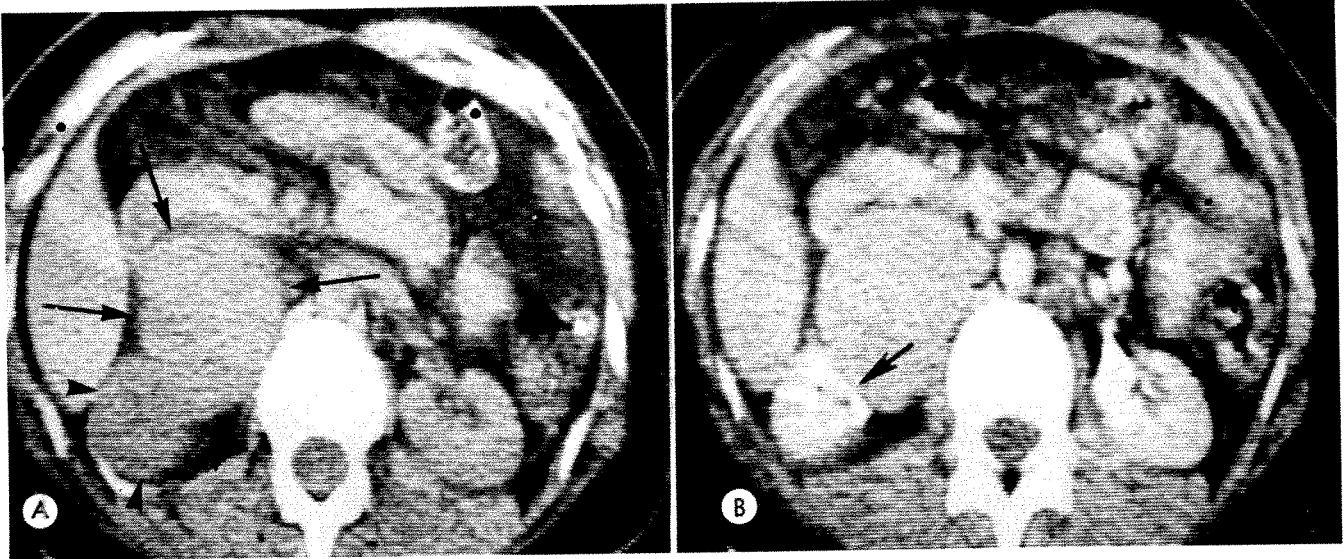


Fig. 15.—55-year-old woman with vague right-sided abdominal pain. Urogram demonstrated mass appearing to arise from medial aspect of right kidney; nephrotomography and angiography suggested avascular mass most consistent with cyst. A, CT scan showing mass 5 cm in diameter (arrows) in right retroperitoneum contiguous (anterior and slightly medial) and of equal absorption number to right kidney (arrowheads). Faint cleavage plane suggested between solid mass and right kidney. B, Scan after intravenous administration of 100 ml of Conray 400 showing marked enhancement of both kidneys. Note definite tissue plane (arrow) separating retroperitoneal mass and posterolaterally displaced right kidney. Surgery (approach altered by CT findings) disclosed histiocytic lymphoma in retroperitoneum unattached to kidney.

TABLE 10
Analysis of CT Scans in Chest Cases

CT Diagnosis	No. Cases	Scan Beneficial*
Normal	0	0
Tumor	11	4†
Inflammatory lesion	9	2
Vascular lesion	4	1
Cardiac abnormality	1	1
Mediastinal lesion	7	4

* Provided diagnostic information not apparent on chest radiograph.

† In two cases, diffuse pulmonary nodules could be seen in retrospect on the chest roentgenogram.

Of the 20 lesions diagnosed as cysts by CT, an ultrasound examination was performed in 12. In 11, the ultrasound diagnosis was cyst and in one the study was indeterminate (fig. 18). When cancer occurs in a kidney with coincident multiple cysts, ultrasound may be unable to provide a definitive answer (fig. 19).

Polycystic renal disease could also be easily diagnosed by (1) the lobulated contour of the enlarged kidneys, (2) the innumerable cysts of varying sizes, (3) the distorted intervening parenchyma and calyces, and (4) the bilaterality of the process.

Two patients, both with acute painful upper urinary tract infections, were found to have poorly defined areas of low density within an enlarged upper pole. The margin of the kidney in the same area was not as sharply defined as usual, and diminished contrast was present in the draining calyces

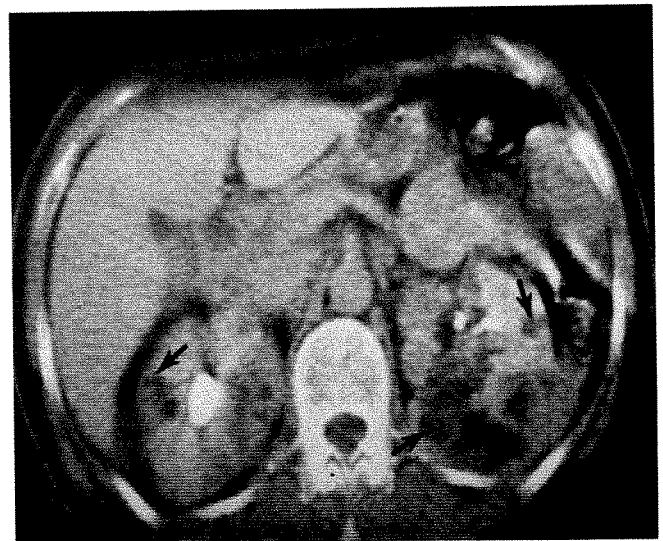


Fig. 16.—65-year-old woman with left flank pain. Urography demonstrated large left renal mass with suggestion of splaying of right pyelo-calycal system; renal angiography interpreted as showing bilateral renal cell carcinoma. CT scan performed after angiography to assess extent of neoplasm demonstrated multiple masses of low attenuation coefficients (arrows; -10 EMU units) within both kidneys. CT findings of fat density within kidneys changed presumptive diagnosis from carcinoma to angiomyolipomas; confirmed by surgical biopsy of left kidney.

compared to the rest of the kidney. The first encounter with these findings resulted in the erroneous diagnosis of abscess. At operation marked nephric and perinephric edema was present, accounting for the low tissue density on CT scan. Biopsy revealed acute and chronic inflammation. The second similar case was interpreted as changes of acute

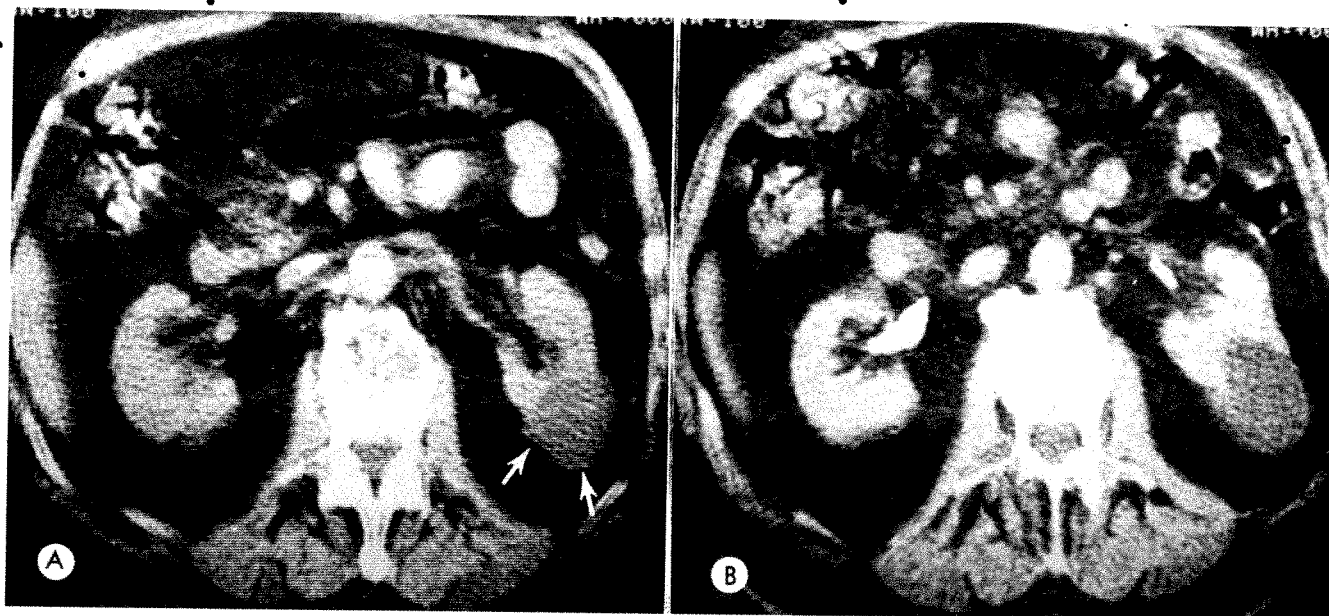


Fig. 17.—CT scans of markedly obese 60-year-old man without urinary tract symptoms. Urography demonstrated left renal mass; ultrasonography unsuccessful on two occasions to delineate nature of mass. A, Sharply demarcated smooth mass (arrows) of low attenuation (5 EMI units) characteristic of benign renal cyst. B, Enhancement of normal renal parenchyma after intravenous administration of 100 ml of Conray 400 without change in attenuation of cyst. Sharp demarcation between cyst and renal parenchyma maintained.

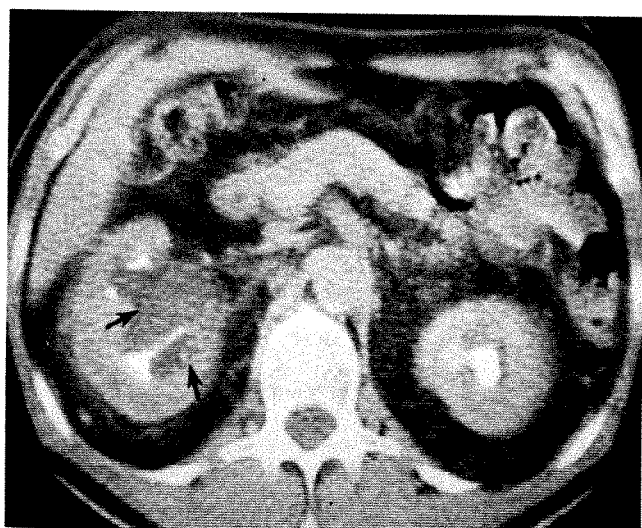


Fig. 18.—64 year-old man without urinary tract symptoms; urography disclosed distortion of calyceal systems centrally in both kidneys. CT scan showing large area of low absorption density (arrows; 5 EMI units) in hilum of right kidney characteristic of benign parapelvic cyst. Similar parapelvic cyst in left kidney was seen on higher level cuts.

inflammation and, under appropriate medical therapy, the kidney returned to a normal appearance. Obstruction, renal atrophy, focal infarctions in a transplant kidney, and normal variations of anatomy produced changes on the CT scan which were virtually diagnostic.

Extraperitoneal Space (table 8)

Deviations from the normal anatomy of the retroperitoneum can be easily recognized. The aorta and inferior

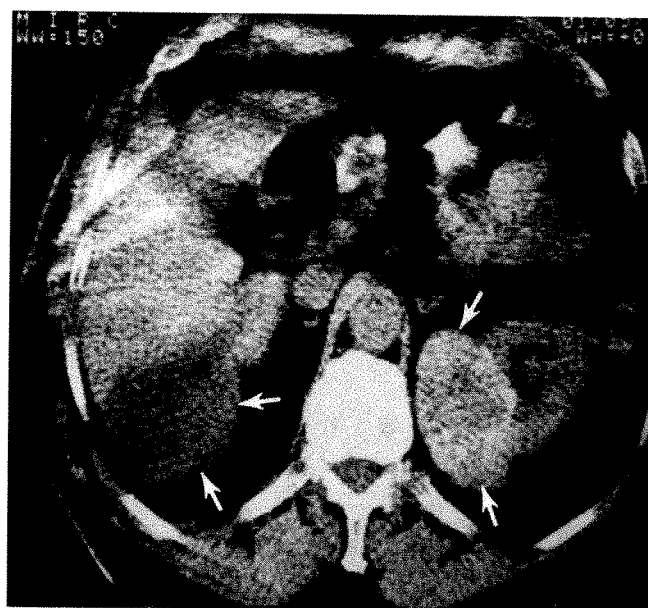


Fig. 19.—69-year-old man without urinary tract symptoms. Urography demonstrated multiple masses in both kidneys. Because of high location of lesions under rib cage, ultrasonography unsatisfactory despite angling of transducer. Angiography disclosed multiple avascular masses in both kidneys. CT findings: right kidney—low density (arrows; 5 EMI units) oval mass characteristic of benign renal cyst; left kidney—solid density (arrows; 36 EMI units) elliptical mass consistent with neoplasm. CT scans of other masses characteristic of benign cysts.

vena cava, which are sharply defined structures in the normal patient, can serve as indicators of disease by their (1) compression or displacement by a mass; (2) disappearance due to enlargement of surrounding nodes or envelopment by tumor (figs. 20A and 21); and (3) in-

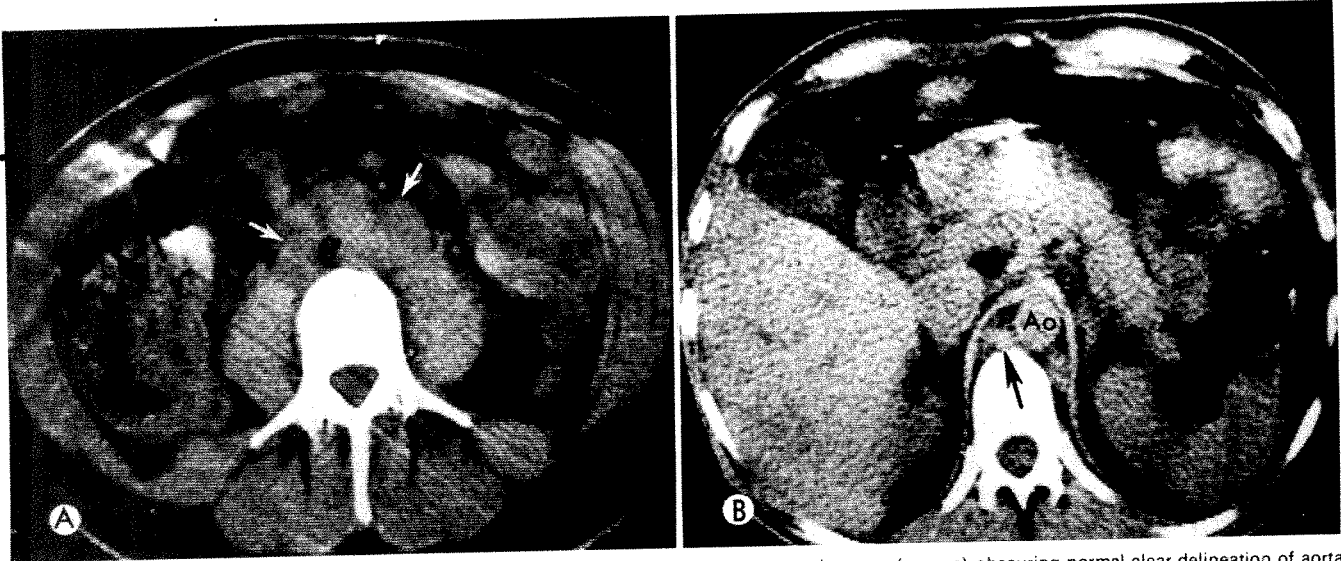


Fig. 20.—CT scans of 40-year-old man with fever of unknown origin. *A*, Masses in retroperitoneum (arrows) obscuring normal clear delineation of aorta and vena cava. *B*, Scan at higher level showing moderately enlarged lymph nodes posterior to diaphragmatic crura (arrow) on either side of aorta (Ao). With increasing enlargement of these nodes, widened paravertebral stripe becomes apparent on conventional plain films of chest or upper abdomen. Laparotomy disclosed enlarged paraaortic and paracaval retroperitoneal lymph nodes secondary to histiocytic lymphoma.

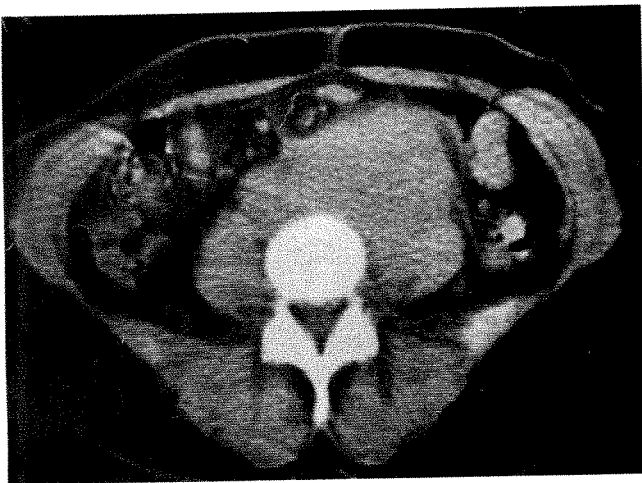


Fig. 21.—Asymptomatic 56-year-old woman treated 3 years previously for Hodgkin's disease of neck with radiation therapy; lymphangiography and laparotomy normal at that time. Questionable left-sided midabdominal mass palpable on routine examination. CT scan showing 6 cm mass within retroperitoneum, predominantly on left side, obscuring aorta, inferior vena cava, and anterior margin of left psoas muscle, consistent with recurrent Hodgkin's disease.

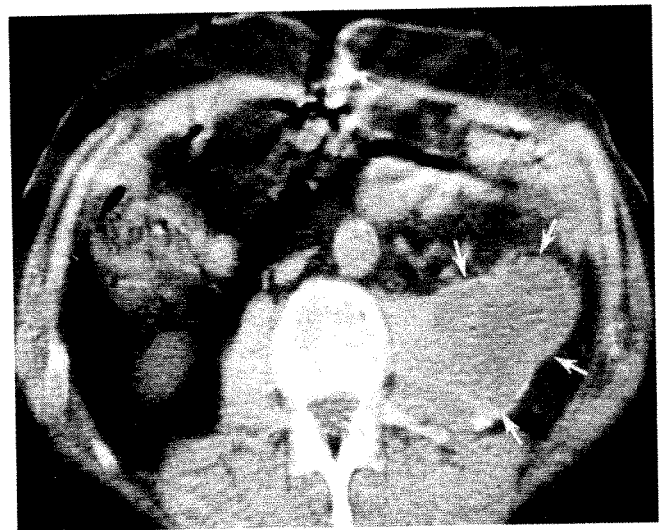


Fig. 22.—64-year-old man with dull ache in left flank 2 years post left nephrectomy for carcinoma. No mass palpable; conventional radiographic studies normal. CT scan showing large mass in left retroperitoneum (arrows) contiguous with left psoas muscle. Mass, consistent with recurrent carcinoma, has central low attenuation coefficients suggesting some necrosis.

trinsic abnormal appearance (i.e., aneurysmal dilatation). Tumor masses themselves are generally well profiled by surrounding fat and present little diagnostic problem on the CT scan (figs. 15 and 22). Enlarged paraaortic nodes beneath the diaphragmatic crura have been demonstrated by CT to be the cause of a widened paravertebral stripe at the level of T12–L2 (fig. 20*B*) seen on the chest and abdominal radiographs in several patients.

Of the 24 cases in which the extraperitoneal space (primarily retroperitoneum) was evaluated by CT, 14 were proven correct. Ten cases remain unconfirmed.

Pelvis (table 9)

The diagnostic accuracy of CT scans in the pelvis is comparable to that achieved in the retroperitoneum. The anatomy is well defined and quite constant compared to the variable relationship of the organs in the upper abdomen (fig. 23). Solid tumors (figs. 24 and 25), cystic masses (fig. 26) or alterations in the size or shape of normally encountered pelvic structures are detectable. In this regard, the relative confinement of the bony pelvis is analogous to the cranial vault and allows for more subtle judgments related to the lateral or anteroposterior displace-

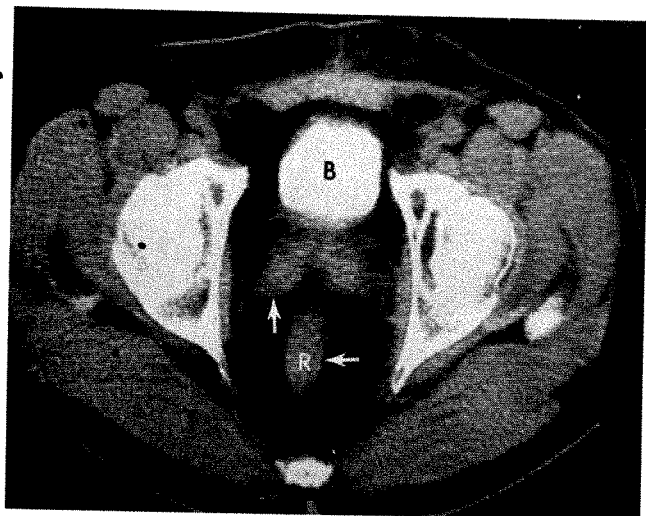


Fig. 23.—CT scan of normal pelvis in 75-year-old man. Opaque bladder (B) filled with contrast media sharply delineated by surrounding peripelvic fat. Seminal vesicles (vertical arrow) seen on either side posterior to bladder. Rectum (horizontal arrow; R) clearly demarcated by surrounding fat.

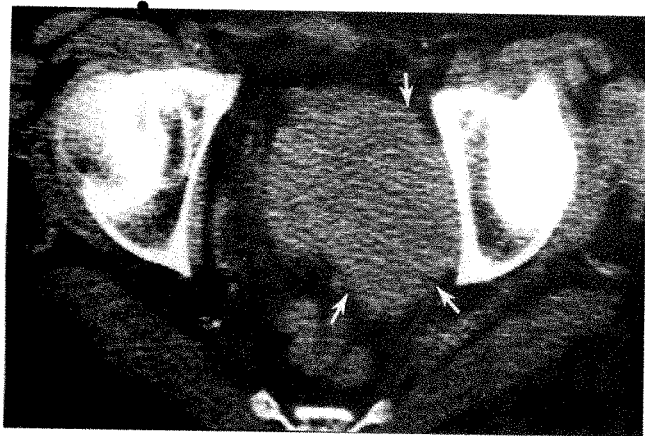


Fig. 24.—75-year-old man with hematuria. Extensive transitional cell carcinoma involving left side of bladder seen on cystoscopy; uncertain extravesical extent. CT scan showing large tumor mass arising from bladder and extending through peripelvic fat to left lateral pelvic wall (arrows). Surgical confirmation.

ment of anatomic structures than in the upper abdomen (fig. 27).

Thorax (table 10)

All patients studied with CT scans had abnormal plain chest roentgenograms. Sixteen patients with solitary pulmonary lesions were evaluated. In three patients with indeterminate conventional radiographs, CT scans strongly suggested the correct diagnosis (calcification indicative of benignity in two, irregularity and infiltration without calcification consistent with malignancy in another). In the remaining 13 cases, the CT scan was no more definitive or correct than plain radiographic or conventional tomographic examination.

In one patient with intrathoracic malignancy previously proven by aspiration needle biopsy, the extent of the lesion



Fig. 25.—21-year-old woman with palpable right adnexal mass; barium enema and urogram normal. CT scan showing 4 cm soft tissue mass (arrows) contiguous with right lateral pelvic wall. Surgery disclosed fibrosarcoma.

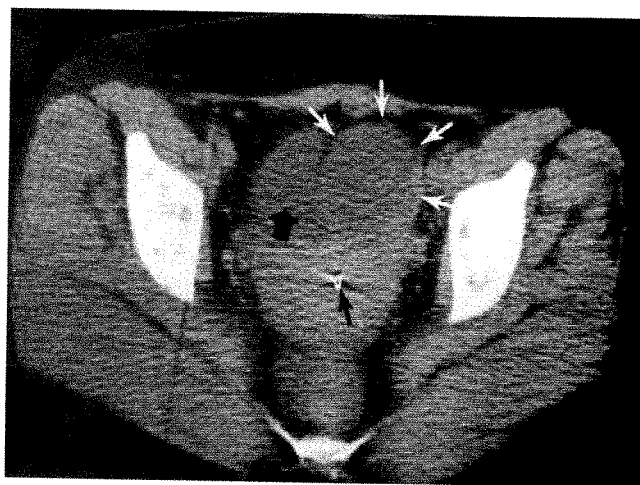


Fig. 26.—Asymptomatic 27-year-old woman with palpable left adnexal mass. CT scan showing sharply demarcated round 5 cm mass (white arrows) of low attenuation (5 EMU units) in left anterolateral aspect of pelvis. Urinary bladder (large black arrow) of identical attenuation to mass is displaced to right. Mass consistent with cyst. High density contraceptive device (small black arrow) present in center of uterus. Surgery disclosed benign left ovarian cyst.

demonstrated on the CT scan aided the referring surgeon in a decision to substitute radiation therapy for resection. Two patients with proven bronchogenic carcinoma who were being evaluated prior to radiation therapy had multiple small pulmonary metastases discovered on CT scanning which were seen only in retrospect on the plain chest radiograph.

CT scanning was valuable in determining the etiology of four of nine mediastinal lesions studied. Cases precisely diagnosed were mediastinal extension of multiple myeloma (fig. 28), pericardial fat pad, herniated retroperitoneal fat, and a bronchogenic cyst. Further workup was obviated by the CT findings in the first three cases. In a case of aortic dissection, it was seen on the CT scan that the widened mediastinum was due to an aortic aneurysm; but it was

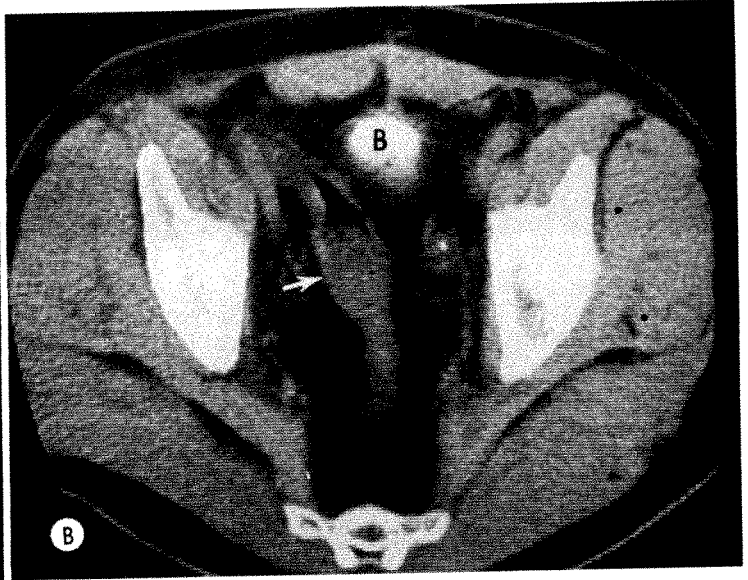


Fig. 27.—61-year-old man with vague abdominal pain. A. Barium enema demonstrating elevation of sigmoid colon out of pelvis; etiology uncertain (? mass, ? adhesion). Urogram normal. B. CT scan showing no evidence of mass surrounding sigmoid colon (arrow). Abundance of fat present within pelvis; bladder (B) filled with contrast media. CT findings obviated need for further diagnostic workup of questionable pelvic mass.

impossible, even after intravenous injection of contrast media, to diagnose the presence of a dissection. No mediastinal lesion was discovered in seven patients with known bronchogenic carcinoma or lymphoma in whom the mediastinum was normal on the plain chest radiograph.

Pericardial effusion was diagnosed by CT scanning in the one patient studied for this problem. Both ultrasonography and fluoroscopy were also positive in this patient.

Although more cases will be investigated (including controlled studies), it is not anticipated that the impact of CT, at least in its current state, will be as great in the evaluation of cardiopulmonary disease as in diseases involving the solid abdominal and pelvic organs.

Discussion

The disproportionately large number of scans of the abdomen (table 1) are a reflection of several factors: (1) the preferential selection by radiologists of liver and pancreas studies after initial experience suggested that these studies were the most efficacious; (2) the large number of diagnostic problems involving the upper abdomen as experienced by the referring physicians; (3) the much higher level of diagnostic accuracy of conventional radiologic studies in the chest and extremities in comparison to the solid abdominal organs; and (4) the availability of two EMI brain scanners within the radiology department to handle the bulk of the brain cases.

Of the 48 proven liver cases (table 3), the CT diagnosis was correct in 46 (95.8%). The majority of the unconfirmed

cases (66%) are from the "normal" category. Based on their clinical course, many of these patients are presumed to have normal livers or diseased livers which would appear normal by CT scan.

The lowest level of accuracy occurred in the pancreas studies (table 6) in which there were six errors in 37 proven cases (83%). In general, the diagnostic information was present on the CT scan but because of minimal experience the interpretation was faulty. Findings could be seen in retrospect which were not readily apparent to the examiners at the time of the study. It is anticipated that the current accuracy rate will improve significantly as experience is gained. Note that the majority of unconfirmed cases is again from the normal category, the presumption being the same as in the liver cases.

Only patients with abnormal excretory urograms were referred for CT scans of the kidney. In view of the fact that the conventional workup of renal masses (employing urography, ultrasound, and arteriography) has a diagnostic accuracy approaching 98%, it was not anticipated that CT would play a significant role in this area. However, experience now shows that CT scans can resolve indeterminate (mixed echo patterns) or technically unsatisfactory ultrasound scans and obviate the need for arteriography in a significant number of cases.

Of the 17 proven renal cases, the CT diagnosis was correct in 16 (94%). Sixteen of the 18 unconfirmed cases were diagnosed as cyst(s) by CT scan. This suggests that the clinicians started to accept the CT scan results, often

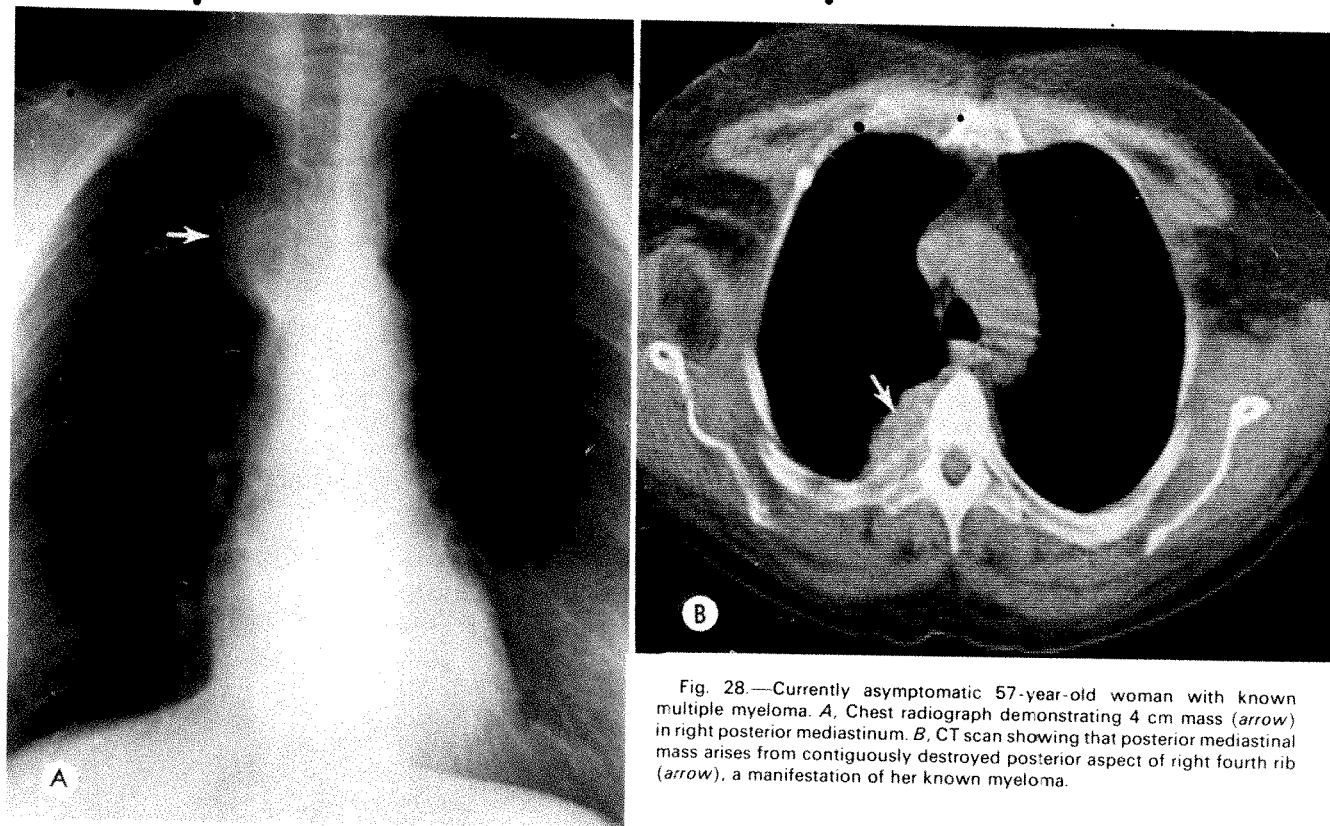


Fig. 28.—Currently asymptomatic 57-year-old woman with known multiple myeloma. *A*, Chest radiograph demonstrating 4 cm mass (arrow) in right posterior mediastinum. *B*, CT scan showing that posterior mediastinal mass arises from contiguously destroyed posterior aspect of right fourth rib (arrow), a manifestation of her known myeloma.

conjunction with ultrasound findings, as definitive, electing to forego needle aspiration which has been the standard procedure until now.

The 27 proven cases from the CT scans of the pelvis and extraperitoneal space (tables 8 and 9) were all correctly interpreted. Eleven of the 18 unconfirmed cases are considered normal by CT. Six masses clinically presumed to be neoplasms have not yet been biopsy proven.

The initial studies on a variety of pelvic tumors suggest that gross extension toward or to the pelvic wall can be assessed quite accurately. In several cases the bulk of the tumor mass, as seen on the CT scan, far exceeded clinical impressions and resulted in an alteration of the radiation therapy plan. In one instance a suspected mass elevating the sigmoid colon out of the pelvis was shown by CT to be simply increased pelvic fat (fig. 28).

One of the most difficult factors to assess is the actual effect of CT on patient management. Specific statements in the patient's record regarding the influence of the CT scan on subsequent management were infrequent. However, an analysis of the charts showed that CT results influenced management in the following ways: (1) made the definitive diagnosis when other nonoperative methods had failed, leading to specific therapy; (2) brought a potentially lengthy evaluation to a halt, thereby expediting or obviating surgery; and (3) in a few instances caused a change in radiation port size or obviated the need for continued therapy. (In one of the two cases where therapy was terminated, CT detected occult pulmonary metastases, and in

the other the presence of a clinically suspected retroperitoneal mass was disproved.) A systematic study of the effect of CT scanning on decision making by the referring physician is in progress.

Problems encountered in CT scanning of the abdomen include the two extremes of body weight. Very obese patients do not fit within the scanning ring if the part of their body to be scanned has a circumference exceeding 45 inches. As already mentioned, cachectic patients are poor subjects for CT scans because they lack the perivisceral fat needed to delineate organs and related anatomic structures. The resultant scans may or may not be interpretable depending upon which organ is being studied. The visibility of the pancreas and retroperitoneum is affected the most when body fat is absent.

If the patient is unable to hold his or her breath for 18 sec, the quality of the scan is compromised and the images resemble those obtained with scanners requiring 2 min or more of scanning time [6, 7]. Diagnostic information can still be obtained if the lesion is large enough or the organ being studied moves only minimally with respiration.

High density material such as barium, highly concentrated iodinated contrast agents (Pantopaque, Ethiodol), opaque nasogastric tubes, metallic surgical clips, and internal pacemakers degrade the quality of the image by producing star or streak artefacts. If barium is present on the scout film in the area of interest, a single test scan should be processed. If no bowel or respiratory motion is present, the barium will not interfere. However, slight motion of the

barium results in significant degradation.

Conclusions

The initial data from CT scans of the abdomen indicate that this diagnostic method may prove to be the primary radiologic test for evaluation of the liver, pancreas, and retroperitoneum. Prospective studies are underway to compare CT with (1) radionuclide scans of the liver and spleen, (2) abdominal ultrasound, (3) lymphangiography in lymphoma patients, and (4) conventional contour determination and tumor localization for treatment planning in radiation therapy.

In view of the demonstrated ability of CT to define pancreatic tumors, arteriography to evaluate the pancreas will rarely be indicated when the CT scan is positive. There are currently no data to indicate what the tumor detection rate of arteriography would be when the CT scan of the pancreas is "normal."

It is already apparent that CT will aid in the evaluation of renal masses and nonfunctioning kidneys. As the validity of CT diagnosis becomes established, the need to percutaneously aspirate renal cysts or perform arteriography for indeterminate renal masses will diminish.

The role of CT in the chest is less clear. In the majority of cases studied, CT yielded no more information than conventional radiologic examinations. Definitive diagnosis was possible in a few lesions of the lung and mediastinum when specific composition of the lesion was revealed (i.e., fat, water density, or calcification not discernible on radiographic film). Additional experience should serve to identify those clinical situations in which CT scanning might be beneficial.

ACKNOWLEDGMENTS

We wish to express our gratitude to Drs. Ronald G. Evens and

Michel Ter-Pogossian for advice and assistance and to Timothy Aly, Judith Cortner, and Sue Day for their untiring effort.

REFERENCES

1. Paxton R, Ambrose J: The EMI scanner. A brief review of the first 650 patients. *Br J Radiol* 47:530-565, 1974
2. New PFJ, Scott WR, Schnur JA, Davis KR, Taveras JM: Computerized axial tomography with the EMI scanner. *Radiology* 110:109-123, 1974
3. Baker HL Jr, Campbell JK, Houser OW, Reese DF: Early experience with the EMI scanner for study of the brain. *Radiology* 116:327-333, 1975
4. Evens RG: New frontier for radiology: computed tomography. *Am J Roentgenol* 126:1117-1129, 1976
5. Baker HL Jr: The impact of computed tomography on neuro-radiologic practice. *Radiology* 116:637-640, 1975
6. Alfidi RJ, Haaga J, Meaney TF, MacIntyre WJ, Gonzalez L, Tarar R, Zelch MG, Boller M, Cook SA, Jelden G: Computed tomography of the thorax and abdomen; a preliminary report. *Radiology* 117:257-264, 1975
7. Twigg HL, Axelbaum SP, Schellinger D: Computerized body tomography with the ACTA scanner. *JAMA* 234:314-317, 1975
8. Hounsfield GN: Computerized transverse axial scanning (tomography). I. Description of system. *Br J Radiol* 46:1016-1022, 1973
9. Sagel SS, Stanley RJ, Evens RG: Early clinical experience with motionless whole body computed tomography. *Radiology* 119:321-331, 1976
10. Brooks RA, DiChiro G: Theory of image reconstruction in computed tomography. *Radiology* 117:561-572, 1975
11. Haaga JR, Alfidi RJ, Zelch MG, Meaney TF, Boller M, Gonzalez L, Jelden GL: In vivo computed tomography of the pancreas. *Radiology*. In press, 1976

Computed Tomography of the Liver

RALPH J. ALFIDI,¹ JOHN R. HAAGA,¹ THOMAS R. HAVRILLA,¹ RICHARD G. PEPE,¹
AND SEBASTIAN A. COOK²

This work examines the scope and accuracy of CT in the detection of tumors, abscesses, cysts, and parenchymal disorders of the liver. While CT remains an emerging modality, it is shown to be equal to nuclear medicine in detecting mass lesions. It has also been possible to distinguish obstructive from nonobstructive jaundice. Presently, CT is not well suited to the study of cirrhosis. Technological advances in CT design and contrast agents offer promise of significantly improved resolution.

Recent investigations [1, 2] have shown the capability of CT in the diagnosis of a variety of abdominal and thoracic disorders. In the liver, primary and metastatic neoplasms, abscesses, cysts, and certain stages of cirrhosis are demonstrable. This communication includes a comparison of CT with nuclear medicine and a discussion of the use of contrast agents as well as CT as an adjunct in transhepatic cholangiography, biopsy, and drainage procedures.

Materials and Methods

This work was performed using an Ohio Nuclear Delta scanner which obtains two simultaneous 13 mm thicknesses in approximately 2½ min. Other characteristics of the machine have been described [1].

No attempt was made to limit respiratory motion. Patients were simply instructed to remain as motionless as possible for the duration of the scan. Between eight and 16 thicknesses were obtained depending upon the dimensions of the liver.

Scanning patients in the right lateral decubitus position appeared to be helpful in decreasing motion artifacts. When large amounts of gas were present in the stomach, nasogastric suction was of some value. The use of antiperistaltic drugs was also partially successful.

Biopsies were performed by localizing the area of pathology, marking the skin with an intraepidermal needle, and progressively advancing a biopsy needle into the site of pathology as monitored by repeated scans. Transhepatic CT cholangiograms were performed in several patients. Films were obtained with mobile equipment once the contrast was instilled into the biliary tree. Abscess aspirations were performed in the same manner.

The use of contrast material greatly enhances differential attenuation coefficients in normal and abnormal liver tissue. When contrast enhancement was desired, 50–100 ml of Renografin 60 was injected intravenously in a bolus. Scans were performed immediately thereafter.

A total of 76 patients were studied. In 61, both CT and nuclear medicine scans were available; in 15, only CT scans were performed.

Results

Results of CT and nuclear medicine scans are listed in table 1. Table 2 shows a separate group of patients having either common bile duct or cystic duct obstruction.

TABLE 1

Results of CT and Nuclear Medicine

Diagnosis	No. Cases	Correct by CT	Correct by Nuclear Medicine
Normal	10	9	8
Provisionally normal*	10	8	9
Total	20	17	17
Mass Lesions of liver:			
Primary and metastatic tumors:			
Biopsy proven	10	9	9
Clinical and laboratory evidence	9	7	7
Surgically proven	3	1	1
Abscess	2	1	1
Regenerating nodules	1	1	1
Polycystic renal and liver disease	1	1	1
Total	26	20	20
Cirrhosis (biopsy proven)	11	8	10
Toxic hepatitis	2	0	2
Triaditis	2	0	2

* Patients with a proven disorder that could produce an imaging abnormality in the liver. However, based on final clinical diagnosis the liver was not believed to be involved.

TABLE 2

Diagnosis of Cystic or Common Bile Duct Obstruction

Diagnosis	No. Cases	CT Positive
Cystic duct obstruction (stones)	3	3
Common bile duct obstruction:		
Stone	1	1
Tumor	3	3
Pancreatitis	1	0
Total	5	4

Normal Liver

In 20 patients there were three false positive interpretations by both CT and nuclear medicine scans; the remaining 17 were correctly interpreted as normal. Two of the false positive CT diagnoses occurred in a group of 10 patients who had a proven disorder which could produce an imaging abnormality in the liver. However, based on final clinical diagnosis the liver was not believed to be involved. Because of the equivocal nature of this group and the fact that there were more false positives by CT than nuclear medicine in this group, they are listed separately in table 1.

Received March 1, 1976.

¹ Department of Radiology, Cleveland Clinic Foundation, 9500 Euclid Avenue, Cleveland, Ohio 44106.

² Department of Radiation Therapy and Nuclear Medicine, Cleveland Clinic Foundation, Cleveland, Ohio 44106.

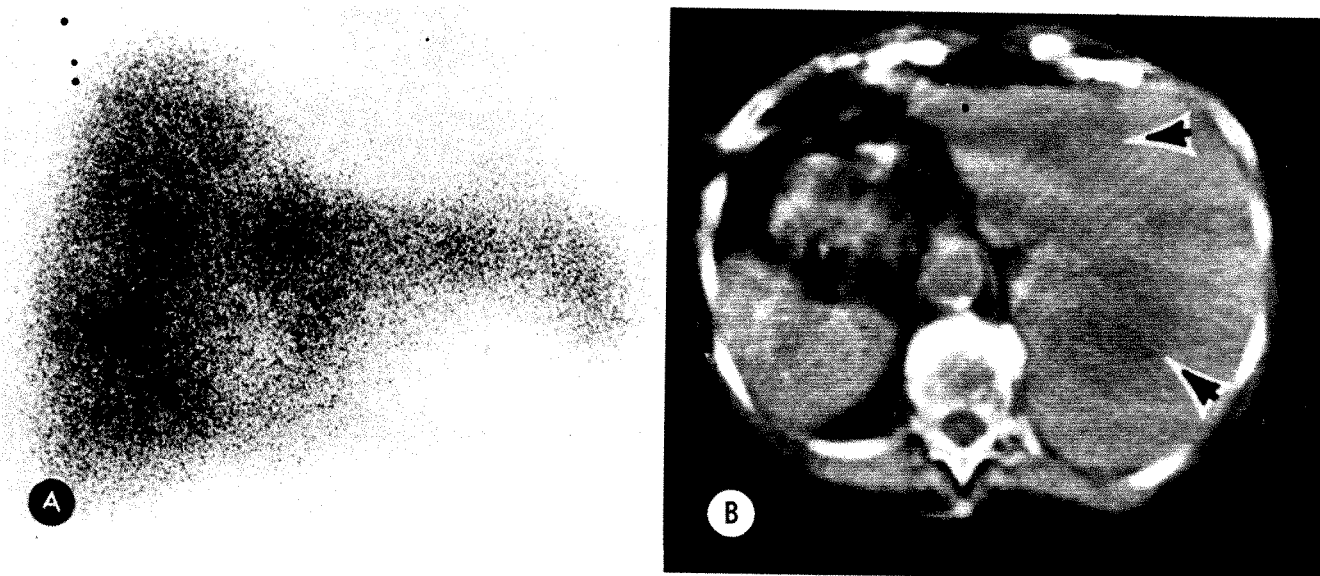


Fig. 1.—A. Technetium scan of metastases in liver. B. CT scan showing metastases in left and right lobe of liver.

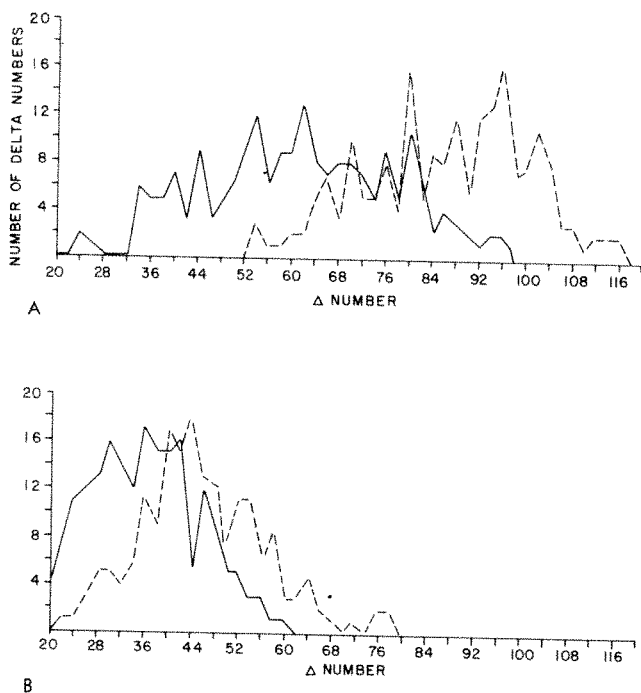


Fig. 2.—Histogram of hepatoma studied with and without contrast medium. A. Normal liver parenchyma without (solid line) and with (dashed line) contrast. B. Tumor parenchyma without (solid line) and with (dashed line) contrast. Although tumor parenchyma increased slightly in attenuation coefficient, normal liver parenchyma virtually doubled in attenuation after contrast enhancement.

Tumors

In the investigation of primary and metastatic liver tumors, CT and nuclear medicine studies proved identical in accuracy. Seventeen of 22 were correctly detected by CT and nuclear scans (fig. 1). Contrast enhancement made visual search much simpler in the detection of abnormalities (fig. 2). The majority of lesions were of lower density

(attenuation coefficient) than normal liver parenchyma (figs. 3 and 4). In one patient with extensive renal cell carcinoma metastatic to the liver, no evidence of differential density was seen with or without contrast enhancement.

Cysts

Cystic lesions of the liver were present in five patients. The absorption coefficients of cysts varied from 4 to 25 Delta units (fig. 5). When cystic lesions were large and their density closely approximated that of water (zero), the diagnosis was virtually pathognomonic. However, this does not imply that neoplastic lesions with large cysts and a small solid tumor in the wall are detectable by means of CT. Polycystic liver and renal disease was obvious in the several cases scanned to date (fig. 6).

Cirrhosis

Eleven patients were studied by CT and nuclear scans. CT showed an abnormality in only eight. This was characterized by a decrease in density of the hepatic parenchyma as a result of fatty infiltration (fig. 7). Conversely, nuclear scans were positive in 10 of the 11 cases. This diagnosis was made primarily as a result of reversal of the liver-spleen ratio in the technetium sulfur colloid scan. In retrospect, it would have been possible in several cases to implicate cirrhosis by CT based on increased splenic size relative to that of the liver.

Abscess

Five patients were found to have either intrahepatic or parahepatic abscess. In only two were both nuclear medicine and CT scans performed. Both studies were correct in the diagnosis of one. Intrahepatic abscesses demonstrated by CT were of lower attenuation coefficient (fig. 8) than the normal hepatic parenchyma either with or without contrast material. Two abscesses were aspirated by CT and one was surgically opened. One was treated primarily by

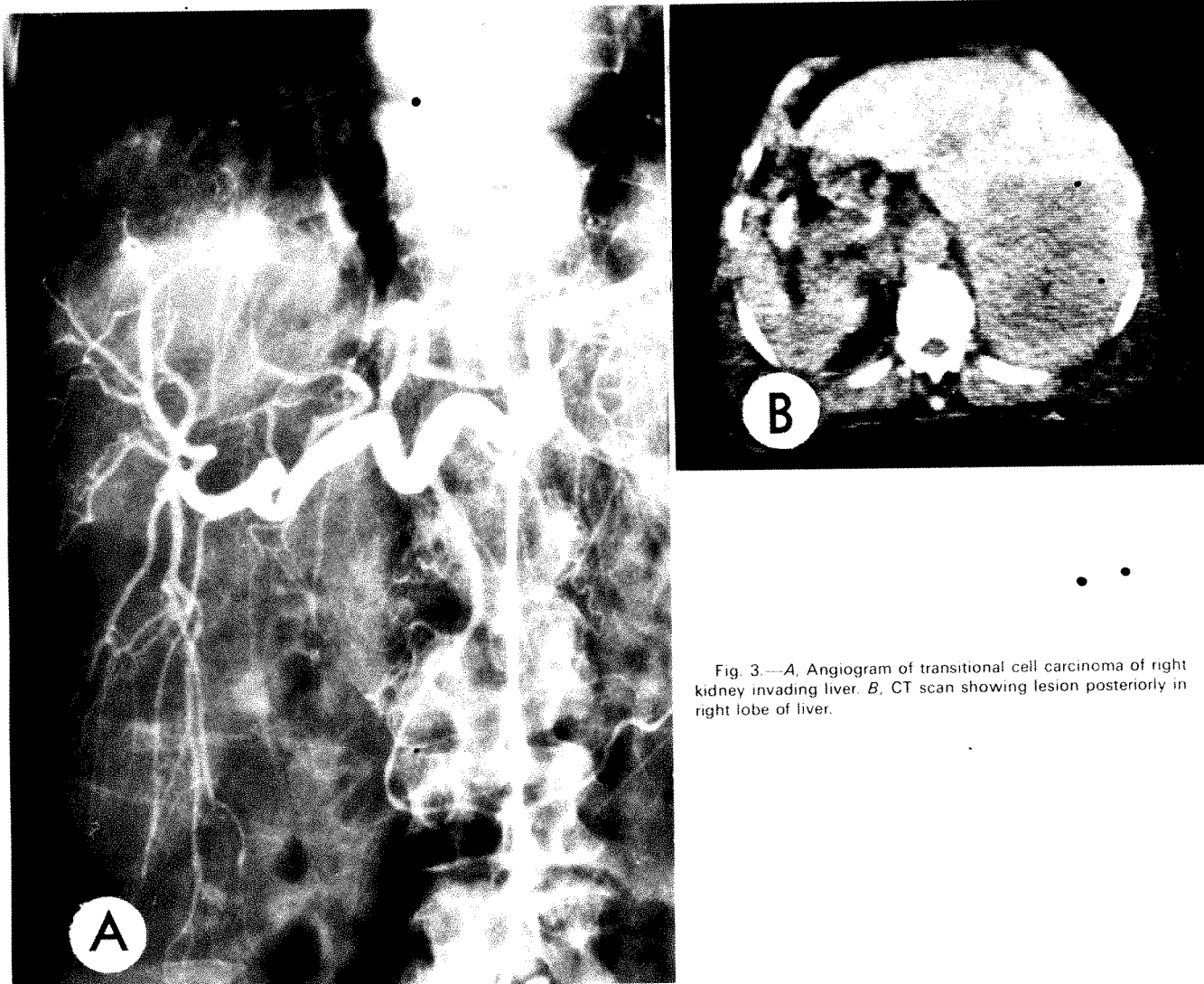


Fig. 3.—A, Angiogram of transitional cell carcinoma of right kidney invading liver. B, CT scan showing lesion posteriorly in right lobe of liver.

CT drainage following percutaneous placement of a trocar and balloon catheter in the abscess cavity. This resulted in cure of the abscess.

Obstructive Jaundice

CT studies were performed in five patients with obstructive jaundice. Dilated intrahepatic bile ducts were evident in the liver parenchyma and seen as low density branching structures (fig. 9A). This is due to the fact that bile has a considerably lower attenuation coefficient than normal liver parenchyma. In four of the five patients, CT correctly diagnosed the presence of obstructive jaundice. Two patients underwent transhepatic cholangiography "guided" by CT (fig. 9B).

Obstruction of the cystic duct was correctly diagnosed in all three patients with hydrops of the gallbladder. The gallbladder was seen as larger than normal, suggesting the presence of hydrops. Nonopaque gallstones were seen in the gallbladder in one case (fig. 10).

Discussion

This study establishes CT as a clinically useful entity in studies of the liver. At present, the usefulness of CT is hampered by (1) Z axis motion blurring; (2) superimposed motion artifacts; (3) lack of organ-specific contrast agents; and (4) failure to identify cirrhosis when significant amounts of fat are absent in the liver parenchyma. Experience should improve accuracy.

This study, performed on a $2\frac{1}{2}$ min scanner, will have to be reevaluated when shorter scan times become available. It has already been established that up to 50% of spatial and contrast resolution is lost as a result of respiratory motion [3, fig. 2]. Shorter scan times will significantly reduce motion blurring and eliminate or at least reduce superimposed peristaltic and respiratory motion artifacts.

Contrast Agents

Contrast agents have been shown to be quite useful in CT studies of hepatic parenchymal disorders [1]. As a general principle, the density of normal liver parenchyma in-

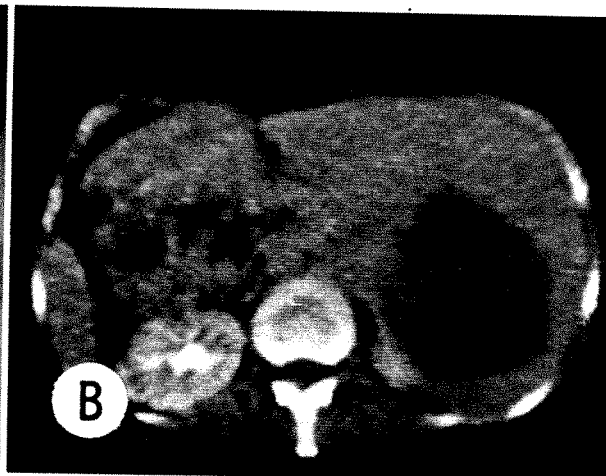
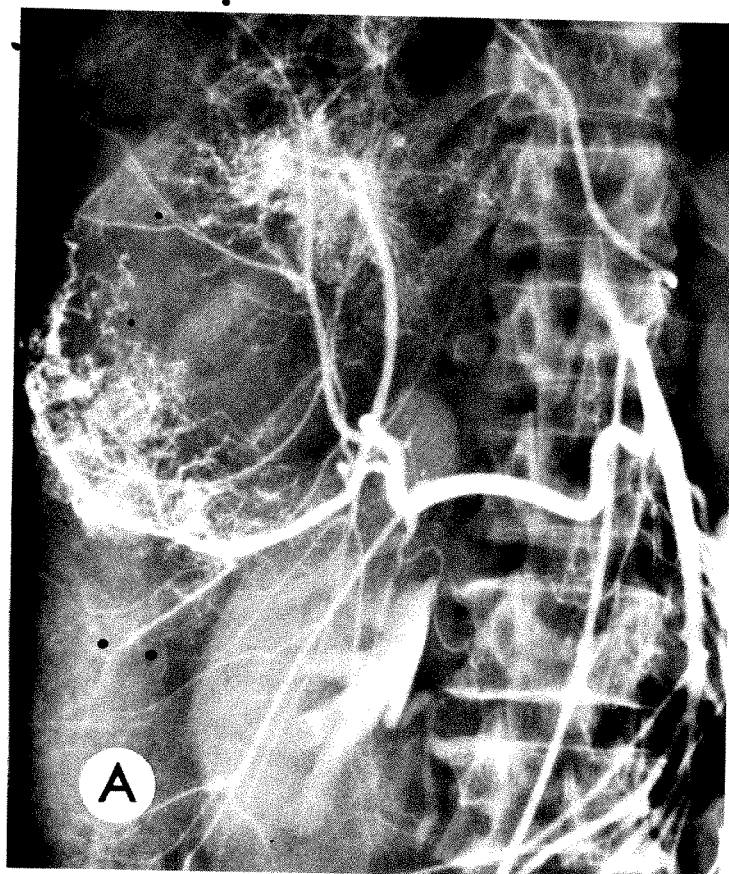


Fig. 4.—A, Angiogram showing vascular hepatoma in right lobe of liver. B, CT scan showing hepatoma as low density structure in posterior aspect of right lobe of liver.

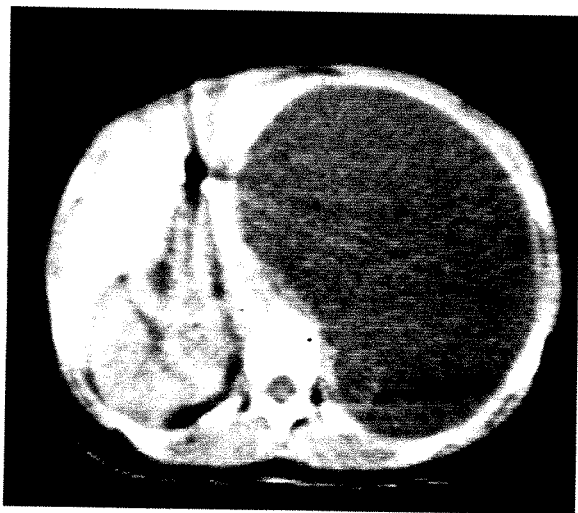


Fig. 5.—Large cystadenoma in right lobe of liver.

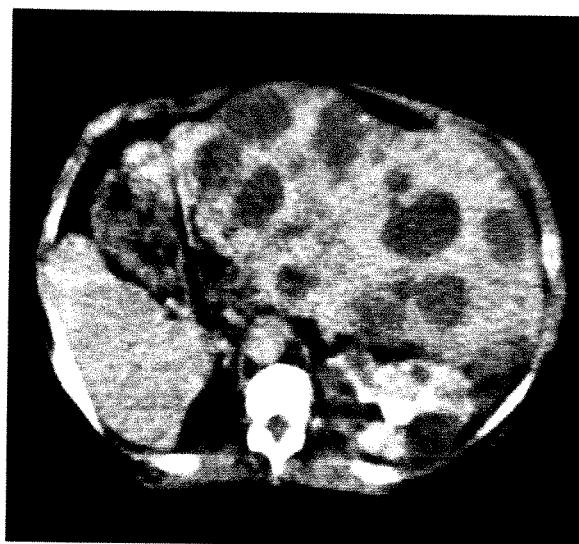


Fig. 6.—Polycystic liver and renal disease.

creases significantly, while that of abscesses, cysts, and bile ducts increases slightly or not at all. The increase in density of tumor parenchyma is intermediate between the two. In general, the effect is opposite that which occurs in the central nervous system when contrast material is used to enhance visualization of neoplasms. There have been several exceptions to date, so that CT studies should be conducted both with and without contrast enhancements

for the highest accuracy. When conventional contrast agents are used, the normal hepatic parenchyma increases in density proportionally to the dosage of iodine.

Three patients were studied using 20 ml of intravenous Cholografin. The increase in density of liver parenchyma was less than that observed using a 100 ml bolus of 60% Renografin. Since there is also a higher risk of adverse reactions with Cholografin, its use was abandoned.

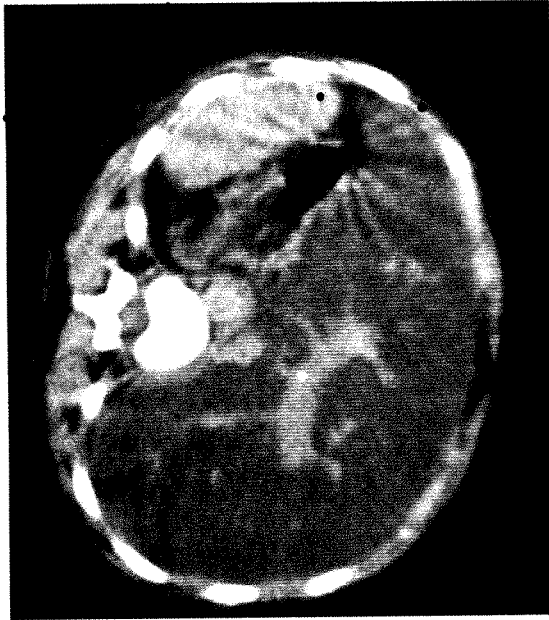


Fig. 7.—Scan of patient in right lateral decubitus position showing liver of considerably lower density than spleen due to fatty degeneration. Portal vein (never previously visualized in normal parenchyma) stands out clearly due to deposition of fat in liver.



Fig. 8.—Abscess in left lobe of liver (arrow).

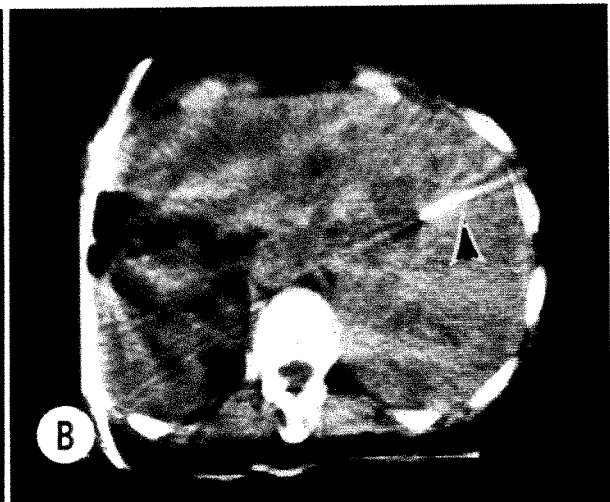


Fig. 9.—A, Multiple branching low density structures in hilum of liver are dilated bile ducts of obstructive jaundice. B, Guided transhepatic cholangiogram of same patient. Needle (arrow) inserted directly in confluence of dilated right and left hepatic bile ducts.

An experimental contrast agent (AG 60.99; Guerbet-Aulnay-sous-Bois, France) has been recently evaluated in animals [4]. It is a stable iodinated emulsion which promises improved visualization of mass lesions, the biliary tree, and even intrahepatic vasculature. It may also make possible the distinction between cirrhosis and normal parenchyma by CT.

Transhepatic Cholangiography

Presently, transhepatic cholangiograms are performed under "blind" conditions. CT offers the opportunity for guided transhepatic needle placement. The bile ducts are

routinely shown in opacified and nonopacified liver parenchyma as structures of low attenuation coefficient. Although time consuming and somewhat cumbersome, CT visualization of the bile ducts combined with CT-guided transhepatic cholangiography might be expected to reduce the incidence of complications of this procedure. With the aid of CT, failure to enter the dilated bile ducts should theoretically be eliminated.

CT Biopsy

As with cholangiography, "blind" biopsies of the liver may result in a missed diagnosis. With CT, an imaged ab-

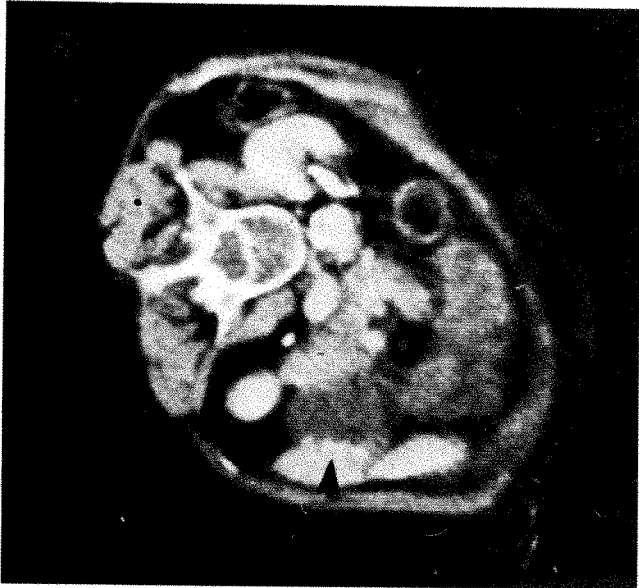


Fig. 10.—Scan of patient in right lateral decubitus position showing layered gallstones (arrows) within gallbladder.

normality can be biopsied with three-dimensional precision. Utilization of this modality may preclude the morbidity, mortality, and expense of laparotomy. This is also true of cyst aspiration and abscess drainage and culture.

To date, one intrahepatic abscess has already been treated primarily by CT puncture and insertion of a large drainage catheter with an attached balloon. No surgery was required, and the patient was discharged from the hospital cured of his intrahepatic abscess within 3 weeks.

In several cases, the extent of neoplastic involvement of liver by adjacent tumors could not be appreciated by means other than CT. Very recently, a case of metastatic neoplasm studied by both angiography and CT was not evident on prospective viewing of angiograms but was obvious on CT (fig. 3).

The future of CT is promising considering the advances in machine design and contrast medium technology. Although struggling through the problems of infancy, this modality offers outpatient imaging and histologic diagnosis in a variety of hepatic disorders.

REFERENCES

1. Alfidi RJ, Haaga JR, Meaney TF, MacIntyre WJ, Gonzalez L, Tarar R, Zelch MG, Boller M, Cook SA, Jelden G: Computed tomography of the thorax and abdomen; a preliminary report. *Radiology* 117:257-264, 1975
2. Philips RL, Stephens DH: Computed tomography of liver specimens. *Radiology* 115:43-46, 1975
3. Alfidi RJ, MacIntyre WJ, Haaga JH: The effects of biological motion on CT resolution. *Am J Roentgenol* 127:11-15, 1976
4. Alfidi RJ, Laval-Jeantet M: A liver-spleen CT contrast agent. Submitted for publication.

Computed Tomographic Evaluation of Aortic Aneurysms

STEWART P. AXELBAUM,¹ DIETER SCHELLINGER,¹ MARIO N. GOMES,² ROBERT A. FERRIS,¹
AND HALAPPA G. HAKKAL¹

Applications of computed tomography are being extended from the brain to other body parts. This report describes CT scanning of abdominal and thoracic aortic aneurysms in 30 patients. CT shows greatest promise in abdominal aortic scanning, where reliable identification of the aorta can be achieved even in the absence of enlargement or calcification. However, current limitations prevent visualization of internal detail such as intimal plaques or mural thrombi. Technical advances are described which should have an important bearing on this.

This paper describes our experience with CT as a method of delineating aortic aneurysms.

Materials and Methods

CT scans were obtained by means of an ACTA scanner in 32 patients [1, 2]. The majority were referred with known (by physical examination, x-rays, or ultrasound) aortic aneurysms in an effort to investigate the quality of aneurysm imaging with CT. As experience was gained, a smaller number, the remainder of this group, were referred for CT scanning as a primary diagnostic aid.

Abdominal aneurysms are scanned at the level of maximum

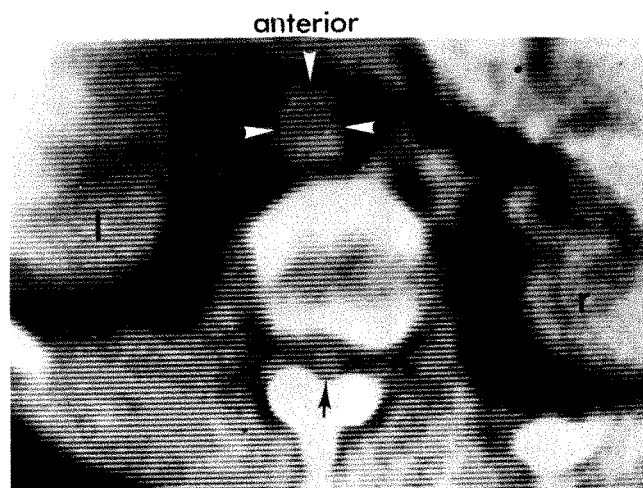


Fig. 1.—Normal aorta (arrowheads). Note also left (l) and right (r) kidneys, vertebra (white), and spinal cord (arrow) with neural foramina lateral to cord.

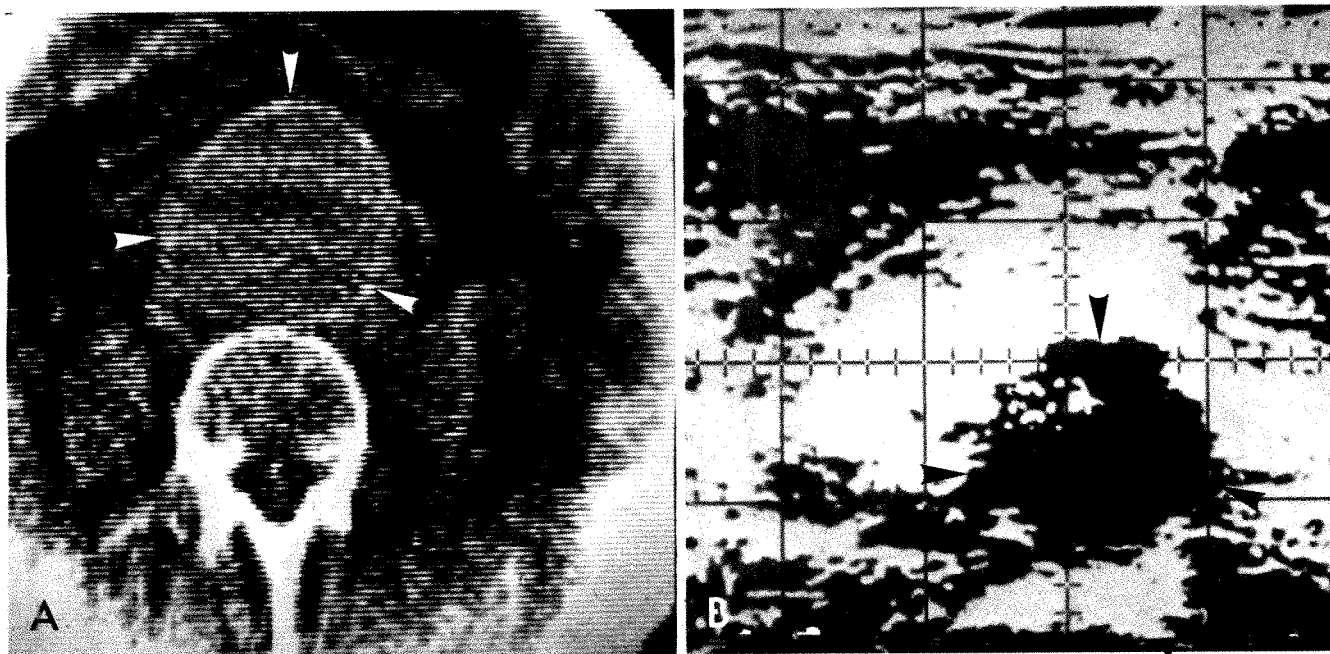


Fig. 2.—A, Abdominal aortic aneurysm (arrows) with calcific wall measuring 8 cm. Size estimate based on 1:4.2 scale measured from Polaroid print. B, Sonogram at same level showing 8 cm aneurysm (arrows). Crosshatches represent 1 cm intervals. Measurement confirmed at surgery.

¹ Department of Radiology, Georgetown University Hospital, 3800 Reservoir Road NW., Washington, D.C. 20007. Address reprint requests to S. P. Axelbaum.

² Department of Surgery, Georgetown University Hospital, 3800 Reservoir Road N.W., Washington, D.C. 20007.

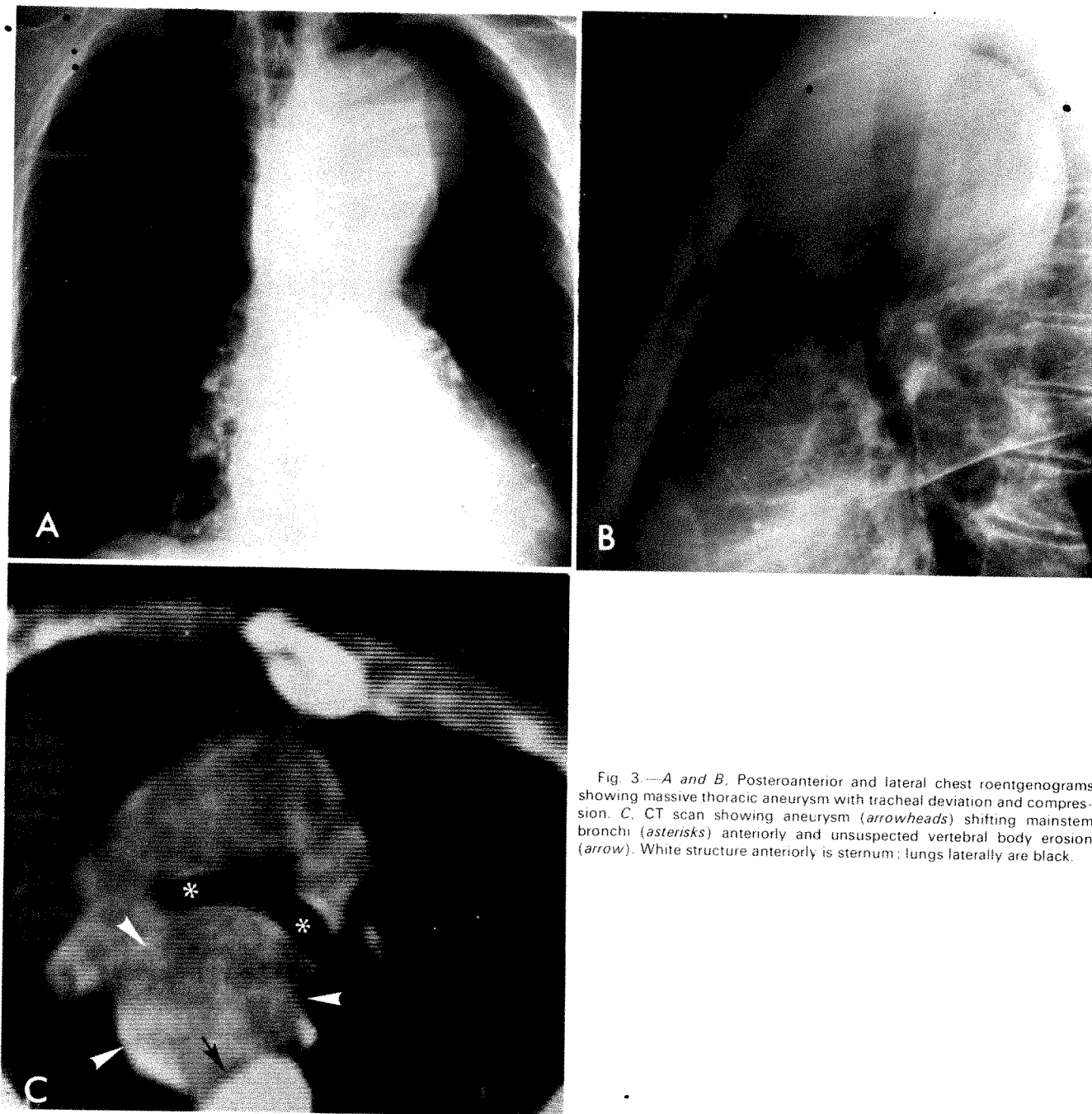


Fig. 3.—*A and B*, Posteroanterior and lateral chest roentgenograms showing massive thoracic aneurysm with tracheal deviation and compression. *C*, CT scan showing aneurysm (*arrowheads*) shifting mainstem bronchi (*asterisks*) anteriorly and unsuspected vertebral body erosion (*arrow*). White structure anteriorly is sternum; lungs laterally are black.

palpable aortic diameter. For thoracic and nonpalpable abdominal aneurysms, the plain x-rays serve as a guide for the section level. A minimum of three scans are made at 2 cm intervals. Each scan results in a pair of transverse images 7.5 mm thick. The radiation dose at the skin is approximately 2 rads.

All patients had conventional radiographs of the abdomen in anteroposterior and lateral projections. Ten of the abdominal aneurysms were also evaluated with A- and B-mode ultrasound, the latter in both horizontal and longitudinal orientation.

Results

Five thoracic and 25 abdominal aortic aneurysms were visualized with CT. Scans in two patients clinically sus-

pected of having abdominal aortic aneurysms demonstrated abdominal aortas of normal size.

The aorta, whether calcified or not, is nearly always visible as a discrete structure on ACTA scan sections. The normal descending thoracic and abdominal aorta is easily recognized anterior and to the left of the spine as a homogeneous round moderately dense image (fig. 1). The vessel wall is indistinguishable from intraluminal blood content unless the wall is calcified (fig. 2). We have as yet been unable to detect the presence of arteriosclerotic plaques or thrombi. When the aorta dilates, it becomes eccentrically shaped; and, of course, its relation to the spine may change markedly with increasing aortic tortuosity. In some cases, vertebral

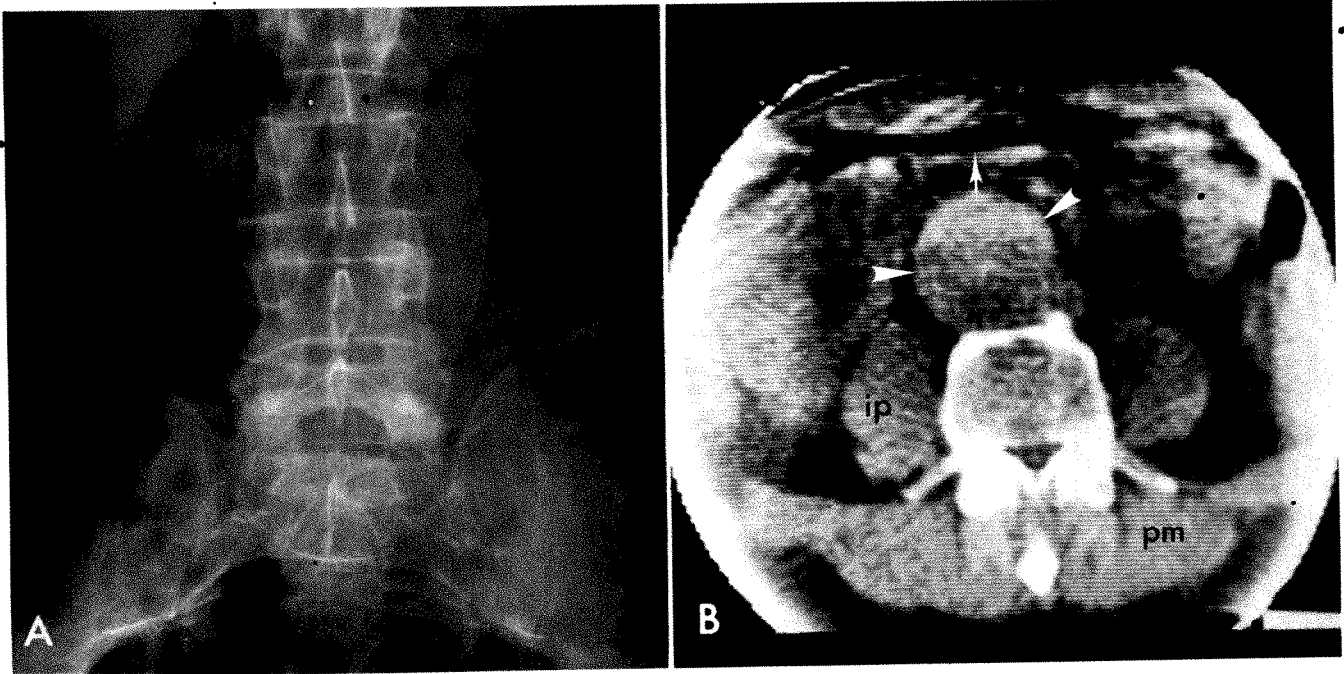


Fig. 4.—A, Abdominal aneurysm delineated laterally by its calcific wall; medial wall not recognized. B, CT scan showing more accurate depiction of transverse extent of aneurysm (arrowheads). Note air-fluid level in stomach (arrow), prominent iliopsoas (ip), and posterior paravertebral muscles (pm) in this mesomorphic individual.

body erosion is evident as well as pressure effects on other adjacent structures (fig. 3).

The 10 sonograms performed visualized abdominal aortic aneurysms as sonolucent structures, some with internal echoes thought to represent thrombus. With plain roentgenography the calcified portions of abdominal aneurysms were visualized in the majority of cases, although the full extent of the aneurysm was often not apparent (fig. 4).

Estimates of aneurysm size were made at surgery in 10 patients. There was no discrepancy greater than 2 cm between the surgical finding and CT predictions. Similarly, measurements of size and extent of aortic aneurysms by CT and sonography correlated very well.

Discussion

Calcification is usually a prerequisite to plain x-ray visualization of abdominal aneurysms. However, in some series visible calcification has been absent in 14%–45% of aneurysms [3, 4]. CT has the advantage of delineating the aorta regardless of calcification.

The scan is quite helpful in defining an aneurysm in patients with an abdominal mass lacking the usual clinical features of an aneurysm. It is also helpful in excluding aneurysm, as was true in two of our patients. The value of serial scanning in nonoperative management of aneurysms is self evident.

Thoracic aortic aneurysms are also consistently visualized on CT scans. On plain films the medial wall of the descending thoracic aorta is sometimes difficult to visualize, whereas it is easily seen on CT. Thus differentiation of aortic tortuosity and aneurysmal dilatation should be facilitated. In gen-

eral, however, CT has had less impact in the thorax than the abdomen because the thoracic aorta is usually displayed well enough with plain x-rays to allow at least a presumptive diagnosis of aneurysm.

While opaque media and air in the gastrointestinal tract cause streaks on abdominal scans, some information about the aorta can still be obtained. This is a potential advantage over sonography, a technique substantially restricted by these sources of artifact.

Technologic advances on the horizon may soon alleviate the difficulties currently experienced with CT scanning. In our experience thus far, current resolution does not permit the recognition of mural thrombus and luminal patency. A second problem is the limited view of the aorta afforded by a single scan. Only a 2 cm length of this structure is included in a scan resulting from a full 5 min exposure. The more encompassing image provided by the longitudinal sonogram or plain x-ray is lacking. A third restricting factor is the cost of the examination. At the current level of acquisition and staffing costs, a charge of \$200.00 is considered average for 30 min of machine time.

Instruments with shorter scanning cycles and numerous x-ray source detector combinations have already been introduced. These will allow larger areas of the body to be studied in less time and will improve resolution by minimizing the effects of visceral motion. Computer reconstruction of anatomy in the sagittal and coronal planes from multiple horizontal scans has been achieved in CT brain imaging [5], and we are currently attempting to extend the technique to the aorta.

ACKNOWLEDGEMENT

We thank Dr. Giovanni Di Chiro for reviewing the manuscript.

Computed Tomography of the Heart

M. M. TER-POGOSSIAN,¹ E. S. WEISS,² R. E. COLEMAN,³ AND B. E. SOBEL²

In an attempt to evaluate the possible usefulness of transmission computed tomography, CT scans of the chest of a series of dead dogs were obtained by means of an EMI body scanner. The sections thus obtained with and without the injection of contrast material reveal a great deal of cardiac morphology. Infarcts of the heart produced prior to scanning were imaged as regions of lower x-ray attenuation. The hearts of a series of live dogs following infarction were imaged by means of a positron emission transverse tomograph (PETT) following administration of ¹¹C-palmitate. The images permitted assessment of the relative size of the infarct. The relative advantages of transmission and emission tomography in cardiac visualization are discussed.

Introduction

Visualization of the myocardium and the cardiac chambers by transmission and emission CT to assess their anatomic and functional integrity is an attractive goal, but a formidable challenge. Transverse tomographic sections of the myocardium obtained by these noninvasive techniques offer promise of supplying information about the structure of the heart as a pump and the nature and extent of injury sustained by myocardium. However, the motion of the heart during the cardiac cycle interferes with presently available CT reconstruction methods. At least two approaches have been proposed to minimize the effect of cardiac motion: (1) synchronizing the tomographic data acquisition with the cardiac cycle, and (2) decreasing the CT data acquisition time sufficiently so that cardiac motion no longer interferes. Accordingly, it is probable that the heart will soon be amenable to CT investigation in keeping with the already impressive array of organs imaged by this technique.

We have utilized emission transaxial tomography, an approach employing a reconstruction technique similar to that used in transmission tomography to provide a quantitative picture of the distribution of a radionuclide in a transverse section. Emission transaxial tomography has already been used to evaluate myocardial perfusion and metabolism with a number of radiopharmaceuticals. The purpose of this report is to outline, on the basis of a few very preliminary experiments, the relative merits of transmission and emission CT for the evaluation of the myocardium itself as well as cardiac chamber dimensions and morphology and functional imaging of the heart.

Transmission Tomography

Presently available body scanners provide images of the heart in vivo with no distinguishable morphology other than its outline. The motion of the heart during the few

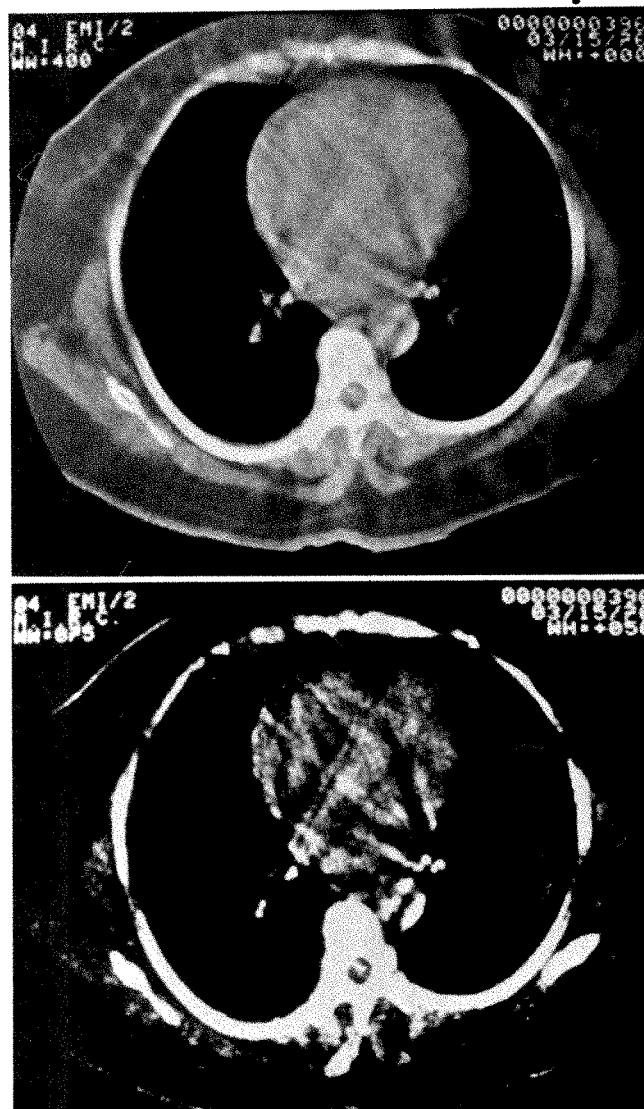


Fig. 1.—Transmission CT scans of beating human heart. Images differ by window setting. Section thickness 13 mm; scan time 20 sec per section.

seconds needed for data collection interferes with the reconstruction process and leads to obliteration of nearly all distinguishable features (fig. 1). This difficulty can be overcome either by reducing the data collection time to a few milliseconds, as proposed by the Mayo Clinic group who performed promising pioneering work in this direction [1], or by synchronizing the data collection system so as to

Received March 24, 1976.

This work was supported by U. S. Public Health Service grants 5 PO1 HL13851 and HL17646.

¹ Division of Radiation Sciences, Mallinckrodt Institute of Radiology, Washington University School of Medicine, 510 South Kingshighway, St. Louis, Missouri 63110. Address reprint requests to M. M. Ter-Pogossian.

² Cardiovascular Division, Department of Medicine, Washington University School of Medicine, St. Louis, Missouri 63110.

³ Division of Nuclear Medicine, Mallinckrodt Institute of Radiology, St. Louis, Missouri 63110.

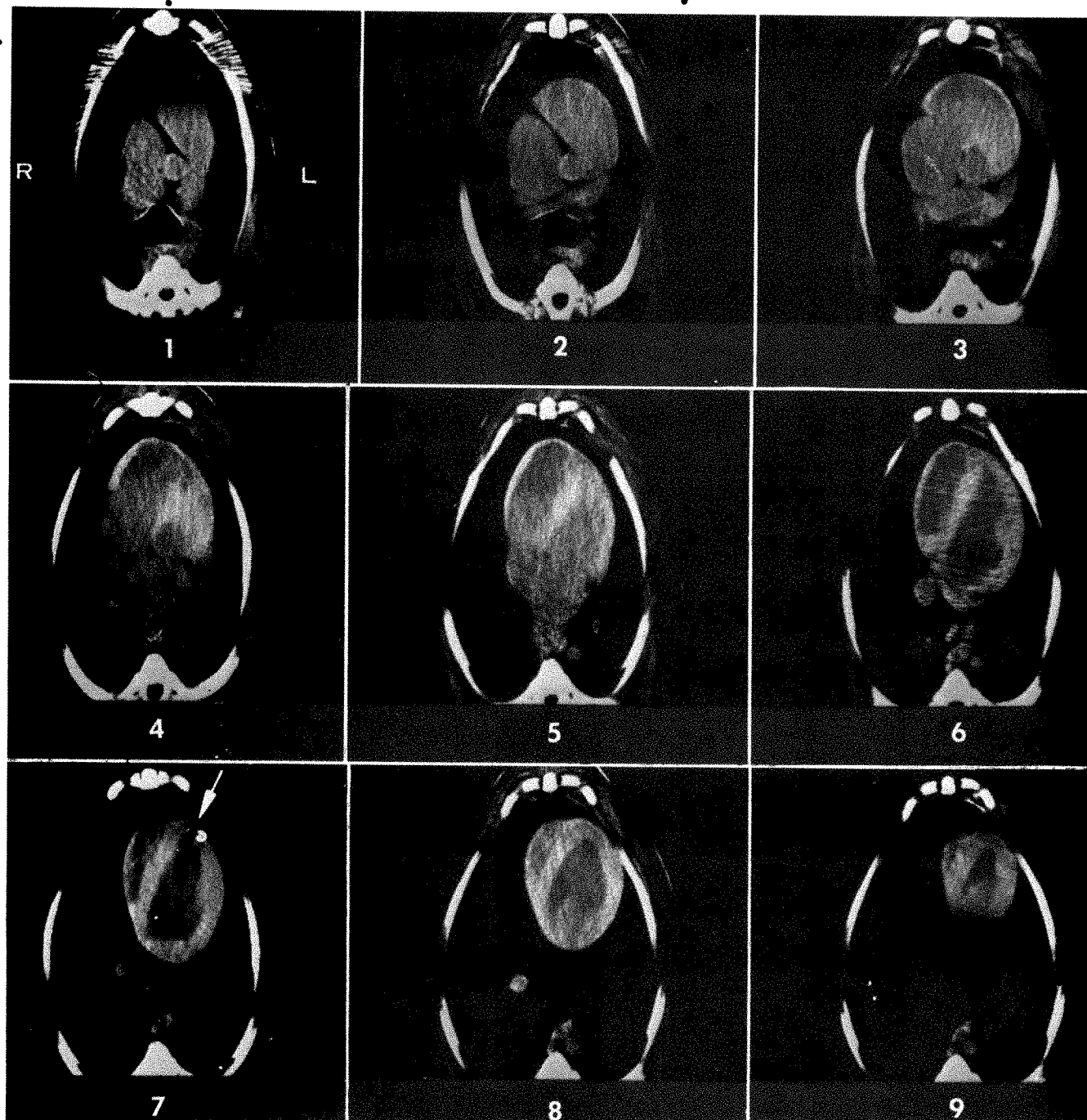


Fig. 2.—Transmission CT scans of dead 30 kg mongrel dog (no. 22) 13 days post LAD coronary occlusion. Dog heparinized before death and scanning. Section thickness 13 mm; scan time 80 sec per section. Small left ventricular infarct visible anteriorly (arrow).

integrate during the data collection period of the CT system different profiles of the heart taken during the same phase of its cycle. The latter approach is presently under investigation in our laboratory. As a first step in evaluating the possible usefulness of this synchronization approach, we have stopped the heart motion of dogs during CT data acquisition, not by synchronization, but by sacrificing the animal.

Experimental Procedure

The CT apparatus used in our studies is the prototype of the EMI CT 5000 body scanner (EMI Ltd., Hayes, England). In all experiments the field scanned was 10 inches in diameter, with a measured resolution of approximately 1.5 mm. The thickness of the slice was either 13 or 6 mm (specified in figure legends).

The animals used in the experiments were large mongrel dogs (17–30 kg body weight). Prior to imaging, each animal except one underwent ligation of the left anterior descending coronary artery.

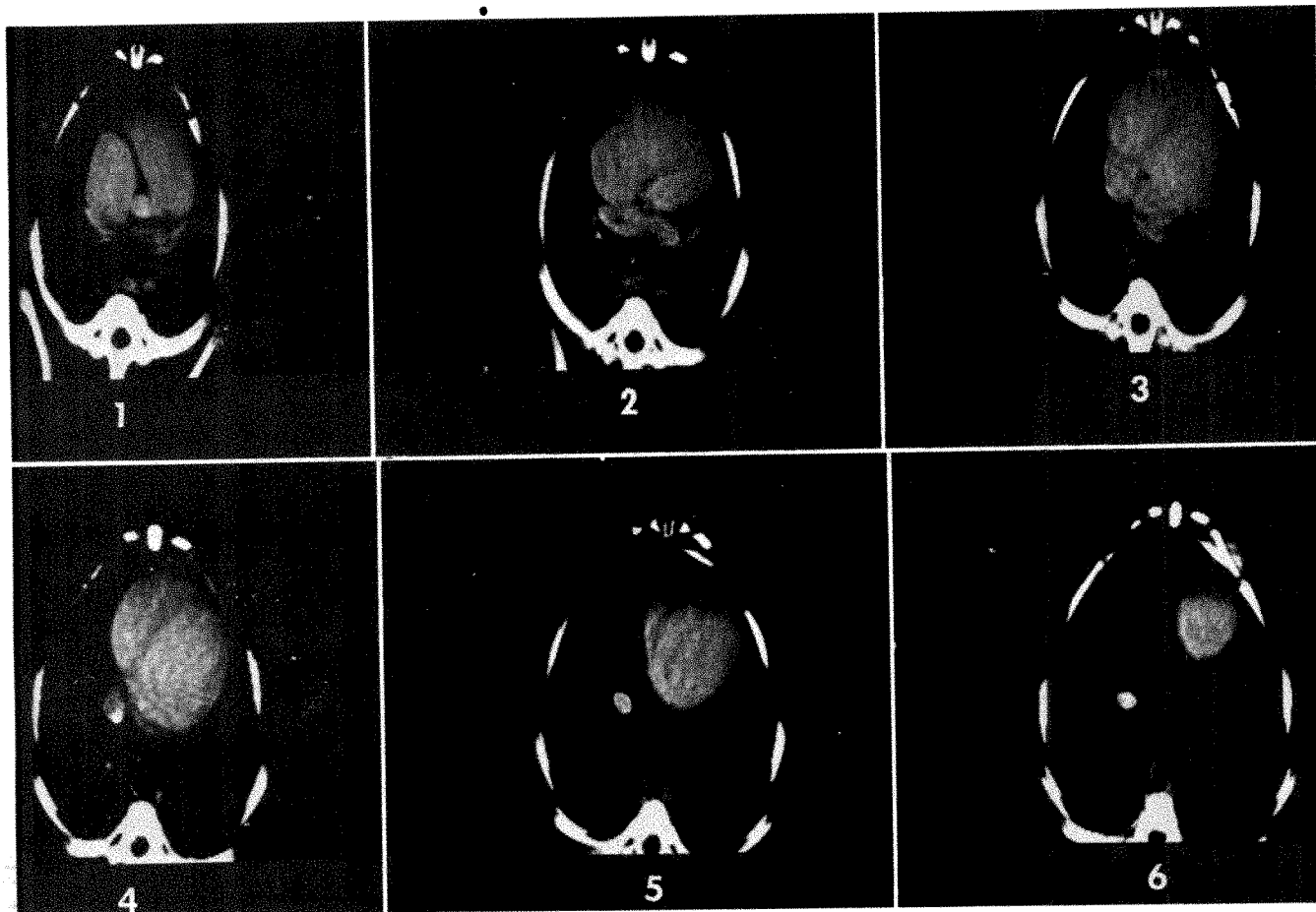


Fig. 3.—Transmission CT scans of dead 17 kg mongrel dog (no. 24). Dog heparinized before scanning and injected with contrast before death (see text). Section thickness 13 mm; scan time 20 sec per section; orientation as in fig. 2.

The time interval from coronary occlusion to scanning is indicated in the figure legends. The scans were performed with the dogs in the supine position, with scanning times from 20 to 80 sec.

Animals were anesthetized by intravenous injection of sodium pentobarbital (30 mg/kg). An anteroposterior radiograph of the chest was obtained, with lead markers placed on the chest for correlation with CT sections. The animal was placed in the CT device, scanned in the living state, and then sacrificed by rapid intravenous administration of sodium pentobarbital (60 mg/kg). Some of the animals were heparinized prior to death by intravenous administration of 3,000 U of heparin. As soon as cardiac motion had ceased, between five and eight CT scans were obtained from the base to the apex of the heart, at intervals of approximately 1 cm. The total time elapsed between the beginning of the first scan and the end of the last was approximately 40 min.

Six dogs were scanned without contrast and two after administration of meglumine iohalamate (Conray-60, 600 mg/ml). The contrast material (approximately 1 mg/kg) was infused over a period of approximately 15 sec. Ten seconds after starting the intravenous infusion of contrast, the dog was sacrificed by simultaneous administration of pentobarbital into a separate venous catheter. Termination of the infusion of contrast corresponded approximately to the cessation of heart beat.

Results

None of the CT images obtained in living animals demonstrated any cardiac structure other than a general outline of the heart. The images obtained in the sacrificed animals are

shown in figures 2–8. The window settings were selected as a compromise between the emphasis on cardiac morphology and the dynamic range required to show a broad range of structures within the heart. In all figures, the scans are numbered consecutively from the base of the heart to the apex.

These images clearly visualize cardiac morphology, even without the use of contrast (figs. 2, 4, 6, and 7). The injection of contrast material (figs. 3 and 5) does not appear to provide any more information than that obtained without contrast. *It should be noted, however, that the very small number of animals studied does not permit any conclusion on this point.*

The images obtained without contrast provide excellent visualization of ventricular morphology, the intraventricular septum, and, in some cases, papillary muscle. In one animal not heparinized before scanning, blood clots in the cardiac chambers were clearly identifiable (fig. 4) and subsequently verified at autopsy. In the images obtained in dogs with infarct of 3–13 days' duration (fig. 8), the infarcted area is visualized as a zone of lower x-ray attenuation than normal myocardium. In these animals the area of infarct on the image correlated well with autopsy findings.

The clear delineation observed between the myocardium

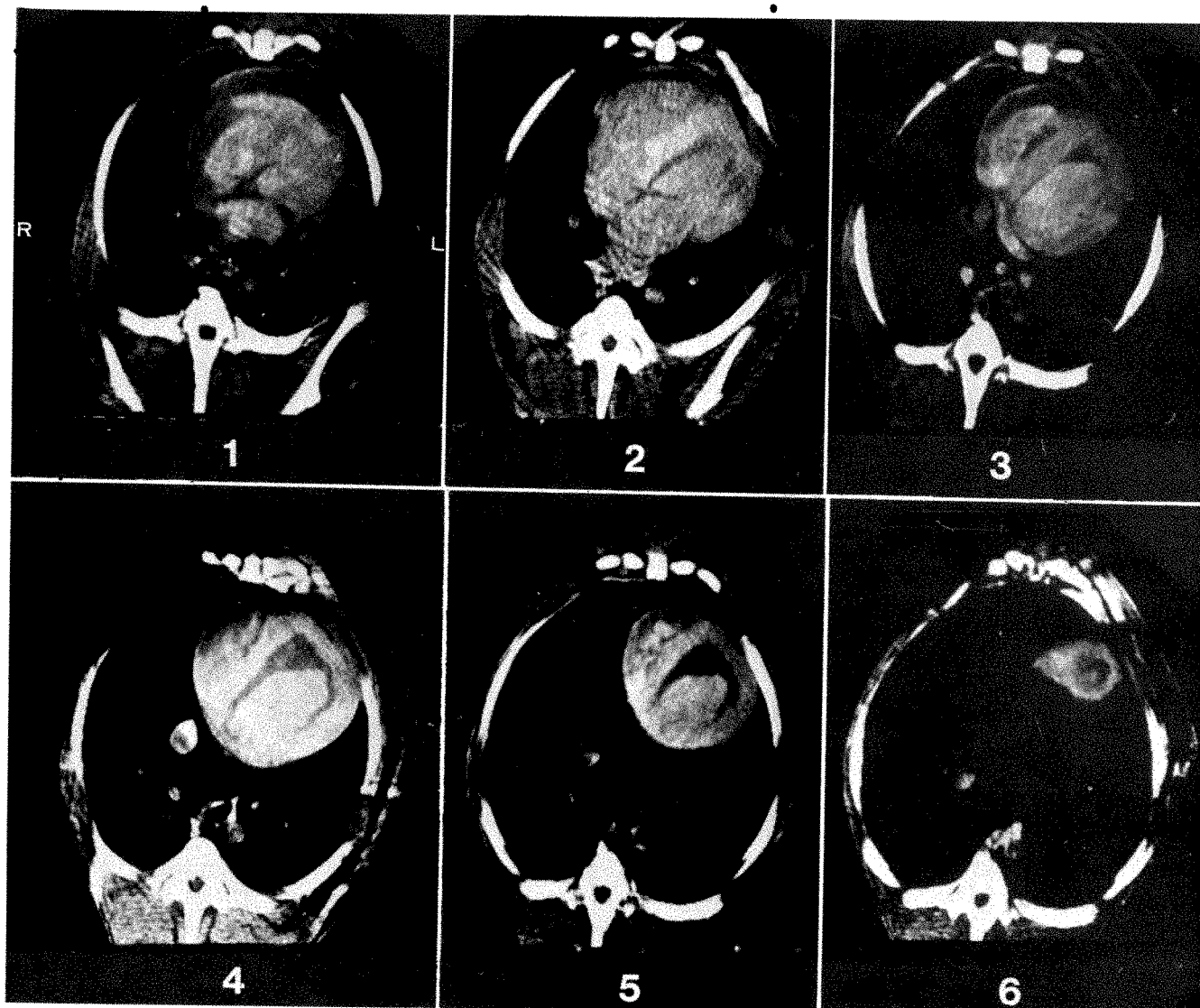


Fig. 4.—Transmission CT scans of dead 27 kg mongrel dog (no. 26) 7 days post LAD coronary occlusion. Dog not heparinized before scanning. Section thickness 13 mm; scan time 20 sec per section; orientation as in fig. 2. Note blood clots in heart chambers.

and blood in the cardiac chambers was unexpected. Indeed, the measured linear x-ray attenuation coefficients for heart and blood (table 1) appear to deny the possibility of visualizing cardiac morphology without contrast enhancement. An attractive explanation for this discrepancy is blood clotting and/or sedimentation in the dead animals which we studied. This is certainly the correct explanation for the images obtained in nonheparinized dogs (figs. 4 and 7); in one of them (fig. 4), the presence of the visualized clots was verified at autopsy.

However, this explanation does not easily fit the results obtained in heavily heparinized dogs (figs. 2 and 6) in which no clotting in the heart was identified at autopsy. Sedimentation of cells does, of course, occur in heparinized dead animals. However, the images were obtained only minutes after death, and sedimentation would presumably be identified in the pictures by a visible level between plasma and cells. Such a level was not observed in heparinized dogs, although it was clearly visible in at least two un-

heparinized animals (figs. 4 and 7). Despite these arguments, we are not ready to abandon this explanation, which

TABLE 1
Linear X-ray (or Gamma Ray) Attenuation Coefficients
of Human Specimens

Human Specimen	Photon Energy (keV)			
	59.6*	60†	84.3*	122†
Heart.....212165
Blood.....214-.222168-.70
Plasma.....	.20631816	...
RBC.....	.22241942	...
Evaporated blood.....223
Clotted blood.....	.22191919	...

*Data from [2].

†Data from [3].

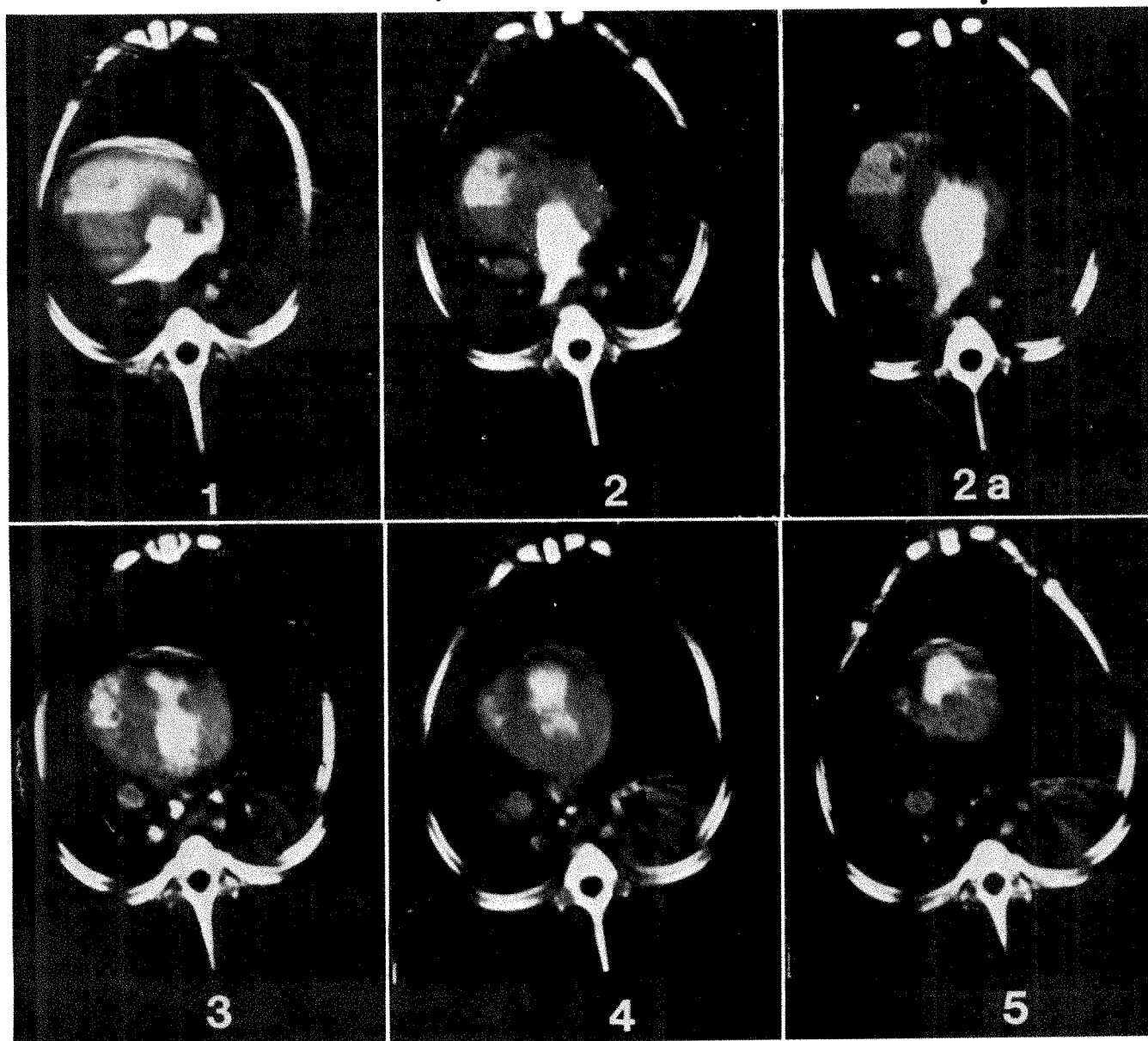


Fig. 5.—Transmission CT scans of dead 22 kg mongrel dog (no. 27) 24 hr post LAD coronary occlusion. Dog heparinized and injected with contrast material before death and scanning. Section thickness 13 mm; scan time 20 sec per section; orientation as in fig. 2. Scan 2a, taken approximately 15 min before scan 2, shows different distribution of contrast material.

we consider correct.

Another possibility is that the x-ray attenuation coefficients of the blood in our preparations were affected by dilution from the sodium pentobarbital administered to kill the dog. At this time we do not have sufficient evidence to either adopt or disprove this hypothesis.

There remains the least attractive explanation that dog myocardium is more opaque to x-rays than the specimen shown in table 1. At this time we are unable to reconcile our images with the information shown in table 1, and we are carrying out further experiments to explain this apparent paradox.

The above results indicate that transmission CT of the still heart in the dead dog provides an image in which the

myocardium and cardiac chambers are identified even without administration of contrast material. Furthermore, in some instances areas of myocardium infarcted for more than 24 hr demonstrate a decrease in x-ray attenuation coefficients compared to normal myocardium. However, this decrease does not appear sufficient to permit reliable quantitative delineation of the injured tissue. This difficulty in quantitating myocardial injury on the CT scan is not surprising, since there is little reason to believe that recently infarcted myocardium would exhibit measurable differences in x-ray attenuation from normal myocardium. We feel that these preliminary results are encouraging for the possible clinical usefulness of a CT scanner gated to the cardiac cycle.

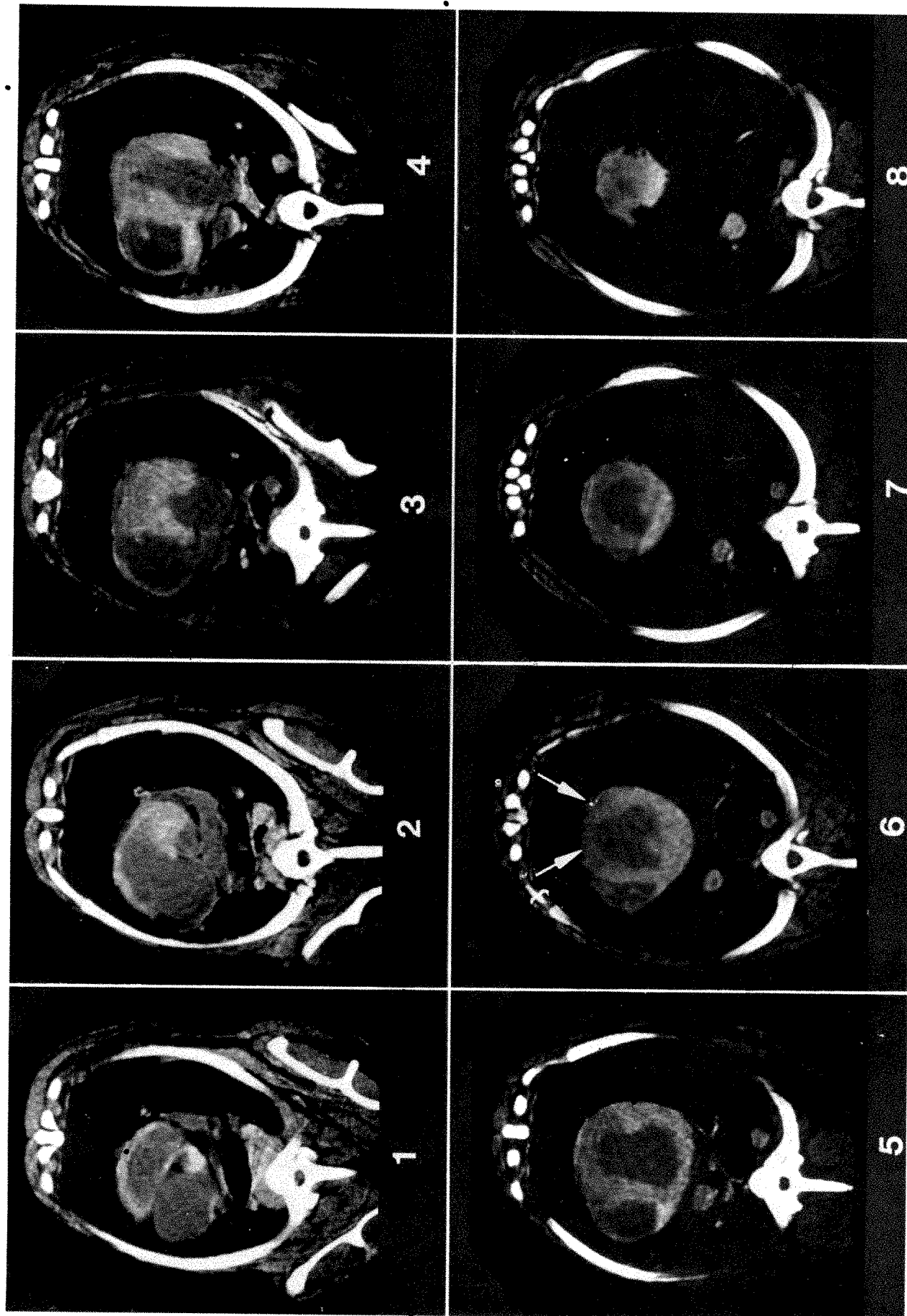


Fig. 6.—Transmission CT scans of dead 27 kg mongrel dog (no. 28) 72 hr post LAD coronary occlusion. Dog heparinized before death and scanning. Section thickness 6 mm; scan time 80 sec per section; orientation as in fig. 2. Large infarct in anterior left ventricular wall (arrows).

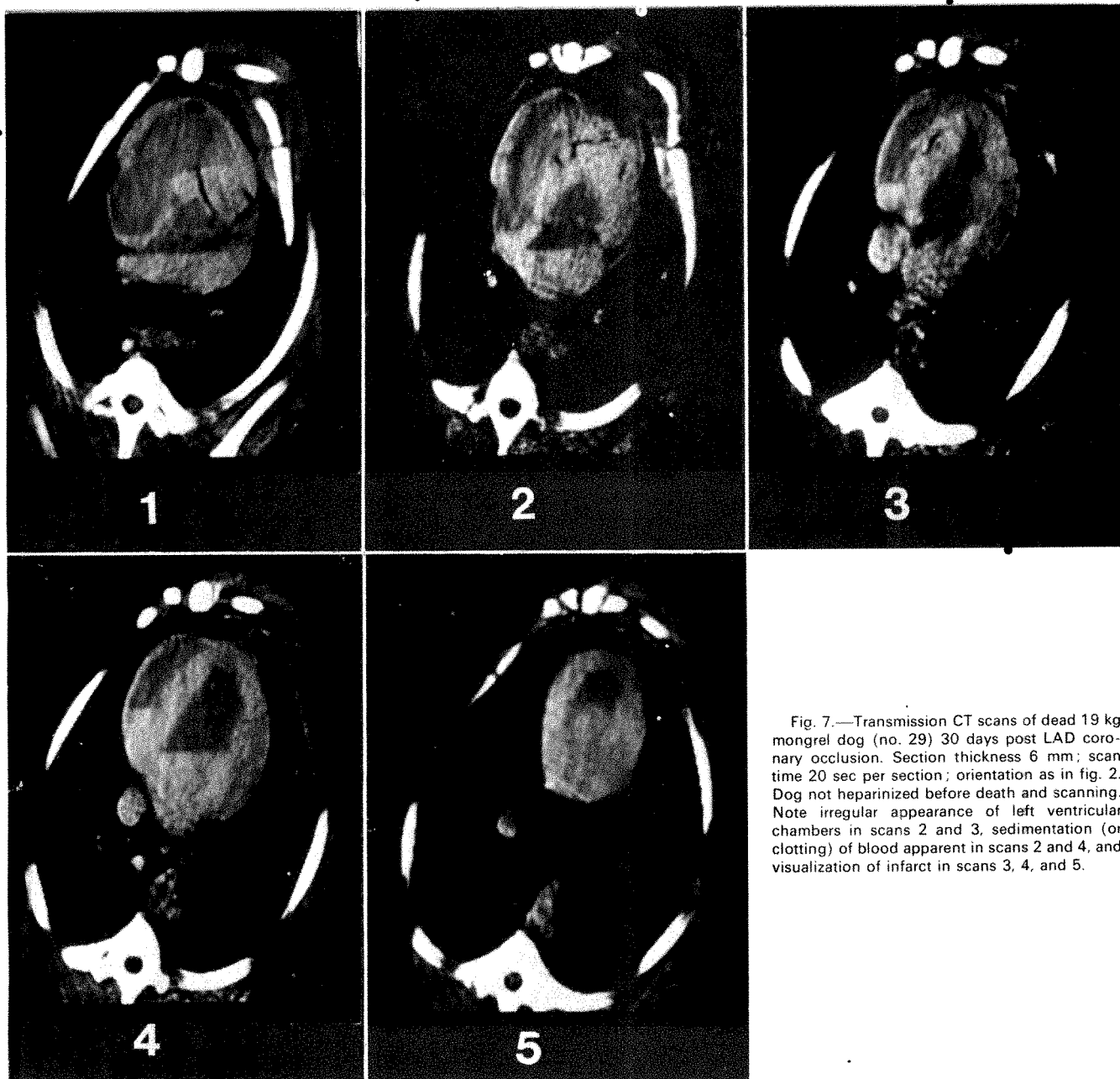


Fig. 7.—Transmission CT scans of dead 19 kg mongrel dog (no. 29) 30 days post LAD coronary occlusion. Section thickness 6 mm; scan time 20 sec per section; orientation as in fig. 2. Dog not heparinized before death and scanning. Note irregular appearance of left ventricular chambers in scans 2 and 3, sedimentation (or clotting) of blood apparent in scans 2 and 4, and visualization of infarct in scans 3, 4, and 5.

Emission Tomography

The external identification of infarcted and/or ischemic myocardium with radionuclides has already been implemented with considerable efficacy [4]. The ability to image a structure on the basis of its content of a previously administered radiopharmaceutical offers fundamental advantages over transmission methods of imaging. While transmission imaging must rely on often small differences in x-ray attenuation properties resulting from structural changes in tissue secondary to ischemia, emission imaging can provide considerably greater sensitivity by detecting altered metabolism leading to the selective increase or decrease in accumulation of a suitable radiopharmaceutical. While infarction and ischemia may or may not be ac-

companied by the alteration of x-ray attenuation properties necessary for visualization by transmission CT, the circulatory or biochemical changes are potentially identifiable with a suitable radiopharmaceutical.

The feasibility of imaging myocardial infarction and ischemia using a scintillation camera and radiopharmaceuticals such as $^{99m}\text{Tc}(\text{Sn})$ -pyrophosphate [5] and ^{201}Tl [6] has been well documented. However, routine imaging methods compress the three-dimensional distribution of the radioactive label into a two-dimensional image. Activity contained in tissues overlying and underlying the region of interest are super-imposed in the image, drastically reducing the contrast of the examination and interfering seriously with quantitative studies. Furthermore,

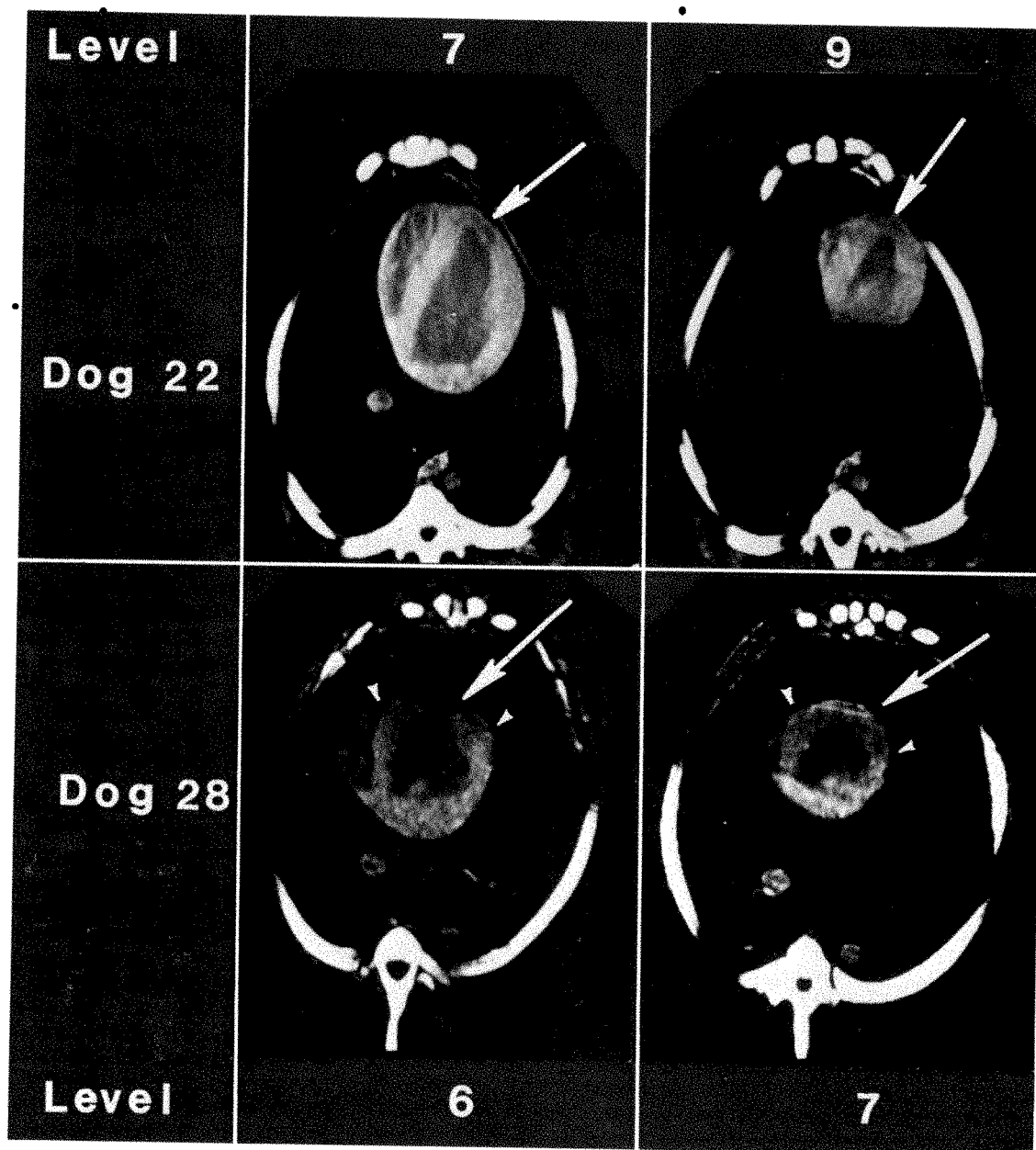


Fig. 8.—Selected CT scans of dogs 22 and 28 (figs. 2 and 6) showing visualization of infarcted tissues. Note use of different CT window settings.

attenuation of the radiation by tissues located between the lesion and the scintillation camera further interferes with reliable quantitation by the usual imaging techniques.

Fortunately, the weaknesses of the projection imaging technique can be overcome by the use of CT, which brings to nuclear medicine the advantages so well recognized in diagnostic radiology: images of transverse sections without the interference of tissues overlying and underlying the region of interest and a three-dimensional representation of the structures examined.

Since the principles of operation of emission CT have been extensively described, this subject will not be treated here. We do agree that positron-emitting radionuclides lend themselves better to emission CT through the coincidence

detection of the annihilation radiation than single photon emitters [7–9], particularly for cardiac imaging where the tissue attenuation correction is complicated by inhomogeneities. Furthermore, some positron-emitting radionuclides such as ^{11}C , ^{13}N , and ^{15}O are particularly well suited to functional imaging because of their kinship to nuclides involved in metabolic processes [10, 11]. There have already been several reports of the qualitative visualization of the myocardium by means of ^{13}N -ammonia [11, 12] and ^{11}C -palmitate [11].

Recently, we have utilized a radioactively labeled physiological substrate of myocardium, ^{11}C -palmitate (produced in the Washington University Medical Center cyclotron), to evaluate ischemia qualitatively in isolated per-

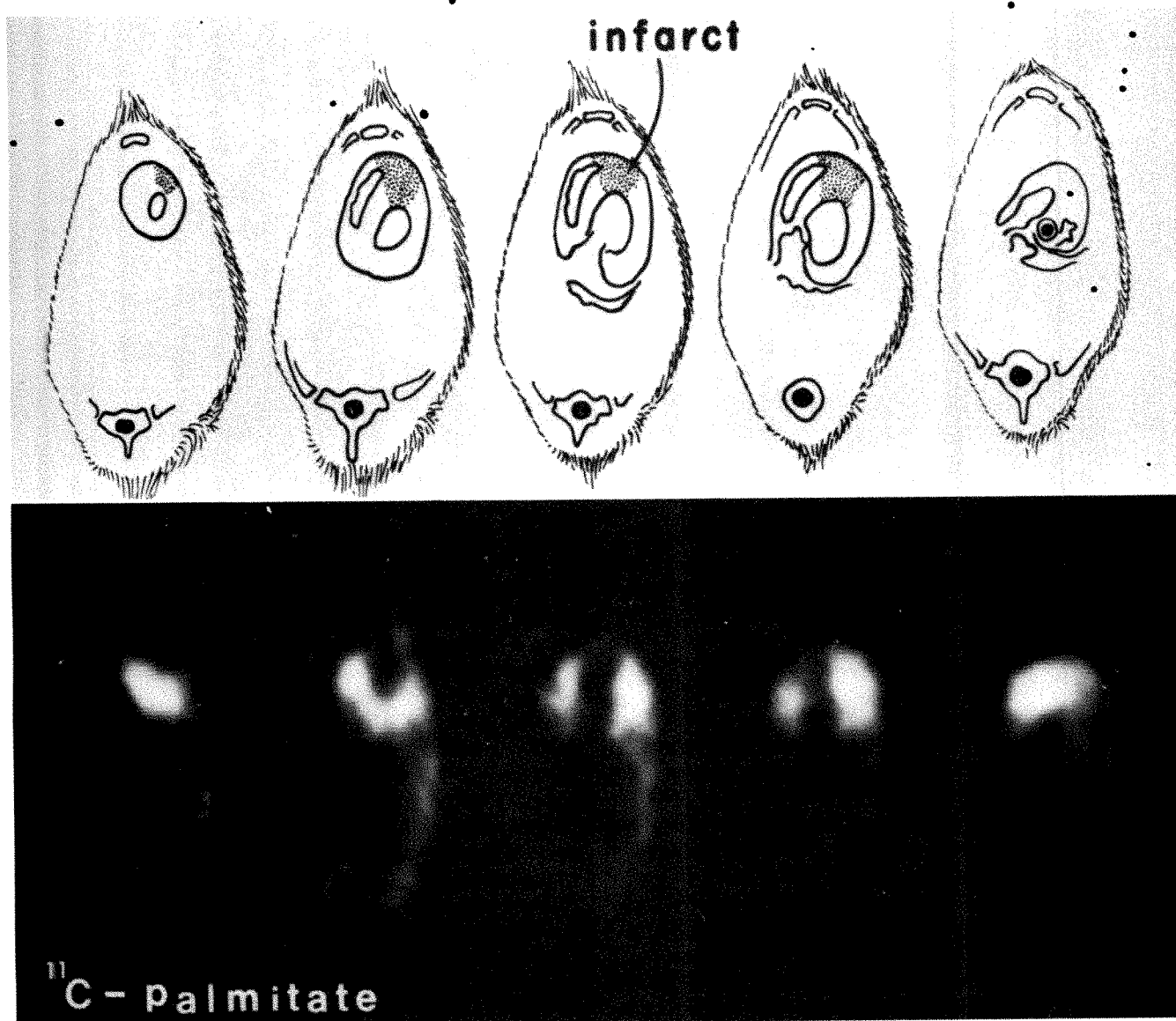


Fig. 9.—Emission CT scans of anesthetized 31 kg mongrel dog 48 hr post LAD coronary occlusion. Scan obtained by means of positron emission transverse tomograph (PETT III) subsequent to intravenous injection of approximately 6.2 mCi of ^{11}C palmitate. Each image contains between 500,000 and 700,000 counts accumulated in periods from 4 to 12 min. Sections spaced by approximately 1.5 cm. Note visualization of infarcted area as zone of lower concentration of activity compared to images obtained in normal dog (see fig. 11).

fused hearts and intact dogs [13]. Results of initial studies in isolated perfused hearts demonstrated a diminished rate of ^{11}C -palmitate accumulation in ischemic myocardium, which was based on decreased utilization of fatty acids rather than exclusive dependence on low flow.

We employed the same radiopharmaceutical in preliminary experiments to measure the extent of infarction in transverse sections of the canine heart in vivo (fig. 9) by means of a positron emission CT device (PETT) [7, 13–15]. In intact dogs, ^{11}C -palmitate localized within the thorax to heart muscle [11]. These studies showed a diminished regional uptake of ^{11}C within minutes after coronary occlusion. The numerical printout provided by the PETT represents quantitatively the distribution of ^{11}C in a CT section

of the infarcted heart and permits measure of the fraction of infarcted tissues [16].

The extent of presumably intact myocardium is delineated as a zone of high activity (fig. 10). This zone is identified as 50% of maximum isocount, after subtraction of extra cardiac activity. The borders of the zone thus established were found empirically to correspond well with the outline of the heart section.

The infarct is identified as the difference between the outlined normal myocardium and the presumed outline of the total section of the heart obtained by extrapolating the outline of the normal myocardium to a doughnut shape (fig. 11, scan 2) or horseshoe shape (figure 11, scan 1) for sections of the heart at the level of the left atrium. After 48

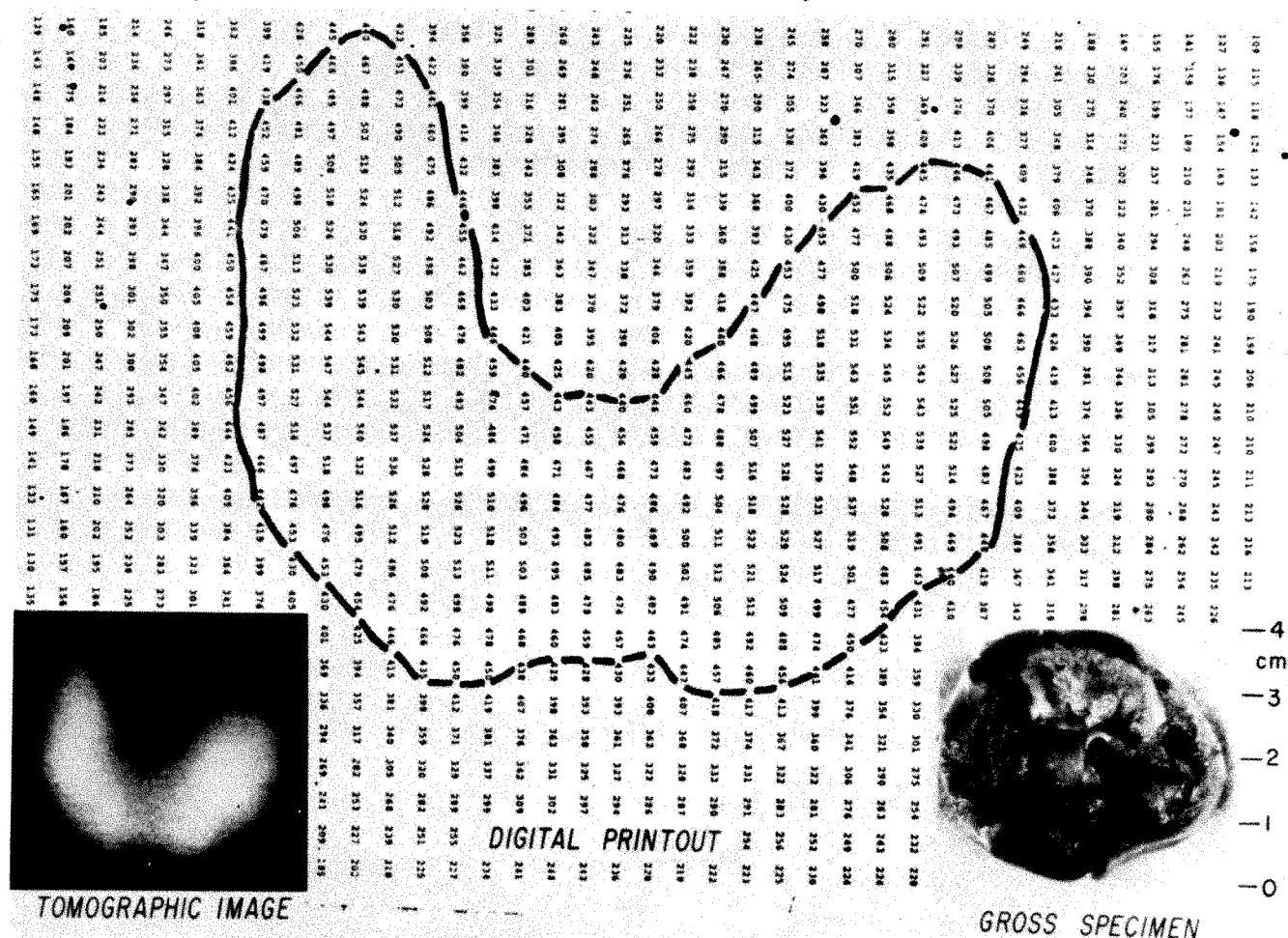


Fig. 10.—Emission CT scan image, digital printout, and gross specimen of section of 48 hr infarcted dog heart. Tomographic image and printout obtained by PETT III system in living dog subsequent to administration of ^{11}C -palmitate.

hr of ischemia, the decreased uptake demonstrable in the computer-reconstructed cross-sectional image of the heart reflected the percentage of infarction in a 15 mm cross section—verified morphometrically (table 2) and by analysis of CPK activity in corresponding regions of the heart at necropsy [16, 17].

TABLE 2

Comparison of Infarct Size Measured In Vivo and Morphometrically in Dogs

% Infarction Tomographically	% Infarction Morphometrically
5.....	0
17.....	10
21.....	23
36.....	39
35.....	42
43.....	58
54.....	60

Note.—Tomographic estimation derived from CT PETT sections in vivo, morphometric estimation from corresponding cross section at necropsy 48 hr after coronary occlusion. $r = .97$.

The spatial and contrast resolution which are presently achieved in emission CT are considerably lower than those of transmission CT. This is because of the considerably lower number of photons in the emission image. Typically, an emission CT image of the heart is formed by about 10,000 recorded photons per pixel with a spatial resolution of approximately 1 cm and a contrast resolution of no better than a few percentage points. Transmission images, on the other hand, are formed by millions of photons per pixel, with a spatial resolution of about 1 mm and a contrast resolution of about 0.5%.

However, cardiac motion does not affect the emission CT images as much as the transmission CT reconstruction. This is because the lower resolution of the emission examination is more tolerant of the relatively small displacements of the heart with respect to image reconstruction. In nuclear medicine CT, stilling the motion of the heart by synchronization is easier to achieve because of the long data acquisition period imposed by low counting rates, with a consequent penalty of respiration unsharpness, than in the exquisitely high resolution transmission CT image.

The combined use of positron emission transverse tomography and of a suitable radiopharmaceutical allows

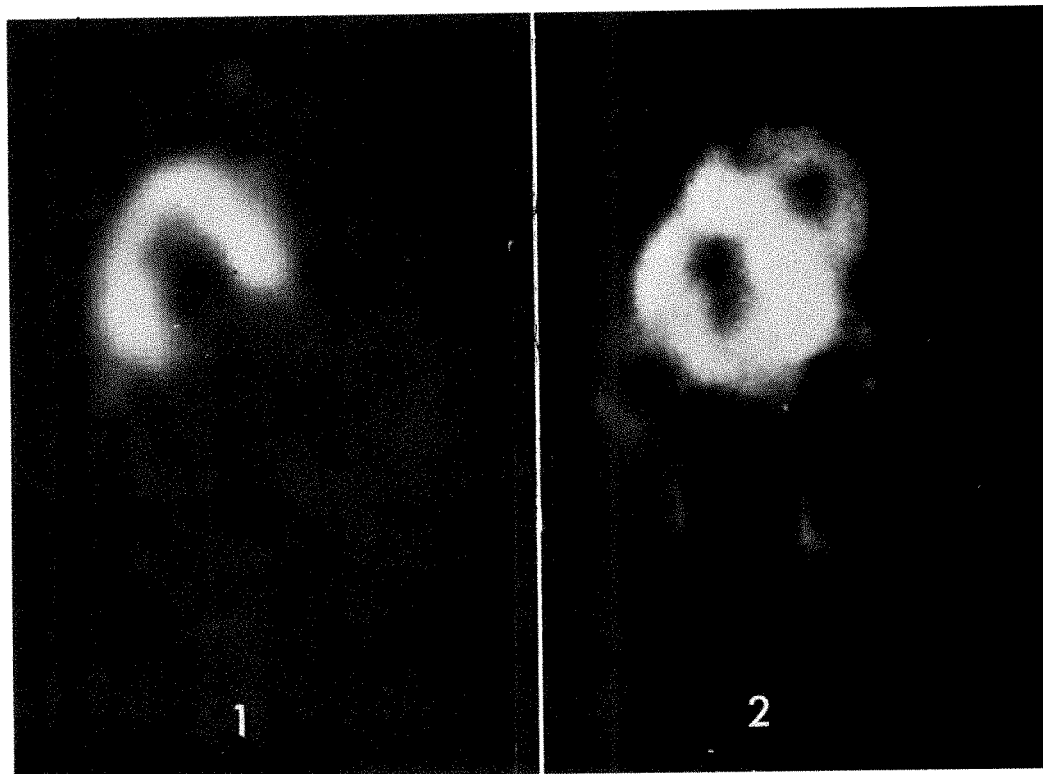


Fig. 11.—Emission CT scans (PETT III) of dog hearts obtained in vivo in two normal dogs following administration of ^{13}N -ammonia. Scan 1 obtained at level of left atrium; Scan 2 closer to cardiac apex. Both show mainly left ventricle with typical horseshoe and doughnut shapes. These two scans correspond approximately to transmission CT scans 4 and 6 in fig. 6.

not only the striking visualization but also the reliable quantitative assessment of recent and old myocardial infarction.

Conclusions

From a limited number of observations, it appears that transmission CT is a promising technique, with or without the administration of contrast material, for the non-invasive visualization of the cardiac chambers. It also offers the possibility of identifying infarcted myocardium. The clinical application of this method must await the technical developments permitting either synchronization of data acquisition with the heart cycle or data acquisition sufficiently fast to image the heart in a short phase of its cycle.

Emission CT has already demonstrated its capabilities in imaging areas of myocardial ischemia and infarction. We feel that both techniques will be used in the assessment of cardiac pathology in the very near future.

REFERENCES

1. Wood EH: New horizons for the study of the cardio-pulmonary and circulatory systems. *Chest* 69:394-408, 1976
2. Phelps ME, Hoffman EJ, Ter-Pogossian MM: Attenuation coefficients of various body tissues, fluids, and lesions at photon energies of 18 to 136 keV. *Radiology* 117:573-583, 1975
3. Rao PS, Gregg EC: Attenuation of monoenergetic gamma rays in tissues. *Am J Roentgenol* 123:631-637, 1975
4. Holman BL: Radionuclide methods in the evaluation of myocardial ischemia and infarction. *Circulation* 53:1112-1119, 1976
5. Willerson JT, Parkey RW, Bonte FJ, Meyer SL, Atkins JM, Stokeley EM: Technetium stannous pyrophosphate myocardial scintigrams in patients with chest pain of varying etiology. *Circulation* 51:1046-1052, 1975
6. Strauss HW, Harrison K, Langan JK, et al: Thallium-201 for myocardial imaging: relation of thallium-201 to regional myocardial perfusion. *Circulation* 51:641-645, 1975
7. Ter-Pogossian MM, Phelps ME, Hoffman EJ, Mullani NA: A positron emission transaxial tomograph for nuclear imaging (PETT). *Radiology* 114:89-98, 1975
8. Phelps ME, Hoffman EJ, Mullani NA, Ter-Pogossian MM: Application of annihilation coincidence detection to transaxial reconstruction tomography. *J Nucl Med* 16:210-224, 1975
9. Brownell GL, Burnham CA: MGH positron camera, in *Tomographic Imaging in Nuclear Medicine*, edited by Friedman GS, New York, Society of Nuclear Medicine, 1972, pp 154-164
10. Ter-Pogossian MM: Discussion: Limitations of present radionuclide methods in the evaluation of myocardial ischemia and infarction. *Circulation* 53:1119-1121, 1976
11. Ter-Pogossian MM, Hoffman EJ, Weiss ES, Coleman RE, Phelps ME, Welch MJ, Sobel BE: Positron emission reconstruction tomography for the assessment of regional myocardial metabolism by the administration of substrates labeled with cyclotron-produced radionuclides. Paper presented at the meeting on Cardiovascular Imaging and Image Processing, Stanford University, July 1975
12. Hoop B Jr, Smith TW, Burnham CA, Correll JE, Brownell GL, Sanders CA: Myocardial imaging by means of $^{13}\text{NH}_4^+$ and multicrystal positron camera. *J Nucl Med* 14:181, 1973
13. Ter-Pogossian MM, Phelps ME, Hoffman EJ, Coleman RE:

- The performance of PETT III, in *Reconstructive Tomography in Diagnostic Radiology and Nuclear Medicine*, Baltimore, University Park Press. In press, 1976
14. Phelps ME, Hoffman EJ, Mullani NA, Higgins CS, Ter-Pogossian MM: Some performance and design characteristics of PETT III, in *Reconstructive Tomography in Diagnostic Radiology and Nuclear Medicine*, Baltimore, University Park Press. In press, 1976
 15. Hoffman EJ, Phelps ME, Ter-Pogossian MM, Mullani NA, Higgins CS: Design and performance characteristics of a whole body positron transaxial tomograph. *J Nucl Med*. In press, 1976
 16. Weiss ES, Welch MJ, Ter-Pogossian MM, Sobel BE: External quantification of myocardial infarction in vivo (abstr.). *Clin Res*. In press, 1976
 17. Weiss ES, Ahmed SA, Welch MJ, Williamson JR, Ter-Pogossian MM, Sobel BE: Quantification of infarction in cross sections of canine myocardium in vivo with positron emission transaxial tomography and ^{11}C -palmitate. Submitted for publication

Cardiac Reconstruction Imaging in Relation to Other Ultrasound Systems and Computed Tomography

RAYMOND GRAMIAK¹ AND ROBERT C. WAAG²

A computer-controlled system is described for the generation of two-dimensional motion images of the heart. A standard B scanner is used to scan the area of interest during 40–50 cardiac cycles, and the computer controls recording of the ultrasound signals, beam position indicators, and physiologic data. The ultrasonic echoes are reformatted by the computer into sequential frames by reference to the ECG. Images are displayed in motion on a large monitor, and hard copy is obtained on 35 mm cine film. Off-line computer-controlled signal processing is utilized for image enhancement of clinical studies.

Real-time systems for the production of two-dimensional motion images of the heart are discussed and compared to computer reconstruction of ultrasound cardiac imaging. The advantages of ultrasound imaging of the heart and other body areas are presented, and perspectives are offered by which the present and future roles of ultrasound can be evaluated in respect to computed tomography.

It is concluded that ultrasound will remain the primary noninvasive modality for cardiac motion study and that ultrasound will continue to provide important clinical information in all parts of the body where it is currently employed.

Introduction

Ultrasound is an established method for the clinical evaluation of patients with heart disease [1]. Though initial development utilized one-dimensional information for recording cardiac structures and motion, several systems are being developed along different lines to produce two-dimensional images of the heart in motion. The system we are developing is based on image reconstruction employing a computer to store and process pulse echo ultrasound data into frames using the ECG as a reference signal [2, 3]. Computerized ultrasound reconstruction of the heart resembles computed tomography (CT) since a computer is used to reconstruct images, but it differs in that CT requires calculation of absorption differences to show structure. In ultrasound, this information is contained in the unprocessed signal. Also, the ultrasound method allows identification of signals according to temporal characteristics to display time-varying changes not currently available from the algorithms employed in CT.

The purpose of this presentation is to describe computer-based cardiac reconstruction of images as performed in our laboratory and to demonstrate our preliminary imaging capability. Comparison will be made to other existing ultrasound two-dimensional motion imaging systems for

the heart, and perspectives will be presented by which ultrasound can be compared to CT to determine its eventual role in the clinical practice of total body imaging.

Description of System

The system we have assembled for the production of two-dimensional motion images of the heart using ultrasound is extremely flexible and provides a research as well as clinical examination capability [4, 5]. The underlying principle is identification of echo returns by their temporal position in the cardiac cycle by reference to a simultaneously recorded ECG. Patient examination consists of a slow, manually directed scan over the heart during a series of cardiac cycles using a single ultrasonic beam. All echo returns which occur at the same point in the cardiac cycle are grouped into individual frames which represent a stop action image of all structures illuminated by the beam. Individual frames can be produced as often as the data are sampled within the span of one cardiac cycle.

A commercially available B scanner with a standard 2.0 MHz transducer attached to a scanning arm is used to generate and detect ultrasound signals. The scanning arm allows free transducer motion and angulation in a designated plane and generates signals indicative of beam position and angulation. These signals, as well as incoming physiological signals such as the ECG and respiratory excursions, may be recorded in analog or digital form. Images are displayed on a large monitor, and hard copy is obtained on 35 mm motion picture film.

Equipment

The computer in our system functions as a controller of peripherals needed to record the wide bandwidth and high dynamic range of the ultrasound signals which exceed the capabilities of direct recording systems. Matching the high data rates of the incoming signal to recording media capabilities is accomplished by stretching the time interval for recording (fig. 1). The returning echoes are first digitized with a high speed A/D converter, stored in a buffer memory, and then read during the relatively long interpulse interval at a rate compatible with recording capabilities. The wide dynamic range is accommodated by using 8 bit resolution, and the high volumes of data are stored by reversion into analog signals or directly on disk or digital tape. Paths of signal flow are diagrammed in figure 2, and equipment specifications are listed in table 1.

Received March 24, 1976.

This work was supported in part by U. S. Public Health Service grants 1 R01 HL 16260-01 and 2 R01 HL 15016-04 from the National Heart and Lung Institute, National Institutes of Health.

¹ Department of Diagnostic Radiology, School of Medicine and Dentistry, University of Rochester, Rochester, New York 14642. Address reprint requests to R. Gramiak.

² Department of Electrical Engineering, College of Engineering and Applied Science, University of Rochester, Rochester, New York 14642.

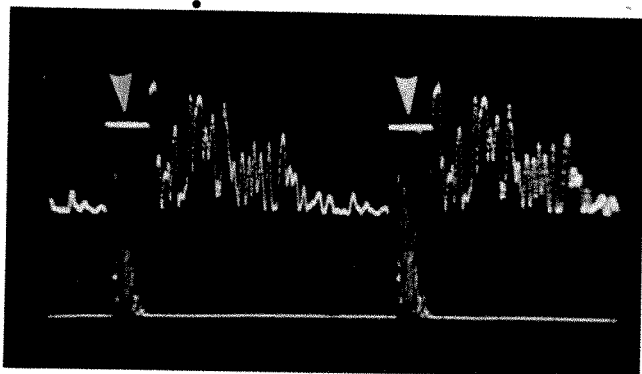


Fig. 1.—Waveform stretching. Lower trace shows two received video waveforms separated by interpulse interval. Upper trace shows stretched version of these video signals along with range gate during which sampling occurred (arrows).

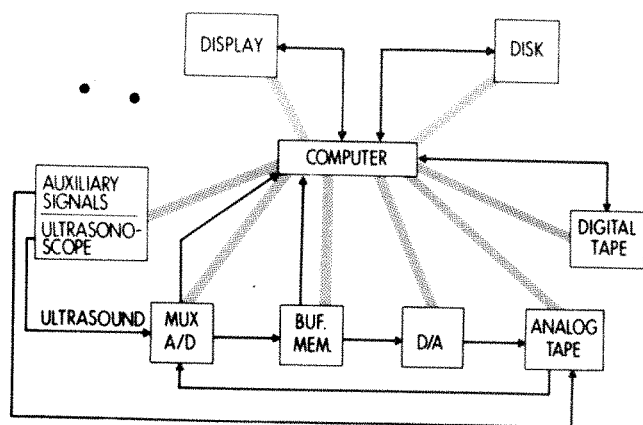


Fig. 2.—Computer-controlled data acquisition, processing, and display. Components, signal flow, and computer peripheral control links are shown. Computer functions as controller of data acquired during patient examination, produces a digital record on tape or disk, displays a processed, re-assembled image, and controls hard copy production on 35 mm cine film. Auxiliary signals=beam position and physiological signals such as electrocardiogram and respiratory excursion; MUX=multiplexer; A/D=analog to digital converter; D/A=digital to analog converter.

TABLE 1
Equipment

Equipment	Characteristics
Computer	Nova 800 with 32 K words of core
A/D and D/A converters	10 MHz
Buffer memory	2,000 8-bit words
Multiplexer	8 channel
Analog tape recorder	7 channel wideband II with up to 500 KHz bandwidth
Digital tape recorder	75 IPS, 9 track, 800 CPI
Disk	160 megabyte, 2 spindle, random access
Display monitor	1024 × 1024 16-level matrix, 30,000 points 30 times/sec refresh capability

The recent availability of rapid, high volume disk storage units has permitted us to record the stretched version of the ultrasound pulses directly in digital form along with the physiologic and beam position data, thereby eliminating the delay associated with intermediate analog tape recording formerly used [3]. The one-pass conversion is accomplished by a specially designed interface that controls the ultrasound sampling and the multiplexing of auxiliary information. With the disk system, motion images of the heart can be displayed on a large monitor within a few minutes of scanning, while the patient is still in the examining room. This display, which consists of a 1,024×1,024 grid containing 16 levels of amplitude, is refreshed from core through an interface and can show intensity-modulated lines at very rapid rates. Hard copy is obtained from a high resolution slave oscilloscope viewed by a 35 mm cine camera which automatically operates as images are displayed (fig. 3). The film is spliced into loops for projection or optical printing for efficient, economic display and archival storage of processed images.

Processing

Algorithms have been implemented to reformat the ultrasound data into frames, to display these frames for inspection and photography, and to permit the interactive application of various image processing techniques directed at image enhancement. The goals of image processing include enhancement of boundary definition, improvement of structure characterization from signal amplitude or frequency, and the elimination of image clutter produced by the reverberation of sound in tissues.

The reorganization of data acquired during patient examination into time-equivalent images requires several processing steps. Initially, the ECG is scanned, the QRS complexes are identified, and the R-R intervals measured. All cardiac cycles which vary in length beyond specified limits are rejected. Portions of the scan recorded during unusually deep breathing are degraded because cardiac displacement introduces returns from different portions of the heart into the image. These can be recognized from simultaneously recorded respiratory excursion and eliminated by respiratory gating. The result of this processing is a record that consists of data blocks containing ultrasonic waveforms and their vector coordinates sequenced according to position in the cardiac cycle.

The number of frames produced in this process is theoretically limited by the pulse repetition frequency and can be selected for clinical viewing of cardiac motion. We ordinarily use frame rates of 50–100 per cardiac cycle. Processing time is proportionate to the number of frames and is around 3 min for a typical 50-frame study encompassing 40 heart cycles. Our usual pulse repetition frequency of 1 kHz generates many additional frames that can be used for slow motion viewing or image processing.

This reformatted ultrasound data may be viewed in motion utilizing the intensity-modulated line drawing capability of our display (fig. 4). The construction of a display file on disk adds an additional 3 min for a 50-frame

study so that rapid assessment of scan quality and scanning plane selection may be made.

Processing can be carried out on arrays of ultrasound waveforms or ultrasound data distributed in an X-Y matrix. Interpolation can be used to generate additional lines or points to improve structure continuity for better depiction of cardiac boundaries (fig. 5). Frame overlays are also used to provide additional data points through summation and allow peak detection or point averaging. Filtering techniques include lowpass, highpass, bandpass, band rejection, and differentiation based on Fourier transform frequency domain or time domain processing. Various moving target indicator techniques based on pulse-to-pulse subtraction or more sophisticated waveform differentiation are available to detect signal amplitude fluctuation for improved visualization of moving structures and rejection of signals which do not fluctuate in intensity (fig. 6).

After processing, data are displayed in a matrix format for cine photography. In this mode, the ultrasound image is presented as a field of 256×256 points displayed with 16 levels of gray.

Thresholding, compression, and expansion through logging or specification of break points in the image may be readily accomplished for optimal display of recorded signal amplitude from the 8 bit, 256 level data (fig. 7).

Provision has been made for variable magnification of designated portions of the image as well as variable frame rates. In addition to the ultrasound image, an ECG waveform is displayed with an indicator of the position of the frame in the cardiac cycle along with patient identification information, processing parameters, date, frame number, and a measurement scale.

Programs are also available for the display of the frequency content of signals, and random-line M modes can be generated between any two points in the displayed image, including those not directly obtainable from the chest wall.

Clinical Studies

Patient examination begins with selection of the cardiac plane to be studied by observation of A-mode signals and survey B-scan images stored on an oscilloscope with or without ECG and respiratory gating. A range window of interest is determined, and two points are identified along the lines of information to specify beam position and angle for display. This allows flexible beam angulation, especially at the margins of the field where the signal is limited to remain within the dynamic range of the A/D converter. In addition to the ECG, a signal corresponding to respiratory excursion is obtained from a pneumograph.

We have examined a variety of patients primarily for system testing and to provide data for various processing techniques. Motion picture images of the long and short axes of the left ventricle as well as other planes passing through various portions of the heart have been produced. Cycle-related contour changes of the left ventricle have been clearly shown (fig. 8) and the movement of papillary muscles depicted within the left ventricular cavity. Pa-

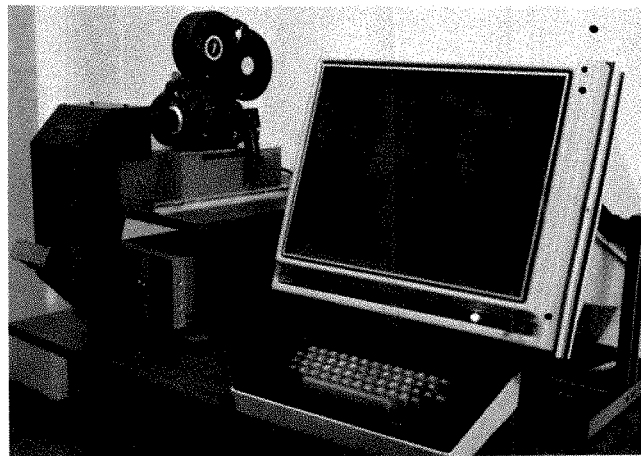


Fig. 3.—Image display and recording. Large monitor displays processed and unprocessed ultrasound image in response to keyboard entries. A 35 mm cine camera views slave oscilloscope through periscope. As image is displayed, computer operates camera automatically.



Fig. 4.—Display of unprocessed ultrasound data. Long-axis view of left ventricle with apex down is shown. This uninterpolated image can be viewed in motion or stop action within minutes following recording. LV=left ventricle.

tients with pericardial effusion have been studied and the swinging motion of the heart in the pericardial sac demonstrated. In one patient with traumatic pericardial effusion, an isolated clump of echoes in the pericardial space appeared to correspond to clots found at surgery (fig. 9). A large left atrial myxoma has been imaged as it moved in the left atrial cavity. Several patients with rupture of the chordae tendineae of the mitral valve have been studied and a dramatic inversion of leaflets into the left atrial cavity demonstrated in systole (fig. 10).

Immediate areas of clinical application appear to be left ventricular function and wall motion, valve function, chamber size evaluation, and distortions of cardiac anatomy resulting from congenital malformations.

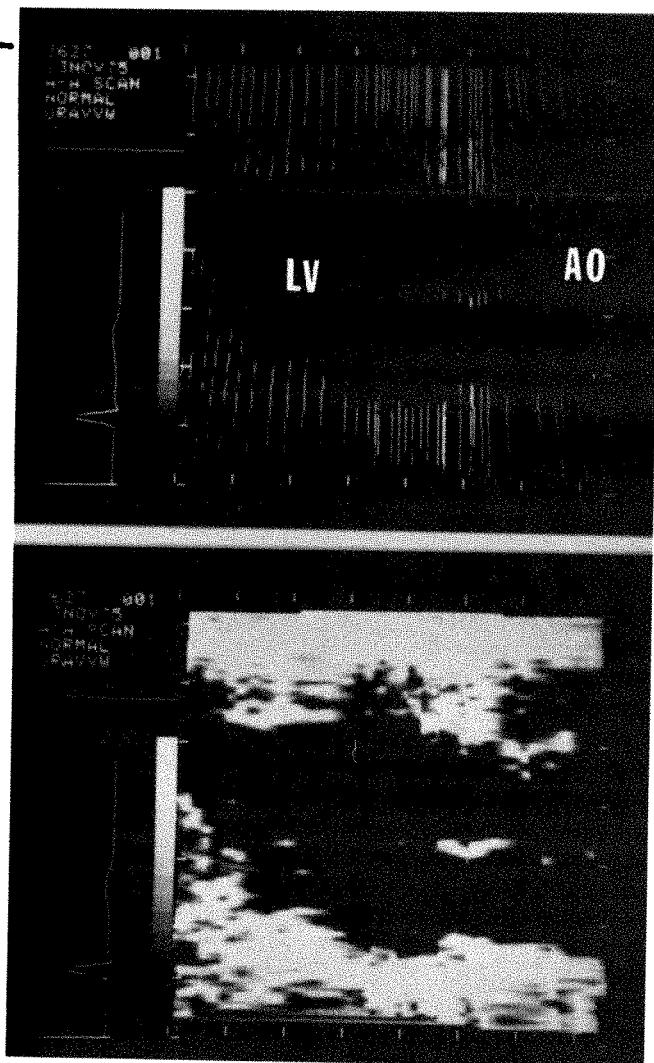


Fig. 5.—Image interpolation. Upper panel contains 37 lines of original data. Lower panel shows same image after interpolation to produce better structure continuity. Image was produced in matrix format which includes examination information, ECG with marker indicating phase of cardiac cycle, and gray scale of logarithmic compression employed in display. LV=left ventricle; AO=aorta.

Comparison of Cardiac Motion Imaging Systems

Two-dimensional ultrasound cardiac motion imaging systems are now commercially available and can be compared to computer-based reconstruction of the heart.

Real-time Systems

Fixed beam multielement arrays. The transducer consists of a multielement linear array in which 20 individual elements are excited sequentially, and the returns to each element are used to modulate intensity of a corresponding line of a raster display at a rate of 80 lines/sec [6]. Transducers either 5 or 8 cm long have been produced to display depth up to 16 cm. Videotape is used to record the image for subsequent study.

Display of a single line as it changes with time conveniently produces M-mode recordings from selected portions

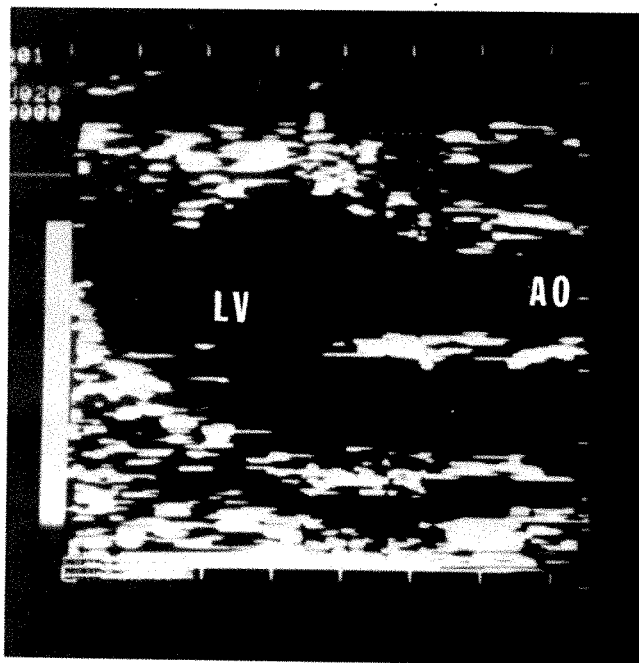


Fig. 6.—Moving target indicator processing. Images, separated in time by 6 msec, were subtracted to demonstrate those portions in which signal amplitude changed. Echoes from relatively stationary structures, such as the chest wall and left ventricular myocardium shown in fig. 5, are suppressed.

of the heart. The image is produced in real time, and the routine extraction of aortic and mitral valve data is easy since these structures are more readily recognized in two-dimensional motion viewing than in one-dimensional M mode. Applications in pediatric echocardiography appear promising where the presence or absence of a structure or its intracardiac relationship to other structures may represent vital diagnostic data.

Since the individual transducer elements are necessarily small to maintain as many lines of display as possible over a given linear distance, the system is primarily limited by beam width. Individual elements produce broad beams which tend to overlap, so that an omnidirectional reflector may be imaged by several beams on their respective axes, producing lateral distortion. This effect can be reduced by the simultaneous excitation of several adjacent crystal elements. These transducers also tend to be large and bulky and lack the maneuverability of single element transducers. The fixed perpendicular relationship of the beam to the transducer precludes beam angulation for image drop-out control, and there is no provision for compound scanning nor for flexible signal processing.

Beam scanning systems. Beam scanning devices have also been developed for real-time two-dimensional motion recording of the heart [7, 8]. Mechanical scanning of a standard single-element transducer through angles up to 45° and at scanning rates of 30/sec produces wedge-shaped images of cardiac anatomy in motion. Beam geometry improves image quality over that obtained with

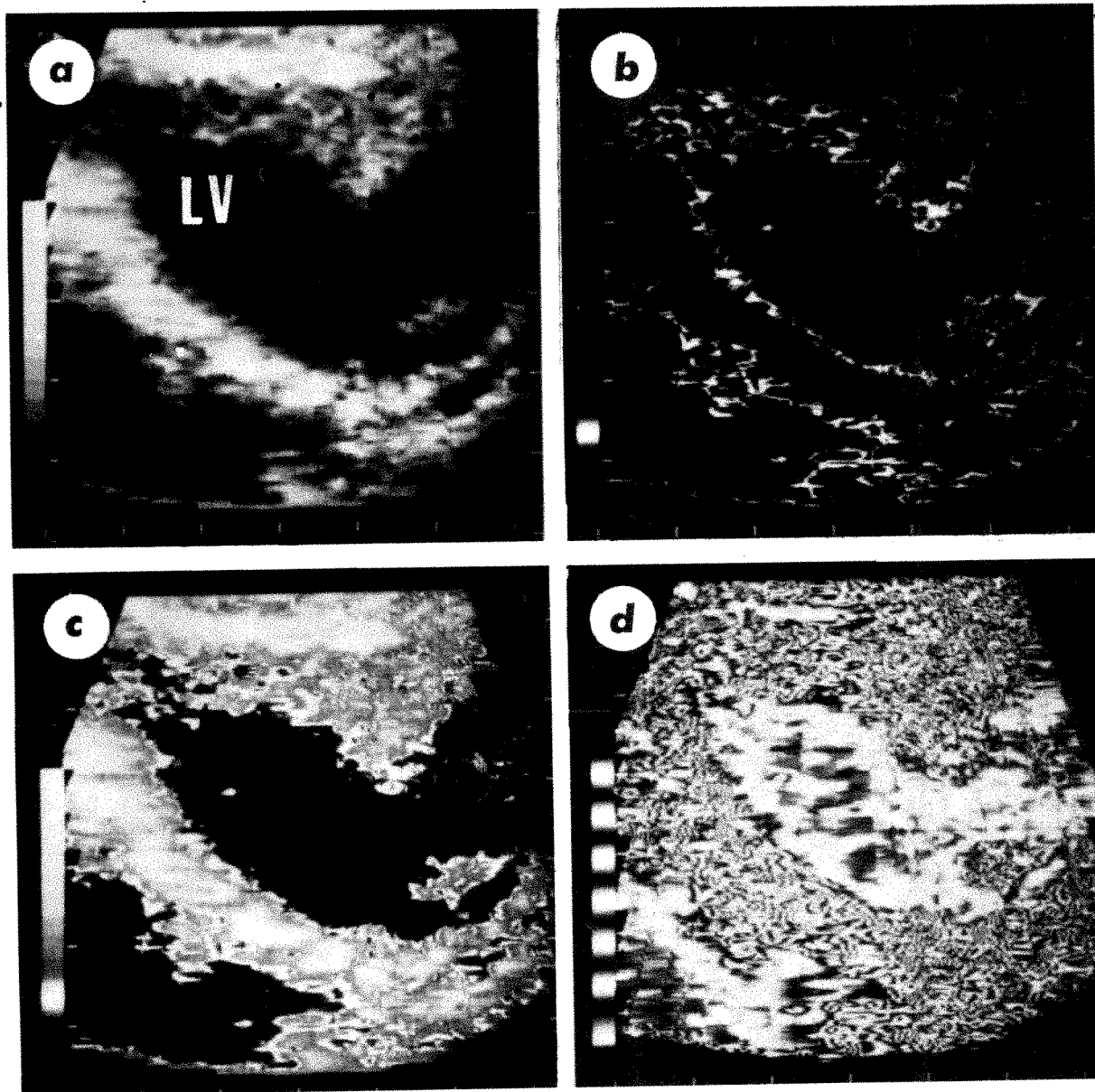


Fig. 7.—Variable signal amplitude display. *A*, Long axis of left ventricle with conventional logarithmic compression of 256 signal amplitudes into 16 shades of gray. *B*, Signal amplitudes 63–79 imaged with maximal brightness to show edge enhancement in low amplitude range. *C*, Same signal amplitude range imaged for maximum brightness and superimposed on conventional logarithmic compression of image. *D*, Alternate suppression and maximum brightness representation of amplitude bands in available signal range. These images depict flexible nature of computer processing of two-dimensional cardiac images.

fixed beam multielement arrays. Mobility and angulation of these devices are comparable to standard single transducers.

An electronically steered beam-scanning multielement array, intended primarily for cardiac examination, has been produced by Thurstone and von Ramm [9] and can be considered representative of other similar devices now available commercially. The transducer is a linear array consisting of 16 elements with an overall length of 24 mm and width of 14 mm. The beam can be steered through an angle of 60° by computer-controlled analog delay lines which delay the output of the individual elements successively to pro-

duce a wavefront which propagates at an angle to the face of the transducer.

Dynamic focusing is effected during the receive phase by crossing the margins of the angled, received "beam" to correspond to the range of the returning signals. As a result, a beam width of about 3 mm is achieved over the 15 cm range of operation. The 60° field of view is usually scanned at a rate of 20/sec and contains 250 lines of information. Changes in field size and scanning rate can be easily implemented through panel controls.

Logarithmic RF amplification is used to provide a wide dynamic range displayed in about 10 levels of gray. Hard

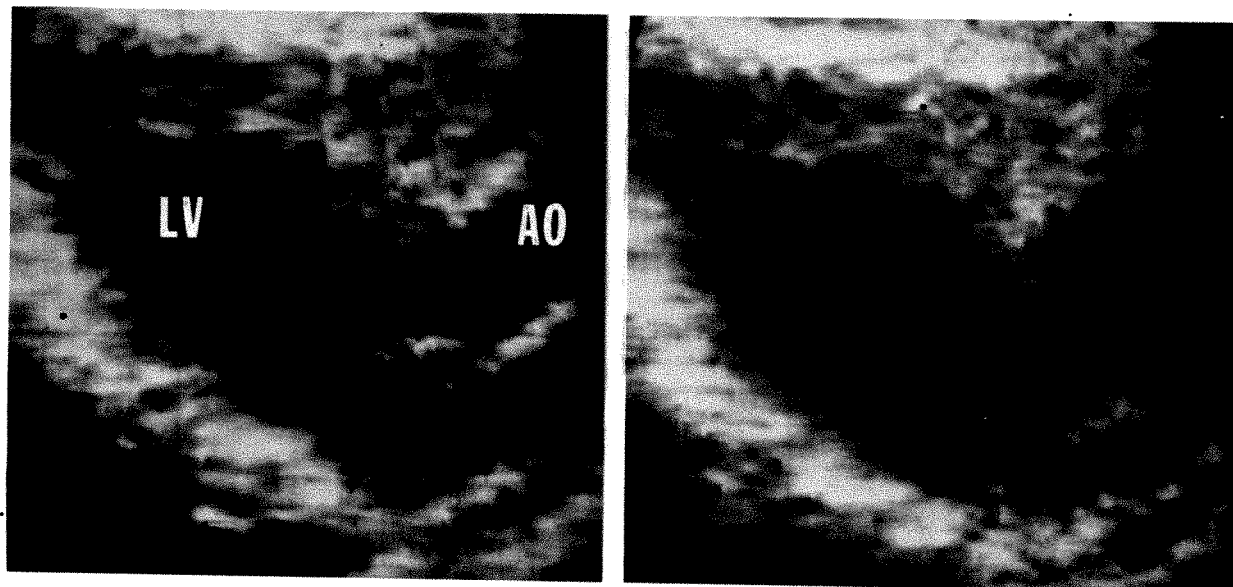


Fig. 8.—Left ventricular systole and diastole, same subject as fig. 7. Frames selected to demonstrate maximal systolic contraction (*left*) and maximal diastolic expansion (*right*). Data displayed with conventional logarithmic compression except that small signals suppressed to enhance contours of ventricular cavity.

copy is obtained from a cathode ray tube by videotape recording. Excellent resolution in both radial and lateral directions has been demonstrated. High temporal resolution, radially oriented M-mode traces can be obtained from any portion of the 60° angle of view.

Certain physical constraints govern the operation of beam scanning systems. Mechanical scanners must maintain some overlap of the sending and receiving beams, which imposes an upper limit on the rate at which the crystal may be oscillated. M modes with high temporal resolution cannot be obtained, and the device produces a buzzing sensation when applied to the chest, which might upset an apprehensive child.

Both mechanical and electronic scanners must cope with the same fundamental problem, namely, the achievement of a sufficient number of lines of information to produce a satisfactory image. Increasing the pulse repetition frequency to about 4,000/sec helps somewhat. However, higher pulse repetition rates create a problem because the interpulse interval is shortened so that echoes returning from deeply situated structures overlap those from subsequent pulses and degrade image quality. The number of lines per image can be increased by narrowing the angle of view, but this decreases the system aperture. Similarly, the number of frames per second can be reduced with resultant degradation of temporal resolution. Thus a compromise must be achieved between the pulse repetition frequency, the angle of view, and the number of frames per second to maintain satisfactory image quality. In general, the aperture limitation is the most important constraint; thus the entire long axis of the left ventricle is difficult to image.

Compound scanning for ideal structure illumination is not possible with either the mechanical or electronic system, and there are no provisions for flexible image process-

ing. In addition, transducers and electronics are not interchangeable.

Computer Reconstruction

Computer reconstruction of the heart in motion was developed to produce images of maximum aperture and temporal resolution. The aperture of our system is controlled by patient anatomy; the contact scan principle utilized allows imaging of hearts of all sizes. Temporal resolution is a function of the pulse repetition frequency, and frame rates can be obtained up to the usable limit (4,000). The number of lines per image is related to the number of cardiac cycles recorded during the scan since one line of information is obtained from each cycle. We usually scan the heart over an interval of 40–50 cardiac cycles and expand the raw data by a factor of eight during processing. Thus, by trading real-time capability for rapid off-line processing, the inherent constraints associated with beam scanners can be resolved.

Compound scanning for optimal structure illumination can be readily accomplished. Transducers and electronics can be changed as technology evolves, and it is conceivable that one of the real-time imaging devices could be incorporated into the computer-based system to combine the desirable features of both methods of imaging. The potential for enhanced image quality appears greatest with the computer system since it can accept the input of any other device and add image processing. Another attractive capability of the computer is the extraction of M-mode information along any line in the two-dimensional image. The movement patterns of both short axes of the left ventricle or of the papillary muscles could be studied along lines not obtainable from the chest wall.

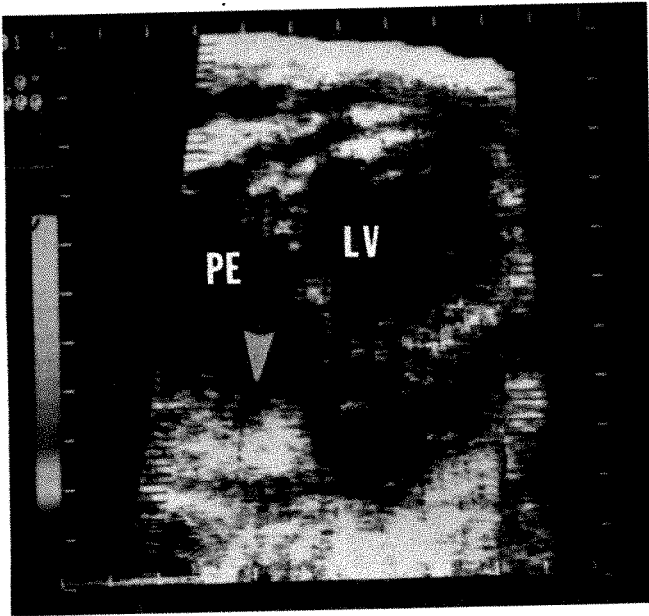


Fig. 9.—Short-axis view of left ventricle in patient with traumatic pericardial effusion. Circular cross-sectional view of left ventricular cavity seen in upper right portion of image. Small echoes within cavity arise from papillary muscles which could be seen to move dramatically to a grouped central position with systole and toward periphery in diastole. Arrow indicates clump of echoes within pericardial space believed to originate from clotted blood. Gray scale display demonstrates variable amplitude imaging employed. PE=pericardial effusion.

The emerging technology in computer graphics can be utilized to construct, manipulate, and image three-dimensional data obtained from ultrasonic devices which record multiple orthogonal planes through the heart. From these data, cardiac volumes, detailed evaluation of the motion of all portions of the cardiac wall, and accurate assessment of the size of stenotic valve orifices may be obtained.

The simultaneous motion display of blood-flow patterns along with solid structures of the heart represents an achievable goal for future development. Doppler information extracted from pulse signals [10] can be used to detect flows directly in planes passing through the chambers and great vessels of the heart. Gray scale or pseudocolor display of flow velocities, added to the system for two-dimensional viewing of the heart, would produce information analogous to that obtained by invasive techniques such as angiocardiology. Anticipated complexity of such a system suggests that only a computer would be capable of processing the large volumes of data required.

Computer reconstruction is not a real-time method, but the delay between scanning and viewing the motion image has been reduced to an acceptable span of minutes. The image obtained is a highly processed single cardiac cycle which is viewed repetitively. Consequently beat-to-beat variations cannot be studied, and arrhythmias require computer-based cycle length selection and normalization to permit viewing. Commercial systems are not available, and individual investigators must custom build their own apparatus.

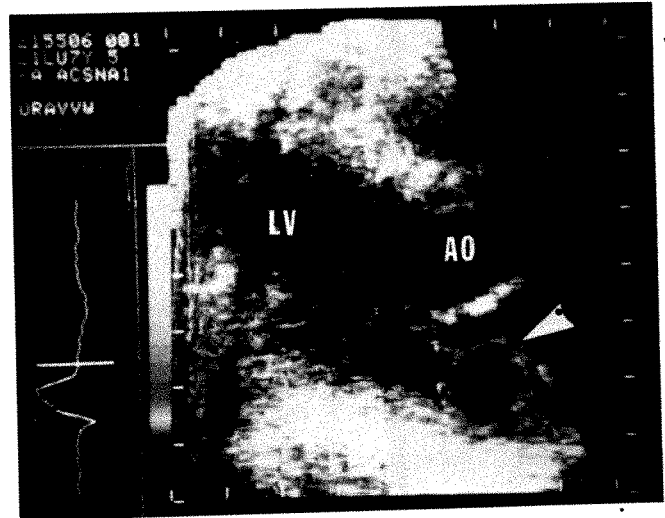


Fig. 10.—Chordae rupture. Systolic frame from long-axis view of left ventricular cavity of patient with bacterial endocarditis and severe mitral regurgitation. In systole, anterior leaflet of mitral valve was imaged as it fluttered wildly in left atrial cavity (arrow). In diastole, untethered leaflet swung freely in left ventricle.

Ultrasonic Imaging and CT

Anatomic Imaging

Heart. Although CT is not limited by the lung or the ossified sternum, there are several other problems which require solution before it can approach the present level of development of cardiac ultrasound. Structure motion, which is readily imaged by current ultrasonic methods, complicates present reconstruction algorithms used in CT and produces artifacts in the image [11]. Preliminary images of the heart and abdominal vessels obtained by CT reveal no detail in the blood-tissue interface [12]. Contrast injection will probably be required for demonstration of cardiac cavities and great vessels.

CT is an orthogonal transverse scanning system not readily modified to produce longitudinal or oblique planes. Thus various nonorthogonal planes known to be desirable from current clinical ultrasound activity are not obtainable directly. Consequently ultrasound is and probably will remain the method of choice for study of heart chamber and valve motion using existing one-dimensional and emerging two-dimensional techniques.

Head. CT has revolutionized imaging of the brain and ventricular system [13]. Ultrasound, on the other hand, appears to be limited in the head to the determination of midline position and ventricular size measurement [14]. However, the equipment required for these studies is small and portable which allows use in the emergency room or at the bedside. Two-dimensional imaging of the brain has been severely hampered by the skull which causes scattering and refraction of the ultrasonic beam [15]. Reverberation artifacts are a major problem, and refraction results in the imaging of off-axis reflectors in erroneous positions obscuring anatomical relationships. However, large aperture transducer systems are being investigated and appear to

show considerable potential in their ability to overcome imaging difficulties caused by the skull [16].

Eye. Ultrasonic imaging of the eye is also a well established clinical entity which uses transducers of high frequency (up to 25 MHz) to produce axial resolution under 0.1 mm and exceeding that available with CT [17]. In the orbit, both systems produce excellent information concerning retrobulbar pathology [18].

Obstetrical imaging. In obstetrical imaging, ultrasound appears to be firmly established as the examination of choice because of its nonionizing nature. Its flexible multiplanar capability makes it ideal for imaging the fetal biparietal diameter, useful for estimation of fetal development. The natural contrast which exists between the placenta and amniotic fluid makes placental localization relatively easy [19]. In addition, fetal movements, which are reliable indicators of fetal viability, are readily detected by ultrasound. It is difficult to envision the routine application of CT to problems in obstetrics.

Abdominal structures. It appears that CT and ultrasound will play complementary roles in abdominal structure imaging. Ultrasound can readily provide definitive clinical data for the evaluation of intraabdominal mass, aortic aneurysm, or other condition. However, in a significant number of instances, the ultrasonic examination may be complicated by the presence of bowel gas which blocks beam transmission. These patients can probably be better studied by CT. In cases where interpretation of ultrasonic data may be confusing or difficult, the ultrasound study may be used to designate the specific planes requiring CT, thereby lessening the examination time and radiation exposure. Thus ultrasound represents the ideal initial examining modality for the evaluation of patients with abdominal diseases [20].

Ultrasonic systems are less expensive, generally smaller in size than apparatus for CT, and may be portable. Devices are available to permit bedside examination in all areas of clinical application.

Other Aspects

In addition to the foregoing advantageous features of ultrasound, there are other aspects which are important. Ultrasound detects differences in mechanical properties of tissues, while CT recognizes differences in x-ray absorption. In combination, these systems provide complementary information by which improved structure recognition and tissue characterization may be obtained.

Ultrasound can be used in ways that appear unattainable by CT. The coherent nature of ultrasound allows the creation of ultrasonic holograms for two- and three-dimensional imaging [21]. The frequency content of ultrasonic signals has yet to be thoroughly analyzed and exploited as a diagnostic parameter. Common frequency-based observations such as musical instrument identification by tonal quality have not yet been applied in diagnostic ultrasound but offer the prospect that tissues may be characterized by frequency analysis of ultrasonic signals [22].

The utilization of wave interference effects, such as those

employed in x-ray crystallography, also promise to yield information about the size and spacing of tissue elements which scatter ultrasound [23]. Furthermore, this concept may be applied to image tissues in two or three dimensions on a scale corresponding to commonly employed ultrasonic wavelengths (1.5–0.1 mm) by computation from scattered ultrasound signals obtained by angle and frequency scanning.

Blood flow can be detected as well as imaged by observing the frequency shift of signals scattered from blood. These concepts have been applied to imaging peripheral vessels and the aortic arch [24] but have not yet been extended to imaging intracardiac blood flow patterns. It appears that Doppler imaging will extend the capabilities of echocardiography by producing two-dimensional displays of intracardiac blood flow patterns in motion.

Ultrasonic transmission systems have been developed to produce acoustic images corresponding to conventional radiographs [25]. These systems have the potential to image soft tissues according to their acoustic absorption characteristics or propagation velocities [26] which are distinct from the impedance variations detected by pulse echo techniques and also different from the tissue properties which control x-ray absorption. Thus ultrasound can provide a broad variety of tissue parameters to differentiate between normal and disease states.

In view of demonstrated present capabilities as well as anticipated development, we believe ultrasound will remain the primary noninvasive cardiac imaging modality and that it will continue to provide important clinical information for diagnosis in all current applications.

REFERENCES

1. Gramiak R, Waag RC: *Cardiac Ultrasound*. St Louis, Mosby, 1975
2. Gramiak R, Waag RC, Simon W: Cine ultrasound cardiography. *Radiology* 107:175, 1973
3. Gramiak R, Waag RC: Ultrasound cine cardiography, in *Ultrasonics in Medicine*, Proceedings 2d World Congress on Ultrasonics in Medicine, Rotterdam, June 1973, edited by de Vlieger M, White DN, McCready VR, Amsterdam, Excerpta Medica, 1974, pp 244–249
4. Waag RC, Gramiak R: New concepts for acquiring, processing, and imaging cardiac ultrasound data, in *Ultrasonics in Medicine*, Proceedings 2d World Congress in Ultrasonics in Medicine, Rotterdam, June 1973, edited by de Vlieger M, White DN, McCready VR, Amsterdam, Excerpta Medica, 1974, pp 239–243
5. Waag RC, Gramiak R: Computer-controlled two-dimensional cardiac motion imaging, in *Proceedings 1974 Ultrasonics Symposium*, Milwaukee, IEEE Catalog no. 74 CHO 896-1SU, 1974, p 12
6. Bom N: *New concepts in Echocardiography*. Leiden, Stenfort Kroese, 1972
7. Griffith JM, Henry WL: A sector scanner for real-time two-dimensional echocardiography. *Circulation* 49:1147, 1974
8. Eggleton RC, Feigenbaum H, Johnston KW, Weyman AE, Dillon JC, Chang S: Visualization of cardiac dynamics with real-time B-mode ultrasonic scanner, in *Ultrasound in Medi-*

- cine, vol. 1, Proceedings 19th Annual Meeting of the American Institute of Ultrasound in Medicine, edited by White D. New York, Plenum, 1975, pp 385-393
9. Thurstone FL, von Ramm OT: A new ultrasound technique employing two-dimensional electronic beam steering, in *Acoustical Holography*, vol 5, edited by Green PS, New York, Plenum, 1974
10. Johnson SL, Baker DW, Lute RA, Dodge HT: Doppler echocardiography: the localization of cardiac murmurs. *Circulation* 48:810, 1973
11. Paxton R, Ambrose J: The EMI scanner: a brief review of the first 650 patients. *Br J Radiol* 47: 530-565, 1974
12. Alfidi RJ, Haaga J, Meaney TF, MacIntyre WJ, Gonzalez L, Tarar R, Zelch MG, Boller M, Cook SA, Jelden G: Computed tomography of the thorax and abdomen: a preliminary report. *Radiology* 117:257-264, 1975
13. New PFJ, Scott WR, Schnur JA, Davis KR, Taveras JM, Hochberg FH: Computed tomography with the EMI scanner in the diagnosis of primary and metastatic intracranial neoplasms. *Radiology* 114:75-87, 1975
14. McKinney WM: Echoencephalography, in *Diagnostic Ultrasound*, edited by King DL, St. Louis, Mosby, 1974, pp 52-71
15. White DN: *Ultrasonic Encephalography*. Kingston, Ontario, Medical Ultrasonic Laboratory, Queen's University, 1970
16. Fry FJ, Eggleton RC, Heimburger RF: Transkull visualization of brain using ultrasound: an experimental model study, in *Ultrasonics in Medicine*, Proceedings 2d World Congress on Ultrasonics in Medicine, Rotterdam, June 1973, edited by de Vlieger M, White DN, McCready VR, Amsterdam, Excerpta Medica, 1974, pp 97-103
17. Coleman DJ: Ophthalmic ultrasonography, in *Diagnostic Ultrasound*, edited by King DL, St. Louis, Mosby, 1974, pp 273-281
18. Momose KJ, New PFJ, Grove AS, Scott WR: The use of computed tomography in ophthalmology. *Radiology* 115:361-368, 1975
19. Kobayashi M, Hellman LM, Cromb E: *Atlas of Ultrasonography in Obstetrics and Gynecology*. New York, Appleton-Century-Crofts, 1972
20. Leopold GR, Asher WM: *Fundamentals of Abdominal and Pelvic Ultrasonography*. Philadelphia, Saunders, 1975
21. Metherell AF: Acoustical holography and ultrasonic cameras, in *Cardiac Ultrasound*, edited by Gramiak R, Waag RC, St. Louis, Mosby, 1975, pp 286-298
22. Namery J, Lele PP: Ultrasonic detection of myocardial infarction in dog, in *Proceedings 1972 Ultrasonics Symposium*, Boston, IEEE Catalog no. 72 CHO 708-8 SU, 1972, p 491
23. Waag RC, Gramiak R, Lerner RM: Ultrasonic determination of cardiac macrostructure, in *Cardiac Ultrasound*, edited by Gramiak R, Waag RC, St. Louis, Mosby, 1975, pp 277-285
24. Baker DW, Johnson SL, Strandness DE: Prospects for quantitation of transcutaneous pulsed Doppler techniques in cardiology and peripheral vascular disease, in *Cardiovascular Application of Ultrasound*, Proceedings International Symposium at Janssen Pharmaceutica, Beerse, Belgium, edited by Reneman RS, New York, American Elsevier, 1974, pp 108-124
25. Green PS, Schaefer LF, Jones ED, Suarez JR: A new, high-performance ultrasonic camera, in *Acoustical Holography*, vol 5, Proceedings 5th International Symposium on Acoustical Holography, edited by Green PS, New York, Plenum, 1974, pp 493-503
26. Greenleaf JF, Duck FA, Samayoa WF, Johnson SA: Ultrasonic data acquisition and processing system for atherosclerotic tissue characterization, in *Proceedings 1974 Ultrasonics Symposium*, Milwaukee, IEEE Catalog no. 74 CHO 896-1SU, 1974, pp 738-743

Computed Tomography and Neuroradiology: A Fortunate Primary Union

HILLIER L. BAKER, JR.¹

Computed tomography (CT) has led to extensive re-assessment of and alterations in the practices of neuroscientists. Many of these alterations and their implications are described. The progress and problems encountered in the past 36 months are reported as well as the trends of future investigations. The principles evolving should apply in many situations as the benefits of CT are extended to other portions of the body.

Introduction

In 1976, only 4 years after the advent of computed tomography (CT) in medical diagnosis, there seems little doubt that within the coming decade the technique will have a major general impact on both radiologic and clinical practice. To date, the greatest benefits have accrued to the neurosciences and patients with neurologic disorders, simply because the first CT instrument available for clinical use was designed specifically for examination of the head. That occurrence was not entirely fortuitous, for Godfrey Hounsfield [1], who conceived and supervised construction of the first clinical scanner unit, was dedicated to extreme accuracy and sensitivity of measurement. He recognized that the physical principles relating to ionizing radiation, imaging, density discrimination, and spatial discrimination could be served best if a stationary, compact, and anatomically constant portion of the body (such as the cranium) was made the object of interest. His views were enthusiastically endorsed by Ambrose [2], a neuroradiologist, whose early clinical trials of the unit indicated that a major advance in radiology was at hand.

Thus was an idea, tentatively put forward in 1961 by Oldendorf [3] (a clinical neurologist) but conceived and developed independently by Hounsfield [1], given to neuroradiologists for clinical application and investigation. Even though neuroradiologists are numerically one of the smaller subspecialty groups within radiology, their abilities, enthusiasm, inquisitiveness, dedication, and willingness to accept new ideas provided an ideal climate for the full exploration of the method. Similar attributes among collaborating colleagues in other of the neurosciences have assured a thorough, impartial, and extensive evaluation of CT as a clinical diagnostic and investigational tool. More than 100 articles in the scientific literature since January 1973 attest to this fact. It is germane, at this time, to review this work, to identify the progress made, to study problems encountered, and to suggest directions for future investigations. I shall base my findings on the background of my experience and that of my colleagues at the Mayo Clinic, which encompasses a period of 36 months.

Clinical Progress

As one looks at the rapidly developing field of CT neurodiagnosis, there is ample documentation [4-10] that the technique is, in general, superior to the traditional neuro-radiologic examinations (cerebral angiography, cerebral pneumography, radionuclide brain scan, and echoencephalography) in the detection and localization of lesions as well as in accuracy and specificity of diagnosis. This superiority exists despite comparison of results backed by experience and sophistication reckoned in months with those supported by a decade or more of tradition and by refinements. It is not surprising, therefore, that the advent of CT should affect the utilization of all neurodiagnostic procedures [11].

From the beginning, including a 6-month familiarization period (fig. 1), CT investigations of neurologic disorders have steadily increased (saturating the capacity of one and then two instruments). At present, about one in every four patients seen by neurologists and neurosurgeons at the Mayo Clinic is examined by this modality. Perhaps predictably, the electroencephalogram (fig. 2), a unique indicator of cortical electrophysiologic activities, has been employed at a fairly steady rate in keeping with a 15%-20% increase of clinical load. Neuroradiologic examinations have not fared as well (figs. 3-6); their utilization has decreased. Pneumography, the most disagreeable and hazardous examination, was affected most in spite of a record of greatest accuracy. Echoencephalography and radionuclide scans, which yield less specific information, fell to intermediate levels. Cerebral angiography, the source of highly specific diagnostic information concerning the status of individual vessels and the vascularity of masses, was least affected, although the number of investigations of trauma to the head and of nonspecific convulsive disorders decreased dramatically.

As the patterns of cerebral angiographic diagnoses over the recent 4-year period are examined, it is interesting to note that negative findings have become less common—30% of the total in 1972 but only 22% in 1975 (table 1), a decrease of slightly more than 25%. In addition, the variety of pathologic processes delineated showed a distinct change. There was a 50% decrease in diagnoses related to traumatic hematomas and edema, whereas those identifying tumors increased by one-half and vascular lesions by one-fourth. Although the total number of tumors encountered in our practice increased dramatically (table 2), lesions in or adjacent to the skull base increased disproportionately. To me these data tangibly illustrate the present superiority of

Received April 19, 1976.

This investigation was supported in part by U.S. Public Health Service grants CA-15902 and CB-43982 from the National Institutes of Health.

¹ Mayo Clinic and Mayo Foundation, Rochester, Minnesota 55901.

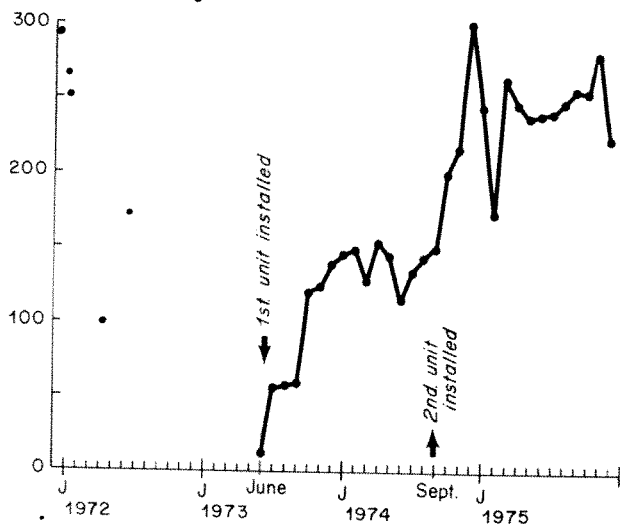


Fig. 1.—Monthly volume of CT scans per 1,000 neurologic patient registrations (1972-1975).

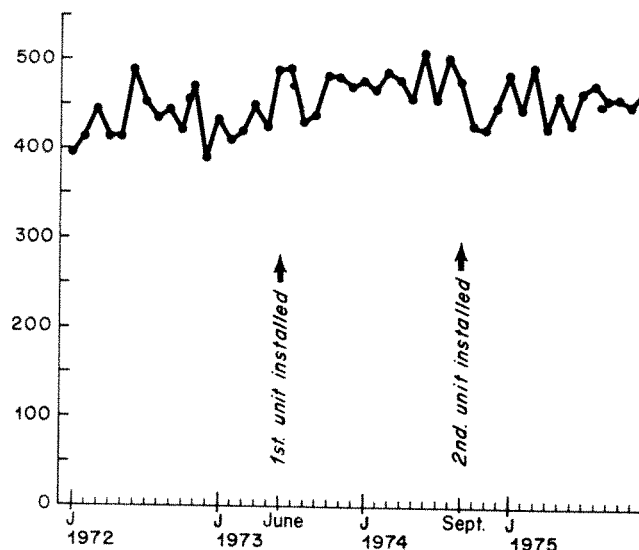


Fig. 2.—Monthly volume of electroencephalographic examinations per 1,000 neurologic patient registrations (1972-1975).

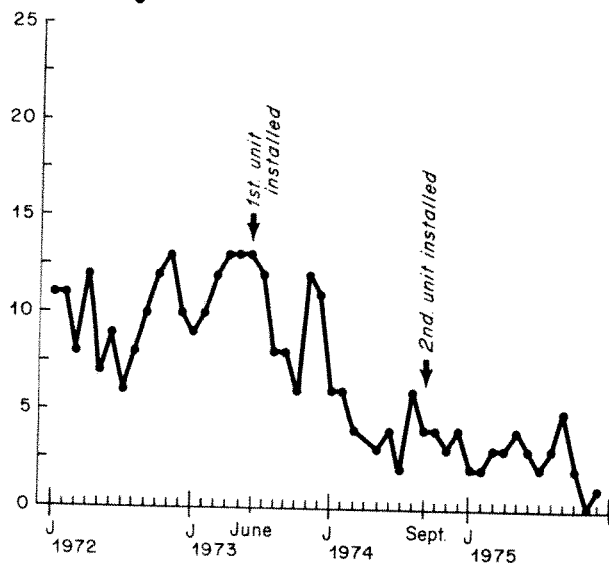


Fig. 3.—Monthly volume of cerebral pneumograms (ventriculograms and encephalograms) per 1,000 neurologic-patient registrations (1972-1975).

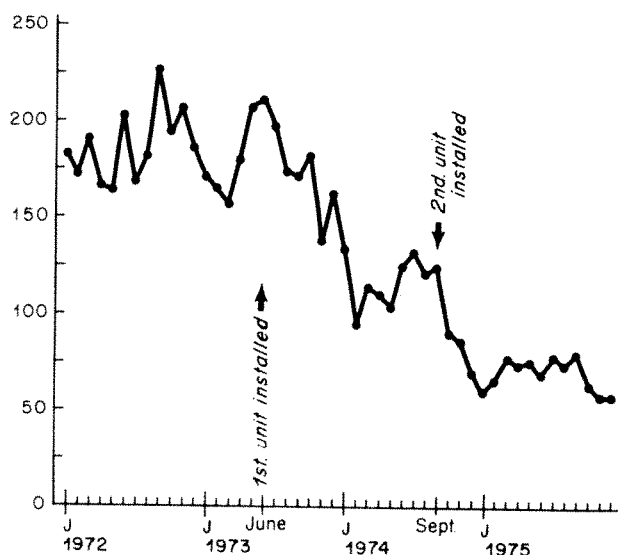


Fig. 4.—Monthly volume of A-mode echoencephalograms per 1,000 neurologic patient registrations (1972-1975).

angiography over CT for the investigation of vascular lesions of all types and of certain intracranial masses. They also highlight the importance of CT in the management of head trauma. The findings also suggest that our clinicians have high regard for CT findings to reveal structural lesions of the brain worthy of further definition through angiography and are less likely to pursue additional neuroradiologic investigation if the CT scan is normal.

Other changes in our practices are evolving and are under constant study. Still on the increase are the numbers of patients referred for CT with the tentative clinical diagnoses of cerebrovascular disease, subarachnoid hemorrhage, orbital mass, and possible postoperative complications. In the hemiplegic patient the rapid differentiation of tumor, infarct, and intracerebral hemorrhage is frequently possible. Orbital

pathologic masses, vascular lesions, and endocrinopathies can be sorted out, and postoperative edema, infection, or hemorrhage may be pinpointed so that appropriate therapeutic measures can be applied. Evaluation of the functional integrity of a shunt apparatus can easily be carried out before a patient's symptoms become severe; early and logical corrective measures can then be initiated.

Another trend has been an apparent change in the supratentorial gliomas encountered in our practice. In 1972, low grade (grades 1 and 2) astrocytomas were verified in only 5%-7% of operative cases, whereas in 1975 more than 30% of histologically verified gliomas were of this more benign variety. We are presently analyzing our material in search of a possible explanation and shall report our findings in a future publication.

TABLE 1
Cerebral Angiographic Diagnoses

Diagnosis	% of Total			
	1972	1973	1974	1975
Negative	30	26	25	22
Vascular disease	28	29	31	35
Tumor	21	24	29	32
Traumatic hematoma and edema	12	12	10	6
Vascular anomalies	5	4	3	3
Atrophy, hydrocephalus	3	3	2	2
Inflammation	1	2

TABLE 2
Tumor Diagnoses by Neuroangiography

Tumor	1972	1973	1974	1975
Glioma	125	118	122	163
Meningioma	30	44	40	47
Metastasis	44	51	26	51
Pituitary	4	38	54	72
Miscellaneous*	18	33	26	43
Total	221	284	268	376

* Includes angioblastoma, craniopharyngioma, pinealoma, colloid cyst, epidermoid, sarcoma, chemodectoma, myeloma, chordoma, chondrosarcoma, and fibrous dysplasia.

TABLE 3
Indications for Contrast Enhancement of CT Scans

Indications
1. Possible brain tumor clinically: Primary intradural mass Meningioma Known tumor (postoperative recheck) Metastatic disease Lymphoma, leukemia, or Hodgkin's disease Pineal region mass
2. Lesion in posterior fossa, including acoustic neuroma
3. Sellar or parasellar lesion
4. Brainstem lesion
5. Stroke
6. Possible aneurysm or arteriovenous malformation
7. Possible abscess or cerebritis
8. Possible orbital tumor
9. Possible subdural hematoma if routine CT negative or equivocal
10. Special circumstances if ordered by radiologist or clinician

Clinical Problems

Along with the progress I have described, problems in diagnosis have developed. The most pressing of these [12-18] has been determination of the role that intravenous injection of contrast medium should play in CT neurodiagnosis. Many workers have noted that certain lesions become more dense and therefore more easily demonstrable after the

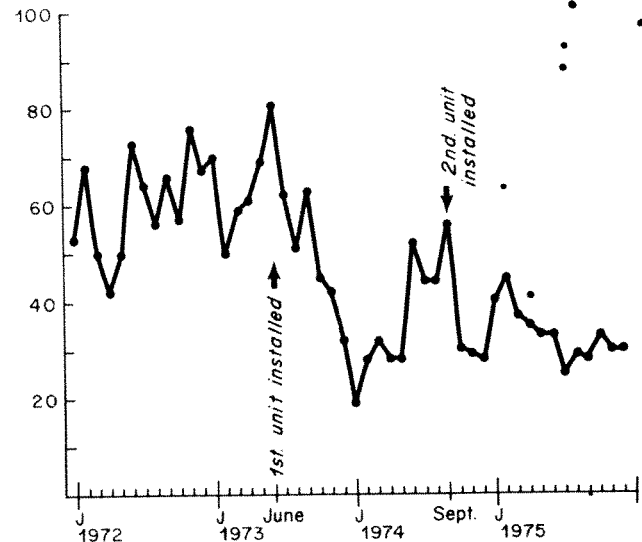


Fig. 5.—Monthly volume of radionuclide brain scans per 1,000 neurologic patient registrations (1972-1975).

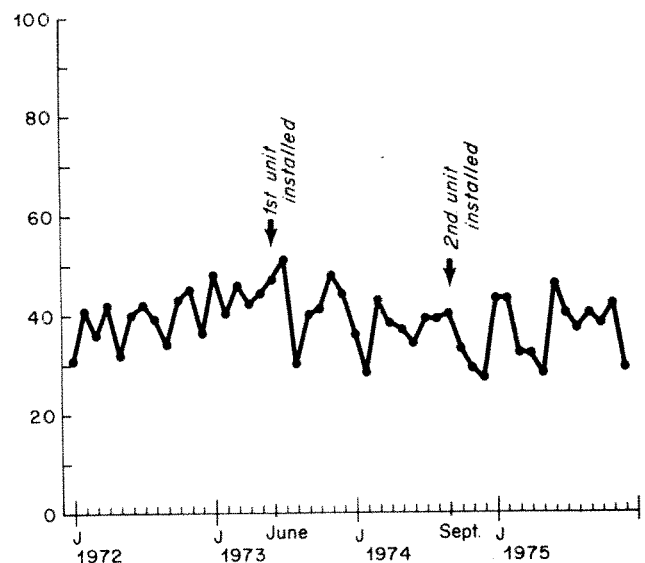


Fig. 6.—Monthly volume of cerebral angiograms per 1,000 neurologic patient registrations (1972-1975).

administration of iodinated contrast agents. The effect is apparently proportional to the vascularity of the tissues, the permeability of the blood-brain barrier, and the blood concentration of iodine. Some investigators have advocated routine "contrast enhancement" in all cases.

At the Mayo Clinic, we have taken a more conservative approach, employing the technique in our early experience only for tumor suspects. It soon became apparent that both accuracy and specificity of diagnosis could be positively influenced in additional situations, and over the months we have continually added to our list of indications for contrast enhancement (table 3). At this time, 50% of the CT examinations we conduct involve scanning both before and after the intravenous administration of iodinated medium.

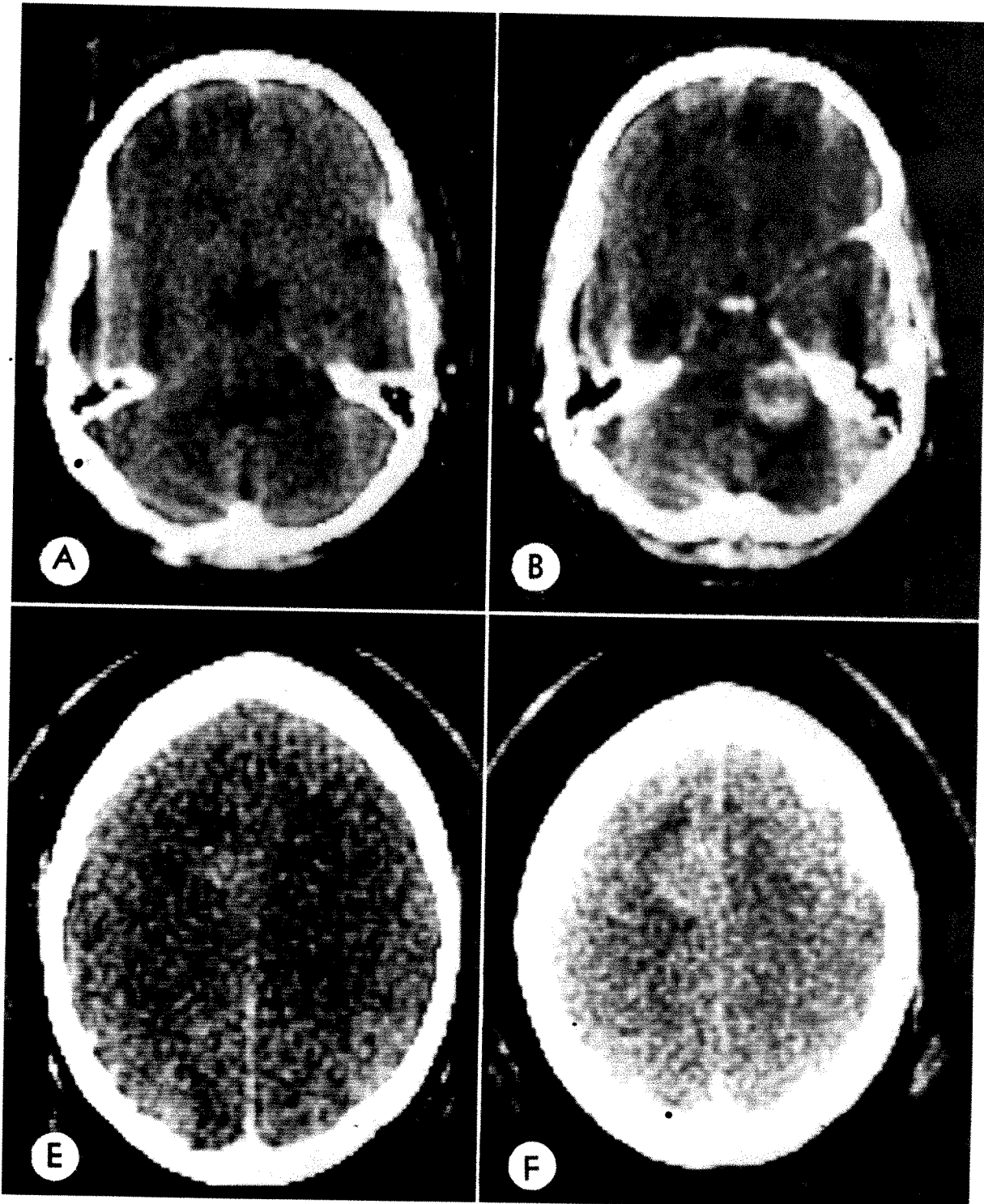


Fig. 7.—Enhancement of pathologic CT changes through intravenous injection of iodinated contrast medium. *A and B*, 1.5-cm right acoustic neurinoma; low absorption area before contrast (*A*) is precisely outlined and dense after contrast (*B*). *C and D*, Grade 2 astrocytoma of pons; area of slightly increased absorption, barely visible before enhancement (*C*) is easily discernible after (*D*). *E and F*, Grade 3 astrocytoma, left frontoparietal parasagittal region, in patient

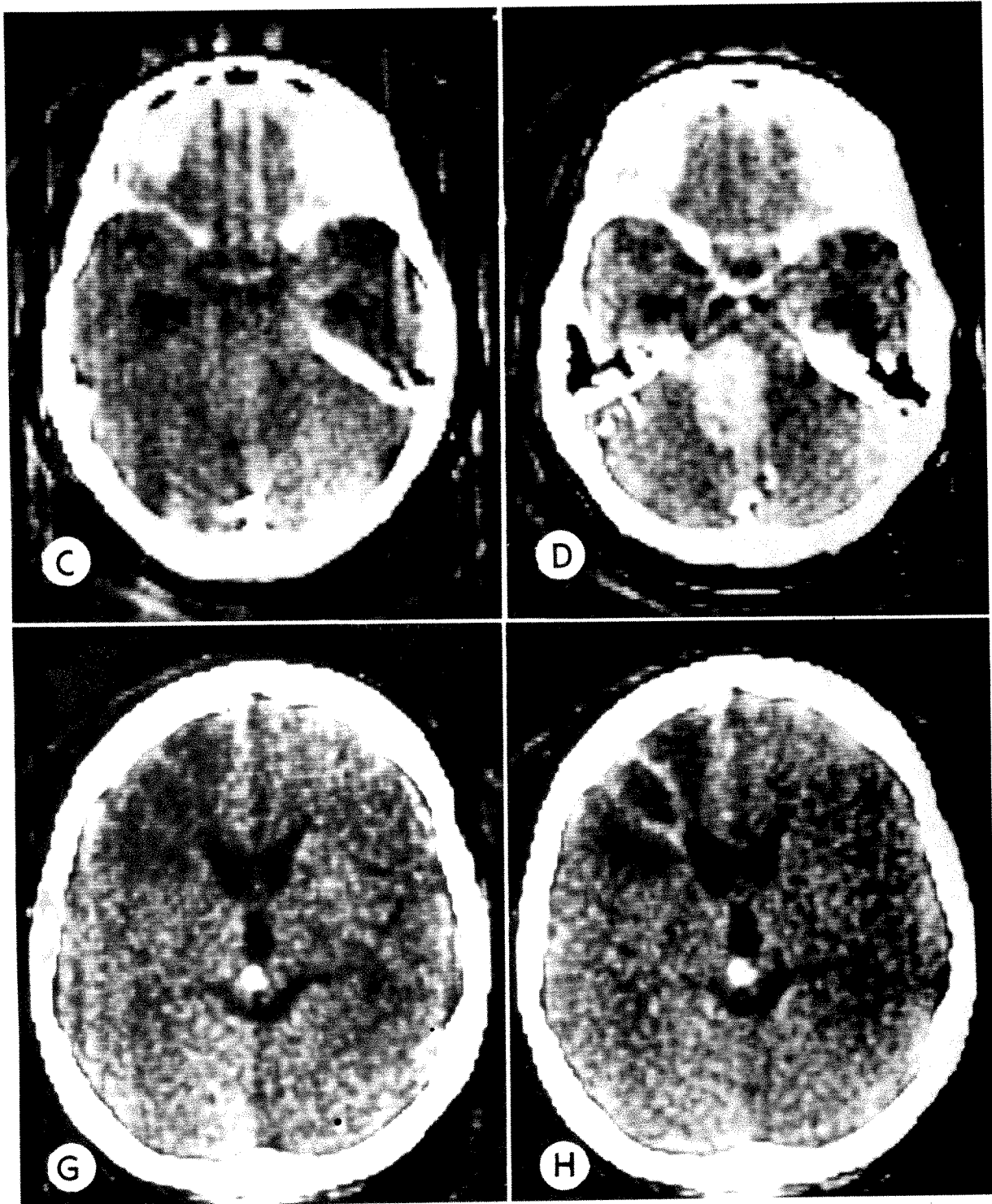


Fig. 7. (*cont.*)—with seizure disorder; note more obvious visible changes in scan after administration of contrast (F) compared to baseline series (E). G and H. Left frontoparietal infarct in patient with polyarteritis nodosa and sudden onset of headaches 4 days before examination; infarct easily seen before (G) and after (H) contrast. There is convincing evidence of "luxury perfusion" within lesion.

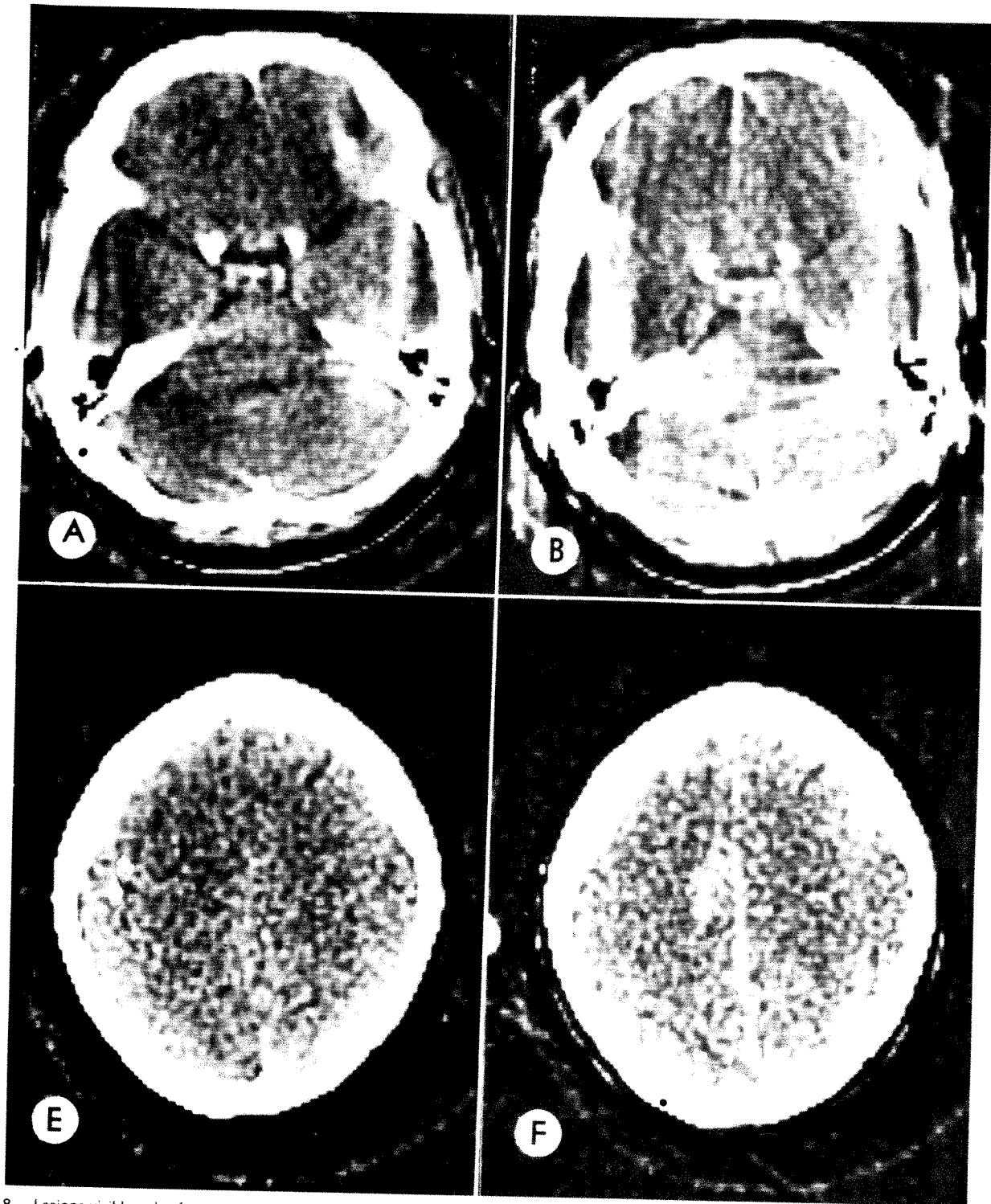


Fig. 8.—Lesions visible only after contrast enhancement. *A and B*, 3.5-cm left acoustic neurinoma; lesion not evident before contrast (*A*) but visible after (*B*). *C and D*, Huge right middle fossa meningioma; lesion has absorption coefficient similar to normal brain before contrast (*C*) but is densely opacified after contrast (*D*). *E and F*, 72-hour infarct in left frontoparietal parasagittal scans before (*E*) and after (*F*) contrast. Cerebral angiogram negative; radionuclide

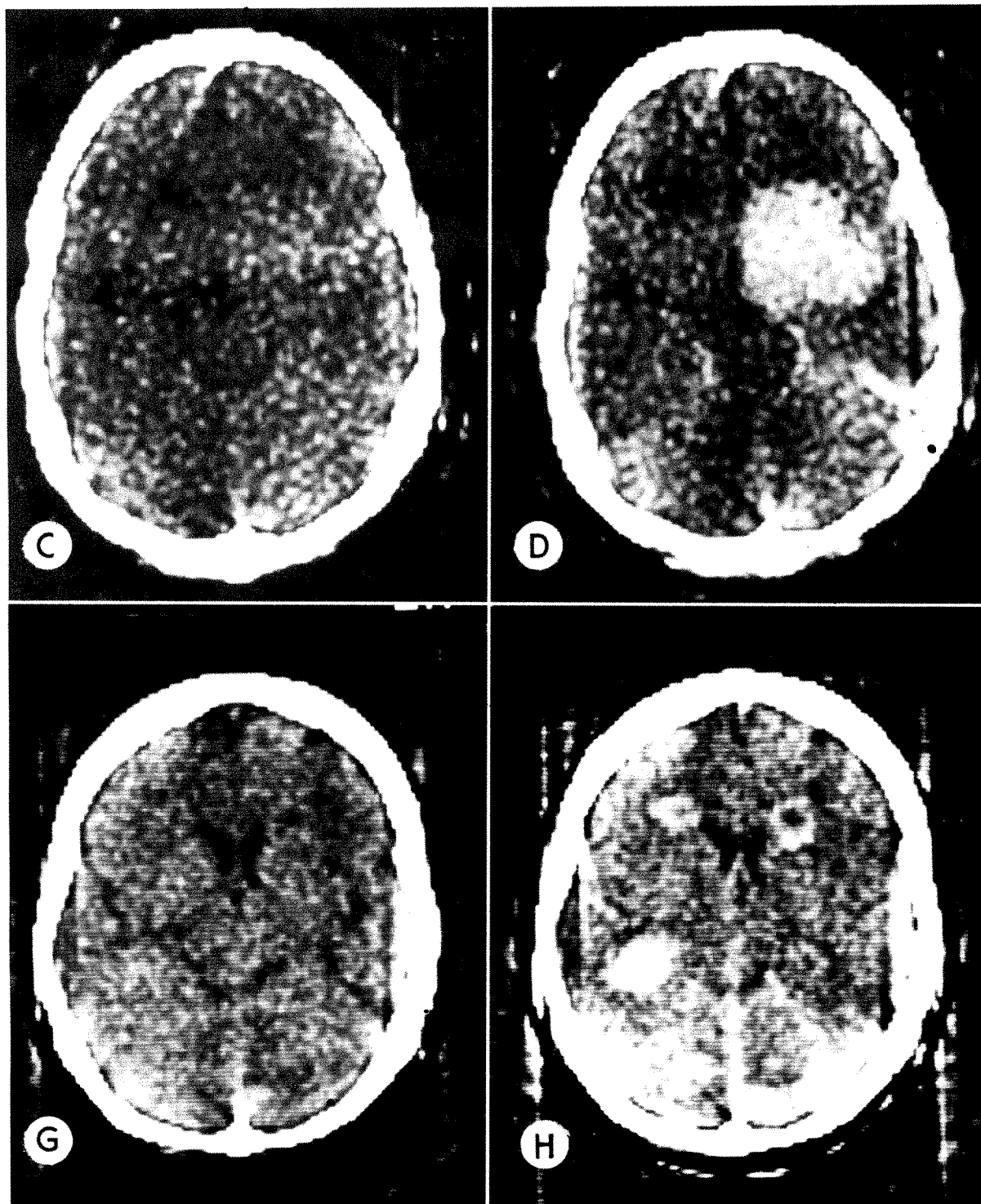


Fig. 8. (cont.)—scan positive. Surgical biopsy yielded infarcted brain tissue. Note similarity in appearance to tumor in figs. 7E and 7F. G and H, Metastatic small-cell bronchogenic carcinoma; positive identification not possible before contrast (G) even though at least eight nodules obvious after contrast (H).

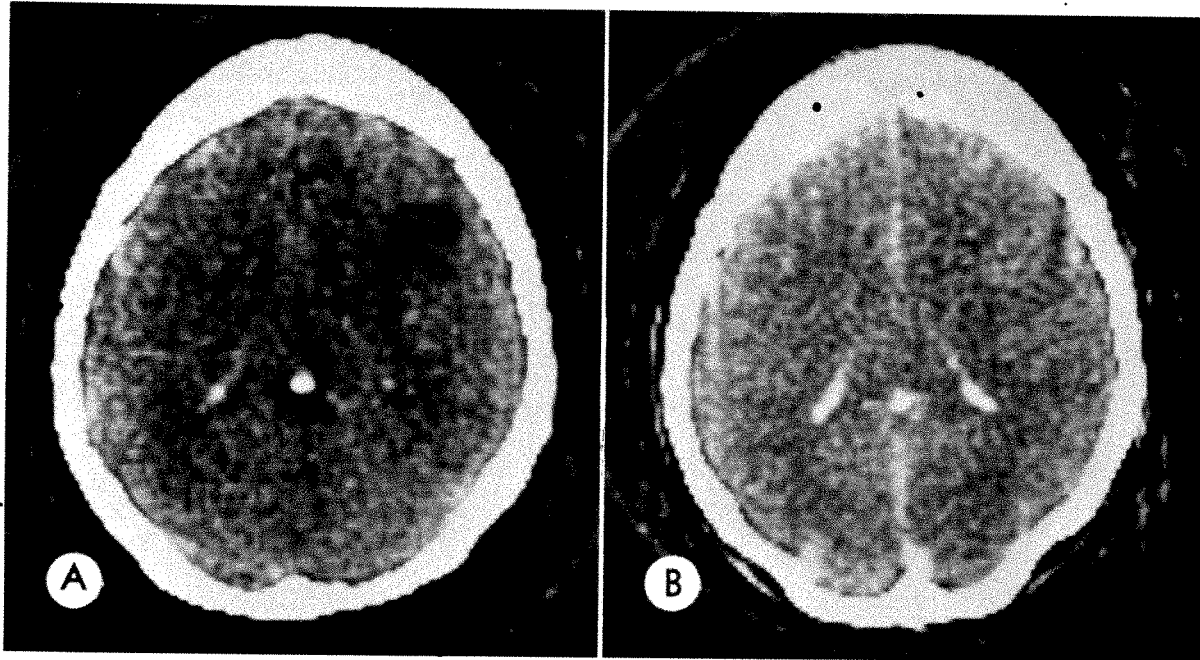


Fig. 9.—A, Obvious low density lesion in right frontal lobe (8-day-old infarct according to history). B, Administration of contrast brings absorption coefficient of lesion to that of surrounding brain so that it "disappears."

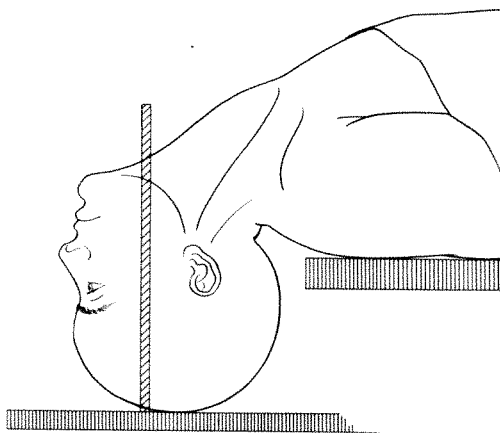


Fig. 10.—Head positioning of patient for coronal CT sections of the brain, possible with large opening in a body scanner.

We have been impressed by the work of Gado and associates [17, 18] who studied iodine concentrations in blood after infusion and bolus injection of equivalent quantities of iodine. Their results indicate that iodine levels reach a higher peak more quickly and are sustained for the same period with the bolus method. We accordingly employ the bolus technique, giving 19.5 g of iodine in the form of meglumine diatrizoate. We have used as much as 23 g and as little as 12.75 g, but have found that our present practice yields adequate "enhancement" while minimizing patient discomfort and consequent motion artifact.

When applied for the foregoing clinical indications, the following results were noted in 1,049 recent enhanced scans: 51% of the studies were negative on scans both before and after adding contrast medium, while 45% were

positive on both. Although contrast medium was not mandatory for the assessment of positivity in this latter group, certain tumors (figs. 7A–7F), inflammatory processes, and infarcts (figs. 7G and 7H) became more obvious with its usage and a differential diagnosis could be made with greater confidence. We are also more certain of our negative assessments if enhancement has been employed in cases with unequivocal neurologic signs and symptoms.

Probably of more importance are the remaining 4% of cases, half of which had negative scans before the injection of medium but positive findings on the sequence after injection. For the other half, lesions with a low absorption coefficient (μ) disappeared as enhancement raised their absorption coefficient to that of the normal surrounding brain tissue. Lesions seen only in the enhanced scan included acoustic neurinomas (figs. 8A and 8B), meningiomas (figs. 8C and 8D), infarcts (figs. 8E and 8F), metastasis (figs. 8G and 8H), and arteriovenous malformations. Lesions that disappeared included infarcts (fig. 9), cerebritis, and metastasis. We presume that additional entities with similar characteristics will be discovered and believe it proper to insist vigorously on adequate procedures (scans before and after adding contrast medium) if erroneous diagnoses are to be avoided.

Future Investigations

Continued investigation is vital to realize the full potential of CT. Two areas that we are now pursuing are the augmentation of imaging and display capabilities and the extraction of maximal information from CT scan data.

Altered image processing and display techniques, which seem to have attracted most attention, are sought in order to contribute additional anatomic information for better interpretation of CT studies. Several investigators [19–22]

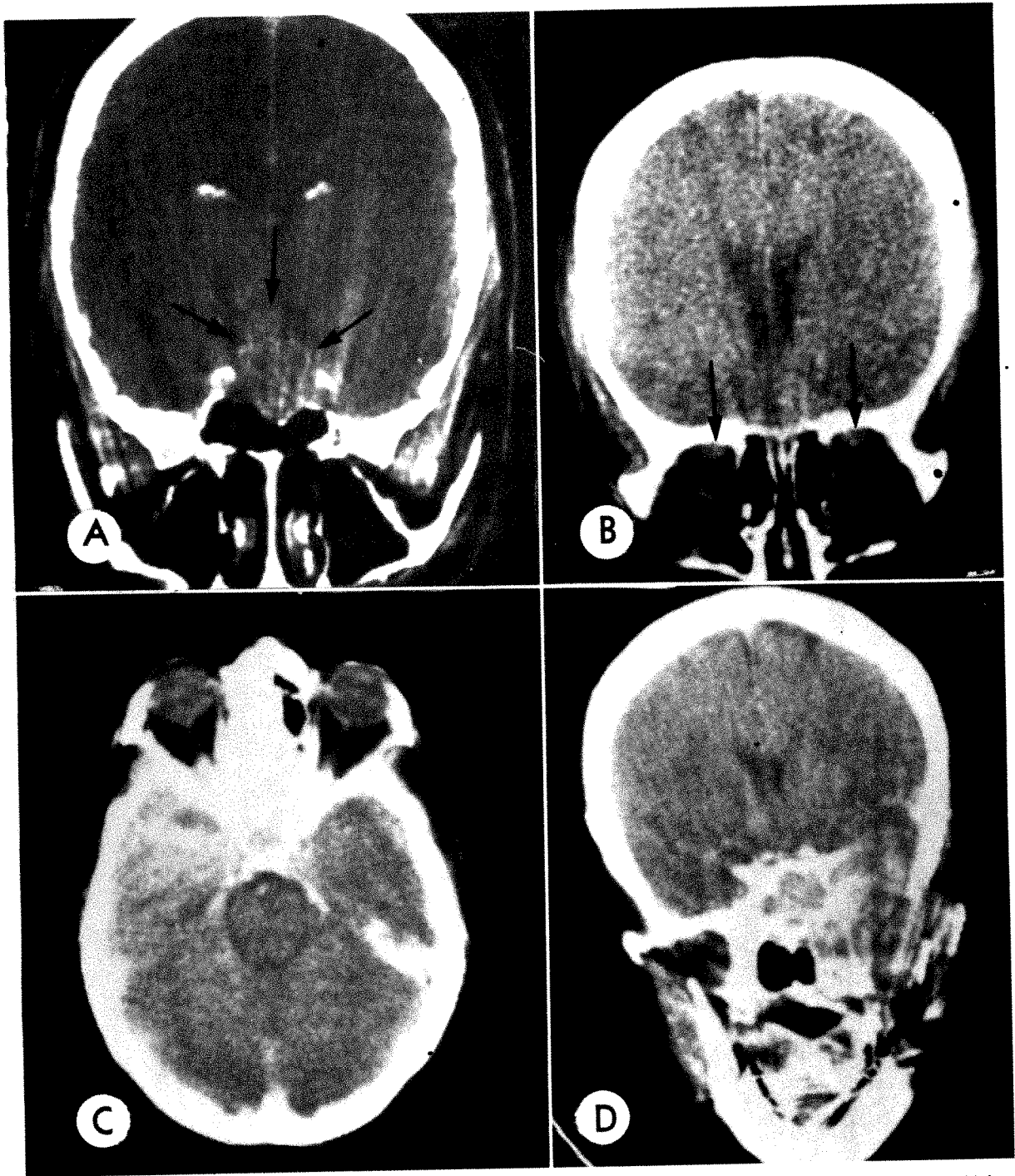


Fig. 11.—Coronal CT sections of intracranial pathologic processes. *A*, Large pituitary tumor expanding inferiorly into sphenoid sinus and left parasellar and suprasellar regions (*arrows*). Note how full extent of mass is visualized. *B*, Graves' ophthalmopathy with thickening of ocular muscles and proptosis. On routine transverse sections, muscle thickening not well appreciated, especially in superior group, but was easily visible (*arrows*) in coronal slices. *C*, Large left middle fossa and nasopharyngeal neurolemmoma seen as diffuse mass filling temporal fossa. *D*, Coronal section of same patient revealing full extent of mass, bony destruction of middle fossa floor, and invasion of sphenoid sinus. Note distortion of pterygoid plate.

have developed systems for manipulation and redisplay of CT image data in the more or less conventional format. Promising innovations have resulted from the work of Glenn et al. [23] who have devised methods for generating a large number of thin nonoverlapping tissue "slices" resulting in improved resolution and the capability of reconstructing image planes perpendicular to (coronal and sagittal) the original transverse scans. Our work [24] has addressed the production of coronal sections of the head with the EMI-CT 5000 body scanner by simple alterations in the position of the subject's head (fig. 10). Coronal sections have been most useful in the evaluation of sellar and parasellar masses (fig. 11A), orbital processes (fig. 11B), nasopharyngeal masses (figs. 11C and 11D), and lesions in the cerebellopontine angle. The additional anatomic information, so easily obtained, has been invaluable for diagnosis and warrants further study and utilization.

The extraction of maximal information from CT absorption data has attracted little attention from investigators [25-28]. Our efforts [29] involve comparison of absorption coefficients of the two cerebral hemispheres in terms of means, standard deviations, skewed coefficients, frequency polygons, and CSF-brain ratios to assist the radiologist in classifying scans as normal or abnormal. Early studies show promise of being more sensitive than visual inspection, and we are evolving more refined methods to characterize density profiles in smaller subsegments of the brain in health and disease. Our goal is to develop an on-line system so that all CT scans might be analyzed in a prospective manner.

REFERENCES

- Hounsfield GN: Computerized transverse axial scanning (tomography). I. Description of system. *Br J Radiol* 46:1016-1022, 1973
- Ambrose J: Computerized transverse axial scanning (tomography). II. Clinical application. *Br J Radiol* 46:1023-1047, 1973
- Oldendorf WH: Isolated flying spot detection of radiodensity discontinuities: displaying the internal structural pattern of a complex object. *IEEE Trans Biomed Electronics* 8:68-72, 1961
- Baker HL Jr, Campbell JK, Houser OW, Reese DF, Sheedy PF, Holman CB, Kurland RL: Computer assisted tomography of the head: an early evaluation. *Mayo Clin Proc* 49:17-27, 1974
- Baker HL Jr, Campbell JK, Houser OW, Reese DF: Early experience with the EMI scanner for study of the brain. *Radiology* 116:327-333, 1975
- New PFJ, Scott WR, Schnur JA, Davis KR, Taveras JM: Computerized axial tomography with the EMI scanner. *Radiology* 110:109-123, 1974
- Paxton R, Ambrose J: The EMI scanner: a brief review of the first 650 patients. *Br J Radiol* 47:530-565, 1974
- Pendergrass HP, McKusick KA, New PFJ, Potsaid MS: Relative efficacy of radionuclide imaging and computed tomography of the brain. *Radiology* 116:363-366, 1975
- Gado M, Coleman RE, Alderson PO: Clinical comparison of radionuclide brain imaging and computerized transmission tomography. I., in *Noninvasive Brain Imaging: Computed Tomography and Radionuclides*, edited by De Blanc HJ, Sorenson JA, New York, Society of Nuclear Medicine, 1975, pp 147-171
- Passalacqua AM, Braunsberg P, Kricheff II, Naidich TP, Chase NE: Clinical comparison of radionuclide brain imaging and computerized transmission tomography. II., in *Noninvasive Brain Imaging: Computed Tomography and Radionuclides*, edited by De Blanc HJ, Sorenson JA, New York, Society of Nuclear Medicine, 1975, pp 173-181
- Baker HL Jr: The impact of computed tomography on neuro-radiologic practice. *Radiology* 116:637-640, 1975
- Davis DO, Pressman BD: Computerized tomography of the brain. *Radiol Clin North Am* 12:297-313, 1974
- Huckman MS: Clinical experience with the intravenous infusion of iodinated contrast material as an adjunct to computed tomography. *Surg Neurol* 4:297-318, 1975
- Kramer RA, Janetos GP, Peristein G: An approach to contrast enhancement in computed tomography of the brain. *Radiology* 116:641-647, 1975
- Ambrose J, Gooding MR, Richardson AE: Sodium iothalamate as an aid to diagnosis of intracranial lesions by computerized transverse axial scanning. *Lancet* 2:669-674, 1975
- Yock DH Jr, Marshall WH Jr: Recent ischemic brain infarcts at computed tomography: appearances pre- and postcontrast infusion. *Radiology* 117:599-608, 1975
- Gado MH, Phelps ME, Coleman RE: An extravascular component of contrast enhancement in cranial computed tomography. II. Contrast enhancement and the blood-tissue barrier. *Radiology* 117:595-597, 1975
- Gado MH, Phelps ME, Coleman RE: An extravascular component of contrast enhancement in cranial computed tomography. I. The tissue-blood ratio of contrast enhancement. *Radiology* 117:589-593, 1975
- Shields RA, Isherwood I, Pullan BR: The use of an off-line static display system with a computerized transverse axial tomographic unit. *Br J Radiol* 47:893-895, 1974
- Huang HK, Ledley RS: Three-dimensional image reconstruction from in vivo consecutive transverse axial sections. *Comput Biol Med* 5:165-170, 1975
- Larsen LE, Evans RA: An off-line image processing system for digital tomography. Paper presented at the annual meeting of the American Society of Neuroradiology, Vancouver, British Columbia, June 1975
- Thompson CJ: Cited in *Computed Tomography of the Brain and Orbit (EMI Scanning)*, edited by New PFJ, Scott WR, Baltimore, Williams & Wilkins, 1975, pp 48-51
- Glenn WV Jr, Johnston RJ, Morton PE, Dwyer SJ: Image generation and display techniques for CT scan data: thin transverse and reconstructed coronal and sagittal planes. *Invest Radiol* 10:403-416, 1975
- Baker HL Jr: CT scanning: its impact on radiology (RSR 5203, audiovisual course). Paper presented at the annual meeting of the Radiological Society of North America, Chicago, November 1975
- Penn RD, Walser R, Ackerman L: Cerebral blood volume in man: computer analysis of a computerized brain scan. *JAMA* 234:1154-1155, 1975
- Fox JH, Huckman MS: Computerized tomography: a recent advance in evaluating senile dementia. *Geriatrics* 30:97-100, 1975
- Huckman MS, Fox J, Topel J: The validity of criteria for the evaluation of cerebral atrophy by computed tomography. *Radiology* 116:85-92, 1975
- Rutherford RA, Pullan B, Isherwood I, Goddard J: Quantitative aspects of computer assisted tomography (abstr.). *Br J Radiol* 48:605, 1975
- Reese DF, O'Brien PC, Beeler GW Jr, Gerding PR, McCullough EC: An investigation for extracting more information from computerized tomography scans. *Am J Roentgenol* 124:177-185, 1975

Some Limitations of Computed Tomography in the Diagnosis of Neurological Diseases

KENNETH R. DAVIS,¹ JUAN M. TAVERAS, GLENN H. ROBERSON, AND ROBERT H. ACKERMAN

Some of the limitations of CT in the diagnosis of neurologic disease are reported. Problem areas include small lesions; lesions obscured by adjoining structures; small vascular structures and detail of large vessels; cases in which the diagnosis is made but information is incomplete for treatment; cases of incorrect diagnosis; non-neoplastic lesions mistaken for neoplasms; some subdural hematomas; occasional false negative findings; and misinterpretation due to technical errors. Knowledge and use of the clinical presentation, the performance of other comple-

mentary diagnostic procedures, repeat CT scans tailored to the region of interest, and repeat serial scans may assist in reaching the proper diagnosis and diminishing potential error.

Introduction

Use of the EMI head scanner during the past 3 years has helped considerably in the diagnosis and management of many patients suffering from neurological disorders [1, 2].

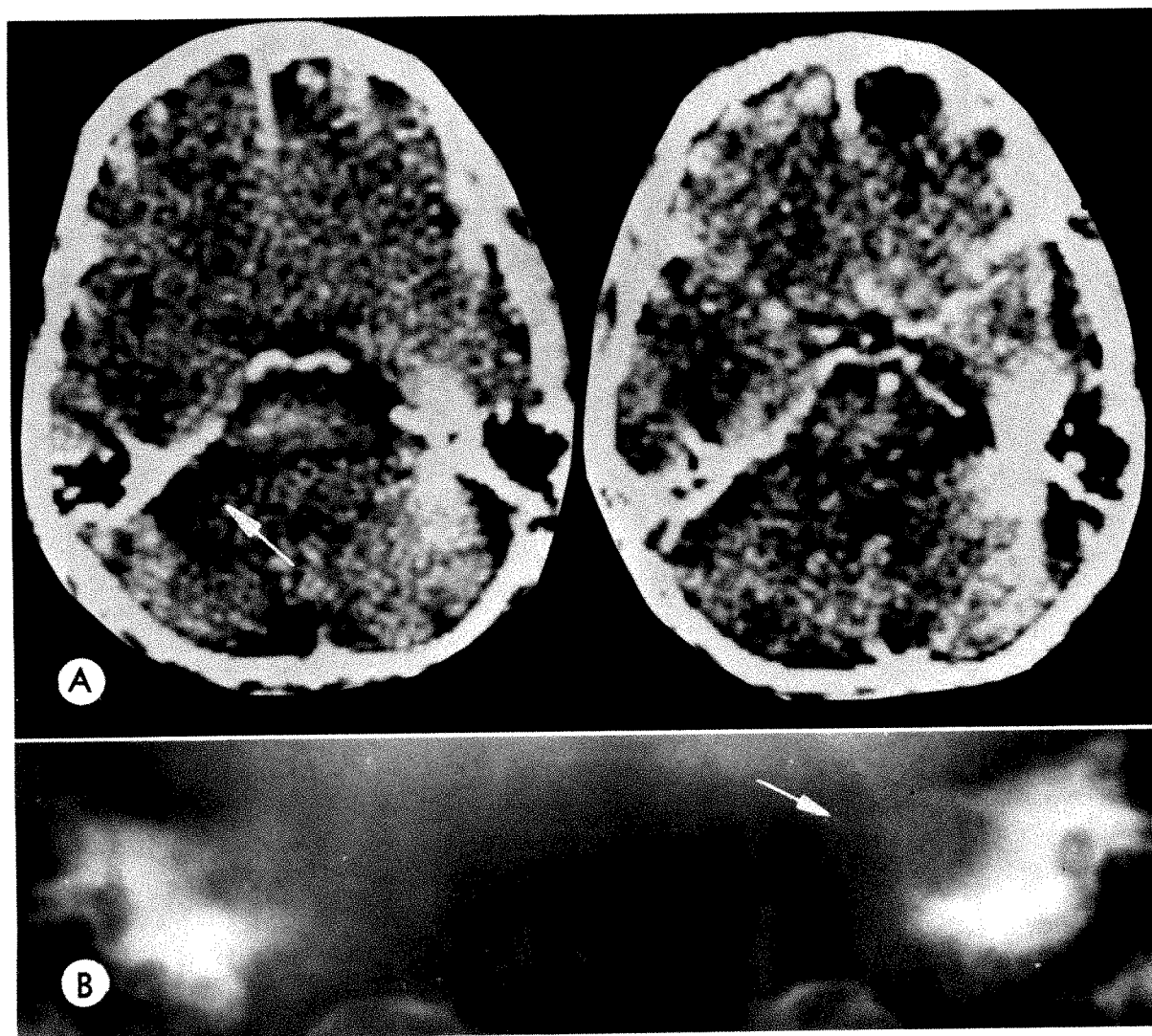


Fig. 1.—Left acoustic neuroma. A, CT scans without contrast (*left*) and following 300 ml meglumine diatrizoate (*right*). Normal left cerebellopontine angle (*arrow*); right cerebellopontine angle artifact. Undisplaced fourth ventricle. B, Coronal polytome laminogram showing widened abnormal left auditory meatus (*arrow*). Left-sided 1.5 cm neuroma confirmed at surgery.

Received March 25, 1976.

¹ All authors: Department of Radiology, Massachusetts General Hospital and Harvard Medical School, Boston, Massachusetts 02114. Address reprint requests to K. R. Davis.

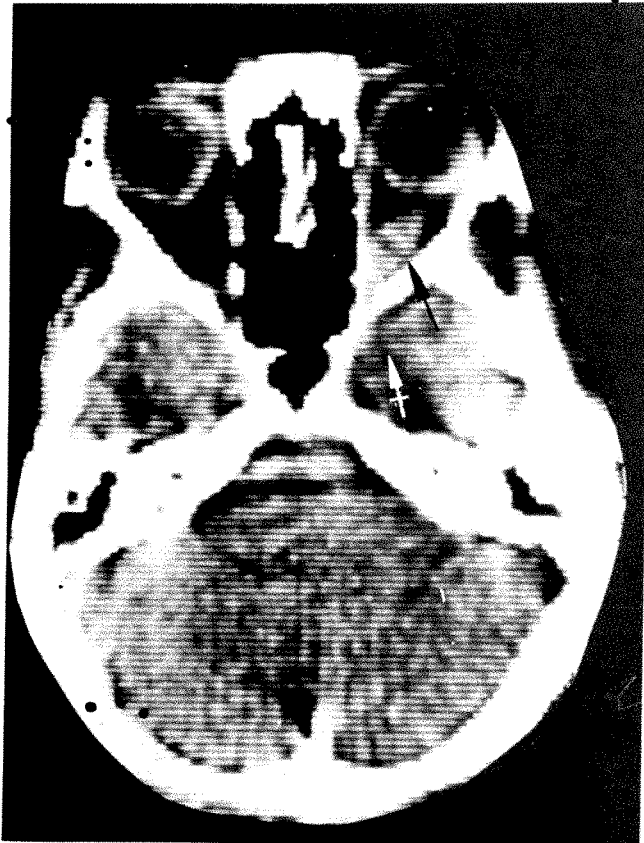


Fig. 2.—Meningioma. CT scan with contrast (300 ml meglumine diatrizoate) showing retrobulbar high absorption abnormality (arrow). Normal right orbitocranial junction behind anterior clinoid (hatched arrow). At surgery 2 cm intracranial meningeoma extension in region of anterior clinoid found which was not seen on CT.

←

While the advantages of the technique are numerous, the shortcomings have not received sufficient attention. It has taken some time to accumulate enough experience to determine the types of cases in which CT information may be erroneous or incomplete. While this paper demonstrates some of the limitations of CT diagnosis, no doubt other limitations will be reported in the future.

Diagnostic Categories

CT fails to give complete information in the following situations.

Small Lesions

The CT scan may fail to detect a lesion either because it is too small or because there is little difference between the absorption coefficient of the lesion and that of surrounding brain both before and after intravenous contrast enhancement. Excessively high or low absorption values of adjacent structures may also limit detectability of a lesion (see below) [3]. Some examples are lacunar infarcts (involving deep penetrating vessels), small foci of metastatic tumor,

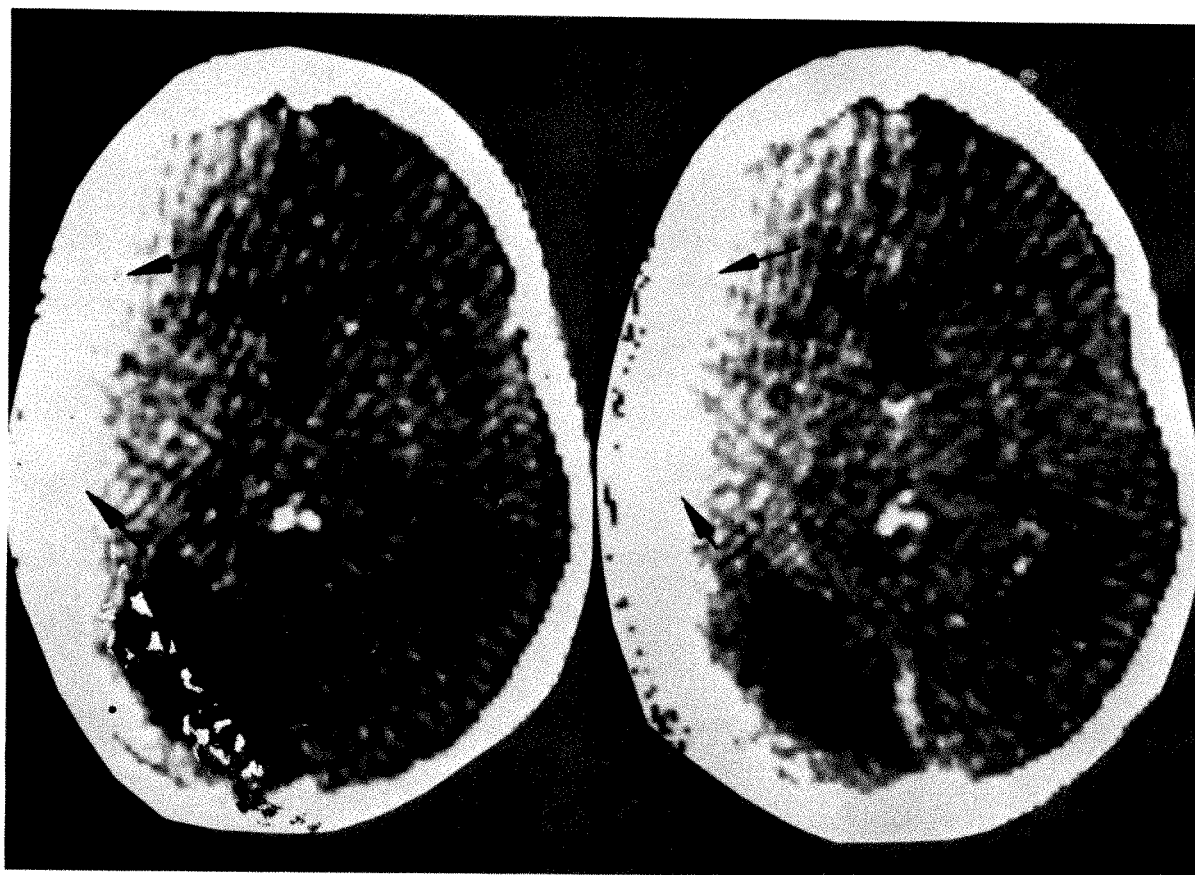


Fig. 3.—Recurrent meningeoma. CT scans without contrast (left) and after 300 ml meglumine diatrizoate (right). Arrows show scatter from tantalum. At surgery 3 cm recurrent meningeoma found near pterion which was not seen on CT.

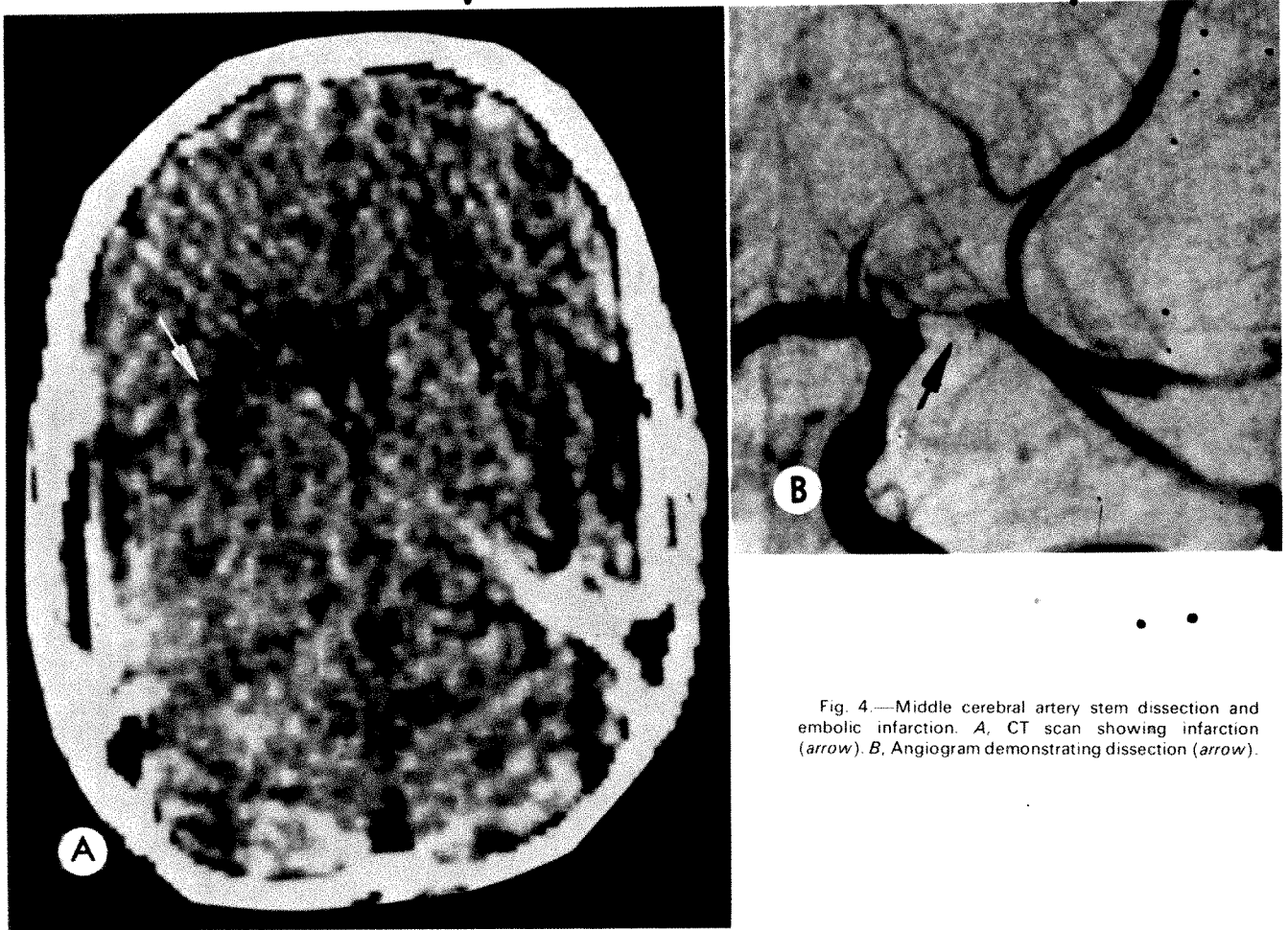


Fig. 4.—Middle cerebral artery stem dissection and embolic infarction. A, CT scan showing infarction (arrow). B, Angiogram demonstrating dissection (arrow).

pituitary microadenomas, and small acoustic neuromas (fig. 1).

Polytome laminography, rather than CT, is the procedure of choice for detection of pituitary microadenomas because they usually do not protrude into the suprasellar region. Small acoustic neuromas that are clinically suspected and not seen on CT scan even after intravenous contrast enhancement may be detected by Pantopaque cisternography. Laminography of the internal auditory meati may be negative or positive in these cases.

Lesions Obscured by Adjoining Structures

Very high or low absorption values of structures adjacent to small lesions may interfere with detection of the lesion [3]. For example, dense bone at the base of the skull may interfere with detection of a pituitary adenoma, whereas pneumoencephalography may demonstrate suprasellar extension. Other types of lesions may be overlooked in this region (fig. 2), and, similarly, the petrous bone may obscure a small acoustic neuroma. High absorption substances such as tantalum or the presence of many metallic clips may prevent detection of an underlying lesion, whereas angiography will depict the abnormality (fig. 3).

Vascular Lesions and Vascular Structures

Small vessels and detail of larger vessels are not observed on CT scans even after intravenous injection of contrast medium [4]. Figure 4 illustrates a patient in whom angiography demonstrated middle cerebral artery dissection and CT showed cerebral infarction. The collateral vessels of occlusive vascular disease (fig. 5) and even the rich vascular telangiectasis seen in multiple progressive intracranial arterial occlusions (moyamoya) are not seen (fig. 6). CT provides no information on cervical carotid bifurcation in cases of occlusive disease or the vascular spasm secondary to subarachnoid hemorrhage.

Although the presence of an aneurysm measuring more than 5 mm in diameter may be suspected following intravenous contrast enhancement, the fine detail of the aneurysmal sac and its relation to the parent vessel cannot be shown. Cerebral angiography is required in all these cases. However, CT may show infarction in many cases of vascular occlusive disease, and, in addition, may depict hematoma, major subarachnoid blood, hydrocephalus, or intraventricular hemorrhage in cases of intracranial bleeding [5].

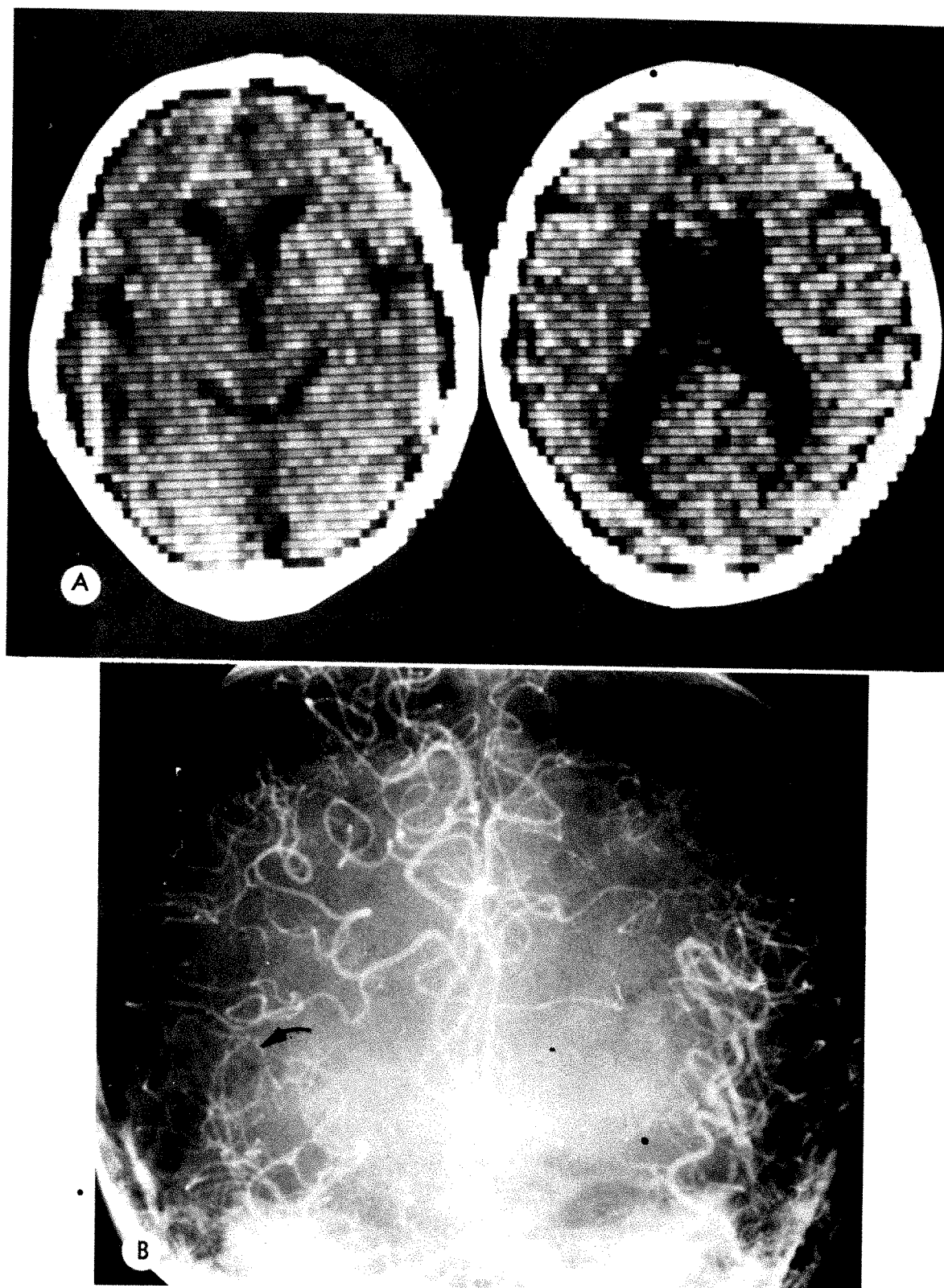


Fig. 5.—Arteriosclerotic vascular occlusive disease. *A*, CT scans showing minimal atrophy only. *B*, Left carotid AP angiogram showing retrograde filling from right anterior cerebral artery into right middle cerebral artery (*arrow*).

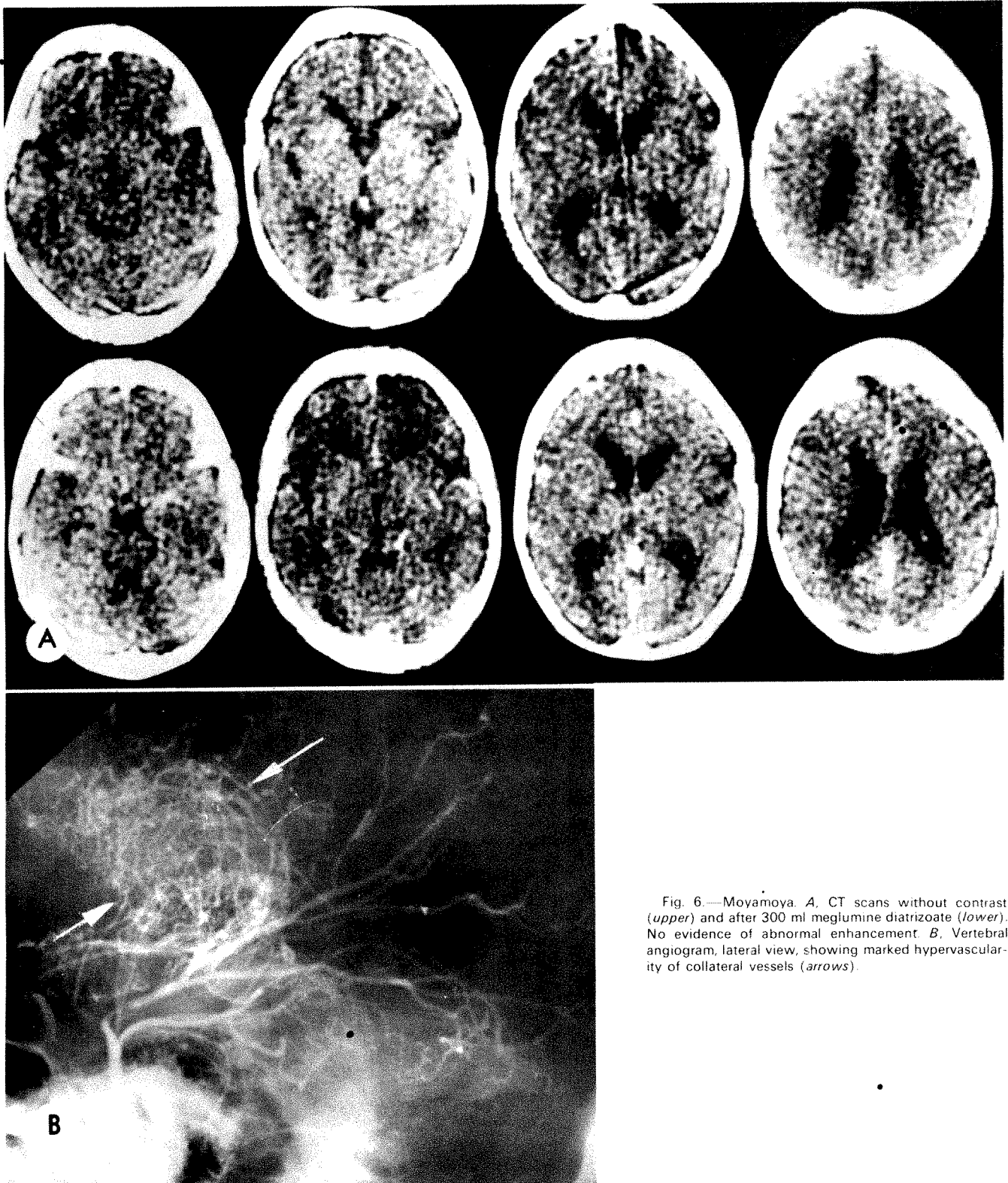


Fig. 6.—Moyamoya. A. CT scans without contrast (*upper*) and after 300 ml meglumine diatrizoate (*lower*). No evidence of abnormal enhancement. B. Vertebral angiogram, lateral view, showing marked hypervascularity of collateral vessels (*arrows*).

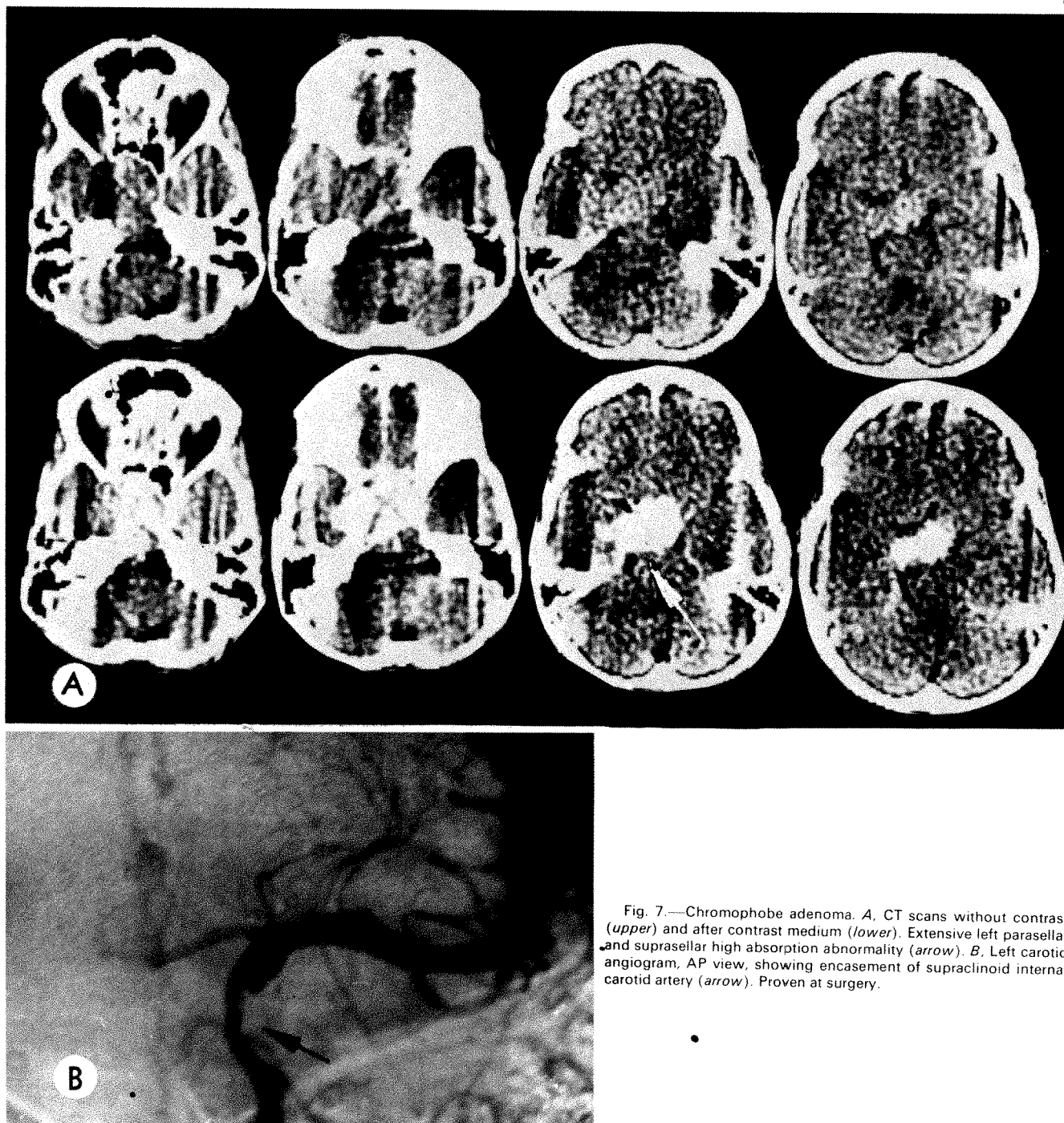


Fig. 7.—Chromophobe adenoma. A, CT scans without contrast (*upper*) and after contrast medium (*lower*). Extensive left parasellar and suprasellar high absorption abnormality (*arrow*). B, Left carotid angiogram, AP view, showing encasement of supraclinoid internal carotid artery (*arrow*). Proven at surgery.

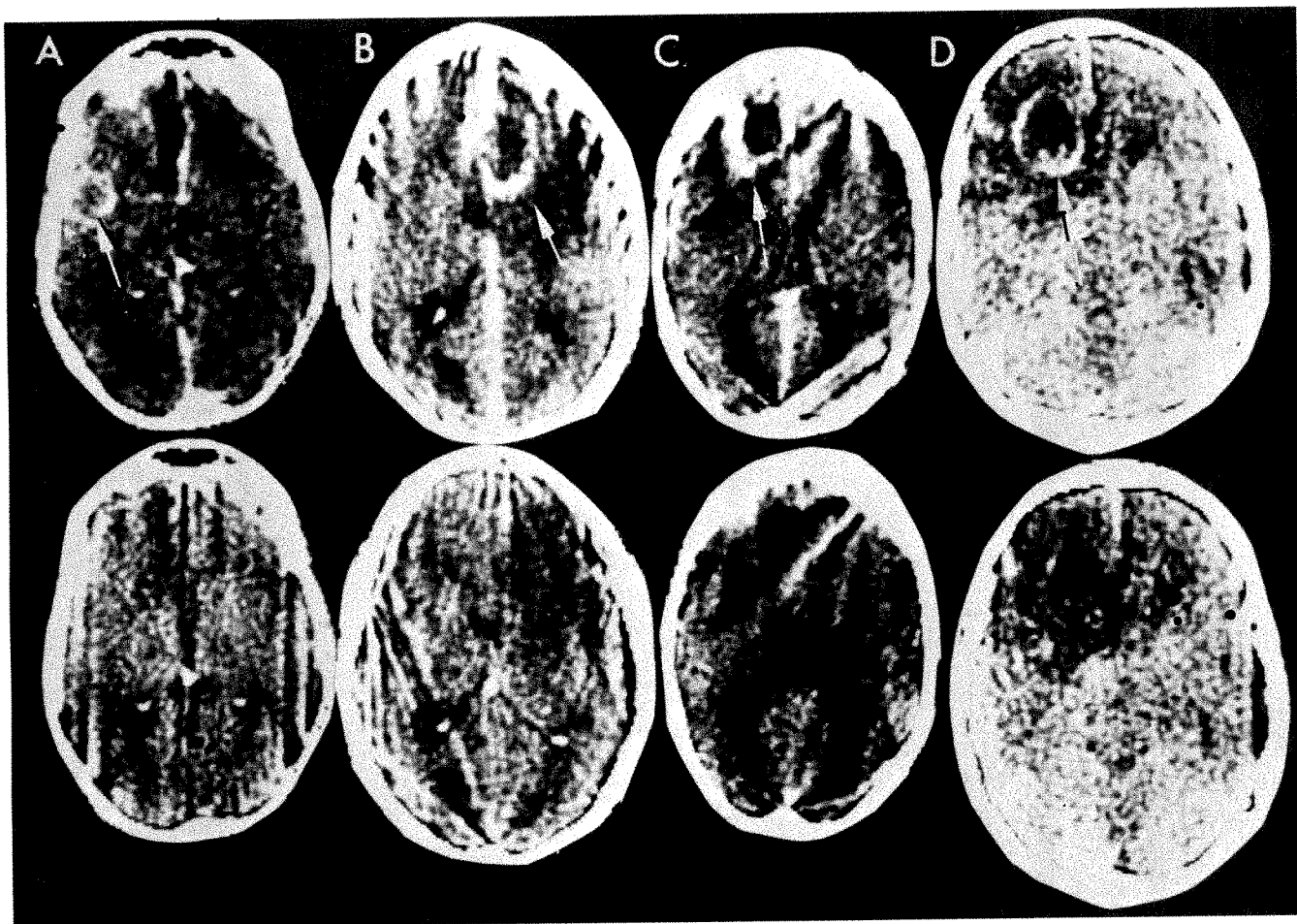


Fig. 8.—Four cases showing ringlike enhancement. CT scans after 300 ml meglumine diatrizoate (*upper*) and without contrast (*lower*). A, Proven infarction at surgery; preoperative diagnosis, abscess. B, Surgically proven right frontal glioblastoma. C, Surgically proven left frontal abscess. D, Left frontal undifferentiated lung metastasis.

Diagnosis Made but Information Incomplete for Treatment

Other procedures may be necessary in order to provide sufficient information for treatment. For example, encasement of a vessel may only be identified at angiography. This is most often present in cases of meningioma or chordoma, but may also be seen in unsuspected instances of large chromophobe adenomas (fig. 7) or intradural epidermoid tumors. Cases of suprasellar extension of a chromophobe adenoma may show high absorption after contrast medium, but pneumoencephalography combined with detailed laminography is necessary to depict the exact position of the optic chiasm and third ventricle. Involvement of the optic chiasm by an optic glioma, although the optic nerve involvement is evident on CT, may be definitively shown in some cases only by pneumoencephalography.

Incorrect Diagnosis

Since many lesions appear similar on CT scans, an error in interpretation is possible. In some cases the clinical history and other examinations will lead to the correct diag-

nosis. Figure 8 shows several different types of lesions characterized on CT by a ring of high absorption after contrast infusion. Figure 9 depicts a variety of pathological conditions with high absorption in the suprasellar region.

A craniopharyngioma (fig. 9A) was clinically felt to represent a rare hypothalamic tuberculoma because of fever, hypothalamic signs, and signs of low-grade meningitis. In our experience, tuberculoma will show contrast enhancement. Another case, a child with obstructive hydrocephalus at the level of the aqueduct due to a pinealoma that did not enhance after intravenous contrast, may have been confused with aqueductal stenosis were it not for pneumoencephalography and the clinical presentation. Figure 10 is an additional case thought to be an arteriovenous malformation on CT scan until angiography revealed partial embolic occlusion of a branch of the left posterior cerebral artery.

Nonneoplastic Lesions Mistaken for Neoplasm

Patients have been brought to surgery because of a mistaken CT diagnosis of neoplasm. Sometimes the addition of

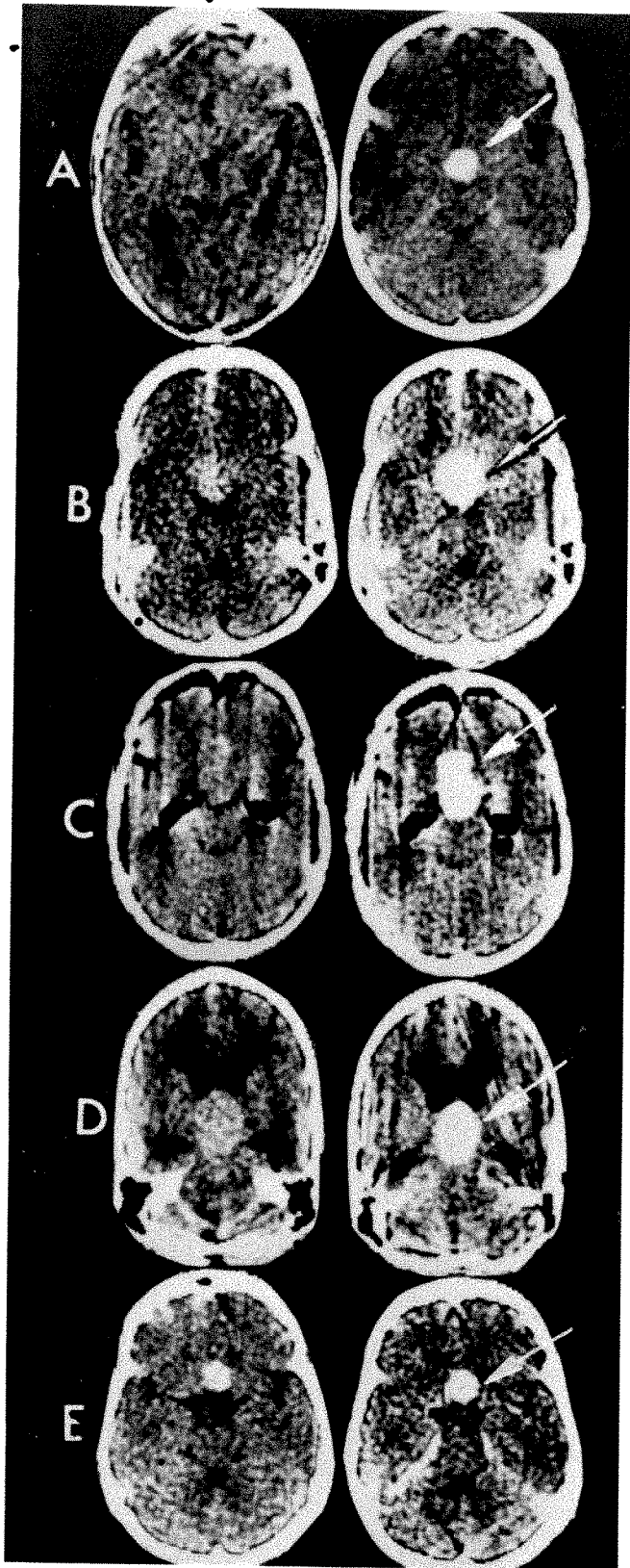


Fig. 9.—Five cases showing suprasellar high absorption abnormality. CT scans without contrast (left) and after 300 ml meglumine diatrizoate (right). A, Craniopharyngioma, no calcification. B, tuberculum meningioma. C, Chromophobe adenoma with suprasellar extension. D, Germinoma of pineal origin. E, Aneurysm with calcified wall.

other neuroradiologic procedures combined with the clinical findings will complement the CT appearance and clarify the diagnosis. Figure 11 demonstrates a case in which radiation necrosis was found at surgery rather than the suspected neoplasm. The angiogram in this case did not help to make the correct diagnosis. Another patient suspected of tumor of the inferior vermis because of high absorption in the vermis on CT and a defect in the region of the choroid plexus of the fourth ventricle at pneumoencephalography was found to have no abnormality upon surgical exploration.

A patient with multiple sclerosis in an active demyelinating phase was at first suspected of tumor until repeat studies were obtained and the high absorption area could no longer be seen after intravenous contrast enhancement (not on steroids) (fig. 12). Another patient, following his first seizure, was interpreted on CT as having neoplasm, but subsequent normal neurological status and repeat normal CT scans indicated that the high absorption value of the lesion after enhancement was either vascular, inflammatory, or possibly related to the seizure (fig. 13). A small equivocal low absorption residual raised the possibility of an infarct with transient enhancement. Another patient with high absorption at the lateral margin of the tentorial incisura was at first thought to have a meningioma until angiography revealed an aneurysm (fig. 14).

Subdural Hematoma

Occasionally a subdural hematoma may not be detected because the absorption values do not differ enough from adjacent brain. Rather than occurring in the acute or chronic stages when the absorption values of the collection are usually higher or lower than that of the adjacent brain, respectively, the error most often occurs in the intermediate stage between 30 and 90 days from onset. A poorly visualized large unilateral subdural collection will demonstrate a mass effect, and angiography may be performed to definitely detect the collection. A small acute or chronic unilateral collection may be overlooked and its clinical significance questionable in some cases; but bilateral, symmetrical subdural collections are usually significant.

Bilateral subdural hematomas with essentially imperceptible absorption values may only result in subtle compression of the ventricles without midline shift (fig. 15). The ventricular compression can be easily missed on CT interpretation. Angiography (or radionuclide scan, usually after the first week from onset) will usually demonstrate the bilateral extracerebral collections. Sometimes the clinical history and findings are strongly indicative of a subdural hematoma when the CT scan is equivocal. Occasionally, atrophy rather than chronic subdural hematoma may be the cause of a low absorption extracerebral space on CT as well as angiography. Intracranial structures may be shifted ipsilaterally, and the ventricle on that side may be enlarged.

False Negative Findings

If a lesion is very highly suspected clinically but the CT scan is negative, other neurodiagnostic studies, repeat CT

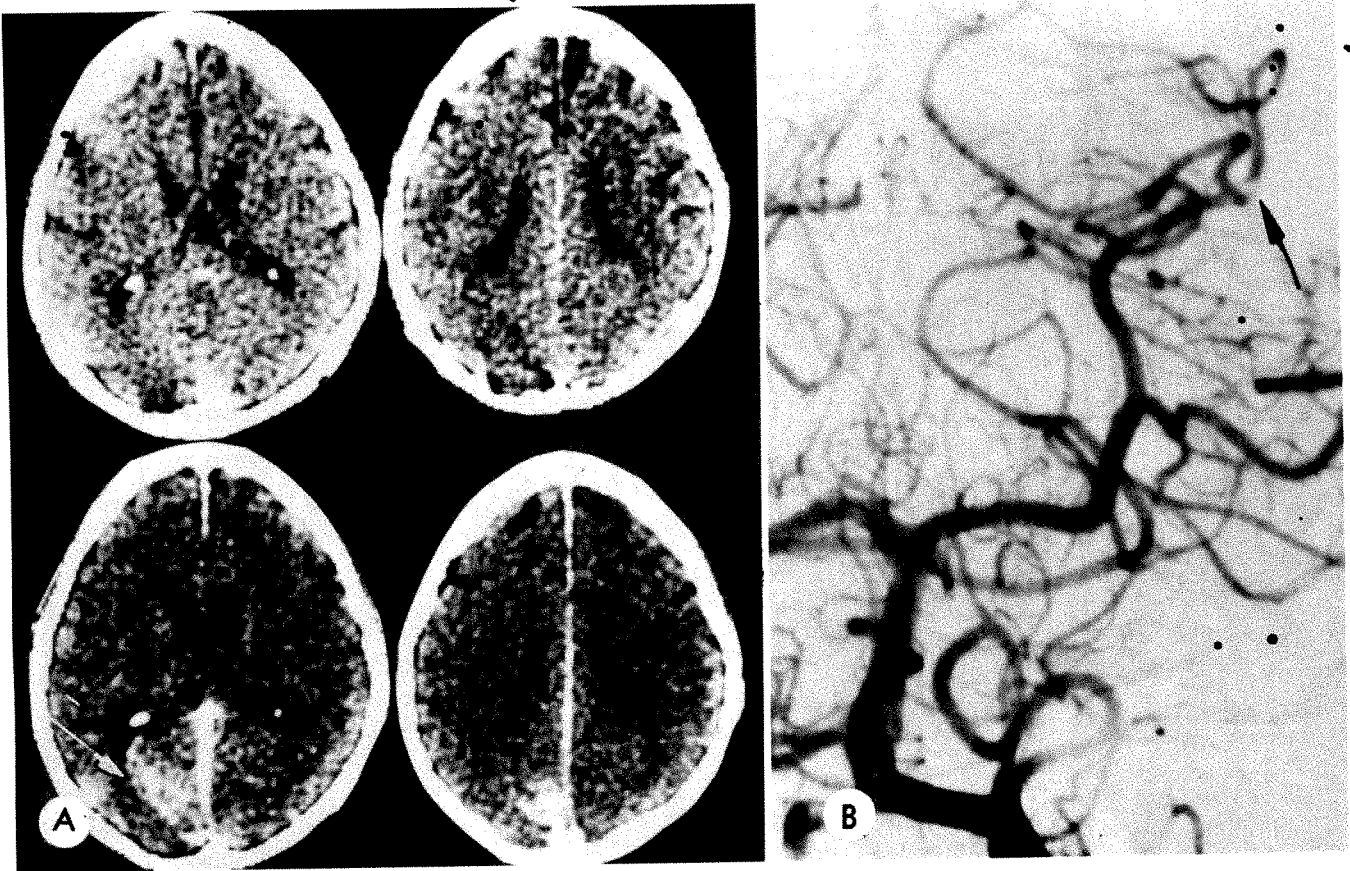


Fig. 10.—Contrast enhancement of infarction. *A*, CT scans without contrast (*upper*) and after 300 ml meglumine diatrizoate (*lower*). Negative plain study but high absorption after contrast medium (*arrows*). Thought to be arteriovenous malformation. *B*, Subsequent vertebral angiogram showing embolus producing partial occlusion of parietal occipital branch of left posterior cerebral artery (*arrow*).

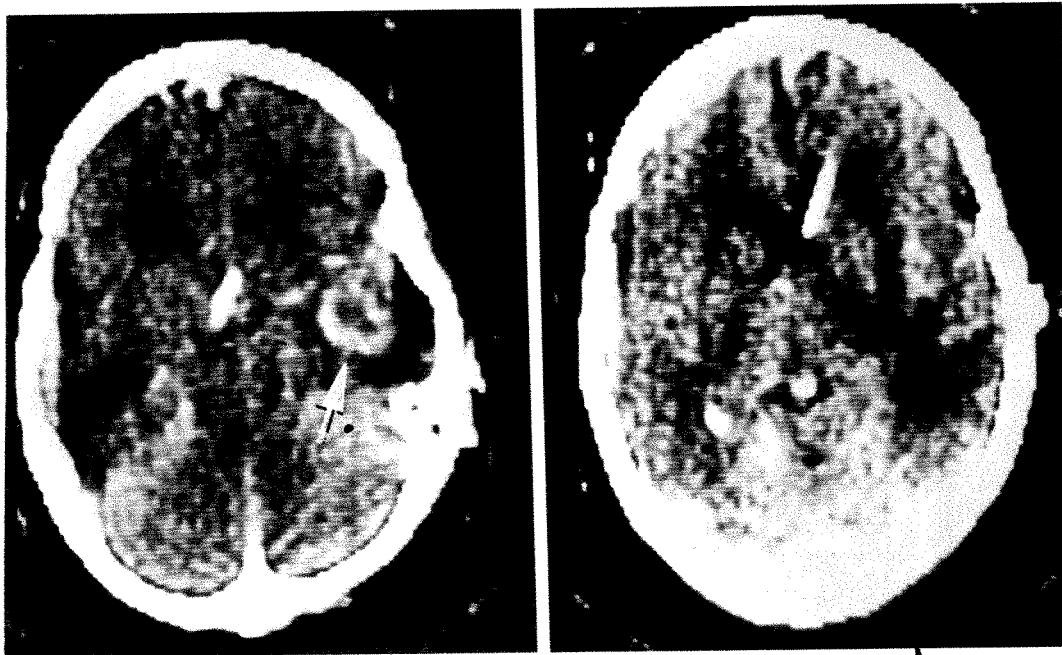


Fig. 11.—Radiation necrosis. CT scans after 300 ml meglumine diatrizoate (*left*) and without contrast (*right*). Doughnut-shaped area in right temporal lobe with ring of high absorption (*arrow*) thought preoperatively to represent neoplasm. Patient received radiation treatment of pituitary adenoma incompletely resected surgically 18 months previously.

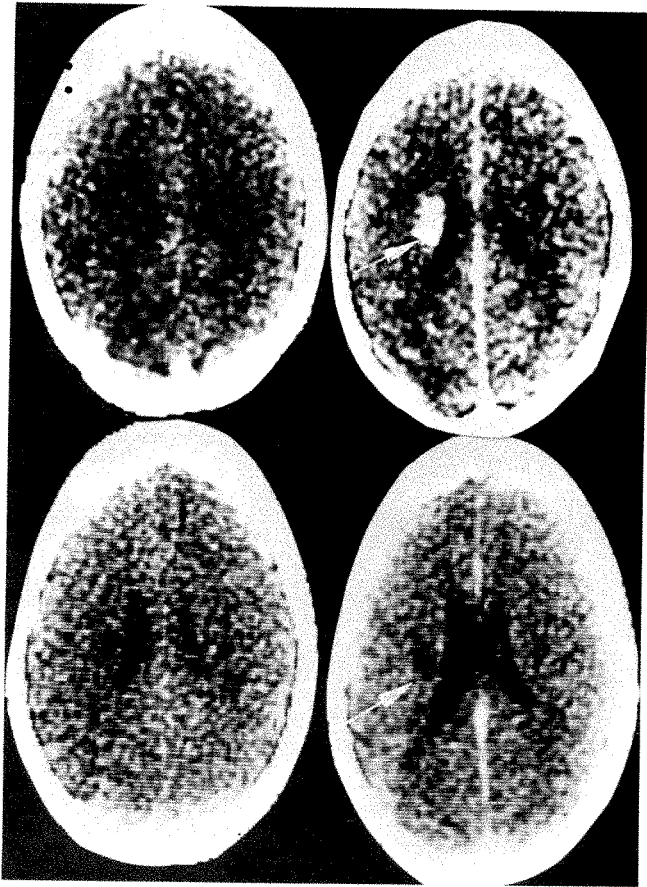


Fig. 12.—Clinically suspected multiple sclerosis. CT scans without contrast (*left*) and after 300 ml meglumine diatrizoate (*right*). *Upper*, Scans 1 week after onset of right hemiparesis showing high absorption abnormality in left corona radiata (*arrow*). *Lower*, Low absorption residual showing no enhancement 4 months later (*arrow*). (Scan 23 days after onset also showed no enhancement.) Early symptoms cleared and spinal cord signs appeared later. No steroids taken before later CT.

scans tailored to the area of interest (change of angle or overlapping thin slices), or serial CT scans may be indicated. Figure 16 shows a case of glioblastoma initially negative on CT scan but positive on scans shortly thereafter. The angiogram also converted from negative to positive in the same temporal sequence. A similar situation occurred in a patient with medulloblastoma metastatic to the cerebellopontine angle.

CT studies tailored to show temporal tip abnormality have usually been nonrevealing, whereas pneumoencephalography with polytome laminography demonstrated a small proven glioma in one case and atrophy in many others. A patient with meningeal carcinomatosis in the cerebellopontine angle (at autopsy) showed no abnormality on CT, and there was no hydrocephalus. Cases of cerebellopontine angle adhesions have been negative on CT scans but positive on pneumoencephalograms or Pantopaque studies. Under these circumstances, careful consideration of the apparent size of the lesion by pneumoencephalography or Pantopaque cisternography may lead to the correct diagnosis, thus obviating the need for surgical intervention.

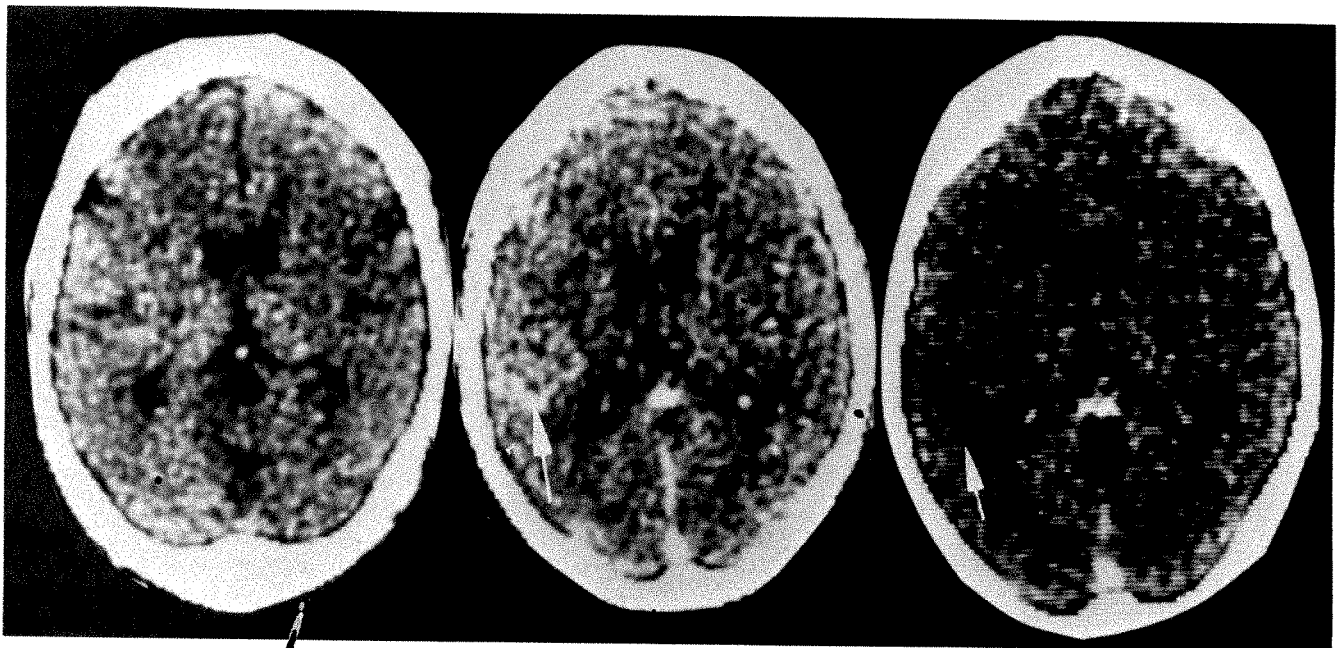


Fig. 13.—Seizure (or infarction); 38-year-old male with solitary left temporal seizure on day of scan without sequelae, who remained well. *Left*, Normal scan without contrast. *Center*, Scan after 300 ml meglumine diatrizoate showing left posterior temporal irregular ring of high absorption (*arrow*). *Right*, Scan 6 months later showing no enhancement but question of minimal low absorption abnormality (*arrow*), raising possibility of previous infarction.

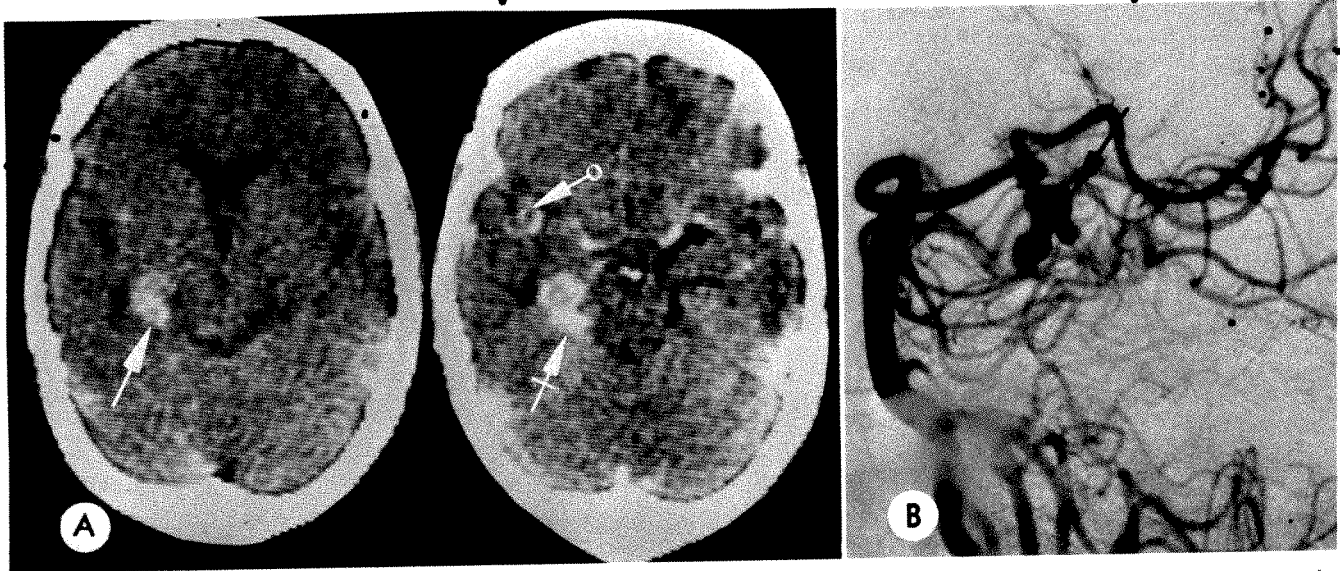


Fig. 14.—Vessel tortuosity and aneurysm. A, Left medial temporal high absorption abnormality on plain scan (arrow) shows slight enhancement after contrast medium (hatched arrow), thought at first due to tumor. [Incidental left middle cerebral artery aneurysm (top arrow) also seen at angiography.] B, Vertebral angiogram (lateral view) showing aneurysm projecting inferiorly from left posterior cerebral artery (arrow). Confirmed at surgery.

Technical Errors

Commonly, errors occur when plain studies are not obtained for comparison prior to using contrast medium. Figure 17 is a hemorrhagic infarct that was initially interpreted as tumor following the first study performed after intravenous contrast. Overinterpretation and incorrect diagnoses due to the presence of motion or other artifacts are other common sources of error.

Discussion

The overall accuracy of CT in lesion detection has been high. In our hands intracranial neoplasms have been detected with an accuracy of approximately 98% [6] (excluding a selected category of lesions less than 1.5 cm in diameter and in difficult regions such as the base of the skull). In the diagnosis of cerebral infarction, accuracy has varied depending on the type of infarction and the time between onset of symptoms and CT examination [4]. The range is around 75%. In the diagnosis of hematomas larger than 1.0 cm in diameter, the accuracy is 100% in terms of lesion discovery.

Most often the problem is not whether the lesion has been detected but whether all the anatomical information necessary to institute therapy is available (in the case of surgically treatable lesions) or whether the "obvious" diagnosis is correct. Because many lesions are so easily visualized by CT, there is a temptation to cut short the diagnostic workup, sometimes to the detriment of optimum therapeutic result.

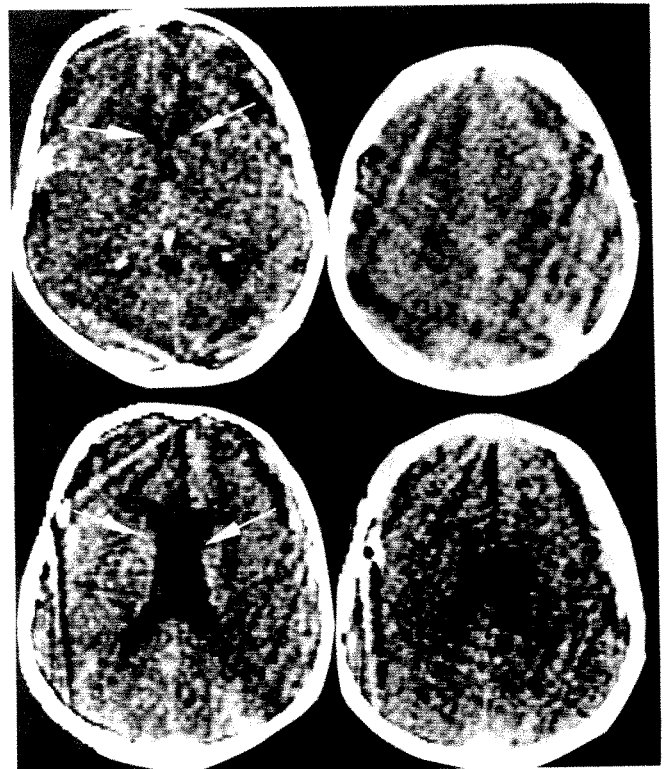


Fig. 15.—Bilateral subdural hematomas. Upper, Small ventricles (arrows) and no evidence of subdural hematoma on preoperative scan. Lower, Post-operative CT scan after removal of bilateral subdural hematomas showing ventricular reexpansion (arrows) and small reaccumulation on right.

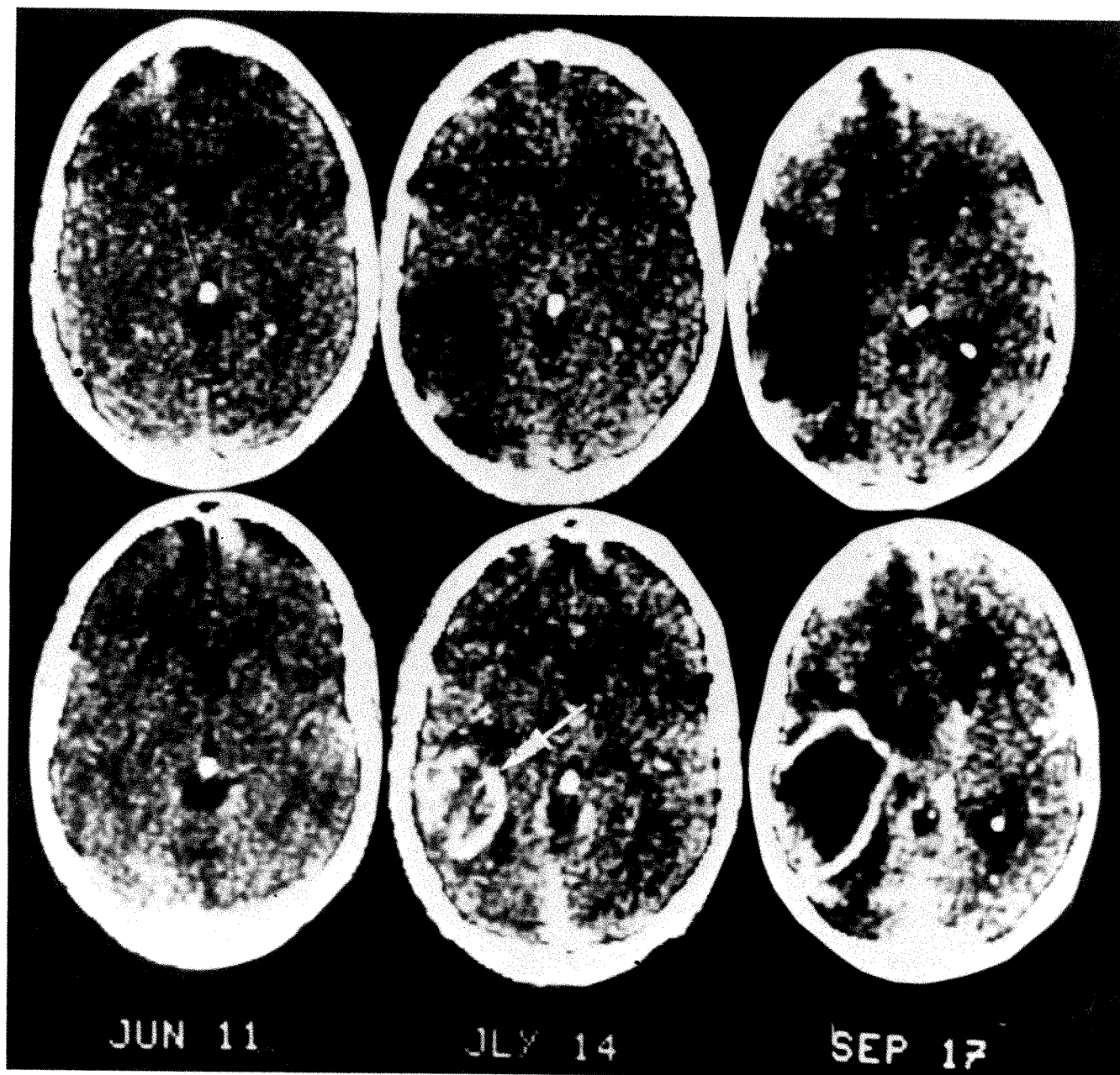


Fig. 16.—Glioblastoma. CT scans without contrast (*upper*) and after 300 ml meglumine diatrizoate (*lower*). *Left*, Normal study. *Center*, Scan 1 month later showing left temporal abnormality with definite enhancement (*arrow*). *Right*, Scan 2 months later showing marked progression.

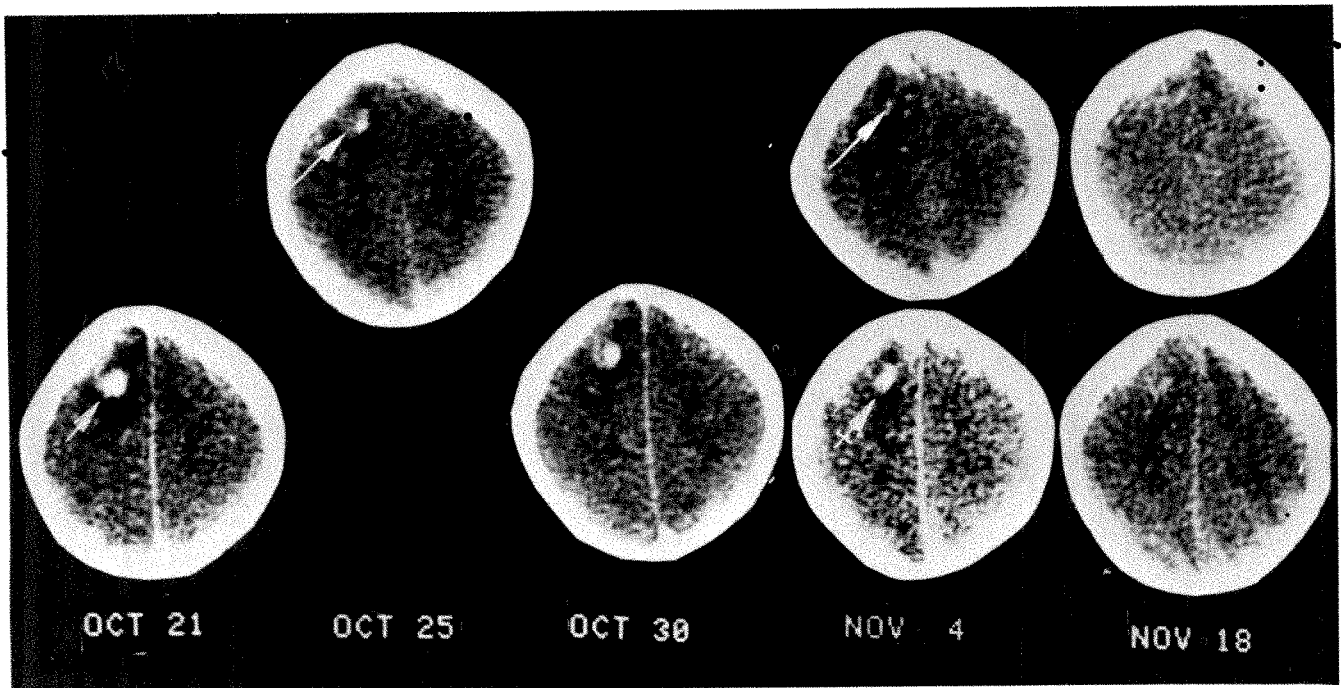


Fig. 17.—Hemorrhagic infarction. CT scans without contrast (*upper*) and after 300 ml meglumine diatrizoate (*lower*). *Oct. 21*, High absorption with low absorption rim (*arrow*); neoplasm questioned. *Oct. 25*, High absorption abnormality without contrast. *Oct. 30*, Less enhancement than originally. *Nov. 4*, Less high absorption hemorrhage (*arrow*) and enhancement of lesion (*hatched arrow*). *Nov. 18*, Essentially normal CT.

REFERENCES

1. New PFJ, Scott WR, Schnur JA, Davis KR, Taveras JM: Computerized axial tomography with the EMI scanner. *Radiology* 110:109-124, 1974
2. Paxton R, Ambrose J: The EMI scanner. A brief review of the first 650 patients. *Br J Radiol* 47:530-565, 1974
3. Ambrose J: Computerized transverse axial scanning (tomography). II. Clinical application. *Br J Radiol* 46:1023-1047, 1973
4. Davis KR, Taveras JM, New PFJ, Schnur JA, Roberson GH: Cerebral infarction diagnosis by computerized tomography. Analysis and evaluation of findings. *Am J Roentgenol* 124:643-660, 1975
5. Scott WR, New PFJ, Davis KR, Schnur JA: Computerized axial tomography of intracerebral and intraventricular hemorrhage. *Radiology* 112:73-80, 1974
6. New PFJ, Scott WR, Schnur JA, Davis KR, Taveras JM, Hochberg FH: Computed tomography with the EMI scanner in the diagnosis of primary and metastatic intracranial neoplasms. *Radiology* 114:75-87, 1974

Trends in the Development of Reconstruction Tomography in Neuroradiology

TORGNY GREITZ¹

Because of the new uses of CT, it is difficult to accurately forecast the future balance between it and conventional radiologic techniques. However, the relatively low frequency resolution of CT makes it unlikely that conventional radiology will be completely replaced. Photon noise and the iodine concentration of the contrast medium limit the size of the cerebral vessels which can be studied by CT. Thus angiography is likely to remain the method of choice for fine-detail study of these vessels. For optimal measurements and comparative studies, improved head fixation is required. Given precisely reproducible positioning, stereotaxic surgery and radiation therapy become a reality.

Computerized axial tomography introduced by Hounsfield [1] and Ambrose [2] in 1972 has been greeted as the most important advancement in the history of clinical radiology. Like many other improvements in technique such as arteriography, tomography, film subtraction, and isotope scanning, this new method was first applied to examinations of the head. Therefore, at present, our most reliable experience in assessing the usefulness of CT is in neuroradiology. The number of achievements made are already sufficiently great to warrant acceptance of CT as an indispensable tool in clinical neurological work.

There have been a number of reports on the impact of CT on conventional neuroradiologic techniques [3-7]. Almost invariably they describe a marked drop in the number of pneumoencephalographic and ventriculographic procedures and a less marked but still significant decrease in the number of angiographic examinations as well as isotope studies. The present trends would almost indicate a complete disappearance of these procedures. Such extrapolations have raised questions as to the limitations of CT scanning and prompted attempts to infer the ultimate fate of conventional neuroradiologic techniques.

However, CT has not only gained ground at the expense of old methods but is also likely to be used in certain patients who were rarely tested before. For example, in patients suffering from cerebrovascular disorders CT enables the important differential diagnosis between cerebral infarcts and cerebral hemorrhages to be made with a high degree of significance [2, 4, 8-10].

The new uses of CT make it impossible to accurately forecast the future balance between CT and conventional radiography. When discussing the impact of the total body scanner it has been pointed out that 50% of all radiologic examinations involve bones and joints and, hence, are not very likely to fall within the domain of CT. On the other hand, bone is the only tissue (with the exception of fat) which differs in attenuation from other body tissues to such a degree as to be seen in a conventional radiogram.

Irrespective of whether we are dealing with a trauma to the head or to the ankle, it is more frequently the soft tissues which are a matter of concern. When examining bone in search for metastases we are not primarily concerned about bone destruction but would rather have information on pathological soft tissue masses within as well as outside the bony system. Thus it seems likely that the present relationship between x-ray examinations of bone and those of soft tissue will be altered. As a consequence, the panorama of diagnostic radiology may be changed dramatically.

The relatively low frequency resolution of CT (about 3 lines/cm) [11, 12] makes it unlikely that conventional radiology will be completely replaced. Even by using refined methods for image reconstruction in various planes and projections, it is doubtful that CT could ever achieve the same precise diagnosis of a partial aqueduct stenosis as through pneumoencephalography and ventriculography. Many of the early difficulties in diagnosing small lesions such as tumors close to the skull base [1-4, 13] have now mostly been overcome by the use of new algorithms, a new matrix, and increased use of intravenous injection of contrast media [2, 4, 7, 14, 15]. However, very small tumors within the basal cisterns may still have to be diagnosed by pneumoencephalography or by positive contrast cisternography using a suitable water-soluble contrast medium [16].

The two major factors limiting the size of the cerebral vessels which can be studied by CT are photon noise and the iodine concentration of the contrast medium. The only way to increase the resolution and discernibility of the vessels in computer intravenous angiography [17] is to increase the amount of iodine for a given tonicity of the contrast medium. However, even if such contrast media were available, the smallest demonstrable intracranial vessel would be 1 mm in diameter [12]. Therefore, angiography is likely to remain the method of choice for fine-detail study of cerebral vessels. However, the demonstration of an operable saccular aneurysm (2 mm in diameter or more) and its parent vessel is quite feasible using coned down tomography with a finer matrix and reconstruction of several sections in several planes [18, 19].

The potential of CT in neuroradiology is not limited to studies of normal and pathologic anatomy. A functional study made possible by CT is that of the movement of the optic nerve in normal and pathological conditions ([20]; G. Di Chiro, personal communication). Another dynamic study is that of the CSF circulation [21, 22] in which the same type of information on CSF dynamics was obtained as by isotope cisternography, but with a higher resolution and a lower radiation dose to the spinal cord. This method could probably be used to quantify the flow of CSF and, using compartmental analysis, to provide interesting data

Received February 27, 1976.

¹ Department of Neuroradiology, Karolinska Sjukhuset, S-104 01 Stockholm, Sweden.

on the circulation and absorption of CSF, especially in patients with hydrocephalus. Important contributions to the study of the extracranial CSF circulation may be obtained using the body scanner (G. Di Chiro, personal communication).

Computer cisternography also provides interesting data for the study of the pharmacokinetics of contrast media [23]. Using the principles of dye dilution, the blood volume of the brain may be assessed following intravenous injection of contrast media. By maintaining a steady state concentration of contrast medium within the blood, physiological and pathophysiological blood volume alterations may be studied quantitatively [24; G. du Boulay, personal communication]. Focal hyperemia as a sign of regional loss of autoregulation leading to so-called luxury perfusion has been demonstrated [25] in cases with subarachnoid hemorrhage and a focal encephalitis. In these cases damage to the blood-brain barrier occurs which leads to an uptake of contrast medium in the brain tissue. Such damage to the blood-brain barrier also occurs in tumors and is in part responsible for the increased uptake of contrast medium seen in various kinds of tumors [2, 4, 5, 7, 14, 15].

Contrast enhancement varies with time and with type of tumor due to variations in the degree of vascularization and damage to the blood-brain barrier. The enhancement response curve may become a means of differentiating various types of tumor [14, 15]. As the blood volume within the tumor is computed, the time constant for the uptake through the blood-brain barrier could be calculated for each "CT element" of the tumor (M. Bergström and M. Riding, personal communication), and the ensuing pattern may serve as a guide for the differential diagnosis.

To take full advantage of the method in dynamic studies, a satisfactory fixation of the skull is mandatory. The position in which the patient has been fixed should be reproduced with a very high degree of accuracy. This is usually not the case with the fixation methods used so far. If this reproducibility is achieved, the comparison of subsequent examinations may be made by the computer and hence fully automated. This would not only allow dynamic studies using observations over time (hours or days) but also make objective comparisons possible in the evaluation of various forms of treatment (e.g., cortisone therapy for cerebral edema, chemotherapy and radiotherapy of intracranial tumors). In principle each tomographic cut might have its own dose planning chart, and the shape of the treated area could be varied to correspond to the shape of the tumor, this procedure being repeated for each tomographic cut. This would result in stratigraphic radiotherapy.

A method for exact fixation of the patient should be applicable in radiotherapy as well as in any stereotaxic procedure including radiosurgery according to Leksell [26]. At our institution a fixation method has been worked out which allows the x-ray scanner to include a diagnostic coordinate system which can be directly transferred to a therapeutic coordinate system such as those currently used for stereotaxic treatment [27]. At the Karolinska Sjukhuset, stereotaxic radiosurgery is used in the treatment of mainly small central tumors (e.g., pinealoma, pituitary tumor, and acoustic neuroma) for occluding the parent and feeding

vessels of arteriovenous malformations, and, occasionally, intracranial arterial aneurysms. Stereotaxic CT scanning provides a simple and exact way of choosing the target point in radiosurgery and other stereotaxic procedures.

REFERENCES

1. Hounsfield GN: Computerized transverse axial scanning (tomography). I. Description of system. *Br J Radiol* 46:1016-1022, 1973
2. Ambrose J: Computerized transverse axial scanning (tomography). II. Clinical application. *Br J Radiol* 46:1023-1047, 1973
3. Baker HL, Campbell JK, Houser OW, Reese DF, Sheedy PF, Holman CB, Kurland RL: Computer assisted tomography of the head. An early evaluation. *Mayo Clin Proc* 49:17-26, 1974
4. Gawler J, du Boulay GH, Bull JWD, Marshall J: Computer-assisted tomography (EMI scanner). Its place in investigation of suspected intracranial tumours. *Lancet* 2:419-423, 1974
5. New PFJ, Scott WR, Schnur JA, Davis KR, Taveras JM: Computerized axial tomography with the EMI scanner. *Radiology* 110:109-123, 1974
6. Wortzman G, Holgate RC, Morgan PP: Computed cranial tomography: an evaluation of cost effectiveness. *Radiology*. In press, 1976
7. Paxton R, Ambrose J: The EMI scanner. A brief review of the first 650 patients. *Br J Radiol* 47:530-565, 1974
8. Cronqvist S, Brismar J, Kjellin K, Söderström CE: Computer assisted axial tomography in cerebrovascular lesions. *Acta Radiol [Diagn]* (Stockh) 16:135-145, 1975
9. Söderström CE, Kjellin KG, Cronqvist S: Computer tomography compared with spectrophotometry of cerebrospinal fluid in cerebrovascular diseases. *Acta Radiol [Suppl]* (Stockh) 346:130-142, 1975
10. Davis KR, Taveras JM, New PFJ, Schnur JA, Roberson GH: Cerebral infarction diagnosis by computerized tomography. Analysis and evaluation of findings. *Am J Roentgenol* 124:643-660, 1975
11. Goodenough DJ, Weaver KE, Davis DO: Physical measurements of the EMI imaging system. Paper presented at the workshop on Reconstruction Tomography in Diagnostic Radiology and Nuclear Medicine, San Juan, Puerto Rico, 1975
12. Bergström M, Riding M, Greitz T: The limitations of definition of the blood vessels in computer intravenous angiography. *Neuroradiology*. In press, 1976
13. Greitz T: Computer tomography for diagnosis of intracranial tumours compared with other neuroradiologic procedures. *Acta Radiol [Suppl]* (Stockh) 346:14-20, 1975
14. Gado MH, Phelps ME, Coleman RE: An extravascular component of contrast enhancement in cranial computed tomography. II. *Radiology* 117:595-597, 1975
15. Hatam A, Bergvall U, Lewander R, Larsson S, Lind M: Contrast medium enhancement with time in computer tomography. Differential diagnosis of intracranial lesions. *Acta Radiol [Suppl]* (Stockh) 346:63-81, 1975
16. Grepe A: Cisternography with the non-ionic water-soluble contrast medium metrizamide. A preliminary report. *Acta Radiol [Diagn]* (Stockh) 16:146-160, 1975
17. Riding M, Bergström M, Bergvall U, Greitz T: Computer intravenous angiography. *Acta Radiol [Suppl]* (Stockh) 346:82-90, 1975
18. Glenn WV, Taveras JM, Johnston BJ, Morton PW, Dwyer SJ: Clinical feasibility of reconstructing coronal, sagittal and thin transverse sections from overlapped 8.0 mm CT scans. Paper presented at the workshop on Reconstruction Tomography in

Diagnostic Radiology and Nuclear Medicine, San Juan, Puerto Rico, 1975

19. Bergström M, Sundman R: Picture processing in computed tomography. *Am J Roentgenol* 127:17-21, 1976
20. Möller A: Movements of the optic nerve in normal and pathological conditions studied by computer tomography. Submitted for publication
21. Greitz T, Hindmarsh T: Computer assisted tomography of intracranial CSF circulation using a water-soluble contrast medium. *Acta Radiol [Diagn]* (Stockh) 15:497-507, 1974
22. Hindmarsh T, Greitz T: Computer cisternography in the diagnosis of communicating hydrocephalus. *Acta Radiol [Suppl]* (Stockh) 346:91-97, 1975
23. Hindmarsh T: Elimination of water-soluble contrast media from the subarachnoid space. Investigation with computer tomography. *Acta Radiol [Suppl]* (Stockh) 346:45-50, 1975
24. Bergström M, Gordon E, Greitz T: Intracranial blood volume changes estimated by computer tomography. Submitted for publication
25. Riding M, Greitz T: Focal hyperemia (luxury perfusion) in subarachnoid hemorrhage and encephalitis studied by computer tomography. Submitted for publication
26. Leksell L: Cerebral radiosurgery. *Acta Chir Scand* 134:585-595, 1968
27. Bergström M, Greitz T: Stereotaxic computed tomography. *Am J Roentgenol* 127:167-170, 1976

Computed Tomography in Infants and Children: Intracranial Neoplasms

PAUL E. BERGER,^{1,2} DONALD R. KIRKS,^{1,3} DAVID L. GILDAY,¹ CHARLES R. FITZ,¹
AND DEREK C. HARWOOD-NASH¹

Cranial CT proved exceptionally accurate in detecting and localizing cerebral neoplasms in children, with only one false negative case in 40 tumors. CT had its greatest diagnostic value in cerebral and cerebellar hemispheric lesions, tuberous sclerosis, and as a screening device for craniopharyngiomas. While CT may provide a definitive diagnosis, additional information from other neuroradiologic studies is often necessary.

Introduction

Initial reports [1-3] have clearly demonstrated the usefulness of computed tomography (CT) in the investigation of patients with cerebral neoplasms. However, few of the cases presented have been children. Houser et al. [4] recently described their initial experience in infants and children. The purpose of this report is to present our experience with CT in children highly suspected of having cerebral neoplasms and to correlate the findings with those of the radionuclide brain scan, pneumoencephalogram, ventriculogram, and angiogram.

Subjects and Methods

From the first 225 patients who underwent CT we selected 44 in whom a diagnosis of cerebral neoplasm was strongly suspected (either clinically, on skull roentgenogram, and/or radionuclide brain scan) or who had been previously operated on for a neoplasm and recurrence was suspected. A total of 45 CT scans were performed on these 44 infants and children, and 40 intracranial neoplasms were diagnosed. All patients had either (1) tumor suspected or diagnosed on a CT scan or (2) tumor not diagnosed on a CT scan but subsequently shown to be present on an air study, angiogram, or at surgery. All cases are pathologically proven either surgically or at postmortem. Patients with purely cystic lesions such as porencephalic cysts, arachnoid cysts, or encysted ventricles were excluded.

Results

Computed Tomography

The 44 patients underwent a total of 45 CT scans and 40 neoplasms were diagnosed. One child had bilateral acoustic neuromas, each presenting on separate occasions and each as a new neoplasm. Consequently this case was considered as two patients for this report. The location and pathology of these 40 neoplasms is presented in table 1. Forty CT scans were interpreted as positive, and in 37 of

these a tumor was present. There were three false positive CT scans (table 2), and four were judged equivocal. By equivocal we mean that a tumor is suspected but further investigation with either an air study or angiogram is definitely indicated. Of the four cases with equivocal scans, three were shown to have tumors and one was negative on additional study. One patient with a negative scan at the time of initial presentation became positive on repeat testing 2 months later. This is the only false negative scan in this series and will be discussed in detail. Patients with a negative radionuclide and CT brain scan and who had no additional examination or surgery are not included, since follow-up in these patients has been less than 1 year.

Thus at the time of initial presentation, 39 of 40 patients (97.5%) with tumors were detected by CT, with one false negative case (2.5%).

Radionuclide Brain Scans

Complete nuclear medicine evaluation was performed in 36 of these children. Each study consisted of a radionuclide angiogram, immediate blood pool images (1,000 counts/cm²) and delayed scans at 2-4 hr, using 8.3 mCi of ^{99m}Tc pertechnetate per square meter of body surface area following oral administration of 8 mg/kg of potassium perchlorate.

In this group there were two false positive scans, both in children with false positive CT scans. There were three false negative brain scans. Two of the normal scans were in brain stem tumors and the other in a cystic craniopharyngioma. Both false positive studies remain enigmas, since focal encephalitis, which may mimic a neoplasm, was excluded clinically.

We have found that the complete nuclear medicine evaluation complements the CT examination. In infants and young children who may require general anesthesia or heavy sedation for CT scanning, the nuclear medicine study is usually the screening procedure of choice. Contrast-enhanced CT and radionuclide blood pool images may delineate the amount of blood within the neoplasm, whereas the radionuclide angiogram indicates the *relative amount* of blood flow to the lesion. If the angiogram suggests an arteriovenous malformation rather than a tumor or a tumor with a very high blood flow, then cerebral angiography is the neuroradiological procedure of choice. Thus, we feel that complete nuclear medicine evaluation remains an excellent screening modality especially in the younger age group.

¹ Division of Neuroradiology, Department of Radiology, Hospital for Sick Children, Toronto, Ontario, Canada M5G 1X8. Address reprint requests to D. C. Harwood-Nash.

² Present address: Children's Hospital of Buffalo, Buffalo, New York 14222.

³ Present address: Children's Hospital Medical Center, Oakland, California 94609.

TABLE 1

Pathology and Location of Cranial Neoplasms

Type	No.
Infratentorial:	
Cerebellar hemisphere:	
Cystic astrocytoma	6
Solid astrocytoma	1
Medulloblastoma	4
Brain stem (glioma)	2
Cerebellopontine angle (acoustic neuroma)	2
Total	15
Supratentorial:	
Intracerebral:	
Astrocytoma, high grade*	5
Astrocytoma, low grade†	1
Ganglioglioma (parietooccipital)	2
Choroid plexus papilloma (trigone)	1
Primitive neuroectodermal tumor (frontal lobe)	1
Para-third ventricular region:	
Posterior:	
Atypical teratoma	1
Pinealoblastoma	1
Dermoid	1
Anterior (craniopharyngioma)	6
Total	19
Miscellaneous:	
Tuberous sclerosis	3
Extracerebral:	
Myxofibromatous sarcoma of dura (occiput)	1
Schwannoma (temporal fossa)	1
Orbit (optic nerve glioma)	1
Total	6

* III-IV (basal ganglia, thalamic).

† I-II (temporal lobe).

Cerebral Angiography

Of the 44 patients, 28 had angiograms and 21 were positive. In all these patients a tumor was present. Of the four patients with negative angiograms, none had a tumor. Three were interpreted as equivocal, and in each case a tumor was found (one dermoid in the posterior third ventricle, one thalamic glioma, and one craniopharyngioma).

Air Studies

Of the 23 air studies performed, 13 were pneumoencephalograms and 10 were ventriculograms. Nineteen were positive and all patients had tumors. Four were negative and one of these patients had a tumor (acoustic neuroma).

Discussion

In performing any neuroradiologic investigative procedure, two factors of paramount importance are the safety

TABLE 2

Results of CT Scanning

Result	No.
CT positive:	
Tumor present	37
Tumor absent	3
CT equivocal:	
Tumor present	3
Tumor absent	1
CT negative:	
Tumor present	1
Tumor absent	0

of the procedure and the accuracy of the examination. Problems unique to small children are the possibility of tracheal kinking with flexion of the head necessary to obtain satisfactory CT scans of the posterior fossa and excess patient motion in the uncooperative child resulting in an unsatisfactory nondiagnostic examination. Because of this we have found it necessary to use general anesthesia with the younger uncooperative child (generally 4 years of age or less) and especially with small infants. This assures a patent airway for the child and eliminates motion artefacts which will result in a nondiagnostic and confusing scan.

A CT examination in any child strongly suspected of neoplasm must consist of a routine scan followed by contrast enhancement and repeat of the cuts in the planes of interest. We have been using 3 ml/kg meglumine diatrizoate—60 up to a maximum of 60 ml in a bolus injection with good results.

The value of CT scans in detecting and localizing neoplasms and the interrelationship of CT with the other investigative modalities of radionuclide brain scanning, air studies (pneumoencephalography and ventriculography), and angiography is dependent primarily on the location of the tumor.

Infratentorial Tumors

Cerebellar Hemisphere

The CT scan was positive in all 11 cerebellar hemisphere tumors. Cystic astrocytomas demonstrated a well-defined area of decreased density representing the cystic component of the tumor with the mural nodule being of density similar to normal surrounding cerebellum. However, with contrast enhancement the mural nodule could be clearly defined (fig. 1). Medulloblastomas (fig. 2) demonstrated an ill-defined area of slightly decreased density relative to normal cerebellum and mass effect with shift of the fourth ventricle. However, the tumor density was at times indistinguishable from normal cerebellum and only with contrast enhancement was the tumor visible. An area of surrounding decreased density, when present, represented surrounding edema or tumor necrosis. One of our patients demonstrated calcification within the medulloblastoma not recognizable on plain films. One astrocytoma without cystic

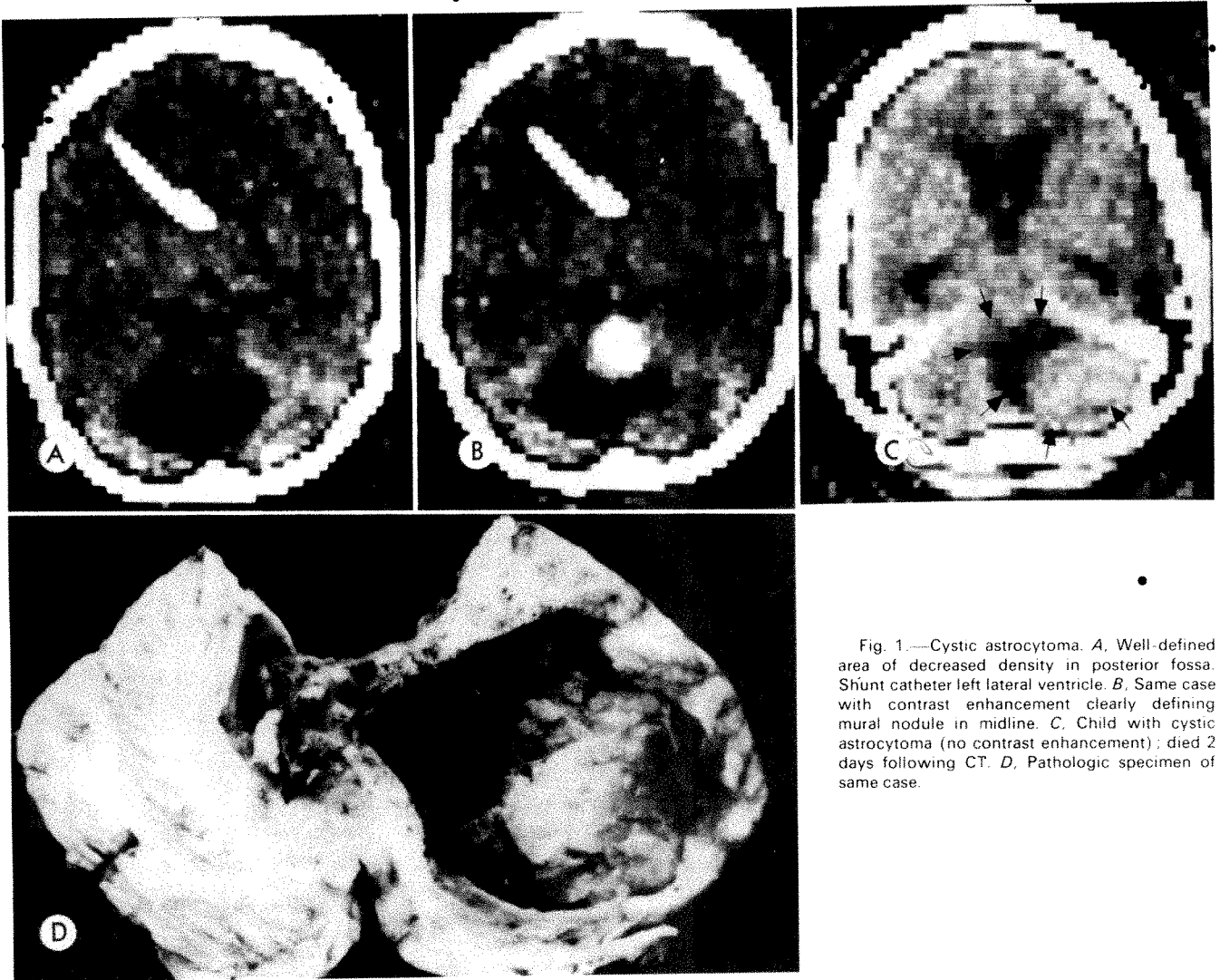


Fig. 1.—Cystic astrocytoma. *A*, Well-defined area of decreased density in posterior fossa. Shunt catheter left lateral ventricle. *B*, Same case with contrast enhancement clearly defining mural nodule in midline. *C*, Child with cystic astrocytoma (no contrast enhancement); died 2 days following CT. *D*, Pathologic specimen of same case.

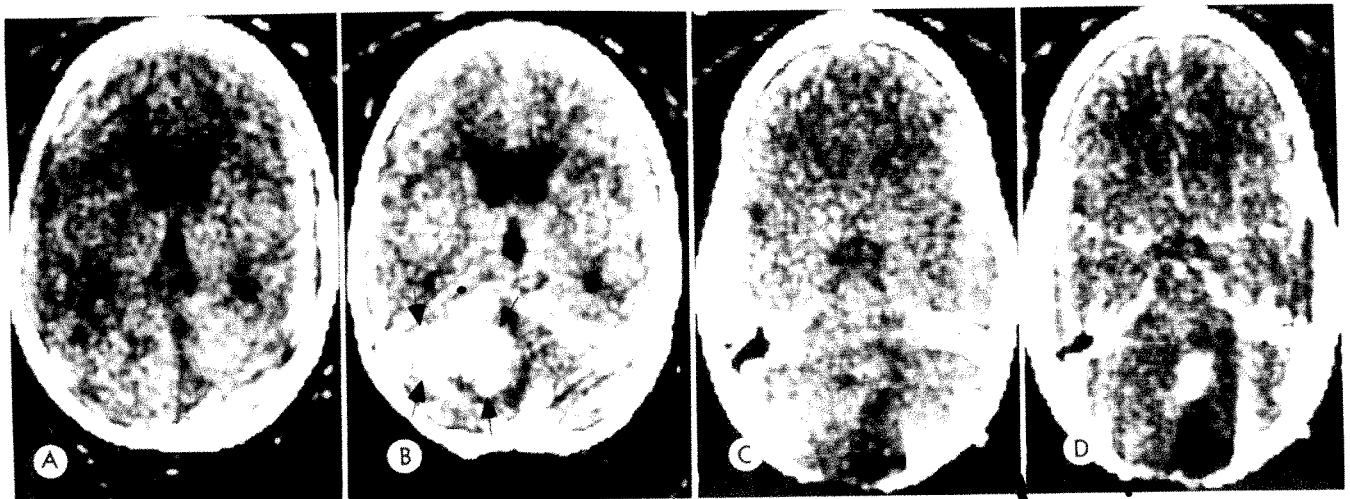


Fig. 2.—Medulloblastoma. *A*, Tumor indistinguishable from normal surrounding cerebellum on routine study; 6-year-old boy. *B*, Same case with contrast enhancement demonstrating medulloblastoma (arrow). *C*, Routine scan of 2-year-old boy, post removal and radiation therapy to medulloblastoma. Uncertain whether area of decreased density post-fossa is due to tumor or postoperative changes. *D*, Same case with contrast enhancement clearly defining recurrent medulloblastoma.

component was indistinguishable from medulloblastoma. There were no patients in this series with ependymoma.

The relationship of the mass to the fourth ventricle and any intrinsic involvement of the fourth ventricle by the tumor mass is important anatomical information to the neurosurgeon in planning his operative approach and resection. This information is currently best obtained by ventriculography. This was performed in seven of our patients and was positive in all. Ventriculography demonstrates the degree of hydrocephalus, kinking of the cerebral aqueduct at the collicular plate, and relationship of the tumor to the fourth ventricle.

Angiography was performed on five patients and was positive in all. This was valuable as a diagnostic technique and as a confirmatory procedure following CT. However, in general, angiography did not provide additional information with regard to tumor location, extent, or type and was not of significant additional help prior to surgery. No posterior fossa arteriovenous malformations or aneurysms are included in our group of patients; in these patients angiography would be of paramount importance.

Brain Stem Tumors

Two patients had CT scans. One was positive with an ill-defined area of decreased density extending into one brachium pontis. The second was interpreted as equivocal with a question of increased size of the brain stem with a tissue density indistinguishable from normal brain. Contrast enhancement was of no value in this second case. Radionuclide brain scan was negative in both of these patients. The procedure of choice in these patients was pneumoencephalography, which beautifully outlines the increased size of the brain stem as well as extraaxial extension of the tumor. We feel this is still the procedure of choice in suspected brain stem neoplasms. A CT scan may be helpful in defining a cystic component to the brain stem neoplasm. All our brain stem neoplasms are operated on looking for a cyst which may be aspirated. In our experience 10% of brain stem tumors in children have a cystic component at operation or on postmortem examination.

Cerebellopontine Angle Tumors

Two acoustic neuromas in the same patient were evaluated by CT. The left neuroma presented first, at which time the presence of his subsequent right neuroma was equivocal. Each neuroma was indistinguishable on routine CT scan but very well demonstrated on contrast enhancement (fig. 3). Sixteen months prior to CT scan, a pneumoencephalogram with polytomographic cuts of the cerebellopontine angle was negative. Posterior fossa myelography could not be performed because of a high cervical block to flow of contrast material by a large cervical neuroma. Each tumor was angiographically avascular, although there was displacement of the anterior inferior cerebellar artery. The procedure of choice in the detection of small acoustic neuromas is still felt to be posterior fossa myelography [5-7].

However, CT as well as angiography may be of great value in the detection of large neuromas.

Supratentorial Tumors

Cerebral Hemisphere

Ten patients had primary intracerebral hemispheric neoplasms, including five with tumor principally involving the thalamus and basal ganglia regions extending to involve the frontal or temporoparietal regions. The initial CT scan was positive in all except one patient. This boy had a repeat CT scan 2 months later which was strongly positive. This is the only initial false negative finding (see later). The pathologic diagnosis in the hemispheric tumors was variable and is presented in table 1. The CT scan demonstrated either an area of increased density, often calcification as seen on roentgenogram or hemorrhage, and ill-defined areas of decreased density representing tumor necrosis or surrounding edema. Mass effect with ventricular shift was also present. Contrast enhancement is imperative in these patients and serves to delineate vascular tumor from adjacent necrotic tissue and edema. In several of our cases the tumor was of similar density to normal brain and was appreciated only by its mass effect and with use of contrast enhancement (fig. 4). We cannot overemphasize the importance of contrast enhancement in evaluating children with suspected cerebral neoplasm.

Para-Third Ventricular Tumors

Posterior. Three patients had posterior third ventricular tumors (fig. 5). One, a very large pinealoblastoma, was seen to invade brain stem and extend into the temporal lobe. It was of slightly increased density compared to surrounding brain tissue, with a faint vascular rim seen on contrast enhancement; the remainder was relatively avascular. A second patient had a dermoid in the posterior third ventricle. The CT scan was equivocal, showing what appeared to be calcification within the third ventricle along the left lateral wall and a question of soft tissue density posteriorly which did not increase significantly in density with contrast enhancement. A ventriculogram demonstrated the large mass lesion. The third patient had a "double midline tumor" [8] with a posterior third ventricular tumor partially calcified and a second tumor at the anteroinferior aspect of the third ventricle which was not calcified. Both tumors were seen on CT scan and were slightly enhanced by contrast. Histology was atypical teratoma. This patient had an angiogram which demonstrated the posterior third ventricular tumor but did not show the anteroinferior third ventricular tumor, which was demonstrated by pneumoencephalography. There were abnormal vessels seen over the convexity with a progressive variation in caliber suggesting metastases via the CSF pathways. Tumors in the posterior third ventricular region may represent a diagnostically difficult CT scan. We currently feel that additional studies with air and angiography are necessary to delineate their precise geography and character toward successful neurosurgical removal.

Anterior (craniopharyngioma). All six of our patients with craniopharyngiomas had positive CT scans (fig. 6).

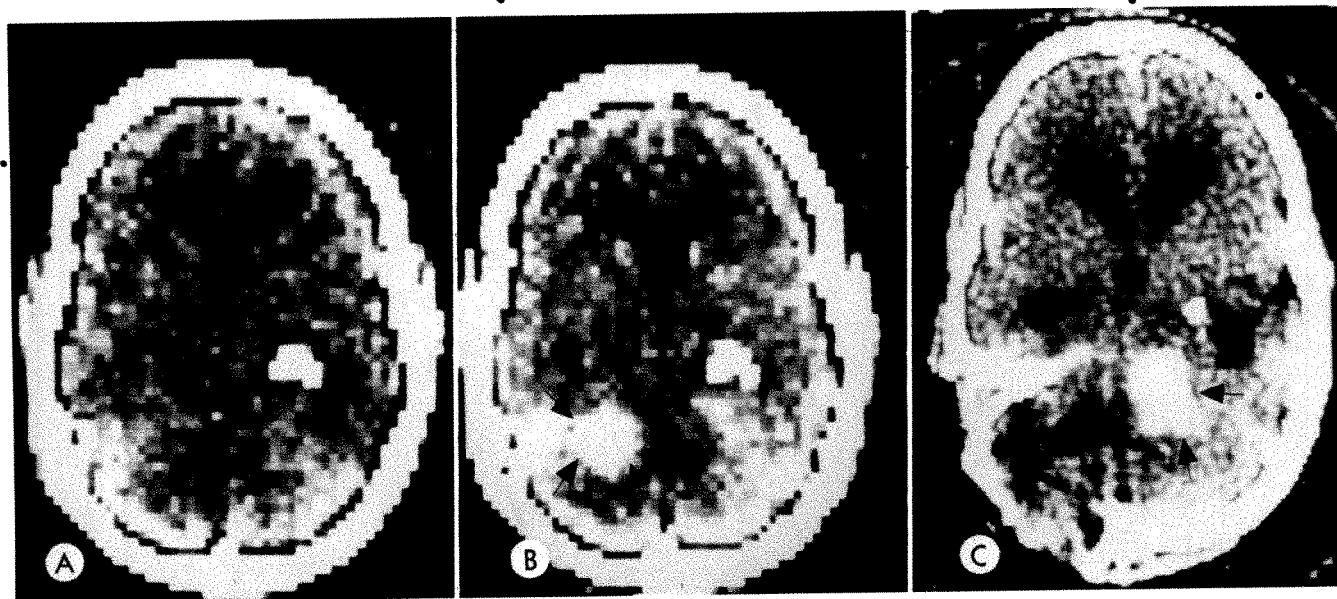


Fig. 3.—Acoustic neuroma. A, Routine scan of 16-year-old boy with neurofibromatosis, ataxia, and no auditory abnormality showing calcification of glomus of right choroid plexus. Otherwise negative. B, Same patient with contrast enhancement. Well-defined left acoustic neuroma (arrow) and question of ill-defined increased density on right. C, Same patient 3 months later with contrast enhancement. Postoperative changes on left; well-defined large acoustic neuroma on right.

Most were cystic tumors with a calcific rim, although two were more solid and calcified without definite cystic component. These showed some contrast enhancement. Pneumoencephalography was the procedure of choice, beautifully demonstrating the geography of the lesion and its relation to surrounding anatomic structures such as the basilar artery, optic chiasm, and internal carotid arteries. Angiography is indicated to rule out the possibility of an aneurysm and to determine the position of the carotid and basilar arteries with respect to the tumor mass. Thus although CT appears to be a good screening aid, pneumoencephalography is still felt to be the procedure of choice.

Miscellaneous

Of the additional six patients, three had tuberous sclerosis, one a sarcomatous dural tumor in the occipital region, one an extradural schwannoma in the temporal fossa, and one an optic nerve glioma. In patients with uncomplicated tuberous sclerosis CT is the procedure of choice, showing calcified and noncalcified subependymal and subcortical tubers which may be missed on conventional skull roentgenogram (fig. 7). However, pneumoencephalography [9] is also of diagnostic value.

The patient with the dural sarcoma was a 3-month-old infant thought initially to have a leptomeningeal cyst in the occipital region. The CT scan showed a low density solid tumor (10–15 EMI units) (figs. 8A and 8B), and angiography demonstrated vascular supply via hypertrophied meningeal vessels and a tumor blush. The schwannoma in the temporal fossa was seen to be an area of increased density on contrast enhancement but was best demonstrated on selective external carotid angiography. These last two cases demonstrate the complementary nature of CT and other diagnostic modalities in the investigation of difficult diagnostic neuroradiological problems.

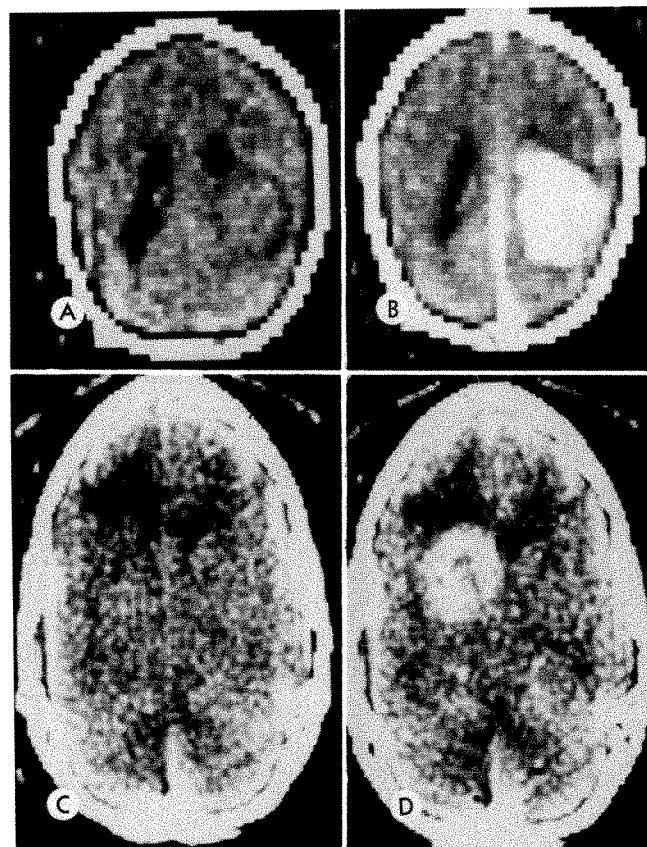


Fig. 4.—Cerebral hemisphere. A, Choroid plexus papilloma. Routine CT showing asymmetry of trigone and occipital horn of right lateral ventricle. B, Same patient with contrast enhancement clearly delineating large tumor in trigone. Also note enhancement of falx. C, Glioblastoma multiforme. Routine CT showing ill-defined area of decreased density in left frontal lobe. Left lateral ventricle not visualized. D, Same patient with contrast enhancement. Tumor in basal ganglia and thalamus extending to frontal lobe with edema (low density) anterior to tumor mass.

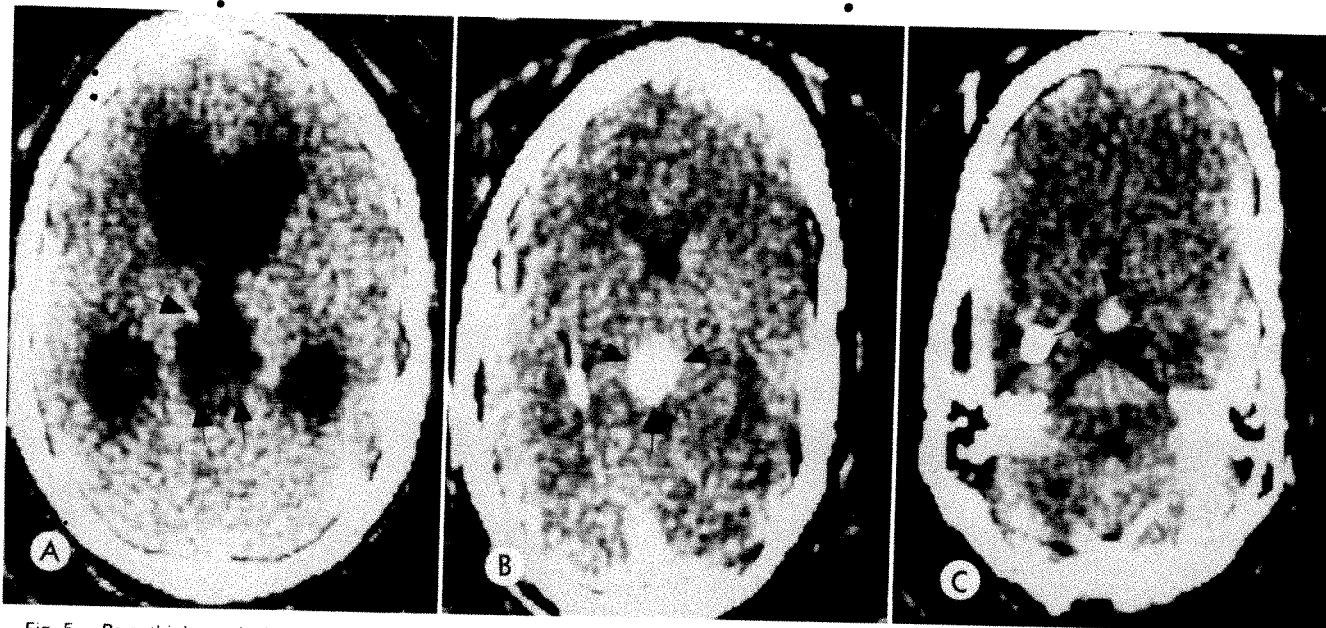


Fig. 5.—Para-third ventricular tumors. A, Dermoid. Small calcific density (arrow) apparently inside wall of enlarged third ventricle. Ill-defined area in posterior third ventricle (double arrows) of uncertain etiology. Scan interpreted as equivocal. Ventriculogram demonstrated large mass within posterior third ventricle. B, Atypical teratoma in 12-year-old boy with diabetes insipidus. Contrast enhancement showing increased density in pineal region. Shunt catheter to left. C, Same patient showing small mass in anteroinferior aspect of third ventricle (arrows). Tumor confirmed on pneumoencephalography.

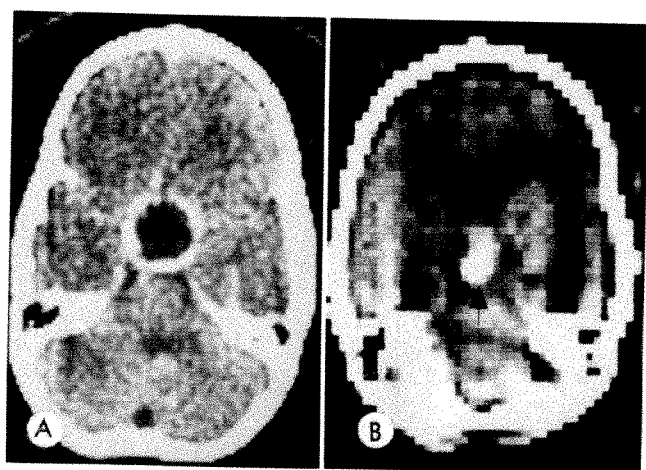


Fig. 6.—Craniopharyngioma. A, Well-defined cystic craniopharyngioma with calcified rim. B, Calcified craniopharyngioma without cystic component causing obstruction at foramen of Monro with enlarged lateral ventricles.

An orbital optic nerve glioma was clearly demonstrated on CT scan (fig. 8C); however, pneumoencephalography with tomography is still the procedure of choice in intracranial optic gliomas. Axial views of the optic canals [10] followed by polytomographic pneumoencephalography provides the finest delineation of anatomic detail in the region of the optic nerves, chiasm, and hypothalamus and certainly still remains the neuroradiologic investigative procedure of choice.

Accuracy of CT

CT proved very accurate in detecting and localizing intracranial neoplasms. There were four false positive and only

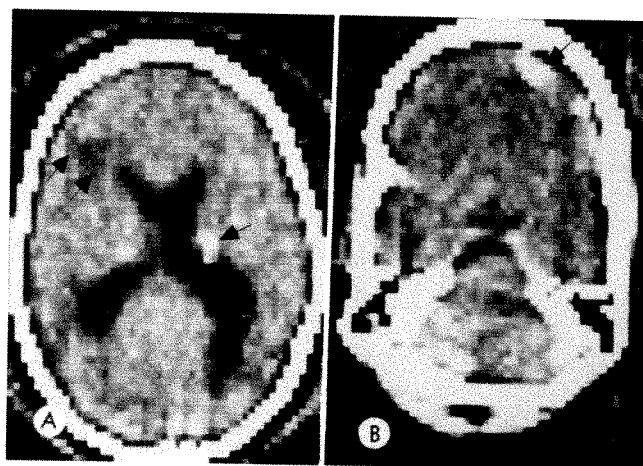


Fig. 7.—Tuberosclerosis. A, Calcified subependymal (arrow) and noncalcified tuber (double arrows). B, Calcified subcortical tubers, frontal region (arrows).

one false negative scan in 43 patients with 40 tumors. These 40 neoplasms occurred in 39 patients, one patient having bilateral acoustic neuromas.

False Positive Cases

Of the four false positive CT scans, one was interpreted as possible suprasellar neoplasm. Brain scan was also suggestive of an abnormality in this area. Pneumoencephalography and angiography were normal. This was early in our series and in retrospect the CT scan would now be considered normal.

The second case showed a very small area of increased density in the left thalamic region on contrast enhance-

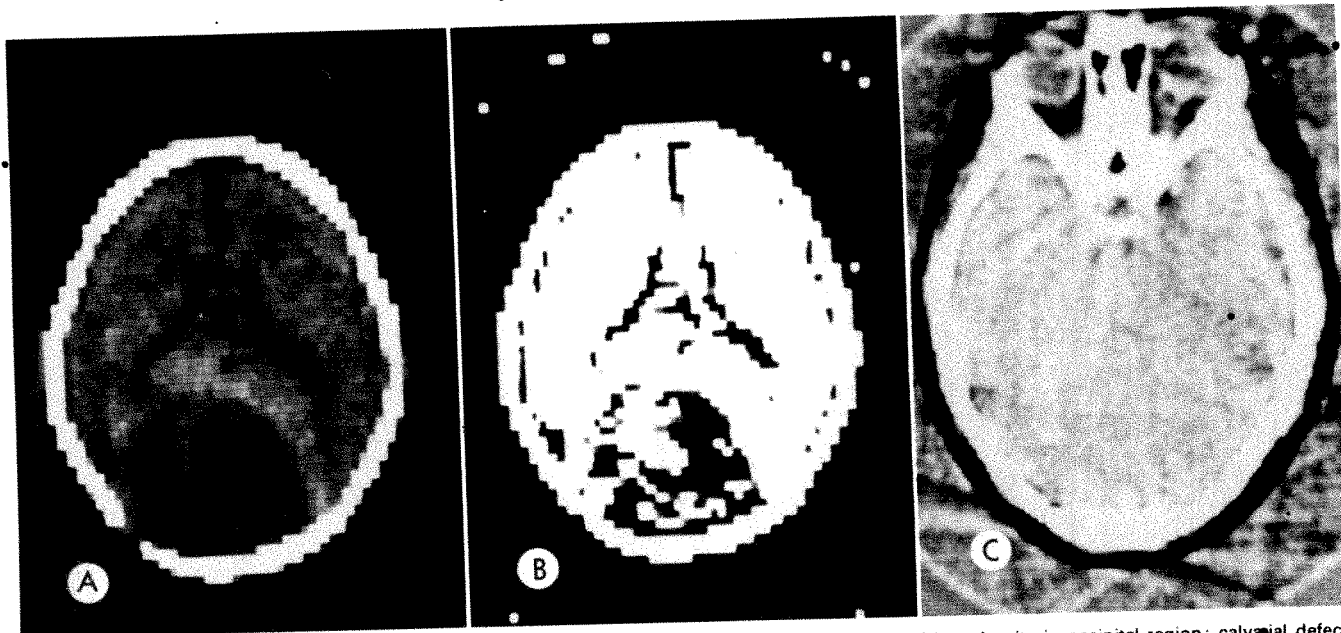


Fig. 8.—Miscellaneous tumors. A, Dural sarcoma in occipital region. 3-month-old child with area of low density in occipital region; calvarial defect. Clinically thought to be leptomeningeal cyst. B, Same patient with scanner set at density of 14 EMI units, suggesting a low density solid tumor. Surgically proven dural myxofibroma with sarcomatous changes. C, Right optic nerve glioma in 5-year-old female, confirmed by pneumoencephalography.

ment. There was no mass effect. An arteriovenous malformation or a neoplasm was suspected, but angiography was normal.

The third patient was thought clinically to have a posterior fossa tumor. The CT scan, although suboptimal because of patient motion, showed markedly enlarged lateral and third ventricles with an area of increased density in the mid-portion of the posterior fossa (fig. 9A). This was interpreted as posterior fossa tumor. Radionuclide brain scan was normal. Carotid and vertebral angiography showed hydrocephalus without evidence of posterior fossa tumor, and ventriculography and pneumoencephalography revealed aqueductal stenosis. The area of increased density is presumably brain stem associated with motion artefact. This case points up the hazards of interpreting suboptimal CT scans.

The fourth patient had previous surgery for cerebellar astrocytoma and presented with headaches. The CT scan showed a large low density cystic midline area in the posterior fossa with an area of increased density in the region of the right cerebellar hemisphere (figs. 9B and 9C). With contrast enhancement the area of increased density enlarged slightly. This was interpreted as recurrent tumor. Brain scan was also interpreted as abnormal and a recurrent tumor suspected. At surgery the patient was found to have a blocked ventricular shunt with the cystic midline mass being an enlarged fourth ventricle. The area of increased density on the scan was found to be ossified dura. Skull roentgenograms did not show the dural ossification.

False Negative Cases

There was one false negative CT scan in our series. This was an 11-year-old boy who presented with headaches and vomiting and an abnormal electroencephalogram in the

left temporal area. The radionuclide brain scan was normal as was the CT scan without and with contrast enhancement (fig. 10). The patient returned 2 months later with the same symptoms having worsened. Repeat radionuclide brain scan was abnormal, and repeat CT scan demonstrated a very large tumor in the left temporal lobe region extending to involve the thalamus and basal ganglia with shift of the ventricles to the right. On contrast enhancement the tumor increased in density with a central area of necrosis and surrounding edema well seen. Carotid angiography confirmed the very vascular neoplasm with arteriovenous shunting. This neoplasm was a glioblastoma multiforme. The patient's clinical status deteriorated rapidly and 4 months after initial presentation he died. At the time of initial CT examination the neoplasm must have been small since there was no ventricular shift. Even in retrospect no abnormality can be seen on the routine or contrast-enhanced scans. This was an aggressive glioblastoma as demonstrated on follow-up study and short clinical course until demise.

Conclusions

Most workers would agree that as much information as possible should be obtained prior to the attempted biopsy or removal of any intracranial neoplasm. To this end, air and angiographic studies as well as CT are now virtually always performed to define the exact geography and character of the neoplasm. CT also provides information on whether the neoplasm contains a cyst.

It is premature to state definitively the relative value of radionuclide brain scans, air studies, and angiography as adjunctive procedures to CT in the neuroradiologic investigation of children with cerebral neoplasms. However, some generalizations may be made.

In cooperative children, generally those 5 years of age

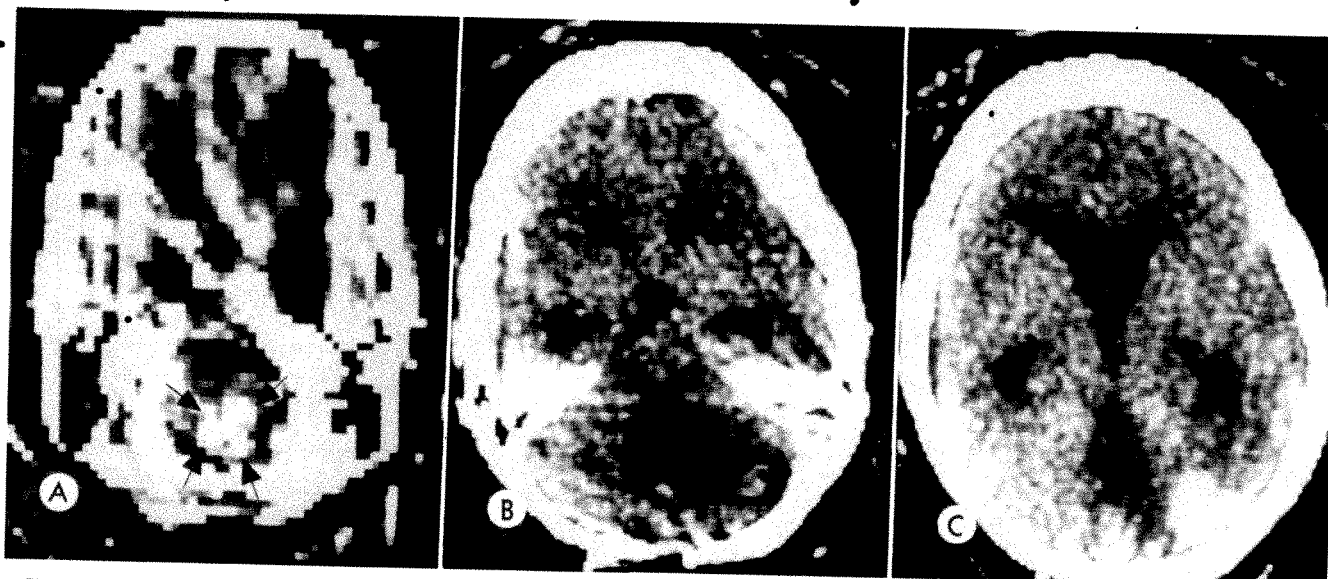


Fig. 9.—False positive cases. *A*, Suboptimal CT due to patient motion. Area of increased density in posterior fossa (arrows) thought to be tumor. Subsequent studies showed only aqueductal stenosis with normal fourth ventricle. *B* and *C*, Previous surgical removal of cystic astrocytoma. CT interpreted as recurrent tumor. At surgery no tumor present. There was an obstructed ventriculoperitoneal shunt with large fourth ventricle (area of decreased density on CT) and dural ossification (area of increased density) which was not visible on skull roentgenograms.

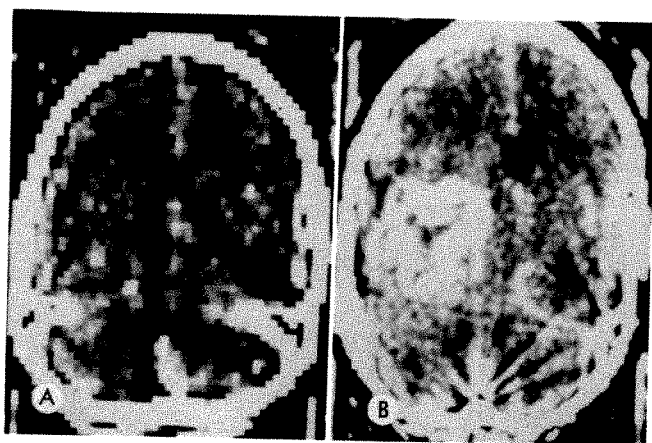


Fig. 10.—False negative case. *A*, Initial CT with contrast enhancement interpreted as normal. *B*, Same patient 2 months later with contrast enhancement. Large tumor mass with central necrosis, left basal ganglia, and temporal lobe. Glioblastoma multiforme.

and older, we feel CT with contrast enhancement will replace the radionuclide brain scan as a screening procedure for neoplasms. However, in infants and uncooperative children who would require either heavy sedation or general anesthesia to obtain a satisfactory CT scan, complete nuclear medicine evaluation remains an excellent screening modality. Nuclear medicine can define physiologic parameters of intracranial abnormalities such as relative blood flow to a neoplasm or arteriovenous malformation, and it is this aspect of the nuclear medicine study which we feel will assume greatest importance.

Tumors of the cerebellum are demonstrated well on CT. The study we found most helpful in confirming CT findings was the air ventriculogram, which shows the relationship of the mass to the fourth ventricle and the exact location of

the fourth ventricle. This latter information is important to the surgeon, is not always available on CT, and may be less accurate on angiography than the direct visualization of the fourth ventricle containing air.

Based on our experience with 53 tumors involving the brain stem, we feel that the geography of the tumor is best delineated by pneumoencephalography. Although frequently angiography is also performed in these patients, little additional information is obtained. Our experience with CT is too limited, and two brain stem tumors were missed on radionuclide brain scans. Thus we feel the initial procedure of choice in suspected brain stem neoplasm is still pneumoencephalography.

Tumors in the posterior third ventricular region may pose very difficult diagnostic problems. We have performed both air studies and angiography as well as CT scans and have found all of value.

Craniopharyngiomas were demonstrated well on CT. However, based on experience with 60 craniopharyngiomas, it is our feeling that pneumoencephalography best demonstrates the precise geography of the neoplasm and its relationship to surrounding anatomic structures. Although we have had no false negative craniopharyngiomas on CT, if a lesion in the region of the sella turcica is suspected clinically and the CT scan is negative, we still proceed with a pneumoencephalogram.

Tumors involving the cerebral hemispheres were well demonstrated with CT and contrast enhancement. As an adjunctive and confirmatory procedure we currently perform angiography which may provide additional information with regard to the character of the neoplasm (for example, arteriovenous shunting in a high grade glioma and demonstration of major feeding and draining vessels if surgical extirpation is contemplated).

These generalizations are based on our early experiences.

We suspect that as experience with CT scanning increases and with the remarkable technological advances being made in this modality, approaches will be appropriately modified.

REFERENCES

1. Ambrose J: Computerized transverse axial scanning (tomography). II. Clinical application. *Br J Radiol* 46:1023-1047, 1973
2. New PFJ, Scott WR, Schnur JA, Davis KR, Taveras JM, Hochberg FH: Computed tomography with the EMI scanner in the diagnosis of primary and metastatic intracranial neoplasms. *Radiology* 114:75-87, 1975
3. Baker HL, Campbell JK, Houser OW, Reese DF, Sheedy PF, Holman CB, Kurland RL: Computer assisted tomography of the head. An early evaluation. *Mayo Clin Proc* 49:17-27, 1974
4. Houser OW, Smith JB, Gomez MR, Baker HL Jr: Evaluation of intracranial disorders in children by computerized transaxial tomography: a preliminary report. *Neurology* 25:607, 1975
5. Gilday DL, Ash J: Accuracy of brain scanning in pediatric craniocerebral neoplasms. *Radiology*. In press, 1976
6. Valvassori GE: The abnormal internal auditory canal: the diagnosis of acoustic neuroma. *Radiology* 92:449-459, 1969
7. Hanafey WN, Wilson GH: Pontocerebellar angle tumors, newer diagnostic methods. *Arch Otolaryngol* 92:236-243, 1970
8. Swischuk LE, Bryan RN: Double midline intracranial atypical teratomas: a recognizable neuroendocrinologic syndrome. *Am J Roentgenol* 122:517-524, 1974
9. Fitz CR, Harwood-Nash DCF, Thompson JR: Neuroradiology of tuberous sclerosis in children. *Radiology* 110:635-642, 1974
10. Harwood-Nash DC: Axial tomography of the optic canals in children. *Radiology* 96:367-374, 1970

Computed Tomography: The Anatomic Basis of the Zone of Diminished Density Surrounding Meningiomas.

RICHARD M. SIGEL^{1,2} AND ALBERT V. MESSINA¹

Computed tomography of meningiomas often demonstrates a zone of diminished density surrounding the actual tumor. This zone may be related to widening of the subarachnoid space, cerebral edema, tissue necrosis, or demyelination. A case is presented in which the anatomic basis of the zone of diminished density was shown on pneumoencephalography and at surgery to be an enlarged subarachnoid space.

Of the various neuroradiologic diagnostic modalities, computed tomography (CT) allows direct demonstration not only of a brain tumor but also of related abnormalities in the surrounding brain parenchyma, subarachnoid spaces, and associated structures. Meningiomas generally appear as more or less homogeneous, occasionally lobulated masses of density equal to or greater than that of the surrounding brain tissue. These tumors almost uniformly increase in density after intravenous injection of iodinated contrast media [1-3]. They are usually surrounded by a well-circumscribed zone of diminished, noncontrast-enhancing density of variable width [2, 4]. While correlation of the pathology of the various density changes seen in meningiomas has been previously discussed [1, 5], there is very little mention of the structural changes in the surrounding low density zone which has been associated with these lesions. Paxton and Ambrose [2] suggested that this zone might represent either loculated or trapped subarachnoid fluid or edema of the adjacent brain tissue.

This report details one patient studied by CT, nuclide scan, angiography, and pneumoencephalography because of a difficult clinical problem. The structural basis for the zone of diminished density was demonstrated radiographically and surgically.

Case Report

This 60-year-old woman presented with numbness and episodic pain involving the entire left side of her face for 4 months. She had dermatomyositis with Raynaud's phenomenon for 12 years and had been on steroids until 1 year prior to admission. A diagnosis of trigeminal neuralgia was made, but treatment with Tegretol and Valium afforded no relief. She then developed a mild gait disturbance. Tomograms of the petrous bones were negative, but a brain scan showed a left parasagittal mass.

Admission neurologic examination confirmed hypesthesia in all three divisions of the left trigeminal nerve. The motor division of the fifth nerve was spared. She had a left facial paresis without involvement of taste or lacrimation. The remainder of her examination was essentially negative.

Four-vessel cerebral angiography demonstrated a small left

posterior frontal parafalcine meningioma supplied by meningeal branches of both internal and external carotid arteries (fig. 1). The superior sagittal sinus appeared to be uninvolved. No abnormality of the posterior fossa was shown. It was felt that her facial pain had not been explained; therefore, a pneumoencephalogram was performed. The posterior fossa structures were normal. The supratentorial mass effect of the meningioma was demonstrated. A collection of air was seen over the left cerebral convexity in a widened subarachnoid space adjacent and posterior to the tumor (fig. 2). No subdural air was present.

Computed tomography performed 5 days after the pneumoencephalogram demonstrated a left parasagittal contrast-enhancing tumor (fig. 3). Surrounding the tumor, predominantly posteriorly and inferiorly, was a zone of diminished density with absorption coefficients ranging from 0 to 8 EMI units, a density consistent with cerebrospinal fluid. This corresponded to the expanded subarachnoid space shown on the prior pneumoencephalogram, again filled with cerebrospinal fluid, the air having been absorbed.

At surgery a meningioma was found arising from the junction of the falx and superior sagittal sinus. Although the tumor was partially embedded in brain tissue, the adjacent subarachnoid space over the cerebral convexity was markedly widened. The surgeon noted no evidence of cerebral edema. Microscopic examination of the tumor was reported as "angioblastic meningioma."

The patient has had no facial pain since the operation, although the left side of her face has remained numb.

Discussion

There has been little radiologic-pathologic correlation of the observations of CT. The zone of diminished density surrounding tumors may commonly represent cerebral edema, but fluid-filled spaces and areas of necrosis and demyelination may have similar appearances [2].

Before the routine use of angiography, air encephalography was an important modality in the evaluation of patients with meningiomas [6, 7]. It was not unusual to demonstrate widening of the subarachnoid spaces around meningiomas. There are numerous examples in the literature, particularly concerning parafalcine meningiomas [7-9].

While a zone of low density is very frequently noted around meningiomas on CT scans, cerebral edema is less commonly noted around meningiomas at surgery [7]. Venous compression or occlusion may be a factor in such edema. Cushing noted considerable edema around some convexity meningiomas with a cystic component [10]. He not uncommonly observed "xanthogranulomatous cysts" and large cavities at the periphery of meningiomas without evidence of tumor degeneration. At ventriculography, air may be injected into these cystic spaces [6, 10]. In the experience of others, however, cysts are rare [11].

Received February 17, 1976.

¹ Division of Neuroradiology, Department of Radiology, New York Hospital-Cornell University Medical Center, 1300 York Avenue, New York, New York 10021. Address reprint requests to A. V. Messina.

² James Picker Fellow in Academic Radiology.

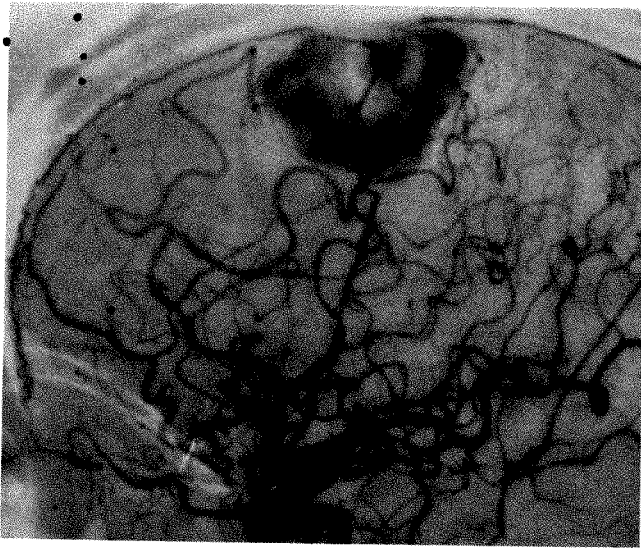


Fig. 1.—Left common carotid angiogram, subtraction film. Lobulated vascular blush in posterior frontal region. Central relatively nonvascular zone is supplied from right carotid branches.

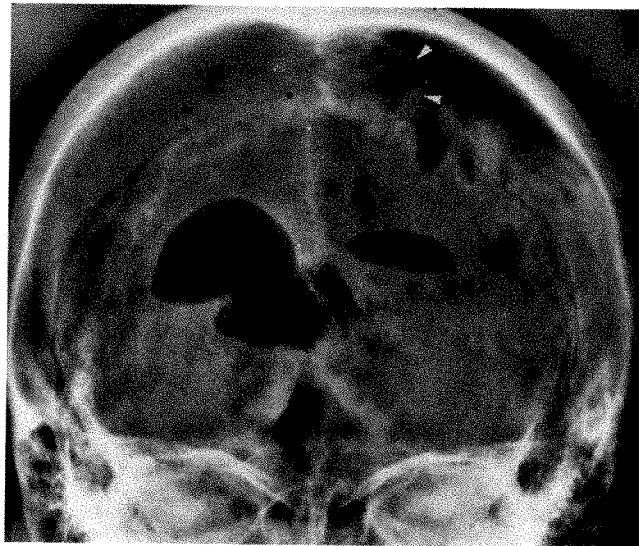


Fig. 2.—Pneumoencephalogram, sitting position, posteroanterior view. Note large collection of subarachnoid air over left convexity. Contralateral displacement of midline structures and depression of left lateral ventricle are apparent. Arrows indicate tumor.

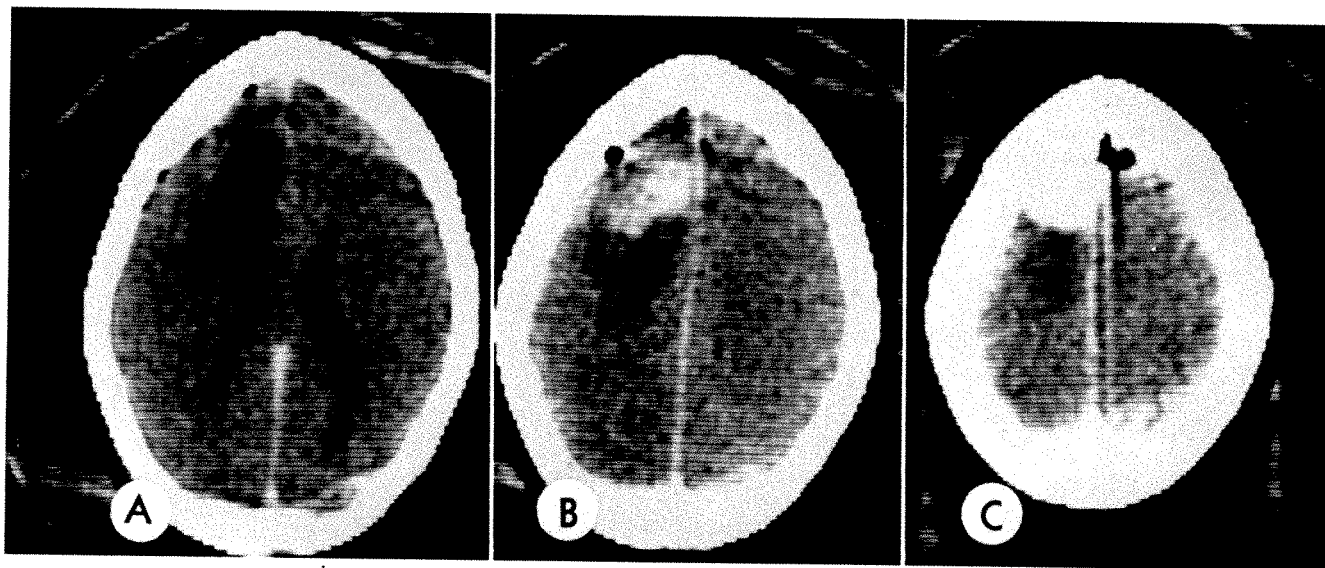


Fig. 3.—CT with contrast, contiguous slices. *A*, Large area of reduced tissue density in left posterior frontal region. *B* and *C*, Slices superior to 3A. Lobulated dense left frontal meningioma anterior to zone of reduced tissue density.

The CT scan in this case demonstrates a large, irregular zone of diminished density around a meningioma. The diminished density correlated in extent and position with widening of the subarachnoid space noted on pneumoencephalography and at surgery. Such widening of the subarachnoid space is also seen with other extraaxial masses (e.g., cerebellopontine angle tumors) and may be a simple mechanical effect or may be related to focal atrophy.

In view of the number of pathologic processes which can occur at the margins of a meningioma, extensive work is needed to correlate the CT scan appearance with pathologic anatomy. It is not now possible on CT scan alone to,

definitely determine the cause of the diminished density around a meningioma.

REFERENCES

1. Ambrose J: Computerized transverse axial scanning (tomography). II. Clinical application. *Br J Radiol* 46:1023-1047, 1973
2. Paxton R, Ambrose J: The EMI scanner: a brief review of the first 650 patients. *Br J Radiol* 47:530-565, 1974
3. New PFJ, Scott WR, Schnur JA, Davis KR, Taveras JM, Hochberg FH: Computed tomography with the EMI scanner in the diagnosis of primary and metastatic intracranial neoplasms. *Radiology* 114:75-87, 1975

4. Baker HL, Campbell JK, Houser OW, Reese DF, Sheedy PF, Holman CB, Kurland RL: Computer assisted tomography of the head: an early evaluation. *Mayo Clin Proc* 49:17-27, 1974
5. Ambrose J: Computerized x-ray scanning of the brain. *J Neurosurg* 40:679-695, 1974
6. Traub S: *Roentgenology of Intracranial Meningiomas*. Springfield, Thomas, 1961
7. Gauten-Smith PC: *Parasagittal and Falx Meningiomas*. New York, Appleton-Century-Crofts, 1970
8. DiChiro G: *An Atlas of Pathologic Pneumoencephalographic Anatomy*. Springfield, Thomas, 1967
9. Andersson T: Pneumographic diagnosis of meningioma of the falx. *Acta Radiol* 40:195-210, 1953
10. Cushing H: *Meningiomas: Their Classification, Regional Behavior, Life History, and Surgical End Results*. Springfield, Thomas, 1938
11. Russell DS, Rubenstein LJ: *Pathology of Tumors of the Nervous System*. Baltimore, Williams & Wilkins, 1971

Computed Tomographic Evaluation of Hemorrhage Secondary to Intracranial Aneurysm

KENNETH R. DAVIS,¹ P. F. J. NEW,¹ ROBERT G. OJEMANN,² ROBERT M. CROWELL,²
RICHARD B. MORAWETZ,² AND GLENN H. ROBERSON¹

Angiography in patients with subarachnoid hemorrhage secondary to aneurysm gives precise information on the location and size of the aneurysm and the presence of spasm but gives incomplete information on ventricular size, size and location of hematoma, and extent of infarction. CT demonstrates precisely brain or intraventricular hematoma and, at times, subarachnoid hemorrhage; indicates the extent of infarction; and rapidly documents the degree of hydrocephalus. Infarction secondary to spasm, hematoma, and hydrocephalus are readily differentiated.

The CT examination may be repeated as often as necessary without patient discomfort or morbidity. Serial scans allow rapid assessment of change in ventricular size, development and persistence of infarction, and change in size of hematoma.

Computed tomography may be of considerable assistance in the management of subarachnoid hemorrhage due to aneurysm. A graphic representation of intracranial anatomy and pathology may easily and frequently be obtained without recourse to repeated angiography when clinical circumstances dictate.

Subjects and Methods

Anatomic clarity was improved after installation of the 160×160 matrix, enabling visualization of some abnormalities which had not been fully appreciated on the 80×80 matrix [1]. Consequently only those patients with subarachnoid hemorrhage due to aneurysm who were studied using the 160×160 matrix are included in this report; 45 cases studied with the 80×80 matrix were eliminated.

A total of 3,000 CT examinations using the 160×160 matrix were reviewed; 24 patients with subarachnoid hemorrhage secondary to aneurysm were found (table 1). All patients had the diagnosis established by history, examination, and appropriate studies. Six of the 24 cases came to autopsy; angiograms had not been performed in three (table 2). One other patient died before an angiogram was obtained. Of the 24 patients, 12 had a single CT scan and the remainder had serial studies, for a total of 46 CT scans.

Findings

Origin of Hemorrhage

The location of subarachnoid, intraventricular, or intracerebral hemorrhage may suggest the approximate site of the aneurysm which bled (fig. 1). This occurred in nine of the 12 patients in this series who showed some evidence of hemorrhage (table 3). Multiple aneurysms were present in one case, and the area of infarction suggested the location of the bleeding aneurysm.

TABLE 1
Age and Sex of Patients

Age (Yr)	Sex	
	Females	Males
20-39.....	0	4
40-49.....	0	3
50-59.....	5	5
60-69.....	3	1
70-79.....	2	0
80-89.....	1	0
Total.....	11	13

Note.—58% had hypertension.

TABLE 2
Studies Performed

Study	No.
CT, angiogram.....	10
CT, angiogram, surgery.....	7
CT, angiogram, autopsy.....	3
CT, autopsy.....	3
CT only.....	1

Neurologic Deficit

The neurologic deficit at the time of the scan was related to the CT findings (table 4). The neurologic deficit was classified according to the following grades as modified from Botterell et al. [2]: grade 1—alert, mild headache, no neurologic deficit; grade 2—neurologically intact or nerve palsy only with moderate to severe symptoms and signs of blood in the subarachnoid space; grade 3—drowsy or obtunded without major focal deficit; grade 4—major neurological deficit; grade 5—decerebrate or decorticate posturing; and grade 6—moribund, no spontaneous respirations, essentially dead.

In the drowsy or obtunded patients (grade 3), six of eight had hydrocephalus and three had infarction. In the grade 4 cases, eight of 14 had hydrocephalus, three had intracerebral hemorrhage, and five had infarction, four with a mass effect.

Received February 6, 1976; revised April 5, 1976.

This work was supported in part by U.S. Public Health Service grant NS10828-02 from the National Institutes of Health.

¹ Department of Radiology, Massachusetts General Hospital and Harvard Medical School, Boston, Massachusetts 02114. Address reprint requests to K. R. Davis.

² Department of Neurosurgery, Massachusetts General Hospital and Harvard Medical School, Boston, Massachusetts 02114.



Fig. 1.—Subarachnoid hemorrhage. *A*, Left carotid, right posterior oblique angiogram on day of onset showing no evidence of anterior communicating artery aneurysm (later found at autopsy). *B*, CT scan (80 × 80 matrix) on day 18 showing left frontal hematoma (*arrow*). This case not included in tabulation.

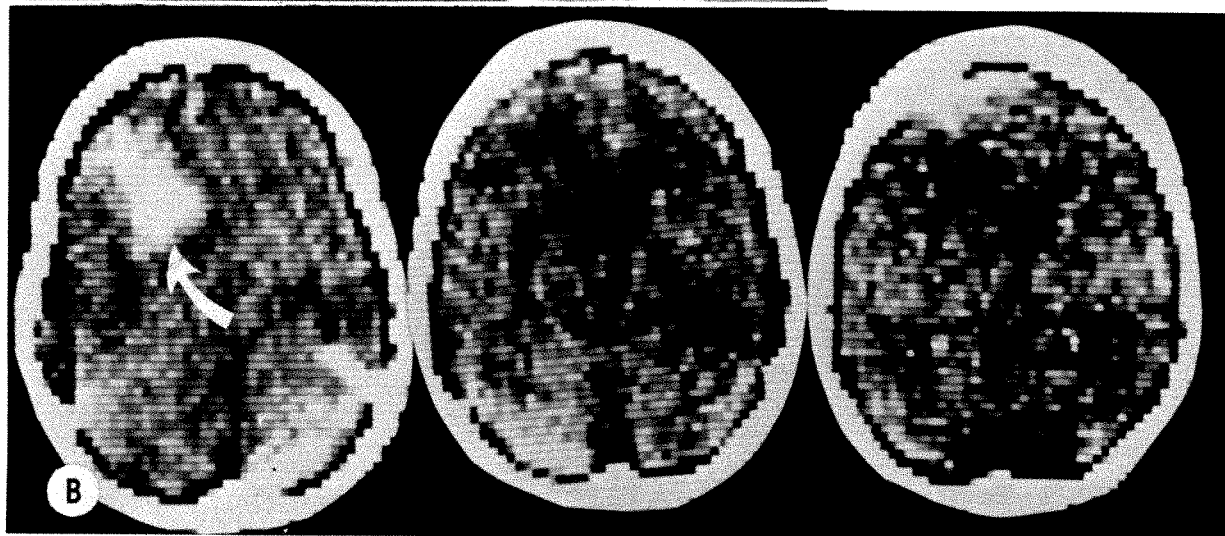


TABLE 3
Determination of Origin of Hemorrhage with CT

CT Finding	No. Patients	Site of Aneurysm Suggested				
		ACA	PCA	MCA	PICA	None
Subarachnoid hemorrhage.....	2	1	1
Subarachnoid and intraventricular hemorrhage.....	4	1	1	2
Subarachnoid, intraventricular, and intracerebral hemorrhage.....	2	2
Subarachnoid and intracerebral hemorrhage.....	2	2
Intraventricular hemorrhage.....	2	1	1	...

Note.—ACA=anterior communicating aneurysm; PCA=posterior communicating aneurysm; MCA=middle cerebral artery aneurysm; PICA=posterior inferior cerebellar artery aneurysm.

TABLE 4
Comparison of Neurologic Deficit and CT Findings

CT Finding	Neurologic Deficit (Grade)					Total
	1	2	3	4	5	
Hydrocephalus		1	6	8	4	19
Subarachnoid hemorrhage			1	2	1	4
Subarachnoid and intraventricular hemorrhage				5	1	6
Intraventricular hemorrhage			1	2	1	4
Intracerebral hemorrhage			1	3	1	5
Infarct:						
With mass		1	1	4		6
Without mass	1		2	1	2	6
Aneurysm	1	1				2
Negative CT	2	1	1			4
Total	4 (4)	4 (4)	13 (8)	25 (14)	10 (6)	56

Note.—Grade is at time CT was obtained. Patient may be tabulated more than once if grade changed when repeat CT scan was done. Multiple CT scans on same patient with same deficit and CT findings were listed only once. More than one or none of the above pathologic findings may be present on a scan at the time of a given neurologic deficit. Numbers in parentheses indicate scans in each grade having a specific CT abnormality.

Infarction

In some cases, serial scans showed the infarct developing. One patient had CT scans on days 6, 34, and 78 and was classified as grades 3, 2, and 1, respectively. The subarachnoid hemorrhage was due to an aneurysm arising from the left posterior communicating artery. The scans showed an evolving infarction in the distribution of the superior division of the left middle cerebral artery. Spasm of this vessel was seen at angiography. In another case, an infarct was suspected but the scan was negative and the patient remained well. In a third patient, reduction in mass effect was associated with good neurologic recovery.

Intraventricular Hemorrhage

One of the most important observations relates to intraventricular hemorrhage. Six patients (five grade 4 and one grade 5) had massive subarachnoid (basal cisterns) and intraventricular hemorrhage, and all died. However, four other patients (one grade 3, two grade 4, and one grade 5) with only intraventricular hemorrhage survived. Of the patients with major subarachnoid hemorrhage (blood in basal cisterns visible on CT), 50% died.

Intracerebral Hematoma

CT delineated the exact location and configuration of the hematoma. In one patient with a grade 4 neurologic status after subarachnoid hemorrhage from an anterior communicating aneurysm, CT scans were obtained 4 and 38 days after onset. Hematoma anterior to the lamina terminalis region and anterior interhemispheric fissure was present on the first scan and had been resorbed except for a small amount in the lamina terminalis cistern on the second study. The neurologic status did not improve during this time.

Another patient had three CT scans after subarachnoid hemorrhage from a posterior inferior cerebellar artery aneurysm. The neurologic deficit was grade 3 at the time of the CT scan on the first day. This scan showed blood in the fourth ventricle and hydrocephalus (fig. 2). The patient

TABLE 5
Relation of Ventricular Size to Time from Hemorrhage

Days from Onset	Ventricular Size		
	Normal	Minimal Enlargement	Moderate Enlargement
0-2	5		7
3-8	5	3	
9-14	1	2	
15-21	1	2	
22-30	1	1	
30-60	4	5	1
60-90	1	2	
90-120	1	1	1

Note.—One scan in the same time period and one following shunt not included.

rebled and had respiratory arrest on day 6. The second CT scan just before this time showed no blood in the fourth ventricle and no sign of hydrocephalus. The neurologic deficit was then grade 4. The last scan (day 13) showed no change in ventricular size but minimal blood in the fourth ventricle; the neurologic status remained unchanged.

Hydrocephalus

The CT scan is of great value in assessing the degree and cause of hydrocephalus (table 5, figs. 2 and 3). One patient with subarachnoid hemorrhage from a right posterior communicating aneurysm had three CT scans: day of onset (grade 5), day 6 (grade 4), and day 34 (grade 4). The first scan showed only hydrocephalus, and a ventriculostomy was performed which was removed on the next day. The ventricles were progressively smaller on the next two scans (normal size on the last scan). One of the most striking observations from table 5 is that more than half of the patients scanned within 48 hr of onset of hemorrhage had ventricular enlargement.

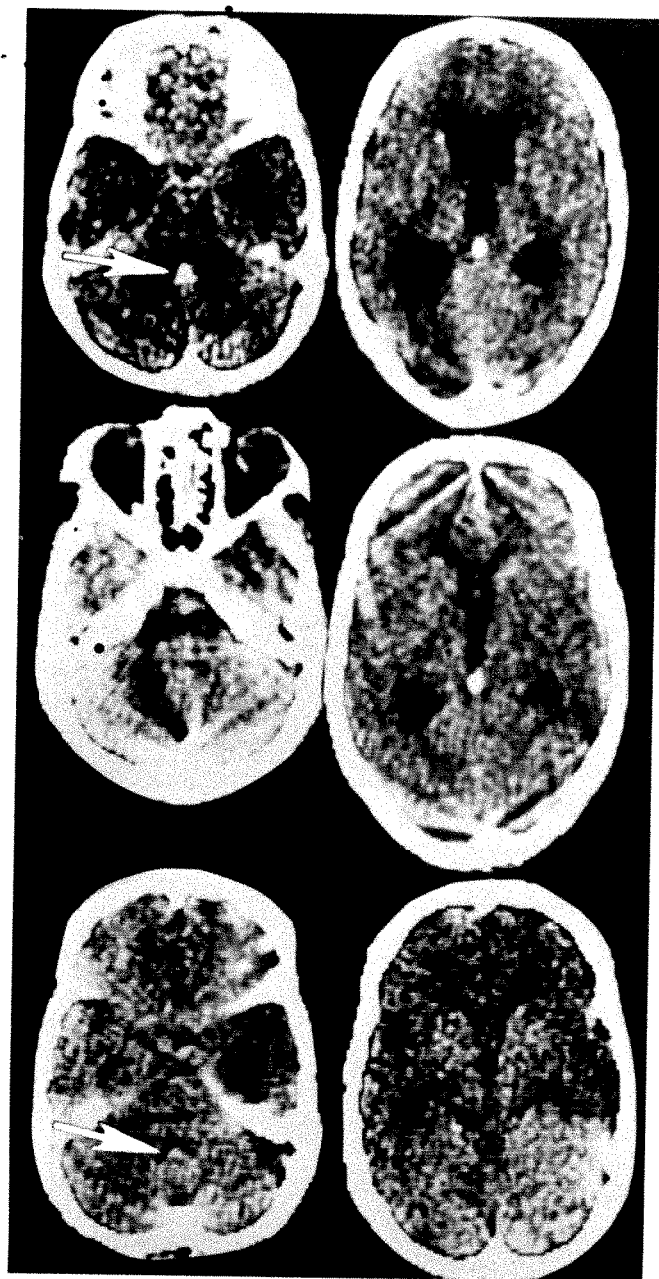


Fig. 2.—Evaluation of ventricular size. *Upper*, Scan on day 1 showing hydrocephalus and blood in fourth ventricle (arrow). *Middle*, Scan on day 4 showing no hydrocephalus and no blood in fourth ventricle. *Lower*, Scan on day 13 after rebleed on day 6. Minimal blood in fourth ventricle (arrow); no hydrocephalus.

Correlation of CT and Angiography

Angiographic and CT findings were compared in 11 cases in which the studies were performed within 24 hr of each other (table 6). In nine cases, CT provided additional information. In general, CT provided better visualization of intracerebral and intraventricular hemorrhage, infarction, subarachnoid hemorrhage, and partial thrombosis of aneurysm (fig. 4). CT studies could also definitely exclude the presence of hematoma.

TABLE 6
Additional Information Provided by CT

Information Provided	No. Cases
Improved visualization of:	
Intracerebral hematoma	3
Intraventricular hemorrhage	1
Infarction	2
Subarachnoid hemorrhage	4
Partial thrombosis of aneurysm	1
Exclusion of hematoma	2

Note.—Data from 11 cases in which angiography and CT performed within 24 hr of each other. CT provided additional information in nine. One patient had both CT and angiography on two separate days. A case may be listed in more than one category.

Most aneurysms are not large enough to permit assessment of size, but one striking case was seen (fig. 4). Another case of a multilobulated aneurysm from the ambient cisternal segment of the left posterior cerebral artery did not show a change in apparent size on CT scans before and after contrast infusion. The CSF was negative, but at the time of operative clipping, the sac wall showed changes consistent with a recent bleed.

CT rather than angiography was used for evaluation of the presence of hydrocephalus, intracerebral hematoma, or infarction in many patients with severe or increasing neurologic deficit or increased intracranial pressure (figs. 5–8). The CT scan often obviated the need for repeated angiographic studies.

In the following section, CT findings are compared with findings at autopsy (six cases) and surgery (seven cases).

Case Reports

Autopsied Cases

Case 1. A 45-year-old hypertensive male was found comatose. Examination revealed bilateral subhyaloid hemorrhages and no signs of neurological function except respiration. CT scan showed blood in the subarachnoid spaces and swelling of both cerebral hemispheres, compressing the ventricles (fig. 6). He died 8 hours later.

At autopsy, marked subarachnoid hemorrhage was found, especially at the base of the swollen brain as seen on CT. Buried in the blood clot was a 5 mm aneurysm of the anterior communicating artery, not seen on CT. Some blood was present in the fourth ventricle near the foramina. A CT projection at that level was not done.

Case 2. A 50-year-old male had sudden right frontal headache and then became comatose. CT scan on admission showed a right frontal hematoma (a portion of which was the blood pool of the aneurysmal sac), blood in the right sylvian and interhemispheric fissures with compression of the body of the right ventricle, and right-to-left shift of the septum pellucidum. Angiography demonstrated a giant aneurysm of the right middle cerebral artery and a deep right avascular frontal mass. Three days after onset left hemiparesis developed. CT scan on that day showed enlargement of the hematoma and greater mass effect. The aneurysm was excised. On day 9 the patient became obtunded and the right pupil dilated. The third CT scan on day 11 showed massive right hemispheric swelling. A frontotemporal decompression lobectomy was

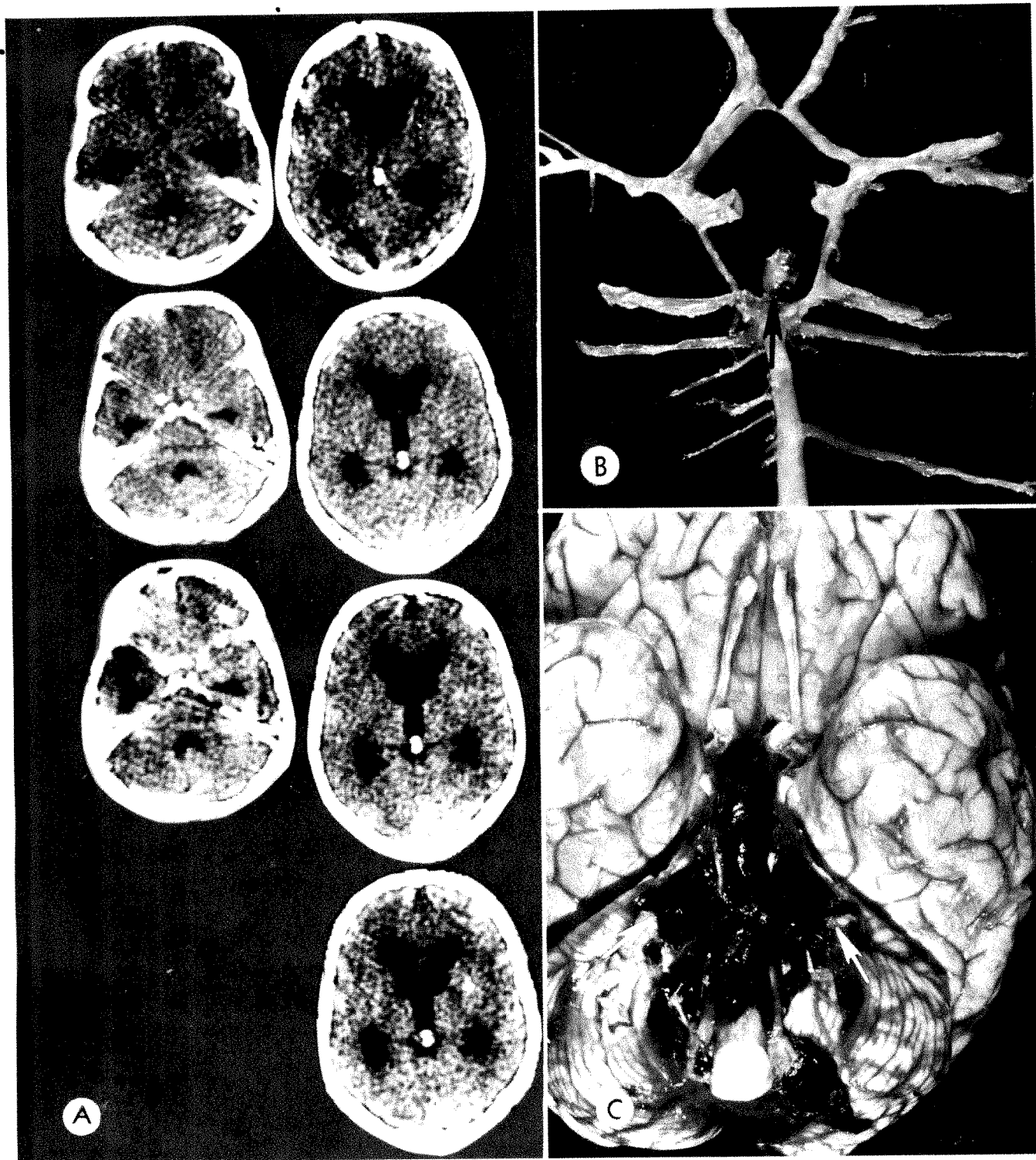


Fig. 3. —Case 4: evaluation of ventricular size. *A*, Upper to lower, CT scans on days 1, 6, 14, and 22. Only transient decrease in hydrocephalus: sylvian fissures not visualized. *B* and *C*, Aneurysm (arrow) and clot in cisterns (arrows) found at autopsy on day 25.

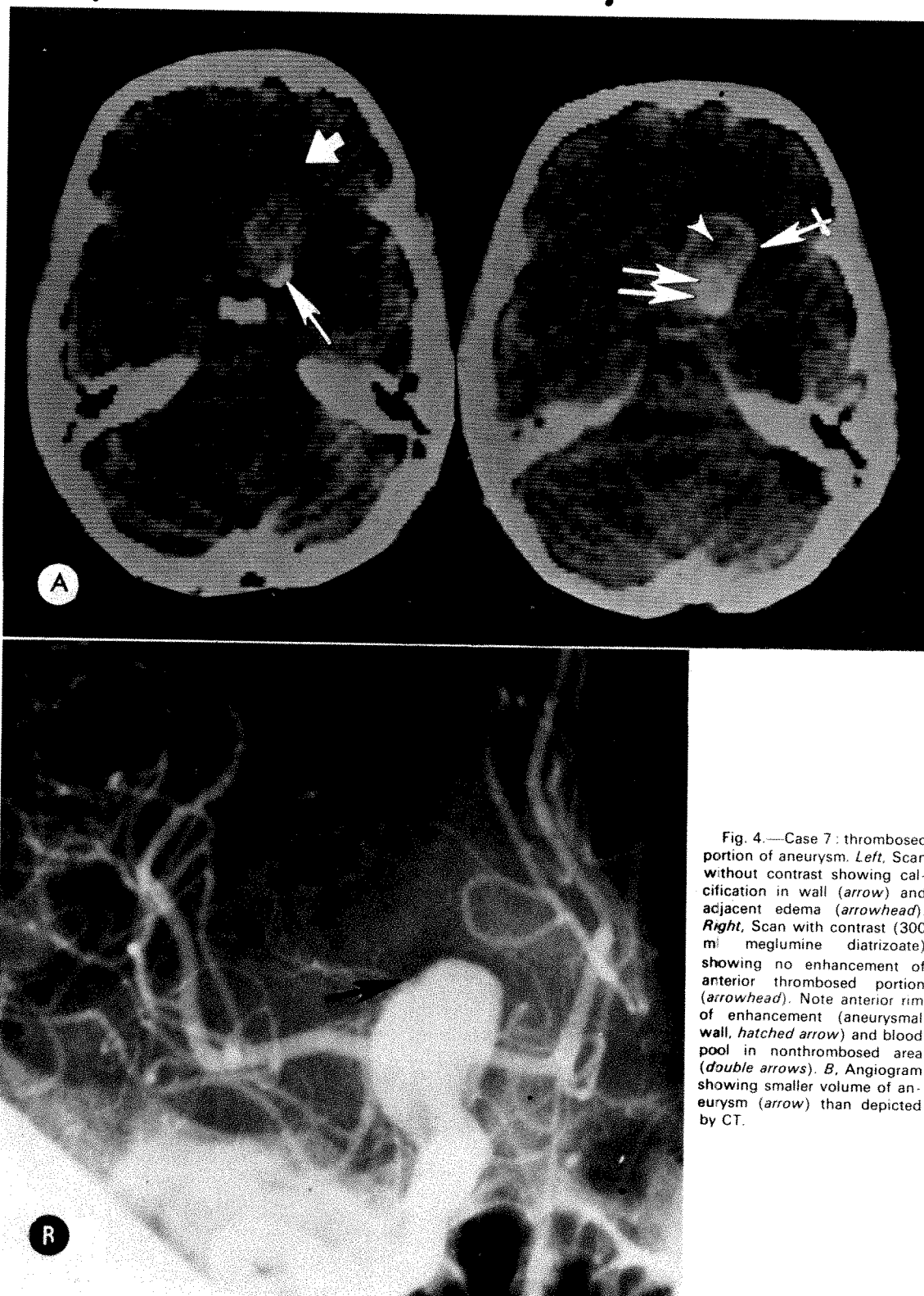


Fig. 4.—Case 7: thrombosed portion of aneurysm. *Left*, Scan without contrast showing calcification in wall (arrow) and adjacent edema (arrowhead). *Right*, Scan with contrast (300 ml meglumine diatrizoate) showing no enhancement of anterior thrombosed portion (arrowhead). Note anterior rim of enhancement (aneurysmal wall, hatched arrow) and blood pool in nonthrombosed area (double arrows). *B*, Angiogram showing smaller volume of aneurysm (arrow) than depicted by CT.

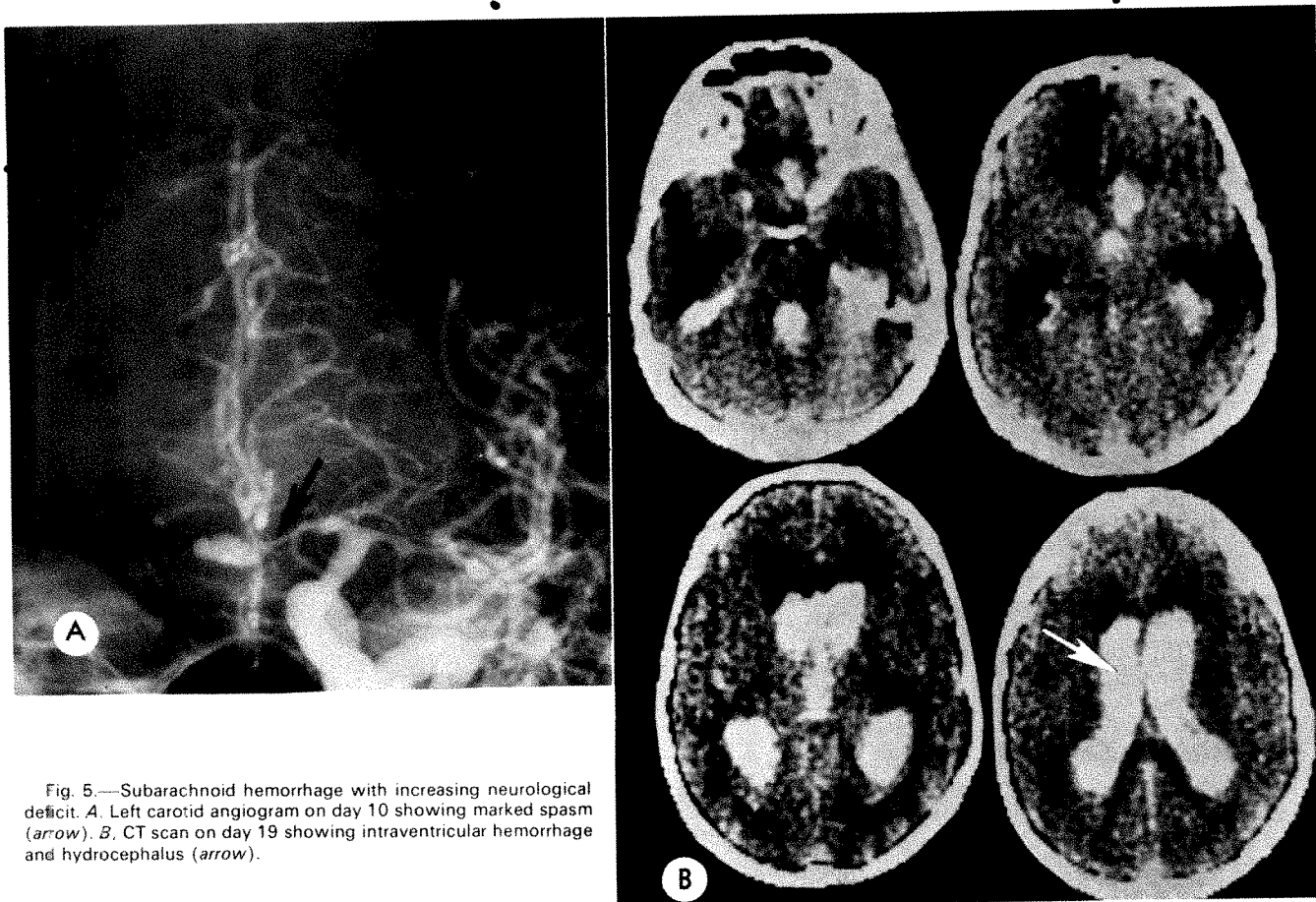


Fig. 5.—Subarachnoid hemorrhage with increasing neurological deficit. A. Left carotid angiogram on day 10 showing marked spasm (arrow). B. CT scan on day 19 showing intraventricular hemorrhage and hydrocephalus (arrow).

performed, but he did not improve. CT scan on day 44 showed a large cavity in the right frontal region. He died on day 53.

At autopsy a large amount of subarachnoid blood was found, especially in the chiasmatic, interpeduncular, pontine, and medullary cisterns. Clot was found in the lateral and fourth ventricles.

Case 3. A 57-year-old female had sudden onset of headache and nuchal rigidity. There was a bilateral sixth nerve palsy, limitation of upward gaze, and a positive left Babinski. The cerebrospinal fluid was bloody. Twelve hours after onset, she was unresponsive and had bilateral papilledema. CT scan showed subarachnoid blood in the basal cisterns and interhemispheric fissure, blood in the third ventricle and both occipital horns, and hydrocephalus. Fifteen hours after onset, the pupils dilated and became nonreactive. She died the next day.

At autopsy a large amount of subarachnoid blood was present, especially in the chiasmatic interpeduncular, pontine, and medullary cisterns. An aneurysm 6 mm in diameter was found, originating 2 mm beyond the takeoff of the left posterior inferior cerebellar artery. Clot was found in the lateral and fourth ventricles.

Case 4. A 38-year-old hypertensive male had sudden headache, light-headedness, and bizarre behavior. A seizure occurred, and then he became comatose. The spinal fluid was bloody. The next day he was awake and responsive. CT scan on that day showed hydrocephalus (fig. 3). Angiography demonstrated a bilobed basilar bifurcation aneurysm without spasm. Paralysis on upward gaze and disorientation developed on the sixth day. CT scan on that day showed slightly less hydrocephalus. CT scans on days 14 and 22 showed mild progressive hydrocephalus. He died of recurrent hemorrhage on day 24.

At autopsy a clot was present in the cisterns anterior to the brain-stem, cisterna magna, and interpeduncular and chiasmatic cisterns. There was an aneurysm at the point of basilar bifurcation and ventricular enlargement.

Case 5. A 59-year-old male became hypertensive during an extra-cranial surgical procedure and remained unresponsive in the recovery room. CT scan on the following day showed hemorrhage in the lateral (left greater than right), third, and fourth ventricles, subarachnoid blood in the basal cisterns, ambient cisterns, interhemispheric fissure, and hematoma in the rostrum of the corpus callosum. He died on that day.

At autopsy a small anterior communicating aneurysm was found to have ruptured, resulting in blood within and around the anterior corpus callosum, within the anterior interhemispheric fissure, ambient cisterns, circle of Willis and pontine cistern, and over the convexities. The brain was swollen. Massive intraventricular hemorrhage was seen in all four ventricles.

Case 6. A 34-year-old male became dizzy and then comatose. An angiogram obtained 5 days after onset of symptoms showed an aneurysm of the left anterior communicating artery. The left anterior cerebral artery was clipped 9 days after onset. He was akinetic and mute postoperatively. Five weeks later, still comatose, he was transferred to the Massachusetts General Hospital. CT scan at that time showed communicating hydrocephalus and left anterior cerebral and right middle cerebral infarctions. A radionuclide cerebrospinal fluid study showed ventricular stasis, and a ventriculoatrial shunt was done. CT scan 8 days after the shunt showed smaller ventricles, but there was no change in his neurological status. Fifteen days after the shunt, he developed dilatation of the left pupil and was

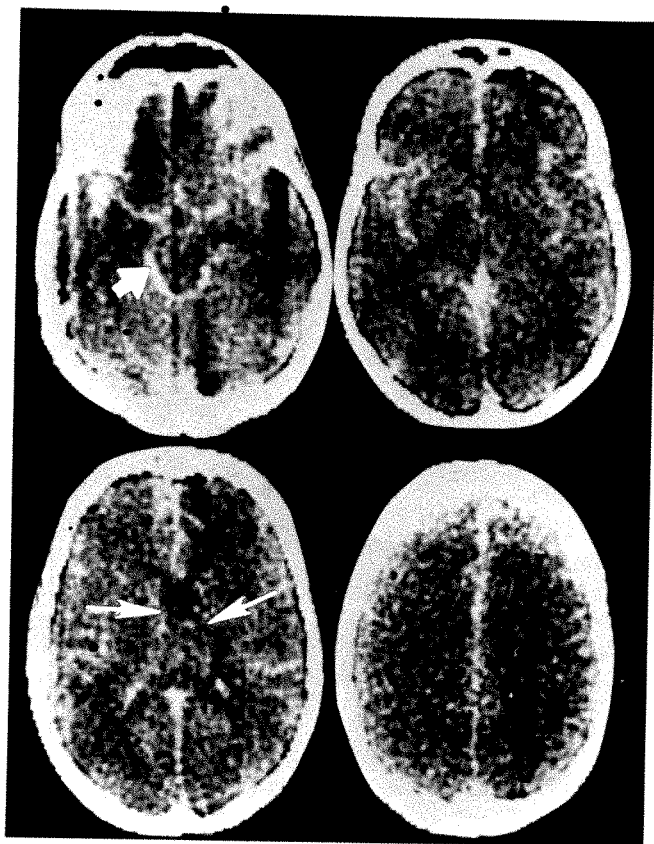


Fig. 6.—Case 1: subarachnoid hemorrhage with edema. CT scan on day of onset showing bilateral swelling with compression of ventricles (arrows). Note subarachnoid hemorrhage (arrowhead). Aneurysm not identifiable.

flaccid with intermittent decerebrate posturing. He died 3 days later.

At autopsy a saccular aneurysm (7.5 mm diameter) of the anterior communicating artery and a 10×20 mm aneurysm of the right anterior cerebral artery were found. There was massive hemorrhage into both frontal lobes and the ventricular system. Subarachnoid hemorrhage was also found, due to a rebleed after the last CT scan. Recent massive left frontoparietal and moderate right parietal infarctions were seen. Both frontal areas were swollen.

Surgical Cases

Case 7. A 54-year-old male had a seizure. The cerebrospinal fluid was clear and the neurological examination normal. CT scan (fig. 4) showed a right supraclinoid inferior frontal abnormality with absorption values in the lower blood range (18–27 EMI units). Calcification was present posteriorly (31–66 EMI units). Following infusion of 300 ml of meglumine diatrizoate, the posterior portion and anterior rim of the abnormality showed enhancement (18–41 and 27–31 EMI units, respectively). A low absorption region in the central anterior aspect (18–27 EMI units) was consistent with a partially thrombosed aneurysm. Angiography showed an aneurysm arising from the right internal carotid artery, just above the origin of the ophthalmic artery. The size of the aneurysm was smaller than the total volume of the high absorption abnormality on CT scan. This was consistent with thrombus anteriorly. The low absorption changes were interpreted as compressed edematous frontal lobe.

Surgical findings correlated well with CT findings, whereas the angiogram had incompletely revealed the size of the aneurysm.

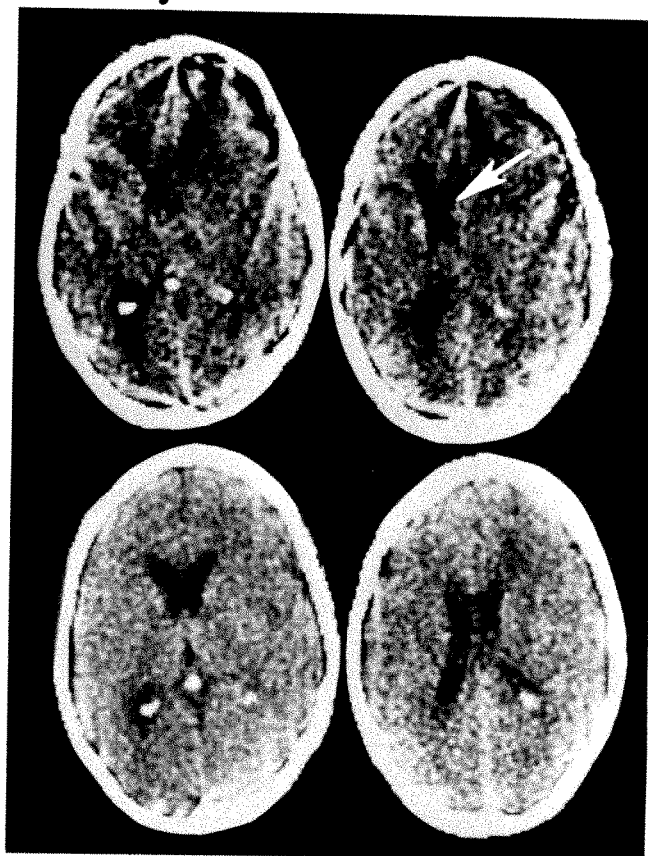


Fig. 7.—Case 9: infarction following clipping of aneurysm of anterior communicating artery. *Upper*, Scan 9 days postoperatively showing mass effect (arrow). *Lower*, Scan almost 1 month later showing less mass effect.

The sac was not entered, but the neck of the aneurysm was clipped.

Case 8. A 38-year-old male had a seizure followed by a right hemisensory deficit. Lumbar puncture was negative. CT scan showed a high absorption abnormality in the lower blood range (18–30 EMI units) adjacent to the lateral and inferior aspect of the left ambient cistern. Absorption values elevated to 24–44 EMI units after infusion of contrast medium. An angiogram showed a multilobulated aneurysm of the ambient segment of a left posterior cerebral artery, projecting inferiorly.

At surgery a 5–8 mm multilobulated aneurysm of the posterior cerebral artery was clipped. No thrombosis or adjacent hematoma was present, and the appearance suggested a recent bleed.

Case 9. A 67-year-old female had sudden syncope followed by left hemiparesis and aphasia, which cleared rapidly. Angiography demonstrated an aneurysm of the anterior communicating artery. The neurologic status was grade 1 at the time the aneurysm was clipped. Nine days after surgery she developed left hemiparesis and drowsiness. The CT scan (fig. 7) showed mass effect from a right middle cerebral artery infarct and slight ventricular enlargement. There was progressive improvement, and a second scan was obtained 26 days later to check ventricular size. There was no hydrocephalus and less mass effect. One year after surgery she remained grade 1.

Case 10. A 51-year-old hypertensive male had sudden left facial weakness, slurred speech, and nuchal rigidity. A multilobulated aneurysm of the right middle cerebral artery was seen at angiography. The aneurysm was coiled when the patient was grade 1. The first CT study was obtained postoperatively 22 days after onset. The patient was grade 1, and the scan was negative. A month later the patient developed a cough and left hemiparesis

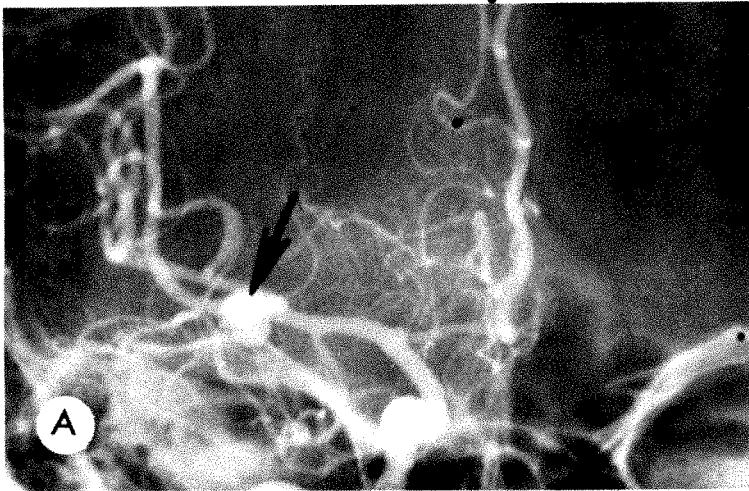


Fig. 8.—Subarachnoid hemorrhage; development of neurologic deficit without recurrent hemorrhage. *A*, Right carotid angiogram on day 1 showing middle cerebral artery aneurysm (arrow), spasm, and midline shift. *B*, CT scan 6 days later showing infarct with swelling in distribution of right middle cerebral artery (arrow). Note resorbing (previously present) hematoma (arrowhead).

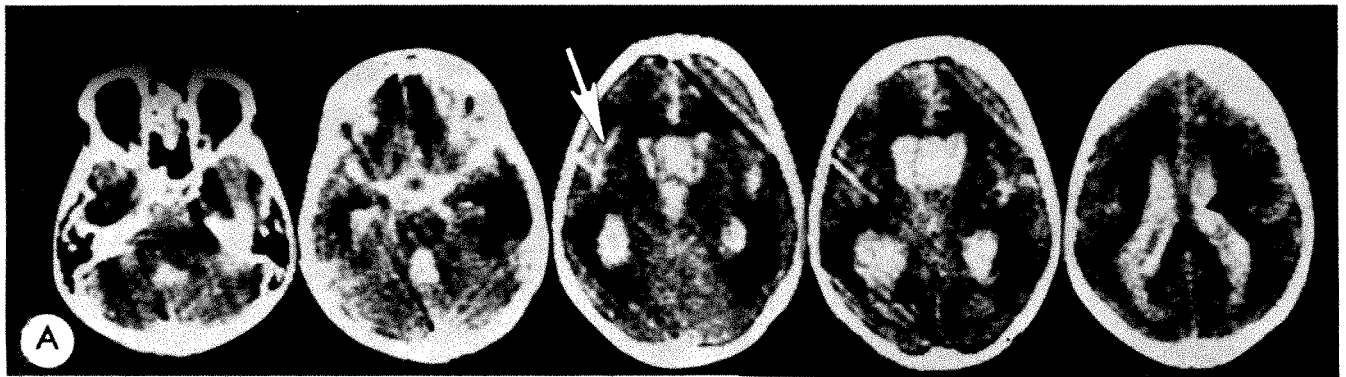


Fig. 9.—Criteria for poor prognosis. *A*, CT scan showing marked subarachnoid (arrow) and intraventricular (arrowhead) hemorrhage and blood in distended cavum of septum pellucidum. *B*, Left carotid angiogram, AP view, on same day showing aneurysm of communicating artery (arrow).

and dysarthria. Angiography showed occluded right middle cerebral artery branches, thought to be secondary to a dislodged clot from the aneurysm. A CT scan 4 days later showed infarction with mass effect in the right frontotemporal region. He was grade 4 at this time but subsequently improved.

Case 11. A 57-year-old hypertensive female had subarachnoid hemorrhage secondary to an aneurysm of the anterior communicating artery. The aneurysm was clipped. The patient was confused and drowsy postoperatively. CT scans were obtained 1 and 2 months postoperatively to assess ventricular size. The confusion and drowsiness persisted even though both scans showed the ventricles to be only minimally enlarged. There was no evidence of infarction.

Case 12. A 55-year-old female was shown to have an aneurysm of the right posterior communicating artery and severe spasm of the superior division of the right middle cerebral artery 4 and 8 days, respectively, after subarachnoid hemorrhage. When the aneurysm was clipped 12 days after onset, the patient's neurologic status was grade 1. On the fourth postoperative day, angiography was performed, showing marked spasm in the right anterior and middle cerebral arteries and a mass effect. In an effort to exclude hematoma, a CT scan was obtained; mass effect from infarct was seen. The patient was comatose. Three additional scans were obtained at monthly intervals for evaluation of ventricular size. A grade 3 neurologic deficit persisted, whereas the CT studies showed slight ventricular enlargement and evolution of the infarction. Use of serial CT scans to assess ventricular size and define the infarction eliminated the need for angiography.

Case 13. After subarachnoid hemorrhage, a 51-year-old female was shown by angiography to have an aneurysm of the posterior communicating artery. There was a question of a small mass effect, but two preoperative CT studies showed no abnormality. A grade 1 neurologic deficit persisted before and after surgery. Two months later there was a question of rebleed, but the scan was negative. The patient subsequently returned to grade 1 neurologic status.

Discussion

The advent of CT has revolutionized the diagnostic and therapeutic approach to many intracranial problems [3, 4], including subarachnoid hemorrhage due to aneurysm. However, one difficulty is that the very sick patient is often not able to hold his head motionless for the required time. Use of short-acting sedatives has proved valuable in obtaining a satisfactory study. Hopefully, newer equipment with shorter scanning times will obviate the need for sedation.

Origin of Hemorrhage

Usually the origin of hemorrhage is determined by angiography. However, the CT scan may suggest the origin of the bleed. At times an aneurysm is not seen on the first angiogram but may be visualized on a later study. Spasm or an avascular mass effect from probable intracerebral hematoma, if present, may suggest the location of the angiographically invisible aneurysm. The CT scan may demonstrate subarachnoid, intraventricular, or intracerebral hemorrhage [5] confined to one particular region and thereby suggest the site of origin of the bleed (fig. 1, table 3).

Occasionally, multiple aneurysms are found at angiography without angiographic or neurologic criteria to suggest which aneurysm has bled. The CT scan may show an intra-

cerebral hematoma or subarachnoid or intraventricular blood in the vicinity of one of the aneurysms, suggesting that particular aneurysm as the cause of the bleed.

Patient Management

Subarachnoid hemorrhage may be accompanied by varying neurological symptoms. If the patient is alert or drowsy with little neurologic deficit, angiography is indicated. If the patient has severe or increasing neurological deficit or increased intracranial pressure, the CT scan may demonstrate the presence of hydrocephalus, intracerebral or intraventricular hemorrhage, or cerebral edema [5, 6] (figs. 5-7), which could obviate the need for angiography (table 4) and lead to prompt, appropriate treatment.

The patient with moderate to severe but stable neurologic deficit who has subarachnoid hemorrhage will be medically treated for a period of time. The CT scan allows assessment for infarction and evaluation of hydrocephalus [5] as well as resolution of associated edema.

Some patients who are alert develop deficit without evidence of recurrent hemorrhage. CT allows evaluation for developing hydrocephalus or infarction (fig. 8).

If some type of shunt is needed for hydrocephalus, CT permits evaluation of ventricular size (figs. 2 and 3). In patients with a seizure disorder but no history of subarachnoid hemorrhage, CT with contrast medium may depict a large aneurysm or arteriovenous malformation [5].

The CT scan may demonstrate a larger aneurysmal volume than the angiographic representation, due to thrombosis in a portion of the sac (fig. 4). This information may be very helpful if surgery is contemplated. Without use of contrast medium, absorption values in the range of blood may be seen. This can represent a thrombosed portion of the aneurysm, a sufficiently large blood pool in the aneurysm, or an adjacent hematoma [5].

Calcification in the wall of the aneurysm may be seen. The blood pool of an aneurysm, if large enough to be detected, will be noted as an area of enhancement following administration of contrast medium. This region may be subtracted from the remainder of the adjacent elevated absorption values seen on the baseline study. The difference between the two areas will either represent thrombus in the sac or adjacent hematoma. A rim of enhancement may be seen, representing the wall of the aneurysm (fig. 4).

Angiography requires a shorter period of head immobilization for a filming sequence and is obviously superior to the CT scan in demonstrating an aneurysm and blood vessels. But since angiography is an invasive study associated with potential morbidity and discomfort, the CT scan is valuable for repetitive studies (e.g., for assessing ventricular size during the course of management). The CT scan is superior to the angiogram in depicting the presence of intracerebral or intraventricular hemorrhage [5]. The two studies are complementary in showing the presence of infarction when the clinical status has deteriorated and spasm has been demonstrated angiographically [6] (table 6).

An initial CT scan revealing a marked amount of subarachnoid blood from an aneurysm suggests that com-

communicating hydrocephalus may develop at a later date (fig. 2). The finding of marked subarachnoid and intraventricular blood usually correlates with poor neurologic status and a poor prognosis. Deterioration of neurologic status, marked spasm, hydrocephalus, or angiographic demonstration of extravasation of contrast medium into the ventricle also suggest a poor prognosis; depiction of large amounts of subarachnoid and intraventricular blood by CT are now used as additional criteria (fig. 9). An occasional patient may do well after ventriculostomy has been performed based on findings of intraventricular hemorrhage on CT scan. The patient may need a shunt for communicating hydrocephalus and is best followed by CT scan for ventricular visualization, as indicated by clinical status.

REFERENCES

1. New PFJ: Computed tomography: experience at the Massachusetts General Hospital, in *Cerebral Vascular Diseases*, edited by Whisnant JP, Sandok BA, New York, Grune & Stratton, 1975, pp 203-219
2. Botterall EH, Loughhead WM, Scott JW, Vanderwater SL: Hypothermia and interruption of carotid, or carotid and vertebral circulation in the surgical management of intracranial aneurysms. *J Neurosurg* 13:1-42, 1956
3. New PFJ, Scott WR, Schnur JA, Davis KR, Taveras JM: Computerized axial tomography with the EMI scanner. *Radiology* 110:109-123, 1974
4. Paxton R, Ambrose J: The EMI scanner: a brief review of the first 650 patients. *Br J Radiol* 47:530-565, 1974
5. Scott WR, New PFJ, Davis KR, Schnur JA: Computerized axial tomography in intracerebral and intraventricular hemorrhage. *Radiology* 112:73-80, 1974
6. Davis KR, Taveras JM, New PFJ, Schnur JA, Roberson GH: Cerebral infarction diagnosis by computerized tomography: analysis and evaluation of findings. *Am J Roentgenol* 124:643-660, 1975

Demonstration of Purulent Bacterial Intracranial Infections by Computed Tomography

ROBERT A. ZIMMERMAN,¹ SURESH PATEL, AND LARISSA T. BILANIUK

Computed tomography is shown to be an important modality in both diagnosis and management of cerebral infections. Representative findings from CT scans of patients with purulent bacterial infection of the meninges, cerebrum, ventricles, and adjacent structures are presented. Material is taken from 2,645 CT scans done in a 1 year period at the Hospital of the University of Pennsylvania. It is hoped that the use of CT will lead to a decrease of morbidity and mortality in entities such as brain abscess and subdural empyema.

Introduction

CT, a highly accurate, noninvasive technique of examining the brain [1-5], is proving to be of great value in the investigation of patients with cerebral infection. As of December 1975, there have been two published accounts of the use of CT in diagnosis of cerebral infection [2, 5]. These authors report primarily their experience with brain abscess.

The present work deals with CT manifestations of purulent bacterial meningitis, cerebritis, cerebral abscess, ventriculitis, and epidural, subdural, and subgaleal infection. Neuropathology of these entities is discussed briefly.

The material is selected from 2,645 cranial CT scans performed in a 1 year period at the Hospital of the University of Pennsylvania. Our results indicate that CT is both sensitive and accurate in detecting, characterizing, and delineating the purulent bacterial infectious process. It also is most useful in following the course of the infectious disease and in the evaluation of therapy.

Intracranial Infections

Meningitis

CT manifestations of purulent bacterial infection of the leptomeninges correlate well with neuropathological findings. In early meningitis and in successfully treated cases,

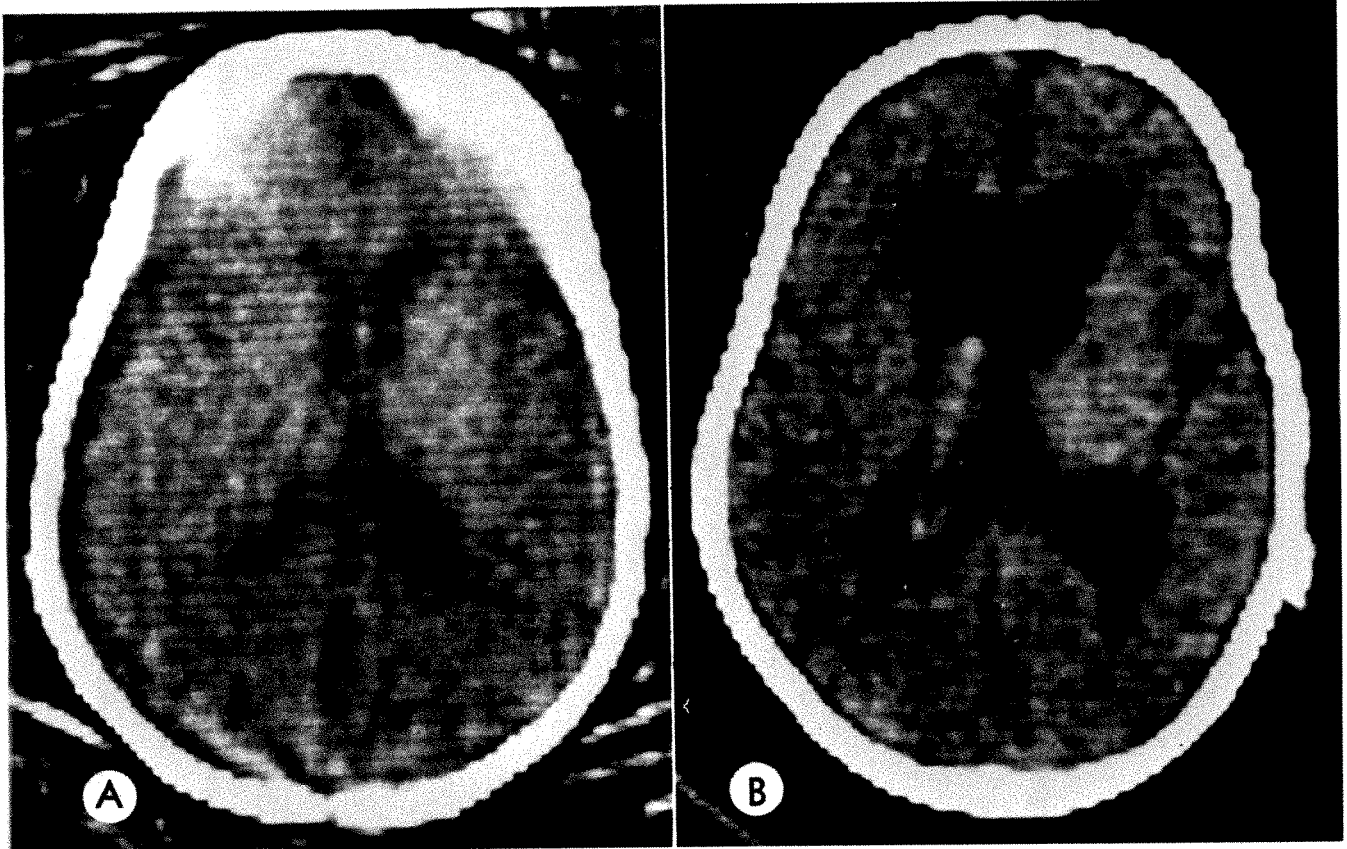


Fig. 1.—Meningitis. 7-month-old female with *H. influenzae* meningitis who developed signs of increased intracranial pressure. A, Left extracerebral collection manifested by thin rim of decreased density around temporal occipital lobes. Note slight compression and shift of left lateral ventricle. B, Scan 20 days later showing hydrocephalus but absence of extracerebral collection. Fresh periventricular hematoma noted at attempted ventriculography.

Received February 6, 1976; revised April 5, 1976

¹ All authors: Department of Radiology, Hospital of the University of Pennsylvania, 3400 Spruce Street, Philadelphia, Pennsylvania 19104. Address reprint requests to R. A. Zimmerman.

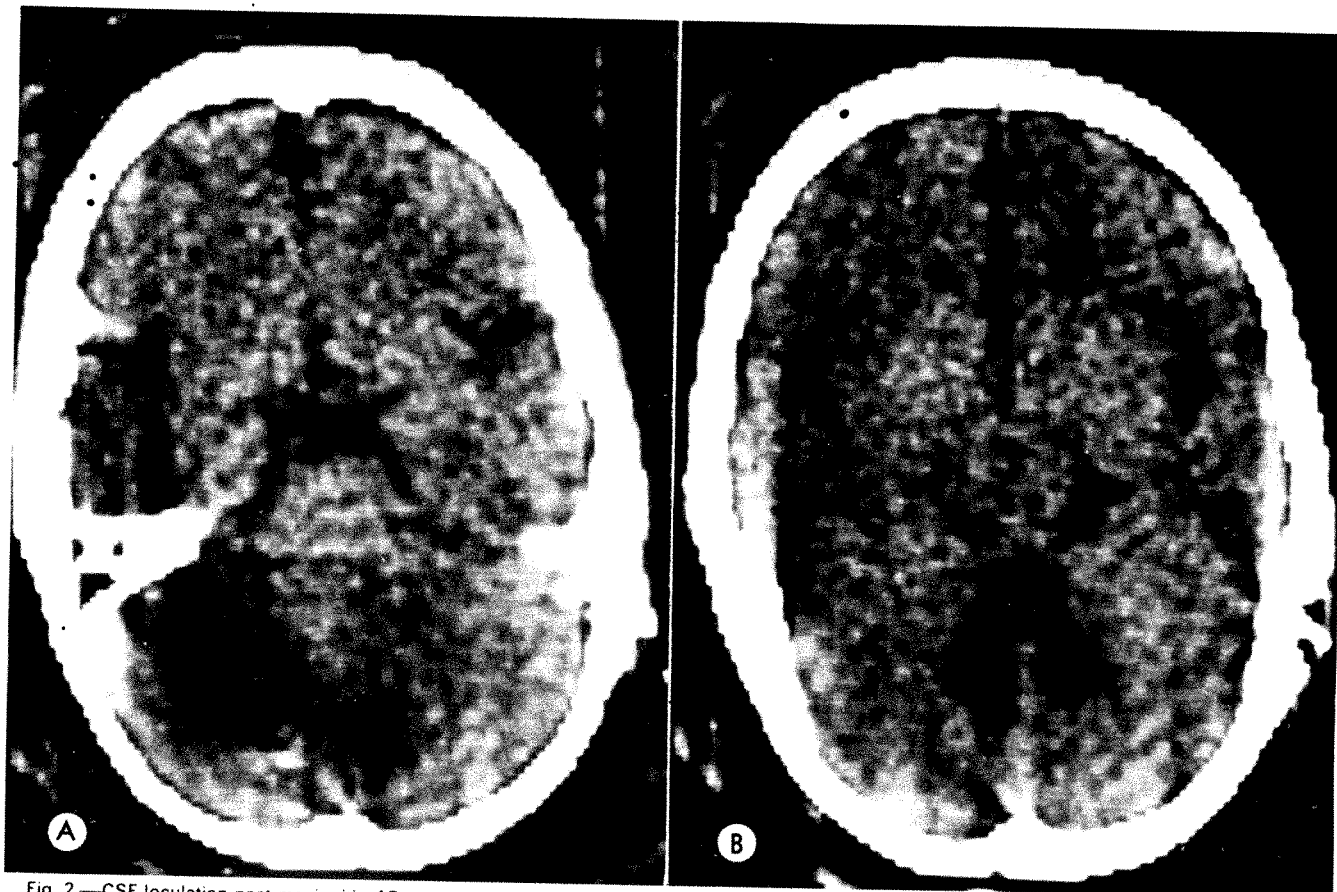


Fig. 2.—CSF loculation post meningitis. 15-year-old female with prior shunt for hydrocephalus secondary to meningitis. *A*, Dilated subarachnoid space related to left cerebellopontine cistern and cerebellar hemisphere. *B*, Scan 13 mm higher showing dilated superior cerebellar cistern.

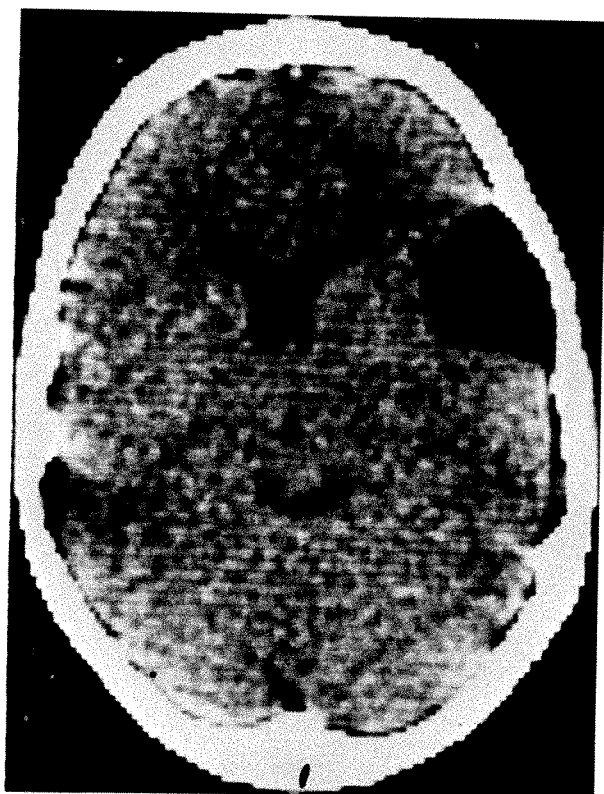


Fig. 3.—Arachnoidal cyst post meningitis. 11-year-old male with history of meningitis at age 2. Well delineated area of decreased density consistent with presence of CSF in anterior portion of right middle cranial fossa. Associated with this is mass effect on right lateral ventricle and localized outward bowing of cranium.

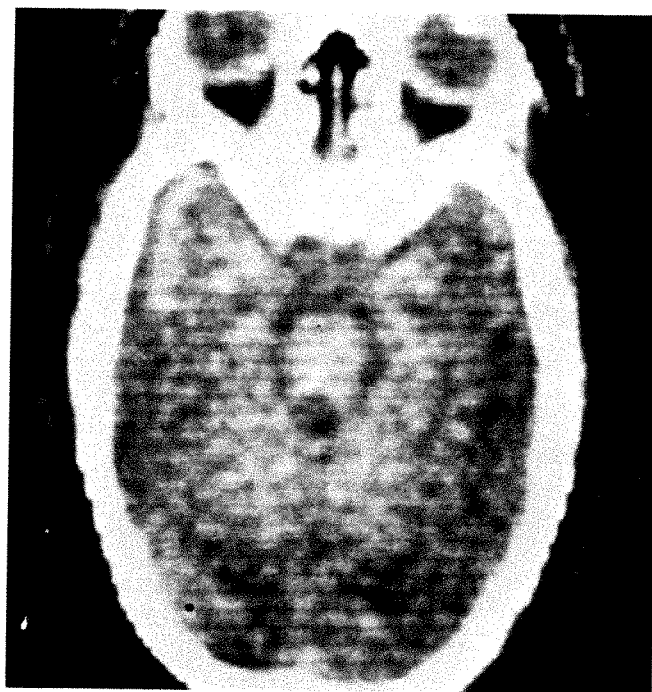


Fig. 4.—Meningitis. 2-month-old female febrile and comatose with bulging fontanel and focal right-sided seizures; diagnosis of *B*-streptococcal meningitis by culture of purulent cerebrospinal fluid. Clinical diagnosis of cortical infarction secondary to vasculitis made and supported by electroencephalogram which showed delta waves consistent with severe brain damage. Radionuclide brain scan showed diffuse peripheral uptake from frontal to occipital regions bilaterally. CT scan shows nonhomogeneous regions of decreased density consistent with infarction present diffusely in cortical areas of temporal lobes and in cerebellar hemispheres. Two months later patient remains in vegetative state.

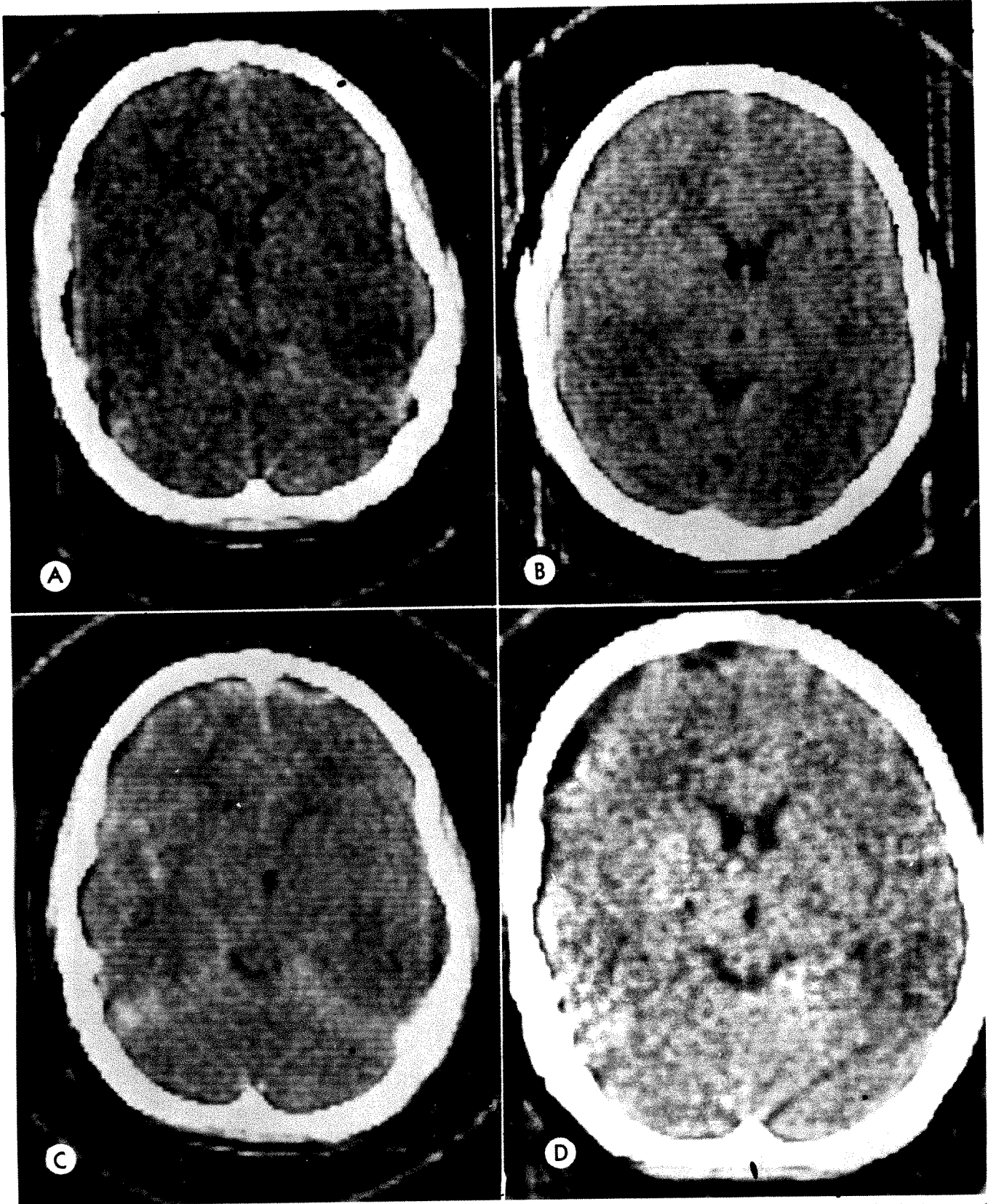


Fig. 5.—Cerebritis. 14-year-old male with diagnosis of frontal sinusitis; transferred to hospital because of lethargy, fever, right-sided focal seizures, and right hemiparesis. *A*, Normal initial scan. *B*, Scan 7 days later showing shift of lateral ventricles from left to right. *C*, Scan after injection of contrast showing multiple scattered areas of enhancement in left frontal and temporal lobes consistent with cerebritis. *D*, Scan 14 days later demonstrating left frontal subdural collection of decreased density.

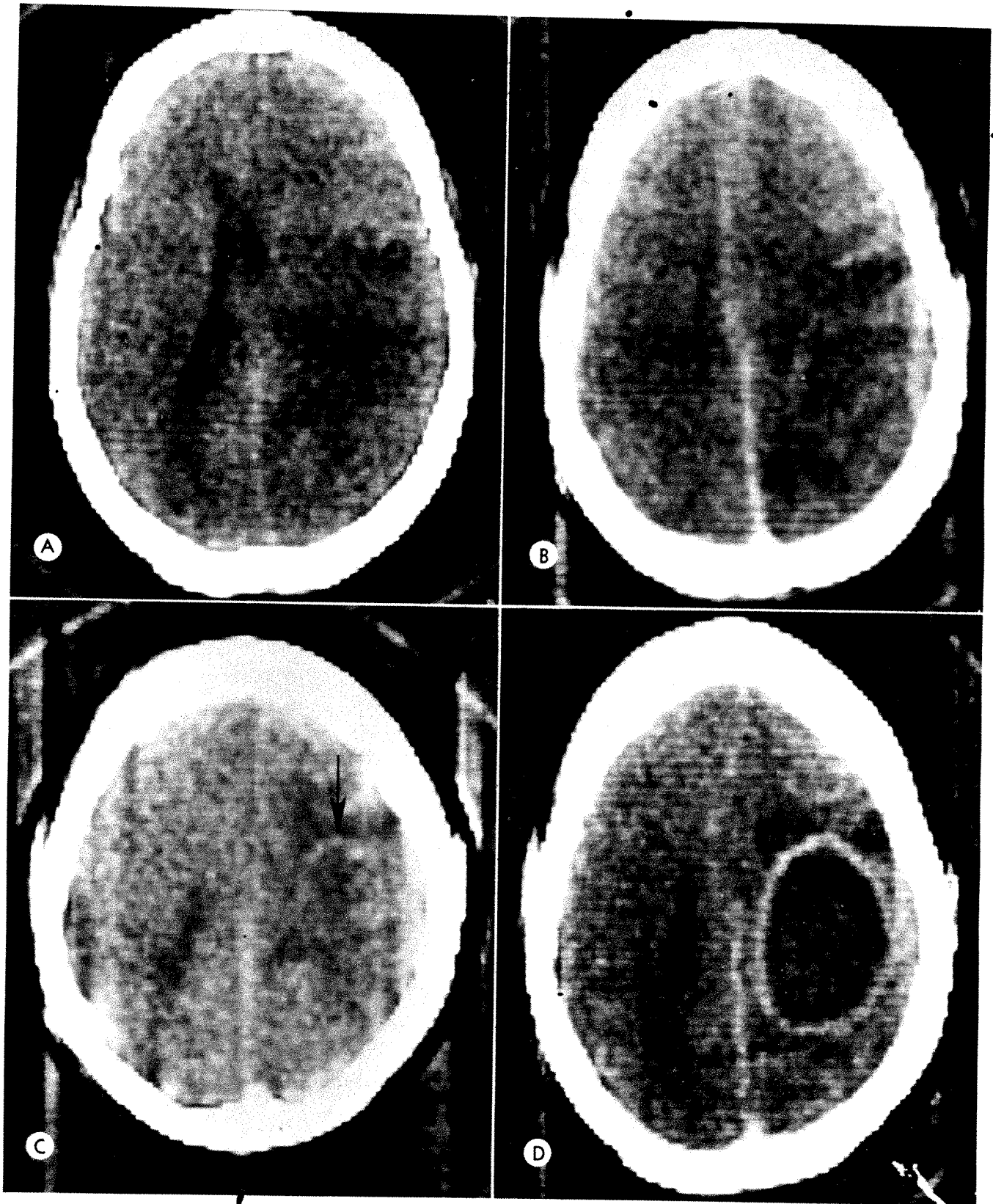


Fig. 6.—Brain abscess in right parietal lobe. 26-year-old female with 2 day history of headaches and left arm paresthesia 2 weeks after upper respiratory infection. A, Precontrast scan showing decreased density in right parietooccipital area with displacement of ventricles and compression of body of right lateral ventricle. B, Postcontrast scan on admission showing enhancement of cortical gyri surrounded by zones of edema. C, Postcontrast scan 11 days after admission showing faint oval rim (arrow) consistent with abscess capsule. D, Postcontrast scan 25 days after admission showing well defined abscess capsule.

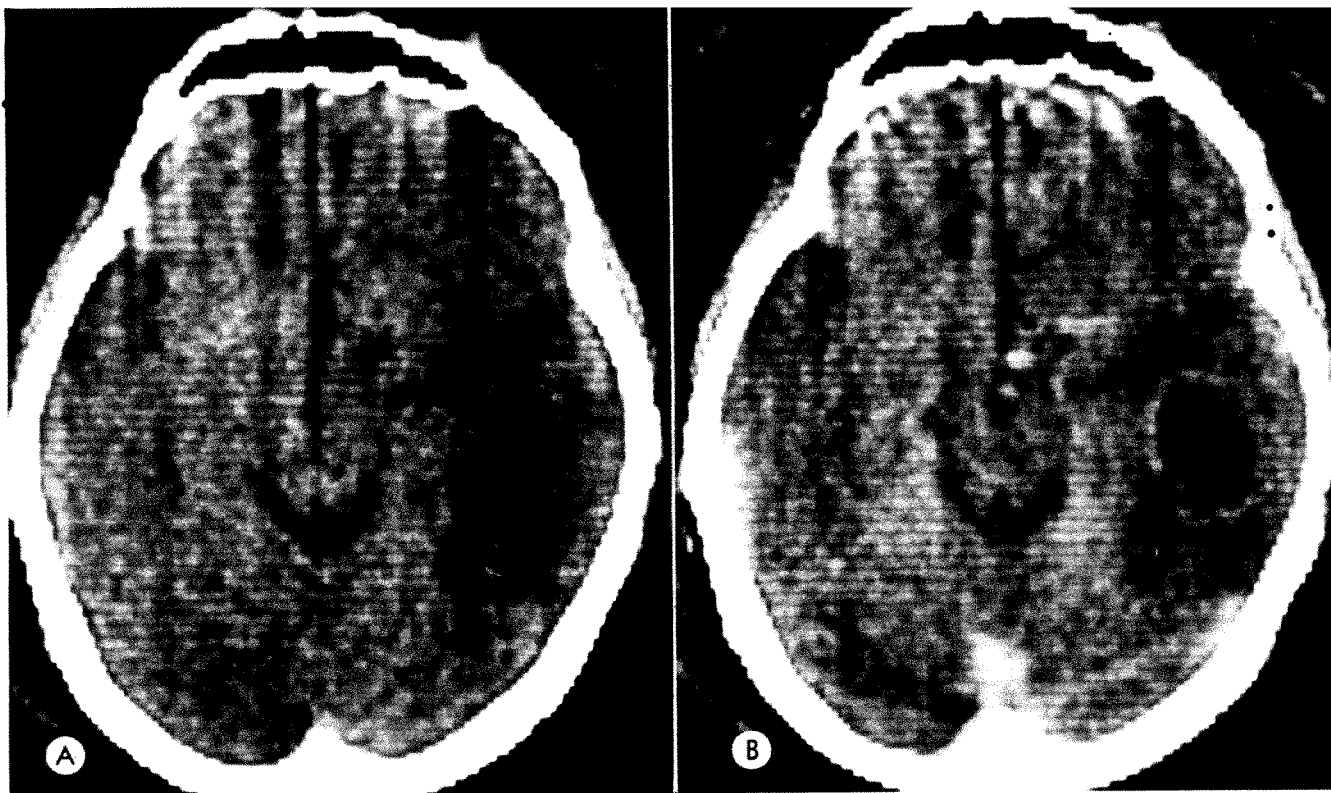


Fig. 7.—Brain abscess in right temporal lobe. 69-year-old male with localized headaches 10 days, memory and speech difficulty 2 days, and low-grade fever on admission. *A*, Scan without contrast showing zone of decreased density within temporal lobe. *B*, Scan with contrast showing enhancement of thin abscess capsule. Area of decreased density surrounding capsule compatible with edema.

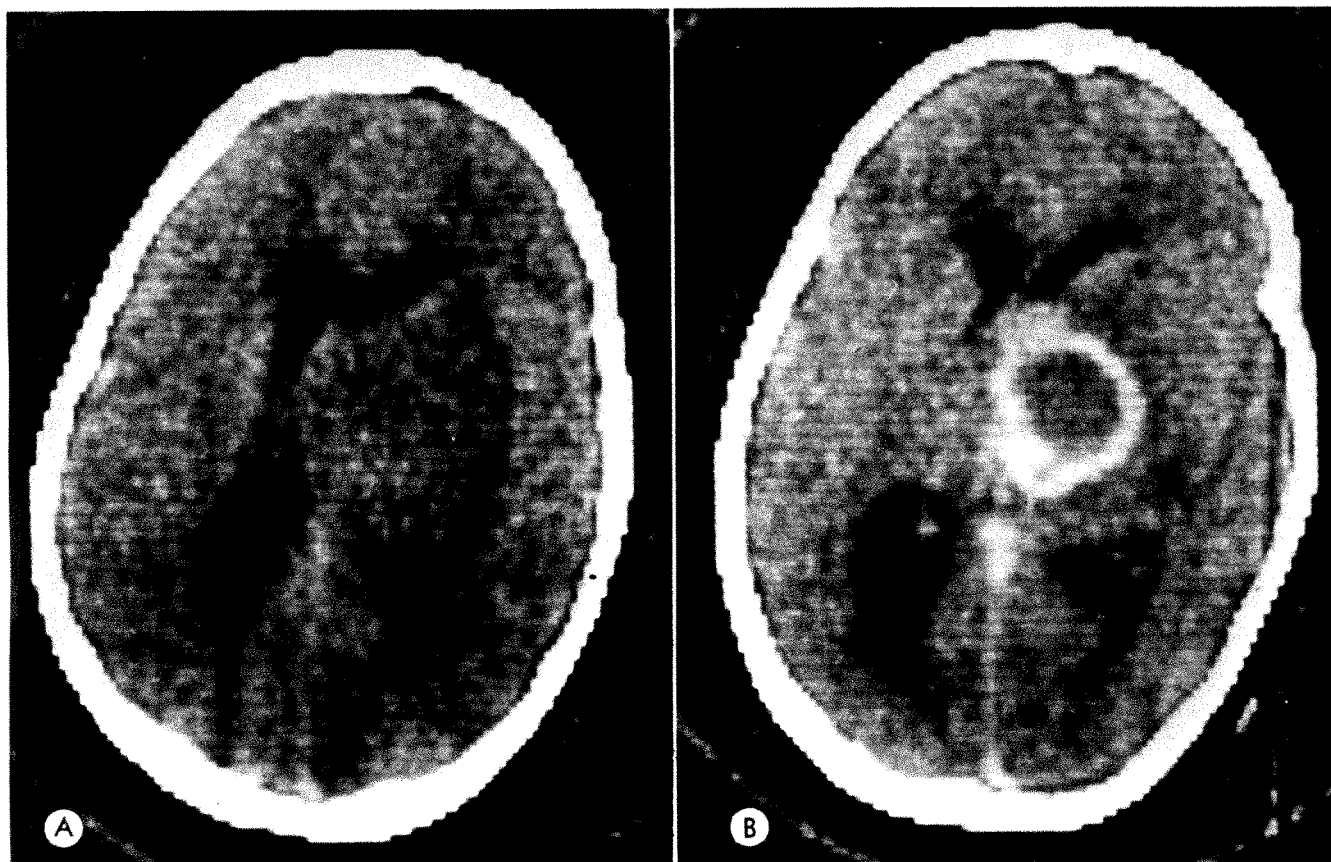


Fig. 8.—Brain abscess in right thalamus. 7-year-old female with tetralogy of Fallot who had Waterston shunt performed during first year of life. Eleven days prior to admission, the patient began to have headaches, fever and increasing cyanosis. She did not respond to antibiotic prescribed and developed left hemiparesis and left homonymous hemianopsia. *A*, Scan at level of lateral ventricles showing large nonhomogenous area of decreased density in right basal ganglionic and thalamic regions; associated mass effect manifested by marked shift of lateral ventricles to left, posterior displacement of right atrium, and obliteration of third ventricle and quadrigeminal plate cistern. *B*, Scan with contrast demonstrating round rim of contrast enhancement consistent with capsule. Because abscess projected into right lateral and third ventricles, surgical drainage was performed immediately.

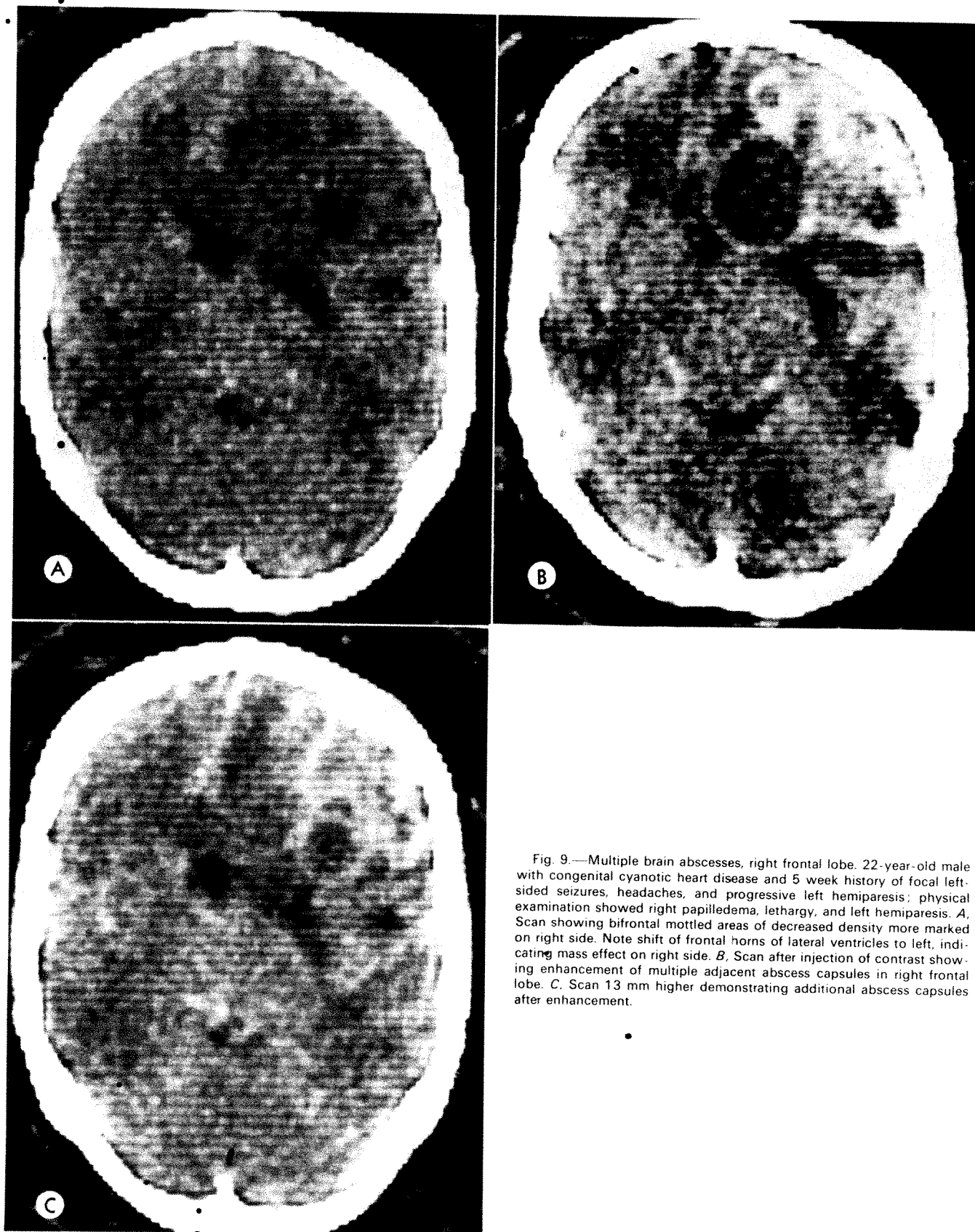


Fig. 9.—Multiple brain abscesses, right frontal lobe. 22-year-old male with congenital cyanotic heart disease and 5 week history of focal left-sided seizures, headaches, and progressive left hemiparesis; physical examination showed right papilledema, lethargy, and left hemiparesis. *A*, Scan showing bifrontal mottled areas of decreased density more marked on right side. Note shift of frontal horns of lateral ventricles to left, indicating mass effect on right side. *B*, Scan after injection of contrast showing enhancement of multiple adjacent abscess capsules in right frontal lobe. *C*, Scan 13 mm higher demonstrating additional abscess capsules after enhancement.

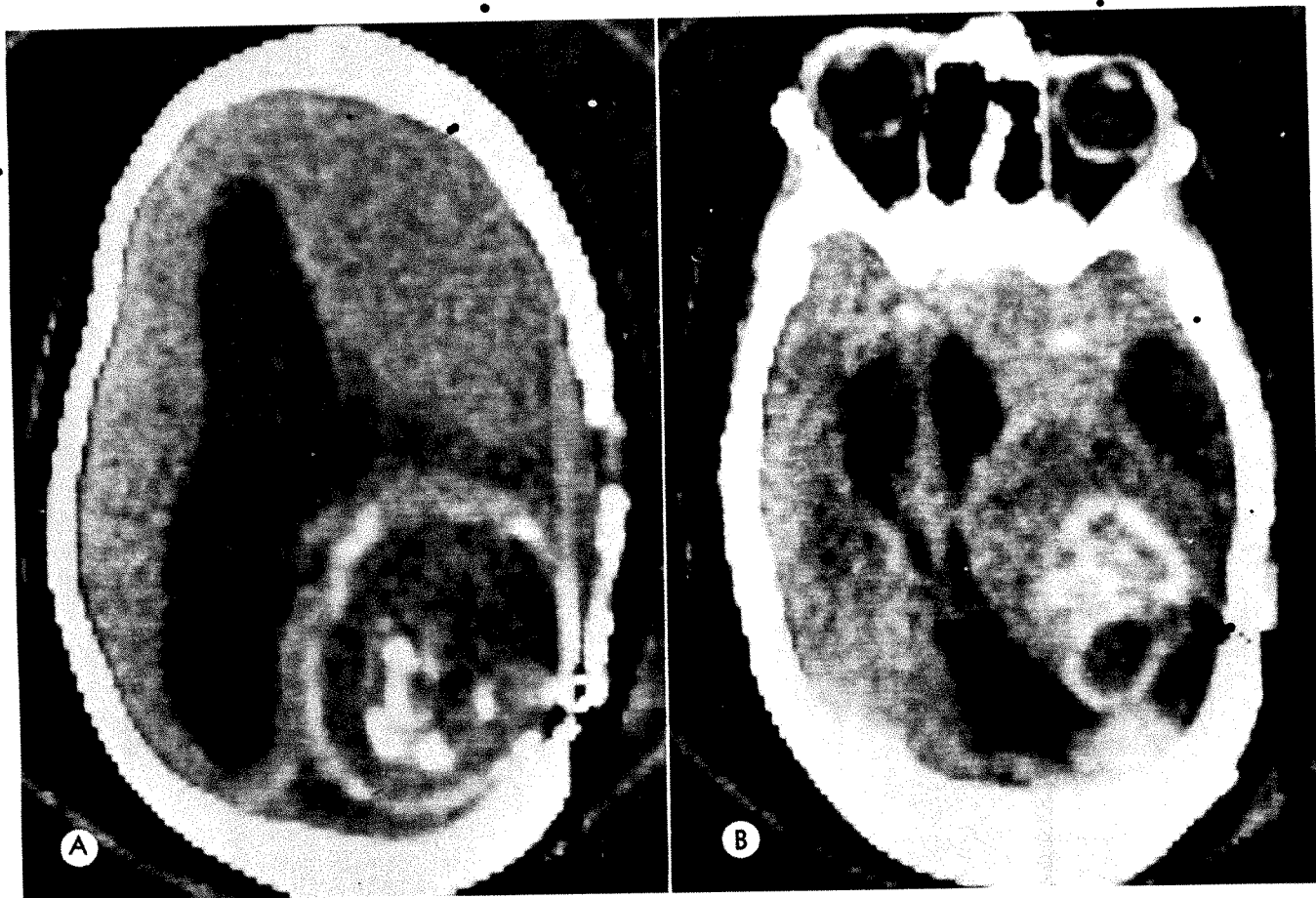


Fig. 10.—Chronic abscess with daughter abscesses. 7-year-old male with repeated infection of shunts for hydrocephalus post meningitis. Right parieto-occipital abscess operated on 1 year ago. Presents now with clinical deterioration. A, CT scan at level of occipital horns showing calcified chronic abscess capsule with calcified debris within it, effaced right lateral ventricle, and markedly dilated left lateral ventricle. Craniotomy site and shunt hardware over abscess capsule. B, Scan after contrast showing multiple enhanced daughter abscesses extending inferiorly and forward into basal ganglionic region.

CT findings were normal. In inadequately treated cases, fulminant cases, and in cases of the sequelae of meningitis, CT helped delineate the disease process. Leptomeningeal inflammation may be associated with sterile subdural effusion [6, 7] (fig. 1). Such effusions may become bacterially infected leading to subdural empyema [8]. Pia-arachnoidal adhesions may cause loculation of cerebrospinal fluid chiefly in the basilar cisterns [9, 10] (fig. 2) but in other locations as well (fig. 3). Communicating hydrocephalus [9, 10] (fig. 1) can result secondary to these adhesions, while obstructive hydrocephalus can result secondary to aqueductal occlusion [11].

Meningitis causes congestion in leptomeningeal capillaries. Increased blood volume, along with slow blood flow in these capillaries, may lead to cortical infarction [6, 9]. Infarction may also occur secondary to vasculitis in these vessels, in which case it may be extensive (fig. 4). Septic thrombosis of cortical veins can be another cause of infarction.

Cerebritis

Neuropathologically, septic cerebritis consists of vascular congestion, petechial hemorrhages, cerebral softening,

and edema [10, 12]. Sequential CT examinations in a case of cerebritis revealed progression of the disease. The initial pre- and postenhancement CT scan was normal (fig. 5A). A subsequent scan showed mottled areas of enhancement associated with a mass effect consistent with cerebritis (figs. 5B and 5C). Finally, when the cerebritis led to meningeal inflammation, the CT scan demonstrated the presence of a subdural collection (fig. 5D).

Cerebral Abscess

The area of cerebral softening in cerebritis may undergo liquefaction, resulting in an abscess. The abscess capsule consists of three layers: the inner granulation tissue, the large middle collagen layer, and the surrounding reactive glial tissue [12]. Formation of the collagen layer is dependent on fibroblasts which are found in vessel walls and meninges but not otherwise within the cerebral tissue [10, 13]. For this reason, abscess capsule formation may be slow. CT scan on a patient with a 4 day clinical course showed cerebritis postenhancement (figs. 6A and 6B). A follow-up CT scan 11 days later suggested the beginning of an abscess capsule (fig. 6C). Subsequent CT scan 25 days after admission demonstrated a well formed abscess

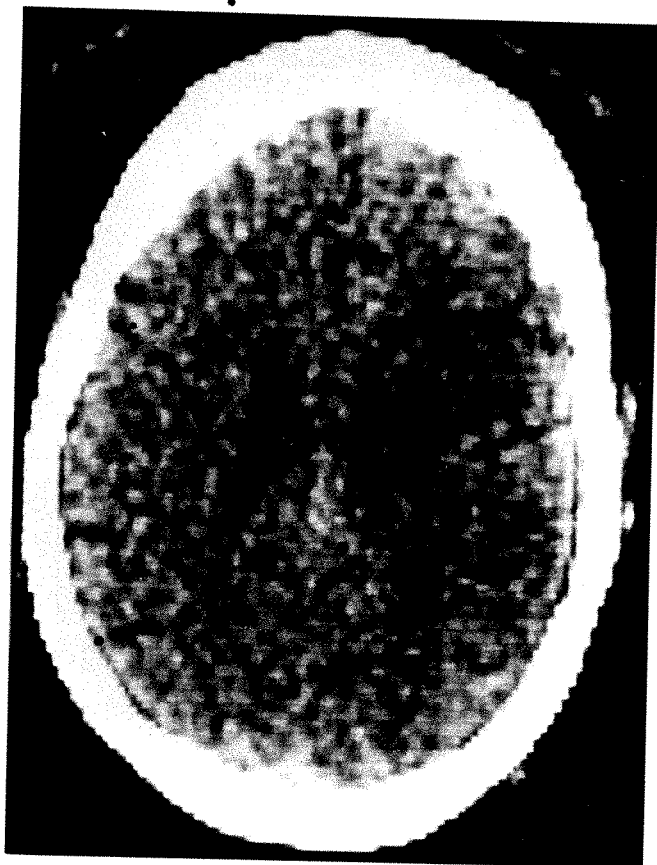


Fig. 11.—Infarction. 30-year-old male juvenile diabetic with sudden onset of left hemiparesis followed by progressive obtundation 30 days after onset of acute staphylococcal endocarditis with aortic insufficiency. Clinical diagnosis of brain abscess based on positive radionuclide brain scan. CT scan shows area of decreased density lateral to right lateral ventricle without mass effect. Subsequent hospital course prior to discharge showed slow improvement in neurological status and negative cultures of cerebrospinal fluid. Follow-up CT and radionuclide brain scans demonstrated infarction.

capsule (fig. 6D). Demonstration of the abscess capsule by CT is important because it indicates to the neurosurgeon when to drain and subsequently when to excise the abscess capsule. There is significant morbidity and mortality when surgery is performed prematurely. Surgical results are considerably better when the abscess capsules are excised [9, 14, 15].

The vascularity of cerebral gray matter is richer than that of white matter. Because abscess capsule collagen formation is related to the availability of blood vessels, capsular formation tends to be slower and weaker on the inner or white matter side [10, 12]. This explains the tendency for abscess to rupture into the ventricular system. The CT scan can show the exact location of the abscess capsule, including its relationship to the ventricles and the degree of formation of its wall within the white matter.

A patient with a temporal lobe abscess (fig. 7) succumbed due to intraventricular rupture before surgical intervention. However, if a child with a thalamic abscess (fig. 8), CT demonstration of the para-third ventricular position of the abscess prompted emergency drainage which resulted in a complete cure.

Slower development of the collagen in the white matter portion of the abscess capsule may lead to formation of daughter abscesses [12, 15]. Detection of all daughter abscesses is of utmost importance. In the case shown in figure 9, the CT scan alerted the neurosurgeon to the presence of seven abscess cavities, which were all drained. The patient recovered completely. Chronic abscesses as well as newly formed daughter abscesses associated with them are also detected (fig. 10).

Hematomas and Infarcts

Septic emboli from bacterial endocarditis may lead to cerebritis (which may result in abscess) and to the formation of mycotic aneurysms [9]. Mycotic aneurysm rupture can produce acutely both intracerebral and subdural hematomas, lesions which for the most part are detectable with CT [2, 5]. Emboli in patients with acute or subacute bacterial endocarditis may not be septic and may produce only bland infarction (fig. 11). In case of infarction, follow-up CT scans can be utilized to detect evolution of septic infarcts into cerebritis or abscess. Infarction secondary to meningitis has been discussed (see above).

Ventriculitis

Chronic bacterial ventriculitis results in ependymitis [9], which leads to hydrocephalus secondary to blockage of the foramen of Monro or cerebral aqueduct or secondary to a meningitis which results from the ventriculitis [11, 16]. Loculation within the ventricular system can occur [11] (fig. 12). Chronic fungal and tuberculous ventriculitis can produce subependymal gliosis which leads to hydrocephalus [11, 16] (fig. 13).

Epidural and Subdural Infection [6, 8, 10]

Epidural abscess is usually due to paranasal or mastoid sinus infection, osteomyelitis of the skull, postcraniotomy infection, or septic phlebitis of emissary veins. The CT scan would be expected to show an extracerebral area of decreased density with a mass effect.

Subdural empyema occurs predominantly over the cerebral convexities and rarely at the skull base. The etiologies are paranasal sinusitis, osteomyelitis of the calvarium, otic infection, postcraniotomy infection, and purulent bacterial meningitis. Again, the CT scan would be expected to show an extracerebral collection of decreased density associated with a mass effect. The mortality rate in subdural empyema has been reported to be 25%–40% [8]. Prompt surgical evacuation achieves good results.

Subgaleal infection is an example of a lesion that can progress to subdural or epidural abscess if prompt surgical treatment is not instituted. Infection of the subgaleal space may be secondary to craniotomy, osteomyelitis, and scalp injury [7, 8]. Figure 14 shows a CT scan of a patient with osteomyelitis of a bone graft after surgical repair of an encephalocele. It demonstrates a soft tissue mass with enhancement, without evidence of intracranial involvement.

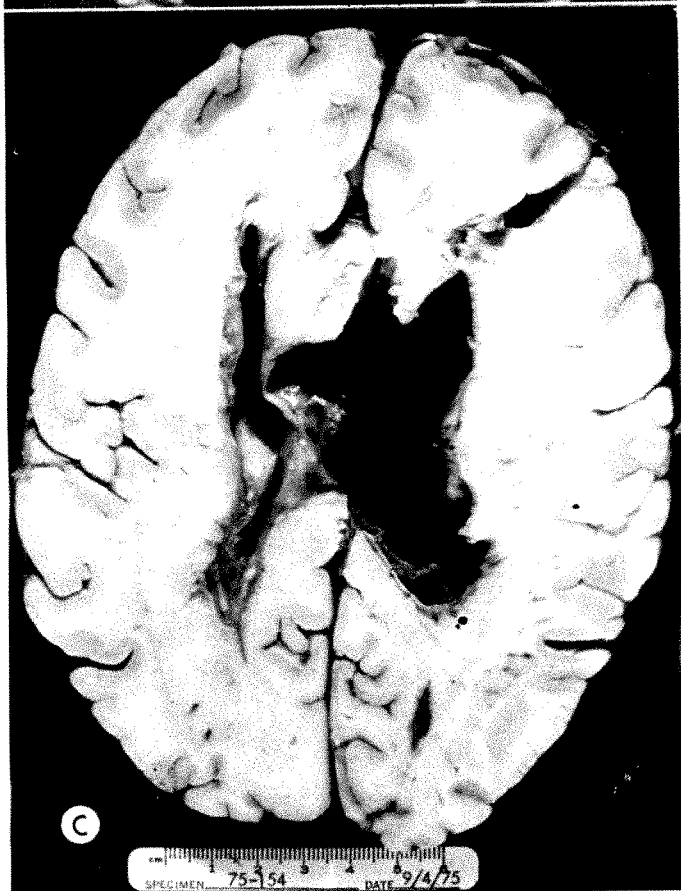
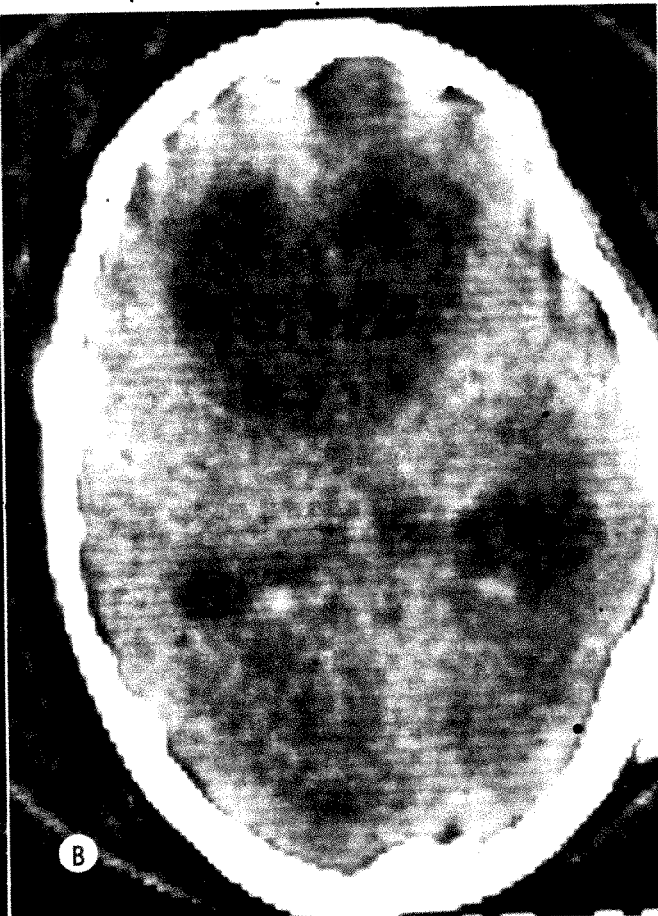
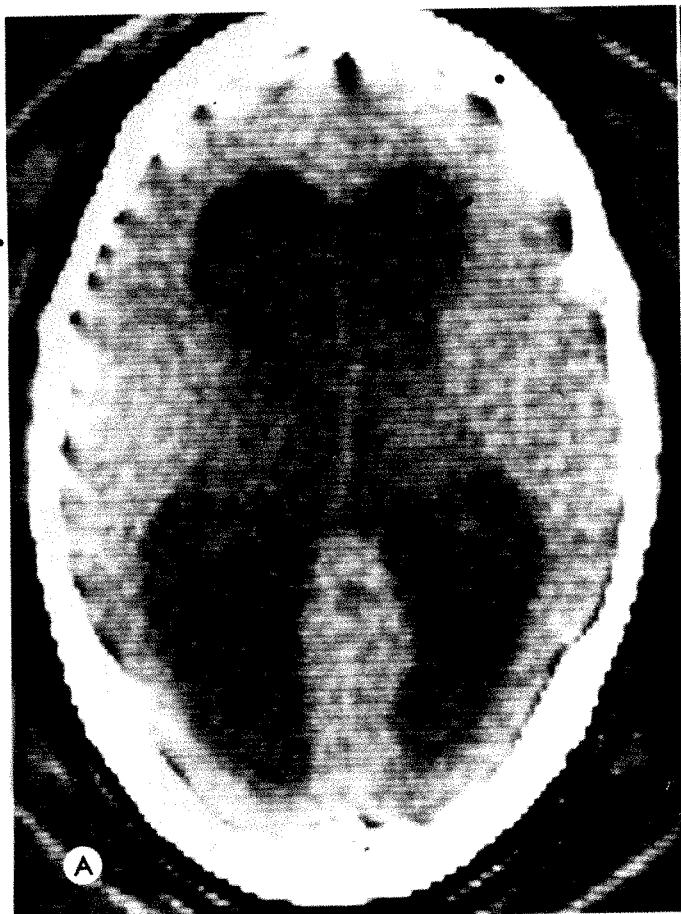


Fig. 12.—Ventriculitis. 30-year-old woman who developed *Staphylococcus coagulase* ventriculitis after shunt procedure for treatment of aqueductal stenosis, followed by *Klebsiella* ventriculitis. Both lateral ventricles were shunted after Conray ventriculogram revealed obstruction of both foramina of Monro. Patient did not respond to therapy and expired. A, CT scan prior to initial shunt procedure revealing marked hydrocephalus. B, Scan after development of infection revealing hydrocephalus and material of higher density than CSF occupying both occipital horns (cf. fig. 12A). At autopsy, this was found to be pus material and necrotic debris. C, Brain section demonstrating location of infection in dependent occipital horns. Note lack of irregularity of occipital horns (cf. fig. 13.) Bacterial infection does not lead to subependymal gliosis.

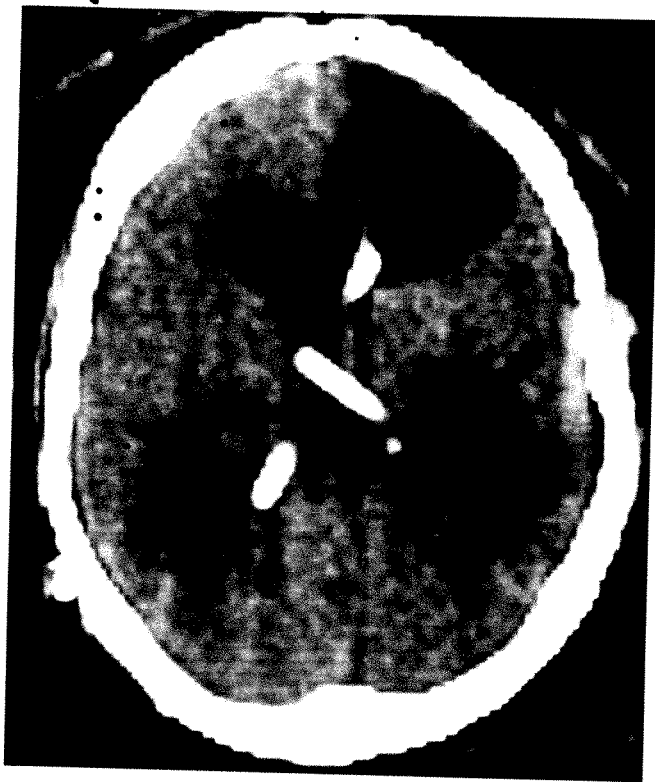


Fig. 13.—Ventriculitis Chronic ventriculitis in 17-year-old male with long history of CNS infections which began with right frontal monilia abscess and meningitis secondary to depressed fracture. Hydrocephalus followed initial infection and was treated with shunts; repeated *Monilia* infections necessitated many shunt revisions. CT shows hydrocephalus and multiple ventricular shunts. Focal dilatation of right frontal horn consistent with porencephaly at site of previous abscess. Marked irregularity of ventricular margins in atria and occipital horns reflects subependymal gliosis characteristic of chronic granulomatous or fungal infection. Right temporal lobectomy performed subsequent to CT scan because of seizures. Subependymal gliosis with adjacent old microabscess found.

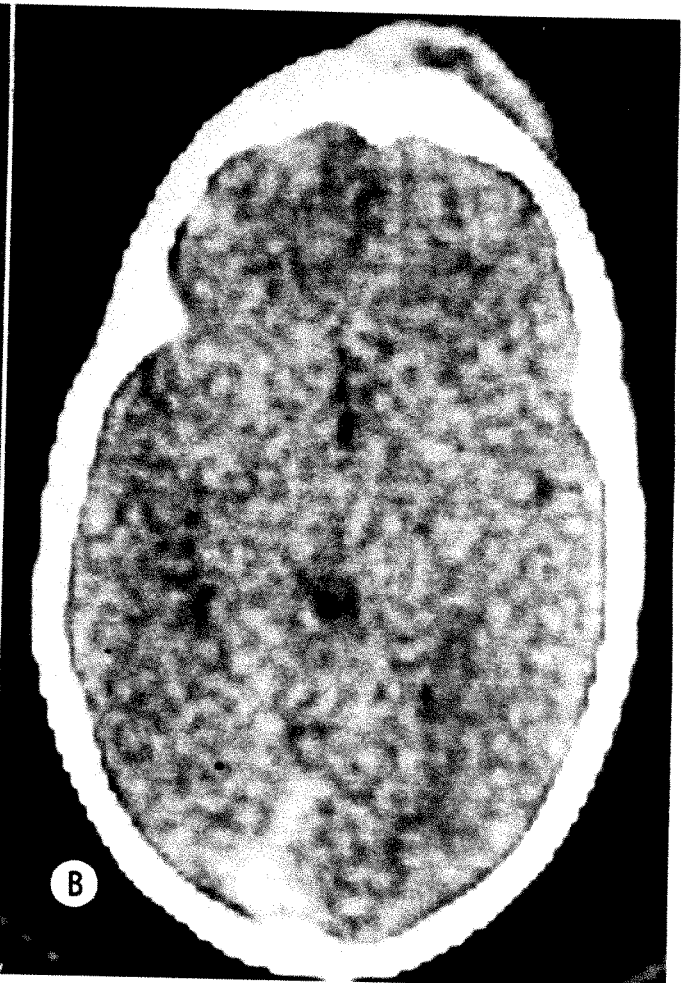
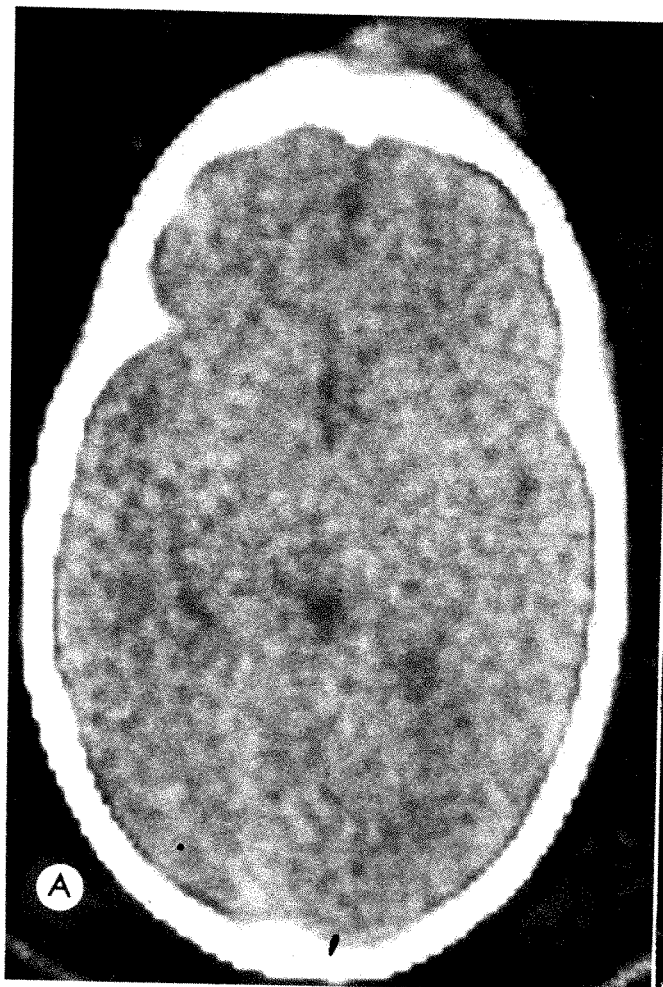


Fig. 14.—Subgaleal abscess secondary to osteomyelitis. 15-month-old boy with history of surgery for nasofrontal encephalocele and nasal glioma during newborn period. Patient developed right frontal fluctuant mass and fever; plain roentgenograms showed lytic area in frontal bone. A, CT scan showing crescentic region of soft tissue density projecting extracranially from right frontal bone. B, Scan after contrast showing enhancement of margin. Subsequently, pus drained from mass and infected bone graft removed.

Discussion

It was hoped that with the advent of antibiotics and advances in neurosurgical techniques, the morbidity and mortality rates from cerebral infection would decrease. However, the success achieved in the treatment and management of noncerebral infection has not been realized for infections of the central nervous system. The mortality rate due to brain abscess alone ranges from 32% to 45% [14, 17-21].

Therapeutic success has been hampered by incorrect diagnosis, failure to detect the disease process early, and incorrect localization of the lesion before or during surgery. Diagnostic tests such as lumbar puncture or pneumoencephalography carry some risk in the presence of increased intracranial pressure [12, 14, 15, 17]. A combination of the cerebral angiogram and radionuclide brain scan has been reported to be accurate in identifying an abnormality in 90% of brain abscesses [14, 17]. However, even these procedures do not indicate the exact nature of the lesion or its stage of evolution [9].

Initial data, while too limited for definitive conclusions, indicate that CT contributes significantly to the diagnosis and management of purulent bacterial central nervous system infections. Cerebritis can be identified, and its resolution to normal or its evolution to abscess can be followed. Exact localization of an abscess is possible, as well as identification of its stage of development and determination of the thickness of its capsule. Also, a mature cerebral abscess can be differentiated from the surrounding edema. The presence of daughter abscesses may be detected and their number determined.

Intracerebral hematomas from mycotic aneurysms, infarctions from bland emboli, and abscess can be differentiated in patients with bacterial endocarditis. In acute meningitis, interhemispheric accumulations of pus may be recognized, as well as the presence of subdural collections and infarction secondary to vasculitis. In follow-up of meningitis cases, hydrocephalus, and loculated CSF collections are easily identified.

REFERENCES

- Ambrose J: Computerized transverse axial scanning (tomography). II. Clinical application. *Br J Radiol* 46:1023-1047, 1973
- Paxton R, Ambrose J: The EMI scanner: a brief review of the first 650 patients. *Br J Radiol* 47:530-565, 1974
- New FJ, Scott WR, Schnur JA, Davis KR, Taveras JM: Computerized axial tomography with the EMI scanner. *Radiology* 110:109-123, 1974
- Baker HL, Campbell JK, Houser OW, Reese DF: Early experience with the EMI scanner for study of the brain. *Radiology* 116:327-333, 1975
- New PF, Scott WR: *Computerized Tomography of the Brain*. Baltimore, Williams & Wilkins, 1975
- Butler IJ, Johnson RT: Central nervous system infections. *Pediatric Clin North Am* 21:649-668, 1974
- Youmans JR: *Neurological Surgery*. Philadelphia, Saunders, 1973
- Galbraith JG, Barr VW: Epidural abscess and subdural empyema. *Adv Neurol* 6:257-267, 1974
- Segall HD, Rumbaugh CL, Bergeron RT, Teal JS, Gwinn JL: Brain and meningeal infections in children. Radiological considerations. *Neuroradiology* 6:8-16, 1973
- Greenfield's Neuropathology*. Baltimore, Williams & Wilkins, 1963
- Salmon JH: Ventriculitis complicating meningitis. *Am J Dis Child* 124:35-40, 1972
- Moore GA, Thomas LM: Infections including abscess, of the brain, spinal cord, intraspinal and intracranial lesions. *Surg Annu* 6:413-437, 1974
- Waggner JD: The pathophysiology of bacterial meningitis and cerebral abscesses: an anatomical interpretation. *Adv Neurol* 6:1-17, 1974
- Beller AJ, Sahar A, Praiss I: Brain abscess: review of 89 cases over a period of 30 years. *J Neurol Neurosurg Psychiatry* 36:757-768, 1973
- Yoshikawa TT: Brain abscess. *West J Med* 121:207-219, 1974
- Leeds NE, Shultz P: The radiographic pattern in ventriculitis. Paper presented at the 10th annual meeting of the American Society of Neuroradiology, Mexico City, February 1972
- French LA, Chous SN: Treatment of brain abscesses. *Adv Neurol* 6:269-275, 1974
- Morgan H, Wood MW, Murphey F: Experience with 88 consecutive cases of brain abscess. *J Neurosurg* 38:698-704, 1973
- Garfield J: Management of supratentorial intracranial abscess: a review of 200 cases. *Br Med J* 2:7-11, 1969
- Kiser J, Kendig JH: Intracranial suppuration. *J Neurosurg* 20:494-511, 1963
- Jooma OV, Pennybacker JB, Tutton GK: Brain abscess: aspiration, drainage, or excision. *J Neurol Neurosurg Psychiatry* 14:308-313, 1951

Stereotaxic Computed Tomography

MATS BERGSTRÖM¹ AND TORGNY GREITZ¹

A method for stereotaxic computed tomography is described. A head fixation system has been devised enabling the exact transfer of information from the diagnostic coordinate system of the scanner to other therapeutic or diagnostic coordinate systems.

Several authors have pointed out the potential of using CT to plan examinations such as biopsies [1] as well as types of treatment such as dose planning in radiotherapy [2]. An accurate fixation device is the necessary link connecting CT with other diagnostic and therapeutic procedures. We are now developing a fixation system flexible enough to fit various types of examinations and treatment which require accurate localization of the lesion. The prototype described has yielded good results in transferring information obtained at CT investigation to the planning of radiosurgical treatment [3, 4] and conventional neurosurgery.

Method

Diagnostic and Therapeutic Coordinate Systems

A diagnostic coordinate system is attached to the scanner in such a way that the position of each element in the tomographic picture is defined by a set of coordinates (x, y, z). This coordinate system has a fixed relationship to the opening of the scanner, and consequently any point in the tomographic picture may be related to it. The patient's head is held in a fixed relationship to the coordinate system by a fixation device that immobilizes him in a given position in relation to the opening of the scanner.

A therapeutic coordinate system is attached in an analogous manner to the therapeutic device so that any target point is defined by a set of coordinates (x', y', z'). By connecting the fixation device used for the diagnosis to the therapy unit in a well-defined manner, the coordinates of the diagnostic system may be transferred to the therapeutic system. An anatomical detail with coordinates (x, y, z) is chosen as target point and will have the coordinates (x', y', z') which are given by a simple calculation (fig. 1). Hence the target point will be precisely defined in both coordinate systems without any reference to anatomical structures.

Fixation Device

A modified version has been developed of a fixation device used for radiosurgery at Karolinska Sjukhuset (L. Leksell, B. Jernberg, and G. Hammarström, personal communication, 1975). A piece of thermoplast (Kerr®) is shaped to fit the root of the nose. A band of another type of thermoplast (Orthoplast®) is firmly applied around the patient's head. Notches are made to leave the eyes free. The plastic

material usually becomes rigid within 10 min and the patient is then placed in a simulated EMI scanner, the position and angulation of the head being adjusted (fig. 2A). The orthoplast bandage is fixed using aluminium hooks onto a ring which may be applied to the front of the scanner (fig. 2B). The patient walks over to the scanner with the orthoplast bandage and the ring attached to the head (fig. 2C) and is placed in position in such a manner that the holes in the ring are guided into the holds (fig. 2D). The entire procedure takes about 30 min. After the scan, the patient is transferred with the fixation device still on the head and is attached to another diagnostic device or therapy unit (fig. 3). The orthoplast bandage can be cut through and stored for future use.

Use of Scanner to Localize Target Point

The coordinates of the chosen target point in the plane of the image may be determined from the printout. A faster approach is to use the polaroid picture. The length A of the picture matrix across the picture and the distance a from the target point to the edge of the matrix are measured. The coordinate is calculated from $x = a \times 160/A$ (fig. 4). Using this procedure the influence of variations in picture size due to inconstancy of the oscilloscope is eliminated. A check of this coordinate is later made by computer (see below). The vertical coordinate is determined from the picture achieved by reconstruction of an orthogonal plane using densely applied, partly overlapping cuts [5, 6] (fig. 5). The vertical coordinate is defined by the cut intersecting the target point and may be expressed as a given measurement on a vernier scale mounted between the scanner gantry and its

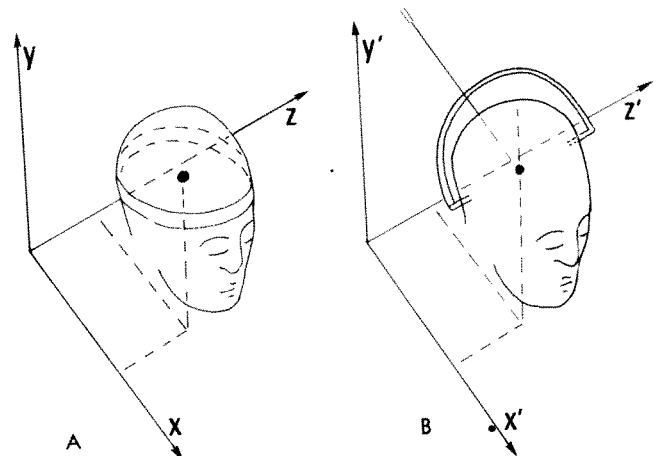


Fig. 1.—Information transfer from diagnostic coordinate system (A) to therapeutic coordinate system (B). Tomographic cut (indicated by ellipse) defines vertical coordinate.

Received February 27, 1976.

This work was supported by a grant from the research funds of the Karolinska Institutet.

¹ Department of Neuroradiology, Karolinska Sjukhuset, S-104 01 Stockholm, Sweden.

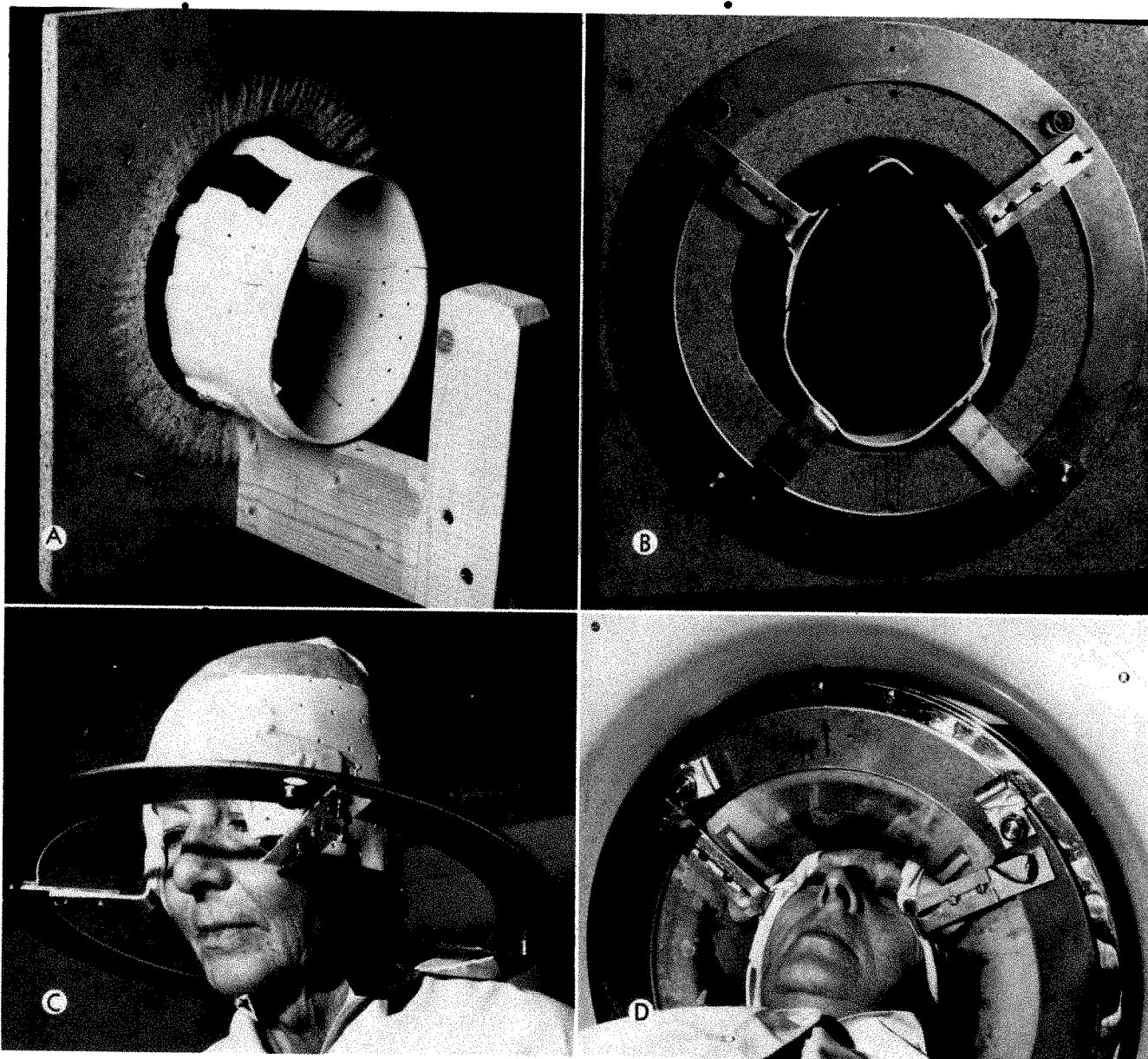


Fig. 2.—A, Simulated scanner opening and water box. B, Plastic bandage fixed by adjustable aluminium hooks to metal ring fitting scanner opening. C, Fixation of helmet to ring. D, Patient attached to scanner opening. Since in this case fixation of helmet was improved by inserting screws into calvarium, no plastic mold over nose root was needed.

water box and used for accurate determination of the tomographic cuts.

Delineation of Target Area

To check the coordinates of the target area obtained by tomography, they are fed into the computer which plots them back into the picture. The geometry of the gamma lesion is well anticipated in radiosurgical procedures. With the aid of the computer a 50% isodose curve can be plotted into the picture, roughly indicated as an ellipse or a circle [6] (fig. 6). Because the size of the picture element is 1.5×1.5 mm, no precise isodose curve can be plotted at present. However, by using a magnified EMI picture (e.g., with the aid of a television system) and by placing trans-

parencies with isodose curves over the monitor, a crude appreciation of the dose distribution can be obtained. When checking the target area, a simultaneous calculation of the coordinates of the therapeutic system is automatically made by computer.

Discussion

A fixation device for stereotaxic CT scanning should meet the following criteria: (1) be efficient enough to cause a significant decrease in the occurrence of artifacts due to patient movement; (2) allow reproducible positioning during procedures of long duration; (3) enable constant positional relationship of the patient (target) to various interrelated diagnostic and therapeutic devices and allow a simple and accurate transformation of coordinates be-

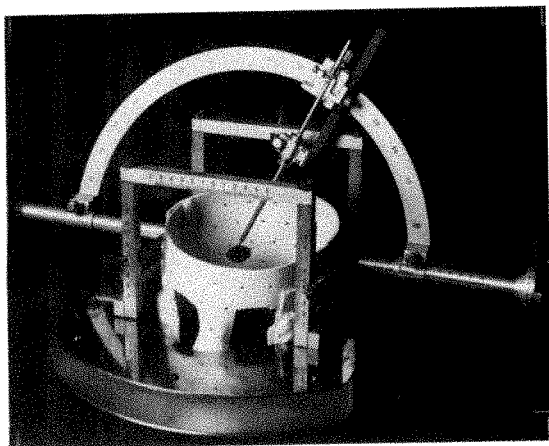


Fig. 3.—Procedure for attaching Leksell stereotaxic instrument to fixation device. Coordinates of target point obtained at CT scanning are directly transferred to this system without reference to anatomical landmarks.

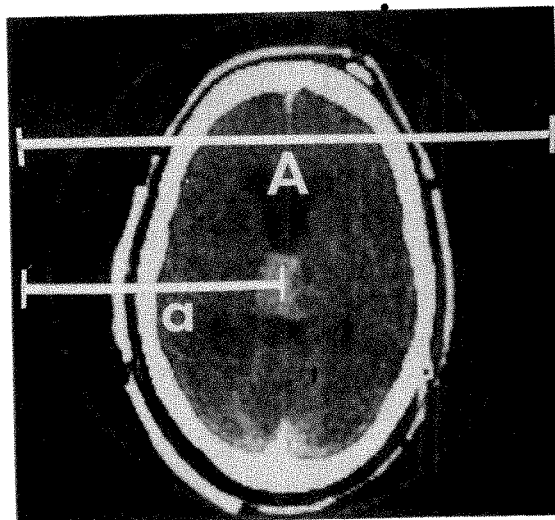


Fig. 4.—Determination of horizontal coordinate. Distance in number of matrix elements from edge = $a \times 160/A$.

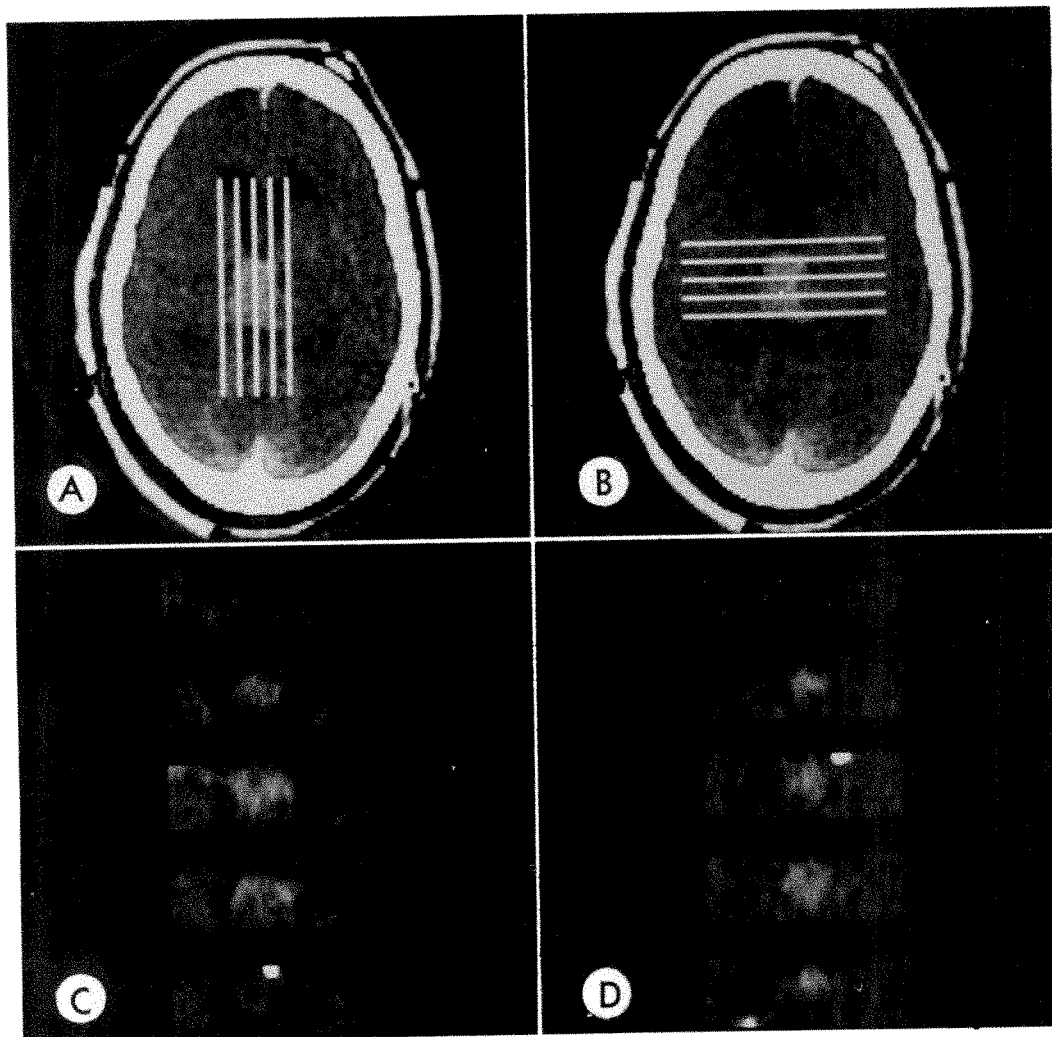


Fig. 5.—Determination of vertical coordinate using reconstruction pictures in lateral and frontal planes. *A and B*, Reconstruction planes. *C and D*, Corresponding results, *C*=lateral projections, *D*=frontal projections. Size and extension of pinealoma is clearly visible. Small white spots in *C* (bottom) and *D* (middle) represent tip of shunt catheter, not seen in planes of *A and B*.

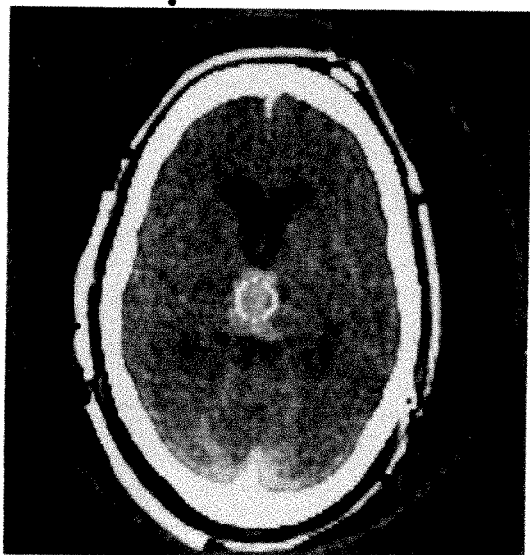


Fig. 6.—Pinealoma. Target point and rough estimation of 50% isodose curve plotted into picture by computer.

tween these systems; and (4) give an acceptable reproducibility of positioning for examinations at different times.

The methods of fixation and transformation of coordinates presented have been used in a limited number of patients. The results are promising and indicate that the fixation obtained in many respects meets the requirements listed above. Accordingly, EMI pictures of improved quality have been obtained due to the decrease in patient movement. It has been possible to pursue time-consuming procedures with good reproducibility of the tomographic cuts. Some improvement in the method is necessary since vertical movement of the head was observed in repeat examinations. The mean vertical movement was 3 mm but in one case was 13 mm. Work is now in progress to considerably reduce this error.

The fixation of the plastic bandage may be improved by inserting two or three metal screws into the calvarium, the plastic being molded around the screws. If these measures

are taken, the error in transforming the coordinates from the diagnostic to the therapeutic coordinate system is considerably reduced. In experimental models, tumors have been punctured with a standard deviation from the target point of 1.1 mm. Movement between the plastic helmet and the skull was not taken into account in these studies. Also the center of the tumor model was determined more accurately by plotting attenuation profiles which allowed a target point to be chosen between the centers of adjacent elements.

For many purposes the fixation requirements are not this exacting. The plastic helmet may then be applied without screws, becoming a simple procedure which requires no preparation of the patient and can be done outside the scanning room. This less elaborate fixation method has been used in CT examinations of about 50 patients.

Three patients have been treated with radiosurgery based on information obtained from stereotaxic CT using the principles described here. The results will be published [7].

REFERENCES

1. Alfidi RJ, Haaga J, Meaney TF, MacIntyre WJ, Gonzalez L, Tarar R, Zelch MG, Boller M, Cook SA, Jelden G: Computed tomography of the thorax and abdomen; a preliminary report. *Radiology* 117:257-264, 1975
2. Chernak ES, Rodriguez-Antunez A, Jelden GL, Dhaliwal RS, Lavik PS: The use of computed tomography for radiation therapy treatment planning. *Radiology* 117:613-614, 1975
3. Leksell L: The stereotaxic method and radiosurgery of the brain. *Acta Chir Scand* 102:316-319, 1951
4. Leksell L: A note on the treatment of acoustic tumours. *Acta Chir Scand* 137:763-765, 1971
5. Glenn WV, Taveras JM, Johnston BJ, Morton PW, Dwyer SJ: Clinical feasibility of reconstructing coronal, sagittal and thin transverse sections from overlapped 8.0 mm CT scans. Paper presented at the workshop on Reconstruction Tomography in Diagnostic Radiology and Nuclear Medicine, San Juan, Puerto Rico, 1975
6. Bergström M, Sundman R: Picture processing in computed tomography. *Am J Roentgenol* 127:17-21, 1976
7. Norén G, Backlund EO, Bergström M, Greitz T: Radiosurgery of acoustic neuromas using stereotaxic computerized tomography. Submitted for publication

Computed Tomography and Radionuclide Studies in the Diagnosis of Intracranial Disease

JAMES H. CHRISTIE,¹ HIROFUMI MORI, RAYMUNDO T. GO, STEVEN H. CORNELL,
AND ROLF L. SCHAPIRO

The accuracy of CT and radionuclide studies in the diagnosis of intracranial disease is analyzed based on experience in 641 patients. Results indicate that both modalities give reasonably similar precision and that a modest improvement in diagnosis can be expected if both techniques are employed. It is emphasized that the radionuclide studies used routinely included what are rightfully considered adjunctive scanning procedures, so that results must be considered in this light.

Computed tomography (CT) introduced by Hounsfield [1] and initially reported by Ambrose [2] in 1973 has rapidly achieved widespread acclaim in the diagnosis of intracranial disease. At first glance, it appears to provide in a noninvasive manner information comparable to that previously obtained by the combination of radionuclide brain scans, angiography, and pneumoencephalography. While CT is certain to have an effect on the utilization of all neuro-radiologic techniques, the unique anatomic information it provides threatens to replace the radionuclide brain scan in its traditional role as the screening test for suspected intracranial disease.

The purpose of this report is to compare our initial experience in CT with radionuclide scintigraphy and to attempt to assess the usefulness and limitations of each technique.

Subjects and Methods

Between November 1973 and April 1975, relatively concurrent CT and radionuclide studies were performed on 657 patients. Time intervals between the two examinations varied from 1 week in patients with trauma, suspected brain abscess, or cerebrovascular disease; 2 weeks in patients with other discrete intracranial lesions; to 3 weeks in patients in whom discrete pathologic lesions were ultimately not established.

The radionuclide studies were all made on a Nuclear Chicago Pho-gamma III camera utilizing ^{99m}Tc pertechnetate after a blocking dose of 400 mg of potassium perchlorate. Adult doses were in the range of 20–25 mCi, with proportionately smaller doses for children. Anterior dynamic images as well as four-view static images at 10 min and 2 hr after injection were routinely obtained. Commonly 3 or 4 hr delayed and/or posterior stereoscopic images were obtained to clarify equivocal earlier findings or to confirm earlier normal studies on patients who were strongly suspected of harboring intracranial disease.

The CT technique used (EMI) is essentially as described elsewhere [3, 4]. Image enhancement by the injection of contrast material initially was used sparingly but increased to approximately 20% of examinations by July 1975. Contrast material was only given after review of the initial nonenhanced CT images. During the first 12 months, CT images were displayed on an 80×80 matrix system and thereafter by a 160×160 matrix system.

It is important to emphasize that during the time interval of this

comparison only 25% of patients with initial radionuclide studies had subsequent CT studies; conversely, 40% of patients with initial CT studies had subsequent radionuclide studies. The reasons for this selectivity are varied, including frequent malfunctions initially of the EMI scanner which necessitated a return to the traditional diagnostic approach to intracranial disease. During the early months of this study, patients with positive findings demonstrated by either technique often had the other examination for the sake of comparison. Later, patients with negative or equivocal results on either technique frequently had the other examination to satisfy a high index of clinical suspicion. It should also be emphasized that because of the function of this referral center, patient selectivity is quite high. To a large degree, this selectivity accounts for the number of patients with neoplasms compared to those with cerebrovascular disease; the latter are not referred to us except in unusual circumstances.

Sixteen patients were excluded from the study because 15 CT images and one radionuclide image were technically unsatisfactory. In the remaining 641 patients, radionuclide and CT studies were reviewed as well as patient charts.

In the early months of this study, there were 71 patients in whom one study was initially considered positive while the other was negative, and 24 patients in whom one of the studies (primarily CT) was considered equivocal. All of these studies were retrospectively reviewed independently without clinical information by four radiologists. Increased experience in CT interpretation resolved this disagreement in 54 patients. In the remaining 38 patients, disagreement remained. In all patients, the final diagnosis was confirmed by surgery, autopsy, angiography, pneumoencephalography, or the subsequent clinical course. Equivocal CT studies on three patients (one ultimately proved to have disease, two proved normal) are considered one false negative and two false positive in this analysis. To date, disease cannot be established in six patients with contradictory results by the two techniques. Therefore, positive radionuclide scans on three of these patients and positive CT scans on the other three patients are considered false positives in this analysis.

Of the 641 patients, 135 were diagnosed by the CT study as having hydrocephalus, porencephaly, cerebral atrophies, benign cysts, or developmental abnormalities such as agenesis of the corpus callosum. Since these conditions cannot be diagnosed by the radionuclide study, they were excluded in the calculation of percentages. Similarly, we have excluded diagnoses of reduced carotid flow in patients without clinical manifestations of cerebrovascular occlusive disease. These exclusions are not intended to minimize the importance of these findings but rather to permit a reasonable comparison of the two techniques.

Results

Among the 641 patients, 114 had intracranial tumors (table 1). A breakdown of the lesions which were false negative by one or both techniques is shown in table 2.

The results in 86 patients with nonneoplastic disease are

Received March 15, 1976.

¹ All authors: Department of Radiology, University of Iowa Hospitals and Clinics, Iowa City, Iowa 52242. Address reprint requests to J. H. Christie.

TABLE 1
Neoplastic Disease

Location	No. Cases	CT + RN +	CT - * RN - *	CT - * RN +	CT + RN - *	Total		
						CT +	RN +	% +
Supratentorial	79	68	5	3	3	71	71	94
Base of brain †	11	5	3	1	2	7	6	73
Posterior fossa	24	17	4	1	2	19	18	83
Total	114	90 (79)	12 (11)	5 (4)	7 (6)	97 (85)	95 (83)	89

Note.—Numbers in parentheses are percentages. RN=radionuclide study.

* False negative.

† Supratentorial though in juxtaposition to bony structures at base of skull.

TABLE 2
Analysis of False Negative Examinations

Examination	No.
False negative CT and RN:	
Supratentorial:	
Microglioma of corpus callosum (autopsy)	1
3 mm parasagittal meningioma, right frontal (autopsy)	1
Metastatic tumor, breast (clinical diagnosis not confirmed)	2
Frontal parietal mass (diagnosis: malignant by angiography)	1
Supratentorial, base of skull:	
Pituitary adenoma	2
Craniopharyngioma	1
Posterior Fossa:	
Brain stem glioma	3
Metastatic tumor, cerebellopontine angle	1
Total	12
False negative CT, positive RN:	
Supratentorial:	
Metastatic tumor	1
Primary tumors (diagnosed malignant by angiography)	2
Supratentorial, base of skull (sphenoid wing meningioma using image enhancement)	1
Posterior fossa (malignant cerebellar glioma)	1
Total	5
Positive CT, false negative RN:	
Supratentorial:	
Low grade glioma	2
Focal proliferation of leukemic cells	1
Supratentorial, base of skull:	
Pituitary adenoma	1
Craniopharyngioma	1
Posterior fossa:	
Brain stem glioma	1
Cerebellar medulloblastoma	1
Total	7

shown in table 3. The patients with occlusive cerebrovascular disease have been categorized according to the time between onset of clinical symptoms and examination.

Discussion

CT failed to detect 17 of the 114 neoplasms; that is, 15% of the CT scans yielded false negative results. Four of these failures occurred early in our experience and probably could have been avoided by the use of image enhancement with circulating contrast material. Two of the missed lesions were found incidentally at necropsy and proved to be of a size rendering detection unlikely. Pituitary adenomas which are in most instances readily detected on plain skull radiographs are difficult to diagnose by both CT and radionuclide techniques; diagnosis by the scintiscan is especially hampered by the normal background activity at the base of the calvarium. Posterior fossa neoplasms that have always proved difficult to demonstrate on radionuclide studies have also been difficult to diagnose on CT studies [2, 5].

Notwithstanding these observations, our results indicate a 90% detection probability with each technique individually or a 95% probability for both examinations combined, provided lesions confined to the brain stem are excluded. The present state of the art does not permit demonstration of brain stem lesions by scintigraphy unless the tumor extends beyond the normal confines of the brain stem [6]. A greater potential for detection of brain stem lesions has been anticipated for the CT technique [7] but must await further confirmation. Finally, the diagnosis of neoplasm is rendered more likely if both the radionuclide and CT techniques are utilized; this view is currently held for supratentorial lesions, including those near the base of the brain, as well as for infratentorial lesions. However, the improvement in detection is moderate at best.

While others have reported that CT studies are more efficient than radionuclide studies in following postoperative cases [8, 9], in our limited comparison all six recurrent tumors were detected utilizing both techniques. In one case, interpretation of the CT study was handicapped by artifacts produced by a metallic shunt in the same plane. Recently, Leonard et al. [10] have reemphasized the ability to differentiate on postoperative radionuclide images between surgical changes and recurrent tumor in 21 of 30 patients; in eight of the remaining nine cases, the presence or absence

TABLE 3
Nonneoplastic Disease

Type	No. Cases	CT + RN +	CT - * RN - *	CT - * RN +	CT + RN - *	Total		
						RN +	CT +	% +
Vascular occlusive disease:†								
<1 week	10	4	2	1	3	5	7	80
1-4 weeks	27	14	5	8	...	22	14	81
4-8 weeks	5	2	2	1	...	3	2	60
>8 weeks	10	2	6	0	2	2	4	40
Brain hemorrhage	13	7	0	0	6	7	13	100
Arteriovenous malformation	3	2	0	1‡	0	3	2	100
Large aneurysm	2	1	0	0	1	1	2	100
Subdural hematoma	9	7	0	1	1	8	8	100
Cerebral contusion	2	0	0	1	1	1	1	100
Cerebral abscess	5	5	0	0	0	5	5	100
Total	86	44	15	13	14	57	58	83

* False negative.

† Categorized according to time between onset of clinical symptoms and examination.

‡ No image enhancement with contrast material.

of tumor could be determined by subsequent repeat studies. In those instances where metallic clips or shunt valves produce CT images of poor quality [8, 9], it is reasonable to believe that radionuclide studies will continue to be useful.

Our comparative results in cerebrovascular occlusive disease are essentially as expected. Since the majority of our patients were referred because of atypical or unusual clinical manifestations, the lack of histologic proof in most cases renders an analysis presumptive at best. Our results support previous reports [11] indicating that static radionuclide images tend to be normal in the first week after onset of symptoms, become grossly abnormal 1-3 weeks later, and return to normal in most cases after 8 weeks. Our data also conform to those of Paxton and Ambrose [5] who found CT studies 100% accurate in diagnosis during the first 7 days, while positive findings decrease progressively to about 50% or less of cases 1 to 3 weeks thereafter.

CT studies are clearly superior to the radionuclide technique in cerebral, cerebellar, or intraventricular hemorrhage. In our series as well as in those reported by others [5, 12, 13], the diagnosis of hemorrhage within the brain has been 100% accurate. While positive radionuclide images in brain hemorrhage have been reported by many investigators, considerable disagreement persists as to the ultimate value of scintiscans in this regard [14-16].

The detection of arteriovenous malformations by dynamic radionuclide studies is well established. While these lesions are readily identified in CT images after enhancement with contrast material, our results and those of Pressman et al. [17] suggest that the nonehanced CT study for the unsuspected arteriovenous malformation is not as sensitive as desirable.

Our results pertaining to the evaluation of acute and chronic head trauma are similar to those described elsewhere [1, 7, 18-20]. In acute subdural or epidural hematomas, CT is specific, while the radionuclide technique oc-

asionally may be useful provided dynamic studies are performed. In chronic subdural hematoma, both techniques are useful and were found to be complementary in the present series.

The few brain abscesses in our series were readily detected by both techniques, although one could only be demonstrated by CT after image enhancement with contrast material. Davis et al. [21] have suggested that the radionuclide study may be more sensitive in early abscess formation.

A word of caution seems appropriate in using these data to evaluate the relative efficiency of scintigraphy and CT as screening procedures for brain disorders. Because of our longstanding interest in nuclear brain imaging and because of the extensive preselection of patients referred for brain imaging in this tertiary referral center, the "routine" nuclear scan as performed in this department cannot realistically be viewed as a screening procedure. Virtually every brain scan includes what are rightfully considered adjunctive scanning procedures such as dynamic images, immediate static scans, and, commonly, sequential scans and delayed scans as deemed necessary during the progress of the continually monitored examination. In the usual clinical setting, this inclusive examination routine may be impractical and difficult to justify in terms of present day medical economic realities.

These considerations suggest that the sensitivity and accuracy attributed to the nuclear study in the present series cannot always be extended to the screening radionuclide study which traditionally includes only static images obtained at a single fixed time interval 1-2 hr after injection of the nuclide. In an earlier communication [22], we presented data showing that adjunctive scanning procedures on 108 selected patients made possible the delineation of 40 lesions that escaped detection on "routine" static views obtained 1 hr after nuclide injection. Thus these data probably significantly underestimate the relative efficacy of CT

TABLE 4
Review of Cases

	No.	%
True positive CT and RN	134	26.5
True negative CT and RN	297	58.7
False negative:		
CT and RN	27	5.3
CT alone	19	3.8
RN alone	21	4.2
False positive:		
CT alone	5	1.0
RN alone	3	.6
Subtotal	506	
Exclusively diagnosed by CT*	135	
Total	641	

* Hydrocephalus, porencephaly, cerebral atrophies, benign cyst, and developmental abnormalities such as agenesis of the corpus callosum.

scans as a screening procedure compared to the more traditional "routine" brain scans.

The discussion so far has dealt with brain disorders that can usually be expected to be diagnosed by both techniques. CT has the capability of providing significant information on additional disorders in which the ineffectiveness of radionuclide studies has long been recognized. These conditions include entities such as porencephaly, hydrocephalus, brain atrophies, benign cysts, and developmental abnormalities such as agenesis of the corpus callosum. In the present series, these disorders comprise 21% of all patients.

This study suggests that both radionuclide and CT imaging give reasonably similar precision in the diagnosis of intracranial disease (table 4) and that the combination of both techniques is superior to either alone (table 5); in this sense, each modality complements the other. The improvement in diagnosis to be expected using both techniques appears to be on the order of 5% for neoplasms and somewhat greater for vascular anomalies and trauma. However, this conclusion must be considered in the light of a relatively limited experience.

REFERENCES

1. Hounsfield GN: Computerized transverse axial scanning (tomography). I. Description of system. *Br J Radiol* 46:1016-1022, 1973
2. Ambrose J: Computerized transverse axial scanning (tomography). II. Clinical application. *Br J Radiol* 46:1023-1047, 1973
3. Ambrose J: Computerized x-ray scanning of the brain. *J Neurosurg* 40:679-695, 1974
4. New PFJ, Scott WR, Schnur JA, Davis KR, Taveras JM: Computerized axial tomography with the E.M.I. scanner. *Radiology* 110:109-123, 1974
5. Paxton R, Ambrose J: The E.M.I. scanner: a brief review of the first 650 patients. *Br J Radiol* 47:530-565, 1974
6. Feigin DS, Welch DM, Siegel BA, James AE Jr: The efficacy

TABLE 5
Comparative Accuracy

Type of Lesion	No. Cases	Accuracy (%)		
		RN	CT	Both
Neoplasm	114	83	85	89
Vascular occlusive disease	52	62	52	71
Brain hemorrhage	13	54	100	100
Vascular anomalies	5	80	80	100
Infection	5	100	100	100
Trauma	11	82	82	100

of the brain scan in diagnosis of brain-stem gliomas. *Radiology* 116:117-120, 1975

7. Davis DO, Pressman BD: Computerized tomography of the brain. *Radiol Clin North Am* 12:297-313, 1974
8. New PFJ, Scott WR, Schnur JA, Davis KR, Taveras JM, Hockberg FH: Computed tomography with the E.M.I. scanner in the diagnosis of primary and metastatic intracranial neoplasms. *Radiology* 114:75-87, 1975
9. Pendergrass HP, McKusick KA, New PFJ, Potsaid MS: Relative efficacy of radionuclide imaging and computed tomography of the brain. *Radiology* 116:363-366, 1975
10. Leonard JR, Witherspoon LR, Mathaley MS Jr, Goodrich JK: Value of sequential postoperative brain scans in patients with anaplastic gliomas. *J Neurosurg* 42:551-556, 1975
11. Quinn JL III: Aids for the diagnosis of cerebral vascular disease brain scanning, in *Cerebral Vascular Diseases*, 6th Conference, edited by Siekert RT, Whisnant JP, New York, Grune & Stratton, 1968, pp 179-189
12. Scott WR, New PFJ, Davis KR, Schnur JA: Computerized axial tomography of intracerebral and intraventricular hemorrhage. *Radiology* 112:73-80, 1974
13. Wise G, Brockenbrough EC, Marty R, Griep R: The detection of carotid artery obstruction: a correlation with angiography. *Stroke* 2:105-113, 1971
14. Burrows EH: False negative results in brain scanning. *Br Med J* 1:473-476, 1972
15. Cronqvist S, Muller R: Brain scanning cerebrovascular lesions. *Acta Radiol [Diagn]* (Stockh) 13:659-671, 1972
16. Shivers JA, Adcock DE, Cuinto FC, Radcliffe WB: Radionuclide imaging in primary intracerebral hemorrhage. *Radiology* 111:211-212, 1974
17. Pressman BD, Kirkwood JR, Davis DO: Computerized transverse tomography of vascular lesions of the brain. I. Arteriovenous malformations. *Am J Roentgenol* 124:208-214, 1975
18. Baker HL Jr, Campbell JK, Houser OW, Reese DF, Sheedy DF, Halman CB: Computer assisted tomography of the head: an early evaluation. *Mayo Clin Proc* 49:12-37, 1974
19. Baker HL Jr, Campbell JK, Houser OW, Reese DF: Early experience with the E.M.I. scanner for study of the brain. *Radiology* 116:327-333, 1975
20. Hopkins GB, Kristensen KAB: Rapid sequential scintiphotography in the radionuclide detection of subdural hematomas. *J Nucl Med* 14:288-290, 1973
21. Davis KR, Taveras JM, New PFJ, Schnur JA, Roberson GH: Cerebral infarction diagnosis by computerized tomography: analysis and evaluation of findings. *Am J Roentgenol* 124:643-660, 1975
22. Christie JH, Go RT, Suzuki Y, Tonami N, Schapiro RL: Sequential brain scanning as an adjunctive scanning procedure. *Radiology* 114:381-387, 1975

High Resolution Computed Tomography of the Orbit with the Ohio Nuclear Delta Head Scanner

MEREDITH A. WEINSTEIN,¹ ALLISON J. BERLIN, JR.,² AND PAUL M. DUCHESNEAU¹

The orbit is an ideal structure to examine by CT because of large differences between absorption values of retro-orbital fat and other structures such as muscle, optic nerve, and ophthalmic artery. Spatial resolution in CT is dependent upon the volume of each pixel (individual picture element). Whereas the pixel volume of the original EMI scanner was 117 mm³, that of the Ohio Nuclear Delta head scanner employed in this paper is only 5 mm³.

Over 200 patients have been examined using this scanning instrument, including 32 patients in whom the orbits were specifically examined with a scan plane parallel to Reid's baseline. Representative abnormalities are discussed and illustrated. Orbital tumors such as hemangiomas, lymphomas, meningiomas, and inflammatory pseudotumors can be accurately localized while still very small.

Spatial resolution in computed tomograph (CT) is in part a function of the volume of the individual picture elements (pixels). With each report of decreased pixel volume in examination of the orbit, resolution of orbital content has improved. The orbit has been examined with CT pixel volumes of 117, 72, 29.25, 18, and 13.5 mm³ [1-5]. We have demonstrated increased resolution of the orbital contents using the Delta head scanner (Ohio Nuclear) with a pixel volume of 5 mm³.

Materials and Methods

The patient lies on a reclining chair. The head is secured by Velcro straps around a plexiglass head holder. Two slices are obtained simultaneously. Three calcium fluoride detectors per section are used. Slice thicknesses of 13, 8, or 5 mm are selected by a dial on a control console. The 5 mm slices, used to examine the orbits, are separated by a gap of 3 mm. The chair is advanced in alternating increments of 5 and 15 mm. The two scan speed times available are 2 min, 10 sec and 3 min, 5 sec. The photon flux with the slow scan speed is twice that of the fast scan. The slow scan was used to examine the orbits in order to maximize the contrast resolution of the parts examined. The first section is presented as it is constructed during the scan and is available immediately after the scan is completed. The second section can be viewed 6 sec after scan completion.

The opening in the gantry for the patient's head has a diameter of 10 inches. The distance between x-ray source and detector is 24.23 inches. The matrix is 256×256. Each matrix element is 0.98 mm square. The scan is made at 130 kV, 30 mA with 3 mm of aluminum filtration. A total of 256 readings of transmissions through the body are made each time the machine is indexed 3° (1° for each detector) around the head. The 46,080 readings generated for each slice are then processed by the PDP 11-05 computer. The average scan time per patient is 30 min. The scale of the scanner is from +1,000 units for bone to -1,000 units for air. With the sections 5 mm thick, the percentage deviation of the mean in a water phantom and the spatial resolution determined with a Siemens star approxi-

mate the findings with the Ohio Nuclear body scanner and the EMI head scanner with 13 mm slices.

A circular or elliptical area of interest can be enclosed within a cursor. The computer calculates the average density, the standard and root mean square deviation of the density, the number of square centimeters, and the number of matrix elements within the cursor (fig. 1). The distance in millimeters and pixels and the angle between any two points on the slice can be displayed (fig. 2). A portion of an image can be magnified to fill the viewing screen (figs. 2 and 3). Over 200 patients have been examined on this scanner. The orbits were specifically examined in 32 of these patients with the scan plane parallel to Reid's baseline.

Results and Discussion

The first commercial CT unit (EMI) had picture elements 3×3 mm in cross section. Picture elements less than 1 mm² in cross section are now available with the EMI body scanner CT5005 (0.75×0.75 mm), the Ohio Nuclear Delta body scanner (0.74×0.74 mm with a 20 cm scan length), and the Ohio Nuclear Delta head scanner (0.98×0.98 mm). Spatial resolution in CT is dependent upon the volume of each pixel. Reducing the slice thickness (Z axis) increased volume resolution. Adjacent volumes of different attenuation coefficients are averaged in the thickness of the slice.

The EMI and Ohio Nuclear body scanners are supplied with optional collimators which reduce the scan slices from 13 to 8 mm in thickness. The slices in the Ohio Nuclear Delta head scanner can be collimated to 13, 8, or 5 mm nominal thickness. The pixel volume of the original EMI

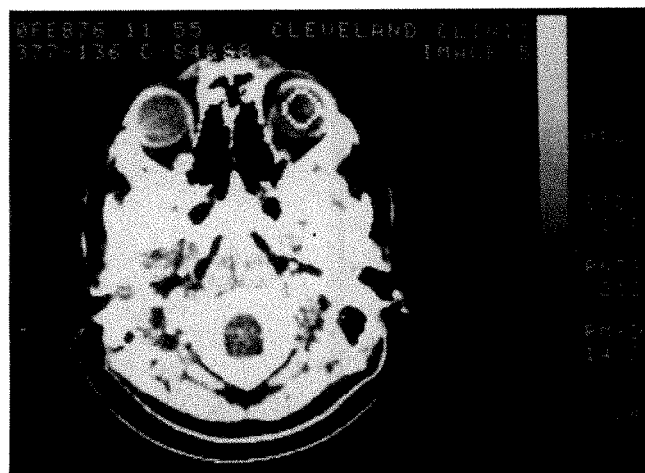
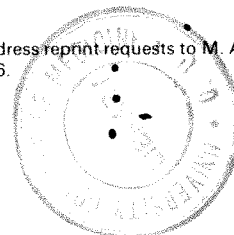


Fig. 1.—Cursor superimposed upon right globe. Mean density of portion of globe within cursor, standard and root mean square deviations of this density, number of pixels, and square centimeters within cursor are displayed.

Received March 24, 1976.

¹ Department of Radiology, Cleveland Clinic Foundation, 9500 Euclid Avenue, Cleveland, Ohio 44106. Address reprint requests to M. A. Weinstein.

² Department of Ophthalmology, Cleveland Clinic Foundation, 9500 Euclid Avenue, Cleveland, Ohio 44106.



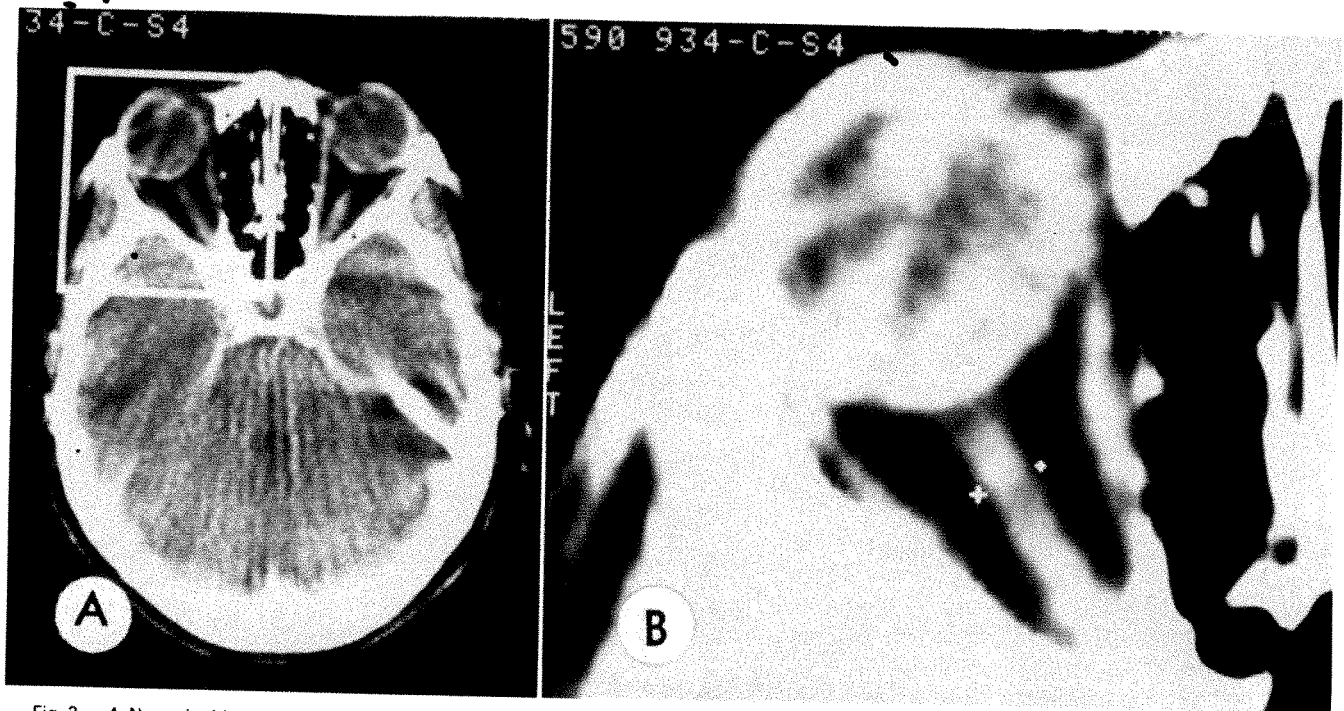


Fig. 2.—A, Normal orbits with area to be expanded enclosed in cursor. B, Magnified left orbit with markers on sides of optic nerve. Nerve is 5.44 mm wide. Magnified nerve extends over 21 pixels.

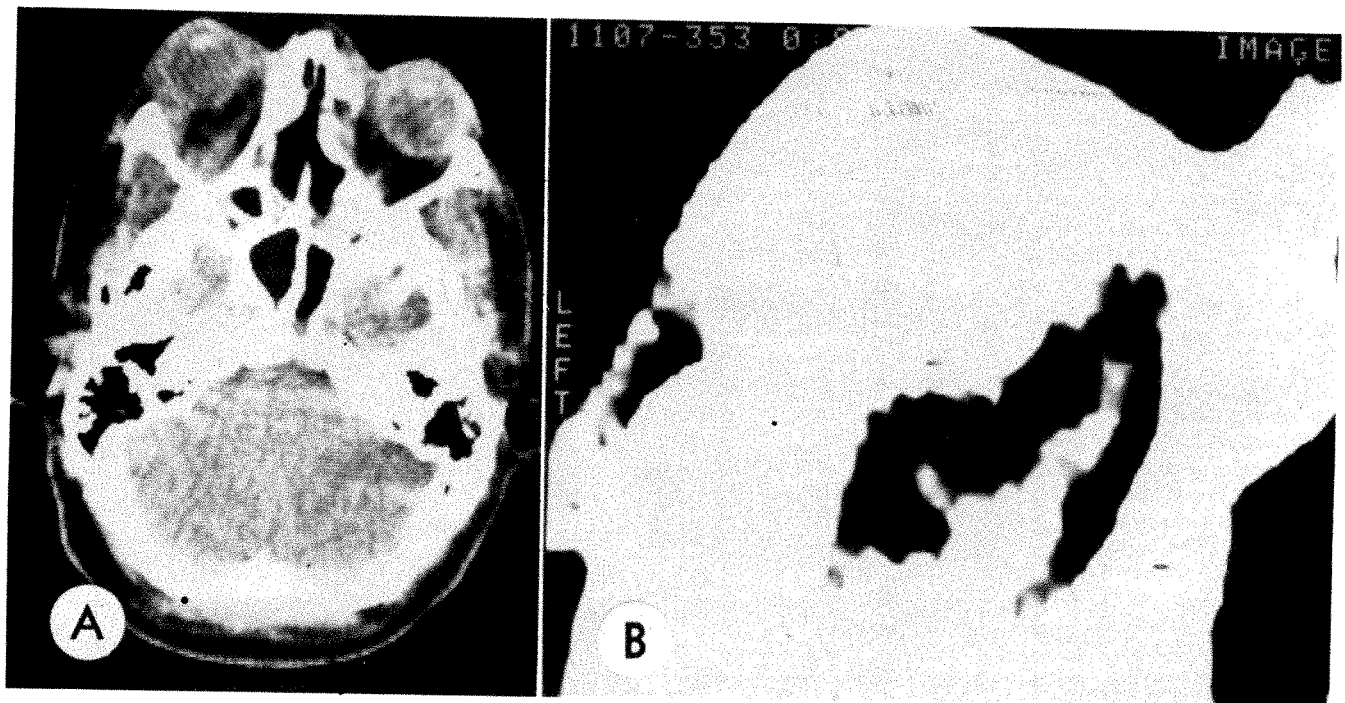


Fig. 3.—A, Irregular mass posterior and inferior to globe which is displaced anteriorly. Clinical diagnosis is pseudotumor. B, Magnified view of mass in retroorbital space.

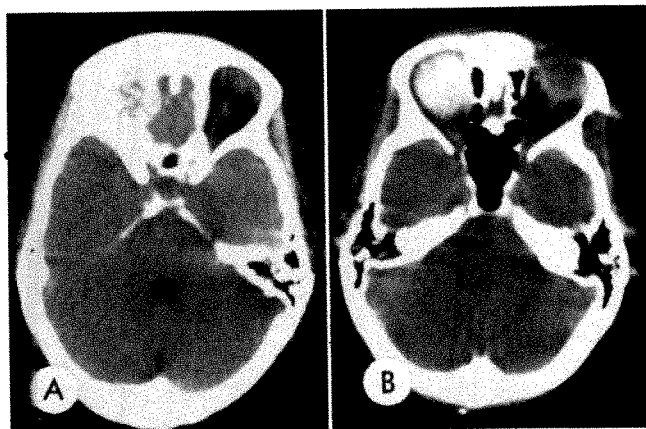


Fig. 4.—A, Hemangioma in roof of left orbit with expansion of bone. B, Inferior section showing extent of inferior expansion of hemangioma. Ethmoid sinuses medial to orbit are intact.

scanner was 117 mm^3 ($3 \times 3 \times 13 \text{ mm}$). The pixel volume of the Ohio Nuclear head scanner used to examine the orbits is 5 mm^3 ($0.98 \times 0.98 \times 5$). Although reducing the thickness of each slice increased volume resolution, contrast resolution may be decreased because of the reduction of photon flux through each pixel with a resultant increase in the noise-to-information ratio. The tube-to-detector distance has been reduced from 48 inches in the Ohio Nuclear body scanner to 24.23 inches in the Ohio Nuclear head scanner. This increases the photon flux fourfold.

The patient dosage with the Ohio Nuclear head scanner is 26 rads to the back of the head and 11 rads to the center of the head with the 5 mm slow scan. This dosage is for eight sets or 16 adjacent scans. The corresponding dosage rates for the 8 mm sections are 17 and 7 rads for eight scans. For the 13 mm sections the dosages are 14 and 5 rads for six scans. The dosages for the fast scan speed are one-half those of the slow scan. We now use the fast scan for screening and the slow scan to determine finer anatomical details.

Within the orbit the muscles, lens [2], optic nerves, and ophthalmic artery measure only a few millimeters in diameter. Retroorbital fat envelops the structures. The large difference between the absorption values of fat (-100 units) and muscle, optic nerves, and ophthalmic artery (approximately 30 units) makes the orbit an ideal structure to examine with CT. Orbital tumors such as hemangiomas, lymphomas, meningiomas, and inflammatory pseudotumors can be accurately localized while small in size. (figs. 3 and 4). Small foreign bodies can be detected (fig. 5)

With increasing resolution, the effects of systemic disease upon the orbit can be evaluated. Hilal et al [6] have reported on the detection of enlargement of the orbital muscles in hyperthyroidism by CT. The effects of systemic disease and aging upon the density of the globe and lens can be evaluated by enclosing them in the cursor and mea-

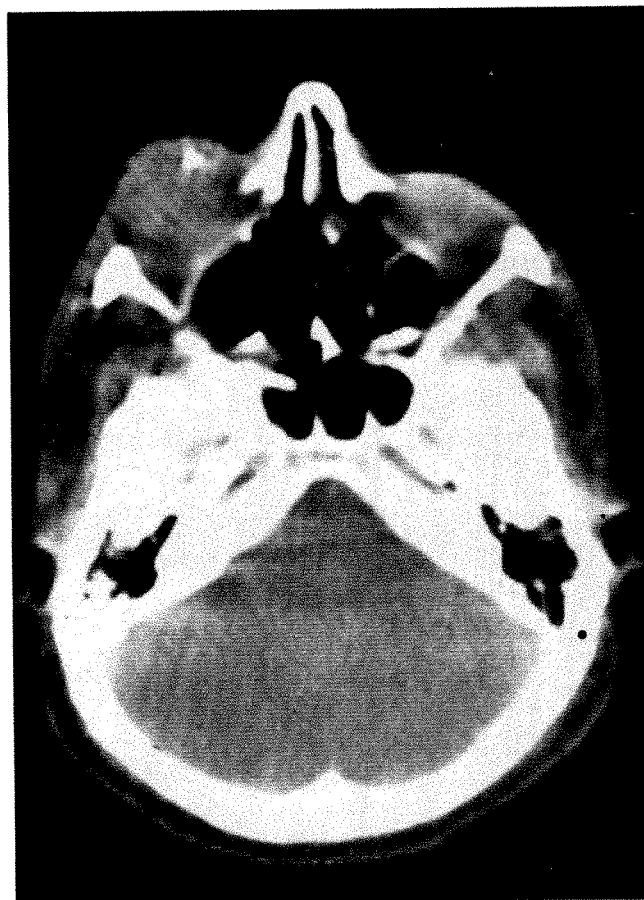


Fig. 5.—Metallic foreign body in inferior anterior aspect of left globe. Globe is proptotic.

suring their density (fig. 1). With faster scanning time, patients will be able to fix their globe during the scan enabling the diagnosis of pathology within it.

REFERENCES

1. Lampert VL, Zelch JV, Cohen DN: Computed tomography of the orbits. *Radiology* 113:351-354, 1974
2. Gawler J, Sanders MD, Bull JWD, duBoulay G, Marshall J: Computer assisted tomography in orbital disease. *Br J Ophthalmol* 58:571-587, 1974
3. Ambrose JAE, Lloyd GAS, Wright JE: A preliminary evaluation of fine matrix computerized axial tomography (Emiscan) in the diagnosis of orbital space-occupying lesions. *Br J Radiol* 47:747-751, 1974
4. Momose KJ, New PFJ, Grove AS Jr, Scott WR: The use of computed tomography in ophthalmology. *Radiology* 115:361-368, 1975
5. Hayward RW, Zatz LM: A thin-section collimator for the EMI scanner. *Radiology* 117:475-478, 1975
6. Hilal SK, Trokel SL, Kreps SM: High resolution computerized tomography of the orbit. Paper presented at the annual meeting of the Radiological Society of North America, Chicago, December 1975

Further Progress in CT Scanning and Computerized Radiation Therapy Treatment Planning

GWYNN L. JELDEN,¹ EDWARD S. CHERNAK,¹ ANTONIO RODRIGUEZ-ANTUNEZ,¹
JOHN R. HAAGA,² PAUL S. LAVIK,¹ AND RANJIT S. DHALIWAL¹

Total body computed tomography has introduced a unique method of obtaining body contours as well as anatomical representations for radiation therapy treatment planning. CT scanning combined with computerized radiation therapy treatment planning has improved accuracy and contributed greatly to the solution of complex treatment problems. CT scans can also be used to evaluate the progress of patients undergoing radiation therapy.

Since the introduction of external radiation beams in therapeutic radiology, various techniques have been developed to improve treatment planning. It was realized that the patient's contour was vital in calculating the dose of radiation to an underlying tumor. Various methods from lead wires to mechanical jigs have been used in radiation therapy to obtain a contour. The contours obtained by these methods are both time consuming and inaccurate.

The next step was to transfer this artificial contour onto paper, refer to a book of cross-sectional anatomy, and hopefully find a drawing that would correspond to the area to be treated. The resulting drawing also introduced error in dosage calculations since there was no differential between normal, pathological, or the individual patient's anatomy.

Another device that held only a fleeting glimmer for improvement of treatment planning was conventional radiologic transverse tomography. This proved hardly more successful because the contour obtained was indistinct and the anatomical representations were of poor quality.

In the past few years ultrasound has provided a means of obtaining a contour which is reasonably accurate. However, anatomical representation is limited primarily to the abdomen, retroperitoneal area, pelvis, neck, and chest wall measurements.

With CT it is now possible to make precise contours and detailed representations of normal and pathologic anatomy throughout the entire body. This can be done with the patient in treatment position, thus individualizing the treatment plan.

Small computers used for radiation therapy have become available and have assumed an important role in treatment planning. They have greatly increased accuracy and offered determinative technique, with a corresponding reduction in time when compared with manual techniques.

We have developed a method of treatment planning which uses the imaging technique of the CT scan combined with a radiation therapy computer.

Method

The initial step in treatment planning is to obtain a series of CT scans throughout the entire tumor-involved area. The scan that occupies the central axis of the therapy beam is then chosen as the representative scan (fig. 1A). Additionally, off-axis scans and beam dosimetry are reviewed. Window settings on the CT scanner are then selected so as to offer a contrast accurately representing the contour of the patient section under study (fig. 1B).

The second step is to enter the information obtained from the CT scan into a computer used for radiation therapy treatment planning. Presently, the information may be entered by three possible methods: (1) using a calibrated transparency of the CT image and densitometrically scanning it, thus transferring the information through an interface into the computer; (2) tracing an image using a calibrated rho theta (or theta phi) device, provided the image is of sufficient size; or by (3) preprocessed data entry.

If method 1 is used, a density scan is made by calling up from the computer between three and five density levels on a density range scale of 0-1000. The densities are chosen to represent tumor, bone, air (as in sinuses), or any other density corresponding to areas of critical anatomy. The density scan can be viewed on the display monitor of the computer (fig. 1C). If the density levels chosen include all the vital anatomy, a digital or analog printout can be made.

Since the density scan has too many data points to routinely calculate and plot isodose curves, we have created a computerized scan (fig. 1D). The rho theta tracing arm is used to outline the patient contour and vital anatomy shown in the density scan. This simplified representation of the contour and anatomy allows more efficient use of the computer. This step (method 2) may be omitted if preprocessed data entry is used (method 3). Presently, we are perfecting this program to accept the CT scan data, determine tissue densities, and present only the density contours.

Figure 2 demonstrates how beam entry and angulation can be controlled by viewing the treatment plan on the display monitor. Tissue inhomogeneity produced by bone and structures containing air present no difficulties in dosage calculations with the combination of CT scanning and radiation therapy computers.

There is a program especially designed for tissue inhomogeneities. The CT scan provides the useful information of body composition in the radiation field for tissue inhomogeneity calculations.

Received March 2, 1976

¹ Department of Radiation Therapy and Nuclear Medicine, Cleveland Clinic Foundation, 9500 Euclid Avenue, Cleveland, Ohio 44106. Address reprint requests to A. Rodriguez-Antunez.

² Department of Radiology, Cleveland Clinic Foundation, Cleveland, Ohio 44106.

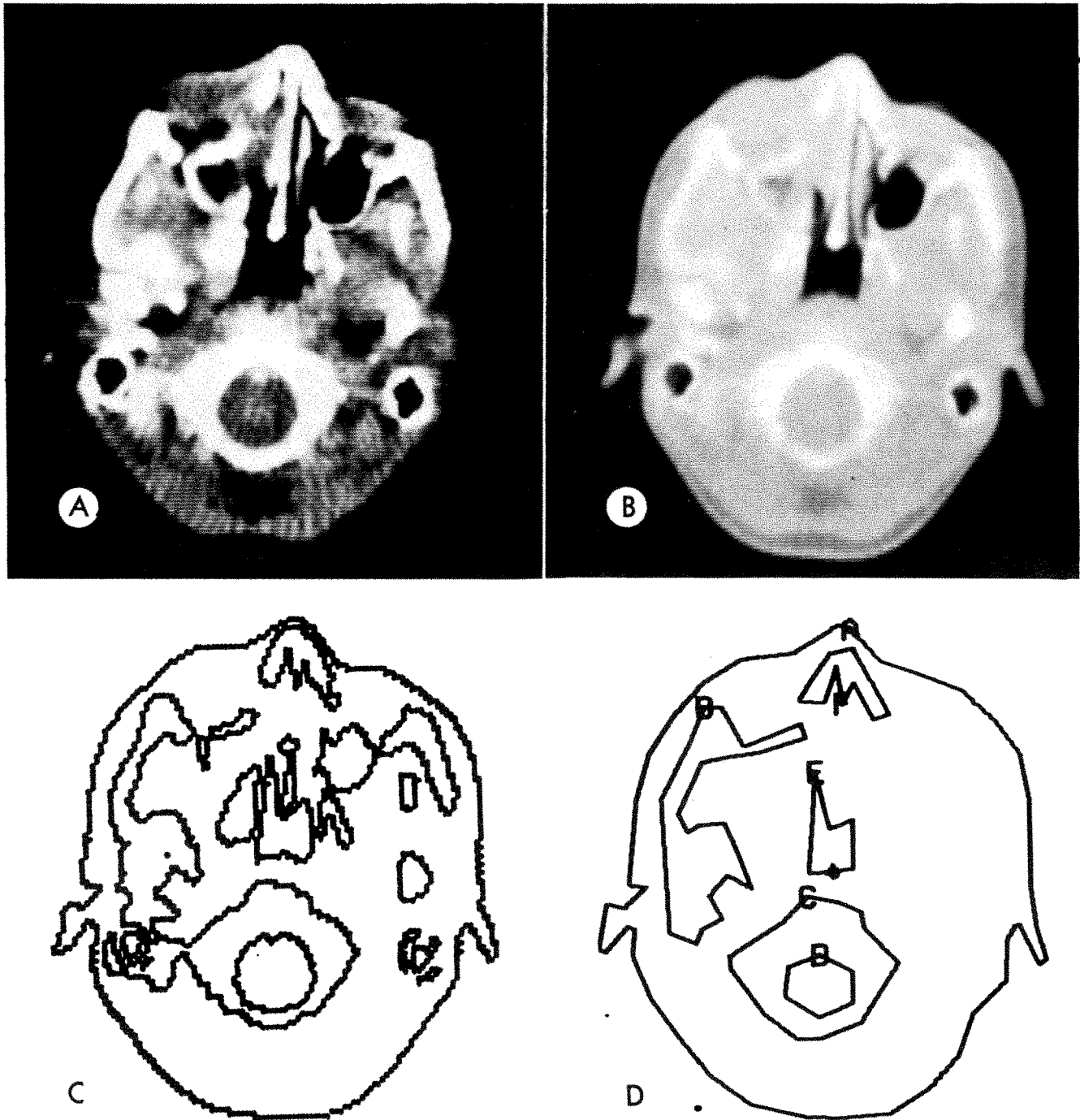


Fig. 1.—Esthesioneuroepithelioma. *A*, CT scan demonstrating esthesioneuroepithelioma of left side of nose, extending anteriorly into orbit and inferiorly into antrum, eroding bone and causing asymmetry of face. *B*, Same cross-sectional area but different window settings on scanner to lighten density to obtain contour. *C*, Density scan representation displayed on screen of treatment planning computer. Anatomical landmarks and patient contour readily identified. *D*, Computerized scan obtained by placing density scan with rho theta arm. Patient contour and anatomical structures of interest are in simplified form to reserve core in computer for calculating isodose curves.

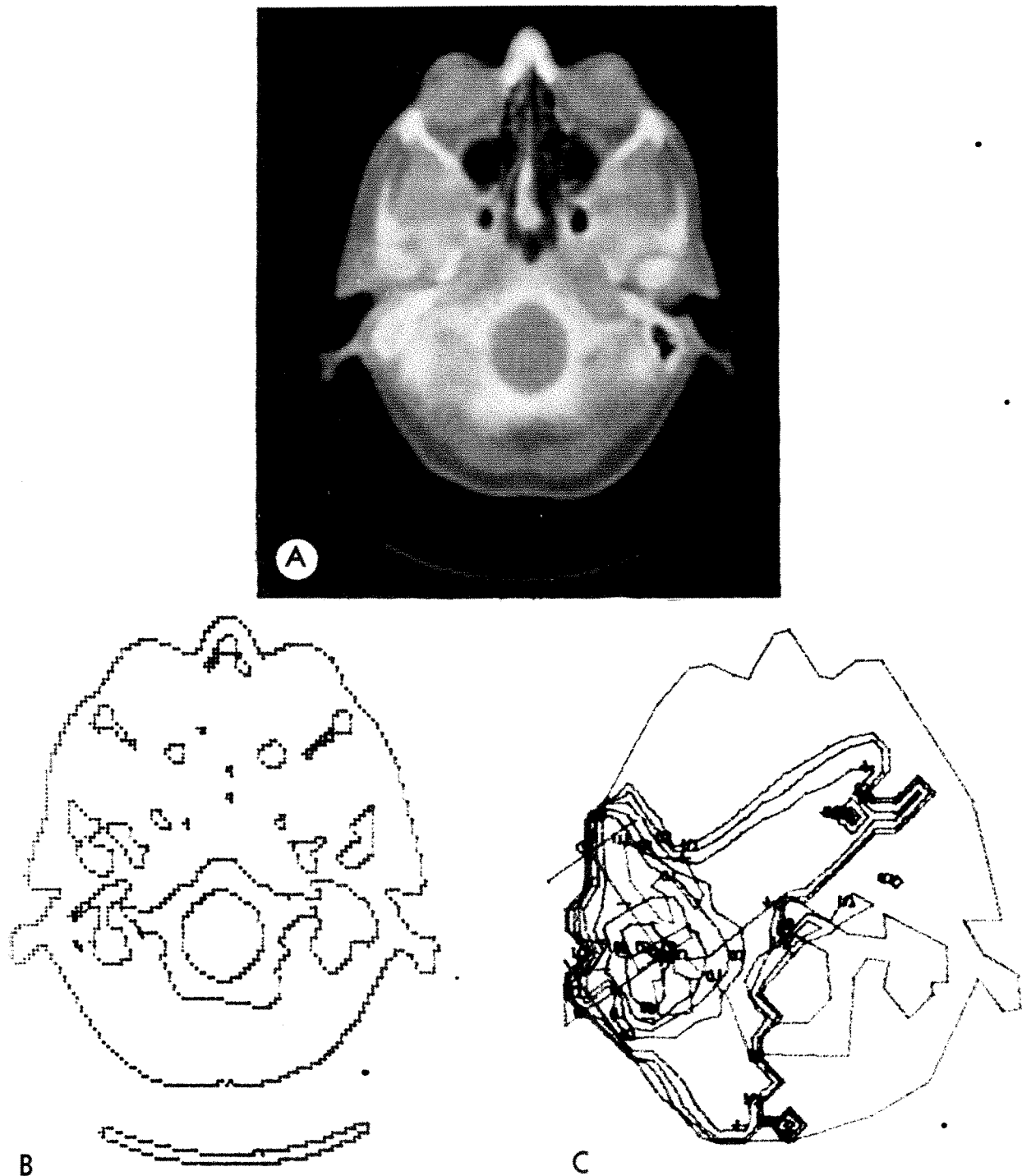


Fig. 2.—Squamous cell carcinoma of left external auditory canal. A, CT scan showing no erosion of bone and rather indistinct tumor mass. Accurate information obtained on tumor volume and position of structures that should receive minimal radiation (e.g., eyes and brain stem). B, Density scan. C, Isodose curve corrected for tissue inhomogeneities from anatomical information supplied by CT scan.

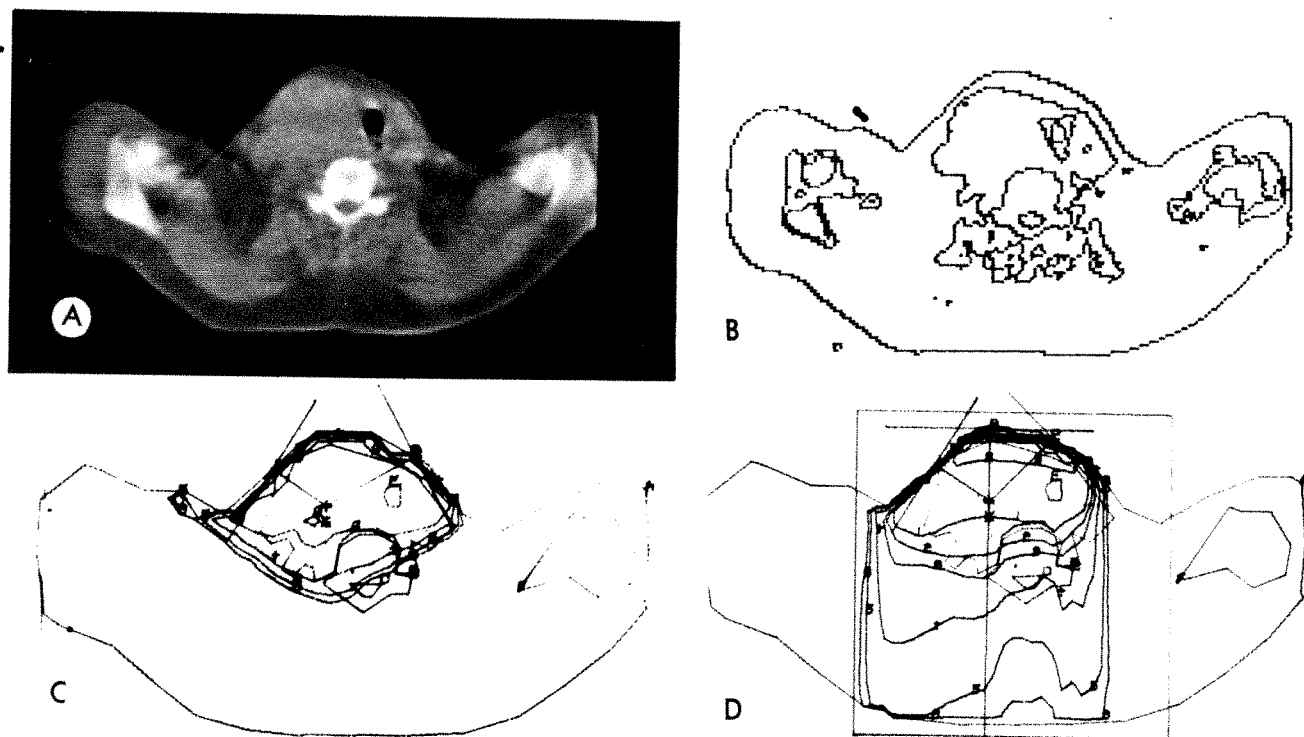


Fig. 3.—Recurrent follicular cell carcinoma of thyroid. *A*, CT scan showing displacement of trachea. *B*, Density scan. *C*, Treatment plan using angles, beams, and wedges. *D*, Composite isodose distribution from three combined fields. Corrected for tissue inhomogeneity.

Results and Discussion

With the capabilities of the present generation of treatment planning computers, beams of various sizes can be entered and positioned to suit individual anatomy. The isodose distribution can be extracted for various therapy units, tailored to the patient's individual anatomy (figs. 2–5). Combinations of beams and wedges can be added with resultant isodose distributions for each (figs. 2, 3, and 5).

CT scanning is also useful in evaluating treatment progress. Treatment progress can be followed in scans with or without contrast agents (fig. 5).

In addition to the excellent imaging capabilities of the CT scanners, the scanners can be used to obtain a histologic diagnosis. CT-guided biopsies present the most accurate means of positioning an instrument for percutaneous

biopsy. The biopsy instrument can be placed in any desired area of the suspected neoplasm (fig. 6). We have performed this type of biopsy in most abdominal organs, including liver (fig. 7), kidney, pancreas, and retroperitoneum (fig. 8). The technique consists of positioning the needle and positioning the instrument in the skin and subcutaneous tissue, followed by repetitive scans and repositioning of the instrument until it is within the desired area. The needle biopsy is then taken.

With the rapid progress in medical imaging, the next step will be the ability to obtain longitudinal body sections. With this potential future development, three-dimensional anatomical reconstruction can further improve radiation therapy treatment planning.

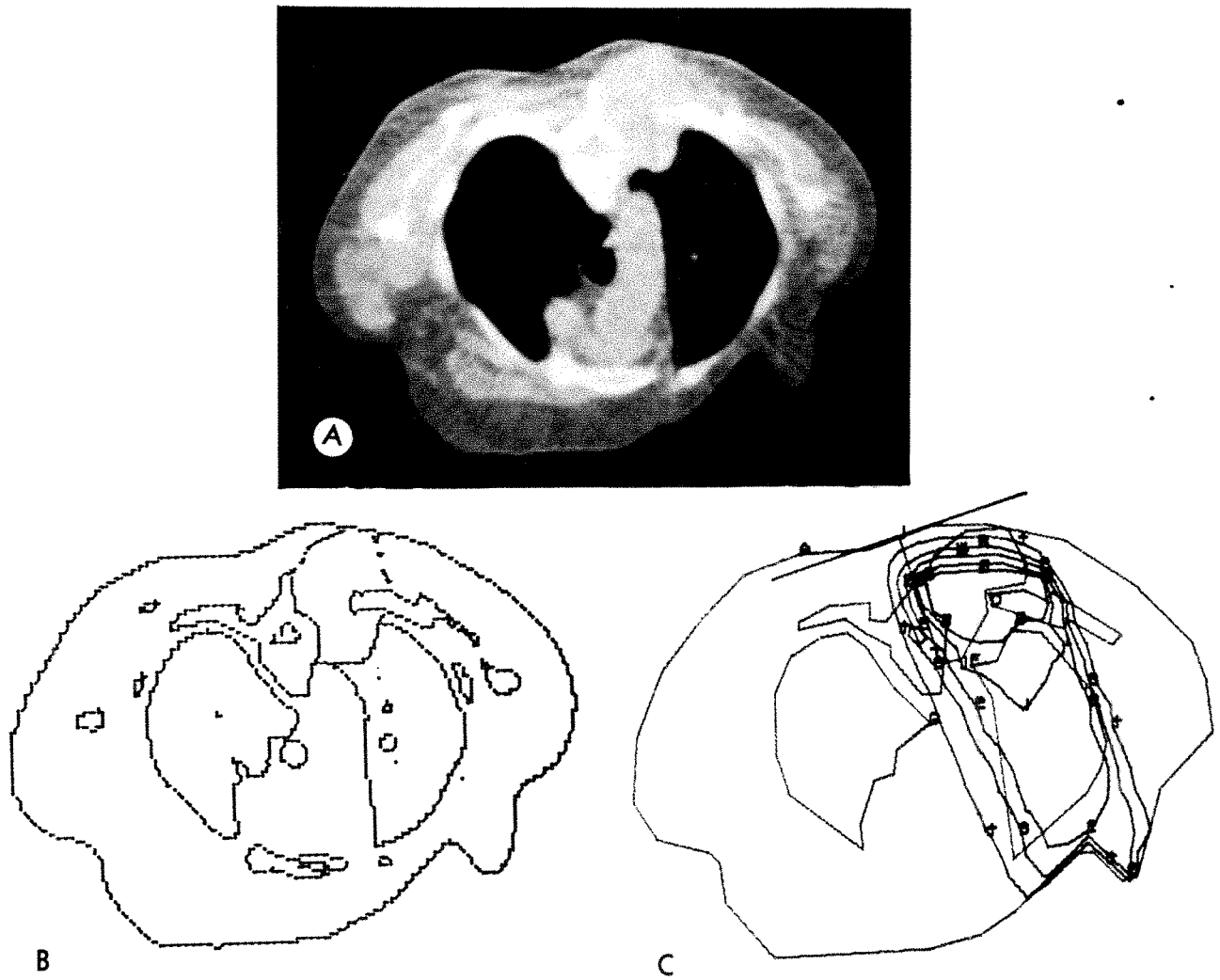


Fig. 4.—Recurrent fibrosarcoma. A, CT scan showing involvement of postcentral aspect of midthorax. Note that mass has eroded rib and penetrated thoracic cavity. B, Density scan. C, Isodose distribution with 15° angulation of single port.

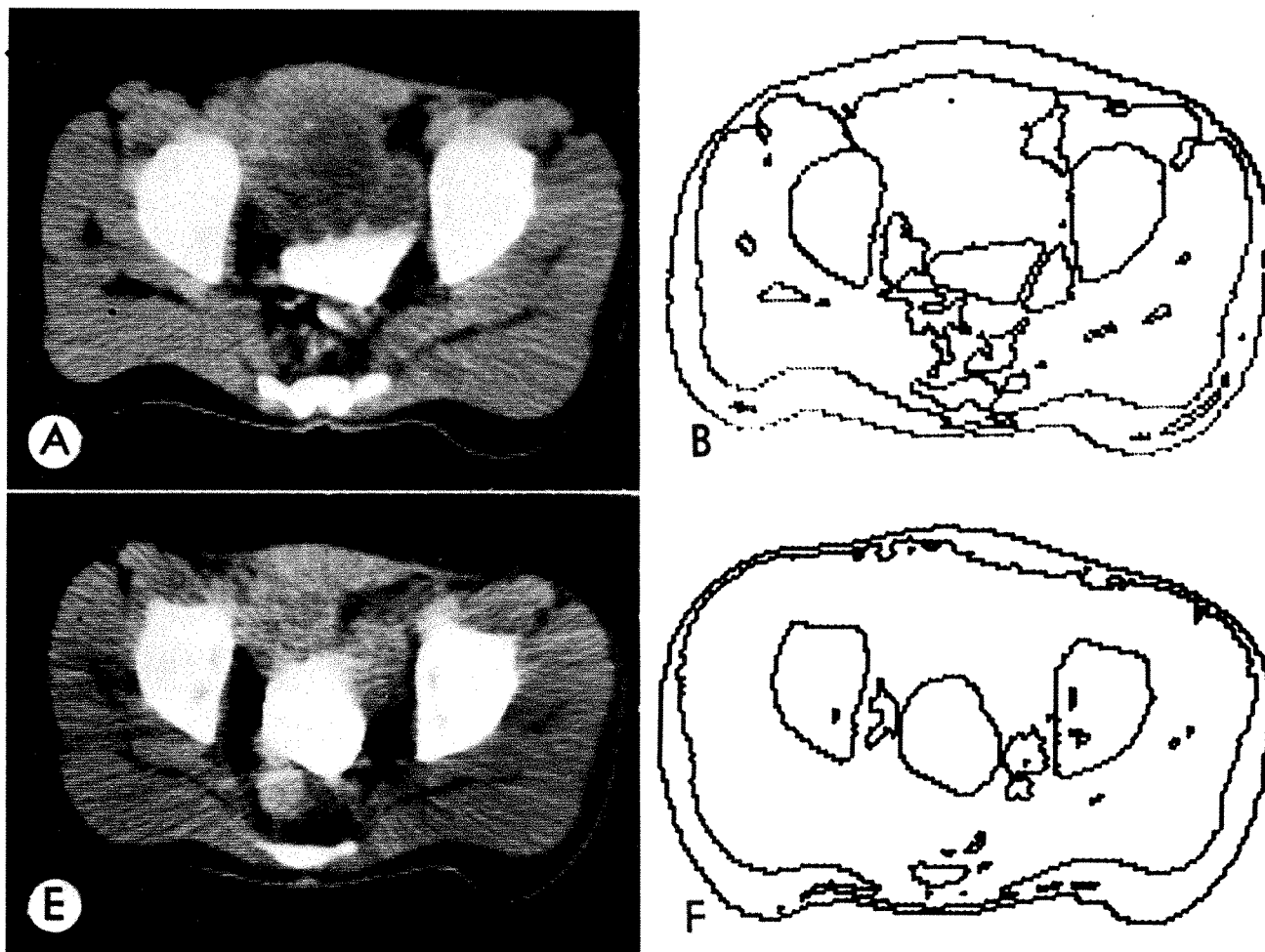


Fig. 5.—Transitional cell carcinoma of bladder. *A*, CT scan. *B*, Density scan with delineation of tumor. *C*, Computerized scan. *D*, Isodose distribution using anteroposterior parallel opposed portals. *E*, Midtreatment scan with contrast to evaluate progress. *F*, Midtreatment density scan. *G*, Change of treatment plan

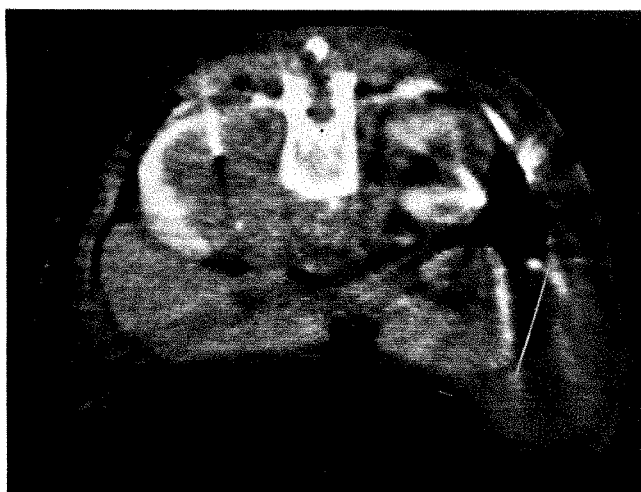


Fig. 6.—CT scan showing position of needle biopsy.

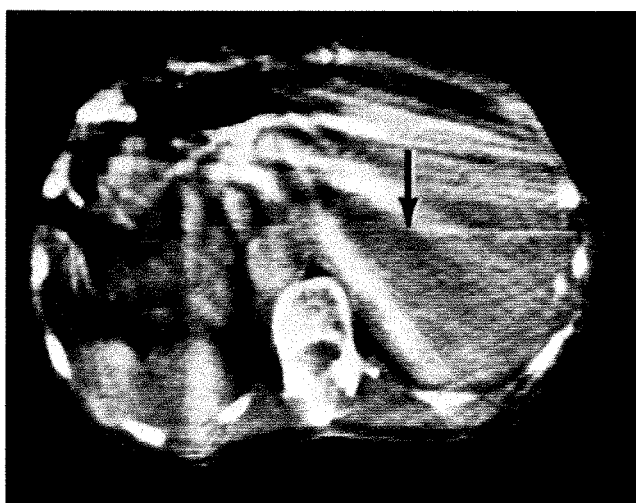


Fig. 7.—CT biopsy of liver neoplasm. Arrow points to tip of needle placed within mass. Biopsy positive for hepatocellular carcinoma.

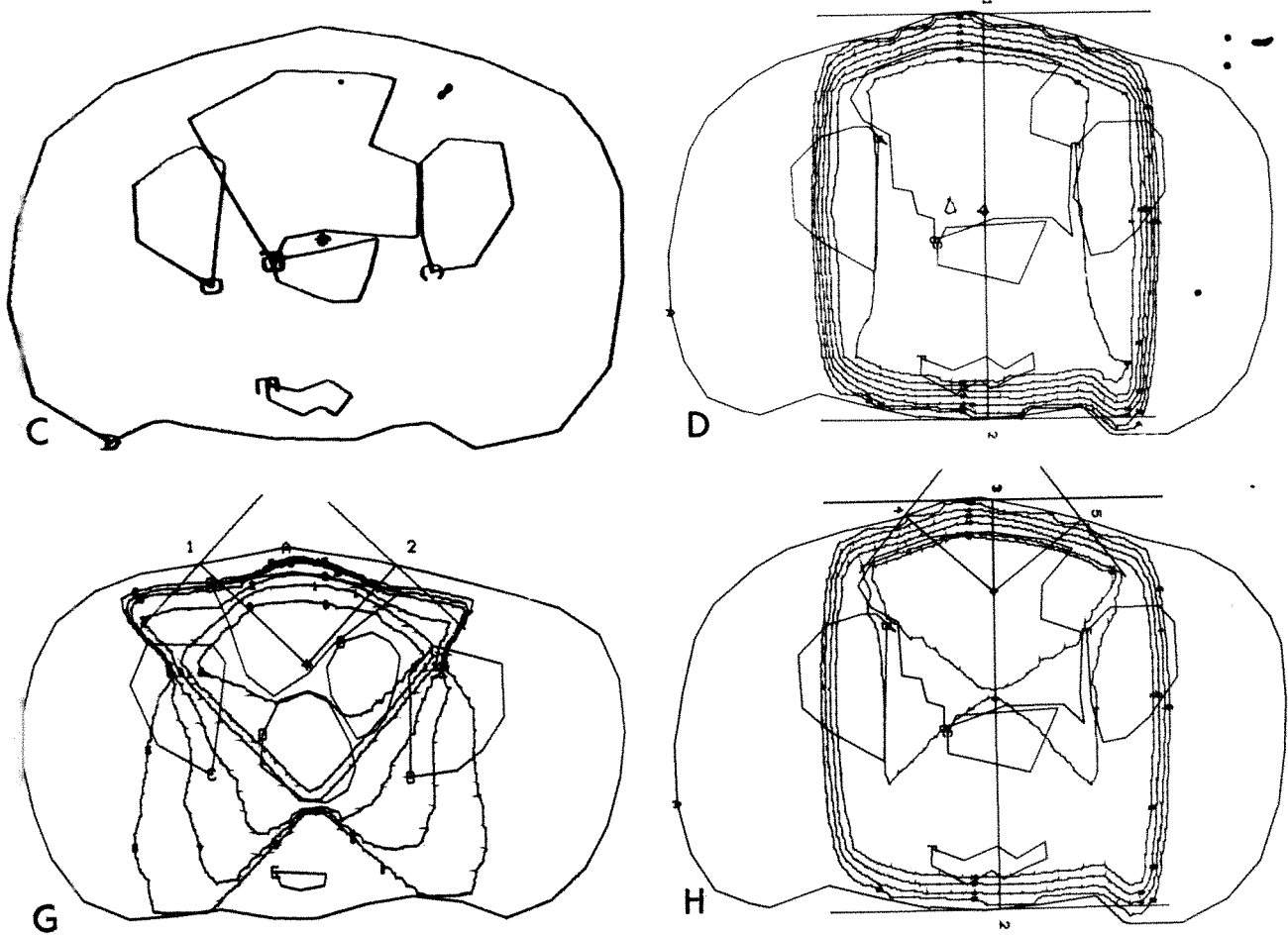
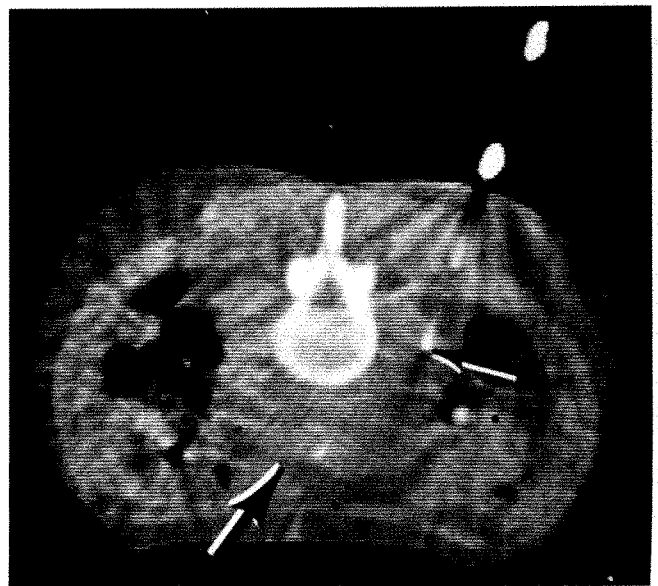


Fig 5. (cont.)—to two anterior oblique portals at 45° with 45° wedges. H, Composite isodose distribution of entire treatment.

Fig. 8.—CT scan demonstrating biopsy of retroperitoneal mass. Small arrow designates tip of biopsy needle within mass. Note calcified aorta displaced anteriorly from spine by mass (large arrow).



Health Planning for Computed Tomography: Perspectives and Problems

LEE E. CLOE¹

Computed tomography has been introduced to the health care system at a time when health care planning is still evolving. Unlike the recent past, final authorization of large expenditures and new services such as CT now lies outside the providers of care and is based on laws and regulations that are not familiar to many physicians. A brief review of the principal federal statutes is presented from the Hill-Burton Act to the National Health Planning and Resources Development Act of 1974. Recognizing the unique problems in certain special service areas such as CT, the state of Indiana has formed committees to collect information and develop recommendations to assist its health planners in their actions and decisions under the federal statutes. The quantitative problems which the Indiana CT committee must address are presented in some detail, problems that other health planners face as well.

Computed tomography has been hailed as a technological advance nearly equal in importance to Roentgen's original discovery of x-rays. Great optimism exists for its eventual beneficial applications once CT technology is fully developed and widely dispersed. Quality medical care for every citizen has come to be viewed as an obligation of society. Yet increasing concerns about cost as well as availability have led to laws and regulations that affect the introduction of CT even before its full medical promise has been defined. Many physicians who enthusiastically anticipate access to CT are unaware of the background of health planning efforts and the current requirements for authorization of such high cost expenditures.

Modern Genesis of Health Planning

Health planning began after World War II when the federal government enacted and funded the Hill-Burton program (P.L. 88-443). The country proceeded to go on a hospital building spree during which many fine and much-needed facilities were built. Conversely, others turned out to be inefficient, poorly planned, and poorly located; while still others resulted in duplicated and consequently underutilized services. Such shortcomings resulted from planning with a microcosmic rather than a macrocosmic perspective. From this experience, local health facilities planning committees developed. Initially, they were supported by the health care providers since they were the health care industry's response to local health planning. But again, most problems were examined in a narrow sense.

Critics of local health facilities planning committees charged they were provider controlled (many were funded, controlled, and under the full-time direction of persons employed by hospitals), lacked consumer representation, and had no legal enforcement.

Subsequently, the federal government, under the 1966 law P.L. 89-749, brought about the Comprehensive Health Planning (CHP) movement. This law required development of local comprehensive health planning councils and established a Certificate of Need review process for proposed projects. However, comprehensive health planning councils did little planning, instead voting on the planning done by health care providers.

In October 1972, Section 1122 of the Social Security Act was implemented in P.L. 92-603. This section authorized individual states to control capital expenditures in health services and facilities. Under its provisions, if a health care facility will be reimbursed for depreciation of capital expenditures under Title V, Maternal and Child Health; Title XVIII, Medicare; or Title XIX, Medicaid, and if the capital expenditure exceeds \$100,000 or if it relates to a significant change in clinical services, then the facility must present a statement of need for review. Local health planning agencies make the review and recommend to the secretary of Health, Education, and Welfare that the project be either approved or disapproved for reimbursement of services under these Titles.

In the review process, agencies must look at four areas: need, manpower, financial feasibility from the viewpoint of both the facility and the community, and cost containment or improved quality of care (what is the most effective and productive way to provide the service).

With the requirements of the law as set forth in P.L. 92-603, a wide range of projects must be reviewed, including the construction of a completely new facility, the addition or deletion of beds from existing facilities, and any major change of services. States that participated in the Section 1122 program were mandated to develop criteria, standards, plans, and programs that would enable the various projects to be judged. Initially, projects were examined from a broad-brush viewpoint. The Hill-Burton plans could be utilized in some cases since they are essentially planning inventories of hospitals and hospital beds. Such plans also include nursing homes (on a limited basis) and some other facilities, but they basically relate to hospitals.

Very quickly, the states found areas that posed particular difficulty in the review process. One such area was that of highly specialized services. Many were costly not only in initial expenditure but also in personnel and equipment maintenance. In addition, many of these were emotionally charged situations which became almost a life or death issue as far as the applicant was concerned. It was also apparent that many states had very little data upon which to base decisions in the specialty areas. As a consequence,

Received April 15, 1976.

¹ Health Plan and Program Development Division, Indiana State Board of Health, 1330 West Michigan Street, Indianapolis, Indiana 46206.

the review process was focused on one project, and the project's relationship to the entire state often was overlooked. The same microcosm problem that affected the early Hill-Burton program was apparent.

The Indiana Approach

In Indiana, the director of the 1122 program for the Indiana State Board of Health, David J. Edwards, saw the need for statewide development of criteria, standards, and guidelines in specialty areas. Through the Indiana Public Health Foundation, Inc., a grant from the Indiana Regional Medical Program was obtained to study seven specialized medical services in four specialty areas. These were (1) end-stage renal disease and kidney transplant; (2) radiation therapy and therapeutic radioisotopes; (3) cardiac catheterization, cardiac angiography, and open-heart surgery; and (4) burns.

A committee designed to represent the entire state was selected to develop a CT planning document. This document was to define the problem, develop a model to indicate work load; set standards and criteria for head as well as whole body CT units; inventory existing facilities and services plus a projected inventory of services; and to review current literature.

The committee is comprised of five Indiana physicians with specialties in neurology, neurosurgery, neuroradiology, or diagnostic radiology, and two out-of-state physicians, qualified and recognized authorities in the field; an executive director of an established and recognized comprehensive health planning agency; and an administrator of an Indiana hospital. In addition, representatives from the Radiological Health Section of the Indiana State Board of Health, the health insurance industry, and the Indiana Regional Medical Program act as consultants to the committee.

Some may criticize the makeup of the committee as being provider controlled and not having consumer representation. However, the purpose of the committee is to develop necessary medical and technical criteria and standards for future health planning organizations so that Indiana residents will have the best CT services at the least possible cost. Future planning agencies that will approve new services in the area will have adequate consumer representation under P.L. 93-641.

The committee developed an interim plan for CT in Indiana, which was adopted by the executive board of the Indiana State Board of Health in September 1975. This plan is limited primarily to head CT units. With completion of the clinical evaluation of the whole body scanner, the committee has begun to develop criteria and standards for all CT units. The final plan will not pertain to the medical treatment of patients, since the Indiana State Board of Health is not concerned with clinical management of individual patients. The plan is designed primarily for the provider concerned with community needs and the health care planner who must judge their validity. The plan also is designed for lay people to use as an independent resource document.

After the initial plan has been adopted by the Indiana State Board of Health, the committee will be designated as a permanent technical advisory committee to the Board of Health. The committee is mandated to meet at least annually, to review the latest data, and then update the plan to keep it current.

Some obvious questions must be faced by persons charged with CT planning. These include: What is the effectiveness of the scanners? How many are needed? How great will the demand be for their use? How will they affect health care costs? and What is the rate of obsolescence for the current models?

Other specific areas of medicine and technology must be addressed by planning groups.

1. Community standard of practice. Since CT provides physicians with more knowledge about the brain and body than was previously possible, will the practice of defensive medicine (brought on by malpractice cases) increase the demand for a supplemental service such as CT?

2. What procedures does CT complement or replace?

Experience with head scanners shows that cerebral angiograms, pneumoencephalograms, nuclear brain scans, and other procedures are performed on patients who are also potential candidates for CT scans. Which procedures identify candidates for CT scans? What percentage of each procedure can be used to develop a formula for CT utilization?

3. Utilization rates. At present, operating time is used for less than one patient per hour. Although scan speed time has been reduced from $4\frac{1}{2}$ min to 20 sec (and even faster in newer prototypes), the processing time per scan remains approximately the same. Until processing times are reduced or alternatives are found, increased utilization can only come through additional hours of operation or additional installations. What should be the minimum utilization rate? What percentage of normal scans to the total number of scans would be acceptable?

4. Private ownership of CT units. Since present planning guidelines and certificate of need programs focus on the institutional location and exempt private offices and clinics from project review, how does a planning group judiciously address the issue of privately owned units in noninstitutional settings? Currently, if an institution does not meet the criteria, private ownership is a permissible alternative. If, in agreement with an institution, such a private office installation is utilized for inpatient service, transportation as well as medical backup in emergency situations are important considerations.

5. Distribution of CT units. Should guidelines be based on a geographical and/or population basis? Should institutions only be considered for the placement of CT units? Should CT units in noninstitutional settings be included in the inventory? If it is determined that two CT units are needed for a medical service area and there are two privately-owned units in operation, should an institution be denied a unit if that institution meets all the criteria and standards developed?

6. Cost of a scan. Since patient volume has a significant effect on the cost per patient, as patient volume increases

above a certain point, should costs to the patient be reduced? What is a reasonable utilization ratio/charge? Considering that the present average cost per basic scan in the United States (including both technical and professional charges) is \$220, can a CT unit be considered a primary screening device? In many third-party payor contracts in the health care insurance industry, the total diagnostic outpatient charges are limited to \$200 per year. After this point, the charges can be placed against a major medical policy. This usually carries a \$100 deductible charge and is then reimbursed at 80% of charges over the deductible.

7. Radiation hazard levels. What are the acceptable dosage rates that should be used for head units? For total body units?

8. Staffing. What personnel are needed to adequately staff a CT unit? Should this include physicians, radiation physicists, computer technologists, radiology technologists, secretary, etc.? What are the qualifications needed by each?

9. Cost effectiveness. What is the number of CT examinations required to evaluate effectiveness? Any valid study of cost effectiveness must be done on the basis of costs—not charges. Areas that must be examined to determine cost effectiveness include reduction of staffing and costs within institutions. The savings in charges in avoidance of admissions by CT procedures can be misleading since the empty beds could actually increase the per diem rate.

An Added Impetus

While Indiana was in the process of developing the specialized medical services plans, the National Health Planning and Resources Development Act of 1974 (P.L. 93-641) became law. In developing this legislation, Congress listed the following assumptions:

1. Achievement of equal access to quality health care at a reasonable price is a priority of the federal government.

2. Massive infusion of federal funds into the existing health care system has contributed to inflationary increases in the cost of health care and failed to produce an adequate supply or distribution of health resources; and, consequently, has not made possible equal access for everyone to such resources.

3. Many and increasing responses to these problems by the public sector (federal, state, and local) and the private sector have not resulted in a comprehensive, rational approach to the present problems.

4. Increases in the cost of health care, particularly of hospital stays, have been uncontrollable and inflationary, and there are presently inadequate incentives for the use of appropriate alternative levels of health care, and for the substitution of ambulatory and intermediate care for inpatient hospital care.

5. Since the health care provider is one of the most important participants in any health care delivery system, health policy must address the

legitimate needs and concerns of the provider, and it is imperative that the provider be encouraged to plan an active role in developing health policy at all levels.

6. Large segments of the public are lacking in basic knowledge regarding proper personal health care and methods for effective use of available health services.

A solution to the problems listed by Congress is made even more urgent by the potential enactment of a National Health Insurance Program in the future. Such legislation would place an extra burden on existing health care facilities and manpower at the same time demanding a rational approach to the controlled growth of resources without creating costly surpluses.

Discussion

Abstract issues in the health care system are facing each of us today. Some of the most compelling questions are: Can and should medical science advances be regulated? How can costs and benefits in health care be balanced? and Who should decide what to spend on new technology in health care?

In search of answers to these and related questions, debate seems to place medical personnel on one side and bureaucrats on the other. But, in any event, it appears that federal leadership, direction, and regulation are inevitable.

To maintain some measure of local authority, committees such as the Indiana CT committee have been appointed. With input from both sides as well as the health insurance industry and others concerned, such committees seek realistic and viable criteria and standards. Hopefully, these will accomplish what P.L. 93-641 was designed to do—build on what is good about the system today and negate that which is deficient.

Some critics of health planning claim that CT planning standards, criteria, and guidelines may be premature since there is no way to predict the need for the service. On the other hand, the Indiana State Board of Health believes that planning (as imperfect as it may be) is a necessary alternative to uncontrolled proliferation of CT units at an unknown cost.

While health care planners realize the great potential medical value of CT, they worry that institutions and other facilities may acquire more units than needed. If this happens, patients will pay the price for expensive and underutilized equipment. In the institutional setting, rates would be adjusted to pay for underused equipment, shifting the cost to all patients. Some surveys indicate that the more scanners that are available, the more the demand will be for them. CT may be a technology that generates its own demand and is used simply because it is available—whether it is necessary or not. In this respect, it would not be unique.

It is the hope of health care planners that standards, criteria, and guidelines can be developed that will allow CT units to be placed in adequate numbers in proper locations to serve the patient without unnecessary duplication

and expenditure. Currently there are more questions than facts. Only experience will determine whether criteria and guidelines formulated now will have been appropriate when viewed in retrospect. But a start must be made and it must be undertaken by those most knowledgeable in the

field: health professionals, the health insurance industry, and health care administrators. Their assistance to local health planning agencies has already been generous and must continue if local conditions are to determine rationally distributed local CT services.

Economic Analysis of Computed Tomography Units

RONALD G. EVENS¹ AND R. GILBERT JOST¹

All operating CT installations in the United States were surveyed in January 1976; data were obtained from 98 of 140 installations. Although the respondents represented 80 head units and 18 head and body units, the overwhelming experience was with head CT studies. CT equipment was installed in an average of 1.3 months, operated 64 hr per week and examined 50–55 patients per week. A downtime of 7 hr per week was reported. Radiologists are responsible for 92 of 98 installations, and 90% of installations are in a hospital. The scheduling delay averages 1.6 days for inpatients and 11.5 days for outpatients. The delay is increasing in many installations. The estimated total yearly technical cost is \$325,000–\$371,000 per installation, depending upon patient volume. The estimated technical cost per patient (when 50 patients per week are studied) compares favorably with the estimated net revenue per patient from the average basic technical charge (\$130 compared to \$138). A separate billing method is used by 59% of installations, and 76% have an extra charge for contrast injection and additional studies; 60% of patients receive contrast. The reported total charges during the last 3 months were higher in installations that (1) charged additionally for contrast, (2) were located in outpatient settings, and (3) had non-radiologists as the responsible physician. It should be emphasized that most CT installations are not independent activities and should be considered an integral part of a diagnostic radiology department or office.

Introduction

Computed tomography (CT) was introduced in 1972 [1, 2] and has rapidly gained acceptance as an important new diagnostic method. The first generation radiologic computer system required several minutes for patient scanning with a water bag surrounding the anatomy under study. The initial clinical experience was limited to the cranial vault. Thousands of head CT studies have now been performed [3–6], and the examination has proven its diagnostic value in patients with neurologic disease.

In a short time, CT body scanners were developed [7, 8]. Initially each scan required more than 1 min, making it impossible to suspend respiration during the examination. In 1975, CT equipment became available which could scan in less than 20 sec without the need for a water bag, so that it is now possible to scan the entire body with respiration suspended [9]. The availability of high quality CT images of the abdomen, chest, head and neck, and extremities has generated great excitement among radiologists. While many important clinical observations have been made [10], the exact position of CT body scanning in the patient's diagnostic workup has not yet been completely established.

The impact of CT on medical practice has been accompanied by a definite financial impact. The purchase price for

each unit of equipment is several hundred thousand dollars, and more than 300 units have already been sold. Some sales estimates number 1,000 or more units. Radiologic diagnostic equipment purchases of this magnitude have a decided effect upon diagnostic costs, hospital budgets, third party payer reimbursement, and the purchase of other x-ray equipment. Equipment utilization requires additional costs for operation (including space, personnel, maintenance, contrast, etc.) which have not been quantitated. Questions regarding the economics of CT have increased with the announcement of whole body equipment and the immediate interest by radiologists (in both hospital and outpatient practice) in their purchase. Data related to the financial operation of CT equipment can be of primary importance in decisions regarding purchase [11]. This study was undertaken to obtain utilization, cost, and revenue data from current users of CT equipment.

Materials and Methods

The location of CT equipment (or anticipated location by January 1976) was obtained from the known equipment manufacturers (ACTA, Pfizer; Delta, Ohio-Nuclear; and EMI Limited) at the meeting of the Radiological Society of North America in November 1975.

A total of 147 installations were expected to be in operation by January 1976, and a four-page economic survey was sent to the physician responsible for each unit. By March 1, 1976, 98 surveys were returned and are the basis for this study. We were notified by the physicians responsible for seven potential installations that the units were not in operation by January 1976, so the actual number of units for study was 140 (or less since some of the "no responses" may not have been installed). The exceptionally high percentage of surveys returned (70%) indicates the interest in this information by physicians responsible for CT and their willingness to cooperate in an economic evaluation.

The survey dealt with detailed questions on the location of equipment, utilization of equipment, costs, and revenues. Data from each respondent were entered into a PDP-11/40 computer system in order that a series of tabulations and comparisons could be made.

Results

CT Equipment, Location, and Administration

Of the 98 units studied, 80 are used entirely for examinations of the head, while 18 are used for both head and body. A large majority of current CT installations are manufactured by EMI; however, several physicians with ACTA and Delta units responded to the survey. When appropriate, the data are tabulated by manufacturer and in total. Since only a small number of ACTA and Delta units are operational at this time, statistical comparisons between manufacturers

Received March 26, 1976.

R. G. Jost is a James Picker Scholar in Academic Radiology.

¹ Department of Radiology, Washington University School of Medicine, and Mallinckrodt Institute of Radiology, 510 South Kingshighway, St. Louis, Missouri 63110.

TABLE 1
Equipment Data

	Total	ACTA	Delta	EMI
Location :				
Hospital	87	8	9	70
Outpatient	11	0	0	11
Total	98	8	9	81
Installation time (mo)	1.3	1.1	.9	1.3
Maintenance (hr/week) :				
Regular	1.9	1.5	1.5	2.0
Unscheduled	5.2	6.0	4.6	5.3
Total	7.1	7.5	6.1	7.3

Note.—Mean values.

have not been developed. All units for the head only are EMI, 17 head and body units are ACTA or Delta, and one body unit is EMI.

The average time from delivery to full operation was 1.3 months (range 1 week to 7 months) (table 1). The average time per week that equipment was "down" for regular maintenance or unscheduled breakdown was 7.1 hr.

The location of 95% of units is in the radiology department of a hospital or in a radiology outpatient office (table 2). Nearly all hospital units are in the radiology department, but four of 11 outpatient units are located in nonradiology offices. Scan interpretation and reporting is the responsibility of radiologists in 92 of the 98 installations. In the six locations where a radiologist is not responsible for interpretation, the responsible physicians are neurologists, neurosurgeons, or both. The hospital installations included hospitals with a range of 75–1,800 beds. The mean bed number was 595. Figure 1 shows the location of units by hospital size.

CT Utilization

All units were in operation 5 or more days per week (mean 5.4 days) (fig. 2). Some respondents who indicated 7 days probably meant on an emergency basis rather than standard operation. Mean operating time per day is 11.8 hr, and 90 of 98 units were available for urgent cases 24 hr per day.

Utilization data are shown in table 3. All units schedule examinations (with the exception of emergency cases); the average scheduling delay is 1.6 days for inpatients and 11.5 days for outpatients. The scheduling delay for inpatients is increasing in 21% of installations and decreasing in 9%, whereas the scheduling delay for outpatients is increasing in 35% of installations and decreasing in only 6%.

The survey also asked about any effect on utilization as a result of new CT equipment in the nearby area. Seventeen installations (18%) reported no other units in the area, 49 (53%) reported no effect, 27 (29%) reported a decrease in scheduling delays after the availability of other units, and five did not answer.

TABLE 2
Location and Responsible Physician

	No.
Location :	
Hospital :	
Radiology department	85
Other	2
Outpatient :	
Radiology department	7
Other	4
Responsible physician :	
Radiologist	92
Other specialist	6

Cost Data

Data on equipment and space costs are shown in table 4. The cost of equipment varies by manufacturer and also with the selection of accessories, time of purchase, and method of purchase (whether interest costs are incurred). The equipment was purchased with capital funds in 52 installations, by lease arrangement in 25 installations, borrowed funds in seven, and various combinations in nine. The equipment was the gift of major donors in five installations. Straight-line depreciation methods were utilized in 68 cases and accelerated means in 10; 20 respondents did not answer. The mean number of years for depreciation is 5.8 years; nearly half of all installations have selected 5 years.

Most equipment is maintained by arrangement with the manufacturer (69 with manufacturer alone, 17 by a combination of manufacturer and owner, and four by owner alone). The average cost of a "full" maintenance contract is \$25,000 per year (range \$21,000–\$28,000).

The average space allocation is 537 square feet, and remodeling costs average \$19,903. We excluded the three respondents who listed remodeling costs of greater than \$50,000 since these figures were probably related to new construction.

Personnel were estimated in full-time equivalents. The average personnel assigned to each CT unit is 0.96 radiologists, 2.3 x-ray technologists, 1.1 aide, and 1.2 "other" personnel.

The mean cost of contrast was \$7.70 for each use, and the cost of other supplies (polaroid film, magnetic tape, "floppy" discs) had a mean value of \$10 per patient.

Most respondents recognized a variety of indirect costs that included administration, billing, collection, transcription, training, messenger service, and hospital and university overhead; however, few respondents could report the actual cost of overhead items. The estimated overhead costs ranged from \$1,000 to \$208,000 per year.

Revenue Data

Data on the number of patients examined per week and per month, amount of charges, and information relating to charges for contrast injection are shown in table 5. Fifty-

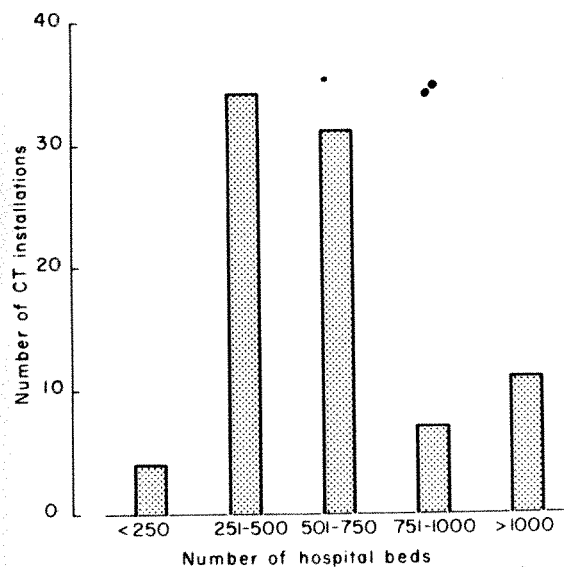


Fig. 1.—Location of units by hospital size. Only four of 87 units are in hospitals with fewer than 250 beds.

TABLE 3
Utilization Data

	Total	ACTA	Delta	EMI
Usual operation (hr/day)	11.8	9.2	10.6	12.2
Patients/week:				
Scheduled	55	40	64	57
Examined	58	38	60	61
Studies with contrast (%)	60	68	67	59

Note.—Mean values.

TABLE 4
Cost Data

	Total	ACTA	Delta	EMI
Equipment cost (\$)	387,000	277,000	378,000	397,000
Years depreciated	5.8	5.8	5.2	5.9
% using 5 year depreciation	49	60	43	51
Space allocation (ft ²)	537	564	423	543
Remodeling cost (\$)	19,303	15,055	34,000	18,524

Note.—Mean values.

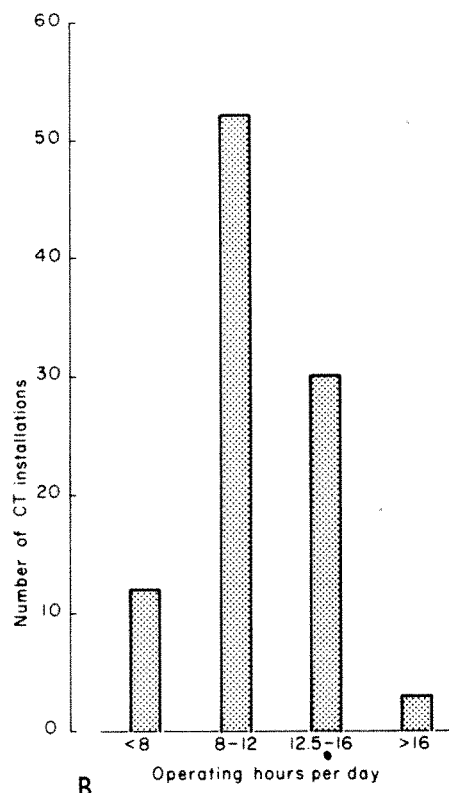
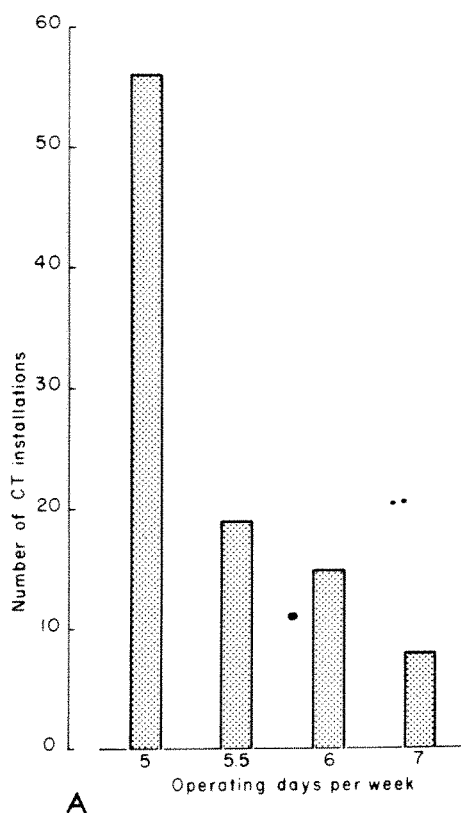


Fig. 2.—Usual operating week (A) and day (B) of CT installations. Mean operating time is 11.8 hr/day, 5.4 days/week.

TABLE 5
Revenue Data

	Total	ACTA	Delta	EMI
Patients examined:				
Per week.....	58	38	60	61
Per month.....	228	110	195	241
Separated charges (\$):				
Technical.....	157	158	157	157
Professional.....	63	55	102	60
Total.....	220	213	257	217
Single charge (\$):.....	226	223	243	223
Additional charge for con-				
trast (%).....	76	86	60	78
Charge for contrast (\$):..	67	68	48	68
% studied with contrast..	60	68	67	59
Charges last 3 months				
(\$)*.....	136,000	99,000	129,000	138,000

Note:—Mean values.

* Data from 48 installations operating more than 6 months.

seven of 96 responders (59%) separated charges into a technical and professional component, while 39 (41%) submitted one charge for both technical and professional services. The total basic charge is slightly less with the separate method (\$220 vs. \$226).

The method for charging is quite complex and varies considerably. Most installations (76%) charge extra for contrast injection and additional studies, with the average total charge for contrast being \$67. Other extra charges and the number of installations using them are: additional views, 13; limited study or follow-up, 13; with and without contrast, 10; orbit study, nine; patient sedation, four; and other, two.

Ten respondents have a charge for a study without contrast, another charge for a study with contrast, and a higher charge for studies with and without contrast. The charge for an examination with and without contrast ranged from \$156 to \$410.

Of the 98 respondents, 54 reported information on their partial pay and bad debt reduction as a percentage of gross revenues (mean value 12.2%). Sixty listed their total charges for the last 3 months; however, since many units were in operation for relatively short periods of time, the information shown in table 5 is from 48 installations in operation for 6 months or more. Note the discrepancy between calculated total charges (patients examined per week \times usual charge \times 13 weeks) and the reported 3 month charges.

Discussion

Between 1972 and January 1976, approximately 140 CT systems were installed throughout the United States. This report summarizes data from 98 installations. We have studied the utilization and economics of CT operation at the Mallinckrodt Institute (two EMI head units and one EMI body unit) in detail, and these data compare closely to our

TABLE 6
Estimated Technical Costs per Year

Item	Cost (\$)
Direct costs:	
Fixed:	
Equipment*	77,400
Maintenance contract.....	25,000
Space remodeling*.....	3,860
Space upkeep†.....	6,229
Personnel‡.....	49,200
New developments (equipment).....	25,000
Total.....	186,689
Variable (at 50 patients/week):	
Contrast (\$4.60/patient)\$.....	11,960
Other (\$10.00/patient).....	26,000
Total.....	37,960
Total direct costs.....	224,649
Indirect costs (if 50% of direct).....	112,324
Total costs.....	336,973

* 5 year straight/line depreciation.

† 537 ft² \times \$11.60/ft².

‡ See text.

\$ \$7.70 per contrast injection times 60% of patients requiring contrast.

experience. This study should be considered an evaluation of head CT experience, even though 18 of 98 installations were classified as head and body units. ACTA and Delta units have body capabilities, but recent publications indicate a high percentage and head studies with the equipment [8]. The only EMI body unit reported here was in operation 4 months and was utilized for clinical protocol studies. Our early experience predicts certain differences between body and head utilization (e.g., higher equipment cost, more radiologist time, and fewer patients examined per day). Consequently, economic analysis of body CT must be postponed until more data are available.

CT Equipment, Location, and Administration

The majority of respondents have experience with EMI equipment (the actual situation as of January 1976); however, several respondents practice with ACTA and Delta equipment, and the data have been shown by manufacturer. Downtime (scheduled maintenance as well as breakdown) was significant, averaging 7.1 hr per week for all units. Equipment installation required an average of 1.3 months and is similar for all three manufacturers.

Approximately 90% of installations are located in hospitals, and essentially all hospital units are located in a radiology department. Of the 10% in the outpatient setting, four of 11 are located in nonradiology offices. Examinations are interpreted and reported by radiologists in 94% of cases. This overwhelming predominance of radiologic responsibility is undoubtedly related to many factors, including the basis of CT in diagnostic radiation physics and

the expertise of radiologists in interpreting visual and anatomical data. The selection of radiologists as the responsible physician for CT should be even more justifiable with body scanning because of the required diagnostic abilities and experience in several anatomical regions.

CT Utilization

This study documents the great clinical demand for CT. All units were in operation an average of 5.4 days per week and 11.8 hr per day. More than 90% are available for emergency cases. The clinical demand for CT scans has not been met, as indicated by the increasing scheduling delay for inpatients and outpatients in 21% and 35% of installations, respectively. An increase in scheduling delay is significant because average delay times are already 1.6 days for inpatients and 11.5 days for outpatients. Of the 76 installations reporting additional CT units in their geographic area, only one-third indicated a decrease in scheduling delay because of the increased CT capability. The literature supports the fact that clinical demand is based on diagnostic utility and improvement in patient care [10, 12]. Some scheduling delay can be diminished by an increase in operation time or the throughput of patients per day. Unfortunately, we have found great difficulty in improving these factors at the Mallinckrodt Institute, in spite of significant effort. (Installations are already operating an average 11.8 hr day.) We believe the answer must be with an increased number of installations.

An average of 58 patients per week are examined, and 60% of patients receive intravenous iodinated contrast and additional scans (table 3). Most institutions perform the contrast-enhanced study after a routine study, so the examination time is considerably lengthened for these patients (time to inject contrast and obtain appropriate views). Although respondents reported an average of 58 patient examination per week, they also reported an average of 228 cases per month or 53 patients per week (table 5). This apparent discrepancy is probably explained by a continually increasing demand in some installations and by fluctuation in the number of scheduled and emergency cases. The amount of charges in the last 3 months also suggests an average patient volume of less than 58 per week. We believe the average number of patients per week per CT unit is between 50 and 55.

CT Costs

Costs vary among installations due to such factors as depreciation method, maintenance requirements, number of personnel, differing costs in geographic areas, utilization of equipment, and overhead allocation. In addition, there is no average or typical installation; individual variations develop with varying medical settings and practice methods. Nevertheless, we believe it is important to develop approximate costs per installation. We estimated technical costs since our survey did not encompass direct and indirect costs of the professional responsibility.

An outline of our approach in estimating technical costs is shown in table 6. The average equipment cost has been allocated on a yearly basis by the straight-line depreciation

method over 5 years since it was the most common method chosen by respondents. The average cost of a maintenance contract (the most common method for maintenance) is shown. Initial space-remodeling costs were allocated by a straight-line depreciation method. Yearly space upkeep is calculated by the average number of square feet per unit times the average cost per square foot. The reported mean number of technical personnel was multiplied by \$14,000 per technologist, \$7,000 per aide, and \$7,000 per other employee. These estimates are reasonable personnel costs but certainly vary around the United States. A value of \$25,000 per year is added for updating equipment, since this has been our experience during the past 3 years and is probably conservative. These costs total \$186,689 per year and are classified as fixed costs since they remain constant in spite of changes in number of examinations.

The variable costs (costs which change with the number of examinations) are calculated at an examination rate of 50 patients per week and refer to the cost of items such as contrast, Polaroid film and magnetic tape. The sum of fixed and variable costs directly related to CT examinations is \$224,649 per installation.

Indirect costs (sometimes called overhead) are the cost of activities that are shared among several radiology procedures or are difficult to identify with a specific installation. These activities include administration, transcription, billing, collection, transportation, training, and hospital or university overhead. While these costs must be allocated to CT, the survey respondents were unable to quantify them (estimates varied from \$1,000 to \$208,000 per year). We have discussed various allocation methods with accountants, hospital administrators, economists, and radiology department business managers and have found no standard or "best" method. We set indirect costs at 50% of direct costs because this is the approximate percentage at the Mallinckrodt Institute. The interested reader can determine his own indirect cost amount [13]. Thus the total cost of a single CT installation is \$336,973 per year when an average of 50 patients per week are examined.

Patient volume has minimal effect on total costs because only the variable costs (and some indirect costs) increase with more procedures. On the other hand, increased patient volume has a *significant* effect on reducing the cost per patient (table 7). As discussed above, the average number of patients studied per week is between 50 and 55 (12 hr day), and the estimated technical cost is \$120 to \$130 per patient. In actual practice, some of the fixed costs may increase with activity (personnel or maintenance), and the variable costs may decrease with activity (reduced prices with quantity purchases); however, within a certain range of patient volume, the definition of fixed and variable costs holds. This concept is illustrated in figure 3.

This study was designed to provide information on CT cost with CT equipment as a specific cost center. However, CT installations are not a separate entity but an integral part of diagnostic radiology. Thus there are many required costs in addition to the usual calculated direct costs. Additional costs can be partially estimated by indirect cost allocation methods, but there are other considerations. For

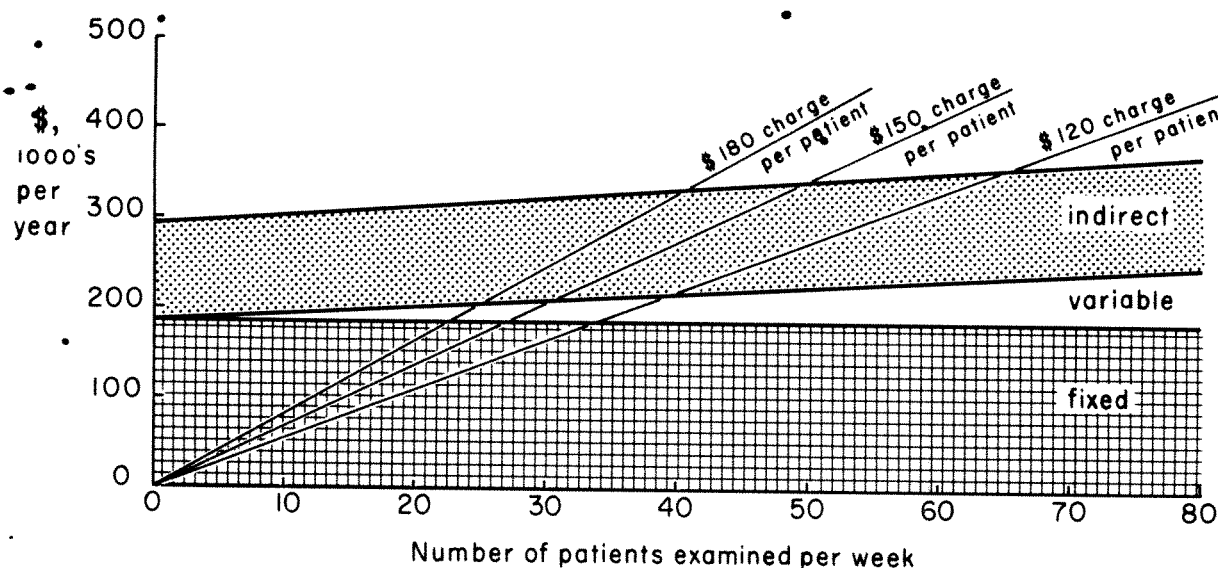


Fig. 3.—Break-even points for CT technical cost and revenues. Net revenues obtained from technical charges of \$120, \$150, and \$180 per patient shown by diagonal lines using partial pay-bad debt reduction of 12.2%. Costs are as estimated in table 7. Break-even point occurs where diagonal revenue line meets total cost (fixed+variable+indirect).

TABLE 7
Effect of Patient Volume on Technical Costs

	Patients/Week			
	80	60	50	40
Costs:				
Fixed.....	186,689	186,689	186,689	186,689
Variable.....	60,736	45,552	37,960	30,368
Indirect.....	123,712	116,125	112,324	108,528
Total.....	371,137	348,375	336,973	325,585
Cost/patient (\$)...	89.21	111.65	129.60	156.53

TABLE 8
Typical Revenues per Patient

	Gross (\$)	Net (\$) *
Technical:		
Basic exam charge.....	157	137.85
Plus extra charge for contrast †	186	163.31
Professional:		
Basic exam charge.....	63	55.31
Plus extra charge for contrast †	74	64.97

* Utilizing partial pay-bad debt reduction of 12.2%.

† Assume similar ratio of professional/technical components as standard charge and 60% of patients receive contrast.

example, CT examinations have diminished the number of pneumoencephalograms, cerebral arteriograms, and brain scans by 30%–70% in many institutions [10, 12]. Nevertheless, these tests remain necessary in certain patients, and the facilities to perform them must be maintained. The high fixed costs of these procedures will continue while examinations, billings, and revenues decrease, becoming an even greater financial burden to radiology departments. There must be some mechanism for recovering these fixed costs, and this point should be considered when analyzing CT installations.

CT Revenues

Charges per installation should be a product of the number of patients examined and the average charge per patient. The average charge per patient is a complex value since many installations charge extra for contrast injection and some have other extra charges. Utilizing the simplest example (a basic examination charge without additional charges), the estimated total charges for 3 months is con-

siderably higher than the charges reported for the same period: 58.4 patients per week \times 13 weeks \times \$220 (total of separated charges) or \$226 (single charge) = \$167,000 or \$171,000 for 3 months, and the average charge reported was \$136,000. This discrepancy can be explained by one or more of the following considerations:

1. The actual number of patients examined per week is less than 58. This is probably a major consideration since the reported number examined per month (228) is equal to 53 patients per week.
 2. Every patient examined is not charged, or some patients are charged less than the basic charge.
 3. Some installations reported only technical charges or only professional charges.
 4. The reported charges were collections (net revenue).
- Since we do not know the reason for this discrepancy, actual charges (and therefore actual revenues) from CT installations cannot be determined.

The average charge per patient allows the calculation of net revenue per patient by using the reported average partial

TABLE 9
Revenue Effect of Charging for Contrast

	Additional Charge for Contrast	No Additional Charge for Contrast
Patients examined:		
Per week	61	55
Per month	236	204
Separated charges (\$):		
Technical	154	160
Professional	59	69
Total	213	229
Single charge (\$)	230	219
Separated/combined*	50/26	6/13
% studied with contrast	62	54
Other charges†	27/35	1/13
Charges last 3 months (\$)‡	148,000	92,000

Note.—Mean values.

* Ratio of respondents that separated charges to respondents that have a combined charge.

† Ratio of respondents with additional charges (other than contrast) to respondents having no additional charges.

‡ Data from installations operating more than 6 months.

pay—bad debt reduction of 12.2% (table 8). The average technical basic examination charge compares closely to the estimated technical cost per patient at a patient volume of 50 per week (\$137.85 compared to \$129.60). The major reported additional charge (contrast injection in 76% of installations) adds a significant amount to the calculated net revenue per patient because contrast injection is required in 60% of patients and the average additional charge for contrast is \$67.

The effect of an additional charge for contrast on revenue is shown in table 9. Installations charging for contrast examined more patients per week and month, more frequently used a separated method of billing, utilized contrast in a higher percentage of patients, commonly had other additional charges, and reported higher total charges for the last 3 months (\$148,000 vs. \$92,000) than installations without an additional charge. Accordingly, a typical charge in installations with an additional charge for contrast is \$213 per patient for a study without contrast (38% of patients) and \$280 (\$213+\$67) for patients with and without contrast (62% of patients), for an average \$254.50 per patient. For installations without the additional charge, the cost is \$219 per patient. Since this study demonstrates that the standard CT examination usually includes contrast, we suggest that instead of an additional charge for contrast injection, a basic technical charge of appropriate amount be used.

The amount of charge is obviously an important factor; the calculated revenues from technical charges of \$120, \$150, and \$180 are illustrated in figure 3. A financial break-even point [13, 14] occurs when the revenue line crosses total costs for a specific number of patients studied per week. With CT installations, the estimated break-even points for technical charges of \$120, \$150, and \$180 occur at 65, 49, and 40 patients per week, respectively. A similar

TABLE 10
Data Comparison by Location

	Hospital Location	Outpatient Location
No. units	87	11
Usual operation (hr/day)	11.9	11
Patients/week:		
Scheduled	53	69
Examined	58	61
Accelerated depreciation	6/68	4/10
Assigned space (ft ²)	516	713
Remodeling costs (\$)	19,579	17,433
% studied with contrast	61	55
Separated charges (\$):		
Technical	156	166
Professional	63	52
Total	219	218
Single charge (\$)	228	213
Additional charge for contrast (%)	75	63
Charge for contrast (\$)	65	82
Other charges*	23/44	5/5
Partial pay and bad debt (%)	12.5	10.6
Charges last 3 months (\$)†	129,000	161,000

Note.—Mean values.

* Ratio of respondents with additional charges (other than contrast) to respondents having no additional charges.

† Units in operation more than 6 months.

analysis can be performed for a specific installation using the actual costs and charges.

We have not analyzed professional revenues because we do not have data to analyze professional costs. Gross and net professional revenues can be estimated from the values in table 8 and the number of examinations performed. The estimated net professional revenues in an installation studying 50 patients per week are \$143,806 with the average basic examination charge and \$168,922 with an extra charge for contrast.

Additional Considerations

Location (hospital versus outpatient). The data were analyzed according to whether CT units were located in a hospital or outpatient facility (table 10). Many of the observations are predictable by the usual differences in hospital and outpatient medical care. For example, outpatient CT units were in operation fewer hours per day yet examined slightly more patients per week. Outpatient medicine services ambulatory patients, so the average time for examination should be less.

A higher percentage of outpatient locations used accelerated methods of depreciation and remodeling costs were lower, even though the outpatient units have more assigned space. Indirect costs are traditionally less in outpatient practice, although we were unable to quantitate this. There was a 22% difference in total charges during the last 3 months between outpatient and inpatient locations. This is partially explained by higher patient volume, higher extra charge for contrast, and the use of extra charges

TABLE 11
Revenue Analysis by Responsible Physician

	Radiologists	Other Specialists
Patients examined :		
Per week	59	66
Per month	227	239
Separated charges (\$) :		
Technical	154	166
Professional	61	55
Total	215	221
Single charge (\$)	226	227
Separated/combined*	52/36	4/2
Additional charge for contrast (%)	80	66
Charge for contrast (\$)	64	98
% studied with contrast	61	60
Other charges†	25/45	3/3
Charges last 3 months (\$)‡	133,000	163,000

Note.—Mean values.

* Ratio of respondents that separated charges to respondents that have a combined charge.

† Ratio of respondents with additional charges (other than contrast) to respondents having no additional charges.

‡ Data from installations operating for more than 6 months.

(in addition to contrast) at the outpatient locations.

Responsible physician. Table 11 compares installations with radiologists as the responsible physician to installations where other specialists assume responsibility for interpretation. Installations where the radiologist was responsible performed fewer examinations per week and month, had smaller total separated charges and a similar single charge, more frequently charged extra for contrast, had a considerably smaller charge for contrast (\$64 vs. \$98), and had lower total charges during the last 3 months. The data are similar to those comparing hospital and outpatient locations since all but two of 87 hospital locations had radiologists as responsible physicians, while four of 11 outpatient locations were under the responsibility of other specialists.

Cost Effectiveness

These data enable a discussion of costs but not of cost effectiveness. Future investigations must define the number of CT examinations required to detect a disease process, to save life or postpone death, or to improve the quality of life before we can begin to evaluate effectiveness.

A recent study [15] predicts cost savings based on a reduction in hospital days and diagnostic procedures. The analysis was based on charges rather than costs, and the predicted reduction in pneumoencephalograms, angiograms, and hospital days was validated only with pneumoencephalograms. At the Mallinckrodt Institute we have documented a 66%, 34%, and 29% reduction in pneumoencephalograms, cerebral angiograms, and radionuclide brain scans, respectively, since installation of CT head scanning equipment. Costs have not been diminished by the same percentage because of the continued need for

certain studies with associated high fixed costs. A reduction of $\frac{1}{2}$ day in average hospital stay on the neurology service has been noted, but a similar reduction occurred in our hospital on other services.

Further discussion of cost effectiveness must be postponed until additional data are available. However, CT has been demonstrated to be an effective examination that has markedly improved diagnostic capabilities and reduced pain and hazard in many patients. We believe the economic parameters described in this study bring us one step closer to analyzing cost effectiveness.

ACKNOWLEDGMENTS

We gratefully acknowledge the advice and counsel of Drs. Benham, Gado, Sagel, Stanley, and Ter-Pogossian. A special note of thanks to the three corporations that provided lists of active installations and the 98 physicians who responded to the survey.

REFERENCES

1. Hounsfield GN: Computerized transverse axial scanning (tomography). I. Description of system. *Br J Radiol* 46:1016-1022, 1973
2. Ambrose J: Computerized transverse axial scanning (tomography). II. Clinical application. *Br J Radiol* 46:1023-1047, 1973
3. Baker HL Jr, Houser OW, Campbell JK, Reese DF, Holman CB: Computerized tomography of the head. *JAMA* 233:1304-1308, 1975
4. Gado M, Coleman RE, Alderson PO: Clinical comparison of radionuclide brain imaging and computerized transmission tomography of the brain. I., in *Noninvasive Brain Imaging: Computed Tomography and Radionuclides*, edited by DeBlanc HJ Jr, Sorenson JA, New York Society of Nuclear Medicine, 1975, pp. 147-172
5. New PFJ, Scott WR, Schnur JA, Davis KR, Taveras JM: Computerized axial tomography with the EMI scanner. *Radiology* 110:109-123, 1974
6. Davis DO, Pressman BD: Computerized tomography of the brain. *Radiol Clin North Am* 12:297-313, 1974
7. Alfidi RJ, Haaga J, Meaney TF, MacIntyre WJ, Gonzalez L, Tarar R, Zelch MG, Boller M, Cook SA, Jelden G: Computed tomography of the thorax and abdomen: a preliminary report. *Radiology* 117:257-264, 1975
8. Twigg HL, Axelbaum SP, Schellinger D: Computerized body tomography with the ACTA scanner. *JAMA* 234:314-317, 1975
9. Sagel SS, Stanley RJ, Evens RG: Early clinical experience with motionless whole body computerized tomography. *Radiology* 119:321-330, 1976
10. Evens RG: New frontier for radiology: computed tomography. *Am J Roentgenol* 126:1117-1129, 1976
11. Evens RG: Financial accounting in radiology and nuclear medicine. *CRC Crit Rev Clin Radiol Nucl Med* 6:57-66, 1975
12. Baker HL Jr: The impact of computed tomography on neuro-radiologic practice. *Radiology* 116:637-640, 1975
13. Evens RG: Cost accounting in radiology and nuclear medicine. *CRC Crit Rev Clin Radiol Nucl Med* 6:67-79, 1975
14. Downham MC, Evens RG: Economic analysis of scintillation camera usage in nuclear medicine facilities. *Radiology* 101:643-649, 1971
15. Wortzman G, Holgate RC, Morgan PP: Cranial computed tomography: An evaluation of cost effectiveness. *Radiology* 117:75-77, 1975

Editorial

Orientation of CT Images

Most radiologists study radiographs as if they were facing the patient. This derives from the customary supine position for many examinations whether they be fluoroscopic or radiographic. Thus in film viewing, the patient's right is to the observer's left.

In dealing with transverse body section images as produced by ultrasound and CT, the same relationship would be preserved if the images were viewed as if from below (i.e., patient's right on the observer's left with anterior structures at the top of the image). This would have great merit for ease of comparison of images of a given organ whether they be radiographic films, ultrasound, CT scans, or radionuclide scans.

This orientation has been followed by the majority of those working in ultrasound. Bean and Geshner [1] surveyed 82 papers published in 1971–1973. By a ratio of 3:1, transverse scans of the abdomen were presented as though reviewed from below. A mail ballot of members of the American Institute of Ultrasound revealed a similar preference in 77% of those responding (P. Carlson, personal communication).

On the other hand, important anatomical references are inconsistent in this regard. The splendid atlas of cross-sectional anatomy by Eycleshymer and Schoemaker [2] presents images as if viewed from above with the supine patient's right on the viewer's right, while Pernkopf's textbook [3] shows the subject prone and viewed from above. Sobotta-Figge's anatomy textbook [4] and Takahashi's atlas of transverse tomography [5] both display the subject supine and viewed from below.

A further inconsistency exists in that both the initial brain imaging and whole body imaging CT units display the patient as seen from above, and a great deal of information has been published with this orientation. On the other hand, more recent whole body CT units present the image as viewed from below as demonstrated in some papers in this issue.

This matter has been dealt with very recently by several groups, and it appears that a consensus has developed. At the International Symposium and Course on Computerized Tomography (San Juan, Puerto Rico, April 1976), a general consensus was reached that all transverse displays of the body be oriented as though viewed from below, with the patient's right to the viewer's left. This group also recom-

mended the same orientation for CT images of the head, a departure from current practice. If this recommendation is followed, there will be no discontinuity in orientation from head to torso as would otherwise exist.

The Executive Committee of the Society for Neuro-radiology has endorsed this suggestion and recommends that CT images of the head be viewed as if from below.

Also meeting subsequent to the San Juan Symposium, the Executive Committee of the American Institute of Ultrasound in Medicine recommended that all transverse images by ultrasound be viewed from below.

Considering these developments, the editors of *Radiology* and the *American Journal of Roentgenology* have jointly declared that the preferred orientation of transverse section images for publication in those journals is that of the supine patient viewed from below [6]. This statement is a reaffirmation of that preference.

Thus it would appear that the great majority of physicians involved in transverse section imaging by ultrasound or CT are in agreement on the preferred orientation of the images for viewing. Further endorsement of this preference would be desirable by larger radiological organizations at their next annual meetings—the Radiological Society of North America, the American Roentgen Ray Society, and the American Institute for Ultrasound in Medicine. In the meantime, manufacturers should take cognizance of this preference in the design of equipment, and authors should be prepared to follow the convention.

Melvin M. Figley
William R. Eyler

REFERENCES

1. Bean WJ, Geshner J: Letter to the editor. *J Clin Ultrasound* 2:169–171, 1974
2. Eycleshymer AC, Schoemaker DM: *A Cross-Section Anatomy*. New York, Appleton-Century-Crofts, 1970
3. Pernkopf E: *Atlas of Topographical and Applied Human Anatomy*, vols 1 and 2. Philadelphia, Saunders, 1963
4. Sobotta, J, Figge HG: *Atlas of Human Anatomy*, 9th ed. New York, Hafner Press, 1974
5. Takahashi S: *An Atlas of Axial Transverse Tomography and Its Clinical Application*. New York, Springer, 1969
6. Eyler WR, Figley MM: Editorial: Computed tomography display. *Radiology* 119:487–488, 1976

Abstracts of Current Literature

Miscellaneous

Multidirectional tomography in reconstructive middle ear surgery. Wildbrand HF, Ekvall L (University of Uppsala, Uppsala Sweden) *Acta Radiol* 16:436-448, Sept 1975

Experience is reported with pre- and postoperative tomography in reconstructive surgery of the ossicular chain in 65 selected, operated cases. The main interest is concentrated on the long term appearance and position of bony transplants in the middle ear. Incus transposition and columella bone graft operations and their post operative tomographic appearances are described. Details of tomographic technique and patient positioning to visualize various aspects of the grafts are recommended. Causes of secondary hearing loss may be due to malposition of columella grafts on the stapedial foot plate, inclination of the graft, contact of the graft with environmental structures, or penetration of the columella through the foot plate. Tomographic reproductions and accompanying annotated figures illustrate these surgical complications.

J. D. Harley

Radiologic detection of breast cancer: review and recommendations. Sadowsky NL et al. (Massachusetts General Hospital, Boston, MA 02114). *N Engl J Med* 294:370-373, 1976

In response to recent public demand for mammographic examinations especially after the discovery of breast cancer in two nationally prominent women, the Ad Hoc Committee on Mammography at the Massachusetts Radiological Society reviewed the present indications, benefits, and risks of radiological techniques used in the detection of neoplastic breast disease. Either low dose film mammography or xeromammography can provide diagnostic information with minimal radiation hazard. Thermography is a sensitive, although nonspecific technique for interim followup observations and for screening of large groups of well patients. Mammographic examination should be performed prior to any contemplated breast surgery, and in women at high risk for the development of breast cancer. This latter group includes those with previous breast cancer, a strong family history for breast cancer, no children (or first child after the age of 35 years of age), certain other breast diseases (such as papillomatosis or ductal hyperplasia) endometrial or ovarian carcinoma, and women with more than 35 years of menstrual activity. Symptomatic patients should undergo mammography to evaluate solitary lesions, since the accuracy of this technique approaches 90% and can provide guidance regarding aspiration, excision under local or general anesthesia, etc. Both breasts should be included since 1.7% of patients have simultaneous bilateral carcinomas and up to 16% of breast cancer patients will develop a second primary in the opposite breast during their lifetime. Routine mammographic studies on healthy women may be initiated after age 35, the frequency of periodic reexamination being determined by clinical and mammographic findings.

Since potential induction of breast cancer by repeated exposure to ionizing radiation is a serious concern to mammographers, it is felt that collimation, compression, and low kV technique should be used. For screening purposes, only two projections on each breast should be necessary. It is felt that the benefit of discovering breast cancer in its earliest stage far outweighs any possible risk of carcinoma induction. At present there are four xeromammographic training centers in the U.S. (Boston, Detroit, Houston, and Los Angeles), as well as seven other primary breast training centers sponsored by the National Cancer Institute. These programs should be capable of providing an adequate supply of well trained physicians.

Lester Kalisher

The detection and significance of calcifications in the breast: a radiological and pathological study. Millis RR, Davis R, Stacey AJ (Institute of Cancer Research and Royal Marsden Hospital, London, SW 3, England. *Br J Radiol* 49:12-26, Jan 1976

This study investigated the optimal conditions required to demonstrate breast calcification as well as the significance of these particles within the breast. The radiological detection of calcification was compared using Xeroradiography, non-screen film, and a film-screen combination. In order to provide a wide range of sizes of naturally occurring calcifications, sections of breast tissue of known histology as well as whole mastectomy specimens were employed. The "threshold" values for Xeroradiography were 100 μm and for conventional radiography, 400 μm . The comparatively large exposure latitude of the Xeroradiographic plate and the "edge" effect combined to give better detection of calcification. The incidence of calcification seen on preoperative mammograms of 68 patients with carcinoma of the breast was 48.5%. Eleven (17%) of these showed predominantly fine calcification (less than 500 μm), emphasizing the importance of detection technique. Further calcification revealed by histological examination raised the overall incidence of calcification in mammary carcinomas to 63%. The incidence of calcification on preoperative mammograms of 135 patients with benign breast disease was 20%. The radiological features of calcification occurring in malignant and benign breast lesions were recorded and no definitive distinguishing features were established.

T. Noel K. Allan

The impact of computerized radiological reporting systems on the radiologist. Seltzer RA (Stanford University, Stanford, California). *Radiology* 118:737-739, March 1976

Although the advantages of automated reporting systems in diagnostic radiology far outweigh the disadvantages, radiologists have been slow to accept them because of their reluctance to work with the systems, i.e., assume a secretarial function, or to abandon *ad lib.* dictation. To realize the benefits of automated reporting, it is necessary for the radiologist to change his reporting style from one of "dictating while reading" to one of "reporting" only after searching the films and drawing a conclusion, and to appreciate that in this era of information overload, rapid delivery of a crisp, pertinent summary of his findings to the referring physician maximizes his influence on patient care.

Author's Abstract

Anatomic variation of the thoracic duct and visualization of mediastinal lymph nodes. Cha EM, Sirijintakarn P (Mount Sinai Hospital Medical Center, Chicago, Illinois). 119:45-48, April 1976

Of 243 thoracic ducts (TD) demonstrated during pedal lymphography, 65 (26.8%) had anatomic variations. In 58 of 65 cases with TD variants, mediastinal lymph nodes were visualized. This suggests that the radiographic appearance of mediastinal nodes is associated with TD anatomic variations. Two or more channels in the cervical portion of the thoracic duct were seen in 195 of the 243 cases. A classification of these anatomic variations is proposed.

Author's Abstract

Ultrasonics

Ultrasonics in the diagnosis of thyroid disease. Ramsey I, Meire H (King's College Hospital, London, England). *Clin Radiol* 26:191-198, April 1975

The authors report on the use of ultrasound A scans carried out in 47 patients with thyroid disease. Thirteen cases in which pathological examination was performed revealed a very close correlation. Information which could be obtained by ultrasound included whether or not thyroid tissue could be found, the anteroposterior diameter of various parts of the thyroid and echo characteristics of the thyroid tissue. Three basic patterns of the latter could be recognized: cystic, nodular, and homogeneous. In addition there

were two other groups which consisted of mixtures of cystic and nodular and of nodular and homogeneous. The size of individual cysts could also be measured. The normal thyroid gland was found to average 0.6–1.6 cm in anteroposterior diameter with a homogeneous ultrasound pattern. Asymmetry in the thyroid gland was found in both the normal and abnormal. Ultrasound has been found valuable in estimating the size of a mass, as well as differentiating a solid from a cystic lesion. Because of the absence of echoes within a cystic mass, it is valuable in studying enlargement of the thyroid gland both as an initial diagnostic tool and as a means of observing changes in thyroid size during therapy.

James F. Martin

The application of ultrasound to the study of thyroid enlargement: management of 450 cases. Rosen IB, Walfish PG, Miskin M (Mount Sinai Hospital, Suite 445, 600 University Avenue, Toronto M5G 1X5, Canada). *Arch Surg* 110:940–944, Aug 1975

The authors report on 450 cases of thyroid enlargement studied by B-mode ultrasonography. Tissue diagnosis was established by operation or aspiration cytology in 155 cases. They have shown that ultrasonography produces characteristic patterns correlative with specific thyroid disease and can be used to define surgical indications for the patient with a thyroid nodule. They describe the usual ultrasonic characteristics of the thyroid cyst, the solid lesion, cystadenomas, multinodular goiters and subacute thyroiditis. They also stress the value of this method of study in the pediatric age group and in pregnant patients. A comparison of the tissue diagnosis and the ultrasonic method revealed the latter to have a 94% reliability in the preoperative ultrasound assessment. Their series revealed a 16% incidence of malignancy, while 46% were benign adenomas (including the cystic variety) with a total incidence of 62% for tumors among the patients. There was a 20% incidence of non-neoplastic cystic lesions.

James F. Martin

Preoperative identification of tumor of the parathyroid by ultrasonotomography. Arima M, Yokoi H, Sonoda T (Osaka University Hospital, Osaka, Japan). *Surg Gynecol Obstet* 141:242–244, Aug 1975

The authors described their results in 10 patients who underwent ultrasonography of the parathyroid gland to correlate preoperative detection with the findings at operation. The examination was performed with a 5 megahertz transducer using a vinyl water bath. Parathyroid echograms were carried out in 10 patients with clinical hyperparathyroidism. The preoperative examination was capable of detecting and localizing enlarged parathyroid glands in seven cases. The small adenomas of 0.2 g could not be detected. The preoperatively detected tumors were oval-shaped and either more than 1 g in weight or larger than 1 cm diameter. The echograms of the adenoma and carcinoma showed cystic changes and appeared indistinguishable: both show a characteristic cystic pattern, for which the term hollow pattern is the most suitable description.

James F. Martin

Ultrasonic cholangiography: gray-scale B-scan evaluation of the common bile duct. Goldberg BB (Episcopal Hospital, Philadelphia, Pennsylvania 19125). *Radiology* 118:401–404, Feb 1976

Using commercially available gray-scale equipment, 12 patients with unexplained jaundice were evaluated ultrasonically for dilatation of the bile ducts. In seven patients, there was no evidence of bile duct dilatation. In five patients, bile duct dilatation was demonstrated by ultrasound, and confirmed at surgery or autopsy. Stones in the common duct and gallbladder were demonstrated in one patient. Longitudinal and multiple oblique scans were used to identify portions of the common duct. Skin marks were placed to outline its course. Then, transverse scans and scans along the course of the common duct were performed. The portal vein was distinguished from the common duct by identifying the confluence with superior mesenteric and splenic veins. In one patient, an experiment confirmed the ability of ultrasound to detect a dilated

common duct. This patient was scanned pre-operatively with demonstration of the dilated common duct with stones. The patient was again scanned postoperatively with a T-tube in place. No stones were shown postoperatively either by ultrasound or by T-tube cholangiography. Air bubbles mixed in contrast material injected via the T-tube were visualized as echoes within the common duct by ultrasound. While bile ducts, especially normal ones, are not clearly defined in all patients, ultrasound is recommended as the initial procedure when trying to distinguish hepatocellular jaundice from posthepatic obstruction.

J. M. Stoeber

Echographic evaluation of splenic injury after blunt trauma. Asher WM, Parvin S, Virgilio RW, Haber K (Kai Haber, University of Arizona Medical Center, Tucson, Arizona 85724). *Radiology* 118:411–415, Feb 1976

The subtle signs of blunt abdominal trauma and the relatively high frequency of splenic injury seems to make sonographic evaluation an appropriate non-invasive examination. A total of 70 blunt abdominal trauma patients underwent sonographic examination. There were 61 true negative cases, one false negative, four true positive, and four false positives. The sonographic findings of a double contour splenic outline, progressive splenic enlargement, and splenomegaly were the most prominent findings. Because of the 61 true negative cases and only one false negative, the authors considered sonography an excellent screening procedure for possible splenic rupture. They add that if the sonographic findings are abnormal, further evaluation is needed.

Robert F. Kuhnhein

Placental aging monitored by gray scale echography. Fisher CC, Garrett W, Kossoff G (Ultrasonic Institute, 5 Hickson Road, Millers Point, 2000 N.S.W., Australia.) *Am J Obstet Gynecol* 124:483–488, March 1976.

Using prototype gray scale ultrasound equipment, changes in placental anatomy were studied in an undisclosed number of placentas that were examined pathologically in 1 cm slices and x-rayed post delivery. The echo-free spaces, previously described by Winsberg, occur after 36 weeks gestation and correspond pathologically to the center of the lobules which are avillous spaces. These varied in size from 0.5 to 3.0 cm in diameter. The strong echos between these echo-free spaces corresponded to fibrous septa separating the lobules which histologically and radiographically showed reticular calcification on the placentas examined post delivery. The authors suggest that if these echo-free areas are seen earlier than 36 weeks gestation the fetus may be small for dates. One example of this situation is presented. In this case the enlargement of the echo-free spaces in the placenta was associated with a decrease in the volume of amniotic fluid surrounding the fetus.

Catherine Cole-Beuglet

The identification of IUD by ultrasound in the uterine cavity. Quakernack K, Schmidt EH, Lieder B, Beller FK (Department of Obstetrics and Gynecology, Westfälische Wilhelms University, Munster, Federal Republic of Germany). *Obstetrical and Gynecological Survey* 31:222–223, 1976. (This was an original article taken from *J Gynecol Obstet Biol Reprod (Paris)* 4:203, 1975, and subsequently abstracted in the *Obst Gynecol Surv*)

Eighty patients were examined by ultrasound B-scans in the longitudinal and transverse and slightly oblique positions for localization of IUDs. It was found that proper location of an IUD in the uterine cavity is dependent on the position of the uterus and the surface structure of the IUD. Loops were easily identifiable if uterus is in the anteverted-flexed position. In the retro-flexed uterus it is difficult to visualize the IUD in its entire length. If the uterus is in a mid-position a misinterpretation is possible if the IUD is in a transverse position. The authors also obtained ultrasonic echoes from the string. Proper location of an IUD in the uterine cavity failed in this series in 10% of examinations, especially in obese patients and in the presence of intra-abdominal adhesions. The editors suggest ultrasonic examination of IUDs to check the position of the device following insertion. This would improve the performance of the

IUD as the most important contribution to the failure rate of an IUD is poor positioning. Insertion requires that the device reaches the fundus for proper functioning. If the device is not high enough this predisposes to pregnancy or expulsion.

Catherine Cole-Beuglet

Ultrasound of the parotid gland. Neiman HL, Phillips JF, Jaques DA, Brown TL (Walter Reed Medical Center, Washington, D.C.). *J Clin Ultrasound* 4:11-13, Feb 1976

Five cases of parotid gland masses were studied using a bistable scanner with a 5 MHz transducer with a 5 cm internal focused crystal. The only masses which were sonolucent at both low and high gain settings were retention cysts and true cysts of the parotid gland. The Warthin's tumor was sonolucent at low gain settings but showed a lattice of internal echoes at higher gain. The remaining benign and malignant tumors presented as solid masses. These included a mixed tumor and an adenoid cystic carcinoma.

Stephen J. Carter

Evaluation of renal transplants with ultrasound. Barm J Jr, Smith EH, D'Orsi CJ, Tilney NL, Dantonio J (Peter Bent Brigham Hospital, Boston, Massachusetts). *Radiology* 118:405-410, Feb 1976

The application of ultrasound in the renal transplant patient is demonstrated in a number of cases. The transplanted kidney and associated structures are readily visualized with a conventional B-scanner with a 2.25-MHz transducer. Complications of lymphocele, pararenal hematoma, abscess, urinoma, and obstruction are shown with photographs of B-mode scans. Renal transplant volume obtained by integrating the cross-sectional areas of serial transverse sections obtained during the B-scan are demonstrated with graphs on four different patients. These show a normal response as well as an acute increase in renal volume associated with rejection and show responses to therapy. Other uses described include: (1) ultrasonically guided percutaneous aspiration to verify the diagnosis of pararenal abscess; (2) mapping of therapy ports; (3) following lesions (e.g. lymphoceles may be electively observed and followed rather than surgically drained). B-mode imaging is an atraumatic method which is independent of renal function forming an integral part of the evaluation of the renal transplant patient along with excretory urography, radio nuclide imaging and angiography.

Stephen J. Carter

Nuclear Medicine

Gallium-67 citrate in cerebral infarction. Poulou KP, Reba RC, Goodyear M (Department of Nuclear Medicine, Washington Hospital Center, Washington, DC 20037). *Invest Radiol* 2:20-23, Jan-Feb 1976

Cerebral scans were obtained on 30 "stroke" patients first with ^{99m}Tc pertechnetate and subsequently with ^{67}Ga citrate. Of the 26 patients with abnormal ^{99m}Tc static scans, 17 (65%) showed the same abnormality in gallium citrate scans also. In 4 patients with positive technetium flow studies but negative static scans, no abnormality was seen in the scans obtained after gallium citrate injection. In none of the patients was the relative concentration of radioactivity in the lesion greater in the gallium image than in the technetium image. This study proves the nonspecificity of gallium citrate and thus its inability to differentiate cerebral tumor from cerebral infarction just on the basis of localization of gallium.

Author's Abstract

Diagnosis of osteomyelitis in children by combined blood pool and bone imaging. Gilday DL, Eng B, Paul DJ, Paterson J (The Hospital for Sick Children, Toronto, Ontario, Canada). *Radiology* 117:331-335, Nov 1975

Differentiation of osteomyelitis from cellulitis or septic arthritis can be difficult. The radiological examination often does not have the characteristic features. Seventy of 71 children with osteomyelitis had focal areas of increased radioactivity at the site of the infection.

The addition of "blood pool" images aids in the interpretation of the study as they permit evaluation of the effect of hyperemia. The 13 children with cellulitis had diffuse increase in radioactivity involving both the bones and soft tissues. Bone imaging as the initial screening procedure for osteomyelitis is recommended.

Author's Abstract

Internal mammary lymphoscintigraphy: the rationale, technique, interpretation and clinical application. A review based on 848 cases. Ege GN (Princess Margaret Hospital, 500 Sherbourne Street, Toronto, Ontario, M4X 1K9, Canada). *Radiology* 118:101-107, Jan 1976

The diagnostic significance of the lymphatic system, and the limitation of contrast lymphography to certain anatomic sites has called for new means of investigating this system. Sherman first reported the selective concentration of interstitially injected colloidal radiogold in regional lymph nodes, and this has been used to study pan-aortic lymph nodes following radiocolloid injection in the dorsum of the feet. Both Rossi and Schenk described the application of this method to the internal mammary lymphatics in 1966. From November 1972 to December 1974 internal mammary lymphoscintigraphy was used to study 848 patients. A total of 1,269 lymphoscintigrams were performed and evaluated. The questions were: is it reproducible and reliable; do scintigrams correlate with the anatomy; what are normal and abnormal patterns?

A successful procedure appears to depend on injection site, and particle size of the radiocolloid. Bilateral subcostal injections medial to the midclavicular lines, and 3.0 cm below the level of the tip of the xyphoid, should be made so that the radiocolloid is deposited just anterior to the posterior rectus sheaths. The particle size of the colloid should be uniformly small precluding the use of ^{99m}Tc sulfur colloid (5,550-2,000 m μ). The colloid of ^{99m}Tc antimony, as developed by Garzon, with a particle size of 4-12 m μ is more suitable. Individual injections of 500 μCi of this radiocolloid in a volume of 0.3 ml, or less, were made into the sites described above. Of the 1,269 lymphoscintigrams, the only complications were hematomas in two patients. No local anesthetic or hyaluronidase was used. There did not appear to be any improvement in image formation when delayed beyond 3 hours. Camera images with xyphoid marker to include the injection sites and the mediastinum were routinely employed. Rectilinear scans were performed when greater correlation with anatomic landmarks was desired. Dual lymphoscintigrams were performed on 140 patients at intervals varying from 3 days to 3 weeks to ascertain reproducibility. An interval of 4-8 days is suggested to allow the lymphatics to "recover" from the first procedure. From 100 lymphoscintigrams that were judged to be normal, the total of all visualized lymphatic aggregates was diagrammed and correlated with the results of four autopsy studies covering 299 subjects. The anatomic validity of the lymphoscintigram is considered satisfactory when the relative ability of the two procedures to "resolve" lymphoid foci are considered. The normal parasternal lymphoscintigram is characterized by considerable individual variation. Perfect symmetry between right and left parasternal lymph nodes is rare. Commonly there is similarity of configuration of the two chains, but numbers of nodes in each chain may vary. However, if no lymphatic aggregates are visualized after either subcostal injection, one must repeat the procedure.

Lymphoscintigrams on patients with carcinoma of the breast, may be misleading due to temporary physiological changes in the immediate postoperative period, but changes which persist 3-4 weeks may indicate disease. The proper selection of parasternal treatment field size for radiation therapy may be greatly facilitated by this procedure. Intractable ascites in patients with carcinoma of the ovary probably indicates obstruction of the diaphragmatic and mediastinal lymphatics by tumor emboli. The identification of this change would provide additional therapeutic assistance. In lymphoma, the pattern is distinctly different. Involved lymph nodes appear larger and concentrate colloid to a greater extent than normal creating a disorganized, non-uniform configuration with additional, ill-defined aggregates being demonstrated.

F. C. Petty

Comparative assessment of scintillation camera performance. Moretti JL, Mensch B, Guey A, Desgrez A (Service de Médecine Nucleaire, Hôpital Henri Mondor, Creteil, France). *Radiology* 119:157-165, April 1976

The performance characteristics of 5 scintillation cameras were compared: Searle 19, Searle 37, Ohio Nuclear, Picker 2C and Toshiba GCA 202. Inherent characteristics including spatial resolution, field uniformity and distortion, energy resolution, count-rate capability and paralyzing time were measured. Extrinsic characteristics such as spatial resolution with emission tests and sensitivity with high resolution, low energy collimators also were measured. The Ohio Nuclear camera gave the best results for most of the parameters studied, followed by Searle 37 PMT, Searle 19 PMT, Picker, and Toshiba. The size of the crystal must also be a criterion for choosing a camera.

Author's Abstract

Radiation Oncology

A study of childhood non-Hodgkin's lymphoma. Murphy SB, Frizzera G, Evans AE (St. Jude Children's Research Hospital, P. O. Box 318, Memphis, Tennessee 38101). *Cancer* 36:2121-2131, 1975

The authors have reported a retrospective review of the pathologic and clinical features of 31 cases of childhood non-Hodgkin's lymphoma using the Rappaport classification. Only two patients had nodular lymphoma. Using a modified classification system, 35.4% of the patients had large basophilic cell (LBC) lymphomas and 16% had convoluted T-lymphocyte (CTL) lymphomas. CNS involvement occurred in 10 children (32%) and a leukemia picture developed in six (19%). The CTL lymphomas were confined to the mediastinum and the LBC lymphomas arose mostly in Waldeyer's ring and Peyer's patches. No correlation with histopathologic type could be established regarding CNS involvement or leukemic transformation.

Herbert C. Berry

Non-Hodgkin's lymphoma in children. Hutter JJ, Favara, BE, Nelson M, Holton CP (The Children's Hospital, 1056 East 19th Avenue, Denver, Colorado 80218). *Cancer* 36:2132-2137, 1975

The authors review, retrospectively, the clinical and histopathological findings in 26 children with non-Hodgkin's lymphoma without marrow involvement. All had diffuse lymphomas. Of 12 patients with initial involvement of the mediastinum, five developed CNS lymphomatous involvement. The question is raised of the use of prophylactic measures against CNS recurrence in the initial therapy of children with mediastinal diffuse lymphocytic lymphoma.

Herbert C. Berry

The results of radiotherapy for Hodgkin's disease. Peckham MJ, Ford HT, McElwain TJ, Harmer CL, Atkinson K, Austin DE (The Royal Marsden Hospital, Sutton, Surrey, England). *Br J Cancer* 32:391-400, 1975

The authors retrospectively review 212 patients with stage I and II Hodgkin's disease (majority clinically staged) and a group of 78 patients with pathological stages Ia-IIIa. Post-irradiation survival statistics were reviewed for all groups of patients. Clinical stage I and II patients showed a 60% 3-year disease-free survival. Pathologic stage I and II groups showed an 80% rate at 3 years. Of the pathologic stage IIIa patients, 76.7% receiving "total nodal irradiation" remain in complete remission post-irradiation. A total of 79 of the clinical and pathologic stage I and II patients relapsed, with 42 of these relapses being transdiaphragmatic and 37 of 42 occurring in clinically staged patients.

Herbert C. Berry

External radiotherapy and radioiodine in the treatment of 359 thyroid cancers. Tubiana M, Lacour J, Monnier JP, Bergiron C, Gerard-Marchant R, Rouyeay J, Bok B, Parmentier C (Institut Gustave-Roussy, Villejuif (94), France). *Br J Radiol* 48:894-907, 1975

The authors review, retrospectively, 359 selected patients with carcinoma of the thyroid treated between 1943-1965 by external radiotherapy or radioiodine (not randomized). In 65 patients receiving prophylactic post-operative external irradiation (most with papillary or follicular histology), the 10-year survival was 85%. Of 85 inoperable patients, 60 were treated with external irradiation with a 10-year survival of 8.5% versus 4.5% 10-year survival for the 25 inoperable patients treated with radioiodine. The supervoltage-treated patients (mean dose 5000 rads) had a significantly higher 10-year survival than the orthovoltage-treated patients (mean dose 2800 rads), 53% compared to 32%. A dose of 5000 to 6000 rads delivered by megavoltage external radiotherapy in 5-6 weeks was well tolerated and effective mostly in differentiated carcinomas and medullary carcinomas.

Herbert C. Berry

Carcinoma of the urinary bladder. Fish JC, Fayos JV (JV Fayos, Division of Radiation Therapy, University Hospital, 1405 East Ann Street, Ann Arbor, Michigan, 48104). *Radiology* 118:179-182, 1976

The authors have selected, retrospectively, two groups of patients with comparable bladder carcinoma from 249 patients irradiated with telecobalt therapy from 1955 through 1971. Group I (45 patients) and Group II (127 patients) were comparable with regard to histology, tumor size and stage, although 44.4% of the tumors in Group I were stage D₁ versus 31.5% in Group II. Group I received a mean isocentric dose of 6,060 rads in 6 weeks to volume of about 1050 cm³. Group II received a mean isocentric dose of 6,542 rads in 6.5 weeks to a volume of approximately 1700 cm³. Information regarding local control was available in about 50% of the patients but was determined in 23.9% of the Group I patients and 21.3% of the Group II patients. Overall 5-year survival rates were 12.6% (Group I) and 25.5% (Group II). Regarding histology, the only statistically significant improvement was in transitional cell carcinoma for which the 5-year survival was 15.3% (Group I) and 27.4% (Group II). Five-year survival by stage was better in Group II at all levels except Stage A. There were no 5-year survivors with Stage C or D₁ tumor in Group I. The major complication rate in Group I was 4.4% versus 7.1% in Group II.

Herbert C. Berry

Malignant melanoma. Southwick HW (Department of Surgery, Rush-Presbyterian-Saint Lukes Medical Center, 1725 West Harrison Street, Chicago, Illinois 61612). *Cancer* 37:202-205, 1976

The author has retrospectively reviewed 259 patients with malignant melanoma, with 150 patients as the determinate group. A regional node dissection was performed on 121 patients (64 patients in continuity, 57 patients in discontinuity). Staging based upon the depth of invasion at the primary site is not reported. Clinically negative but microscopically positive lymph nodes occurred in 11% (13/121) of the patients. Patients having excision and those having excision in continuity with clinically and microscopically negative lymph nodes had a 5 year NED rate of 61% (30/49) versus clinically negative microscopically positive lymph nodes (45% or 4/9). Discontinuous regional node dissection in an unmatched group of patients yielded a 5 year NED rate of 33% (16/48).

Herbert C. Berry

Subclavian artery occlusion following radiotherapy for carcinoma of the breast. Budin JA, Casarella WJ, Harisiadis L (Columbia-Presbyterian Medical Center, 622 West 168th Street, New York, New York 10032). *Radiology* 118:169-173, Jan 1976

The adverse effect of radical mastectomy and radiation therapy upon the upper extremity in patients with carcinoma of the breast is a common and often frustrating clinical problem. Although pain, limitation of motion and lymphedema are well recognized complications of treatment, arterial insufficiency in the upper extremity is a rare sequelae of therapy. The authors found only three published examples of subclavian artery occlusions. Here they present four additional cases. In each patient there was focal subclavian artery

occlusive disease occurring in the field of irradiation from 5 to 17 years after postoperative radiation therapy for breast carcinoma. The authors suggest that this complication is not often reported because many patients who receive postoperative irradiation for breast cancer will not survive a sufficient time to develop subclavian arterial occlusion. Moreover, clinicians may fail to recognize that arterial insufficiency is causing or contributing to the arm symptoms, but blame the pain on lymphedema or nerve root irritation from fibrosis. Factors implicating irradiation as the cause of the arterial occlusions in these cases include location of the lesion in the supraclavicular portal and distal to the origin of the subclavian artery (spontaneous atherosclerotic plaques typically occur in the origin itself) and normal vessels (by angiography) outside of the field of irradiation. Tumor recurrence, as the cause of occlusion, was excluded either by surgical exploration (for correction) or by lack of progression on long-term follow-up (untreated cases).

Radiation doses ranged from 1,466 to 1,798 rets. There was a possibility that radiation field overlap increased the dose, however. Other possible etiologies are discussed and comparisons with experimental studies are offered.

The importance of recognizing postirradiation subclavian artery occlusion is stressed because if this condition is the source of arm pain and disability, it can then be easily diagnosed by angiography and successfully treated by surgery.

Paul M. Kroening

Pathological staging of 100 consecutive untreated patients with non-Hodgkin's lymphomas. Lotz M, Chabner B, DeVitta V, Johnson RE, Berard CW (Clinical Pathology Department, Clinical Center, National Institutes of Health, Bethesda, Maryland 20014). *Cancer* 37:266-270, 1976.

The authors review the results of the pathological staging of 100 consecutive patients with non-Hodgkin's lymphoma. Only diffuse lymphomas were seen in patients under 20 years of age and were twice as common as nodular lymphomas in patients over 60. Nodular lymphomas were most commonly lymphocytic (61%) while diffuse lymphomas were commonly histiocytic (43%). Hepatic involvement was documented in 40 patients. Of 49 patients having staging laparotomy 37 (75%) had abdominal involvement. All negative spleens weighed less than 270 g. The results support earlier studies.

Herbert C. Berry

The role of upper gastrointestinal endoscopy in patients with cancer. Winawer SJ, Sherlock P, Hajdu SI (Memorial Sloan-Kettering Cancer Center, 1275 York Avenue, New York, New York 10021). *Cancer* 37:440-448, 1976

The authors describe the so-called upper gastrointestinal panendoscope, utilizing fiberoptics with complete tip control and sufficient length to allow examination of the esophagus, stomach, duodenum with a single instrument. The results of endoscopic biopsy and brush cytology in upper gastrointestinal cancer are reviewed in 94 patients. A positive diagnosis of cancer was made in 100% of the patients with esophageal carcinoma, 92% of the patients with gastric adenocarcinoma exophytic, 50% of the patients with gastric adenocarcinoma infiltrative, and 71% of the patients with secondary gastric lymphoma. Comparison of brush cytology and tissue biopsy in the diagnosis of upper esophageal cancers revealed that the brush cytologies were more often positive in secondary gastric lymphoma (54% vs. 42%), esophageal epidermoid or adenocarcinoma (97% vs. 67%) and gastric adenocarcinoma (68% vs. 50%). Their studies also demonstrate that carcinoembryonic antigen (CEA) is measurable in gastric lavage and is much lower in concentration than in colonic lavage, but is not clearly diagnostic of the presence of gastric cancer. Prediction of the mucosa at risk for neoplasia is also possible by studying isotopic incorporation within epithelial cells obtained by lavage and biopsy as has been done in the colon.

Herbert C. Berry

New horizons in lung cancer diagnosis. Marsh BR, Frost JK, Erozan YS, Carter D (U.S. Public Health Service Hospital, 3100

Wyman Park Drive, Baltimore, Maryland 21211). *Cancer* 37:437-439, 1976

The authors outline the endoscopic observations and methods they have developed in successfully localizing 17 consecutive, radiologically occult carcinomas discovered in the sputum of 15 patients. Two of the patients were found to have occult tumors in the upper respiratory tract on direct laryngoscopy. Fifteen bronchogenic carcinomas were discovered in 13 patients, two having simultaneous second primary lesions in the opposite lung. Two or more endoscopic procedures were required to localize the lesion in four patients. In 12 of 15 bronchogenic carcinomas, the site of origin seemed to be segmental or subsegmental. These observations tend to correlate with the striking localization improvement resulting from studies of the segmental bronchus now possible with the fibroscope.

Herbert C. Berry

Mammography of the definitively irradiated breast. Bloomer WD, Berenberg AL, Weissman BN (Joint Center for Radiation Therapy, 50 Binney Street, Boston, Massachusetts 02115). *Radiology* 118:425-428, Feb 1976

The role of mammography in the evaluation of patients treated solely by radiation therapy for breast cancer is not well defined. Post-irradiation mammography may be a particularly useful adjunct to physical exam of the irradiated breast in order to assess tumor response. Of 27 patients treated definitively by radiation therapy for localized breast cancer pre- and post-irradiation, mammograms were available for 23, post-irradiation mammograms for only 4. Using a 4MEV linear accelerator, minimum tumor dose to the breast and chest wall range from 4,500 rads in 4.5 weeks to 6,000 rads in 6 to 7 weeks. Progressive skin thickening, fibrosis of the subcutaneous tissue, and breast retraction were observed in the post-irradiation breast. Pre-irradiation mammography showed gross residual tumors in 11 patients. Seven of these patients were examined more than 6 months post-irradiation, five having no identifiable residual mass. Persistence of a mass much beyond 6 months after completion of irradiation suggests a locally uncontrolled tumor. In the Joint Center for Radiation Therapy series of 39 patients with Stage I and Stage II disease, there have been no local failures thus far, while 50 of 61 patients with Stage III disease have remained under local control. It is in this latter group of patients with locally advanced lesions requiring extensive irradiation that serial mammograms may be especially important in detecting tumor recurrence.

Herbert C. Berry

Regional lymph node metastases and the level of invasion of primary melanoma. Carmack EH, Clark W, Morton DL, Eilber F, Bochow A (Division of Oncology, UCLA School of Medicine, University of California, Los Angeles, California 90024). *Cancer* 37:199-201, 1976

The authors review 119 patients with primary malignant melanoma classified according to Clark's level of invasion. All but 30 patients (level II) underwent regional lymph node dissection. The degree of lymph node invasion in level III, IV, and V patients was 32%, 67% and 66% respectively. Pathologically positive regional lymph nodes in patients with clinically negative nodes were noted in 16% (6/38) of the level III and 45% (10/22) of the level IV patients. The authors feel the data support regional lymph node dissection for patients with level IV and V invasion and probably level III invasion also. Regional lymph node dissection is felt unnecessary for patients with level II invasion.

Herbert C. Berry

Physics

The effect of x-ray spectra from molybdenum and tungsten target tubes on image quality in mammography. Haus AG, Metz CE, Chiles JT, Rossmann K (Center for Radiologic Image Research, Department of Radiology, University of Chicago, Chicago, Illinois). *Radiology* 118:705-709, March 1976

The measured x-ray spectra from a molybdenum anode Senographe mammography unit and a tungsten anode unit were used to calculate the x-ray energy spectra transmitted through various thicknesses of fat and water (breast-equivalent materials). The effect of breast tissue on the transmitted primary x-ray spectrum and hence on radiographic contrast depends upon the amount of fat relative to fibrous and glandular tissue present. Breasts composed primarily of fat yield images of higher radiographic contrast when imaged with the molybdenum rather than the tungsten anode tube at the same kVp, although the patient exposure required with molybdenum increases relatively faster with breast thickness. When the breast is very thick, or contains a large percentage of fibrous and glandular tissue, the contrast obtained with the molybdenum anode tube will be similar to that obtained with the tungsten anode tube and patient exposure will be greater.

Author's Abstract

An evaluation of screen-film speed characteristics. Reynolds J, Skucas J, Gorski J (Department of Radiology, University of Rochester School of Medicine and Dentistry, Rochester, New York). *Radiology* 118:711-713, March 1976

The relative speeds of six commercially available screen-film combinations were evaluated. There is a nonlinear relationship throughout the kVp range between the calcium tungstate, barium strontium sulfate, and rare earth screens. The efficiency of the rare earth screens and screens composed of barium strontium sulfate decreases at lower kVp ranges when compared to calcium tungstate screens. This decrease can become critical when subject contrast is being enhanced by the use of a lower kVp.

Author's Abstract

Performance evaluation of phototimers. Chaney EL, Hendee WR, Hare DL (Department of Radiology, University of Colorado Medical Center, Denver, Colorado). *Radiology* 118:715-717, March 1976

Phototimers detect x-rays impinging on or emerging from an x-ray film cassette and terminate the exposure after a predetermined amount of radiation has been received by the film. A phototimer must provide reproducible film exposures over a wide range of target-to-film distances, patient thicknesses, and technique variables. A method is needed which verifies that the phototimer is functioning properly and identifies exposure techniques and practices which are compatible with its use. Several techniques are presented for evaluating phototimer performance, and data accumulated during application of these techniques to the use of three spot-film phototimers are presented.

Author's Abstract

Radiobiology

Cure of a solid tumor by simultaneous administration of microwaves and x-ray radiation. Yerushalmi A (Radiation Unit, The Weizmann Institute of Science, Rehovot, Israel). *Radiat Res* 64:602-610, 1975

Mice bearing an SV-40-induced fibrosarcoma were treated with simultaneous 250 kVp x-irradiation and localized hyperthermia (44°C) produced by 2.450 Mc/sec microwaves. Since this tumor, if left untreated, causes death in 30-50 days with no evidence of metastases, it is an appropriate choice for evaluation of localized treatment in terms of tumor cure or life extension of the tumor-bearing host. Using these endpoints, it was found that a single heat treatment had virtually no effect while a single dose of 800 R x-rays cured 1.75% of the tumors. Twenty-eight minutes of heating (10 minutes at 44°C) plus 800 R given during the last 8 minutes of heating cured 20% of the tumors. Treatment with x-rays (800 R/fraction) and simultaneous heating, two fractions 7 days apart, cured 80% of the tumors. Two heat treatments one week apart cured no tumors while 2×800 R x-rays cured 7.85%. Treatment with up to 4000 R x-rays (single fraction) or 8000 R (two fractions, 7 days apart) without heating cured very few tumors, indicating that this is a fairly radioresistant neoplasm. Hyperthermia enhanced

the curability of a single dose of 800 R x-rays by a factor of 10.28 and of 2×800 R by a factor of 10.25. This augmentation, coupled with well localized tumor heating indicates microwave hyperthermia may be a useful adjuvant to radiation therapy.

Janet S.R. Nelson

Damage and recovery assessment of the mouse jejunum to abdominal x-ray and adriamycin treatment. Burholt DR, Hagemann RF, Cooper JW, Schenken LL, Leshner S (Clinical Radiation Therapy Research Center, Allegheny General Hospital, Pittsburgh, Pennsylvania 15212). *Br J Radiol* 48:908-912, 1975

In planning combined modality (drug plus radiation) treatment of cancer, one must also consider effects on normal tissue. Intestinal crypts produce cells that migrate onto the villi. Following radiation damage to the intestinal crypts two separate mechanisms of injury occur: (1) crypt stem cells are killed, leading to crypt attrition, and (2) rate of cell proliferation is temporarily reduced in those crypts which do survive. Interaction of drug radiation damage at these two levels is the subject of this paper.

Mice received abdominal radiation with 270 kVp x-rays only or abdominal radiation followed immediately by intraperitoneal injection of adriamycin (5 or 10 mg/kg body weight). This drug dose alone causes no animal deaths. The lethal dose for 50% of the mice at 7 days ($LD_{50/7}$) is 1575 R of x-rays alone which is reduced to 1200-1300 in the presence of the drug. Survival of jejunal crypts following radiation or drug-radiation treatment is assessed by two methods. One is the histological microcolony assay of Withers and Elkind (*Int J Radiat Biol* 17:261, 1970) in which crypts/circumference of jejunum is determined microscopically 4 days after treatment. The other is the crypt isolation technique of Hagemann et al (*Radial Res* 46:533, 1971). Intestinal jejunum is removed from 3H -thymidine injected mice. By determining dpm/mg wet weight of tissue and dpm/isolated crypt, crypts/mg of intestine can be determined by scintillation counting of gut samples. Estimates of crypt survival by the two methods are in good agreement, and it is shown that the injection of adriamycin after radiation does not reduce the number of crypts surviving four days posttreatment, relative to animals treated with x-rays alone. Further studies examined dpm/mg of jejunum in animals injected with 3H -thymidine at various times after receiving 1000 R x-rays or 1000 R x-rays plus adriamycin (5 or 10 mg/kg body weight). The addition of the drug delays the compensatory hyperplasia which normally occurs during recovery from radiation damage. This must be considered if adriamycin and radiation are given in combination in treating abdominal tumors.

Janet S.R. Nelson

Enhancement of radiation response of a murine mammary carcinoma by two nitrofur derivatives. Stone HB, Withers HR (Section of Experimental Radiotherapy, M. D. Anderson Hospital & Tumor Institute, Houston, Texas 77025). *Radiat Res* 64:443-451, 1975

NF-131 [1-(5-nitro-2-furyl)-3-piperidino-1-propanone semicarbazone hydrochloride] and nifuroxime (anti-5-nitro-2-furaldoxime) are nitrofur derivatives which, like many other compounds with high electron affinity, have been shown to sensitize hypoxic cells treated in vitro with gamma or x-irradiation. These compounds have now been shown to make mammary carcinomas of C3H mice more sensitive to ^{137}Cs gamma radiation. The dose of γ rays which cures 50% of the tumors (TCD_{50}) was determined in mice which received no additional treatment and was then remeasured in animals which were injected with sensitizing drug at various times prior to irradiation. Since the presence of radioresistant hypoxic tumor cells may prevent cure by radiation therapy, these experiments are of interest.

NF-131 (2 mg/mouse) reduced the TCD_{50} by a factor of 1.21 to 1.23 when given 3, 10 or 30 minutes prior to irradiation. The drug given alone caused no change in tumor growth, suggesting its effect with radiation is truly one of sensitization. Nor did the presence of the drug alter the response of the mouse intestinal jejunum to radiation as determined by a microcolony crypt survival assay. However, the drug was lethal to 3% of the animals. Nifuroxime

(0.05 mg/g body weight) given to mice 10 minutes prior to radiation reduced the TCD₅₀ for the tumor by a factor of 1.36, and 0.1 mg/g body weight gave a dose modification factor of 1.48. A time interval of 3 or 30 minutes between drug injection and radiation yielded a smaller sensitization factor. Both drug doses temporarily inhibited tumor growth when given alone, indicating that cytotoxicity and sensitization were interacting. Nifuroxime did not enhance intestinal radiation damage and the lower dose may have a protective effect. However, a dose of 0.05 mg/g killed 22% of the mice and 0.10 mg/g was lethal to 37% of the animals. The higher mortality and greater dependence of dose modification factor on time-dose relationships make nifuroxime a less useful sensitizer than is NF-131.

Janet S.R. Nelson

Human cell survival as a function of death for a high-energy neon ion beam. Raju MR, Blakely E, Howard J, Lyman JT, Kalofonos DP, Martens B, Yang CH. (Los Alamos Scientific Laboratory, University of California, Los Alamos, New Mexico 87545). *Radiat Res* 65:191-194, 1976

Neon ion and other heavy charged particle beams are currently of interest to radiotherapists. As a charged particle beam passes through tissue, the particles are continuously slowed as the ions undergo many small atomic interactions. The specific energy loss and LET maximize at several centimeters depth at the Bragg peak, where both the physical dose, relative to surface dose, and the biological effectiveness per unit dose are maximal. Beyond this peak, the dose drops off very sharply to a few per cent of the maximum dose. The high RBE of radiation in the Bragg peak is of therapeutic interest but the narrow width of this region in the Berkeley BEVALAC's 400 MeV/u neon ion beam would limit its usefulness for therapy. A ridge-shaped filter was used to modulate the energy of the beam, widening the Bragg peak to 4 cm. The survival of cultured human kidney cells suspended in gelatin-solidified medium was studied as a function of depth in this beam. The RBE for cell killing relative to 250 kVp x-rays was determined at the 10% survival level. For neon ion beam radiation in the plateau region (0-3 cm depth), the RBE is 1.8 but for radiation in the broadened peak region (10-14 cm depth) the RBE is 3.0. The authors conclude that broadening the Bragg peak by added filtration does not sacrifice the higher biological effectiveness of radiation from this portion of the beam.

Janet S.R. Nelson

Collagen content of lungs of mice after irradiation. Law MP, Hornsey S, Field SB (Medical Research Council, Cyclotron Unit, Hammersmith Hospital, London W12 0HS, England). *Radiat Res* 65:60-70, 1976

Fibrosis in irradiated mouse lungs as a function of time and dose was studied by determining tissue levels of hydroxyproline, an amino acid limited to collagen and possibly elastin. Mice received single x-ray doses of up to 4000 rads to the right half of the thorax while the left half was shielded. A dose of 1000 rads had little permanent effect on lung weight or collagen content. At doses of 2000-4000 rads, the dry weight and total hydroxyproline content of the irradiated right lobes decreased with time after treatment. The

amount of hydroxyproline per gram dry weight of irradiated lung relative to controls, however, increased between 24 and 36 weeks after doses of 2000-4000 rads. The maximum effect was not reached until 36 weeks, with no further change at 48 weeks. The atrophy of the irradiated portion was accompanied by hypertrophy of the untreated left half. The greatest changes in collagen deposition and lung atrophy occurred between 1000 and 2000 rads, which is in the range of the LD_{50/80}-180 days of 1100 to 1250 rads following whole thorax irradiation in mice. But the collagen replacement occurs later than the time of animal deaths following whole lung irradiation and therefore probably is not the major contributing factor in lethality due to lung damage.

Janet S.R. Nelson

Radiosensitization of C3H mouse mammary tumors using fractionated doses of x-rays with the drug RO-07-0582. Sheldon PW, Hill SA, Foster JL, Fowler JF (Gray Laboratory of the Cancer Research Campaign, Mount Vernon Hospital, Northwood, Middlesex HA6 2RN, England). *Br J Radiol* 49:76-80, 1976

This paper is one in a series on the response of early generation transplants of C3H mouse mammary tumors to fractionated radiation. Like others in the sequence, it describes attempts at maximizing effect by modifying fractionation scheme. The tumor radiation response to a given dose is expressed as probability of local control at 150 days posttreatment ("cure"). All such results are evaluated relative to normal tissue damage, specifically acute skin response, at different doses, to allow calculation of therapeutic gain factors. In this group of experiments, C3H mammary tumors as well as skin on the feet of nontumor-bearing mice were treated with 240 kV x-rays given in three fractionation schemes either without or with concurrent injection of the hypoxic cell sensitizer RO-07-0582. Five fractions in 9 days, three fractions in 4 days, and five fractions in 4 days were used. In previous experiments these fractionation schemes gave respectively, good, mediocre and poor local control of tumors for a given level of skin damage. The authors expected the addition of the hypoxic cell sensitizer to give some improvement. However, because reoxygenation of hypoxic cells occurs in these tumors between fractions of radiation, one would not expect the addition of RO-07-0582 to give enhancement ratios as high as 1.8, the value obtained when it is injected into tumor-bearing mice concurrently treated with single fractions of x-rays. The enhancement ratio is the radiation dose without a sensitizer necessary to give 50% "cures" divided by the radiation dose given with a sensitizer, necessary to give 50% "cures." The addition of the drug increased to good the radiocurability of tumors by all three fractionation schemes, with the enhancement ratios ranging from 1.1 to 1.2. There was no exacerbation of skin damage, thereby giving a therapeutic gain. The tumor cure results produced by the three fractionation regimes + RO-07-0582 showed little variability from one scheme to another, suggesting that this sensitizer removes some of the unreliability from short fractionated x-ray treatment, which ordinarily allows incomplete or variable reoxygenation between fractions.

Janet S.R. Nelson

American Roentgen Ray Society Section on Instruction

EUGENE GEDGAUDAS, DIRECTOR
HAROLD O. PETERSON, ASSOCIATE DIRECTOR

Instruction courses for the seventy-seventh annual meeting of the American Roentgen Ray Society, at the Washington, D.C. Hilton Hotel, will be offered afternoons, Monday–Thursday, September 20–23, and on the morning of Friday, September 24. Each course is scheduled for 90 min. No other activities are scheduled simultaneously.

In addition to 54 periods of regular courses, there will be a series of courses dealing entirely with bones. This 16 hr categorical course will take place over 6 days. It will not be possible to take other courses in addition to the bone program. The Categorical Course on Bone will begin Sunday, September 19, and will be the only subject presented that day. There will be seven other courses on Monday, 13 daily Tuesday, Wednesday, and Thursday, and nine Friday morning. A complete listing of course titles, faculty, and abstracts is presented on the following pages as is a complete description of the Categorical Course on Bone.

A pink registration form is located at the end of this section. It should be completed and mailed promptly because tickets will be mailed only to those whose forms have been received at the Office of the Director by Monday, September 6. Tickets will be mailed in an envelope marked "SECTION ON INSTRUCTION, AMERICAN ROENTGEN RAY SOCIETY—TICKETS ENCLOSED." Ticket requests that arrive after the deadline will not be honored, although tickets will be available at the instruction course registration desk in

the hotel for courses that have not been sold out. The first ticket mailing will be in early September.

Registration Information

After reviewing the abstracts on the following pages, make three choices for each day, then fill out the order form with the course number and instructor's name. For each course selected, a \$3 registration fee is required from *nonmembers*. For example the cost for nonmembers if five courses are selected, one each day, will be \$15. There is no charge for courses to members of the American Roentgen Ray Society, graduate students or residents in radiology, or nonmembers who are contributing to the program by presenting an instruction course, a paper on the scientific program, or a scientific exhibit. However, everyone must fill out a registration form indicating their choices, and check the proper box opposite their name and address.

All who register for the Categorical Course on Bone Diseases must take the entire series and pay the \$25 fee, including members of the American Roentgen Ray Society. The categorical course totals 16 hr instruction and includes a syllabus.

Please promptly mail the registration form to: Eugene Gedgaudas, Director of Instruction Courses, American College of Radiology, 20 North Wacker Drive, Chicago, Illinois 60606.

Condensed Schedule of Courses

Sunday through Friday

Categorical Course on the Skeletal System, six sessions, 16 hr, fee \$25. Registration in this course precludes registration in any of the other courses. Members as well as guests must pay the course fee.

Monday, 3–4:30 p.m.

101. Cowan. Brain Imaging
102. Dodd. The Radiological Aspects of Certain Familial Cancers
103. Goldberg. An Introduction to Diagnostic Ultrasound
104. Chase, Kricheff. Computerized Axial Tomography
105. Elliott. Plain Film Approach to Pulmonary Venous Congestion
106. Payne. Basic Principles of CT Scanners

Tuesday 3–4:30 p.m.

201. Handmaker. The Applications of Nuclear Medicine in Pediatrics
202. Meyers. Dynamic Radiology of the Abdomen: Normal and Pathologic Anatomy
203. Carson. Basic Principles of Ultrasound Imaging
204. Chase, Kricheff. The Angiographic Diagnosis of Intracranial Mass Lesions
205. Dunbar. The Small Bowel in Pediatric Radiology
206. McCullough. Performance Evaluation of CT Scanners
207. Baker, Berdon. Varied and Unusual Sequelae in Both Systemic and Primary Bone Disease in Children
208. Potts. The Radiological Investigation of Hydrocephalus
209. Marshak. Radiologic-Pathologic Correlation of Interesting Lesions of the Gastrointestinal Tract
210. Theros. Granulomatous Diseases of the Lung
211. Thornbury. Renal Cystic Disease in Adults and Children
212. MacMillian. Sinuses, Nasopharynx and Base of Skull
213. Wolfe. Mammography, Part I

Wednesday, 3–4:30 p.m.

301. O'Mara. What is New In Radiopharmaceuticals and Instrumentation
302. Rice. Radiologic Evaluation of the Acute Abdomen
303. Leopold. Abdominal Ultrasonography
304. Singleton. Pediatric Pulmonary Abnormalities
305. Hattery, Stephens. CT Scanning of the Abdomen
306. Leeds. Diagnosis of Spinal Lesions
307. Martel. Interesting and Significant Lesions of the Alimentary Tract
308. Felson. Pattern Recognition In Disseminated Pulmonary Diseases
309. Judkins. Coronary Angiography
310. Becker. Radiology of the Urinary Tract
311. Jacobson, Siegelman. Skeletal Radiology—Newer Concepts and Provocative Challenges
312. MacMillian. The Neck (Pharynx, Cervical Esophagus, Larynx and Trachea)
313. Wolfe. Mammography, Part II

Thursday, 3–4:30 p.m.

401. Polcyn. Radionuclide Imaging Studies of Lungs and Heart
402. King. Cardiac Ultrasound
403. Swischuk. Neonatal Chest Problems
404. Schechter, Marc. A Simplified Approach to Posterior Fossa (Vertebral) Angiography
405. Reese, Muhm, Sheedy. CT Scanning of the Breast, Chest and Head
406. Jacobson. The Gastrointestinal Tract: Radiological Challenges
407. Vix. Roentgenographic Spectrum of Pleural Disease
408. Greenspan. Pulmonary Circulation and Embolism
409. Gehweiler. Pitfalls in the Diagnosis of Cervical Spine Trauma

410. Potter. What Every Radiologist Should Know About the Ear
 411. Egan. Detection of Early Breast Cancer
 412. Kattan. Tricks and Treats in Tomography
 413. Ružicka. Normal Arterial Anatomy of the Gastrointestinal Tract and Related Organs

Friday, 11 a.m.—12:30 p.m.

501. Muroff. Liver, Spleen, and Bone Imaging; Tumor and Abscess Localization
 502. Tenner. Echoencephalography

503. Wesenberg. The Newborn Chest: State of the Art—1976
 504. Gold. Computerized Tomography (CT) of the Head
 505. Whalen, Kazam. Radiology of the Abdomen: Anatomic Approach (Conventional Radiology, Ultrasound and CT Scanning)
 506. Sagel, Forrest. Special Procedures in Pulmonary Radiology
 507. Heitzman. Roentgen Pathologic Correlations in Common Pulmonary Disorders
 508. Weber. Radiological Evaluation of Eye and Orbital Lesions
 509. Carlson. The Esophagus

Categorical Course on the Skeletal System

September 19–24, 1976

Sidney W. Nelson, general chairman; Jerome F. Wiot, course co-ordinator; and Robert H. Freiburger, program chairman

Please note: This course extends over 16 hr using all available time for instructional courses. If you select this course, do not register for any of the others. Fee is \$25 and must be paid by everyone.

Course Outline

Sunday, 1–5 p.m., Arthritis

Precise Descriptive Terms and the Round Cell Tumors. Gwilym S. Lodwick, professor and chairman, Radiology, University of Missouri School of Medicine, Columbia.

Osteoid Matrix Tumors. Jack Edeiken, professor and chairman, Radiology, Thomas Jefferson University Hospital, Philadelphia.

Chondroid Matrix Tumors. Harold G. Jacobson, professor and chairman, Radiology, Albert Einstein College of Medicine; radiologist-in-chief, Montefiore Hospital, Bronx, NY.

Fibrous Matrix Tumors. Elias G. Theros, professor, Radiological Sciences, University of California, Los Angeles.

Monday, 1–5 p.m., Bone Tumors

Inflammatory Arthritis of Peripheral Joints. William Martel, Radiology professor, University of Michigan Medical Center, Ann Arbor.

Osteoarthritis, Osteonecrosis, and Neuropathic Arthritis. Alex Norman, professor of medicine, Mount Sinai School of Medicine CUNY; director, Radiology, Hospital for Joint Diseases, both New York City.

Axial Arthritis. Donald L. Resnick, assistant radiology professor in residence, University of California; chief, orthopedic division, Radiology, Veterans Administration Hospital, both San Diego.

Metabolic and Miscellaneous Arthritis. Frieda Feldman, radiology professor, Columbia University College of Physicians and Surgeons; attending radiologist, Columbia Presbyterian Medical Center, New York City.

Tuesday, 3–5 p.m., Systemic Bone Disease

Bone-Fundamentals and Physiology. Joseph P. Whalen, radiology professor, New York Hospital-Cornell Medical Center, New York City.

Osteomalacia, Hyperparathyroidism, Osteoporosis, etc. Pamela S. Jensen, associate radiology professor, Yale University School of Medicine, New Haven.

Wednesday, 3–5 p.m., Nuclear Medicine and Bone Quality Determination

Nuclear Medicine of the Skeletal System. Raymond Mary, assistant clinical professor of radiology (nuclear medicine), University of Washington, Seattle.

Bone Quality Determination by Other Means. John Cameron, professor of radiology and physics, University of Wisconsin, Madison.

Thursday, 3–5 p.m., Trauma

Trauma. Sidney W. Nelson, radiologist, Swedish Hospital, Seattle.

Trauma. John H. Harris, Jr., chairman, Radiology, Carlisle Hospital, Carlisle, PA.

Angiography in Trauma. Stanley Baum, professor and chairman, Radiology, University of Pennsylvania Hospital, Philadelphia.

Friday, 11 a.m.—1 p.m., Arthrography

Arthrography of the Knee. Jeremy J. Kaye, section head, Bone and Joint Radiology; radiology professor, Vanderbilt University Hospital, Nashville.

Arthrography of the Shoulder, Hip and Ankle. Robert H. Freiburger, radiology professor, Cornell University Medical College; director, Radiology, Hospital for Special Surgery, both New York City.

Description of Courses

101

Brain Imaging. Robert J. Cowan, associate professor nuclear medicine, Bowman Gray School of Medicine of Wake Forrest, Winston Salem, NC. The current status of brain imaging will be discussed including cerebral dynamic studies, static brain imaging, and transmission techniques. Emphasis will be placed on newer developments and correlation of multiple studies.

102

The Radiological Aspects of Certain Familial Cancers. Gerald D. Dodd, professor and chairman, Radiology, M. D. Anderson Hospital, Houston. Familial aggregations of tumors may occur in virtually all organ systems. Prominent among these are certain gastrointestinal

cancers, neoplasms of the endocrine system, and the nevroid basal cell carcinoma syndrome. Recognition of these tumors is of importance with respect to cancer control and prevention. Detailed studies of affected individuals, particularly in the early stages of disease, may produce information relative to carcinogenesis. The radiologist has a unique opportunity to assist in the diagnosis and identification of these hereditary syndromes. The clinical and genetic aspects will be summarized and pertinent radiologic features described.

103

An Introduction to Diagnostic Ultrasound. Barry B. Goldberg, head, Diagnostic Ultrasound, Episcopal Hospital; professor, Temple Uni-

versity Health Sciences Center, both Philadelphia. Diagnostic ultrasound has assumed ever increasing importance in medicine, particularly as an adjunct to many radiological procedures. This course will provide information on the diagnostic uses of ultrasound utilizing all four established modes of display, i.e., A-mode, M-mode, Doppler and B-scan including gray scale. The basics of physics and instrumentation will be provided. Emphasis will be placed on the established uses of ultrasound in all areas of the body including the head, chest, abdomen, and pelvis. A course outline as well as a list of available books will be distributed.

104

Computerized Axial Tomography. Norman E. Chase, professor and chairman, Radiology, New York University Medical Center School of Medicine, and director, Radiology, Bellevue Hospital, both New York City; and Irwin I. Kricheff, radiology professor, New York University Medical Center School of Medicine, and neuroradiology director, New York University Medical Center, Bellevue Hospital. A presentation of the technique and principles of the CT scanner will be given and a number of areas where the CT scanner is particularly useful in the diagnosis of diseases of the brain will be presented. In addition, a number of typical cases of various types of cerebral disease, neoplasm, atrophy, vascular disease, etc., will be demonstrated.

105

Plain Film Approach to Pulmonary Venous Congestion. Larry P. Elliott, professor, Cardiac Radiology, University of Florida College of Medicine, Gainesville. Heart and lung disease accounts for the vast majority of deaths in the U.S. especially over the age of 40. Every radiologist must deal daily with patients who present in some form of congestive failure. This course is a sequential approach to the plain chest film in an adult who presents with pulmonary congestion. The importance and type of physiologic data that can be derived from an analysis of the pulmonary vessels is emphasized. A roentgenologic-anatomic classification of common forms of heart disease will be given. Entities that will be stressed are rheumatic mitral valve disease (stenosis, insufficiency, associated valve lesions, giant left atrium etc.). The other large category includes lesions which stress the left ventricle (calcific aortic stenosis, coronary ischemia and its manifestations, lesions of the aorta and myocardiopathies).

106

Basic Principles of CT Scanners. J. Thomas Payne, assistant professor, Radiology, University of Minnesota Hospitals, Minneapolis. This course will discuss the basic operating principles of first, second, and third generation CT scanners. Problems associated with X-ray tube operation, detectors, and mechanical alignment will also be covered. The contrast scale or CT numbering scale as it relates to a change in linear attenuation for the different commercial units will be discussed. The relative merits of different forms of image readout (transparency films, various types of hardcopy, etc.) will be evaluated. Possible tradeoffs between body and head type CT units as well as matrix size versus noise will be discussed. Finally, common artifacts as well as radiation dose for single and multiple scans for different CT units will be presented.

Tuesday

201

The Applications of Nuclear Medicine in Pediatrics. Hirsch Handmaker, director, Nuclear Medicine, Childrens Hospital; assistant clinical professor, Radiology, University of California, San Francisco. The increasing applications of diagnostic nuclear medicine techniques in clinical pediatrics are directly related to several technological advances that have occurred in the past decade. Routine availability of short half-life radionuclides with appropriate gamma ray emissions, resultant lower radiation exposure to tissues, and improved detector systems with higher resolution have been instrumental in bringing about these increases. Improvements in data storage and analysis systems have led to useful quantitative tech-

niques for the evaluation of dynamic functions of the brain, lung, heart, and kidney. In addition to the evaluation, staging and followup of children with malignancies, there has been a marked increase in radionuclide studies in children with congenital and infectious diseases. The discussion of Pediatric Nuclear Medicine will include considerations of technique, well-established and newer procedures, and abundant clinical examples of the more commonly performed studies in everyday practice. Comparative dosimetry data with other diagnostic procedures will be included in this presentation. Emphasis will be placed on those pediatric conditions which might be encountered by physicians in practice and outside of large pediatric centers and that involve routinely available radio-pharmaceuticals and imaging equipment.

202

Dynamic Radiology of the Abdomen: Normal and Pathologic Anatomy. Morton A. Meyers, professor, Radiology, New York Hospital-Cornell Medical Center, New York City. This course emphasizes the practical application of knowledge of anatomic relationships and the dynamics of spread of disease in the abdomen to precise radiologic diagnosis. Anatomic sections will provide basic correlation with plain films, conventional contrast studies, ultrasonography, and computerized transverse tomography. Features of the intraperitoneal and extraperitoneal spaces will be stressed leading to specific diagnostic criteria. Clinical applications include abscesses, perforations, traumatic lesions, and malignancies.

203

Basic Principles of Ultrasound Imaging. Paul L. Carson, Assistant Professor of Radiology, University of Colorado Medical Center, Denver. The nature of ultrasound propagation in tissue will be discussed, with emphasis being placed on the origin and masking of diagnostic information in ultrasound waves in tissue. Several fundamental, practical and unnecessary limitations of imaging with pulse echoes and other reflected and transmitted ultrasound waves also will receive attention. For example, the types of information and artifacts arising from single and multiple reflections, scattering, phase distortion, dispersion, refraction, mode conversion and absorption will be described as will the effects of the necessarily finite ultrasound beam size or resolution in the diagnosis of small lesions.

204

The Angiographic Diagnosis of Intracranial Mass Lesions. Norman E. Chase and Irwin I. Kricheff (see 104). This course will include a logical approach to the study and differential diagnosis of supratentorial intracranial mass lesions with an analysis of localization by shift, vascular displacements and physiologic changes. The techniques of angiography and supplemental studies will also be included.

205

The Small Bowel in Pediatric Radiology. J. Scott Dunbar, Children's Hospital, Cincinnati. When should the small bowel be examined in the course of a "routine upper G.I. study"? What place does the study have in the evaluation of abdominal pain in childhood? What sort of lesions are we looking for? How specific are the findings in celiac disease or in "malabsorption syndrome"? Do all infants have small bowel patterns which look like malabsorption? Are the problems and x-ray findings related to them in the small bowel the same for infants and children as they are in the adult, for the most part? What is a reasonable study of the small bowel in a child?

206

Performance Evaluation of CT Scanners. Edwin C. McCullough, Department of Oncology, Mayo Clinic, Rochester, MN. The performance measurement of CT scanners is of interest for a variety of reasons. In addition to the obvious use in a quality assurance program, performance data is of potential value when several CT scanners are being considered for purchase. In this course we review various measures of performance for a CT scanner, being careful to empha-

size their importance relative to clinical needs. Representative data from several CT scanners will be presented. The major emphasis of this course will be to provide easy-to-understand guidance for the radiologist who is in the position of deciding on the purchase of a CT scanner. Some familiarity with CT scanning will be presumed; for example, at the level of course 106 Basic Principles of CT Scanners given by J. Thomas Payne.

207

Varied and Unusual Sequelae in Both Systemic and Primary Bone Disease in Children. David H. Baker, director and professor, Radiology; and Walter E. Berdon, associate director and professor, Radiology both Babies Hospital, Columbia-Presbyterian Medical Center, and Columbia College of Physicians and Surgeons, New York City. This course will discuss the important aspects in new developments as they relate to bone infection, the inflammatory arthritides, and other acquired local and system disease in children. The difference between the child and the adult will be stressed, the emphasis will be clinical and the approach practical.

208

The Radiological Investigation of Hydrocephalus. D. Gordon Potts, professor, Radiology, The New York Hospital-Cornell Medical Center, New York City. The diagnostic approach to hydrocephalus has been markedly changed by computed tomography. This new study must be used in conjunction with one or more of the older procedures—plain skull films, angiography, pneumoencephalography and ventriculography. Many of the lesions that cause hydrocephalus are of special interest since they are near or beyond the resolution limits of modern computed tomography. A practical plan for the investigation of hydrocephalus will be presented. The information derived from computed tomography, and the use of other procedures to provide information that is not obtained from computed tomography will be considered.

209

Radiologic-Pathologic Correlation of Interesting Lesions of the Gastrointestinal Tract. Richard H. Marshak, clinical professor, Radiology, Mount Sinai School of Medicine, New York City. Despite the pathologists and clinicians skepticism as to the radiologists ability to make a cytologic diagnosis, the author will demonstrate how histologic diagnosis can be achieved with a considerable degree of accuracy. Interesting cases involving the stomach, the small intestine, and colon will be presented with their pathologic counterparts. They will include such diverse material as polypoid lesions of the stomach, superficial spreading carcinoma, Menetrier's disease, and the "narrowed stomach," etc. In the small bowel, tumors, immunoglobulin deficiency diseases, retractile mesenteritis and related entitis, ischemic disease, and lymphosarcoma will be discussed. Colonic lesions will include lymphosarcoma, scirrhous carcinoma of the colon, colitis cystica profunda, Kaposi's sarcoma, amebiasis, and the problem of colonic polyps. Possible etiology and management of some of these difficult cases will also be discussed.

210

Granulomatous Diseases of the Lung: A Radiologic-Pathologic Correlative study. Elias G. Theros, professor, Radiological Sciences, University of California, Los Angeles. Man is beset by a multitude of agents that may trigger granulomatous reactions in the pulmonary tissues. The variation in his ability to resist and contain them gives rise to a number of localized and diffuse morphological changes which are reflected in a wide gamut of roentgenographic patterns. A spectrum of such patterns will be presented and correlated with the gross and histological findings. Although such roentgen patterns are frequently not diagnostic enough for specific labeling they are often reliably characteristic. Such characteristics will be stressed and explanations for them sought in the pathogenesis of these diseases or in the disturbed morphology noted by the pathologist. In any such review, the fungi are of great importance, not only because they yield a veritable panorama of roentgen patterns for considera-

tion, but also because they are an increasing clinical problem resulting from the recent widespread use of immunosuppressive agents, steroids, and cytotoxic agents. The fungi, therefore, will be given special attention but a survey will be made of the important categories of agents that cause granulomatous response in the lungs: the pneumoconioses, histiocytosis, sarcoidosis, acid-fast disease, and the collagen diseases.

211

Renal Cystic Disease in Adults and Children. John R. Thornbury, professor, Radiology, University of Michigan Medical Center, Ann Arbor. A brief review of current thoughts about the embryologic basis for the pathogenesis of cystic renal disease will be presented. The first portion of the course will be devoted to a presentation of the spectrum of the infantile polycystic disease/renal dysplasia/adult polycystic disease diagnostic problem. Subsequently, medullary cystic disease, benign simple cyst (single and multiple), and medullary sponge kidney will be discussed and put into perspective. Current concepts of the hereditary aspects of the various entities will be included. The aim of the course will be to present all you want to know about this ambiguous area of renal disease so that you can solve the diagnostic problems in reasonable fashion in daily practice.

212

Sinuses, Nasopharynx, and Base of Skull. A. S. MacMillian, Jr., assistant clinical professor, Radiology, Harvard Medical School, Radiologist, Massachusetts Eye and Ear Infirmary and Harvard Medical and Surgical Services, Boston City Hospital. Five standard views provide an accurate scout film evaluation with optic canal projections the principal accessory views. Fluoroscopic control of catheter and other techniques is routine. Tomography is principally AP and lateral with some basal and supine optic canal positions. Anatomical variations and no disease, trauma-fracture, inflammation and infection, sinus and nasopharyngeal neoplasms are seen in descending order. Involvement of the orbit, facial bones, nasal bones, and cranial nerves I-VI may occur. A Le Forte III stress line fracture is a prime example of the total involvement of the facial area in disease states.

213 and 313

Mammography, Part I and II. John N. Wolfe, chief, Radiology, Hutzel Hospital, Detroit. The following subjects will be discussed: (1) diagnosis of carcinoma; (2) risk for developing breast carcinoma; (3) selected short subjects as problems in diagnosis—skin thickening, areolar thickening, axilla, male breast. The subject of the radiographic diagnosis of carcinoma of the breast will be discussed at some length with some emphasis on the subtle signs and problems. Some of the recent work done at Hutzel Hospital regarding the prediction of risk for developing breast cancer on the basis of mammography will be presented. Short subjects, which are often problems in diagnosis, will be discussed as listed, depending on available time. Most of the graphic material will be xeroradiographs. We will be discussing morphologic changes and there should be no problem in the translation of information from x-ray to conventional film mammography.

Wednesday

301

What is New in Radiopharmaceuticals and Instrumentation. Robert E. O'Mara, radiology professor and chief, Division Nuclear Medicine, University of Rochester Medical Center, NY. This instruction course will deal with new developments in radiopharmaceuticals for bone, tumor, inflammatory disease and kidney studies. In addition, newer developments within instrumentation will be discussed. These will include large field of view cameras, scanning cameras, tomographic and positron units. The relationship to newer development in medical imaging such as ultrasonography and computerized axial tomography in transmission mode will be discussed.

302

Radiologic Evaluation of the Acute Abdomen. Reed P. Rice, associate radiology professor, Duke University Medical Center, Durham, NC. This course is designed to illustrate the value of radiology in the evaluation of the patient with acute abdominal symptomatology. This will include the value of the plain abdominal roentgenogram in the specific diagnosis of diseases, but will also provide a guide to the contrast examination of choice in appropriate situations. An aggressive approach to the use of simple contrast examinations can result in significantly earlier diagnosis.

303

Abdominal Ultrasonography. George R. Leopold, Associate professor, head, Division Diagnostic Ultrasound, University of California Hospital, San Diego. This course will emphasize the wide applicability of ultrasonic radiography in the diagnosis of abdominal disorders. Following a discussion of the normal anatomy of the various organ systems, pertinent examples of pathological disturbances will be presented. Abdominal imaging has been greatly facilitated by the introduction of the gray scale technique which permits display of intra-organ parenchymal echoes and a large number of vascular structures that previously could not be discerned. The resultant image enhancement is certain to assure greater popularity of the technique among radiologists interested in gastrointestinal disease.

304

Pediatric Pulmonary Abnormalities. Edward B. Singleton, director, Radiology, St. Luke and Texas Children's Hospital, Texas Heart Institute; clinical professor, Baylor University, Houston. The course will consider causes of respiratory distress in the newborn and young infant. This age group is important not only to the obstetrician, pediatrician, and pediatric radiologist, but also to the general radiologist in his contact with the hospital maternity and newborn sections. The causes of respiratory distress in this young age group are numerous and include extrapulmonary conditions such as congenital heart disease, intestinal obstruction, diaphragmatic hernia and central nervous system damage. Conditions to be discussed include: primary pulmonary diseases producing respiratory distress in the newborn and young infant—transient tachypnea of the newborn (wet lung syndrome) respiratory distress syndrome; chronic pulmonary insufficiency of prematurity; aspiration syndrome; pulmonary hemorrhage; intrauterine infectious pneumonia; aspiration pneumonia; Wilson-Mikity syndrome; bronchopulmonary dysplasia; pulmonary lymphangiectasia; and pulmonary agenesis. Other conditions covered will include surgical or mechanical abnormalities producing respiratory distress in the newborn and young infant—obstruction of upper air passages; esophageal atresia and tracheoesophageal fistula; bronchopulmonary foregut malformations; pulmonary sequestrations; pneumomediastinum and pneumothorax; congenital lobar emphysema; congenital cystic adenomatoid malformation; phrenic nerve paralysis and eventration; diaphragmatic hernia; accessory diaphragm; vascular ring; chylothorax; and congenital deformities of the thorax. If time permits, some of the common and rare pulmonary infections encountered in the young infant will be included.

305

Computerized Tomography of the Abdomen. Robert R. Hattery and David H. Stephens, both Diagnostic Roentgenology, Mayo Clinic, Rochester, MN. In the brief time period that computerized tomography (CT) has been available for examination of the abdomen, a variety of valid and potentially valid clinical applications of the method has become apparent. The principles and techniques of abdominal CT scanning, the use of oral and intravenous contrast medium, and the manipulation of width and window height will be discussed. Pertinent cross-sectional normal anatomy of the abdomen will be reviewed. Information gained from 1 year's clinical experience with a prototype model of the EMI body scanning system will be presented. Using illustrative clinical material, the CT features of a variety of disorders of abdominal organ systems will be pre-

sented and correlated with other imaging procedures. Capabilities as well as current limitations of abdominal CT will be discussed.

306

Diagnosis of Spinal Lesions. Norman E. Leeds, Professor, Radiology; head, Neuroradiology Section, Montefiore Hospital and Medical Center, Bronx, NY. The course will deal with radiographic changes that enable one to distinguish between benign and malignant lesions of the spine. A variety of lesions will be shown to prove the validity of these observations. The many causes and significance of scalloping of vertebral bodies will also be demonstrated including the physiologic occurrence. Neurofibromatosis with its protean manifestations will be demonstrated including scalloping, scoliosis, meningocele, as well as the frequent occurrence of cord tumors in these patients.

307

Interesting and Significant Lesions of the Alimentary Tract. William Martel, professor, Radiology, University of Michigan Medical Center, Ann Arbor. This will deal with a variety of lesions. Some are unusual manifestations of common disorders, other were chosen because they serve as a springboard for discussion of current concepts, while some illustrate lesions which are often confused with other conditions or missed entirely. Differential diagnosis will be stressed where appropriate.

308

Pattern Recognition of Disseminated Pulmonary Disease. Benjamin Felson, professor, Radiology, University of Cincinnati College of Medicine, Cincinnati General Hospital. There are a number of patterns of widespread pulmonary involvement recognizable on the chest film, including vascular, alveolar, honeycomb, miliary, small irregular shadow, bronchial, and destructive patterns. Each has its own causes. This presentation will emphasize how to distinguish the different patterns and why it is important to do so.

309

Coronary Angiography. Melvin P. Judkins, professor and chairman, Radiology; director, Cardiovascular Laboratories, Loma Linda University Medical Center, CA. Abstract not available at press time.

310

Radiology of the Urinary Tract. Joshua Becker, professor and chairman, Radiology, State University of New York, Downstate Medical Center, Brooklyn. The Course will cover the approach to the optimal urogram in the examination of urinary tract pathology. Dose and salt of the contrast agent will be discussed not only in regard to opacification of the kidney and collecting system but also in relationship to their toxic effects. Developmental anomaly inflammatory processes, neoplastic diseases and trauma will be reviewed in regard to their differential diagnoses for similar appearances at urography, nephrotomography, and angiography. A section will be devoted to the evaluation of the solitary mass lesions of the kidney with emphasis upon needle aspiration. The application of interventional radiology will be discussed reviewing renal embolization for bleeding and neoplasms.

311

Skeletal Radiology, Newer Concepts and Provocative Challenges. Harold G. Jacobson, professor and chairman, Radiology, Albert Einstein College of Medicine, and radiologist-in-chief, Montefiore Hospital and Medical Center, Bronx, NY; and Stanley S. Siegelman, professor and director, Diagnostic Roentgenology, Johns Hopkins University School of Medicine, Baltimore. This course will be divided into two approximately equal sections. In the first, the subject of the plasma cell dyscrasias will be discussed. The clinical manifestations of plasma cell dyscrasias will be shown to be due to the physical effect of expanding masses of cells plus the consequences of circulating plasma cell products. A brief review of normal immunoglobulin synthesis will be presented, followed by a series of cases illustrating radiological manifestations of myeloma, amyloido-

sis, Waldenström's macroglobulinemia, plasma cell granuloma, and heavy chain disorders. The significance of peripheral skeletal lesions in myeloma will be described, the concept of myeloma as a "scar tumor" will be discussed, any osteomalacia as a clinical presentation of myeloma will be illustrated. The dynamics, pathophysiology and interrelationships of the various plasma cell dyscrasias will be emphasized.

In the second half, some interesting manifestations of the skeletal features of various metabolic and endocrine disorders will be considered. These will be selected from a group of abnormalities including hyperparathyroidism, the hypoparathyroid complex, acromegaly, Cushing's syndrome, familial hyperphosphatasemia, osteomalacia, hypophosphatasia, gout, pseudogout and hemochromatosis. In each group of disorders unusual or even esoteric examples of a specific entity will be presented, to serve as a springboard for the demonstration of more frequently encountered manifestations of the abnormality under discussion. The pathogenesis of the skeletal changes in each disorder will be stressed and newer concepts will be advanced when appropriate. In this latter course section, registrants will be encouraged to offer diagnostic possibilities.

312

The Neck (Pharynx, Cervical Esophagus, Larynx and Trachea). A. S. MacMillan, Jr. (see 212). Patients presenting with any of the "Three D's"—Dysphagia, Dysphonia and Dyspnea—require evaluation of the upper digestive tract and the airway. An orderly protocol has been developed which can be interrupted when the question in mind is answered. An AP 1 mm copper filtered 130 kV 7×17 inch film and a series of lateral neck films, soft tissue technic, begins the evaluation. It is well to include four chest films—PA, lateral and both obliques, with no barium in the esophagus. These initial films will answer most problems. With dysphagia a barium swallow is routine. It may be used in dysphonia, but only judiciously in dyspnea where aspiration poses a risk. Next in sequence is a special set of laryngeal tomograms. Tracheal tomography in AP and lateral projections may be required. Then a detailed fluoroscopic study of the pharynx, larynx, trachea, and chest is performed. After TV monitoring, recording is carried out by conventional spot films, 100 mm cine cut film, videotape, and overhead films. Laryngeal carcinomas are routinely evaluated by positive contrast laryngography prior to biopsy, in addition to all of the above. Tracheal contrast studies are best done with air.

313

Mammography, Part II, John N. Wolfe (see 213).

Thursday

401

Radionuclide Imaging Studies of Lungs and Heart. Robert E. Polcyn, associate professor, Radiology; director, Nuclear Medicine Section, University of Wisconsin Center for Health Sciences, Madison. Perfusion lung imaging has for many years been one of the primary diagnostic tools for evaluating patients with suspected pulmonary embolic disease. Our substantial experience with this study has resulted in a high level of understanding of the pathophysiological conditions which result in aberrations in pulmonary perfusion. Ventilation studies performed with ^{133}Xe enhance the reliability of radionuclide investigation of patients with pulmonary embolic and other categories of lung disease. Radiotracer labelled aerosols and other radionuclide approaches to the study of the lungs are under current investigation. Nuclear Cardiology is currently a rapidly expanding aspect of the practice of Nuclear Medicine. Radiopharmaceuticals are currently available which reliably localize to normal myocardium and experience with $^{99\text{m}}\text{Tc}$ -pyrophosphate localization in recently infarcted myocardium points to an important clinical role for this radiopharmaceutical. Electronic advances and the availability of $^{99\text{m}}\text{Tc}$ -labelled albumin have made it possible to generate high quality cinematic displays of myocardial wall motion allowing for noninvasive evaluation of ventricular dyskinesias and measurement of ejection fraction. Significant patient benefit appears likely to follow from routine performance of these studies in the general hospital setting.

402

Cardiac Ultrasound. Donald L. King, associate professor radiology; director, Ultrasound Division, College of Physicians and Surgeons, Columbia University, New York City. Discussion will include conventional techniques of echocardiography, real-time imaging and newer advances in technology. Routine clinical applications and clinical reporting of derived diagnostic information will be emphasized.

403

Neonatal Chest Problems. Leonard E. Swischuk, professor, radiology and pediatrics, University of Texas Medical Branch, Galveston. The radiologist plays a key role in the diagnosis of neonatal chest disease. His basic job is to determine whether a surgical or medical condition exists, but may times this can be problematic. It is not so much that one is not familiar with such conditions as hyaline membrane disease, TRDN—wet lung syndrome, congenital diaphragmatic hernia, meconium aspiration, etc., but rather that one is often not able to come up with a useful differential diagnosis for certain abnormal roentgenographic patterns. For example: What does one think of when one is presented with: (1) a large, opaque hemithorax; (2) a large, hyperlucent hemithorax; (3) a small, densely opaque hemithorax; (4) a small, slightly opaque hemithorax; (5) bilateral fluffy infiltrates; (6) bilateral bubbly lungs, small bubbles, large bubbles; (7) bilateral granular lungs; or (8) bilateral parahilar, streaky, congested appearing lungs? Each disease will be dealt with in enough detail so as to allow differentiation of one from the other, but grouping according to abnormal pattern is the place to start.

404

A Simplified Approach to Posterior Fossa (Vertebral) Angiography. M. M. Schecter, director, Neuroradiology Section, Radiology Albert Einstein College of Medicine, Bronx, NY; and Joseph A. Marc, director, Neuroradiology Section, Radiology Grady Memorial Hospital of Emory University, Atlanta. A practical guide to interpretation of angiography of the posterior fossa will be presented. The normal arterial and venous angiographic anatomy will be shown and correlated with specimens and simplified with line drawings and geometric designs. The angiographic findings in pathologic conditions involving the brain stem, cerebellum, fourth ventricle cerebellopontine angle, foramen magnum and tentorium will be correlated with gross pathology. An outline summary of the course will be distributed.

405

CT Scanning of the Breast, Chest, and Head. David F. Reese, J. R. Muhm, and Patric F. Sheedy, all Diagnostic Roentgenology, Mayo Clinic, Rochester, MN. Abstract not available at press time.

406

The Gastrointestinal Tract: Radiological Challenges. Harold G. Jacobson, (see 311). In this presentation a variety of highly interesting and even infrequently encountered abnormalities of the gastrointestinal tract will be demonstrated. Unusual manifestations of more commonplace conditions will also be included. These entities will be organized into appropriate categories, e.g., congenital, infective, neoplastic, etc. The concept will be stressed that even in the most difficult cases, radiological criteria are often so definitive that a careful analysis of films should ensure that the correct diagnosis is, at least, seriously considered and often offered categorically. It is also anticipated that this course will demonstrate that diagnostic challenges which test the acumen of clinical radiologists constitute an important impetus to the learning process. Barium studies of the gastrointestinal tract still occupy a large part of clinical diagnostic radiology in this rapidly changing era, and the gastrointestinal tract provides a fertile and fascinating source of exciting challenges.

407

Roentgenographic Spectrum of Pleural Disease. Vernon A. Vix, radiology professor, University of Indiana Medical Center, Indianapolis. Radiologic abnormalities both functional and anatomical

Section on Instruction Order Sheet

It is important to register for the Instruction Courses early since the number admitted to each course will be limited. It is also important that first, second, and third choices be listed for each period. All ticket orders will be filled according to postmark.

Nonmembers of the American Roentgen Ray Society will pay \$3 for each course period. *Nonmembers' fees must accompany this sheet and will not be returned unless cancellation is received before September 13, 1976.*

Members of ARRS, residents in radiology, and nonmembers who are contributing to the program, either by way of an instruction course, a paper, or a scientific exhibit, are not required to pay for these courses but must submit this form.

Tickets for courses will be mailed to those whose order reaches the office of the director on or before Monday, September 6. They will be sent to the address below unless directed otherwise. Tickets for late registrants will be available at the Registration Desk of the Section on Instruction at the Washington Hilton Hotel on and after Sunday morning, September 19.

Please type or print:

Last Name First Name or Initials

Street Address

City State Zip Code

Check one:

- ☐ Member
- ☐ Guest
- ☐ Resident in radiology at: _____
- ☐ Scientific exhibitor/paper



I wish to take the Categorical Course on Bones, 6 periods, Sunday-Friday ☐
Fee: \$25

Period	First Choice	Second Choice	Third Choice
	Course No.	Course No.	Course No.
Monday			
Tuesday			
Wednesday			
Thursday			
Friday			

Mail to:

Dr. Eugene Gedgaudas
Director of Instructional Courses
American Roentgen Ray Society
c/o American College of Radiology
20 North Wacker Drive
Chicago, IL 60606

If mailing late, send to:

Dr. Eugene Gedgaudas
Washington Hilton Hotel
Washington, D.C. 20009

Make checks payable to
American Roentgen Ray Society

Be sure to fill out second and third choices for each period

SECTION ON INSTRUCTION

are commonly seen when changes in the pleura occur. These changes may be either primary or secondary to other disease. This pleural participation in disease may present as an easily recognized pattern or may modify the appearance of an underlying disease. This course will discuss some of the physiology of the pleura as well as present correlated clinical radiographic material in which the recognition of pleural pathology may in itself be diagnostic, aid in diagnosis, or determine the clinical approach to the patient.

408

Pulmonary Circulation and Embolism. Richard H. Greenspan, professor and chairman, Radiology, Yale University School of Medicine, New Haven. This course will analyze pulmonary blood flow distribution in five main categories: normal, pulmonary venous hypertension, pulmonary arterial hypertension, modifying factors for distribution, and pulmonary embolism. Normal appearances will be affected by variations in patient position, phase of respiration, on going muscular activity, and state of hydration. The radiographic findings in pulmonary venous hypertension include haziness of vessel margins, redistribution of flow to upper lobes, septal lines, pulmonary edema, and pleural effusion. In pulmonary arterial hypertension, the features are large central arteries, rapidly tapering peripheral arteries, and flow redistributions with vessel caliber similar in upper lobes and bases. A major modifying factor in distribution will be chronic obstructive pulmonary diseases. Discussion of pulmonary embolism will include epidemiology, clinical findings, and study methods including laboratory, chest film, isotope perfusion and ventilation scans, and pulmonary angiography.

409

Pitfalls in the Diagnosis of Cervical Spine Trauma. John A. Gehweiler, Jr., associate radiology professor, Duke University Medical Center, Durham, NC. Many radiologists and surgeons feel fallible when confronted with patients having sustained traumatic injuries of the cervical spine. Thus, the emphasis in this instructional course will be to simplify the problem and to provide the practicing radiologist with the practical points that he may use daily to diagnose the various injuries of the cervical spine. In order to accomplish this goal, the following topics will be discussed: (1) roentgen techniques used to examine the severely injured patient, and patients with chronic symptoms having a "normal routine" radiologic examination; (2) a review of the normal anatomy of the cervical spine with special emphasis on rarely used radiographic projections—this is a fundamental prerequisite for the accurate interpretation of injuries; and (3) an analysis of the mechanisms of injury to the spine and the resulting roentgen patterns. The atlas and axis will be considered separately from the remainder of the cervical vertebrae.

410

What Every Radiologist Should Know About the Ear. Guy D. Potter, radiology professor, College of Physicians and Surgeons, Columbia University and Columbia-Presbyterian Medical Center, New York City. The radiographic examination should be keyed to the particular condition with which a patient presents, such as congenital atresia, trauma, inflammatory disease, and neoplasm. Radiographic description of these conditions will be presented in contrast with normal radiographs and tomograms. Information which the radiologist should include in his report to the treating physician will be discussed.

411

Detection of Early Breast Cancer. Robert L. Egan, chief, mammography Section, Radiology, Emory University School of Medicine, Atlanta. A review of mammography, and other modalities it has engendered, and the study of breast diseases will be presented. The value of mammography, its pitfalls and how to obtain the most from the procedure will be stressed. Also frankly discussed will be mammographic equipment, radiographic detail and dosage, compression, screen-film combinations, processing, collimation and requirements for an occasional as well as a busy mammographic room. If desired, discussion can extend into thermography and modified radiographic techniques for breast examination.

412

Tricks and Treats in Tomography. Kenneth R. Kattan, associate radiology professor University of Cincinnati Medical Center. The course describes the different pitfalls in tomography and how to avoid them. The law of tangent is stressed and its clinical applications are described. Mention is also given to the application of law of tangent to a curved surface. Parasitic and phantom shadow formations are explained in diagrams and clinical examples of each are given. The importance of proper rotation of the patient and the proper direction of the tube in order to decrease distortion of the image is mentioned. This is feasible only if proper examination of the study is initiated. The conventional roentgenogram (and sometimes fluoroscopy) is done before initiation of the tomographic study. The various tube movements, the different thickness of the cut and the degree of spacing between the cuts in different studies are reviewed.

413

Normal Arterial Anatomy of the Gastrointestinal Tract and Related Organs. Francis F. Ruzicka, professor and associate chairman, Radiology, University of Wisconsin Medical Center, Madison. This course is designed first to present in simplified form the prevailing patterns of variations of the visceral arteries. In addition to the variations of the major trunks, the arteries of the liver, gallbladder, pancreas, spleen and gastrointestinal tract will be discussed in detail. Further, major collateral routes that involve the visceral arteries will be illustrated: (1) the vertical pathways between the celiac and superior mesenteric artery systems; (2) the vertical pathways between the superior mesenteric and the inferior mesenteric artery systems; and (3) the horizontal collateral routes between the right and left sides of the celiac artery system. Secondly, the predominate normal portal venous pattern and the more common variations as seen radiologically will be described and illustrated. Thirdly, test cases will be presented for audience participation for the sake of repetitive instruction.

Friday

501

Liver, Spleen, and Bone Imaging; Tumor and Abscess Localization. Lawrence R. Muroff, clinical assistant professor, University of Southern Florida College of Medicine; director, Nuclear Medicine, University Community Hospital, Tampa. The course will emphasize the increased applicability of radionuclide imaging in the evaluation of patients with specific diagnostic problems. The practical nature of these studies will be explored and limitations of the various procedures, as well as, their indications will be discussed. Radiopharmaceuticals that are available to most nuclear medicine departments will be covered, and the differential utilization of each will be enumerated. The course will be geared to the private practitioner of nuclear medicine who is interested in becoming acquainted with the newer, expanded practical applications of nuclear imaging.

502

Echoencephalography. Michael Tenner, associate radiology professor, State University of New York, Downstate Medical Center, Brooklyn. Ultrasonographic characterization of different brain structures can be satisfactorily accomplished only after achieving a thorough understanding of the underlying neuroanatomy pertinent to this modality. The echoencephalogram is usually done by A-mode techniques and only in a small portion of cases is the more anatomically explicit B-mode technique used. In order to obtain reliable results by A-mode techniques, a systematic search for certain intracranial structures must be made. This requires the identification of the third ventricle, a well known technique, followed by a search for the position of the lateral ventricles, and the midline structures at this higher level. The methodology in characterizing mass lesions will also be presented as well as the value of studying the midbrain in a midline sagittal plane. It is becoming evident that this technique is an excellent adjunct to computerized tomography for several reasons. It is an effective screening tool in patient selec-

SECTION ON INSTRUCTION

tion for computerized tomography. Some lesions are characterized better by ultrasound reflections than by averaged radiation absorption, and it is often the only noninterventional procedure that can be done in the agitated patient. Also, it is a useful screening procedure particularly in the very young when radiation dosage at any level should be avoided.

503

The Newborn Chest: State of the Art, 1976. Richard L. Wesenberg, pediatric radiologist, University of Colorado Medical Center, Denver. The latest concepts in newborn chest film interpretation will be presented. Components of the normal neonatal chest will be analyzed, utilizing logical and practical radiologic criteria. These criteria will then be applied to a discussion of the major types of respiratory distress in the newborn: (1) wet lung disease—T.R.D.N.; (2) drowned newborn syndrome (D.N.S.)—aspiration of clear amniotic fluid *in utero*; and (3) hyaline membrane disease—R.D.S. Practical points concerning new developments in newborn chest radiography and film interpretation to be presented are: radiation dosage in the newborn from routine radiographic examinations; low dosage radiography via rare-earth screens; the effect of early intubation on hyaline membrane disease; perinatal asphyxia syndrome (P.A.S.); meconium aspiration syndrome; persistent fetal circulation syndrome (P.F.C.); bronchopulmonary dysplasia; and infant of a diabetic mother (I.D.M.)

The course is designed as a primer for those radiologists who are in the uncomfortable position of having to occasionally interpret newborn chest films, despite never having had any training in this highly specialized field. For those radiologists beyond the tyros stage, it is also intended to be a refresher course, as well as an introduction to the latest concepts and modifications pertaining to the common forms of newborn chest disease. As usual, rare and exotic entities will not be discussed as this is intended to be a practical course.

504

Computerized Tomography of the Head. Lawrence H. A. Gold, associate radiology professor, University of Minnesota Medical Center, Minneapolis. A complete and comprehensive discussion of the principles and technique of CT scanning will be presented. Neuro anatomy will be dealt with in detail. The course will be amply illustrated with a wide assortment of pathological material from the University of Minnesota Hospitals. Anatomy and pathology of orbital lesions will be discussed.

505

Radiology of the Abdomen: Anatomic Approach (Conventional Radiology, Ultrasound, and CT Scanning). Joseph P. Whalen, radiology professor, New York Hospital-Cornell Medical Center; and Elias Kazam, assistant radiology professor, New York Hospital, both New York City. In the past this course has utilized anatomic sections in demonstrating radiologic anatomy and its pathologic alteration, developing an approach to abdominal masses which we have termed the vector approach. Further we have classified abscesses of the abdomen, based on this anatomic approach. In this session we will include ultrasonography and CT correlation. The format of presentation will be a brief review of sectional anatomy correlated with normal roentgen, ultrasound, and scanning anatomy. We will then demonstrate the three modalities in detecting abnormality, both masses and effusions.

506

Special Procedures in Pulmonary Radiology. Stuart S. Sagel, associate professor and director, Chest Radiology, Mallinckrodt Institute, Washington University School of Medicine; and John V. Forrest, associate radiology professor, Washington University, both St. Louis. A large array of diagnostic modalities are available to pursue abnormalities detected on the plain chest radiograph. This seminar will discuss the relative merits of these various procedures—both radiologic and nonradiologic. Which technique to use, when, and why will be scrutinized. In particular the indications and techniques for tomography, bronchography, needle biopsy, and bronchial brushing will be emphasized. The pragmatic and feasible will be stressed. Attention will be directed toward the need for abandoning unproductive examinations, and substituting those which provide definitive information upon which clinical decisions can be based. In addition, the current status of computed tomography of the thorax will be presented.

507

Roentgen Pathologic Correlations in Common Pulmonary Disorders. E. Robert Heitzman, radiology professor, State University of New York, Upstate Medical Center, Syracuse, NY. An analysis and deductive approach to the diagnosis of abnormalities demonstrated on radiographs requires a thorough knowledge of the gross pathologic appearances of these abnormalities. Although this is vitally important in pulmonary radiology, the pathology of many pulmonary diseases is often poorly understood. Roentgen pathologic correlations will be demonstrated to establish a firm pathologic basis for the roentgen appearances in common pulmonary conditions such as pulmonary infarct, pneumonia, emphysema, bronchogenic carcinoma, lymphoma, and some chronic inflammatory diseases of the pulmonary interstitium.

508

Radiological Evaluation of Eye and Orbital Lesions. Albert L. Weber, chief; Radiology Massachusetts Eye and Ear Infirmary, Boston. This course will deal with radiological evaluation of eye and orbital lesions. Different radiologic examinations, such as plain films, polytomography, venography, angiography, ultrasound, CT scan, and dacryocystography, will be discussed, with respect to eye and orbital lesions. After a brief review of the normal orbital anatomy, different topics, including trauma (with major emphasis on blow-out fractures) and the causes and findings in exophthalmos, will be discussed. Examples of lesions arising from the eye and orbit or extending into the orbit from the cranial cavity, facial area, and sinuses will be shown, with a discussion of the radiological findings.

509

The Esophagus. Harley C. Carlson, Diagnostic Roentgenology, Mayo Clinic, Rochester, MN. This will be a review of most of the major disease processes which involve the esophagus. Principles of examination with emphasis on fluoroscopy as well as radiography will be reviewed and any special techniques applicable to the separate disease processes will also be covered. In addition to the characteristic radiographic findings of the various disease processes, emphasis will be placed on pathology, significance of the disease to the patient in terms of morbidity and mortality, and additional procedures which may be used to more precisely define the nature of the disease process. The discussion will include diverticula, webs, esophagitis with its many variations, esophageal hiatal hernia, achalasia, and benign and malignant neoplasms of the esophagus.

News

Particles and Radiation Therapy Conference

The International Conference on Particles and Radiation Therapy, Part II, will be conducted at the Lawrence Berkeley Laboratory of the University of California, September 15-17. Supported by the Division of Cancer Research Resources and Centers, National Cancer Institute, and cosponsored by the American College of Radiology and the American Roentgen Ray Society, the conference is a successor to a 1972 meeting in Los Alamos, New Mexico.

Primary topics are: localization, inhomogeneities and treatment planning for particle therapy; protons and heavy ions; neutrons; negative pi-mesons; and general topics of interest.

Registration fee is \$100 and attendance is limited to 400. For additional information, contact William E. Powers, chairman, Part II Conference, American College of Radiology, 130 South 9th Street, Philadelphia, Pennsylvania 19107.

Computed Tomography Symposium

An international symposium on Computer Assisted Tomography in nontumoral disease of the brain, spinal cord and eye will be held at the Clinical Center of the National Institutes of Health in Bethesda, Maryland, October 11-15. The National Institute of Neurological and Communicative Disorders and Stroke is the sponsor. The symposium is intended as a forum for investigators who work on the development or have clinical experience in the areas of transmission and emission computed tomography. Scientific and technical exhibits are planned. There is no registration fee.

Investigators who wish to present papers are invited to submit detailed and documented abstracts, including data and illustrations, no later than August 1.

Abstracts should be sent to Giovanni Di Chiro, National Institutes of Health, Section on Neuroradiology, Clinical Center, Room 2D13, Bethesda, Maryland 20041. Registration information is also available from the same address.

In Vitro Nuclear Medicine

The Division of Nuclear Medicine at Johns Hopkins University School of Medicine, Baltimore, will offer a postgraduate course in "In Vitro Nuclear Medicine," October 11-13, 1976. Procedures such as radioimmuno-assay, competitive protein-binding assay, immunoradiometric assay, enzymatic assay, and other radiometric techniques will be presented. The course will stress the recent progress and clinical aspects of the field. The cost is \$200 and the course is approved for Category I credit. Additional information may be obtained from the Office of Continuing Medical Education, Johns Hopkins Medical Institutions, Turner Building, Room 17, 720 Rutland Avenue, Baltimore, Maryland 21205.

Radiological Department Planning

The Second International Symposium on the Planning of Radiological Departments is scheduled for September 26-30 in Philadelphia. Sponsors are the American College of Radiology, the Committee on Department Planning, and Temple University Health Sciences Center Department of Radiology. Sessions will cover: trends in radiology; department design; radiological equipment; follow-up of first symposium; management systems; and specialized areas including equipment for developing countries, nuclear

medicine departments, oncology centers, and specialized diagnostic rooms. The symposium is approved for Category I credit.

Information is available from Francis J. Shea, Temple University Health Sciences Center, 3401 North Broad Street, Philadelphia, Pennsylvania 19140.

Gastrointestinal Refresher Course

The Department of Radiology and the A. Webb Roberts Center for Continuing Education of the University of Texas are sponsoring a 2½ day refresher course in gastrointestinal radiology. The course will be October 22-24 at the Fairmont Hotel in Dallas, and will include a review of all aspects of gastrointestinal radiology, including ultrasound. Faculty are: R. N. Berk, J. Brinley, M. Conrad, H. M. Goldstein, J. O. Janes, W. J. Kilman, D. Kirks, M. Landay, P. J. Loeb, L. R. Radford, C. Richardson, and H. Smith. The course meets criteria for Category I credit.

For further information, please contact: R. N. Berk, Department of Radiology, Parkland Memorial Hospital, 5201 Harry Hines Boulevard, Dallas, Texas 75235.

Radiology Postgraduate Course

Faculty from the Duke University Medical Center Radiology Department and a distinguished guest faculty will conduct a 5-day radiology postgraduate course, October 25-29, at the Southampton Princess Hotel in Bermuda. The disease-oriented format will cover pediatric and adult radiology, nuclear medicine of the chest, genitourinary tract, gastrointestinal tract, and the skeletal system. The course will carry 25 hours Category One accreditation.

Guest faculty members are: E. R. Heitzman, chest; R. E. Miller, gastrointestinal tract; J. A. Evans, genitourinary; A. Gottschalk, nuclear medicine; J. S. Dunbar, pediatric radiology; and E. G. Theros, skeletal system. Faculty from Duke University are: H. Grossman, I. S. Johnsrude, R. McLelland, and R. A. Older.

Inquiries should be directed to Robert McLelland, Radiology—Box 3808, Duke University Medical Center, Durham, North Carolina 27710.

Team Approach to Cancer Health Care

A symposium called "The Professional Team Approach to Cancer Health Care," will be held in San Francisco, California, October 29-30. Presented by the Claire Zellerbach Saroni Tumor Institute of Mount Zion Hospital and Medical Center, the conference is open to all medical and professional personnel involved in the care of cancer patients. Fees range from \$110 to \$50 and include a copy of the symposium proceedings. Pre-registration is required. For additional information, contact the Department of Continuing Education, Mount Zion Hospital and Medical Center, P. O. Box 7921, San Francisco, California 94120.

Midsummer Radiological Conference

The 38th Midsummer Radiological Conference, sponsored by the Rocky Mountain Radiological Society, will be held August 19-21 at the Brown Palace Hotel, Denver, Colorado. Faculty members are: J. R. Thornbury, J. N. Wofle, R. L. Wesenberg, A. B. Crummy, M. J. Schneider, C. T. Dotter, J. F. Roberts, M. T. Korobkin, and W. J. Steines. Additional information is available from Lorenz R. Wurtzebach, 4200 East 9th Avenue, Denver, Colorado 80220.

Radiologic Societies

International Societies

Fleischner Society. Secretary, E. Robert Heitzman, State University of New York Upstate Medical Center, Syracuse NY 13210. Annual Meeting: 1977, Town and Country Convention Center, San Diego CA, Feb 27-Mar. 2.

Inter-American College of Radiology. Secretary, Gaston Morillo, Department of Radiology, Jackson Memorial Hospital, 1611 NW 12th Avenue, Miami FL 33136.

International Skeletal Society. Secretary-Treasurer, Jack Edeiken, Radiology Dept, Thomas Jefferson University Hospital, 11th and Walnut Sts, Philadelphia PA 19107. Third annual refresher course: Sept 13-15, 1976, Queen Elizabeth Hotel, Montreal, Canada

International Society of Radiology. Hon. Secretary-Treasurer, W. A. Fuchs, Department of Diagnostic Radiology, University Hospital, Inselspital, CH-3010 Bern, Switzerland.

U.S. National Societies

American Association of Physicists in Medicine. Secretary, John Wright, Radiology Department, Geisinger Medical Center, Danville PA 17821.

American Board of Radiology. Secretary, C. Allen Good, Kahler East, Rochester MN 55901.

American College of Radiology. Executive Director, William C. Stronach 20 N. Wacker Drive, Chicago IL 60606.

American Institute of Ultrasound in Medicine. Executive Secretary, Donna LaMaster, PO Box 25065, Oklahoma City OK 73125.

American Nuclear Society. Program Chairman, Ted D. Tarr, U.S. Energy Research and Development Administration, Mail Station A-436 Office of Assistant Administrator for Nuclear Energy, Washington DC 20545.

American Osteopathic College of Radiology. 1976 Program Chairman, Joseph C. Andrews, 13355 East Ten Mile Road, Warren MI 48089. 1977 Program Chairman, George O. Faerber, 1087 Dennison Avenue, Columbus OH 43201. Annual Meeting: Oct 17-21, 1976, New Orleans LA.

American Radium Society. Secretary, Richard H. Jesse, Dept of Surgery, M.D. Anderson Hospital and Tumor Institute, Houston TX 77025.

American Roentgen Ray Society. Secretary, James Franklin Martin, 300 S. Hawthorne Rd., Winston-Salem NC 27103. Annual Meeting: Washington Hilton, Washington D.C., Sept 20-24, 1976.

American Society of Neuroradiology. Secretary, Arthur E. Rosenbaum, University of Pittsburgh School of Medicine, Pittsburgh PA 15261.

American Society of Therapeutic Radiologists. Secretary, Robert W. Edland, 1836 South Ave., LaCrosse WI 54601. Annual Meeting: Oct 13-17, 1976, Hyatt Regency, Atlanta GA.

Association of University Radiologists. Secretary-Treasurer, Gerald T. Scanlon, Milwaukee County Medical Center, Milwaukee, WI 53226. Annual Meeting: April 30-May 4, 1977, Kansas City KA.

Health Physics Society. Executive Secretary, Richard J. Burk, Jr., 4720 Montgomery Lane, Bethesda MD 20014.

North American Society of Cardiac Radiology. Secretary-Treasurer, Erik Carlsson, University of California, San Francisco CA 94143.

Radiation Research Society. Executive Director, Richard J. Burk, Jr., 4720 Montgomery Lane, Bethesda MD 20014.

Radiological Society of North America, Inc. Secretary, Theodore A. Tristan, Fifteenth Floor, One MONY Plaza, Syracuse NY 13202, Annual Meeting: 1976 Nov 14-19; 1977, Nov 27-Dec 2; 1978, Nov 26-Dec 1, all in Chicago IL.

Section on Radiology, American Medical Association. Secretary, Antolin Raventos, Dept of Radiology, School of Medicine, University of California, Davis.

Society of Gastro-Intestinal Radiologists. Secretary-Treasurer, Walter Whitehouse, Dept of Radiology, University of Michigan, Ann Arbor MI 48104. Annual Meeting: Sept 16-19, 1976, Princess Hamilton Hotel, Bermuda.

Society of Nuclear Medicine. President, 475 Park Avenue S, New York NY 10016.

Society for Pediatric Radiology. Secretary-Treasurer, John P. Dorst, 601 N Broadway, Baltimore MD 21205. Annual Meeting: Sept 19-20, 1976 Washington Hilton, Washington, D.C.

The Society of Uroradiology. Secretary-Treasurer, Howard M. Pollack, Dept of Radiology, Episcopal Hospital, Front St at Lehigh Ave, Philadelphia PA 19125. Annual Meeting: Sept 20, 1976, Washington Hilton, Washington DC

U.S. State and Local Societies

Alabama

Alabama Academy of Radiology. Secretary-Treasurer, Lawrence E. Fetterman, 1720 Springhill Ave, Suite 201, Mobile AL 36604.

Section of Radiology, National Medical Association. Secretary, Ivy Brooks, Dept of Radiology, Veterans Administration Hospital, PO Box 511, Tuskegee AL 36083.

Southern Radiological Conference. Secretary-Treasurer, J. W. Maxwell, PO Box 2144, Mobile AL 36601. Annual Meeting: Jan 28-30, 1977, Grand Hotel, Point Clear AL 36564.

Alaska

Alaska Radiological Society. Chapter ACR. Secretary-Treasurer, John J. Kottra, 3200 Providence Ave. Anchorage AK 99504.

Arkansas

Arkansas Chapter of ACR. Secretary-Treasurer, Richard Seibold, Jr., Wadley Hospital, Texarkana AR-TX 75501.

Arizona

Arizona Radiological Society. Chapter of ACR. Secretary, Irwin M. Freundlich, 1501 N Campbell Ave, Dept of Radiology, Tucson AZ 85724.

California

California Radiological Society, California Chapter of ACR. Executive Secretary, J. Michael Allen, 1225 8th St, Suite 590, Sacramento CA 95814.

East Bay Radiological Society. Secretary-Treasurer, Richard H. Culhane, 4 Vista del Mar, Orinda CA 74563.

Los Angeles Radiological Society. Secretary, Arthur F. Schanche, 333 N Prairie Ave, Inglewood CA 90301.

Northern California Radiological Society. Secretary, Patrick J. Grinsell, 1207 Fairchild Ct, Woodland CA 95695.

Northern California Radiotherapy Association. Secretary-Treasurer, John D. Earle, Stanford Medical Center, Stanford CA 94305.

Orange County Radiological Society. R. Lawrence Argue, 100 E Valencia Mesa Dr, Fullerton CA 93632.

Radiological Society of Southern California. Secretary-Treasurer, Duane Eugene Blickenstaff, La Jolla Radiology Medical Group, Inc, 7849 Fay Ave, La Jolla CA 92037. Meetings: Oct 1976, Santa Barbara; Dec 1976, Newport; Feb 1977, Palm Springs.

Redwood Empire Radiological Society. Secretary, Hal B. Peterson, 357 Perkins St, Sonoma CA 95476.

San Diego Radiological Society. President, Donald J. Fleischli, 7849 Fay Ave, La Jolla CA 92037.

South Coast Radiological Society Chapter of ACR. Secretary-Treasurer, Brian R. Schnier, Dept of Radiology, Cottage Hospital, Pueblo at Bath, Santa Barbara CA 93105.

Southern California Radiation Therapy Society. Secretary-Treasurer, Jerome Stuhlberg, 514 N Prospect, Redondo Beach CA 90277.

Colorado

Colorado Radiological Society, Chapter of ACR. Secretary, John Pettigrew, 2215 N Cascade, Colorado Springs CO 80907.

Rocky Mountain Radiological Society. Secretary-Treasurer, Lorenz R. Wurtzebach, 4200 E 9th Ave., Denver CO 80220.

Connecticut

Connecticut Valley Radiologic Society. Secretary-Treasurer, Gerald N. LaPierre, 759 Chestnut St, Springfield MA 01107.

Radiological Society of Connecticut, Inc. Secretary, Gerald L. Baker, 85 Jefferson St, Hartford CN 06106.

Delaware

Delaware Chapter of ACR. Secretary, Ekkehard S. Schubert, Wilmington Medical Center, PO Box 1951, Wilmington DE 19899.

District of Columbia

Section on Radiology, Medical Society of the District of Columbia. Secretary-Treasurer, Albert M. Zelna, 21 Masters St, Potomac MD 20854.

Florida

The Florida Radiological Society, Chapter of ACR. Secretary, Alfred Schick, 1350 S Hickory St, Melbourne FL 32901.

The Florida West Coast Radiological Society, Inc. Secretary-Treasurer, Aaron Longacre, 501 E Buffalo Ave, Tampa FL 33606.

Greater Miami Radiological Society. Secretary, David C. Hillman, PO Box 610544, North Miami FL 33161.

North Florida Radiological Society. Secretary, Charles E. Bender, 1430 16th Ave S, Jacksonville Beach FL 32250.

Georgia

Atlanta Radiological Society. Secretary-Treasurer, James H. Larose, Dept of Nuclear Medicine, South Fulton Hospital, East Point GA 30344.

Georgia Radiological Society, Chapter of ACR. Secretary, E. P. Rasmussen, Piedmont Professional Bldg, 35 Collier Rd NW, Atlanta GA 30309.

Hawaii

Hawaii Radiological Society, Chapter of ACR. Secretary-Treasurer, Michael J. McCabe, Straub Clinic and Hospital, Honolulu HI 96813.

Illinois

Chicago Radiological Society, Division of the Illinois Radiological Society, Chapter of ACR. Secretary-Treasurer, Harold J. Lasky, 55 E Washington St, Suite 1735, Chicago IL 60602.

Illinois Radiological Society, Inc., Chapter of ACR. Secretary, Robert D. Dooley, Hinsdale Medical Center, Hinsdale IL 60521.

Indiana

Tri-State Radiological Society. Secretary Thomas Harmon, St. Mary's Hospital, Evansville IN 47750.

Iowa

Iowa Radiological Society, Chapter of ACR. Secretary-Treasurer, Dale L. Roberson, 1948 First Ave NE, Cedar Rapids IA 52402.

Kansas

Kansas Radiological Society, Chapter of ACR. Secretary-Treasurer, Ralph H. Baehr, 310 Medical Arts Bldg, Topeka KA 66604.

Kentucky

Bluegrass Radiological Society. Secretary-Treasurer, James King, 3313 Overbrook Dr, Lexington KY 40504.

Kentucky Chapter of ACR. Secretary-Treasurer, John Hummel, Jr., Kentucky Baptist Hospital, Louisville KY 40204.

Louisiana

Ark-La-Tex Radiological Society. Secretary, Erich K. Lang, Confederate Memorial Medical Center, LSU School of Medicine, Shreveport LA 71101.

Louisiana Radiological Society, Chapter ACR. Secretary-Treasurer, Stover L. Smith, 250 Vincent Ave, Metairie LA 70005.

Section on Radiology, Southern Medical Association. Secretary, Michael Sullivan, 4514 Jefferson Highway, New Orleans LA 70121. Annual Meeting: Nov 7-10, 1976, New Orleans.

Maine

Maine Radiological Society, Chapter of ACR. Secretary-Treasurer, Peter E. Giustra, Dept of Radiology, Penobscot Bay Medical Center, Rockland ME 04841.

Maryland

Maryland Radiological Society, Chapter of ACR. Secretary, David S. O'Brien, Anne Arundel Hospital, Annapolis MD 21401.

Massachusetts

Massachusetts Radiological Society, Chapter of ACR. Secretary, Joseph T. Ferrucci, Jr., Massachusetts General Hospital, Boston MA 02114.

New England Roentgen Ray Society. Secretary, Melvin E. Clouse, 185 Pilgrim Rd, Boston MA 02115.

Northeastern Society for Radiation Oncology. Secretary, C. C. Wang, Massachusetts General Hospital, Boston MA 02114.

Michigan

Michigan Radiological Society, Chapter of ACR. Secretary-Treasurer, Francis P. Shea, Bon Secours Hospital, 468 Cadieux, Grosse Pointe MI 48230.

Michigan Society of Therapeutic Radiologists. Secretary-Treasurer, William T. Knapp, St. Mary's Hospital, 830 S Jefferson, Saginaw MI 48601. Annual Meeting: Sept 1976, Ann Arbor.

Minnesota

Minnesota Radiological Society. Secretary-Treasurer, Marvin E. Goldberg, Box 292, Mayo Memorial Health Sciences Center, Minneapolis MN 55455.

Missouri

Greater Kansas City Radiological Society. President-Secretary, Jay I. Rozen, Suite 216, 6400 Prospect, Kansas City MO 64132.

Greater St. Louis Society of Radiologists. Secretary-Treasurer, William B. Hutchinson, 2821 Ballas Rd, St. Louis MO 63131. Annual Meeting: Oct 1976, St. Louis.

Missouri Radiological Society, Chapter of ACR. Secretary-Treasurer, Ronald G. Evens, Mallinckrodt Institute of Radiology, 510 S. Kingshighway, St. Louis MO 63110.

Mississippi

Mississippi Radiological Society, Chapter of ACR. Secretary-Treasurer, James B. Barlow, 514B E Woodrow Wilson, Jackson MS 39216.

Nebraska

Nebraska Chapter of ACR. Secretary-Treasurer, Charles A. Dobry, Dept of Radiology University of Nebraska Medical Center, 42nd at Dewey, Omaha NB 68105.

New Hampshire

New Hampshire Chapter of ACR. Secretary-Treasurer, Edward P. Kane, Claremont General Hospital, Claremont NH 03743.

New Jersey

Radiological Society of New Jersey, Chapter of ACR. Secretary, Fred M. Palace, 2424 Morris Ave, Union NJ 07083.

New Mexico

New Mexico Society of Radiologists, Chapter of ACR. Secretary, W. M. Jordan, 1100 Central Ave SE, Albuquerque NM 87106.

New York

Bronx Radiological Society, New York State, Chapter of ACR. Secretary-Treasurer, Leon J. Corbin, 1369 Rosendale Ave, Bronx NY 10472.

The Brooklyn Radiological Society. Secretary-Treasurer, Ralph Brancaccio, 7901 4th Ave, Brooklyn NY 11209.

Buffalo Radiological Society. Secretary, Jerald P. Kuhn, 9267 Jennings Rd, Eden NY 14057.

Central New York Radiological Society. E. Mark Levinsohn, Radiology Dept, Upstate Medical Center, 750 E Adams St, Syracuse NY 13210.

Kings County Radiological Society. Secretary, Melvin Moore, 7815 Bay Parkway, Brooklyn NY 11214.

Long Island Radiological Society. Secretary, Harry L. Stein, North Shore University Hospital, 300 Community Dr. Manhasset NY 11030.

Mid-Hudson Radiological Society. Secretary-Treasurer, William D. Stiehm, 37 Flower Hill Rd, Poughkeepsie NY 12603.

New York Roentgen Society. Secretary-Treasurer, Thomas C. Beneventano, 111 E 210th St, Bronx NY 10467.

New York State Chapter of ACR. Secretary-Treasurer, Albert F. Keegan, 6 Secor Dr, Port Washington NY 11050.

Northeastern New York Radiological Society. Secretary, Donald R. Morton, Dept of Radiology, St. Clare's Hospital, Schenectady NY 12304.

Rochester Roentgen Ray Society. Secretary-Treasurer, Robert J. Bruneau, 1441 East Ave, Rochester NY 14610.

Westchester County Radiological Society. Secretary, Leonard Cutler, 16 Guion Pl, New Rochelle NY 10802.

Nevada

Nevada Radiological Society, Chapter of ACR. Secretary, Charles F. Veverka, Carson Tahoe Hospital, Carson City NV 89701.

North Carolina

Catawba Valley Radiological Society. Secretary, J. N. Owsley, 18 13th Ave. NE, Hickory NC 28601.

North Carolina Chapter of ACR. Secretary-Treasurer, Ernest B. Spangler, Wesley Long Hospital, Greensboro NC 27402. Annual Meeting: Nov 1976, Mid-Pines Club, Southern Pines NC.

North Dakota

North Dakota Radiological Society, Chapter of ACR. Secretary, H. C. Walker Jr., PO Box 624, Devils Lake, ND 58301.

Ohio

Cleveland Radiological Society. Secretary-Treasurer, Charles M. Greenwald, 7007 Powers Blvd, X-ray Department, Parma OH 44129.

Northwestern Ohio Radiological Society. Secretary, Gerald Marsa, 3939 Morroe St, Toledo OH 43606.

Ohio State Radiological Society, Chapter of ACR. Secretary, James Farmer, 3461 Warrensville Center Rd, Cleveland OH 44122.

Oklahoma

Northeastern Oklahoma Radiological Society. Secretary, William L. Lavendusky, 100 Center Plaza Suite, C, Tulsa OK 74119.

Oklahoma State Radiological Society, Chapter of ACR. Secretary, Bob G. Eaton, 2508 Stillmeadow Rd, Edmond OK 73034. Annual Meeting: Oct 1-3, 1976, Shangri-La Lodge on Grand Lake, Afton OK.

Oregon

Oregon State Radiological Society, Chapter of ACR. Secretary-Treasurer, Ray F. Friedman, 3324 SW 44th St, Portland OR 97221.

Pennsylvania

Philadelphia Roentgen Ray Society. Secretary, Marvin E. Haskin, 230 N Broad St, Philadelphia PA 19102.

Pittsburgh Roentgen Society. Secretary, Klaus M. Bron, Presbyterian-University Hospital, Pittsburgh 15261.

Rhode Island

Radiological Society of Rhode Island, Chapter of ACR. Secretary, Stefan Frater, Rhode Island Hospital, Providence RI 02902.

South Carolina

South Carolina Radiological Society, Chapter of ACR. Secretary, George W. Brunson, 4315 Woodleigh Rd, Columbia SC 29206.

Tennessee

Memphis Roentgen Society. Secretary-Treasurer, D. Randolph Ramey, Baptist Memorial Hospital, 899 Madison Ave., Memphis TN 38140.

Tennessee Radiological Society, Chapter of ACR. Secretary-Treasurer, Jerry W. Grise, Methodist Hospital, 1265 Union Ave, Memphis TN 38104.

Texas

Central Texas Radiology Society. Secretary-Treasurer, E. Jerome Schollar, Scott and White Clinic, Temple TX 76501.

Dallas-Fort Worth Radiological Society. Secretary-Treasurer, William V. Bradshaw, 777 W Rosedale Suite 260, Ft. Worth TX.

Houston Radiological Society. Secretary, Thomas S. Harle, 103 Jesse H. Jones Library Bldg, Texas Medical Center, Houston TX 77030.

Louisiana-Texas Gulf Coast Radiological Society. Secretary-Treasurer, J. Gardiner Bourque, 3155 Stagg Dr, Suite 230, Doctors Bldg, Beaumont TX 77701.

San Antonio Civilian Military Radiological Society. Secretary, Jose Maria Chao, Diagnostic Clinic, San Antonio TX.

Texas Radiological Society, Chapter of ACR. Secretary-Treasurer, Donald N. Dysart, Scott and White Clinic, Temple TX 76501. Annual Meeting: March 17-19, 1977, Fairmont Hotel, Dallas TX.

Vermont

Vermont Radiological Society, Chapter of ACR. Secretary, Peter Dietrich, Medical Center Hospital of Vermont, Burlington VT 05401.

Virginia

Mid-Shenandoah Valley Radiological Society. Secretary, Kenneth L. Dwyer, King's Daughters Hospital, Staunton VA 24401.

Richmond Radiological Society. Secretary, Melvin Vinik, 9504 Carterwood Rd, Richmond VA 23229.

Virginia Chapter of ACR. Secretary-Treasurer, Charles P. Winkler, 3500 Kensington Ave Suite 2-A, Richmond VA 23221.

Washington

Pacific Northwest Radiological Society. Secretary-Treasurer, Kenneth D. Moores, 1118 9th Ave, Seattle WA 98101. Annual Meeting: May 6-8, 1977, Victoria, B.C., Canada.

Washington State Radiological Society, Chapter of ACR. Secretary-Treasurer, Donald J. Hesck, 3216 NE 45th Pl, Seattle WA 98105.

West Virginia

West Virginia Radiological Society, Chapter of ACR. Secretary-Treasurer, Andrew W. Goodwin II, 200 Medical Arts Bldg., Charleston WV 25301.

Wisconsin

Milwaukee Roentgen Ray Society. Vice President, Thomas C. Lipscomb, 1004 N 10th St, Milwaukee WI 53233.

Wisconsin Radiological Society, Chapter of ACR. Secretary-Treasurer, June Unger, Wood VA Hospital, Wood WI 53193.

Wisconsin Society of Therapeutic Radiologists. Secretary, M. Greenberg, Milwaukee County General Hospital, 8700 W Wisconsin Ave, Milwaukee WI 53222.

Wyoming

Wyoming Radiological Society, Chapter of ACR. Secretary, Thomas E. Hettinger, 1609 E 19th St, Cheyenne, WY.

Canada

Canadian Association of Radiologists. Honorary Secretary, C. Germain Beauregard, Suite 806 1440 St. Catherine St W, Montreal, Quebec Canada.

Edmonton and District Radiological Society. Secretary B. Caplan, 12320 103rd Ave, Edmonton, Alberta T5N 0R2, Canada.

Toronto Radiological Society. Secretary, H. Shulman, Sunnybrook Hospital, 2075 Bayview Avenue, Toronto, Ontario, Canada.

Central and South America

Sociedad Chilena de Radiología. Secretary, Manuel Neira, Casilla 13426, Santiago, Chile.

Sociedad Colombiana de Radiología. Secretary-General, Gustavo Sanchez Sanchez, Bogotá, Colombia. Annual Meeting: Feb 1977, Manizales (Caldas) Colombia.

Sociedad de Radiología del Atlantico. Secretary, Raul Fernandez, Calle 40 #41-110, Baranquilla, Colombia. Annual Meeting: Feb 3, 1977, Baranquilla, Colombia.

Sociedad de Radiología, Radiotherapéutica y Medicina Nuclear de Rosario. Secretary-General Marcela Muñoz, Santa Fe 1798, Rosario, Argentina.

Europe

Bavarian-American Radiologic Society. Secretary, Stuart A. O'Byrne, Radiology Service, Stuttgart, West Germany, 5th General Hospital, APO NY 09154.

British Institute of Radiology. Honorary Secretaries, D. H. Trapnell, P. N. T. Wells, 32 Welbeck St, London, W1M/7PG, England.

Československá Radiologická Společnost. Secretary, Jaromír Kolář, Radiological Clinic, Parha 2, Unemocnice 2, Czechoslovakia.

Danish Radiological Society. Secretary General, Johannes Praestholm, Radiological Department I, Bispebjerg Hospital, DK-2400, Copenhagen NV.

Deutsch Röntgengesellschaft. President, Wolfgang Frik, Dept of Radiology, Techn Univ Aachen, D-5100 Aachen, Goethestrasse 27/29, West Germany.

Faculty of Radiologists. Honorary Secretary, M. Ryan, Faculty of Radiologists, Royal College of Surgeons in Ireland, Stephen's Green, Dublin 2, Ireland.

The Hospital Physicists' Association. Honorary Secretary, R.F. Mould, Westminster Hospital, Physics Department, Page St. Wing, London SW1P 2AR, England.

Norsk Forening for Medicinsk Radiologi. General Secretary, Arnulf Skjennald, Ullevål sykehus, Oslo, Norway.

Nederlandse Vereniging voor Radiologie. Secretary, H.E. Schütte, Department of Radiology, Elizabeth Gasthuis, Haarlem, Netherlands.

Royal College of Radiologists. Secretary, P.D. Thomson, 28 Portland Pl, London, W1N 4DE, England.

Scandinavian Radiological Society. Secretary-General, C-E. Unnéus, Havsvindsv. 5C., 02120 Esbo 12 (Hagalund-Tapiola) Finland.

Schweizerische Gesellschaft für Radiologie und Nuklearmedizin. **Société Suisse de Radiologie et de Médecine Nucléaire.** Secretary, Gustav A. Schoch, 7 Gellerstrasse, CH-4052 Basel, Switzerland.

Sociedad Española de Radiología y Electrológica Médicas y de Medicina Nuclear. Secretary-General, Pilar Gallar Barberá, Villanueva, Madrid 1, Spain.

Società Italiana di Radiologia Medica e Medicina Nucleare. Administrative Secretary, R. Dall'Acqua, Ospedale Mauriziano, 10128, Torino, Italy. Annual Meeting: Sept 25-28, 1976, XXVII Congresso Nazionale, SIRMN—BARI—Campus Universitario Via Re Daviol, Italy.

Société Européenne de Radiologie Pédiatrique. Secretary, J. Corbaton, Clinica Infantil "La Paz," Av. Generalísimo, 117 Madrid 34, Spain.

Société Française de Radiologie Médicale, Médecine Nucléaire et Electrológica. Secretary-General, J. Sauvegrain, Hôpital des Enfants-Malades, 149 Rue de Sèvres, 75730 Paris Cedex 15, France. Annual Meetings: 1976, Nov 15-18, Centre International de Paris (Porte Maillot); 1977, Nov 15-18, Centre International de Paris.

Société Française de Neuroradiologie. Secretary-General, R. Djindjian, 16, rue de l'Université 75, Paris 7^e, France.

Society of Pediatric Radiology. Secretariat, PO Box 272, S-101 23 Stockholm, Sweden.

Svensk Förening för Medicinsk Radiologi. Secretary, Hans Ringertz, Department of Pediatric Radiology, Karolinska Sjukhuset, S-104 01 Stockholm, Sweden. Annual Meeting: Dec. 1-4, 1976, Stockholm, Sweden.

Africa

Association of Radiologists of West Africa. Honorary Secretary, A. A. Obisen, Department of Radiology, University College Hospital, Ibadan, Nigeria. Annual Meeting: Feb 4-5, 1977, Accra, Ghana.

Radiological Society of South Africa. Secretary, Dr. A. Visser, P.O. Box 8850, Johannesburg, South Africa.

South African International Radiological Congress. Director, Dr. Paul Sneider, P. O. Box 4878, Johannesburg, South Africa. Annual meeting: Sept 1976, Durban Annual Congress; Oct 1978, International and National Congress.

Near East and Asia

Bengal Radiological Association. Honorary Secretary, B. Chatterji, 262 Rash Behari Ave, Calcutta 700019, India. Annual Meeting: Dec 10, 1976, 3-1 Madan St, Calcutta 700013, India.

Indian Radiological Association. Honorary General Secretary, S. P. Aggarwal, 10-B Kasturba Ghandi Marg, New Delhi 110001, India. Annual Meeting: Jan 1977, Chandigarh, India.

Indonesian Radiological Society. Secretary, Gani Iljas Sasmitaatmadja, Radiology Department, Faculty of Medicine, University of Indonesia, Salemba 6, Jakarta, Indonesia.

Iranian Radiological Society. Secretary Majid Rooholamini, P.O. Box 14-1151

Israel Radiological Society. Secretary, Izkovitch Izhak, Haifa Betharofe, Israel. Annual Meeting: April 1977, Haifa, Israel.

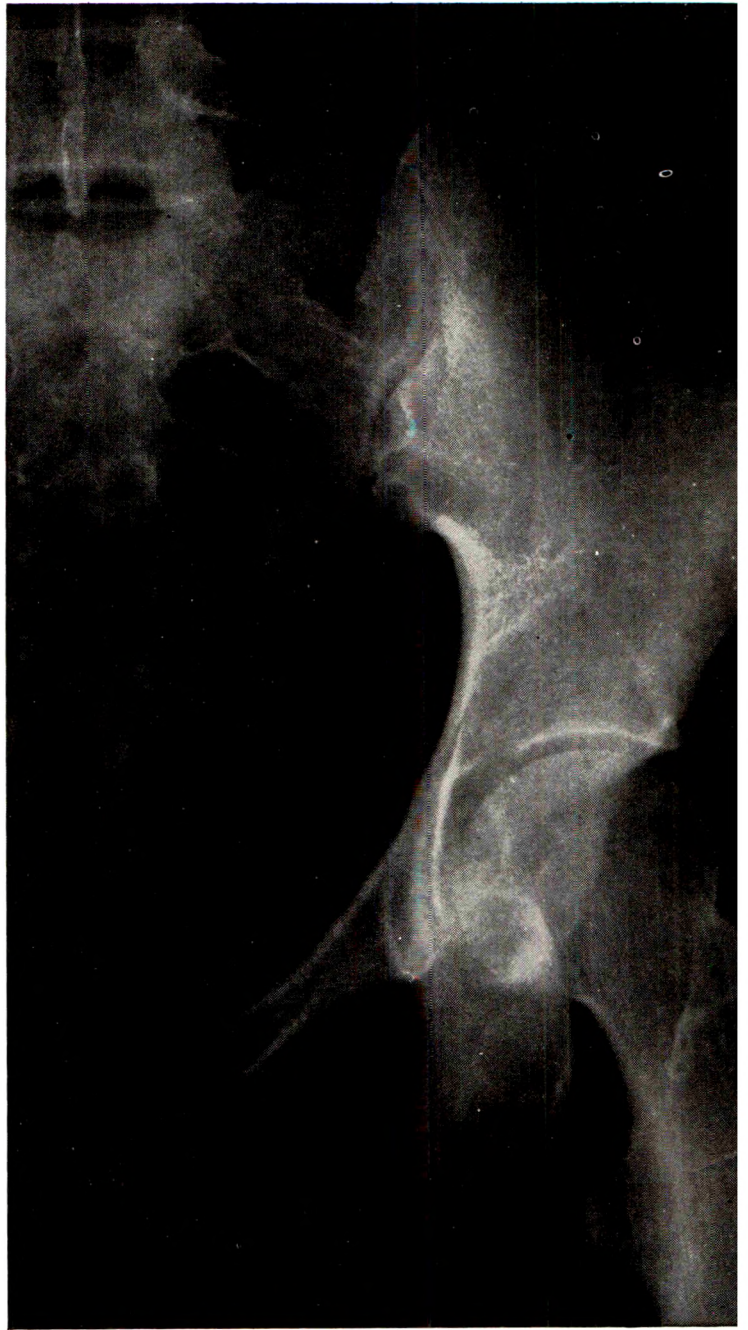
Philippine College of Radiology. Secretary-Treasurer, Antonio Chavez, Box 1284, Commercial Center, Makati, Rizal, D-708, Philippines.

Radiological Society of Thailand. Secretary, Dusdee Prabbasawat, Department of Radiology, Siriraj Hospital Faculty of Medicine, Mahidol University, Bangkok 7, Thailand.

Royal Australasian College of Radiologists. Honorary Secretary, T. P. Loneragan, 45 Macquarie St, Sydney NSW 2000, Australia. Annual Meeting: Oct 10-15, 1976, Jakarta, Indonesia.



Hysterosalpingogram with Salpex Contrast Medium.



24-hour postinjection x-ray of same patient.

now you see it

now you don't

With Salpex as your contrast medium, your gynecologic patient needn't undergo the 24-hour postinjection x-ray usually required with iodized oils. Water-soluble Salpex leaves virtually no irritating radiopaque residue to produce foreign-body reactions, yet it provides the viscosity needed for adequate visualization.

Contraindications: Contraindications to hysterosalpingography include the presence of severe vaginal or cervical infections, existing or recent pelvic infection, marked cervical erosion or endocervicitis, and pregnancy. The procedure is contraindicated during the immediate pre- or post-menstrual phase.

Sensitivity Test: If indicated in the patient's history, an intracutaneous skin test or sublingual absorption observation may be done with 0.1 cc Salpex.

Warning: Not for intravenous use.

© ORTHO PHARMACEUTICAL CORPORATION 1970

Salpex CONTRAST MEDIUM
TRADEMARK

EACH CC CONTAINS:
sodium acetrizolate 0.53 g and
polyvinylpyrrolidone 0.23 g



ORTHOPHARMACEUTICAL CORPORATION • RARITAN, NEW JERSEY 08869

Accuracy. It's good therapy.

Because complete therapy planning is unquestionably beneficial to patients, more and more therapy centers rely on therapy simulators. It's good sense and it's good therapy. Since the TherX™ simulator has no equal, TherX is a logical choice.

TherX pinpoint accuracy makes pinpoint treatment easier. TherX localizes tumors, confirms entry/exit ports and verifies beam coverage with an isocentric accuracy of $\pm 1\text{mm}$.

TherX frees therapy equipment for full time therapy use. And most important, patients receive safe and undeniably thorough treatment.

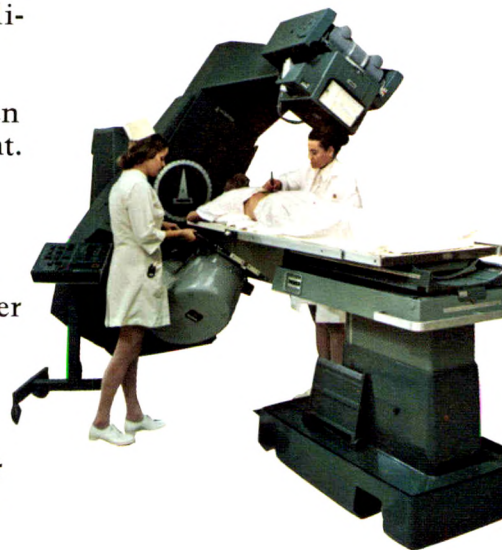
The versatile TherX reproduces the relative movements of teletherapy units, linear

accelerators and betatrons. A unique combination of radiographic, fluoroscopic and positioning capabilities make TherX particularly useful in brachytherapy.

A new TherX stretcher duplicates all the features of the stretcher used with Picker's C-12 Co⁶⁰ therapy unit for even more precise planning/treatment.

TherX is a product of Picker's synergy — the complete interfacing of systems and services for improved therapy and therapy planning. No other therapy simulator available today can match it.

For complete information contact your local Picker representative. Or write Picker Corporation, 595 Miner Road, Cleveland, OH 44143.



PICKER®
ONE OF THE C.I.T. COMPANIES



Picker'synergy



Revitalize Your Tired R-F Equipment.

Add a Machlett Cesium Iodide Image Intensifying System

- **IRIS 100** TV Viewing & 100mm Spotfilming
- **DYNAVISION** TV Viewing
- **DYNAVIEW** Optical Viewing

Superior performance at the right price.
Ask your x-ray dealer for complete
information or contact:



The Machlett Laboratories, Incorporated

1063 Hope Street
Stamford, Connecticut 06907
(203) 348-7511

A Raytheon Company

CHARLES C THOMAS • PUBLISHER

ADMINISTRATION OF A RADIOLOGY DEPARTMENT: Hints for Day-to-Day Operation by Murray L. Janower, *St. Vincent Hospital, Worcester, Massachusetts*. Various systems which can be applied to the radiology department to insure efficient functioning are presented in this book. In addition to a general overall look at a totally functioning diagnostic radiology department, the various subunits in a department are dissected and discussed in detail. All of these discussions are supplemented by a great deal of statistical data. Specific attention has been given to the methods used in handling patients, the establishment of a quality control program, efficient production of radiological reports, methods of film interpretation, and darkroom operations. '76, 72 pp., 8 il., 7 tables, \$7.50

CARDIAC CATHETERIZATION AND ANGIO-CARDIOGRAPHY IN SEVERE NEONATAL HEART DISEASE by Michael T. Gyepes, *UCLA, Los Angeles*, and William R. Vincent, *Pennsylvania State Univ., University Park*. Organized around the acts of cardiac catheterization (CC) and angiocardiology (ACG) this book is divided into three parts. Part I covers the preliminary clinical and laboratory examination which must take place prior to catheterization. Part II deals with the technical aspects of CC and ACG, with particular emphasis on the special needs and problems of the unstable infant. The final section discusses the all-important question of what to do with the obtained information. '74, 184 pp., 317 il., \$14.50

THE PHYSICS OF RADIOLOGY (3rd Ed., 3rd Ptg.) by Harold Elford Johns and John Robert Cunningham, *both of the Univ. of Toronto, Toronto, Ontario, Canada*. Emphasis in this edition has been shifted from 200 kv and caesium 137 radiation toward higher energy radiations. Also expanded is the section on diagnostic radiology including many of the modern techniques of TV in radiology. Recent information concerning the nature of radiation damage, repair processes in cells and fractionation are included. '74, 812 pp. (6 3/4 x 9 3/4), 398 il., 92 tables, \$24.75

Prepaid orders sent postpaid, on approval

**301-327 EAST LAWRENCE
SPRINGFIELD • ILLINOIS • 62717**

Hanley Space Saver X-Ray and Medical Record Cabinets are installed in most hospitals in America.

Top quality and low price is the reason.

5 compartment with doors—\$219.25

5 compartment less doors—\$179.50

Bentson Medical Record Files, Lateral, and Card Cabinets
Brochure F.O.B. Factory

AMERICA'S LARGEST DISTRIBUTOR OF X-RAY CABINETS

HANLEY MEDICAL EQUIPMENT CO.

5614 South Grand X-Ray Division St. Louis, Mo. 63111

In reply to advertisers
please mention that you saw
their advertisement in

THE AMERICAN JOURNAL OF ROENTGENOLOGY

published monthly for

The American

Roentgen Ray Society

by

CHARLES C THOMAS • PUBLISHER

Springfield, Illinois 62717

Mental retardation can happen to anyone.

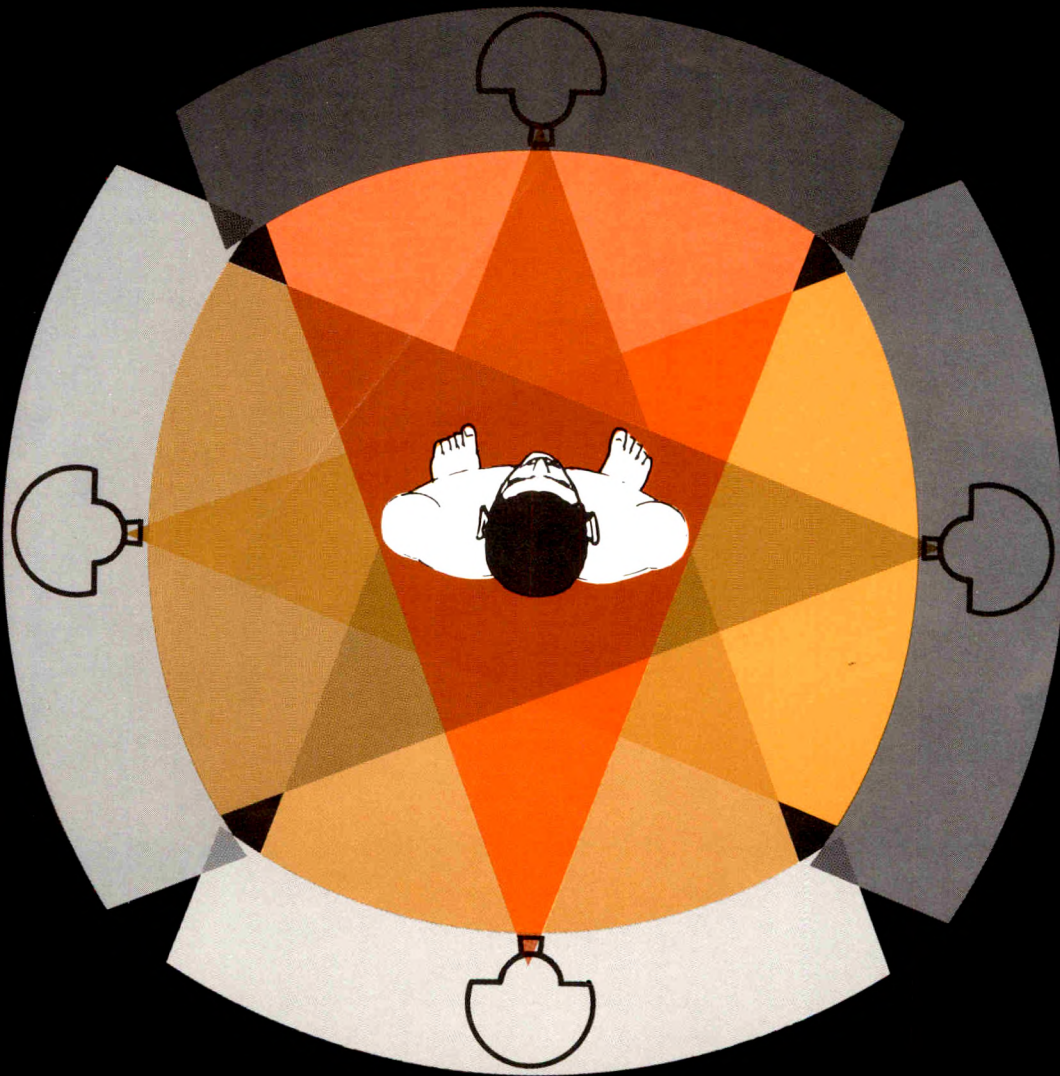
It can happen to you!

But you can prevent mental retardation.

To find out how, write:

National Association for Retarded Citizens,
Civitan Inquiry Program,
P. O. Box 6109, Arlington, Texas 76011.

Varian Introduces the 6-Second Whole-Body CT Scanner



**A New Era in
Computed Tomography...**

CHARLES C THOMAS • PUBLISHER

ADMINISTRATION OF A RADIOLOGY DEPARTMENT: Hints for Day-to-Day Operation by Murray L. Janower, *St. Vincent Hospital, Worcester, Massachusetts*. Various systems which can be applied to the radiology department to insure efficient functioning are presented in this book. In addition to a general overall look at a totally functioning diagnostic radiology department, the various subunits in a department are dissected and discussed in detail. All of these discussions are supplemented by a great deal of statistical data. Specific attention has been given to the methods used in handling patients, the establishment of a quality control program, efficient production of radiological reports, methods of film interpretation, and darkroom operations. '76, 72 pp., 8 il., 7 tables, \$7.50

CARDIAC CATHETERIZATION AND ANGIO-CARDIOGRAPHY IN SEVERE NEONATAL HEART DISEASE by Michael T. Gyepes, *UCLA, Los Angeles*, and William R. Vincent, *Pennsylvania State Univ., University Park*. Organized around the acts of cardiac catheterization (CC) and angiocardiology (ACG) this book is divided into three parts. Part I covers the preliminary clinical and laboratory examination which must take place prior to catheterization. Part II deals with the technical aspects of CC and ACG, with particular emphasis on the special needs and problems of the unstable infant. The final section discusses the all-important question of what to do with the obtained information. '74, 184 pp., 317 il., \$14.50

THE PHYSICS OF RADIOLOGY (3rd Ed., 3rd Ptg.) by Harold Elford Johns and John Robert Cunningham, *both of the Univ. of Toronto, Toronto, Ontario, Canada*. Emphasis in this edition has been shifted from 200 kv and caesium 137 radiation toward higher energy radiations. Also expanded is the section on diagnostic radiology including many of the modern techniques of TV in radiology. Recent information concerning the nature of radiation damage, repair processes in cells and fractionation are included. '74, 812 pp. (6 3/4 x 9 3/4), 398 il., 92 tables, \$24.75

Prepaid orders sent postpaid, on approval

**301-327 EAST LAWRENCE
SPRINGFIELD • ILLINOIS • 62717**

Hanley Space Saver X-Ray and Medical Record Cabinets are installed in most hospitals in America.

Top quality and low price is the reason.

5 compartment with doors—\$210.25

5 compartment less doors—\$179.50

Bentson Medical Record Files, Lateral, and Card Cabinets
Brochure F.O.B. Factory

AMERICA'S LARGEST DISTRIBUTOR OF X-RAY CABINETS

HANLEY MEDICAL EQUIPMENT CO.

5614 South Grand X-Ray Division St. Louis, Mo. 63111

In reply to advertisers
please mention that you saw
their advertisement in

THE AMERICAN JOURNAL OF ROENTGENOLOGY

published monthly for

The American
Roentgen Ray Society

by

CHARLES C THOMAS • PUBLISHER

Springfield, Illinois 62717

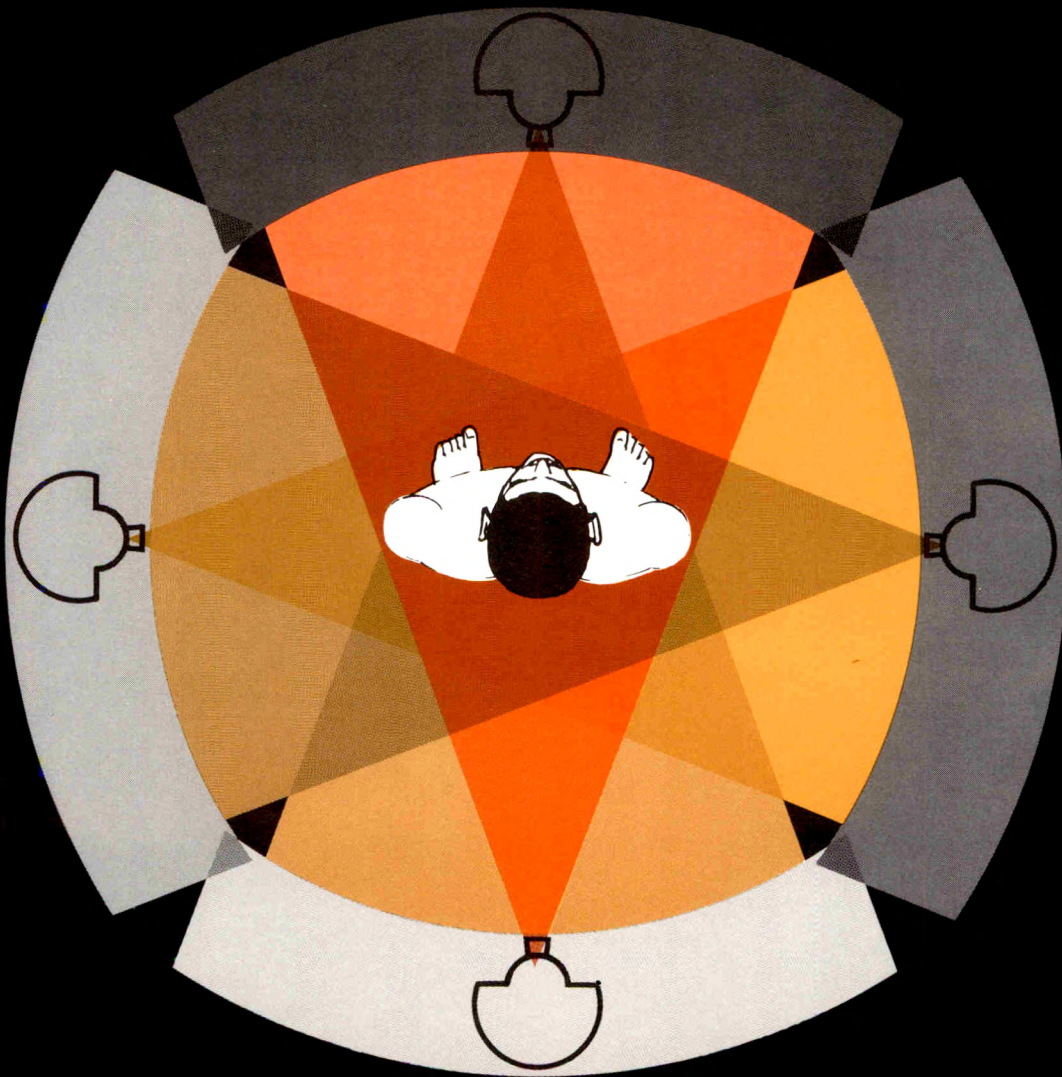
Mental retardation can happen to anyone.

It can happen to you!

But you can prevent mental retardation.

To find out how, write:
National Association for Retarded Citizens,
Civitan Inquiry Program,
P. O. Box 6109, Arlington, Texas 76011.

Varian Introduces the 6-Second Whole-Body CT Scanner



**A New Era in
Computed Tomography...**

Let Varian Introduce You to 6-Second Computed Tomography

A Full 360° Whole-Body Scan in 6 Seconds

The two most important parameters in CT scanning, quality of image and short data-acquisition time, have now been achieved by Varian.

With a 6-second scan, two immediate benefits are realized. First, artifacts resulting from involuntary physiological motion are virtually eliminated. Second, with respiration easily suspended for the brief 6-second scanning period, you get sharp, clear images the first time.

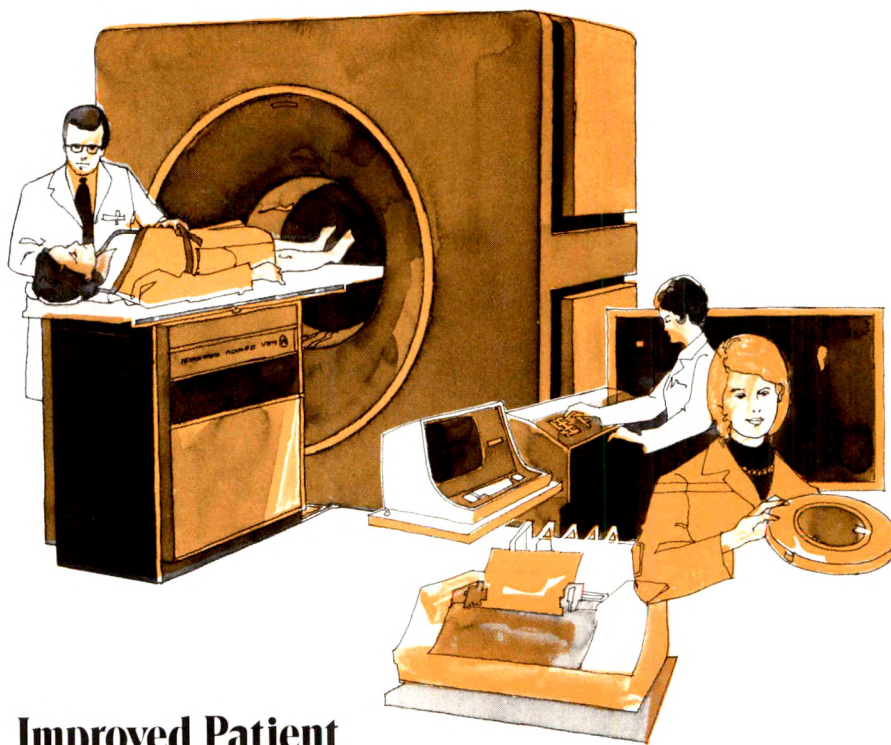
Superior Design

Varian's CT Scanner utilizes fan beam geometry. X-rays are collimated into a fan-shaped beam and collected by approximately 300 high-efficiency Xenon-Krypton detectors. X-ray tube and detectors rotate as a unit, scanning the full patient cross-section throughout the entire 360 degrees.

The Varian-developed slip-ring construction eliminates cable flexing, and provides a base for faster than 6-second data acquisition in the future.

Compatible with the Future

The design concepts of the Varian system assure compatibility with inevitable developments in the rapidly advancing CT technology. Equally important, Varian's total corporate involvement and close control over the major components in the CT Scanner System—Rotating Gantry, Xenon-Krypton Detector, Computer, and X-ray source—facilitate prompt incorporation of new technological advances.



Improved Patient Handling

The new Scanner is a carefully engineered patient and user-oriented system. For example, the 90 cm-diameter aperture will accommodate your largest patients. Patient positioning within the rotating gantry is facilitated by a low-power laser alignment system and computer driven patient couch.

Talk to Varian

Before you make any decision, get the facts on the 6-second era from Varian. Call or write today. Varian Radiation Division, 611 Hansen Way, Palo Alto, CA 94303. Tel: 415/493-4000. Worldwide sales and service.



CHARLES C THOMAS • PUBLISHER

THE RENAL UPTAKE OF RADIOACTIVE MERCURY ($^{197}\text{HgCl}_2$): Method for Testing the Functional Value of Each Kidney, Technique—Results— and Clinical Application in Urology and Nephrology edited by **Claude Raynaud**, *Service Hospitalier Frederic Joliot, Orsay, France*. Foreword by **Pierre Royer**. (41 Contributors) The first chapters of this text describe several techniques of uptake measurement along with simplified systems of external counting, scanners or gamma cameras, and specific problems associated with the deep position of the kidney or Hg metabolism. The rest of the book discusses the normal values of Hg renal uptake and the results obtained in patients. '76, 248 pp., 110 il., 47 tables, \$22.75

ELEMENTS OF RADIATION PROTECTION by **Ronald V. Scheele and Jack Wakley**, both of the *Univ. of Virginia School of Medicine, Charlottesville*. The basic ideas and practical aspects of radiation protection are developed by coordinating material from several disciplines. Preliminary chapters deal with atomic structure, ionizing radiations, radioactivity, x-rays and the interaction of radiation with matter. The mechanisms of biological damage and the factors of radiation damage are outlined along with the acute and long-term biological manifestations of radiation exposure. '75, 112 pp., 15 il., 10 tables, \$7.95, paper

ARTHROGRAPHY OF THE SHOULDER: The Diagnosis and Measurement of the Lesions Visualized by **Julius S. Neviaser**, *George Washington Univ., Washington, D. C.* Normal arthrograms are illustrated in this text, and frequent and unusual lesions are discussed. Individual chapters cover adhesive capsulitis, ruptures of the rotator cuff, ruptures following a dislocation or fracture, chronic and frequently misunderstood ruptures, lesions of the biceps tendon, dislocation of the shoulder, pathologic anatomy of old unreduced dislocations, the "stripping operation," and changes in the joint which cause limitation of motion following fractures of the surgical neck of the humerus. '75, 288 pp., 265 il., \$22.50

AN ATLAS OF POLYTOME PNEUMOGRAPHY by **Taher El Gammal and Marshall B. Allen, Jr.**, both of *Medical College of Georgia, Augusta*. Assisted by **Paul Dyken**. This atlas presents a large number of studies which supplement the study of normal anatomy of the cerebrospinal fluid pathways and provide comparison for the identification of abnormal structures. Concentration is on the findings of polytome pneumography but, where possible, correlations are made with angiography, positive contrast ventriculography, and CAT examinations. '76, 480 pp. (8 1/2 x 11), 729 il., \$39.50

XERORADIOGRAPHY OF THE BREAST (3rd Ptg.) by **John N. Wolfe**, *Hutzel Hospital, Detroit, Michigan*. Foreword by **Wendell G. Scott**. Written for persons working in the field of breast cancer, this text presents a new and significant method for early detection. The mechanics and principles involved in this procedure are clearly defined. Breast anatomy and the normal breast are discussed, providing a thorough understanding necessary to achieve the proper technique and correct interpretation of the xeromammogram. An up-to-date discussion of benign conditions, miscellaneous conditions, and malignancies is presented. The xeroradiographs are accurately reproduced in their original blue color for consistency of detail. '75, 194 pp. (8 1/2 x 11), 242 il. (92 in color), \$23.50

A STUDY GUIDE IN NUCLEAR MEDICINE: A Modern Up-to-Date Presentation compiled and edited by **Fuad Ashkar, August Miale, Jr. and William Smoak**, all of the *Univ. of Miami, Miami, Florida*. (22 Contributors) A comprehensive review of nuclear medicine is provided by this book which is a necessity for persons studying for the examination of the American Board of Nuclear Medicine. Covered are such topics as interaction of gamma rays with matter, control of radiation exposure to man, basic mathematics of nuclear medicine, electrolytes and body composition, essentials of rectilinear scanning, cardiovascular imaging and treatment of thyroid disease with radioiodine. '75, 488 pp., 312 il., 44 tables, cloth-\$22.75, paper-\$17.50

Orders with remittance sent, on approval, postpaid

301-327 East Lawrence Avenue • Springfield • Illinois • 62717

Let Varian Introduce You to 6-Second Computed Tomography

A Full 360° Whole-Body Scan in 6 Seconds

The two most important parameters in CT scanning, quality of image and short data-acquisition time, have now been achieved by Varian.

With a 6-second scan, two immediate benefits are realized. First, artifacts resulting from involuntary physiological motion are virtually eliminated. Second, with respiration easily suspended for the brief 6-second scanning period, you get sharp, clear images the first time.

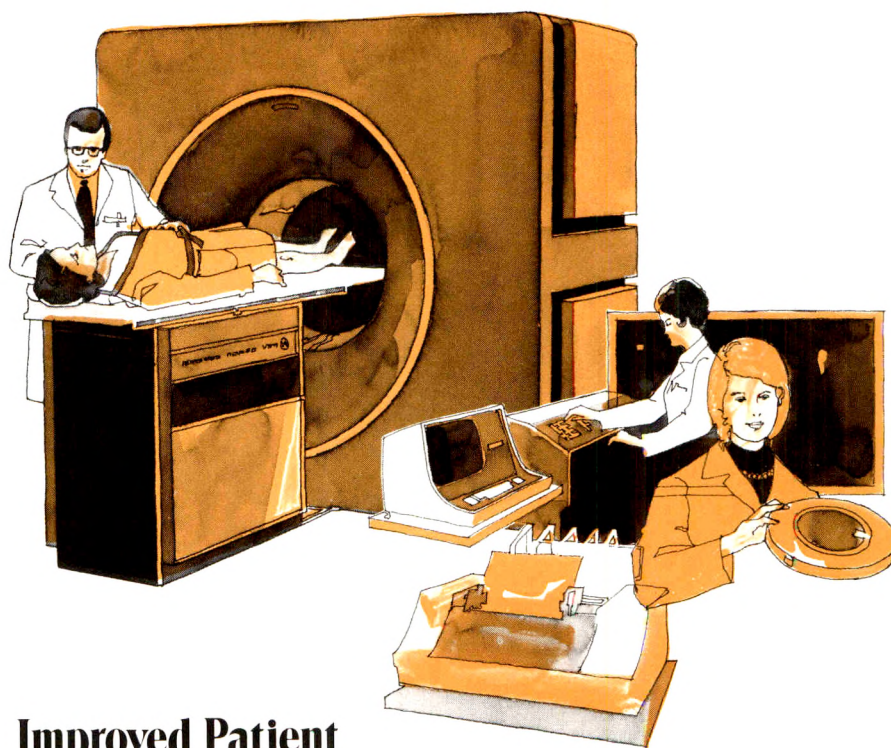
Superior Design

Varian's CT Scanner utilizes fan beam geometry. X-rays are collimated into a fan-shaped beam and collected by approximately 300 high-efficiency Xenon-Krypton detectors. X-ray tube and detectors rotate as a unit, scanning the full patient cross-section throughout the entire 360 degrees.

The Varian-developed slip-ring construction eliminates cable flexing, and provides a base for faster than 6-second data acquisition in the future.

Compatible with the Future

The design concepts of the Varian system assure compatibility with inevitable developments in the rapidly advancing CT technology. Equally important, Varian's total corporate involvement and close control over the major components in the CT Scanner System—Rotating Gantry, Xenon-Krypton Detector, Computer, and X-ray source—facilitate prompt incorporation of new technological advances.



Improved Patient Handling

The new Scanner is a carefully engineered patient and user-oriented system. For example, the 90 cm-diameter aperture will accommodate your largest patients. Patient positioning within the rotating gantry is facilitated by a low-power laser alignment system and computer driven patient couch.

Talk to Varian

Before you make any decision, get the facts on the 6-second era from Varian. Call or write today. Varian Radiation Division, 611 Hansen Way, Palo Alto, CA 94303. Tel: 415/493-4000. Worldwide sales and service.



CHARLES C THOMAS • PUBLISHER

THE RENAL UPTAKE OF RADIOACTIVE MERCURY ($^{197}\text{HgCl}_2$): Method for Testing the Functional Value of Each Kidney, Technique—Results— and Clinical Application in Urology and Nephrology edited by Claude Raynaud, *Service Hospitalier Frederic Joliot, Orsay, France*. Foreword by Pierre Royer. (41 Contributors) The first chapters of this text describe several techniques of uptake measurement along with simplified systems of external counting, scanners or gamma cameras, and specific problems associated with the deep position of the kidney or Hg metabolism. The rest of the book discusses the normal values of Hg renal uptake and the results obtained in patients. '76, 248 pp., 110 il., 47 tables, \$22.75

ELEMENTS OF RADIATION PROTECTION by Ronald V. Scheele and Jack Wakley, both of the *Univ. of Virginia School of Medicine, Charlottesville*. The basic ideas and practical aspects of radiation protection are developed by coordinating material from several disciplines. Preliminary chapters deal with atomic structure, ionizing radiations, radioactivity, x-rays and the interaction of radiation with matter. The mechanisms of biological damage and the factors of radiation damage are outlined along with the acute and long-term biological manifestations of radiation exposure. '75, 112 pp., 15 il., 10 tables, \$7.95, paper

ARTHROGRAPHY OF THE SHOULDER: The Diagnosis and Measurement of the Lesions Visualized by Julius S. Neviaser, *George Washington Univ., Washington, D. C.* Normal arthrograms are illustrated in this text, and frequent and unusual lesions are discussed. Individual chapters cover adhesive capsulitis, ruptures of the rotator cuff, ruptures following a dislocation or fracture, chronic and frequently misunderstood ruptures, lesions of the biceps tendon, dislocation of the shoulder, pathologic anatomy of old unreduced dislocations, the "stripping operation," and changes in the joint which cause limitation of motion following fractures of the surgical neck of the humerus. '75, 288 pp., 265 il., \$22.50

AN ATLAS OF POLYTOME PNEUMOGRAPHY by Taher El Gammal and Marshall B. Allen, Jr., both of *Medical College of Georgia, Augusta*. Assisted by Paul Dyken. This atlas presents a large number of studies which supplement the study of normal anatomy of the cerebrospinal fluid pathways and provide comparison for the identification of abnormal structures. Concentration is on the findings of polytome pneumography but, where possible, correlations are made with angiography, positive contrast ventriculography, and CAT examinations. '76, 480 pp. (8 1/2 x 11), 729 il., \$39.50

XERORADIOGRAPHY OF THE BREAST (3rd Ptg.) by John N. Wolfe, *Hutzel Hospital, Detroit, Michigan*. Foreword by Wendell G. Scott. Written for persons working in the field of breast cancer, this text presents a new and significant method for early detection. The mechanics and principles involved in this procedure are clearly defined. Breast anatomy and the normal breast are discussed, providing a thorough understanding necessary to achieve the proper technique and correct interpretation of the xeromammogram. An up-to-date discussion of benign conditions, miscellaneous conditions, and malignancies is presented. The xeroradiographs are accurately reproduced in their original blue color for consistency of detail. '75, 194 pp. (8 1/2 x 11), 242 il. (92 in color), \$23.50

A STUDY GUIDE IN NUCLEAR MEDICINE: A Modern Up-to-Date Presentation compiled and edited by Fuad Ashkar, August Miale, Jr. and William Smoak, all of the *Univ. of Miami, Miami, Florida*. (22 Contributors) A comprehensive review of nuclear medicine is provided by this book which is a necessity for persons studying for the examination of the American Board of Nuclear Medicine. Covered are such topics as interaction of gamma rays with matter, control of radiation exposure to man, basic mathematics of nuclear medicine, electrolytes and body composition, essentials of rectilinear scanning, cardiovascular imaging and treatment of thyroid disease with radioiodine. '75, 488 pp., 312 il., 44 tables, cloth-\$22.75, paper-\$17.50

Orders with remittance sent, on approval, postpaid

301-327 East Lawrence Avenue • Springfield • Illinois • 62717

OUR LAURA HAS A LEARNING PROBLEM. BUT SHE'S DOING FINE IN SCHOOL.



"Not long ago, if a child had a learning problem, everybody just sort of gave up. I'm glad our Laura wasn't growing up back then."

"Today we know that even children with severe handicaps can learn much more than people used to realize."

"Through special education, Laura is really getting a lot out of school. Just as important, she is getting along well with other children. She's leading a pretty normal, happy life."

If you have a child with any kind of handicap (physical, mental or emotional) who is not getting the special education he needs, we have free information that can help. Just fill in this coupon.

CLOSER LOOK · BOX 1492
WASHINGTON, D.C. 20013

Name _____

Address _____

City _____

State _____

Zip _____

Handicap or Problem _____



CLOSER LOOK

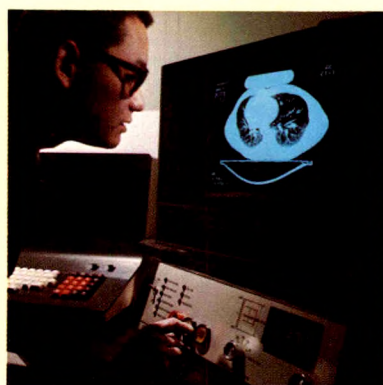
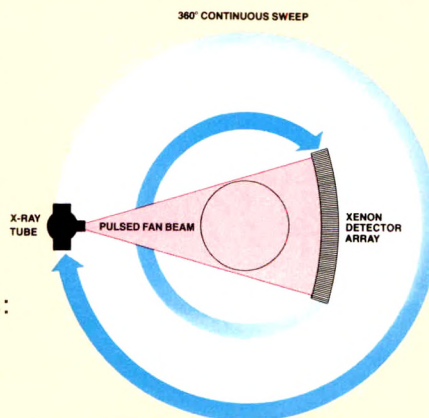
(a free service of the U.S. Office of Education
Department of Health, Education & Welfare)

CT/T fast-scanner: the third generation computed tomography system that's versatile, efficient and consistent.

CT/T system: 4.8-second scans, consistently sharp images.

The CT/T total body scanner has established the third generation of computed tomography: GE fast-scan. With this system, one 360° sweep yields the scan information for a full 320 pixel diameter image in just 4.8 seconds.

This unprecedented speed solves the primary problem of slower units: motion unsharpness caused by patients' respiratory motion. First and second generation systems, using an incremental rotate-and-translate principle, take from 18 seconds to 5½ minutes per scan. But the new GE fast-scan unit features a rotating pulsed fan beam with a 320 element xenon detector array. The tube and detectors rotate around the body in one, smooth 360° motion, taking only 4.8 seconds. Most patients can comfortably hold their breath



during the GE fast-scan procedure, with improved resulting image quality.

The CT/T system offers many other diagnostic advantages. Here are just some of the key features:

Versatile viewing capability.

The viewing console allows precise selection of the range of CT numbers displayed. A special feature on the CT/T system is an IDENTIFY button, which causes the CT numbers at the center of the CT range to "blink." This provides rapid identification of picture elements at a selected CT number without changing window widths.

Photographic recording of selected images is provided by a multi-format camera which accommodates three standard film sizes.

Advantages of GE xenon detectors

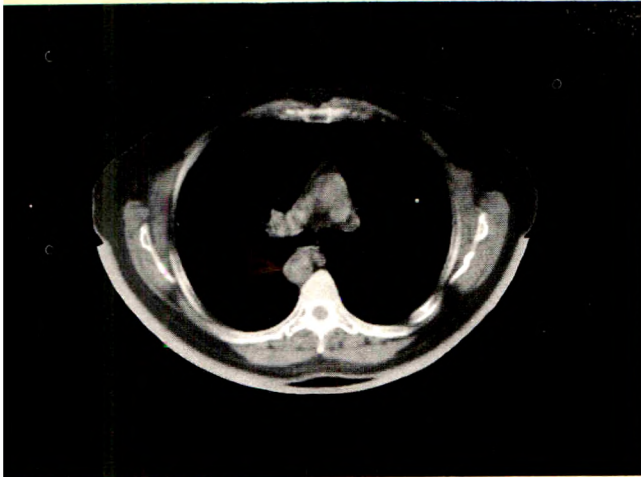
After studying many different detector options for the rotating pulsed fan beam fast-scan system, GE researchers found high-pressure xenon offered numerous advantages over other types of detectors. Here are some of the most important considerations:

Necessary Characteristics. The multi-element xenon detector array possesses the most important requirements for a CT detector: reliability, complete response to x-radiation, and a wide linear dynamic range. Advanced fabricating techniques provide for reliable, consistent detector manufacturing. The detectors are operated in a stable range of voltage and pressure to ensure consistent performance. Unlike vacuum components, impurity contamination is not a problem, and the uniform high pressure of xenon gas within the detector chamber ensures that the response is uniform throughout the detector, and remains so with time. The pulsed mode of operation provides sufficient time for complete response to the incoming x-ray photons. And, the response of the xenon detector is linear over the range of digitization used within the system.

Overall Efficiency. The overall efficiency of the GE rotating fan beam x-ray source and detector system is a product of two main factors: the detection efficiency and the collimation efficiency. The noise

equivalent absorption (NEA) for the xenon detector is about sixty percent that of the best possible scintillator crystal/ photomultiplier tube combination. But the collimation efficiency possible with this system is superior to that of any other. Because of this, at least twice as many unscattered x-rays emerging from the patient actually reach the active area of the detector as in other systems. Also, because the scan is carried out through 360° rather than 180°, the reduction in skin dose required for the same integral dose is calculated to be a factor of about 1.6.

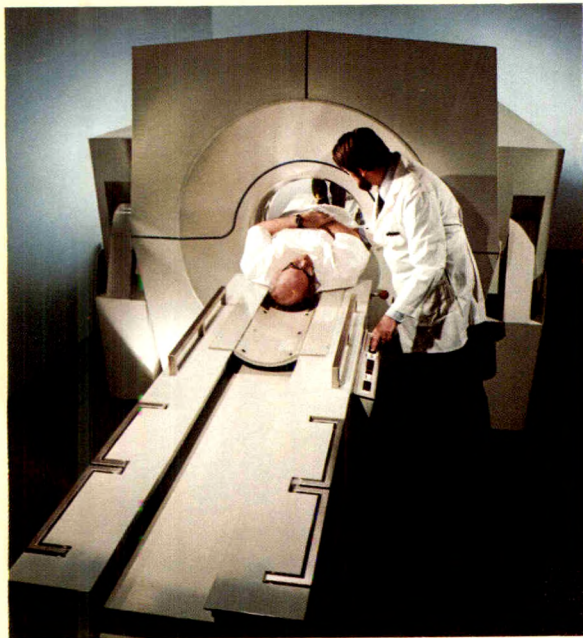
Putting these three factors together (detection efficiency, collimation efficiency and 360° scan) provides an approximate 2X reduction in the skin dose requirement over those systems using a broad x-ray tube focal spot and scintillator crystal/ photomultiplier tube detectors. Thus the pulsed fan beam/multi-element xenon detector array provides the design option of keeping the dose low or increasing the dose to improve resolution. There is considerable latitude in changing the system mAs through changes in the pulse, the pulse mA, and the number of pulses. For the typical patient on the CT/T system, it is expected that the skin dose will be approximately 2-4R, although diagnostic quality images have been produced with skin doses substantially under 1R.



Chest scan of lung area—Level setting is 0; window setting is 200, ranging from +100 to -100. Soft tissue—muscle, heart and subcutaneous fat—is emphasized.



Abdominal scan—Level setting is +27; window setting is 160, ranging from -53 to +107. Scan shows lobulated liver; round tumor near liver; top of right kidney; displaced spleen.



A fast look: fast-scan CT/T system

Scanning speeds—4.8 seconds and 9.6 seconds.

Image reconstruction time—200 seconds.

Matrix dimensions—320 pixel dia. matrix. Each pixel corresponds to a volume element measuring 1.3 mm x 1.3 mm x 10 mm.

Main disc storage—over 200 images.

Archival storage—magnetic tape unit is standard with the system.

Multi-format camera—images may be positioned on film in any order for diagnostic convenience. Film sizes: 8 x 10; 11 x 14; 14 x 17.

Gantry—60 cm opening; 42 cm field of view; $\pm 15^\circ$ gantry angulation; no water bag required.

X-ray tube—Maxiray™ 125.

Generator—3-phase MSI™ 850 II.

Simultaneous reconstruction and viewing.

The display monitor in the viewing console is "refreshed" by a separate high-speed memory, to provide flicker-free images that may be viewed and manipulated without interrupting the computer's image reconstruction. This dual capability allows faster, more efficient diagnosis and speeds patient flow.

Holds more than 200 images.

The CT/T system's main memory disc can hold more than 200 images, 320 pixels in diameter. High-speed random access capability of this disc permits image retrieval in a matter of seconds, compared to minutes for tape systems. All computer functions are directed from a "conversational" keyboard/CRT display to simplify operation. A magnetic tape system for archival storage is included with the system.

If you'd like our new brochure with all the facts on the CT/T system, contact your GE representative or write GE Medical Systems, P.O. Box 414, Milwaukee, Wisconsin 53201. We want you to know more about CT/T: the fast-scan total body system backed by General Electric's corporate commitment to technology, product quality and service.

General Electric Medical Systems,
Milwaukee, Toronto, Madrid.

GE: leading the way in diagnostic imaging.

GENERAL  ELECTRIC

*Improving productivity is important to radiology departments. •
• GE equipment can help make it happen.*

GE: committed to helping x-ray departments do more.

The prime concern of any radiology department is serving patients. And the more efficient that service, the more everyone benefits. That's why GE is committed to providing systems that help your x-ray department make optimum use of time, space, resources and personnel. Here are some examples:

MMX system... optimum capability and efficiency for breast exams, with minimum patient apprehension.

This dedicated, self-contained system offers a wide variety of tube angulations and compression positions for virtually any breast projection. Today,



Axillary view

in hundreds of hospitals, MMX™ is delivering high quality images of the entire area of interest, using xeroradiography or mammography, including new fast screen/low dose film procedures. The technologist can perform exams quickly and confidently, assured of minimum retakes.

Patient confidence is also increased, because the patient can maintain visual contact with the technologist throughout the exam.

Quantamat™ automatic exposure control provides correct exposure, regardless of breast size or firmness. This control assures consistent image density from one exam to the next. Resulting image quality is excellent, from craniocaudad views to axillary and mediolateral.

With this specialized system, any radiology room can become a dedicated breast examination area. Since no wall, ceiling or floor supports are needed, installation is fast and inexpensive. If departmental layout changes at a later date, the MMX system can be easily moved to a different room.

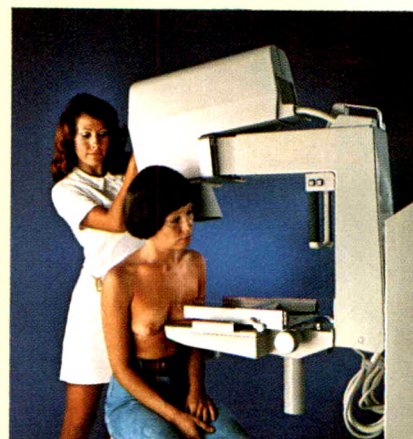
If seeing is believing, here's your opportunity to do so. Now, the ease and versatility of positioning and operating the MMX system are demonstrated in a new desk-top motion picture and related application guide. Featured are positioning directions, suggested techniques, a critique of actual films and more. Ask your GE medical systems representative to arrange for a showing and a supply of application guides for your department.



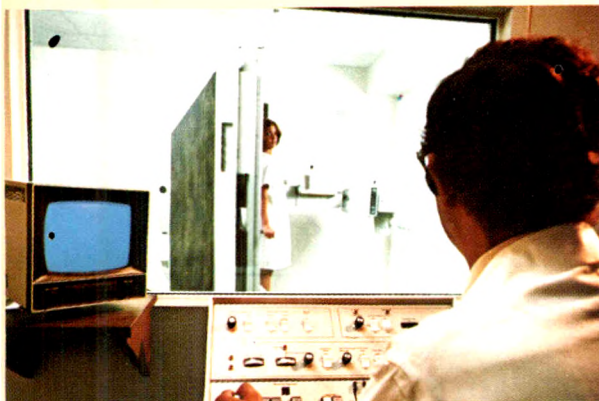
Mediolateral view



Supine mediolateral view



**Craniocaudad view
(with tube unit angulated)**

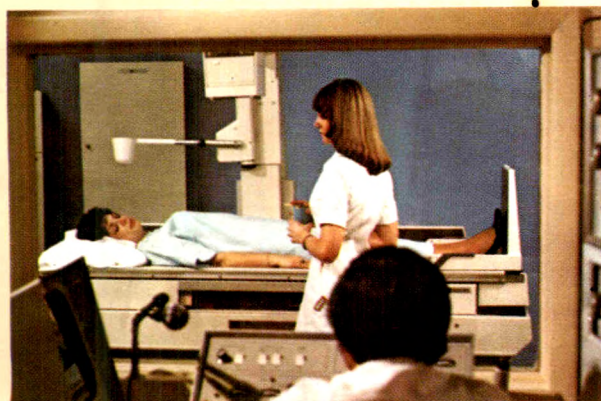


Televis remote control system...technic versatility provides more image information; improves patient flow.

Versatile, proven performance makes the Televis™ system the logical alternative to classical approaches. Any tableside R&F procedure can be handled by Televis remote control, with some very real advantages.

Maximum image information—plus better image quality—result from the system's optimized geometry (43-inch SID). And, there's greater convenience because of integrated multi-procedural capability... immediate changeover between fluoroscopy, Bucky radiography and true linear tomography. This significantly improves patient flow and, in many hospitals, results in operational cost savings up to 25%. In addition, there's reduced radiation exposure to the radiologist, because of total remote control. And, fewer retakes, less total time per examination means less exposure to patients too... the result of sharp fluoro images and immediate recording of precisely what has been viewed, as well as Quantamat™ automatic exposure control that provides the desired density in every image.

Televis system smoothly handles the full range of morning GI studies, including longitudinal oblique angle fluoroscopy in any scanning position, with 105 mm photospotting that can record up to 10 images per second, plus Bucky radiography. Then, in the afternoon, Televis takes on the department's high volume of radiographic and tomographic procedures.

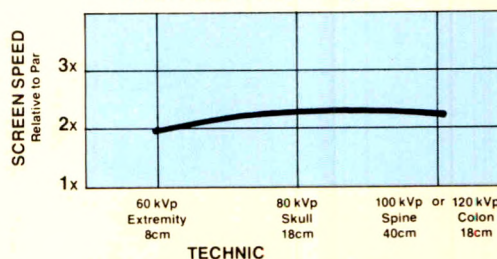


Blue Max screens... precise image quality and reduced radiation without drastic changes in equipment or technic.

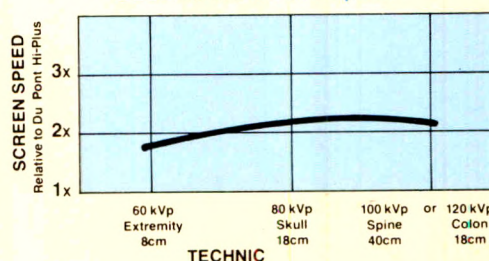


GE Blue Max™ screens provide maximum image quality and diagnostic data at much lower radiation levels than standard screens. Blue Max 1 and 2 intensifying screens feature GE-developed lanthanum oxybromide phosphors which absorb twice the x-rays, compared to standard calcium tungstate screens. Thus, Blue Max screens deliver the same image quality at half the mAs. This allows shorter exposure times, reducing motion unsharpness. Standard cassettes and any blue-sensitive film can be used. Blue Max screens are blue-emitting, so they require no unusual dark-room lighting or special processing techniques.

BLUE MAX 1 Screen Speed



BLUE MAX 2 Screen Speed



Blue Max screens' consistent 2x speed over the diagnostic kVp range makes modification of technic charts simple.

General Electric has many other time-saving, cost-saving systems to improve radiology productivity. Find out how these systems can help your x-ray department do more. Talk to your GE representative. General Electric Medical Systems Milwaukee, Toronto, Madrid

GE: leading the way in diagnostic imaging.

GENERAL  ELECTRIC

Maybe your business needs some new partners



We suggest that you form an alliance with the arts...that your company actively support now some form of the visual or performing arts.

There are vital humanistic reasons for this. All in life is not competition and striving for affluence. And there are sound business reasons for such support. For example: the design industry would be without vitality were there no modern art museums; the fashion industry

uninspired without the great collections of textile artistry; and the advertising business very uncreative without the theater, art, and the world of music to draw upon. In fact, all business and industry need the arts.

Your support can be monetary, of course. You know of the financial crisis in the "labor intensive" field of the arts, and corporate gifts are essential. But there are many other kinds of gifts.

Your support can be the use of a display window to promote a local repertory company. Or the volunteering of interested employees' time, with their "time off" your contribution. There are many ways your company can help, and they're listed in a booklet which we

hope you'll send for.

Start being a patron today! The arts deserve and need your support. And your new partnership will be a thoroughly enjoyable experience.

Support the Arts

Business Committee for the Arts, Inc.
1700 Broadway, New York, N.Y. 10019

Gentlemen:

Please send your booklet "126 Ways To Support the Arts"

Name _____

Address _____

City _____ State _____ Zip _____

From the very beginning, Pfizer Medical Systems has been aware that growing clinical experience and continuing research would dictate certain refinements and improvements in computerized tomography. Pfizer is determined to be in the forefront of such developments and to make them available as economically as possible.

The first result of this effort is the ACTA-Scanner 200, which incorporates a more efficient and comfortable patient handling system and an advanced computer system, firmly establishing a modular approach to changing technology. The 200 user will be able to convert to the 0200FS

when available. The 0200FS will enable completion of a scan in less than 30 seconds and will have other operating refinements described on the back.

This modularity, of course, will make the advanced features of the 0200FS just as readily available to current as well as prospective users.



MEDICAL SYSTEMS, INC.
A SUBSIDIARY OF PFIZER INC.



Distinguishing Features



MEDICAL SYSTEMS, INC.
A SUBSIDIARY OF PFIZER INC.

ACTA-SCANNER[®] 0200 & 0200FS

Operation and Control Advances (0200FS only)

- Under 30-second scan time minimizes artifacts and increases patient throughput
- Immediate image reconstruction
- Industry compatible CT numbering system allows universal comparisons
- Advanced computer system
- Light beam guided patient positioning
- Variable scan slice thickness adjustment
- Tilttable gantry ($\pm 20^\circ$) for increased flexibility of scan position
- 22" tunnel diameter to accommodate most patients

Versatile Patient Record System (0200 & 0200FS)

- *For data storage*—(1) magnetic tape, for low cost mass storage; (2) optional "floppy" disc for easy filing of individual patient scan data
- *For photographic recording*—(1) 105 mm roll or cut film; (2) Polaroid[®] copies; (3) Multiformat Scan Recorder (optional)

Advanced Patient Handling System (0200 & 0200FS)

- Interchangeable bed modules allow maximum patient throughput
- Bed modules may be rolled to patient rooms, simplifying patient transfers
- Head supports on each bed module allow pre-positioning and immobilization
- Human-engineered for increased patient comfort
- Power mechanism raises bed module and locks it into position
- Movements of bed module are remotely controlled after lock-in

Continuing Features (0100, 0200, 0200FS)

- 320 matrix
- Instant image reconstruction
- Pfizer commitment to customer service
- 12 month warranty—labor, parts including tube
- Color and black-and-white viewing
- Selective enlargement

“How many people do you know who have been cured of cancer?”

Almost everybody knows someone who has died of cancer. But the fact is about two million living Americans have been cured. Not only cured but leading active, normal lives. Another fact is millions more could be.

By getting to the doctor in time.

By availing themselves of the most effective methods of treatment today.

By advances made through cancer research. Research made possible with the help of the American Cancer Society.

However, there's much more to be done. To help save more people, the American Cancer Society needs more money. So, please, give. We want to wipe out cancer in your lifetime.

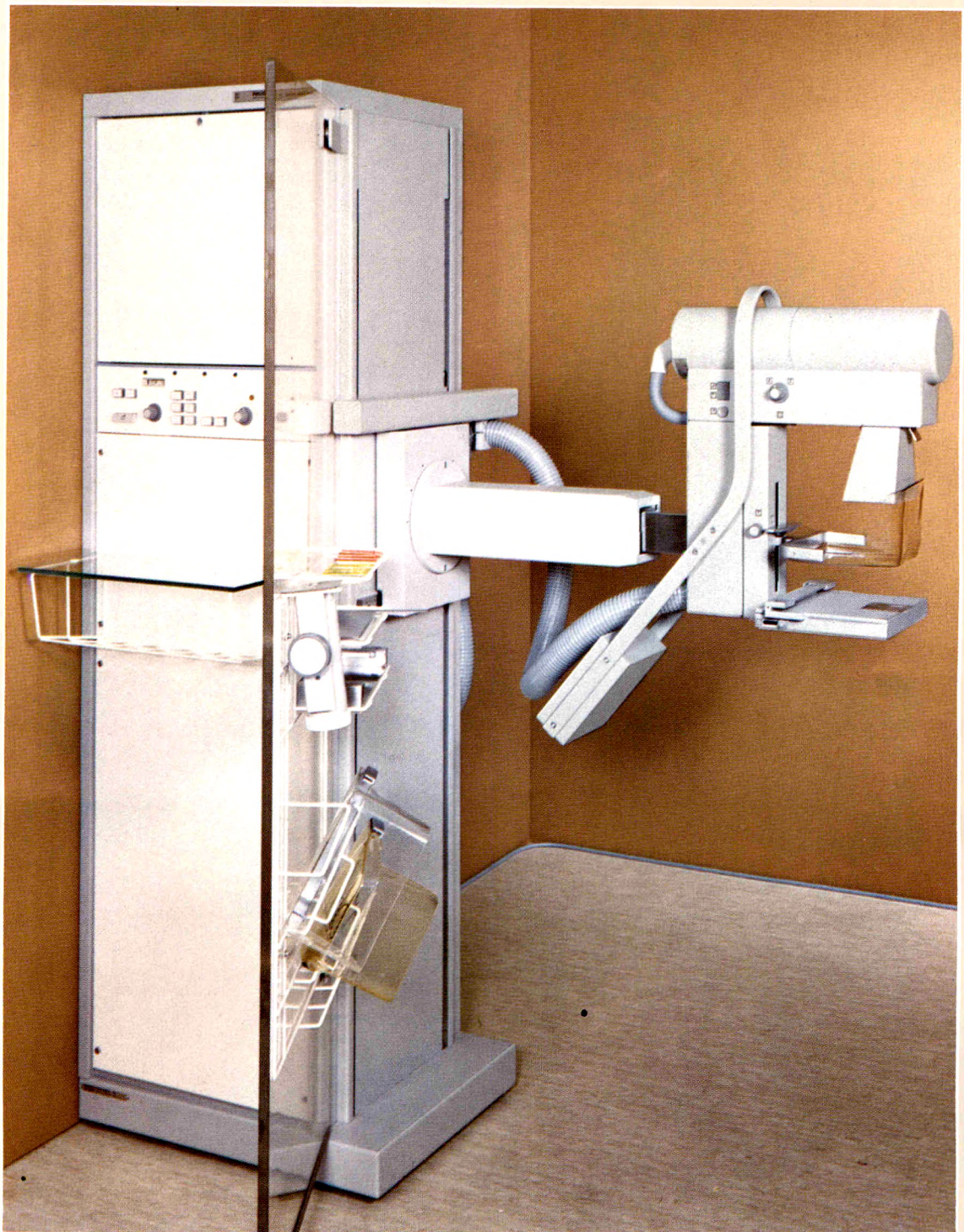
American Cancer Society



Flip Wilson,
National Crusade Chairman

For mammography, take a stand
you can count on:

PHILIPS MAMMO DIAGNOST



Clear detail, the finest contrast and the best possible resolution. All with minimum radiation dose to your patient.

That's what Philips Mammo Diagnost gives you with every film. Whether you use the Mammo Diagnost for radiography or Xeroradiography, you can make your diagnosis with total confidence.

And with convenience. Examinations are easier and faster for you, more comfortable, assuring and relaxing for your patient.

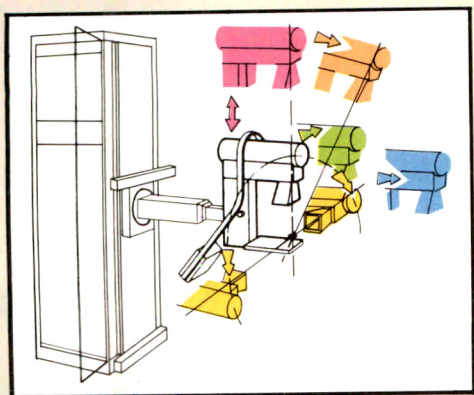
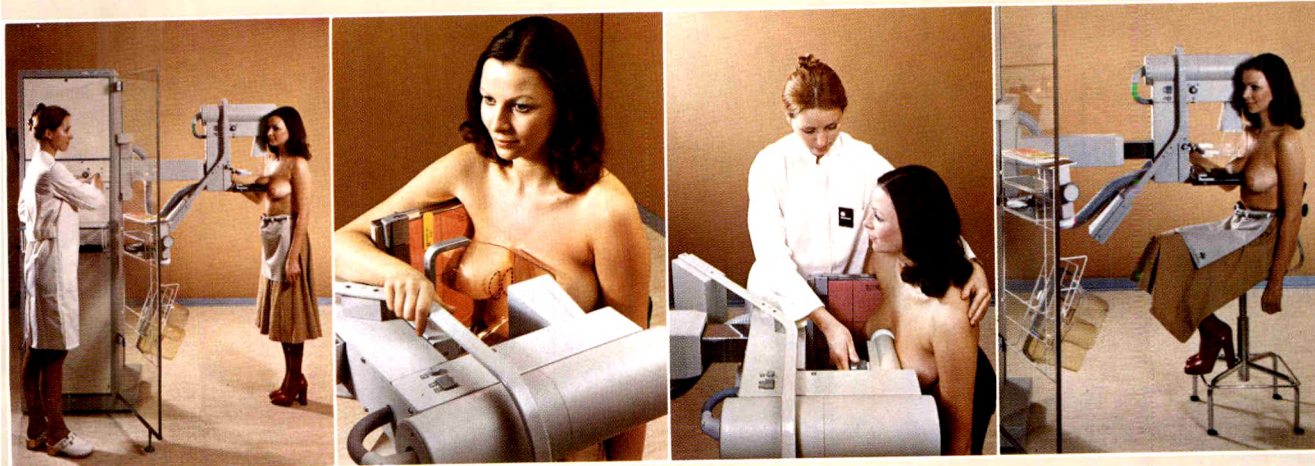
Seated, standing or recumbent patients are examined efficiently, with precise positioning insured by a wide range of tube travel (including caudal angulation).

Self-contained, compact and pre-wired for rapid installation, the Mammo Diagnost also features Automatic Exposure capability, optional water cooling of the X-ray tube, and logically

arranged generator controls for both programmed and manual techniques. Vacuum cassettes and all new low dose films can be used with outstanding results.

For additional information, contact your Philips representative. Or, call or write:

PHILIPS MEDICAL SYSTEMS, INC.
710 Bridgeport Avenue, Shelton, Conn. 06484
Tel. (203) 929-7311



PHILIPS®

We help you help.

An employee of yours has a house fire, a disabled parent, an emergency of any kind.

That's just when Red Cross — America's Good Neighbor — steps in to lend a hand. Because helping people is what we're all about.

You could say all this helps your company, too.

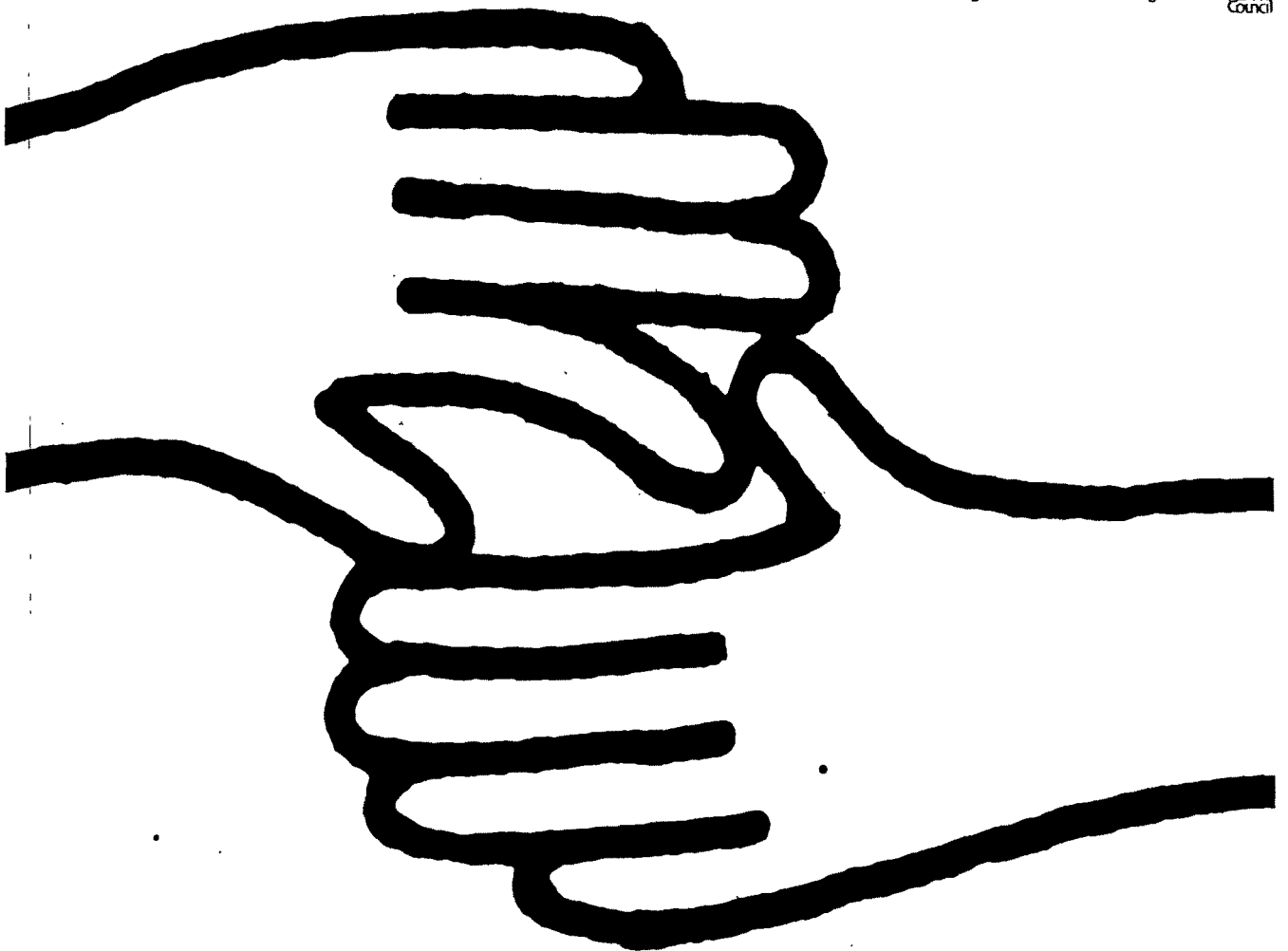
Because easing people over life's rough spots makes them easier in their minds. And no one has to tell you how important that is on the job.

So help Red Cross any way you can.

When you help us, it helps your people.

And when you help your people, you help yourself.

A Public Service of This Magazine & The Advertising Council



 **Red Cross.
The Good
Neighbor.**

Double up, America.



Two can ride cheaper than one.

When people drive to work alone, they spend twice as much money on commuting as they should.

That's too much.

They can cut it in half. They can take a friend.

Not only will that daily commute cost less (and be a lot more pleasant), but when people carpool, they cut pollution, congestion and gasoline usage.

And companies benefit directly, because, obviously, fewer cars will make less demand on the parking spaces in the company lot. And some companies have attributed an increase in punctuality to the fact that more and more of their employees were carpooling.

Help the people in your company carpool. Texas Instruments in Dallas did it. 3M Company in St. Paul did it. Prudential Insurance Company of America in Boston did it.

Do it.

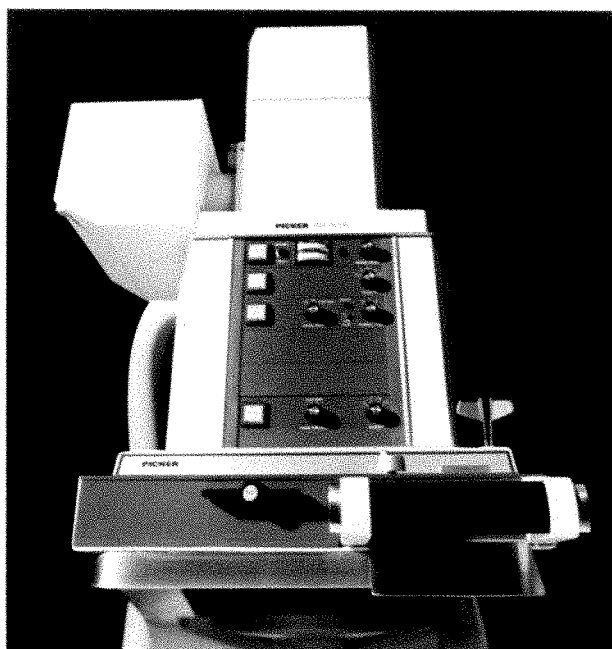
For your "Double up Kit," write to Double up, U.S. Department of Transportation, P.O. Box 1813, Washington, D.C. 20013. It outlines how companies can help organize carpools.

Let's double up. We'll all get where we're going. Faster and cheaper.



A Public Service of This Magazine & The Advertising Council

Technology catches up to a good idea. Flushmount.



Integral mounting of the x-ray imaging system has long been recognized as a good idea. Because of recent technological advances, Picker now brings you Flushmount—cassetteless spotfilming of the future.

The mobility and flexibility of Picker's Flushmounted Multicon image intensifier delivers total system reliability, proven results, and eliminates the need of cassettes.

While Picker's Flushmount concept improves the appearance of your radiology

department, more importantly it provides superior patient-film geometry and reduces the overall film handling procedures.

With Flushmount, there is no need to remove and park the imaging system as with heavier imaging system combinations. Changeover from fluoroscopy to radiography and back again is quick and easy.

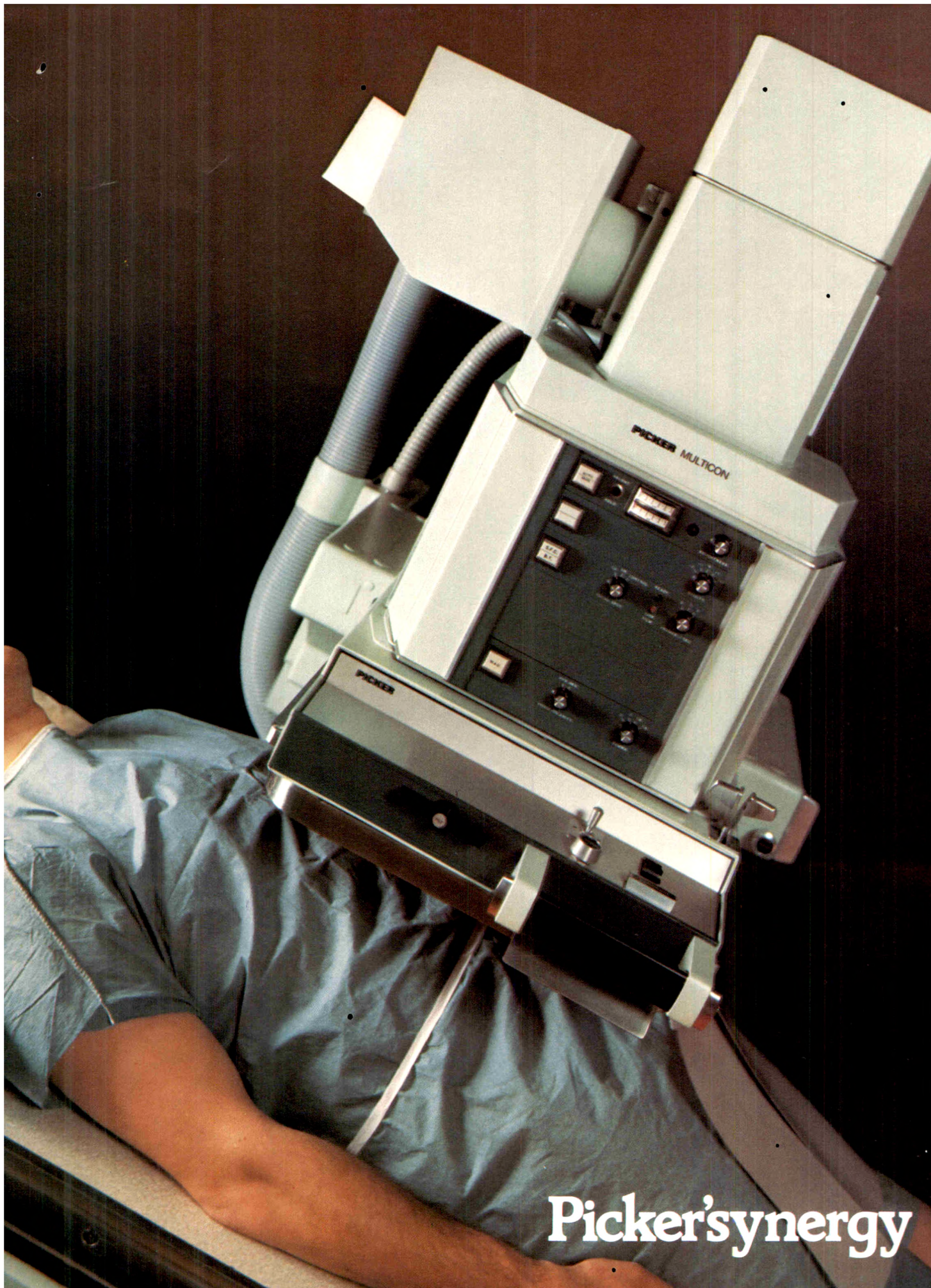
Given Flushmount's reduced mass, "mini-cassetteless" ease of the 100mm film format,

quality results and the field-proven worth of the 90/90 table, Picker today offers the radiologist a hardworking, versatile configuration solid enough to become the backbone of tomorrow's radiology suite.

Flushmount. It's another example of Picker's synergy—the complete interfacing of systems and services for improved diagnostic visualization.

Contact your Picker representative. Or write Picker Corporation, 595 Miner Road, Cleveland, OH 44143.

PICKER®
ONE OF THE C.I.T. COMPANIES



INDEX TO ADVERTISERS

E. I. DuPont de Nemours & Company, Inc.	xii, xiii
Eastman Kodak Company	xviii, xix
EMI Medical, Inc.	xxiv, xxv, xxvi, xxvii, xxviii
E-Z-EM Company	x
C. B. Fleet	vi, vii
General Electric Company	xxxviii, xxxix, xl, xli
Grumman Health Systems	Cover 3
Hanley Medical Equipment Company	xxxiii
Low X-Ray Corporation	xi
Machlett Laboratories	xxxii
Ortho Pharmaceutical Corporation	xxix
Pako Corporation	i
Pfizer Medical Systems	xliii, xlv, xlv, xlv, xlvii, xlviii
Philips Medical Systems, Inc.	1, li
Picker Corporation	xxx, xxxi, liv, lv
The Purdue Frederick Company	v
Searle Radiographics	Cover 2, xvii
SHM Therapy Systems	viii, ix
Siemens Corporation	xxii, xxiii
E. R. Squibb & Sons, Inc.	xiv, xv, xvi, xx, xxi
Charles C Thomas - Publisher	xxxiii, xxxvi
Varian Associates	xxxiv, xxxv
Wolf X-Ray Corporation	ii

We try to present an accurate index. Occasionally this may not be possible because of a last-minute change or an omission.

Now the complete,
flexible ultrasound system:

The RT-400.

For dynamic, two-dimensional,
real-time, high-resolution imaging
(Today and tomorrow.)

For more information, write or call:

Grumman Health Systems
400 Crossways Park Drive
Woodbury, New York 11797
(516/575-3513)



GRUMMAN

American Journal of Roentgenology

Vol. 127

July 1976

No. 1

The Challenge of Computed Tomography. <i>M. M. Ter-Pogossian</i>	1
Picture Quality of Computed Tomography. <i>G. N. Hounsfield</i>	3
The Effects of Biological Motion on CT Resolution. <i>R. J. Alfidi, W. J. MacIntyre, and J. R. Haaga</i>	11
Picture Processing in Computed Tomography. <i>M. Bergström and R. Sundman</i>	17
Computed Tomography of the Body: Initial Clinical Trial with the EMI Prototype. <i>P. F. Sheedy, D. H. Stephens, R. R. Hattery, J. R. Muhm, and G. W. Hartman</i>	23
Computed Tomography of the Body. Early Trends in Application and Accuracy of the Method. <i>R. J. Stanley, S. S. Sagel, and R. G. Levitt</i>	53
Computed Tomography of the Liver. <i>R. J. Alfidi, J. R. Haaga, T. R. Havrilla, R. G. Pepe, and S. A. Cook</i>	69
Computed Tomographic Evaluation of Aortic Aneurysms. <i>S. P. Axelbaum, D. Schellinger, M. N. Gomes, R. A. Ferris, and H. G. Hakkal</i>	75
Computed Tomography of the Heart. <i>M. M. Ter-Pogossian, E. S. Weiss, R. E. Coleman, and B. E. Sobel</i>	79
Cardiac Reconstruction Imaging in Relation to Other Ultrasound Systems and Computed Tomography. <i>R. Gramiak and R. C. Waag</i>	91
Computed Tomography and Neuroradiology: A Fortunate Primary Union. <i>H. L. Baker, Jr.</i>	101
Some Limitations of Computed Tomography in the Diagnosis of Neurological Diseases. <i>K. R. Davis, J. M. Taveras, G. H. Roberson and Robert H. Ackerman</i>	111
Trends in the Development of Reconstruction Tomography in Neuroradiology. <i>T. Greitz</i>	125
Computed Tomography in Infants and Children: Intracranial Neoplasms. <i>P. E. Berger, D. R. Kirks, D. L. Gilday, C. R. Fitz, and D. C. Harwood-Nash</i>	129
Computed Tomography: The Anatomic Basis of the Zone of Diminished Density Surrounding Meningiomas. <i>R. M. Sigel and A. V. Messina</i>	139
Computed Tomographic Evaluation of Hemorrhage Secondary to Intracranial Aneurysm. <i>K. R. Davis, P. F. J. New, R. G. Ojemann, R. M. Crowell, R. B. Morawetz, and G. H. Roberson</i>	143
Demonstration of Purulent Bacterial Intracranial Infections by Computed Tomography. <i>R. A. Zimmerman, S. Patel, and L. T. Bilaniuk</i>	155
Stereotaxic Computed Tomography. <i>M. Bergström and T. Greitz</i>	167
Computed Tomography and Radionuclide Studies in the Diagnosis of Intracranial Disease. <i>J. H. Christie, H. Mori, R. T. Go, S. H. Cornell, and R. L. Schapiro</i>	171
High Resolution Computed Tomography of the Orbit with the Ohio Nuclear Delta Head Scanner. <i>M. A. Weinstein, A. J. Berlin, Jr., and P. M. Duchesneau</i>	175
Further Progress in CT Scanning and Computerized Radiation Therapy Treatment Planning. <i>G. L. Jelden, E. S. Chernak, A. Rodríguez-Antunez, J. R. Haaga, P. S. Lavik, and R. S. Dhaliwal</i>	179
Health Planning for Computed Tomography: Perspectives and Problems. <i>L. E. Cloe</i>	187
Economic Analysis of Computed Tomography Units. <i>R. G. Evens and R. G. Jost</i>	191
Editorial: Orientation of CT Images	207
<i>M. M. Figley and W. R. Eyler</i>	199
Abstracts of Current Literature	200
ARRS Section on Instruction	207
News	217
Radiologic Societies	219

Rec.
15.11.76

AJR

American
Journal of
Roentgenology



August 1976

MAGNIFICATION SUBTRACTION

In super-selective angiography

... magnification and subtraction are methods used for better visualization of small vessels.

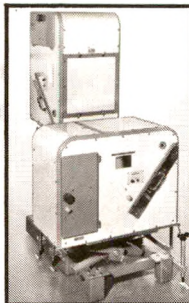
Full-size, direct angiography is the technique. And Schonander Cutfilm Changers are the instruments. World-wide.

Write for illustrated brochures.



elema-schonander, inc.

699 Lively Boulevard
Elk Grove Village, Illinois 60007
(312) 593-6770



PUCK 20 films/3 exp. per sec./14"x14"/24X30 cm



AOT 30 films/6 exp. per sec./14"x14"/24X30 cm

SCHONANDER CUTFILM CHANGERS—
Precision Instruments for Angiography

For faster patient flow, you can buy a compound scanner and a real-time add-on.

Or do it all in one unit for about half the cost with **Siemens Vidoson Ultrasound.**



If you're looking for faster patient flow and superior diagnostic capabilities, there's just one way to do the job with just one machine:

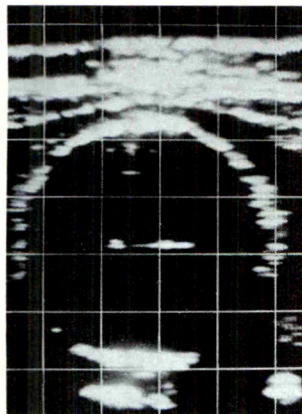
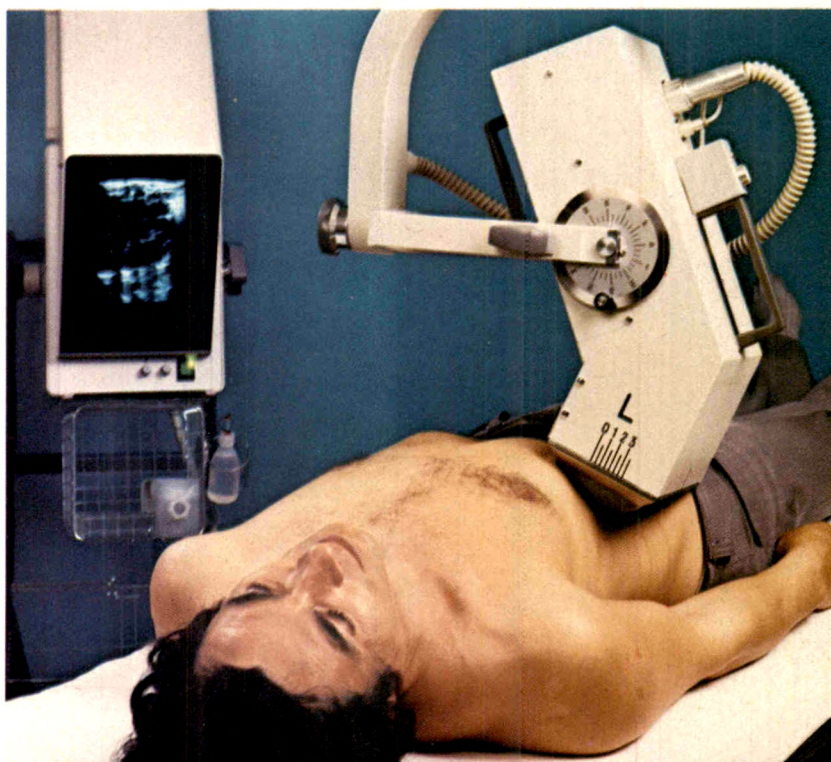
Vidoson Ultrasound by Siemens.

It combines the real-time immediacy of ultrasound with the optimum in gray scale resolution. And it gives you "dynamic and static" pictures in just about one minute.

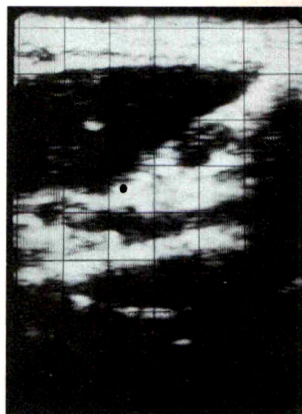
All for about half the cost of a compound scanner and a real-time add-on.

Surprised? You shouldn't be. After all, Siemens has been a pioneer in ultrasound innovation since 1950. Siemens was the first to use it successfully in obstetrics and gynecology. And now, because of the outstanding Siemens gray scale, Vidoson becomes the equipment of choice for internal applications.

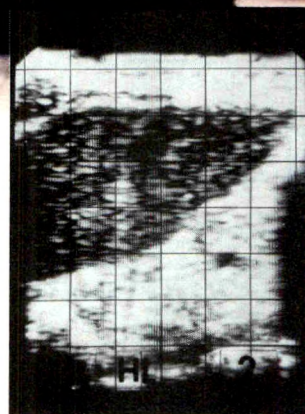
For detailed literature on Siemens Vidoson Ultrasound, write or call:
Siemens Corporation, Medical Systems Division, 186 Wood Avenue South, Iselin, New Jersey, (201) 494-1000.



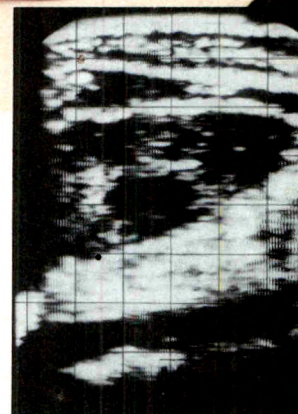
Vidoson embryo assessment; fetal skull with midline echo.



Longitudinal scan through the left lobe of a normal liver.



Left liver lobe showing fatty degeneration.



Black, blurred regions show metastases of the liver.

Sonograms courtesy of: Dr. Rettenmaier, District Hospital of Boeblingen, West Germany and Dr. Lutz, University Clinic of Erlangen, West Germany.

SIEMENS

You are entering a remarkable era of diagnostic advancement. Instead of being limited to a single imaging method, you will take advantage of many techniques, choosing them to meet your specific diagnostic criteria and the condition of your patient.

Searle is helping shape this era of advancement. Over the past decade, guided by your needs, we have developed sophisticated nuclear imaging instruments to a high degree of performance. Now, the knowledge gained during that time is being applied to the creation of instrumentation in the fields of ultrasound and CT scanning.

What Searle developed yesterday in nuclear imaging, the medical community relies on today. And *today* we are planning significant advances in ultrasonic, CT, and nuclear imaging. Tomorrow is in view.

IMAGING:

The Living Art



SEARLE

Searle Radiographics Inc.

AMERICAN JOURNAL OF ROENTGENOLOGY

EDITOR MELVIN M. FIGLEY

ASSISTANT EDITOR ROSALIND H. TROUPIN

ASSOCIATE EDITORS LUTHER W. BRADY
KENNETH L. KRABbenhOFT
E. FREDERICK LANG
RUSSELL H. MORGAN

EDITOR
EMERITUS TRAIAN LEUCUTIA

INCLUDING DIAGNOSTIC RADIOLOGY, RADIATION ONCOLOGY, NUCLEAR
MEDICINE, ULTRASONOGRAPHY AND RELATED BASIC SCIENCES

CONSULTING EDITORIAL BOARD

KENT ELLIS
E. ROBERT HEITZMAN
DONALD L. KING
JOHN A. KIRKPATRICK, JR.
EUGENE C. KLATTE

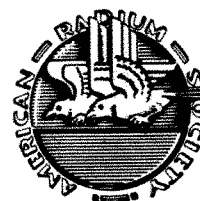
JOHN G. McAFEE
THOMAS H. NEWTON
ROBERT G. PARKER
STEWART R. REUTER
WILLIAM B. SEAMAN

ROBERT J. SHALEK
JOHN STORER
MICHEL M. TER-POGOSSIAN
JOSEPH P. WHALEN
DAVID M. WITTEN

EDITORIAL STAFF: C. P. KAISER, M. J. LEONARD, K. A. MURRAY, M. B. WIECKOWICZ



OFFICIAL JOURNAL
AMERICAN ROENTGEN RAY SOCIETY
AMERICAN RADIUM SOCIETY



The American Journal of Roentgenology is issued monthly by Charles C Thomas, Publisher, 301-327 East Lawrence Ave., Springfield, Illinois 62717. Correspondence regarding subscriptions, advertisements and other business should be addressed to the Publisher. Annual subscription prices: United States and U. S. Possessions \$30.00, Pan America, Canada and others \$35.00. Printed by the George Banta Co., Menasha, Wisconsin. Copyright © 1976 by American Roentgen Ray Society. Second-class postage paid at Springfield, Illinois and at additional mailing offices. Printed in U.S.A.

Guidelines for Authors

The *American Journal of Roentgenology* publishes original and timely contributions to the advancement of radiologic diagnosis and treatment. Although the content is predominantly clinical in origin, laboratory investigations are accepted when their relevance to clinical practice is demonstrable. Contributions are reviewed by two outside consultants and are accepted on condition that they are submitted only to this Journal and that they will not be reprinted or translated without consent of the Editor. Statements within an article are the responsibility of the authors and not the Journal or its publisher.

Address all manuscripts and correspondence to the Editor, Dr. Melvin M. Figley, 403 Pacific National Bank Building, 4545 15th Avenue N.E., Seattle, Washington 98105.

Manuscript Form

Manuscripts should be typed double-spaced throughout, including references, tables, and footnotes. Tables, footnotes, and figure legends should be on separate sheets, and a separate title page should be provided. In addition to the original typewritten copy, a duplicate copy complete with figures, tables, and references is required.

Figures should be submitted as 5" x 7" glossy prints, untrimmed and unmounted. Identifying information (author name, figure number, and indication of the top of the figure) should be attached to the back of each figure with a gummed label. Line illustrations and graphs should be drawn in black ink on white background. Labels on all figures should be of professional quality and sufficiently large to be easily read when reduced in size.

References should be cited in the text by number (e.g., [3, 4]). The bibliography should be arranged in the numerical order that references are cited in the text and typed double-spaced throughout. Data for each reference should be arranged according to the uniform style on bibliographic citations adopted by many biomedical journals. Abbreviations for titles of medical periodicals should conform to those published in *Index Medicus*. Examples:

1. Miller RE, Chernish SM, Skucas J, Rosenak BD, Rodda BE: Hypotonic roentgenography with glucagon. *Am J Roentgenol* 121:264-274, 1974
2. Boijesen E: Superior mesenteric angiography, in *Angiography*, edited by Abrams H, Boston, Little, Brown, 1971, pp 1091-1119

Organization

Title page. Titles should be brief and specific. Include full names and addresses of all authors and acknowledgment of grant support when appropriate.

Abstract. A description of the purpose, methods, results, and conclusions of the study is required. It should be informative to a reader who has not read the text of the article.

Key indexing words. Five to 10 words or short phrases should be supplied to enable cross-indexing of the article.

Introduction. Clearly state the purpose of the investigation including necessary background facts.

Materials and methods. Describe the protocol clearly so that an experienced worker can understand what was done. Use standard abbreviations as presented in the *Council of Biology Editors Style Manual*, 3d edition.

Results. Present results in logical sequence.

Discussion. Interpret the results to lend meaning and importance to the observations. If hypotheses and speculation are included, they must be labeled as such. When results differ from those of previous investigators, an attempt should be made to explain the discrepancy.

References. Only include those references which provide adequate background and present fairly any opposing evidence and concepts. Accuracy of reference data is the responsibility of the author.

Legends. Legends should be brief but should provide sufficient description to interpret the figure.

Special Communications

Case Reports. Concise case reports are accepted if they present unusual experiences that are medically important and educational. Clarity and brevity are essential.

Technical notes. Brief descriptions of new techniques or significant modifications of older ones which are directly applicable to clinical practice will be accepted.

Letters to the Editor. Letters should be limited to between 250 and 500 words. Criticism of published articles should be objective and constructive. Letters may also discuss matters of general interest to radiologists.

Proofs and Reprints

Galley proofs will be sent for correction of errors. The corrected proof, copy-edited manuscript, and the reprint order should be returned directly to the Editor. If the author fails to return proof by the date specified, it may be necessary to publish without the author's approval.



Clean & Clear

Clean bowel means clear picture. X-PREP Liquid is designed specifically for preradiographic bowel cleansing — without enemas, suppositories, or overhydration.

Good-to-excellent visualization is usually obtained with a single, simple dose.* No residual oil droplets (as is often the case with castor oil) obscure the picture.

Pleasant taste of X-PREP Liquid meets with high patient acceptance.* Simplicity and ease of administration are appreciated by the patient at home, by the nursing staff at the hospital.

*References available on request.

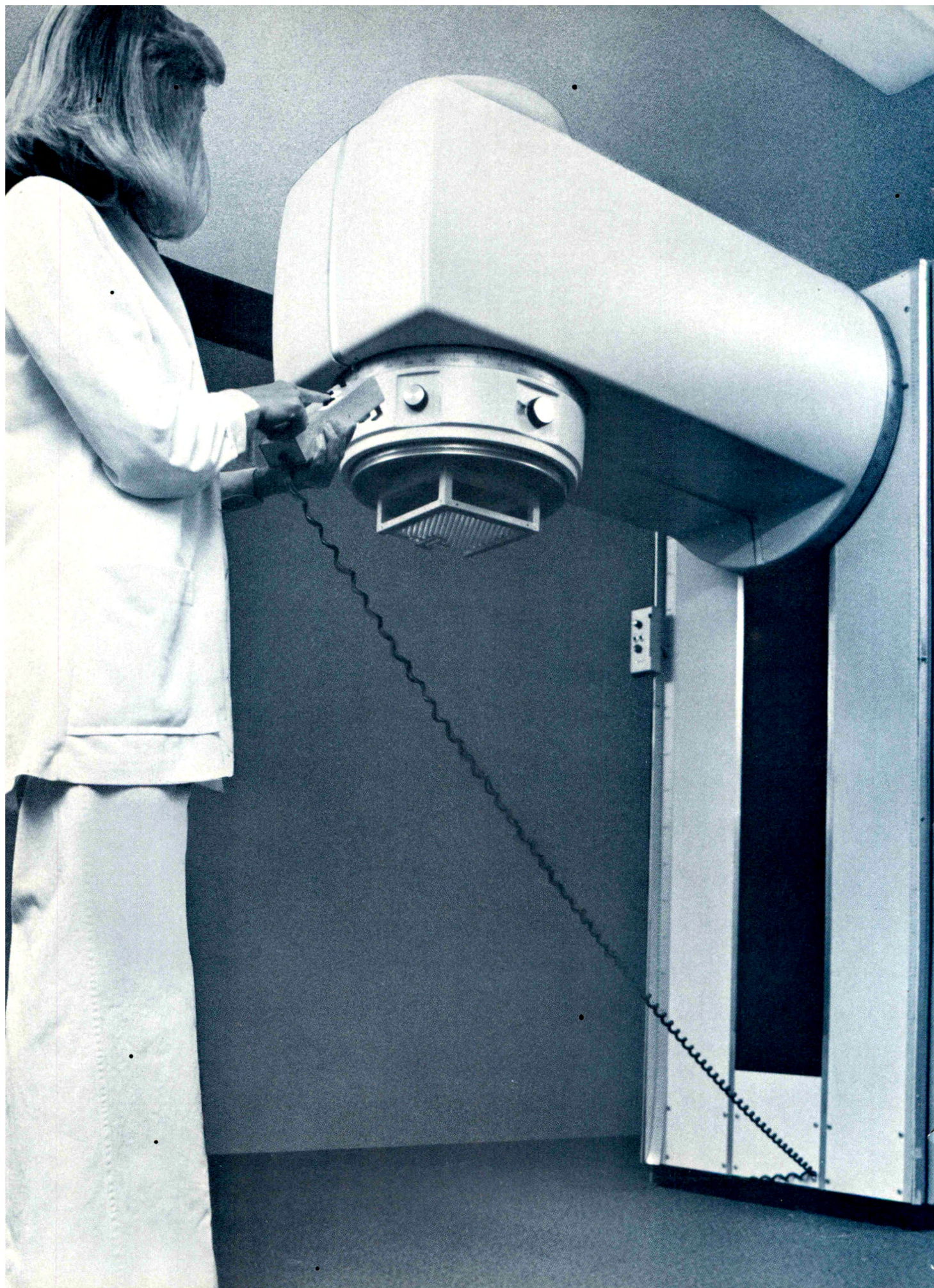
One step • One dose • One bottle

X-PREP Liquid

(standardized extract of senna fruit)

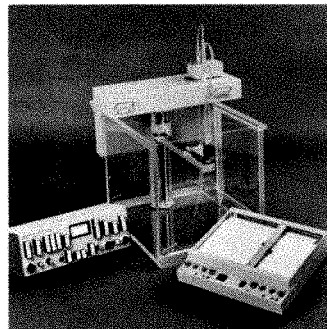
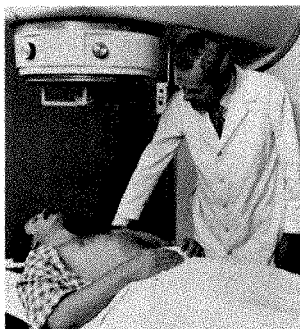
To prep the bowel for radiography

Gray Pharmaceutical Co., Affiliate
The Purdue Frederick Company



THERAPI 4: IT'S BIGGER THAN IT LOOKS.

Therapi 4 is the profession's most economical linear accelerator. It's low in cost; thousands of dollars less than other basic linac systems. It's compact; small enough to fit into existing treatment rooms. And it's easy to install; usually less than two weeks from delivery to operation. □ Yet Therapi 4 rivals much larger and more expensive systems in performance. It offers 4 MeV photons, fully motorized positioning, large field sizes for full body radiation and focal spot size of less than 2mm. It's equipped with an advanced field defining light system, optical range finder for 80 or 100cm treatment distance and many other valuable performance features. And it has advanced solid-state electronics. Electronics that have proven their reliability in over five years of actual therapy service. □ Therapi 4 is built and supported by SHM, a leader in therapy systems and equipment. Call SHM for installation planning information, complete system specifications and a quotation on the most economical linear accelerator available today. □ SHM Nuclear Corporation, 570 Del Rey, Sunnyvale, CA 94086 (408) 245-3136



SHM offers a range of linear accelerator systems, Rad 8 therapy planning systems, isodose plotters and therapy accessories.

SHM Nuclear Corporation



A new series of x-ray generators featuring simple push-button programming: Siemens Organomatic.

Convenience is the idea behind these generators. Any one of 49 preset programs may be selected simply by the turn of the knob and the push of a button.

For ease of identification, push-buttons are organ related. The proper kV, mAs, mA, focus, screen and tube can be selected with only one button. The need to consult reference tables for desired settings is eliminated. Moreover, through automation, the chances of error and the need for time consuming repeats are substantially reduced.

Selection. Available as a single-phase 600 mA generator (model 502) or a three-phase 500 mA generator (model 506), the Organomatic may be customized to meet specific user needs. All automatic programs can be preset during installation to accommodate any desired combination of kV and mAs settings.

Ease of Service. Solid state circuitry guarantees performance reliability. Circuit board and swing-out rack assembly assures accessibility and ease of maintenance.

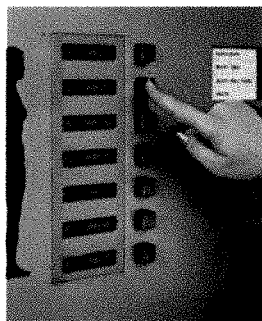
The Organomatic also features an exclusive automatic fault locator/indicator to pinpoint service requirements.

Options. A variety of add-on system features make the Organomatic fully adaptable to specific needs. Among them:

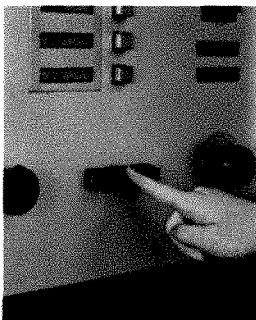
- Automatic exposure timer for correct patient size compensation.
- Planigraphy programming (28 additional programs).
- Fluoroscopy with automatic brightness control.
- Indirect exposure technique with 100 mm cut film camera.
- Over-ride module for free kV and mAs selection.



1 Body region selector.



2 Organ selector buttons.



3 Patient thickness compensation.

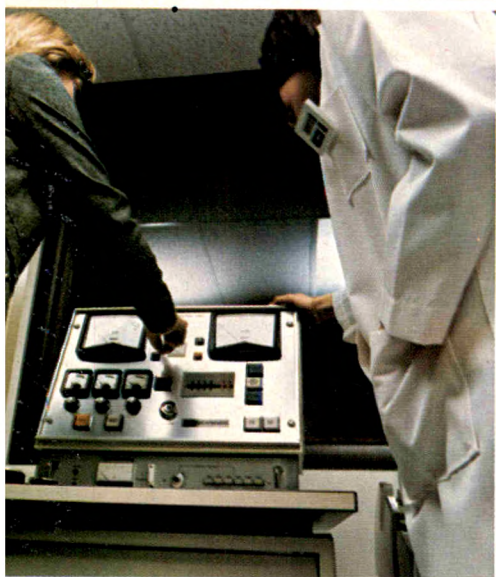
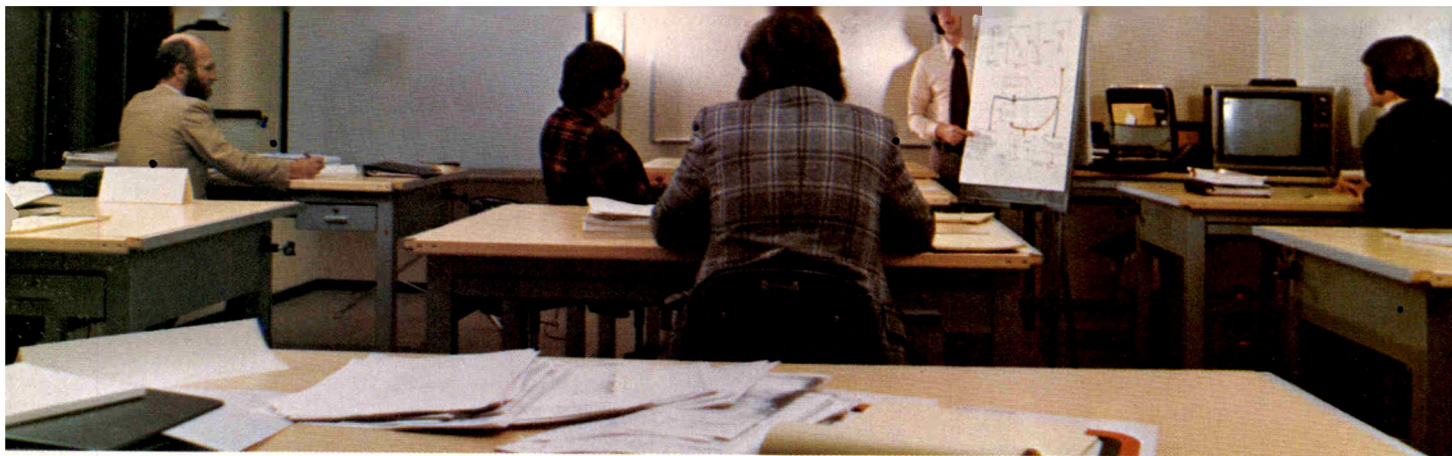


4 Exposure release.

Investigate the Siemens Organomatic and ask about convenient lease financing arrangements. For detailed information, contact your Siemens representative, or you may write to: Siemens Corporation, Medical Systems Division, 186 Wood Avenue South, Iselin, N.J. 08830 (201) 494-1000

In Canada: Siemens Canada Limited, P.O. Box 7300, Pointe Claire 730-P.Q.

SIEMENS



6-212

When you purchase an EMI-Scanner you become

A CT postgraduate at EMI U.

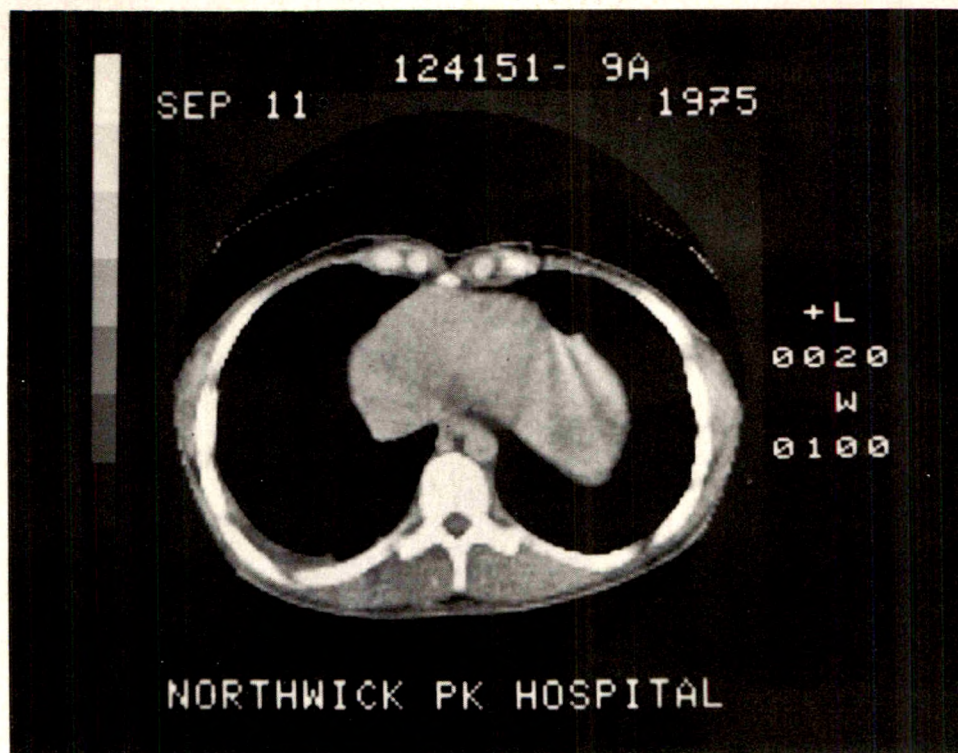
EMI Medical has more experience training more CT scanner operators and maintenance engineers than anyone in the world. Working closely with client institutions, we've developed teaching media and methodology that ensure optimum learning opportunities for your technical staff. An intensive, free-of-charge, 5-day course at EMI's facilities trains your maintenance technician/engineer to perform on-site servicing and routine maintenance. Orientation and training in the use of the EMI-Scanner System is also provided to



First in CT training programs

EMI MEDICAL INC

your technologists and other radiology staff by our registered ASRT personnel at your scanner installation site. The EMI-Scanner System was the world's first CT system. Today, it is the world leader in acceptance and use. When you purchase an EMI-Scanner CT1010 Advanced Neuro C.T. System or CT5005 General Diagnostic System you are assured of a personnel training program that is a direct extension of EMI's continuing commitment to leadership. For more information, call us or write.



Scan taken at the level of the 10th thoracic vertebra, demonstrating a small pleural effusion on the right side. This was not visible on the standard chest radiograph.

6-218

Superior diagnostic information in every EMI-SCAN:

A pleural effusion at T10

The picture you see above is but one example of the wealth of thoracic anatomy which can be demonstrated in one scan by varying the window level setting on the EMI-Scanner CT5005 Advanced General Diagnostic C.T. System. Because of the CT5005's rapid scanning time, the patient can suspend respiration for the duration of the scan, allowing clear views of such detail as the fine vessels at the periphery of the lungs. The EMI-Scanner CT5005 utilizes 300,000 X-ray readings per scan to differentiate between tissue densi-



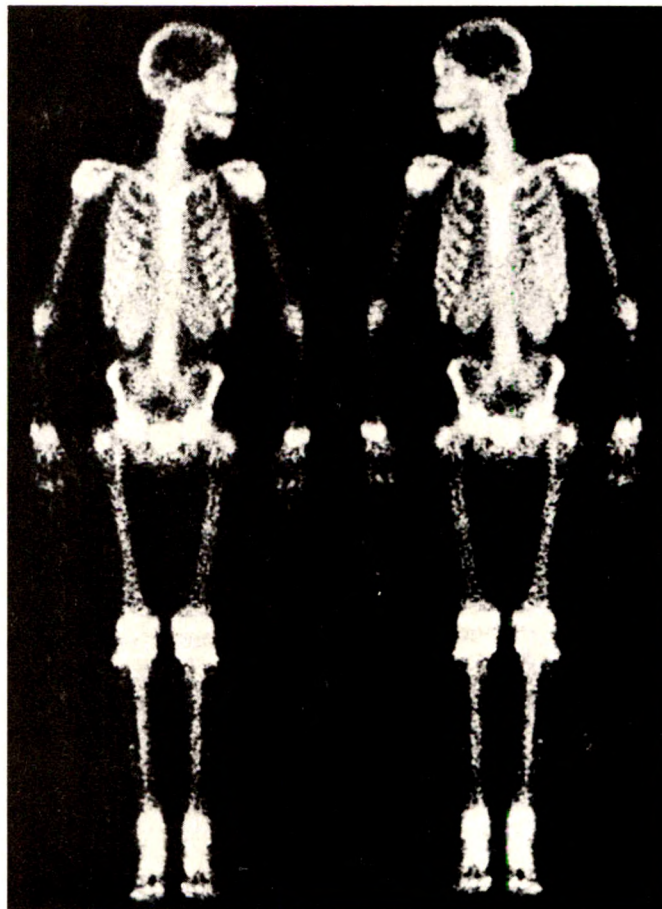
**First in CT
imaging,
worldwide**

EMI MEDICAL INC

ties that vary by as little as one unit in 2000. In the optional high-resolution format, it resolves picture elements 0.75 mm x 0.75 mm in area. A special clinician's Diagnostic Viewing Console enables any quarter section of the total scan picture to be enlarged four times. Additional diagnostic display and data processing options are provided to meet specific clinical needs. The EMI-Scanner is unexcelled in accuracy, resolution, and clinical versatility. It is unrivaled in acceptance and use. For information, call us or write.

**"Wow!
18
whole-body
scans
today!"**

***"Glad
we
have
a
cleon"***



TELEPHONE (617) 444-2494/TELEX 922-552

cleon

CORPORATION ...for maximum patient throughput in whole-body imaging.

SEND FOR THE FACTS:

cleon

AJR

CORPORATION
150 Gould Street
Needham, MA 02192

Yes, I'd like to have the facts about
the Cleon Whole-Body Imager.

NAME _____

DEPARTMENT _____

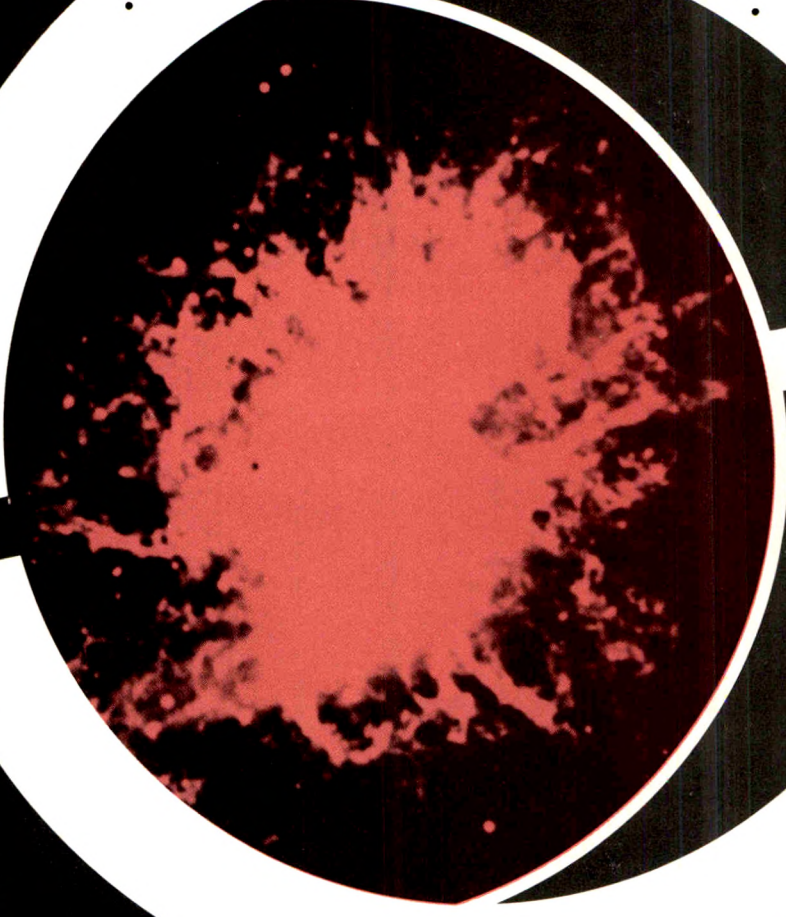
INSTITUTION _____

ADDRESS _____

CITY

STATE

ZIP



e's Pho/Trax CT scanner is the newest most technically advanced instrument of its type available today. But even more important is the fact that Pho/Trax is designed to retain its state-of-the-art status for years to come.

Pho/Trax takes just 5 seconds to travel around a patient's head or torso in a smooth, continuous 360° sweep. Because of this rapid scanning capability, Pho/Trax potentially eliminates blurred exposures due to patient motion, allows breath-holding even with the severely ill and facilitates infant studies.

Pho/Trax has a 23.5" aperture, which means you can perform torso scans on all but the most obese patients. Evaluation of certain structures in the brain, orbits and abdominal organs may require angled or off-axis views. To help you obtain optimum images in these instances, the Pho/Trax gantry can be tilted in both directions over a 30° range.

VARIABLE SLICE THICKNESS

In scanning small structures such as the optic nerve, a narrower slice thickness can often aid accurate diagnosis. With Pho/Trax, the operator can choose any slice thickness from 3mm to 12mm in 1mm increments. A unique beam-shaping technique controls the x-ray fan, keeping it very close to the slice thickness selected.

VARIABLE SCAN SPEED

For most images, a 5 second scan speed is highly desirable; at this speed, radiation exposure is at a new low while resolution is of a very high order. In circumstances where patient motion is not a problem, and where an exceptional degree of clarity is needed, Pho/Trax lets you select a 10 or 20 second scan speed.

FIELD OF VIEW OPTIMIZATION

Advanced computer technology enables Pho/Trax to use a very high number of picture elements (or "pixels") on the 256 x 256 matrix regardless of the actual size of the area of interest. This is not a simple magnification or "zoom" process, but an algorithmic function which uses 100% of the raw data and does not degrade resolution in any way.

A VARIETY OF IMAGING MODES

Reconstruction time with Pho/Trax is 40 seconds for head and torso scans. There is also a 20-second preview mode which allows the operator to evaluate each scan, with subsequent batch image processing after the study is completed. Typically, 6 12mm brain slices can be reconstructed in 4 minutes, while the next patient is being positioned.

Pho/Trax was developed with the dedication to technical superiority that made Searle the recognized leader for in-vivo and in-vitro radionuclide applications. And as with all Searle instrumentation, Pho/Trax is backed by the industry's largest service organization dedicated to medical imaging devices.

For more information, including sample studies, write Searle CT Systems or call our toll-free "800" number.

CALL 800-323-0221 TOLL-FREE

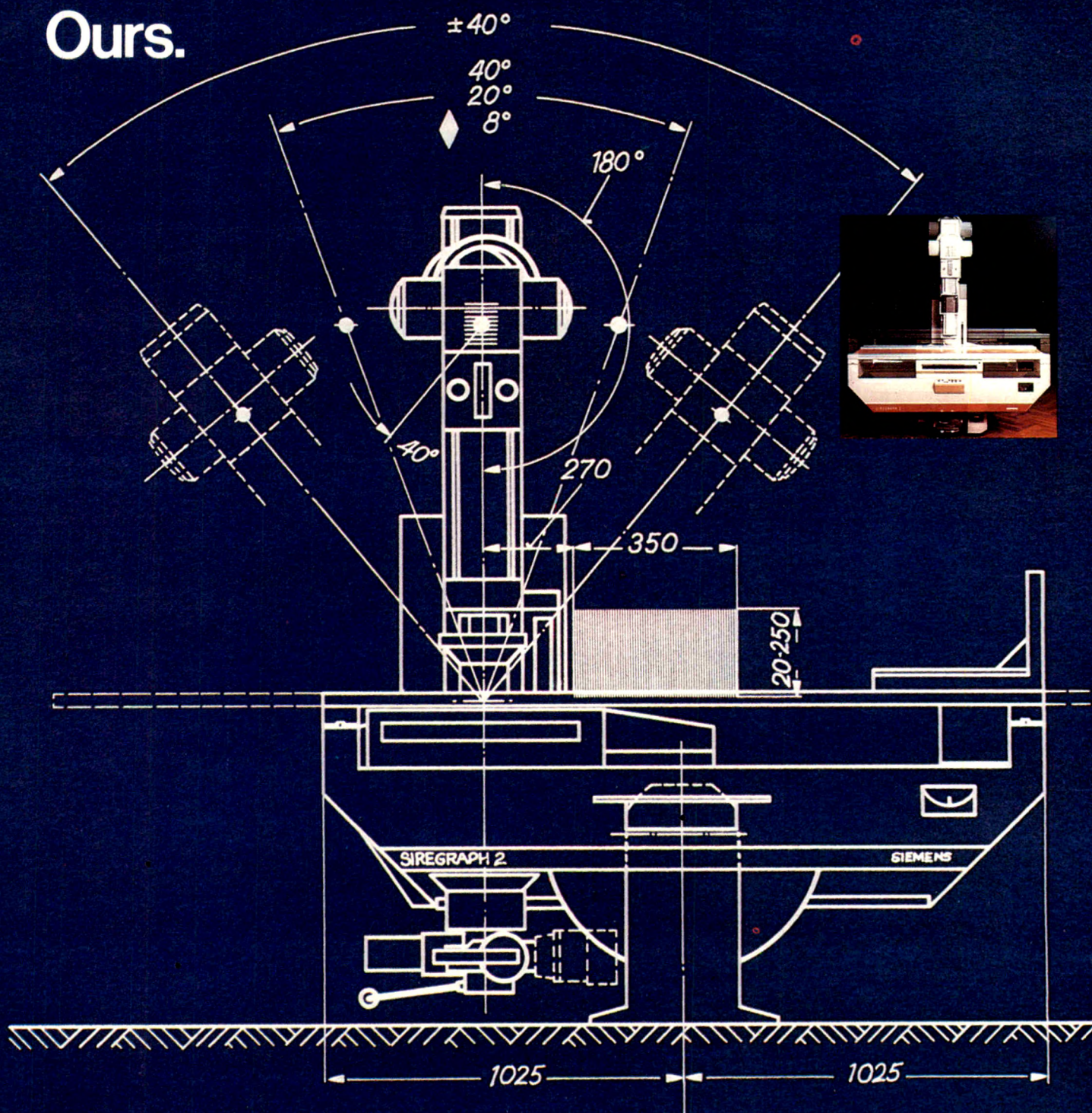
SEARLE

Searle CT Systems
Division of Searle Radiographics, Inc.
4233 North United Parkway
Schiller Park, IL 60176

Designed with the future in mind
New Pho/Trax™ CT scanner

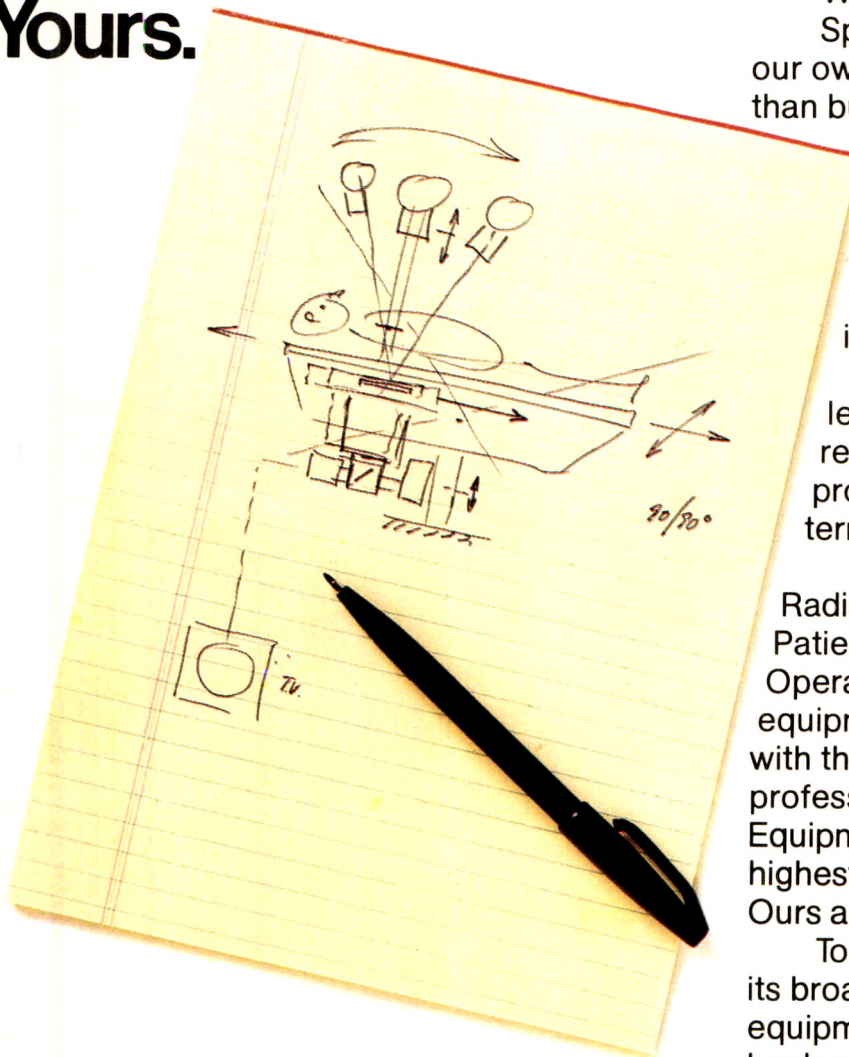
In medical electronics,
every manufacturer aims
at one standard of excellence.

Ours.



**Our excellence
is derived
from one standard.**

Yours.



Siemens became a leader in medical electronics over a century ago by working hand-in-hand with the medical community; we have devoted the same attention to detail in the production of our products as medical professionals exercise in using them.

We still work that way.

Specifically, we emphasize using our own internal components rather than buying outside. This improves quality control and insures that materials work in the system. Also, each production unit is subjected to cumulative testing in the factory as well as in the field.

Siemens customers enjoy less downtime, more reliable and reproducible performance, longer product life and maximum long-term cost-effectiveness.

Whether it be Medical X-ray, Radiation Therapy, Ultrasound, Patient Monitoring, Dental, or Operating and Emergency Room equipment—Siemens products work with the skilled hands of the medical professional—not against them. Equipment that truly meets the highest standards of excellence. Ours and Yours.

To learn more about Siemens and its broad line of medical systems equipment, planning services, service back-up and lease/purchase options, call or write:

Siemens Corporation
Medical Systems Division
Iselin, New Jersey 08830
(201) 494-1000

SIEMENS

**We want to make
gall bladder studies
more convenient.**

For you. For your patients.



Oragrafin®

Calcium Granules

Ipodate Calcium for Oral Suspension U.S.P.

Oragrafin®

Sodium Capsules

Ipodate Sodium Capsules U.S.P.



the
reason
is clear™

Oragrafin (podate) conveniences...

Scheduling flexibility

Diagnostically adequate filling of the gallbladder often takes place within 5 hours or less after ingestion of granules, thereby permitting same-day examinations.

In routine overnight procedures, opacification is attained 10 hours after ingestion of capsules.

Choice of dose forms

Granules or capsules — Rapid absorption of both calcium salt and sodium salt often permits visualization of even poorly functioning gallbladders.

Prepared or unprepared patients

Both salts have been administered to unprepared patients as well as previously prepared patients, with no significant difference in results.

*Please see following page
for brief summary.*



ORAGRAFIN® CALCIUM GRANULES

Ipodate Calcium for Oral Suspension U.S.P.

ORAGRAFIN® SODIUM CAPSULES

Ipodate Sodium Capsules U.S.P.

CONTRAINDICATIONS: Both preparations are contraindicated in patients who are hypersensitive to ipodate salts.

WARNINGS: A history of sensitivity to iodine *per se* or to other iodinated compounds is not an absolute contraindication to the use of these preparations, but calls for extreme caution in administration.

Usage in Pregnancy: The safety of these preparations for use during pregnancy has not been established; therefore, they should be used in pregnant patients only when, in the judgment of the physician, their use is deemed essential to the welfare of the patient.

PRECAUTIONS: Increasing the dosage above that recommended increases the possibility of hypotension. Anuria may result when these preparations are administered to patients with combined renal and hepatic disease or severe renal impairment. Renal toxicity has been reported in a few patients with liver dysfunction who were given oral cholecystographic agents followed by urographic agents. Administration of urographic agents should therefore be postponed in any patient with a known or suspected hepatic or biliary disorder who has recently taken a cholecystographic contrast agent. Gastrointestinal disorders which interfere with absorption and liver disorders which interfere with excretion may result in nonvisualization of the hepatic and biliary ducts and the gallbladder. Contrast agents may interfere with some chemical determinations made on urine specimens; therefore, urine should be collected before administration of the contrast media or two or more days afterwards. Thyroid function tests, if indicated, should be performed prior to the administration of these preparations since iodine-containing contrast agents may alter the results of these tests.

ADVERSE REACTIONS: Mild and transient nausea, vomiting, or diarrhea sometimes occur; the incidence can be reduced by using the calcium granules and restricting the dosage to 3 g. in persons prone to gastrointestinal reactions. Transient headache, dysuria, or abdominal pains may occur.

Hypersensitivity reactions may include urticaria, serum sickness-like reactions (fever, rash, arthralgia), other skin rashes, and rarely anaphylactoid shock. They are more likely to occur in persons with a history of allergy, asthma, hay fever, or urticaria and in those who are known to be hypersensitive to iodine compounds.

Note Concerning Dosage: A total dose of 6 g. (12 capsules or 2 packets of Granules) per 24-hour period should not be exceeded.

For full information, see Package Insert.

HOW SUPPLIED: Oragrafin Calcium Granules (Ipodate Calcium for Oral Suspension U.S.P.) provide 3 g. ipodate calcium per packet; available in boxes of 25 single-dose foil packets. Oragrafin Sodium Capsules (Ipodate Sodium Capsules U.S.P.) provide 0.5 g. ipodate sodium per capsule; available in boxes of 25 vials (each vial contains 6 capsules), in bottles of 100, and in Unimatic® packages of 100.

SQUIBB HOSPITAL DIVISION
E. R. Squibb & Sons, Inc.
©1976 E. R. SQUIBB & SONS, INC. H-36-5011

the reason
is clear™



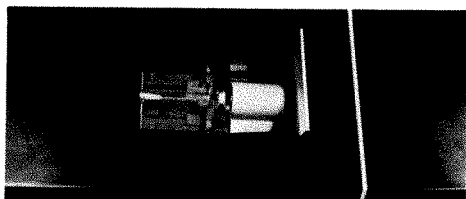
CintiChem™

Automated ^{99m}Tc Unit-Dose Delivery System

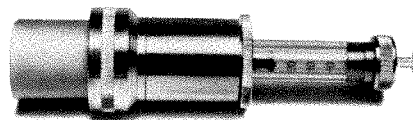
Systematically safer.



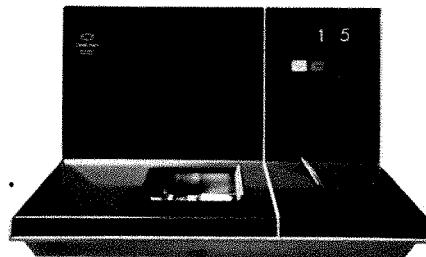
Organ-specific agents for optimum imaging of brain, kidney, bone and lung, and for glomerular filtration rate studies, are provided in kits containing 10 unit-dose vials. Each kit is single step, requiring only addition of technetium to produce the scanning agent.



Preselected amount of ^{99m}Tc activity is automatically dispensed into vial, then diluted with saline to 1.3 ml. Entire dispense/dilute cycle is automatic and shielded, and is completed within 75 seconds.



Unit-dose vial is entered only once for technetium delivery, once for agent withdrawal. Shielded syringe assembly automatically centers disposable syringe with vial. A 1.0-ml patient injection is reproducibly withdrawn into syringe.



Dispenser fully automates isotope measurement, reagent transfer and dose calibration. Eliminates time-consuming manual steps, computations and potential radiation exposure.

**UNION
CARBIDE**

Delivering the future in imaging agents:

The CINTICHEM System, a total unit-dose ^{99m}Tc delivery system...

- ☐ Simplifies radionuclide delivery
- ☐ Improves dosage accuracy and reproducibility
- ☐ Reduces radiation burden
- ☐ Permits precise, contaminant-free administration of agents
- ☐ Reduces labor and cost per test
- ☐ Simplifies record keeping and calculations

The CINTICHEM System includes: an automated technetium dispenser, a high-yield molybdenum 99/technetium 99m generator, organ-specific kits and a unique unit-dose shielded syringe assembly. All integrated for the preparation of sterile, pyrogen-free radio-diagnostic agents—precisely, reliably and with greatly reduced radiation burden to the user.

The CINTICHEM Dispenser automatically delivers a preselected amount of ^{99m}Tc activity (TcO_4^- in saline) into a single-use unit-dose vial. Vial contents

are transferred to a disposable syringe via a shielded syringe assembly that permits reproducible withdrawal of a 1.0-ml patient dose.

The CINTICHEM Generator is an optimized, advanced-technology ^{99m}Tc generator. It offers exceptionally high yields and is available in 500-, 1,000-, 1,500- and 2,000-mCi sizes. (Sodium pertechnetate ^{99m}Tc in isotonic saline.)

A series of organ-specific CINTICHEM Agents incorporates optimum current formulations for organ specificity. Each kit contains 10 unit-dose vials. (Kits containing five multidose vials are also available.) Each kit is single step. Requires only the addition of technetium to produce the imaging agent. And the CINTICHEM Dispenser performs this step automatically.

Kits currently available include: DTPA (diethylene triamine pentaacetic acid [calcium trisodium salt]). For brain and kidney imaging, and glomerular filtration rate (GFR) studies. Unit dose con-

tains 3.3 mg CaNa_3DTPA , 0.17 mg $\text{SnCl}_2 \cdot 2\text{H}_2\text{O}$, pH adjusted to 4 with HCl. HEDSPA (1-hydroxy-ethylidene-1,1 disodium phosphonate). For bone imaging. Unit dose contains 0.75 mg HEDSPA, 0.08 mg stannous ion as tartrate, pH adjusted to 4 with HCl. MAA (macroaggregated albumin). For lung perfusion studies. Unit dose contains 0.11 mg MAA ($0.3\text{--}1.3 \times 10^6$ particles), 0.09 mg stannous tartrate, isotonic saline. HCl and NaOH may be present for pH adjustment. Additional radio-pharmaceuticals will also be offered.

Let us send detailed data on the CINTICHEM System. Simply return the coupon and we'll come back with a glimpse into the future.

CintiChem™

Systematically safer.

Union Carbide Corporation
Clinical Diagnostics
401 Theodore Fremd Avenue
Rye, New York 10580

- ☐ Send brochure on the CINTICHEM System.
- ☐ Have field representative call for an appointment.

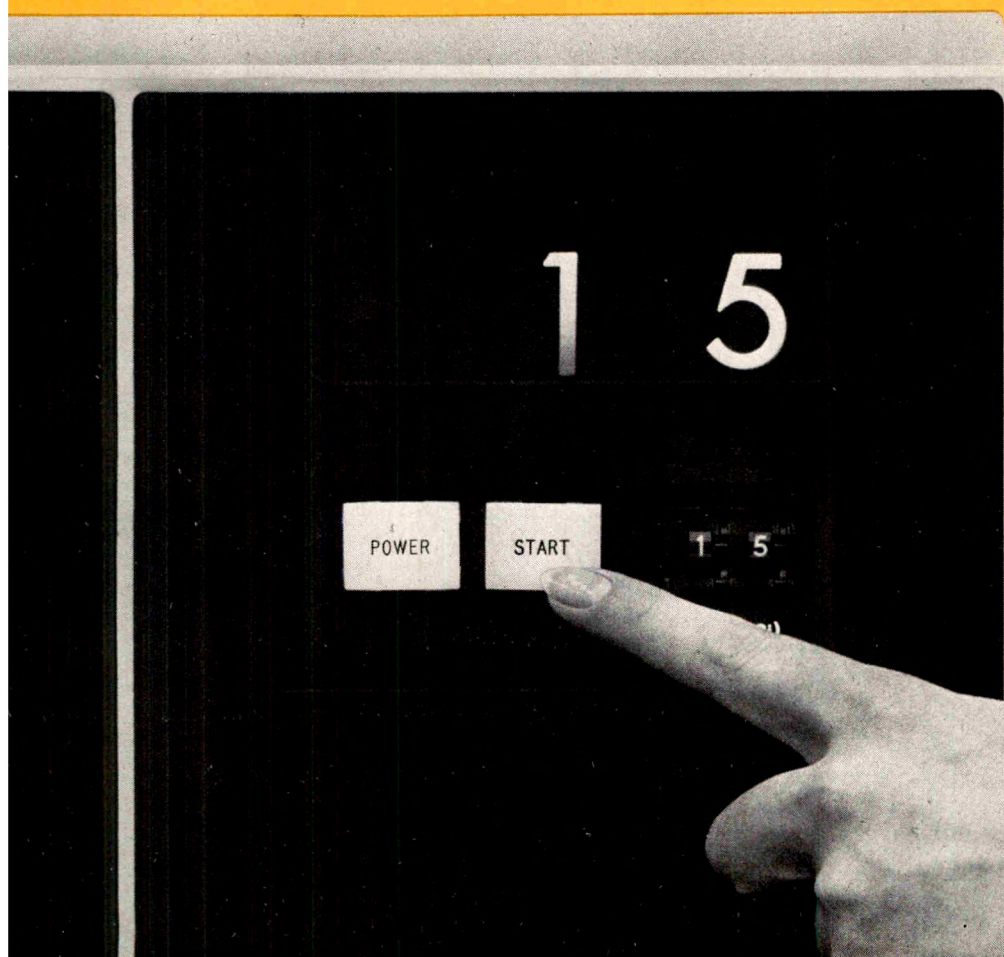
Name _____
(Please print)
Title _____
Institution _____
Address _____
City _____ State _____ Zip _____
Telephone _____
(Area code and number)

RR6



Clinical Diagnostics

Unit-dose.

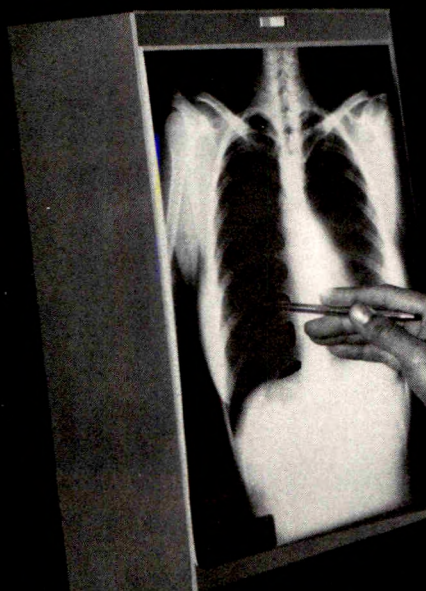


New from Wolf X-Ray Medi-Tex[®] Protective Aprons

This revolutionary new anti-bacterial fabric, exclusive with Wolf X-Ray, is tough and durable for years of continued service, yet lightweight and attractive for maximum personal comfort.

New Medi-Tex safeguards against:

- **Stains**...its specially formulated vinyl surface is extremely stain resistant, yet cleans easily with ordinary soap and water.
- **Tears**...its high strength industrial nylon reinforcement prevents costly rips and tears.
- **Fire**...permanently flame-proof, Medi-Tex will not support combustion.



- **Odors**...Medi-Tex stays fresh, color-fast, and odor-free, even after repeated cleaning.
- **Fluid Absorption**...this tough vinyl fabric is non-absorbing, permanently waterproof.
- **Anti-Bacterial**...Medi-Tex effectively fights cross infection, exceeding, by far, accepted standards.

Plus, proven cost reduction: this tough, durable, lightweight fabric increases wearability, hereby reducing replacement costs!

Wolf Medi-Tex Protective Aprons are available in a variety of sizes and styles to meet your exact requirements: Apronettes, Bib, Conventional Style, Coat, Special Procedure, Mini, and Easy Wrap. Call your local Wolf X-Ray dealer for complete information today.

When you think accessories, think Wolf.

Wolf X-Ray

A Division of IPCO Hospital Supply Corporation

82-20 Liberty Ave., Jamaica, N.Y. 11412

Medi-Tex is a registered trademark of Wolf X-Ray Chemical Corporation.

AGFA-GEVAERT

Mamoray RP-3

*10X faster than conventional non
screen films...up to 33% faster
than the popular "low dose"
system!*

Mamoray RP-3...another new generation film from
Agfa-Gevaert, the world's leader in sophisticated
imaging technology.

Mamoray RP-3 features:

- An exposure speed less than 1/10 that of non screen techniques; up to 1/3 faster than other low dose systems currently in use, and...with a remarkable increase in contrast in all low density areas.
- Fine grain for optimum visualization of minute calcifications.
- A high contrast level that enhances clarity in diagnosing low density areas.

These, and other important features, make Mamoray RP-3
the ultimate film for all fine detail techniques: non screen, single and
double screen.

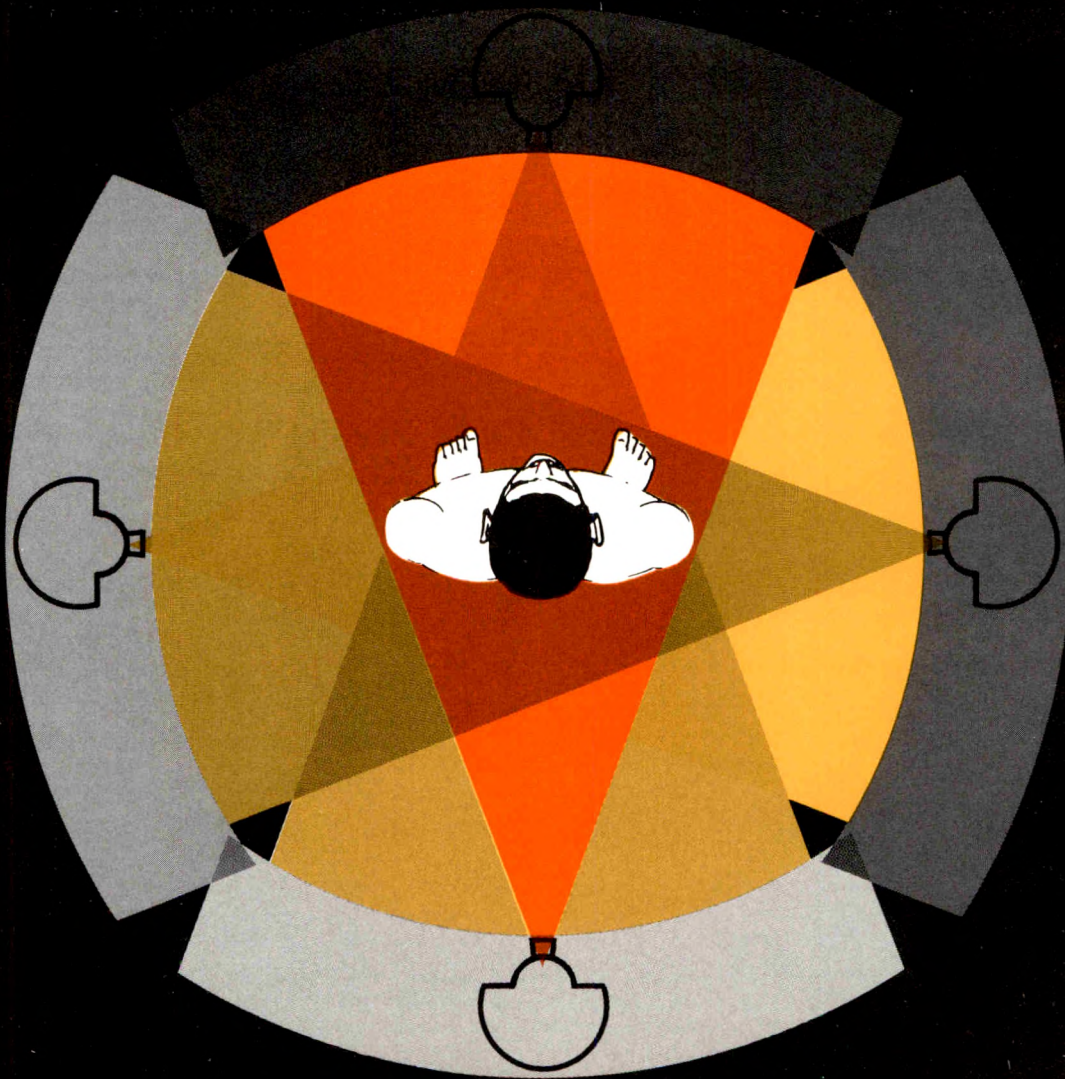
If you're still utilizing older mammographic film techniques it's time
that you looked at Mamoray RP-3. Contact your local Low X-Ray representa-
tive today. He'll gladly discuss these, and other Mamoray RP-3 features
with you.

AGFA-GEVAERT
MAMORAY



Division of IPCO Hospital Supply Corporation
1025 Westchester Avenue
White Plains, New York 10604

Varian Introduces the 6-Second Whole-Body CT Scanner



**A New Era in
Computed Tomography...**

Let Varian Introduce You to 6-Second Computed Tomography

A Full 360° Whole-Body Scan in 6 Seconds

The two most important parameters in CT scanning, quality of image and short data-acquisition time, have now been achieved by Varian.

With a 6-second scan, two immediate benefits are realized. First, artifacts resulting from involuntary physiological motion are virtually eliminated. Second, with respiration easily suspended for the brief 6-second scanning period, you get sharp, clear images the first time.

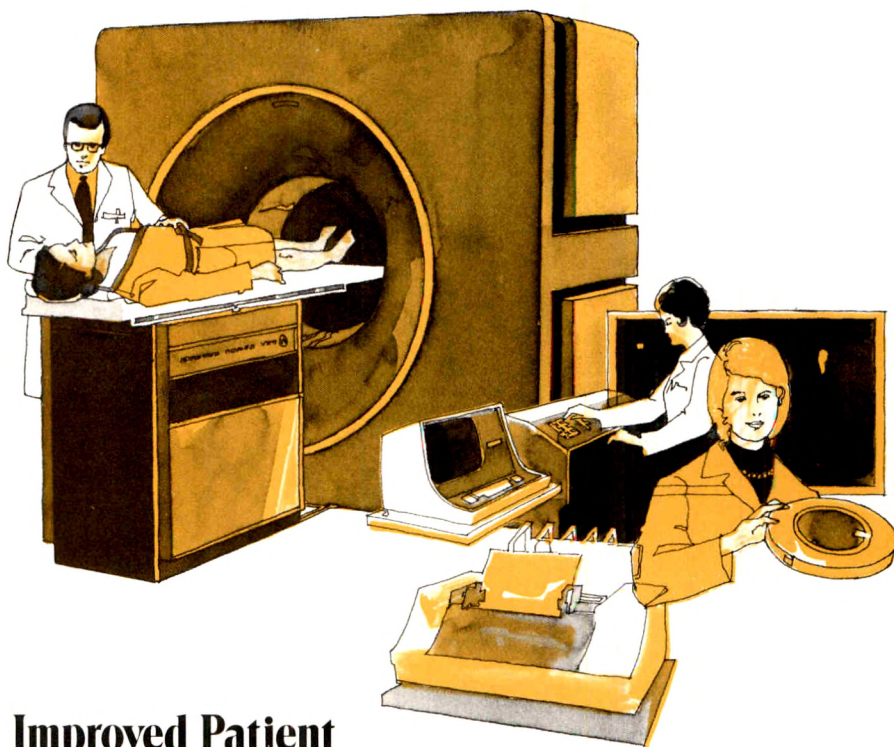
Superior Design

Varian's CT Scanner utilizes fan beam geometry. X-rays are collimated into a fan-shaped beam and collected by approximately 300 high-efficiency Xenon-Krypton detectors. X-ray tube and detectors rotate as a unit, scanning the full patient cross-section throughout the entire 360 degrees.

The Varian-developed slip-ring construction eliminates cable flexing, and provides a base for faster than 6-second data acquisition in the future.

Compatible with the Future

The design concepts of the Varian system assure compatibility with inevitable developments in the rapidly advancing CT technology. Equally important, Varian's total corporate involvement and close control over the major components in the CT Scanner System—Rotating Gantry, Xenon-Krypton Detector, Computer, and X-ray source—facilitate prompt incorporation of new technological advances.



Improved Patient Handling

The new Scanner is a carefully engineered patient and user-oriented system. For example, the 90 cm-diameter aperture will accommodate your largest patients. Patient positioning within the rotating gantry is facilitated by a low-power laser alignment system and computer driven patient couch.

Talk to Varian

Before you make any decision, get the facts on the 6-second era from Varian. Call or write today. Varian Radiation Division, 611 Hansen Way, Palo Alto, CA 94303. Tel: 415/493-4000. Worldwide sales and service.



From start to finish, Fleet systematizes

For cleaner colons, clearer x-rays, and fewer retakes



For preparation,
Fleet Barium Enema
Prep Kits assure
thorough, reliable
colon cleansing by
utilizing a combination
of diet, hydration, and
evacuation.

- Available in two convenient forms with suppository or enema as final step.
- Offering an effective and balanced method of prepping.
- Meeting all criteria for colon preparation as recommended by the American College of Radiology Ad Hoc Committee on Detection of Cancer of the Colon.
- With easy-to-follow instructions.
- With 3 convenient time schedules to fit better into your schedule and your patient's routine.

For the examination

Fleet Barobag offers greater visibility because it contains Ultrasperse™ with a combination of barium sulfate USP (98%) and selected suspending and dispersing agents (2%) for "instantized" mixability.

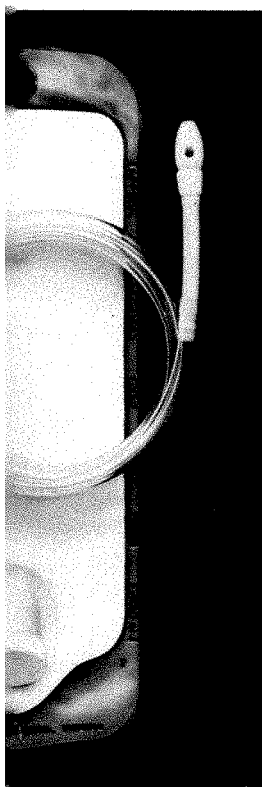
- With excellent suspension stability—up to 2 hours.
- With rapid, free-flow emptying.

barium enema exams...

B. Fleet presents a unique three-part system of products that can help you give quality

barium enema exams. It includes Fleet® Barium Enema Prep Kits for colon preparation, Fleet® Barobag for the actual

barium enema examination, and Fleet® Phospho-Soda for aftercare.



leakproof with screw closures for convenience.

With angled spout (45°) for easier filling and handling.

Available with either 12 or 16 oz. Ultrasperse® barium sulfate USP).

Also available with retention catheter.

For aftercare,

Fleet Phospho-Soda is gentle and most effective for cleansing the colon of barium and for preventing fecal impaction.

- Works in an hour or overnight, according to dosage, for convenience and flexibility in scheduling.
- Usually produces soft, formed stool with no unusual side effects.
- Promotes natural peristalsis to assure thorough action.

- Buffered for gentleness.
- Easy-to-take.
- Safe for use by patients of all ages, as indicated.

In the final note to *Detection of Colon Lesions* by the American College of Radiology Ad Hoc Committee on Detection of Cancer of the Colon, R. E. Miller states: "Almost every recommendation made is part of urging *quality control* by the radiologist in all aspects of his colon examination."

Fleet's new system of products will answer almost every need you'll encounter in barium enema examinations—from start to finish.

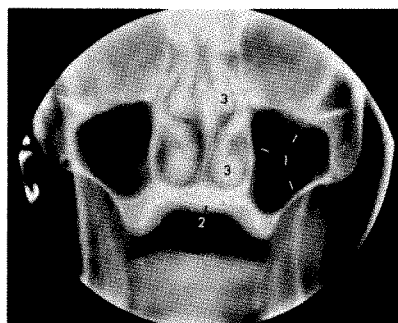
In barium enema exams, quality controls results. And Fleet controls quality.



C. B. FLEET CO., INC.
Lynchburg, Va. 24505

TOMOGRAPHY

PHYSICAL PRINCIPLES and CLINICAL APPLICATIONS



Section 17:
Golden's Diagnostic Radiology Series

By J. T. Littleton, MD, FACR, Chairman,
Section of Radiology, Guthrie Clinic and
Robert Packer Hospital, Sayre, Pennsylvania,
and Professor of Radiology, Hahnemann
Medical Hospital, Philadelphia

The sophistication and specialization that tomography brings to diagnostic roentgenology has created a very real need for one comprehensive volume which recognizes pluridirectional tomography as an aid to the clinical radiologist which cannot be equaled by any other available roentgen film method of imagery. Tomography is that book. In his exposition of the procedure, Dr. Littleton has studded his text with many hundreds of illustrations — line drawings, tables, tomograms — and presents physical concepts in a simplified, nonmathematical, visual form.

Tomography is primarily directed to the practicing radiologist, but is eminently readable and consequently valuable to the training resident, interested technician, veterinarian, and dentist. To the medical physicist, the discussions of dosimetry will be of interest; to the tomographic radiographer, the extensive illustrations of patient-positioning will be insightful aids.

In the most obvious sense, the intent of this book is to identify modern pluridirectional tomography as a distinct and definite dimension in diagnostic radiology. More subtle is the author's attempt to improve the effectiveness of the radiologist's care of the patient by stimulating a more general and routine use of this simple technique.

Tomography is the newest volume in the outstanding Golden's Diagnostic Radiology series, and well meets the requirements for excellence which have come to be expected from that succession of texts.

1976/approximately 850 pages/800
illustrations/\$57.50

WILLIAMS & WILKINS
428 East Preston Street
Baltimore, Maryland 21202

please type or print

NAME _____

ADDRESS _____

CITY _____ STATE _____ ZIP _____

☐ Check enclosed

☐ Bill me

To order titles on 20-day approval, check selections

Save postage and handling by enclosing
payment with order.

Maryland residents please add 4% sales tax.

☐ Littleton: Tomography
[book #5089-3, \$57.50]

The Value of Systemic Arterial Heparinization in Transfemoral Angiography: A Prospective Study

RUZA ANTONOVIC,¹ JOSEF RÖSCH, AND CHARLES T. DOTTER

A prospective, controlled study was done in 400 patients to assess the value of systemic arterial heparinization in relation to complications of transfemoral angiography. The control group was comprised of patients studied conventionally with small amounts of heparin in catheter flushing solutions. Manual compression time required to stop bleeding, the incidence of clinically detectable local or distant complications, and, in the first 200 patients, pullout angiograms were used as criteria for comparison. The use of systemic heparinization required prolonged manual puncture site compression, decreased the incidence of puncture site thrombus formation, eliminated arterial occlusion, but increased the incidence of delayed bleeding at the catheter entry. No substantial differences were found in the incidence of early hematomas or the formation of fibrinous sheaths around the catheter. It is concluded that systemic heparinization offers advantages for transfemoral angiography; its disadvantages can be avoided by intravenous injection protamine sulfate after the procedure.

Systemic arterial heparinization for the prevention of thromboembolic complications in angiography is the subject of several recent reports [1-8]. In most, it is regarded as a worthwhile prophylactic measure, particularly in connection with coronary arteriography [1, 3, 5-7]. However, some workers have questioned its value [4, 9], and stressed the need for a controlled study [9, 10].

This paper reports a prospective, randomized, controlled study of the incidence of complications in 400 consecutive patients who had transfemoral angiography, half with systemic heparinization as described by Wallace et al. [8] and half in which heparin was confined to conventionally used small amounts in the catheter flushing solutions.

Subjects and Methods

Four hundred patients from 6 to 76 years of age (mean 59) undergoing transfemoral angiography were randomly assigned to systemic heparinization (experimental) or conventional (control) study groups. In all, 154 patients had coronary arteriography, 158 visceral or renal arteriography, and 88 aortofemoral arteriography. The series was consecutive except for the deliberate exclusion of 16 patients with acute gastrointestinal bleeding and five on anticoagulant therapy.

In the systemic heparinization group heparin (45 U/kg body weight) was injected into the abdominal aorta at the beginning of the study. Irrigation solution contained 500 U of heparin in 250 ml of saline; flushing was performed every few minutes and after each catheter exchange and guidewire insertion. On the average, during the course of the 1 hr procedure, the average patient in this group received 3,250 U of concentrated intraaortic heparin plus 250 U in the irrigation solution, a total dose of 3,500 U.

In the control group not receiving prophylactic systemic heparin,

TABLE 1
Local Complications

Type	Control Group (N=200)	Systemic Heparinization Group (N=200)	P
Minor hematoma	11	12	...
Major hematoma	2	2	...
Delayed bleeding	3	12	<.05
Femoral artery occlusion . . .	2	0	>.10
Total	18	26	...

1,500 U of heparin were added to 250 ml of flushing solution. Thus, the average control group patient received approximately 750 U of heparin during the course of a 1 hr examination (less than one-fourth of that given to the test group).

Coronary arteriography was done using nos. 7 or 8 French catheters with two or three catheter exchanges; visceral, renal, abdominal, and peripheral studies were performed using no. 6.5 French polyethylene catheters with from zero to three catheter exchanges. The first 100 patients in each group had ileofemoral "pullout" arteriography at the end of the study in which the catheter was pulled down into the external iliac artery, 6-8 ml of contrast material injected in 1 sec, and eight films exposed in 2 sec. After all procedures, manual compression was applied until complete hemostasis was achieved; the required time was recorded. Pressure dressing and bedrest followed for 6 hr, whereupon normal activity was resumed.

Compression time required for hemostasis, postcatheterization clinical follow-up, and pullout arteriograms were used to assess complications. Local complications were classified into four groups: minor hematoma (under 4 cm in diameter); major hematoma (over 4 cm); delayed bleeding (occurring during or after use of the pressure dressing); and femoral artery occlusion. In a search for distant, embolic complications, attention was directed to the possible occurrence of myocardial infarction, stroke, and peripheral embolization. Pullout arteriograms were evaluated blindly and considered abnormal when they disclosed: (1) a distinct radiolucent halo (fibrinous sheath) around the catheter; (2) a localized radiolucent defect (thrombus) at the entry site of the catheter; or (3) femoral artery occlusion (fig. 1). Data were statistically analyzed using χ^2 and unpaired *t* tests.

Results

Manual compression times were 10-15 min in the control group and 15-45 min in the heparin group. No distant complication occurred in either group. There were 18 (9%) local complications in the control group and 26 (13%) in the systemic heparinization group (table 1).

Received March 9, 1976; accepted March 30, 1976.

This study was aided in part by U.S. Public Health Service grants HL05828 and HL03275 from the National Heart and Lung Institute.

¹ Department of Diagnostic Radiology, School of Medicine, University of Oregon Health Sciences Center, Portland, Oregon 97201. Address reprint requests to R. Antonovic.

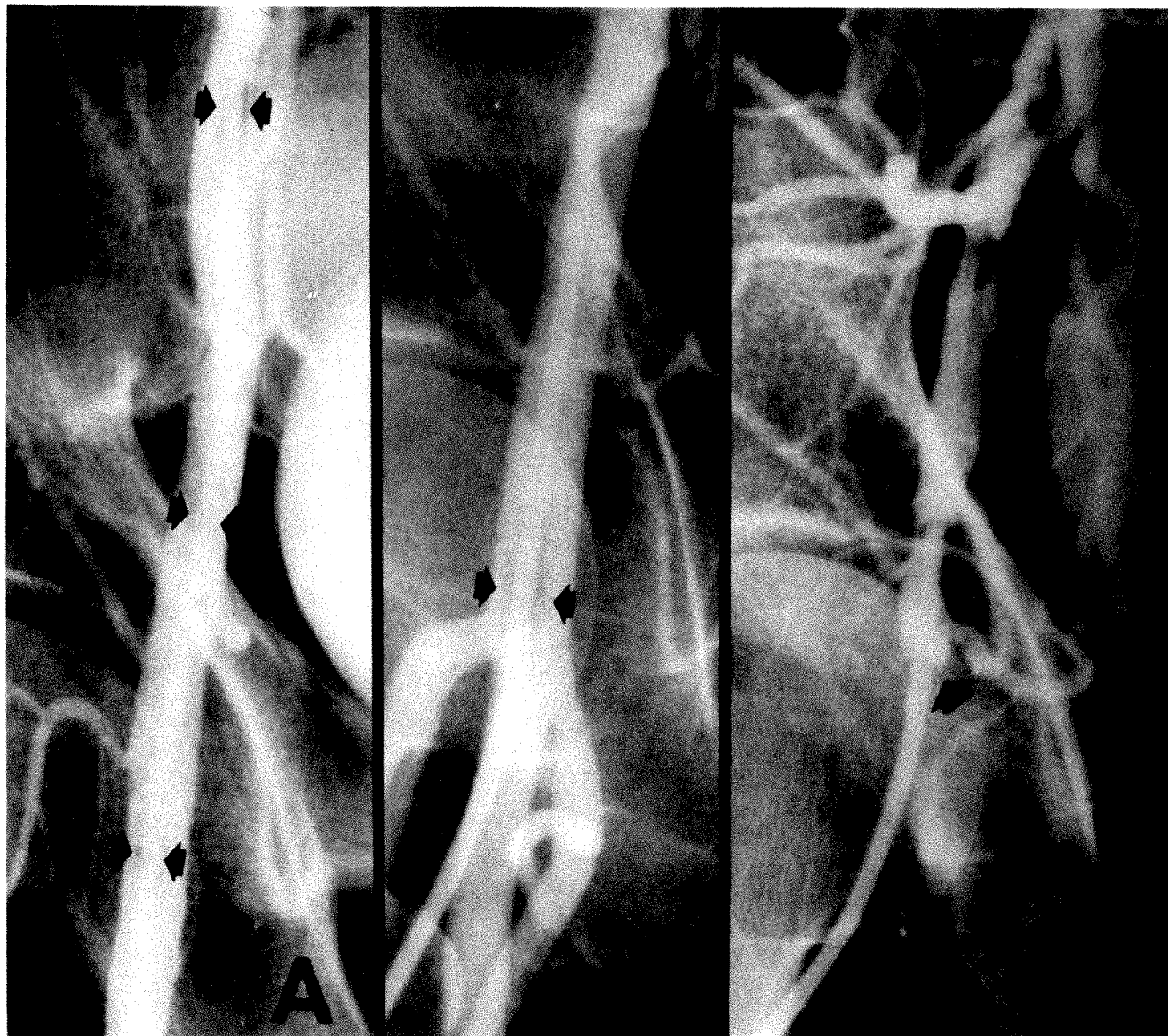


Fig. 1.—Representative abnormal pullout ileofemoral arteriograms of three study patients who had left ventriculogram and selective coronary arteriograms. A, Fibrinous sheath around catheter (arrows) in control group patient. B, Localized thrombus at entry site (arrows) in systemic heparinization group patient. C, Occlusion of femoral artery at entry site (arrow) in control group patient.

Minor hematomas occurred in 11 patients in the control group and 12 in the systemic heparinization group. Major hematomas developed in two patients of each group. In the control group, both patients with major hematomas had advanced atherosclerotic vascular disease; their procedures required three catheter exchanges and lasted 90 and 125 min. In the systemic heparinization group, one patient with a large hematoma had systemic arterial hypertension (200/115), and the other had advanced peripheral vascular disease requiring a 90 min procedure with two catheter exchanges. In the latter two patients, bleeding around the catheter occurred during the procedure, and postprocedural hemostasis required 30–40 min of manual compression.

Delayed bleeding occurred in three patients in the con-

trol group and 12 in the systemic heparinization group. This difference was statistically significant ($P < .05$). In all patients of the control group and 11 of the heparinization group, delayed bleeding took place under the pressure dressing or shortly after its removal. It was controlled by manual compression and reapplication of an external compression dressing for an additional 6 hr. The twelfth patient in the heparinization group, a 14-year-old girl who had a history of arterial hypertension but was normotensive during the procedure, was discharged 24 hr after uneventful abdominal aortography. Three days later she rebled from the puncture site and was readmitted with a hematoma 14×10 cm in size. At surgery a small hole in the femoral artery was found and sutured.

TABLE 2
Abnormalities on Pullout Ileo-femoral Angiograms

Type	Control Group (N=100)	Systemic Heparinization Group (N=100)	P
Fibrinous sheath around catheter.....	12	8	>.25
Nonocclusive thrombus at entry site.....	13	4	<.05
Femoral artery occlusion...	2	0	>.10
Total.....	27	12	...

Note.—Data from first 200 study patients.

Femoral artery occlusion occurred in two patients (1%) in the control group, both during catheterization, and none in the systemic heparinization group. One patient required surgical thromboembolectomy and the other had a successful removal of a soft thrombus by manual compression of the common femoral artery [11].

Pullout arteriograms (table 2) showed fibrinous sheath formation around the catheter in 12 patients in the control group and eight patients in the systemic heparinization group (fig. 1A). Small puncture site thrombi were observed in 13 patients in the control group and four in the heparinization group (fig. 1B). This difference was statistically significant ($P < .05$). As noted, two patients in the control group had occlusion of the femoral artery at the puncture site (fig. 1C).

Discussion

Use of systemic heparinization in angiographic procedures has both advantages and disadvantages. Heparin, a mucopolysaccharide, inhibits coagulation by an anti-thrombin effect. Its value in preventing thrombosis is evidenced by the 4% incidence of entry-site thrombi and absence of arterial occlusion in the systemic heparinization group compared to a 13% and 2% incidence, respectively, in the control group (based on 100 pullout arteriograms in each group). On the other hand, the comparably high incidence of fibrinous sheath formation on the outer wall of the catheter in both groups (control 12%, systemic heparin 8%) leaves room for further improvement.

Disadvantages associated with prophylactic hepariniza-

tion lie in the prolonged manual compression time required to stop bleeding after removal of the catheter and the greater incidence of delayed bleeding (6.5% in the systemic heparinization group compared to 1.5% in the control group). Protamine sulfate, a heparin antagonist not used in this randomized study, can help to eliminate these disadvantages [1, 5, 8]. It can be used routinely [1, 5] or selectively for patients at higher risk of bleeding [8], particularly when hypertension or advanced atherosclerotic disease is present, after difficult or traumatic catheterization, or when bleeding at the puncture site persists after 15 min of manual compression. Wallace et al. [8] report that an intravenous injection of 10 mg protamine sulfate for each 1,000 units of intraarterially injected heparin completely controlled bleeding within 10 min.

REFERENCES

1. Eyer KM: Complications of transfemoral coronary arteriography and their prevention using heparin. *Am Heart J* 86:428, 1973
2. Freed MD, Keane JF, Rosenthal A: The use of heparinization to prevent arterial thrombosis after percutaneous cardiac catheterization in children. *Circulation* 50:565-569, 1974
3. Judkins MP, Gander MP: Prevention of complications of coronary arteriography. *Circulation* 49:599-602, 1974
4. Kaplan MA, Harris CN, Parker DP: Heparinization in coronary arteriography. *Circulation* 52:517, 1975
5. Luepker RV, Bouchard RJ, Burns R, Warbasse JR: Systemic heparinization during percutaneous coronary angiography: evaluation of effectiveness in decreasing thrombotic and embolic catheter complications. *Catheterization Cardiovasc Diagnosis* 1:35-44, 1975
6. Page HL, Campbell WB: Percutaneous transfemoral coronary arteriography: prevention of morbid complications. *Chest* 67:221-225, 1975
7. Walker WJ, Mundall SL, Broderick HG, Prasad B, Kim J, Ravi JM: Systemic heparinization for femoral percutaneous coronary arteriography. *N Engl J Med* 288:826-828, 1973
8. Wallace S, Medellin H, DeJongh D, Gianturco C: Systemic heparinization for angiography. *Am J Roentgenol* 116:204-209, 1972
9. Rich JM, Cobb TC, Leighton RF: Percutaneous transfemoral coronary arteriography without systemic anticoagulation—a review of 648 consecutive procedures. *Catheterization Cardiovasc Diagnosis* 1:275-281, 1975
10. Adams DF, Fraser DB, Abrams HL: The complications of coronary arteriography. *Circulation* 48:609-618, 1973
11. Jeffery RF: A simple method of removing intra-arterial clots formed during catheterization. *Radiology* 103:573-575, 1972

Takayasu's Arteritis and Congenital Coarctation of the Descending Thoracic and Abdominal Aorta: A Critical Review

ADAM LANDE¹

A critical reappraisal of the clinical, arteriographic, and pathologic features of Takayasu's arteritis and so-called congenital aortic coarctations at atypical sites is presented. It is concluded that as an isolated cardiovascular abnormality, cases of atypical congenital coarctations of the descending thoracic and abdominal aorta are probably rare. The majority of atypical aortic coarctations previously reported in the United States and Europe as congenital lesions apparently represent unrecognized cases of Takayasu's arteritis.

In the last 4 decades, approximately 150 cases of congenital coarctation of the descending thoracic and abdominal aorta have been reported in Europe and the United States. At the same time, several hundred cases of Takayasu's arteritis have been reported in Japan and other countries. A curious situation has arisen: congenital coarctation of the descending thoracic and abdominal aorta is virtually unknown in the Orient, while in the United States and Europe, an acquired etiology of the descending thoracic and abdominal coarctations is not seriously considered.

Congenital coarctations at atypical sites have been reported under various names, including elongated stenosis of the aorta [1], hypoplasia of the abdominal aorta [2-4], atresia of the distal aorta [5, 6], infraductal coarctations [7], and atypical coarctation of the aorta [8-10].

This report represents a critical review of Takayasu's arteritis and so-called congenital coarctations at atypical sites.

Takayasu's Arteritis

Takayasu's disease [11] is currently recognized as an arteritis of unknown etiology which may involve the aorta, its branches, and the pulmonary arteries. It can progress to stenosis, occlusion, or aneurysmal dilatation of the affected vessels [12-14].

There is virtually unanimous agreement that Takayasu's arteritis is autoimmune in nature [12, 14-18]. However, definite proof is still lacking [15].

Takayasu's disease is worldwide in distribution [12, 16-20]. Although it has been given a variety of names such as nonsyphilitic or nonspecific aortitis [21], idiopathic arteritis [16, 22], pulseless disease [23], and aortitis syndrome [18], Takayasu's arteritis is the most commonly used designation [24].

The features which differentiate Takayasu's arteritis from other forms of aortitis (syphilitic, rheumatoid, rheumatic, giant cell aortitis, aortitis in association with recurrent poly-chondritis, Reiter's syndrome, etc.) have been described [25]. However, one point deserves emphasis: constrictions and narrowings of the aorta are caused almost ex-

clusively by Takayasu's arteritis. At present there is no published evidence that other forms of aortitis (with rare exceptions such as radiation aortitis) can duplicate this phenomenon. Thus constrictive aortitis is synonymous with Takayasu's disease. On the other hand, the aneurysmal forms of Takayasu's arteritis are nonspecific and may resemble other forms of aortitis.

The anatomic distribution of pathologic lesions in Takayasu's arteritis is unpredictable. Various clinical syndromes may emerge according to the predominant region affected. Involvement of the arch with occlusion or stenosis of the brachiocephalic trunks causes the "pulseless" syndrome with a plethora of visual and cerebral manifestations [23].

Abdominal coarctation is usually associated with renal artery stenosis or occlusion, and severe hypertension overshadows all other signs and symptoms. This clinicopathologic entity has been named the middle aortic syndrome [26]. Coarctation of the infrarenal aorta or the aortic bifurcation may produce Leriche syndrome [17, 26]. Many other syndromes in various combinations may emerge according to the variable localization of lesions. Hence, Takayasu's disease produces a multiplicity of syndromes and truly deserves to be called "one of the great imitators of medicine" [27].

Several Japanese and Indian investigators provided convincing clinical, arteriographic, and pathologic evidence that so-called atypical coarctations of the aorta represent variable localizations of Takayasu's arteritis with or without involvement of the arch [13, 17, 28]. Indeed, when a large series of patients with Takayasu's arteritis is assembled, a gradual transition of anatomic changes can be demonstrated ranging from primary involvement of the arch, to an extensive type of arteritis involving various portions of the aorta, and finally to a form of arteritis primarily confined to the descending thoracic and abdominal aorta (fig. 1). The stenosing variety of this type of arteritis has been named atypical coarctation of the aorta [28, 29].

Clinical Considerations

Takayasu's arteritis is believed to be an autoimmune disease. The original Japanese descriptions stressed the existence of two phases of the disease: an early systemic phase characterized by generalized signs and symptoms [12, 13, 27] and a late occlusive state in which systemic illness has subsided and clinical manifestations have become secondary to arterial occlusions and regional ischemia [12, 13, 27].

Our experience [30-32] and that of others [18] indicates that in the vast majority of patients, onset of Takayasu's

¹ Department of Radiology, New York Medical College, Metropolitan Hospital Center, 1901 First Avenue, New York, New York 10029.

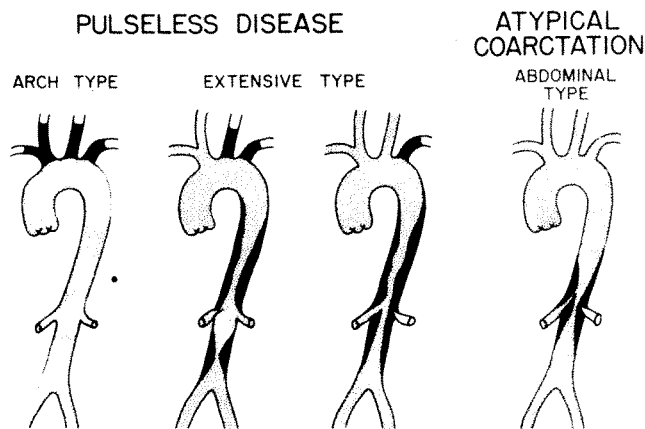


Fig. 1.—Transition of pathologic changes in Takayasu's arteritis. (Modified from Inada et al. [28])

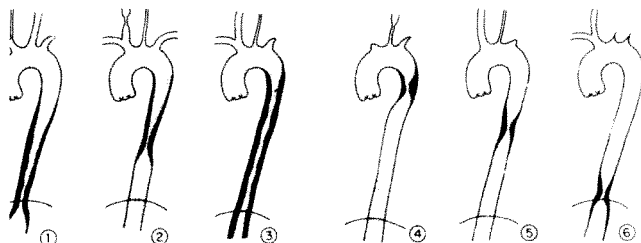


Fig. 2.—Schematic outline of thoracic coarctations. 1 and 2, Gradual tapering of thoracic aorta creating comma-shaped configuration. 3, Entire descending aorta diffusely narrowed. 4–6, Short segmental narrowings located anywhere in descending aorta.

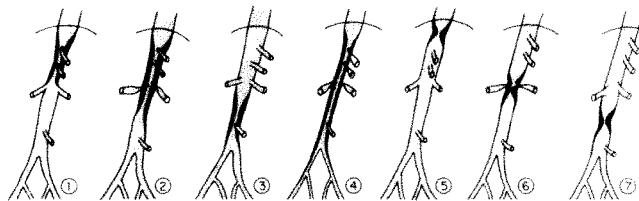


Fig. 3.—Schematic outline of abdominal coarctations. Narrowings may be long and diffuse or short and segmental. 1, 2, 5, and 6, Supra- and interrenal coarctations are frequently associated with severe hypertension. 3 and 7, Infrarenal coarctations which may cause claudication of lower limbs. 4, Constriction of entire abdominal aorta.

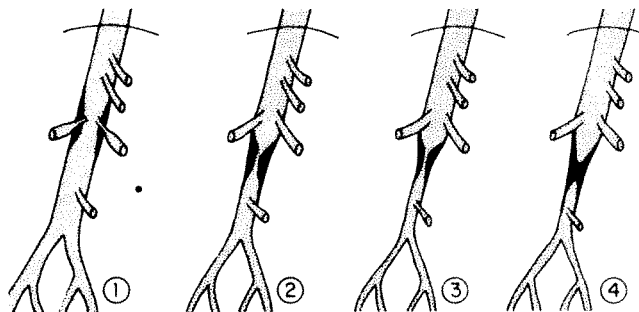


Fig. 4.—Schematic outline of short segmental coarctations. 1, Minimal hemodynamically insignificant aortic narrowing. 2, Moderately severe constriction with some narrowing of distal aorta; common form. 3, Severe coarctation with marked narrowing of distal aorta. Terms "hypoplasia" and "atresia" have been applied to this form of aortic constriction. 4, Extreme forms of aortic constriction which may culminate in total occlusion.

arteritis is insidious, the systemic prodromal manifestations are absent, and the presenting symptoms are of the late occlusive variety.

The age distribution in patients with Takayasu's arteritis and those with so-called congenital atypical coarctations, is approximately the same. Although both range from early childhood to advanced age, the peak incidence remains between 15 and 25 years of age [33, 34]. Similarly, both groups show a definite preponderance of females [33–35].

It must be emphasized that the clinical picture of Takayasu's arteritis is extremely variable. The atypical coarctations of Takayasu's type described in this paper are insidious or chronic forms of Takayasu's arteritis, and many patients have apparently entered an inactive stage of the disease. However, there are numerous reports of severe systemic forms which can lead to a rapid demise, particularly in children [22, 37, 38].

Arteriographic Considerations

Early investigators of so-called congenital coarctations at typical sites, particularly D'Abreu et al. [39], have provided diagrammatic classifications of the atypical aortic narrowings. These diagrams are indistinguishable from coarctations and narrowings produced by Takayasu's arteritis (figs. 2–4). The arteriographic appearance of both entities is the same [4, 40–44].

Since the arteriographic configuration and clinical background of Takayasu's arteritis and so-called congenital coarctations resemble each other closely, the final differentiation can be only achieved by pathologic examination of the lesions.

Pathologic Considerations

In the last 2 decades, the pathologic features of Takayasu's arteritis have been well documented in numerous autopsies from various parts of the world [12, 32, 37, 38, 45–48]. Thorough familiarity with the histologic appearance of Takayasu's arteritis from acute to inactive stage of the disease permitted a critical reevaluation of the pathologic findings as described in congenital coarctations at atypical sites. Invariably, in each instance gross pathological and histological characteristics of Takayasu's arteritis could be identified [40, 49, 50–52].

Our pathologic material consists of two autopsies, three segmental resections of the aorta with graft replacement, and three incisional biopsies at the site of coarctation [53]. In the active phase of Takayasu's arteritis, the media undergoes variable degrees of destruction ranging from mild disruption and fragmentation of the elastic fibers to extensive disintegration of the elastic lamellae with remnants of the elastic tissue scattered in the fibrous stroma [12, 29, 47, 54]. In some instances the media is totally destroyed, and the thickened intima overlies the fibrous thickened adventitia. Gradually, the inflammatory activity in Takayasu's arteritis subsides. The residual damage to the media is depicted in figure 5.

In the chronic stage of the disease, the adventitia and intima are markedly thickened. Fibrous adventitial thickening may be relatively mild and strictly confined to the aortic

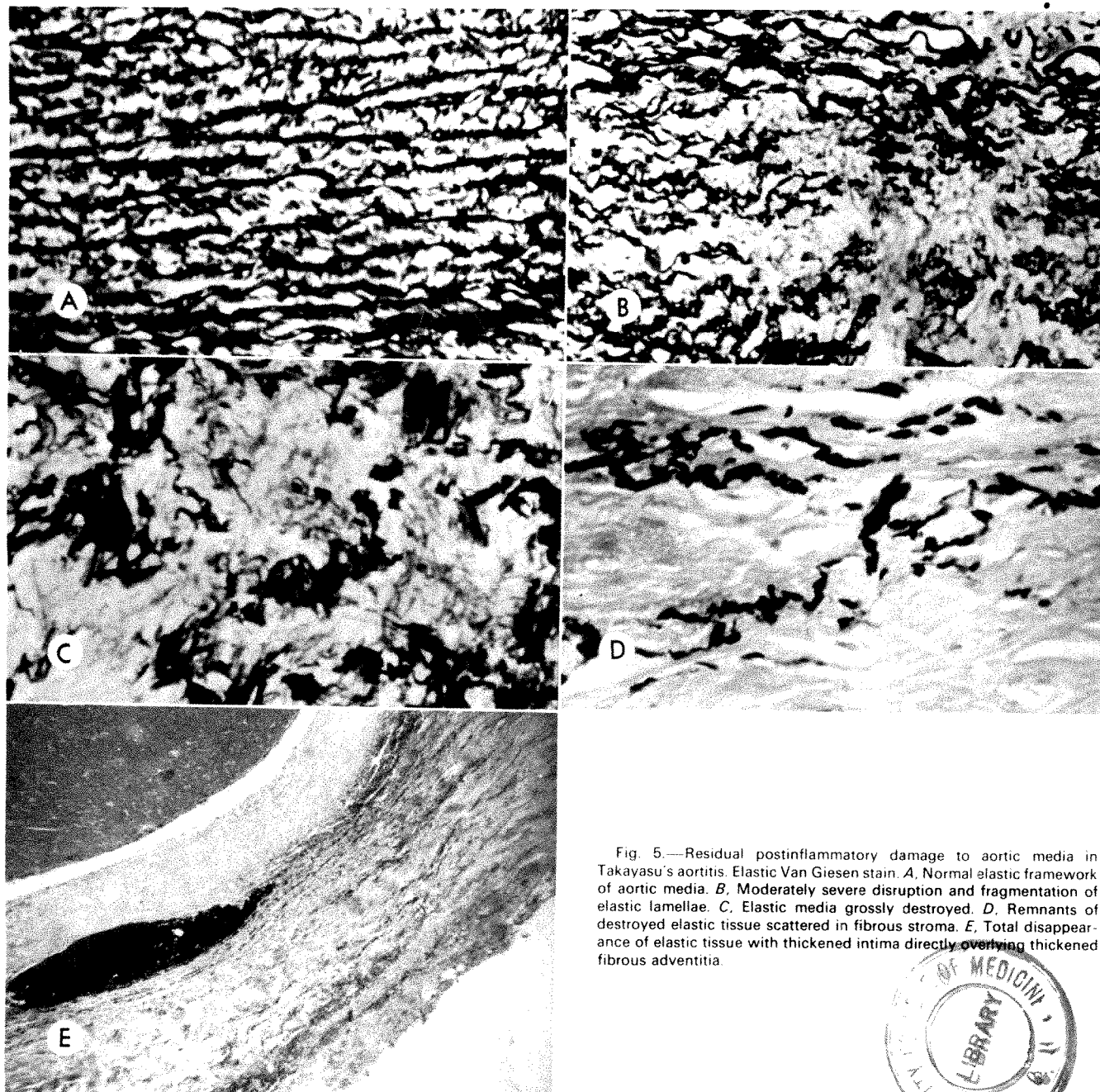
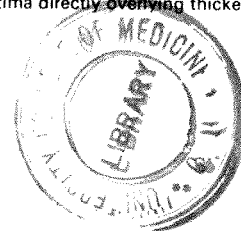


Fig. 5.—Residual postinflammatory damage to aortic media in Takayasu's arteritis. Elastic Van Gieson stain. *A*, Normal elastic framework of aortic media. *B*, Moderately severe disruption and fragmentation of elastic lamellae. *C*, Elastic media grossly destroyed. *D*, Remnants of destroyed elastic tissue scattered in fibrous stroma. *E*, Total disappearance of elastic tissue with thickened intima directly overlying thickened fibrous adventitia.



wall; the aorta can be easily separated from the periaortic fatty tissues [32, 46]. In other instances, however, dense adventitial fibrosis extends into the periaortic tissues, and the presence of periaortic adhesions indicates previous aortitis [8, 9, 47, 55, 56].

Intimal thickening in Takayasu's arteritis may assume enormous proportions, and it is frequently the primary cause of luminal stenosis and occlusion [12, 29, 43, 47, 54]. Occasionally, intimal infoldings may produce diaphragm-like structures [40, 51, 54, 57, 58] which have been mistaken for congenital malformations [7, 40, 59, 60].

In the late and inactive stage of Takayasu's arteritis, the

inflammatory process has resolved and the destroyed elements of the aortic wall are replaced by fibrous tissue [30, 31, 45, 47]. In this stage of the disease, identification of nonspecific fibrosis as postinflammatory scar tissue may present difficulties, and the histological examination is liable to be inconclusive. Thickening and obliteration of the vasa vasorum alone is insufficient evidence of previous aortitis [61].

Because of these limitations, we have searched for a means of identifying aortitis at gross inspection of the aorta.

Since the beginning of this century when the classical

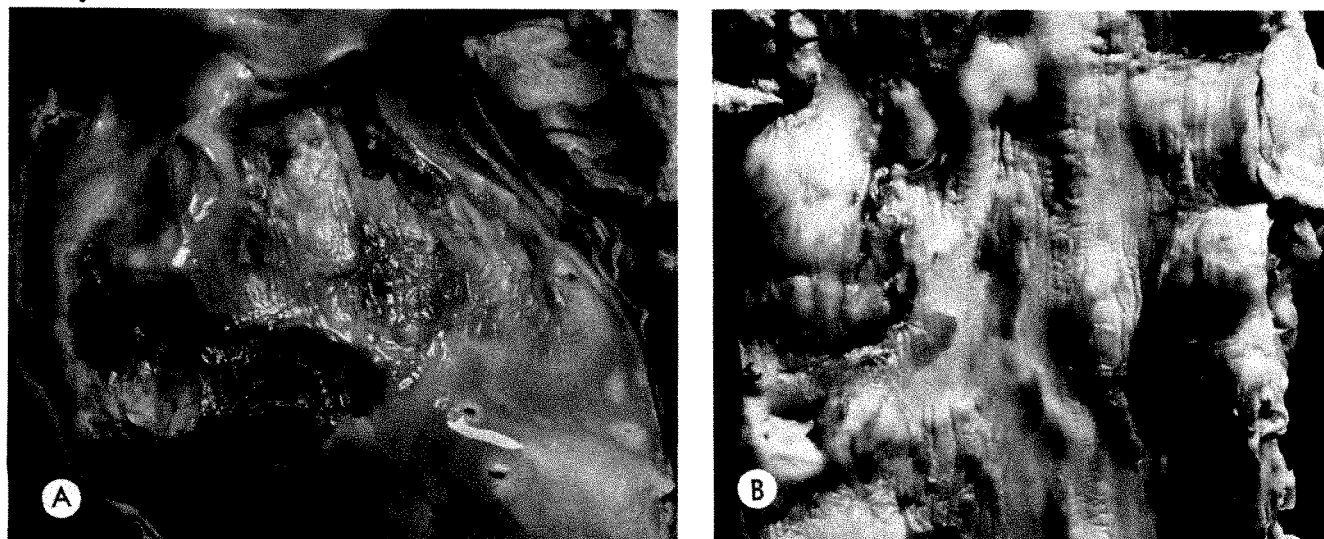


Fig. 6.—Gross specimens of Takayasu's aortitis showing skip areas of aortitis with involvement of root, isthmic portion, and descending aorta. *A*, Localized intimal changes of isthmus with typical longitudinal wrinkling. *B*, Descending aorta diffusely affected. Intima shows characteristic tree bark changes indistinguishable from syphilitic aortitis [32, fig. 7*D*]. (Reprinted with permission from *Radiology*.)

appearance of syphilitic aortitis was first described, the anomaly could be easily recognized. The characteristic changes consist of longitudinal wrinkling of the aortic intima. When transverse furrows appear in addition, the crisscross pattern creates the typical tree bark configuration of syphilitic aortitis (fig. 6).

For several decades, this appearance was considered pathognomonic for syphilis of the aorta. However, in 1937 Mallory [62] reported that rheumatoid aortitis could not be distinguished from syphilitic aortitis. This concept was later expanded by de Takats [63] who showed that all forms of aortitis in advanced stages, irrespective of underlying etiology, resembled each other closely. Sen [17] further amplified this observation, stating that "were it not for the dependable serological tests for syphilis, it would be truly impossible to distinguish one form of aortitis from another."

Thus the longitudinal intimal wrinkling and tree bark appearance of syphilitic aortitis became a characteristic landmark of all forms of aortitis, irrespective of underlying etiology [17, 32, 37, 38, 45, 62, 64–68]. This observation proved very helpful in identifying congenital coarctations at atypical sites as a stenosing form of aortitis, which we believe is synonymous with Takayasu's disease.

"Atypical Congenital Coarctations"

As previously indicated, congenital coarctations at atypical sites and coarctations caused by Takayasu's arteritis are arteriographically indistinguishable. In many instances, the diagnosis of congenital coarctation prior to reconstructive surgery was based solely on the arteriographic appearance of the lesion [4, 44, 69]. The problem is not of purely academic interest, since reactivation of Takayasu's arteritis following surgery has been described [17].

Many reports include only fragmentary pathological descriptions of the aortic lesions, while in others the etiologic

evaluation of the diseased aorta was made at surgical exploration [2, 4, 8, 41, 55, 70]. However, many do provide detailed pathological descriptions. Several studies [40, 50, 52] are commonly referred to by the proponents of congenital etiology of atypical coarctations.

Interest in congenital coarctations at atypical sites began with a paper by Maycock in 1937 [52]. This reference is cited most often and provides gross pathologic and histologic illustrations of the diseased aorta. It includes an excellent gross pathologic illustration of the diseased aorta in a 22-year-old female.

Close inspection of the vessel shows classical features of Takayasu's arteritis. There are skipped areas of aortic involvement with an aneurysm in the ascending portion, patchy aortitis in the descending aorta, and a segmental coarctation of the infrarenal aorta. The coarctation was further complicated by a superimposed thrombosis. Distal to the occlusion, the aorta was thin and hypoplastic. The ascending aorta shows characteristic longitudinal wrinkling of the intima. The microscopic slides were analyzed by Trench et al. [36] and found to be unequivocally inflammatory in nature.

An example of active aortitis in a 24-year-old female was reported by Brust et al. [40, case 2]. The lesion was believed to be congenital in nature. The gross pathological illustration shows the abdominal aorta to be coarcted with markedly thickened walls and pronounced adventitial fibrosis. The aortic intima is hyperplastic and, according to the pathology report, showed longitudinal wrinkling. The histologic description at the site of coarctation is as follows: "Fibrous granulation tissue accompanied by inflammatory infiltrate composed of lymphocytes, plasma cells and giant cells invades the elastic framework of the media. The adventitia was thickened and participated in the inflammatory process."

Fisher and Corcoran [50] described an advanced aortitis

in a 14-year-old male. The aortic narrowing was minimal and hemodynamically insignificant. The aortic involvement was short and segmental, which is characteristic of Takayasu's arteritis. However, the critical location of the lesion between the two renal arteries caused stenosis of the renal orifices and severe hypertension. At autopsy, longitudinal wrinkling of the intima was shown. The intima was markedly hyperplastic, and the elastic tissue of the media was extensively disrupted and fragmented.

The three examples provide a good cross section of the entire group of cases described as congenital coarctations at atypical sites. In each instance, landmarks of Takayasu's arteritis could be identified.

"Congenital Aortic Hypoplasias and Atresias"

Skipped areas of aortic involvement, aneurysms, and narrowings alternating with normal segments are characteristic of Takayasu's arteritis. However, in some instances, Takayasu's arteritis may be limited to a short, localized segment of the aorta (fig. 4). Fibrosis and retraction of the aortic wall combined with marked intimal hyperplasia may produce short segmental coarctations [37, 38, 43, 57, 58, 71-73].

Severe constrictions cause hypertension in the proximal aorta and hypotension in the distal vessel. Since the integrity of the distal aorta is closely related to the blood flow and the mean arterial pressure, extreme reduction of both factors may cause defunctionalization and atrophy of the distal vessel [74, 75]. Indeed, a narrow hypoplastic aorta in an adult patient is indirect evidence of marked obstruction or occlusion in the proximal portion of the vessel. It is probable that severe coarctations and occlusions in association with markedly hypoplastic distal aorta were acquired in early childhood. Aortic coarctations may range from mild, hemodynamically insignificant narrowings to severe constriction and total occlusions (fig. 4). Depending on the severity of constriction, the distal aorta may show variable degrees of "hypoplasia" or "atresia" [2-4, 6, 42, 52, 76].

Histologic examination of the coarcted segment, which is frequently very short and segmental, is of crucial importance for etiologic identification of the lesion. Unfortunately, the presently favored methods of surgical reconstruction employ bypass grafts, and the coarcted segment of the aorta remains untouched [41, 77].

Discussion

Objections to the congenital etiology of atypical aortic coarctations were expressed as early as 1956. After clinical and pathologic analysis of cases of congenital coarctations at atypical sites, Trench et al. [36] concluded that the vast majority were acquired and secondary to aortitis. Similar conclusions were expressed by Bircks et al. [19].

In the largest reported series of atypical aortic coarctations in the United States, Cooley and De Bakey [78] observed that atypical coarctations of the aorta were rare. There appeared to be localized segmental aortitis with secondary atherosclerosis producing an obstructive obliterative aortic process. In a later report on the same series,

Morris et al. [43] concluded that atypical coarctations of the aorta were pathologically distinct from isthmic coarctations. Previously suggested theories of congenital origin were not convincing. There appeared to be some relationship to the syndrome of brachiocephalic arteritis of young females [43].

It must be emphasized that the present report deals only with congenital coarctations at atypical sites that occur as an isolated cardiovascular abnormality. Congenital coarctations of the descending thoracic and abdominal aorta do exist as part of several well defined syndromes: Williams's syndrome or congenital hypercalcemia [79, 80], rubella syndrome [81], and neurofibromatosis [82].

REFERENCES

1. Milloy F, Fell EH: Elongate coarctation of the aorta. *Arch Surg* 78:759-765, 1959
2. Dillon LM, Postlethwait WR: Coarctation of the abdominal aorta. *South Med J* 54:295-298, 1961
3. Mann MB, Gunter JU: Hypoplasia of the abdominal aorta. *NC Med J* 19:485-488, 1958
4. Nennhaus, PH, Hushang J, Hanter AJ: Surgical treatment of renovascular hypertension in children, with a review of infradiaphragmatic arterial hypoplastic anomalies. *J Thorac Cardiovasc Surg* 54:246-258, 1967
5. Ritchie HD, Douglas DM: Atresia of the abdominal aorta. *Br Med J* 1:144-145, 1956
6. Schwartz MB, Kniep CH, Schamroth L: Congenital atresia of the abdominal aorta. *Am Heart J* 54:605-609, 1957
7. Zaroff IL, Krell I, Sobel JJ, Baranofsky DI: Multiple and infraductal coarctations of the aorta. *Circulation* 20:910-917, 1959
8. Bahnson HT, Cooley RN, Sloan RD: Coarctation of the aorta at unusual sites. *Am Heart J* 38:905-913, 1949
9. Baird RJ, Evans JR, Labrosse CL: Coarctation of the abdominal aorta. *Arch Surg* 89:466-474, 1964
10. Grishman A, Sussman LM, Steinberg FM: Atypical coarctation of the aorta with absence of the left radial pulse. *Am Heart J* 27:217-224, 1944
11. Takayasu M: Case with peculiar changes in retinal vessels. *Acta Soc Ophthalmol Jpn* 12:554, 1908
12. Gotsman MS, Beck W, Schrire V: Selective angiography in arteritis of the aorta and its major branches. *Radiology* 88:232-248, 1967
13. Nako K, Ikeda M, Kimata S, Niitani H, Miyahara M, Ishimi Z, Hashiba K, Takeda Y, Ozawa T, Matsushita S, Kuramochi M: Takayasu's arteritis. *Circulation* 35:1141-1155, 1967
14. Paloheimo JA: Obstructive arteritis of Takayasu's type. Clinical, roentgenological and laboratory studies on 36 patients. *Acta Med Scand [Suppl]* 468:7-45, 1967
15. Hirsch MS, Aikat, BK, Basu, AK: Takayasu's arteritis: report of five cases with immunologic studies. *Bull Johns Hopkins Hosp* 115:29-64, 1964
16. Schrire V, Asherson RA: Arteritis of the aorta and its major branches. *Q J Med* 33:439-463, 1964
17. Sen KP: Obstructive disease of the aorta and its branches. *Indian J Surg* 30:289-327, 1968
18. Ueda H, Morooka S., Ito I, Yamacuchi H, Takeda T, Saito, Y: Clinical observations on 52 cases of aortitis syndrome. *Jpn Heart J* 10:277-288, 1969
19. Bircks W, Kort J, Kremer K: Die operative behandlung tiefer aortenstenosen. *Thoraxchirurgie* 10:291-304, 1962-1963
20. Cesarman E, Cardenas M, Escudero J, Zafarias S, Contreras R:

- Arteritis de Takayasu, observaciones clinicas y anatomopatologicas. *Arch Inst Cardiol Mex* 33:690-719, 1963
21. Restrepo, C, Tejeda C, Correa P: Nonsyphilitic aortitis. *Arch Pathol* 87:1-12, 1969
 22. Isaacson C: An idiopathic aortitis in young Africans. *J Pathol* 81:69-79, 1961
 23. Shimizu K, Sano K: Pulseless disease. *J Neuropathol Exp Neurol* 1:37-47, 1951
 24. Hachiya J: Current concepts of Takayasu's arteritis. *Semin Roentgenol* 5:245-259, 1970
 25. Lande A, Berkmen MY: Aortitis: a pathologic, clinical and arteriographic review. *Radiol Clin North Am*. In press, 1976
 26. Sen PK, Kinare SG, Engineer SD, Parulkas GB: The middle aortic syndrome. *Br Heart J* 25:610-618, 1963
 27. Strachan RW: Natural history of Takayasu's arteriopathy. *Q J Med*, 33:57-69, 1964
 28. Inada K, Shimizu J, Kibayashi T, Ishiai S, Kawamoto S: Pulseless disease and atypical coarctation of the aorta. *Arch Surg* 84:306-311, 1962
 29. Nasu T: Pathology of pulseless disease. *Angiology* 2:225-242, 1963
 30. Lande A, Bard R, Rossi P, Passariello R, Castrucci A: Takayasu's arteritis, a worldwide entity (report on 12 Caucasian patients). Submitted for publication
 31. Lande A, Gross A: Total aortography in the diagnosis of Takayasu's arteritis. *Am J Roentgenol* 116:165-178, 1972
 32. Lande A, Rossi P: The value of total aortography in the diagnosis of Takayasu's arteritis. *Radiology* 114:287-297, 1975
 33. Engelsing B: Die abdominale Koarktation der Aorta. *Z Kreislaufforsch* 58:386-396, 1969
 34. Onat T, Zeren E: Coarctation of the abdominal aorta. *Cardiologia* 54:140-157, 1969
 35. Daimon S, Kitamura K: Coarctation of the abdominal aorta. *Jpn Heart J* 5:562-573, 1964
 36. Trench FN, Lengyel L, Maffei EW: Coartacoes e estenoses segmentares da aorta toracica e abdominal, de localizacao atipica. *Arq Hosp Santa Casa Sao Paulo* 3:33-128, 1957
 37. Danaraj JT, Ong HE: Primary arteritis of abdominal aorta in children causing bilateral stenosis of renal arteries and hypertension. *Circulation* 20:856-863, 1959
 38. Danaraj JT, Wong, OH, Thomas AM: Primary arteritis of aorta causing renal artery stenosis and hypertension. *Br Heart J* 25:153-165, 1963
 39. D'Abreu AL, Rob CG, Vollmar JF: Die Coarctation aortae abdominalis. *Langenbecks Arch Chir* 165:830-843, 1959
 40. Brust AA, Howard MJ, Bryant RM, Godwin TJ: Coarctation of the abdominal aorta with stenosis of the renal arteries and hypertension. *Am J Med* 27:793-802, 1959
 41. De Bakey EM, Garrett EH, Howell FJ, Morris CG: Coarctation of the abdominal aorta with renal arterial stenosis: surgical considerations. *Am Surg* 165:830-843, 1967
 42. Ludin H, Elke M: Abdominale Aortenkoarktation aortographische Diagnose in einem Fall. *Fortschr Roentgenstr* 104:34-39, 1966
 43. Morris CG, De Bakey EM, Cooley AD, Crawford ES: Substhenic aortic stenosis and occlusive disease. *Arch Surg* 80:87-104, 1960
 44. Robicsek F, Sanger WP, Daughtery KH: Coarctation of the abdominal aorta diagnosed at aortography. *Ann Surg* 162:227-233, 1965
 45. Ask-Upmark E, Fajers MD: Further observations on Takayasu's syndrome. *Acta Med Scand* 155:275-291, 1956
 46. Beneke R: Ein eigentimlicher Fall Schwieriger Aortitis. *Virchows Arch* 254:723-733, 1925
 47. Harrell EJ, Manion CW: Sclerosing aortitis and arteritis. *Semin Roentgenol* 5:260-266, 1970
 48. Yamada H, Harumi K, Ohta A, Nomura T, Okada R, Ishii M: Aortic arch syndrome with cardiomegaly and aortic calcification. *Jpn Heart J* 2:538-548, 1961
 49. Doberneck CR, Varco LR: Congenital coarctation of the abdominal aorta. *J Lancet* 88:143-150, 1968
 50. Fisher RE, Corcoran CA: Congenital coarctation of the abdominal aorta with resultant renal hypertension. *Arch Intern Med* 89:943-950, 1952
 51. Kittredge DR, Anderson WJ: Coarctation of the lower thoracic and abdominal aorta. *Radiology* 79:799-803, 1962
 52. Maycock W d'A: Congenital stenosis of the abdominal aorta. *Am Heart J* 13:633-646, 1937
 53. Lande A, La Porta A: Takayasu's arteritis: an arteriographic-pathologic correlation. *Arch Pathol*. In press, 1976
 54. Hanson J, Ikkos L, Johansson U, Rudhe U, Senning A: Coarctation of the abdominal aorta. *Acta Chir Scand [Suppl]* 245:315-322, 1959
 55. Beattie JE, Cooke NF, Paul SJ, Orbison AJ: Coarctation of the aorta at the level of the diaphragm treated successfully with a preserved human blood vessel graft. *J Thorac Surg* 21:506-512, 1951
 56. Riemenschneider AT, Emmanouilides CG, Hirose F, Line ML: Coarctation of the abdominal aorta in children: report of three cases and review of the literature. *Pediatrics* 44:716-726, 1969
 57. Deterling AR: Resection of an acquired coarctation of the low thoracic aorta and replacement with a preserved vessel graft. *J Thorac Surg* 26:290-299, 1953
 58. Olin BC: Coarctation of the aorta at the level of the diaphragm. *Ann Surg* 130:1091-1097, 1949
 59. Brust AA, Ferris EB: The diagnostic approach to hypertension due to unilateral renal disease. *Ann Intern Med* 47:1049-1066, 1957
 60. Shapiro JM: Coarctation of the abdominal aorta. *Am J Cardiol* 4:547-550, 1959
 61. Abrahams GD, Cockshott WP: Multiple nonluetic aneurysms in young Nigerians. *Br Heart J* 24:83-91, 1962
 62. Mallory BT: Case records of the Massachusetts General Hospital, case 22141. *N Engl J Med* 214:690-698, 1936
 63. de Takats G: Arterial injuries and arterial inflammation, in *Vascular Surgery*, Philadelphia, Saunders, 1959, pp 130-196
 64. Ansell BM, Bywaters LGM, Doniach I: The aortic lesions of ankylosing spondylitis. *Br Heart J* 20:507-515, 1958
 65. Hope-Ross P, Bien JE, Palladino SV, Graham G: Rheumatoid aortitis: report of an unusual case. *Ann Intern Med* 52:682-693, 1960
 66. McGuire J, Scott CR, Gall AE: Chronic aortitis of undetermined cause with severe and fatal aortic insufficiency. *Am J Med Sci* 235:394-404, 1958
 67. Marquis Y, Richardson JB, Ritchie AC, Wigle ED: Idiopathic medial aortopathy and arteriopathy. *Am J Med* 44:939-954, 1968
 68. Thomas E, Forbus DW: Irradiation injury to the aorta and the lungs. *Arch Pathol* 67:256-263, 1959
 69. Albanese RA, Lasszrini AA: Coarctation of the abdominal aorta-graft of preserved aorta. *Angiology* 4:429-435, 1953
 70. Bjork VO, Intonti F: Coarctation of abdominal aorta with right renal artery stenosis. *Ann Surg* 160:54-60, 1964
 71. Ehrlich A, Brodoff NB, Rubin LI, Berkman IJ: Malignant hypertension in a patient with renal artery occlusions. *Arch Intern Med* 92:591-601, 1953
 72. Kemnitz P, Willgeroth CH: Coarctatio aortae abdominalis vom Takayasu-Typ bei einem 15 jährigen Mädchen. *Zentralbl Allg Pathol* 112:505-513, 1969
 73. Martin JF, Yount EH: Coarctation of the abdominal aorta

- demonstrating value of aortography as diagnostic aid. *Am J Roentgenol* 76:782-786, 1956
74. Heath D, Edwards EJ: Configuration of elastic tissue of aortic media in aortic coarctation. *Am. Heart J* 57:29-35, 1959
 75. Hipona AF, Jamshidi A: Coarctation of the abdominal aorta. *Am J Roentgenol* 110:515-519, 1970
 76. Pyorala K, Heinonen O, Kiskelo P, Heikel PE: Coarctation of the abdominal aorta. Review of twenty-seven cases. *Am J Cardiol* 6:650-662, 1960
 77. Huang TT, Wolma JF, Tyson RK: Coarctation of the abdominal aorta. *Am J Surg* 120:598-601, 1970
 78. Cooley AD, De Bakey EM: Resection of the thoracic aorta with replacement by homograft for aneurysms and constrictive lesions. *J Thorac Surg* 19:66-104, 1955
 79. Ottessen EO, Antia UA, Rowe DR: Peripheral aortic stenosis associated with the supra-avalvular aortic stenosis syndrome. *Radiology* 86:430-435, 1966
 80. Williams JCP, Barratt-Boyes BG, Love JB: Supra-avalvular aortic stenosis. *Circulation* 24:1311-1318, 1961
 81. Siassi B, Klyman G, Emmanouilides CG: Hypoplasia of the abdominal aorta associated with the rubella syndrome. *Am J Dis Child* 120:476-479, 1970
 82. Glenn F, Keefer CBE, Speer SD, Dotter TC: Coarctation of the lower thoracic and abdominal aorta immediately proximal to celiac axis. *Surg Gynecol Obstet* 94:561-569, 1952

Aortoenteric and Paraprosthetic-Enteric Fistulas: Radiologic Findings

WILLIAM M. THOMPSON,¹ DONALD C. JACKSON, AND IRWIN S. JOHNSRUDE

Ten cases of graft-intestinal fistulas occurred in 712 patients who had undergone abdominal aortic reconstructive surgery. Radiographic abnormalities were demonstrated in eight—three by conventional barium gastrointestinal examinations and five by angiography. A high index of suspicion of the condition and an aggressive radiologic workup are recommended.

Fistulas between the gastrointestinal tract and the aorta have been reported following graft replacement for abdominal aortic aneurysms and occlusive vascular disease [1–5]. There are two different types. The first, aortoenteric, is a direct communication between the aortic lumen and the intestine. The second, paraprosthetic-enteric, is a communication between the graft bed and the intestine. These have great clinical importance due to their grave prognosis resulting from difficulties of diagnosis and from problems of management. The clinical picture of gastrointestinal hemorrhage, signs of infection, and abdominal pain has been well documented, while the radiologic findings of graft-intestinal fistulas have received little attention [6, 7]. While some of the more bizarre x-ray manifestations of graft-intestinal fistulas have been reported [6, 8–12], most authors stress difficulty in roentgenologic diagnosis [2, 13].

The usual clinical manifestation is severe gastrointestinal bleeding [14]. Initially this is seldom exsanguinating, and if the diagnosis is suspected and investigated, prompt surgical intervention can be successful [13, 15]. A high index of suspicion is an important factor in making the diagnosis [2]. Any patient with an abdominal aortic graft and subsequent occurrence of gastrointestinal bleeding or obscure signs of infection should be suspected of having a graft-intestinal fistula. The following report deals with the diagnosis of graft-intestinal fistulas, with special emphasis on radiologic manifestations and problems of diagnosis.

Subjects and Methods

Over a 5 year period (1969–1974), 10 of 712 patients who had abdominal aortic surgery for either aneurysm or occlusive vascular disease were seen at Duke University and Durham Veterans Administration Hospitals with graft-intestinal fistulas. The records were reviewed for details of the previous surgery, time from initial operation to onset of symptoms, cause of fistula, and outcome. Methods of diagnosis were critically evaluated.

Results

Eight of the 10 patients had aortoenteric fistulas while two had paraprosthetic fistulas (table 1). Seven had previously undergone surgery for abdominal aortic and/or

iliac artery aneurysms and the other three for occlusive vascular disease. Nine of the 10 patients were males, and the age range was 49–77 years. Dacron interposition grafts were used in all patients. The time to onset of symptoms following the patients' previous surgery varied from 3 weeks to 6 years (average, 24 months).

Nine of 10 patients presented with signs and symptoms of gastrointestinal bleeding, and the other patient had pain and a mass in the left groin (case 2). Two of the patients had signs of infection and three had abdominal pain. The length of symptoms varied from 1 day to 2 months (average, 21 days). One patient had a duodenal paraprosthetic fistula, and one had a sigmoid colon paraprosthetic fistula to the left limb of the aortoiliac bifurcation graft. Erosion by the graft was thought to be the cause for the fistula formation in these two patients. False aneurysm was the cause of the fistulas in the eight patients with aortoenteric fistulas. The differentiation between erosion and false aneurysm formation was determined at surgery. The duodenum was the site of the fistulas in seven patients. The sigmoid colon, jejunum, and ileum were the locations in the remaining three.

The radiologic findings for the 10 patients are listed in table 2. Plain films of the abdomen were obtained in eight of the 10 patients and revealed no specific diagnostic findings. Upper gastrointestinal examinations were performed in five and were helpful in two. A duodenal paraprosthetic fistula was demonstrated in one patient (fig. 1), and a large retroperitoneal mass eroding the third portion of the duodenum in another (see fig. 6B). Barium enemas, performed in five patients, demonstrated left colon diverticulosis in three. The fourth patient had a sigmoid colon paraprosthetic fistula (fig. 2). The fifth study was normal.

Angiographic studies were performed in seven patients; findings were normal in only one (case 2). Obvious extravasation of contrast from the aorta into the intestine was demonstrated in one patient (case 3; fig. 3). False aneurysms and subtle extravasation of contrast were demonstrated in two patients—one prior to surgery (case 4; fig. 4) and one retrospectively (case 5). False aneurysms at the proximal anastomotic site without extravasation of contrast were demonstrated in cases 6 and 7 (fig. 5). In the last patient (case 8), the angiogram showed a patent graft and dilatation of the aorta but no evidence of a fistula (fig. 6A). This patient's upper gastrointestinal examination (fig. 6B) suggested the diagnosis of an aortoduodenal fistula.

The diagnosis was considered preoperatively in eight of the 10 patients but was only established with certainty

Presented at the annual meeting of the American Roentgen Ray Society, Atlanta, Georgia, October 1975.
W. M. Thompson is a Picker Scholar, James Picker Foundation.

¹ All authors: Department of Radiology, Duke University Medical Center, Durham, North Carolina 27710.

TABLE 1
Clinical Features

Case No.	Sex and Age	Original Surgery	Time from Surgery to Onset of Symptoms (Mo)	Presenting Symptoms	Cause of Fistula		Site	Primary Diagnostic Method
					Graft Erosion	False Aneurysm		
1 (fig. 1) M, 51		Resection AAA	10	Septicemia and lower GI bleeding, 2 mo	+	...	Duodenum	Upper GI
2 (fig. 2) F, 59		Aortofemoral bypass for OVD	7	Pain, mass left groin, and septicemia, 4 wk	+	...	Sigmoid	Barium enema
3 (fig. 3) M, 77		Resection false AAA	3 wk	Severe upper GI bleeding, 1 day	...	+	Duodenum	Angiography
4 (fig. 4) M, 65		Aortofemoral bypass for OVD	18	Severe upper GI bleeding, 2 days	...	+	Duodenum	Angiography
5 M, 76		Resection AAA	10	Lower GI bleeding, 6 wk	...	+	Jejunum	Angiography, surgery
6 (fig. 5) M, 49		Aortoiliac bypass for OVD	15	Lower GI bleeding, 8 days; abdominal pain, 12 days	...	+	Duodenum	Angiography, surgery
7 M, 72		Resection AAA	6 yr	Severe upper GI bleeding, 2 days	...	+	Duodenum	Angiography, surgery
8 (fig. 6) M, 53		Resection AAA	5 yr	Abdominal pain, 6 wk; jaundice and hematemesis, 1 day	...	+	Duodenum	Upper GI
9 M, 64		Resection iliac aneurysms	12	Lower GI bleeding, 1 day	...	+	Duodenum	Surgery
10 M, 58		Resection AAA	36	Lower GI bleeding, 3 wk	...	+	Ileum	Surgery

Note.—Three patients survived initial surgery: cases 1, 2, and 10. AAA=abdominal aortic aneurysm; OVD=occlusive vascular disease.

prior to surgery in five (cases 1–4 and 8). Since the aortograms in cases 6 and 7 demonstrated only false aneurysms and no extravasation, the diagnosis of aortoenteric fistula was not made. In case 5, a suspicious blush of contrast appeared over the midportion of the left kidney on the patient's flush aortogram which was initially thought to represent bleeding from a colonic diverticulum. However, subsequent selective injections of the superior mesenteric and celiac arteries failed to confirm a definite bleeding site. Subsequent review of the films and subtraction technique following surgery confirmed the presence of this extravasation. In retrospect, this likely represented the aortoenteric fistula. Therefore, although the diagnosis was made preoperatively in five patients, eight had radiologic abnormalities suggesting graft-intestinal fistulas.

One patient (case 9) had no radiographic studies. The diagnosis was suspected clinically based on a past Dacron graft and the presence of severe upper gastrointestinal bleeding. He was taken directly to surgery. Left colon diverticulosis was thought to be the cause of the rectal bleeding in case 10; however, at surgery a false aneurysm with an aortoileal fistula was discovered.

Three of the 10 patients survived the initial surgery; however, one (case 2) has had numerous operative procedures secondary to recurrent infections. The other two patients have had an uncomplicated postoperative course.

Discussion

The incidence of fistulas following abdominal aortic surgery has been reported as high as 5%–10% [4, 16]. This figure has decreased to approximately 1% in most recent series [2, 17, 18]. In the present series, the initial surgery in one patient was performed at an outside hospital, so only nine of 712 patients (1.3%) initially operated on at this institution developed graft-intestinal fistulas. The decrease in incidence of postoperative fistulas is due to the following: improved surgical technique; more suitable Dacron grafting material replacing homografts and Teflon grafts; more durable synthetic, rather than silk, suture; and the recognition that tissues must be interposed between the patient's intestine and the Dacron grafts [2, 3].

A total of 80% of aortoenteric fistulas occur in the duodenum [2, 4, 18]. Aortoenteric fistulas, secondary to aneurysms and following aortic surgery, have been reported involving all portions of the gastrointestinal tract, including the esophagus [15], stomach [19], jejunum [1], ileum [20], colon [6, 8], and even the appendix [21].

The most common causes of graft-intestinal fistulas are perforation of the duodenal wall, which is usually caused by impairment of the duodenal blood supply during surgical dissection, erosion by the graft, or false aneurysm at the anastomotic site. A large abdominal aortic aneurysm makes dissection more difficult, and this increases the likelihood

TABLE 2
Radiologic Findings

Case No.	Upper GI	Barium Enema	Angiogram
1	Fistula from duodenum to graft (fig. 1)	Normal	N.D.
2	Normal	Fistula from sigmoid to graft (fig. 2)	Normal
3	N.D.	N.D.	Extravasation into intestine (fig. 3)
4	N.D.	N.D.	Subtle extravasation into intestine (fig. 4)
5	Normal	Diverticulosis	Subtle extravasation into intestine
6	N.D.	Diverticulosis	False aneurysm (fig. 5)
7	N.D.	N.D.	False aneurysm
8	Mass compressing duodenum (fig. 6)	N.D.	Dilatation of aorta, no evidence of bleeding sites (fig. 6)
9	N.D.	N.D.	N.D.
10	Normal	Diverticulosis	N.D.

Note.—Plain films were obtained in cases 1–6, 8, and 10 and yielded no specific diagnostic findings. N.D. = not done.

of compromising the duodenal blood supply. The posterior wall of the third portion of the duodenum is the most common site of fistulas. This is due both to the close apposition of the anterior aortic wall to the duodenum and the location of the third duodenal segment between the aorta and superior mesenteric artery (fig. 3C). Fistulas may occur at other sites if there is direct contact of the graft with the intestinal wall.

Whatever the cause of the defect in the bowel wall, the escape of intestinal contents causes localized infection around the graft. The clinical picture is that of retroperitoneal abscess with or without septicemia. Should the infection established along the graft reach a suture line, hemorrhage will occur [1, 2, 4]. This can be retroperitoneal, but most commonly the hemorrhage is into the duodenum through the communication established between the lumen of the gut and the paraprosthentic abscess. False aneurysms often form at anastomotic sites due to infection. However, they may occur without an obvious infectious process due to abnormal aortic tissue at the anastomosis. False aneurysms may lead to an aortoenteric fistula. Once there is intestinal contamination of the graft, it may be impossible to determine the exact cause of the fistula.

The majority of patients with aortoenteric fistulas will present with some form of gastrointestinal bleeding, varying from intermittent to acute hemorrhage. Signs of infection may occur. Another reported finding is a painful and/or pulsatile abdominal mass [2–4, 13, 16, 22].

The signs and symptoms of the patients in the present series (table 1) compare closely with previous reports. The

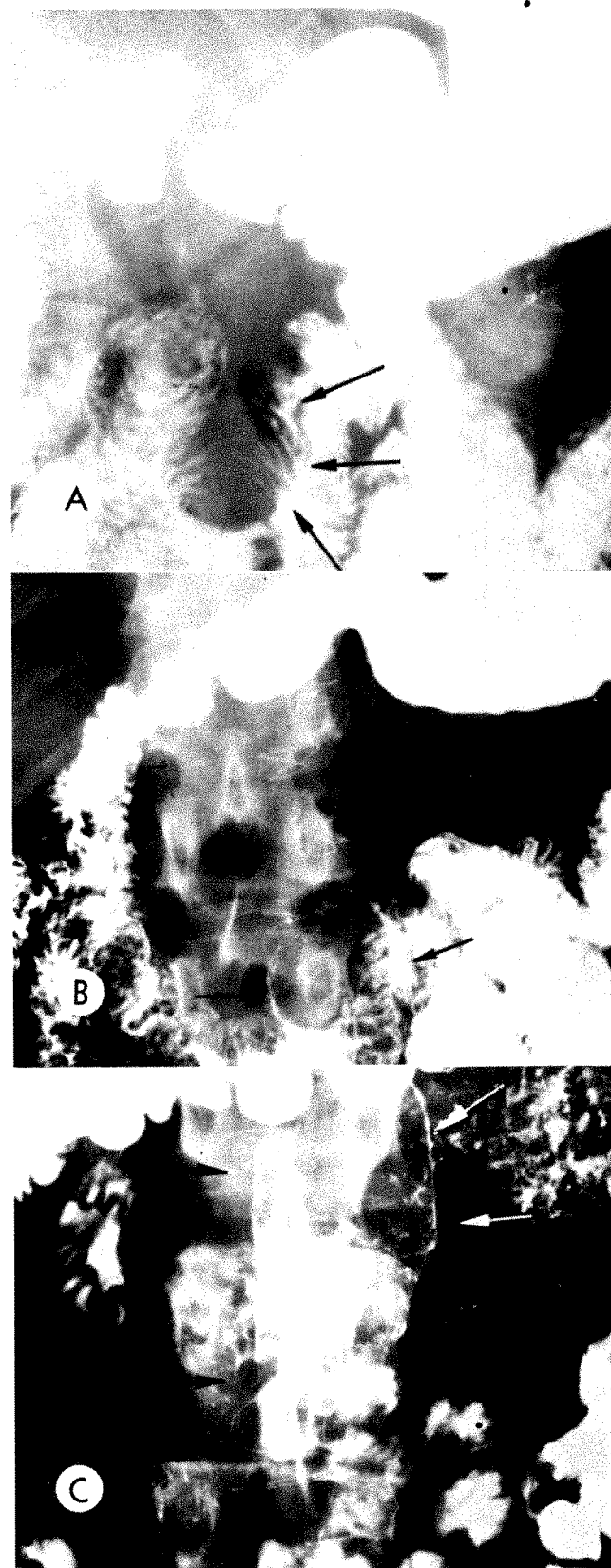


Fig. 1.—Case 1. A, Corrugated filling defect in third portion of duodenum (arrows). B, Repeat barium meal 3 months later demonstrating enlargement of filling defect (arrows). C, Delayed film showing extravasation of barium outlining prosthetic graft (arrows). Infected graft was removed.

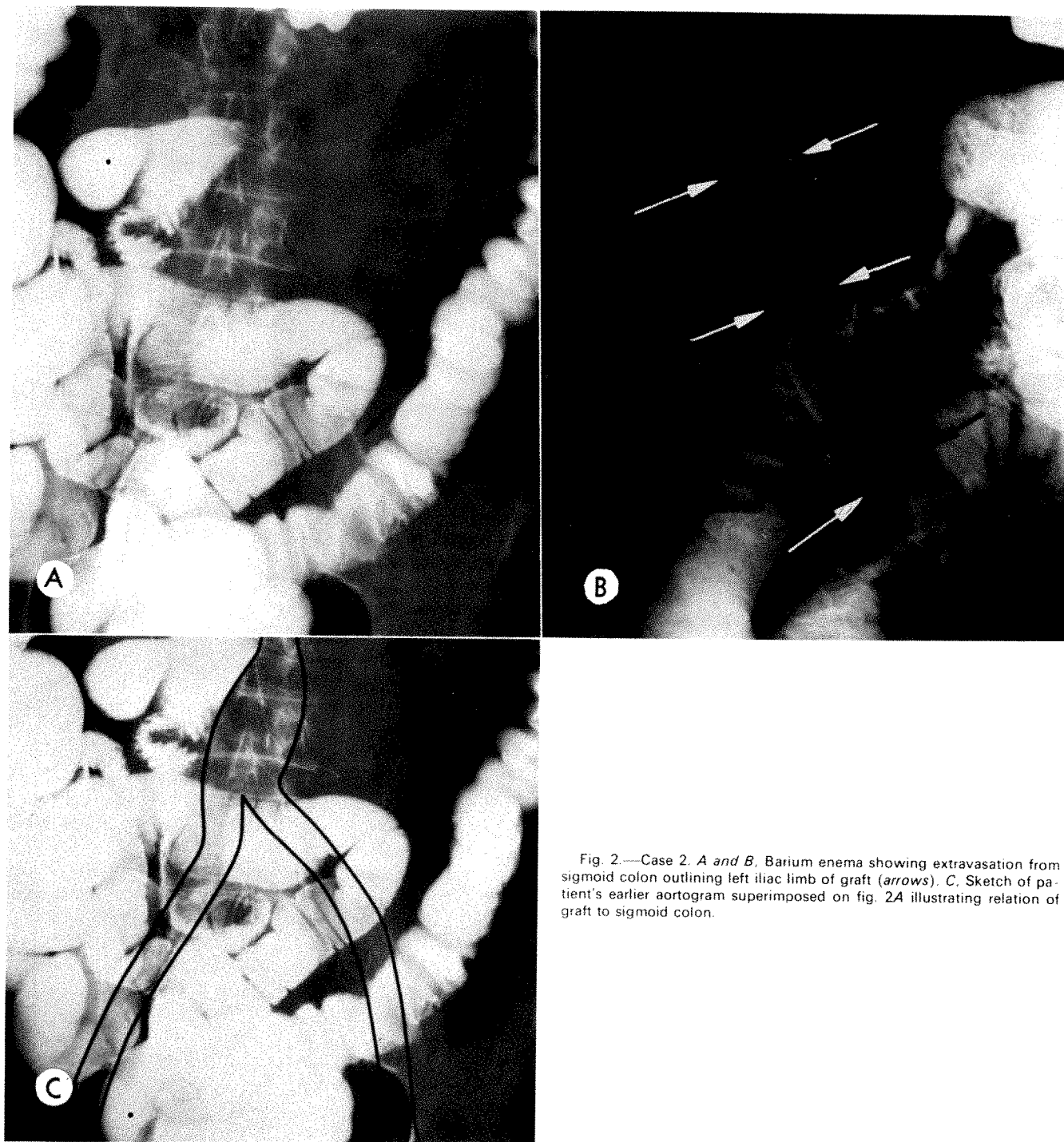


Fig. 2.—Case 2. *A and B*, Barium enema showing extravasation from sigmoid colon outlining left iliac limb of graft (*arrows*). *C*, Sketch of patient's earlier aortogram superimposed on fig. 2*A* illustrating relation of graft to sigmoid colon.

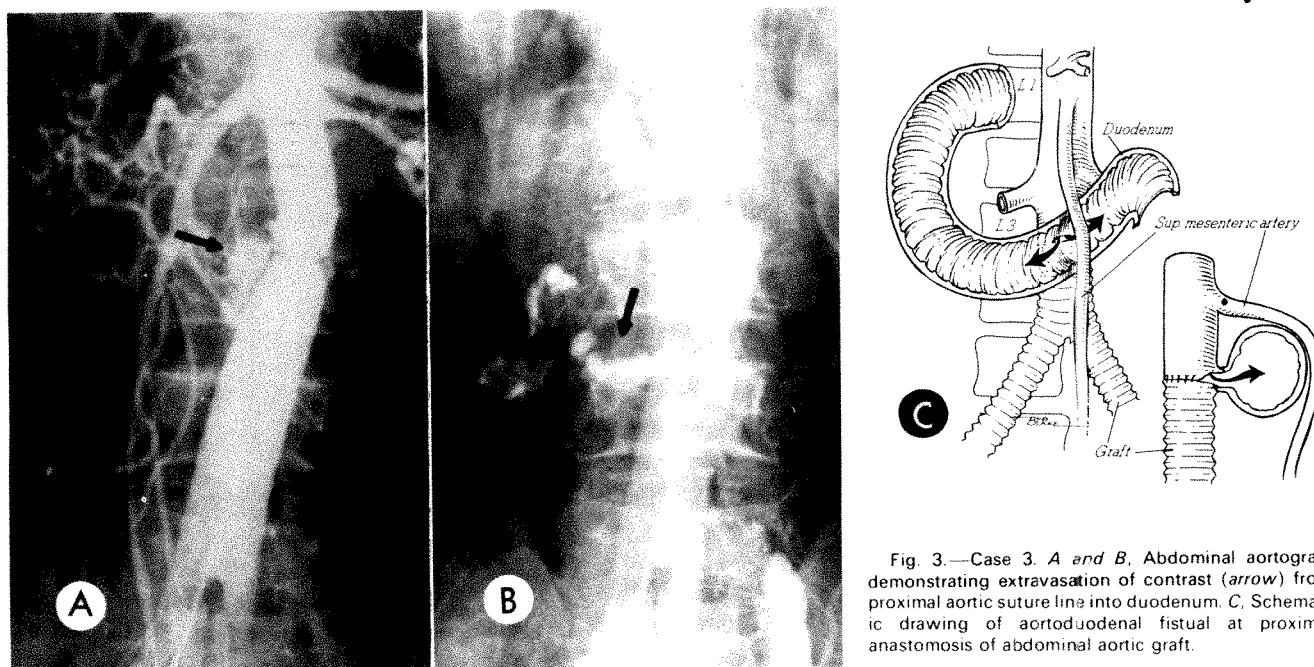


Fig. 3.—Case 3. A and B, Abdominal aortogram demonstrating extravasation of contrast (arrow) from proximal aortic suture line into duodenum. C, Schematic drawing of aortoenteric fistula at proximal anastomosis of abdominal aortic graft.

chronic nature of the disorder and the latent interval to the onset of symptoms are a well documented feature of graft-intestinal fistulas [2–5, 13, 16, 22].

The diagnostic studies have two goals: (1) to eliminate causes of retroperitoneal sepsis and gastrointestinal hemorrhage other than aortoenteric or paraprosthesis-enteric fistulas, and (2) to relate the hemorrhage or sepsis to the presence of the prosthesis. If the hemorrhage is massive, immediate surgery precludes diagnostic studies. Most authors have stated that if the bleeding is intermittent and in small amounts, radiologic examination of the alimentary tract and angiography of the abdominal aorta may be permissible but will seldom be useful [2, 13, 23]. This is because the duodenal defect is difficult to demonstrate by conventional barium meal, and during quiescence the communication with the vascular wall is temporarily obliterated by clot. Also, in many instances, the fistula is due to a defect in the proximal suture line, without any evidence of false aneurysm formation or graft irregularity to suggest the diagnosis of an aortoenteric fistula [23].

Our series differs from previous reports concerning the value of diagnostic studies. Eight of the 10 patients had radiographic abnormalities; in the remaining two a complete diagnostic workup was not undertaken (table 2). In five of the eight, a diagnosis of a graft-intestinal fistula was made preoperatively on the basis of radiologic findings. In three, the specific abnormalities were not interpreted to indicate graft-intestinal fistulas (tables 1 and 2).

Patients who present with sepsis should have studies directed toward localizing the site of infection. In those without an obvious site and a history of abdominal aortic surgery, exploration of the graft should be undertaken [2].

In the radiologic workup of a suspected aortoenteric fistula, plain films of the abdomen are usually not helpful.

A mass in the abdomen secondary to a false aneurysm, retroperitoneal hematoma, or abscess may be demonstrated. The patients should undergo an upper gastrointestinal examination, since this study may show a mass displacing or occluding the duodenum and/or erosion with extravasation of barium [2, 6, 9, 10, 24, 25]. A small bowel study should be included since small bowel loops may be displaced by a false aneurysm or hematoma. Barium enema examinations are necessary in the majority of patients with lower intestinal bleeding to rule out other causes for the bleeding. In patients with graft-intestinal fistulas, a mass or area of ulceration with or without extravasation along the limb of the graft may be demonstrated [6, 24].

Angiographic studies should be performed on all patients with intermittent gastrointestinal bleeding who have had previous abdominal aortic surgery. If extravasation is demonstrated on the angiogram (fig. 3), the diagnosis is clearly established. This is not a frequent finding, as demonstrated in the present series (table 2). Subtraction film techniques will clarify questionable areas of extravasation of contrast overlying bony structures or organs such as the kidneys (fig. 4).

In patients who are having severe gastrointestinal bleeding, there is a tendency to proceed directly to selective angiography of the celiac and mesenteric vessels without performing a flush abdominal aortogram. Failure to opacify the aorta will prevent detection of an aortoenteric fistula [12]. We recommend that all patients undergoing angiography for gastrointestinal bleeding, especially those suspected of having an aortoenteric fistula, have an abdominal aortogram done routinely. Since the bleeding point is on the anterior aortic wall (fig. 3B), the fistula may be shown in the lateral rather than the frontal projection and also may

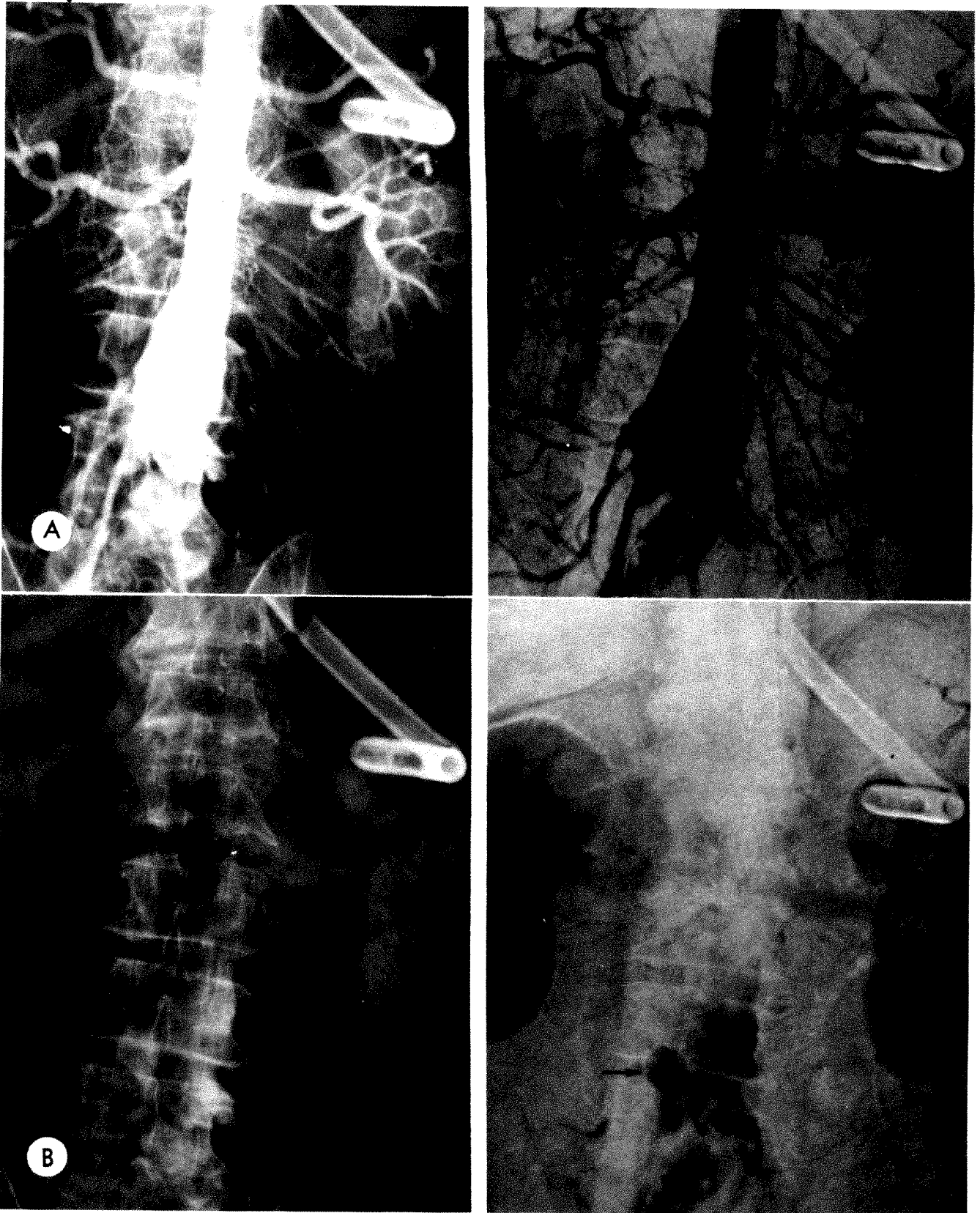


Fig. 4.—Case 4. *A*, Single film from abdominal aortogram showing false aneurysm at proximal anastomosis. *B*, Later film in aortogram illustrating circular area of contrast thought to represent aortoduodenal fistula. Subtraction films clarify findings.

be better seen with the patient prone. We recommend a biplane prone abdominal aortogram in all patients suspected of having an aortoenteric fistula, even though these technical variations did not demonstrate the fistulas in the present series.

A much higher correlation between angiographic abnormalities and the finding of a fistula was noted in this series compared to previous reports.

Our data indicate that if a patient admitted with gastrointestinal bleeding has a false aneurysm demonstrated at angiography but no evidence of extravasation, surgical exploration of the graft should be performed. The presence of false aneurysm suggests that the proximal anastomotic site has weakened and may be involved with infection. In these circumstances, surgery is best undertaken as an elective procedure rather than as an emergency during massive hemorrhage.

Abdominal ultrasound was not utilized in this group of patients or in other series of graft-intestinal fistulas. Ultrasound is a valuable procedure in patients with abdominal aortic aneurysms [17]. It is a recommended procedure in patients with possible graft-intestinal fistulas, since a false aneurysm or retroperitoneal abscess may be demonstrated.

Graft-intestinal fistulas have a grave prognosis: a 70% mortality rate has been reported [1, 2, 4, 5, 14]. The mortality is related both to the delay in diagnosis and the technical difficulties of repairing an aortoenteric fistula. A high index of suspicion and an aggressive diagnostic workup are important factors in reducing the mortality of this condition.



Fig. 5.—Case 6. Aortogram showing false aneurysm at proximal anastomosis (arrow). No bleeding site noted. At surgery, aortoduodenal fistula was found.

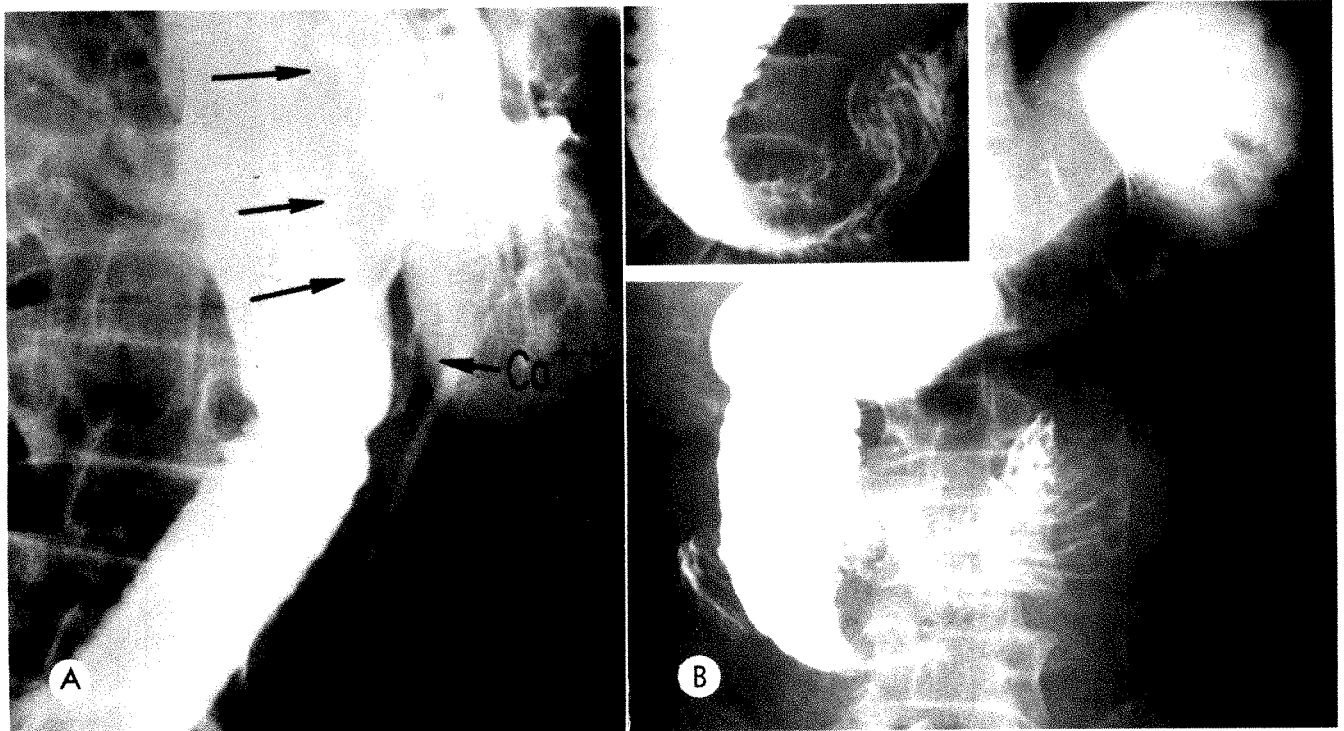


Fig. 6.—Case 8. A, Abdominal aortogram revealing marked ectasia and dilatation of aorta above patent graft. Filling defect (arrows) represents large thrombus. Calcification (Ca^{++}) is present in aortic wall. No bleeding site identified. B, Barium study revealing large mass eroding duodenum, which was thought to represent aortoduodenal fistula found at surgery.

ACKNOWLEDGMENT

We thank Dr. Don Munson for contributing case 1.

REFERENCES

1. De Weese MS, Fry WJ: Small-bowel erosion following aortic resection. *JAMA* 179:882-886, 1962
2. Elliott JP Jr, Smith RF, Szilagyi DE: Aorto-enteric and para-prosthetic-enteric fistulas. *Arch Surg* 108:479-488, 1974
3. Garrett HE, Beall AC Jr, Jordan GL Jr, De Bakey ME: Surgical considerations of massive gastrointestinal tract hemorrhage caused by aortoduodenal fistula. *Am J Surg* 105:6-12, 1963
4. Humphries AW, Young JR, de Wolfe VG, LeFevre FA: Complications of abdominal aortic surgery. *Arch Surg* 86:43-50, 1963
5. Javid H, Julian OC, Dye WS, Hunter JA: Complications of abdominal aortic surgery. *Arch Surg* 85:650-661, 1962
6. Ferris EJ, Koltay MRS, Koltay OP, Sciammas FD: Abdominal aortic and iliac graft fistulae. *Am J Roentgenol* 94:416-420, 1965
7. Nevin IN, Bump WS, Thuerer GR: Preoperative diagnosis of rupture into the duodenum of an aortic-homograft anastomosis. *N Engl J Med* 263:243-245, 1960
8. Beach M, Risley TS: Aorticosigmoid fistulization following aortic resection. *Arch Surg* 92:805-807, 1966
9. Case records of the Massachusetts General Hospital (case 45282). *N Engl J Med* 261:92-96, 1959
10. Case records of the Massachusetts General Hospital (case 45522). *N Engl J Med* 261:1339-1342, 1959
11. Case records of the Massachusetts General Hospital (case 38-1971). *N Engl J Med* 285:739-745, 1971
12. Case records of the Massachusetts General Hospital (case 21-1974). *N Engl J Med* 290:1248-1253, 1974
13. Reckless JPD, McColl I, Taylor GW: Aorto-enteric fistulae: an uncommon complication of abdominal aortic aneurysms. *Br J Surg* 59:458-460, 1972
14. Pinkerton JA Jr: Aortoduodenal fistula. *JAMA* 225:1196-1199, 1973
15. Rosato FE, Barker C, Roberts B: Aorto-intestinal fistula. *J Thorac Cardiovasc Surg* 53:511-514, 1967
16. Donovan TJ, Bucknam CA: Aorto-enteric fistula. *Arch Surg* 95:810-818, 1967
17. Lee RK, Walls WJ, Martin NL, Templeton AW: A practical approach to the diagnosis of abdominal aortic aneurysms. *Surgery* 78:195-201, 1975
18. Schramek A, Weisz GM, Erlik D: Gastro-intestinal bleeding due to arterio-enteric fistula. *Digestion* 4:103-108, 1971
19. Youmans CR, Derrick JR: Gastrointestinal erosion after prosthetic arterial reconstructive surgery. *Am J Surg* 114:711-715, 1967
20. Claytor H, Birch L, Cardwell ES, Zimmerman SL: Suture-line rupture of a nylon aortic bifurcation graft into the small bowel. *Arch Surg* 77:965-969, 1956
21. Tyson RR, Maier WP, D Pietrantonio S: Iliaco-appendiceal fistula following Dacron aortic graft. *Am Surg* 35:241-243, 1969
22. Lise M, Yacoub MH: Aorto-duodenal fistula: a complication of abdominal aortic grafts. *J Cardiovasc Surg (Torino)* 10:1196-1199, 1969
23. Levy MJ, Todd DB, Lillehei CW, Varco RL: Aortointestinal fistulas following surgery of the aorta. *Surg Gynecol Obstet* 120:992-996, 1965
24. Ng E, Cooperman LR: Erosion of the small intestine with hemorrhage following aortic resection: roentgen findings. *Clin Radiol* 21:87-89, 1970
25. Sondheimer FK, Steinberg I: Gastrointestinal manifestations of abdominal aortic aneurysms. *Am J Roentgenol* 92:1110-1122, 1964

Angiography of Mediastinal Parathyroid Adenomas

CHARLES J. TEGTMEYER,¹ E. MEREDITH ALRICH,² AND THEODORE E. KEATS¹

Two cases with mediastinal parathyroid adenomas are presented. Both patients had undergone previous unsuccessful neck explorations. Angiography correctly localized the parathyroid adenomas in each case, substantiating the value of parathyroid angiography in mediastinal tumors.

We seek him here, we seek him there,
Those Frenchies seek him everywhere.
Is he in heaven?—Is he in hell?
That demmed, elusive [parathyroid] Pimpernel? [1]

The problem of parathyroid disease has become one involving the close cooperation of many disciplines of medicine. Until recently, the radiologist contributed in the diagnosis of parathyroid disease but not to the localization of the adenoma. Despite the fact, the first angiographic localization of a parathyroid adenoma was reported by Seldinger [2] in 1954.

The localization of parathyroid adenomas in patients who have undergone previous neck explorations presents a difficult problem. The localization of mediastinal parathyroid adenomas is especially difficult. The cases presented here illustrate the value of preoperative angiography in the localization of mediastinal parathyroid adenomas in two patients with previous unsuccessful neck surgery.

Case Reports

Case 1

R. C., a 55-year-old male, was readmitted to the hospital following a neck exploration for hyperparathyroidism. A bilateral subtotal thyroidectomy was performed, and two parathyroid glands were removed. One parathyroid was normal and the other was hyperplastic. His hypercalcemia persisted (10.7–17.6 mg/100 ml).

Parathyroid angiography showed an enlarged left inferior thyroid artery. A prominent branch of this artery descended into the mediastinum and supplied a 4.0 × 2.0 cm vascular mass (fig. 1A and 1C). The intense vascular blush in the tumor appeared early and persisted (fig. 1B).

The patient was explored through a median sternotomy incision, and an adenoma was removed from the anterior mediastinum. Postoperatively, hypoparathyroidism developed; however, it was readily controlled with medical therapy.

Case 2

D. M., a 75-year-old female, underwent a neck exploration and removal of the left lobe of her thyroid for hyperparathyroidism. Her hypercalcemia persisted (11.3–13.2 mg/100 ml).

Parathyroid angiography demonstrated an enlarged branch of the right inferior thyroid artery descending into the upper mediastinum (fig. 2A and 2C). It curved around the medial border of a densely stained mass which is supplied (fig. 2B).

The patient was reexplored. The abnormal branch of the inferior thyroid artery was identified and traced to a 4.0 × 2.5 × 1.5 cm

parathyroid adenoma. The mediastinal adenoma was located behind the trachea, anterior to the esophagus. Postoperatively, the serum calcium returned to normal.

Discussion

The operative discovery of a parathyroid tumor, especially one located in the mediastinum, can be a difficult and frustrating surgical exercise [3, 4]. It required seven operations and 6 years to locate and remove the first parathyroid adenoma treated in this country because it lay in the mediastinum [3].

The difficulties encountered in the localization of the parathyroid glands stem from embryologic development. Embryologically, the superior pair of glands derive from the fourth branchial pouch. They migrate only a short distance to the adult position, which is posterior to the superior poles of the thyroid gland at the level of the lower border of the cricoid cartilage.

The inferior pair of glands derive from the third branchial pouch. They traverse a greater distance to reach the usual position overlying the recurrent laryngeal nerve somewhat lateral and inferior to the lower poles of the thyroid gland. However, the inferior parathyroids migrate in intimate relationship with the thymus gland, and this initial wide range of migration contributes to the relative inconsistency of their location. They may be located anywhere from the larynx to the pericardium.

An overlooked adenoma is usually in the neck and not in the mediastinum [5]. However, the mediastinum is the site of parathyroid adenomas in from 1% to 10% of cases [6, 7].

Angiographic demonstration of parathyroid adenomas depends upon the vascular supply of the adenoma. The blood supply of the cervical parathyroid glands is usually from the inferior thyroid arteries [8, 9]. Intrathoracic parathyroid adenomas also often derive their blood supply from a branch of the inferior thyroid artery [4, 10]. Mediastinal parathyroid adenomas, however, are occasionally supplied by the internal mammary artery [10, 11] or by an anomalous artery arising from the innominate artery [12, 13]. In both of our patients an enlarged branch of the inferior thyroid artery supplied the mediastinal parathyroid adenomas.

The angiographic findings previously reported in cervical parathyroid adenomas are abnormal vessels, displacement or stretching of the branches of the inferior thyroid artery, increased size of the ipsilateral thyroid artery, and a vascular blush or stain of the adenoma [2, 13, 14]. Displacement of the cranial and caudal loops of the inferior thyroid artery has also been described [13]. "The single most important finding has been the demonstration of a capillary stain sufficiently far removed from the thyroid gland as outlined

¹ Department of Radiology, University of Virginia Medical Center, Charlottesville, Virginia 22901. Address reprint requests to C. J. Tegtmeier.

² Department of Surgery, University of Virginia Medical Center, Charlottesville, Virginia 22901.

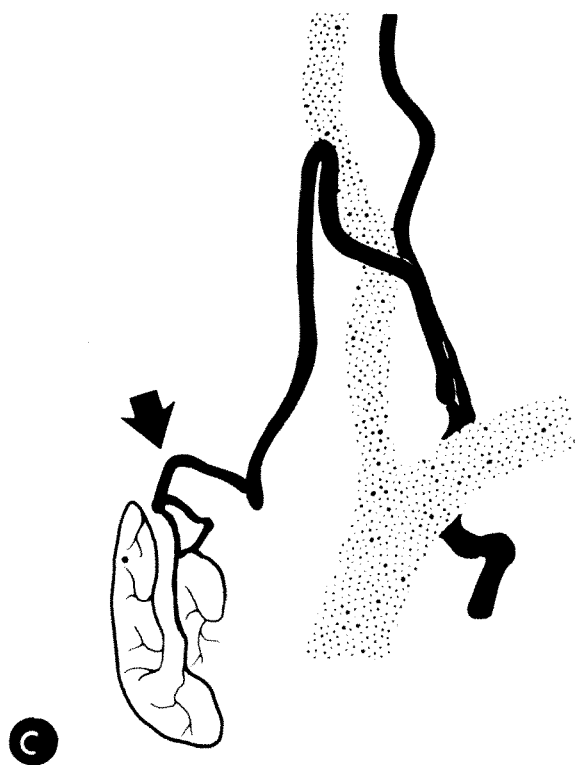
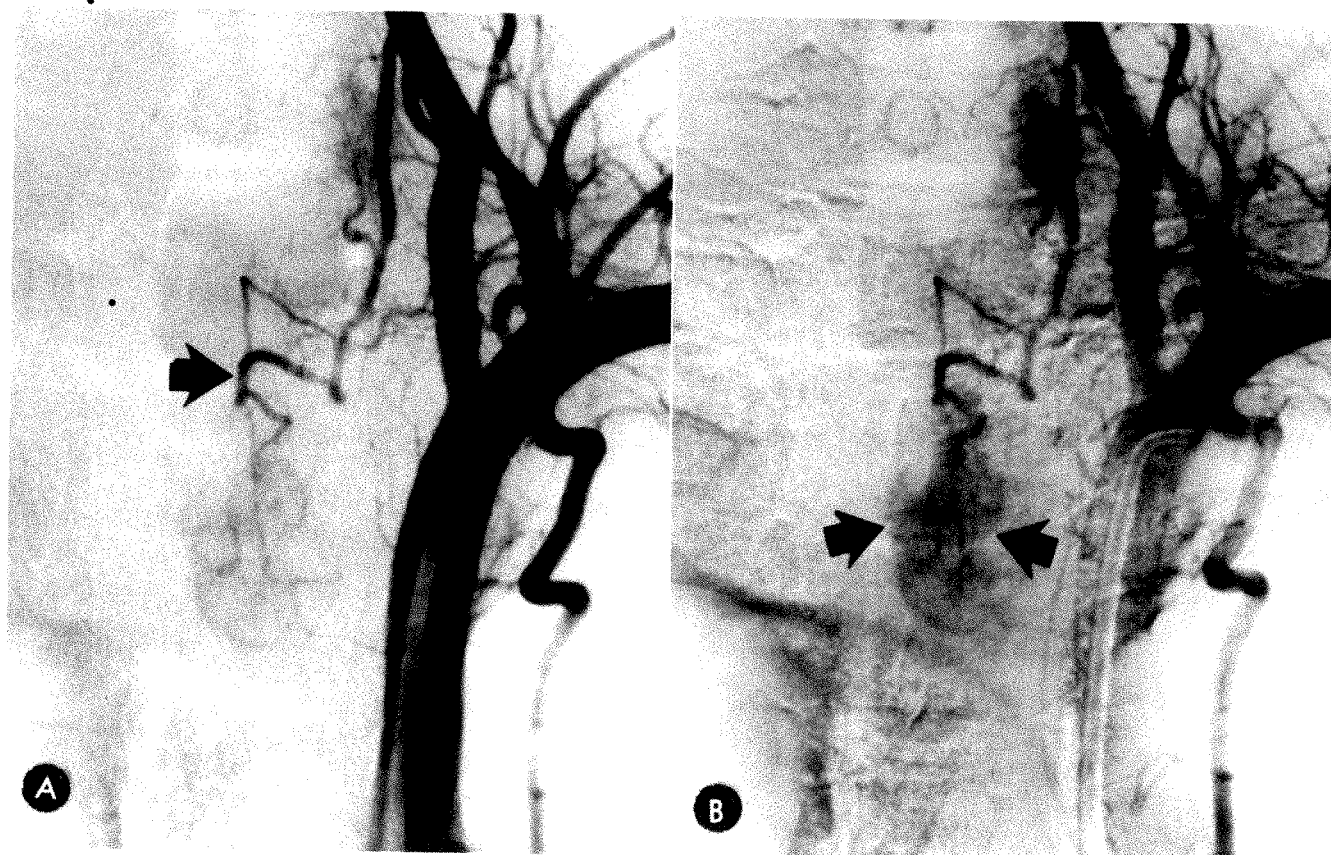


Fig. 1.—Case 1. *A* and *B*, Early and late arterial phase subtraction films of left subclavian arteriogram showing large branch (*arrow*) of inferior thyroid artery descending into mediastinum to supply parathyroid adenoma. *C*, Diagrammatic representation.

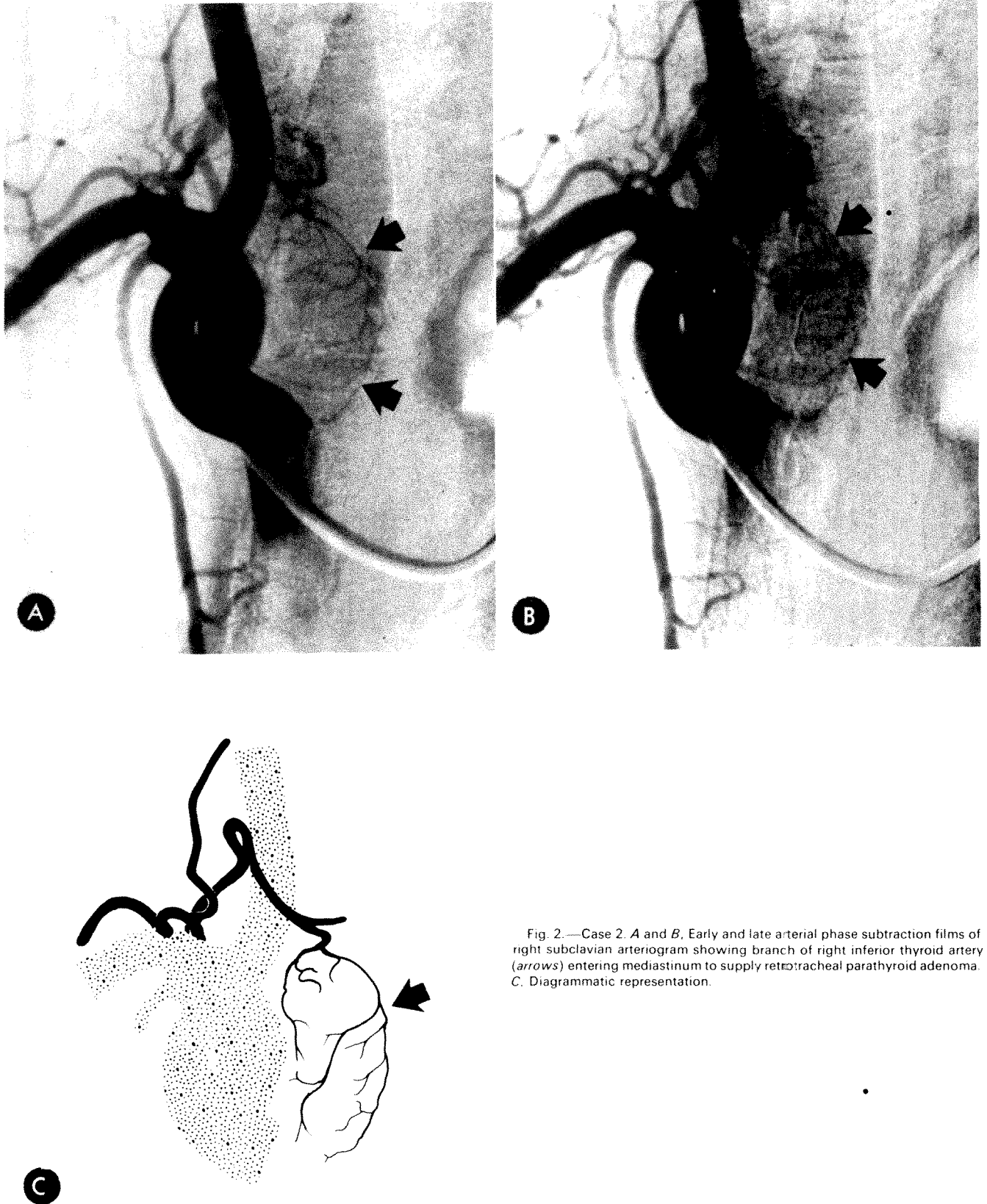


Fig. 2.—Case 2. *A* and *B*, Early and late arterial phase subtraction films of right subclavian arteriogram showing branch of right inferior thyroid artery (arrows) entering mediastinum to supply retrotracheal parathyroid adenoma. *C*, Diagrammatic representation.

on the scan that it cannot be considered thyroid tissue" [15].

Unlike cervical parathyroid adenomas, mediastinal adenomas are well separated from the thyroid gland, and interpretation of the angiograms is simplified. In both of our patients an anomalous enlarged branch of the inferior thyroid artery supplied the adenoma. The angiographic diagnosis was confirmed by the intense capillary staining of the adenoma. The adenomas are sufficiently far removed from the thyroid gland as outlined on the scan to permit easy separation of the adenoma blush from the thyroid blush.

A review of the literature reveals that arteriography has been performed to locate 14 mediastinal adenomas, including the present cases. Two of these angiographic studies were undertaken during surgery [4, 12], and both studies correctly localized the adenomas. The remaining 12 studies were performed prior to surgery, and the preoperative angiographic localization was correct in 10 of these cases [10, 11, 16–18]. The other two cases were incorrectly diagnosed [10, 13]. However, in one of these the blush of the adenoma was appreciated in the mediastinum in retrospect [10]. Arteriography has been attempted in 14 mediastinal parathyroid adenomas and has located 13 of them.

Selective catheterization of the neck veins for parathyroid hormone (PTH) immunoassay has also proven to be a valuable aid in the preoperative localization of parathyroid adenomas residing in the neck [19–22].

Selective venous PTH sampling has been proposed as a method for locating mediastinal adenomas. However, Doppman et al. [10] found that elevated concentrations of PTH in selectively sampled inferior thyroid veins could lateralize a source of excess PTH production but could not assure a cervical (as opposed to mediastinal) location. This is because most mediastinal glands drain cranially into the inferior thyroid veins or into the thymic veins which frequently anastomose with the thyroid veins. This corroborates the surgical observation that most mediastinal adenomas are supplied by a vascular pedicle from the neck. Selective parathyroid arteriography, however, directly demonstrates the mediastinal adenomas.

Reexploration of patients for elusive parathyroid adenomas is usually very difficult because of scar tissue. Angiography correctly localized the adenomas in both of our cases, and similar favorable results have been reported. Tracing the course of the arterial supply provides a road map for the surgeon. This greatly simplifies surgical localization of mediastinal adenomas.

REFERENCES

1. Orczy B: *The Scarlet Pimpernel*. New York, Putnam, 1905.
2. Seldinger SI: Localization of parathyroid adenomata by arteriography. *Acta Radiol* 42:353–366, 1954
3. Nathaniels EK, Nathaniels AM, Wang CA: Mediastinal parathyroid tumors: a clinical and pathological study of 84 cases. *Ann Surg* 171:165–170, 1970
4. Steiner RE, Fraser R, Aird I: Operative parathyroid arteriography for localization of parathyroid tumour. *Br Med J* 2:400–401, 1956
5. Doppman JL, Wells SA, Shimkin PM, Pearson KD, Bilezikian JP, Heath DA, Powell D, Ketcham AS, Aurbach GD: Parathyroid localization by angiographic techniques in patients with previous neck surgery. *Br J Radiol* 43:403–418, 1973
6. Black BM: Problems in the treatment of hyperparathyroidism. *Surg Clin North Am* 41:1061–1068, 1961
7. Goldman L, Gordan GS, Roof BS: The parathyroids: progress, problems and practice. *Curr Probl Surg*, August 1971, pp 1–64
8. Curtis GM: The blood supply of the human parathyroids. *Surg. Gynecol Obstet* 51:805–809, 1930
9. Halsted WS, Evans HM: The parathyroid glandules: their blood supply and their preservation in operation upon the thyroid gland. *Ann Surg* 46:489–506, 1907
10. Doppman JL, Mallette LE, Marx SJ, Monchik JM, Broadus A, Spiegel AM, Beazley R, Aurbach GD: The localization of abnormal mediastinal parathyroid glands. *Radiology* 115:31–36, 1975
11. Dodds WJ, Newton TH, Enloe LJ: Parathyroid adenoma of anterior mediastinum demonstrated by preoperative selective arteriography. *Radiology* 91:923–924, 1968
12. Hardy JD, Snively JR, Langford HG: Low intrathoracic parathyroid adenoma: large functioning tumor representing fifth parathyroid, opposite eighth dorsal vertebra with independent arterial supply and opacified at operation with arteriogram. *Ann Surg* 159:310–315, 1964
13. Newton TH, Eisenberg E: Angiography of parathyroid adenomas. *Radiology* 86:843–850, 1966
14. Doppman JL, Hammond WG, Melson GL, Evens RG, Ketcham AS: Staining of parathyroid adenomas by selective arteriography. *Radiology* 92:527–530, 1969
15. Kuntz CH, Goldsmith RE: Selective arteriography of parathyroid adenomas. *Radiology* 102:21–28, 1972
16. Bradley EL, McGarity WC: Surgical evaluation of parathyroid arteriography. *Am J Surg* 126:67–73, 1973
17. Eisenberg H, Pallotta J, Sherwood LM: Selective arteriography, venography and venous hormone assay in diagnosis and localization of parathyroid lesions. *Am J Med* 56:810–820, 1974
18. Wanke R: Epithelkörperchen—Chirurgie bei primärem Hyperparathyreoidismus. *Chirurg* 33:53–57, 1962
19. O'Riordan JL, Kendall BE, Woodhead JS: Preoperative localization of parathyroid tumors. *Lancet* 2:1172–1175, 1971
20. Palmer JA: Exploration of the neck for hyperparathyroidism. *Can J Surg* 18:10–13, 1971
21. Reitz RF, Pollard JJ, Wang CA, Fleischli DJ, Cope O, Murray TM, Deftos LJ, Potts JT: Localization of parathyroid adenomas by selective venous catheterization and radioimmunoassay. *N Engl J Med* 281:348–351, 1969
22. Wells SA, Ketcham AS, Marx SJ, Powell D, Bilezikian JP, Shimkin PM, Pearson KD, Doppman JL: Preoperative localization of hyperfunctioning parathyroid tissue: radioimmunoassay of parathyroid hormone in plasma from selectively catheterized thyroid veins. *Ann Surg* 117:93–98, 1973

Systemic to Pulmonary Venous Communication in the Superior Vena Caval Syndrome

EDWIN S. WILSON¹

A case of superior vena caval obstruction due to bronchogenic carcinoma is presented. Upper extremity venography demonstrated shunting of contrast media from systemic veins to the right pulmonary veins. This collateral pathway has not been previously described in the superior vena caval syndrome. A proposed mechanism for this flow pattern is discussed.

Obstruction of the superior vena cava was first reported in 1747 by Hunter [1] in a patient with aortic aneurysm. Schechter [2] summarized the world literature in 1954 and noted that over 500 cases of superior vena caval obstruction had been reported since the original description of Hunter. The mechanism of obstruction in over 80% of patients with the superior vena caval syndrome is mediastinal neoplasm [3, 4]. Less frequent causes of caval obstruction include tuberculosis, histoplasmosis, pyogenic mediastinitis, aneurysm, and idiopathic thrombophlebitis of the innominate veins and/or superior vena cava.

Obstruction from any cause may produce the superior vena caval syndrome, and the severity of the clinical manifestations depends largely upon the degree or completeness of caval obstruction. The superior vena caval syndrome consists of swelling and edema of the head and neck, orbital proptosis, venous distention of the neck and trunk, cyanosis, headache, dizziness, and syncope. Upper extremity phlebography may be used to document the site and extent of venous occlusion and may provide clues to the obstructing agent in undiagnosed cases [3, 4]. Venography in advanced cases of caval obstruction will graphically demonstrate the venous collateral channels and pathways which develop in an attempt to bypass the obstructed caval segment.

There are four generally recognized collateral pathways which may develop in patients with obstruction of the superior vena cava [3-6]. The case presented demonstrates these classic collateral pathways as well as flow of contrast medium from systemic chest wall veins to pulmonary veins of the right lung. This apparently represents a fifth possible collateral pathway for venous return, which to my knowledge has not been previously reported.

Case Report

A 36-year-old female was admitted to the hospital because of progressive dyspnea, cyanosis, facial edema, and dizziness. She had received 4,000 rads to the right hilum and mediastinum 12 months earlier because of inoperable carcinoma of the lung. The patient had smoked one pack of cigarettes daily since age 15.

Physical examination revealed a mildly cachectic female with dyspnea and moderate respiratory distress. The respiratory rate was 28/min. There was cyanosis of the head and shoulders, venous dis-

tention of the neck and upper thorax, and bilateral orbital proptosis. Blood pressure in the semirecumbent position was 125/75 mm Hg, and the apical pulse was 100/min. Excursion of the right thorax was limited, and there was dullness to percussion and absent breath sounds; the left thorax was resonant with normal breath sounds. Prominent veins were present over the chest and abdomen, but the abdomen was soft and liver and spleen were normal size. Peripheral pulses were normal.

Hemoglobin was 14.6 g/100 ml, white blood cell count was 14,600 cells/mm³, and blood urea nitrogen was 24 mg/100 ml.

Chest radiograph on admission revealed complete opacification of the right thorax (fig. 1). Upper extremity phlebography demonstrated apparently complete bilateral obstruction of the subclavian veins and opacification of numerous dilated collateral veins over the chest and abdomen (fig. 2). There was filling of the azygos, lateral thoracic, and internal mammary collateral pathways as well as reflux of contrast medium into the vertebral collateral veins. An unexpected finding was opacification of the right pulmonary veins, which occurred early in the examination prior to visualization of the right atrium, ventricle, or pulmonary artery. Visualization occurred synchronously with opacification of small veins within the right chest wall. The patient experienced marked dyspnea during the examination, and further study was not feasible.

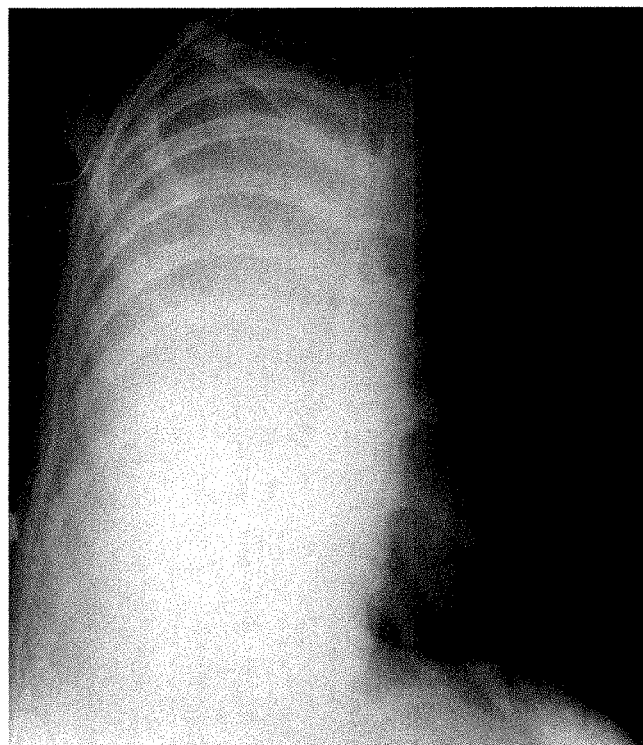


Fig. 1.—Frontal chest radiograph showing complete opacification of right hemithorax.

Received January 5, 1976; accepted after revision March 20, 1976.

¹ Department of Radiology, Burlington County Memorial Hospital, 175 Madison Avenue, Mt. Holly, New Jersey 08060.

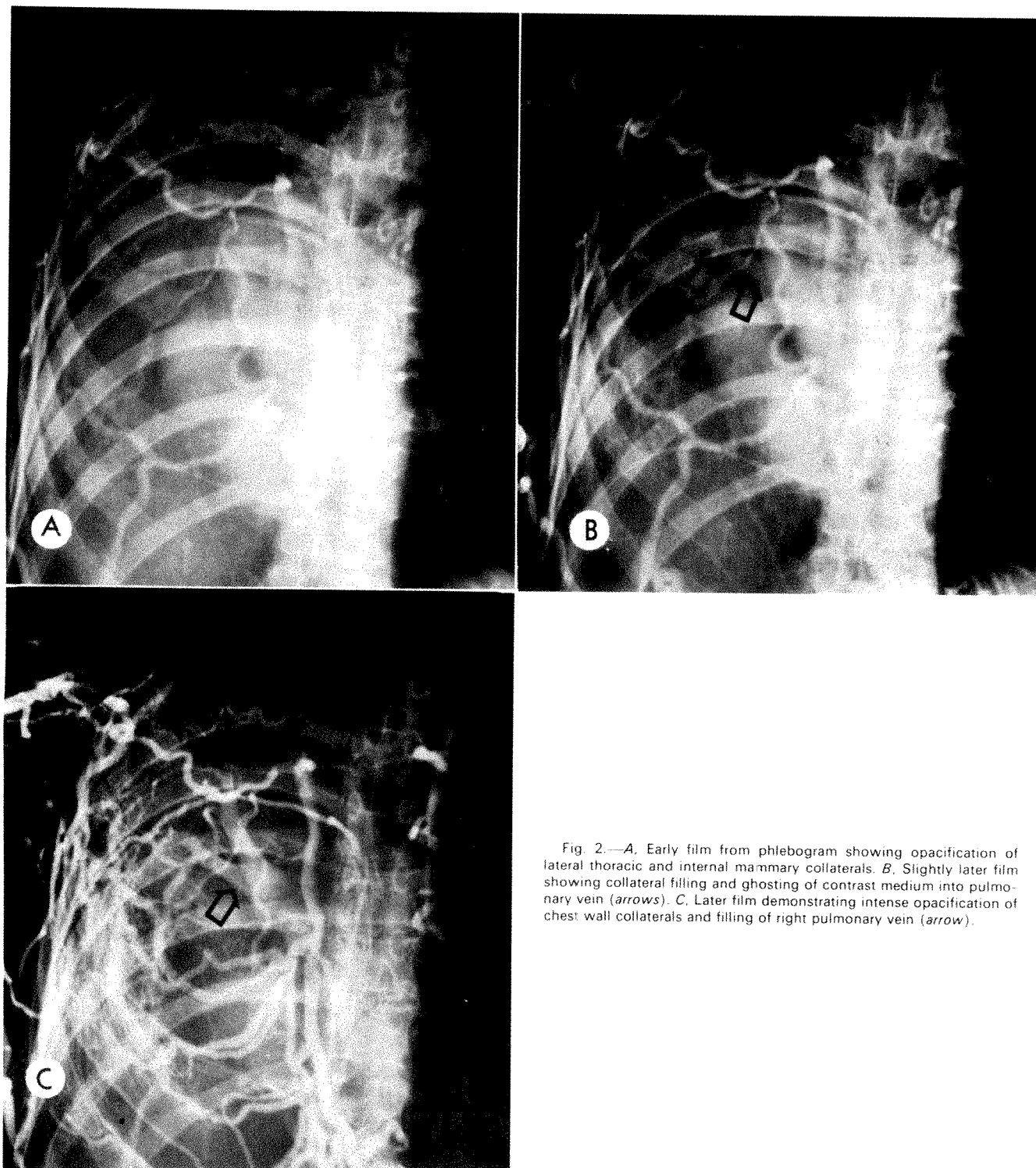


Fig. 2.—*A*, Early film from phlebogram showing opacification of lateral thoracic and internal mammary collaterals. *B*, Slightly later film showing collateral filling and ghosting of contrast medium into pulmonary vein (*arrows*). *C*, Later film demonstrating intense opacification of chest wall collaterals and filling of right pulmonary vein (*arrow*).

Because of the previous irradiation, the patient received emergency medical therapy with intravenous diuretics and corticosteroids. Despite these measures, the patient continued to deteriorate and expired 5 days after admission.

Autopsy revealed extensive malignancy of the right lung, pleura, and mediastinum; multiple adhesions between the right lung and the chest wall; and compression and infiltration of the superior vena cava, with thrombosis of the innominate and subclavian veins. Histologic sections confirmed the previous diagnosis of adenocarcinoma of the lung.

Discussion

Obstruction of the superior vena cava provides the stimulus for the development of at least four generally recognized collateral pathways for the return of venous blood to the heart [1].

Internal mammary pathway. This pathway consists of the internal mammary, superior epigastric, inferior epigastric, musculophrenic, and superficial veins of the thorax. These collaterals fill the iliac veins and inferior vena cava.

Azygos pathway. This consists of the azygos, hemiazygos, intercostal, and lumbar veins.

Lateral thoracic pathway. This includes the lateral thoracic, thoracoepigastric, superficial epigastric, superficial circumflex, long saphenous, and femoral veins to the inferior vena cava.

Vertebral pathway. This consists of the innominate, vertebral, vertebral plexus, intercostal, lumbar, and sacral veins to the azygos and internal mammary pathways.

Blood may return to the right atrium by any one of these routes or, as more frequently happens, by various combinations of the collateral pathways. Phlebography demonstrates the obstruction, and delayed films of the thorax and/or abdomen demonstrate the collateral pathways described above. Although obstruction is easily seen,

retrograde thrombosis superimposed upon the neoplastic infiltration of the cava may prevent visualization of the precise point at which it occurs.

Opacification of the pulmonary veins as a collateral pathway during phlebography in patients with caval obstruction has not been previously described to my knowledge. While the mechanism in this patient is not proven it certainly seems related to the development of venous anastomoses within pleural adhesions described at autopsy. The development of the venous anastomoses between the systemic and pulmonary systems provided the mechanism whereby blood could flow from the dilated systemic veins of the chest wall to the theoretically lower pressure venous collaterals on the outer surface of the lung, and thereby to the right pulmonary veins observed radiographically. Although unusual, this fifth theoretical pathway should be added to the generally recognized collateral venous channels in patients with superior vena caval obstruction.

REFERENCES

1. Hunter W: History of aneurysm of aorta with some remarks on aneurysm in general. *Med Observations Inquiries*, 1:323-357, 1747
2. Schechter MM: Superior vena cava syndrome. *Am J Med Sci* 227:46-56, 1954
3. Abrams HL: *Angiography*, 2d ed. Boston, Little, Brown, 1971
4. Roberts DJ Jr, Dotter CT, Steinberg I: Superior vena cava and innominate veins: angiographic study. *Am J Roentgenol* 66:341-352, 1952
5. Brown RC, Nelson CMK, Lerona PT: Angiographic demonstration of collateral circulation in a patient with the superior vena caval syndrome. *Am J Roentgenol* 119:543-546, 1973
6. Okay NH, Bryk D: Collateral pathways in occlusion of the superior vena cava and its tributaries. *Radiology* 92:1493-1498, 1969

Pseudocavitary Granulomas of the Lung

NICHOLAS BANCKS¹ AND JESUS ZORNOZA²

Due to the high lipid content of the caseous material in granulomas of the lung, these lesions may radiographically mimic truly cavitated pulmonary neoplasms or granulomas. Four cases of pseudocavitation within granulomas of the lung are presented along with their clinical, radiographic, and pathologic features. In all four cases diagnosis was made only after surgery.

Very little has been written about pseudocavitary granulomas of the lung [1, 2]. Although the radiographic demonstration of this entity is uncommon, it is of interest to realize that not all apparently excavated coin lesions are truly cavitated. This presentation includes the clinical, pathologic, and radiographic findings of pseudocavitary granulomas of the lung seen in four patients.

Case Material

Clinical Findings

All four cases were referred to the M. D. Anderson Hospital with a diagnosis of probable bronchogenic carcinoma.

The patients, three male and one female, ranged in age from 38 to 54 years. In all cases the pulmonary lesions were incidental radiographic findings. Except for one patient with a positive PPD 2 years before, history and routine screening tests for granulomatous disease (bronchoscopy in all patients, mediastinoscopy in two, and bronchial brushing in one) were negative for positive cytology or organisms. All four patients ultimately underwent wedge resections of the lungs.

Radiographic Findings

In all cases the lesion was solitary and ranged in size from 1 to 3 cm. No characteristic segmental distribution was found, although all of the lesions were posteriorly located. In only one case was calcification seen; it was ring shaped (fig. 1). No satellite lesions were found, even on tomography. In all cases, the wall of the apparent cavity was thick and had a smooth outer contour without surrounding infiltrate (fig. 2), with an inner wall that was irregularly nodular (fig. 3). There was no air-fluid interface or free intracavitary material in any of the cases, nor was there associated hilar or mediastinal adenopathy.

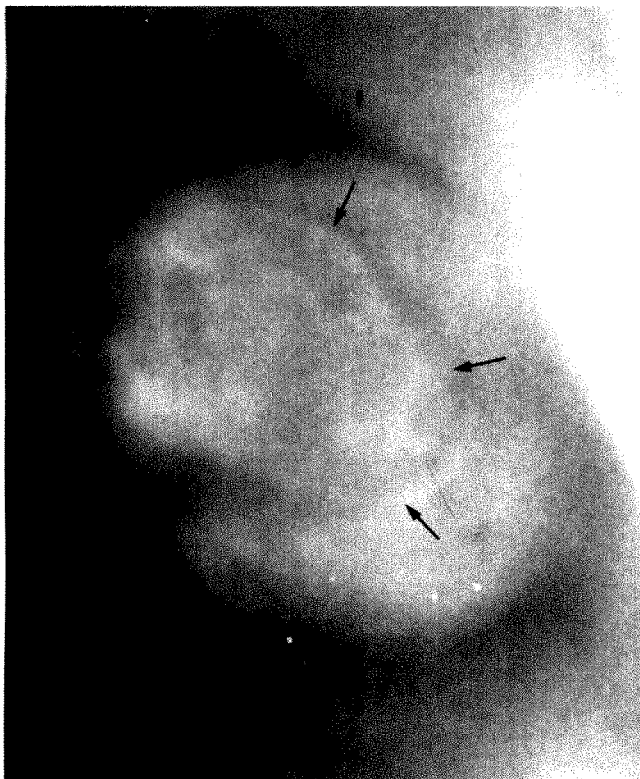


Fig. 1.—Granuloma (3×2 cm) in left lower lobe. Tomogram showing calcific ring (arrows) surrounding caseous necrosis.

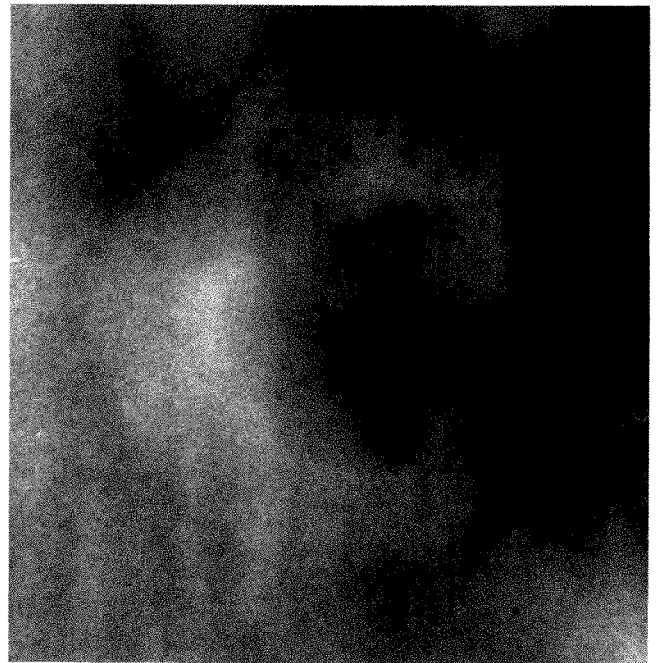


Fig. 2.—Granuloma (3×3 cm) in left lower lobe. Tomogram demonstrating sharply margined zone of relative lucency.

¹ Resident in Diagnostic Radiology, University of Texas Medical School at Houston, Houston, Texas 77030.

² Department of Diagnostic Radiology, University of Texas System Cancer Center, M. D. Anderson Hospital and Tumor Institute, Houston, Texas 77030. Address reprint requests to J. Zornoza.



Fig. 3.—Granuloma (3×3 cm) in right lower lobe. Relatively lucent zone has irregular inner margin.

Pathologic Findings

The lesions in all four cases were found to be benign granulomas. In one case spheroid bodies within the granuloma were strongly suggestive of coccidiomycosis. However, in all cases bacteriologic workup failed to demonstrate viable organisms. None of the specimens demonstrated a true cavity, and no evidence of communication between the nodule and bronchial tree could be demonstrated. Rather the lucency within the lesion was due to caseation in three of our cases and to fat necrosis within the granuloma in the other (fig. 4).

Discussion

Though the roentgenographic presentation of pseudo-cavitating granuloma was described in 1955 [2], the entity

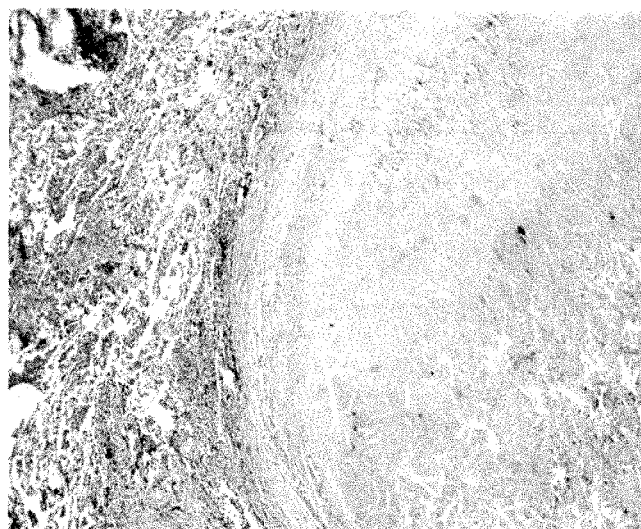


Fig. 4.—Section of lung showing fibrocaseous granuloma with fat necrosis. Hematoxylin and eosin stain, ×20.

has since received little attention. The radiolucent appearance can be readily understood in view of the high lipid content of caseous material [3, 4]. The difficulty in radiologic differentiation of this lesion from truly cavitating neoplasms or granulomas of the lung is obvious; the diagnosis must ultimately rest on histologic verification. However, as our experience indicates, this is a lesion which does occur in clinical practice and which should be included in the differential diagnosis of an apparently cavitating coin lesion.

REFERENCES

1. Fraser RG, Pare JAP: *Diagnosis of Diseases of the Chest. An Integrated Study Based on the Abnormal Roentgenogram*, vol 1. Philadelphia, Saunders, 1970
2. Maylock RL, Dillon RF, Stead WW: Roentgenographic simulation of cavitation by caseous material in lung lesions. *Am Rev Tuberc Pulm Dis* 71:529-543, 1955
3. Boyd W: *A Textbook of Pathology*. Philadelphia, Lea & Febiger, 1961
4. Lang ER: *The Chemistry and Chemotherapy of Tuberculosis*, 3d ed. Baltimore, Williams & Wilkins, 1958

Percutaneous Spot Localization of Nonpalpable Breast Lesions

JOHN W. HORNS¹ AND ROLF D. ARNDT²

The spot method of localization is applied to nonpalpable breast lesions detected at mammography. This percutaneous procedure is easy to perform, comfortable for the patient, and highly accurate in facilitating surgical excision of the smallest amount of breast tissue for microscopic examination.

The primary goal of the mammographer is detection of breast carcinoma in an early stage. Achieving this often means finding a lesion which cannot be palpated in the intact breast. Prior to biopsy, it is essential that the mammographer localize the lesion to facilitate surgical excision of a small portion of breast tissue containing the suspicious lesion for examination by the pathologist.

The first requirement for accurate localization of a nonpalpable lesion by mammography is high quality film or xeroradiographs made during compression of the breast. Craniocaudad and mediolateral radiographs are essential, and sometimes axillary views are helpful. Beyond this, several methods for more precise localization have been described:

1. The drawing of coordinates on the mammogram to localize the lesion according to its relationship with vertical and transverse midnipple lines and/or plotting such coordinates on a paper mammographic map which in turn displays the lesion in mediolateral, craniocaudad, and frontal projections. This map is then taken to surgery [1, 2].

2. Taping to the breast strips of plastic numbers at regular intervals and then performing mammography, thus allowing direct coordinates to be taken off the films with minimal distortion [3].

3. X-ray photogrammetry, which consists of localizing a lesion in three dimensions by taking stereo craniocaudad mammograms of the breasts to which appropriate skin markers have been attached. The suspect lesion is then localized by peripheral coordinates, and its depth in the breast may also be determined [4].

4. Use of a Plexiglas compression device with multiple precisely separated perforations attached directly to a Senograph mammography unit. The breast remains in position while the films are taken and studied, and the lesion is identified according to its location beneath a given hole. By passing a needle through the hole under which the lesion appears, biopsy may be performed directly in the mammography suite. This method may be used for open biopsy by inserting one or two needles (at right angles to one another) and leaving them in place, while the patient is sent to the operating room [5].

5. A type of percutaneous needle localization where one long 25-gauge needle is inserted into the breast at or near

the lesion from the coordinates plotted on the preceding mammograms. Upon accurate positioning, the needle is taped in place and the patient sent to surgery [6, 7].

6. A percutaneous needle localization similar to above, using two needles at right angles to one another [8].

7. The so-called spot method, first introduced by Rabin [9] in 1941 to localize lung abscesses. This has been applied to the breasts and consists of injecting a mixture of colored dye and radiopaque contrast at or very near a suspicious lesion [10, 11]. We have used this method successfully on over 70 patients and have been pleased with the results, as have our referring surgeons. A description of the technique follows.

Technique

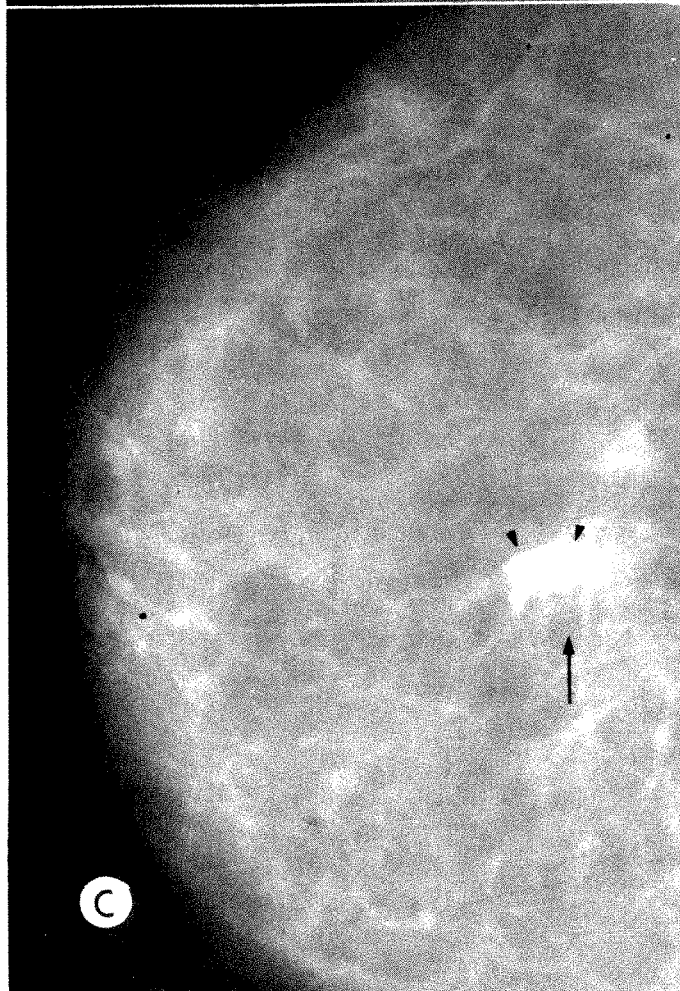
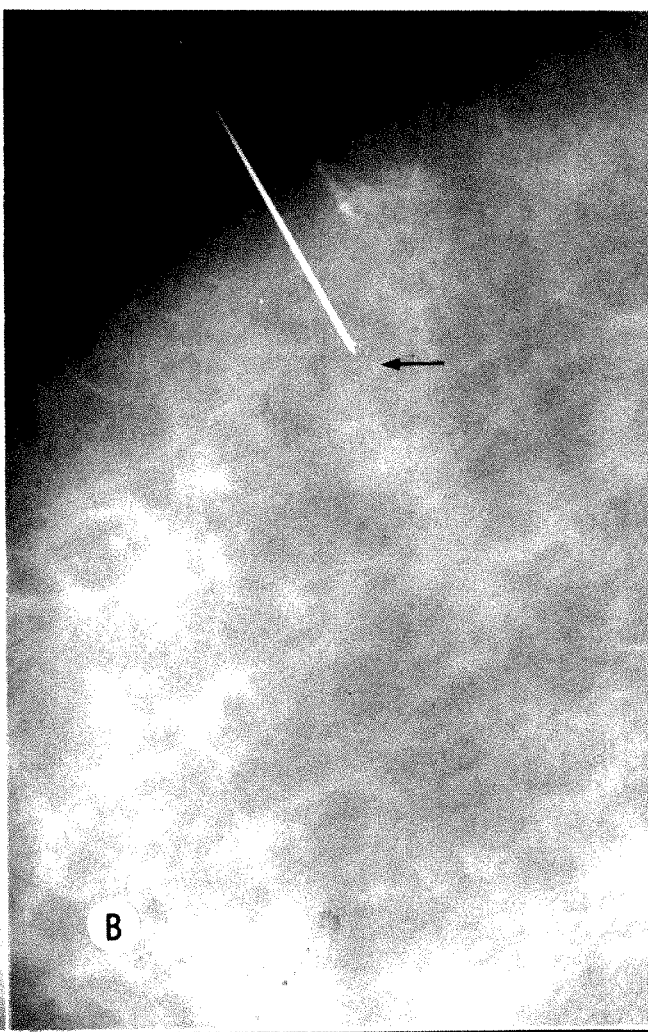
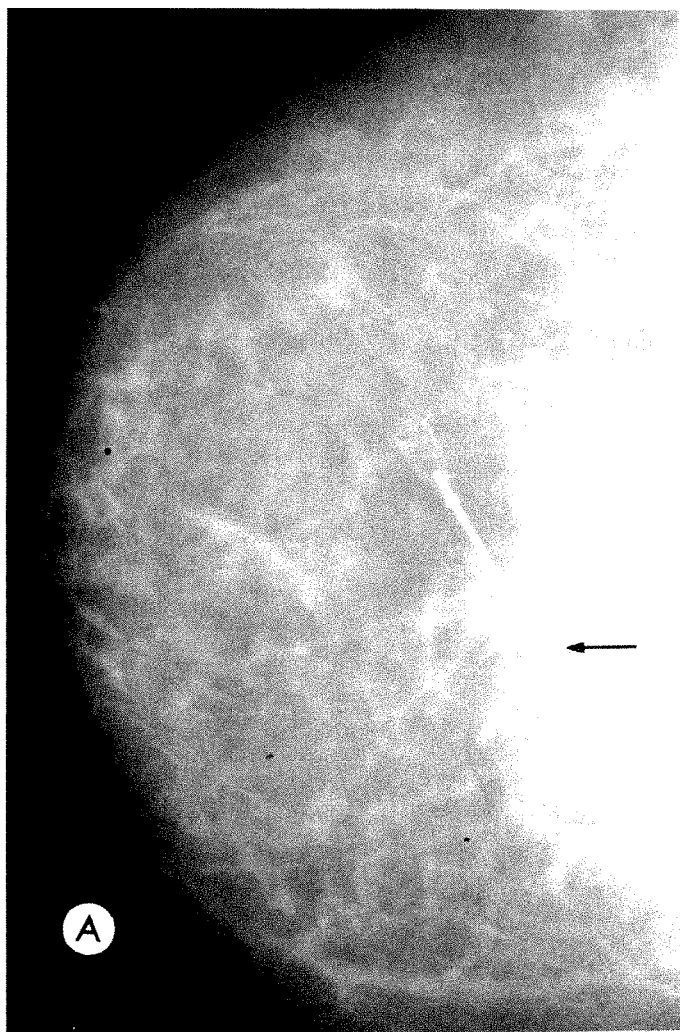
The site for insertion of the localizing needle is selected by using coordinate measurements in relation to the nipple taken from the craniocaudad and mediolateral mammograms. The length of needle to be used is determined by the depth of the lesion. When the suspect area is at 3, 6, 9, or 12 o'clock position, the depth can be measured directly from the mammograms. If the lesion is elsewhere, the depth is usually not as great as it appears on the radiographs.

Skin and subcutaneous tissues are infiltrated with 1% Xylocaine. In most women there is little or no pain sensation in the breast tissue deep to the subcutaneous layers; thus local anesthesia may be limited to the skin. The localization needle is then inserted in the direction and depth determined by the coordinate measurements made on the mammograms. Repeat craniocaudad and mediolateral mammograms (xeroradiography or film) are obtained with the needle in place (figs. 1A and 1B). These show the relationship of the needle tip to the lesion and indicate changes in position that might be needed. Often there is increased resistance as the needle enters abnormal breast tissue. When the needle tip has been satisfactorily positioned, 0.1 ml of a solution of equal parts of colored dye (Evans or Sky Blue) and radiopaque contrast agent previously drawn up and mixed in a tuberculin syringe is injected. A small amount of air is flushed through the needle to expel the contents. The needle is withdrawn and repeat craniocaudad and mediolateral mammograms are taken to determine the distance and direction of the lesion from the radiopaque dye (figs. 1C, 1D, and 2). The surgeon is advised of these measurements, and this final pair of mammograms is sent with the patient to the operating room. At surgery, with the patient supine, the breast will be in a different position than during mammography. However, the relationship of

Received January 26, 1976; accepted after revision April 23, 1976.

¹ Department of Radiology, Saint John's Hospital and Health Center, 1328 22d Street, Santa Monica, California 90404. Address reprint requests to J. W. Horns.

² Department of Radiology, UCLA Center for the Health Sciences, Los Angeles, California 90024.



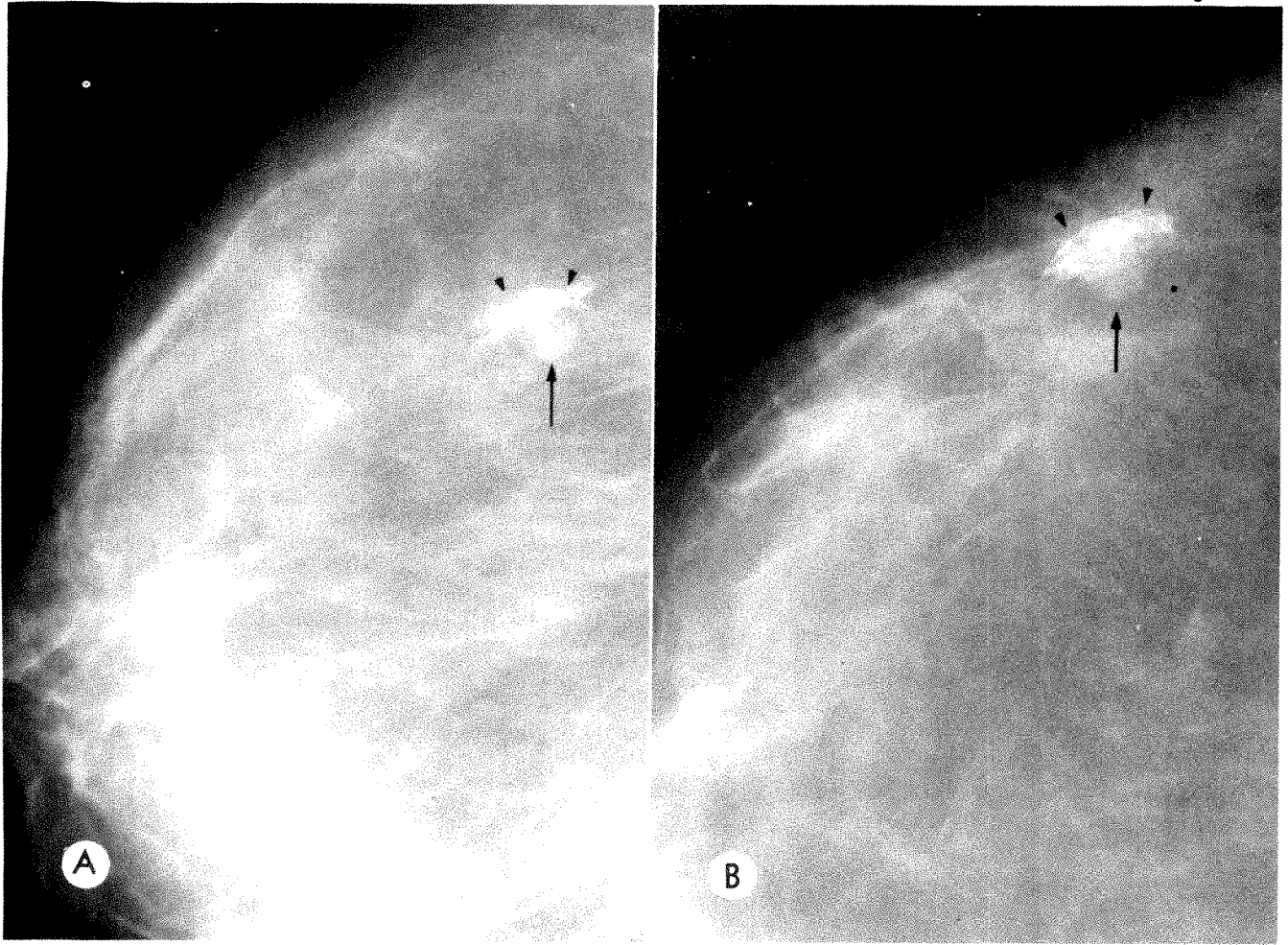


Fig. 2.—Fibroadenoma. Mediolateral (A) and craniocaudal (B) mammograms showing preoperative spot localization (arrowheads) of small nonpalpable breast mass (arrow).

the colored dye to the lesion will remain nearly the same.

The surgeon explores the appropriate quadrant of the breast and, upon finding the colored dye, excises the most economical section of breast tissue corresponding to the relationships with the dye given by the mammographer. The excised tissue is then sent for specimen radiography to verify that it contains the lesion.

Discussion

We have found that the spot method is easy for the radiologist to perform, is not unpleasant to the patient, and is an accurate guide to the biopsy site for the surgeon. The main disadvantage of localization methods based on the transfer of coordinates either directly to the breast at surgery or onto a paper mammographic map is that mammograms are taken in the sitting position, while the patient is supine at surgery. The breast thus falls laterally and supe-

riorly, especially if large. The spot method overcomes this problem.

While localization with indwelling needles also overcomes the sitting-to-supine distortion, securing a needle with tape risks movement and subsequent displacement. The average breast is predominantly fat, which at body temperature is nearly liquid. There is little solid tissue to hold the needle, and we have observed shifts in position with respiration alone. We prefer the method by which a needle is inserted and properly positioned with the aid of mammograms, followed by injection of dye and contrast agent. Since there is some diffusion of the blue dye at the injection site, surgery should follow within 4 hr of injection.

It should be noted that any localization method for suspicious calcifications should be accompanied by specimen radiography. However, this is only occasionally helpful in identification of a noncalcified lesion because of tissue dis-

Fig. 1.—Sclerosing adenosis. Mediolateral (A) and craniocaudal (B) mammograms showing position of localization needle relative to clustered microcalcifications (arrow). C and D, Films following injection of iodinated contrast and colored dye indicating exact relationship of dye spot (arrowheads) to calcifications (arrows). Films enhanced for purposes of publication.

tortion during resection. We prefer the method by which the entire specimen is radiographed, surrounded by lead numbers as on the face of a clock. The wedge containing the lesion (usually microcalcifications) is identified by the corresponding number. The section is then dissected by the pathologist or by us, radiographed again to verify the pathological tissue, and sent for microscopic examination.

We have had no complications in over 70 successful localizations. Review of surgical and pathological reports on noncalcified lesions and our own correlation with specimen radiographs of calcified lesions indicates that the suspicious tissue was indeed localized and removed in all cases. Among the localizations performed, 57% were for noncalcified lesions. The incidence of malignancy in the total series is 17%.

ACKNOWLEDGMENT

We are grateful to Ms. Jean Kossuth for excellent technical assistance.

REFERENCES

- Berger SM, Curcio BM, Gershon-Cohen J, Isard HJ: Mammographic localization of unsuspected breast cancer. *Am J Roentgenol* 96:1046-1052, 1966
- Stevens GM, Jamplis RW: Mammographically directed biopsy of nonpalpable breast lesions. *Arch Surg* 102:292-295, 1971
- Frankl G, Rosenfeld DD: Breast xeroradiography: analysis of our first seventeen months. *Ann Surg* 178:676-679, 1973
- Price JL, Butler PD: Steroscopic measurement in mammography. *Br J Radiol* 44:901, 1971
- Muehlow A: A device for precision needle biopsy of the breast at mammography. *Am J Roentgenol* 121:843-845, 1974
- Threatt B, Appleman H, Dow R, O'Rourke T: Percutaneous needle localization of clustered mammary microcalcifications prior to biopsy. *Am J Roentgenol* 121:839-842, 1974
- de Sevilla EQ, Debnam JW, Staple TW: Preoperative localization of nonpalpable breast lesions. Symposium exhibit presented at the American College of Radiology annual conference on Detection and Treatment of Early Breast Cancer, San Juan, Puerto Rico, March 1975
- Dodd G: Preoperative radiographic localization of nonpalpable lesions. Paper presented at the American College of Radiology annual conference on Detection and Treatment of Early Breast Cancer, Lake Buena Vista, Florida, March 1974
- Rabin CB: Precise localization of pulmonary abscesses by the spot method. *J Thorac Surg* 10:662-664, 1941
- Simon N, Lesnick GJ, Lerer WN, Bachman A: Roentgenographic localization of small lesions of the breast by the spot method. *Surg Gynecol Obstet* 134:572-574, 1972
- Shepard D, Soder P, Cooper D, Eaton B, Godwin J: Mammography: an aid in the treatment of carcinoma of the breast. *Ann Surg* 179:749-756, 1974

Double-blind Comparison of Meglumine Iodoxamate (Cholovue) and Meglumine Iodipamide (Cholografín)

ALAN H. ROBBINS,¹ E. NICHOLAS SARGENT,² MIRIAM E. VINCENT,¹
WILLIAM BOSWELL,² AND HARVEY I. MEYERS²

A double-blind comparison of two intravenous cholangiocholangiographic agents of similar molecular structure, meglumine iodoxamate and meglumine iodipamide, was carried out in 90 patients. Each produced a comparably high percentage of satisfactory examinations. A similar pattern of excretion speed and intensity was noted for each, though meglumine iodoxamate appeared to be slightly more effective in patients with elevated serum bilirubin. Less evidence of hepatic toxicity and fewer and less serious adverse side effects were observed in patients given the newer agent, meglumine iodoxamate.

Meglumine iodoxamate is a new intravenous cholecysto-cholangiographic agent currently being evaluated in the United States. Its molecular structure is not unlike that of meglumine iodipamide. The major difference lies in the composition of the linkage between the two triiodinated benzoic acid rings. The two molecules in their acid forms are depicted in figure 1.

Preclinical studies in animals demonstrated greater biliary excretion of iodoxamate when compared to iodipamide. The animal studies also demonstrated less toxicity to the central nervous system, kidneys, and formed elements in the blood as well as significantly less severe cardiovascular side effects [1]. No electrocardiographic abnormalities of significance were noted with the newer agent, whereas marked ST segment and T-wave changes were noted with iodipamide.

Because of these characteristics, it was anticipated that iodoxamate would be potentially a superior agent for clinical use in human patients. Clinical trials performed in Europe documented both its effectiveness and relative safety [2].

The early clinical studies in the United States have further substantiated these impressions. Sargent et al. [3] studied 18 patients with essentially normal biliary function. The agent was found to be rapidly excreted and produced highly effective visualization of the biliary tree and gallbladder. No important adverse effects were noted. Robbins et al. [4] studied 18 patients, all of whom had elevated serum bilirubin. Successful examinations were obtained with serum bilirubin elevations as high as 6.5. Again, no important adverse effects were noted either clinically or by a wide variety of laboratory parameters.

This report is presented to document the results of a double-blind comparison of meglumine iodoxamate and meglumine iodipamide with respect to the quality of the radiographic examination and relative toxicity of the two agents.

Materials and Methods

A total of 90 patients were given an intravenous injection of either 20 ml of 52% meglumine iodipamide containing the equivalent of 260 mg/ml of organically bound iodine or 20 ml of 40% meglumine iodoxamate containing 183 mg/ml of organically bound iodine. The 20 ml dose was given intravenously over a 10 min interval. Patients received no premedication of any kind.

The study plan involved media assignment and labeling in accordance with a predesigned and balanced randomized assignment schedule so that by the end of the study each of the two agents was administered to 45 patients. Examinations were performed only when there was a clear-cut clinical indication for the procedure. Specifically, no clinically normal individuals were included in this study.

The films were independently evaluated by a radiologist who did not conduct the actual examination and who had no knowledge of the agent used. The scheduling of examinations was random.

Excluded from the study were pregnant females, patients with a history of hypersensitivity to intravenous contrast agents, patients below the age of 18, any patient who had an intravenous cholecysto-cholangiographic agent within 1 month prior to the study, and moribund patients. Also excluded were those with hyperthyroidism, sickle cell disease, pheochromocytoma, or multiple myeloma.

Clinical evaluation included a physical examination prior to the study, after 24 hr, and approximately 72 hr afterward. Vital signs were monitored before, during, and for 4 hrs immediately after administration of the contrast agent. In addition, a full laboratory profile was performed prior to the contrast study, after 24 hr, and after approximately 72 hr. This included CBC, platelets, urinalysis, serum creatinine, cholesterol, calcium, phosphorus, total bilirubin, albumin, total protein, uric acid, BUN, LDH, glucose, alkaline phosphatase, SGPT, and SGOT. Any laboratory abnormality occurring subsequent to administration of the drug was followed until the value returned to the predose level.

Of the 90 patients studied, 70 had creatinine clearances performed at the intervals noted above. The same 70 patients had electrocardiographic examinations performed prior to the study, during the injection, and within 10 min after the injection of contrast agent. Any patient who developed an electrocardiographic abnormality during the examination was restudied by ECG after 2 and 24 hr, respectively.

An abdominal scout film was obtained prior to drug administration. Serial radiographs of the right upper quadrant were then made at 10, 20, 30, 50, and 60 min after injection. If no opacification occurred within 30 min, laminography was employed after 40, 50, or 60 min. If no visualization was obtained by 60 min, follow-up films were obtained at 90, 120, and 240 min as well as after 24 hr.

Films were evaluated initially on the basis of technical adequacy. Those deemed adequate were then subjected to two evaluations. First, the quality of radiocontrast density of each portion of the biliary tree was studied separately (i.e., left and right subhepatic

Presented at the annual meeting of the American Roentgen Ray Society, Atlanta, Georgia, October 1975.

¹ Department of Radiology, Tufts University School of Medicine, and Veterans Administration Hospital, 150 South Huntington Avenue, Boston, Massachusetts 02130. Address reprint requests to A. H. Robbins at the Veterans Administration Hospital.

² Department of Radiology, Los Angeles County—University of Southern California Medical Center, Los Angeles, California 90033.

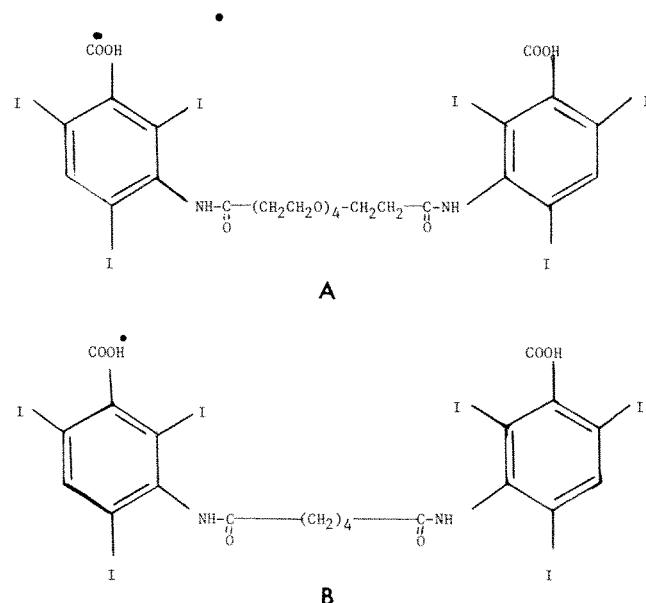


Fig. 1.—Molecular structure of iodoxamic acid (A) and iodipamide (B).

ducts, left and right hepatic ducts, cystic duct, gallbladder, and common bile duct). These were graded on the following basis: 0=no opacification; 1=faint opacification inadequate for diagnosis; 2=adequate opacification for diagnosis; and 3=superior opacification permitting diagnosis easily.

Second, after taking into account the available clinical and laboratory data, the suspected pathology, and the radiocontrast density, an overall evaluation was made as to whether the examination was indeed satisfactory.

All adverse reactions were noted, and, as far as could be determined, a judgment was made as to whether they were drug related. Reactions were graded on the following basis: mild=reactions disappearing spontaneously without treatment; moderate=reactions necessitating treatment with patients responding immediately to such treatment; and severe=alarming or life-threatening reactions with patients responding poorly, slowly, or not at all to treatment.

Results

Of the 45 patients studied with meglumine iodoxamate, 24 were male and 21 female. The group included 40 Caucasians and five blacks. Their ages ranged from 20 to 71 years (mean 46.0).

For the men, average weight and height were 71.5 kg and 173.3 cm; for the women, 77.2 kg and 162.8 cm.

Among the 45 patients who received meglumine iodipamide, 32 were male and 13 female. The group included 35 Caucasians, nine blacks, and one Oriental. Their ages ranged from 19 to 83 years (mean 50.5). The average weight and height for the men were 66.7 kg and 173.3 cm and for the women, 64.1 kg and 158.5 cm.

The preliminary clinical diagnoses are listed in table 1 and the radiologic diagnoses in table 2. Where surgical proof was obtained (eight who received iodoxamate and five iodipamide), the radiologic diagnoses were confirmed in all cases with the exception of one in the iodipamide group where duct disease was diagnosed but not confirmed at surgery. The only false negative in either series occurred in one patient given iodoxamate whose study was

TABLE 1
Preliminary Clinical Diagnoses

Preliminary Diagnosis	Agent Used	
	Meglumine iodoxamate	Meglumine iodipamide
Cholecystopathy	29	29
Cholangiopathy	14	13
Miscellaneous	2	3

TABLE 2
Radiologic Diagnoses

Diagnosis	Agent Used	
	Meglumine iodoxamate	Meglumine iodipamide
Normal	20	20
Cholecystopathy	10	9
Cholangiopathy	5	8
Undetermined	10	8

radiologically normal but was found to have cholesterosis at surgery.

Satisfactory Examinations

Successful examinations were obtained with iodoxamate in 35 of 45 patients (78%) and with iodipamide in 37 of 45 patients (82%).

In those patients with either normal or minimally abnormal serum bilirubin (0.1–1.5 mg/100 ml), a roughly equivalent pattern was noted. Satisfactory examinations were obtained in 31 of 33 patients (93.9%) who received iodoxamate and in all 35 patients (100%) given iodipamide. Failures with iodoxamate occurred in one patient who weighed in excess of 400 pounds and in another who had what turned out to be an acutely rising serum bilirubin.

In those patients with more marked elevation of serum bilirubin (greater than 1.5 mg/100 ml), iodoxamate appears to be somewhat better. Thus four of 12 patients (33.3%) showed satisfactory examinations (serum bilirubin range 1.8–6.0 mg/100 ml) as opposed to the iodipamide patients in whom only two of 10 (20%) were visualized satisfactorily (serum bilirubin range 2.0–4.3 mg/100 ml). It is worth noting that the patient in the iodoxamate group with serum bilirubin of 6.0 mg/100 ml was one who did satisfactorily opacify and that laboratory follow-up showed the serum bilirubin level to be stable.

The status of preexisting renal function did not seem to affect the success of the examination. Thus three of four patients in each study group with impaired renal function had satisfactory cholangiograms.

Opacification

To minimize confounding factors, the speed of excretion and maximum opacification obtained were assessed only

TABLE 3
Speed of Excretion and Maximum Opacification

Examination and Agent Used	Patients Who Opacified		Initial Visualization		Maximum Opacification within				Rated Superior or Adequate	
			within 20 min		60 min		90 min			
	No.	%	No.	%	No.	%	No.	%	No.	%
Hepatic ducts :										
Iodoxamate	26/33	78.8	22	84.6	26	100	16	61.5
Iodipamide	26/32	81.3	23	88.5	24	92.3	17	65.4
Common bile duct :										
Iodoxamate	30/33	90.9	30	100	28	93.3	30	100	30	100
Iodipamide	32/32	100	30	93.8	32	100	32	100	30	93.8
Gallbladder :*										
Iodoxamate	19/27	70.4	11	57.9	10	52.6	16	84.2	19	100
Iodipamide	22/27	81.5	11	50	16	72.7	19	86.4	20	90.9

Note.—Data on patients with normal bilirubin levels who opacified.

* Because 11 patients were cholecystectomized (six given iodoxamate and five iodipamide), opacification was evaluated in only 54 patients.

TABLE 4
Patients with Evidence of Hepatic Toxicity

Agent Used and Patient	Bilirubin	Alkaline Phosphatase	SGOT	SGPT	LDH
Iodoxamate:					
A	Slight, 24
B	Slight, 24	...	Slight, 24
C	Slight, 24	...
Iodipamide:					
A1	Moderate, 24, 72
B1	Moderate, 24	...	Slight, 24
C1	...	Marked, 24, 72	Marked, 24, 72	Marked, 24, 72	Marked, 24, 72
D1	Moderate, 72
E1	...	Slight, 72	Moderate, 72	Moderate, 72	...
F1	Slight, 72
G1	Slight, 24, 48	Slight, 48	Slight, 48

Note.—Slight=less than 50% elevation; moderate=50%-100% elevation; marked=more than 100% elevation. Numbers indicate time at which measurement taken.

in patients with normal bilirubin levels. A total of 65 patients had pretreatment serum bilirubin levels within the normal range (1.3 mg/100 ml or less). The results of this analysis are summarized in table 3.

Electrocardiographic Studies

Most of the patients studied had normal baseline electrocardiograms. Three of the iodoxamate group and eight of the iodipamide group had preexisting abnormalities. Each group included ischemic changes, arrhythmias, and evidence of ventricular hypertrophy. No alterations of the electrocardiograms were encountered in any of the patients studied with either agent (see table 5).

Renal Function

No striking evidence of renal toxicity was seen in either group based on observations of BUN, serum creatinine, and/or creatinine clearance. Of 38 patients with normal renal function given iodoxamate, two showed slight impairment of renal function at 24 hr only. The seven patients with abnormal renal function given iodoxamate showed no change.

Of 39 patients with normal renal function given iodipamide, three showed alterations in renal function: one mild impairment at 24 hr only, one moderate impairment at 24 hr only, and the third slight impairment at both 24 and 72 hr. The six patients with abnormal function at the outset who received iodipamide showed no change.

Hepatic Function

Alterations in hepatic function were noted in both study groups (table 4). In the iodoxamate group, three patients (7%) showed chemical evidence of hepatic toxicity. Serum bilirubin rose in two patients but returned to normal range within 72 hr. One of these two showed a transient elevation of SGOT. The third patient showed only a transient elevation of SGPT at 24 hr. No alterations were noted in serum LDH or alkaline phosphatase values.

Seven patients in the iodipamide group (16%) showed chemical alterations attributable to the contrast agent. One patient (G1) showed elevation of serum bilirubin which continued to rise at 48 hr, at which point he was lost to follow-up. There was concomitant slight elevation of alkaline phosphatase and SGOT.

TABLE 5
Summary of Adverse Reactions

Adverse Reaction	Iodoxamate	Iodipamide
Death	0	0
ECG abnormality	0	0
Nausea	2	3
Urticaria	2	2
Wheezing	0	1
Hypotension	1*	1†
Pruritus	2	1
Miscellaneous	0	3‡
Total	7	11
No. patients involved	4	6

* Mild.

† Severe.

‡ One tingling of face, one nasal congestion, one coughing.

Hematology and Urinalysis

Minor changes were noted in peripheral blood studies in both groups: 12 (26.7%) in the iodoxamate group and eight (17.8%) in the iodipamide group. These changes included minor alterations of hemoglobin, white blood cell count and differential, and platelet count. While all had to be ascribed to the drug used, many were of such minor degree that they could easily reflect laboratory error. No serious hematologic abnormalities were noted. It is interesting to note that six patients developed eosinophilia: five in the iodoxamate group (11.1%) and one in the iodipamide group (2.2%).

Four patients in the iodoxamate group and six in the iodipamide group (8.9% and 13.3%, respectively) showed minor changes in the urine up to 72 hr. These included proteinuria, microscopic pyuria, microscopic hematuria, and occasional casts. No serious findings were noted.

Adverse Reactions

Adverse reactions were reported in four of the patients given meglumine iodoxamate (8.9%) and in six (13.3%) given iodipamide. They are summarized in table 5.

Discussion

Little difference was found in the percentage of satisfactory examinations obtained with the two agents. Although the numbers are small, the data tend to support the earlier impression that iodoxamate offers some improvement in study of the jaundiced patient. Recent preliminary data on a larger series of patients showed satisfactory results in 161 of 185 (87%) patients given iodoxamate and 134 of 172 (77.9%) patients given iodipamide. A breakdown by bilirubin values is not yet

available [5].

Whereas previous studies have suggested a more intense and rapid biliary excretion of the newer agent, such a finding was not documented in this study. In fact, some of the data seem to suggest the opposite. However, the numbers involved are too small to draw any valid conclusions. Perhaps the present protocol was not sensitive enough to detect subtle differences in the degree of density or the speed of appearance of contrast in the biliary tree. If that is the case, then such a difference is probably so small as to be of little clinical significance.

In the area of patient safety, however, there does appear to be a pattern favoring the use of iodoxamate. Clearly a greater number of hepatic function abnormalities occurred in the iodipamide group. The abnormalities involved more patients, were of a more marked degree, and tended to persist longer. The frequency of such laboratory abnormalities is similar to that observed by Scholz et al. [6] in a recent toxicologic assessment of iodipamide.

A similar pattern is noted when other adverse reactions are considered. The adverse reactions that occurred in the iodipamide group tended to be greater in severity and number and occurred in a greater percentage of patients than those in the iodoxamate group. In a larger series from the Squibb Institute [5], a similar pattern was noted: 32 adverse reactions in 21 of 185 patients (11.4%) given iodoxamate compared to 43 in 29 of 172 patients (16.9%) given iodipamide.

In conclusion both drugs demonstrated a high degree of safety and overall effectiveness. There is a suggestion of advantage to using iodoxamate in the patient with elevated bilirubin. Preliminary results also suggest lower toxicity with the new agent. This may well prove to be its strongest asset.

REFERENCES

1. Tirone P, Rosati G: Radiopaque contrast media. 28. Toxicologic studies with iodoxamic acid, a new intravenous cholegraphic agent. *Farmaco [Sci]* 28:1011-1023, 1973
2. DiFazio LT: Summary of preclinical studies, in *Clinical Pharmacology Investigator's Brochure for SQ 21, 982*, Princeton, N. J., Squibb Institute for Medical Research, Sept 1973, pp. 1-14
3. Sargent EN, Schulman A, Meyers HI, Gutler RB, Nicoloff JT, DiFazio LT: A new contrast medium for cholangiocholangiography: meglumine iodoxamate. *Am J Roentgenol* 125:251-258, 1975
4. Robbins AH, Earampamoorthy S, Koff RS, DiFazio LT, Wickis EA, Gertler AN: Successful intravenous cholecystocholangiography in the jaundiced patient using meglumine iodoxamate (Cholovue). *Am J Roentgenol* 126:70-76, 1976
5. Zaki A, Frost D, Wasas K: Preliminary report: comparison of meglumine iodoxamate and Cholografin meglumine for intravenous cholecystography. Unpublished data, Princeton, N.J., Squibb Institute for Medical Research, August 1975
6. Scholz FJ, Johnston DO, Wise RE: Intravenous cholangiography. *Radiology* 114:513-518, 1975

Lymphoreticular Hyperplasia of the Stomach (Pseudolymphoma)

WILLIAM MARTEL,¹ MURRAY R. ABELL,² AND T. N. K. ALLAN^{1,3}

Three histologically proved cases of gastric lymphoreticular hyperplasia with long term follow-up are reported. This condition is often confused radiologically with ulcerating carcinoma and pathologically with malignant lymphoma. The presence of a large ulcer surrounded by a mass and associated with thick rugal folds and additional gastric or duodenal ulcers is not diagnostic but should suggest the possibility of this condition.

Recent interest in lymphoproliferative lesions of the stomach was stimulated largely by Smith and Hellwig [1] who reviewed 131 cases of "malignant lymphoma of the stomach" and noted in retrospect that 42 were in reality benign lymphoproliferative disorders. Attention has since been focused on the necessity of distinguishing these lesions, and a number of pathologic criteria have been suggested [2-4]. Many terms have been applied to this disorder, including chronic lymphoid gastritis [5], chronic atrophic "lymphoblastamoid" gastritis [6], reactive lymphoid hyperplasia [1], pseudolymphoma [2], and lymphoid hyperplasia [3]; this has contributed to problems of nosology and diagnosis.

Most papers dealing with this condition have emphasized pathologic features. This report emphasizes both the radiologic and pathologic findings in three histologically verified cases.

Case Reports

Case 1

A 17-year-old white male was seen 13 years ago at the University of Michigan Medical Center following a 9 month illness characterized by epigastric pain relieved by food, weight loss, and anemia. Radiologic examination of the upper gastrointestinal tract 2 months after onset of symptoms revealed a large gastric ulcer on the lesser curvature and a small ulcer in the pyloric region. He responded well to medical management but required hospitalization 1 month later due to continued blood loss. A second radiologic examination showed a decrease in the size of the larger ulcer and a deformity of the pyloroduodenal junction. He remained asymptomatic while under medical treatment, but his stools were repeatedly guaiac positive. Free gastric acid was present. Multiple gastric cytologic examinations were negative for malignant cells.

Radiologic examination of the stomach in February 1962 showed a crescentic gastric ulcer 4.5 cm in diameter on the lesser curvature of the body, surrounded by a thick ridge of tissue. The findings suggested an ulcerating neoplasm. There were prominent rugal folds throughout the stomach, particularly in the body. A smaller ulcer was noted high on the lesser curvature. The antrum tended to be contracted but was distensible. There was deformity at the pyloroduodenal junction and a question of a small duodenal ulcer (fig. 1).

The patient was treated conservatively. Reexamination of the stomach 4 weeks later showed considerable reduction in the size of the ulcer and adjacent mass (fig. 2). No other ulcers were evi-

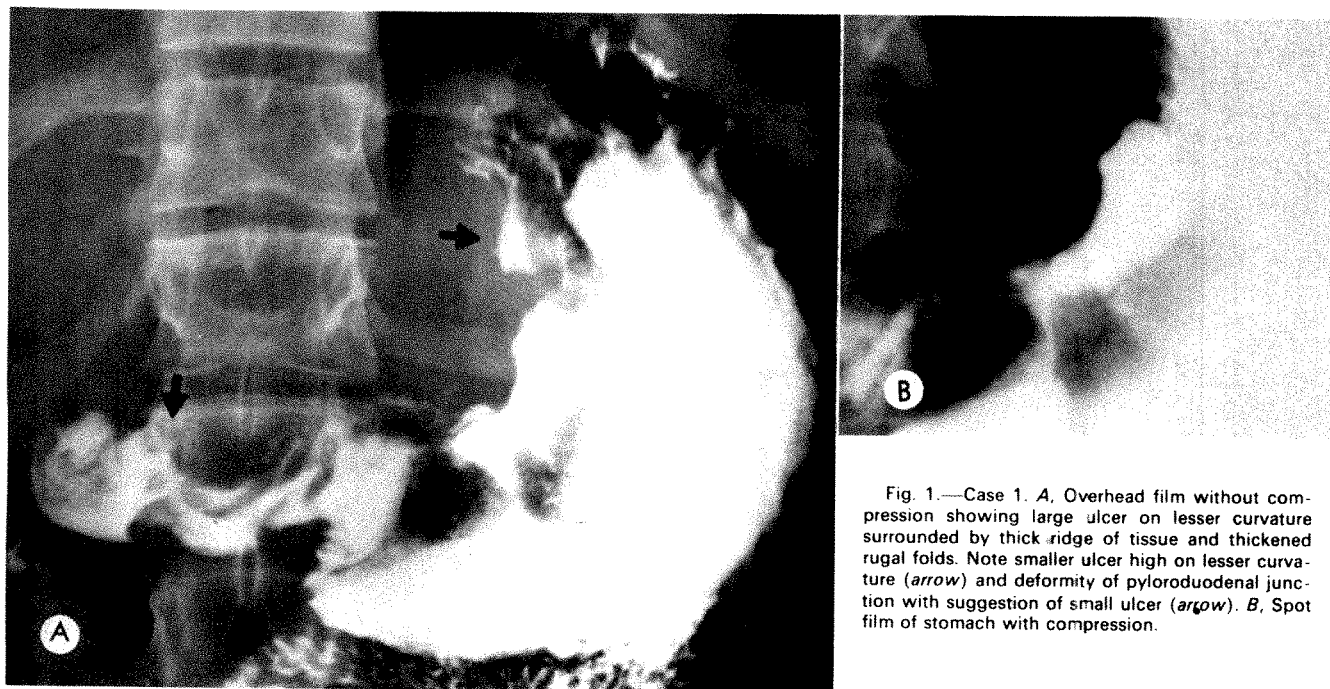


Fig. 1.—Case 1. A, Overhead film without compression showing large ulcer on lesser curvature surrounded by thick ridge of tissue and thickened rugal folds. Note smaller ulcer high on lesser curvature (arrow) and deformity of pyloroduodenal junction with suggestion of small ulcer (arrow). B, Spot film of stomach with compression.

¹ Department of Radiology, University of Michigan Medical Center, Ann Arbor, Michigan 48104.

² Department of Pathology, University of Michigan Medical Center, Ann Arbor, Michigan 48104.

³ Present address: Harborview Medical Center, Seattle, Washington 98104.



Fig. 2.—Follow-up 4 weeks later showing considerable reduction in size of ulcer and mass. No other ulcers evident. Note contracted antrum and persistent deformity of duodenal cap.

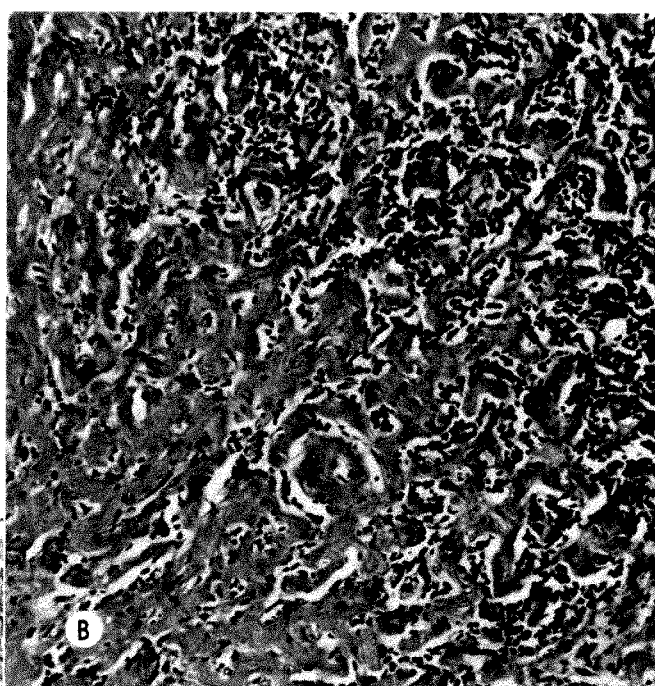


Fig. 3.—Microscopic studies, case 1. *A*, Chronic peptic ulcer with overhanging darkly stained mucosal margin heavily infiltrated with lymphoreticular cells. Cords of similar cells extend throughout scar tissue beneath its base. H & E, $\times 45$. *B*, Hyaline scar tissue from deep in base of ulcer infiltrated by clusters of proliferating lymphoreticular cells. H & E, $\times 200$.

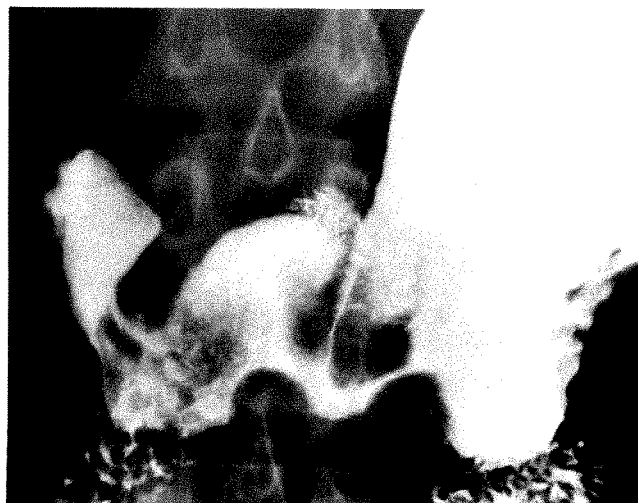


Fig. 4.—Case 2. Film showing mass on greater curvature of antrum with central, poorly defined ulcer associated with massively thickened rugal folds.

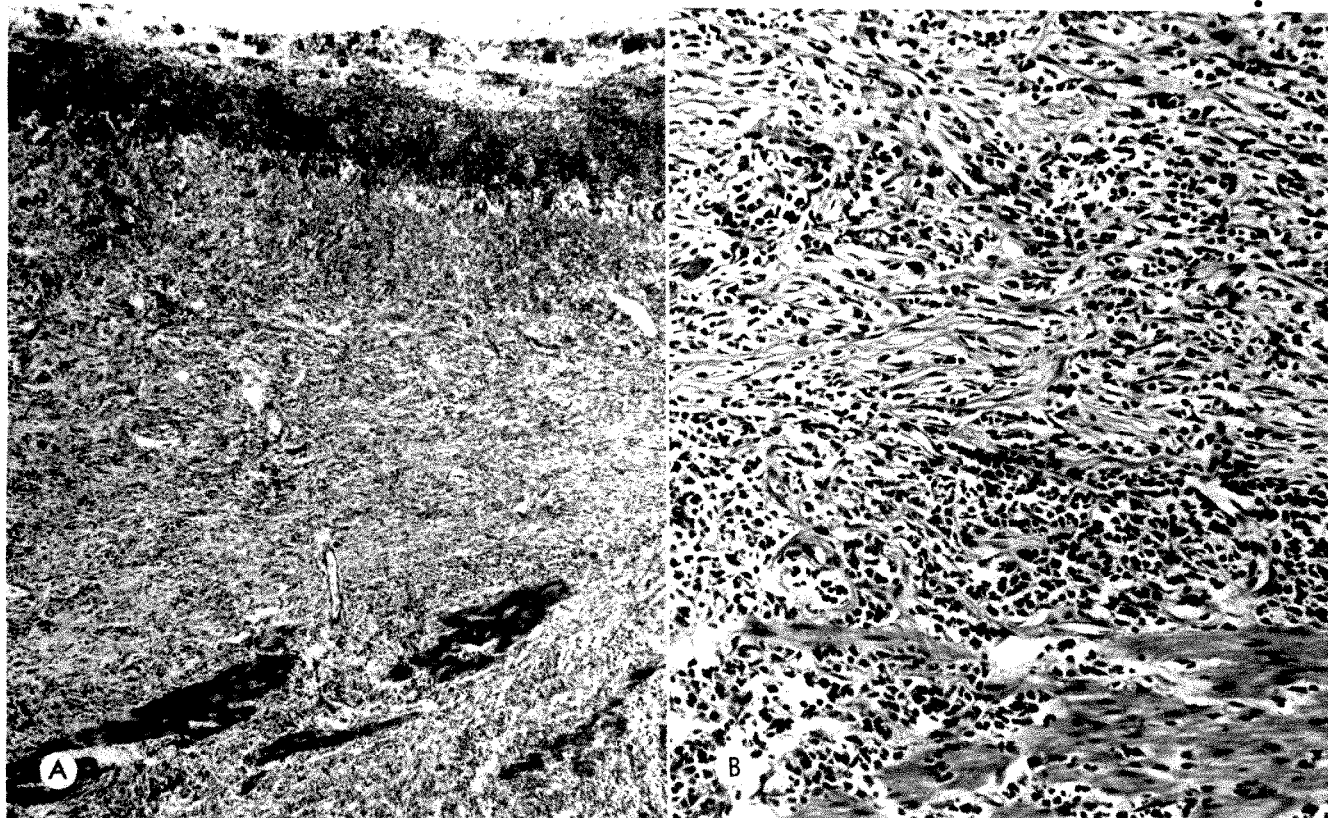


Fig. 5.—Microscopic studies, case 2. A. Section through base of ulcer. Darkly stained zone on the surface is fibrinopurulent exudate. Beneath it is chronic granulation and scar tissue with lymphoreticular infiltrate. Process extends into muscularis, isolating bundles of darkly stained smooth muscle. Masson's trichrome stain, $\times 65$. B. Scar tissue in base of ulcer showing muscularis infiltrated by lymphoreticular cells. H & E, $\times 200$.

dent, either in the stomach or duodenum, but there was a deformity of the superior aspect of the base of the duodenal cap. Reexamination 3 weeks later showed no change, but gastroscopic examination suggested an ulcerating neoplasm.

Surgical exploration in April 1962 revealed an 8×5 cm mass on the lesser curvature of the stomach adjacent to multiple enlarged soft lymph nodes. The gastric wall at the site of the ulcer was greatly thickened and hard. Biopsy and frozen sections of the gastric ulcer suggested lymphoma. A subtotal gastrectomy and gastroenterostomy were performed. Follow-up evaluation 13 years later showed the patient to be free of symptoms, and repeat radiologic examination of the upper gastrointestinal tract showed no evidence of recurrence.

The microscopic sections of the stomach confirmed the presence of a chronic peptic ulcer whose base was covered by a thin purulent and a fibrinous exudate (fig. 3A). Hyaline fibrous scar tissue extended deep into the underlying wall, replacing much of the muscularis. Throughout this scar there were nodules and cords of hyperplastic lymphoreticular cells and scattered plasma cells (fig. 3B). The mucosa and submucosa at the margin of the ulcer were infiltrated by proliferating lymphoreticular cells and plasma cells. Nodular collections of lymphoid cells with prominent reactive germinal centers extended peripherally along the muscularis mucosae.

Although the cells of the infiltrate were hyperplastic, neither the pattern of involvement nor the cytologic features were those of malignant lymphoma. Similarly, the regional lymph nodes showed follicular hyperplasia but no evidence of malignant lymphoma. The pathologic diagnosis was "chronic peptic ulcer with atypical lymphoreticular hyperplasia (pseudolymphoma)."

Case 2

A 59-year-old white male was seen in November 1963 at the Wayne County General Hospital (Eloise, Mich) with a history of postprandial nausea, vomiting, and epigastric pain of 3 weeks' duration and a recent 20 pound weight loss. He had epigastric tenderness. Free gastric acid was absent; hematocrit was 39%. Gastric cytology was negative for malignant cells. Radiologic examination of the stomach showed a mass on the greater curvature of the antrum 4 cm in diameter with a central poorly defined ulcer. The adjacent rugal folds were markedly thickened (fig. 4). Medical management did not provide relief of symptoms.

Surgical exploration 1 month later disclosed an antral mass extending to the serosa and several discrete enlarged soft pyloric lymph nodes. Subtotal gastrectomy and gastroenterostomy were performed. He was reevaluated clinically 9 years later and found asymptomatic.

A firm raised gastric lesion (3×2.5 cm) having a central ulcer involved the mucosa just proximal to the antrum. Microscopically, the base of the ulcer was covered by a purulent exudate (fig. 5A). A chronic granulation scar tissue extended from the base into the inner layer of the muscularis (fig. 5B). Throughout this scar and the adjacent mucosa and submucosa was a polymorphous inflammatory cell infiltrate consisting largely of lymphoreticular and plasma cells with a scattering of eosinophils and neutrophils. Near the periphery of the scarred area lymphoid nodules were prominent, some with reactive germinal centers. The lymph nodes showed hyperplasia and chronic inflammation with no evidence of malignant lymphoma. The pathologic diagnosis was chronic peptic ulcer with atypical lymphoreticular hyperplasia.

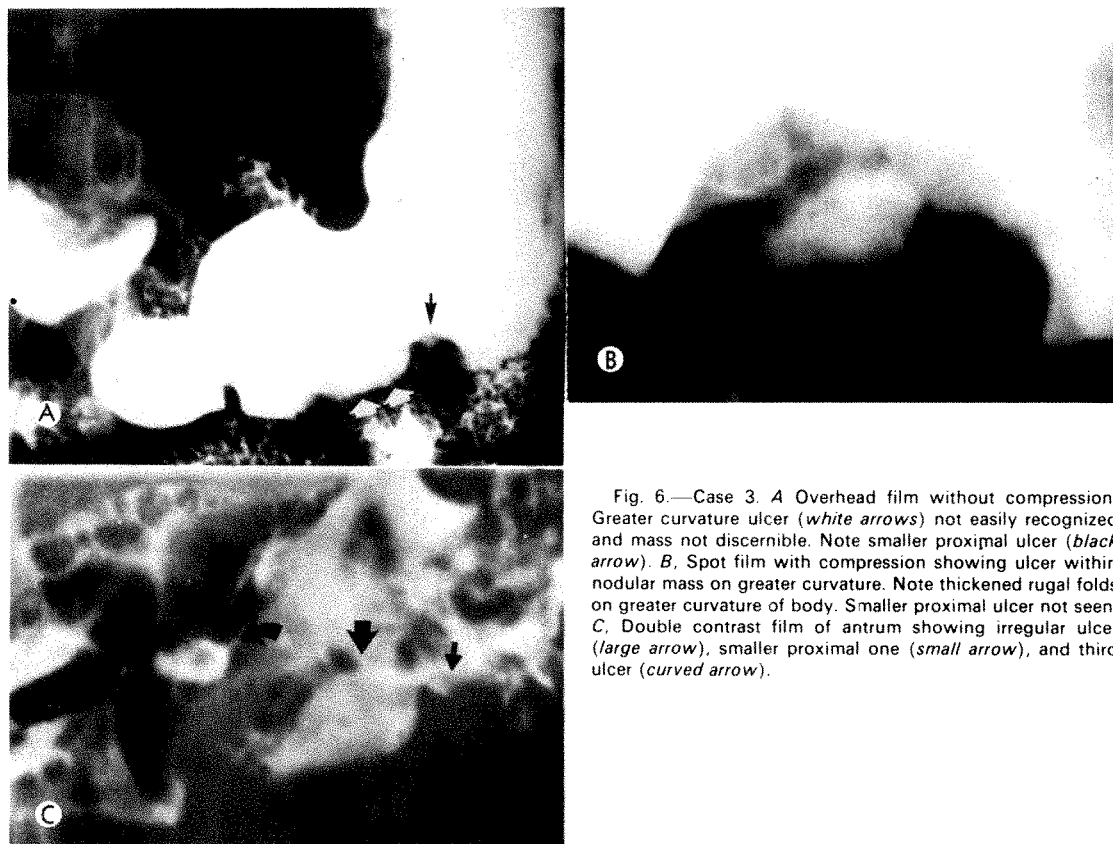


Fig. 6.—Case 3. A Overhead film without compression. Greater curvature ulcer (*white arrows*) not easily recognized and mass not discernible. Note smaller proximal ulcer (*black arrow*). B, Spot film with compression showing ulcer within nodular mass on greater curvature. Note thickened rugal folds on greater curvature of body. Smaller proximal ulcer not seen. C, Double contrast film of antrum showing irregular ulcer (*large arrow*), smaller proximal one (*small arrow*), and third ulcer (*curved arrow*).

Case 3

A 56-year-old white male was hospitalized in April 1974 because of a 10 day history of epigastric pain and tarry stools. Recurrent upper abdominal pain had been present for 2 years but had worsened in the past 2 weeks. There was no nausea or vomiting but a recent 5 pound weight loss. Radiologic examination of the stomach at this time was said to show a large antral ulcer. Hemoglobin was 8.7 g. No tests were done for gastric acidity. A subtotal gastrectomy and gastrojejunostomy were performed in April 1974. The pathology report stated "malignant lymphoma of the stomach."

The patient was referred to the University of Michigan Medical Center for possible radiation therapy. Review of the x-ray films showed an irregular ulcerated lesion on the greater curvature of the stomach. The ulcer measured 3 cm in diameter and was within a mass projecting into the lumen. The nodular mass could only be discerned on spot films with compression (fig. 6B). An additional ulcer 5 mm in diameter was present at the proximal margin of the mass (figs. 6A and 6C), and a third discrete ulcer 1 cm in diameter was evident in the antrum adjacent to the distal edge of the mass (fig. 6C). The rugal folds in the antrum were diffusely thickened and had a polypoid configuration, particularly near the greater curvature of the body.

Microscopic slides of the resected segment showed a chronic peptic ulcer with dense hyaline scar tissue extending into the underlying muscularis. Throughout this tissue was a nodular lymphocytic infiltrate composed of well differentiated small lymphocytes and a few histiocytes and plasma cells. Some of the proliferating nodules had well defined germinal centers. A similar nodular infiltrate involved the mucosa and the submucosa at the margin of the ulcer. There was no evidence of malignant lymphoma. The changes were

interpreted as chronic peptic ulcer with lymphoreticular hyperplasia.

Discussion

The differentiation of gastric lymphoreticular hyperplasia from lymphoma or carcinoma may be difficult. Clinical manifestations are not useful in this regard. The duration of symptoms tends to be longer in patients with hyperplasia than in those with neoplasms, but there are exceptions (case 2). Men have been affected more often than women, and the average age of the patients in one series was 57 years [7]. To our knowledge, case 1 (17 years old) is the youngest patient thus far reported. While abdominal pain, hematemesis, and melena are common, a palpable abdominal mass is unusual [4, 8]. Anemia is frequent. Free acid is usually present, but some patients have had achlorhydria [8].

Perez and Dorfman [7] noted a variety of radiologic findings in this condition, including "tumor" mass with ulceration, infiltrating constrictive lesions associated with ulceration, solitary well defined ulcer craters, and enlarged gastric rugae. Approximately half of their 15 cases were erroneously diagnosed as polypoid, infiltrating, or ulcerating carcinoma. Indeed, the two neoplasms most frequently confused radiologically with this entity are carcinoma and lymphoma.

The fact that the large ulcer in case 3 could be identified as such only with compression indicates that it represented

an ulcer within an intraluminal mass. This is a salient feature of Carmen's sign [9-11], which has been regarded as pathognomonic of an ulcerating carcinoma. Although it is admittedly difficult to reconstruct with certainty a three-dimensional view of the lesion in retrospect, the observations suggest that this case represents an exception to the rule. The detectability of the ulcers in cases 1 and 2 *without compression* indicates that they were located within the gastric wall. Nevertheless, the irregularity of the surrounding tissue in these cases did justify the suspicion of an infiltrating neoplasm associated with ulceration.

An essential point is that all of our cases had an "ulcerating tumor mass" associated with regional or generalized enlargement of the rugal folds. Two of our patients had other gastric or duodenal ulcers. It is conceivable that multiple ulcers are more likely to occur in this condition than in patients with the usual variety of peptic disease. Duodenal deformity due to earlier ulcer was noted to be associated with this disease in three cases [7].

Although gastric lymphoreticular hyperplasia has no specific radiologic features, this diagnosis should be considered in patients with gastric lesions if the pathology report suggests lymphoma. An erroneous initial diagnosis of gastric lymphoma was made on the basis of frozen sections in case 1 and as a final diagnosis in case 3.

Faris and Saltzstein [3] considered gastric lymphoid hyperplasia to be a nonspecific late stage of peptic ulceration of the stomach. In support of this concept is the frequent finding of varying degrees of lymphofollicular gastritis in patients with chronic peptic ulcers. Why some patients should develop a marked and atypical lymphoreticular response, unless it represents an abnormal immunologic reaction to mucosal ulceration or retained partly digested food, is not known. It is theoretically possible that patients with gastric lymphoid hyperplasia are predisposed to the development of discrete chronic peptic ulcers. However, the demonstration of chronic ulcers prior to the appearance of lymphoreticular masses, at least in some cases, tends to discount this thesis.

Atypical lymphoreticular hyperplasias are not restricted to the stomach but have been found in the small intestine, frequently in association with ulcers. A report [12] on lymphoid hyperplasias of stomach, duodenum, and terminal ileum characterized the lesions as small and polypoid without ulceration and without significant associated inflammation. The relationship of these particular lesions to the ones presented here is equivocal. On the other hand, lesions identical to those in our patients have been described

in other portions of the alimentary tract, including the small intestine [13].

The microscopic differentiation of atypical lymphoreticular hyperplasia from malignant lymphoma is not always easy, particularly on frozen sections. In such cases, the surgeon should be encouraged to remove some of the regional lymph nodes for study. Important microscopic features which aid in distinguishing this condition from lymphoma include lymphoid follicle formation with true reactive germinal centers, the presence of mature lymphocytes as the predominant cell, and an admixture of plasma cells and sometimes eosinophils. In the presence of a chronic peptic ulcer with scar tissue replacing the underlying muscularis, the probability of the lymphoid infiltrate being lymphoma is remote.

ACKNOWLEDGMENT

We are grateful to Dr E. C. Swint for providing clinical information relevant to case 3.

REFERENCES

1. Smith JL Jr, Helwig EB: Malignant lymphoma of the stomach: diagnosis, distinction, and biological behavior (abstr.). *Am J Pathol* 34:553, 1958
2. Jacobs DS: Primary gastric lymphoma and pseudolymphoma. *Am J Clin Pathol* 40:379-394, 1963
3. Faris TD, Saltzstein SL: Gastric lymphoid hyperplasia: a lesion confused with lymphosarcoma. *Cancer* 17:207-212, 1965
4. Wright CJE: Pseudolymphoma of the stomach. *Hum Pathol* 4:305-318, 1973
5. Konjetzny GH: Eine besondere Form de chronischen hypertrophischen Gastritis unter dem klinischen und roentgenologischen Bilde des Carcinomas. *Chirurg* 10:260-268, 1938
6. Schindler R: *Gastroscopy*. Chicago, Univ. Chicago Press, 1950
7. Perez CA, Dorfman RF: Benign lymphoid hyperplasia of the stomach and duodenum. *Radiology* 87:505-510, 1966
8. Nelson RS, Lanza FL, Bottiglieri NG: Lymphoreticular hyperplasia of the stomach (pseudolymphoma). *Gastrointest Endosc* 19:183-186, 1973
9. Carman RD: Benign and malignant gastric ulcers from a roentgenologic viewpoint. *Am J Roentgenol* 8:695, 1921
10. Carman RD: A new roentgen-ray sign of ulcerating gastric cancer. *JAMA* 77:990-992, 1921
11. Wolf BS, Sherkow CJ: Carman sign of ulcerating gastric carcinoma. *Am J Dig Dis* 2:467-477, 1957
12. Bahk YW, Ahn JS, Choi HJ: Lymphoid hyperplasia of the stomach presenting as umbilicated polypoid lesions: report of two cases. *Radiology* 100:277-280, 1971
13. Artinian B, Lough JO, Palmer JD: Idiopathic ulcer of the small bowel with pseudolymphomatous reaction. *Arch Pathol* 91:327-333, 1971

Cholecystokinetic Cholecystography: Efficacy and Tolerance Study of Sincalide

E. NICHOLAS SARGENT,¹ HARVEY I. MEYERS,¹ AND JEROME HUBSHER²

The intravenous administration of sincalide, the C-terminal octapeptide fragment of cholecystokinin, affords a safe and effective means for gallbladder contraction with resultant cystic and common bile duct visualization. Intravenous sincalide circumvents the problem of unpredictability of response of the gallbladder to a fatty meal and variability in the rate of release of endogenous cholecystokinin. Peak gallbladder contraction occurs earlier than with a fatty meal.

The normal physiologic mechanism resulting in gallbladder contraction is set in motion by food ingestion, which initiates neural and hormonal stimuli that stimulate the biliary system. Cholecystokinin is released from the duodenal mucosa in response to the presence of fat and lipolytic products in the small intestine and, to a lesser degree, by amino acids and small peptides. It stimulates contraction of the gallbladder and simultaneous relaxation of the sphincter of Oddi, inhibits gastric emptying, and increases intestinal motility [1]. Contraction of the gallbladder in conjunction with cholecystography may permit an additional assessment of gallbladder function.

Cholecystokinin is a polypeptide comprised of 33 amino acids [2]. The C-terminal octapeptide fragment (sincalide) reproduces all the known biologic activities of the intact molecule [2, 3]. The purpose of this study was to determine the effect of sincalide administration on gallbladder contraction in patients undergoing cholecystography.

Subjects and Methods

A total of 40 patients were studied, 11 males and 29 females. Ages ranged from 22 to 61 years (average, 41 years); weights ranged from 54 to 145 kg (average, 81.3 kg). All patients had symptoms which required cholecystography as part of their clinical evaluation. Individuals with a recent history of acute cardiovascular, hematologic, renal, metabolic, or allergic disorders and those found to have numerous biliary calculi were excluded from the study.

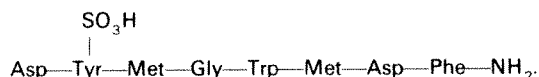
Patient preparation consisted of a fatty meal for lunch on the day prior to the examination and a fat-free evening meal. A 3 g dosage of sodium ipodate (Oragrafin®) was administered orally 12 hr prior to examination. If the gallbladder was not visualized adequately, an additional 3 g was given and the patient reexamined the following day.

Clinical and laboratory tests included physical examination, vital signs, complete blood count, urine, liver and renal function tests, serum electrolytes, and serum calcium, phosphorous, and blood sugar. These tests were performed prior to and 24 hr after drug administration. Electrocardiograms were performed on 33% of the patients immediately before and after the study.

A preliminary film was obtained with the patient recumbent, left side elevated, to determine the optimal position for gallbladder

visualization. Other views included anteroposterior recumbent, right lateral decubitus, and upright compression spot films.

Sincalide (Kinevac®) is a sterile lyophilized powder of the C-terminal octapeptide of cholecystokinin, prepared by synthesis. At the time of manufacture it is placed in vials in which the air has been replaced with nitrogen. The vials are stored at -4°C until use. The chemical structure of sincalide is



Since it is supplied in vials containing 5 µg of drug and 45 mg of sodium chloride, it was reconstituted with 5 ml of sterile water for injection (U.S.P.; pyrogen free, no preservatives). When reconstituted, each milliliter of solution contained 1 µg of sincalide. The drug was administered intravenously over a 60 sec interval (20 ng/kg body weight). Thus an average adult patient weighing 70 kg required 1.4 µg (1.4 ml) of the reconstituted solution.

Gallbladder radiographs were obtained at 0, 1, 3, 5, 10, and 15 min after injection. Gallbladder size (area) was determined by multiplying the maximum length and width.

The minimum criterion for a satisfactory response was a 40% reduction of the gallbladder area on at least one radiograph after injection of sincalide. If reduction in gallbladder size was less than 40%, a repeat intravenous dose of 20 ng/kg was administered. Radiographs were again obtained at the same time intervals.

Results

Of the 40 patients studied, five showed evidence of cholelithiasis after cholecystography. All other patients showed a normal gallbladder.

Maximum gallbladder contraction occurred with a dose of 20 ng/kg in 24 of 40 patients, or 60% (fig. 1). The remaining 16 patients (40%) required a second injection of 40 ng/kg to achieve maximum gallbladder contraction (fig. 2). The total dose administered to each patient ranged from 1.0 to 7.8 µg (average, 2.5 µg).

The average reduction in gallbladder size was 52% of the preinjection area (range 5.5%–100%). Six of 40 patients (15%) showed complete emptying of the gallbladder (fig. 3). Cystic duct visualization occurred in 31 of 40 (78%), and common bile duct visualization in 88% (35 of 40).

Transient mild abdominal pain, cramps, or nausea occurred in 48% of patients. No definite evidence of drug-related cardiac, renal, hepatic, or hematologic abnormalities was found, except for one patient who had a mild leukopenia 24 hr after injection (the white blood cell count fell from 5,000 to 4,300 cells/mm²). One other patient had a rise in the eosinophil count from 7% to 10% and a rise in serum lactic dehydrogenase from 330 to 530 U/ml.

Received February 12, 1976; accepted after revision March 29, 1976.

¹ Los Angeles County—University of Southern California Medical Center, 1200 North State Street, Los Angeles, California 90033. Address reprint requests to E. N. Sargent.

² Squibb Institute for Medical Research, Princeton, New Jersey 08540.

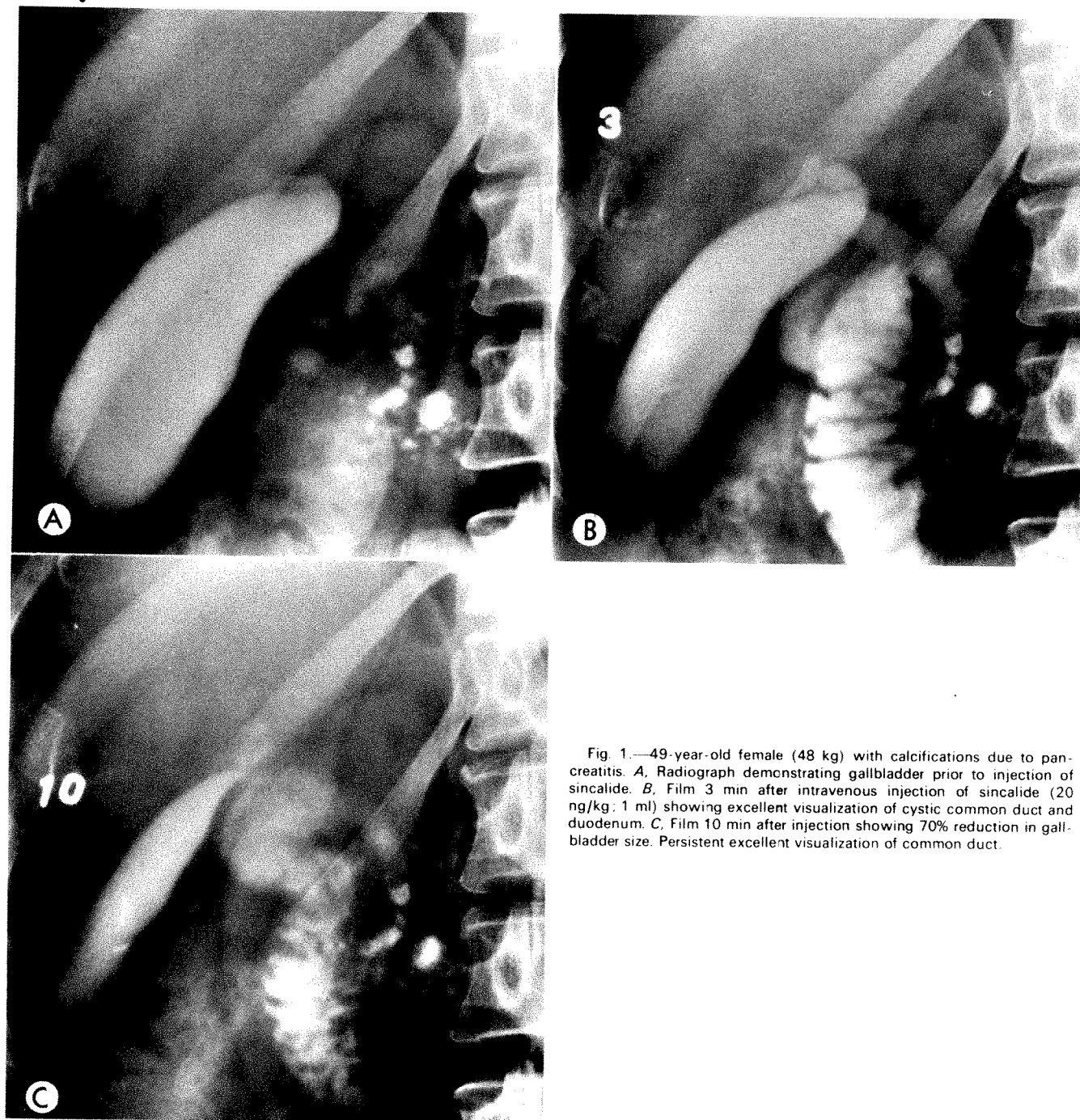


Fig. 1.—49-year-old female (48 kg) with calcifications due to pancreatitis. A, Radiograph demonstrating gallbladder prior to injection of sincalide. B, Film 3 min after intravenous injection of sincalide (20 ng/kg; 1 ml) showing excellent visualization of cystic common duct and duodenum. C, Film 10 min after injection showing 70% reduction in gallbladder size. Persistent excellent visualization of common duct.

Discussion

When injected intravenously, sincalide produces a substantial contraction of the gallbladder with a measurable reduction in gallbladder size. The evacuation of bile that results is similar to that which occurs physiologically in response to endogenous cholecystokinin. Maximum contraction (40% or greater reduction in size) occurs within 5–15 min after injection and is limited in duration. By comparison, a fatty meal causes a progressive contraction of the gallbladder that becomes maximal after approximately 40 min [4].

For prompt contraction of the gallbladder, a dose of 20 ng/kg of sincalide administered as an intravenous bolus over a 1 min period is recommended. If contraction of the gallbladder does not occur within 15 min, a second dose of 40 ng/kg may be administered. For visualization of the cystic and common duct it is usually necessary to take radiographs at 1 min intervals during the first 5 min after injection. Radiographs are then usually taken at 5 min intervals up to 15 min.

The results of this study are similar to those reported by Levant and Sturdevant [5]. They studied 30 patients using a slightly different formulation of sincalide. In their study,

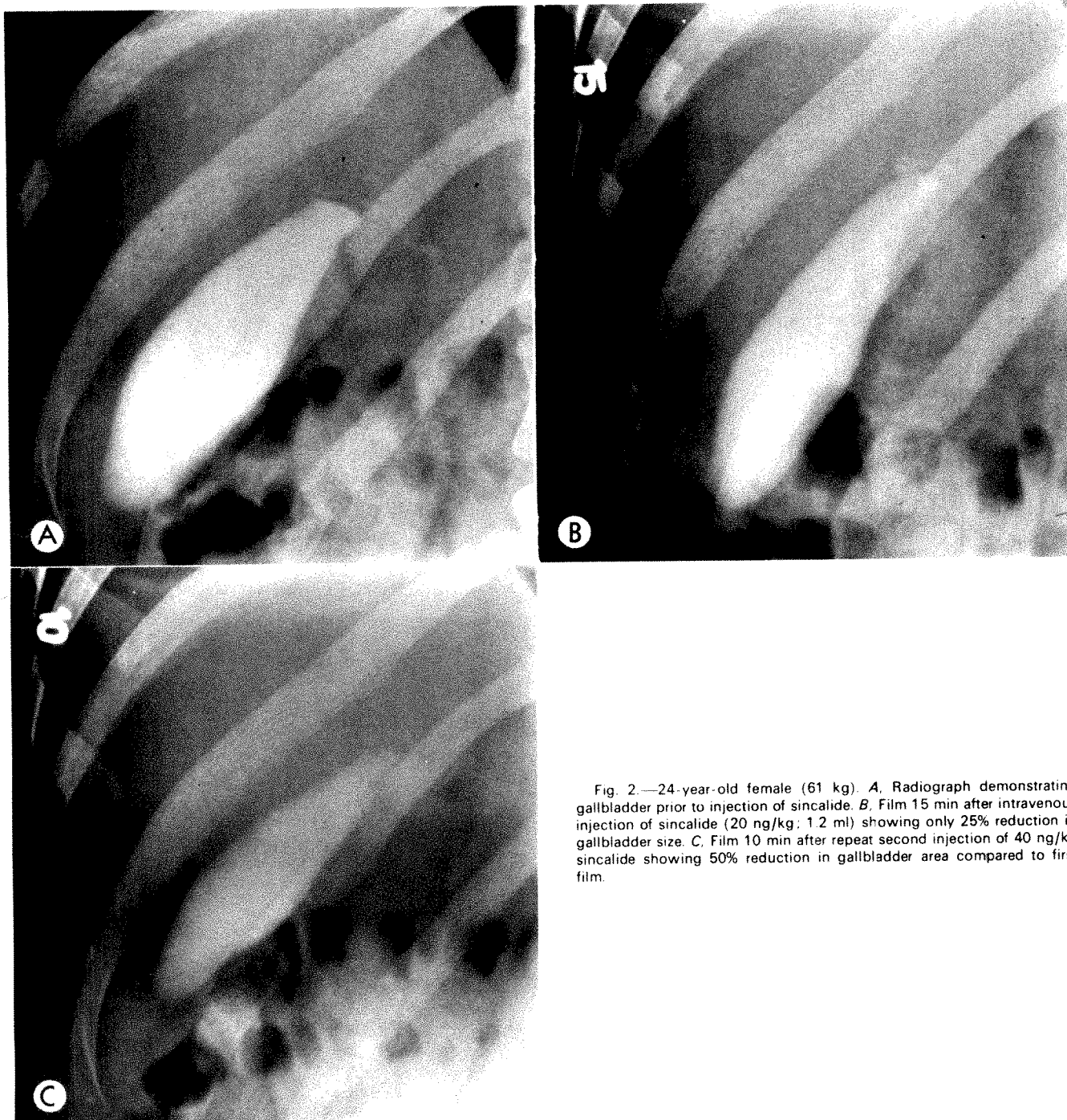


Fig. 2.—24-year-old female (61 kg). A, Radiograph demonstrating gallbladder prior to injection of sincalide. B, Film 15 min after intravenous injection of sincalide (20 ng/kg; 1.2 ml) showing only 25% reduction in gallbladder size. C, Film 10 min after repeat second injection of 40 ng/kg sincalide showing 50% reduction in gallbladder area compared to first film.

each vial contained 5 μ g of the drug with 1 mg of cysteine hydrochloride as carrier. The present formulation using 45 mg of sodium chloride as carrier appears to provide a more stable product.

Gastrointestinal symptoms such as transient mild abdominal pain, cramps, or nausea occurred in almost one-half of the patients studied. These phenomena are manifestations of the physiologic actions of the drug (i.e., delayed gastric emptying and/or increased intestinal motility). Other investigators have also reported occasional transient dizziness and flushing.

Sincalide is contraindicated in patients sensitive to the drug, and its safety for use in pregnant women or in children has not yet been established. Since cholecystokinesis in patients with small biliary calculi could result in passage of stones with lodgement in the cystic or common duct, sincalide should be used cautiously in such cases.

Several potential clinical uses exist for sincalide. The diagnostic value of gallbladder contraction following cholecystography is still uncertain. Cholecystokinetic cholecystography may be helpful in the diagnosis of acalculus cholecystitis [6] if a relationship can be established be-

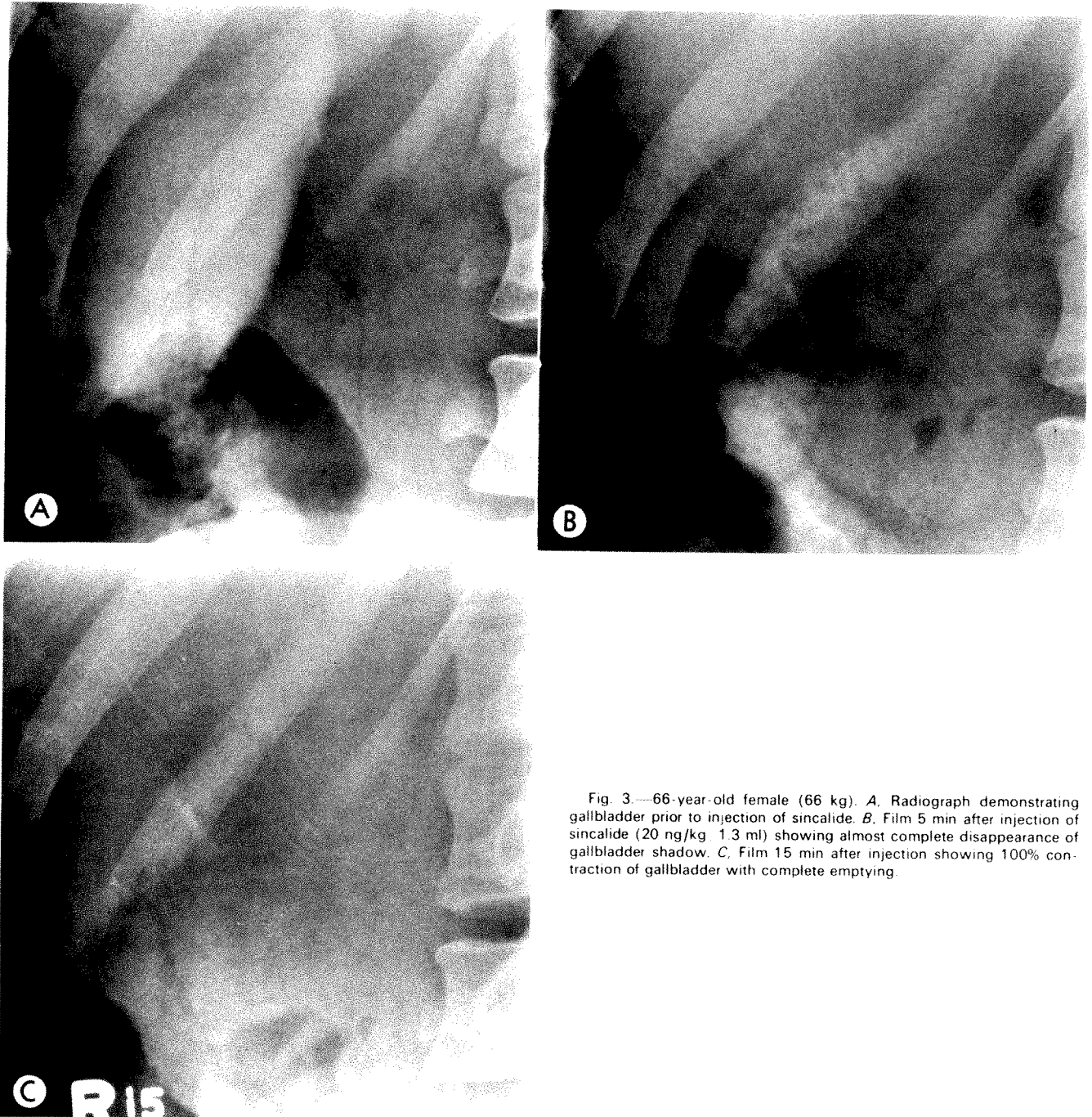


Fig. 3.—66-year-old female (66 kg). A, Radiograph demonstrating gallbladder prior to injection of sincalide. B, Film 5 min after injection of sincalide (20 ng/kg, 1.3 ml) showing almost complete disappearance of gallbladder shadow. C, Film 15 min after injection showing 100% contraction of gallbladder with complete emptying.

tween gallbladder contractility and cholecystitis. It may be helpful in visualizing small gallstones not seen without gallbladder contraction. In some instances, it might eliminate the need for intravenous cholangiography by affording good visualization of the cystic duct and common bile ducts.

Correlation of the pain pattern produced following injection of cholecystokinin in patients without gallstones has been suggested as possibly helpful in predicting the future occurrence of cholelithiasis [7]. In future studies of patients with suspected biliary dyskinesia, the spontaneous

pain pattern may possibly be reproduced [8] following controlled gallbladder contraction with sincalide. Contraction of the gallbladder provides bile that may be aspirated from the duodenum for diagnostic purposes. Sincalide can also be used with secretin as an adjunct to stimulate pancreatic secretion for diagnostic purposes [9].

ACKNOWLEDGMENTS

We are indebted to Dr. Andre Schulman, Neal K. Duenas, and Betty J. Burton for technical assistance and to Patricia McColgan for preparation of the manuscript.

REFERENCES

1. Sleisenger MH, Fordtran J: *Gastrointestinal Disease: Pathophysiology, Diagnosis and Management*. Philadelphia, Saunders, 1973
2. Ondetti MA, Rubin B, Engel SL, Pluscec J, Sheehan JT: Cholecystokinin-pancreozymin: recent developments. *Am J Dig Dis* 15:156-159, 1970
3. Rubin B, Engel SL, Drungis AM, Dzelzkalns M, Grigas EO, Waugh MH, Yiacas E: Cholecystokinin-like activities of C-terminal octapeptide of cholecystokinin in guinea pigs and dogs. *J Pharmacol Sci* 58:955-959, 1969
4. Sacchetti G, Madelli V, Roncoroni L, Montanari G: Influence of age and sex on gallbladder emptying induced by a fatty meal in normal subjects. *Am J Roentgenol* 119:40-45, 1973
5. Levant JA, Sturdevant RAL: Use in C-terminal octapeptide of cholecystokinin in cholecystography. *Am J Roentgenol* 121:380-383, 1974
6. Nora PF, McCarthy W: Cholecystokinin cholecystography in acalculus gallbladder disease. *Arch Surg* 108:507-511, 1974
7. Backlund V: Cholecystokinin vid Röntgenundersökningar. *Läkartidningen* 64:2473-2476, 1967
8. Valbert LS, Jabbari M, Kerr JW, Curtis AC, Ramehand S, Prentice RSA: Biliary pain in young women in absence of gallstones. *Gastroenterology* 60:1020-1026, 1971
9. Jorpes JE, Mutt V (eds): Secretin, cholecystokinin, pancreozymin, and gastrin, in *Handbook of Exp Pharmacology*, vol. 34, Berlin, Springer-Verlag, 1973, pp 234-240

Colonic Changes of Herpes Zoster

LESLIE S. MENUCK,¹ FOLKE BRAHME,¹ JOHN AMBERG,¹ AND HOWARD P. SHERR²

The lesions of herpes zoster of the colon were observed in three cases. Small polygonal mucosal blebs or small ulcerations involving a short segment of the colon and appearing in a reasonable time relationship with the cutaneous manifestations either in a corresponding or noncorresponding dermatome should enable diagnosis of this unusual condition. Recognition of this entity in the presence of these skin lesions should be obvious and therefore helpful in avoiding more aggressive and invasive diagnostic procedures.

Colonic changes in herpes zoster are uncommon. Even though these lesions do not usually cause severe symptoms, it is important to recognize the radiologic manifestations of this entity and its differentiation from other colonic abnormalities in order to avoid more invasive diagnostic procedures. Three cases of herpes zoster with colonic abnormalities are presented to illustrate the radiographic manifestations and the development of these changes.

Case Reports

Case 1

A 43-year-old male had been in good health until he noted the sudden onset of nonspecific migratory abdominal pain which was followed by a fullness in the right lower quadrant. There was no diarrhea or hematochezia. Several weeks later, he developed skin lesions of herpes zoster involving a single dermatome along the inner aspect of the left thigh. On physical examination, there was a suggestion of right lower quadrant abdominal mass.

A barium enema was done which disclosed multiple, sharply angular filling defects within the cecum. Examination of the remainder of the upper gastrointestinal tract and small bowel showed no abnormality. At colonoscopy, the cecum was not reached but no abnormalities were seen in the distal colon. Two weeks after resolution of the skin lesion, a double contrast colonic examination was repeated and showed a normal cecum (fig. 1).

Case 2

This 57-year-old schizophrenic female had a previous history of eczema of the arms, legs, and back which had been treated with steroids over a long period of time. Five weeks prior to admission, her appetite diminished. This lasted for 2 weeks, at which time the vesicular lesions of herpes zoster developed along the T8 dermatome on the left. Except for the cutaneous lesions, the physical examination was unremarkable. Her hematocrit was 18%, and a white blood cell count was 1,400. Hematologic evaluation suggested an iron deficiency anemia and a Coombs-positive hemolytic anemia with a probable drug-related leukopenia.

A barium enema was obtained because of the anemia. Multiple small filling defects with angular margins were found in the cecum. After clearing of the skin lesions, colonoscopy was done, showing only a very small residual polypoid abnormality in the cecum. A repeat barium enema 2 weeks later disclosed a normal cecum (fig. 2).

Case 3

A 54-year-old male who had previously been in good health suddenly developed an acute onset of intense, deep pain in the left side of his abdomen. Blood was noted in the stool. An air contrast barium enema was performed 6 days after the onset of symptoms. In the descending colon a narrowed segment was found with some irregularity to the mucosa, felt to represent small ulcerations. Two weeks later the patient developed skin lesions typical of herpes zoster on the inner aspect of the left lower limb. By this time the abdominal symptoms of bleeding had resolved, and a second radiographic study of the colon demonstrated healing of the ulcerations with moderate residual narrowing of the involved segment. A follow-up examination 2 months later showed further resolution of the colonic changes (fig. 3).

Discussion

Herpes zoster is an exanthematous neurocutaneous disorder secondary to reactivation or reinfection by a large pox virus that also gives rise to varicella. It occurs at a rate of from three to five cases per 1,000 persons per year. The skin changes are associated with segmental inflammation of the posterior root ganglion or extramedullary ganglion of the cranial nerve and along the peripheral sensory nerve distribution [1, 2]. The portal of entry of this virus has not been established, but observations of Cheatham [3] suggest that the gastrointestinal tract rather than the skin is initially invaded. The virus may then propagate from the myenteric plexus to the sympathetic ganglion by way of visceral nerves and involve the posterior nerve roots by way of the white rami communicantes.

In the usual case of herpes zoster, a prodromal phase of chills, fever, and malaise with associated pain and hyperesthesias over the involved dermatome may precede the skin changes by several days or weeks. The cutaneous lesions which follow are grouped, clear vesicles which are usually distributed unilaterally along the course of one or more dermatomes. These eruptions may then either become purulent and form crusts, simply dry up, or become hemorrhagic and ulcerate and then subsequently heal [1]. In patients with an altered immune state (usually patients on antimetabolite or steroid medications or patients with lymphoma or leukemia), skin eruptions may be diffuse causing "herpes zoster generalisatus."

Extracutaneous visceral manifestations involving the respiratory tract, gastrointestinal tract, genitourinary tract, the liver, and serous membranes of the pleura and peritoneum have been described both in patients with an altered immune response and in patients who are otherwise healthy [2, 4-9]. The true incidence of these extracutaneous manifestations is unknown, probably because such

¹ Department of Radiology, University Hospital, University of California at San Diego, and Veterans Administration Hospital, 3350 La Jolla Village Drive, San Diego, California 92161. Address reprint requests to L. S. Menuck at the Veterans Administration Hospital.

² Department of Gastroenterology, University Hospital, University of California at San Diego, La Jolla, California 92037.

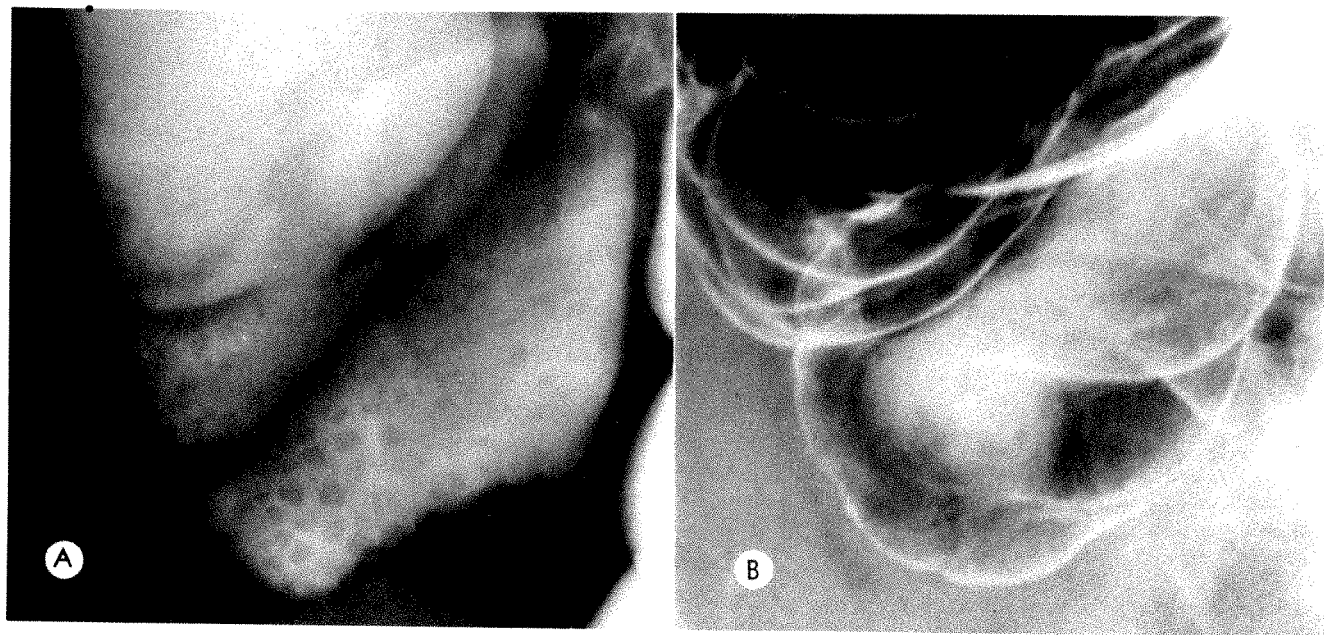


Fig. 1.—Case 1. *A*, Double contrast barium enema showing multiple polygonal filling defects within cecum. *B*, Repeat examination 1 month later showing normal cecum.

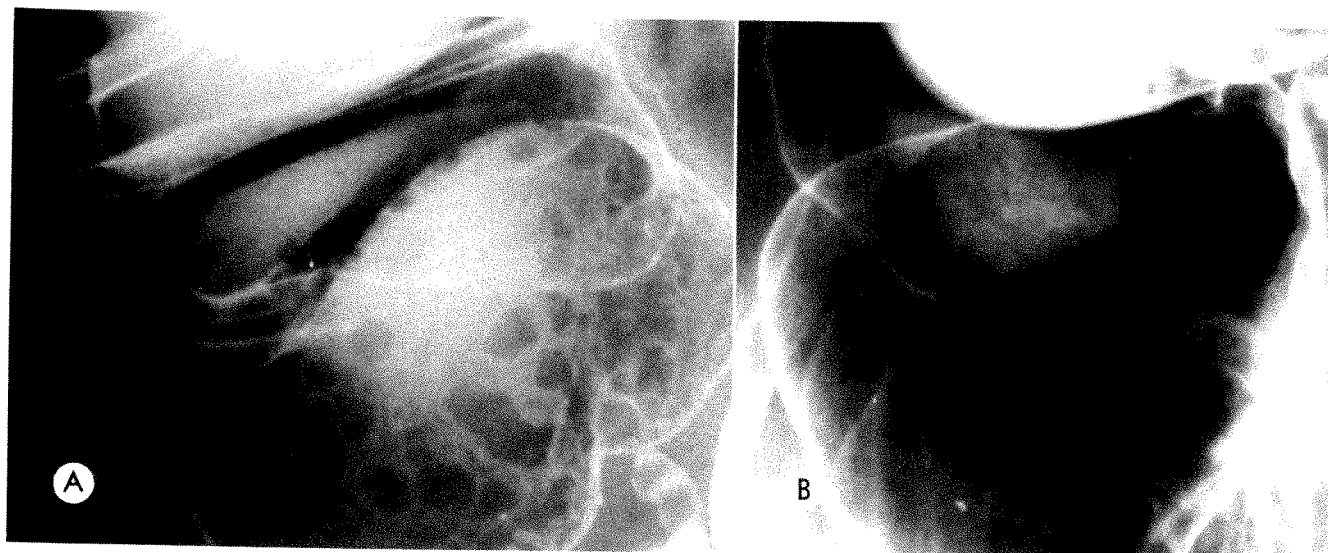


Fig. 2.—Case 2. *A*, Double contrast barium enema showing sharply angular polygonal filling defects of cecum. *B*, Repeat examination 3 weeks later showing total resolution of cecal filling defects.

findings are usually asymptomatic or unrecognized. Since the disease is self limited in most instances, biopsy material is usually not obtained. The presence of gastrointestinal tract involvement has been substantiated by the demonstration of intranuclear inclusion bodies of the virus itself within the ganglion cells of the myenteric plexus and in inflammatory and epithelial cells within the mucosa [2].

The onset of the colonic lesions may coincide with the skin manifestations (as in cases 1 and 2), though they may precede (as in case 3) or follow them by as long as several weeks [9]. Resolution of the colonic lesions may lag

behind the skin changes, especially if there has been mucosal ulceration. The segment of involved colon may correspond to the associated cutaneous dermatome (as in case 3), although in our other two cases there was no real correlation. There have been rare cases where skin lesions have been totally absent (*zoster sine herpette*) and the diagnosis has only been established by the finding of the virus or intranuclear inclusion bodies within the involved gastrointestinal segment [2, 10].

The radiographic appearance of the lesions in the colonic herpes zoster will depend on the stage of the disease at the

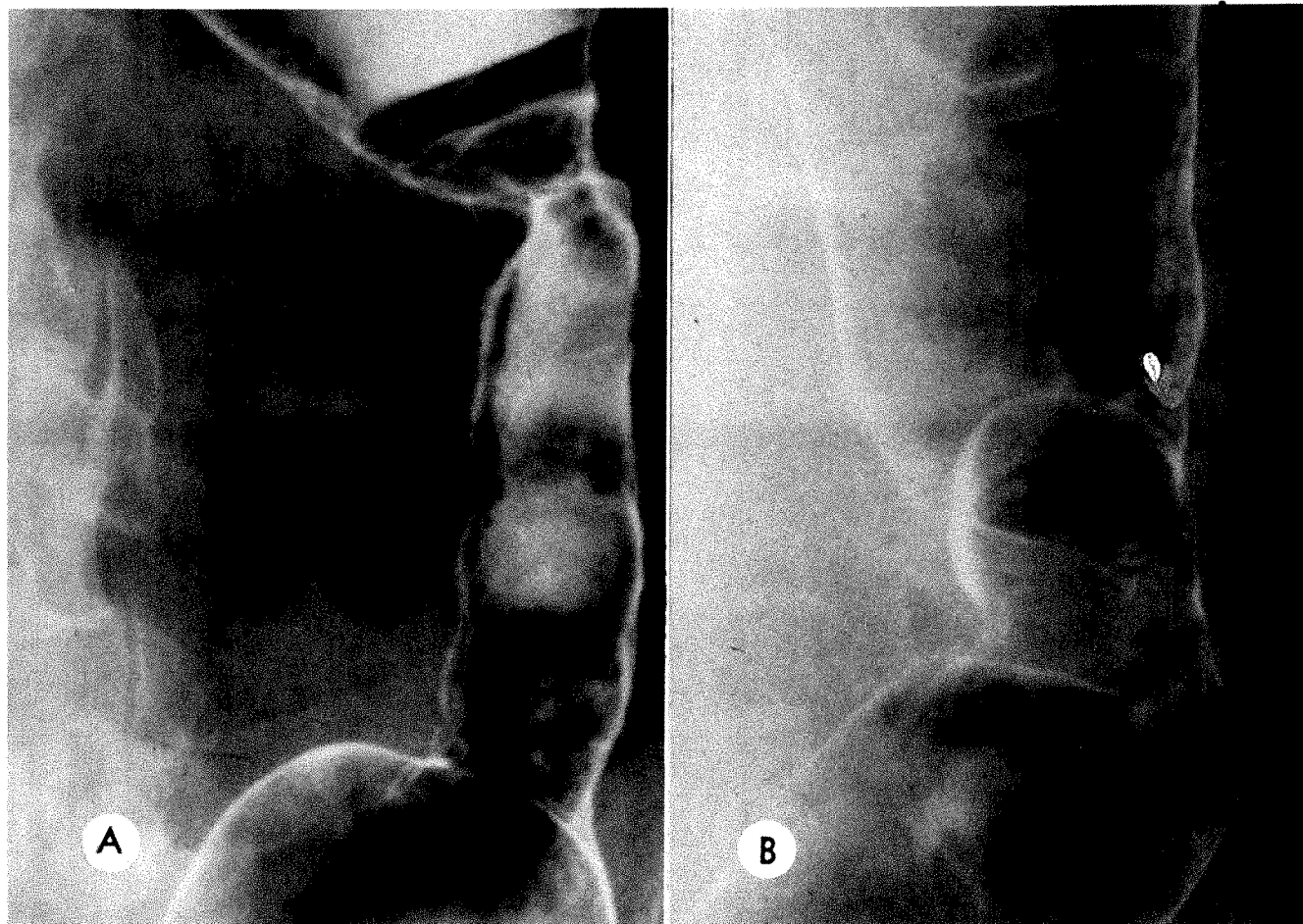


Fig. 3.—Case 3. A, Double contrast barium enema showing short focal narrowing with mucosal irregularity in mid descending colon. B, Repeat examination 2 months later showing some residual narrowing of involved segment.

time of the barium examination. The small discrete polygonal filling defects with sharp angular margins correspond morphologically to the vesicular phase of the cutaneous lesions. This appearance was noted in two of our cases and also in the case reported by Khilnani and Keller [11]. The presence of minute ulcerations in a short segment of the colon as seen in case 3 is felt to represent progression from the vesicular to the ulcerative phase. Similar small ulcerating lesions were found at autopsy in the case presented by Khilnani and Keller [11], even though filling defects had been seen on the previous barium study 6 days earlier; again, this was felt to correspond to the progression of the disease from the vesicular to the ulcerative stage. The presence of focal narrowing as observed by Figiel and Figiel [12] and by Wyburn-Mason [9] was also seen later in case 3. This probably represents a stage of interim residual narrowing following the resolution of the small ulcerations.

The differential diagnosis of the herpetic changes in the colon will depend on whether the vesicular or ulcerative phase is present and on the extent of the colonic involvement. These vesicular lesions have a somewhat different appearance from true polyps in that the margins are quite angular and straight with a polygonal appearance. The

pattern is similar to colonic urticaria as described by Berk and Millman [13]. The focal segmental involvement and the angular polygonal appearance of the lesions will differentiate colonic herpes from inflammatory pseudopolyposis or any of the polyposis syndromes, including lymphoma. (The differentiation from lymphoma is especially important since there is a significant increase in incidence of herpes zoster in patients with lymphoma). The lack of uniformity in the size and shape allows one to differentiate colonic herpes from lymphoid nodular hyperplasia.

The finding of a narrowed segment with small ulcerations is similar to that of a segmental colitis, although the short length of the lesion and the clinical history would be quite atypical. Segmental infarction of the colon is another diagnostic possibility, though one would anticipate the presence of more marked submucosal edema with thumb printing [14]. The rapid disappearance of the small lesions as well as their relationship in time to the typical cutaneous lesions will be helpful in making the diagnosis of herpes zoster.

As in the present three cases, the diagnosis of colonic herpes will usually depend on (1) radiographic appearance, (2) temporal correlation with the cutaneous lesions, and

(3) the inference that the colonic and cutaneous lesions are of the same etiology.

REFERENCES

1. Domonkos AN: *Andrew's Diseases of the Skin; Clinical Dermatology*, 6th ed, Philadelphia, Saunders, 1971
2. Lever WF, Schaumburg G: *Histopathology of Skin*, 5th ed. Philadelphia, Lippincott, 1975
3. Cheatham WJ: Relationship of heretofore unrecognized lesions to pathogenesis of herpes zoster. *Am J Pathol* 29:401-411, 1953
4. Curtin RG: Herpes zoster and its relation to internal inflammations and diseases, especially of the serous membranes. *Am J Med Sci* 73:264-268, 1902
5. Darget R: Deux cas d'herpes zoster de en vessie. *J Urol Nephrol (Paris)* 27:229-231, 1929
6. Eisenbad M: Chickenpox with visceral involvement. *Am J Med* 12:740-746, 1952
7. Reifferscheed M: Herpes Zoster und paralytischer Ileus. *Zentralbl Chir* 74:931-934, 1949
8. Schirduan M, Dietze HH: Über einen blinisch und pathologisch-anatomisch ungewöhnlichen Herpes Zoster Multiplex mit eigenartigen Ileitis. *Arch Dermatol Syphilis* 194:366-375, 1952
9. Wyburn-Mason R: Visceral lesions in herpes zoster. *Br Med J* 1:678-681, 1957
10. Lewis GW: Zoster sine herpate. *Br Med J* 2:418-421, 1958
11. Khilnani MT, Keller RJ: Roentgen and pathological changes in the gastrointestinal tract in herpes zoster generalisata. *Mt Sinai J Med NY* 38:303-310, 1971
12. Figiel SJ, Figiel LS: Herpes zoster with ileus simulating intestinal obstruction. *Am J Med* 23:999-1002, 1957
13. Berk RN, Millman SJ: Urticaria of colon. *Radiology* 99:539-540, 1971
14. Marshak R, Maklansky D, Calem SH: Segmental infarction of the colon. *Am J Dig Dis* 10:86, 1965

Pseudoobstruction in Ceroidosis

MARIELLA BOLLER,¹ CLAUDIO FIOCCHI,¹ AND CHARLES H. BROWN²

Diffuse deposition of ceroid pigment in the muscularis propria of the gastrointestinal tract in a patient with a long history of malabsorption of unknown origin is reported. The deposition of this waste pigment is not reversible and is related to prolonged depletion of vitamin E. Progressive dilatation and hypomotility of the entire gastrointestinal tract are demonstrated by radiographic studies and possibly related to infiltrate of ceroid pigment in the smooth muscle cell with resulting functional impairment. In the differential diagnosis of ceroidosis with other disease, scleroderma has the closest roentgenographic similarity. Pseudoobstruction of the small bowel which can develop must be treated conservatively to avoid unnecessary bowel resection.

Ceroidosis is diffuse accumulation of ceroid pigment in the muscularis propria of the gastrointestinal tract [1-3]. It is not a primary disease but a consequence of long-standing malabsorption. The main clinical manifestations are chronic steatorrhea, malabsorption, and intestinal obstruction without mechanical cause.

Although the literature contains numerous descriptions of ceroidosis, the radiologic features of this condition have not been described.

Case Report

A 39-year-old black male with a diagnosis of Whipple's disease, was admitted to the Cleveland Clinic in April 1964 following laparotomy at another hospital. On physical examination, the abdomen was distended. A diagnosis of intestinal obstruction was made and a laparotomy performed. At laparotomy, the small bowel, large intestine, and the mesenteric lymph nodes appeared to have extensive brown coloration. An ileotransverse colostomy bypassing 4 feet of completely atonic terminal ileum was performed.

Pathologic diagnosis was ceroid pigment accumulation in smooth muscle cells of the muscularis propria of the jejunum, terminal ileum, and colon. The patient was discharged with a diagnosis of malabsorption and intestinal ceroidosis. During further evaluation between October 1964 and January 1965, cystic fibrosis was ruled out by a normal sweat test with pilocarpine iontophoresis; secretion-induced pancreatic amylase, bicarbonate, and juice volume were normal. Alpha tocopherol levels were 58 and 64 $\mu\text{g}/100$ ml (normal, 500 $\mu\text{g}/100$ ml).

In May 1968 he was readmitted for intestinal obstruction which was managed conservatively. In January 1970 he was readmitted because of chronic steatorrhea, peripheral edema, and cachexia. Broad-spectrum antibiotic therapy was begun because of suspected blind-loop syndrome. No improvement was noted.

The patient has been followed as an outpatient for the past 11 years. Abdominal distention and severe malabsorption persist, despite therapy.

Radiologic Findings

A barium study done in 1964 showed dilatation of the

stomach, duodenum, and small bowel, with thickening of the valvulae conniventes; no nodular lesions were recognized (fig. 1). Diagnosis of mechanical small bowel obstruction was made. Examination of the large intestine showed megacolon (fig. 2).

Striking progressive changes were noted in the barium examination done in 1974. Megaesophagus without peristalsis was present (fig. 3). Massive dilatation of the stomach and duodenum was present with loss of normal mucosal folds (fig. 4A). The 24-hr film showed that barium was still in the small bowel and in a very dilated large bowel (fig. 4B). A diagnosis of pseudoobstruction was made.

Discussion

Reports of diffuse accumulation of ceroid pigment in the muscularis propria of the small and large intestine have appeared over the past 30 years [4-7]. The macroscopic findings can be so striking at operation or postmortem that the term brown bowel syndrome has been proposed [3].

Ceroid is a lipofuchsin pigment and it is related to long-standing vitamin E deficiency [1, 8-10]. Ceroidosis has been found in a variety of diseases such as cystic fibrosis, biliary atresia, celiac diseases [10, 11], sprue [4, 12, 13], chronic pancreatitis [9], granulomatous enterocolitis [14], resection of the stomach and small bowel [2, 8], biliary cirrhosis [8], intestinal lymphangiectasia [15], and Whipple's disease [8].

Both ceroid and the material found within the macrophages of the lamina propria in Whipple's disease react positively to periodic acid-Schiff (PAS); this can lead to an erroneous diagnosis as in this case initially. Melanosis coli should be differentiated also; this involves only the mucosa of the colon, appears secondary to prolonged use of cascara, and is reversible [3]. Ceroidosis is not reversible. The patient showed no improvement after tocopherol administration. This has also been demonstrated in animal studies [3].

It has been postulated but not proven that ceroid deposits affect the function of smooth muscle. The clinical and radiologic manifestations of intestinal pseudoobstruction would thus be explained in our case and in all cases of cystic fibrosis, sprue, and chronic pancreatitis [9]. Radiographically, the most striking features in our case were hypomotility and massive dilatation of the entire gastrointestinal tract. No organic occlusion was present.

The diffuse deposition of ceroid is believed to be the cause of these radiologic findings, which are strikingly similar to those in scleroderma. In both conditions megaesophagus, megaduodenum, and megacolon are present, but the absence of skin changes and the typical histological

¹ Department of Radiology, Cleveland Clinic Foundation, 9500 Euclid Avenue, Cleveland, Ohio 44106.

² Department of Gastroenterology, Cleveland Clinic Foundation, Cleveland, Ohio 44106.

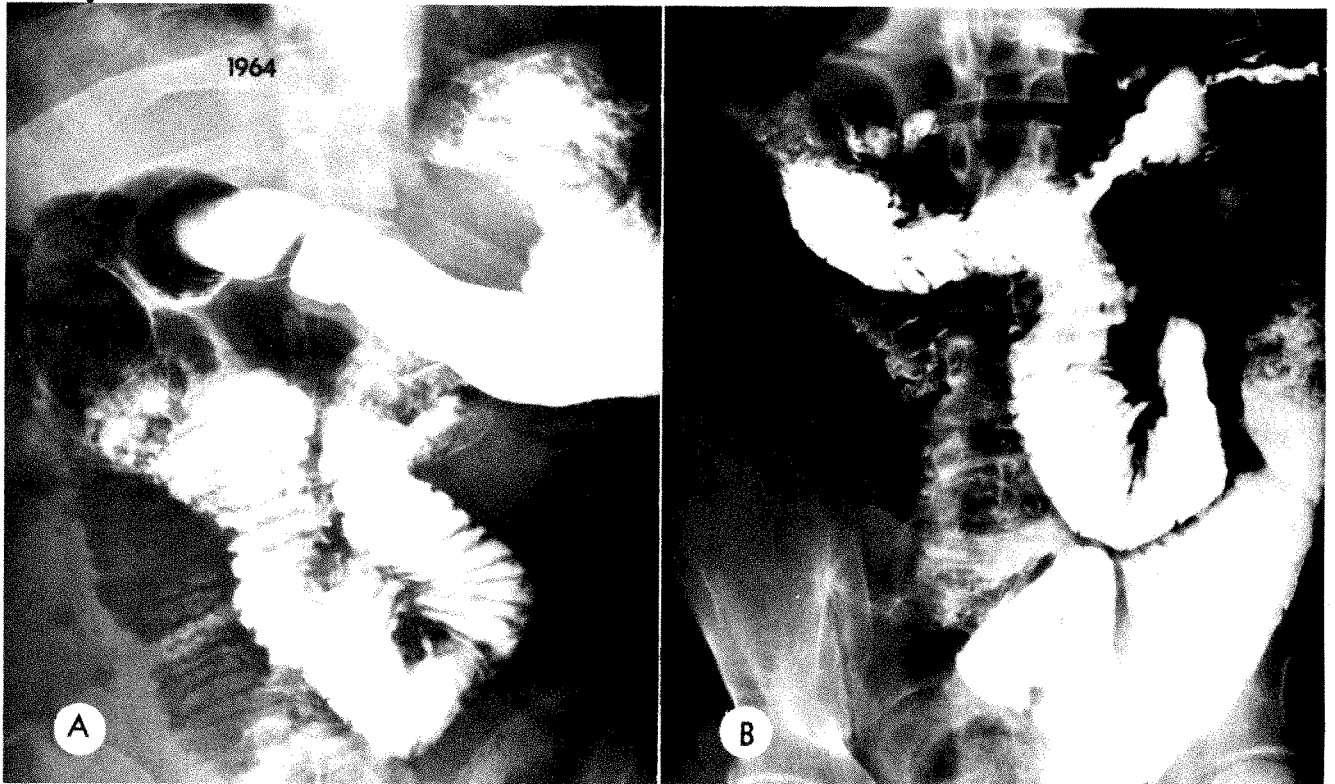


Fig. 1.—A, Barium study showing dilatation of stomach, duodenum, and proximal jejunum with thickening of valvulae conniventes. B, Follow-up 8½ hr later showing barium still in diffusely dilated jejunum and proximal ileum. Thickening of valvulae conniventes again apparent.

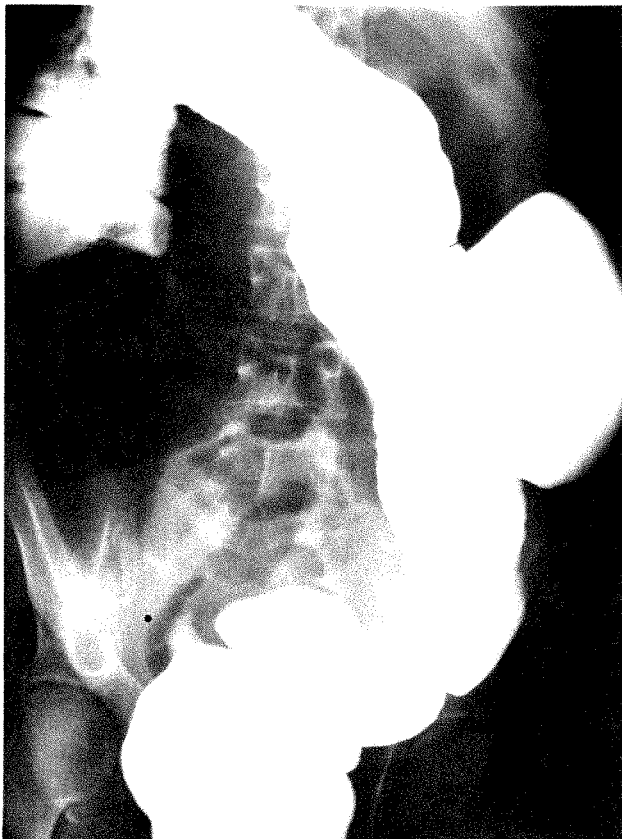


Fig. 2.—Megacolon; no pseudodiverticula are recognized.

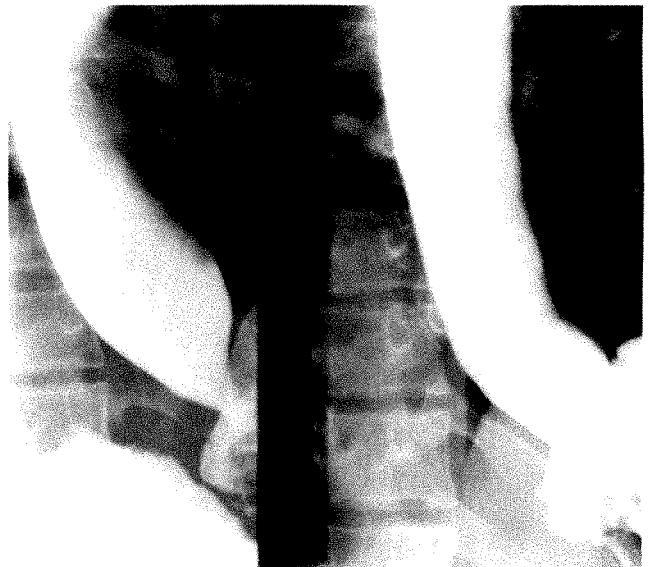


Fig. 3.—Barium study showing massive dilatation of esophagus without stricture formation. Free reflux was noted during fluoroscopic examination.

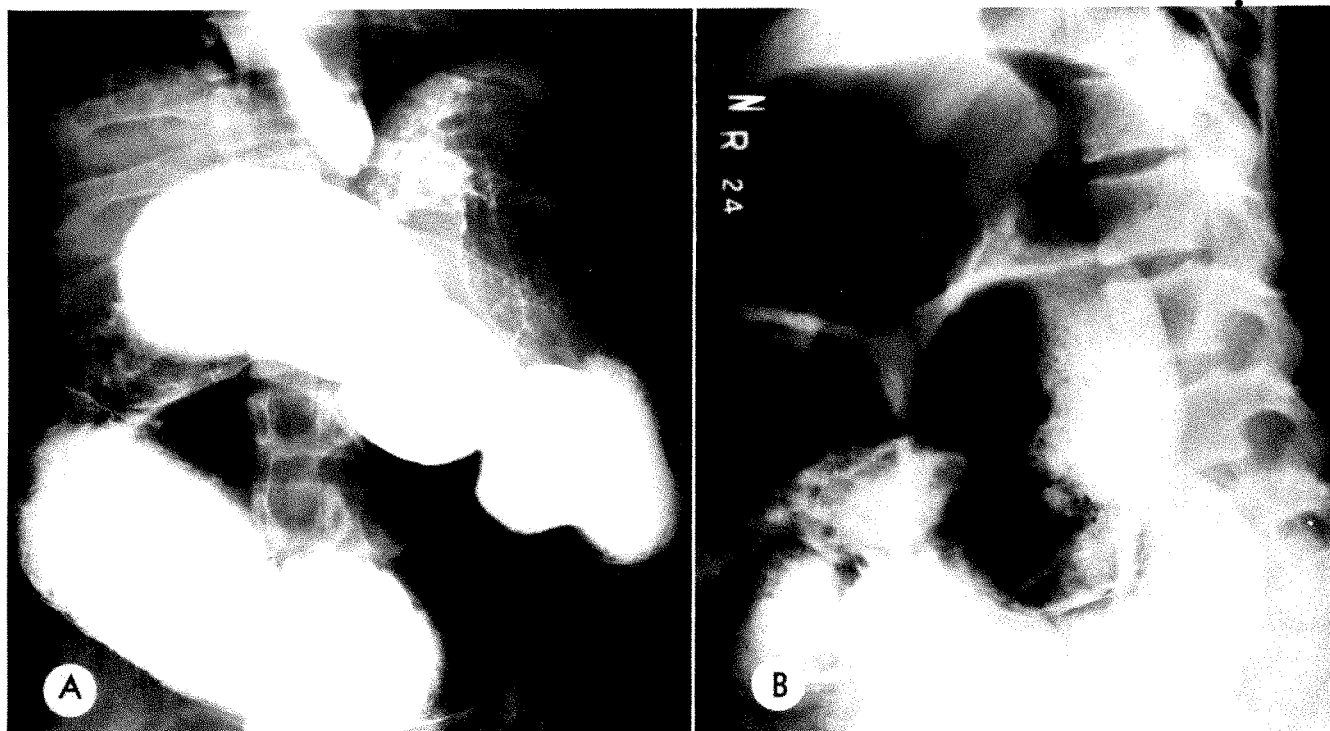


Fig. 4.—A, Barium study showing stomach dilated, occupying entire upper abdomen. Duodenum shows more striking widening, measuring 10 cm in diameter, and loss of normal mucosal pattern. B, 24 hr follow-up showing barium in bowel. Impossible to differentiate small from large bowel. Note again massive dilatation of duodenum.

findings of scleroderma in the bowel clearly differentiate the two diseases [16, 17].

Chagas' disease and myotonia dystrophica [16] are other entities which can cause megaesophagus and megacolon, but the stomach and small bowel are not affected. Numerous other diseases can cause pseudo-obstruction of the small bowel: pneumonia, renal failure, pancreatitis, myxedema, sprue, amyloidosis, lesions of the myenteric plexus [18, 19], and idiopathic steatorrhea [20].

When dilatation and hypomotility of the entire gastrointestinal tract are present in a patient with a long history of malabsorption and intestinal obstruction, ceroid deposition should be suspected. This can be proven by small bowel biopsy. Major surgery in pseudoobstructed patients may thus be avoided.

REFERENCES

1. Ansanelli V Jr, Lane N: Lipochrome (ceroid) pigmentation of the small intestine. *Am J Surg* 146:117-123, 1957
2. Richards WCD: Pigmentation of gastrointestinal muscle. *Lancet* 1:683, 1959
3. Toffler AH, Hukill PB, Spiro HM: Brown bowel syndrome. *Ann Intern Med* 58:872-877, 1963
4. Gresham GA, Cruickshank JG, Valentine JC: Pigmentation of intestinal muscle in steatorrhea. *Nature* 181:538-539, 1958
5. Hooper CW, Whipple GH: Bile pigment metabolism. VIII. Bile pigment output influenced by hemoglobin infection, splenectomy and anemia. *Am J Physiol* 43:275-289, 1917
6. Lillie RD, Daft FS, Sebrell WH: Cirrhosis of the liver in rats on a deficient diet and the effect of alcohol. *Public Health Rep* 56:1255-1258, 1941
7. Pappenheimer AM, Victor J: Ceroid pigment in human tissue. *Am J Pathol* 22:395-413, 1946
8. Binder HJ, Herting DC, Hurst V, Finch SC, Spiro HM: Tocopherol deficiency in man. *N Engl J Med* 273:1289-1297, 1965
9. Braunstein H: Tocopherol deficiency in adults with chronic pancreatitis. *Gastroenterology* 40:224-231, 1961
10. Kerner I, Goldbloom RB: Investigation of tocopherol deficiency in infancy and childhood. *Am J Dis Child* 99:597-603, 1960
11. Blanc WA, Reid JD, Anderson DH: Avitaminosis E in cystic fibrosis of the pancreas. *Pediatrics* 22:494-506, 1958
12. Adlesberg D, Shein J: Clinical and pathological studies in sprue. *JAMA* 134:1459-1467, 1947
13. Paulley JW: Observations on the etiology of idiopathic steatorrhea. *Br Med J* 2:1313-1321, 1954
14. Papp JP, Farmer RG, Hawk W: Ceroid Deposition in the muscularis of the small intestine associated with regional enteritis. *Cleve Clin Q* 36:190-194, 1969
15. Jarnum S: *Protein-Losing Gastroenteropathy*. Oxford, Blackwell Scientific Publications, 1963
16. Margulis AR, Burhenne HJ: *Alimentary Tract Roentgenography*. St. Louis, Mosby, 1973
17. Poirier TJ, Rankin GB: Gastrointestinal manifestation of progressive system scleroderma based on a review of 364 cases. *Am J Gastroenterol* 58:30-44, 1972
18. Dyer NH, Dawson AM, Smith BF, Todd IP: Obstruction of the bowel due to lesion in myenteric plexus. *Br Med J* 1:686-689, 1969
19. Seaman WB: Motor dysfunction of the gastrointestinal tract. *Am J Roentgenol* 116:235-244, 1972
20. Naish JM, Capper WM, Brown NJ: Intestinal pseudo-obstruction with steatorrhea. *Gut* 1:62-65, 1960

Anomalies of the Craniovertebral Border

ROBERT SHAPIRO¹ AND FRANKLIN ROBINSON²

Pertinent embryology is reviewed as a background for understanding anomalies of the craniovertebral border. These anomalies constitute a variable spectrum due either to incomplete assimilation or abnormal fusion.

The occipital bone develops from the fusion of at least four primitive somites which correspond to the primary roots of the hypoglossal nerve [1-3] (fig. 1). In amphibia and some fishes, the hypoglossal nerve is a true spinal nerve which does not pass through the skull. In vertebrates, however, the hypoglossal nerve is transformed into a cranial nerve. The first somite quickly disappears.

In some lower vertebrates (e.g., reptiles), the cranial half of the first cervical sclerotome remains as a separate bone, the proatlas between the occiput and C1 (fig. 2). In man, however, it becomes assimilated into the occipital condyles and also forms the tip of the dens [4]. The body of C1 disappears early, giving rise to all but the tip of the dens. Thus the dens represents the body of C1 and a portion of the proatlantal half segment.

The caudal half of the first cervical sclerotome gives rise to the lateral masses and the anterior and posterior arches of C1. The body, posterior arch, and transverse processes of C2 are derived from the second cervical sclerotome.

In the evolutionary scale, the craniovertebral articulation moves caudally as various vertebrae are assimilated into the postotic segment of the skull. It is helpful, therefore, to think of the craniovertebral border as an embryologically unstable region, subject to variation much like the lumbosacral region where lumbarization of S1 and sacralization of L5 are common.

If the cranial half of the first cervical sclerotome is incompletely assimilated into the occiput, various expressions of an occipital vertebra occur [5-7]. On the other hand, if normal segmentation fails to occur, atlantooccipital fusion results [8-15]. Thus an occipital vertebra and atlantooccipital fusion represent opposite ends of a continuous spectrum.

Incomplete Assimilation

The following are manifestations of an occipital vertebra.

Transverse Basioccipital Fissure

The simplest form of incomplete assimilation of the primitive occipital somites is a transverse cleft in the basiocciput (fig. 3). The fissure may be unilateral or bilateral, partial or complete [7, 16].

Third Occipital Condyle

This anomaly is characterized by a single midline bony

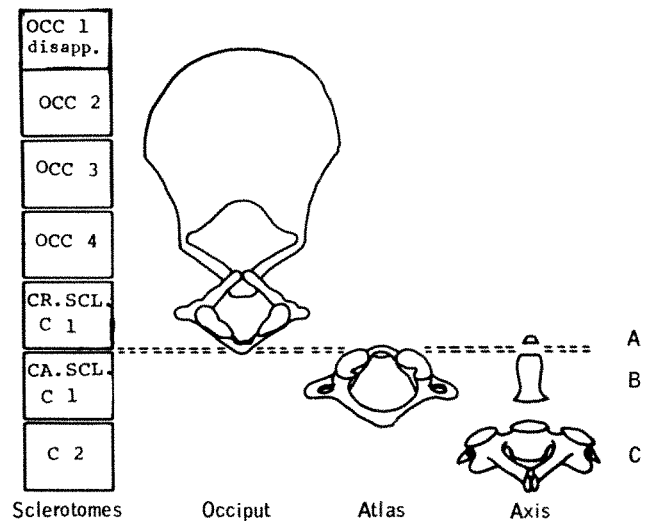


Fig. 1.—Diagrammatic schema of development of occipital bone and first two cervical vertebrae (Modified from List [4]).

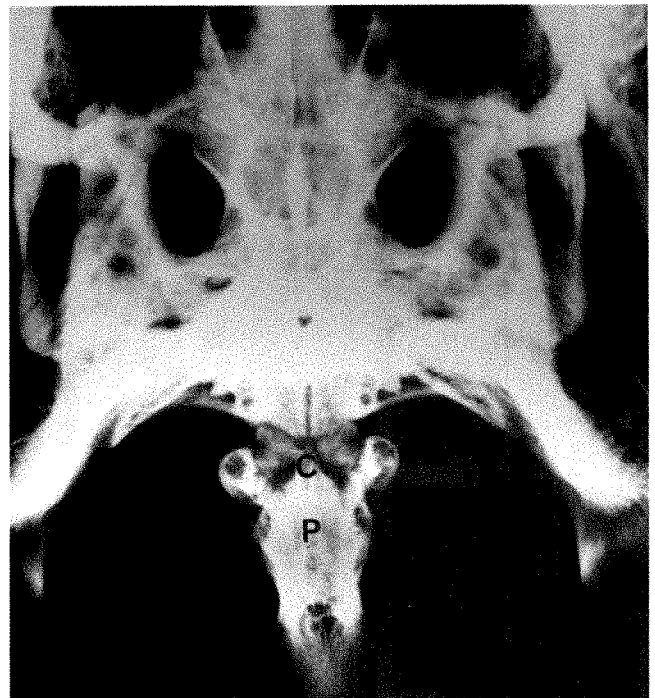


Fig. 2.—Radiograph of craniovertebral border of alligator skull demonstrating proatlas (P) articulating with single occipital condyle (C).

Presented at the annual meeting of the American Roentgen Ray Society, Atlanta, Georgia, October 1975.

¹ Department of Radiology, Hospital of St. Raphael and Yale University School of Medicine, New Haven, Connecticut 06511.

² Department of Neurosurgery, Hospital of St. Raphael and Yale University School of Medicine, New Haven, Connecticut 06511.

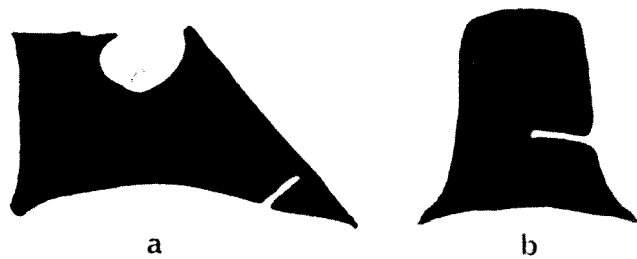


Fig. 3.—Diagram of a transverse basioccipital fissure in lateral (a) and submentovertical (b) projections.

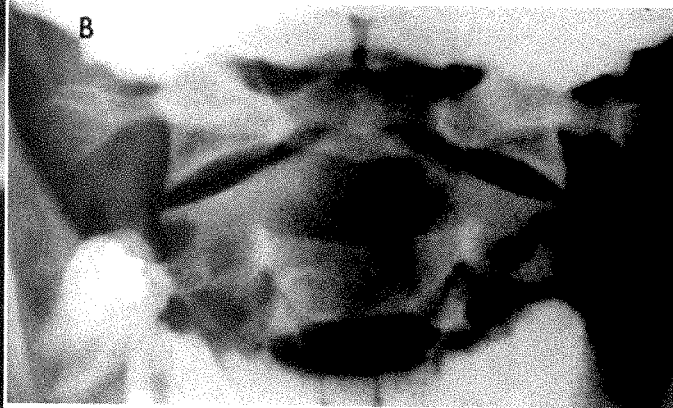
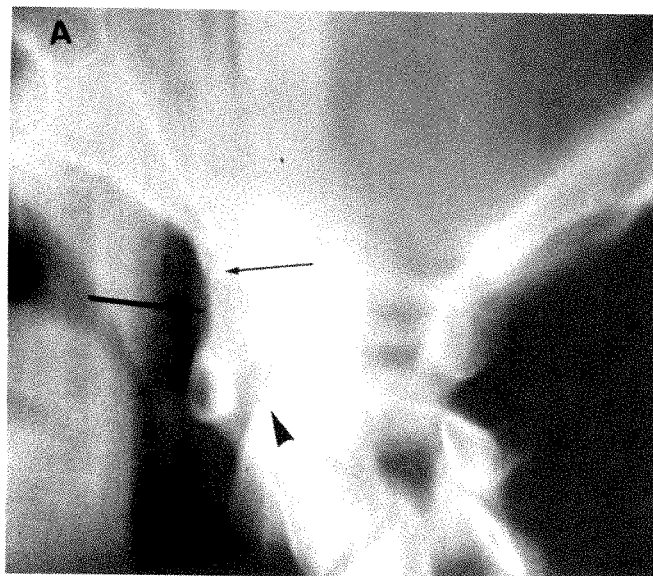


Fig. 4.—Lateral (A) and anteroposterior (B) radiographs of craniovertebral region in 31-year-old male with multiple upper cervical anomalies. Note absent dens, moundlike summit of C2 (*arrowhead*), and third occipital condyle (*thin arrow*) articulating with an os odontoideum (*thick arrow*). Patient also had coarcted foramen magnum (see fig. 13).



Fig. 5.—A and B. Lateral tomograms in two patients showing separate basilar process (*arrow*) inferior to anterior rim of foramen magnum. in B, basilar process articulates with superior rim of anterior arch of C1 by a pseudarthrosis.

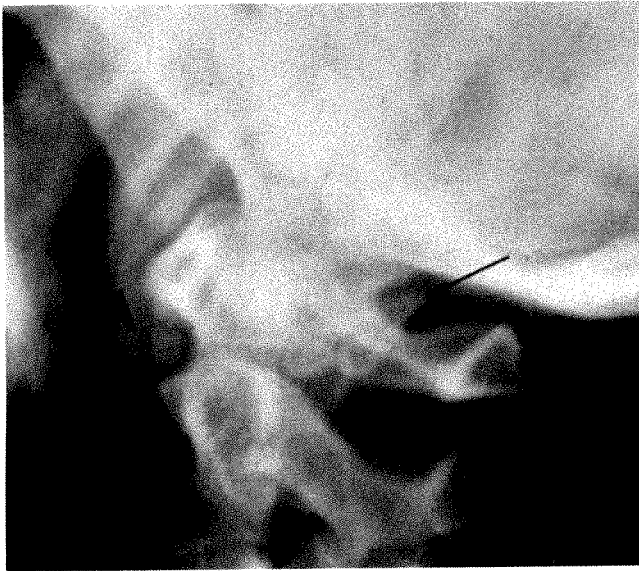


Fig. 6.—Lateral radiograph demonstrating ossicle (*large arrow*) below anterior arch of C1. Note incomplete development of posterior atlantal arch on one side (*small arrow*).

knob projecting down from the inferior aspect of the basiocciput along the anterior aspect of the foramen magnum (fig. 4). The bony projection may be separate or attached to the anterior margin of the foramen magnum. The third occipital condyle may have a facet for articulation with the dens or with the anterior arch of C1, especially in the presence of atlantooccipital synostosis.

Basilar Processes

At times there are dual paramedian tubercles along the anterior margin of the foramen magnum which may be separate or attached (fig. 5). These processes may have articular facets for the anterior rim of C1. We include in the broad category of basilar processes the small ossific foci visualized in the lateral projection between the anterior arch of C1 and C2 (fig. 6). These ossicles can readily be differentiated from the posterior calcification or ossification in the atlantooccipital ligament (fig. 7).

Os Odontoideum

This is a separate bone always associated with a cupola-shaped, hypoplastic dens. It may lie directly above the hypoplastic dens or more anteriorly and superiorly closer to the basiocciput (fig. 8). It may be attached to the anterior arch of C1 in the midline or slightly laterally. Occasionally, the os odontoideum articulates with the basiocciput by a pseudarthrosis.

Bipartite Atlantal Facets

These are a vestige of the cranial half of the first cervical sclerotome which normally forms the dorsal portion of the lateral atlantal masses (fig. 9).

Atlantooccipital Fusion

Atlantooccipital Synostosis

Fusion of C1 with the occiput may be unilateral (fig. 10)

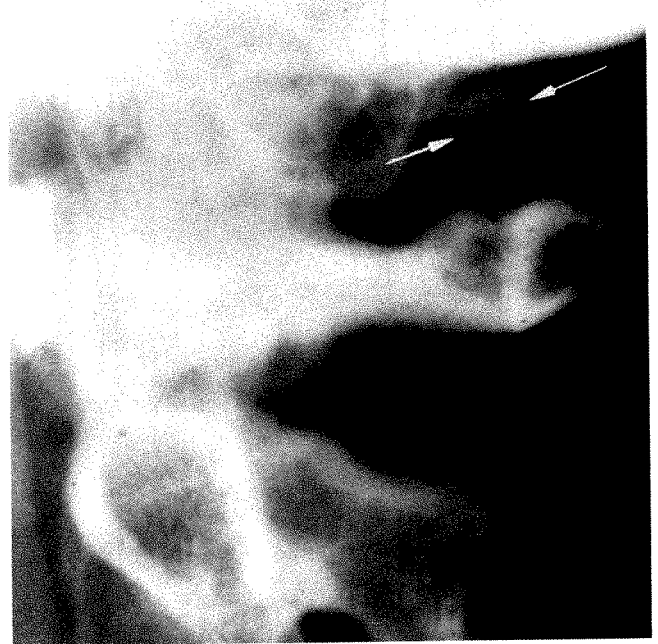


Fig. 7.—Posterior ossicle in atlantooccipital ligament (*arrows*). Latter may show focal areas of calcification or ossification which are acquired.

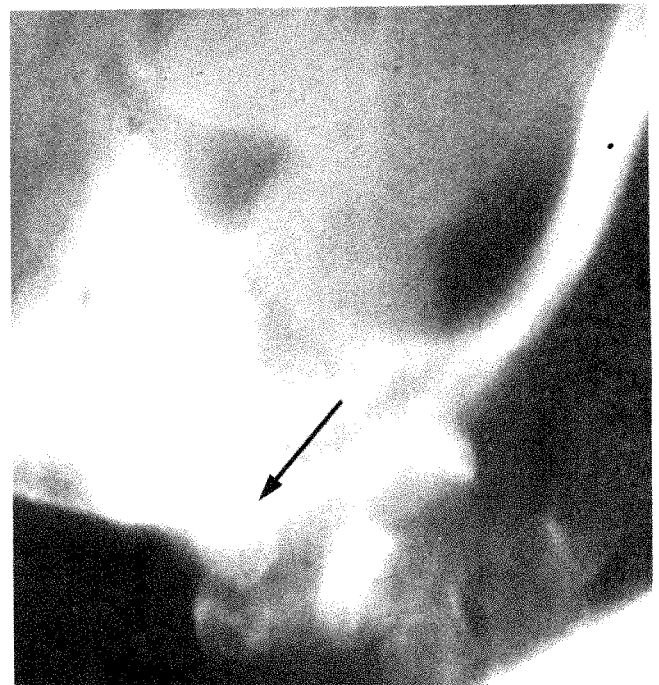


Fig. 8.—Os odontoideum (*arrow*) in 1-year-old girl with Down syndrome.

or bilateral. When bilateral, the fusion is not necessarily symmetrical. Thus the transverse process of C1 may be fused with the styloid process of the temporal bone unilaterally, or one atlantal mass may be larger and more cranially displaced. The fusion may involve the anterior or posterior atlantal arch, or both. It may occur as an isolated anomaly or together with other vertebral abnormalities (e.g., failure of segmentation, particularly at C2–C3; fig.



Fig. 9.—Photograph of normal single atlantal articulation (A, 1) and bipartite atlantal articulations (B, 1).

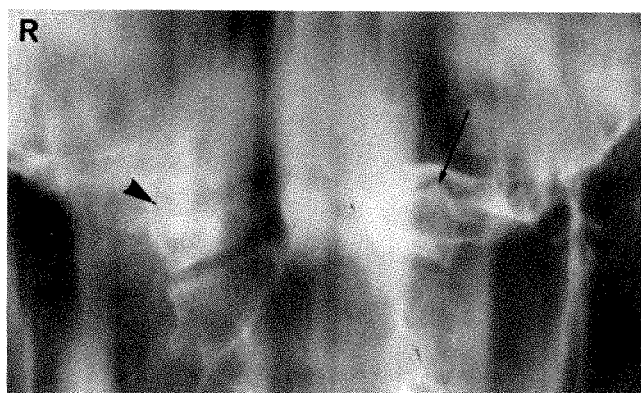


Fig. 10.—Anteroposterior tomogram demonstrating unilateral assimilation of C1 on right (arrowhead). Note normal left atlantooccipital joint (arrow). Patient also had constriction of foramen magnum.

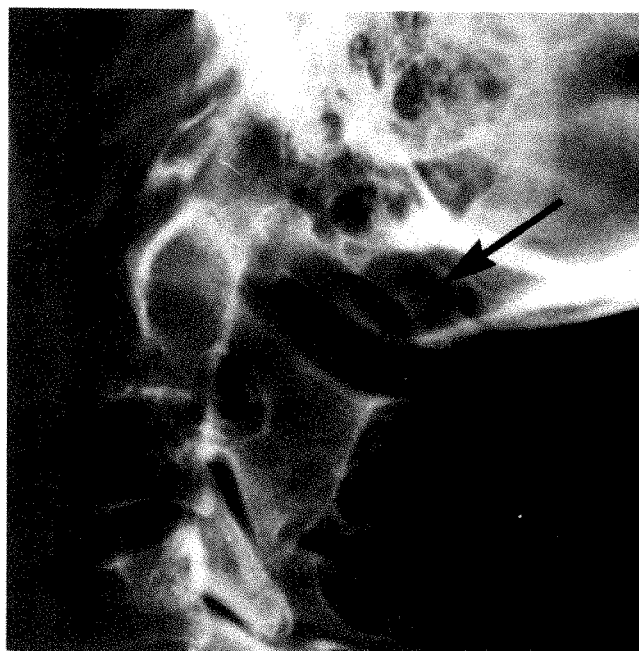


Fig. 11.—Bilateral assimilation of posterior arch of atlas in 40-year-old female (arrow). Note associated segmentation anomaly at C2–C3.

11). Lateral radiographs in flexion and extension demonstrate absence of motion between C1 and the occiput.

Atlantooccipital synostosis may or may not be associated with neurological findings (cerebellar, brain stem, cranial nerve, cervical root signs). When neurologic involvement is present, it is secondary to the effects of one or more of the following associated abnormalities: (1) constriction of the foramen magnum; (2) basilar impression; or (3) hydrocephalus due to adhesions, Arnold-Chiari malformation, Dandy-Walker syndrome, or syringohydromyelia.

Atlantooccipital Ossification [8, 17]

Paracondylar process. The paracondylar process is a broad-based, cone-shaped bony mass projecting down from the lateral aspect of the occipital condyle toward the transverse process of C1 (fig. 12). The term paramastoid process is inappropriate in man since the bony process is not connected to the mastoid tip of the temporal bone.

Epitransverse process. The epitransverse process is a thinner strut of bone arising from the transverse process of the atlas, projecting craniad toward the occipital condyle.

In a sense, the epitransverse process is a mirror image of the paracondylar process.

Both processes may be unilateral or bilateral; they may exist singly or together. They may occur as isolated anomalies or as part of a complex craniovertebral junction abnormality (e.g., atlantooccipital synostosis). These bony projections represent vestiges of the cranial half of the first cervical sclerotome.

Occipital Dysplasia

Constriction of Foramen Magnum

A small foramen magnum is characteristic of achondroplasia. However, it may also be secondary to premature fusion of one or more occipital synchondroses. Constriction

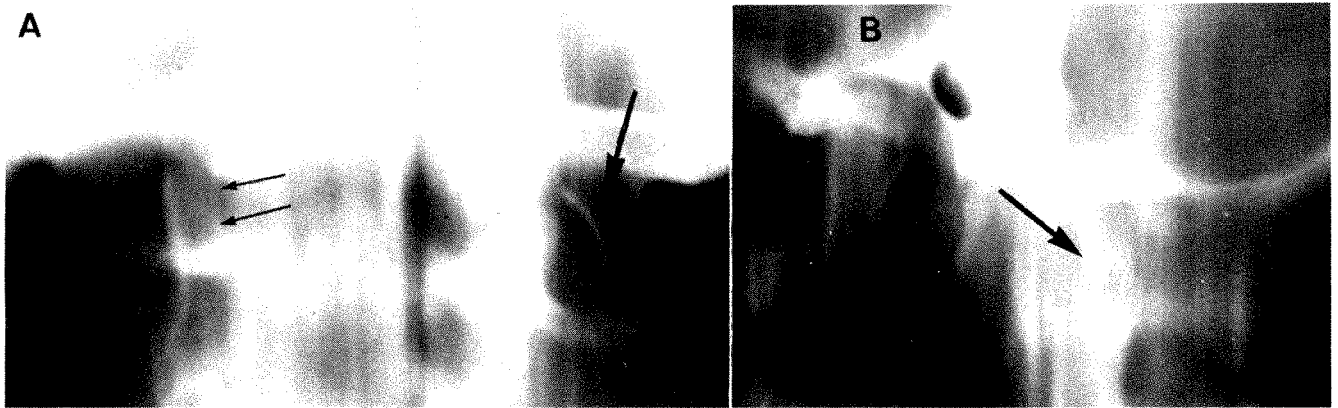


Fig. 12.—Anteroposterior (A) and oblique (B) tomograms in 32-year-old female showing right epitransverse process (*small arrows*) and left paracondylar process (*large arrow*).

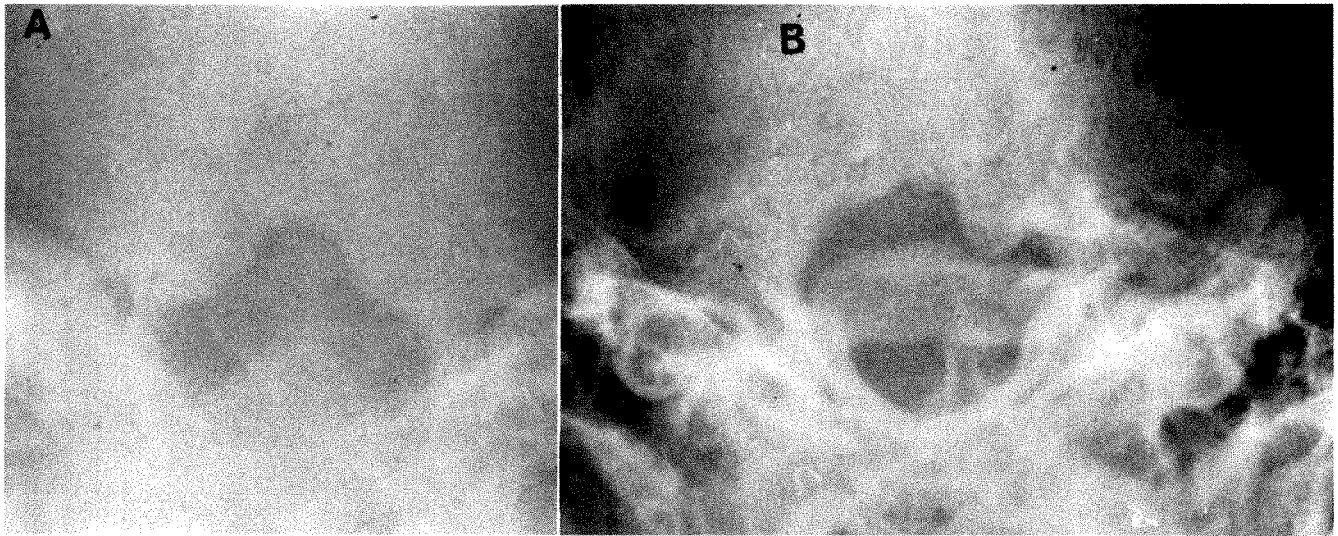


Fig. 13.—A, Cloverleaf deformity of foramen magnum in 31-year-old male with multiple occipitocervical abnormalities (see fig. 4). B, Asymmetrical constriction of foramen magnum as an isolated anomaly.

tion of the foramen magnum may also accompany atlantooccipital fusion (fig. 13).

Condylar Hypoplasia

Condylar hypoplasia occurs as an isolated anomaly or as part of a complex atlantooccipital abnormality [17, 18]. Flattened, underdeveloped condyles result in elevation of C1 and C2 (fig. 14). The height of the occipital condyles may be estimated on an anteroposterior tomographic film from the angle formed by the axes of the atlantooccipital joints. The normal angle is 125° ; an increased angle indicates condylar flattening (fig. 15).

Basilar Impression

Basilar impression means elevation of the floor of the posterior fossa. The congenital type is a form of occipital hypoplasia often associated with other craniovertebral abnormalities, particularly atlantooccipital synostosis [19–22].

Unfortunately, Chamberlain [19] used the terms basilar impression and platybasia interchangeably, which has served to perpetuate the confusion with regard to these

entities. Virchow employed the term platybasia to describe flattening of the skull base. The normal basal angle is 132° ; an angle greater than 140° indicates platybasia. Platybasia may occur as an unimportant normal variant or along with other forms of dysplasia of the occiput and dens (fig. 16).

Basilar impression can be diagnosed from various craniometric data. If half of the dens lies above Chamberlain's line or McGregor's line, basilar impression is present (fig. 17). Although the bimastoid line is unreliable, the digastric (biventer) line is helpful (fig. 18). Normally, the latter lies above the dens and approximately 40 mm above the middle of the atlantooccipital joints. Basilar impression is present if the digastric line lies at or below the level of the atlantooccipital joints.

ACKNOWLEDGMENT

We are grateful to Dr. E. Leon Kier for permission to use his rich collection of craniovertebral abnormalities.

REFERENCES

1. Forriep A: Über ein Ganglion des Hypoglossus und Wirbel-

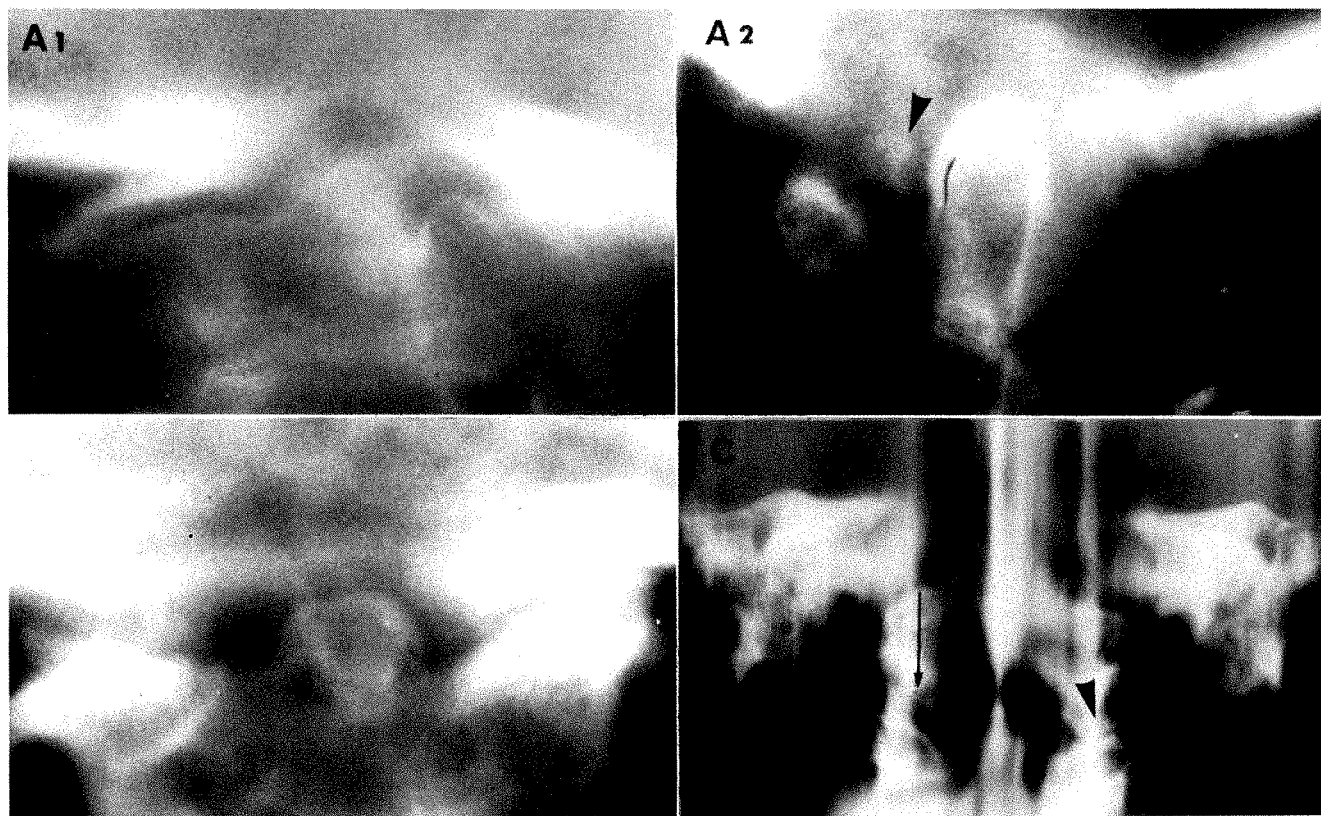


Fig. 14.—Tomographic studies of three patients with condylar hypoplasia. Anteroposterior (A1) and lateral (A2) tomograms in 8-year-old girl demonstrating third occipital condyle (arrowhead) and abnormal dens displaced craniad into foramen magnum. B, Tomogram in young female with limited motion at atlantooccipital region. C, Unilateral hypoplasia of left occipital condyle (arrowhead) in 54-year-old female. Note unilateral arthritic changes in left C1–C2 joint and normal slope of right occipital condyle (arrow).

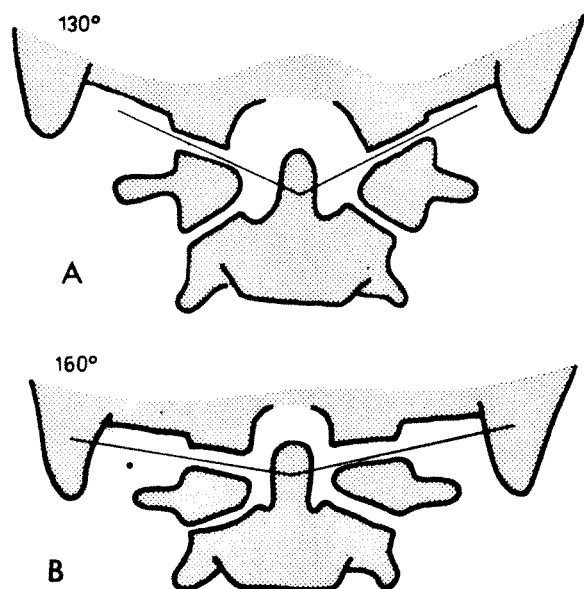


Fig. 15.—Diagram of normal angle formed at intersection of both atlanto-occipital joints (A) and increased angle in condylar hypoplasia (B).

anlagen in der Occipitalregion. *Arch Anat Entwicklungsgesch* 6:279–302, 1882

2. Froriep A: Zur Entwicklungsgeschichte der Wirbelsäule, insbesondere des Atlas und Epistropheus und der Occipitalregion. I. Beobachtung an Hühnerembryonen. *Arch Anat Entwicklungsgesch* 7:177–233, 1883
3. Sensenig EC: Development of occipital and cervical segments and their associated structures in human embryos. *Contrib Embryol Carnegie Inst* 36:143–151, 1957
4. List CF: Neurological syndromes accompanying developmental anomalies of occipital bone, atlas and axis. *Arch Neurol Psychiatr* 45:577–616, 1941
5. Gladstone RI, Erickson-Powell W: Manifestation of occipital vertebra and fusion of atlas with the occipital bone. *J Anat Physiol* 49:190–209, 1914–1915
6. Gladstone RI, Wakeley CPG: Variations of occipito-atlantal joint in relation to metameric structure of craniovertebral region. *J Anat Physiol* 59:195–216, 1924–1925
7. Lombardi G: Occipital vertebra. *Am J Roentgenol* 86:260–269, 1961
8. Brocher JEW: *Die Occipito-Cervical-Gegend*. Stuttgart, Georg Thieme Verlag, 1955
9. Bystrow AP: Morphologische Untersuchungen über die Occipitalregion und die ersten Halswirbel der Säugetiere und des Menschen. I. Über den Proatlas und AnteproAtlas bei der Ratte. *Z Anat Entwicklungsgesch* 100:362–386, 1933
10. Bystrow AP: Morphologische Untersuchungen über die Occipitalregion und die ersten Halswirbel der Säugetiere und des Menschen. II. Die Assimilation des Atlas und deren phylo-

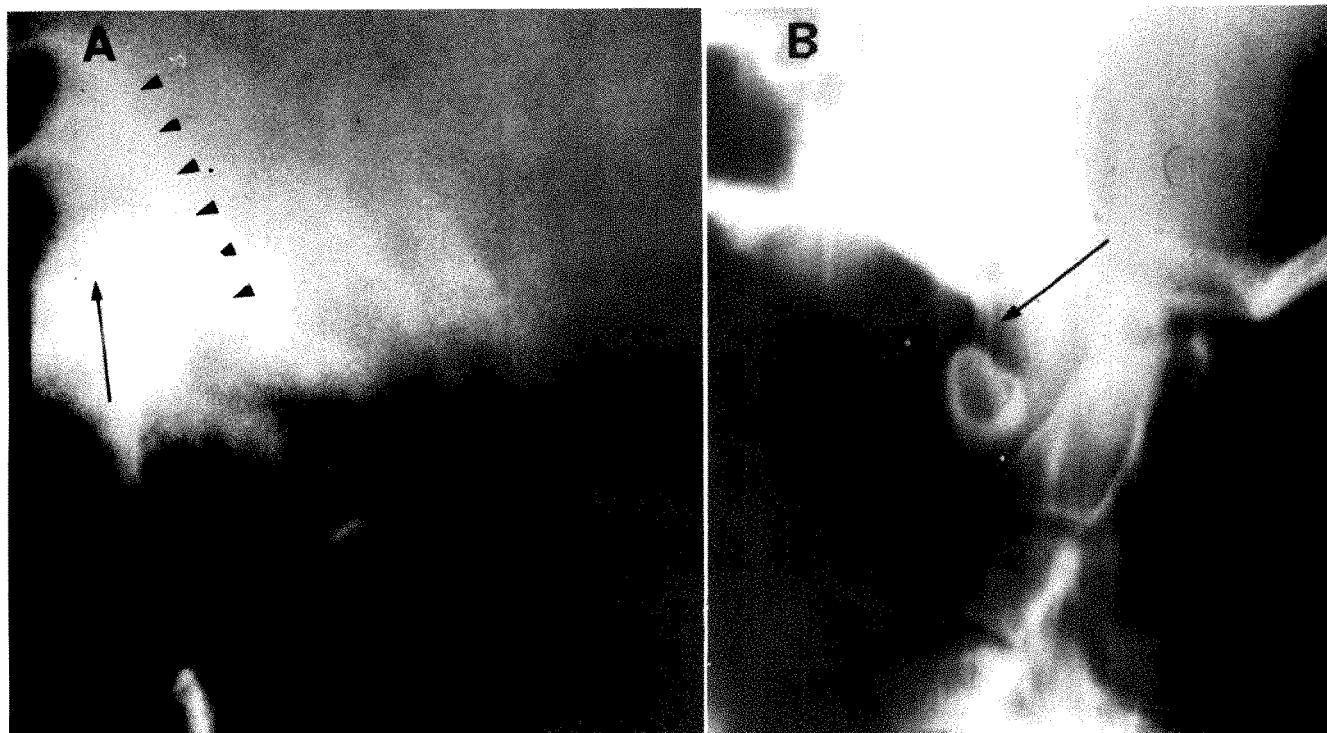


Fig. 16.—A, Patient with marked dysplasia of dens. Note elongation and displacement of dens beneath anterior arch of atlas (arrow); clivus delineated by arrowheads. B, Posterior and craniad displacement of dens in patient with third occipital condyle (arrow).

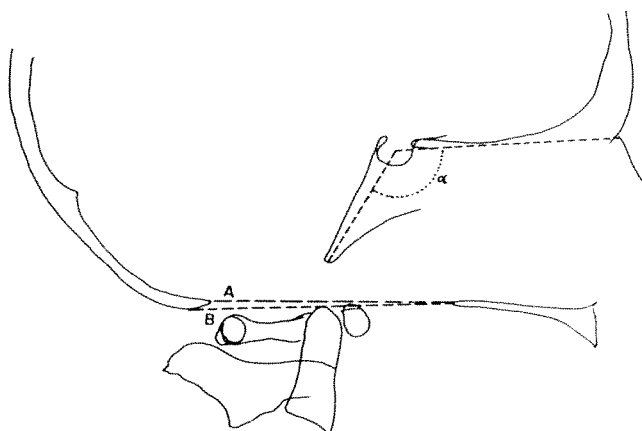


Fig. 17.—Diagram of Chamberlain's and McGregor's lines. Chamberlain's line: line drawn on lateral skull film from posterior margin of hard palate to posterior aspect of foramen magnum (opisthion). McGregor's line: line drawn on lateral skull film from posterior margin of hard palate to most caudal point of occipital curve.

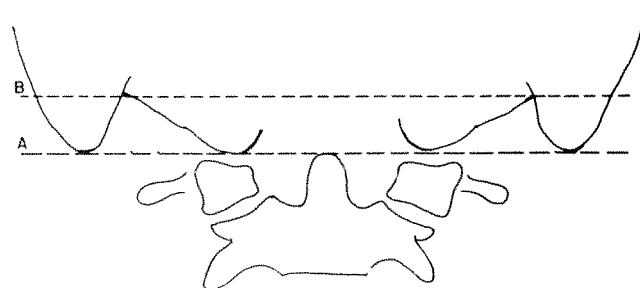


Fig. 18.—Diagram demonstrating digastric and mastoid lines. Digastric line (Fischgold and Metzger) is line drawn on anteroposterior film joining digastric grooves at junction of medial aspect of mastoid processes with base of skull.

genetische Bedeutung. *Z Anat Entwicklungsgesch* 102:307–334, 1933–1934

11. Hadley LA: Atlanto-occipital fusion, ossiculum terminale and occipital vertebra as related to basilar impression with neurological symptoms. *Am J Roentgenol* 59:511–524, 1948
12. Harrower G: Variations in region of foramen magnum. *J Anat* 57:178–192, 1922–1923
13. McCrae DL: Bony abnormalities in region of foramen magnum: correlation of anatomic and neurologic findings. *Acta Radiol* 40:335–354, 1953
14. McCrae DL, Barnum AS: Occipitalization of the atlas. *Am J Roentgenol* 70:23–45, 1953

15. Weigner K: Über die Assimilation des Atlas und über Variationen am Os Occipitale beim Menschen. *Anat Hefte* 45:81–195, 1911–1912
16. Wackenheim A: *Roentgen Diagnosis of the Craniovertebral Region*. Berlin, Springer-Verlag, 1974
17. Schmidt H, Fischer E: *Die Occipitale Dysplasie*. Stuttgart, Georg Thieme Verlag, 1960
18. Kruffy E: Occipital dysplasia in infancy. *Radiology* 85:501–507, 1965
19. Chamberlain WC: Basilar impression (platybasia). *Yale J Biol Med* 11:487–496, 1939
20. Ebenius B: Roentgen appearance in four cases of basilar impression. *Acta Radiol* 15:652–656, 1934
21. Peyton WT, Peterson HO: Congenital deformities in the region of the foramen magnum. *Radiology* 38:131–144, 1942
22. Saunders WW: Basilar impression: position of the normal odontoid. *Radiology* 41:589–590, 1943

An Early Rim Sign in Neonatal Adrenal Hemorrhage

PAULA W. BRILL,¹ IRWIN H. KRASNA,² AND HAROLD AARON³

Neonatal adrenal hemorrhage can usually be diagnosed on excretory urography without resorting to surgical exploration or invasive diagnostic procedures. In the typical case an avascular mass is seen between the liver and kidney. A case is presented in which a vascular rim surrounded the avascular mass, giving an appearance similar to that of an obstructed upper pole renal duplication. This early vascular rim, not as well known as the calcified rim which develops days to weeks after the acute hemorrhage, is probably created by compression and displacement of adrenal tissue by the central hemorrhage.

The presenting signs of adrenal hemorrhage in the newborn are highly variable [1, 2]. Some infants suffer severe exsanguinating hemorrhage with intraperitoneal or retroperitoneal rupture of the gland. Others are asymptomatic, and the diagnosis is assumed when adrenal calcification is discovered as an incidental radiographic finding [3]. Between the extremes are those infants who are studied radiologically because of an abdominal mass alone [4] or mass in association with jaundice [5]. In such cases the avoidance of surgical exploration and extensive diagnostic procedures is possible if a secure radiologic diagnosis can be made.

The radiographic diagnosis of neonatal adrenal hemorrhage is based on observing renal displacement by an avascular suprarenal mass demonstrated on high dose intravenous urography with "total body opacification" [6, 7]. Days or weeks later the diagnosis is confirmed as the mass calcifies and shrinks.

We wish to call attention to an additional early sign of neonatal adrenal hemorrhage: the demonstration of a vascular (dense) rim around an avascular (lucent) suprarenal mass on high dose excretory urography. Subsequent calcification of the rim distinguishes this condition from a hydronephrotic upper pole renal duplication which may give a similar urographic appearance. In the case presented, tomography was useful in showing this calcification at a time when it was not demonstrated on plain abdominal radiographs.

Case Report

A 4,510 g female was born at term to a 37-year-old multipara. Delivery was by midforceps, and left shoulder dystocia resulted in a fractured clavicle. Soon after birth a right upper quadrant mass was palpated. Excretory urography demonstrated flattening and depression of the right kidney by a lucent mass with a dense but noncalcified rim.

Severe indirect hyperbilirubinemia starting at 3 days of age necessitated three exchange transfusions. There was no blood

group incompatibility, anemia, or evidence of sepsis, and the infant was vigorous and fed well.

At 16 days of age the mass was unchanged on physical examination and excretory urography (fig. 1). At 22 days a plain film of the abdomen failed to reveal calcification, but the following day a tomographic cut of the right upper quadrant demonstrated a calcific rim in the suprarenal area (fig. 2). At 2 months of age an excretory urogram showed definite decrease in the size of the rim-like suprarenal calcification and only minimal renal displacement. At 8 months a plain film showed continued increase in the density of the calcification and reduction in its size (fig. 3).

Discussion

During the "total body opacification" phase of excretory urography [7], hemorrhage of the right adrenal gland appears as a round, well defined lucent area between the dense liver and kidney [8]. The radiographic diagnosis is more difficult on the left side due to the obscuring effect of adjacent bowel gas. In the present case a dense rim was demonstrated on "total body opacification" surrounding the lucent suprarenal mass and separate from the liver (fig. 1A). The appearance was similar to that of a hydronephrotic upper pole renal duplication.

Only three previous cases of uncomplicated neonatal adrenal hemorrhage have been reported to show vascular rims. Two were seen on excretory urography [4] and were similar to the present case. These infants presented with mass alone and were not jaundiced. The third case was a 7-day-old infant with a rim of compressed tissue around an adrenal mass, demonstrated on aortography [9]. Neonatal adrenal abscesses have been described both with and without opaque rims [10-12].

The main lesion to be considered in the differential diagnosis of an adrenal hemorrhage with urographic demonstration of a lucent center and dense rim is a double collecting system with obstruction of the upper pole system. In the latter, the central lucency may fill with contrast medium on delayed films if there is sufficient functioning renal parenchyma. With an associated ectopic ureterocele, the typical lucent defect in the bladder would indicate a renal rather than adrenal origin of the mass.

Neuroblastoma is distinguishable from adrenal hemorrhage on the basis of radiographic findings and elevation of urinary catecholamines; angiography is not often necessary [13]. Neuroblastomas tend to appear dense or to contain mottled lucencies on "total body opacification." When calcifications are present they are finely granular and not rimlike. The unusual cases in which *in situ* neuroblastoma has been detected in association with neonatal

¹ Department of Radiology, New York Hospital-Cornell Medical Center, 525 East 68th Street, New York, New York 10021. Address reprint requests to P. W. Brill.

² Department of Surgery, Mount Sinai School of Medicine, New York, New York 10029.

³ Department of Pediatrics, Jewish Memorial Hospital, New York, New York 10040.

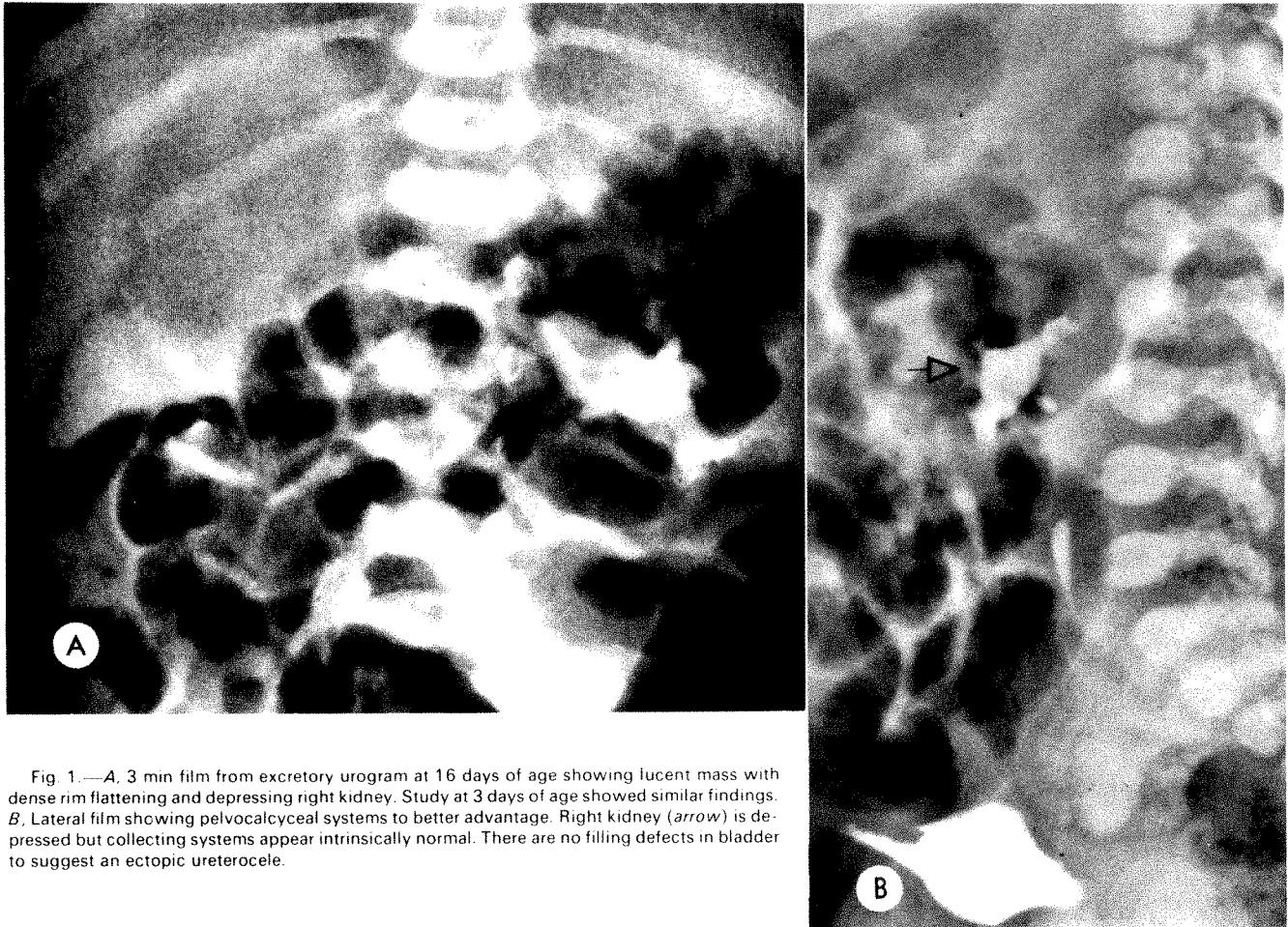


Fig. 1.—A, 3 min film from excretory urogram at 16 days of age showing lucent mass with dense rim flattening and depressing right kidney. Study at 3 days of age showed similar findings. B, Lateral film showing pelvocalyceal systems to better advantage. Right kidney (arrow) is depressed but collecting systems appear intrinsically normal. There are no filling defects in bladder to suggest an ectopic ureterocele.

adrenal hemorrhage [14, 15] are of doubtful significance in view of the fact that such foci can be found in 0.5%–1.5% of postmortem examinations on stillborns and infants up to the age of 3 months [16, 17]. There are no known cases of death due to metastatic neuroblastoma in patients presenting at birth with adrenal hemorrhage.

The jaundice frequently seen with adrenal hemorrhage [5] is the result of the hemolysis which occurs in any closed space hemorrhage coupled with the inability of the liver to conjugate the bilirubin due to transient deficiency of glucuronyl transferase in the neonatal period.

In a stable infant with a clinical picture strongly suggestive of adrenal hemorrhage and urographic findings of a lucent suprarenal mass, with or without a dense rim, conservative management is indicated in the absence of clinical or chemical evidence of neuroblastoma. Subsequent calcification, usually appearing initially in a faint rimlike configuration at the periphery, confirms the diagnosis (fig. 2). The youngest patient in whom calcification was demonstrated radiographically was 12 days old [18]. The calcifications coalesce as the hemorrhage is resorbed (fig. 3).

In the present case the demonstration of calcification was felt to be important because of the close resemblance of the urographic findings to upper pole renal duplication and the paucity of other cases of adrenal hemorrhage in

which vascular rims have been reported. While plain abdominal radiographs failed to demonstrate the calcification, tomography of the renal-adrenal area at 23 days of age convincingly showed a faint calcific rim around the entire periphery of the large gland (fig. 2).

REFERENCES

1. Black J, Williams DI: Natural history of adrenal haemorrhage in the newborn. *Arch Dis Child* 48:183–190, 1973
2. Gross M, Kottmeier PK, Waterhouse K: Diagnosis and treatment of neonatal adrenal hemorrhage. *J Pediatr Surg* 2:308–312, 1967
3. Jarvis JL, Seaman WB: Idiopathic adrenal calcification in infants and children. *Am J Roentgenol* 82:510–520, 1959
4. Eklöf O: Large asymptomatic adrenal haematomas in the neonate. *Acta Radiol [Diagn]* 11:481–488, 1971
5. Rose J, Berdon WE, Sullivan T, Baker DH: Prolonged jaundice as presenting sign of massive adrenal hemorrhage in newborn. *Radiology* 98:263–272, 1971
6. Katzman D, Vanhoutte JJ: Total body opacification technique in neonatal adrenal haemorrhage. *S Afr Med J* 45:1370–1372, 1971
7. O'Connor JF, Neuhauser EBD: Total body opacification in conventional and high dose intravenous urography in infancy. *Am J Roentgenol* 90:63–71, 1963
8. Dunbar JS, Nogrady B: Excretory urography in the first year of



Fig. 2.—Tomographic cut of right upper quadrant without contrast medium at 23 days of age. Note calcific rim in position of vascular rim which had been shown on excretory urography. Plain films the previous day failed to demonstrate calcium.

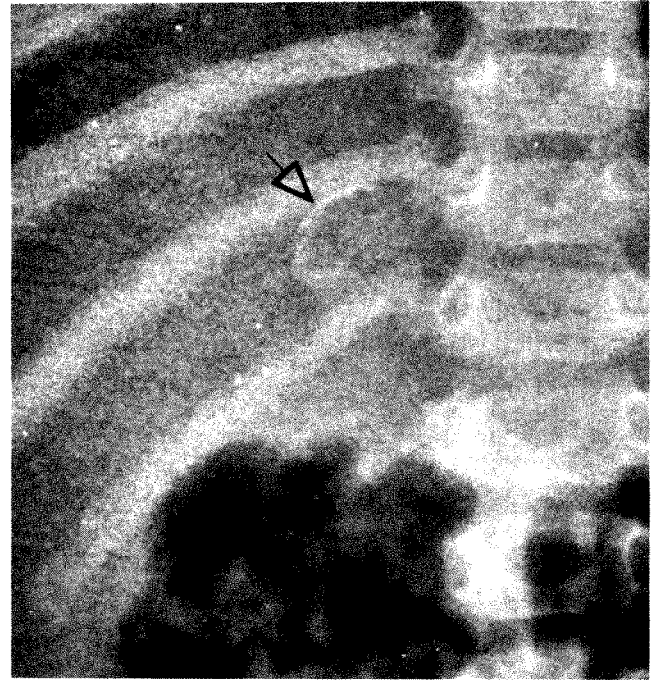


Fig. 3.—Plain radiograph of right upper quadrant at 8 months of age showing rimlike adrenal calcification (arrow) which has become smaller and denser.

life. *Radiol Clin North Am* 10:367-391, 1972

9. Iancu T, Elian E, Lerner MA: Angiography and the conservative management of neonatal adrenal haemorrhage. *Pediatr Radiol* 2:47-50, 1974
10. Blankenship WJ, Bogren H, Stadalnik RC, Vitale DE: Suprarenal abscess in the neonate: a case report and review of diagnosis and management. *Pediatrics* 55:239-243, 1975
11. Carty A, Stanley P: Bilateral adrenal abscesses in a neonate. *Pediatr Radiol* 1:63-64, 1973
12. Favara BE, Akers DR, Franciosi RA: Adrenal abscess in a neonate. *J Pediatr* 77:682-685, 1970
13. Fellows KE Jr: The uses and abuses of abdominal and peripheral arteriography in children. *Radiol Clin North Am* 10:349-366, 1972
14. Sober I, Hirsch M: Unilateral massive adrenal hemorrhage in newborn infant. *J Urol* 93:430-434, 1965
15. Tubergen DG, Heyn RM: In situ neuroblastoma associated with an adrenal cyst. *J Pediatr* 76:451-453, 1970
16. Beckwith JB, Perrin EV: In situ neuroblastomas: a contribution to the natural history of neural crest tumors. *Am J Pathol* 43:1089-1104, 1963
17. Guin GH, Gilbert EF, Jones B: Incidental neuroblastoma in infants. *Am J Clin Pathol* 51:126-136, 1969
18. Wagner AC: Bilateral hemorrhagic pseudocysts of the adrenal glands in the newborn. *Am J Roentgenol* 86:540-544, 1961

Autonomic Dysreflexia in Patients with Spinal Cord Lesions: Complication of Voiding Cystourethrography and Ileal Loopography

ZORAN L. BARBARIC¹

Autonomic dysreflexia is a pathologic reflex which occurs in patients with a spinal cord lesion above T7. The most dangerous manifestation of this reflex is marked increase in systolic and diastolic blood pressure. The trigger is the distension of the urinary bladder, urethra, rectum, or intestine. It can and does occur during radiological examinations such as cystourethrography, loopography, and probably during the barium enema. Because of possible deleterious consequences of marked hypertension, blood pressures in these patients should be continuously monitored during the examinations and appropriate measures immediately instituted should the reaction occur.

Many radiologists are unfamiliar with potentially life threatening complications that may occur during the performance of cystourethrography or loopography in patients with spinal cord lesions above T7. The most pronounced manifestation of this complication is uncontrollable hypertension which, if unrecognized, may lead to convulsions, cerebral hemorrhage, retinal hemorrhage, renal failure, and even death. Autonomic dysreflexia is quite unpredictable. It need not recur during the second examination, or it might occur during the second examination even if the first examination was uneventful. The purpose of this paper is to familiarize radiologists with this peculiar complication, since it is not mentioned in basic urologic textbooks.

Case Reports

Case 1

C. G. (89-31-02) was an 18-year-old quadriplegic male with spinal injury at the level of C2 and with recurrent urinary tract infections. He was evaluated in the radiology department for possible vesicoureteric reflux and for the cause of unacceptable bladder residuum. A no. 12 Foley catheter was placed in the navicular fossa, and the urethra and the bladder were filled in a retrograde fashion. After introduction of 120 ml of contrast material, the patient complained of stuffiness of the nasal passages, profuse sweating of the face and neck, and sudden onset of severe headache.

On physical examination he had a flushed, red face and profuse sweating over the forehead. There was sudden increase in the blood pressure from a baseline of 100/70 mm Hg to 210/100 mm Hg. Pulse rate changed from baseline 75 to 60/min. The bladder was immediately emptied. The blood pressure remained high for the next 5 min and gradually returned to normal within the next 30 min. At the same time the patient's subjective symptoms also subsided.

Case 2

W. W. (70-81-06) was a 23-year-old male quadriplegic with a spinal injury at the level of C4. Urinary tract diversion by means of an ileal conduit was performed several years ago. Recently a right ureteral calculus causing obstruction was removed, and several

weeks after the surgery the patient was referred to the radiology department for a loopogram to check the patency of the right ureter.

The loopogram was performed using a Foley catheter with the balloon inflated in the distal end of the loop with 20 ml of normal saline connected to a drip infusion bottle placed 30 cm above the level of the loop. After receiving 50 ml of contrast, the patient complained of facial flushing and sweating, pounding headache, and nausea. The loop was immediately drained.

Physical examination revealed profuse sweating of the face and elevation of the blood pressure from a baseline of 100/70 mm Hg to 190/100 mm Hg. The pulse rate decreased from baseline 72 to 65/min. The blood pressure and pulse rate returned to normal within 5 min after emptying of the loop; at the same time the patient's subjective symptoms disappeared. At a later date the examination was repeated without recurrence of dysreflexia.

Discussion

Autonomic dysreflexia is a peculiar neurologic phenomenon that occurs only in patients with a spinal cord lesion at T7 or above [1-3]. Pathologic autonomic reflexes are triggered by distension of the bladder, urethra, and rectum and, to a lesser extent, by distension of the small and large bowel.

The patient's subjective symptoms will usually include sudden onset of severe headache, flushing and sweating of the face and neck, and blockage of the nasal passages sometimes associated with difficulty in breathing. These symptoms are not always present and some may be more pronounced than others. Physical findings include increase in systolic and diastolic blood pressure (as much as 100-200 mm Hg and 50-100 mm Hg, respectively); bradycardia; and redness and sweating of the face and neck along with paleness of the skin of the abdomen and the lower extremities.

The pathologic reflex begins during the distension of the bladder, urethra, rectum, or intestine, and the afferent pathways lead to the spinothalamic tracts and dorsal columns of the spinal cord. While traversing the spinal cord, the afferent impulses excite the sympathetic motor neurons of the intermediolateral horns in the spinal grey matter. This results in vasoconstriction, particularly in the splanchnic vascular bed, kidney, skin, and legs [4] (fig. 1). As a result of the vasoconstriction occurring below T7, there is marked increase in the systemic blood pressure.

The normal individual would control the blood pressure rise through the baroreceptors in the carotid sinus and aortic wall. These would send afferent impulses to the vasomotor center in the medulla. The inhibitory impulses from the vasomotor center decrease the blood pressure in two ways: (1) by slowing the heart rate and mildly decreasing myo-

¹ Department of Radiology, University of Rochester School of Medicine and Dentistry, Rochester, New York 14642.

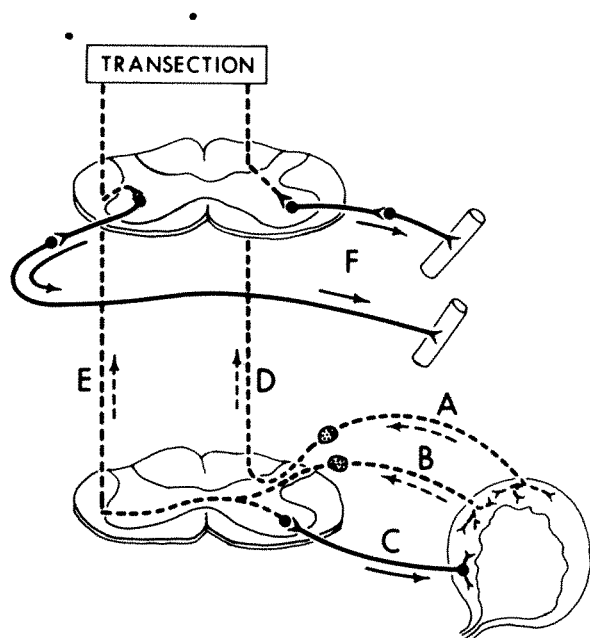


Fig. 1.—A and B, Afferent pathways from the bladder; C, efferent pathway to the bladder; D, dorsal column; E, spinothalamic tract; F, sympathetic efferent pathways to splanchnic vascular bed (T7–L1). Transection at T7 or above.

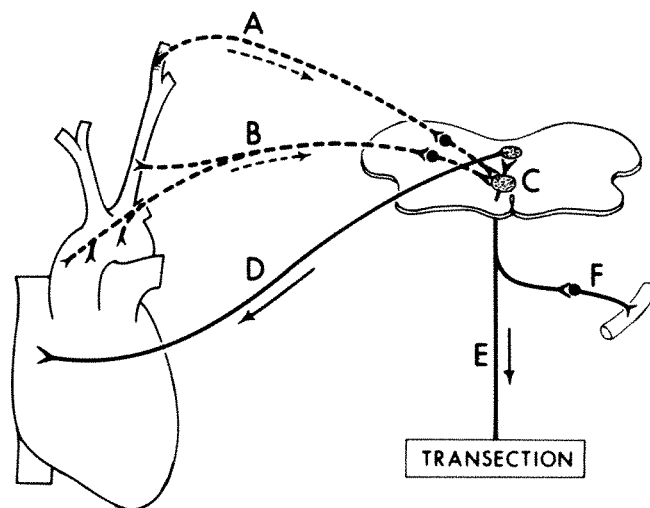


Fig. 2.—A, Afferent pathways from carotid sinus via Hering's and glossopharyngeal nerves. B, Afferent pathways from baroreceptors in aortic wall via vagus. C, Vasomotor center in medulla. D, Efferent pathways carrying inhibitory impulses to heart via vagus. E, Efferent sympathetic pathways from vasomotor center carrying inhibitory impulses to thoracolumbar spinal cord and splanchnic vasculature; these pathways are ineffective below transection. F, Efferent sympathetic pathways to upper half of body carrying inhibitory impulses causing vasodilation and sweating. Transection at T7 or above.

cardiac contractility via efferent vagal impulses, and (2) by dilating the splanchnic and skin vasculature through the sympathetic pathways of the cord. These impulses would effectively balance the sympathetic excitation caused by the bladder distension.

However, in the patient with high spinal cord lesion, the inhibiting impulses from the vasomotor center are unable to reach the splanchnic circulation due to the cord lesion. Hence the sympathetic excitation below the lesion continues uncontrolled. In such a patient, the only means available for the vasomotor center to combat increased blood pressure is to decrease the heart rate (fig. 2).

According to Poiseuille's formula, pressure in tubes is only linearly affected by rate of flow but is affected to the fourth power by the diameter of the tube. Thus the decreased flow due to the slowed heart rate will only minimally affect the high blood pressure. The inhibitory sympathetic impulses above the transection will result in vasodilatation in the head and neck, explaining the stuffy nose, flushing of the face and neck, and marked perspiration in these regions. In addition, there is significant increase of the catecholamine metabolites in the urine after the hypertensive episode. This indicates accelerated release of norepinephrine from sympathetic nerve endings and epinephrine from adrenal medulla during dysreflexia [5].

The radiologist must be aware of this complication since it could have a potentially deleterious effect on the patient. Generally, the higher the spinal cord lesion above T7, the more apt the patient is to experience dysreflexia and the more severe the manifestations. The patient should be questioned prior to the procedure regarding previous episodes of dysreflexia. Constant blood pressure monitoring during the examination is mandatory.

If autonomic dysreflexia occurs during radiologic examination of the bladder, urethra, ileal loop, or intestine, the procedure should be stopped immediately and the structure completely emptied [6]. If this has no effect on the blood pressure, the patient should be propped up in a sitting position. Another procedure is to instill 5–10 ml of 1% lidocaine hydrochloride (Xylocaine, Astra) into the viscus, thereby breaking the afferent limb of the dysreflexia [4, 7].

Should the pressure still remain dangerously high, more drastic measures are needed. An ultrafast ganglionic blocking agent, trimethaphan camsylate (Arfonad, Roche), can be administered with the patient in a semisitting position up to at least 45°. A 0.1% concentration (1 mg/ml) of Arfonad in 5% dextrose solution is administered intravenously starting at an average rate of 60 drops/min. The rate of administration is then adjusted to maintain the desired level of hypotension. This pharmacologic agent blocks transmission in autonomic ganglia by occupying receptor sites on the ganglion cells and by stabilizing the postsynaptic membranes against the action of acetylcholine liberated from presynaptic nerve endings. In addition, it may exert a direct peripheral vasodilator effect. Other useful pharmacological agents that can be used instead are diazoxide (Hyperstat, Schering; 5 mg/kg body weight i.v.) or hydralazine hydrochloride (Apresoline, CIBA; 15 mg i.v.).

Prior to and at the time of the examination some patients may already be on some form of medication, most likely phenoxybenzamine, an alpha-adrenergic blocking agent. This is likely to reduce the incidence of dysreflexia during the examination [8, 9].

The examining physician should be thoroughly familiar

with the drugs described and approach these patients with due care and diligence.

REFERENCES

1. Guttman L, Whitteridge D: Effects of bladder distension on autonomic mechanisms after spinal cord injuries. *Brain* 70:361–404, 1947
2. Kurnick ND: Autonomic hyperreflexia and its control in patients with spinal cord lesions. *Ann Intern Med* 44:678–686, 1956
3. Lapidus J: Autonomic hyperreflexia, in *Urology*, edited by Campbell MF, Harrison JH, Philadelphia, Saunders, 1971, pp 1361–1362
4. Roussan MS, Abramson AS, Lippmann HI, D'Oronzio G: Somatic and autonomic responses to bladder filling in patients with complete transverse myelopathy. *Arch Phys Med Rehab* 47:450–456, 1966
5. Sell HG, Naftchi NE, Lowman EW, Rusk HA: Autonomic hyperreflexia and catecholamine metabolites in spinal cord injury. *Arch Phys Med Rehab* 53:415–417, 1972
6. McCallum RW: The radiologic assessment of the lower urinary tract in paraplegics—a new method. *J Can Assoc Radiol* 25:34–38, 1974
7. Bors E, French JD: Management of paroxysmal hypertension following injuries to cervical and upper thoracic segments of the spinal cord. *Arch Surg* 64:803–812, 1952
8. Sizemore GW, Winternitz WW: Autonomic hyper-reflexia—Suppression with alpha-adrenergic blocking agents. *N Engl J Med* 2:795, 1970
9. Krane RJ, Olsson CA: Phenoxybenzamine in neurogenic bladder dysfunction. II. Clinical considerations. *J Urol* 110:653–656, 1973

Roentgenologic Abnormalities of the Urinary Bladder Secondary to Crohn's Disease

NORMAN JOFFE¹

Urinary tract symptoms and signs may result from secondary involvement of the urinary bladder in patients with Crohn's disease. In a small but significant proportion of these individuals, urinary tract symptoms represent the initial or predominant mode of presentation. Such patients may be erroneously treated for primary infection of the lower urinary tract for prolonged periods before the intestinal origin of the disease process is discovered. Roentgenologic abnormalities of the urinary bladder may provide early and important clues to the correct diagnosis. The various abnormalities of the urinary bladder which may occur secondary to Crohn's disease are described and illustrated, and the roentgenologic differential diagnosis is discussed.

Introduction

A variety of abnormalities of the urinary tract may be observed in patients with Crohn's disease of the small bowel and/or colon [1, 2]. They include: an increased incidence of nephrolithiasis, especially in patients who have undergone resection of diseased small or large bowel [3, 4]; the nephrotic syndrome secondary to amyloidosis [5]; retroperitoneal, psoas, or perirenal abscesses [6, 7]; and ureteric obstruction with hydroureter and hydronephrosis [8]. These complications generally occur in association with disease which is severe or of long duration. Urinary tract complications such as ureteric obstruction may not be recognized unless specifically searched for by excretory urography [9].

Urinary tract symptoms may also occur as a result of secondary involvement of the urinary bladder in patients with Crohn's disease [6, 10-12]. Such symptoms in patients with known inflammatory bowel disease generally provide no serious diagnostic problem, since the primary cause is already established. However, in some patients urinary tract symptoms are the initial or predominant mode of presentation, and failure to recognize the intestinal origin of the disease may result in serious complications. Since roentgenologic abnormalities of the urinary bladder may facilitate correct diagnosis, it is important for radiologists to be aware of them. This paper describes and illustrates the roentgenologic changes.

Material

Urinary tract symptoms were the initial or predominant mode of presentation in 12 patients with roentgenographic abnormalities of the urinary bladder secondary to regional enteritis. Eight were male and four female; ages ranged from 19 to 44 years (mean, 32). Difficulty with micturition, increased frequency, dysuria, nocturia, and penile or suprapubic pain were the initial symptoms in six patients. While urinary symptoms also dominated the clinical picture in the remaining six, Crohn's disease had been diagnosed

1-16 years earlier.

Lower abdominal cramps and/or diarrhea were frequently absent or relatively mild. Such complaints were often elicited only by direct questioning following excretory urography. Pneumaturia and fecaluria were never the initial presenting complaints, although one or the other subsequently developed in three patients in whom enterovesical fistulae were demonstrated by radiology or surgery.

Prior to referral to our hospital, most of the patients in this group, including the six with undiagnosed Crohn's disease, were treated for "acute or chronic cystitis," "recurrent lower urinary tract infection," or even "prostatitis." In all 12 cases, Crohn's disease of the ileum was the primary disease process responsible for the abnormalities of the bladder and the associated urinary symptoms. One of three patients with extrinsic involvement of the rectosigmoid region secondary to adjacent ileal disease had rectal pain and tenesmus; an ileosigmoid fistula was demonstrated in one case.

Discussion

Involvement of the urinary bladder secondary to Crohn's disease is generally the result of direct extension of the inflammatory process from a contiguous loop of bowel with or without an intervening abscess. Initially there is fixation of the inflamed bowel to the peritoneal surface of the bladder with tethering of the bladder wall. This may interfere with normal muscular contraction and cause difficulty in micturition [13]. Secondary inflammatory changes develop within the wall of the bladder and may progress over a period of weeks, months, or even years resulting in thickening of all its layers with associated mucosal edema or polypoid changes.

Clinically there is frequency of micturition, dysuria, and urgency. The patient may also experience suprapubic pain or discomfort. Infection and ulceration of the bladder mucosa may give rise to gross or microscopic hematuria. If the secondary nature of the lesion is not recognized, further progression of the inflammatory process may result in perforation into the bladder lumen with the establishment of a vesicointestinal fistula. Fecal particles may be detected in the urine, or bubbles of gas may escape, especially at the end of micturition.

Fistulous tracts may be direct or indirect and generally involve the posterior and superior aspect of the bladder. In the former there is a direct communication between the bladder and an adherent loop of bowel. Indirect fistulae are generally transperitoneal with an intervening abscess between the bowel and the bladder. If an incipient or established fistula is present, cystoscopy may reveal localized hyperemia, bullous edema, or polypoid epithelial proliferation; the latter may simulate a vesical neoplasm [14]. The fistulous opening is frequently not visualized by cystoscopy,

¹ Department of Radiology, Beth Israel Hospital and Harvard Medical School, 330 Brookline Avenue, Boston, Massachusetts 02115.



Fig. 1.—33-year-old male with 3 week history of urinary tract complaints. Excretory urogram showing smooth, extrinsic pressure deformity of bladder dome. Barium studies revealed Crohn's disease of distal ileum.

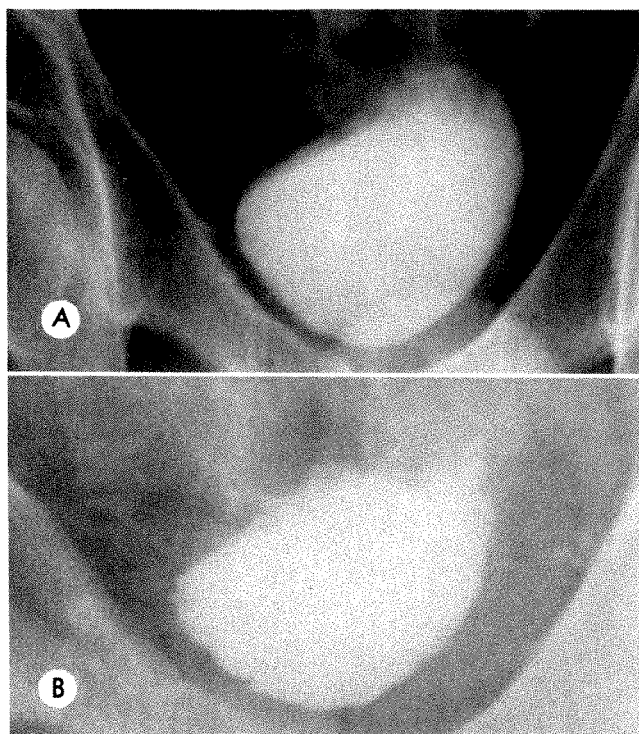


Fig. 2.—31-year-old male with urinary tract complaints and one episode of hematuria; no intestinal symptoms but Crohn's disease of terminal ileum demonstrated 4 years earlier. A, Excretory urogram showing extrinsic pressure deformity of bladder dome. B, Postvoid film showing defect and residue of contrast. Surgery revealed Crohn's disease of distal ileum with abscess and ileovesical fistula.

even in the presence of pneumaturia or fecaluria [12, 15, 16].

Roentgenologic Findings

The roentgenologic abnormalities depend on the stage and degree of the secondary inflammatory process. They

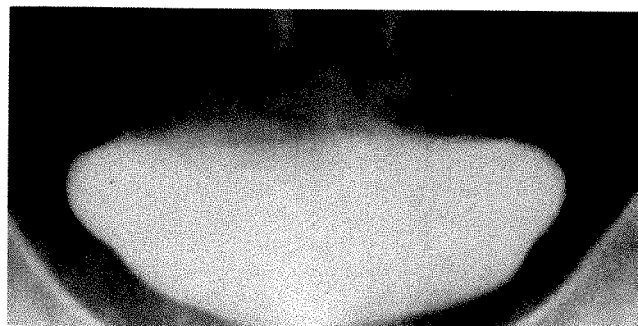


Fig. 3.—19-year-old female with urinary tract complaints and no intestinal symptoms. Excretory urogram showing deformity of bladder dome with spiculated appearance due to fixation and tethering of bladder wall. Barium studies revealed Crohn's disease of distal ileum.

are essentially the same whether the urinary symptoms represent the initial or predominant mode of clinical presentation or develop late in the course of known inflammatory bowel disease.

Roentgenologic abnormalities are generally well demonstrated by excretory urography but may be confirmed or further evaluated by retrograde cystography. Initially, fixation of the inflamed bowel to the bladder wall may result in deformity of the dome of the contrast-filled bladder. This may appear as a smooth extrinsic pressure defect (figs. 1 and 2) or there may be a spiculated appearance (fig. 3). The deformity may be localized or involve the entire superior contour and may be associated with a soft tissue mass. Since the changes are commonly secondary to inflammatory disease of the distal ileum, they are often limited to the right side of the bladder (figs. 1–3).

In the early stages the deformity may be relatively mild; it frequently is attributed to incomplete distention of the bladder on the excretory urogram (fig. 4A). If the deformed contour persists following voiding, the observer should be alerted to its pathologic significance (figs. 2B and 5B). Since the bladder-bowel fixation interferes with normal muscular contraction, a moderate or large postvoid residue of contrast in the bladder may also be observed (figs. 2B and 5B).

Extrinsic deformity of the bladder dome may also occur in association with pelvic abscess secondary to Crohn's disease (fig. 4B). Despite marked abnormalities of the bladder, the ureters and upper urinary tracts are usually normal. Only one of our 12 cases demonstrated evidence of partial unilateral ureteric obstruction.

After the inflammatory process has extended into the bladder wall, two further types of roentgen abnormality may be observed. There may be a diffuse nodular deformity of the bladder dome (figs. 5 and 6) or a localized, smooth, or irregular filling defect simulating a vesical neoplasm (figs. 7 and 8). The latter abnormality is particularly common in association with an incipient or established vesico-intestinal fistula. Demonstration of a fistulous communication by excretory urography, retrograde cystography, and barium studies of the bowel is uncommon, probably due to their long tortuous nature or the valvelike effects produced by the lining inflammatory tissue.

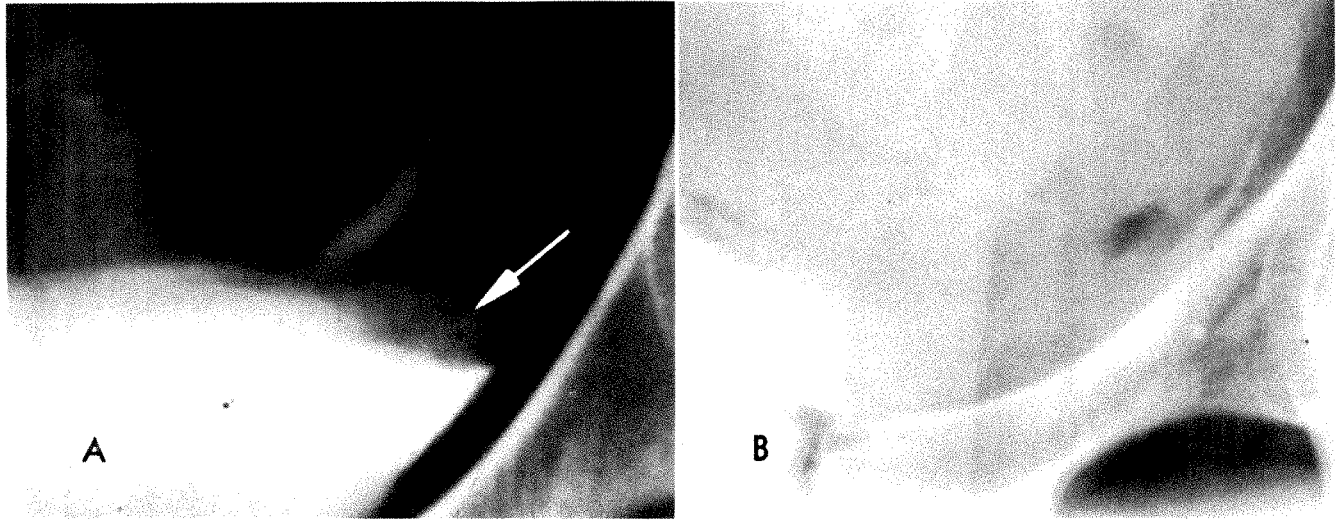


Fig. 4.—30-year-old female with lower urinary tract infection. Two months later, onset of fever, lower abdominal pain, and tender suprapubic mass. *A*, Excretory urogram showing minimal deformity of bladder dome (*arrow*). *B*, Repeat excretory urogram 2 months later showing large soft tissue mass compressing left superior contour of bladder. Small gas collection present just medial to distal portion of normal left ureter. Surgery revealed extensive Crohn's disease of ileum and cecum with large pelvic abscess.

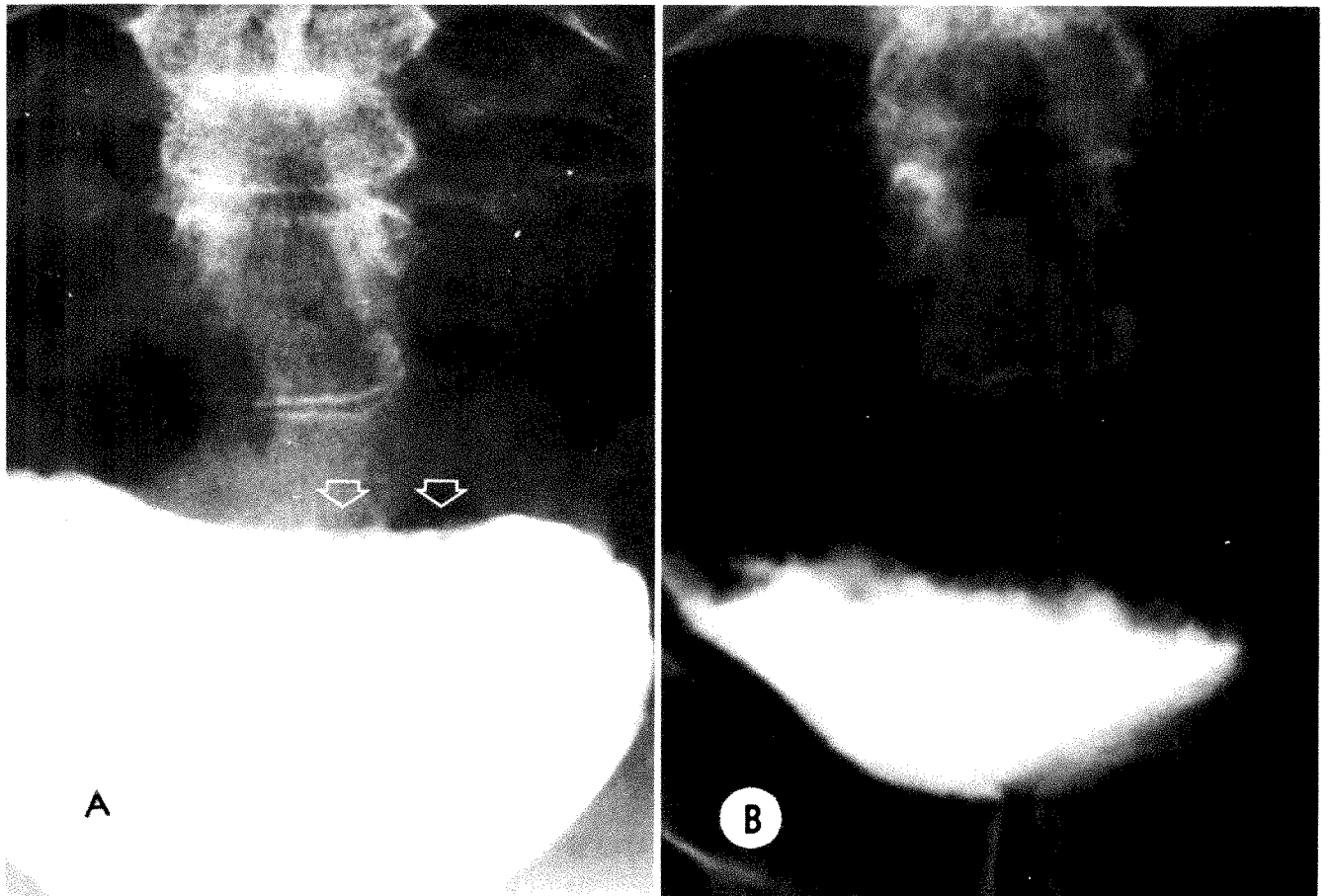


Fig. 5.—40-year-old male with urinary tract complaints and suprapubic pain. *A*, Excretory urogram showing nodular deformity (*arrow*) of bladder dome. *B*, Postvoid film showing persistence of deformity and large residue of contrast. Barium studies demonstrated Crohn's disease of distal ileum. At surgery, chronic abscess cavity found between diseased bowel and bladder wall but no fistula.

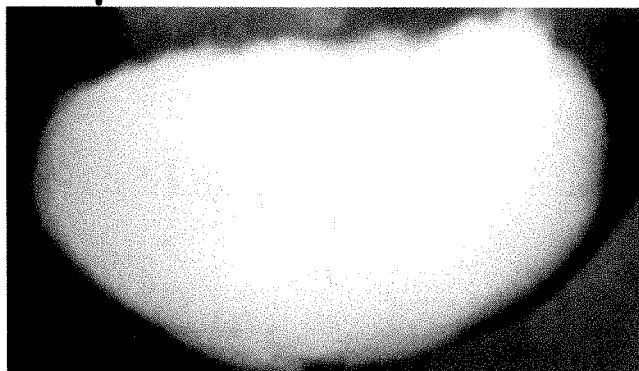


Fig. 6.—36-year-old male with urinary tract complaints and penile pain; no intestinal symptoms. Excretory urogram showing irregularity and nodularity of bladder dome. Barium studies showed Crohn's disease of distal ileum with secondary involvement of sigmoid colon.

Roentgenologic Differential Diagnosis

The roentgenographic abnormalities must be differentiated from both primary and secondary inflammatory or neoplastic processes involving the bladder. These primarily include inflammatory disease of the female genital tract (e.g., tuboovarian or other pelvic abscesses), acute appendicitis with or without periappendiceal abscess formation, cysts and neoplasms of the female genital tract, primary bladder carcinoma, tuberculous cystitis, and benign proliferative lesions (e.g., cystitis cystica and cystitis glandularis).

Differentiation from inflammatory or neoplastic disease of the female genital tract is largely based on associated clinical symptoms and signs and bimanual pelvic examination. Ultrasound may be helpful. If the diagnosis is still uncertain, exclusion of primary bowel disease by barium studies should always be undertaken. Barium enema examination may be helpful in the diagnosis of appendiceal abscess. Tuberculous cystitis is differentiated by associated involvement of the ureters and kidneys and identification of the causative organism in the urine.

Cystitis cystica and cystitis glandularis represent metaplastic changes in the epithelium and are frequently associated with inflammation of the bladder. Both tend to occur in the region of the trigone but may occur elsewhere and give rise to filling defects or irregularity of the bladder contour [17, 18]. Diagnosis depends on cystoscopy, biopsy, and exclusion of primary bowel disease by barium studies. Primary vesical neoplasms are differentiated by cystoscopy and biopsy.

If urinary symptoms include pneumaturia or fecaluria, the differential diagnosis consists essentially of vesicointestinal fistula. The reported incidence of such fistulae in large series of patients with Crohn's disease is shown in table 1, while the comparative incidence of nontraumatic causes of vesicointestinal fistulae is summarized in table 2. In patients over the age of 50, diverticulitis of the sigmoid colon or carcinoma of the rectosigmoid are the most likely causes. The diagnosis is generally established by barium enema examination, although the fistulous communication itself may not always be demonstrated. If the barium enema

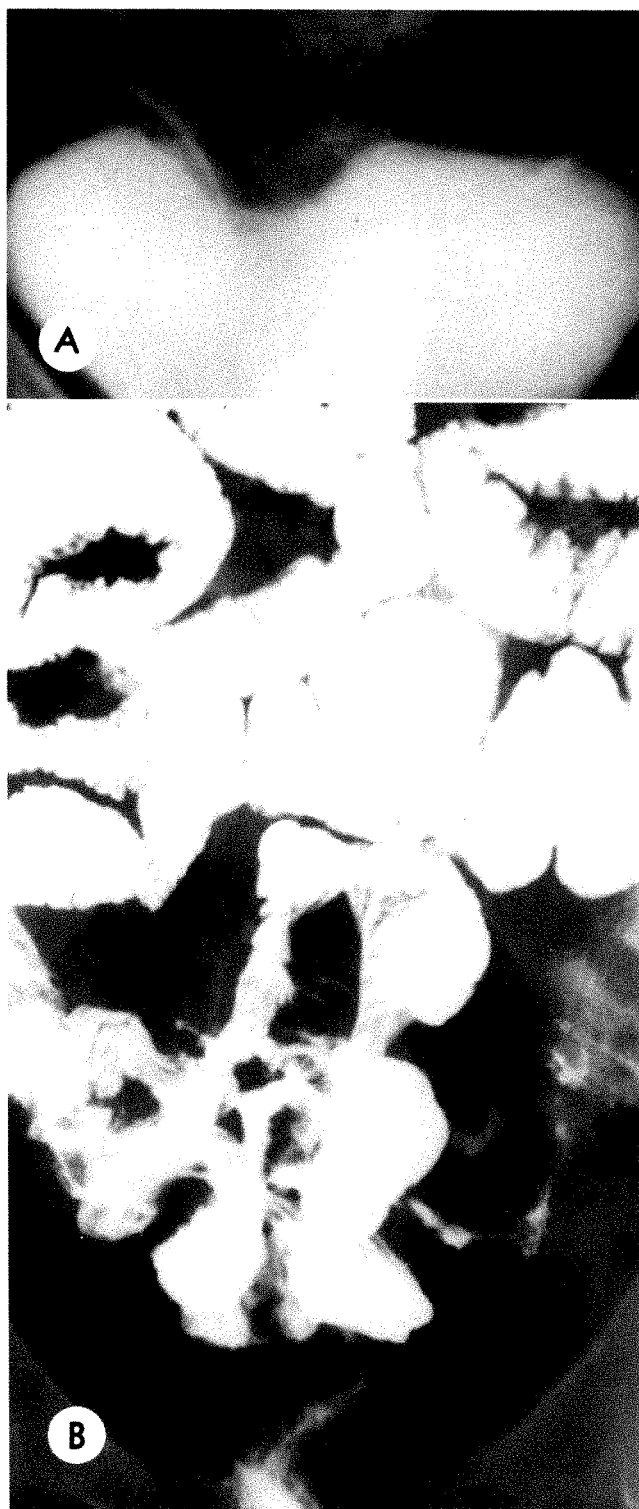


Fig. 7.—27-year-old male with 8 month history of suprapubic pain (diagnosed "prostatism"), urinary tract complaints, and cloudy urine. A, Excretory urogram showing smooth defect on bladder dome. Retrograde cystogram showed similar localized defect; cystoscopy revealed area of polypoid mucosal proliferation. B, Small bowel examination showing Crohn's disease of distal ileum with ileoileal and ileosigmoid fistulae. These findings and ileovesical fistula demonstrated at surgery.

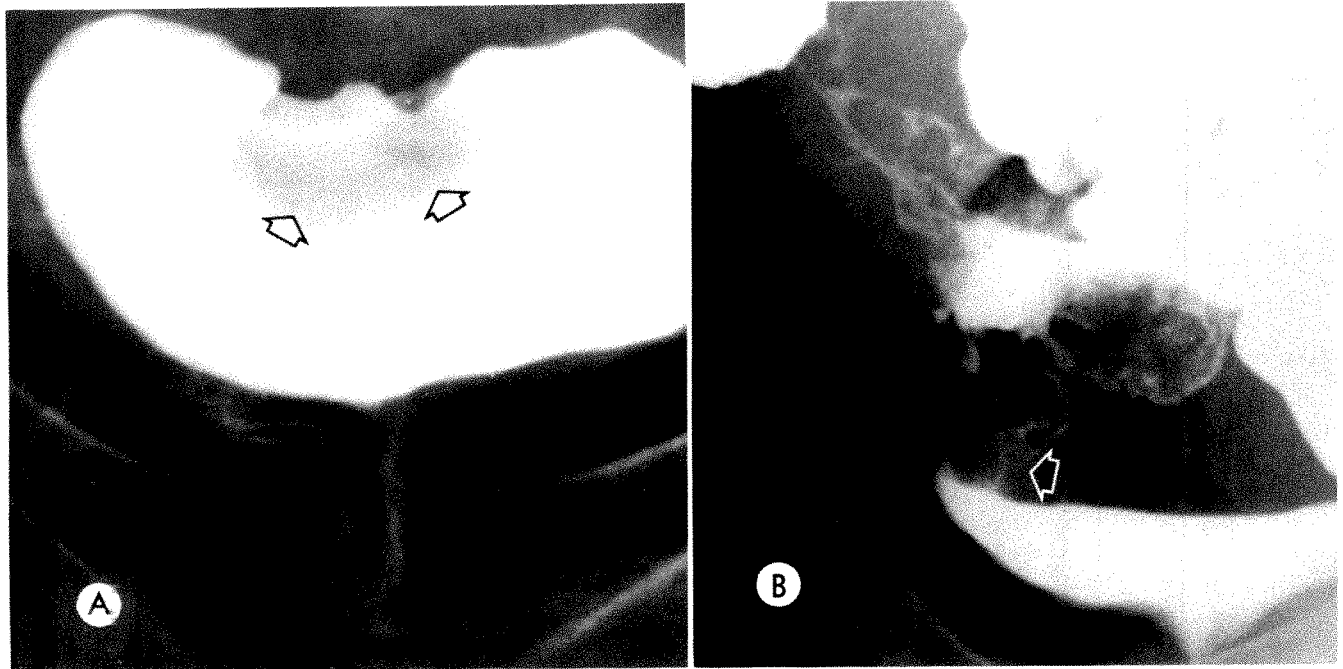


Fig. 8.—26-year-old female with urinary tract complaints and cloudy urine; no intestinal symptoms. Cystoscopy revealed 4 cm necrotic mass on anterior wall of bladder; no fistula visualized. A, Retrograde cystogram showing filling defect (arrows) on bladder dome. B, Small bowel examination showing Crohn's disease of distal ileum with fistulous communication (arrow) to anterosuperior aspect of bladder. Findings confirmed at surgery.

is normal, the possibility of Crohn's disease should be considered, especially in younger patients. Barium examination of the small bowel is mandatory. Other causes of non-traumatic vesicointestinal fistulae include primary bladder carcinoma, acute perforative appendicitis, tuberculosis, amebiasis, actinomycosis, perforated Meckel's diverticulum, and foreign body perforations of the bowel.

REFERENCES

1. Bagley RJ, Clements JL Jr, Patrick JW, Rogers JV, Weens HS: Genitourinary complications of granulomatous bowel disease. *Am J Roentgenol* 117:297-306, 1973
2. Chapin LE, Scudmore HH, Bagenstoss AH, Bagen JA: Regional enteritis: associated visceral changes. *Gastroenterology* 30:404-411, 1956
3. Deren JJ, Porush JG, Levitt MS, Khilani MT: Nephrolithiasis as a complication of ulcerative colitis and regional enteritis. *Ann intern Med* 56:843-852, 1962
4. Grossman MS, Nugent FW: Urolithiasis as a complication of chronic diarrheal disease. *Am J Dig Dis* 12:491-498, 1967
5. Werther JL, Schapira A, Rubenstein O, Janowitz HD: Amyloidosis in regional enteritis. *Am J Med* 29:416-422, 1960
6. Ginzburg L, Oppenheimer G: Urologic complications of regional enteritis. *J Urol* 59:948-952, 1948
7. Kyle J: Psoas abscess in Crohn's disease. *Gastroenterology* 61:149-155, 1971
8. Rominger CJ, Flandreau RH, McGinnis FT, Schnell C: Ureteral obstruction from regional enteritis. *Am J Roentgenol* 86:114-118, 1961
9. Enker WE, Block GE: Occult obstructive uropathy complicating Crohn's disease. *Arch Surg* 101:319-326, 1970
10. Kyle J, Murray CM: Ileovesical fistula in Crohn's disease. *Surgery* 66:497-501, 1969

TABLE 1

Incidence of Ileovesical Fistulae in Crohn's Disease

Reference	No. Cases Crohn's Disease	Incidence of Fistulae	
		No.	%
Van Patter et al. [19]	600	10	1.6
Crohn and Yarnis [20]	546	12	2.2
Daffner et al. [21]	100	1	1.0
Atwell et al. [22]	172	8	4.6
Kyle and Murray [10]	440	10	2.2

11. Robinson RHOB: Vesico-intestinal fistula with special reference to Crohn's disease. *Br J Urol* 25:127-131, 1953
12. Williams RJ: Vesicointestinal fistula and Crohn's disease. *Br J Surg* 42:179-187, 1954
13. Scorer CG: Vesicointestinal fistula. *Proc R Soc Med* 51:1042-1044, 1958
14. Goldstein MH, Bragg D, Sherlock P: Granulomatous bowel disease presenting as bladder tumor: report of a case. *Am J Dig Dis* 16:337-341, 1971
15. Abeshouse BS, Robbins MA, Gann M, Salik JO: Intestino-vesical fistulas. Report of seven cases and review of the literature. *JAMA* 164:251-257, 1957
16. Pugh JI: On the pathology and behaviour of acquired non-traumatic vesicointestinal fistula. *Br J Surg* 51:644-657, 1964
17. Brogdon BG, Sebbiger ML, Colston JAC: Cystitis glandularis. *Radiology* 85:470-473, 1965
18. Dann RH, Arger PH, Enterline HT: Benign proliferative processes presenting as mass lesions in the urinary bladder. *Am J Roentgenol* 116:822-829, 1972
19. Van Patter WN, Bagen JA, Dockerty MB, Feldman WH, Mayo CW, Waugh JM: Regional enteritis. *Gastroenterology* 26:347-450, 1954

TABLE 2
Nontraumatic Causes of Vesicointestinal Fistulae

Reference	Total Cases with Fistulae	Etiology		Cause of Inflammation
		Neoplastic	Inflammatory	
Pugh [16]	30*	13 (43.3)	17 (56.6)	Sigmoid diverticulitis, 13; Crohn's disease, 2; appendicitis, 1
Couris and Block [23]	383	133 (35)	199 (51.9)	Sigmoid diverticulitis, 169; Crohn's disease, 5; appendicitis, 7
Williams [12]	148	64 (43.2)	51 (34.4)	Sigmoid diverticulitis, 23; Crohn's disease, 8; appendicitis, 4
Abeshouse [15]	665	216 (33)	310 (47)	Individual causes not indicated

Note.—Numbers in parentheses are percentages.

* Acquired nontraumatic only.

20. Crohn BB, Yarnis H: *Regional Ileitis*, 2d ed. New York, Grune & Stratton, 1958
21. Daffner J, Brown C: Regional enteritis. Clinical aspects and diagnosis in 100 patients. *Ann Intern Med* 49:580–594, 1958
22. Atwell JD, Duthie HL, Goliger JC: The outcome of Crohn's disease. *Br J Surg* 52:966–972, 1965
23. Couris CD, Block MA: Intestinovesical fistula. *Surgery* 54: 736–742, 1963

Unilateral Hematocolpos and Ipsilateral Renal Agenesis: Report of Two Cases and Review of the Literature

ISABEL C. YODER¹ AND RICHARD C. PFISTER¹

Two cases are presented of a partially duplicated vagina characterized by a one-sided hematocolpos associated with renal agenesis on the same side. A review of the English literature reveals 39 previously reported cases. Invariably this complex of anomalies is seen in adolescents and young women with progressively severe abdominal pain, menstrual irregularities, and a pelvic mass. It is important to make an early accurate diagnosis since they are usually managed as having an ovarian mass and submitted to multiple laparotomies and occasionally to mutilating surgery. An analysis is presented of the salient embryologic, clinical, and radiologic features of the 41 cases gathered. The need for definitive preoperative evaluation of both the urinary tract [urography and cystoscopy] and the genital tract [hysterosalpingography] cannot be overemphasized.

We recently had the occasion to study two young women with partial duplicated vagina, one-sided hematocolpos, and ipsilateral renal agenesis. This paper deals with their case histories, a review of the reported cases in the English literature, followed by a discussion of the embryologic, clinical, and radiologic features relevant to this interesting disease complex.

Case Reports

Case 1

M. J., a 20-year-old white female, was admitted in 1973 with a right-sided pelvic mass. At age 12 she had an imperforate hymen opened. At that time, laparotomy revealed a septate uterus; a metroplasty was done, and a urogram (fig. 1) showed a slightly enlarged single left kidney, with cystoscopy confirming absence of the right hemitrigger. In view of the multiple congenital anomalies, the diagnosis of ovarian cyst was questioned. She underwent salpingography (fig. 2) which demonstrated an irregular filling defect of the fundus reflecting the previous metroplasty. A sinuslike tract filled at the level of the endocervix and led into a large right paravaginal cavity (fig. 3). At laparotomy a heart-shaped uterus was seen, and a paravaginal cystic mass containing many black oval solid stones was excised. The upper part of this pouch was lined with mucinous columnar epithelium consistent with endocervix; the lining of the lower part was squamous epithelium consistent with vagina.

Case 2

B. B., a 15-year-old white female, was admitted with abdominal pain and a large pelvic mass. Urography showed a slightly enlarged single left kidney (fig. 4). No right ureteral orifice was found at cystoscopy. Prior to laparotomy, an intraoperative salpingogram showed a left horn and fallopian tube of a bicornuate uterus. At laparotomy, brownish material was adherent to the right ovary, tube, and mesentery, resembling endometriosis. A right hematometra and hematocolpos was evacuated and the common vaginal septum

widely excised. Pathology confirmed that this was vaginal epithelium. The brownish deposits were described as organizing thrombus and had disappeared at laparoscopy 4 months later. Seven months after surgery a salpingogram (fig. 5) demonstrated a normal left endocervix through which the left uterine horn and fallopian tube were filled. There was a flattened right cervix with a patulous slit-like os. The right uterine horn and tube were enlarged and distorted due to the previous hematometra. A sinuslike tract provided communication between the two uterine cavities at the level of the endocervix (fig. 6).

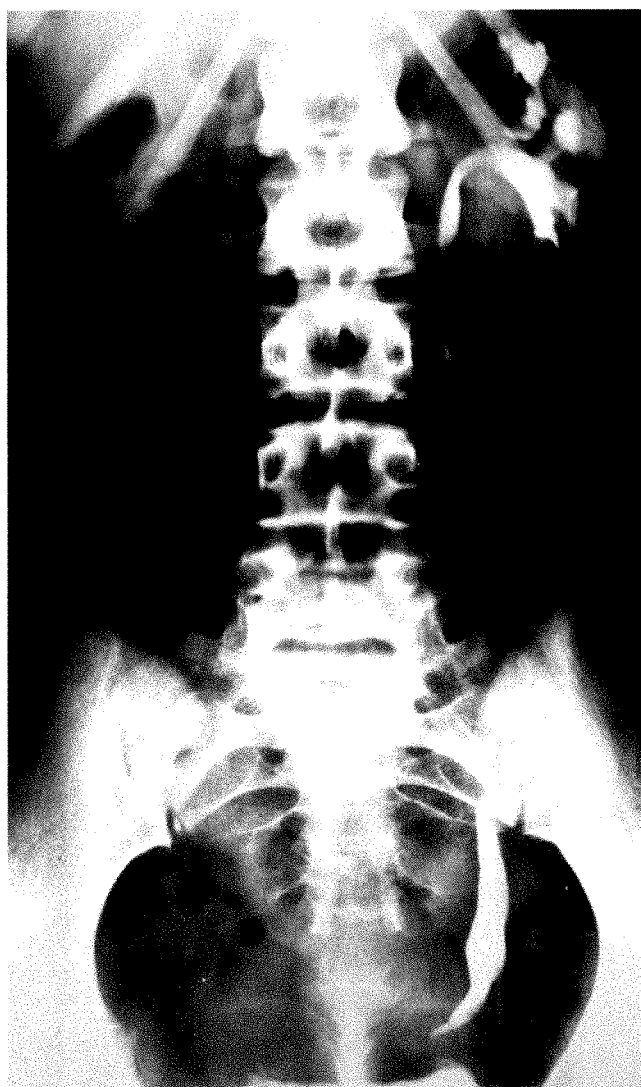


Fig. 1.—Intravenous urogram of case 1 demonstrating solitary left kidney with associated mild primary megaloureter.

¹ Department of Radiology, Harvard Medical School and Massachusetts General Hospital, Boston, Massachusetts 02114. Address reprint requests to R. C. Pfister, Radiology Research Office, Massachusetts General Hospital, Boston, Massachusetts 02114.

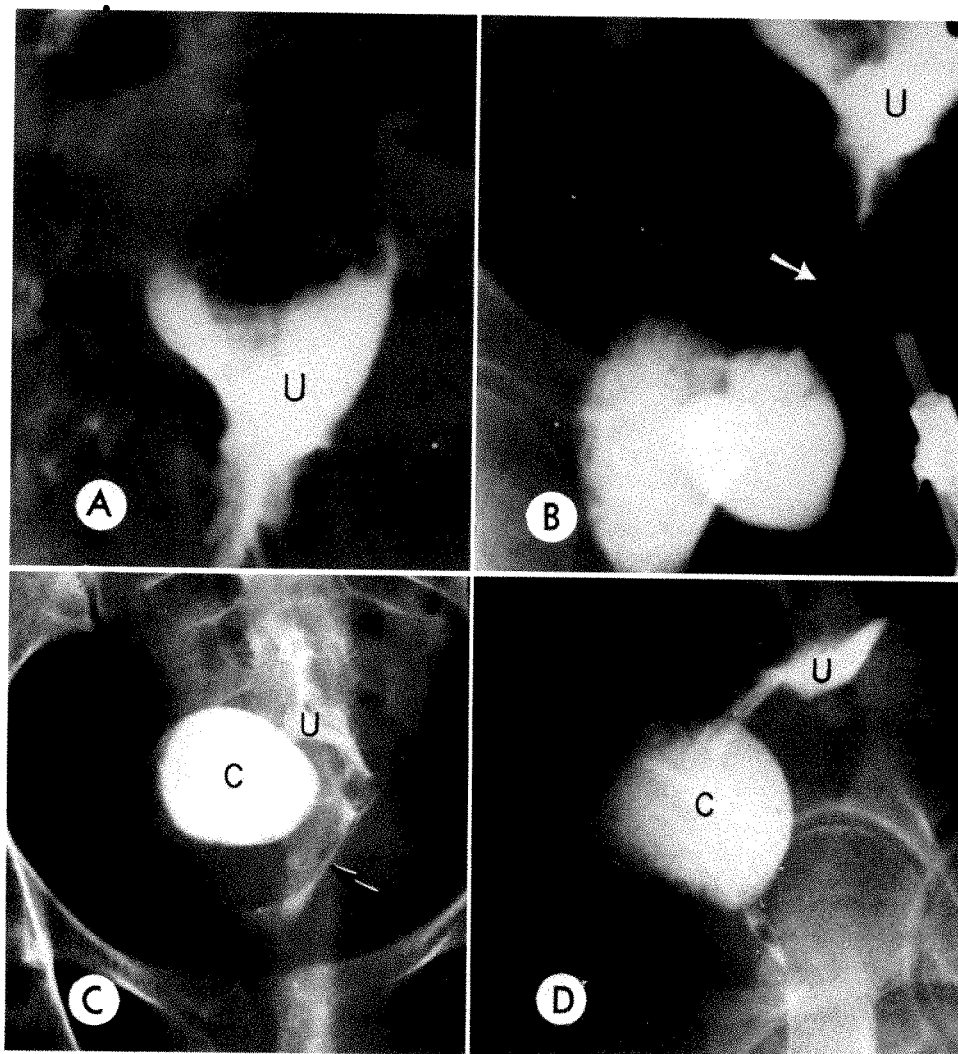


Fig. 2.—Hysterosalpingogram of case 1. *A*, Irregular uterine cavity (U) reflecting previous metroplasty. *B*, Tract (arrow) leading from endocervical canal to partially filled paravaginal cystic structure. *C* and *D*, drainage views in frontal and lateral projections. *C*=filled cavity of incomplete vaginal duplication; *U*=semi-emptied uterus; arrow=vaginal vault.

Literature Review

Table 1 summarizes data on the 39 cases reported in the English literature and the two present cases. Patient age ranged from 11 to 38 years with an average age of 17 years. Clinical presentation was that of a young woman, usually a teenager, who, after going through a normal menarche, began having menstrual irregularities and lower abdominal pain of increasing severity usually associated with menses but occasionally not. On physical examination a pelvic mass of variable size was felt and usually diagnosed as ovarian in origin, since occult hematocolpos or hemato-metrocolpos is seldom considered in a menstruating young woman.

The hematocolpos was on the right side in 28 cases and on the left in 12; side was not specified in one case.

No data were available on the kidneys in 12 cases. Unilateral renal agenesis occurred on the right side in 20 cases and on the left in nine cases. In these 29 cases, the kidney was invariably absent on the side where the hematocolpos was found. Demonstration of an apparent solitary kidney on urography is not conclusive evidence of unilateral agenesis; absence of the ureter and renal vessels

must be confirmed by cystoscopy and angiography, respectively. In only 19 of the 41 cases was unilateral renal agenesis confirmed by cystoscopy and/or laparotomy. In the remaining 10 cases, probable unilateral renal agenesis was assumed on the basis of the intravenous urogram alone.

The uterus was described as double, bicornuate, or didelphys in 36 cases, septate in two cases, and unicornuate in one case. No data were given for two patients. The classification of uterine duplications is confusing. For example, the term bicornuate is loosely used to describe several entities. Strictly speaking, a *bicornuate* uterus refers to an incomplete fusion of the fundal elements resulting in paired uterine horns with a single cervix. *Septate* or *sub-septate* uterus refers to persistence of the median septum in the body and fundus of the uterus with a single cervix, while *uterus didelphys* describes a total duplication of the uterus with two independent horns, two cervices, and a double vagina [21]. If contrast media is placed into only one of these double cavities, an erroneous diagnosis of unicornuate uterus will result.

Both cases presented here as well as eight of those reviewed demonstrated a communication or short sinus

tract between the duplex uteri at the level of the endocervical canal.

Salpingograms were performed on 16 of the 41 cases, eight preoperatively and eight postoperatively.

In eight patients, surgery was confined to excision of the common vaginal septum. The other 33 had at least one laparotomy; of these, nine had two laparotomies, 11 had partial hysterectomies and/or salpingoophorectomies, and two had total hysterectomy. Laparoscopy was done in three patients. In 20 of the patients who underwent laparotomy, some degree of hematometra and hematosalpinx caused by the backup of retained menses in the site of the hematocolpos was described.

Another interesting finding reported in five cases was the presence of brownish deposits studding the pelvic organs and peritoneum, resembling endometriosis. These deposits were adherent to the tissues; however, when our case 2 was examined pathologically, the deposits were described as old blood and on follow-up laparoscopy were no longer seen. Thus rather than true endometriosis, this finding probably represents a backflow of menstrual blood through the fallopian tube into the peritoneal cavity.

Discussion

The incidence of unilateral renal agenesis ascertained at autopsy averages between one in 600 [14] and one in 1,200 [22]. Concomitant genital anomalies are very common. In males, anomalies of the genital tract are less frequent and functionally less striking, the most common being cryptorchidism [23]. In females, the incidence of associated genital anomalies has been conservatively estimated as 50% [14]. In most women, the genital anomaly consists of some degree of duplication of the uterus, cervix, and/or vagina, and less commonly some form of partial atresia [9].

Embryology

Duplication of the female reproductive tract results from a lack of fusion of the paired müllerian ducts which appear at the sixth week of embryonic development. The müllerian ducts develop just lateral to the mesonephric (urinary) ducts, which have been postulated to act as a guide to the growth of the müllerian ducts [24]. As they course caudally, the müllerian ducts cross over the mesonephric ducts ventrally and fusion of the lowermost portion occurs. The cranial unfused portions form the paired fallopian tubes; the caudal fused ducts form the uterus, cervix, and approximately the upper three-quarters of the vagina. The distal vagina is formed by invagination of the urogenital sinus whose endoderm then replaces the entire original vaginal epithelium [24].

All mammals below the primates exhibit some form of nonfusion of the müllerian ducts as evidenced by usual double uterus and sometimes vagina. However, it is hard to explain the lack of fusion of the human reproductive system as an atavistic step to a more primitive form, since in none of these lower mammals is a kidney absent [9]. Because the urinary and genital systems are derived from a common embryonic mesoderm, it is easy to imagine an early

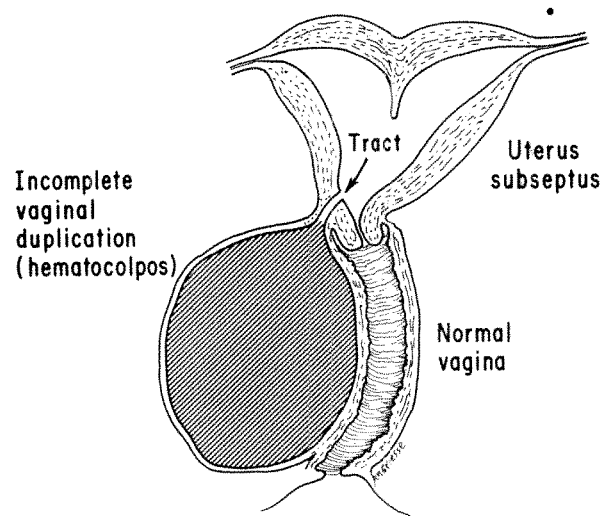


Fig. 3.—Drawing of anatomic relationships (case 1).

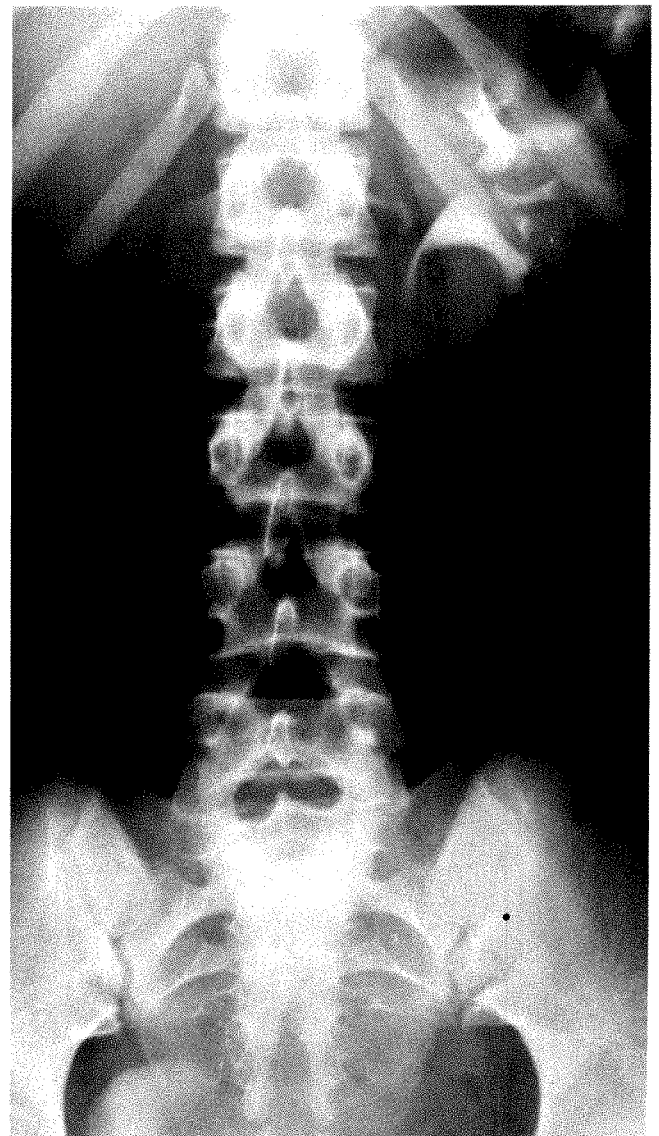


Fig. 4.—Intravenous urogram illustrating absence of right kidney.



Fig. 5.—Left and right hysterosalpingogram of case 2. *A*, Left uterine horn and tube and early filling of right deformed uterine horn (arrow) and duplicated vagina (open arrow) from tract. *B*, Dilated right tube (arrow), uterus (open arrow), incomplete vaginal duplication (*R*), and displaced left vaginal vault (*L*) (postoperative vaginal septum removal).

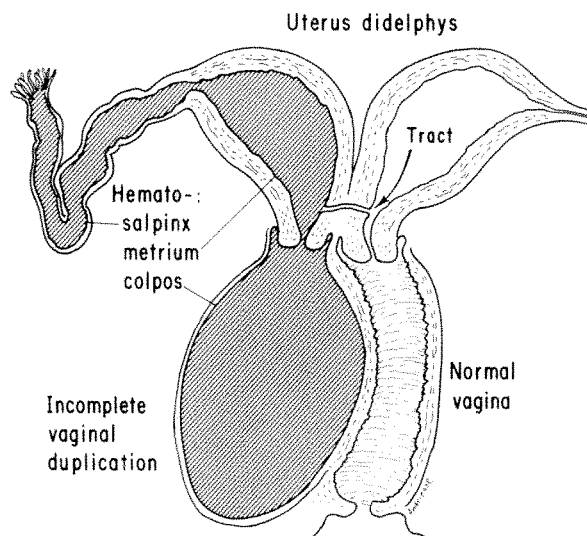


Fig. 6.—Drawing of normal left and dilated right genital duplication (preoperative, case 2).

teratogenic influence leading to simultaneous defects in both systems. Woolf and Allen [9] suggest that the mesonephric duct is the crux of the matter, and without its normal development a normal müllerian tract seems unlikely.

The above speculations do not entirely explain the unilateral hematocolpos seen in this series of patients. The lack of caudal (perineal) opening on one side of the duplicated vagina was clearly not due to an imperforate hymen in any of these cases. The hymen is a transverse perforate membrane formed where the müllerian tubercle (caudal end of the müllerian ducts) meets the urogenital sinus. Cases of simple imperforate hymen usually present

with primary amenorrhea and are not associated with other congenital anomalies [25]. In this series of patients, the vaginal septum causing obstruction extends longitudinally from the lower vagina up to and separating the two cervices. It must represent a lack of reabsorption of the median wall of the fused müllerian ducts, and it must be further postulated that the urogenital sinus invaginated only one side of the vagina, leaving a blind-ending pouch on the other side.

Toaff [20] views the small isthmic communication seen in all of his cases and in a total of 10 cases reviewed in this paper as evidence of early partial resorption of this median wall of the müllerian ducts. He offers this finding as proof that embryologically resorption begins at the endocervical canal and proceeds both cranially and caudally.

Radiology

Hysterosalpingograms were done on both of our patients. Case 1 (figs 1–3) had the study done prior to operation, and case 2 (figs. 4–6) had a complete salpingogram done postoperatively. (A modified one had been performed intraoperatively.) Usually a Swedish vacuum cannula is used for our routine salpingograms. However, in both cases, we had to modify techniques and revert to the use of a tenaculum to pull the cervix toward the midline.

The main differential diagnosis is that of a Gartner's cyst or mesonephric duct remnant. Gartner's cysts occur anywhere between the hymen and the ovary along the vagina and uterine walls or the broad ligament. They represent an incomplete normal resorption of the mesonephric duct in the female and may communicate with the vagina or uterus at any level. Gartner's cysts are lined with a single layer of cuboidal epithelium, while vaginal duplications have a stratified squamous epithelial lining. Usually Gartner's

TABLE 1
Summary of Reported Cases

Reference	Hematocolpos		Renal Agenesis	Uterus	Surgery	Comments
	Right	Left				
Hadden [1]	1	...	N.D.	N.D.		
Purslow [2]	1	...	N.D.	Double	Right hemihysterectomy, vaginal septum incision	...
Wilson [3]	1	N.D.	Double	Total hysterectomy, salpingoophorectomy	Picture of gross specimen
Brown and Brews [4]	1	N.D.	Double	Laparotomy, vaginal septum incision	Patient died 8 days post- operatively of peritonitis
Masson and Mueller [5]	1	...	N.D.	Didelphys	Laparotomy, excision vaginal septum	...
Carrington and Burlington [6]	1	N.D.	Didelphys	Partial hysterectomy, salpingoophorectomy	Picture of gross specimen painted with sodium iodide
Martindale [7]	1	...	N.D.	Double	Excision vaginal septum	...
Embrey [8]	1	...	Yes	Didelphys	Right hemihysterectomy, excision vaginal septum	...
Woolf and Allen [9]	2	2	Yes	Didelphys	Excision vaginal septum, 4 ; salpingoophorectomy, 2	...
Semmens [10]	1	...	Yes	Didelphys	Excision vaginal septum	Pathology : stratified squamous epithelium
Gibberd [11]	1	Yes	Double	Laparotomy, excision vaginal septum	...
Hill [12]	1	...	Yes	Didelphys	Laparotomies, right hemihysterectomy	Pathology : vaginal mucosa
Allen and Cowan [13]	3	1	Yes, 3 ; N.D., 1	Didelphys, 3 ; double, 1	Laparotomy, 4 ; excision vaginal septum, 4	...
Thompson and Lynn [14]	2	1	Yes	Double, 2 ; bicornuate, 1	Laparotomy, 3 ; hemihysterectomy and hemicolpectomy, 3	Four patients reported : N.D. 1 ; picture of gross specimen, 3
Lewis and Brent [15]	1	...	Yes	Unicornuate	Laparotomy	...
Burton [16]	1	Yes	Didelphys	Laparotomies, hemihyster- ectomy and hemicolpectomy	...
Johansen [17]	7	...	Yes, 4 ; N.D., 3	Didelphys, 5 ; double, 2	Laparotomy, 6 ; excision vaginal septum, 6 ; hemihysterectomy, 1	Pathology, 1 : stratified squamous epithelium
Vinstein and Franken [18]	1	1	Yes	Septate, 1 ; didelphys, 1	Laparotomy, 2	...
Konig [19]	1	Yes	Didelphys	Excision vaginal septum, laparoscopy	...
Toaff [20]	3	1	Yes	Didelphys	Laparotomy, 2 ; excision vaginal septum, 3 ; hysterectomy, 1 ; laparoscopy, 1	Picture of surgical specimen, 1
Present report	2	...	Yes	Septate, 1 ; didelphys, 1	Laparotomy, 2 ; excision vaginal septum, 1 ; laparoscopy, 1	Pathology, 1 : vaginal epithelium

Note:—Numbers indicate number of patients N.D. = no data.

cysts do not attain the size of a hematocolpos and do not contain blood. Ipsilateral renal agenesis may also occur with Gartner's duct cysts [26, 27].

REFERENCES

1. Hadden D: Double uterus and vagina. *Am J Obstet Gynecol* 3:526, 1922
2. Purslow CE: A case of unilateral haematokolpos, hematometra and hematosalpinx. *J Obstet Gynaecol Br Emp* 28:643, 1922
3. Wilson J St G: A case of double uterus and vagina with unilateral haematocolpos and hematometra. *J Obstet Gynaecol Br Emp* 32:127-128, 1925
4. Brown AC, Brews A: Congenital retention of the menses. *J Obstet Gynaecol Br Emp* 37:233-255, 1930
5. Masson JC, Mueller SC: Uterus duplex bicornis with septate vagina open only on one side: report of case. *Surg Clin North Am* 13:857-861, 1933
6. Carrington GL, Burlington NC: Incomplete bipartite uterus with unilateral hematocolpos and salpingitis. *Am J Obstet Gynecol* 25:924-925, 1933
7. Martindale L: A case of uterus didelphys associated with haematocolpos of the right vagina and simulating appendicitis. *Lancet* 1:1389-1390, 1935
8. Embrey MP: A case of uterus didelphys with unilateral gynatresia. *Br Med J* 1:820-821, 1950
9. Woolf RB, Allen WM: Concomitant malformations. The frequent simultaneous occurrence of congenital malformations of the reproductive and urinary tracts. *Obstet Gynecol* 2:236-265, 1953
10. Semmens JP: Uterus didelphys and septate vagina. Review; report of a case with gynatresic right vagina and associated hematoceles. *J Obstet Gynecol* 8:620-626, 1956
11. Gibberd AA: Unilateral hematocolpos haematometra. *Br Med J* 1:213, 1957
12. Hill RM: Uterus didelphys with hematocolpos and hematometra on one side and normal menses from the other. Report of an unusual case. *J Int Coll Surgeons* 29:422-428, 1958
13. Allan N, Cowan L: Uterus didelphys with unilateral imperforate vagina. *Obstet Gynecol* 22:422-426, 1963
14. Thompson DP, Lynn HB: Genital anomalies associated with solitary kidney. *Mayo Clin Proc* 41:538-548, 1966
15. Lewis BV, Brent HA: Obstetric and gynecologic complications associated with mullerian duct abnormalities. *Obstet Gynecol* 28:315-322, 1966
16. Burton E: Bicornuate uterus treated by hemihysterectomy and hemicolpomy. *Proc R Soc Med* 61:40, 1968
17. Johansen K: Uterus didelphys with unilateral haematocolpos. Review of 7 cases. *J Obstet Gynecol Br Commonw* 79:85-89, 1972
18. Vinstein AL, Franken EA: Unilateral hematocolpos associated with agenesis of the kidney. *Radiology* 102:625-627, 1972
19. Konig HLE: Uterus didelphys and septate vagina presenting as haematocolpos. *S Afr Med J* 47:98-102, 1973
20. Toaff R: A major genital malformation—communicating uteri. *Obstet Gynecol* 43:221-231, 1974
21. Siegler AM: *Hysterosalpingography*, 2d ed. New York, Medcom Press, 1974
22. Felding C: Obstetric studies in women with congenital solitary kidneys. *Acta Obstet Gynecol Scand* 44:555-562, 1965
23. Doroshow LW, Abeshouse BS: Congenital unilateral solitary kidney: report of 37 cases and a review of the literature. *Urol Survey* 11:219-229, 1961
24. Arey LB: *Developmental Anatomy*, 6th ed. Philadelphia, Saunders, 1965, pp 295-341
25. Reed MH, Griscom NT: Hydrometrocolpos in infancy. *Am J Roentgenol* 118:1-13, 1973
26. Gadbois WF, Duckett JW: Gartner's duct cyst and ipsilateral renal agenesis. *Urology* 4:720-721, 1974
27. Goldstein AI, Ackerman ES, Woodruff R: Vaginal and cervical communication with mesonephric duct remnants: relationship to unilateral renal agenesis. *Am J Obstet Gynecol* 116:101-105, 1973

Gallium Scanning in Cerebral and Cranial Infections

ALAN D. WAXMAN¹ AND JAN K. SIEMSEN¹

Eighteen patients with cranial or intracranial infections were studied with technetium and gallium brain scans. Seven of 18 lesions were noted with gallium and not with pertechnetate, while the reverse pattern was not seen. Brain abscesses were visualized with gallium but not with pertechnetate in two of five cases. Osteomyelitis of the skull and mastoiditis showed intense gallium uptake in all cases, while meningitis or cerebritis gave inconsistent results.

⁶⁷Ga citrate scanning has been used for the detection and differential diagnosis of intracranial lesions. Its effectiveness for this purpose is under current active investigation [1-5]. Numerous reports on gallium localization in extra-cranial sites of inflammation have also been published [6-10]. This report deals with gallium scanning in patients with cranial and intracranial infections.

Subjects and Methods

Eighteen patients with cranial or intracranial infection were studied. Patient selection was prospective and was based on a clinical suspicion of cerebral or cranial infection. Scans were done 3-48 hr following intravenous injection of 3-5 mCi of ⁶⁷Ga citrate, using either an Anger type scintillation camera or a double-headed 5 inch crystal rectilinear scanner. A delayed (2-4 hr) ^{99m}Tc pertechnetate scan with 20 mCi preceded each ⁶⁷Ga citrate study by 24-48 hr. The same instrument was used for both radionuclides in each case. The pathologic process was documented in 10 cases by surgery-biopsy, angiography, or postmortem findings. In six cases of meningitis and/or cerebritis, diagnosis was based on clinical course and laboratory findings in the CSF. Two cases of sinusitis were diagnosed by x-ray findings and clinical course.

Results

The results are summarized in table 1. Visualization of inflammatory foci was better with gallium than with technetium in nine of 18 cases and equal in seven. In no instance was technetium superior to gallium in this series. Figures 1-6 illustrate representative cases.

In the patient with biopsy proven osteomyelitis following craniotomy (fig. 5), the decision to biopsy the skull was based upon the positive gallium scan, and antibiotic treatment was begun after the extensive abnormalities were noted. At the time of the scan, skull x-rays showed non-specific changes attributed to the craniotomy. However, osteomyelitis was also considered a possibility.

In the patient with sinusitis and meningitis (fig. 6), antibiotic therapy was begun 24 hr prior to gallium injection. Sinusitis was not diagnosed as the source of infection until the 4 hr gallium scan was completed. Sinus x-rays confirmed the diagnosis.

Discussion

In this small series, the yield of positive findings on gallium scans in patients with suspected inflammation of the brain, skull, or sinuses was high. Seven of the 18 lesions were detected only with gallium; the reverse pattern was not found. In the five brain abscesses, the gallium study was superior to the ^{99m}Tc study in three and equal in two cases.

A problem in suspected abscess cases is the urgent need for diagnosis. This makes the usual 48 hr delay between gallium administration and scan frequently impractical. The feasibility of an early gallium scan is illustrated in figure 4 and was previously demonstrated by Littenberg et al. [8]. It appears that gallium localizes quite early in at least some inflammatory lesions and in such high concentration that the high early general body background level does not interfere with scan interpretation. However, at this time we have insufficient data to determine the relative effectiveness of early scans compared to delayed ones in brain abscesses.

Postcraniotomy patients with suspected abscess or osteomyelitis are prime candidates for a ⁶⁷Ga study. It has been shown that gallium is very useful in evaluating postcraniotomy tumor recurrence, since gallium will not show significant uptake at or near the craniotomy site unless tumor is also present [11, 12]. However, inflammation in the craniotomy site may give a positive gallium scan (fig. 5), thus providing another indication for combined gallium and technetium studies of the skull.

TABLE 1

Relative ⁶⁷Ga Citrate Uptake in Cranial and Intracranial Infections

Type	Ga Positive Tc Negative	Ga > Tc	Ga = Tc	Tc Negative Ga Negative	Total
Brain abscess . . .	2	1	2	...	5
Meningitis/ cerebritis	2	...	2	2	6
Tuberculoma	1	...	1
Osteomyelitis . . .	1	...	1	...	2
Mastoiditis	2	2
Sinusitis	1	1	...	2
Total	7	2	7	2	18

Note. —Ga > Tc = visualization better with ⁶⁷Ga than with ^{99m}Tc. In no case was visualization better with ^{99m}Tc.

REFERENCES

1. Henkin RE, Quinn JL, Weinberg PE: Adjunctive brain scanning with ⁶⁷Ga in metastases. *Radiology* 106:595-599, 1973

¹ Department of Radiology, Nuclear Medicine Section, Los Angeles County—University of Southern California Medical Center, 1200 North State Street, Los Angeles, California 90033. Address reprint requests to A. D. Waxman.

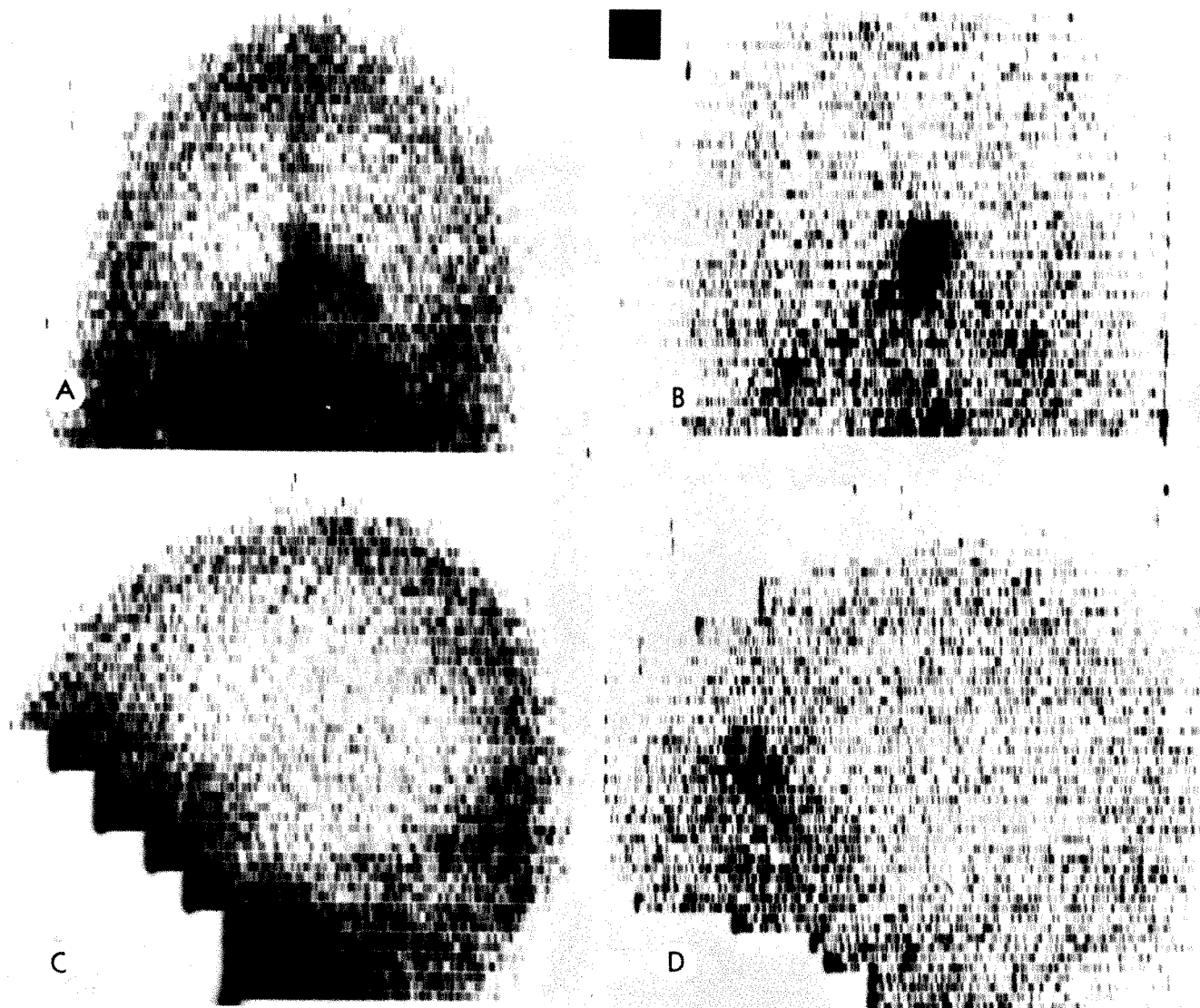


Fig. 1.—Brain abscess detected by both ^{99m}Tc and ^{67}Ga . A and C, 4 hr delayed anterior and left lateral ^{99m}Tc scans. B and D, Same projections with ^{67}Ga at 48 hr.

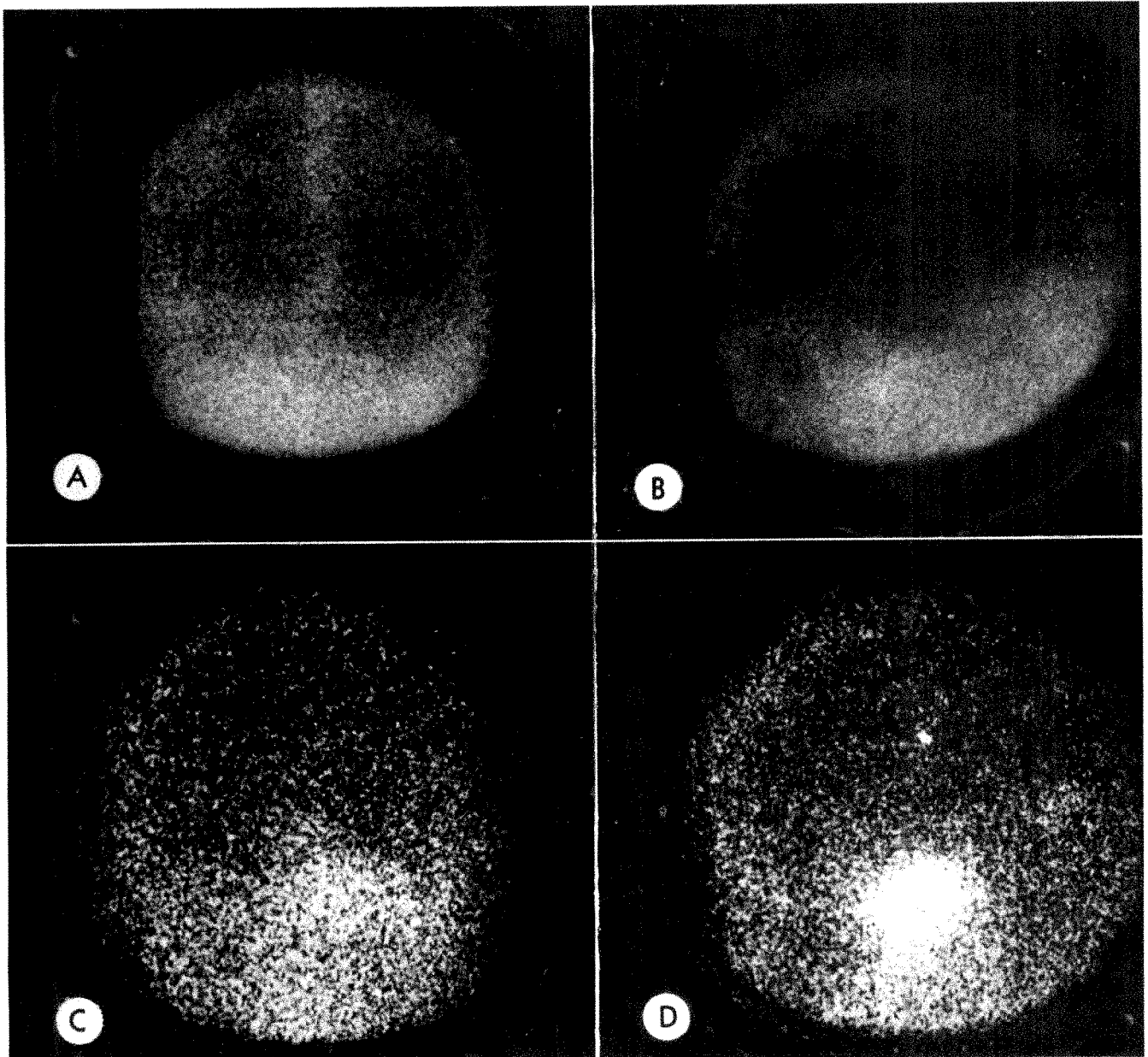


Fig. 2.—Extracerebral pseudomonas abscess, right jugular foramen. *A and B.* Posterior and right lateral ^{99m}Tc scans. *C and D.* Same projections with ^{67}Ga at 48 hr. Case surgically proven.

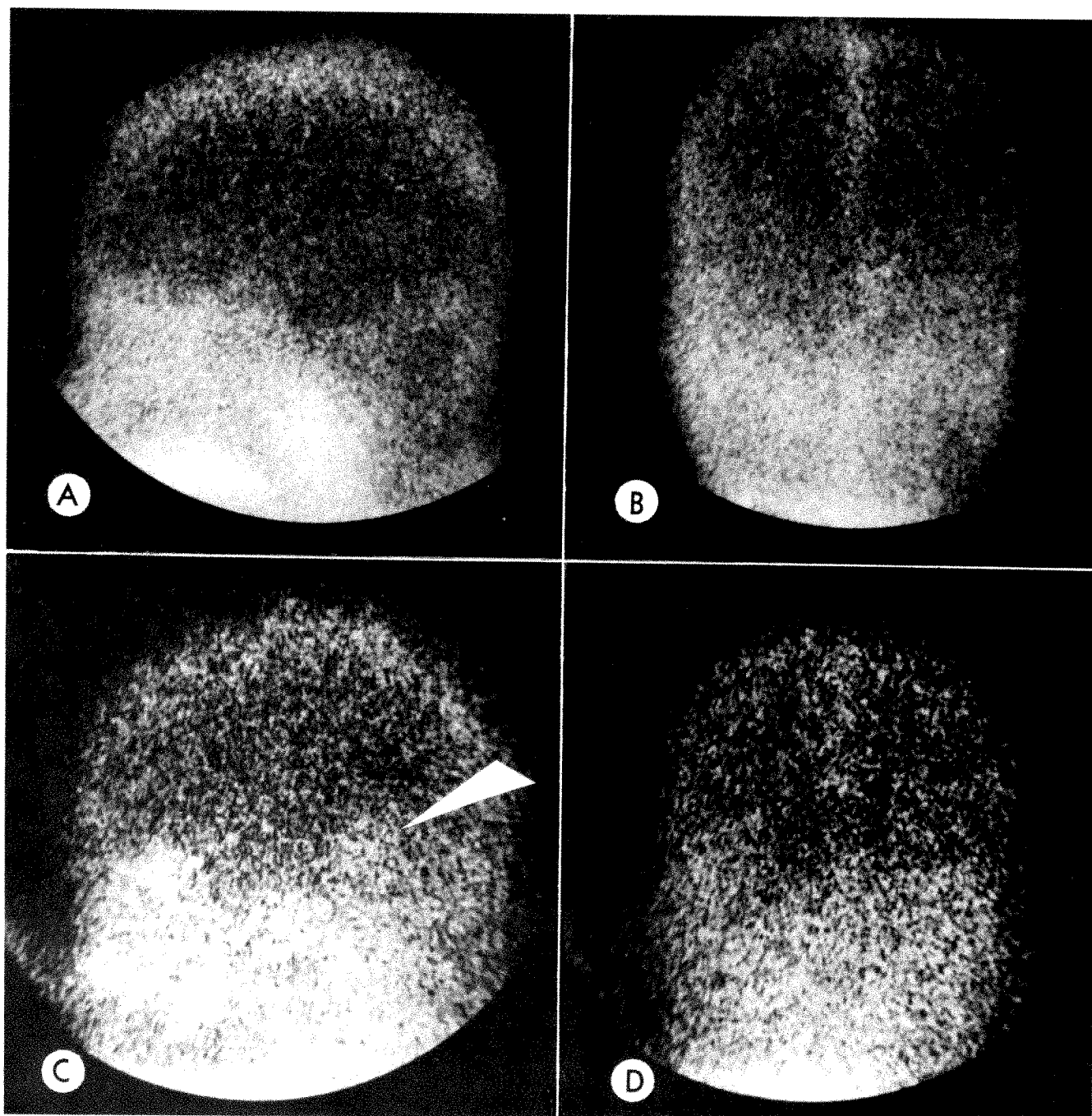


Fig. 3.—Small abscess, left posterior temporal region, detected only by ^{67}Ga . *A and B*, 4 hr delayed left lateral and posterior $^{99\text{m}}\text{Tc}$ scans showing no sign of abscess. *C and D*, Same projections with ^{67}Ga at 48 hr demonstrating abscess (arrow).

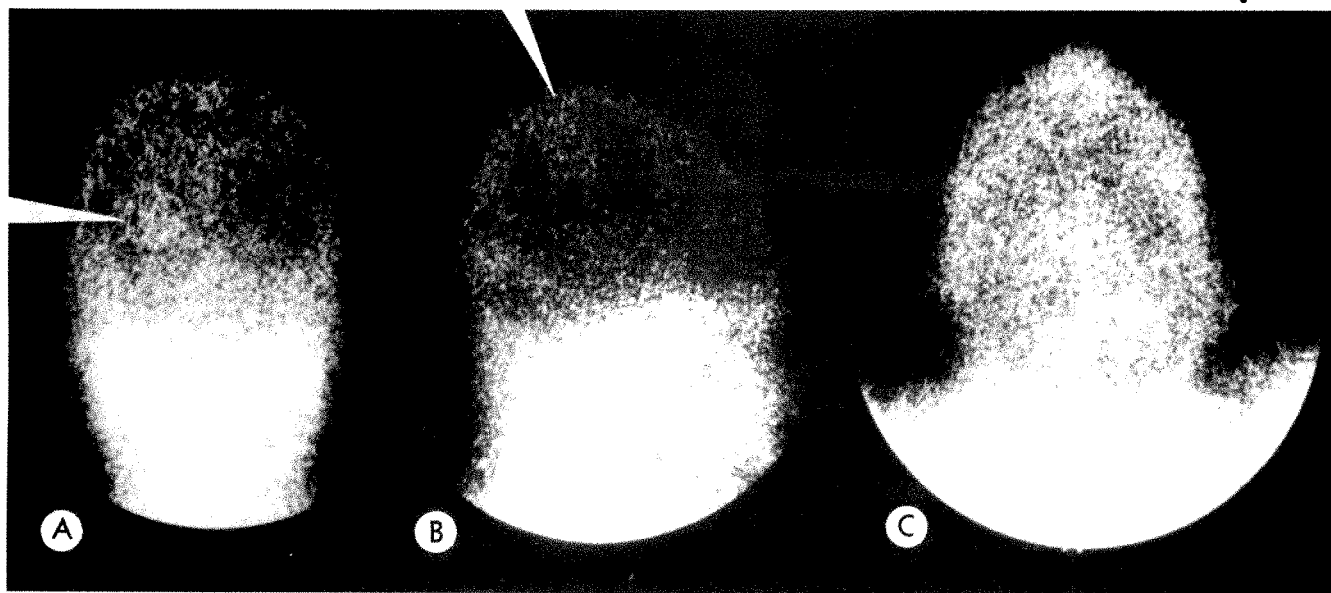


Fig. 4.—Bilateral abscess demonstrated by ^{67}Ga scan 3 hr postinjection. *A*, Posterior view showing left posterior accumulation; *B* and *C*, Right lateral and vertex views showing additional site in right parietal region. $^{99\text{m}}\text{Tc}$ scans also positive. Case proven at autopsy.

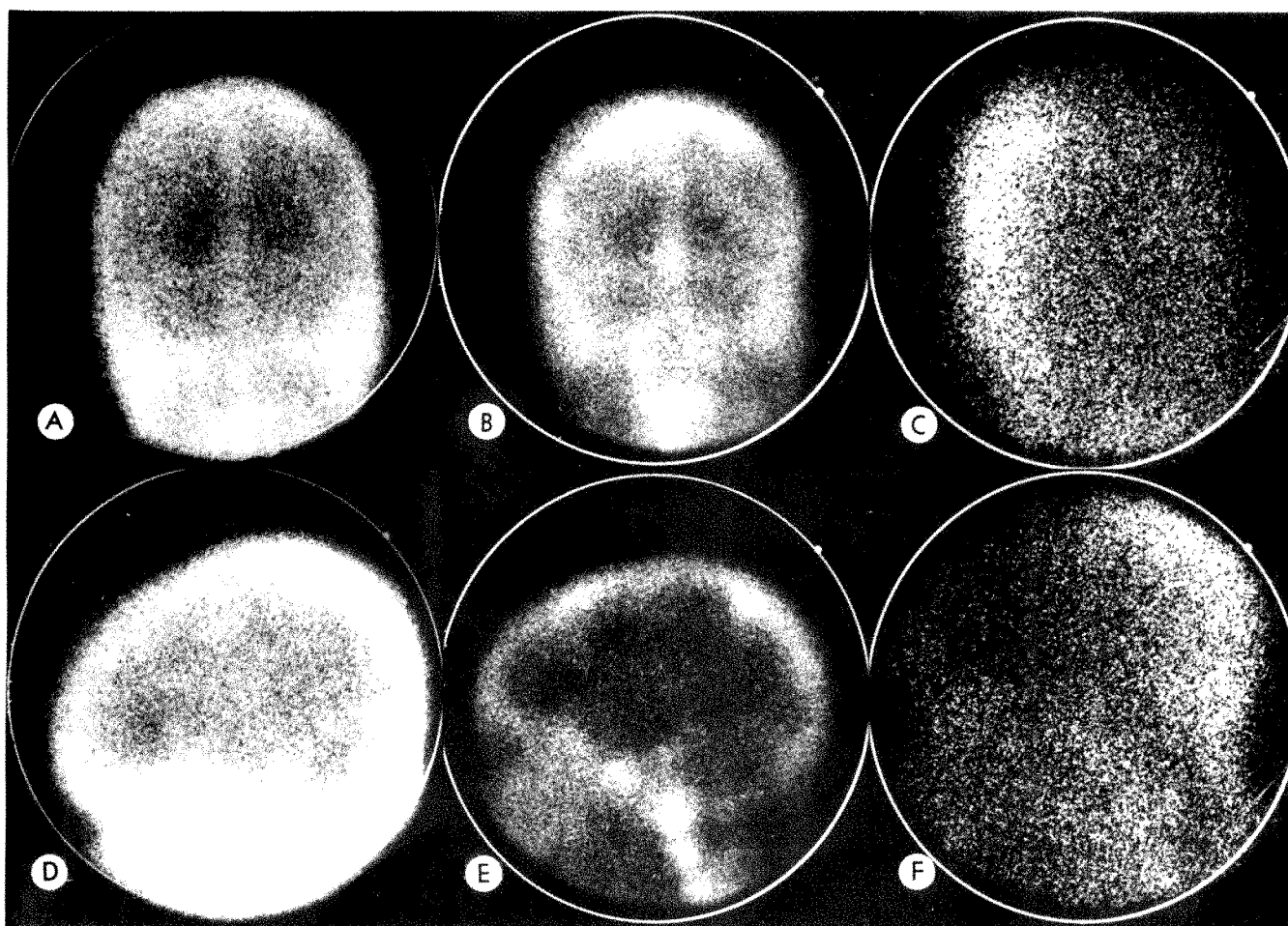


Fig. 5.—Biopsy proven osteomyelitis. *A* and *B*, Posterior and left lateral $^{99\text{m}}\text{Tc}$ scans 3 hr after injection. *D* and *E*, $^{99\text{m}}\text{Tc}$ diphosphonate bone scan 3 hr after injection; *C* and *F*, ^{67}Ga scan 48 hr after injection.

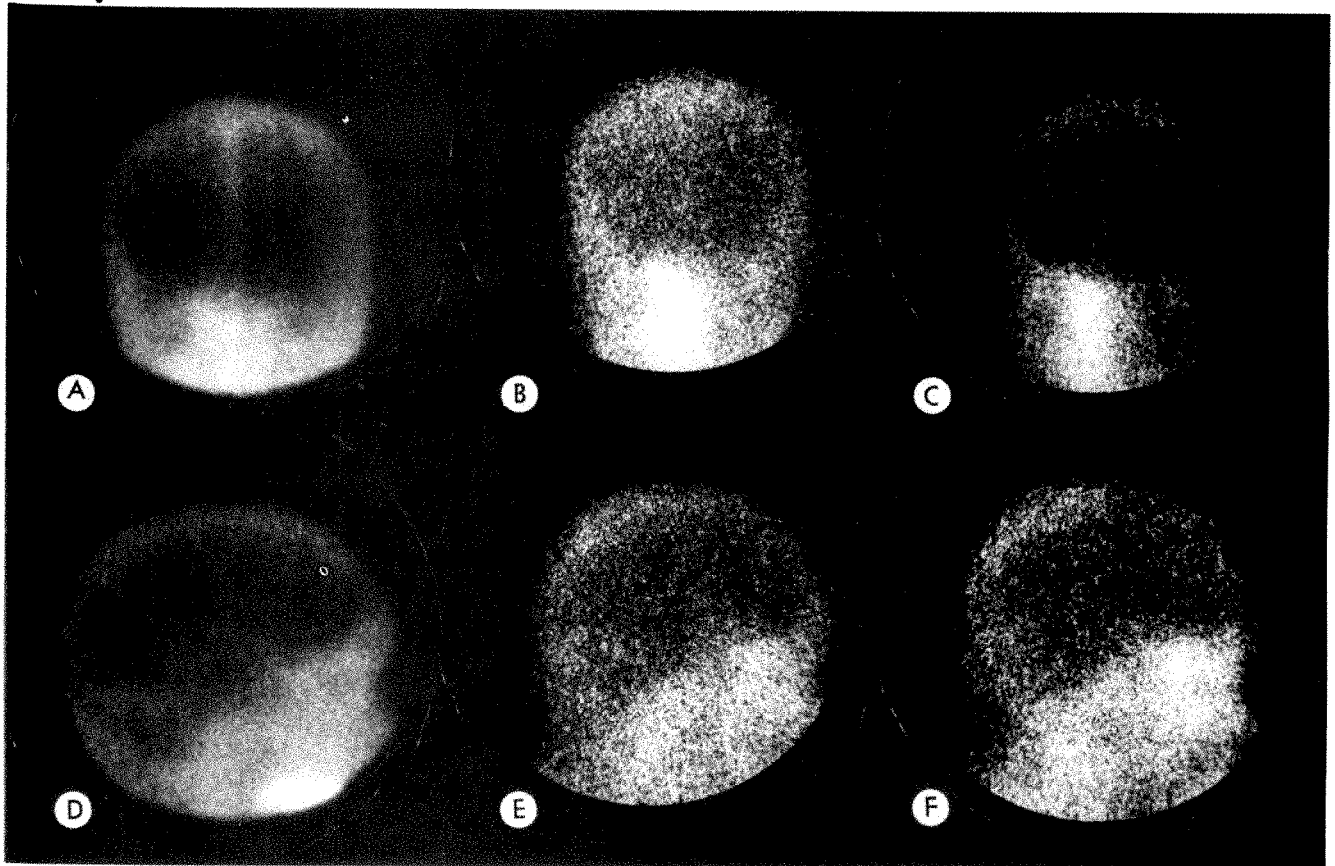


Fig. 6.—Sinusitis and meningitis. *A and D*, Anterior and right lateral ^{99m}Tc scans. *B and E*, ^{67}Ga scans 4 hr after injection. *C and F*, ^{67}Ga scans 24 hr after injection. Note asymmetry along right calvarium and right paranasal sinuses.

- Jones AE, Koslow M, Johnston GA: ^{67}Ga citrate scintigraphy of brain tumors. *Radiology* 105:693–697, 1972
- Reba RC, Poulose KP: Nonspecificity of gallium accumulation: gallium-67 concentration in cerebral infarction. *Radiology* 112:639–641, 1974
- Waxman AD, Lee G, Wolfstein R, Siemsen JK: Differential diagnosis of brain lesions by gallium scanning. *J Nucl Med* 14:903–904, 1973
- Waxman AD, Siemsen JK, Lee GC, Wolfstein RS, Moser L: Reliability of gallium brain scanning in the detection and differentiation of central nervous system lesions. *Radiology* 116:675–678, 1975
- Blair DC, Carrol M, Fekety FR Jr: Localization of infectious processes with gallium citrate ^{67}Ga . *JAMA* 230:82–85, 1974
- Lavender JP, Lowe J, Barker JR, Burn JI, Chaudhri MA: Gallium-67 citrate scanning in neoplastic and inflammatory lesions. *Br J Radiol* 44:361–366, 1971
- Littenberg RL, Taketa RM, Alazraki NP, Halpern SE: Gallium-67 for localization of septic lesions. *Ann Intern Med* 79:403–406, 1973
- Lomas F, Wagner HN: Accumulation of ionic ^{67}Ga in empyema of the gallbladder. *Radiology* 105:689–692, 1972
- Waxman AD, Siemsen JK: Gallium gallbladder scanning in cholecystitis. *J Nucl Med* 16:148–150, 1975
- Jones AE, Frankel RS, De Chiro G, Johnson GS: Brain scintigraphy with ^{99m}Tc polyphosphate and ^{67}Ga citrate. *Radiology* 112:123–129, 1974
- Waxman AD, Siemsen JK, Wolfstein RS, Kurze T: A combined radionuclide approach in the evaluation of postcraniotomy patients. *J Neurosurg* 43:471–475, 1975

Pseudocyst Formation in Acute Pancreatitis: Ultrasonographic Evaluation of 99 Cases

A. C. GONZALEZ,¹ E. L. BRADLEY,² AND J. L. CLEMENTS, JR.¹

A total of 99 patients admitted with a diagnosis of acute pancreatitis were studied by abdominal A- and B-mode ultrasonography in an effort to detect pseudocyst formation. Positive ultrasonic scans were noted in 52 cases. In three patients with positive sonography, surgical exploration did not demonstrate pseudocysts, giving a false positive rate of 8.3%. Of the negative studies four were proven incorrect at surgery or autopsy, yielding a false negative rate of 8.5%. Approximately one-fifth with cystic lesions underwent spontaneous resolution. Three additional patients with pseudocysts had spontaneous cyst-enteric fistulization demonstrated by radiography. The sensitivity and accuracy of pancreatic ultrasound demonstrated by this study established ultrasonography as the procedure of choice in detecting pseudocyst formation in patients with acute pancreatitis.

Pancreatic pseudocysts have been reported to occur in from two to 12 patients per 100,000 hospital admissions [1-3]. However, incidence statistics have been derived from operative or postmortem studies and may not reflect the entire spectrum of the disease process. This study reviews our experience in the ultrasonic investigation of a large number of patients with acute pancreatitis. We have attempted to determine the actual incidence of acute pseudocyst formation by using abdominal ultrasound scanning.

Subjects and Methods

Over a 2 year period, 99 patients were evaluated. The case material was obtained from Grady Memorial Hospital in Atlanta. Sonography was performed in the ultrasonic laboratory of the radiology department of this institution. All patients had a clinical diagnosis of acute or exacerbated pancreatitis, supported by history, physical findings, and laboratory studies. Their clinical profile is outlined in table 1. Each of these patients was referred for an evaluation of pancreatic morphology by ultrasound. A- and B-mode abdominal ultrasonography was obtained with 2.25 MHz, 13 mm transducer using conventional, bistable oscilloscopic display (Picker Echoview VIII). All examinations were done with the patient supine; transverse and longitudinal sonic tomograms were obtained of the entire abdominal cavity at 2 cm intervals. The standard criteria for identification of cystic abdominal mass were used [4]. Including: (1) identification of a cystic structure 2 cm or larger in or near the region of the pancreas; (2) identification of the cyst in two or more coincident planes; (3) confirmation of B mode cystic appearances by simultaneous A mode cystic pattern obtained at low and at high sensitivity instrumental settings; and (4) differentiation of the gallbladder, fluid-filled stomach, or other nonpancreatic cystic structures by anatomic position, changes with patient rotation, overnight restudy, and/or complementary radiographic data.

Findings

The clinical profile is summarized in table 1. Of the 99

patients studied, 59 were male and 40 female, ranging in age from 14 to 81 years (average 40 years). A high percentage (92.9%) were known or suspected alcoholics. Abdominal pain, the most common presenting complaint, occurred in 79 of 99 cases (79.8%). Low grade fever was also common. Fifty-seven patients (57.5%) were febrile, with temperatures ranging from 99°F to 103.2°F (average, 100.4°). A definite palpable mass was noted in 38 of 99 cases (38.3%). There were 57 patients (57.5%) with leukocytosis on admission; counts ranged from 11,000 to 22,000/ml (average, 13,400/ml). There were 84 patients with elevated amylase on admission; Somogyi units ranged from 210 to 2,400 (normal 40-200 units).

Upper GI series was done on 74 patients (74.7%); there was radiographic suspicion of a mass in 64 instances. In 30 of these cases, there was sonographic evidence of pseudocyst; in 23 there was not (table 1). Three cases had radiographic evidence of spontaneous cyst-enteric communication and are reported elsewhere [5].

Excluding the false positive ultrasonic studies, conventional barium studies detected the lesion in only 33 of 49 cases with positive ultrasound (67.3%). In contrast, a mass was palpated in only 38 of the 99 patients studied (38.3%). In those instances where no pseudocyst was found at sonography, the x-ray examination showed gastric and small bowel displacement in 23 of 33 cases examined. In these 23, there was sonographic evidence of pancreatomegaly without pseudocyst in 18 instances, solid tumors in the pancreas in two, retroperitoneal adenopathy in one, marked emaciation with exaggerated lumbar lordosis in one, and an aneurysm of the abdominal aorta in one. There were 10 cases of ultrasonic evidence of pancreatomegaly without radiographic displacement of stomach or bowel.

The ultrasonographic findings are summarized in table 2. Of the 99 cases, 52 (52.5%) had sonographic evidence of pseudocyst. In 47 (47.4%) no mass was identified by sonography. In 16 of the patients with positive ultrasounds, exploration was not done. Excluding the three cases of cyst-enteric rupture, spontaneous resolution of pseudocyst was sonographically documented in 10 of 49 patients (20.5%). Two of the cases that showed spontaneous resolution subsequently recurred. Of 49 cystic lesions, 3 proved to be cystic degeneration within malignancies and one was a retroperitoneal salmonella abscess.

Discussion

Contrast radiography has been considered the most sensitive technique to demonstrate the presence of a pancreatic pseudocyst [2, 3, 6, 7]. Significant displacement of

Received December 19, 1975; accepted after revision March 30, 1976.

¹ Department of Radiology, Emory University School of Medicine, Grady Memorial Hospital, 80 Butler Street SE., Atlanta, Georgia 30303.

² Department of Surgery, Emory University School of Medicine, Grady Memorial Hospital, Atlanta, Georgia 30303.

TABLE 1
Clinical and Laboratory Profile of
Patients with Acute Pancreatitis

Profile	Patients with Positive Ultrasound N=52	Patients with Negative Ultrasound
Sex:		
Male.....	28	31
Female.....	24	16
Age (range).....	43 (14-81)	37 (18-62)
Known or suspected alcoholics.....	48	44
Abdominal pain on admission.....	41	38
Elevated temperature on admission.....	25	32*
Palpable abdominal mass:		
Definite.....	16	22
Questionable.....	8	11
Negative.....	28	14
Leukocytosis on admission†.....	29	28
Elevated amylase on admission‡.....	43	41
Upper GI series:		
Marked displacement.....	30	23§
No displacement.....	8	10
Spontaneous cyst-enteric communication.....	3	...

* Average, 100.4°; range, 99-103.2.

† Positive ultrasound: average, 13,100; range, 11,000-20,700. Negative ultrasound: average, 13,700; range, 11,000-22,000.

‡ Positive ultrasound: average, 478 Somogyi units; range, 210-1,680. Negative ultrasound: average, 474 Somogyi units; range, 260-2,400.

§ Gastric or small bowel displacement.

the stomach and small bowel has been reported to occur in as many as 82% [7] to 86% [3] of cases. However, many other anatomic formations may cause extrinsic gastric or duodenal compression. Arteriography may be of assistance in establishing the diagnosis [8-11]. In Rösch and Bret's series [11] the diagnosis was confirmed in 100% of cases (eight of eight). However, in Ranniger and Saldino's study [10] only half of the operatively proved pseudocysts were demonstrated by arteriography. Though it is possible to increase the diagnostic yield by using angiography, it is an invasive procedure which limits the selection of patients and the performance of serial studies.

Retrograde pancreatography is reported to show filling of the pseudocyst in 10 of 16 patients [12]. However, like angiography, this procedure does not lend itself to serial study, and we have had one instance of pancreatitis developing after this type of procedure. (Retrograde pancreatography was not used in any of the present cases.)

In the present series, cystic abnormalities were found by ultrasonography in 52 of 99 cases. There were three false positive cases in which the diagnosis was not confirmed at surgery and 16 cases in which exploration was not done. Thus our false positive rate was 8.3%. The false negative rate was 8.5%. It appears, therefore, that pseudocyst formation is a relatively common complication of acute pancreatitis, since it was demonstrated in 49 of 99 cases, or nearly 50% (see table 2).

TABLE 2
Ultrasonographic Evaluation of Patients
with Clinical Pancreatitis

Evaluation	No. Patients
	<i>Positive Ultrasound</i>
Cystic configuration not documented.....	16*
False positive (not found at surgery).....	3
Spontaneous resolution documented by serial ultrasonography.....	10†
Documented at surgery:	
Pseudocyst.....	15
Cystic malignancy.....	3
Salmonella abscess.....	1
Total.....	19
Cyst documented at autopsy.....	1
Cyst-enteric rupture documented by upper GI series.....	3
Total.....	52
	<i>Negative Ultrasound</i>
False negative cases:	
Pancreatic abscess.....	2‡
Cyst.....	2§
Total.....	4
Recovery without evidence of pseudocyst.....	29
Absence of pseudocyst documented.....	14
Total.....	47

* Surgery refused, three; lost to follow-up, 13.

† Two subsequently recurred, one proved by surgery.

‡ One found at surgery and one at autopsy.

§ Both found at surgery, less than 5 cm.

|| 10 at surgery, four at autopsy.

Another interesting and significant finding is the sonographic demonstration of gradual, spontaneous regression of these lesions in 10 of 49 cases (20%). This sonographic observation deserves special consideration in the clinical management and follow-up of patients with acute pseudocysts. In three instances, spontaneous drainage took place through dissection into the gastrointestinal tract. Neither regression nor spontaneous drainage appeared to depend upon the size or location of the cyst. There were no instances in this series of cystic intraperitoneal rupture.

The radiograph was positive in 67.3% of our cases, and three radiographic false positives were demonstrated. Thus, contrast studies were shown to be at a considerable disadvantage to ultrasound. In those cases where pancreatomegaly or other disease process accounted for the radiographic report of a mass effect, ultrasound proved a more specific and descriptive test of the mass formation. As previously suggested [13], pancreatitis with peripancreatitis accounted for the clinical and radiographic mass ab-

normality in most instances. However, in eight instances there was evident pancreatic enlargement by ultrasound which was not detected radiographically.

Finally, the overall accuracy of ultrasound in the diagnosis of pancreatic disease has been considerably enhanced with the introduction of scanning in a gray scale with a video-scan converter [14, 15]. The bistable unit used in this and other studies [16–18], is blind in detecting normal pancreas. The gray-scale scanning of this organ allows for differentiation between normal and inflamed tissue. In our opinion ultrasound is the most definitive diagnostic test presently available for detecting pseudocyst formation in acute pancreatitis.

REFERENCES

1. Connolly EA, McGreevey EJ: Internal drainage of pancreatic cyst. *Am J Surg* 87:575–582, 1970
2. Judd ES, Mattson H, Mahorner HR: Pancreatic cysts: a report of 47 cases. *Arch Surg* 22:838–849, 1931
3. Thomford NR, Jesseph JE: Pseudocyst of the pancreas. A review of fifty cases. *Am J Surg* 118:86–94, 1969
4. Goldberg BB, Kotler MN, Ziskin MC, Waxham MB: *Diagnostic Uses of Ultrasound*. New York, Grune & Stratton, 1975
5. Clements JL Jr, Bradley EL III, Eaton SB Jr: Spontaneous internal drainage of pancreatic pseudocysts. *Am J Roentgenol* 126:985–991, 1976
6. Kommani S, Clark JM: Pancreatic pseudocyst: a review of 17 cases with emphasis on radiologic findings. *Am J Roentgenol* 122:385–397, 1974
7. Caravati CM, Ashworth JS, Frederick P: Pancreatic pseudocysts: a medical evaluation. *JAMA* 197:572–576, 1966
8. Fu WR, Stanton LW: Angiographic study of pseudocysts of the pancreas. *J Can Assoc Radiol* 20:176–179, 1969
9. Kadell BM, Riley JM: Major arterial involvement by pancreatic pseudocysts. *Am J Roentgenol* 99:632–636, 1967
10. Ranniger K, Saldino RM: Arteriographic diagnosis of pancreatic lesions. *Radiology* 86:470–474, 1966
11. Rösch J, Bret J: Arteriography of the pancreas. *Am J Roentgenol* 94:182–193, 1965
12. Rohrman C, Vennes J, Silver S: Evaluation of the endoscopic pancreatogram. *Radiology* 113:297–304, 1974
13. Bradley EL, Clements JL: Implications of diagnostic ultrasound in the surgical management of pancreatic pseudocyst. *Am J Surg* 127:163–173, 1974
14. Kossoff G: Improved techniques in ultrasonic cross-sectional echography. *Ultrasonics* 10:221–227, 1971
15. Taylor K, Carpenter D, McCready V: Gray scale echography in the diagnosis of intrahepatic disease. *J Clin Ultrasound* 1:284–287, 1973
16. Filly A, Freimanis A: Echographic examination of pancreatic lesions. *Radiology* 96:575–582, 1970
17. Leopold GR: Pancreatic echography: a new dimension in the diagnosis of pseudocyst. *Radiology* 104:365–369, 1972
18. Walls WJ, Gonzalez G, Martin NJ, Templeton AW: B-scan ultrasound evaluation of the pancreas. *Radiology* 114:127–133, 1975

Preoperative Radiation Therapy in Endometrial Carcinoma: Preliminary Report of a Clinical Trial

IRVING J. WEIGENBERG¹

A total of 91 patients with stage I endometrial adenocarcinoma who were referred for radiation prior to hysterectomy were randomly allocated to receive either intracavitary or external beam irradiation. Total abdominal hysterectomy was done 4–8 weeks later. The 53 patients who received intracavitary irradiation had an actuarial 5 year disease-free survival rate of 75%; the survival rate of the 38 patients in the external beam group was 48%. Nine patients in the external beam group had recurrence or metastases compared to two in the intracavitary group. These recurrences were predominantly pelvic. Complications were also more frequent in the external beam group. These results demonstrate that intracavitary radiation is superior to external beam radiation using the regimens described.

Preoperative radiation therapy has been utilized in the management of endometrial carcinoma for many years. Classically, this has been done by packing the uterus with multiple Heyman capsules containing radium [1, 2]. However, recent studies [3–5] have shown excellent results with external beam radiation. These reports show 90%, 79%, and 83% 5 year survival rates, respectively, without evidence of disease. Orthovoltage equipment was used in two of the studies [3, 4] to deliver a depth dose of 3,000–4,000 rads, whereas cobalt 60 was utilized with a depth dose of 5,000–6,000 rads in the most recent report [5]. The purpose of this study is to compare results using intracavitary and external beam preoperative radiation therapy in the treatment of endometrial carcinoma.

Subjects and Methods

The study was carried out personally in a private practice of radiation therapy at two community hospital settings; initially at Lutheran Hospital and a private office in St. Louis, Missouri, and subsequently at Methodist Hospital in Peoria, Illinois. The latter hospital is also a regional radiation therapy facility, servicing an area within a radius of 30–50 miles and a population of approximately 600,000. It was the general policy of physicians in both locales to treat all patients with endometrial adenocarcinoma by radiation followed by hysterectomy.

All patients with stage I endometrial adenocarcinoma (as defined by FIGO [6]) referred for radiation therapy prior to hysterectomy were randomly allocated to one of two treatment groups. No patient thought suitable for hysterectomy was rejected for preoperative radiation on the basis of such factors as histologic grade, uterine size, obesity, or other medical problems. All had a histologic diagnosis, with a D and C and additional workup including chest x-ray, intravenous pyelogram, and barium enema. Randomization was carried out using year of birth: those born in odd-numbered years received intracavitary curietherapy, while those born in even-numbered years received teletherapy. Referring physicians had no

knowledge of the randomization scheme.

The group to receive intracavitary irradiation received a single implant, usually with multiple Heyman capsules packed into the fundus, a tandem into the lower uterine segment, and ovoids into the lateral vaginal fornices (figs. 1 and 2). The exposure ranged between 5,300 and 6,500 mg hr. In smaller uteri, only a tandem and ovoids were employed with appropriate reduction in exposure.

The external beam irradiation was carried out via opposing anterior and posterior 15×15 cm portals initially utilizing cobalt 60. For the past 2½ years a 4 MeV linear accelerator with TSD of 80 cm has been employed (fig. 3). Generally, one treatment port was used each day, but more recently we have been using both portals daily.

Total abdominal hysterectomy with salpingo-oophorectomy was carried out 4–8 weeks after completion of the radiation therapy. The surgery was performed by board-certified general surgeons or gynecologists.

Results

Between January 1967 and November 1974, 91 patients were studied: 38 in the external beam group and 53 in the intracavitary group. The age distribution of the two groups is shown in figure 4. There is a slight shift toward a younger age in the group receiving intracavitary irradiation. In the intracavitary group, 42% were older than 60 compared to 61% in the external beam group. The mean and median ages were also slightly greater in the external beam group.

Obesity was evaluated according to the following semi-quantitative scale: 1=normal weight, 0=under-weight, 2=mild obesity, 3=moderate obesity, and 4=marked obesity. There was no evident significant difference between the two groups with respect to this factor (fig. 5).

Because of the prevalence of obesity, uterine size could not be reliably assessed by palpation. Thus to assure reliable and consistent measurements, uterine size was evaluated by sounding at the time of initial evaluation for radiation therapy. No consistent, significant difference between the two groups was found (fig. 6).

All slides were reviewed by the same pathologist to determine the degree of differentiation. The criteria specified by FIGO [6] were used. The distribution of histologic grades is virtually identical in both groups (fig. 7). The preponderance of grade 1 carcinoma seen here has been observed elsewhere [7].

Figure 8 demonstrates the actuarial disease-free survival in the two groups. After the first 9 months, there is a clear and persistent survival advantage in the intracavitary group. The 3 and 5 year survival rates are 86% and 75%, respectively, for the intracavitary group compared to 75% and 48% for the external beam group. The difference at 3 years

Presented at the annual meeting of the American Radium Society, San Juan, Puerto Rico, May 1975.

¹ Department of Radiology, Peoria School of Medicine, University of Illinois and Methodist Hospital, 221 Northeast Glen Oak Avenue, Peoria, Illinois 63136.

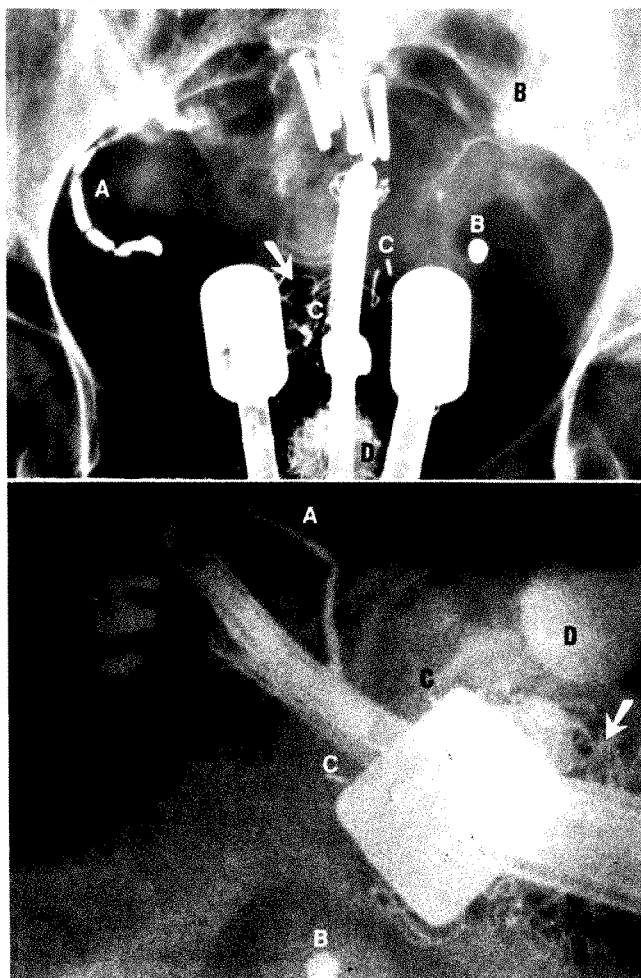


Fig. 1.—Roentgenograms of representative intracavitary implant. Note residual barium in appendix (A) and sigmoid diverticula (B), cervix as indicated by submucosally placed gold seeds (C), bladder neck as demarcated by contrast medium in bulb of Foley catheter (D), and radiopaque marker in vaginal packing (arrow).

was not significant ($P=.13$), but the difference at 5 years was highly significant ($P<.003$). In addition, the two survival curves were found to be significantly different ($P<.005$) by the modified Wilcoxon test [8, 9].

This difference is emphasized by examination of the treatment failures (table 1). There were nine failures among the 38 patients treated with external beam compared to two failures in the 53 patients receiving intracavitary radiation ($P<.02$). One of the two failures in the intracavitary group represents a failure of staging and clinical evaluation rather than of treatment, since at surgery she was found to have extrauterine pelvic extension. However, this case is balanced in the external beam group by a patient who developed a palpable supraclavicular lymph node metastasis in the fourth week of external beam treatment.

The main site of failure in both groups is the pelvis, the remainder occurring in either the upper abdomen (liver, peritoneum, periaortic nodes) or distantly (e.g., lungs, supraclavicular lymph node). The upper abdominal and distant metastases may have been present in occult form at the time of treatment and merely required additional time

HEYMAN CAPSULES	7 X 10 Mg Ra	EQUIV.
FLETCHER A-L TANDEM	2 X 10 Mg Ra	EQUIV.
FLETCHER A-L OVOID	2 X 21 Mg Ra	EQUIV.
6500 Mg Hrs		

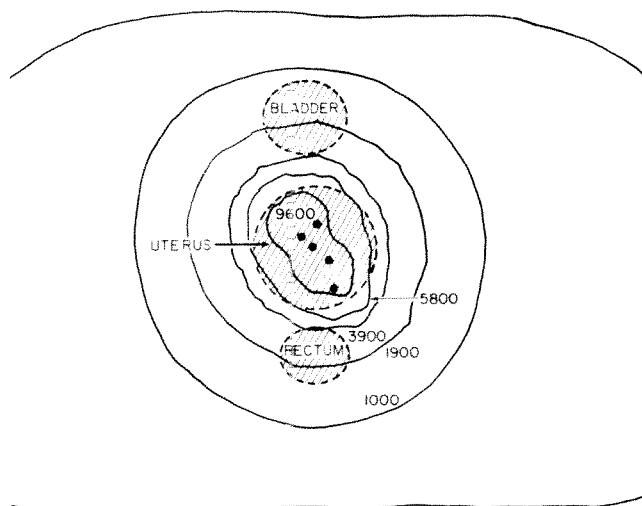


Fig. 2.—Dose distribution resulting from implant (fig. 1). Dots within uterus represent points where radiation source pierces plane of computation.

to become clinically manifest. However, the pelvic failures inescapably represent failure of the treatment method. Appearance of the metastases as late as 55 and 73 months after treatment is noteworthy, being well beyond the time usually noted [10].

An attempt was made to identify factors predisposing to recurrence. No relationship could be identified between tumor recurrence and histologic grade: the distribution of histologic grades in the recurrent group closely paralleled that in the entire external beam group. Similarly, there was no significant difference in the frequency of residual tumor in the excised uterus among those who had recurrence or metastases and those who did not. However, six of the nine recurrences in the external beam group (67%) were in uteri which sounded to a depth of 8 cm or greater, whereas only 42% of the entire external beam group had uteri of this size (table 2). Uterine size was the only factor observed to have any relationship to tumor recurrence.

Tables 3 and 4 demonstrate the increased frequency of complications in the external beam group compared to the intracavitary group. Only the differences based on total number of patients with complications and on number of minor complications were statistically significant ($P=.01$ and $.02$, respectively). Some of the complications were not directly related to the radiation: a fistula due to surgical trauma to the ureters; the fatal hepatic necroses possibly related to general anesthesia; the hepatitis evident only by nonspecific abnormalities in liver function studies at the time of the implant 2 weeks after the D and C; and the small bowel infarction. Nevertheless, because the type of irradiation may be a contributing factor to the complication (e.g., via general anesthesia, dehydration), these complications must be counted against each treatment technique.

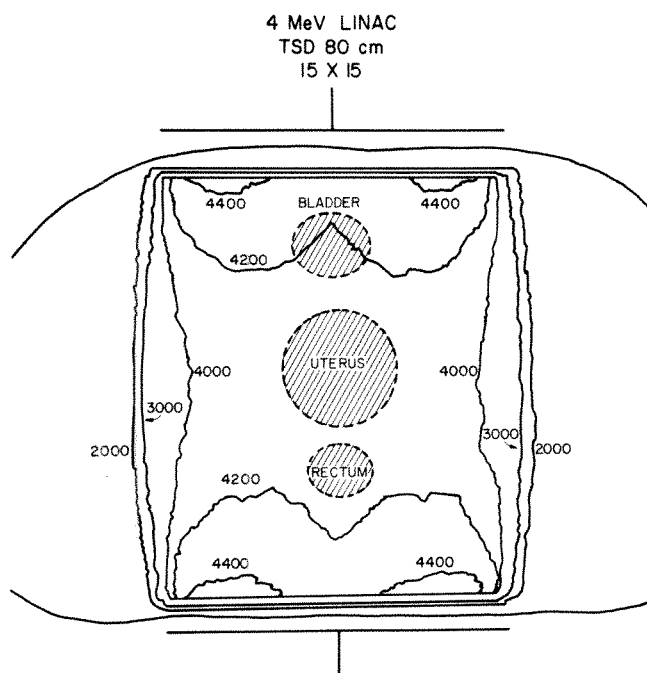


Fig. 3.—Representative dose distribution from characteristic external beam treatment plan.

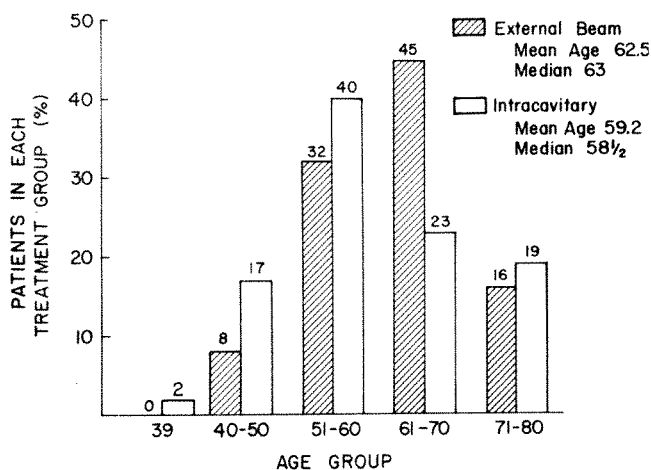


Fig. 4.—Age distribution of patients studied.

No relationship could be established between the excess of complications in the external beam group and age, obesity, subcutaneous fibrosis, or the presence of diverticular disease of the colon.

Discussion

This study does not attempt to answer the fundamental question of the indications for preoperative radiation nor the related question of whether preoperative irradiation is superior to postoperative. It merely compares results using two techniques of preoperative radiation.

The study was carried out in a community hospital, private practice setting where a large number of such cases are being treated today. In this respect, the study may be

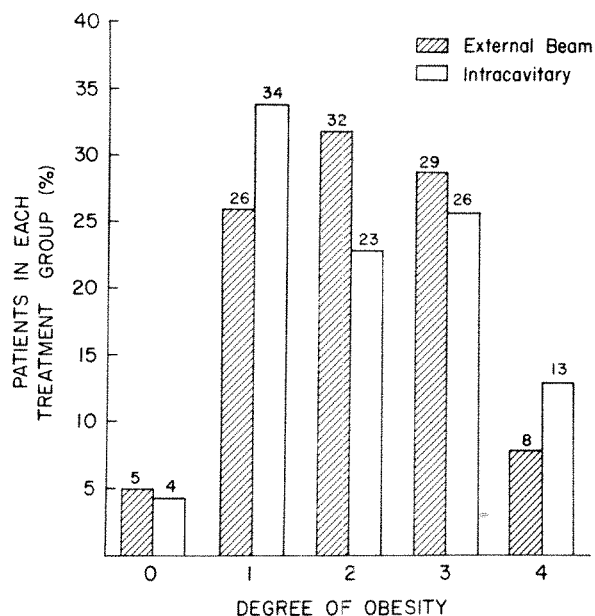


Fig. 5.—Distribution of obesity in study population. 0=underweight, 1=normal weight, 2=mild obesity, 3=moderate obesity, 4=markedly obese.

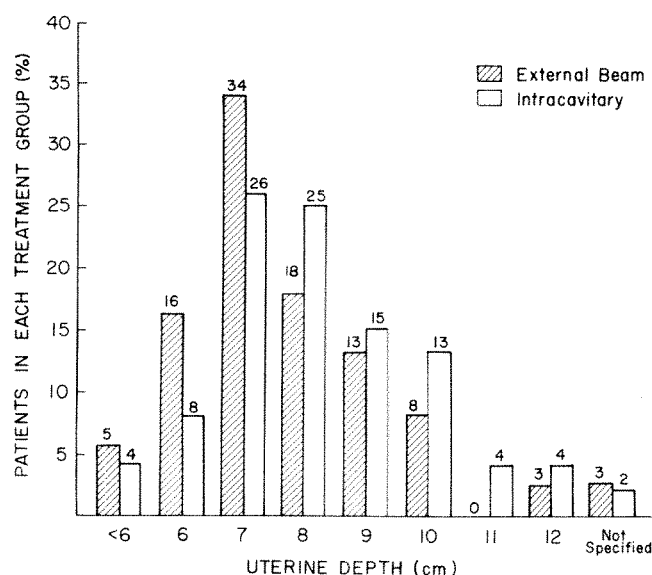


Fig. 6.—Distribution of cases by uterine size.

more representative than one carried out in the highly specialized atmosphere of a university hospital or a cancer center.

These preliminary results show that intracavitary irradiation is superior to external beam radiation at the dose levels tested. Intracavitary radiation, characterized by intense intrauterine dose with rapid extrauterine falloff (fig. 2), appears to be superior to the external beam which delivers a higher dose to the lateral pelvis and pelvic lymph nodes (fig. 3). Increasing the dose of external radiation to 5,000 rads or more may make tumor control rates equivalent. However, the increased dose is likely to further in-

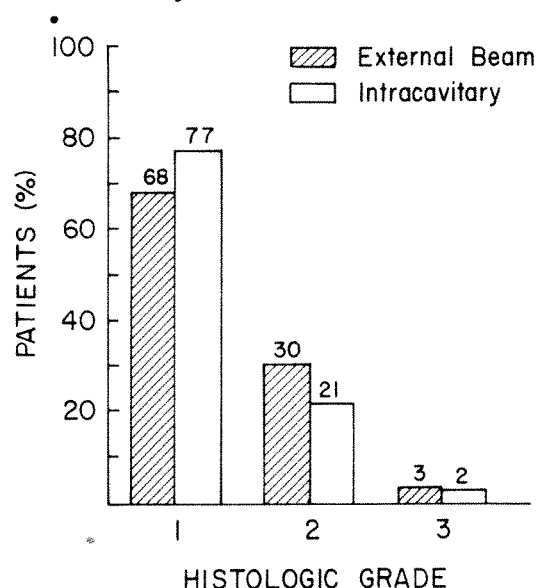


Fig. 7.—Distribution of cases by histologic grade.

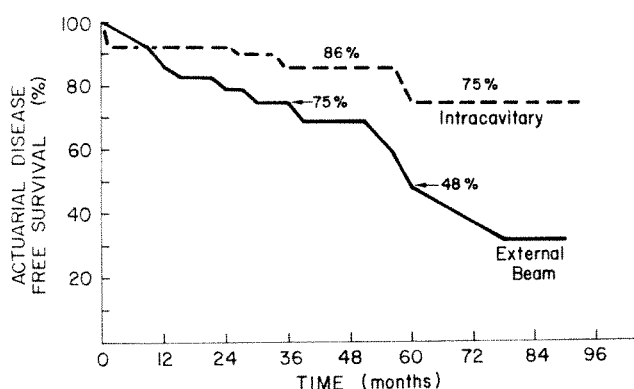


Fig. 8.—Cumulative disease-free survival rates.

crease the rate of complications. Another alternative would be to add an intracavitary implant to the external beam radiation [11]. However, either of these variations would have to be tested against use of intracavitary radiation alone.

Although good prognoses are usually associated with well differentiated grade 1 tumors, six of the 11 recurrences (55%) were in patients with grade 1 histology. This observation, together with the fact that most of the cases fell into the grade 1 category, may reflect a limitation of the histological grading system described by FIGO [6]. Perhaps the requirement that a tumor must have partly solid areas to be classified as grade 2, regardless of cytologic characteristics, needs reconsideration.

The only factor identified as predisposing to recurrence was uterine size. Although it is generally thought that larger uteri are associated with a poorer prognosis, published data do not consistently support this [12]. This may well be attributable to the difficulties inherent in accurately estimating uterine size. These include patient obesity, variations in size estimations among different observers, and failure to routinely record the depth to which the

TABLE 1
Treatment Failures

Type	No. Cases	Time after Treatment (Yr)
External beam:		
Pelvic recurrence	5	6 1/3, 4 7/12, 2 1/2, 1 1/4, 1
Pelvic persistence and distant metastases	1	1/12
Upper abdomen with or without distant metastases	2	1, 7/12
Distant metastases	1	1/3
Total	9	
Intracavitary:		
Pelvic (extrauterine spread)	1	1/6
Pelvic and hepatic	1	3
Total	2	

TABLE 2
Relationship of Recurrences to Uterine Size

Uterine Depth (on)	No. Cases	% of Recurrences	% of Entire Group
External Beam			
4	1	11	5
6	1	11	16
≥8	6	67	42
Not sounded	1	11	3
Intracavitary			
8	1
12	1

uterus sounds at D and C. In addition, any effect associated with uterine enlargement from tumor might well be blurred out by enlargement from benign conditions such as fibroids.

The estimates of uterine size in this study are susceptible to two obvious sources of error, both which tend toward underestimation. With the patient awake, minor or transient obstruction to the passage of the sound can be a greater problem than with the patient asleep. Second, evacuation of the uterine tumor at the time of D and C can result in the cavity being smaller when the patient is evaluated several days later for radiation therapy.

ACKNOWLEDGMENTS

I wish to thank Dr. Alan Campbell for reviewing the histologic material and Mr. V. K. Moses for aid in the statistical evaluation of the data.

REFERENCES

1. Heyman J, Benner S: Further experience with radiotherapy in

TABLE 3

Complications in External Beam Group

Complication	No.
Major:	
Small bowel infarction	1
Wound dehiscence postoperatively, adynamic ileus, late radiation sigmoiditis, and sigmoid-cutaneous fistula*	1
Severe enteritis	2
Perforation of sigmoid colon	1
Fever—reactivation of old PID (1) or diverticulitis (1) postoperatively	2
Total	7
Minor:	
Thrombophlebitis	2
Mild wound healing problems	4
Urinary tract infection	3
Postoperative pleuritic pain	1
Prolonged moderate diarrhea	2
Breakdown of skin over subcutaneous fibrosis	1
Total	13

Note.—Complications occurred in 18 of 38 patients.

* Occurred in same patient.

cancer of corpus uteri. *Acta Radiol* 27:328–333, 1946

2. Heyman J, Reuterwall O, Benner S: Radiumhemmet experience with radiotherapy in cancer of corpus of uterus. *Acta Radiol* 22:11–98, 1942
3. Lampe I: Endometrial carcinoma. *Am J Roentgenol* 90:1011–1015, 1963
4. Sala JM, del Regato JA: Treatment of carcinoma of the endometrium. *Radiology* 79:12–17, 1962
5. del Regato JA, Chabazian CM: External pelvic irradiation as a preoperative surgical adjuvant in treatment of carcinoma of the endometrium. *Am J Roentgenol* 114:106–109, 1972
6. International Federation of Gynaecology and Obstetrics (FIGO): Classification and staging of malignant tumors in the

TABLE 4

Complications in the Intracavitary Group

Complication	No.
Major:	
Ureterovaginal fistula	1
Fatal hepatic necrosis	2
Hepatitis*	1
Wound dehiscence	1
Severe cystitis with necrosis and ulceration	1
Total	6
Minor:	
Thrombophlebitis	3
Mild wound healing problems	2
Adynamic ileus	1
Proctitis	1
Total	7

Note.—Complications occurred in 10 of 53 patients.

* Incipient at time of implant.

female pelvis. *Int J Gynecol Obstet* 9:174–176, 1971

7. Frick HC II, Munn EW, Richart RM, Berger AP, Lawry MF: Carcinoma of the endometrium. *Am J Obstet Gynecol* 115:663–672, 1973
8. Burdette WJ, Gehan EE: *Planning and Analysis of Clinical Studies*. Springfield, Ill., Thomas, 1970
9. Gehan EE: Generalized Wilcoxon test for comparing arbitrarily singly-censored samples. *Biometrika* 52:203–223, 1965
10. Monson RR, MacMahon B, Austin JH: When may endometrial cancer be considered cured? *Cancer* 30:419–425, 1972
11. Marcial VA, Tome JM, Ubinas J: The combination of external irradiation and curietherapy used preoperatively in adenocarcinoma of the endometrium. *Am J Roentgenol* 105:586–595, 1969
12. Shah CA, Green TH: Evaluation of current management of endometrial carcinoma. *Obstet Gynecol* 39:500–509, 1972

The Role of Postoperative Irradiation in the Management of Stage I Adenocarcinoma of the Endometrium*

C. PAUL MORROW,¹ PHILIP J. DI SAIA,² AND DUANE E. TOWNSEND¹

A comparison of treatment protocols for endometrial carcinoma is presented. Valid conclusions regarding optimum approach are virtually precluded because of variability of such factors as clinical staging, incidence of vaginal metastases, patient selection, and histologic grade. While hysterectomy is the established definitive treatment, the superiority of adjuvant irradiation can be demonstrated only by randomized, prospective studies.

The management of endometrial carcinoma remains controversial after more than 25 years of experience accumulated by radiation therapists and pelvic surgeons in Europe and North America. No sense of urgency has appeared to critically evaluate the treatment of this disease, apparently because most cases are diagnosed "early" and the degree of curability is relatively satisfactory to the physician-therapist. In the United States endometrial carcinoma has far surpassed cervical cancer as the most common malignancy of the female genital tract (table 1), a fact which should generate renewed interest in defining its optimal therapy.

The data of Bickenbach et al. [1] and Joelsson et al. [2] refute the obstinate but fading belief that radiation therapy alone can compete with surgery and radiation therapy in the management of stage I endometrial carcinoma. These studies reveal clearly inferior survival results for patients treated entirely by radiation after corrections are made for prognostic factors and noncancer deaths (table 2). While hysterectomy is generally acknowledged as the managerial keystone of stage I adenocarcinoma of the endometrium, most treatment centers utilize, in addition, some variety of adjuvant radiation.

In many quarters the superiority of combination therapy is accepted as established dogma, and reexamination of treatment policies viewed as heretical. Despite the confident air of this position, a life-sparing effect specifically attributable to the radiotherapeutic component of combination regimens has not been proven. Even though unequivocal evidence is lacking that adjuvant irradiation improves survival in endometrial carcinoma, its use is widespread. This is understandable because of the known capability of radiotherapy to cure a substantial portion of medically inoperable cases and its efficacy in reducing the incidence of local recurrences following surgery alone. The demonstrated radiosensitivity of endometrial carcinoma strongly suggests that survival should be improved by adjuvant irradiation.

Literature Critique

Countless clinical reports have demonstrated beyond a reasonable doubt that survival in adenocarcinoma of the endometrium is influenced by clinical stage, extent of myometrial penetration, and histologic (and nuclear) grade of the lesion. It is not clear whether the age of the patient or the depth of the uterine cavity has prognostic significance after corrections are made for stage, muscle invasion, and grade. While many articles purport to show the value of a particular treatment protocol, meaningful interpretation of results is complicated by the variability of prognostic factors among study groups. A brief survey of these discrepancies will demonstrate the magnitude of this problem.

Clinical Staging

There are three common deficiencies in this area.

1. Most reports prior to 1967 utilized the old international staging system [3]. Thus cases with cervical involvement, the equivalent of the current FIGO stage II, were often included in stage I.

2. Few authors describe the method of diagnosing cervical involvement. Clinical examination, cervical biopsies (cone or punch), and fractional curettage undoubtedly will yield different results.

3. Clinical staging is corrected by surgical-pathologic staging in some reports, while others utilize only clinical information. Surgical-pathologic stage correction could up-stage as many as 15% of cases [4, 5].

Vaginal Metastases

The incidence of vaginal metastases in stage I endometrial cancer is of great importance in assessing treatment results since it is the only verified justification for adjuvant radiation. Combination therapy is attended by a lower incidence of vaginal recurrences than is surgical therapy. However, the reporting of this event and the interpretation of the reports have been inexact. Consequently, the benefit from adjuvant radiation therapy is probably less than advertised.

In some series only isolated, apical recurrences are considered in the incidence tabulation of vaginal metastases, while others include all vaginal metastases, isolated or not, regardless of the level of vaginal involvement. An example of misinterpretation concerns the incidence of vaginal recurrences in the series of Meigs [6] and Way [7]. These authors reported metastases which appeared in the vagina before treatment in addition to those occurring after treat-

Presented at the annual meeting of the American Radium Society, San Juan, Puerto Rico, May 1975.

¹ Department of Obstetrics and Gynecology, Los Angeles County—University of Southern California Medical Center, Women's Hospital, 1240 North Mission Road, Los Angeles, California 90033. Address reprint requests to C. P. Morrow.

² Departments of Obstetrics and Gynecology and Radiology, Los Angeles County—University of Southern California Medical Center, Los Angeles, California 90033.

TABLE 1
Cancer Incidence and Death in U.S. Females

Site	Incidence		Deaths	
	No.	% Total	No.	% Total
Breast	88,000	27	32,600	20
Colorectum	51,000	15	25,400	15
Corpus uteri	27,000	8	3,300	2
Lung	19,000	6	17,600	11
Cervix	19,000	6	7,800	5
Ovary	17,000	5	10,800	6

Note.—Data from the American Cancer Society, 1975.

TABLE 2
Corrected 5 Year Survival in Stage I Endometrial Carcinoma

Reference	Surgery with or without Radiation		Radiation Only		P
	No.	% 5 Yr Survival	No.	% 5 Yr Survival	
Bickenbach et al. [1]	137	87	136	69	<.005
Joelsson et al. [2]	517	90	197	71	<.0005

ment. It is obvious from table 3 that the posttherapy rate of vaginal recurrences is approximately half that usually attributed to these series. While these recurrence rates are significantly higher than those usually reported following combination therapy for stage I disease, it must be pointed out that these series were unstaged.

Patient Selection

The allocation of patients to a treatment group on the basis of physician preference, medical problems, or other selective basis will invalidate comparison of treatment series. For example, Lampe [8] reported an overall 87.8% corrected 5 year survival rate for 173 patients with stage I, group 1 carcinoma of the endometrium. Of the 173 cases, 121 received 4,000 rads whole pelvis radiation preoperatively without intracavitary therapy. In this group a 90% 5 year survival rate (93% corrected survival rate) was achieved, and only one patient developed vaginal recurrence. The results for this subgroup rather than for the entire series have been cited to support the use of external beam therapy in the management of endometrial carcinoma [9, 10].

Similarly, the report of Keller et al. [11] states that a 95% corrected 5 year survival rate was achieved utilizing surgery alone in the management of 95 patients with stage I carcinoma of the endometrium. However, 10 patients treated with combined therapy because of "physician's preference" were excluded from the series as were an additional seven patients (medically inoperable) who received only

TABLE 3
Incidence of Vaginal Metastases

Reference	No Cases	Total Metastases *		Posttherapy Metastases	
		No.	%	No.	%
Meigs [6]	206	25	12.1	13	6.7
Way [7]	102	14	13.7	4†	4.3

Note.—Endometrial carcinoma, unstaged surgical series.

* Includes pre- and posttherapy vaginal metastases.

† One case had x-ray therapy at initial treatment.

radiotherapy. The survival of the entire group of 112 patients was 88% at 5 years.

Histologic Grade

Prognosis in endometrial carcinoma is strongly influenced by the degree of histologic differentiation. Nevertheless, clinical reports frequently do not include this information. The survival rate in any study group will depend largely upon the proportion of cases having poorly differentiated tumors, which may vary considerably. In addition, difficulty in discriminating between well differentiated adenocarcinoma and severe atypical hyperplasia or carcinoma in situ is well known.

Variations in interpretation could influence the end results to a greater degree than differences in management. For example, Keller et al. [11] reported that three pathologists who reviewed their histopathology data were unable to concur on the diagnosis of cancer in 48 of 208 cases. The inclusion of these 48 patients in their study group would significantly alter the results. Most reports do not state whether a review of the histopathology has been carried out.

Survival Data

Endometrial carcinoma is a disease which usually afflicts postmenopausal women. Characteristically they also suffer from numerous medical disorders which reduce life expectancy independent of their malignant neoplasm. Gross (crude) survival data, therefore, do not accurately reflect curability or treatment effect. The differences in crude and corrected survival rates can be extreme, as the experience of Nilsen and Koller [12] demonstrates. Their crude survival rate for stage I, group 1 adenocarcinoma of the endometrium was 85%, but after corrections were made for deaths due to intercurrent disease, the 5 year survival rate rose to 98%. Another source of bias occurs when patients lost to follow-up are counted as dead with disease.

These and other discrepancies in reporting all but preclude valid conclusions regarding the specific, life-sparing effect of adjuvant irradiation without employing a randomized clinical trial. Any treatment plan which includes hysterectomy can be proposed as superior to others and supported by selected papers from the literature. As table 4 illustrates, surgery alone and hysterectomy followed by irradiation are apparently superior to irradiation followed

TABLE 4
End Results of Stage I Endometrial Carcinoma

Treatment	No. Cases	Corrected 5 Yr Survival (%)	% Grade 3
Hysterectomy only	407	94	9-26
X-ray therapy+hysterectomy	354	86*	22-26
Hysterectomy+x-ray therapy	747	95	7-38

Note.—Data from [5, 11-13].

* Difference may reflect selection and surgical staging.

TABLE 5
Vault Recurrences

Treatment	No. Cases	Vault Metastases	
		No.	%
Heyman capsules+hysterectomy*	65	4	6.2
Hysterectomy only	55	4	7.3

Note.—Stage I endometrial carcinoma. Data from [16].

* No residual tumor in uterus.

by hysterectomy ($P < .005$). However, the differences are undoubtedly due to bias with regard to histologic grade and surgical staging.

Adjuvant Radiation Therapy

In the minds of many authorities, preoperative irradiation is the standard of therapy. Whether it should be considered the standard is questionable. The most recent issue of the Annual Report [14] indicates that 43% of 3,025 stage I cases were treated by hysterectomy with or without postoperative irradiation, nearly double the number receiving preoperative radiotherapy.

Among the proposed advantages of preoperative irradiation are the following: shrink tumor; seal lymphatics and vascular channels; reduce viable tumor cell population; impair implantability of tumor; treat microscopic disease peripheral to surgical field; reduce incidence of cuff recurrences; and provide a means of optimal parametrial irradiation (intracavitary therapy). Its only unique feature compared to postoperative radiotherapy is the potential to prevent tumor spread at the time of surgery.

The best clinical evidence that preoperative irradiation reduces the spread of tumor at the time of surgery is the lower frequency of vaginal cuff recurrences associated with combination therapy than with surgery alone. However, the incidence of such recurrences after postoperative radiation therapy is comparable to that achieved by preoperative irradiation [9, 15]. The mechanisms might be different: that is, tumor spread to the vagina could occur at the time of surgery in the postoperative irradiation group but the local irradiation destroys it, while spread is prevented by the

TABLE 6
Myometrial Invasion

	Surgery+X-ray*Therapy		X-ray Therapy+Surgery	
	No.	%	No.	%
None	86	27.5	160	78
Superficial	148	47.5	34	16.5
Moderate	74	23.8*	10	4.8*
Deep	2	1.0	2	1.0
Total	311		206	

Note.—Stage I endometrial carcinoma. Data from [2].

* $P < .0005$.

TABLE 7
Late Complications in Endometrial Carcinoma

	Postoperative X-ray Therapy (N=347)	Pre- and Post-operative X-ray Therapy (N=257)	X-ray Therapy Only (N=407)
Injuries:			
Rectal	2	11	14
Bladder	1	8	11
Ureter	0	1	0
Ileum	1	1	2
Total	4	21	27
No patients	3 (0.8)	13 (5.0)	25 (6.1)
Injured cases/pelvic x-ray therapy	2/113 (1.8)	10/63 (15.9)	18/210 (11.7)

Note.—All stages. Data from [2]. Numbers in parentheses are percentages.

effect of preoperative therapy on the primary tumor.

However, the traditional theme that cuff recurrences are due to drop implantation or "squeezing" tumor into the vaginal lymphatics or veins at the time of surgery seems to be refuted by the report of Truskett and Constable [16]. They noted that the incidence of vault recurrences in patients having no residual tumor in the uterus following Heyman packing was essentially the same as that following surgery alone (table 5). With no residual uterine disease it was not possible that the vaginal recurrences resulted from operative spread. This finding is in harmony with other reports [17-19] indicating that the incidence of vaginal recurrences reflected the depth of myometrial invasion, degree of tumor dedifferentiation, and extension of tumor to the isthmus or cervix.

Although radiation does not appear to be important in the prevention of tumor spread at the time of surgery, it has an established role in the management of extrauterine endometrial carcinoma. As previously noted, "prophylactic" irradiation of the upper vagina and paracervical tissue does reduce the incidence of local recurrences. When isolated, these vaginal lesions have little apparent effect on the overall survival rate [20]. Nevertheless, as a matter of principle

it is more desirable to treat microscopic disease than clinical recurrences.

A second region at risk for occult spread of endometrial carcinoma is the pelvic wall. Among 369 collected cases of stage I endometrial carcinoma treated by hysterectomy and lymphadenectomy, 39 (10.6%) had positive pelvic nodes. Some of those with node metastases survived 5 years [21]. This relatively low incidence of pelvic node involvement does not warrant routine whole pelvis irradiation, but high risk patients should be treated. Several studies [e.g., 22, 23] have demonstrated a relationship between the risk of pelvic node metastasis, the depth of myometrial penetration, and the degree of histologic differentiation among surgically verified stage I cases.

While histologic grading can be done preoperatively, evaluation of myometrial invasion can only be carried out after hysterectomy. Invasion is a function of differentiation, but even grade 1 tumors occasionally invade deeply. Because tumor regression alters the depth of myometrial invasion, preoperative irradiation will prevent the identification of most cases which need pelvic wall irradiation (table 6). Furthermore, tumor involving the isthmus, cervix, or adnexae may be obliterated by preoperative radiation. The obfuscation of muscle invasion can be avoided if hysterectomy is done within 1 week following intracavitary therapy as recommended by Boronow [24]. Nevertheless, routine preoperative radiation necessarily overtreats many patients.

Among the advantages of postoperative radiation are accurate surgical-pathologic staging; optimal individualization of adjuvant radiotherapy; and reduced treatment time and cost. There is also a suggestion of reduced treatment complications (see later). Obviously, the major advantage is the accuracy with which the risk of extrauterine disease and, therefore, the need for adjuvant therapy can be assessed. Some selection can be incorporated into the basic preoperative irradiation treatment plan, but the individualization is necessarily more limited than with postoperative radiotherapy. Several workers [4, 25, 26] have recommended hysterectomy without preoperative irradiation for patients with well differentiated stage 1 adenocarcinoma of the endometrium in a small uterus. The association of significant myometrial invasion with grade 1 lesions is low so that few of these individuals will require adjuvant therapy. (These patients commonly have no residual disease at surgery.)

There has been concern that postoperative pelvic irradiation is attended by a higher risk of treatment complications than preoperative radiotherapy because of adhesions, particularly involving the small bowel, and impaired tissue vascularity. This is undoubtedly true when both intrauterine and whole pelvis irradiation are utilized but evidently does not pertain to pelvic irradiation alone or use of vaginal radium. In table 7 the complication rate among 1,011 cases of endometrial carcinoma treated at the Radiumhemmet in Stockholm is displayed. The postoperative irradiation group had a 1.8% incidence of late complications compared to 15.9% in the group treated with pre-

operative intrauterine radium plus postoperative whole pelvis irradiation.

Finally, the entire concept of extending therapy to the pelvic wall has been challenged because autopsy studies [27] suggested that iliac node metastases were always accompanied by extrapelvic disease. Regrettably, there are no data from surgical studies on the incidence of aortic node metastases in adenocarcinoma of the endometrium or the relationship of pelvic and aortic node metastases. Until this information is available, it is illogical to withhold treatment to probable sites of pelvic spread in early endometrial cancer on the basis of necropsy findings.

Conclusions

1. Hysterectomy is the established definitive treatment for stage I corpus cancer.
2. Vaginal cuff recurrences result from lymphatic spread prior to hysterectomy and not from spread at the time of hysterectomy.
3. Adjuvant irradiation reduces the incidence of vaginal recurrences but its effect on survival is not known.
4. There are no convincing clinical data that preoperative irradiation, despite its theoretical advantages, is superior to postoperative irradiation.
5. Adjuvant irradiation administered postoperatively permits optimal individualization of therapy. It offers the advantages of less treatment, less expense, and, perhaps, a lower complication rate than routine preoperative radiation.
6. The end results of therapy for stage I corpus carcinoma with any treatment plan which includes hysterectomy will be good. The superiority of adjuvant irradiation (pre- or postoperative, whole pelvis or intracavitary, Heyman packing or linear source) can be demonstrated only by randomized, prospective studies.

REFERENCES

1. Bickenbach W, Lochmuller H, Dirlich G, Ruland G, Thurmayr R: Factor analysis of endometrial carcinoma in relation to treatment. *Obstet Gynecol* 29:632-636, 1967
2. Joelsson I, Sandri A, Kottmeier HL: Carcinoma of the uterine corpus: a retrospective survey of individualized therapy. *Acta Radiol [Suppl]* (Stockh) 334:3-63, 1973
3. Kottmeier HL (ed): Annual report on the results of treatment in carcinoma of the uterus, vol 13, Stockholm, 1963
4. Kottmeier HL: Individualization of therapy in carcinoma of the corpus, in *Cancer of the Uterus, Tubes and Ovaries, Proceedings 11th Annual Clinical Conference on Cancer*, Houston, 1966, Chicago, Yearbook Medical Publishers, 1968, pp 102-108
5. Welander C, Griem ML, Newton M, Marks JE: Staging and treatment of endometrial carcinoma. *J Reprod Med* 8:41-46, 1972
6. Meigs JV: Adenocarcinoma of the fundus of the uterus: a report concerning the vaginal metastases of this tumor. *N Engl J Med* 201:155-160, 1929
7. Way S: Vaginal metastases of carcinoma of the body of the uterus. *J Obstet Gynecol Br Emp* 58:558-572, 1951
8. Lampe I: Endometrial carcinoma. *Am J Roentgenol* 90:1011-1015, 1963
9. Goodman R, Hellman S: The role of postoperative irradiation in

- carcinoma of the endometrium. *Gynecol Oncol* 2:354-361, 1974
10. Moss WT, Brand WN, Battifora H (eds): *Radiation Oncology: Rationale, Technique, Results*, 4th ed. St. Louis, Mosby, 1973
 11. Keller D, Kempson RL, Levine G, McLennan C: Management of the patient with early endometrial carcinoma. *Cancer* 33:1108-1116, 1974
 12. Nilsen PA, Koller O: Carcinoma of the endometrium in Norway 1957-1960 with special reference to treatment results. *Am J Obstet Gynecol* 105:1099-1109, 1969
 13. Monson RR, MacMahon B, Austin JH: Postoperative irradiation in carcinoma of the endometrium. *Cancer* 31:630-632, 1973
 14. Kottmeier HL (ed): Annual report on the results of treatment in carcinoma of the uterus, vagina, and ovary, vol 15, Stockholm, 1973
 15. Shah CA, Green TH: Evaluation of current management of endometrial carcinoma. *Obstet Gynecol* 39:500-509, 1972
 16. Truskett ID, Constable WC: Management of carcinoma of the corpus uteri. *Am J Obstet Gynecol* 101:689-694, 1968
 17. Brown JM, Dockerty MB, Symmonds RE, Banner EA: Vaginal recurrence of endometrial carcinoma. *Am J Obstet Gynecol* 100:544-549, 1968
 18. Boutsellis JG, Ullery JC, Bair J: Vaginal metastases following treatment of endometrial carcinoma. *Obstet Gynecol* 21:622-626, 1963
 19. Prem KA: Adenocarcinoma of the endometrium with special reference to vaginal involvement: a staff meeting report. *Univ Minn Med Bull* 24:512-528, 1958
 20. Carmichael JA, Bean HA: Carcinoma of the endometrium in Saskatchewan. *Am J Obstet Gynecol* 97:294-307, 1967
 21. Morrow CP, Di Saia PJ, Townsend DE: Current management of endometrial carcinoma. *Obstet Gynecol* 42:399-406, 1973
 22. Javert CT: The spread of benign and malignant endometrium in the lymphatic system with a note on coexisting vascular involvement. *Am J Obstet Gynecol* 64:780-806, 1952
 23. Lewis BV, Stallworthy JA, Cowdell R: Adenocarcinoma of the body of the uterus. *J Obstet Gynecol Br Commonw* 77:343-348, 1970
 24. Boronow RC: A fresh look at corpus cancer management. *Obstet Gynecol* 42:448-451, 1973
 25. Gusberg SB, Jones HC, Tovel HMM: Selection of treatment for corpus cancer. *Am J Obstet Gynecol* 80:374-380, 1960
 26. Rutledge FN: Cited in *Textbook of Radiotherapy*, 2d ed, edited by Fletcher GH, Philadelphia, Lea & Febiger, 1973, p. 670
 27. Henriksen E: The lymphatic spread of carcinoma of the cervix and of the body of the uterus: a study of 420 necropsies. *Am J Obstet Gynecol* 58:924-942, 1949

Fast Neutron Beam Radiotherapy of Glioblastoma Multiforme

ROBERT G. PARKER,¹ HERBERT C. BERRY¹, ARTHUR J. GERDES,¹
MICHAEL D. SORONEN,¹ AND CHENG MEI SHAW²

Twenty-one patients with glioblastoma multiforme were treated with fast neutron beam irradiation of the whole brain. Therapy was well tolerated up to calculated doses of 1,850 rad_{n+γ} in 12–18 increments over 6 weeks. The survival rate 6 months after initiation of treatment was 62%, not significantly different from conventional photon therapy; average posttreatment survival appears to be shortened compared to photon therapy. No improvement or prolonged maintenance of existing neurologic function was observed.

Autopsy findings in seven patients showed replacement of tumor by coagulative necrosis persisting at least 16 months posttreatment, paucity of tumor cells with infrequent mitoses, and suppression of macrophage response. These findings differ from those in conventionally irradiated patients. No treatment-related changes were documented by conventional gross and histologic studies of the irradiated brains distant from the tumors. Thus the deaths of patients in this study appear to be related to unexplained causes other than progressive growth of tumor.

Introduction

Glioblastoma multiforme is rarely controlled by any treatment. Relentless local growth of tumor, rather than metastases, kills the host. Since there are theoretical biological bases for better responses of these tumors to high LET radiations [1], a pilot study of fast neutron beam radiotherapy was begun at the University of Washington.

Materials and Methods

Treatment Techniques

A clinically useful fast neutron beam generated by cyclotron-produced 21 MeV deuterons incident on an intermediate (70% of incident deuterons absorbed), directly water-cooled beryllium target was developed during the first 2 years of a study supported by the National Cancer Institute initiated in June 1971. This beam has a mean energy of 8 MeV, depth dose characteristics comparable to ⁶⁰Co teletherapy, and a potential output of 1 rad_{n+γ} min/μA at 125 cm from the target. The treatment beam can be defined by borated, water-extended (B/WEP) collimators which weigh about 35 pounds, can be rotated about the long axis of the beam, and have custom-shaped apertures [2].

In each patient with cerebral glioblastoma multiforme, the entire intracranial contents were irradiated through lateral opposing 20×20 cm fields with the patient in a sitting position at 150 cm TSD. Both fields, which include the base of the skull and exclude the orbits, were irradiated each treatment day.

The pattern of treatment for 17 patients was 150 rad_{n+γ} fractions twice weekly (Monday and Friday), while the other four patients were treated with 100 rad_{n+γ} fractions three times weekly (Monday,

Wednesday, and Friday). In 14 of 17 patients completing treatment, the total dose was 1,800 ± 50 rad_{n+γ}. The lowest dose was 1,550 rad_{n+γ} in 10 fractions over 43 days. The highest dose was 1,850 rad_{n+γ} in 17 fractions over 43 days. During this initial phase of the study, the tumor site did not receive a preferentially higher dose.

Patient Population

The first patient with glioblastoma multiforme began treatment on September 10, 1973, and as of November 8, 1974, 21 patients had been treated. All patients referred during this interval with the diagnosis substantiated were accepted for neutron beam radiotherapy regardless of their condition in order to avoid selection bias. All received neutron beam irradiation as the primary post-operative therapy, except for one patient who entered the study after conventional ⁶⁰Co teletherapy had been interrupted when the dose to the whole brain had reached 2,600 rad.

Pretreatment evaluation included history, physical examination with assessment of neurologic function according to the classification of Order et al. [3] (table 1), ophthalmologic examination, and complete blood count. Interval examinations were completed weekly during treatment and at least every 1–2 months thereafter.

All tumor specimens obtained prior to irradiation were reviewed microscopically by neuropathologists. Fourteen patients had grade IV astrocytomas and seven had grade III according to the classification of Kernohan [4]. Autopsies were performed on seven patients, and the gross and histologic CNS material was reviewed.

Results

Because of neurologic deterioration, four patients did not complete fast neutron beam radiation therapy. These patients died 3, 7, and 10 weeks and 14 months after initiation of treatment. One of the four had only a biopsy of the tumor prior to neutron beam irradiation. At least two of the four may not have been accepted for treatment with conventional photon techniques because of their poor condition.

The other 17 patients completed treatment. Although several showed slight neurologic improvement during and after irradiation, none improved enough to change functional classification (table 1).

The average survival currently for the entire group, including the four patients not completing treatment, is 7.2 months from the start of treatment. The seven with grade III tumors have survived 6.6 months and the 14 with grade IV, 7.3 months. Three patients are alive more than 12 months after initiation of radiation therapy: one with a grade IV tumor 17 months after receiving 871 rad_{n+γ} in six fractions over 17 days following 2,600 rad_{n+γ} of ⁶⁰Co teletherapy; another with a grade III tumor 14 months

Presented at the annual meeting of the American Radium Society, San Juan, Puerto Rico, May 1975.

This work was supported by National Cancer Institute grant CA-12441.

¹ Department of Radiology, University of Washington School of Medicine and Hospital, Seattle, Washington 98195. Address reprint requests to R. G. Parker.

² Department of Pathology, University of Washington School of Medicine and Hospital, Seattle, Washington 98195.

TABLE 1
Functional Classification of Patients with Brain Metastases

Class	Definition
I	Intellectually and physically able to work; neurologic findings minor or not present
II	Intellectually intact and physically able to be home, although nursing care may be required; neurologic findings present but not a major factor
III	Major neurologic findings requiring hospitalization and medical care and supervision
IV	Requires hospitalization and is in serious physical and neurologic state

Note.—Classification of Order et al. [3].

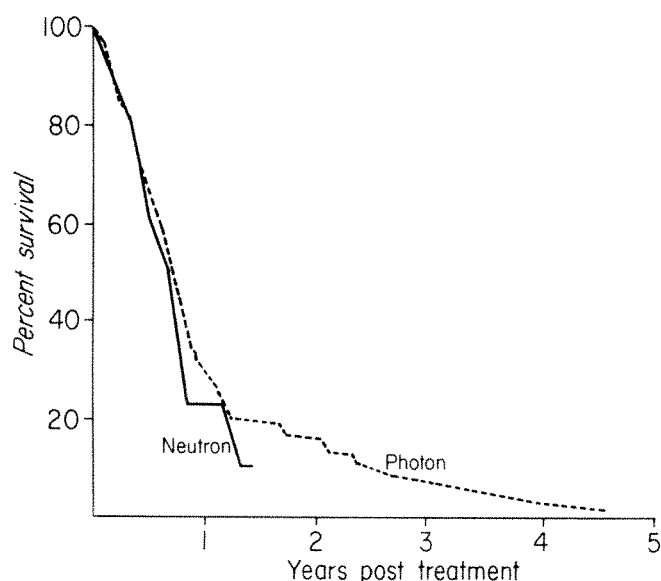


Fig. 1.—Survival of patients with glioblastoma multiforme treated with photon and neutron beam irradiation at the University of Washington. For neutron group, survival after 6 months projected by life table method.

after receiving 1,850 rad_{n+y} in 18 fractions over 43 days; and the third with a grade III tumor 12 months after receiving 1,800 rad_{n+y} in 18 fractions over 46 days. Three others are alive 7, 7, and 6 months after initiation of therapy (fig. 1).

Acute reactions of the scalp became visible by days 17–20, reached a maximum (3+ erythema) by days 25–35, and grossly completely healed 45–70 days after start of treatment. Most patients had dryness and dark pigmentation of the scalp for several months. All patients were epilated, and regrowth of hair has been minimal. Except for one patient with a surgically inserted mesh, the scalp incisions healed promptly and completely. There was no clinically detectable problem with the irradiated skull. The eyes were unchanged on repeated ophthalmologic examinations. Although the estimated doses to the trunk and extremities may have reached 20 rad, including neutrons of reasonably

high relative biologic effectiveness [5], no changes were detected in the peripheral blood.

Seven patients were studied at autopsy. In each, a central discrete mass of coagulative necrosis replaced the bulk of the tumor. Surrounding this discrete necrosis, there was a grossly granular rim of tissue which contained tumor cells less numerous than in the preirradiation biopsy specimen or in specimens from other patients irradiated with x-ray or ⁶⁰Co gamma ray teletherapy (figs. 2 and 3). These remaining tumor cells contained infrequent mitoses and were intermixed with scattered multinucleated giant cells. In contrast to those patients treated conventionally with photon radiations, the macrophage response was markedly reduced in the brain immediately surrounding the coagulative necrosis.

A mass effect with moderate edema of adjacent brain and slight transtentorial herniation was noted in only two of the seven patients.

Although the entire brain was irradiated in all patients, the gross and microscopic appearance distant from the tumor was within normal limits except for slight gliosis in two patients attributable to other causes.

Discussion

There are two likely reasons for the failure of radiation therapy to control glioblastoma multiforme: (1) relative insensitivity of the tumor cells to ionizing radiations, and (2) underestimation of tumor extent with consequent failure to include the entire tumor in the irradiated tissue volume.

Tumor cell insensitivity to irradiation at a clinical level may be related to a small therapeutic ratio based on normal brain tolerance. Tumor cell response may be reduced by hypoxia in a neoplasm which frequently contains foci of necrosis. High LET radiations are less oxygen dependent and thus have a theoretical advantage in the treatment of glioblastoma multiforme [1]. However, adjuvant high pressure oxygen has not significantly improved survival in one study [6].

The importance of irradiating a large volume of the brain to insure inclusion of a tumor with ill-defined margins has been stressed [7–11]. In this series, the entire brain was irradiated to a uniform dose.

The contributions of radiation therapy to lengthened survival and improved quality of life of patients afflicted by glioblastoma multiforme have been discussed [12–14]. As a standard of comparison for our patients treated with fast neutron beams, patients previously conventionally irradiated with 8 MeV x-rays or ⁶⁰Co gamma rays were reviewed (table 2, fig. 1). In these patients, survival frequencies from the start of treatment were 67% at six months, 33% at 12 months, and 17% at 24 months (fig. 1). These frequencies are comparable to those reported in other studies (table 3) [7, 10, 13, 14].

Survival of our first 21 patients irradiated with fast neutron beams apparently has not been lengthened nor quality of life improved, although patient selection may have been an adverse factor (table 4, fig. 1). The average survival currently is 7.2 months, although six patients are alive at 17, 14, 12, 7, 7, and 6 months from the start of treatment.

Fig. 2.—Gross cross section through tumor treated by whole-brain fast neutron beam.

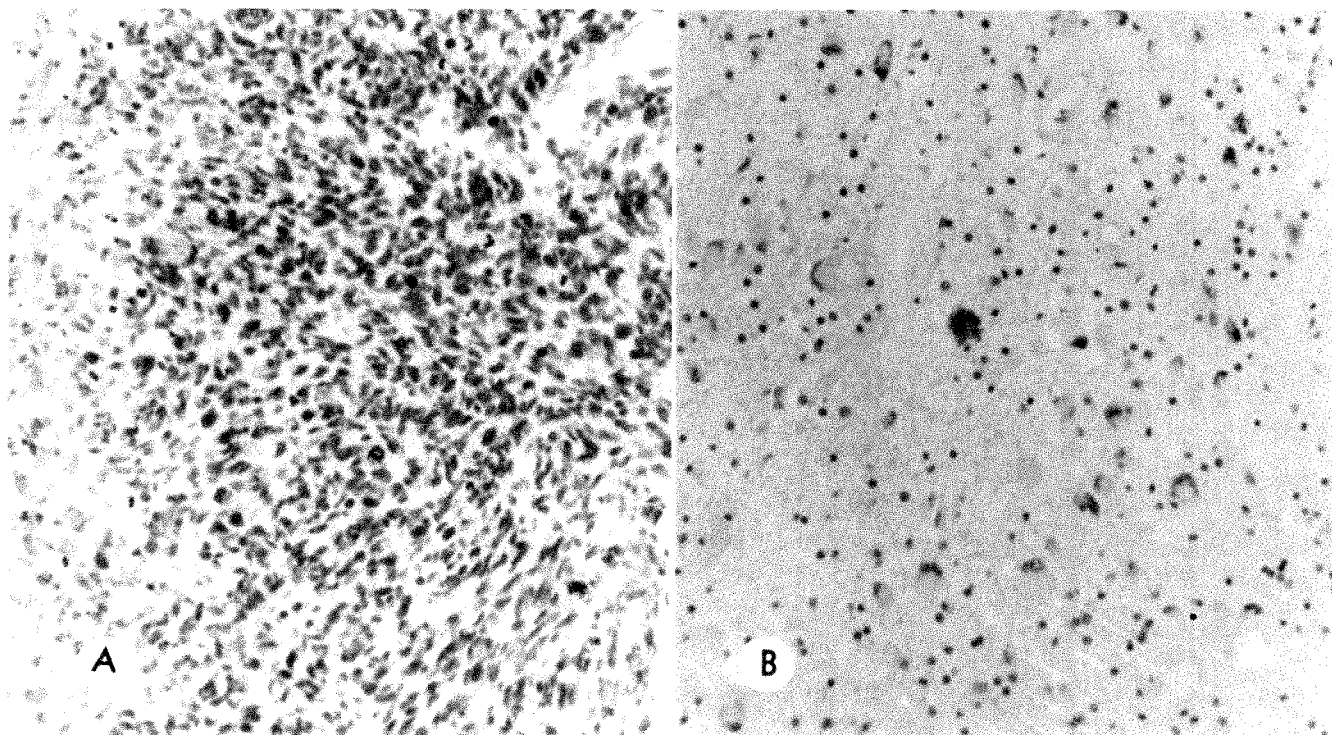
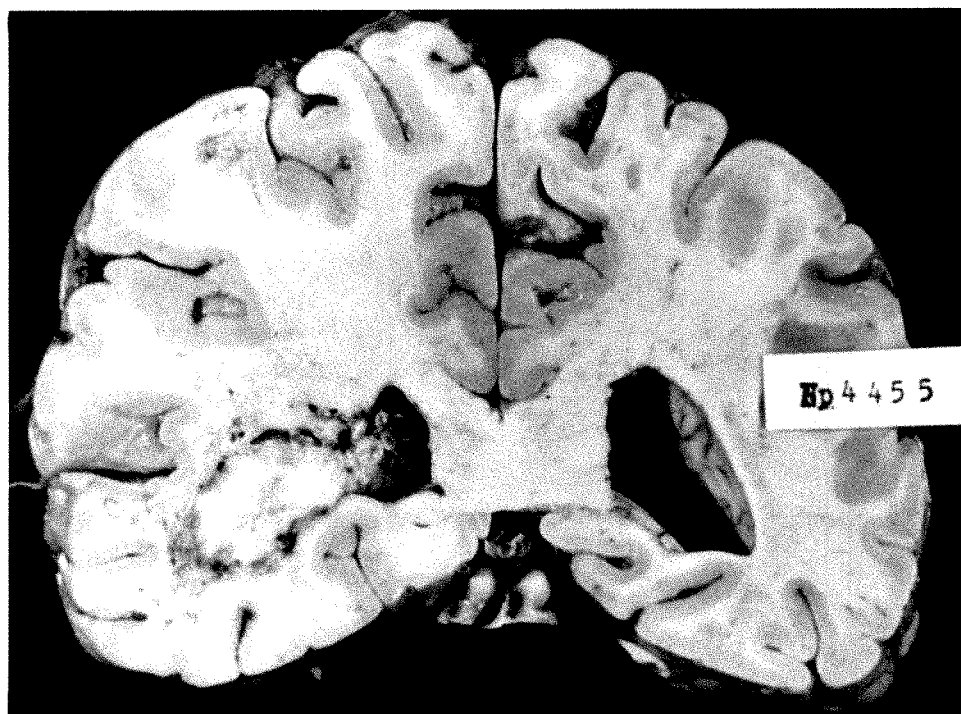


Fig. 3.—Microscopic sections of grade III astrocytoma before (A) and after (B) neutron irradiation.

TABLE 2
Results of Photon Irradiation Therapy in Patients
with Glioblastoma Multiforme

Grade	No. Patients	Survival (mo)	
		Average	Range
III	15	26.0	2.5-55
IV	53	9.9	1-38
Total	68	13.5	1-55

Note.—Patients treated at the University of Washington.

TABLE 3
Survival Rates in Patients with Glioblastoma Multiforme
Treated with Photon Irradiation

Study	Survival (%)		
	6 mo	12 mo	24 mo
Bourchard and Pierce [12]	39	20
Kramer [13]	55	33	13
Stage and Stein [14]			
Grade III	60	35	20
Grade IV	55	27	8
Present report (photon)	67	33	17

TABLE 4
Comparative Survival of Patients with Glioblastoma Multiforme

Irradiation Method	6 mo		12 mo		Average (mo)
	No.	%	No.	%	
Photon	45	67	22	33	13.4
Neutron	13	62	...	23*	7.0

Note.—Patients treated at the University of Washington. Total number receiving photon and neutron irradiation was 68 and 21, respectively.

* Projected by life table method.

Survival at 6 months for the group of 21 patients is 62% (13/21), not statistically different from the 67% for our patients irradiated conventionally. For those 17 patients completing fast neutron beam irradiation, the average survival is 8 months with 65% (11/17) alive at 6 months.

The apparent shorter average survival of our fast neutron beam irradiated patients compared to those treated conventionally (7.2 compared to 13.4 months) may be based on incomplete data (six patients still living), small numbers, poor patient selection, or it may reflect an actual accelerated mortality rate after 6 months.

Improved quality of life measured by either improved neurologic function or prolonged maintenance of useful function would be a substantial accomplishment of treat-

ment. However, it is unrealistic to expect considerable recovery of neurological function when the deficit is secondary to massive destruction of normal CNS tissue by a large or strategically situated tumor. Therefore, this objective of treatment directly relates to patient selection.

Kramer [13] reported that only 21 of 78 patients (27%) with grade III-IV astrocytomas did not improve following radiation therapy. In our group of 21 patients, four did not complete fast neutron beam irradiation because of neurological deterioration. Of the 17 patients completing treatment, several improved neurologically for several months, although none improved enough to change functional classification [3]. The overall posttreatment course has generally been gradual deterioration with lack of responsiveness to steroids. In three of the six patients still alive, neurologic status has deteriorated since initiation of treatment. We are developing a more detailed classification of neurological function which is more sensitive to slight changes than that of Order et al. [3].

Except for the four patients not completing treatment, tolerance to fast neutron beam irradiation was good. Acute skin reactions were mild to moderately severe. Primary healing was prompt and complete in all patients except the one with a chronic infection in the incision. Epilation was complete in all, and hair regrowth was scanty. No short-term peripheral blood changes were detected even though total body doses were estimated to be up to 20 rad containing a component of neutrons of reasonably high relative biologic effectiveness [5]. No eye changes were recorded.

In at least five of the seven patients autopsied, there was no anatomic explanation for the deteriorating neurological status or death itself. However, the persistence of well defined coagulative necrosis which replaced tumor and the reduced macrophage response indicate substantial impairment of the normal mechanisms which clear necrotic debris from within the brain.

The deaths of patients in this study seem related to as yet unexplained causes other than progressive growth of tumor. The suggested shortened average posttreatment survival may be a reflection of these nontumor-related deaths.

ACKNOWLEDGMENTS

We thank the radiation oncology staffs of the Swedish Hospital Tumor Institute, Group Health Cooperative of Puget Sound, and the Virginia Mason Clinic of Seattle for their cooperation in making patients available for this clinical study. We also thank Drs. Ellsworth Alvord, Jr., Alexander Spence, and Shuzo Sumi for their assistance with the analysis of the pathology in these patients.

REFERENCES

1. Withers HR: Biological basis for high LET radiotherapy. *Radiology* 108:131-137, 1973
2. Wootton P, Bichsel H, Parker RG, Weaver K, Williams DL, Wyckoff WG: The University of Washington fast neutron beam facility. Paper presented at the Workshop on Practical Clinical Criteria for a Fast Neutron Generator, Boston, May 1973

3. Order S, Hellman S, Von Essen C, Kligerman M: Improvement in quality of survival following whole brain irradiation for brain metastases. *Radiology* 91:149-153, 1968
4. Kernohan JW: Simplified classification of gliomas. *Mayo Clin Proc* 24:71-75, 1949
5. Geraci JP, Jackson KL, Christensen GM, Parker RG, Fox MS, Throwe PD: Testes DNA as a biological dosimeter to measure RBE of cyclotron neutrons. Abstract presented at the 5th International Congress of Radiation Research, Seattle, July 1974
6. Chang CH, Seaman WB, Jacox HW: Clinical aspects of hyperbaric oxygen and radiotherapy—New York experience. *Front Radiat Ther Oncol* 1:183-188, 1968
7. Aristizabal SA, Caldwell WL: Time-dose-volume relationships in the treatment of glioblastoma multiforme. *Radiology* 101:201-202, 1971
8. Concannon JP, Kramer S, Berry R: The extent of intracranial gliomas at autopsy and its relationship to techniques used in radiation therapy of brain tumors. *Am J Roentgenol* 84:99-107, 1960
9. Kramer S: Tumor extent as a determining factor in radiotherapy of glioblastomas. *Acta Radiol* 8:111-117, 1969
10. Ramsey RG, Brand WM: Radiotherapy of glioblastoma multiforme. *J Neurosurg* 39:197-202, 1973
11. Todd IDM: Choice of volume in the x-ray treatment of supratentorial gliomas. *Br J Radiol* 36:645-649, 1963
12. Bouchard J, Pierce CB: Radiation therapy in the management of neoplasms of the central nervous system. *Am J Roentgenol* 84:610-628, 1960
13. Kramer S: Radiation therapy in the management of malignant gliomas, in *Proceedings of the 7th National Cancer Conference*, Los Angeles, September 1972, Philadelphia, Lippincott, 1973, pp 823-826
14. Stage WS, Stein JJ: Treatment of malignant astrocytoma. *Am J Roentgenol* 120:7-18, 1974

AJR Bicentennial Issue

Single copies of the special AJR Bicentennial issue, devoted entirely to Computed Tomography, may be ordered for \$3.00 each from Charles C Thomas, Publisher, 301-327 East Lawrence Ave. Springfield, Illinois 62717. Please enclose payment with order.

Transformation Delay of Lymphocytes in Patients Undergoing Radiation Therapy

TIMOTHY MERZ,¹ TAPAN HAZRA,¹ MERRILL ROSS,² AND LINDA CIBOROWSKI²

Two types of assay systems to measure the effect of radiation on immune competence are described. The first, transformation, is measured by blast formation or uptake and incorporation of tritiated thymidine by lymphocytes. This measure is affected by a number of known cell responses to radiation such as division delay and delay in DNA synthesis. The second, called Bactec, is designed to measure lymphocyte metabolic activity. Data gathered on 37 patients with lung cancer show that the Bactec system provides a better index of the patient's immune status before and after radiation therapy.

Introduction

The relationship between immune processes and cancer has resulted in a number of studies designed to determine the immune competence of cell-mediated immunity in patients with malignant tumors before and after various treatments [1-9]. These and other studies of radiation-induced alterations in cell-mediated immunity [10-15] cannot piece together a single simple construct describing a consistent effect of radiotherapy on immune response.

The reasons for the lack of agreement on the effect of radiation on immune competence are many and diverse. This report deals with two: (1) the effect of the assay system on the results obtained, and (2) the well known delayed response of lymphocytes to transformation or tritiated thymidine uptake and incorporation [10] after exposure to radiation.

Cell cycle kinetics differ in irradiated and nonirradiated cells [7]. Thus the lower frequency of transformed cells in an irradiated cell population at 72 hr compared to nonirradiated cells may reflect a delayed response rather than a lower total immune response. To investigate the delayed response of these cells, we analyzed data from 37 patients with lung cancer who are part of a larger study on the effect of radiation on immune competence. The analysis utilizes information from two kinds of assay systems. The first is transformation and the second we have called Bactec. Bactec is a system designed to measure the metabolic response of cells to various stimuli.

Materials and Methods

Blood was drawn from patients before, during, and after radiation therapy. Leukocytes were isolated as a buffy coat. The contaminating red cells were lysed by a 20 sec treatment with distilled water at room temperature; cells were rinsed and resuspended. Ficoll-Hypaque gradients were not used in these experiments because lymphocytes, not contaminating granulocytes, have been considered to be the reactive leukocyte in so far as phytohemagglutinin (PHA) stimulation is concerned, and certainly so in regard

to early blast cell formation or transformation.

For transformation studies, leukocytes were cultured in McCoy's 5A medium with PHA; for metabolic studies, they were suspended in Hanks medium at a concentration of 2×10^6 cells/10 ml. Comparisons of the percentage of transformed cells were made after 72, 96, and 120 hr in culture. Each individual was tested before, during, and after radiation therapy and at all culture times.

The metabolic studies were performed using a machine called Bactec because it was originally designed to measure the metabolic responses of bacteria. It has been used by one of us (T. Merz) as a means of measuring lymphocyte metabolism. The lymphocytes were suspended in glucose-free Hanks balanced salt solution at a concentration of 2×10^6 cells/10 ml of solution in a rubber-stoppered vial. Then 2 μ Ci of 14 C-labeled glucose (in the first position) was added to the vials. Every 2 hr the CO_2 was removed and O_2 injected by needles through the rubber stopper automatically. The labeled gas ($^{14}\text{CO}_2$) is counted and affords a direct method for measuring lymphocyte metabolic activity. The carbon position labeled gives a measure of what pathway is being utilized, the first position being associated with glucose metabolism through the hexose monophosphate shunt.

Results

An interesting change occurs in the time at which the peak number of transformed cells appears before and after radiotherapy (table 1). Most patients show a peak frequency of transformed cells at 120 hr, but some peak at 72 and 96 hr. After radiation treatment there is an increase in the number of patients with peaks at 120 hr and a decrease in the number at 72 hr. Thus these data show a delay in the appearance of transformed cells in individuals after irradiation. This finding could be interpreted as approximately a 15% decrease in transformation capability at 72 hr, or it could merely reflect a delayed rather than a decreased transformation capability.

A question that arises is whether the transformation index increases steadily as a function of time in culture or varies cyclically. Figure 1 shows six theoretical plots of the change in transformation index ratios (ratio of the transformation index of PHA-stimulated cells to those unstimulated). Under each is listed the percentage of patients whose transformation index ratio fits the theoretical plot. It is of interest to note that there is no evidence of a decrease in transformation frequency to 120 hr. An increasing trend to 120 hr was seen in 60% of individuals.

Actually the number of transformed cells observed at 72 hr are largely in their second or third division if they have not been irradiated. Utilizing the squelching of acridine fluorescence produced by BUdR incorporation to identify cells in the first through fourth divisions, we regularly see cells in their second division cycle at 48 hr. Although it has

Presented at the annual meeting of the American Radium Society, San Juan, Puerto Rico, May 1975.

¹ Department of Radiology, Division of Radiation Biology, Medical College of Virginia, Richmond, Virginia 23298.

² Johns Hopkins Medical Institutions, Baltimore, Maryland 21205.

TABLE 1
Time at which Peak Number of Transformed Cells Appears

Patients (%)	Culture Time (Hr)		
	72	96	120
Before radiation therapy	13.0	27.0	60.0
After radiation therapy	0.07	27.0	73.0

TABLE 2
Immune Response of Terminal Patients

Measure Used	% Patients with Insignificant Immune Response at Last Reading before Expiration
Transformation index ratio:	
72 hr	22
Peak	0
Bactec ratio:	
10 hr	100
Peak	81

TABLE 3
Immune Response in Patients of Varying Health

Condition Postirradiation	% Patients with Significant Immune Response	
	Transformation	Bactec
Clinically well	100	50
Tumor present	100	33
Deteriorating	100	20
Terminal	100	0

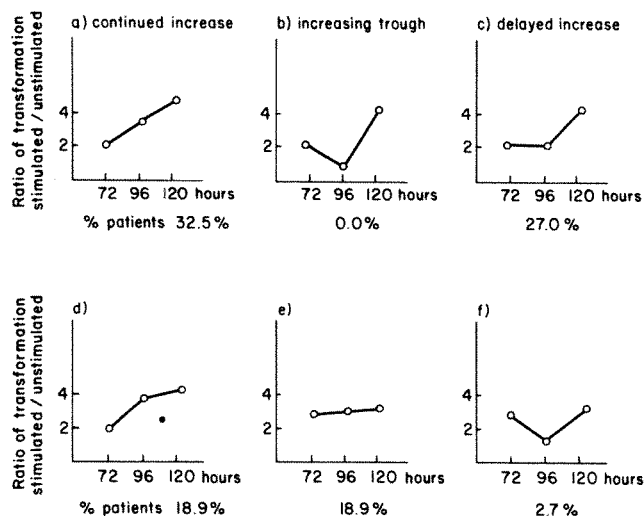


Fig. 1.—Theoretical plots of change in transformation index ratios (ratio of transformation index of PHA-stimulated cells to those unstimulated). Percentage of patients whose transformation index ratio fits theoretical plot shown below each.

been acceptable practice to use 72 hr cultures as a standard for transformation assays, most PHA-stimulated lymphocyte cultures contain a mixture of cells in first, second, and third division.

If one considers the mitotic cycle delay response to radiation over a three-division spectrum and then adds to that the well known effect of synchronization of cells as a result of that delay, one has to question whether simple transformation studies could be useful as an assay technique to determine immunocompetence and/or patient status after radiation therapy.

An easy test of the usefulness of transformation as an assay of patient status is to calculate 72 hr culture transformation in patients just before death. Of the patients who died shortly after the last transformation study, 78% showed significant transformation responses at 72 hr.

The Bactec assay system is apparently a better test of patient status. The system measures the response of lymphocytes and/or granulocytes to stimulation by utilizing an assay which measures the amount of glucose used by the leukocytes after stimulation. This is determined by the amount of labeled carbon dioxide produced from the glucose.

Table 2 presents the measurement of immune responses of terminal patients. The transformation index is shown at 72 hr and at the peak of transformation. At 72 hr, only 22% of terminal patients showed an insignificant immune response before they died. If we look at the peak of transformation, 100% showed significant immune responses at the last reading before expiration.

In contradistinction, the Bactec readings (glucose metabolism) produce precisely the opposite findings. At 10 hr, 100% of the terminal patients showed insignificant immune responses at the last reading before death. At the peak reading, 81% of the terminal patients showed insignificant immune responses before expiration. It appears that the metabolic approach is considerably more accurate in assessing patient status.

In table 3, patients have been categorized as clinically well, tumor present, deteriorating, or terminal. The bulk of the patients were in the second and third category. One would expect to see a deterioration of immune response regardless of assay in such an array of patients. However, postirradiation transformation is significant in all four categories of patients. On the other hand, the Bactec assay of immune response shows a decreasing response from clinically well to terminal patients postirradiation.

Discussion and Conclusions

Transformation indexes are complicated by a number of known radiation responses such as division delay and delay in DNA synthesis. Thus transformation indexes may well not be a good measure of the radiation effect on immune competence and/or patient status at any given time during or after treatment. The data indicate that the metabolic state of leukocytes provides a better index of the patient's immune status before and after radiation therapy.

REFERENCES

1. Braeman J: Lymphocyte response after radiotherapy. *Lancet* 2:683, 1973
2. Braeman J, Deeley TJ: Radiotherapy and immune response in cancer of the lung. *Br J Radiol* 46:446-449, 1973
3. Braeman J, Birch A, Deeley TJ: Depression of in vitro lymphocyte reactivity after radical radiotherapy. *Ann Clin Res* 6:338-340, 1974
4. Blomgren H, Glas U, Melen B, Wasserman J: Blood lymphocytes after radiation therapy of mammary carcinoma. *Acta Radiol* 13:357-367, 1974
5. Clement JA, Kramer S: Immunocompetence in patients with solid tumors undergoing cobalt 60 irradiation. *Cancer* 34:193-196, 1974
6. Dellon AL, Potvin C, Chretien PB: Thymus dependant lymphocyte levels during radiation therapy for bronchogenic and esophageal carcinoma: correlations with clinical course in responders and nonresponders. *Am J Roentgenol* 123:500-511, 1975
7. Dubois JB: Influence of radiotherapy on the immune response of cancer patients. *Bull Cancer (Paris)* 62:11, 1975
8. Lundell G: Effects of radiation therapy on blood-bone leukocytes in patients with mammary carcinoma. *Acta Radiol* 13:307-312, 1974
9. Wara WM, Philips TL, Wara DW, Ammann AJ, Smith V: Immunosuppression following radiation therapy for carcinoma of the nasopharynx. *Am J Roentgenol* 123:482-485, 1975
10. Braeman J, Moore JL: The lymphocyte response to phytohemagglutinin after in vitro radiation. *Br J Radiol* 47:297, 1974
11. Canchi MN, Dawson KB: In vivo radioresistance of activated T cells involved in the graft-versus-host reaction. *Int J Radiat Biol* 27:193-195, 1975
12. Catalona WJ, Chretien PB: Abnormalities of quantitative dinitrochlorobenzene sensitization in cancer patients: correlation with tumor stage and histology. *Cancer* 31:353-356, 1973
13. Jenkins VK, Olson MH, Ellis HN: In vitro methods of assessing lymphocyte transformation in patients undergoing radiotherapy for bronchogenic cancer. *Tex Rep Biol Med* 31:19-28, 1973
14. McCredie JA, Inch RW, Sutherland RM: Peripheral blood lymphocytes and breast cancer: effect of operation and radiotherapy. *Arch Surg* 107:162-165, 1973
15. Vaughn-Smith S, Ling NR: The effects of x-rays on the responses of porcine lymphocytes to the mitogenic stimulus of concanavalin A in vitro. *Int J Radiat Biol* 25:73-85, 1974
16. Carlson JG: Immediate effects on division, morphology, and variability of the cell, in *Radiation Biology*, vol 1, edited by Hollaender S, New York, McGraw-Hill, 1954, pp 763-824
17. Fabrikant JI: *Radiobiology*. Chicago, Yearbook Medical Publishers, 1972

Books Received

Receipt of books is acknowledged as a courtesy to the sender. Books that appear of sufficient interest will be reviewed as space permits.

A Radiographic Index, 5th ed. By Myer Goldman and David Cope. Chicago: Year Book Medical Publishers, Inc., 91 pp., 1975, \$7.95

1976 Year Book of Diagnostic Radiology. Edited by Walter M. Whitehouse. Chicago: Year Book Medical Publishers, 456 pp., numerous illustrations, 1976, \$24.95

1976 Year Book of Nuclear Medicine. Edited by James L. Quinn, III. Chicago: Year Book Medical Publishers, 380 pp., illustrated, 1976, \$23.50

Manual di Radiologia Infortunistica, Patologia Traumatica e Medicina Legale. By Lorenzo Giuntoli. Milan: Casa Editrice Ambrosiana, 413 pp., numerous illustrations, 1976, 18,000 lire

Quantitative Problems in the Biochemical Sciences, 2d ed. By Rex Montgomery and Charles A. Swenson. San Francisco: W. H. Freeman, 370 pp., 1976, \$5.95

Assessment of Skeletal Maturity and Prediction of Adult Height (TW2 Method). By J. M. Tanner, R. H. Whitehouse, W. A. Marshall, M. J. R. Healey, and H. Goldstein. London: Academic Press, 99 pp., illustrated, 1975, \$22.50

M-Mode Echocardiographic Techniques and Pattern Recognition. By Sonia Chang. Philadelphia: Lea & Febiger, 160 pp., 137 illustrations, 1976, \$7

Gynecologic Oncology. By Felix Rutledge, Richard C. Boronow,

J. Taylor Wharton. New York: John Wiley & Sons, 272 pp., illustrated, 1976, \$18.50

Clinical Applications of the Electron Beam. Edited by Norah duV. Tapley. New York: John Wiley & Sons, 274 pp., illustrated, 1976, \$25

Radioisotopes in Medical Diagnosis. Edited by E. H. Belcher, H. Vetter. London: Butterworths, 800 pp., illustrated, 1971, \$73.15

Aseptic Necrosis of Bone. Edited by J. K. Davidson. Amsterdam: Excerpta Medica, 355 pp., illustrated, 1976, \$60.95

X-Ray Equipment for Student Radiographers, 2d ed. By D. Noreen Chesney and Muriel O. Chesney. Philadelphia: J. B. Lippincott Co., 579 pp., 263 illustrations, 11 tables, 1975, \$29

Atlas of Normal Vertebral Angiograms. By Paul Ross and George H. Du Boulay. London: Butterworths, 126 pp., illustrated, 1976, £15

Information Processing in Scintigraphy, Proceedings of the 4th International Conference on Information Processing in Scintigraphy, Orsay, 15–19 July 1975. Edited by C. Raynaud and A. Todd-Pokropek. Orsay, France: Commissariat à l'Energie Atomique, 492 pp., illustrated, 1975, 106 FF

Synopsis of Analysis of Roentgen Signs in General Radiology. By Isadore Meschan. Philadelphia: W. B. Saunders Co., 677 pp., illustrated, 1976

Wilms' Tumor. Edited by Carl Pochedly and Dennis Miller. New York: John Wiley & Sons, 239 pp., illustrated, 1976, \$22.50

Neuroradiologie 2. Edited by J. Metzger, J. Simon, G. Salamon, H. Fischgold. Paris: Masson, 648 pp., 726 figures, 1976, 770 FF

Case Reports

Perforation of the Nasopharynx by Nasogastric Intubation: A Rare Cause of Left Pleural Effusion and Pneumomediastinum

PAUL T. SIEMERS¹ AND ROBERT T. REINKE¹

A case of nasogastric tube perforation of the posterior nasopharynx producing a left pleural effusion and pneumomediastinum is reported. Findings which led to the correct diagnosis were the rapid appearance of a left pleural effusion simultaneous with the initiation of tube feedings, the intrathoracic location of the nasogastric tube, and demonstration of perforation of the posterior nasopharynx. Potentially hazardous intubation techniques are discussed.

Most radiologists are familiar with the complications of indwelling central venous catheters and realize that the rapid appearance of a pleural effusion automatically calls for immediate assessment of the distal position of the catheter [1]. We report an unusual cause of pleural effusion and pneumomediastinum—a perforation of the posterior nasopharynx by a nasogastric tube with its subsequent advancement through the posterior mediastinum into the left pleural space.

Case Report

A 58-year-old white woman was admitted to University Hospital for inanition subsequent to a depression-induced refusal to eat. Past medical history was normal except for tonsillectomy and adenoidectomy in childhood and a rhinoplasty following trauma in 1954.

Physical examination revealed a debilitated, dehydrated woman without other abnormalities. Routine laboratory studies, electrocardiogram, and thoracic roentgenogram were normal. Because of her continued refusal to eat, nasogastric tube feedings were instituted. A polyethylene nasogastric tube was passed through the left naris with some initial difficulty in advancing the tube through the posterior nasopharynx. Before the tube was inserted, it was placed in ice water to increase its rigidity. Air was then injected through the tube while the epigastrium was auscultated. The characteristic sound of air bubbling through fluid was taken as reassurance of its intragastric location. Transtubal feedings of a puree broth were begun. Within 12 hr, left chest pain, dyspnea, diaphoresis, and fever developed.

Physical examination revealed dullness of the left hemithorax with decreased breath sounds. A thoracic roentgenogram showed a large left pleural effusion and pneumomediastinum (fig. 1). The distal tip of the nasogastric tube was at the level of the gastroesophageal junction. Gastrografin instillation through the nasogastric tube revealed extravasation into the left pleural space (fig. 2), without visualization of the esophagus or stomach. Oral ingestion of gastrografin showed that the nasogastric tube had perforated the posterior nasopharynx in the midline (fig. 3) and had dissected along the posterior mediastinum (fig. 4), entering the left pleural space. Closed chest tube drainage, parenteral antibiotics, and vigorous pulmonary toilet led to an uneventful recovery. Subse-

quent endoscopic examination of the posterior nasopharynx revealed a puncture site with adjacent granulation tissue. No local pathology was noted.

Discussion

Iatrogenic perforation of the esophagus is increasing with more aggressive diagnostic and therapeutic instrumentation of the esophagus. Nasogastric intubation is a rare cause of esophageal perforation, which is more frequently a complication of esophagogastrosomy, esophageal dilatation, esophageal biopsy, endotracheal intubation, and esophageal tamponade [2–6]. Such perforations have occurred in the upper-middle to lower esophagus, and some have been associated with predisposing local pathology. Duodenal perforation has been reported as a complication of nasojejunal intubation [7].

The susceptibility of the posterior nasopharynx to trauma has been nicely documented by Wolff and Kessler [8]. Their large series of consecutive autopsies revealed posterior pharyngeal and upper esophageal injury, including submucosal hemorrhage, acute mucosal laceration, post-cricoid ulceration, and organ perforation in 60% of those patients with a history of prior instrumentation. Nasogastric intubation accounted for a significant number of these lesions, both as an acute injury of passage and as a result of the indwelling tubing.

While we are unaware of other reported cases of nasogastric tube perforation of the posterior nasopharynx in adults, this is a recognized cause of pharyngeal pseudodiverticulum in the neonate. More than 12 cases of traumatic perforation of the posterior nasopharynx and upper esophagus in newborns have been described in the past 5 years [9–15]. Traumatic perforation may be confused clinically with esophageal atresia, esophageal diverticulum, and duplication of the esophagus. However, it has a characteristic roentgenographic appearance with barium filling an irregular elongated false channel posterior to the esophagus. In the present case, pseudodiverticulum formation was prevented by advancement of the tube into the left pleural space.

Attempts to increase the rigidity of the nasogastric tubing by placing it in ice prior to insertion, as in this case, increase the likelihood of producing injury. This practice should be discouraged. The fallacy of assessing nasogastric tube position by auscultation of the epigastrium while air is injected into the tubing is obvious. Air bubbling within the

¹ Department of Radiology, University Hospital, University of California at San Diego, and Veterans Administration Hospital, 3350 La Jolla Village Drive, San Diego, California 92161. Address reprint requests to R. T. Reinke at the Veterans Administration Hospital.



Fig. 1.—AP supine film of chest after initiation of tube feedings demonstrating rapid appearance (previously normal chest film) of large left pleural effusion and pneumomediastinum.



Fig. 2.—AP spot film of tip of nasogastric tube showing it in region of gastroesophageal junction with extravasation of gastrografin into left pleural space.

pleural space produces a similar sound. The return of bile-stained gastric contents remains a superior method of assessing tube placement.

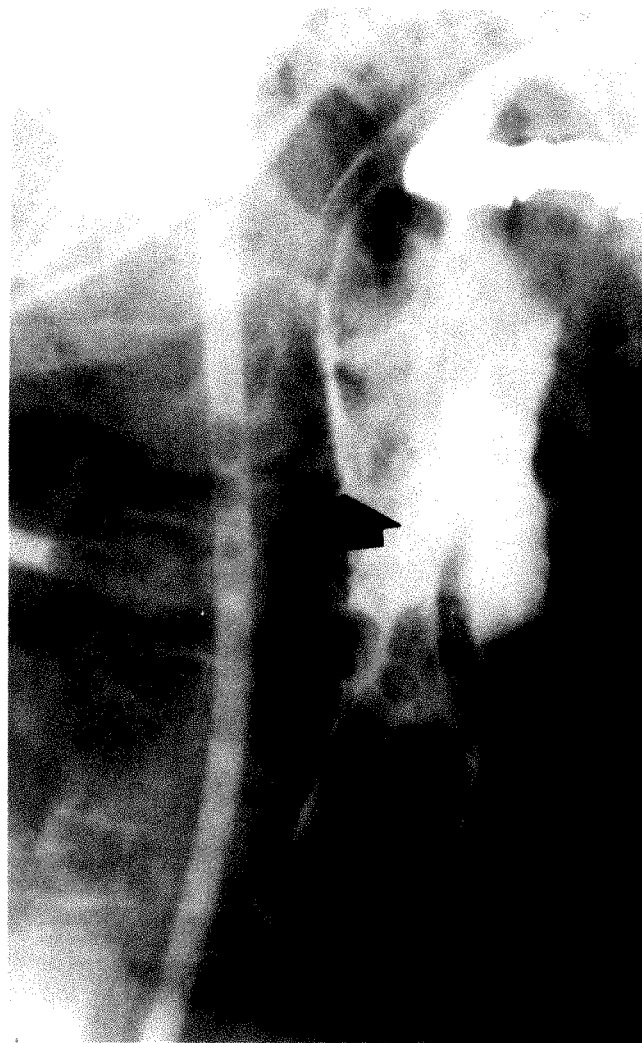


Fig. 3.—Lateral spot film of nasopharynx demonstrating retropharyngeal location of nasogastric tube. Arrow shows posterior wall of pharynx.

The roentgenographic findings which suggest the diagnosis in this case are (1) location of the nasogastric tube at the gastroesophageal junction (but not in the stomach), and (2) a rapidly accumulating left pleural effusion and pneumomediastinum simultaneous with the initiation of tube feeding. While the nasogastric tube was extraesophageal on oblique views, it was only the lateral spot film of the nasopharynx that showed the site of perforation. As with central venous catheters, the radiologist should be wary of a perforation when pleural effusion and/or pneumomediastinum develops in the presence of an intrathoracic nasogastric tube.

REFERENCES

1. Oakes DD, Wilson RE: Malposition of a subclavian line. *JAMA* 233:532-533, 1975
2. Johnson J, Schwegman CW, MacVaugh H III: Early esophago-gastrostomy in the treatment of iatrogenic perforation of the distal esophagus. *J Thorac Cardiovasc Surg* 55:24-29, 1968
3. Mathewson C, Dozier WE, Hamill JP, Smith M: Clinical ex-



Fig. 4.—Supine left anterior oblique film of chest showing nasogastric tube posterior to esophagus in posterior mediastinum. Note extravasation of gastrografin into left pleural space.

- periences with perforation of the esophagus. *Am J Surg* 104: 257–266, 1962
4. Rabinovich S, Smith IM, McCabe BF: Rupture of the esophagus. *Arch Otolaryngol* 85:410–415, 1967
5. Wichern WA: Perforation of the esophagus. *Am J Surg* 119: 534–536, 1970
6. Wolloch V, Zer M, Dintsman M, Tiqva P: Iatrogenic perforations of the esophagus. *Arch Surg* 108:357–360, 1974
7. Boros SJ, Reynolds JW: Duodenal perforation: a complication of neonatal nasojunal feeding. *J Pediatr* 85:107–108, 1974
8. Wolff AP, Kessler S: Iatrogenic injury to the hypopharynx and cervical esophagus: an autopsy study. *Ann Otol Rhinol Laryngol* 82:778–883, 1973
9. Armstrong RG, Lindberg EF, Stanford W, Takamoto RM, Wolfe RD, Dietz JW: Traumatic pseudodiverticulum of the esophagus in the newborn infant. *Surgery* 67:844–846, 1970
10. Astley R, Roberts KD: Intubation perforation of the esophagus in the newborn baby. *Br J Radiol* 43:219–222, 1970
11. De Espinosa H, De Paredes CG: Traumatic perforation of the pharynx in a newborn baby. *J Pediatr Surg* 9:247–248, 1974
12. Ducharme JC, Bertrand R, Devie J: Perforation of the pharynx in the newborn: a condition mimicking esophageal atresia. *Can Med Assoc J* 104:78, 1971
13. Eklöf O, Löhr G, Okmian L: Submucosal perforation of the esophagus in the neonate. *Acta Radiol (Stockh)* 8:187–192, 1969
14. Girdany BR, Sieber WK, Osman MZ: Traumatic pseudodiverticula of the pharynx in newborn infants. *N Engl J Med* 280:237–240, 1969
15. Gwinn JL, Lee FA: Radiological case of the month: pseudodiverticulum of the pharynx. *Am J Dis Child* 121:329–330, 1974

Arthrographic Diagnosis of Synovial Chondromatosis

ROBERT J. PRAGER¹ AND JAY C. MALL¹

A case of synovial chondromatosis without plain film calcifications is presented. The arthrographic findings and differential diagnosis are discussed.

Synovial chondromatosis is a condition affecting the synovial membrane in which metaplasia results in formation of multiple cartilaginous nodules. Characteristic plain film findings are present if the cartilaginous bodies are calcified or ossified [1].

While the arthrographic features are not unique, they are found in a limited number of conditions; consideration of clinical, laboratory, and plain film findings often permits preoperative diagnosis. To our knowledge, the arthrographic findings in synovial chondromatosis have been reported in only one previous case in the English-language literature [2].

Case Report

A 43-year-old male presented with pain and swelling of the left knee of several months' duration. There was no history of locking or giving way. He had sustained a soft-tissue injury in a car accident approximately 22 years earlier.

Examination revealed a markedly swollen left knee with a firm mass on the lateral side of the suprapatellar pouch. Range of motion was restricted by effusion. Arthrocentesis yielded clear, straw colored, sterile fluid with a negative rheumatoid factor, glucose of 85 mg/dl, 1,950 RBC/mm³, and 250 WBC/mm³ (94% mononuclear and 6% polynuclear).

Arthrography revealed a fine nodularity of the prefemoral and suprapatellar synovium. In addition a 4×2 cm mass was noted in the superolateral aspect of the suprapatellar pouch (fig. 1). The menisci and articular cartilage were normal. A diagnosis of synovial chondromatosis was made.

At surgical exploration, multiple cartilaginous nodules both at-

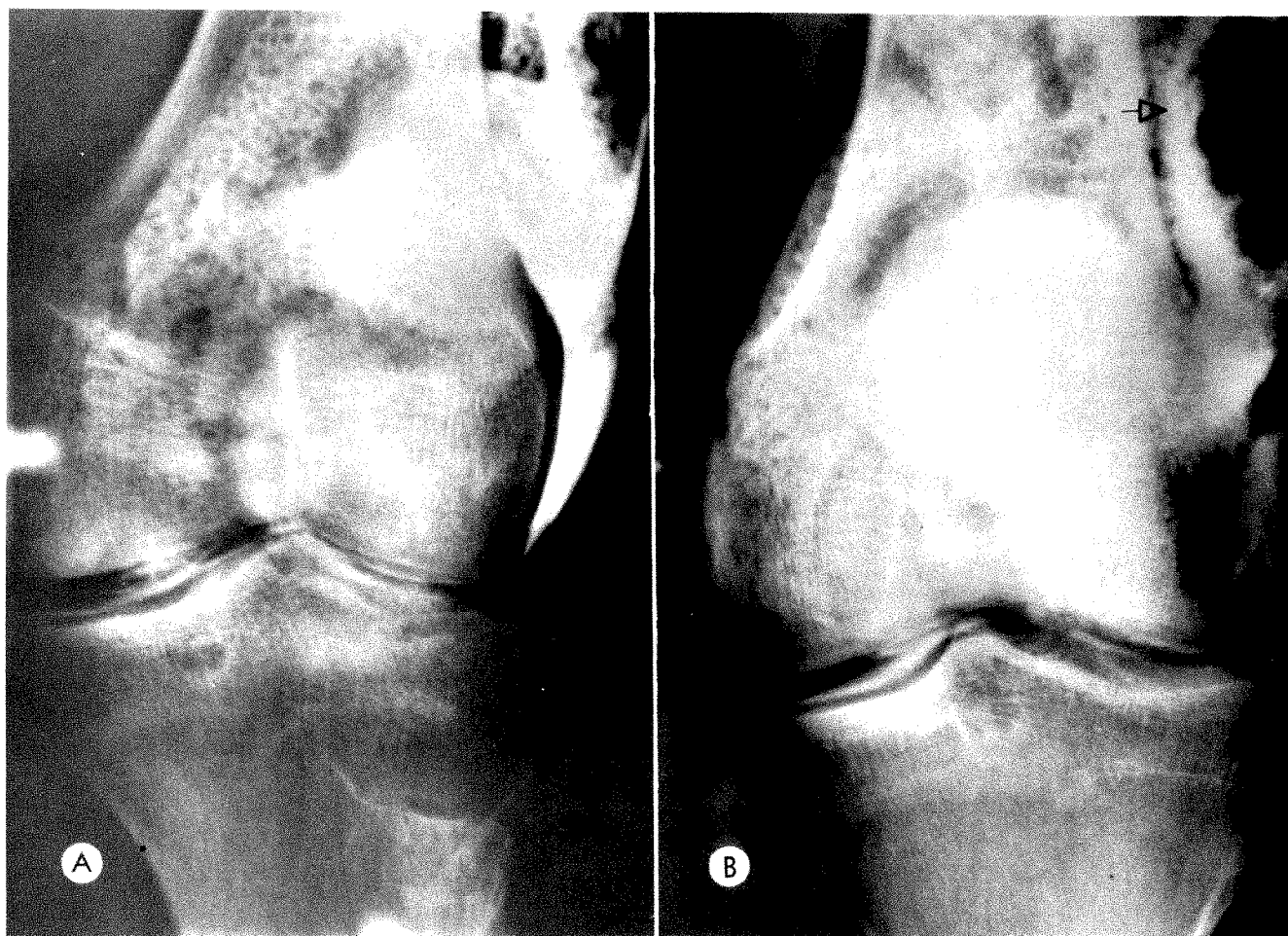


Fig. 1.—AP and oblique views of left knee arthrogram. A, Fine nodularity of synovium in suprapatellar pouch. B, Mass formed by coalescence of small nodules (arrow).

¹ Department of Radiology, University of California at San Francisco, San Francisco, California 94143. Address reprint requests to J. C. Mall.



Fig. 2.—Surgical specimen showing innumerable small white nodules in synovium.

tached to the synovium and loose within the joint were noted. Many small nodules had coalesced to form larger lesions; one such mass measuring 3×4 cm was attached to the synovium on the lateral aspect, corresponding to the clinically palpable mass. An anterior synovectomy and medial and lateral menisectomies were performed. The surgical specimen is shown in figure 2 and a microscopic section in figure 3. The patient's knee was strong and stable 18 months after operation.

Discussion

Synovial chondromatosis occurs most commonly in the knee, but also has been reported in the ankle [3], elbow [4, 5], shoulder [6, 7], and hip [8, 9]. The same process can



Fig. 3.—Microscopic section (×10) showing cartilaginous nodules (arrows).

also affect bursae [10, 11] and tendon sheaths [5, 12]. The etiology is unknown. Pain, swelling, and stiffness are the most common clinical complaints; locking is uncommon in spite of the many loose bodies [1]. Physical findings include limitation of motion, effusion, and tenderness [13, 14]. Although spontaneous regression has occurred and good results have been reported with simple removal of loose bodies [13, 15, 16], the treatment of choice is usually synovectomy [14, 16].

Multiple small, sharply defined defects are noted at arthrography; these may occasionally coalesce to form larger cartilaginous masses (fig. 1). Differential diagnosis includes pigmented villonodular synovitis [17], lipoma arborescens [18], rheumatoid arthritis [19], and synovial hemangioma [20]. The filling defects in pigmented villonodular synovitis are not as sharply outlined and are more frondlike. Dark, serosanguineous, or frankly blood fluid is typically aspirated. The nodules in lipoma arborescens are less regular and also more ill defined than those seen in synovial chondromatosis. In addition, on physical examination the nodular masses are soft compared to the rock-hard cartilaginous and/or bony nodules in synovial chondromatosis. Rheumatoid arthritis can be easily distinguished from synovial chondromatosis by multiple joint involve-

ment, clinical features, laboratory values, and plain film findings. Synovial hemangioma usually presents as a single soft mass with bloody effusion. Occasionally, phleboliths seen on plain film and cutaneous hemangiomas are clues to the correct diagnosis. Synovial hemangioma and synovial chondromatosis have affected the same joint simultaneously [21].

In synovial chondromatosis innumerable hard masses are found both attached to the synovium and free floating. Microscopically, these are areas of proliferating cartilage in the connective tissue below the surface layer of the synovium (fig. 3).

REFERENCES

1. Zimmerman C, Sayegh V: Roentgen manifestations of synovial osteochondromatosis. *Am J Roentgenol* 83:680-686, 1960
2. Crittenden JJ, Jones DM, Santarelli AG: Knee arthrogram in synovial chondromatosis. *Radiology* 94:133-134, 1970
3. Khmeresh O, Weissman SL: Synovial osteochondromatosis of the ankle. *Harefuah* 84:219-220, 1973
4. Leydig SM, Odell RT: Synovial osteochondromatosis. *Surg Gynecol Obstet* 89:457-463, 1949
5. Lichtenstein L: Tumors of synovial joints, bursae, and tendon sheaths. *Cancer* 8:816-830, 1955
6. Addison J: Osteochondromatosis of the shoulder. *Proc R Soc Med* 18:112-113, 1949
7. Freund E: Chondromatosis of joints. *Arch Surg* 34:670-686, 1937
8. Hamada G: Osteochondromatosis of the hip joint. *J Bone Joint Surg* 33-B:85-86, 1957
9. McIvor RR, King D: Osteo chondromatosis of the hip joint. *J Bone Joint Surg* 44-A:87-97, 1962
10. Symeonides P: Bursal chondromatosis. *J Bone Joint Surg* 48-B:371-373, 1966
11. Zadek I: Osteochondromatosis of a popliteal bursa. *Bull Hosp Joint Dis* 5:12-15, 1944
12. Henderson MS, Jones HT: Loose bodies in joints and bursae due to synovial osteochondromatosis. *J Bone Joint Surg* 5:400-424, 1923
13. Jeffreys TE: Synovial chondromatosis. *J Bone Joint Surg* 49-B:530-534, 1967
14. Murphy FP, Dahlin DC, Sullivan CR: Articular synovial chondromatosis. *J Bone Joint Surg* 44-A:77-86, 1962
15. Mussey RD Jr, Henderson MS: Osteochondromatosis. *J Bone Joint Surg* 31-A:619-627, 1949
16. Swan EF, Owens WF Jr: Synovial chondrometaplasia: a case report with spontaneous regression and a review of the literature. *South Med J* 65:1496-1500, 1972
17. Wolfe RD, Giuliano VJ: Double-contrast arthrography in the diagnosis of pigmented villonodular synovitis of the knee. *Am J Roentgenol* 110:793-799, 1970
18. Burgan DW: Lipoma arborescens of the knee: another cause of filling defects on a knee arthrogram. *Radiology* 101:583-584, 1971
19. Taylor AR: Arthrography of the knee in rheumatoid arthritis. *Br J Radiol* 42:493-497, 1969
20. Forrest J, Staple TW: Synovial hemangioma of the knee. *Am J Roentgenol* 112:512-516, 1971
21. Sabanas AO, Ghormley RK: Hemangioma of the knee joint complicated by synovial chondromatosis: report of a case. *Mayo Clin Proc* 30:171-179, 1955

Synovial Osteochondromatosis Involving the Elbow

PETER E. GIUSTRA,^{1,2} ROBERT S. FURMAN,¹ LLOYD ROBERTS,¹ AND PAUL J. KILLORAN¹

Synovial osteochondromatosis is a rare disease of the synovium characterized by the formation of multiple cartilaginous bodies within connective tissue beneath the surface of the synovial membrane [1-3]. The disease is characteristically monoarticular, most commonly involving the knee. Despite frequent mention of elbow involvement in various texts and articles, the most comprehensive documentation of synovial osteochondromatosis of the elbow was published almost 25 years ago [4]. We wish to review the clinical, radiologic, and histologic features of synovial osteochondromatosis of the elbow by presenting a recent case with a correct preoperative diagnosis.

Case Report

S. D., a 55-year-old Caucasian male, had a several-year history of intermittent locking and loss of range of motion of the right elbow. The elbow lacked 20° of full extension and 15-20° of flexion. Pronation and supination were complete; crepitation was noted when the elbow was brought from flexion to extension. Other joints were normal. A radiographic diagnosis of synovial osteochondromatosis was made (fig. 1).

At surgery multiple osteochondromata were found adherent to the thickened synovium and within the joint space. A partial synovectomy and removal of loose bodies was accomplished. Microscopic examination showed the synovial connective tissue to be distorted by irregular masses of bone, osteoid, and cartilage just beneath the synovial lining cell membrane. There was no proliferation of the synovial lining cells and no inflammation (fig. 2).

Discussion

Synovial osteochondromatosis is generally an adult disease, most commonly affecting the knee. The entity is four times more frequent in males than females and can be suspected in a middle-aged patient (30-50 years) with a chronic history of solitary joint pain, swelling, and decreased range of motion [1-3].

The diagnosis is even more suspect if multiple small paraarticular amorphous calcifications are seen on x-ray with good preservation of the articulating surfaces. The radiologic appearance should rarely be confused with other entities giving rise to loose bodies, such as degenerative joint disease, osteochondritis dissecans, neuropathic joint, tuberculous arthritis, or osteochondral fracture. All of these tend to involve the articulating surfaces and generally produce larger, denser loose bodies. Erosion of subchondral bone and osteoarthritis as secondary changes have been described in synovial osteochondromatosis and, when present, permit a less confident preoperative radiologic diagnosis. In the rare instance where calcifications are not present, a correct radiographic diagnosis can be made by the use of arthrography [5].

It must be stressed that the final diagnosis of synovial osteochondromatosis rests with the histologic sections which prove that the synovial connective tissues are the site of formation of the cartilaginous or osteocartilaginous bodies. The cause of these multiple metaplastic cartilaginous foci within the synovial connective tissues is unknown. However, it is fairly characteristic for chondroid bodies to break off from the synovium and thrive and grow within the joint, nourished by synovial fluid, with ultimate calcification or ossification.

Although osteochondromatosis may be self-limiting and undergo spontaneous resolution, presently accepted treatment is surgical. Removal of loose bodies and synovectomy (as extensive as possible to remove the cartilage-producing tissue) is encouraged. Recurrence rate is low. Our patient has done well 2 years following surgery; he is asymptomatic and lacks only 10° of full extension.

Almost 25 years ago, Mussey and Henderson [4] described elbow involvement in 22 of 104 patients with synovial osteochondromatosis seen at the Mayo Clinic from 1910 to 1945. However, only 18 patients had histologic confirmation, and it was not specified which joints were histologically confirmed. Since then, reported experience with synovial osteochondromatosis has not established a high incidence of elbow involvement. The few cases in the literature have been poorly documented. The 32 cases of synovial chondromatosis reported by Murphy et al. [2] from 1910 to 1957 at the Mayo Clinic contained no instances affecting the elbow. Up to 1958, Jaffe [1] had experience with only six cases involving other joints, mentioning the elbow once but not illustrating the case. Radiographs of an elbow labeled "arthrosis of the elbow joint with chondromatosis" are found in Köhler and Zimmer's book [6]; however, the case is not referenced or histologically documented. The series of Zimmerman and Sayegh [3] does not describe or reference a case involving the elbow. Meschan [7] illustrates a patient with "multiple areas of chondromatosis of the joints" with a radiograph of an elbow. Other isolated examples without mention of surgical or histologic documentation also have been reported [8, 9].

The case presented is the only documented instance of synovial osteochondromatosis of the elbow found in 2,000 elbows radiographed at Knox County General Hospital in the past 10 years. Thus synovial osteochondromatosis of the elbow must be considered rare. While it may be more common than has been documented in the literature, the true incidence of elbow involvement has not been established. It is hoped that description of this case will lead to more accurate clinical and radiologic diagnosis of the con-

¹ Knox County General Hospital, Rockland, Maine 04841.

² Present address: Department of Radiology, Penobscot Bay Medical Center, 710-04 Rockland, Maine 04841. Address reprint requests to P. E. Giustra.

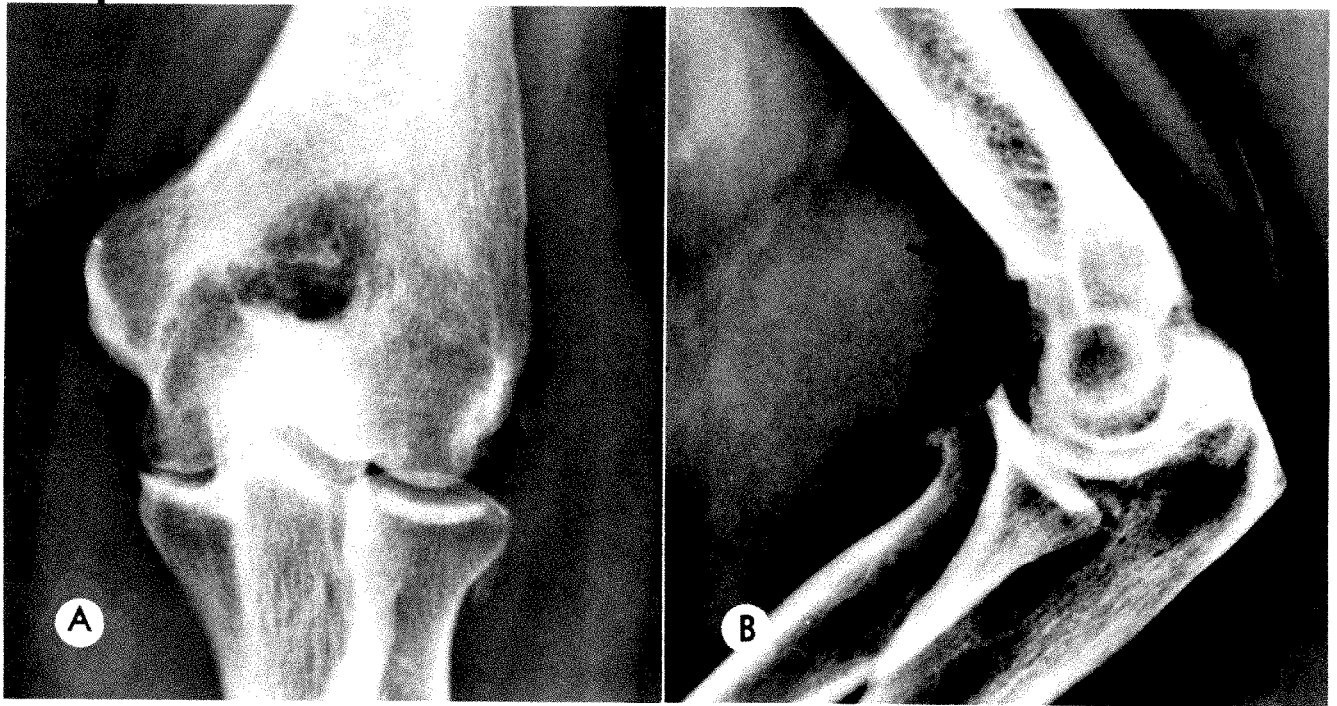


Fig. 1.—AP (A) and lateral (B) roentgenograms of right elbow showing soft tissue swelling about joint. Note multiple small, somewhat rounded and amorphous calcified densities overlying both joint space and capsule (arrows). Only minor degenerative osteophytes are seen. Articular surfaces are smooth and joint spaces are not narrowed.

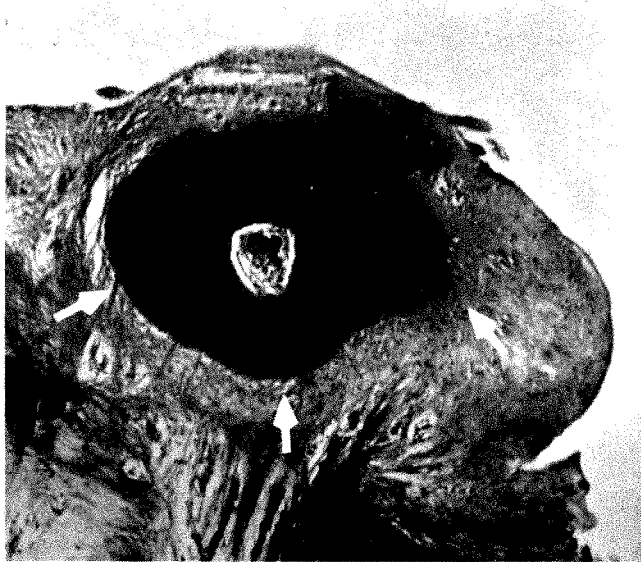


Fig. 2.—Nodule of ossifying cartilage distorting synovial connective tissues (arrows). Nodule just beginning to become polypoid, first step leading to detachment and formation of loose body. Synovial lining intact. H and E, $\times 100$.

dition. Early surgery apparently results not only in cure but in prevention of late degenerative joint disease.

Note added in proof Since submitting this manuscript, a similar case involving the elbow has come to our attention: R. S. Jacob et al., *Clin Orthop* 109:152–154, 1975.

REFERENCES

1. Jaffe HL: *Tumors and Tumorlike Conditions of the Bones and Joints*. Philadelphia, Lea & Febiger, 1959
2. Murphy FP, Dahlin DC, Sullivan CR: Articular synovial chondromatosis. *J Bone Joint Surg* 44-A:77–86, 1962
3. Zimmerman C, Sayegh V: Roentgen manifestations of synovial osteochondromatosis. *Am J Roentgenol* 83:680–686, 1960
4. Mussey RD Jr, Henderson MS: Osteochondromatosis. *J Bone Joint Surg* 31-A:619–627, 1949
5. Crittenden JJ, Jones DM, Santarelli AG: Knee arthrograph in synovial chondromatosis. *Radiology* 94:133–134, 1970
6. Köhler S, Zimmer ES: *Borderlands of the Normal and Early Pathologic in Skeletal Roentgenology*. New York, Grune & Stratton, 1968
7. Meschan I: *Roentgen Signs in Clinical Practice*, vol. 1. Philadelphia, Saunders, 1967
8. Aegerter E, Kirkpatrick JA: *Orthopedic Diseases*. Philadelphia, Saunders, 1968
9. Turek SL: *Orthopedics Principles and their Application*. Philadelphia, Lippincott, 1967

A Mobile Calcified Amputated Appendix Epiploica

SETH A. BORG,¹ GRAHAM H. WHITEHOUSE, AND GLASLYN J. GRIFFITHS

The appendices epiploica are small pouches of peritoneum containing a variable amount of fatty tissue and are usually 0.5–5.0 cm long. They are present along the entire length of the colon, usually in two rows closely related to the anterior and posteroinferior tenia coli. Calcification as a consequence of infarction or inflammation may occur within these appendages. Amputation, presumably as a result of either process, may be roentgenographically apparent as a freely mobile calcific density within the peritoneal cavity. There has not been a description of the calcified and amputated freely mobile epiploic appendage since 1948, and there were only three reports prior to that date.

The purpose of this paper is to document the intriguing roentgenographic appearances and to discuss the differential diagnosis of freely mobile, calcified intraperitoneal lesions.

Case Report

The patient, a 55-year-old obese female, was admitted to Strong Memorial Hospital following a positive cell block for malignancy subsequent to culdocentesis. The latter had been performed following several abnormal Papanicolaou smears and an abnormal cervical cone biopsy. A roentgenogram of the abdomen immediately prior to urography revealed a "ground glass" appearance consistent with ascites, a few pelvic calcifications 1 cm or less in size, and a larger ovoid pelvic calcified opacity measuring 3.9 × 2.1 cm (fig. 1A). The core of this mass was composed of heterogeneous mottled calcification surrounded by a thin lucent zone, which itself was circumscribed by a rim of peripheral calcification. It lay to the right of the midline within the pelvis.

Excretion urography revealed medial deviation of the pelvic portion of the right ureter, with some change in the pelvic position of the larger calcified mass (fig. 1B). During a subsequent barium enema performed immediately after the urogram, the opacity occurred lateral to the descending colon, demonstrating its mobility within the peritoneal cavity (fig. 2).

The site of malignancy remained obscure despite a complete oncologic evaluation; therefore, a laparotomy was performed. At incision, the described calcified mass was seen floating freely within 2,500 ml of ascitic fluid. Bilateral small ovarian tumors, histologically proven to be moderately well differentiated serous carcinoma, were also found. There were extensive secondary implants to other pelvic organs as well as to paraaortic lymph nodes and the omentum. The right ureter was encased and deviated by tumor. Pathologically, the intraperitoneal foreign body was consistent with an infarcted appendix epiploica with fibrous and dystrophic calcification.

Discussion

The first description of a free-lying calcified appendix epiploica is credited by Harrigan [1], to Littre in 1703.

Hunt [2] found 11 examples in the literature and added a further case of his own. Virchow [3] believed that as a result of obesity, the appendices epiploicae increase in fat content and therefore weight, then undergo torsion, infarction, and finally amputation. However, it seems more likely that ischemia as a result of torsion or inflammation is the dominant etiologic factor that leads to infarction and amputation [4]. When torsion and strangulation occur acutely, the resulting symptoms can be identical to those of acute appendicitis. However, if the torsion and strangulation are more chronic, saponification, calcification, and

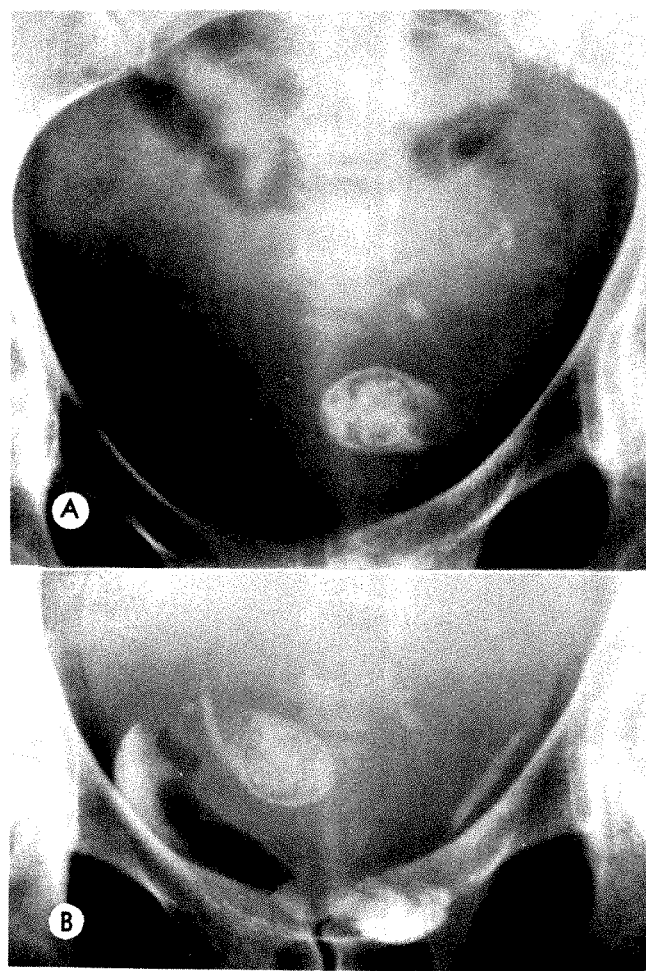


Fig. 1.—A, Anteroposterior roentgenogram of pelvis immediately prior to excretory urography. Large calcified opacity lies left of midline within pelvis. B, AP view during urography showing opacity within right portion of pelvis adjacent to opacified right ureter. Opacification of left ureter and bladder also demonstrated.

Received January 26, 1976; accepted February 10, 1976.

¹ All authors: Department of Radiology, Strong Memorial Hospital, University of Rochester Medical Center, 601 Elmwood Avenue, Rochester, New York 14642. Address reprint requests to S. A. Borg.

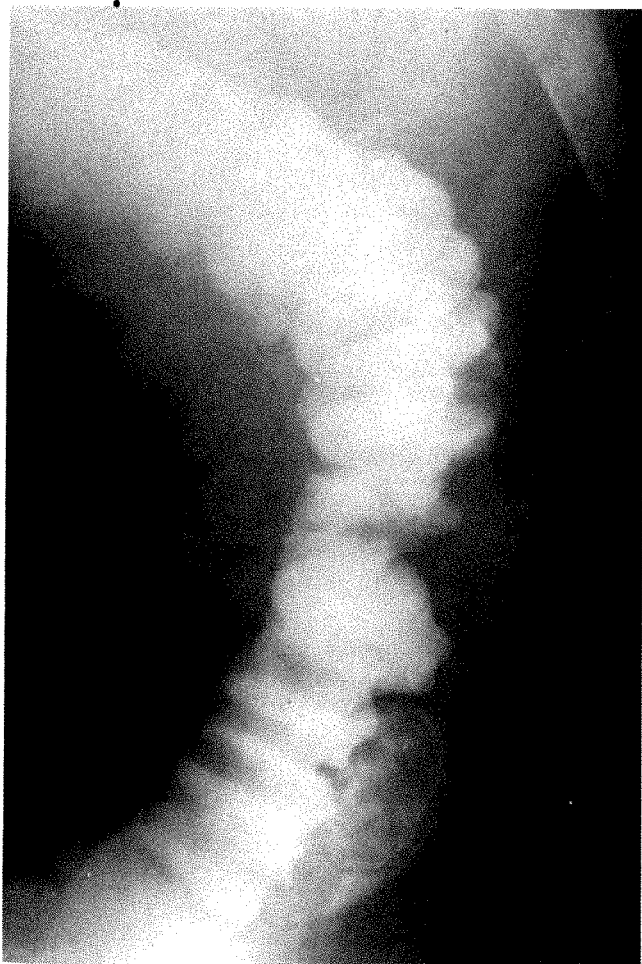


Fig. 2.—Anteroposterior roentgenogram obtained during barium enema. Radiodense mass seen lateral to descending colon.

ultimately amputation can occur insidiously as in our patient.

Calcification of the appendices epiploicae was first described roentgenographically in 1939 by Barden [5]. Two ovoid calcifications, variable in position within the pelvis, were found at laparotomy and were histologically proven to be appendices epiploicae. Morales [6] described another case with verification at autopsy and described a further six cases which were roentgenographically consistent with the diagnosis of appendices epiploicae but lacked pathologic proof. Holt and MacIntyre [7] reported a

pathologically proven amputated calcified epiploic appendage lying freely within the pelvis. Most of the previously reported calcified appendages were small, but sizes ranged from that of a pea to a chicken egg.

Similar mobile ovoid radiodensities seen within the abdomen or pelvis may be due to calcified deposits within the omentum [7]. Considerable mobility may be encountered; the only possible distinguishing characteristic between omental calcification and the calcified appendices epiploicae is the multiplicity seen with the former [2]. Pedunculated uterine fibroids and teratomata, fecoliths, ureteral and bladder calculi, lithopedions, and calcified lymph nodes may have a similar appearance to the epiploic appendage. However, the limited mobility of these entities may help to distinguish them from the amputated calcified epiploic appendage. Rarely, an ovary may become amputated and undergo calcification [8]; it would be impossible to distinguish from the amputated epiploic appendage on a purely roentgenographic basis.

The importance of correct recognition of the mobile calcified amputated epiploic appendage depends upon the ability of the observer to refrain from confusing this entity with other calcified masses of greater clinical importance.

ACKNOWLEDGMENTS

We thank Mrs. Margaret Kowaluk for assistance in preparation of this manuscript, and we are indebted to Dr. Anthony Leone and the Genesee Radiology Group for their kind permission to publish this case.

REFERENCES

1. Harrigan AH: Torsion and inflammation of the appendices epiploicae. *Ann Surg* 66:467-478, 1917
2. Hunt VC: Torsion of appendices epiploicae. *Ann Surg* 69:31-46, 1919
3. Virchow R: *Die Krankhaften Geschwülste*. Berlin, 1863
4. Patterson DC: Appendices epiploicae. *N Engl J Med* 209:1255-1259, 1933
5. Barden RC: Calcified epiploic appendage: a radiologic curiosity. *Radiology* 33:768-769, 1939
6. Morales O: Calcified appendices epiploicae as freely mobile bodies in the abdominal cavity. *Acta Radiol* 25:653-661, 1944
7. Holt JF, MacIntyre RS: Calcified omental fat deposits; their roentgenologic significance. *Am J Roentgenol* 60:612-616, 1958
8. Lester PD, McAllister WH: A mobile calcified spontaneously amputated ovary. *J Can Assoc Radiol* 21:143-145, 1970

Carcinoma of the Urachus

SANG Y. HAN¹ AND DAVID M. WITTEN¹

Characteristic roentgenographic and anatomical features of a mucinous adenocarcinoma of the urachus were observed in two patients. Both presented with a midline anterior abdominal mass in the suprapubic area. The tumor contained fine stippled calcification in one case. The cystogram demonstrated an irregular filling defect in the bladder dome in the other case. Ultrasonographic examination in one case was helpful in delineating the nature, size, and location of the mass in detail.

Carcinoma of the urachus is not as rare as generally believed. In a review of 434 cases of tumors of the urinary bladder, Franksson [1] found that 11 (2.5%) had originated from the urachus. In contrast to carcinoma of the urinary bladder which is mostly transitional cell type, most urachal carcinomas are mucinous adenocarcinomas arising either from the intramural or suprapubic portion of the urachus.

The mode of clinical presentation varies with the site of involvement. When the tumor arises from the intramural portion of the urachus, it may present as irregularity in the dome of the bladder on cystoscopic examination. Unless it ulcerates, it produces no symptoms. When the tumor arises from the suprapubic portion of the urachus, it presents as a midline mass in the anterior wall of the abdomen.

Although sporadic reports of urachal carcinoma have described its clinical course and treatment, radiological findings have not been stressed. This paper reports two cases of carcinoma of the urachus with characteristic radiographic and anatomic features which suggested the correct diagnosis in both cases preoperatively. The ultrasonographic findings which facilitated the diagnosis in the second case are also presented.

Anatomy of the Urachus

The urinary bladder develops from a division of the cloaca by the transverse vertical septum. The fetal bladder extends up to the umbilicus where it continues into the allantoic stalk. Shortly after birth, the upper half of the bladder narrows as the lower half descends to the pelvic cavity. If a remnant of the allantois remains patent, it presents as the patent urachus which may be an open tube from the bladder to the umbilicus or end as a blind pouch with no connection to the urinary bladder [2].

In the anterior abdomen, the urachus lies between the transversalis fascia and peritoneum in the space of Retzius. The upper portion of the urachus together with the obliterated umbilical artery forms the ligamentum commune. The urachus proper is 5–6 cm long. It consists of suprapubic and intramural portions. The latter is 1 cm

long and penetrates the bladder wall. It is divided into intramuscular and intramucosal parts [3].

Cases Reports

Case 1

A 64-year-old man was referred for evaluation of an enlarging abdominal mass. He denied abdominal pain and had no symptoms related to the gastrointestinal or genitourinary system. There was no history of trauma.

Physical examination revealed a 16×17 cm mass in the suprapubic area. It was soft and movable without tenderness or pulsation. Excretory urography demonstrated lateral displacement of both ureters (fig. 1A). Irregularity and small filling defect were detected at the bladder dome on subsequent cystogram (fig. 1B). No connection between the mass and bladder was present.

At surgery, a large cystic mass 15 cm in diameter in the anterior abdominal wall was resected. The posterior inferior portion of the cyst was attached to the bladder dome. Further exploration of the area revealed a 1 cm polypoid mass. The cyst contained about 1,000 ml of mucinous gelatinous fluid.

The pathology report on the removed cyst and mass indicated an urachal cyst and mucinous adenocarcinoma of the urachus arising from the intramuscular portion.

Case 2

A 62-year-old man was admitted with a 6 week history of a gradually enlarging abdominal mass. Except for occasional sharp pain, there were no other symptoms associated with the mass. He denied weight loss or change in appetite or bowel habit. There were no genitourinary tract symptoms.

Physical examination was unremarkable except for a large abdominal mass in the suprapubic area. The mass was fixed to the anterior abdominal wall and was neither tender nor pulsatile. Plain film of the abdomen demonstrated a midline abdominal mass 15 cm in diameter (fig. 2A). Fine stippled calcifications were seen in the mass. An excretory urogram was normal. Ultrasonography demonstrated a cystic mass with some internal echoes (fig. 2B). The mass was clearly separated from the bladder. Cystoscopy and cystogram were normal.

At surgery, a 15 cm knobby mass was resected from the anterior abdominal wall. The omentum and peritoneum were stuck to the mass. There was no invasion of the abdominal viscera or urinary bladder.

On pathologic examination, the mass was found to be multiloculated and relatively well encapsulated. The loculations were filled with mucinous gelatinous material. The bladder wall was not involved. The pathological diagnosis was mucinous adenocarcinoma of the urachus with calcification.

Discussion

There are two types of urachal carcinoma. Those arising from the suprapubic portion of the urachus are often

Received January 9, 1976; accepted February 13, 1976.

¹ Department of Diagnostic Radiology, University of Alabama School of Medicine, 619 South 19th Street, Birmingham, Alabama 35233. Address reprint requests to S. Y. Han.

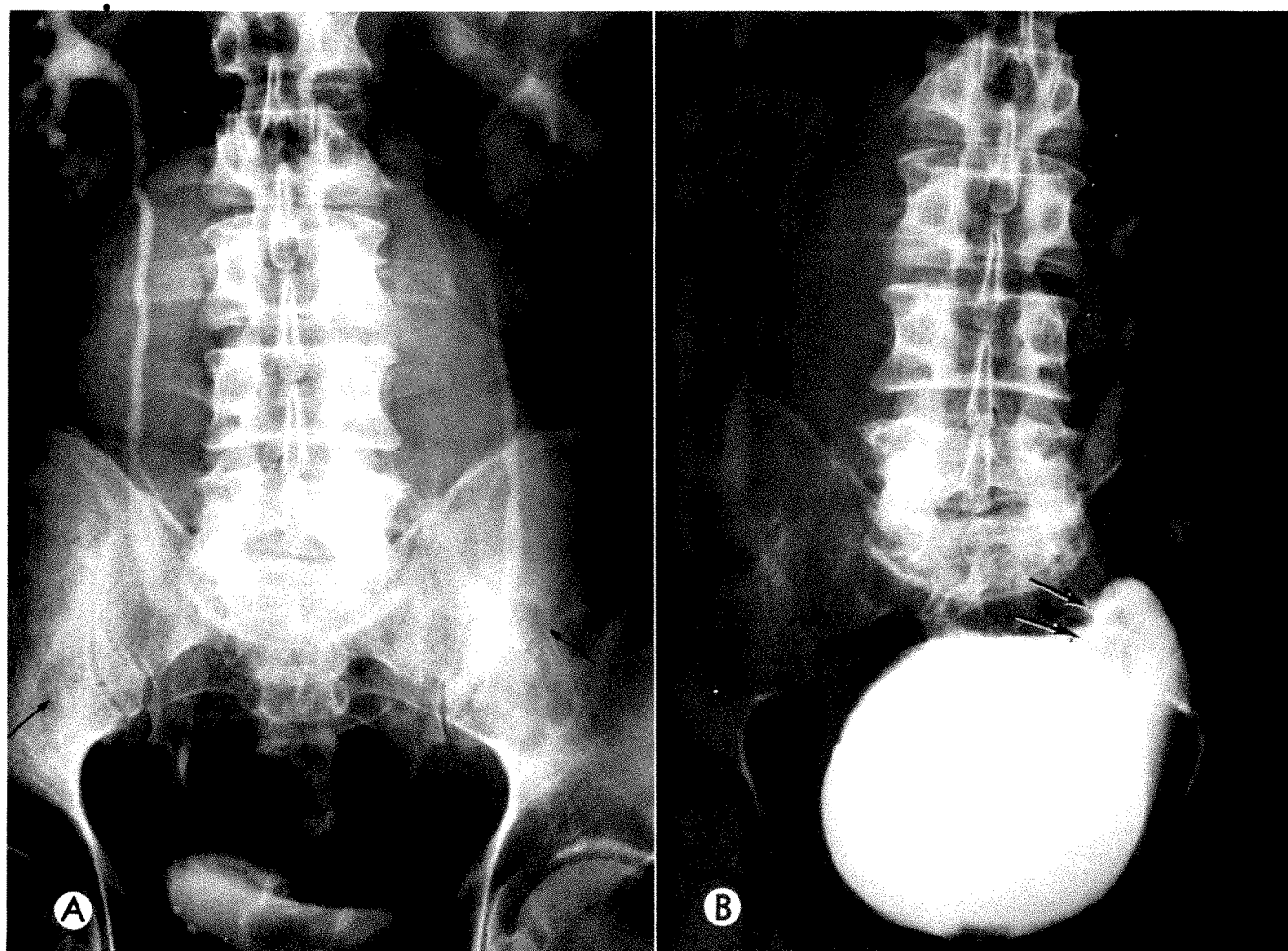


Fig. 1.—Case 1. A, Excretory urogram showing lateral displacement of ureter on both sides. Note large oval shaped mass (arrows). B, Cystogram demonstrating irregularity of bladder wall and small filling defect in bladder dome (arrowheads).

cystic and encapsulated. The other type arises from the intramural portion and is usually small and solid [2].

About 80% of the reported urachal tumors occur in males, most commonly between the ages of 50 and 60 years [4]. Symptoms are those of vague abdominal pain produced by a mass in the suprapubic area. If the tumor invades the mucosa of the bladder, it may cause hematuria [4, 5]. Cystoscopic examination may reveal a mass in the bladder dome.

Although a variety of roentgenographic findings in urachal carcinoma have been published, [5, 6], few reports summarize them for diagnostic purposes. As a result, radiologic diagnosis of urachal tumor has rarely been made preoperatively. The two cases presented here illustrate all the roentgenographic features of urachal carcinoma.

Case 1 is an example of a tumor arising from the intramural portion of the urachus in association with cyst. Roentgenographic findings in this group include a small filling defect in the bladder dome with supraventricular mass. The tumor is frequently associated with cyst [5]. As in case 1, the cyst usually grows cephalad into the space of Retzius. Only the caudal portion of the cystic mass is attached to the

bladder wall. If the tumor is not associated with the cyst, a small defect in the bladder dome is the only roentgenologic finding. A mass in the intramural portion of the urachus protrudes into the bladder and is responsible for the filling defect in the bladder dome on cystogram.

Case 2 is representative of the other group of tumors, those arising from the urachus proper. The principal roentgenographic feature in this group is a midline anterior abdominal mass. It may contain fine stippled calcifications as demonstrated in case 2. Begg [2] described characteristic mucoid degeneration of urachal tumors which are predominantly adenocarcinoma in cell type. As with some of mucinous adenocarcinomas of other abdominal organs, urachal carcinoma may produce typical psammomatous calcifications [4].

Because of their cystic nature and location in the anterior abdominal wall, urachal tumors appear to be ideal lesions for ultrasonographic examination. The filled urinary bladder serves as good echographic reference. Since the tumor is extraperitoneal, the scan is not affected by bowel gas. In case 2, ultrasonographic findings were very suggestive of the diagnosis. The sonogram delineated the size,

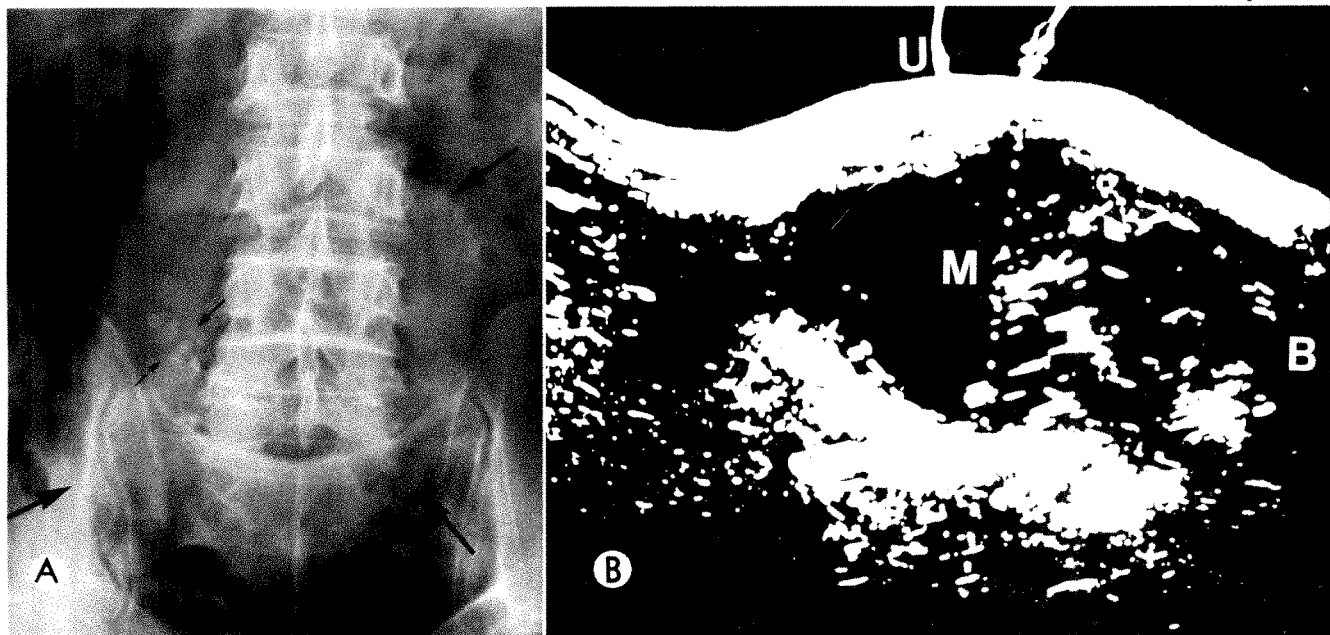


Fig. 2.—Case 2. A, Supine film of abdomen showing large soft tissue mass in supraventricular area (*large arrows*). Note several groups of fine calcification (*small arrows*) in mass. B, Longitudinal sonogram of abdomen at midline. M=mass, U=umbilicus, B=bladder. Note internal echoes within mass.

nature, and location of the mass in detail. The mass was localized in the anterior abdominal wall at the supraventricular area, clearly separated from the bladder. It was sonolucent except for some internal echoes in the lower portion produced by calcification.

REFERENCES

1. Franksson C: Tumors of the urinary bladder. *Acta Chir Scand [Suppl]* 151:1–203, 1950
2. Begg RC: The colloid adenocarcinoma of the bladder vault

arising from the epithelium of the urachal canal. *Br J Surg* 18:422–466, 1931

3. Dreyfuss ML: Benign and malignant lesions of the urachus. *Va Med Mon* 70:200–204, 1943
4. Whitehead ED, Tessler AN: Carcinoma of the urachus. *Br J Urol* 43:468–476, 1971
5. Bandler CG, Roen PR: Mucinous adenocarcinoma arising in the urachal cyst and involving bladder. *J Urol* 64:504–510, 1950
6. Pollock AV: A case of adenocarcinoma of the urachus showing extensive calcification. *Br J Surg* 40:187–188, 1952

Technical Notes

Spinal Needle with Depth Guide: A New Design for Simplifying Subarachnoid Injections

VINCENT C. HINCK¹

In performing a routine spinal tap, the operator palpates the row of lumbar spinous processes to identify midline and select the best level for puncture. The spinal needle is then advanced through overlying soft tissues, traversing the space between adjacent spinous processes, and entering the osseous spinal canal. With further advance, the operator may feel a "pop" as the bevel of the needle penetrates the dura and arachnoid.

At this juncture, flow of cerebrospinal fluid from the needle after removal of the stylet indicates that the subarachnoid space has been entered, but not necessarily that the bevel of the needle is entirely within the subarachnoid space. If the bevel has only partially penetrated the arachnoid membrane, fluid may flow from the subarachnoid space through one-half of its orifice while injected substances may flow partly or entirely into the extraarachnoid space through the other half. All who perform spinal taps for subarachnoid injections are familiar with this problem.

To minimize the uncertainties surrounding the correct placement of the needle, I have designed a blunt-tipped stylet to be used as a depth guide.* It enables the operator to position the needle tip 5 mm above the floor of the osseous spinal canal. There, with rare exception, the bevel should lie entirely within the subarachnoid space (fig. 1). The manner in which this stylet is used is depicted in figure 2 and described in the legend.

Spinal taps for special neuroradiologic procedures on this service are generally performed by house officers with

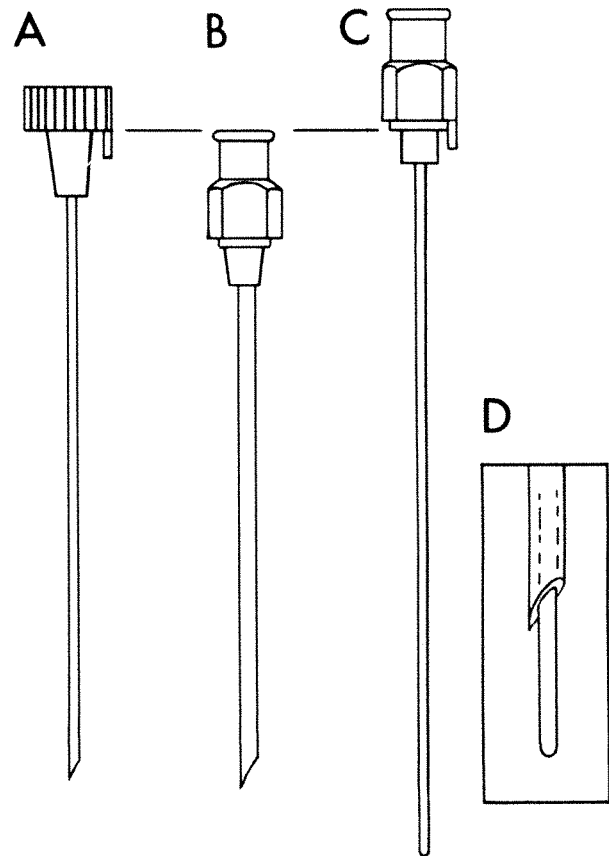


Fig. 2.—*Example 1.* Needle bevel straddling arachnoid in dorsal aspect of spinal canal. *A*, Stylet removed, spinal fluid flowing; *B*, blunt stylet inserted to full extent; *C*, stylet advanced until stopped on floor of spinal canal; *D*, stylet withdrawn leaving needle tip 5 mm above canal floor. *Example 2.* Bevel straddling arachnoid in ventral aspect of canal. *E*, Stylet removed, spinal fluid flowing; *F*, stylet introduced but not advancing to full extent (i.e., key and slot on hub do not engage completely), indicating needle tip near canal floor; *G*, stylet tip held gently but firmly against floor while needle withdrawn along stylet until key and slot engage; *H*, stylet withdrawn leaving needle tip 5 mm above canal floor. Stippled area = subarachnoid space.

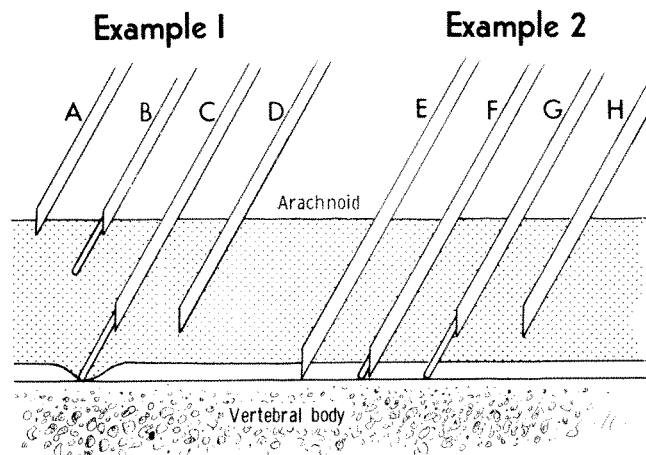


Fig. 1.—*A*, Standard bevelled stylet; *B*, standard spinal needle; *C*, blunt-tipped stylet which, when inserted to full extent, extends 5 mm beyond needle tip (*D*).

Received January 6, 1976; accepted after revision April 6, 1976.

¹ Department of Radiology, Baylor College of Medicine, Texas Medical Center, Houston, Texas 77025.

* Prototypes were provided by Cook, Inc., Box 489, Bloomington, Indiana 47401.

various levels of skill and experience. Extraarachnoid injections were rather common before introduction of the depth guide concept. Subsequently, however, they have actually been rare. In the exceptional instance one can usually identify a point at which the operator failed to follow the procedure described above. This technique has been used in at least 400 pneumoencephalograms and myelograms without complication.

Update on the Independent Radiation Monitor (IRM)

PAUL M. KROENING¹ AND RAYMOND MUCHA²

The new independent radiation monitor (IRM), unlike its predecessor, is a reliable and sensitive safety device for any radiation therapy room. It shows unequivocally that the beam is on, and it is inexpensive and simple to construct.

It has been adroitly stated (A. W. Sommer, personal communication) that for every scientific paper published a follow-up article on the same subject and by the same author should be required. Such a requirement would provide a real opportunity to elaborate on the experience gained and to describe the resulting changes.

This is the case with the independent radiation monitor (IRM). In 1969 we published [1] the reasons for and details of a device that would detect low levels of radiation, alerting those using the radiotherapeutic equipment that the unit was indeed on. On one occasion our teletherapy unit locked in the on position; the original IRM detected this mechanical failure and allowed expeditious removal of the patient with minimal radiation exposure. There also were several times when we were not certain whether a unit was functioning but were assured by the IRM that it was emitting radiation. This device was named the IRM because it would not be affected by an electrical power failure. It was also stressed that such a unit could be constructed easily and inexpensively.

However, in the last 5 years we discovered some less desirable features of the IRM: It was sensitive to humidity, it failed to detect radiation from tiny cones or small fields, it was slow to turn on, and it remained on for several seconds after termination of the irradiation. We have developed another model to correct these defects.

The new IRM is extremely sensitive. It now can detect and respond to single photons. Therefore, transient cosmic rays will trigger the light-emitting diode. This is a most useful side effect because these occasional flashes of light reaffirm that the IRM is functioning even when the unit is not monitoring an emitting therapeutic source of radiation.

The IRM is battery powered so it is truly independent (fig. 1). This is most important for monitoring radiation sources (such as cobalt units or radium storage areas) that could emit photons even during a line power failure. Because the batteries are not sealed inside the unit, they may easily be removed for replacement and recharging on a routine basis. In installations in which the IRM is to service a radiation generator that depends on an AC power supply, the unit can be equipped with a trickle charger. This keeps the batteries fully charged, eliminates routine battery replacement, and permits the addition of a sound alert device if desired.

Technical Description

The cost of the new IRM has increased. The expense for the materials required to assemble this unit now totals ap-



Fig. 1.—Independent radiation monitor (IRM) as it now appears from outside treatment room. Patient and monitor light can be viewed simultaneously. Note that batteries are readily accessible for ease of changing.

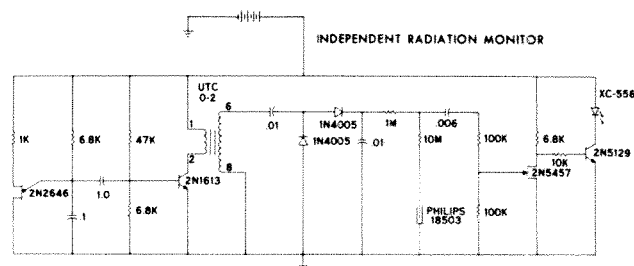


Fig. 2. Circuit diagram of new independent radiation monitor (IRM). Power supply is four 1.2 V nickel-cadmium batteries.

proximately \$57 (from Catalog no. 102, Newark Electronics, 500 North Pulaski Road, Chicago, IL 60624).

The IRM has a flexible design (fig. 2) that can be modified to a specific need. Substitutions for most components are possible. It has three basic sections: the low voltage/high voltage power supply, the detector, and the display.

The power supply is a unijunction-driven transistor conducting through one winding of a high-turn-ratio transformer. The secondary output is then rectified for the bias needed by the Geiger-Müller detector.

The avalanche pulse from the detector is coupled to the gate of a field-effect transistor that drives a final transistor to activate a light-emitting diode. The result is a flash in the diode each time a photon enters the Geiger-Müller tube.

ACKNOWLEDGMENT

We thank L. H. Deiterman for his help in modifying the IRM.

REFERENCE

1. Kroening PM, Mucha R: The independent radiation monitor (I.R.M.). *Am J Roentgenol* 105:900-902, 1969

¹ Department of Therapeutic Radiology, Scott and White Clinic, Temple, Texas 76501. Address reprint requests to P. M. Kroening.

² Scott and White Memorial Hospital, Scott, Sherwood and Brindley Foundation, Temple, Texas 76501.

The Technologic Imperative

Recently, society has come to realize that its most serious problems are unexpected consequences of technologic triumphs (e.g., the population explosion, urbanization, pollution, resource depletion, and health risk factors). The health care system has not been immune to such technology-produced problems. Factors such as uncontrolled costs, specialization, impersonalization, and public disenchantment have their roots in accelerating technology. Newly developed clinical investigative tools have led to an expanding array of diagnostic devices of increasing cost, complexity, and comprehensiveness.

Diagnostic instrumentation is obtaining increasing amounts of clinical data from intrinsic energies developed within the body, including biopotentials, audible sounds, recordable pressures, and temperatures. Chemical analysis of air, blood, body fluids, excreta, and tissue samples has become so automated that diversity and volume of testing have reached staggering proportions. While automation of cytology, histology, and microbiology is developing along predictable lines, energy sources directed or inserted into the body have provided an ever-expanding array of diagnostic energy probes for "nondestructive" testing [1]. Roentgen rays are the most obvious example of the process by which wave energy is transmitted into the body and the emerging energy analyzed to obtain information regarding the location, size, shape, and performance of internal organs. The sequence of development extending from roentgenography, fluoroscopy, image intensification, to biplane radiography have reached a zenith in the recent emergence of computed tomography (CT).

The fanfare and acclaim accompanying the adoption of this relatively untried technology is a truly startling phenomenon. Although CT units provide images containing a great deal of information, potentially wasteful duplication of these devices is already developing at a disquieting rate. Equipment costs range from \$375,000 to \$500,000. Yet these expenditures can be amortized quite easily if 10 patients per day are seen at \$200 each. The very high cash flow that can be generated by CT has attracted financially stressed hospitals to the point that the number of units being ordered in metropolitan areas already exceeds expectation of realistic need. Original expectations called for one scanner for each 300,000 people, but in Florida and southern California the ratio is already one per 75,000. Simultaneously, additional technological developments are rendering models obsolete at a startling rate.

Current ultrasonic echographic equipment is being rapidly refined and supplemented with ultrasonic Doppler flow-detecting techniques [2]; and whole new generations of diagnostic batteries promise enormous versatility in presenting data [3]. The U.S. market for ultrasonic equipment is expected to soar from \$33 million in 1974 to some \$200 million in 1983, and past estimates have been consistently low. In addition, computer storage and analysis of ultra-

sonic data is expected to become widespread along with an eightfold increase in sales of diagnostic ultrasonic instruments led by B-mode scanners and echocardiographs [4]. Similarly, the technologies associated with the use of radioisotopes have attained a high level of sophistication.

The pace of these developments has been so rapid that most physicians who will be ordering and interpreting the new data graduated from medical school long before these complicated devices were conceived. Conceding that these technological triumphs will provide large quantities of clinically relevant data, little attention has been directed to the extent to which these expensive information sources will ultimately influence the course of detected illnesses by therapeutic action.

Our ability to confidently identify metabolic, degenerative, malignant, allergic, genetic, or idiopathic disease states has added little to our ability to effect cures or even to favorably alter the course of illness through direct medical intervention [5]. The public has been effectively imbued with the need for early recognition of ailments in the name of "preventive medicine," but the extent to which these diseases and disabilities can be treated by therapeutic intervention is rarely considered in either mass media or scientific journals. Health professionals, like other scientists and engineers, have an obligation to consider the consequences of development and use of new technologies.

The concept of technology assessment is relatively new. For example, we are now witnessing a more conservative approach to the screening of populations for early stage disease detection [5]. Screening is clearly a worthy goal, particularly if the discovered ailments are accurately identified with reasonable frequency and are treatable. There is an implication that ailments are more effectively treated if discovered early. There is also an assumption that the process of detecting disease will produce no harm or health risk such as iatrogenic symptoms or hazards to health (i.e., carcinogenic mammography) [6].

The availability of technology to elicit information with minimal or negligible risk tends to assure its excess utilization in the current period of high public expectation, third party payments, and threats of litigation. Specifically, Bell and Loop [7] explored the utility of radiographic skull examinations in patients with trauma but without neurologic signs. They concluded that reasonable discrimination could have greatly reduced the number of unnecessary skull x-rays in emergency rooms. There is reason for concern that the general public may exhibit a surge of "iatrogenic" disturbances unless health professionals discriminate in their use of diagnostic technologies, particularly the complex and dramatic ones.

The health care system has many incentives for excessive utilization of diagnostic resources. In contrast there are few, if any, mechanisms or incentives toward conservative and discriminating selection of types and levels of data acquisi-

tion, particularly in relation to the effectiveness of available therapy. Indeed, one interpretation of current usage is that diagnosis is an integral part of therapy and is a suitable end in itself. Health professionals are not very responsive to controls or persuasion designed to influence or modify their professional activities, even by peers. The heads of diagnostic laboratories are among the few control mechanisms in a position to strive for more discriminative utilization of costly technologies.

It is tempting to consider the possible effect of routine inquiry regarding the intent of the physician and his expectations from the tests being ordered. Physicians ordering radiologic tests might be asked to indicate their purpose by checking an appropriate square on an order form. Choices could be: establish diagnosis, evaluate pathology, follow-up management, confirm normality, screen, and avoid liability.

If this approach would stimulate discrimination by the physician and evaluation by the radiologist, one additional step may be considered. Physicians could also indicate whether the conditions were considered to be: curable, treatable, remediable, requiring palliation, or self-limited.

Acquisition of such data on physician intent would have at least three effects. It would cause the referring physician to consider his indications for the request. The radiologist would be in a position to more intelligently review and evaluate the possibility that the physician's intent would be realized. The potential cost/benefit ratio of diagnostic test-

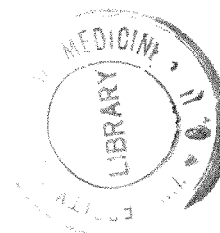
ing could be more effectively assessed using such information in prospective studies.

The ultimate consequences of unrestrained utilization of complex and comprehensive diagnostic testing seem sufficiently threatening to fully justify efforts directed toward providing effective mechanisms and incentives to drive the health professions toward increasing conservatism.

Robert F. Rushmer
University of Washington
Seattle, Washington 98195

REFERENCES

1. Rushmer RF: Medical engineering, in *Projections for Health Care Delivery*, New York, Academic Press, 1972
2. Baker DW: Pulsed ultrasonic Doppler blood flow sensing. *IEEE Trans Sonics Ultrasonics* SU-17:170-185, 1970
3. Barber FE, Baker DW, Nation AC, Strandness DE, Reid JM: Ultrasonic duplex echo-Doppler scanner. *IEEE Trans Biomed Eng BME-21*:109-113, 1974
4. Creative Strategies Inc.: *The Medical Electronics Industry*, special report, San Jose, Creative Strategies, Inc. (4340 Stevens Creek Blvd., San Jose, CA 95129)
5. Sackett DL: Laboratory screening: a critique. *Fed Proc* 34: 2157-2161, 1975
6. Bailar JE, III: Mammography: a contrary view. *Ann Intern Med* 84:77-84, 1976
7. Bell RS, Loop JW: The utility and futility of radiographic skull examination for head trauma. *N Engl J Med* 284: 236-239, 1971



Richard Hall Chamberlain, 1915–1975

With the death of Richard Hall Chamberlain December 4, 1975, at his home in Chestnut Hill, near Philadelphia, the world lost an authentic genius, and radiology and radiologists, a stalwart friend.

He was born in Jacksonville, Florida, in 1915 and had many relatives and "kissing cousins" throughout the South. Chamberlain's schooling and professional accomplishments were impressive. He graduated from Center College in Kentucky in 1934

and received his M.D. degree from the University of Louisville in 1939. After an internship at the Louisville City Hospital, he did 2 years of residency training in radiology under Eugene P. Pendergrass at the University of Pennsylvania Hospital. In 1942 he entered the Army, serving as chief of radiologic services at Army hospitals in the Middle East and India for 4 years.

He rejoined the teaching staff at the University of Pennsylvania in 1946, becoming a full professor in 1952 and department chairman in 1961. He also served as chairman of the university's Hospital Program Planning Committee from 1965–1970.

His contributions to medicine and radiology more than matched the honors he received. At 38, he was invited to give the Carmen Lecture of the Radiological Society of North America. He served as a member of the Board of Chancellors for the American College of Radiology and as chairman of the Commission on Radiologic Units, Standards, and Protection from 1953–1961. He received the Gold Medal of the College in 1969 and Gold Medal of the Radiological Society of North America in 1971.

Chamberlain had been a member of the National Commission on Radiation Protection since 1950 and held numerous offices within that organization. In 1953, he was elected to the International Commission on Radiation Units and Measurements. His work in radiation protection and



R. H. Chamberlain

radiology led to his appointment in 1963 as U.S. delegate to the United Nations Scientific Committee on the Effects of Atomic Radiation. He was a member of the National Advisory Council on Radiation and chaired several of its subcommittees. He was also chairman of the Radiology Training Committee of the National Institute of General Medical Sciences and chairman of the Medical X-ray Advisory Committee of the U.S. Public Health Service, Bureau of Radiological Health.

While an Army radiologist in the Middle East and India, Chamberlain developed an interest in international affairs. He had strong feelings about obligations to developing countries and was a member of the World Health Organization's Expert Advisory Panel on Radiation. He also served as a consultant for the World Health Organization and made several speaking tours in Southeast Asia and the Western Pacific. More recently he participated in the Pan American Health Organization's program for the development of small radiological facilities for the disadvantaged areas in the Americas. From 1968 to 1975, he was counterpart chairman of the Department of Radiology at the University of Saigon and under the auspices of the Americal Medial Association developed a system of basic radiology for use in developing countries which became known as the technamatic system. It is now being used in South American countries after testing in Vietnam proved its suitability for rugged and remote areas where trained personnel are in short supply.

Chamberlain was a man of unbounded energy and astonishing skill and versatility. His superlative artistic accomplishments included painting, handicraft in wood and metal, photography, architecture, and engineering. Sometime in the early 1940s, he took me to see an authentic revolutionary era house he had just purchased. The living room contained a great pile of bricks from the collapsed fireplace. When Dick left that house for good last December, it was a showplace, beautifully kept inside and out. It is only one of his many monuments.

In his way, Richard Hall Chamberlain was a great man who left his mark upon his time as few men ever do.

Robert P. Barden
Ambler, Pennsylvania

Abstracts of Current Literature

Chest

Cavitary pulmonary nodules in systemic lupus erythematosus. Castaneda-Zuniga WR, Hogan MT (West Virginia University School of Medicine, Morgantown, West Virginia 26506). *Radiology* 118:45-48, Jan 1976

It is well known that both pleural and pulmonary involvement are common in systemic lupus erythematosus. The clinical and radiographic manifestations of pleuropulmonary involvement are extremely variable. The authors emphasize the occurrence of cavitary pulmonary nodules and interstitial fibrosis in systemic lupus erythematosus and review the pertinent literature concerning the radiographic manifestations. Significant pathological lesions are found in the lungs, pleura, and heart in 80% of patients with collagen disease. Involvement of the lungs by lupus erythematosus is less frequent than that of the pleura or heart. All of the radiographic findings are nonspecific for the disease. Characteristically, the changes have been described as chronic changes of the pleura, lungs, and pericardium which remain after acute exacerbation of the disease. The authors report two cases of systemic lupus erythematosus with cavitary pulmonary nodules. Before this report, cavitary nodules had not been described as a specific manifestation of pulmonary involvement in systemic lupus erythematosus, although lesions have been mentioned in other necrotizing vasculitides such as periarteritis and Wegner's granulomatosis. Finally, one of the most remarkable aspects concerning the pleuropulmonary manifestations of systemic lupus erythematosus is the rapid response to high-dosage steroid therapy.

E. Jerome Schoolar

Primary and secondary pulmonary artery neoplasia mimicking acute pulmonary embolism. Olsson HE, Spitzer RM, Erston WF (Rochester General Hospital, 1425 Portland Avenue, Rochester, New York 14621). *Radiology* 118:49-53, Jan 1976

Rare forms of primary pulmonary neoplasm directly involving the pulmonary artery may mimic the signs, symptoms, and angiographic findings of pulmonary embolism. The authors report two cases, one a primary pulmonary artery sarcoma and the other a pulmonary carcinoma, presenting as acute pulmonary embolism. The diagnoses were made at a thoracotomy in one instance and at autopsy in the second. Pulmonary blood flow can be altered by bronchogenic carcinoma. However, primary bronchogenic carcinoma is seldom confused with pulmonary embolism because of the lack of direct arterial involvement by the neoplasm. Primary pulmonary artery sarcoma can give both clinical and radiographic findings which can be confused with pulmonary embolism. However, the usual clinical presentation is that of a chronic or recurrent thromboembolic process.

Primary pulmonary carcinosarcoma is of two types, central and peripheral. The central type presents as an endobronchial mass lesion showing signs of bronchial obstruction, rather than arterial plugging. A central lesion is the more frequent presenting form. The peripheral form spreads rapidly and involves the mediastinum, pleura and chest wall as well as the vascular structures. The authors present their case of carcinosarcoma as the first reported in the literature to present mimicking acute pulmonary embolism. The authors suggest that these two forms of rare pulmonary neoplasm be included in the differential diagnosis of atypical types of acute or chronic pulmonary thromboembolism.

J. P. Eberts

Pulmonary edema and respiratory insufficiency in acute pancreatitis. Rovner AJ, Westcott JL (Hartford Hospital, Hartford, Connecticut). *Radiology* 118:513-520, March 1976

Pulmonary edema, cardiac enlargement, and respiratory insufficiency may occur in patients with acute pancreatitis. The

mechanisms are complex and incompletely understood, but probable etiologic factors include fluid overload, left ventricular failure, impaired respiratory excursion and microatelectasis, and a non-specific response of the lung to various types of pulmonary injury including hypotension, intravenous crystalloids, and the effects of circulating pancreatic enzymes. Recognition of the association of pulmonary edema and respiratory insufficiency with pancreatitis is important because early treatment with positive pressure breathing, careful fluid management and diuretics, and corticosteroids may prevent the development of irreversible respiratory failure.

Author's Abstract

Mushroom worker's lung disease. Stolz JL, Arger PH, Benson JM (Community General Hospital, Reading, Pennsylvania). *Radiology* 119:61-63, April 1976

Although usually considered a feature in mushroom worker's lung disease, hilar adenopathy was not found and only 8 of the authors' 26 patients exhibited positive radiographic findings. The etiology of the disease is allergic with a radiographic appearance of alveolitis which may present with consolidation or a reticular pattern. None of the 26 patients exhibited enlargement of the hilar lymph nodes. The acute phase subsides in 10 days to 6 weeks after exposure has ceased.

Author's Abstract

Pulmonary videodensitometry in the diagnosis of carcinoma of the lung. Reinke RT, Silverman NR, Rosen L, Helland DH (University Hospital, University of California at San Diego School of Medicine, La Jolla, California). *Radiology* 118:521-525, March 1976

Pulmonary videodensitometry is the densitometric analysis of pulmonary vascular pulsation. It involves converting the optical fluoroscopic image into an electronic one using a television system with high speed electronic computers for assessing vascular pulsations. Earlier workers demonstrated that centrally placed bronchogenic neoplasms result in impairment of pulmonary vascular pulsation. The phenomenon is obviously not a specific one and abnormalities of pulmonary vascular pulsation will be encountered in chronic bronchitis, asthma, emboli, and heart disease. It may have application, however, in determining operability or resectability of carcinoma once diagnosis has been established.

RHT

Swyer-James (Macleod's) syndrome. Gottlieb LS, Turner AF (Los Angeles County-University of Southern California Medical Center, Los Angeles, California). *Chest* 69:62-66, Jan 1976

Two cases of Swyer-James (Macleod's) syndrome are reported comparing this syndrome to pulmonary embolism and other intrapulmonic disorders. The patients in this report had clinical features suggestive of either pulmonary embolism, bronchiectasis, bronchitis, or a congenital pulmonary disorder. A detailed pulmonary-bronchial arterial investigation of the affected lung was part of the study. The authors point out that the distinctive radiographic signs of the Swyer-James syndrome can simulate other disease and these other etiologies must be excluded (i.e., unilateral hyperlucent lung of normal or decreased size with diminished lung markings, a smaller hilar shadow than the opposite lung, and slight displacement of the mediastinum to the affected side).

Bronchograms, perfusion lung scans, ventilation lung scans, pulmonary arteriograms and bronchial arteriograms were performed in these patients. The authors point out that the two basic pathophysiologic defects in the Swyer-James syndrome, unilateral bronchiectasis and hypoplasia of the pulmonary artery on the same side may result in reciprocal increase in bronchial arterial flow. While the etiology of this entity has not been clearly defined, two theories are postulated. One suggests that the initial abnormality occurs in

the peripheral bronchial tree following infection at an early age with secondary hypoplasia of the pulmonary artery. Another suggests that a primary unilateral pulmonary vascular anomaly exists that predisposes to bronchial and alveolar changes. One of the major warnings in the article is that the disorder may mimic pulmonary embolism and patients may have been subjected to protracted courses of anticoagulant therapy in error.

Anthony G. Peck

Cardiovascular

Diagnostic arteriographie des tumeurs parathyroïdiennes. (Arteriographic diagnosis of the parathyroid tumors.)

Jeukens JM, Delvigne J (Service de Radiodiagnostic de l'Université de Liège, Liège, Belgium). *J Belge Radiol* 58:213-223, May-June 1975

Seldinger first demonstrated the value of angiography in the localization of parathyroid tumors in 1954. Jeukens and Delvigne, employing a transfemoral approach, add nine cases to the 42 previously reported in literature. In the "global" technique, a 10 ml injection was made into the subclavian artery to opacify the inferior thyroid artery. If it was necessary to visualize the most distal branches, the authors introduced 15-20 ml of contrast medium. During injection, a blood pressure cuff was placed on the arm and inflated to above systolic reading. Rapid-sequence angiograms were taken in the anteroposterior and the oblique projections. In the "selective procedure" a rather rigid catheter, ending in a simple curve, was directed from the subclavian artery to the origin of the thyro-cervical branch and 4 ml of contrast was introduced, the blood pressure cuff was applied and followed by delayed roentgenograms. Angiographic findings can be summarized as: (1) increased caliber of the inferior thyroid artery; (2) variations in the course of the inferior thyroid artery; (3) appearance of a "blush"; (4) "staining." The authors believe the presence of two or more of these signs should be considered of definite diagnostic value in the localization of a parathyroid tumor.

A. F. Govoni

Pulmonary perfusion abnormalities and ventilation-perfusion imbalance in children after total repair of Tetralogy of Fallot.

Alderson PO, Boonvisut S, McKnight RC, Hartman AF Jr (Department of Radiology, 510 South Kingshighway Boulevard, Saint Louis, Missouri 63110). *Circulation* 53:332, Feb 1976

Palliative aortic-pulmonary shunts predispose to impaired perfusion of the shunted lung after total correction of Tetralogy of Fallot. The pulmonary perfusion of 25 children who had total surgical correction of Tetralogy of Fallot was evaluated by radio-nuclide perfusion scans. In addition, 18 had Xe ventilation studies. Previously 18 of the children had palliative systemic-pulmonary shunts: 14 had aortic-pulmonary shunts (Waterston or Potts-Smith) and four had Blalock-Taussig shunts. Seven children had single stage total corrections. An asymmetric perfusion pattern was found in 13 of the 18 who previously had systemic-pulmonary shunts, including 12 of 14 with previous aortic-pulmonary shunt. Asymmetric perfusion was significantly less common with single stage correction. Reasons offered for the discrepancy were: (1) elevated vascular resistance in the shunted lung; and (2) strictures of the pulmonary artery where it had been shunted and then taken down. Single stage correction is advocated.

Robert Frech

Traumatic pseudoaneurysms: a review of 23 cases. Bole PV et al. (New York Medical College, 106th Street and 5th Avenue, New York, New York 10029). *J Trauma* 16:63-70, Jan 1976

The authors report a series of 23 patients with traumatic pseudoaneurysms treated during a 5-year period. Twenty occurred as a result of penetrating injury while three occurred with only blunt trauma. Nine were distributed in the trunk, the remainder in the extremities. The clinical diagnosis was evident in all but two patients prior to angiography. A palpable pulsating mass was noted in 19 patients. Four were associated with arteriovenous fistulae. Two

instances of delayed rupture of iliac pseudoaneurysms were encountered. One aortic pseudoaneurysm caused late-onset hypertension because of renal artery compression.

Twenty-one patients were treated surgically while one patient with a hepatic artery aneurysm had spontaneous resolution. The various surgical methods employed were briefly reviewed. Those aortic aneurysm repairs employing intraluminal balloon catheters were described in greater detail. Potential errors in diagnosis, were cited and included (1) failure to perform the appropriate angiographic studies, (2) misinterpretation of the angiograms, and (3) unrecognized additional trauma during surgery. The second arterial injury may be missed because of inadequate exploration or because bleeding stopped during hypotension only to resume following resuscitation.

Curtis Northrop

Right ventricular growth in a case of pulmonic stenosis with intact ventricular septum and hypoplastic right ventricle. Rao PS, Liebman J, Borkat G (Department of Pediatrics, Medical College of Georgia, Augusta, Georgia 30902). *Circulation* 53:389-393, Feb 1976

Adequate growth of the hypoplastic right ventricle in a patient with severe pulmonary stenosis and intact ventricular septum was documented after pulmonary valvotomy in infancy. It is postulated that the growth of the ventricular chamber is largely the result of pulmonary regurgitation resulting from successful pulmonary valvotomy. Based on this and the observations of others on the growth of the hypoplastic right ventricle in patients with pulmonary atresia surgical correction can be planned in stages. Atrial septostomy, systemic pulmonary shunt, and valvotomy are recommended in infancy. Repair is completed at a later time. The staged correction is recommended for hypoplastic right ventricle associated with pulmonary atresia or stenosis with intact ventricular septum.

Robert Frech

Antibodies to radiographic contrast agents: induction and characterization of rabbit antibody. Brasch RC, Caldwell JL, Fudenberg HH (University of California School of Medicine, San Francisco, California). *Invest Radiol* 2:1-9, Jan-Feb 1976

An allergic, immunologic mechanism for certain adverse reactions to radiocontrast agents has been postulated on the basis of clinical and theoretical considerations. One obstacle to the acceptance of this allergic theory has been the inability to demonstrate significant antibodies with specificity for these agents. We attempted the induction of antibodies in the rabbit using analogues of radiocontrast media. The synthesis of four different analogues of commonly used radiocontrast agents allowed for testing the haptenic potential of various portions of the contrast medium molecule. Each analogue was conjugated to a carrier protein, emulsified in a suitable adjuvant, and repeatedly injected into several rabbits. Optimal immunization conditions were selected to increase the probability of antibody induction. Specific antibody was produced in good titer to each of the four haptens and in all injected rabbits. Antibodies were characterized by means of precipitation assays and radioimmunoassay using contrast agents labeled with ¹²⁵I. Antibody concentrations ranged from 0.23 to 2.7 mg/ml and varied with interval and frequency of booster injections. In addition to antibodies specific for the contrast media analogues, antibodies to the carrier protein were also detected. Antibodies were of the IgG class and in selected sera were 83-92% precipitable. The induction of antibodies to radiocontrast agents supports the allergic theory of contrast medium toxicity.

Author's Abstract

Angiographic appearance of the renal vein in a case of fibromuscular dysplasia of the artery. Rosenberger A, Adler O, Litchig H (Rambam University Hospital, Aba Khoushy School of Medicine, Haifa, Israel). *Radiology* 118:579-580, March 1976

Renal venography was performed in a patient suffering from hypertension due to fibromuscular dysplasia of the renal artery.

The venogram revealed morphological changes in the renal veins similar to those seen in fibromuscular dysplasia of the arteries. Histological examination of the veins showed fibrosis of the medial wall layer.

Author's Abstract

Bradykinin-induced changes in caliber of portal vein during splanchnic angiography. Aspelin P, Nylander G, Pettersson H (Roentgendiagnostic Department, Malmö Allmänna Sjukhus, Malmö, Sweden). *Invest Radiol* 2:10-13, Jan-Feb 1976

The caliber of the portal vein was investigated in two groups of patients subjected to celiac and mesenteric angiography. In one group, 10 patients (the controls) two angiographic series were performed without giving any pharmacum but the contrast medium. In the other group, 20 patients, also two angiographic series were performed but bradykinin 10 µg was given in the superior mesenteric artery before the second series. Injection of bradykinin resulted in a dilation of the portal vein in 18 of 20 patients, while there was no change in portal caliber in the controls.

Author's Abstract

Pressure dressings and postarteriographic care of the femoral puncture site. Christenson R, Staab EV, Burko H, Foster J (Vanderbilt University Medical Center, Nashville, Tennessee). *Radiology*, 119:97-99, April 1976

Patient dissatisfaction with prolonged bed rest and the discomfort caused by pressure dressings led to the following evaluation. Alternate application of pressure dressings and band-aids to femoral artery puncture sites was performed in 754 arteriographic examinations. The application of pressure dressings for 16-24 hours, especially in hypertensive patients, was found to be justified by a significant reduction in delayed bleeding requiring further medical attention. A minimum application time of 8 hours is supported because all instances of delayed bleeding occurred within 8 hours of the procedure. Arterial thrombosis is not affected by the use of pressure dressings. The rationale for recommendation of bed rest is largely anecdotal and is supported by almost all experienced angiographers responding to our questionnaire.

Author's Abstract

Effect of bradykinin on portal pressure and portal caliber in the dog: an experimental angiographic study. Aspelin P, Nylander G, Pettersson H (Roentgendiagnostic Department, Malmö General Hospital, Malmö, Sweden). *Invest Radiol* 2:14-19, Jan-Feb 1976

Portal pressure and caliber of the portal vein was examined in dogs after bradykinin injection (0.5 µg/kg bodyweight) into the superior mesenteric artery. Ten experiments were performed. The portal pressure rose from a mean of 10.4 cm H₂O to a mean of 21.2 cm H₂O after bradykinin injection. The portal vein was dilated in 8 of the 10 experiments. Also the portal circulation time was calculated and decreased after bradykinin injection. Thus, because of the increase in portal pressure and increase in portal circulation care should be exercised when injecting bradykinin into the superior mesenteric artery in patients with portal hypertension and imminent bleeding from oesophageal varices.

Author's Abstract

Clinical and angiographic features of pulmonary arteriovenous fistulas in children. Higgins CB, Wexler L (Stanford University Hospital, Stanford, California). *Radiology* 119:171-175, April 1976

Multiple pulmonary arteriovenous fistulas were demonstrated angiographically in 8 patients who exhibited cyanosis and polycythemia during childhood. Cyanosis was first observed during infancy in 5 patients. The diffuse (telangiectatic) type was present in 2 cases, while the remainder were of the multiple discrete type with one or two dominant fistulas. The clinical and angiographic features and surgical implications of multiple pulmonary arteriovenous fistulas in these children and those reported previously are discussed.

Author's Abstract

Velocity of ventricular wall motion determined by fluoroscopic videodensitometry: a noninvasive method for evaluating myocardial contractile state. Higgins CB, Helland DR, Rosen L, Silverman NR (University of California, San Diego, California). *Invest Radiol* 2:24-31, Jan-Feb 1976

Videodensitometry of the margins of the fluoroscopic image of the left ventricle (LV) was used to evaluate LV wall motion and differentiation of the wall motion signal reflected velocity of LV contraction (dV/dt) during various inotropic interventions in six anesthetized dogs. During these interventions heart rate, afterload and preload were maintained constant. Alterations in dV/dt were similar to changes in simultaneously measured LV peak dP/dt and the quotient of dP/dt and developed LV pressure, two widely accepted parameters of LV contractile state. Wide variations in preload and afterload caused no significant changes in dV/dt. Thus, the current study indicates that fluoroscopic videodensitometry provides a specific and reliable noninvasive method for evaluating LV contractile state.

Author's Abstract

The location of increased resistance to portal blood flow in obstructive jaundice. Reuter SR, Chuang VP (University of Michigan, Eloise, MI 48132). *Invest Radiol* 2:54-59, Jan-Feb 1976

The simultaneous measurement of wedged hepatic venous pressure and portal venous pressure at 11 and 28 days following common bile duct and intrahepatic bile duct obstruction reveals a significant elevation of the portal pressure at 28 days which is due primarily to increased presinusoidal resistance to portal blood flow. Portal venograms performed prior to sacrifice revealed moderate narrowing of the portal vein radicles and delayed emptying at 11 days and severe morphological alterations at 28 days. These results confirm the findings of other investigators and help to explain why the hemodynamic alterations occur so rapidly in obstructive jaundice, well before the development of significant biliary cirrhosis.

Author's Abstract

Vasodilator therapy for chronic left ventricular failure. Kovich RB, Tillish JH, Berens SC, Bramowitz AD, Shine KI (Division of Cardiology, UCLA School of Medicine, Los Angeles, California 90024). *Circulation* 53:322-328, Feb 1976

The effects of chronic oral vasodilator therapy were studied in a group of patients with refractory congestive heart failure. Fifteen patients were treated acutely with intravenous sodium nitroprusside and sublingual isosorbide dinitrate. After 72 hours the patients were placed on isosorbide dinitrate and oral phenoxybenzamine. Beneficial effects of the acute vasodilator therapy included reduction in pulmonary capillary wedge pressure and systemic vascular resistance, and increases in cardiac index and stroke work index. Mean arterial blood pressure and heart rate were unchanged. During the period of chronic vasodilator administration no other change in basic therapy was made. In the nine patients restudied after prolonged therapy with isosorbide dinitrate and phenoxybenzamine (3-21 months) the favorable effects observed acutely were maintained. All patients demonstrated symptomatic improvement with minimal side effects.

Robert Frech

Optimal resources for examination of the chest and cardiovascular system. Report of the Inter-Society Commission for Heart Disease Resources, MP Judkins, chairman. (American Heart Association, 7320 Greenville Avenue, Dallas, Texas 75231). *Circulation* 53A:1-37 Feb 1976

An ideal catheterization-angiographic laboratory is described and specifications are given for radiologic and physiologic equipment. The report discusses case loads for safe and effective performance as well as complication rates. Optimal location, affiliated laboratories, professional staff, administration, electrical safety, and radiation protection are among the many details analyzed. In addition, the report analyzes x-ray equipment for operating rooms, intensive care units, and conventional chest examination. This

monograph covers everything technical from power supply to developing and modulation transfer, and discusses roles for engineers, nurses, technicians etc. If you are planning a new catheterization lab or reviewing an existing one, this reference will help.

Robert Frech

Angiographic and radionuclide characteristics of hepatic angiosarcoma found in vinyl chloride workers. Whelan JG Jr, Creech JL, Tamburro CH (University of Louisville School of Medicine, Louisville, Kentucky). *Radiology* 118:549-557, March 1976

Cases of hepatic angiosarcoma have been discovered in Louisville, Kentucky among workers exposed to the polymerization of vinyl chloride, a material essential to the production of plastics. Investigation of the records of deceased employees of two vinyl chloride plants revealed an incidence of death from cancer of the liver and biliary tract 11 times greater than expected when compared to other workers of the same age group and sex. A systematic screening program studying all 1,180 workers of a Louisville vinyl chloride polymerization plant was undertaken.

Radiologic screening procedure included chest x-rays and a ^{99m}Tc -sulfur colloid liver-spleen scan. If the liver scan was positive, or if there were abnormal biochemical liver studies, further examinations were performed. Fifty individuals fell into these categories and were subsequently studied with hepatic and splenic angiography, transjugular hepatic venography, venous pressure studies, and liver biopsies. Four workers were found to have hepatic angiosarcomas. These appear as negative defects on liver scans which are distinctly peripheral in location. This preference for a peripheral site is probably responsible for the surgical finding of early direct extension through the liver capsule. The angiographic characteristics of these tumors appear to be: (a) a normal-sized hepatic artery, (b) peripheral tumor stain and puddling appearing during the midarterial phase and persisting as late as 34 seconds and, (c) some degree of hypovascularity of the central portion of the tumor. In one additional case, wedged hepatic venography apparently resulted in unrecognized hepatic infarction, and at the time of arteriography the following day showed as an area of peripheral stain and central hypovascularity. Surgical resection was carried out because of the pattern resembling angiosarcoma, but this was found to represent an infarct. Hepatic angiosarcoma is a tumor which arises from the endothelial cells lining the sinusoids. In the vinyl chloride workers, subcapsular and portal fibrosis, sinusoidal dilatation, and atypical sinusoidal lining cells have been found to coexist with this tumor. This atypical alteration of the lining cells could represent a precursor stage in the development of angiosarcoma.

RHT

Gastrointestinal

Diagnosis and management of bile duct strictures. Hermann RE (Cleveland Clinic Foundation, 9500 Euclid Avenue, Cleveland, Ohio 44106). *Am J Surg* 130:519-522, Nov 1975

The authors reviewed their experience with biliary strictures in 100 patients at the Cleveland Clinic. Ninety-three of these patients developed a stricture following a cholecystectomy and all strictures were in the common bile duct with one-half in the upper common bile duct. The patients generally presented with classic symptoms (intermittent chills, fever, and jaundice) and the radiologist played an important role in the diagnosis of the stricture. Indirect or intravenous cholangiography is not usually possible, since the patient invariably has increased bilirubin levels. The most valuable technique for bile duct visualization was percutaneous transhepatic angiography, which should be performed the morning of operation. Delay of more than 8 hours following the procedure was felt to markedly increase the danger of bile peritonitis from bile leakage at the site of needle entry into the liver. This technique was most useful in delineating the anatomy of the biliary tract above the stricture and was usually able to well delineate the site of the stricture. The other technique of retrograde cannulation of the ampulla (ERCP) was less useful in the presence of jaundice, because com-

plete occlusion of the duct precluded visualization of the all important proximal ductal system. Their results, using a variety of surgical techniques, were excellent with complete relief of symptoms in 84% of patients. The authors felt that a significant feature of their results was the better preoperative evaluation of the biliary tree using either transhepatic cholangiography or ERCP.

David M. Heimbach
Surgery, U.W.

Radiological and histological findings in six patients with alpha-chain disease. Doe WF, Henry K, Doyle FH (Royal Postgraduate Medical School, London W 12, England). *Br J Radiol* 49:3-11, Jan 1976

The tetrad of diarrhea, weight loss, abdominal pain, and finger clubbing in young patients from parts of the world where intestinal infections and infestations are common should suggest the possibility of alpha-chain disease. The radiologist should, in some circumstances, be able to suggest the diagnosis in his differential diagnosis of certain abnormalities seen on examination of the small bowel. In this series multiple fluid levels, minor degrees of flocculation and segmentation, and slight circular fold thickening, all being more marked proximally, were seen in all six patients. In three patients the changes were more specific showing coarse mucosal nodularity, coarse scalloping, and a spiky contour of the proximal small bowel being somewhat similar to those described in Waldenström's macroglobulinaemia. They corresponded with the small bowel appearances seen in other patients with this disorder. One patient had hypertrophic osteoarthropathy and another developed an ulcerating malignant duodenal tumor with cobblestone mucosa and multiple polypoid tumors extending from the jejunum to the rectum. Heavy chain fragments of IgA, free of light chains, were characteristically demonstrated in the serum of all six patients and in the urine and jejunal fluid of three. The jejunal biopsies in all six patients showed a diffuse and massive proliferation of predominantly plasma cells within the lamina propria associated with absent or short villi and with normal luminal epithelium and few and widely separated crypts. The histological and radiological assessments of severity in this series roughly corresponded.

T. Noel K. Allan

Intravenous cholangiography in the Rhesus monkey. Part I: determination of optimal iodipamide dose during a one-hour infusion. Wittenberg J, Maturi RA, Williams LF Jr, Teplick SK, Preblud SR, O'Brien JJ, Small DM (Boston University School of Medicine, Boston, Massachusetts 02215). *Invest Radiol* 2:45-53, Jan-Feb 1976

One-hour infusion intravenous cholangiography with iodipamide was performed in 3 rhesus monkeys with intact enterohepatic circulations. A series of four different doses including standard (0.3 ml/kg) and "double dose" (0.6 ml/kg) levels were compared. The 0.6 ml/kg dose resulted in significantly higher biliary iodine excretion and concentration than the lower two doses. A 1.2 ml/kg dose probably increased biliary iodine concentration a small amount when compared to the 0.6 ml/kg dose but did not increase iodine excretion. Peak iodine excretion and concentration occurred, on the average, at one hour. The excretion of iodine in the bile demonstrated no inhibitory effect on the concomitant excretion of bile salts.

Author's Abstract

Correlation of endoscopy and double-contrast radiography in the early stages of ulcerative and granulomatous colitis. Laufer I, Mullens JE, Hamilton J (McMaster University Medical Center, Hamilton, Ontario, Canada). *Radiology* 118:1-5, Jan 1976

Early radiological changes in ulcerative colitis include (a) finely granular mucosa due to hyperemia and edema, (b) mucosal stippling due to adherence of barium to superficial ulcers, and (c) coarsely granular mucosa due to ingrowth of granulation tissue. In granulomatous colitis, early changes include discrete, superficial ulcers, often against a background of normal mucosa, seen best *en face*. All of these changes can be demonstrated by the double-contrast technique. The radiological and endoscopic findings were

in agreement in 95% of the examinations in the authors' series. The importance of the technical aspects of the examination is stressed.

Author's Abstract

The role of serum albumin in the hepatic excretion of iodipamides. Song CS, Beranbaum ER, Rothschild MA (New York University School of Medicine, New York, New York 10010). *Invest Radiol* 2:39-44, Jan-Feb, 1976

The contrast agent for biliary tract visualization, iodipamide, is strongly bound to serum albumin. The relationship between the affinity of the contrast agent for albumin and its preferential uptake and excretion by the liver has been unclear. The role of serum albumin on hepatic uptake and excretion of iodipamide therefore was investigated on the isolated perfused rabbit liver. With the perfusate containing fully reconstituted rabbit plasma protein or 3.5 g/100 ml rabbit albumin alone, the iodipamide excretion is initially extremely slow. It then increases gradually to about 6 μ g/g liver per min by 60 minutes and thereafter remains constant. The half-time of transfer to the bile is about 130 min. Without albumin in the perfusate the initial clearance rate of iodipamide is rapid, with half-time transfer to the bile of about 40 min. Rabbit serum globulins have no effect on iodipamide excretion. Thus, binding of iodipamide to albumin retards the transfer of iodipamide from plasma to the bile, probably due to competition between albumin and the anion binding protein of the liver.

Author's Abstract

Plain-film findings in severe pseudomembranous colitis. Stanley RJ, Melson GL, Tedesco FJ, Saylor JL (Mallinckrodt Institute of Radiology, Saint Louis, Missouri). *Radiology* 118:7-11, Jan 1976

Plain-film abdominal changes in 5 patients with severe antibiotic-related pseudomembranous colitis were found to be strikingly similar and distinct from those seen in other colitides. These consisted of moderate gaseous distension of the colon and unusual wide transverse bands of thickened bowel wall associated with giant "thumbprinting" which was universal in distribution, with minimal or absent small-bowel abnormalities. While the radiographic findings were not pathognomonic, they were highly suggestive of advanced pseudomembranous colitis when combined with the clinical data. Prompt recognition of this entity by the radiologist is extremely helpful in management, since such patients frequently present with physical findings of an acute abdomen requiring surgery.

Author's Abstract

Saturation kinetics of iopanoate in dogs with an intact enterohepatic circulation before and after phenobarbital induction. Herzog RJ, Nelson JA, Staubus AE (University of California School of Medicine, San Francisco, California). *Invest Radiol* 2:32-38, Jan-Feb 1976

Capacity-limited elimination of sodium iopanoate and a reproducible apparent transport maximum (T_m) were demonstrated in nonoperated dogs having an intact enterohepatic circulation and normal endogenous bile salt pool. Using a multiple infusion technique, estimation of apparent T_m of iopanoate in the liver was possible without sampling either bile or urine. Values obtained for apparent T_m of iopanoate in dogs with normal bile salt pool were similar to those obtained in studies of dogs with chronic bile fistulas. Use of this technique in 4 dogs demonstrated that pretreatment with phenobarbital significantly increases apparent T_m of iopanoate.

Author's Abstract

Effects of some water-soluble contrast media on the colonic mucosa. Lutzger LG, Factor SM (Albert Einstein College of Medicine, Bronx, New York). *Radiology* 118:545-548, March 1976

Enemas of various solutions were administered to rats to determine if Gastrografin was specifically irritating to the colonic

mucosa. Gastrografin was found to cause considerably more inflammation than Hypaque-25, saline, or barium sulfate. Further studies with hypertonic sorbitol, Renografin-76, and Tween 80 suggested that (a) neither hyperosmolality nor the diatrizoate compound itself were damaging to the colon, and (b) Tween 80 most likely plays a major role in Gastrografin's inflammatory effect.

Author's Abstract

Hypotonic duodenography with glucagon. A clinical comparison study. Carsen GM, Finby N (St. Luke's Hospital Center, College of Physicians and Surgeons, New York, New York). *Radiology* 118:529-533, March 1976

Hypotonic duodenography is a well recognized method of evaluating the duodenum for intrinsic and extrinsic disease, especially that related to the pancreas. Agents employed initially were primarily anticholinergic drugs and then more recently glucagon, a straight-chain polypeptide which is normally produced by the alpha cells of the islets of Langerhans. This is a double-blind study using 39 clinical subjects to evaluate the effectiveness of glucagon as compared to Pro-Banthine. The study employed three intramuscular drug possibilities: 2 mg of glucagon, 45 mg of Pro-Banthine, or a 2 ml placebo. The participating radiologists did not know which drug had been administered. Preinjection base line films were obtained followed by appropriate fluoroscopic and overhead films after drug injection. In addition, patients were carefully questioned the following morning concerning side effects. The onset of action was not significantly different for the two drugs. Seventy-seven per cent of the glucagon patients and 92% of the Pro-Banthine patients had duodenal paralysis adequate for hypotonic study. Peristaltic activity returned to the pre-drug level more rapidly when glucagon was used. Although Pro-Banthine was shown to be slightly more effective as a hypotonic agent, its use was associated with a higher incidence of side effects and patient discomfort.

RHT

The normal endoscopic pancreatogram. Varley PF, Rohrmann CA Jr, Silvius SE, Vennes JA (Veterans Administration Hospital, Minneapolis, Minnesota). *Radiology* 118:295-300, Feb 1976

Pancreatograms of 102 patients with proved normal pancreatic status were reviewed to establish normal standards of pancreatic ductal morphology. Precise details of ductal course, position, length, caliber, and variant anatomy were analyzed. The ampulla was found at the level of the second lumbar vertebra in 75% of cases, while the pancreatic duct crossed the spine at L1 in most cases. Analysis of the course of the main pancreatic duct revealed a wide variety of course patterns. Approximately 75% of ducts ascend from the duodenum to the spine and have a horizontal orientation across the spine. The variance of normal ductal positions emphasizes the caution which must be applied to diagnosing pancreatic abnormalities solely on the basis of ductal position.

The mean maximal main pancreatic ductal diameters with standard deviations were found to be: head 3.1 mm (± 0.9); body 2.0 mm (± 1.7); tail 0.9 mm (± 0.4). The mean ductal length was found to be 169 mm with a range of 107-223 mm and standard deviation of ± 27 mm. The duct of Santorini was opacified in 62% of cases and a ventral pancreas was shown in three cases. Increase in ductal caliber with age was not shown. A pyelogram was seen in 26% of the patients, and was $2\frac{1}{2}$ times more frequent in patients in whom at least partial acinarization of the gland occurred.

Charles A. Rohrmann, Jr.

Diffuse cavernous hemangioma of the colon in the Klippel-Trenaunay syndrome. Ghahremani GG, Kangarloo H, Volberg F, Meyers MA (Virginia Commonwealth University, Medical College of Virginia Hospitals, Richmond, Virginia). *Radiology* 118:673-678, March 1976

The Klippel-Trenaunay Syndrome is a rare entity characterized by cutaneous hemangiomas, bone and soft tissue hypertrophy of the lower extremities, and congenital varicose veins. Diffuse cavernous hemangioma of the colon with striking radiologic find-

ings have not been previously described in this group of patients. The authors present two pediatric cases in which large infiltrative cavernous hemangiomas involved the left side of the colon. Plain films of the abdomen showed numerous phleboliths along the distribution of the rectum and left colon. Barium enema demonstrated nodular mucosal folds resembling esophageal varices as well as scalloped areas of irregular narrowing caused by the extramucosal portion of the hemangioma. Both patients experienced episodes of brisk rectal bleeding, and in one case, selective inferior mesenteric angiography was useful in demonstration of the vascular supply and extent of the hemangioma. Delineation and definition of the lesion is of importance to avoid endoscopic misinterpretation and biopsy.

RHT

Radiographic features of colitis associated with the hemolytic-uremic syndrome. Peterson RB, Meseroll WP, Shrago GG, Gooding CA (Letterman Army Medical Center, San Francisco, California). *Radiology* 118:667-671, March 1976

The hemolytic-uremic syndrome is a clinical entity similar to childhood thrombotic thrombocytopenic purpura. The disease begins in a previously healthy child who contracts gastroenteritis, followed by an intravascular coagulation disorder. Fibrin is deposited in the microvasculature of the kidneys and other organs, following which an anemia with characteristic morphologic red cell abnormalities develops. In the early stages of the gastroenteritis, severe bloody diarrhea predominates and the clinical presentation may mimic ulcerative colitis. The authors present four cases of colitis in this prodromal phase of the hemolytic-uremic syndrome. Abnormalities demonstrated by barium enema consist of filling defects, marginal serrations, and mucosal edema. Focal areas of dilatation and stenosis may also be present. The features are those of submucosal hemorrhage due to vascular occlusion and may be the earliest expression of the intravascular clotting. The appearance of the colon itself is not specific, but correlation with the clinical history and peripheral blood smear may clarify the complex.

RHT

Evaluation of the gastrocolic space in 100 cases of acute pancreatitis. Moreno G, Rivera HH (U.N.A.M. School of Medicine, General Hospital of Mexico, Mexico City, Mexico). *Radiology* 118:535-538, March 1976

From a group of 152 cases of acute pancreatitis, 100 with available abdominal plain films were selected for analysis. Four commonly appreciated plain-film signs of acute pancreatitis included the colon "cutoff" sign, the presence of a sentinel loop, displacement of the stomach, and generalized peritoneal reaction. These four signs occurred with a frequency of only 21%-27%. One of the earliest reported signs of acute pancreatitis was separation of the stomach and transverse colon, first described by Case in 1940. In normal individuals the greater curvature of the stomach is superimposed on the colon; when they are separated by a space, something generally is occupying the lesser sac. Normal variation exists however. Even in obese patients the gastrocolic space as seen on supine AP film does not measure over 3 cm. In 49% of these 100 patients, abnormal gastrocolic separation was demonstrable. The authors showed that if all five of these signs are utilized, 90 of the 100 cases showed diagnostic abnormalities on the plain abdominal film.

RHT

Surgical management of radiation injury to the small intestine. Swan RW, Fowler WC, Doronow RC (Department of Obstetrics Gynecology, University of Mississippi Medical Center, Jackson, Mississippi). *Surg Gynecol Obstet* 142:325, March 1976

The authors relate their experience with 45 patients suffering from radiation enteritis over a 20 year period, and compare their results to a review of other patients in English literature. They point out that while symptoms may develop any time from weeks to 32 years following radiation, the average onset of symptoms is within 2 years. Overall incidence varies from 1% to 5% of patients receiving

significant pelvic or transabdominal radiation therapy. Most common symptoms are those of partial intestinal obstruction, but gastrointestinal bleeding and weight loss are not uncommon. There are two acceptable surgical treatments for severe radiation enteritis: resection of the diseased segment with end to end anastomosis; and side to side bypass of the diseased segment. In the authors' series, the postoperative mortality from resection was 53%, but only 7% for the side to side bypass group. Postoperative anastomotic dehiscence occurred in 65% of the resection patients and 11% in the bypass group. The incidence of subsequent gastrointestinal symptoms was similar in both groups. The authors concluded that side to side anastomosis better preserved the tenuous blood supply to the radiated bowel and, therefore, caused fewer anastomotic leaks. The fear of a subsequent "blind loop syndrome" was not realized in their bypass treatment group, and since the complication rate was considerably lower, they suggest that bypass is the treatment of choice for severe segmental radiation enteritis.

David Heimbach
Surgery, U.W.

Treatment of volvulus of the colon by colonoscopy. Ali Ghazi A, Shinyah, Wolff W (Bethlehem Israel Medical Center, New York, New York 10003). *Ann Surg* 183:263-265, March 1976

Sigmoid volvulus is a disease of elderly and debilitated patients. Initial treatment by reduction with a rigid sigmoidoscope is successful in approximately 70% of cases. The authors feel that the flexible colonoscope may not only be a safer instrument, but that it can also reduce a volvulus occurring at a higher level than can be reached with the sigmoidoscope. The authors report their experience on two occasions with one patient who had a successful reduction by this means. While the colonoscope will undoubtedly prove to be a useful tool for the immediate management of sigmoid volvulus, two cautions should be mentioned. The recurrence rate after reduction will still be in excess of 50%, and, therefore, elective surgical resection should still be recommended during an asymptomatic period. Evidence of ischemia, manifested by bloody drainage or dark purple colonic mucosa, requires prompt abandonment of colonoscopic attempts to reduce the volvulus, and should lead to surgical intervention.

David M. Heimbach
Surgery, U.W.

A diagnostic technique for acalculous cholecystitis. Adams TW, Foxley EG (St. Charles Memorial Hospital, Bend, Oregon). *Surg Gynecol Obstet* 142:168-170, Feb 1976

The authors discuss the dilemma of the patient with a strong history of biliary symptoms but repeatedly normal oral cholecystograms. They studied a group of 26 patients with classic biliary symptoms and a control group of 22 patients with other intraabdominal diseases, but without biliary tract symptoms. All patients underwent a standard oral cholecystogram using six Telepaque tablets, and all gallbladders were radiologically normal. The patients then resumed their normal diets and reported back to the radiologist (36 hours after ingestion of Telepaque). A single plain film of the right upper quadrant was taken in each patient. All 26 patients with biliary symptoms had persistent opacification of the gallbladder, while none of the patients without biliary symptoms had persistent opacification. All patients underwent surgery and every patient with persistent opacification of the gallbladder was found to have significant gallbladder disease. Those without persistent opacification were found to have normal gallbladders.

Comment. The surgeon is very reluctant to remove a gallbladder that has been reported to be normal on oral cholecystogram. Most surgical clinics are filled with patients who have undergone five to 10 normal oral cholecystograms but still suffer from repeated episodes of biliary colic. This simple and noninvasive addition to the cholecystogram in highly suspicious patients may be a real advance in the management of these difficult patients.

David M. Heimbach
Surgery, U.W.

Genitourinary

Percutaneous needle endoscopy of renal cysts. Pollack HM, Goldberg EB (Episcopal Hospital, Temple University Health Sciences Center, Philadelphia, Pennsylvania). *Radiology* 118:723-724, March 1976

The authors have accomplished direct visualization of the interior of renal cysts by means of a tiny endoscope inserted through an ultrasonically guided needle. The endoscope has a diameter of 1.7 mm and fits through a cannula which approximates a 14-gauge needle. It is a fiberoptic system employing a forward-looking field with a 55-degree viewing angle and an inclined field with a 70-degree angle. Special attachments permit small pieces of tissue to be obtained for biopsy. Twelve patients were studied, all of whom had cystic lesions demonstrated by ultrasound. In nine patients these were simple unilocular cysts. One patient had a trilobular cyst, another had a trabecular bridging band, and the final patient had an organized hematoma with a large fibrin ball in its center. The authors view the procedure as experimental, but feel that it is worthy of further study. It is anticipated that as fiberoptic technology improves, development of wider visual angles will improve internal visibility, in addition to which the instruments will be smaller and more flexible.

RHT

Medial deviation of the ureters secondary to psoas muscle hypertrophy. Bree RL, Green B, Keiller DL, Genet EF (USAF Medical Center, Keesler Air Force Base, Mississippi 39534). *Radiology* 118:691-695, March 1976

Bilateral medial deviation of mid and distal portions of the ureters can occur as a normal finding in patients with psoas muscle hypertrophy. Two groups of patients are presented, both composed of young, healthy males. In 13 patients, the distance between the ureters at the narrowest point averaged 3.7 cm. Psoas muscle hypertrophy was evident radiographically and confirmed by ultrasound. In 20 patients with normal psoas muscles, the average minimum distance between the ureters was 7.1 cm. The importance of this observation is to avoid overdiagnosis of retroperitoneal disease in this group of young, muscular men. The differential diagnosis and several examples of this normal variant are presented.

Author's Abstract

The incidence and clinical importance of hystero-graphic evidence of cavities in the uterine wall. Slezak P, Tillinger KG (University School of Medicine, Linköping, Sweden). *Radiology* 118:581-586, March 1976

Filling of cavities in the uterine wall during hystero-graphy was observed in 54 of 320 surgically excised specimens in which metal threads had been inserted at different levels for identification. Adenomyosis may have accounted for these cavities in 24%. Cavities secondary to adenomyosis in one part of the uterus co-existed with cavities not etiologically related to the disease in another part. Adenomyosis is generally not involved in the pathogenesis of cavities in the lower half of the uterus and does not account for cavities of more than 5 mm in diameter.

Author's Abstract

Uriniferous perirenal pseudocyst: new observations. Meyers MA (The New York Hospital-Cornell University Medical Center, New York, New York). *Radiology* 111:539-545, Dec 1975

The chronic encapsulated extravasation of urine, most accurately designated as uriniferous perirenal pseudocyst, causes urine to collect within the cone of renal fascia. This results in a characteristic complex of radiographic findings including an elliptical soft-tissue mass in the flank oriented inferomedially with upward and lateral displacement of the lower renal pole, medial displacement of the ureter, obstructive hydronephrosis, and perhaps evidence of extravasation into the mass. Since the clinical recognition of the mass is typically delayed several weeks following the original traumatic episode, prompt radiological diagnosis is essential before irreparable damage to the kidney occurs.

Author's Abstract

Uterine artery calcification: its association with diabetes. Fisher MS, Hamm R (Temple University Medical School, Philadelphia, Pennsylvania 19140). *Radiology* 117:537-538, Dec 1975

Uterine artery calcification was observed in 26 patients. Fourteen of the 22 with adequate clinical information had diabetes mellitus. This is considered a significant association by the authors and calcification should raise the question of diabetes.

Author's Abstract

Duplication of the urethra. Effmann EL, Lebowitz RL, Colodny AH (Children's Hospital Medical Center, Boston, Massachusetts). *Radiology* 119:179-185, April 1976

Ten patients with patent urethral duplication are presented. Nine patients had two independent patent urethral channels originating from the bladder or the posterior urethra. Both voiding cystourethrography and retrograde urethrography are necessary to completely evaluate this anomaly. In each instance the ventral channel, regardless of the position of its meatus, proved to be the more functional urethra. In those patients whose dorsal channel was in an epispadiac position, the symphysis pubis was abnormally wide. A functionally and anatomically accurate classification is proposed, and the embryology of these anomalies is discussed.

Author's Abstract

Percutaneous nephropylotomy in the management of acute pyohydronephrosis. Barbaric ZL, Davis RS, Frank IN, Linke CA, Lipchik EO, Cockett, ATK (University of Rochester School of Medicine and Dentistry, Rochester, New York). *Radiology* 118:567-573, March 1976

Percutaneous nephropylotomy is a relatively simple procedure which can be readily performed under local anesthesia in any well equipped radiology department. The authors describe their experience with six patients who had urinary tract obstruction complicated by superimposed acute pyelonephritis. At the onset of their acute kidney disease most of these patients would have tolerated surgery poorly. Local anesthesia is introduced with a 15 cm thin 21-gauge needle introduced via a posterolateral approach. The nephropylotomy tube is a #18 Teflon needle catheter preshaped to a 90-degree curve and tailored with two side holes. By means of an angiographic guidewire the catheter is positioned with its tip in the uretero-pelvic junction and urine samples are taken for culture and sensitivity. The obstructed system can be irrigated with an appropriate antibiotic, and excellent antigrade urograms can be obtained by injecting contrast material through the tube. By establishing adequate drainage of the obstructed urinary system, together with adequate antibiotic and other supportive therapy, the patients can be prepared for elective definitive surgery.

RHT

Musculoskeletal

Staphylococcal osteomyelitis, sepsis, and pulmonary disease: observations of 10 patients with combined osseous and pulmonary infections. Felman AH, Shulman ST (University of Florida, Gainesville, Florida). *Radiology* 117:649-655, Dec 1975

Staphylococcal osteomyelitis with sepsis and associated pulmonary emboli is a potentially life threatening disease. In such patients the clinical picture of overwhelming toxicity coupled with the radiologic pattern of pulmonary infection may cause an obscure focus of bone or joint involvement to be overlooked. To be effective however, therapy must be directed toward both the pulmonary and the skeletal infection. Clinical and radiographic findings in 10 pediatric patients were reviewed. In eight patients the initial diagnostic and therapeutic emphasis was directed toward sepsis and pulmonary infection. Associated bone or joint involvement was suspected or proved at the onset of symptoms in only 12 patients. Radiographs of the chest showed definite abnormalities in nine of the 10 patients when first examined. The chest x-rays early in the course of the illness suggested septic embolic disease. One patient was initially normal on chest roentgenography, but diffuse infil-

trates developed within 48 hr. In four patients, soft tissue swelling was apparent at the onset of illness but underlying bones were normal. Three patients demonstrated typical radiologic changes of osteomyelitis from the outset. In six patients the skeletal infection was limited to bone, in one pyoarthritis was also seen, and three had combined bone and joint infection. In two patients, multiple bones were involved. Extreme toxicity and signs of bacteremia were seen in all but one patient. Initial concern with the sepsis and pulmonary disease resulted in delay in recognition and treatment of the primary skeletal infection for days and even weeks in most cases. Only one patient died. Six of the nine survivors exhibited residual pulmonary or skeletal abnormalities at their past examination. The authors emphasize the importance of prompt and accurate recognition of skeletal infections when sepsis and pulmonary septic emboli are present.

J. F. Bergstrom

Postirradiation atrophic changes of bone and related complications. Howland WJ, Loeffler RK, Starchman DE, Johnson RG (Aultman Hospital, 2600 Sixth Street, SW, Canton, Ohio 44710). *Radiology* 117:677-685, Dec 1975

The terms radiation osteitis, radiation necrosis of bone, and osteoradionecrosis have been used to describe bone changes following radiation therapy. The authors believe that the primary uncomplicated event is "atrophy" and that these changes in bone are very similar to atrophic changes of skin and mucous membranes. Bone atrophy is usually followed by reparative efforts, whereas the term necrosis implies irreversible death of tissue.

This study was confined to the shoulder girdle. Three groups of patients were analyzed following irradiation to this area for carcinoma of the breast. The groups were treated with different radiation energies: 200 kV, 25 MeV betatron photon, and cobalt 60-radiation. Atrophic changes were graded in degrees of severity. Mild changes consisted of coarsening of the trabecular pattern, slight to moderate cortical thickening, diffuse demineralization and rib thinning. Moderate atrophy showed significant diffuse demineralization and localized lytic and sclerotic changes. Severe changes were the same except for a greater degree of involvement. Group I received orthovoltage treatment. Bone changes were greatest in this group of 49 patients. Patients received 3,000-3,500 R midplane dose in 3-3½ weeks using opposed portals to the axillary-supraclavicular region. Because of the high ratio of bone to soft tissue absorption, the estimated total dose to bone was 9,540 rads using all correction factors. Mild atrophic changes were noted in 17 cases, moderate changes in 24, and severe changes in six patients. True necrosis with secondary infection of the bone and soft tissue was noted in two patients. One patient developed an example of hematogenous osteomyelitis in the radiation-altered bone. One high grade fibrosarcoma developed in the treatment field.

Group II consisted of 50 patients treated with 25 MeV betatron photon radiation. A tissue dose of 4,200 rads was administered in 4 weeks using a single anterior portal and 20 treatments. Of the 50 patients studied, none developed atrophic changes more marked than those of the "mild" category. Seven anterior rib fractures occurred and none experienced pain. All changes in this group were noted in the area of overlap between the supraclavicular field and tangential chest wall fields.

Group III received Radiocobalt radiation. A total of 4,500 rads was given in 25 treatments over a 5 week period. Mild atrophy was noted in four patients, moderate changes in three, and severe changes in one. All patients were asymptomatic. One patient showed fractures of the clavicle and the anterior ribs but had no significant pain.

The authors conclude that the basic atrophic process of bone seems to have clinical implications similar to the atrophic changes of skin or mucous membranes. Weakened bones should be protected against stress. Biopsies should be avoided. The term "necrosis" and "osteitis" should be avoided since they do not reflect the true pathology. Bone changes are more severe following equivalent exposure to kilovoltage than megavoltage radiation because of the higher ratio of bone to soft tissue absorption. Megavoltage therapy can also cause bone atrophy, but severe atrophy can usually be

avoided in most clinical situations. Differentiation from metastatic disease is usually possible. Metastatic disease gives a localized lytic or lytic and sclerotic area in otherwise normal appearing bone. Radiation atrophy on the other hand is evident in a diffuse manner, confined to the treatment portal. Uncomplicated atrophic changes were not apparent in less than 2 years after therapy.

Odin D. Skinner

Tibiotalar slant: a new observation in sickle cell anemia. Shaub MS, Rosen R, Boswell W, Gordonson J (LAC/USC Medical Center, Los Angeles, California). *Radiology* 117:551-552, Dec 1975

The homozygous form of sickle cell anemia is found in 0.3%-1.3% of the black population in the U.S. and 7%-9% will be affected by the heterozygous form of the disease. The effects of this disorder on the osseous structures, cardiopulmonary apparatus, kidneys, and central nervous system are well known and are not discussed in this article. The authors present several examples of a peculiar tibiotalar deformity process about the ankle joint which has been described in cases of hemophilic arthritis, juvenile rheumatoid arthritis, and multiple epiphyseal dysplasia, but has never been described in conjunction with sickle cell anemia. Sixty-three patients, ranging in age from 18-36 years, with clinical and laboratory evidence of sickle cell anemia were surveyed. Thirty-six (57%) had roentgenograms of one or both ankles and the tibiotalar angulation deformity was demonstrated in 14 (39%). Five patients showed unilateral changes while nine exhibited a definite bilateral tibiotalar slant. Eight occurred in men and six in women. The incidence and etiology of the tibiotalar slant is unknown but it is felt by the authors that the chronic hyperemia present in this condition and also in the previously mentioned conditions leads to an asymmetrical epiphyseal growth, bony and synovial ischemia, and progressive joint cartilage destruction, singly, or in combination, resulting in this wedged-shaped tibiotalar angulation deformity. The authors state that when this deformity is found in black patients, further examination for sickle cell disease should be done.

Donald N. Dysart

Poland's syndrome: a review of forty-three cases. Ireland D, Takayama W, Flatt A (University of Iowa, Iowa City, Iowa). *J Bone Joint Surg* 58A:52-58, Jan 1976

Poland's syndrome, hypoplasia of the hand with congenital aplasia of digits with incomplete syndactyly, is of unknown etiology. The authors reviewed 43 cases seen over the past 40 years at the University Hospital in Iowa City. Poland's syndrome may include hypoplasia of the breast and upper ribs, herniation of the lung, and elevated scapula. Early operative treatment to separate the syndactyly was recommended to fashion a useful hand with independent function.

Gerald R. Smith

Chondromalacia patellae. Insall J, Falvo A, Wise D (535 East 70th Street, New York, New York 10021). *J Bone Joint Surg* 58A:1-8, Jan 1976

In a prospective study of 105 arthrotomies for chondromalacia patellae, an increased Q-angle was found in most knees examined. The Q-angle is measured clinically and is formed by the line of pull of the quadriceps and the line of the patellar ligament. An angle of more than 20 degrees is considered abnormal. The abnormal alignment of the patella contributes to "indirect trauma" to the patella cartilage. The authors believe that trauma, either direct or indirect, is the etiology of chondromalacia patellae. The characteristic symptom was diffuse aching pain in the antero-medial aspect of the knee. Sometimes pain in the popliteal fossa made worse by activity or stair climbing was noted and often the pain was aggravated by prolonged sitting with the knee flexed. The lateral symptom is called "movie sign" or "theater sign." Roentgenograms of the patella were usually normal. Occasionally patella alta, lateral patella displacement, or fractures of the medial margin of the patella were found. Radiographs, therefore, had a role in excluding other disease processes but were not considered a primary diagnostic modality in proving chondromalacia.

Gerald R. Smith

Pulmonary Diseases Congress and Symposium

The Second Brazilian Congress and Third International Symposium on Pulmonary Diseases will be October 24–30 at the Hotel Meridien in Salvador, Bahia, Brazil. Sponsored by the Brazilian Society of Pulmonary Diseases and the Brazilian National Cancer Division, the meetings will be devoted to courses on such topics as chest radiology, acute respiratory insufficiency, oxygen transport, occupational lung diseases, chronic obstructive lung disease, lung morphology, and immunology. Official languages are Portuguese and English. Additional information may be obtained from Prof. Almério de Souza Machado, Centro Medico da Graca, Rua Humberto de Campos, 11–11, Salvador, Bahia, Brazil.

Hounsfield Named Scott Lecturer

Godfrey N. Hounsfield, inventor of the EMI head and body computed tomography scanner, has been named fifth annual Wendell G. Scott Lecturer. Hounsfield will speak at the Mallinckrodt Institute of Radiology on September 13. Hounsfield is a fellow of the Royal Society and has received the MacRobert Award, the Austrian Wilhelm Exner Medal, and the Lasker Award. The Scott lectureship was established at the Mallinckrodt Institute in 1972. Inquiries should be directed to Ronald G. Evens, Mallinckrodt Institute of Radiology, 510 South Kingshighway, St. Louis, Missouri 63110.

Mammography Seminar

A seminar-workshop on mammography is slated for September 30 through October 2 at the University of Wisconsin, Madison. Sponsor is the Department of Radiology and the fee is \$175. For additional information contact Dennis M. Day, 456 WARF, 610 North Walnut Street, Madison, Wisconsin 53706.

Diagnostic Radiology Symposium

The Department of Diagnostic Radiology, Lahey Clinic Foundation, will hold a symposium on general diagnostic radiology at the Copley Plaza Hotel, Boston, September 17–18. A \$100 fee will cover tuition, luncheons, reception, and banquet. The course carries 14 hours of category I credit. For more information, contact Carl R. Larsen, Program Chairman, Department of Radiology, Lahey Clinic Foundation, 605 Commonwealth Avenue, Boston, Massachusetts 02215.

Bone and Joint Seminar

A seminar on bone and joint radiology sponsored by the University of Toronto Faculty of Medicine is scheduled for October 29–30 at Mount Sinai Hospital, Toronto. Guest speakers will be Harold Jacobson and Elias P. G. Theros. Additional information is available from Postgraduate Medical Education, University of Toronto, Medical Sciences Building, Toronto, Canada, M5S 1A8.

Polytomography of the Temporal Bone

The fourteenth symposium on Polytomography of the Temporal Bone will be offered by the Wright Institute of Otology at Community Hospital, Indianapolis, September 11–12. The number of registrants is limited to 20 and course fee is \$250. The symposium is acceptable for 12 AMA Category I credit hours. Subjects to be

covered include basic anatomy of the temporal bone, technique of polytomography of the temporal bone, and pathological conditions revealed by polytomography, such as cholesteatoma, ossicular chain problems, otosclerosis, fractures, foreign bodies, tumors, and congenital anomalies. Inquiries should be directed to the Wright Institute of Otology, Community Hospital of Indianapolis, 1500 North Ritter Avenue, Indianapolis, Indiana 46219.

Diagnostic Ultrasound in Gastroenterology

Faculty has been announced for a symposium on Diagnostic Ultrasound in Gastroenterology and Urology, September 9–10, at the Johns Hopkins Hospital, Baltimore. The program is designed for the practicing ultrasonographer, gastroenterologist and urologist and is approved for 16 hours AMA Category I credit. Fee is \$150, \$100 for residents and technicians. Faculty members include D. Carpenter, B. Doust, T. Hendrix, F. Sample, R. Sanders, E. Smith, L. Von Micsky, P. Walsh, and F. Winsberg. For further details write to Janet B. Hardy, Department of Continuing Education, Johns Hopkins University School of Medicine, Baltimore, Maryland 21205.

Los Angeles Radiological Conference

The 29th annual Los Angeles Midwinter Radiological Conference will be at the Century Plaza Hotel in Los Angeles, January 28–30, 1977. The first day will consist of workshops for small groups covering diagnostic and therapeutic radiology, nuclear medicine, and ultrasound. On subsequent days, a panel of speakers will present scientific sessions. The second largest radiologic technical exhibit in the country will be open each day. A post convention seminar in Hawaii is also planned.

Additional information may be obtained from R. W. Thompson, Cedars-Sinai Medical Center, 4833 Fountain Avenue, Los Angeles, California 90029.

Stable Isotopes Symposium

An International Symposium on Biological Applications of Stable Isotopes will be held December 6–10 in Leipzig, German Democratic Republic. The symposium is sponsored by the International Atomic Energy Agency, Vienna, Austria, and the Council for Mutual Economic Assistance, Moscow, USSR. Topics will include: separation of stable isotopes, isotopic exchange reactions, photochemical reactions; synthesis of labelled molecules by organic synthesis, biosynthesis; isotope analysis methods, particularly mass spectrometry, emission spectrometry, NMR spectrometry, absorption spectrometry, and activation analysis; and applications of stable isotope tracers in biochemistry and pharmacology, biology, medicine, and agriculture.

Symposium participants must be nominated by the government of a member state of IAEA or CMEA or by an international organization that has been invited to participate. Participation forms should be sent to the official national authority (ministry of foreign affairs or national atomic energy commission) for transmission to the symposium's joint secretariat.

Radiobiological Research Symposium

The International Symposium on Radiobiological Research Needed for the Improvement of Radiotherapy will be November 22–26, 1976 in Vienna, Austria. Organized by the International

Atomic Energy Agency, the symposium will cover: problems and limitation of radiotherapy, nature of potential cancerous cells, dosimetric and fractionation aspects, high LET radiations; radiation and modifying agents; radiobiological aspects of clinical experiences; and late effect implications.

Participation in the symposium will be through nomination by the government of a member of the International Atomic Energy Agency or by an international organization that has been invited to participate. Participation forms should be sent to the appropriate national atomic energy authority for transmission to the IAEA.

Program of the Society for Pediatric Radiology

SEPTEMBER 20, 1976
WASHINGTON HILTON HOTEL

Morning

8:15. Primary abdominal sonography in the neonate. PJ Dempsey, AE Robinson, Mobile, Alabama

8:30. Neonatal Gastric Volvulus. JB Campbell, WS Davis, Denver

8:45. Gastric antral diaphragm. GD Shackelford, WH McAlister, St. Louis

9. Investigation of hemangiomas and hemangioendotheliomas of the liver. P Stanley, GF Gates, RT Eto, SW Miller, Los Angeles

9:15. Renovascular hypertension in infancy. D Merten, J Vogel, R Adelman, A Palubinskas, H Bogren, B Goetzman, Sacramento, California

9:30. Bronchopulmonary dysplasia and positive pressure respirator therapy—a changing pattern. GH Bicker, C Severn, Omaha

9:45. Chronic insufficiency of prematurity: roentgenographic and pathologic features. FM Volberg, AN Krauss, P Symchych, P Winchester, P Kleinman, PAM Auld, New York City

10. Radiography of infantile chlamydia pneumonia. KJ Kranzler, Chicago

10:15. Pulmonary sequestration and "pseudosequestration." RI Macpherson, L Whytehead, Winnipeg, Canada

11. Neuhauser Lecture. The lung—its growth and remodeling. L Reid, Boston

Afternoon

1:30. Computerized tomography of the body in pediatric patients. AM Schwartz, JC Leonidas, BL Carter, Boston

1:45. Pediatric tracheostomy: roentgen signs of normal healing and complications. Value of xerography. JR Scott, SS Kramer, Albany, New York

2. Restrictive chest disease: a ? complication of long-term chemotherapy. AS Tucker, AJ Newman, Cleveland

2:15. Multiple bladder diverticula in Williams syndrome. DP Babbitt, J Dobbs, T Good, Milwaukee

2:30. Single ectopic ureter. LH Prewitt, Jr., RL Lebowitz, Boston

2:45. Amputated ovary: a cause of migratory abdominal calcification. GW Nixon, VR Condon, Salt Lake City

3:15. Cholecystography in cystic fibrosis. PR L'Heureaux, JN Isenberg, HL Sharp, WJ Warwick, Minneapolis

3:30. Mucopolipidosis II (I cell disease) in infancy. H Patriquin, Sherbrooke, Canada; A Giedion, Zurich, Switzerland; P Kaplan, Montreal, Canada

3:45. Predicting the type of rickets from roentgenograms: is it possible? LE Swischuk, CK Hayden, Jr, Galveston

4. Histiocytosis X: a clinical and radiographic analysis and method for prognosis. WL Schey, I Garoon, R Port, JJ Conway, Chicago

4:15. Effects of radiation therapy on growing long bones. AA DeSmet, LR Kuhns, JV Fayos, JF Holt, Ann Arbor, Michigan

4:30. Forensic radiology's role in pediatrics. VG Mikity, Los Angeles

Radiologic Societies

International Societies

Fleischner Society. Secretary, E. Robert Heitzman, State University of New York Upstate Medical Center, Syracuse NY 13210. Annual Meeting: 1977, Town and Country Convention Center, San Diego CA, Feb 27-Mar 2.

Inter-American College of Radiology. Secretary, Gaston Morillo, Department of Radiology, Jackson Memorial Hospital, 1611 NW 12th Avenue, Miami FL 33136.

International Skeletal Society. Secretary-Treasurer, Jack Edeiken, Radiology Dept, Thomas Jefferson University Hospital, 11th and Walnut Sts, Philadelphia PA 19107. Third annual refresher course: Sept 13-15, 1976, Queen Elizabeth Hotel, Montreal, Canada.

International Society of Radiology. Hon. Secretary-Treasurer, W. A. Fuchs, Department of Diagnostic Radiology, University Hospital, Inselspital, CH-3010 Bern, Switzerland.

U.S. National Societies

American Association of Physicists in Medicine. Secretary, John Wright, Radiology Department, Geisinger Medical Center, Danville PA 17821.

American Board of Radiology. Secretary, C. Allen Good, Kahler East, Rochester MN 55901.

American College of Radiology. Executive Director, William C. Stronach, 20 N. Wacker Drive, Chicago IL 60606.

American Institute of Ultrasound in Medicine. Executive Secretary, Donna LaMaster, PO Box 25065, Oklahoma City OK 73125.

American Nuclear Society. Program Chairman, Ted D. Tarr, U.S. Energy Research and Development Administration, Mail Station A-436 Office of Assistant Administrator for Nuclear Energy, Washington DC 20545.

American Osteopathic College of Radiology. 1976 Program Chairman, Joseph C. Andrews, 13355 East Ten Mile Road, Warren MI 48089. 1977 Program Chairman, George O. Faerber, 1087 Dennison Avenue, Columbus OH 43201. Annual Meeting: Oct 17-21, 1976, New Orleans LA.

American Radium Society. Secretary, Richard H. Jesse, Dept of Surgery, M.D. Anderson Hospital and Tumor Institute, Houston TX 77025.

American Roentgen Ray Society. Secretary, James Franklin Martin, 300 S. Hawthorne Rd., Winston-Salem NC 27103. Annual Meeting: Washington Hilton, Washington D.C., Sept 20-24, 1976.

American Society of Neuroradiology. Secretary, Arthur E. Rosenbaum, University of Pittsburgh School of Medicine, Pittsburgh PA 15261.

American Society of Therapeutic Radiologists. Secretary, Robert W. Edland, 1836 South Ave., LaCrosse WI 54601. Annual Meeting: Oct 13-17, 1976, Hyatt Regency, Atlanta GA.

Association of University Radiologists. Secretary-Treasurer, Gerald T. Scanlon, Milwaukee County Medical Center, Milwaukee, WI 53226. Annual Meeting: April 30-May 4, 1977, Kansas City KA.

Health Physics Society. Executive Secretary, Richard J. Burk, Jr., 4720 Montgomery Lane, Bethesda MD 20014.

North American Society of Cardiac Radiology. Secretary-Treasurer, Erik Carlsson, University of California, San Francisco CA 94143.

Radiation Research Society. Executive Director, Richard J. Burk, Jr., 4720 Montgomery Lane, Bethesda MD 20014.

Radiological Society of North America, Inc. Secretary, Theodore A. Tristan, Fifteenth Floor, One MONY Plaza, Syracuse NY 13202. Annual Meeting: 1976 Nov 14-19; 1977, Nov 27-Dec 2; 1978, Nov 26-Dec 1, all in Chicago IL.

Section on Radiology, American Medical Association. Secretary, Antolin Raventos, Dept of Radiology, School of Medicine, University of California, Davis.

Society of Gastro-Intestinal Radiologists. Secretary-Treasurer, Walter Whitehouse, Dept of Radiology, University of Michigan, Ann Arbor MI 48104. Annual Meeting: Sept 16-19, 1976, Princess Hamilton Hotel, Bermuda.

Society of Nuclear Medicine. President, 475 Park Avenue S, New York NY 10016.

Society for Pediatric Radiology. Secretary-Treasurer, John P. Dorst, 601 N Broadway, Baltimore MD 21205. Annual Meeting: Sept 19-20, 1976, Washington Hilton, Washington, D.C.

The Society of Uroradiology. Secretary-Treasurer, Howard M. Pollack, Dept of Radiology, Episcopal Hospital, Front St at Lehigh Ave, Philadelphia PA 19125. Annual Meeting: Sept 20, 1976, Washington Hilton, Washington DC.

U.S. State and Local Societies

Alabama

Alabama Academy of Radiology. Secretary-Treasurer, Lawrence E. Fetterman, 1720 Springhill Ave, Suite 201, Mobile AL 36604.

Section of Radiology, National Medical Association. Secretary, Ivy Brooks, Dept of Radiology, Veterans Administration Hospital, PO Box 511, Tuskegee AL 36083.

Southern Radiological Conference. Secretary-Treasurer, J. W. Maxwell, PO Box 2144, Mobile AL 36601. Annual Meeting: Jan 28-30, 1977, Grand Hotel, Point Clear AL 36564.

Alaska

Alaska Radiological Society, Chapter ACR. Secretary-Treasurer, John J. Kottra, 3200 Providence Ave, Anchorage AK 99504.

Arkansas

Arkansas Chapter of ACR. Secretary-Treasurer, Richard Seibold, Jr., Wadley Hospital, Texarkana AR-TX 75501.

Arizona

Arizona Radiological Society, Chapter of ACR. Secretary, Irwin M. Freundlich, 1501 N Campbell Ave, Dept of Radiology, Tucson AZ 85724.

California

California Radiological Society, California Chapter of ACR. Executive Secretary, J. Michael Allen, 1225 8th St, Suite 590, Sacramento CA 95814.

East Bay Radiological Society. Secretary-Treasurer, Richard H. Culhane, 4 Vista del Mar, Orinda CA 74563.

Los Angeles Radiological Society. Secretary, Arthur F. Schanche, 333 N Prairie Ave, Inglewood CA 90301.

Northern California Radiological Society. Secretary, Patrick J. Ginnell, 1207 Fairchild Ct, Woodland CA 95695.

Northern California Radiotherapy Association. Secretary-Treasurer, John D. Earle, Stanford Medical Center, Stanford CA 94305.

Orange County Radiological Society. R. Lawrence Argue, 100 E Valencia Mesa Dr, Fullerton CA 93632.

Radiological Society of Southern California. Secretary-Treasurer, Duane Eugene Blickenstaff, La Jolla Radiology Medical Group, Inc, 7849 Fay Ave, La Jolla CA 92037. Meetings: Oct 1976, Santa Barbara; Dec 1976, Newport; Feb 1977, Palm Springs.

Redwood Empire Radiological Society. Secretary, Hal B. Peterson, 357 Perkins St, Sonoma CA 95476.

San Diego Radiological Society. President, Donald J. Fleischli, 7849 Fay Ave, La Jolla CA 92037.

San Francisco Radiological Society. Secretary-Treasurer, Philip A. Brodey, Dept of Radiology, Mt Zion Hospital, P.O. Box 7921, San Francisco, CA 94120.

South Coast Radiological Society Chapter of ACR. Secretary-Treasurer, Brian R. Schnier, Dept of Radiology, Cottage Hospital, Pueblo at Bath, Santa Barbara CA 93105.

Southern California Radiation Therapy Society. Secretary-Treasurer, Jerome Stuhlberg, 514 N Prospect, Redondo Beach CA 90277.

Colorado

Colorado Radiological Society, Chapter of ACR. Secretary, John Pettigrew, 2215 N Cascade, Colorado Springs CO 80907.

Rocky Mountain Radiological Society. Secretary-Treasurer, Lorenz R. Wurtzbaach, 4200 E 9th Ave., Denver CO 80220.

Connecticut

Connecticut Valley Radiologic Society. Secretary-Treasurer, Gerald N. LaPierre, 759 Chestnut St., Springfield MA 01107.

Radiological Society of Connecticut, Inc. Secretary, Gerald L. Baker, 85 Jefferson St., Hartford CN 06106.

Delaware

Delaware Chapter of ACR. Secretary, Ekkehard S. Schubert, Wilmington Medical Center, PO Box 1951, Wilmington DE 19899.

District of Columbia

Section on Radiology, Medical Society of the District of Columbia. Secretary-Treasurer, Albert M. Zelna, 21 Masters St., Potomac MD 20854.

Florida

The Florida Radiological Society, Chapter of ACR. Secretary, J. T. Johnson, P.O. Box 2075, Sanford, FL 32771.

The Florida West Coast Radiological Society, Inc. Secretary-Treasurer, Aaron Longacre, 501 E. Buffalo Ave., Tampa FL 33606.

Greater Miami Radiological Society. Secretary, David C. Hillman, PO Box 610544, North Miami FL 33161.

North Florida Radiological Society. Secretary, Charles E. Bender, 1430 16th Ave S., Jacksonville Beach FL 32250.

Georgia

Atlanta Radiological Society. Secretary-Treasurer, James H. Larose, Dept of Nuclear Medicine, South Fulton Hospital, East Point GA 30344.

Georgia Radiological Society, Chapter of ACR. Secretary, Theodora Vanderzalm, Dept of Radiology, Medical College of Georgia, Augusta, GA 30902.

Hawaii

Hawaii Radiological Society, Chapter of ACR. Secretary-Treasurer, Michael J. McCabe, Straub Clinic and Hospital, Honolulu HI 96813.

Illinois

Chicago Radiological Society, Division of the Illinois Radiological Society, Chapter of ACR. Secretary-Treasurer, Harold J. Lasky, 55 E. Washington St., Suite 1735, Chicago IL 60602.

Illinois Radiological Society, Inc., Chapter of ACR. Secretary, Robert D. Dooley, Hinsdale Medical Center, Hinsdale IL 60521.

Indiana

Tri-State Radiological Society. Secretary Thomas Harmon, St. Mary's Hospital, Evansville IN 47750.

Iowa

Iowa Radiological Society, Chapter of ACR. Secretary-Treasurer, Dale L. Roberson, 1948 First Ave NE, Cedar Rapids IA 52402.

Kansas

Kansas Radiological Society, Chapter of ACR. Secretary-Treasurer, Stephen J. Tempero, 310 Medical Arts Bldg., Topeka KA 66604.

Kentucky

Bluegrass Radiological Society. Secretary-Treasurer, James King, 3313 Overbrook Dr., Lexington KY 40504.

Kentucky Chapter of ACR. Secretary-Treasurer, John Hummel, Jr., Kentucky Baptist Hospital, Louisville KY 40204.

Louisiana

Ark-La-Tex Radiological Society. Secretary, Erich K. Lang, Confederate Memorial Medical Center, LSU School of Medicine, Shreveport LA 71101.

Louisiana Radiological Society, Chapter ACR. Secretary-Treasurer, Stover L. Smith, 250 Vincent Ave., Metairie LA 70005.

Section on Radiology, Southern Medical Association. Secretary, Michael Sullivan, 1514 Jefferson Highway, New Orleans LA 70121. Annual Meeting: Nov 7-10, 1976, New Orleans.

Maine

Maine Radiological Society, Chapter of ACR. Secretary-Treasurer, Peter E. Giustra, Dept of Radiology, Penobscot Bay Medical Center, Rockland ME 04841.

Maryland

Maryland Radiological Society, Chapter of ACR. Secretary, David S.

O'Brien, Anne Arundel Hospital, Annapolis MD 21401.

Massachusetts

Massachusetts Radiological Society, Chapter of ACR. Secretary, Joseph T. Ferrucci, Jr., Massachusetts General Hospital, Boston MA 02114.

New England Roentgen Ray Society. Secretary, Melvin E. Clouse, 185 Pilgrim Rd., Boston MA 02115.

Northeastern Society for Radiation Oncology. Secretary, C. C. Wang, Massachusetts General Hospital, Boston MA 02114.

Michigan

Michigan Radiological Society, Chapter of ACR. Secretary-Treasurer, Francis P. Shea, Bon Secours Hospital, 468 Cadieux, Grosse Pointe MI 48230.

Michigan Society of Therapeutic Radiologists. Secretary-Treasurer, William T. Knapp, St. Mary's Hospital, 830 S. Jefferson, Saginaw MI 48601. Annual Meeting: Sept 1976, Ann Arbor.

Minnesota

Minnesota Radiological Society. Secretary-Treasurer, Marvin E. Goldberg, Box 292, Mayo Memorial Health Sciences Center, Minneapolis MN 55455.

Missouri

Greater Kansas City Radiological Society. President, Secretary, Jay I. Rozen, Suite 216, 6400 Prospect, Kansas City MO 64132.

Greater St. Louis Society of Radiologists. Secretary-Treasurer, William B. Hutchinson, 2821 Ballas Rd., St. Louis MO 63131. Annual Meeting: Oct 1976, St. Louis.

Missouri Radiological Society, Chapter of ACR. Secretary-Treasurer, Donald G. Evens, Mallinckrodt Institute of Radiology, 510 S. Kingshighway, St. Louis MO 63110.

Mississippi

Mississippi Radiological Society, Chapter of ACR. Secretary-Treasurer, James B. Barlow, 514B E. Woodrow Wilson, Jackson MS 39216.

Nebraska

Nebraska Chapter of ACR. Secretary-Treasurer, Charles A. Dobry, Dept of Radiology, University of Nebraska Medical Center, 42nd at Dewey, Omaha NB 68105.

New Hampshire

New Hampshire Chapter of ACR. Secretary-Treasurer, Edward P. Kane, Claremont General Hospital, Claremont NH 03743.

New Jersey

Radiological Society of New Jersey, Chapter of ACR. Secretary, Fred M. Palace, 2424 Morris Ave., Union NJ 07083.

New Mexico

New Mexico Society of Radiologists, Chapter of ACR. Secretary, W. M. Jordan, 1100 Central Ave SE, Albuquerque NM 87106.

New York

Bronx Radiological Society, New York State, Chapter of ACR. Secretary-Treasurer, Leon J. Corbin, 1369 Rosendale Ave., Bronx NY 10472.

The Brooklyn Radiological Society. Secretary-Treasurer, Ralph Braccaccio, 7901 4th Ave., Brooklyn NY 11209.

Buffalo Radiological Society. Secretary, Jerald P. Kuhn, 9267 Jennings Rd., Eden NY 14057.

Central New York Radiological Society. E. Mark Levinsohn, Radiology Dept, Upstate Medical Center, 750 E. Adams St., Syracuse NY 13210.

Kings County Radiological Society. Secretary, Melvin Moore, 7815 Bay Parkway, Brooklyn NY 11214.

Long Island Radiological Society. Secretary, Harry L. Stein, North Shore University Hospital, 300 Community Dr., Manhasset NY 11030.

Mid-Hudson Radiological Society. Secretary-Treasurer, William D. Stiehm, 37 Flower Hill Rd., Poughkeepsie NY 12603.

New York Roentgen Society. Secretary-Treasurer, Thomas C. Beneventano, 111 E 210th St., Bronx NY 10467. Spring Conference: April 28-30, 1977, Waldorf Astoria Hotel, New York City.

New York State Chapter of ACR. Secretary-Treasurer, Albert F. Keegan, 6 Secor Dr., Port Washington NY 11050.

Northeastern New York Radiological Society. Secretary, Donald R. Morton, Dept of Radiology, St. Clare's Hospital, Schenectady NY 12304.

Rochester Roentgen Ray Society. Secretary-Treasurer, Robert J.

Bruneau, 1441 East Ave. Rochester NY 14610

Westchester County Radiological Society. Secretary Michael K. Kauff, 170 Maple Ave. White Plains, NY 10601.

Nevada

Nevada Radiological Society, Chapter of ACR. Secretary, Charles F. Veverka, Carson Tahoe Hospital, Carson City NV 89701.

North Carolina

Catawba Valley Radiological Society. Secretary, J. N. Owsley, 18 13th Ave. NE, Hickory NC 28601.

North Carolina Chapter of ACR. Secretary-Treasurer, Ernest B. Spangler, Wesley Long Hospital, Greensboro NC 27402. Annual Meeting: Nov 1976, Mid-Pines Club, Southern Pines NC.

North Dakota

North Dakota Radiological Society, Chapter of ACR. Secretary, H. C. Walker Jr., PO Box 624, Devils Lake, ND 58301

Ohio

Central Ohio Radiological Society. Secretary-Treasurer, John Johnson, 3016 Asbury Rd, Columbus, OH 43221

Cleveland Radiological Society. Secretary-Treasurer, Charles M. Greenwald, 7007 Powers Blvd, X-ray Department, Parma OH 44129

Northwestern Ohio Radiological Society. Secretary, Gerald Marsa, 3939 Monroe St. Toledo OH 43606

Ohio State Radiological Society, Chapter of ACR. Secretary, James Farmer, 3461 Warrensville Center Rd, Cleveland OH 44122

Oklahoma

Northeastern Oklahoma Radiological Society. Secretary, William L. Lavendusky, 100 Center Plaza Suite, C, Tulsa OK 74119.

Oklahoma State Radiological Society, Chapter of ACR. Secretary, Bob G. Eaton, 2508 Stillmeadow Rd, Edmond OK 73034. Annual Meeting Oct 1-3, 1976, Shangri-La Lodge on Grand Lake, Afton OK.

Oregon

Oregon State Radiological Society, Chapter of ACR. Secretary-Treasurer, Ray F. Friedman, 3324 SW 44th St, Portland OR 97221

Pennsylvania

Philadelphia Roentgen Ray Society. Secretary, Marvin E. Haskin, 230 N Broad St, Philadelphia PA 19102

Pittsburgh Roentgen Society. Secretary, Klaus M. Bron, Presbyterian University Hospital, Pittsburgh 15261.

Rhode Island

Radiological Society of Rhode Island, Chapter of ACR. Secretary, Stefan Frater, Rhode Island Hospital, Providence RI 02902.

South Carolina

South Carolina Radiological Society, Chapter of ACR. Secretary, George W. Brunson, 4315 Woodleigh Rd, Columbia SC 29206

Tennessee

Memphis Roentgen Society. Secretary-Treasurer, D. Randolph Ramey, Baptist Memorial Hospital, 899 Madison Ave., Memphis TN 38140

Tennessee Radiological Society, Chapter of ACR. Secretary-Treasurer, Jerry W. Grise, Methodist Hospital, 1265 Union Ave, Memphis TN 38104.

Texas

Central Texas Radiology Society. Secretary-Treasurer, E. Jerome Scholar, Scott and White Clinic, Temple TX 76501

Dallas-Fort Worth Radiological Society. Secretary-Treasurer, William V. Bradshaw, 777 W Rosedale Suite 260, Ft. Worth TX.

Houston Radiological Society. Secretary, Thomas S. Harle, 103 Jesse H. Jones Library Bldg, Texas Medical Center, Houston TX 77030

Louisiana-Texas Gulf Coast Radiological Society. Secretary-Treasurer, J. Gardiner Bourque, 3155 Stagg Dr, Suite 230 Doctors Bldg, Beaumont TX 77701

San Antonio Civilian Military Radiological Society. Secretary, Jose Maria Chao, Diagnostic Clinic, San Antonio TX.

Texas Radiological Society, Chapter of ACR. Secretary-Treasurer, Donald N. Dysart, Scott and White Clinic, Temple TX 76501. Annual Meeting March 17-19, 1977, Fairmont Hotel, Dallas TX.

Vermont

Vermont Radiological Society, Chapter of ACR. Secretary, Peter Dietrich, Medical Center Hospital of Vermont, Burlington VT 05401

Virginia

Mid-Shenandoah Valley Radiological Society. Secretary, Kenneth L. Dwyer, King's Daughters Hospital, Staunton VA 24401

Richmond Radiological Society. Secretary, Melvin Vinik, 9504 Carterwood Rd, Richmond VA 23229

Virginia Chapter of ACR. Secretary-Treasurer, Charles P. Winkler, 3500 Kensington Ave Suite 2-A, Richmond VA 23221

Washington

Pacific Northwest Radiological Society. Secretary-Treasurer, Kenneth D. Moores, 1118 9th Ave, Seattle WA 98101. Annual Meeting: May 6-8, 1977, Victoria, B.C., Canada

Washington State Radiological Society, Chapter of ACR. Secretary-Treasurer, Donald J. Hesch, 3216 NE 45th Pl, Seattle WA 98105

West Virginia

West Virginia Radiological Society, Chapter of ACR. Secretary-Treasurer, Andrew W. Goodwin II, 200 Medical Arts Bldg., Charleston WV 25301.

Wisconsin

Milwaukee Roentgen Ray Society. Vice President, Thomas C. Lipscomb, 1004 N 10th St, Milwaukee WI 53233

Wisconsin Radiological Society, Chapter of ACR. Secretary-Treasurer, June Unger, Wood VA Hospital, Wood WI 53193

Wisconsin Society of Therapeutic Radiologists. Secretary, M. Greenberg, Milwaukee County General Hospital, 8700 W Wisconsin Ave, Milwaukee WI 53222

Wyoming

Wyoming Radiological Society, Chapter of ACR. Secretary, Thomas E. Hettinger, 1609 E 19th St, Cheyenne, WY

Canada

Canadian Association of Radiologists. Honorary Secretary, C. Germain Beauregard, Suite 806 1440 St. Catherine St W, Montreal, Quebec Canada

Edmonton and District Radiological Society. Secretary B. Caplan, 12320 103rd Ave, Edmonton, Alberta T5N 0R2, Canada.

Toronto Radiological Society. Secretary, H. Shulman, Sunnybrook Hospital, 2075 Bayview Avenue, Toronto, Ontario, Canada.

Central and South America

Sociedade Brasileira de Radiologia. Secretary, Walter Vieira de Azevedo, Caixa Postal P532, Rio de Janeiro, Brasil.

Sociedad Chilena de Radiologia. Secretary, Manuel Neira, Casilla 13426, Santiago, Chile.

Sociedad Colombiana de Radiologia. Secretary General, Gustavo Sanchez Sanchez, Bogotá, Colombia. Annual Meeting: Feb 1977, Manizales (Caldas) Colombia

Sociedad de Radiologia del Atlantico. Secretary, Raul Fernandez, Calle 40 #41-110, Baranquilla, Colombia. Annual Meeting: Feb 3, 1977, Baranquilla, Colombia.

Sociedad de Radiologia, Radiotherapéutica y Medicina Nuclear de Rosario. Secretary-General, Marcela Muñoz, Santa Fe 1798, Rosario, Argentina

Europe

Bavarian-American Radiologic Society. Secretary, Stuart A. O'Byrne, Radiology Service, Stuttgart, West Germany, 5th General Hospital, APO NY 09154.

British Institute of Radiology. Honorary Secretaries, D. H. Trapnell, P. N. T. Wells, 32 Welbeck St, London, W1M 7PG, England.

Čekoslovenská Radiologická Společnost. Secretary, Jaromír Kolář, Radiological Clinic, Parha 2, Unemocnice 2, Czechoslovakia

Danish Radiological Society. Secretary General, Johannes Praestholm,

Radiological Department I, Bispebjerg Hospital, DK-2400, Copenhagen NV
Deutsch Röntgengesellschaft. President, Wolfgang Frik, Dept of Radiology, Techn Univ Aachen, D-5100 Aachen, Goethestrasse 27/29, West Germany.

European Society of Pediatric Radiology. Secretary, U. Willi, E.S.P.R., Kinderspital, Steinwiesstr. 75, Zurich, Switzerland 8032, CH. Permanent Secretary, C. Fauré Service de Radiologie, Hôpital des Enfants Malades, 149 rue de Sèvres, 75 730, Paris Cedex 15. Fourteenth Annual Congress: May 12-14, 1977, Luzern, Switzerland.

Faculty of Radiologists, Royal College of Surgeons in Ireland. Honorary Secretary, M. J. Ryan, St. Stephen's Green, Dublin 2, Ireland. Annual Scientific Meeting: Oct 8-9, 1976, Dublin. Combined meeting of Radiologists/Radiological Society of Ireland and Radiological Section of Royal Academy of Medicine, March 11-12, 1977, Galway.

The Hospital Physicists' Association. Honorary Secretary, R.F. Mould, Westminster Hospital, Physics Department, Page St. Wing, London SW1P 2AR, England.

Norsk Forening for Medicinsk Radiologi. General Secretary, Arnulf Skjennald, Ullevål sykehus, Oslo, Norway.

Nederlandse Vereniging voor Radiologie. Secretary, H.E. Schütte, Department of Radiology, Elizabeth Gasthuis, Haarlem, Netherlands.

Royal College of Radiologists. Secretary, P.D. Thomson, 28 Portland Pl. London, W1N 4DE, England.

Scandinavian Radiological Society. Secretary-General, C.-E. Unnérus, Havsvindsv. 5C, 02120 Esbo 12 (Hägalund-Tapiola) Finland.

Schweizerische Gesellschaft für Radiologie und Nuklearmedizin.
Société Suisse de Radiologie et de Médecine Nucleaire. Secretary, Gustav A. Schoch, 7 Gellertstrasse, CH-4052 Basel, Switzerland.

Sociedad Española de Radiología y Electrológica Médicas y de Medicina Nuclear. Secretary-General, Pilar Gallar Barberá, Villanueva, Madrid 1, Spain.

Società Italiana di Radiologia Medica e Medicina Nucleare. Administrative Secretary, R. Dall'Acqua, Ospedale Mauriziano, 10128, Torino, Italy. Annual Meeting: Sept 25-28, 1976, XXVII Congresso Nazionale, SIRMN—BARI—Campus Universitario Via Re David, Italy.

Société Française de Radiologie Médicale, Médecine Nucleaire et Electrolologie. Secretary-General, J. Sauvegrain, Hôpital des Enfants-Malades, 149 Rue de Sèvres, 75730 Paris Cedex 15, France. Annual Meetings: 1976, Nov 15-18, Centre International de Paris (Porte Maillot); 1977, Nov 15-18, Centre International de Paris.

Société Française de Neuroradiologie. Secretary-General, R. Djindjian, 16, rue de l'Université 75, Paris 7^e, France.

Society of Pediatric Radiology. Secretariat, PO Box 272, S-101 23 Stockholm, Sweden.

Société Royale Belge de Radiologie (Koninklijke Belgische Vereniging voor Radiologie). Secretaries-General: A. L. Baret, University Hospital, 3000 Leuven, Belgium; L. Jeanmart, Institut Bordet, 1000 Bruxelles, Belgium.

Svensk Förening för Medicinsk Radiologi. Secretary, Hans Ringertz, Department of Pediatric Radiology, Karolinska Sjukhuset, S-104 01 Stockholm, Sweden. Annual Meeting: Dec. 1-4, 1976, Stockholm, Sweden.

Africa

Association of Radiologists of West Africa. Honorary Secretary, A. A. Obisen, Department of Radiology, University College Hospital, Ibadan, Nigeria. Annual Meeting: Feb 4-5, 1977, Accra, Ghana.

Radiological Society of South Africa. Secretary, Dr. A. Visser, P.O. Box 8850, Johannesburg, South Africa.

South African International Radiological Congress. Director, Dr. Paul Snieder, P. O. Box 4878, Johannesburg, South Africa. Annual meeting: Sept 1976, Durban Annual Congress; Oct 1978, International and National Congress.

Near East and Asia

Bengal Radiological Association. Honorary Secretary, B. Chatterji, 262 Rash Behari Ave, Calcutta 700019, India. Annual Meeting: Dec 10, 1976, 3-1 Madan St, Calcutta 700013, India.

Indian Radiological Association. Honorary General Secretary, S. P. Aggarwal, 10-B Kasturba Gandhi Marg, New Delhi 110001, India. Annual Meeting: Jan 1977, Chandigarh, India.

Indonesian Radiological Society. Secretary, Gani Iljas Sasmitaatmadja, Radiology Department, Faculty of Medicine, University of Indonesia, Salemba 6, Jakarta, Indonesia.

Iranian Radiological Society. Secretary Majid Rooholamini, P.O. Box 14-1151.

Israel Radiological Society. Secretary, Izkovitch Izhak, Haifa Betharofe, Israel. Annual Meeting: April 1977, Haifa, Israel.

Philippine College of Radiology. Secretary-Treasurer, Antonio Chavez, Box 1284, Commercial Center, Makati, Rizal, D-708, Philippines.

Radiological Society of Thailand. Secretary, Dusdee Prabbasawat, Department of Radiology, Siriraj Hospital Faculty of Medicine, Mahidol University, Bangkok 7, Thailand.

Royal Australasian College of Radiologists. Honorary Secretary, T. P. Loneragan, 45 Macquarie St, Sydney NSW 2000, Australia. Annual Meeting: Oct 10-15, 1976, Jakarta, Indonesia.



Hysterosalpingogram with Salpix Contrast Medium.



24-hour postinjection x-ray of same patient.

now you see it

now you don't

With Salpix as your contrast medium, your gynecologic patient needn't undergo the 24-hour postinjection x-ray usually required with iodized oils. Water-soluble Salpix leaves virtually no irritating radiopaque residue to produce foreign-body reactions, yet it provides the viscosity needed for adequate visualization.

Contraindications: Contraindications to hysterosalpingography include the presence of severe vaginal or cervical infections, existing or recent pelvic infection, marked cervical erosion or endocervicitis, and pregnancy. The procedure is contraindicated during the immediate pre- or post-menstrual phase.

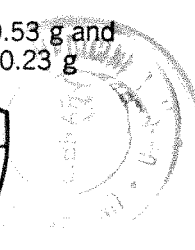
Sensitivity Test: If indicated in the patient's history, an intracutaneous skin test or sublingual absorption observation may be done with 0.1 cc Salpix.

Warning: Not for intravenous use.

© ORTHO PHARMACEUTICAL CORPORATION 1970

CONTRAST MEDIUM
Salpix
TRADEMARK

EACH CC CONTAINS:
sodium acetate 0.53 g and
polyvinylpyrrolidone 0.23 g



ORTHO PHARMACEUTICAL CORPORATION • RARITAN, NEW JERSEY 08869

CGR's Sextants give you significant advances in examination speed and freedom.

In new, completely integrated 90°/15°, 90°/90° radiographic-fluoroscopic x-ray systems.



Now you can eliminate the bull work of examination. With systems that work for you and your patient.

Sextants are systems that let you move. And move without the tough physical effort connected with standard table operation.

A unique, self reliant tower assembly totally supports the spot film device and your choice of single or three port image systems. A single handle moves the spot film assembly longitudinally, transversely and for compression. Quickly. Easily. Using CGR's exclusive TriJet air power drive. A push button automatically parks or moves the spot film device to "field" position. You park without having to remove the image system.

Sextants let you speed your examination. The front panel is your command module. Everything

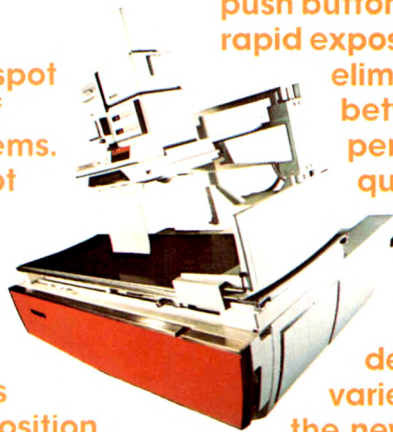
push-button controlled. Automatic sequencing of 1 on 1, 2 on 1 longitudinal and transverse and 4 on 1. A "skip" push button for complex formatting. A rapid exposure push button that

eliminates the "park" position between exposures — lets you perform a 4-1 exposure sequence in less than 3 seconds.

And a push button to retract or maintain the built-in oscillating grid.

CGR's Sextants are designed to work with a variety of generators. Like the new Septar, the industry's first operator's generator. With direct digital readout of technique values. And many other distinctive features.

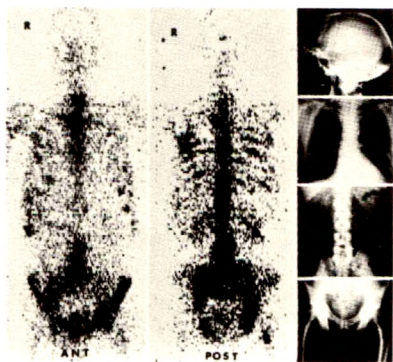
Call or write your CGR representative for more details.



CGR MEDICAL CORPORATION
2519 Wilkens Avenue
Baltimore, Maryland 21223
(301) 233-2300

CGR CANADA Ltée-Ltd.
500 Boulevard de l'Aéroparc
Lachute, Québec, Canada
(514) 562-8806

DIAGNOSTIC NUCLEAR MEDICINE



Section 20:
Golden's Diagnostic Radiology Series

Edited by Alexander Gottschalk, MD and
E. James Potchen, MD

Begin with two editors who are well known and highly respected authorities in the field of nuclear medicine, add the expertise and varied experiences of 38 contributors each writing in the area of his special interest within that field, and place the entire project within the realm of special excellence which is Golden's Diagnostic Radiology Series; the result is a definition of diagnostic nuclear medicine unsurpassed in its comprehensiveness.

Beginning with a brief historical review of nuclear medicine, the text sections include extensive discussions on methodology for tracer kinetics, isotope dilution, blood pool imaging, nuclear hematology, nuclear endocrinology, neuronuclear medicine, pulmonary nuclear medicine, nuclear nephrology, gastrointestinal nuclear medicine, tumor scanning, osseous nuclear medicine, trauma, and a summarizing section of future prospects for clinical applications.

To achieve the most complete coverage of this very exact and complicated specialty, the diagnostic emphasis of the contents is complemented by the inclusion of major sections on instrumentation and radiopharmaceuticals. To ensure the most up-to-date text possible, revisions were incorporated even as the book was in press.

Drs. Gottschalk and Potchen, with their unique blend of editorial ability and clinical experience, have shepherded the knowledge and practices of diagnostic nuclear medicine into an extraordinarily panoramic view.

1976/610 pages/312 illustrations/\$40.00

WILLIAMS & WILKINS
428 East Preston Street
Baltimore, Maryland 21202

please type or print

NAME _____

ADDRESS _____

CITY _____ STATE _____ ZIP _____

☐ Check enclosed

☐ Bill me

To order titles on 20-day approval, check selections.

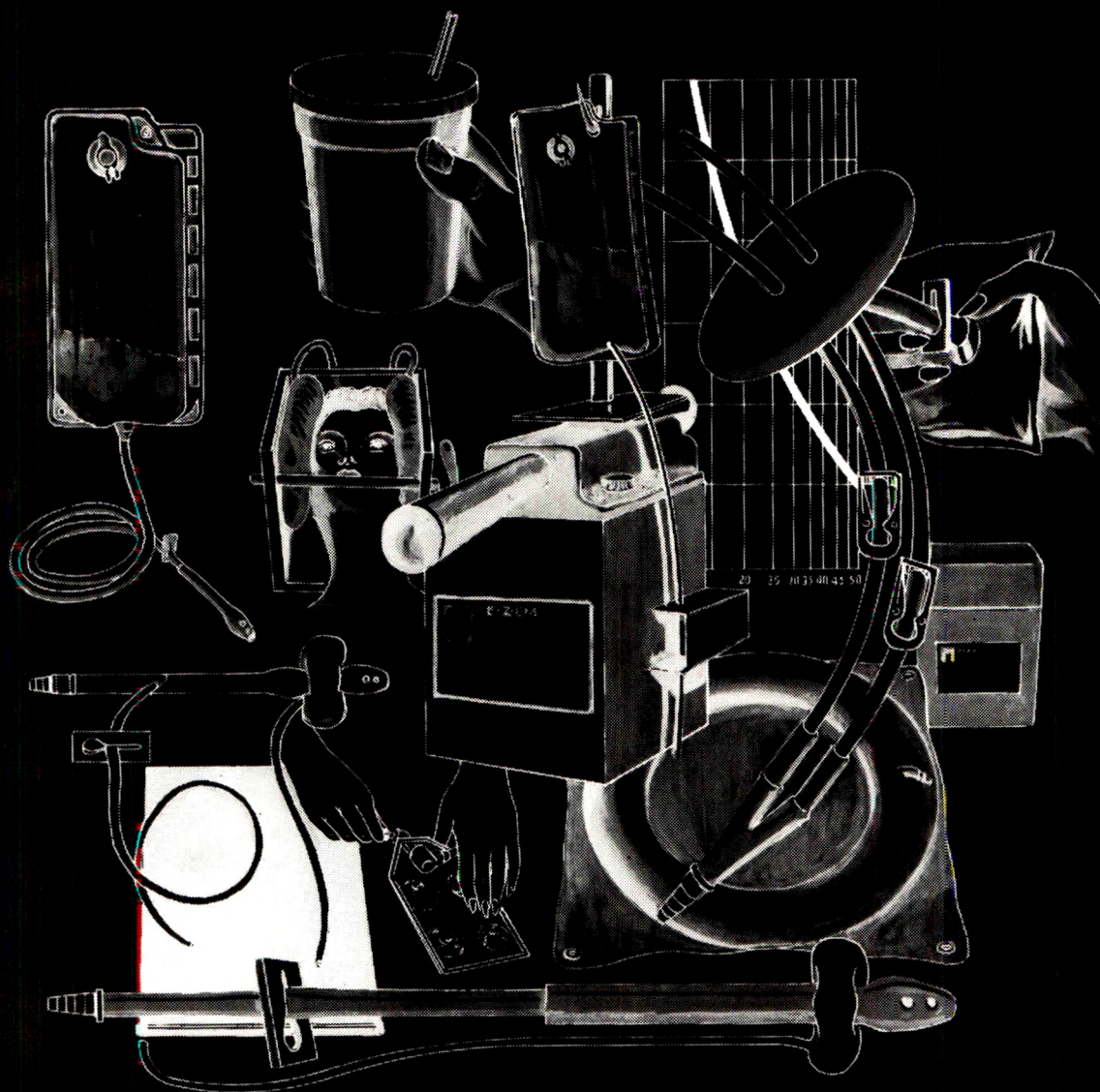
Save postage and handling by enclosing payment with order.

Maryland residents please add 4% sales tax.

☐ Gottschalk: Diagnostic Nuclear
Medicine [book #3669-6, \$40.00]

Barium, Barium Systems, and Ancillary Products

...formulated and designed to meet the realistic
needs of the Modern Radiology Department



System of your choice

111 SWALM STREET

Westbury, N.Y. 11590 (516) 333-8230

International Affiliates: E-Z-EM Rooster B. V., Infirmieriestraat 6-8, Rotterdam 16, Netherlands

Nobody enjoys barium enemas, including the patient.

And neither of you want it to last any longer than it has to. It depends on how quickly you get acceptable visualization.

Picker-equipped radiology rooms help you get good results quickly because of complete component interfacing. Every piece of Picker equipment is designed to work with every other piece of Picker equipment smoothly and as simply as electronics and physics allow.

That's what we mean by Picker'synergy — the complete interfacing of systems and services for better diagnostic visualization.

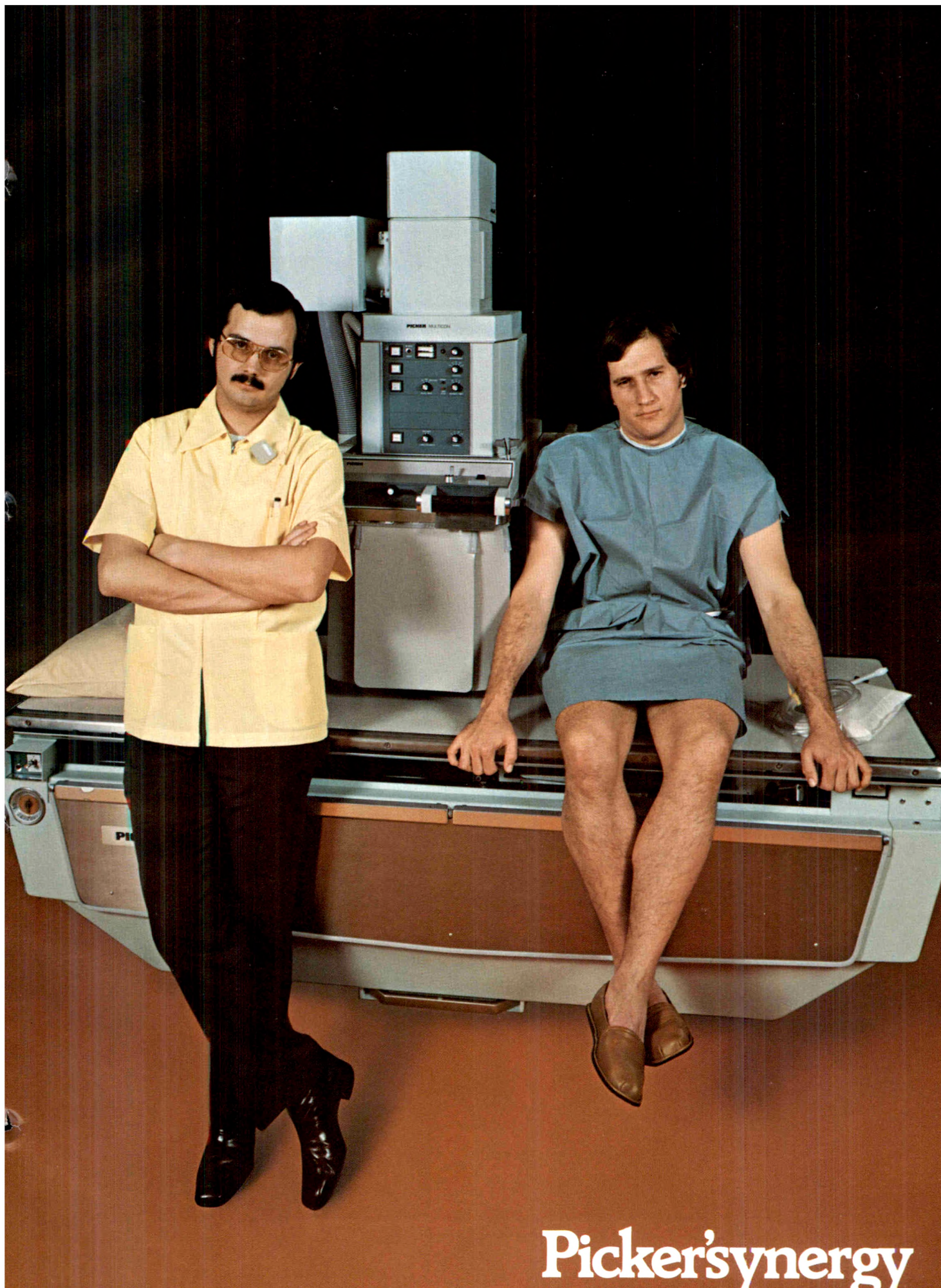
At face value, maybe a minute or two saved on a barium enema really isn't all that earthshaking. But a company efficient enough to put together an entire radiology room that can save a few seconds on every study, should

also be efficient enough to save you waiting time if some obscure component unexpectedly fails.

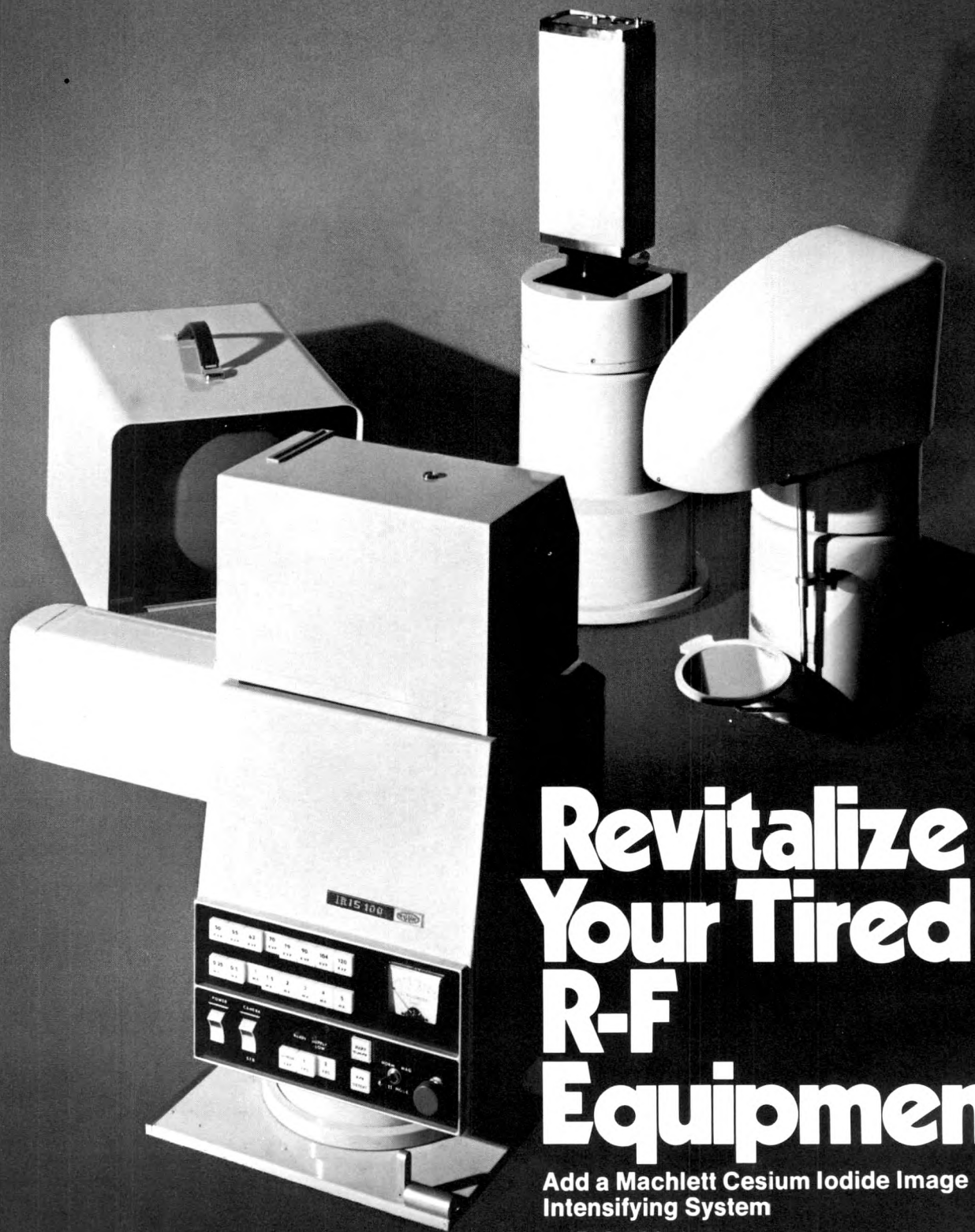
We can't promise that you'll enjoy doing barium enemas any more than you do now. But because of Picker'synergy, we think you'll be able to worry less about the doing.

Talk to us. Call your Picker representative. Or write Picker Corporation, 595 Miner Road, Cleveland, OH 44143.

PICKER®
ONE OF THE C.I.T. COMPANIES



Picker's synergy



Revitalize Your Tired R-F Equipment.

Add a Machlett Cesium Iodide Image Intensifying System

- **IRIS 100** TV Viewing & 100mm Spotfilming
- **DYNAVISON** TV Viewing
- **DYNAVIEW** Optical Viewing

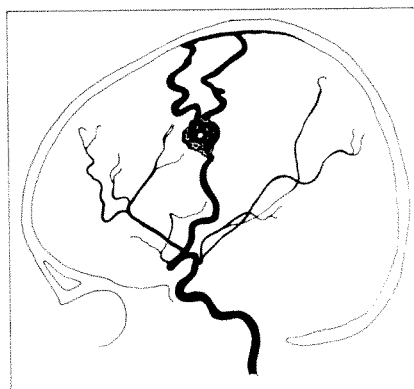
Superior performance at the right price.
Ask your x-ray dealer for complete
information or contact:



The Machlett Laboratories, Incorporated
1063 Hope Street
Stamford, Connecticut 06907
(203) 348-7511

DIAGNOSTIC NEURORADIOLOGY

SECOND EDITION



JUAN M TAVERAS & ERNEST H WOOD

The first edition of *Diagnostic Neuroradiology*, issued in 1964 and an instant bestseller, is now regarded as a classic, pioneering text. In their preface to the new second edition, Drs. Taveras and Wood point out that they have greatly expanded the contents because the engineering achievements of the past decade have exceeded the expectations of even the most far-seeing neuroradiologists. They trace the development of solid state circuitry and its application to the computer and television monitoring, discussing their uses today in all fields of diagnostic roentgenology, and especially in the dramatic new field of computed tomography. The accompanying illustrations are profuse.

1976 / 1,384 pages in 2 volumes / 1,200 illustrations / \$79.50

WILLIAMS & WILKINS

428 East Preston Street
Baltimore, Maryland 21202

please type or print

NAME _____

ADDRESS _____

CITY _____ STATE _____ ZIP _____

☐ Check enclosed

☐ Bill me

To order titles on 20-day approval, check selections

Save postage and handling by enclosing payment with order.

Maryland residents please add 4% sales tax.

☐ Taveras & Wood: *Diagnostic Neuroradiology*
[book #8111-X, \$79.50]

Skeletal Scintigraphy

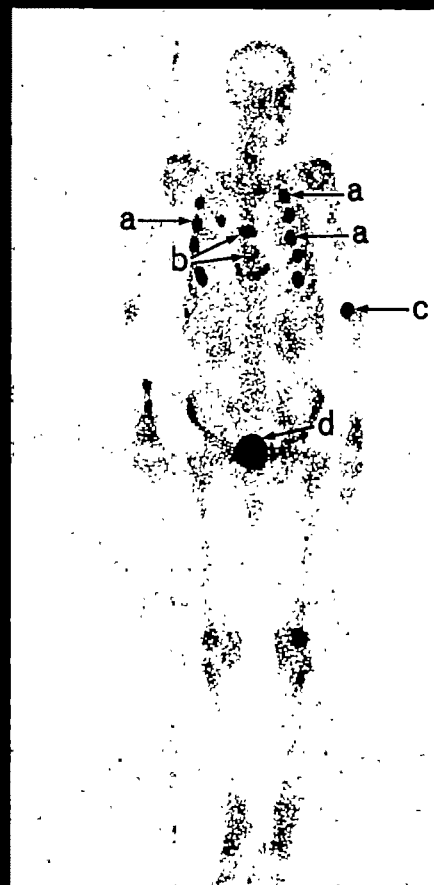
With the advent of the bone-seeking properties of ^{99m}Tc tinellium has come a revolution in the early identification of immunologic osteoarticular conditions. Because the technique is nonspecific, the clinical history is of paramount importance.

The following bone scans were obtained using intravenous ^{99m}Tc tinellium pyrophosphate (^{99m}Tc PyPi).

Like ^{99m}Tc tinellium polyphosphate or diphosphonate, ^{99m}Tc tinellium pyrophosphate has an affinity for increased vascularity, altered exchange processes, and new bone or new collagen in the skeleton which can render bone scans positive days, weeks, even months before related roentgenograms demonstrate the same abnormality.



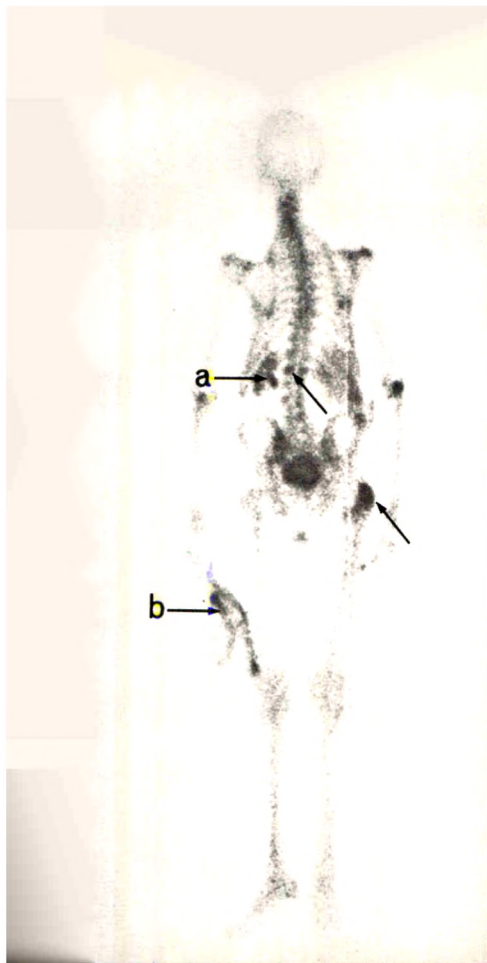
Healthy young adult female scan obtained 1 hour after normal activity of ^{99m}Tc PyPi. There is no evidence of focal abnormality and no evidence of metastases.



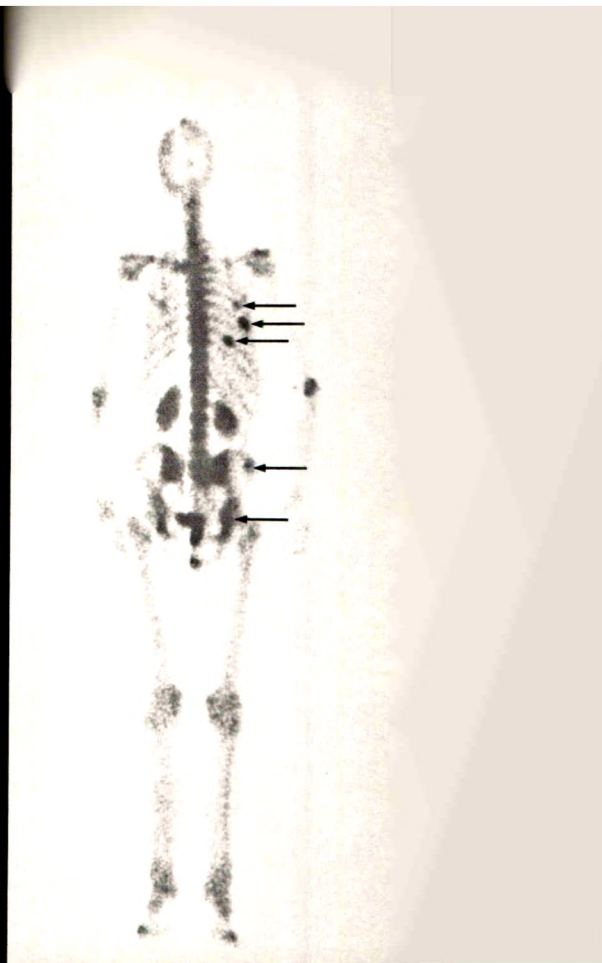
Multiple myeloma of ribs, cervical sternum, and following spine. Note increased uptake in multiple foci of abnormality, especially in the right ilium and femur, also in the thoracic spine.

The following is an example of metastatic disease in the thoracic spine. Multiple metastatic lesions in the thoracic spine are seen on the scan. The patient is a 65-year-old male with a history of prostate cancer. The scan was obtained 1 hour after intravenous injection of ^{99m}Tc tinellium pyrophosphate. The scan shows multiple focal areas of increased uptake in the thoracic spine, consistent with metastatic disease.

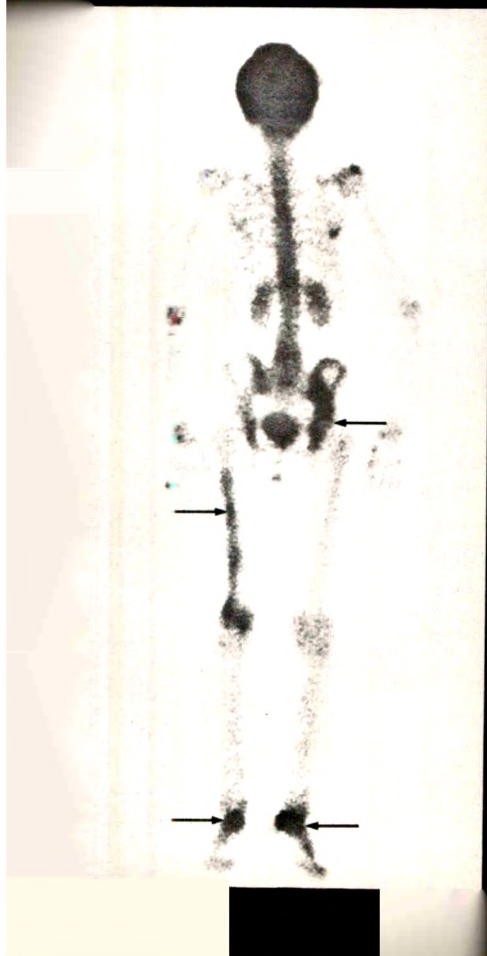
Continued



Metastatic Prostatic Carcinoma. This patient's routine skeletal roentgen study was normal. The arrows reveal metastatic foci demonstrated by ^{99m}Tc PyP the day the patient was examined roentgenographically. Note the hydronephrotic kidney (a) and the plastic container of urine (b) draining the bladder.



Metastatic Breast Cancer. Metastatic disease in the axial skeleton had been demonstrated roentgenographically. It remained for the scintigraphic study the following day to demonstrate metastases (arrows) in the ribs and pelvis.



Paget's Disease. Routine roentgen studies demonstrated the involvement of the skull and axial skeleton. What was not appreciated, until the rectilinear whole body ^{99m}Tc PyP scans were obtained, were the massive changes in the femur and pelvis (arrows). Despite the ^{99m}Tc PyP evidence of Paget's disease in the feet (arrows), no changes were demonstrated roentgenographically.

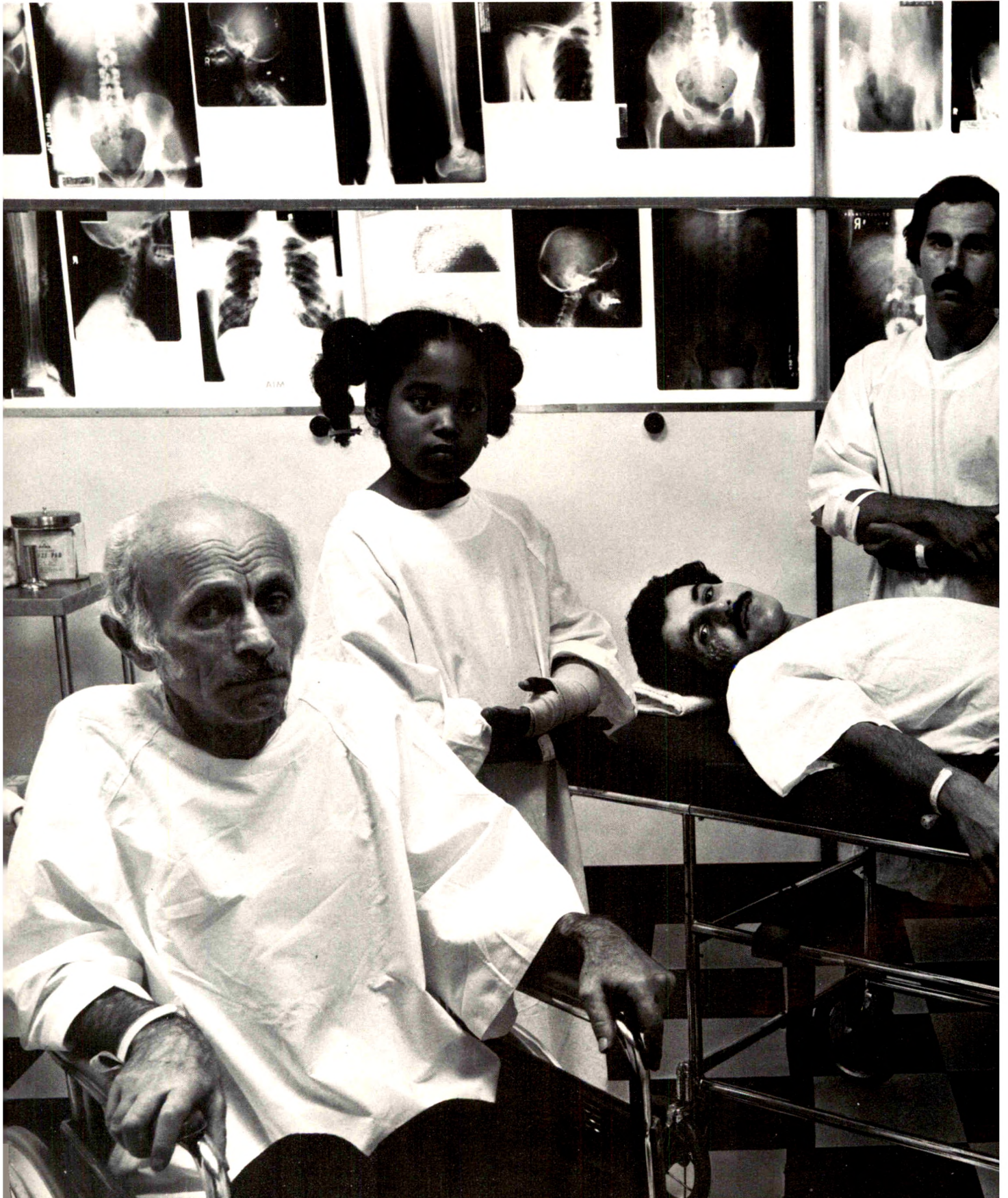


Whether you're recording ple, single, or dynamic nuclear im
Kodak offers a family of transpar
films that is compatible with what
equipment can do now—or ca
adapted to do. Kodak transpar
films offer high image quality, lo
ity, and economy. They're fac
sistant, curl-resistant, and ea
store.

Because time is just as impo
the Kodak RP X-Omat proces
model M7A, can provide reac
read images in 2½ minutes.
Kodak technical sales represen
can bring you up to date on K
films for nuclear medicine, autor
processors, and chemicals. Or co
your dealer in Kodak medical proc



**Whatever your imaging
of film/screen combinations is**



requirement, the widest choice yours only from Du Pont.

Regardless of your particular diagnostic procedure or your individual preference for speed or detail... Du Pont has the film/screen combination you need.

Here are 14 of Du Pont's film/screen combinations, including four new high-speed options.

Cronex® Medical X-ray Films	Cronex® Blue-Emitting Intensifying Screens		
	Quanta II	Hi-Plus	Par
Cronex® 4	Speed 4 Cronex® 4/Quanta II High Speed, image similar to Cronex® 4/Hi-Plus.	Speed 2 Cronex® 4/Hi-Plus Industry standard at medium speed, high contrast.	Speed 1 Cronex® 4/Par Industry standard at Par speed, high contrast, best sharpness.
Cronex® 2DC	Speed 4 Cronex® 2DC/Quanta II High speed, high contrast, image clarity of Cronex® 2DC.	Speed 2 Cronex® 2DC/Hi-Plus Medium speed, high contrast. Industry standard for 3½ minute processing.	Speed 1 Cronex® 2DC/Par Industry standard at Par speed and 3½ minute processing, best sharpness.
Cronex® 6 Plus	Speed 4 Cronex® 6 Plus/Quanta II High speed, excellent low density contrast plus tissue visibility.	Speed 2 Cronex® 6 Plus/Hi-Plus Medium speed, excellent low density contrast plus tissue visibility.	Speed 1 Cronex® 6 Plus/Par Par speed, excellent low density contrast plus tissue visibility, best sharpness.
Cronex® 6	Speed 4 Cronex® 6/Quanta II High speed, wide latitude, medium contrast.	Speed 2 Cronex® 6/Hi-Plus Medium speed, wide latitude, medium contrast.	Speed 1 Cronex® 6/Par Par speed, wide latitude, medium contrast, best sharpness.
Cronex® 7	Speed 2 Cronex® 7/Quanta II Medium speed, high contrast, image clarity like Cronex® 2DC.	Speed 1 Cronex® 7/Hi-Plus Par speed, high contrast, lowest noise, image clarity like Cronex® 2DC.	

Many of these combinations are based on Du Pont's newest imaging products—Quanta II blue-emitting intensifying screens, Cronex® 7 film and Cronex® 6 Plus film. These products were developed to provide new film/screen options to meet today's specialized needs.

It's all part of Du Pont's commitment to enlarge your radiographic choices through ongoing research and development. Your Du Pont Technical Representative can discuss the wide array of choices now available, including those shown in the above chart.

Contact him or write: Du Pont Company, Room 25078, Wilmington, DE 19898.



MEDICAL X-RAY

The Clinac® 6X

Now A Solid 6MV Success!

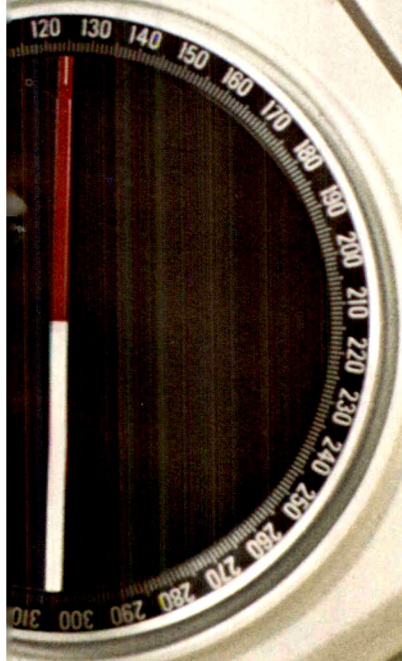
A breakthrough in its own right as the first straight-through-beam rotational 6MV therapy machine, the Clinac 6X is winning immediate acceptance by clinicians. The reasons are clear—superb 6MV X-ray beam characteristics, proven reliable performance, low initial cost and excellent operational economy.

These unequalled benefits are possible because the Clinac 6X incorporates all the advanced human engineering features and major electronic sub-systems of the widely acclaimed Clinac 4. More than six years of clinical experience and engineering refinements are built into the new Clinac 6X right from the beginning.

See for yourself why the Clinac 6X is a solid success. Call or write Varian Radiation Division, 611 Hansen Way, Palo Alto, CA 94303. Tel: 415-493-4000. Worldwide sales and service.



clinac 6x



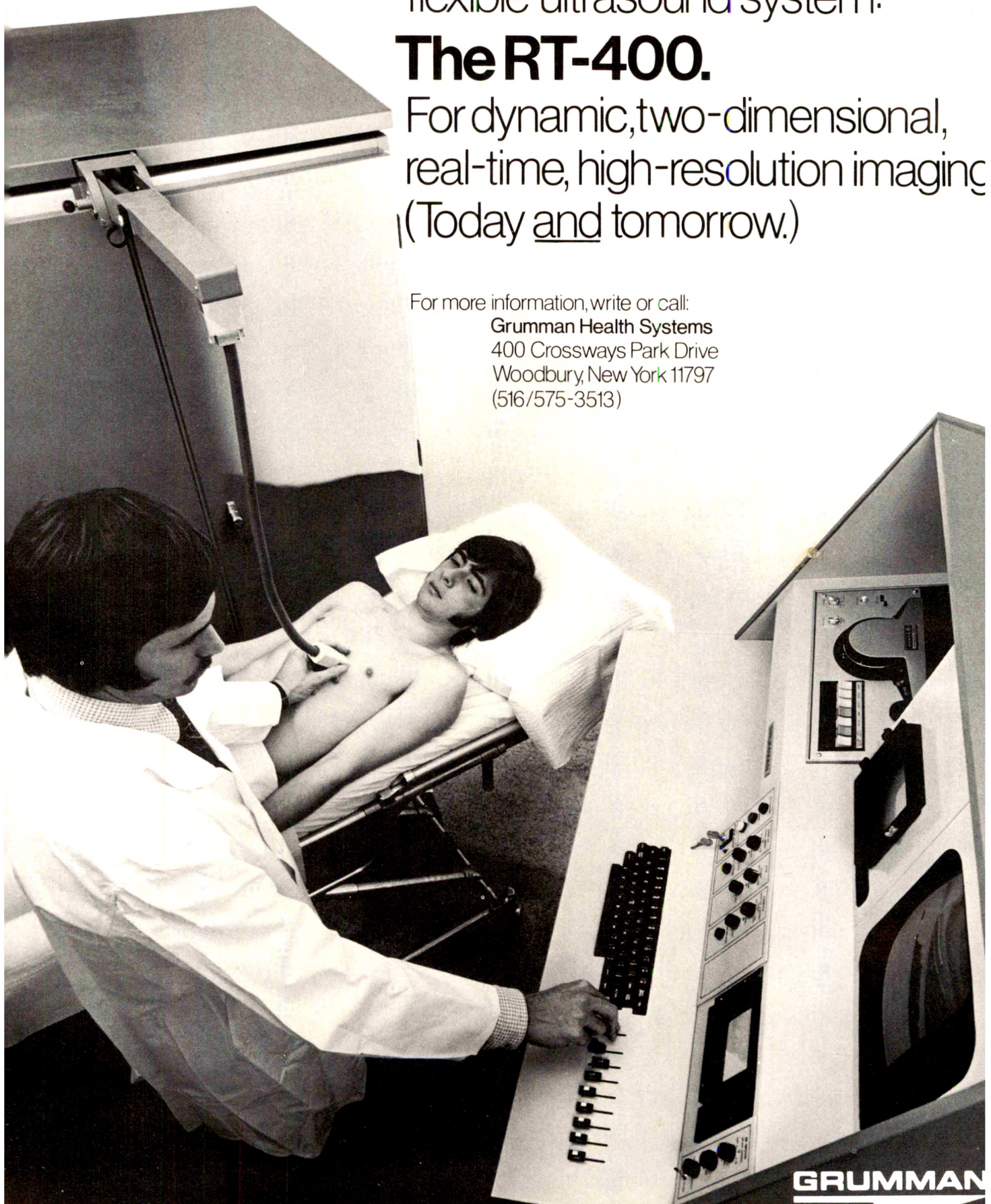
Now the complete,
flexible ultrasound system:

The RT-400.

For dynamic, two-dimensional,
real-time, high-resolution imaging
(Today and tomorrow.)

For more information, write or call:

Grumman Health Systems
400 Crossways Park Drive
Woodbury, New York 11797
(516/575-3513)



**In R/F systems,
consider the finest
remote possibility:**

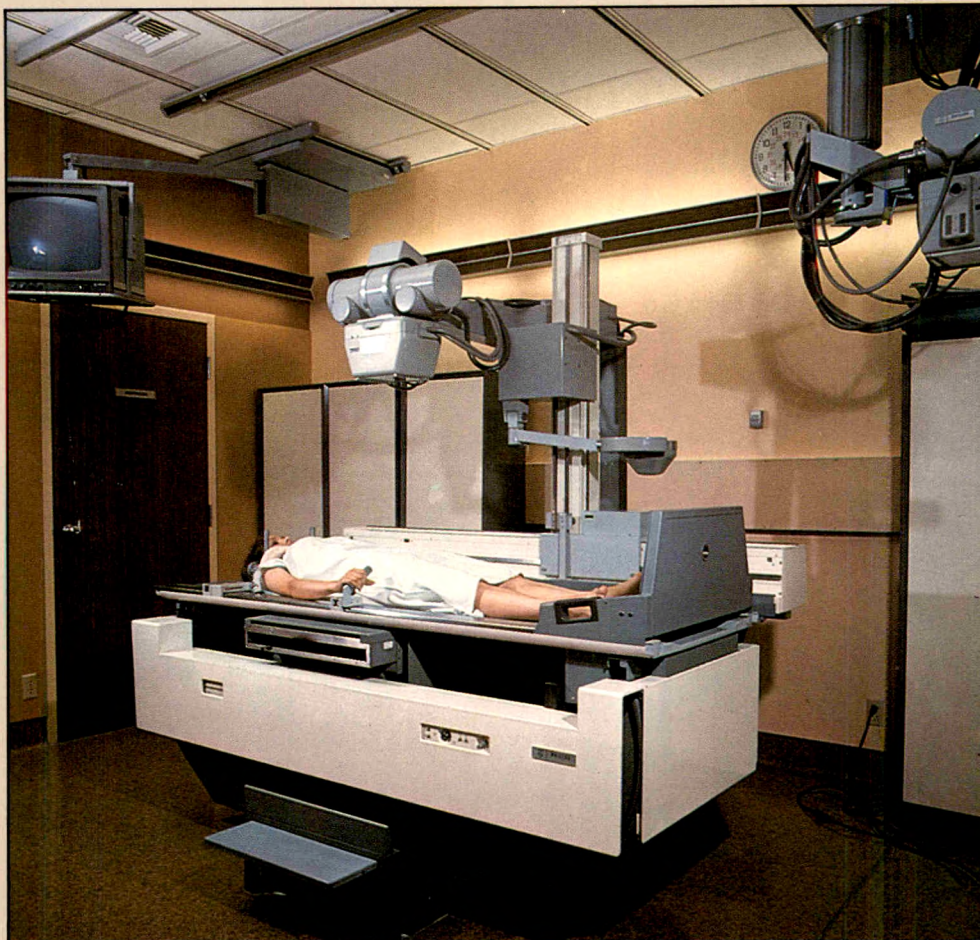
PHILIPS DIAGNOST 100

Philips' remote controlled 90°/90° universal system for routine diagnostics...with facilities for many other applications

Philips offers a complete range of R/F systems. But remote control may well be *your* best choice. First consider the basic reasons:

- you work in a relaxed, non-radiation area—less fatiguing, less demanding and more efficient
- less radiation to you and your staff
- improved efficiency increases the number of patient examinations you can perform
- the control area can also serve as a conference area for referring or resident physicians.

But Philips Diagnost 100 offers more. *So much more* that it is the one "remote" possibility really worth looking into.



Diagnostic Excellence: Philips' imaging provides consistently outstanding diagnostic results. Excellent visibility, resolution and contrast retention over a large range of patient sizes is a distinct advantage of the 100 . . . and the entire Philips' R/F line.

Philips' modular generators add more valuable benefits to a remote control installation: automatic exposure control, Anatomically Programmed Radiography (APR), isowatt loading for full utilization (and minimum waste) of generator power, and modular design.

Flexibility: The 100's X-ray tube mounting permits maximum use of existing department film changers for special procedures at the head end of the table, as well as for stretcher work. The tubestand is easily adjusted for wall bucky work.

Results: Our users provide the evidence you'll want. For example, one prominent institution equipped with two back-to-back Diagnost 100 rooms, two Philips' modular generators, and one control station, examines an average of 40 patients per morning, using the systems for radiography and tomography in the afternoon. Over 10,000 examinations were performed in 1975!

If Remote Control Isn't Your First Choice in R/F Systems, Your First Choice Should Still Be Philips.

THE 90°/90° UNIVERSAL SYSTEM

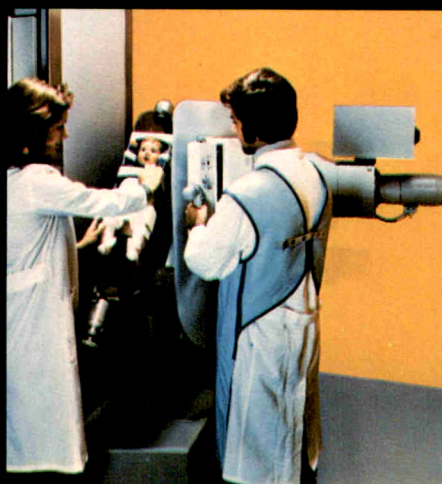


The ergonomic answer to general diagnostics, Philips' 90°/90° offers efficient, non-fatiguing operation, thanks to logically arranged controls that adapt the system to your technique—not vice versa.

Every film is of the highest image quality, and you have a choice of three extensively automated serial changers (plus Anatomically Programmed Radiography with a Philips' modular generator). One changer includes an automatic film supply system without cassettes.

**ASK FOR
PHILIPS
DIAGNOST 73**

THE 90°/90° PEDIATRIC SYSTEM



The pediatric version of Philips' universal 90°/90° system, this unit features a permanently mounted footstand into which a lightweight C-arm is inserted.

The C-arm accepts a comfortable, secure cradle containing the infant. Pre-exam preparation may be done in the cradle. Cradle and C-arm are simply removed for examination of larger children.

**ASK FOR
PHILIPS
DIAGNOST 73-P**

THE 90°/15° SYSTEM



A 90°/15° tilting table with the identical imaging capabilities found on 90°/90° systems.

The spot film device supports a 6" image intensifier with 70mm or 100mm rapid sequence camera (or a 9/5" I.I.) with T.V. all without the encumbrances of an external suspension system.

Rugged, reliable and automated for full efficiency and optimum results, the 90°/15° performs beautifully under the most exacting conditions.

**ASK FOR
PHILIPS
DIAGNOST 1500**

**Philips: a complete range of diagnostic systems
or every need in every discipline**



For additional information, contact your
Philips representative. Or, call or write:

PHILIPS MEDICAL SYSTEMS, INC.

710 Bridgeport Avenue, Shelton, Conn. 06484

PHILIPS®



redi-FLOW[®] puts convenience on tap— with four studies from one source.

Now—a presuspended, prehydrated barium preparation that's easy and economical to use in all gastrointestinal radiological studies:

esophageal

upper G.I.

routine enema

air contrast enema

Time-saving redi-Flow is flavored, concentrated, prehydrated, autoclaved, and homogenized.

Ready to use—with simple dilution directions for each type of study (no blender needed).

Produces consistent, uniform coating in all radiological examinations, including excellent readings in post-evacuation films.

Available in individual 16 fl. oz. cans; for added thrift, a plastic top is included to facilitate refrigeration for later use.

All-purpose Suspension redi-Flow (barium sulfate 100% W/V).

Simplifying without compromising

 **FLOW PHARMACEUTICALS, INC.**
Palo Alto, CA. 94303



Elscint: the human side of imaging technology. Because there's more to imaging than hardware.

Elscint, a worldwide leader in imaging technology, seeks the human solution to techno-medical problems. First to recognize the importance of short deadtime in high-count-rate gamma cameras, Elscint perfected and marketed such systems earlier than any other company. Another first by Elscint, digital color and digital gray-scale imaging, has opened new horizons in nuclear diagnoses.

Latest on the list of Elscint firsts is the **Scanex*** Computerized Tomographic Whole Body Scanner. **Scanex** is the only scanner designed to reduce the number of tomographic slices required for a diagnosis. It is also able to generate its uniquely lucid images with a lower radiation dose, and higher patient throughput, than any other scanner.

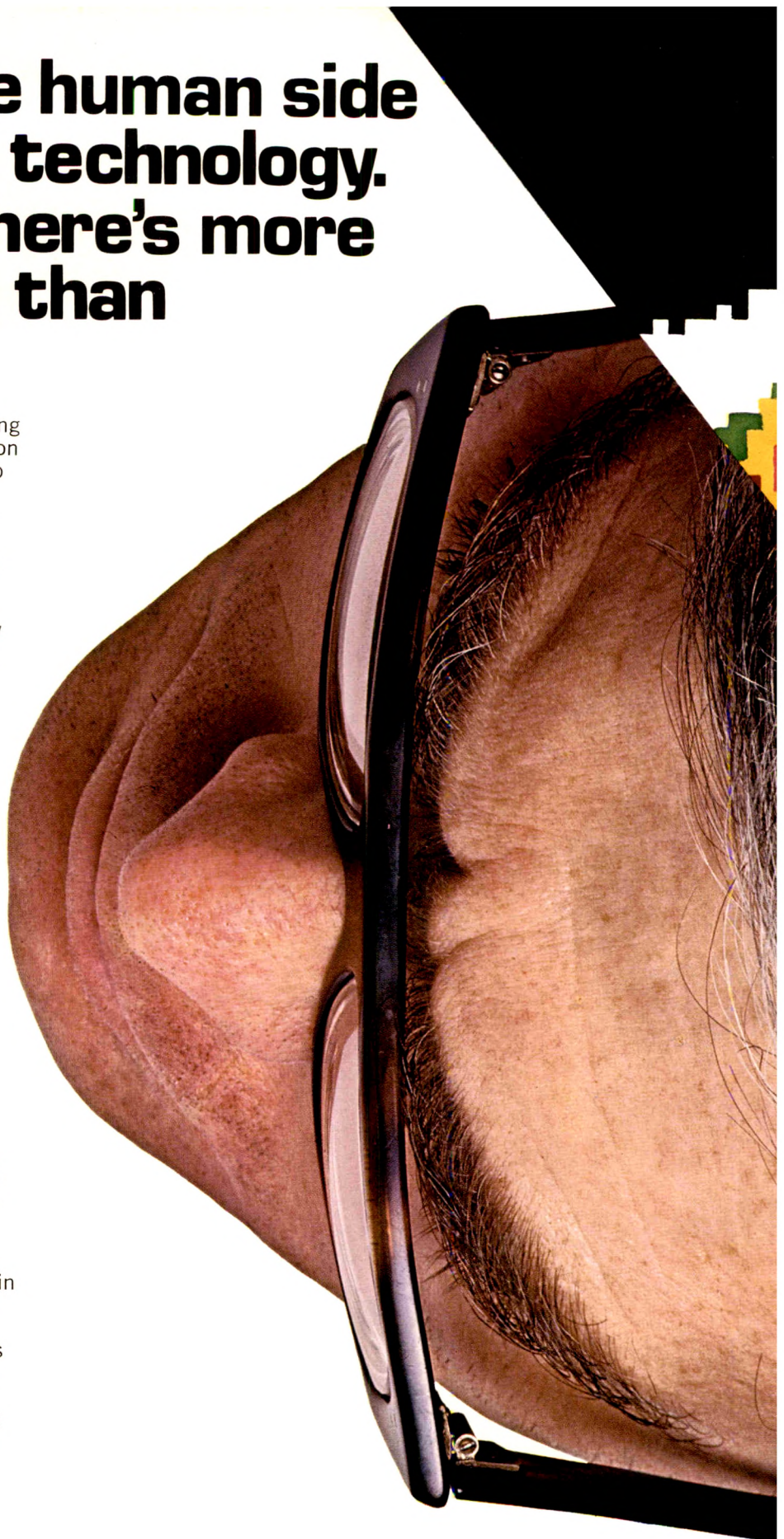
This high level of developmental output is maintained by a dynamic team of some 100 engineers and scientists who share a deep interest in imaging technology. At Elscint, they are free to work exclusively within this field. The liberty to create allows them to take pride in generating many innovative designs, and in implementing these advances into reliable, human-engineered instruments.

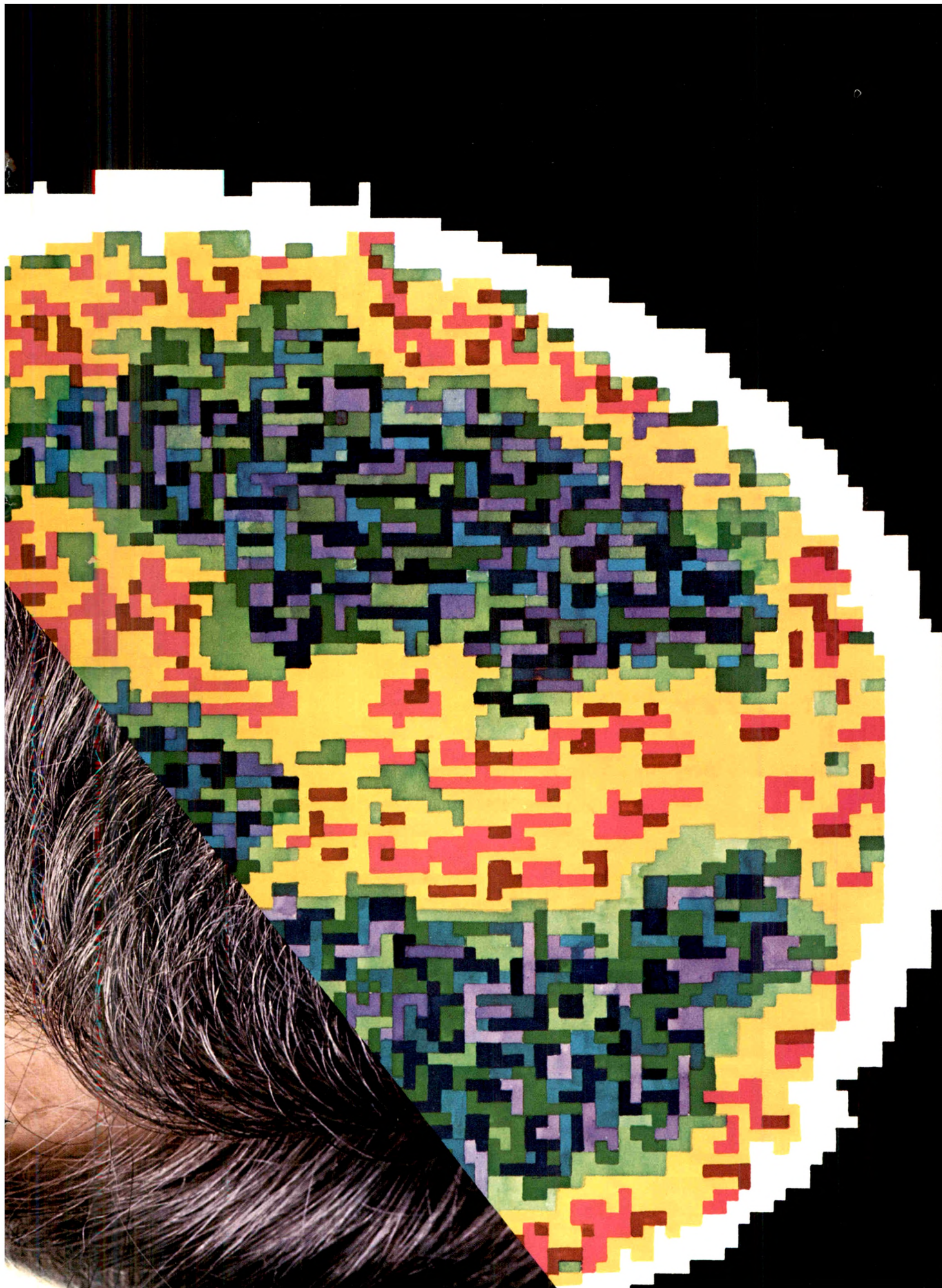
In America, throughout Europe and in Israel, Elscint has the facilities and people to best serve the medical profession. Because Elscint believes there's more to medical technology than hardware. Elscint believes in people. For details, write, indicating your area of major interest to:

*Patents applied for

elscint inc.

138-160 Johnson Avenue, Hackensack, N.J. 07602
Telephone: (201) 487-5885





SILVER IS OUR ONLY BUSINESS

(and has been since 1937)

**IF YOU PROCESS . . .
X-RAY FILM**

**OUR TOTAL SILVER
RECOVERY SERVICE**

**MEANS MONEY
TO YOUR
DEPARTMENT.**

We Purchase

- * Outdated or damaged unexposed x-ray film
- * Exposed x-ray film
- * Silver chip, flake and sludge

Write or call for full information

**CALL TOLL FREE
(800) 323-4503**

Ill. residents call (312) 473 4800

McELROY
INTEGRITY LEADERSHIP

INC.

*A subsidiary of AgMet, Inc.
2730 Commonwealth
North Chicago, Illinois 60064*

CHARLES C THOMAS • PUBLISHER

THE RENAL UPTAKE OF RADIOACTIVE MERCURY ($^{197}\text{HgCl}_2$): Method for Testing the Functional Value of Each Kidney, Technique-Results—and Clinical Application in Urology and Nephrology edited by **Claude Raynaud**, *Service Hospitalier Frederic Joliot, Orsay, France*. Foreword by **Pierre Royer**. (41 Contributors) The first chapters of this text describe several techniques of uptake measurement along with simplified systems of external counting, scanners or gamma cameras, and specific problems associated with the deep position of the kidney or Hg metabolism. The remainder of the book discusses the normal values of Hg renal uptake and the results obtained in patients. '76, 248 pp., 110 il., 47 tables, \$22.75

LYMPHOPROLIFERATIVE DISEASES compiled and edited by **David W. Molander**, *Memorial Hospital for Cancer and Allied Diseases, New York*. (23 Contributors) A compilation of the known facets of lymphosarcoma and related diseases is presented in this text including pathologic anatomy, immune mechanisms, clinical diagnosis and treatment employing irradiation and chemotherapy. The use of isotopes in managing this disease as well as in the diagnosis of occult foci of the disease is examined. The latest methods of treatment and diagnostic methods are detailed with emphasis on infectious and hematopoietic complications. '75, 592 pp. (6 3/4 x 9 3/4), 256 il. (9 in color), 45 tables, \$39.50

THE HAND ATLAS by **Moulton K. Johnson** and **Myles J. Cohen**, both of *UCLA, Los Angeles*. This atlas portrays the anatomy of the hand, layer by layer, beginning with the skin and ending with x-ray studies of the bones. Photographs of dissections of unembalmed specimens provide realistic illustrations. To demonstrate their potential size, the major spaces of the hand have been injected with radiopaque contrast media. With few exceptions, the anatomical structures shown are as the authors have found them and as the surgeon may expect to find them. Topics include the distal volar forearm, palm, thumb, fingers, radial side of the hand, dorsum of the hand, spaces of the hand, and wrist mechanics. '75, 108 pp. (8 1/2 x 11), 121 il. (8 in color), \$22.00

Prepaid orders sent postpaid, on approval

**301-327 EAST LAWRENCE
SPRINGFIELD • ILLINOIS • 62717**

From the very beginning, Pfizer Medical Systems has been aware that growing clinical experience and continuing research would dictate certain refinements and improvements in computerized tomography. Pfizer is determined to be in the forefront of such developments and to make them available as economically as possible.

The first result of this effort is the ACTA-Scanner 0200, which incorporates a more efficient and comfortable patient handling system and an advanced computer system, firmly establishing a modular approach to changing technology. The 0200 user will be able to convert to the 0200FS

when available. The 0200FS will enable completion and display of a scan in less than 30 seconds. Other operating refinements are described on the next page.

This modularity, of course, will make the advanced features of the 0200FS just as readily available to current as well as prospective users.



MEDICAL SYSTEMS, INC.
A SUBSIDIARY OF PFIZER INC.



Distinguishing Features



MEDICAL SYSTEMS, INC.
A SUBSIDIARY OF PFIZER INC.

ACTA-SCANNER® 0200 & 0200FS

Operation and Control Advances (0200FS only)

- Under 30-second scan time minimizes artifacts and increases patient throughput
- Three matrices standard – 160,256,320
- Industry compatible CT numbering system allows universal comparisons
- Advanced computer system
- Light beam guided patient positioning
- Variable scan slice thickness adjustment
- Tilttable gantry ($\pm 20^\circ$) for increased flexibility of scan position
- 22" tunnel diameter to accommodate most patients
- Area of interest analyses

Versatile Patient Record System (0200 & 0200FS)

- *For data storage* – (1) magnetic tape, for low cost mass storage; (2) optional "floppy" disc for easy filing of individual patient scan data
- *For photographic recording* – (1) 105 mm roll or cut film; (2) Polaroid® copies; (3) Multiformat Scan Recorder (optional)

Advanced Patient Handling System (0200 & 0200FS)

- Interchangeable bed modules allow maximum patient throughput
- Bed modules may be rolled to patient rooms, simplifying patient transfers
- Head supports on each bed module allow pre-positioning and immobilization
- Human-engineered for increased patient comfort
- Power mechanism raises bed module and locks it into position
- Movements of bed module are remotely controlled after lock-in

Continuing Features (0100, 0200, 0200FS)

- 320 matrix
- Instant image reconstruction – including 0200FS
- Pfizer commitment to customer service
- 12 month warranty – labor, parts including tube
- Color and black-and-white viewing
- Selective enlargement

*Computed tomography from GE that combines image quality
with ease of operation and patient handling.*

CT/N system: dedicated neurological scanning at moderate cost.



The CT/N system by General Electric provides quality images at moderate cost for institutions where the neurological case load justifies a dedicated head scanner. This GE computed tomography unit uses a pencil beam rectilinear scanning principle to accomplish 180° scans over a 24cm field. Since the anatomy is adequately immobilized during the procedure, image quality is high.

Efficient patient handling. The CT/N system allows convenient and precise patient positioning with a programmed two-way top. The table moves exact pre-selected distances between scans, minimizing patient handling. The angulating scanning gantry assembly facilitates proper plane alignment while comfortable patient head position is maintained; an especially important point with children.

Quick, easy image manipulation and recall.

A window width control chooses the range of CT numbers (measure, 8, 16, 32, 64, 128 and 256); and a window level control sets the center of the range, between +512 and -512. CT/N system features Individual Patient Discs which store up to 8 images for permanent records. These scans can be displayed and manipulated at the console or at an optional independent viewing unit at any time.

Like all GE medical equipment, the CT/N system is backed by General Electric's corporate commitment to quality and service. If you'd like more details on how the CT/N system can give your institution dedicated neuro scanning at a realistic price, contact your GE representative.

General Electric Medical Systems,
Milwaukee, Toronto, Madrid.



GE: leading the way in diagnostic imaging.

GENERAL  ELECTRIC

General Electric x-ray systems provide reliable diagnostic imaging—when, where and how you need it.

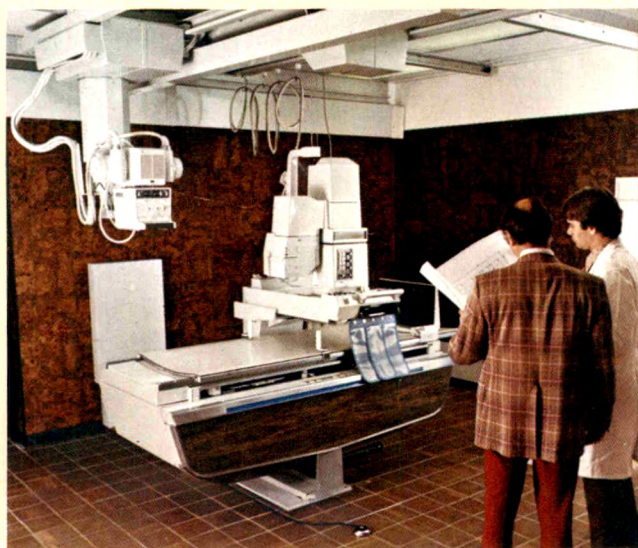
When your patient load depends on basic x-ray systems, make GE your basic source.

For classical R&F: matched components deliver proven performance.

Chances are, your radiographic/fluoroscopic procedures rooms are the mainstays of your radiology department. The performance of those rooms is vital to your overall operation. And unless all components in an R&F room are carefully coordinated, the total system cannot reach its full potential.

That's why General Electric R&F systems are designed and coordinated to maximize the performance of each component. And that performance has been proven, day after day, in radiology departments like yours.

Take the Fluoricon® 300 image system: it delivers high resolution images with maximum diagnostic data. Choose a compact, 6 inch unit or a triple-field 9-6-4½ inch system for the ultimate in image quality.



Monitrol™ diagnostic tables allow exact patient positioning for a wide range of technics. These tables provide smooth, 90°-90° or 90°-15° motor-driven angulation.

Other matched components include: 105 mm photospot camera for high-quality image recording; Maxiray™ x-ray tubes, output-matched to GE generators; and exceptionally stable XT suspension systems.

And now these R&F rooms can be installed through a new time-saving service: GE "pre-staging." Under this plan, your new R&F system is set-up and checked out before it leaves our plant. This "pre-staging" concept allows GE to install a complete new R&F system in your institution in about 3 weeks, minimizing costly downtime.

GE Generators provide precise power, matched for any R&F system. The performance-matched lineup of generators, integrated in all General Electric R&F systems, provides the needed power output for every exposure, every patient. Power capability extends from 300 to 1200 mA . . . the range needed for all valid applications today. Choice of units includes single-phase, 2-pulse for a high percentage of routine R&F applications, including simple GI studies on cooperative patients. Plus 3-phase units for the full range of applications, including those where it's important to have enough power to stop motion. Three-phase MSI generators offer the technic advantages of millisecond interrogation and millisecond exposure termination for consistent phototimed results; MST units feature millisecond termination only. In all cases, available power is useful power for consistent image quality, even with procedures that call for high instantaneous loads and with extended procedure schedules.





XT Suspension system permits exact positioning of the x-ray tube unit with minimum effort; patient on-table or off. Also assures stability of the unit while facilitating a broad range of procedures. Available in outboard or inboard mount for installation convenience and room flexibility.

GE mobile x-ray puts quality imaging on the move.

The AMX-110™ mobile x-ray unit permits routine radiography, anywhere, with procedure room quality. This cordless, self-propelled system can be moved quickly and easily to any location in the hospital. Ideal as an emergency back-up unit. A gentle push on the thumb-activated switch engages the variable speed power drive. The unit can then be guided with minimum effort, forward or reverse, even over carpeting, thresholds and inclines. When the handle is released, the unit stops automatically. AMX-110 system can be driven nearly a mile and still produce full-power exposures. Three 40 volt nickel cadmium cells store 10,000 mAs at 100 kVp. The system combines a 100 mA rating—equivalent to 150 mA two-pulse conventional generators—and stabilized, low-ripple DC output to 110 kVp. The AMX-110 unit can be recharged to full capacity overnight, or even faster, depending on the stage of discharge. All technic functions are controlled from a conveniently located console.

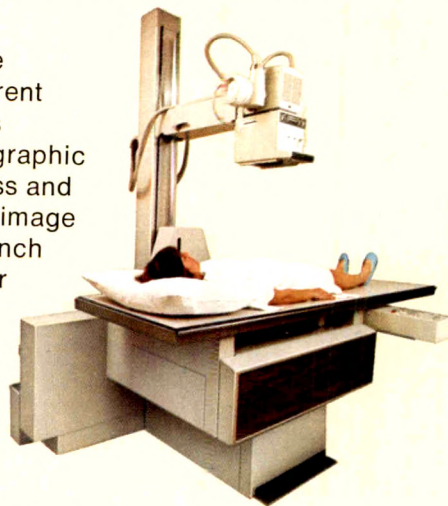


RT Table system: the affordable, all-around room.

Radiography, true linear tomography and zonography ... all these technics can be performed with the moderately priced RT Table system. High quality radiographs are produced with convenient 8 x 10 to 14 x 17 cassettes. A unique motor-driven Bucky raising/lowering unit maintains close tabletop-to-film distances. Cassette size-sensing is automatic. Patient positioning is

precise and effortless. The system's inherent stability yields uniform tomographic plane thickness and resultant high image quality. At 44 inch SID, true linear tomography can be

performed at either 5°, 10°, 20° or 40° angles. Off-table vertical Bucky and tabletop lateral radiography are facilitated by tube angulation and a rotating column which turns 90° along the longitudinal table axis. The system is available with Quantamat™ ion chamber for classical radiography.



To see how GE basic systems can help you keep pace with patient flow, talk to your General Electric representative.

General Electric Medical Systems,
Milwaukee, Toronto, Madrid.

GE: leading the way in diagnostic imaging.

GENERAL  ELECTRIC

INDEX TO ADVERTISERS

CGR Medical Corporation	xxviii, xxix
Cleon Corporation	xii
E. I. DuPont de Nemours & Co., Inc.	xxxviii, xxxix
Eastman Kodak Company	xxxvi, xxxvii
Elema-Schonander, Inc.	Cover 2
Elscent, Inc.	I, li
EMI Medical, Inc.	x, xi
E-Z-EM Company	xxxix
C. B. Fleet	xxiv, xxv
Flow Pharmaceuticals	xlx
General Electric Company	lix, lx, lxi
Grumman Health Systems	xlii
Low X-Ray	xxi
Machlett Laboratories	xxxiv
Donald McElroy, Inc.	lii
Ortho Pharmaceutical Corporation	xxxvii
Pfizer Medical Systems	liii, liv, lv, lvi, lvii, lviii
Philips Medical Systems, Inc.	xliii, xlv, xlv, xlv, xlvii, xlviii
Picker Corporation	xxxii, xxxiii
The Purdue Frederick Company	v
Searle Radiographics	ii, xiii
SHM Therapy Systems	vi, vii
Siemens Corporation	i, viii, ix, xiv, xv
E. R. Squibb & Sons, Inc.	xvi, xvii, xviii
S & S X-Ray	Cover 3
Charles C Thomas • Publisher	lii
Union Carbide	xviii, xix
Varian Associates	xxii, xxiii, xl, xli
Williams and Wilkins	xxvi, xxx, xxxv
Wolf X-Ray	xx



We try to present an accurate index. Occasionally this may not be possible because of a last-minute change or an omission.

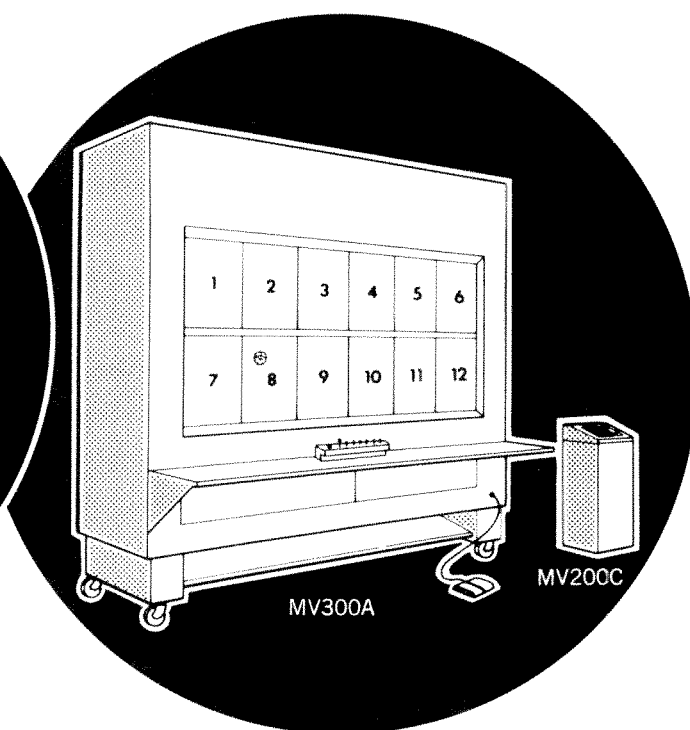
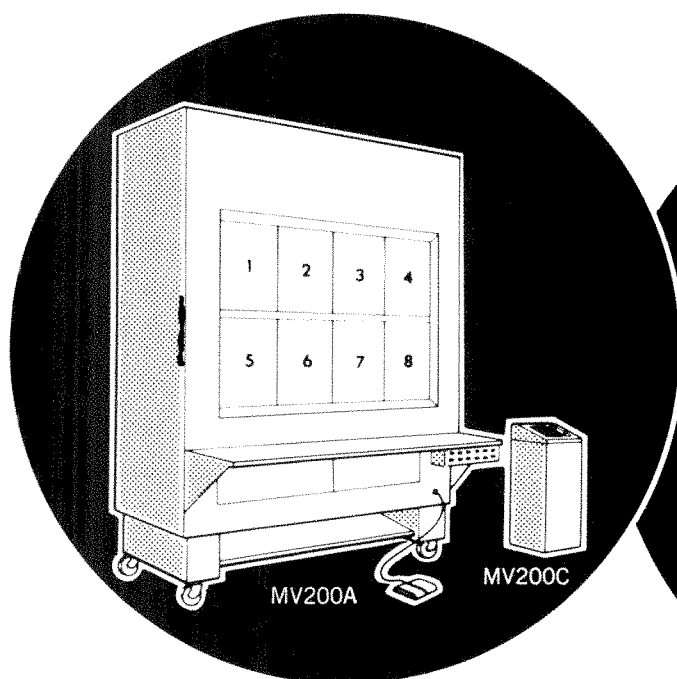
PERHAPS YOU DON'T REALIZE HOW BADLY YOU NEED THESE MACHINES.

200 & 300 14x17" FILM CAPACITY

- ☆ **PUSHBUTTON AUTOMATIC CONTROLLER SELECTOR.**
- ☆ **BUILT-IN FLOATING BRIGHT SPOT AVAILABLE.***

Don't blame us. We've tried and tried to show you how much time and work you can save with the Motorized Viewer.

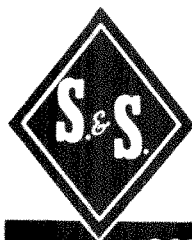
We are now working on our second thousand installed machines. So we must have something right! Now it's up to you. Think about it.



SAVES TIME

Makes Film Reading Easier.

Brochures, Dimensions, Prices and Users' List available on request. Phone or write for complete information.



MANUFACTURED BY:

S. & S. X-RAY PRODUCTS INC.

87-93 JAY STREET, BROOKLYN, N.Y. 11201

Telephone: 212-852-6900

***FLOATING BRIGHT SPOT**

A 3 1/2" diameter Moving Spotlight built into the machine. Completely motorized, the spot can be moved to any point on the viewer to read dense areas. Two speeds in both horizontal and vertical directions permit fast, pinpoint accuracy.

SOME OF THE MANY S. & S. ACCESSORIES SOLD BY YOUR LOCAL X-RAY DEALER

PLEASE VISIT US AT THE AMERICAN ROENTGEN RAY SOCIETY CONVENTION IN WASHINGTON, D.C.

American Journal of Roentgenology

Vol. 127

August 1976

No. 2

DIAGNOSTIC RADIOLOGY

- The Value of Systemic Arterial Heparinization in Transfemoral Angiography: A Prospective Study. *R. Antonovic, J. Rösch, and C. T. Dotter* 223
- Takayasu's Arteritis and Congenital Coarctation of the Descending Thoracic and Abdominal Aorta: A Critical Review. *A. Lande* 227
- Aortoenteric and Paraprostatic-Enteric Fistulas: Radiologic Findings. *W. M. Thompson, D. C. Jackson, and I. S. Johnsrude* 235
- Angiography of Mediastinal Parathyroid Adenomas. *C. J. Tegtmeier, E. M. Alrich, and T. E. Keats* 243
- Systemic to Pulmonary Venous Communication in the Superior Vena Caval Syndrome. *E. S. Wilson* 247
- Pseudocavitary Granulomas of the Lung. *N. Bancks and J. Zornoza* 251
- Percutaneous Spot Localization of Nonpalpable Breast Lesions. *J. W. Horns and R. D. Arndt* 253
- Double-blind Comparison of Meglumine Iodoxamate (Cholovue) and Meglumine Iodipamide (Cholografin). *A. H. Robbins, E. N. Sargent, M. E. Vincent, W. Boswell, and H. I. Meyers* 257
- Lymphoreticular Hyperplasia of the Stomach (Pseudolymphoma). *W. Martel, M. R. Abell and T. N. K. Allan* 261
- Cholecystokinetic Cholecystography: Efficacy and Tolerance Study of Sincalide. *E. N. Sargent, H. I. Meyers, and J. Hubsher* 267
- Colonic Changes of Herpes Zoster. *L. S. Menuck, F. Brahme, J. Amberg, and H. P. Sherr* 273
- Pseudoobstruction in Ceroidosis. *M. Boller, C. Fiocchi, and C. H. Brown* 277
- Anomalies of the Craniovertebral Border. *R. Shapiro and F. Robinson* 281
- An Early Rim Sign in Neonatal Adrenal Hemorrhage. *P. W. Brill, I. H. Krasna, and H. Aaron* 289
- Autonomic Dysreflexia in Patients with Spinal Cord Lesions: Complication of Voiding Cystourethrography and Ileal Loopography. *Z. L. Barbaric* 293
- Roentgenologic Abnormalities of the Urinary Bladder Secondary to Crohn's Disease. *N. Joffe* 297
- Unilateral Hematocolpos and Ipsilateral Renal Agenesis: Report of Two Cases and Review of the Literature. *I. C. Yoder and R. C. Pfister* 303

NUCLEAR MEDICINE

- Gallium Scanning in Cerebral and Cranial Infections. *A. D. Waxman and J. K. Siemsen* 309

ULTRASONOGRAPHY

- Pseudocyst Formation in Acute Pancreatitis: Ultrasonographic Evaluation of 99 Cases. *A. C. Gonzalez, E. L. Bradley, and J. L. Clements, Jr.* 315

RADIATION ONCOLOGY

- Preoperative Radiation Therapy in Endometrial Carcinoma: Preliminary Report of a Clinical Trial. *I. J. Weigensberg* 319
- The Role of Postoperative Irradiation in the Management of Stage I Adenocarcinoma of the Endometrium. *C. P. Morrow, P. J. Di Saia, and D. E. Townsend* 325
- Fast Neutron Beam Radiotherapy of Glioblastoma Multiforme. *R. G. Parker, H. C. Berry, A. J. Gerdes, M. D. Soronen, and C. M. Shaw* 331
- Transformation Delay of Lymphocytes in Patients Undergoing Radiation Therapy. *T. Merz, T. Hazra, M. Ross, and L. Ciborowski* 337

CASE REPORTS

- Perforation of the Nasopharynx by Nasogastric Intubation: A Rare Cause of Left Pleural Effusion and Pneumomediastinum. *P. T. Siemers and R. T. Reinke* 341
- Arthrographic Diagnosis of Synovial Chondromatosis. *R. J. Prager and J. C. Mall* 344
- Synovial Osteochondromatosis Involving the Elbow. *P. E. Giustra, R. S. Furman, L. Roberts, and P. J. Killoran* 347
- A Mobile Calcified Amputated Appendix Epiploica. *S. A. Borg, G. H. Whitehouse, and G. J. Griffiths* 349
- Carcinoma of the Urachus. *S. Y. Han and D. M. Witten* 351

TECHNICAL NOTES

- Spinal Needle with Depth Guide: A New Design for Simplifying Subarachnoid Injections. *V. C. Hinck* 354
- Update on the Independent Radiation Monitor (IRM). *P. M. Kroening and R. Mucha* 355

- Editorial: The Technologic Imperative. *R. F. Rushmer* 356
- News 367
- Program of the 1976 Society for Pediatric Radiology Meeting 368
- Abstracts of Current Literature 359
- Radiologic Societies 369

19.2.77

19.2.77

AJR

American
Journal of
Roentgenology

September 1976

Better yields Better service



with the improved Minitec Generator (Technetium 99m)

Squibb Research recently made modifications in Minitec. As a result, yields are better and more consistent. Small-volume, high-concentration eluates provide maximum flexibility. Wide range of potencies—220, 440, 880, 1330, 1770 and 2220 mCi of ^{99m}Tc—means there's a Minitec generator to meet every lab's needs.

Let CUSTOMTEC™ solve your delivery problems. This free Squibb computer service custom-tailors generator size and delivery schedule to your daily ^{99m}Tc requirements. For more information, mail this coupon to:

Name _____
 Institution _____
 Address _____
 City, State, Zip _____

E. R. Squibb & Sons, Inc. Box 4000 Princeton, N.J. 08540
 CUSTOMTEC™



When Rockford's SwedishAmerican decided to build a complete radiation therapy center, they came to the source.

LEFT: RC-120-Rotational Cobalt Teletherapy Unit gives maximum versatility by means of a broad combination of standard components. Unique features offer field sizes as large as 35 cm. x 35 cm. at 80 cm. SSD. Ram-style couch can be provided, offering the user treatment fields large as 70 cm. x 70 cm. Increased source head capacity of 120000 RHM.

CENTER: LMR-15-Medical Linear Accelerator provides six treatment modes, — two x-ray and four electron. Features ram-style couch, and provides exceptionally large treatment fields. Small scale, ease of operation and low cost. Complete package of options for maximum flexibility. Proven dependability and performance with over fifty operating installations.

RIGHT: LX-8 Universal Therapy Simulator. Provides pinpoint accuracy in simulation. Improved efficiency in therapy-planning. Single generator operation gives substantial initial savings.

Litton Medical Systems and Toshiba. A complete source of radiation therapy systems. Together, offering years of experience, achievement and distinguished technology in this highly complex field.

When you're considering a complete radiation therapy center—consider the source. Litton Medical Systems and Toshiba.



Litton
Medical Systems



TOSHIBA

Toshiba International Corporation
P.O. Box T, Wheeling, Illinois 60090

515 E. Touhy Ave., Des Plaines, Ill. 60018

For faster patient flow, you can buy a compound scanner and a real-time add-on.

Or do it all in one unit for about half the cost with **Siemens Vidoson Ultrasound.**

If you're looking for faster patient flow and superior diagnostic capabilities, there's just one way to do the job with just one machine:

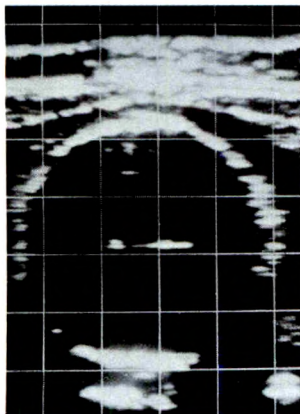
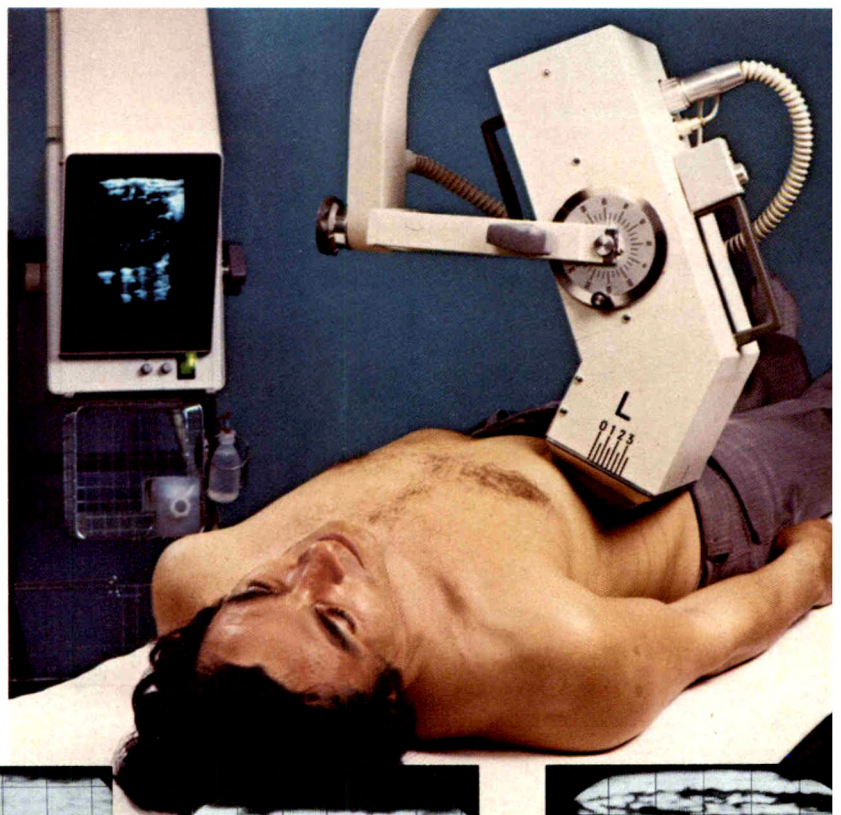
Vidoson Ultrasound by Siemens.

It combines the real-time immediacy of ultrasound with the optimum in gray scale resolution. And it gives you "dynamic and static" pictures in just about one minute.

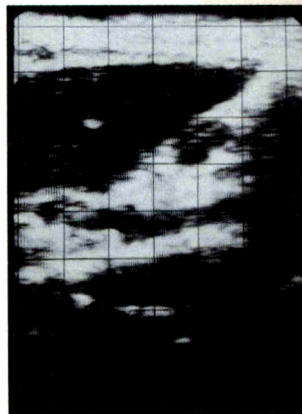
All for about half the cost of a compound scanner and a real-time add-on.

Surprised? You shouldn't be. After all, Siemens has been a pioneer in ultrasound innovation since 1950. Siemens was the first to use it successfully in obstetrics and gynecology. And now, because of the outstanding Siemens gray scale, Vidoson becomes the equipment of choice for internal applications.

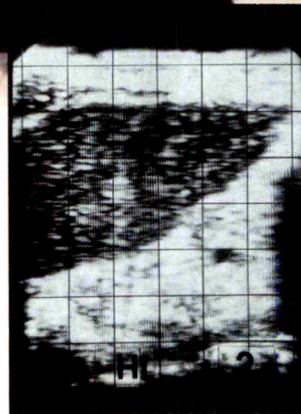
For detailed literature on Siemens Vidoson Ultrasound, write or call:
Siemens Corporation, Medical Systems
Division, 186 Wood Avenue South,
Iselin, New Jersey, (201) 494-1000.



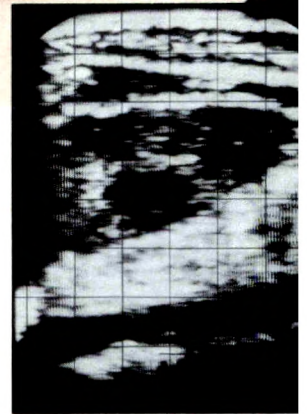
Vidoson embryo assessment; fetal skull with midline echo.



Longitudinal scan through the left lobe of a normal liver.



Left liver lobe showing fatty degeneration.



Black, blurred regions show metastases of the liver.

Sonograms courtesy of Dr. Rettenmaier, District Hospital of Boeblingen, West Germany and Dr. Lutz, University Clinic of Erlangen, West Germany

SIEMENS

AMERICAN JOURNAL OF ROENTGENOLOGY

EDITOR MELVIN M. FIGLEY

ASSISTANT EDITOR ROSALIND H. TROUPIN

ASSOCIATE EDITORS LUTHER W. BRADY
KENNETH L. KRABbenhOFT
E. FREDERICK LANG
RUSSELL H. MORGAN

EDITOR
EMERITUS TRAIAN LEUCUTIA

INCLUDING DIAGNOSTIC RADIOLOGY, RADIATION ONCOLOGY, NUCLEAR
MEDICINE, ULTRASONOGRAPHY AND RELATED BASIC SCIENCES

CONSULTING EDITORIAL BOARD

KENT ELLIS
E. ROBERT HEITZMAN
DONALD L. KING
JOHN A. KIRKPATRICK, JR.
EUGENE C. KLATTE

JOHN G. McAFEE
THOMAS H. NEWTON
ROBERT G. PARKER
STEWART R. REUTER
WILLIAM B. SEAMAN

ROBERT J. SHALEK
JOHN STORER
MICHEL M. TER-POGOSSIAN
JOSEPH P. WHALEN
DAVID M. WITTEN

EDITORIAL STAFF: C. P. KAISER, M. J. LEONARD, K. A. MURRAY, M. B. WIECKOWICZ



OFFICIAL JOURNAL
AMERICAN ROENTGEN RAY SOCIETY
AMERICAN RADIUM SOCIETY



The American Journal of Roentgenology is issued monthly by Charles C Thomas, Publisher, 301-327 East Lawrence Ave., Springfield, Illinois 62717. Correspondence regarding subscriptions, advertisements and other business should be addressed to the Publisher. Annual subscription prices: United States and U. S. Possessions \$30.00, Pan America, Canada and others \$35.00. Single copies, \$3.00. Printed by the George Banta Co., Menasha, Wisconsin. Copyright © 1976 by American Roentgen Ray Society. Second-class postage paid at Springfield, Illinois and at additional mailing offices. Printed in U.S.A.

Guidelines for Authors

The *American Journal of Roentgenology* publishes original and timely contributions to the advancement of radiologic diagnosis and treatment. Although the content is predominantly clinical in origin, laboratory investigations are accepted when their relevance to clinical practice is demonstrable. Contributions are reviewed by two outside consultants and are accepted on condition that they are submitted only to this Journal and that they will not be reprinted or translated without consent of the Editor. Statements within an article are the responsibility of the authors and not the Journal or its publisher.

Address all manuscripts and correspondence to the Editor, Dr. Melvin M. Figley, 403 Pacific National Bank Building, 4545 15th Avenue N.E., Seattle, Washington 98105.

Manuscript Form

Manuscripts should be typed double-spaced throughout, including references, tables, and footnotes. Tables, footnotes, and figure legends should be on separate sheets, and a separate title page should be provided. In addition to the original typewritten copy, a duplicate copy complete with figures, tables, and references is required.

Figures should be submitted as 5" × 7" glossy prints, untrimmed and unmounted. Identifying information (author name, figure number, and indication of the top of the figure) should be attached to the back of each figure with a gummed label. Line illustrations and graphs should be drawn in black ink on white background. Labels on all figures should be of professional quality and sufficiently large to be easily read when reduced in size.

References should be cited in the text by number (e.g., [3, 4]). The bibliography should be arranged in the numerical order that references are cited in the text and typed double-spaced throughout. Data for each reference should be arranged according to the uniform style on bibliographic citations adopted by many biomedical journals. Abbreviations for titles of medical periodicals should conform to those published in *Index Medicus*. Examples:

1. Miller RE, Chernish SM, Skucas J, Rosenak BD, Rodda BE: Hypotonic roentgenography with glucagon. *Am J Roentgenol* 121:264-274, 1974
2. Boijesen E: Superior mesenteric angiography, in *Angiography*, edited by Abrams H, Boston, Little, Brown, 1971, pp 1091-1119

Organization

Title page. Titles should be brief and specific. Include full names and addresses of all authors and acknowledgment of grant support when appropriate.

Abstract. A description of the purpose, methods, results, and conclusions of the study is required. It should be informative to a reader who has not read the text of the article.

Key indexing words. Five to 10 words or short phrases should be supplied to enable cross-indexing of the article.

Introduction. Clearly state the purpose of the investigation including necessary background facts.

Materials and methods. Describe the protocol clearly so that an experienced worker can understand what was done. Use standard abbreviations as presented in the *Council of Biology Editors Style Manual*, 3d edition.

Results. Present results in logical sequence.

Discussion. Interpret the results to lend meaning and importance to the observations. If hypotheses and speculation are included, they must be labeled as such. When results differ from those of previous investigators, an attempt should be made to explain the discrepancy.

References. Only include those references which provide adequate background and present fairly any opposing evidence and concepts. Accuracy of reference data is the responsibility of the author.

Legends. Legends should be brief but should provide sufficient description to interpret the figure.

Special Communications

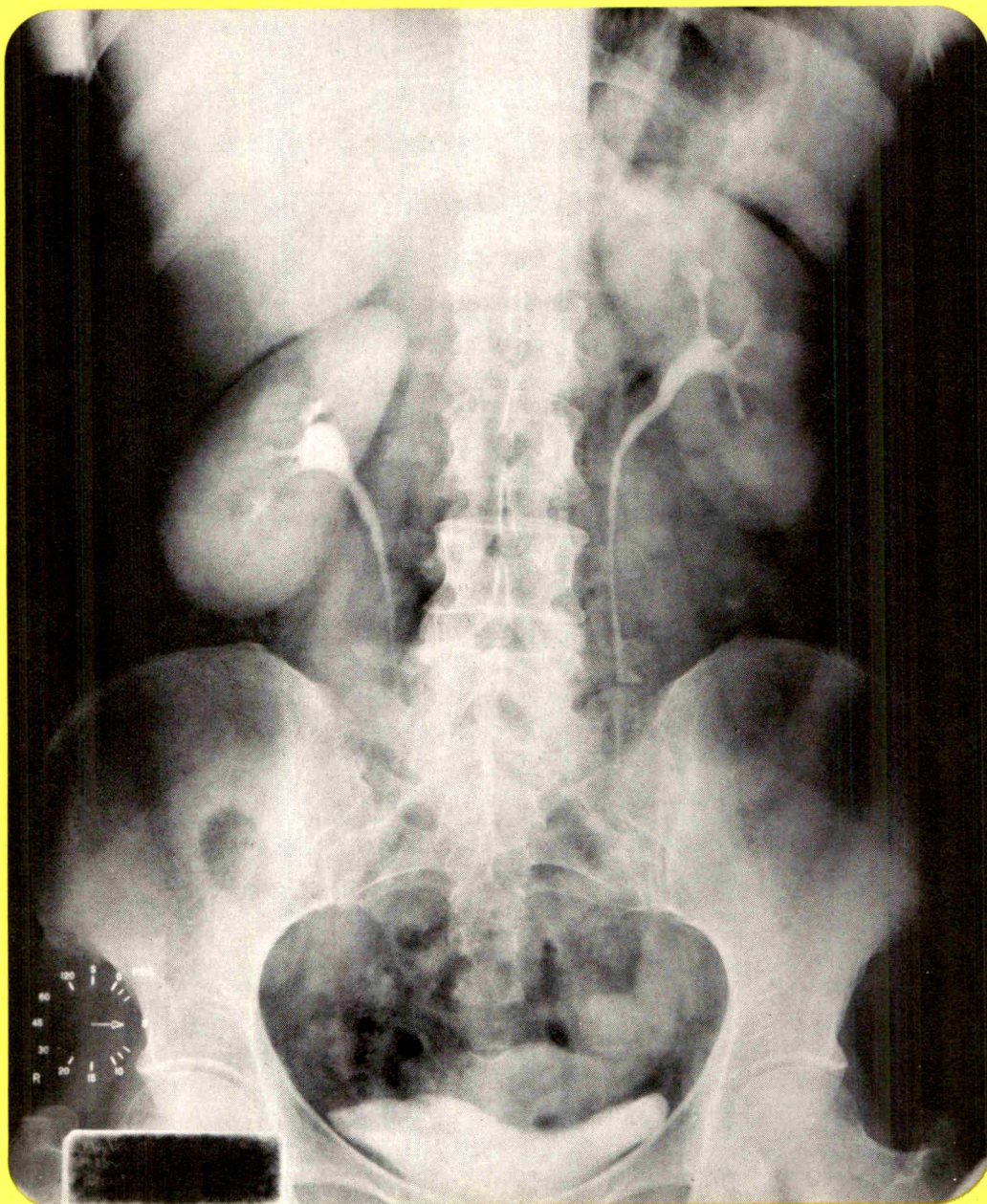
Case Reports. Concise case reports are accepted if they present unusual experiences that are medically important and educational. Clarity and brevity are essential.

Technical notes. Brief descriptions of new techniques or significant modifications of older ones which are directly applicable to clinical practice will be accepted.

Letters to the Editor. Letters should be limited to between 250 and 500 words. Criticism of published articles should be objective and constructive. Letters may also discuss matters of general interest to radiologists.

Proofs and Reprints

Galley proofs will be sent for correction of errors. The corrected proof, copy-edited manuscript, and the reprint order should be returned directly to the Editor. If the author fails to return proof by the date specified, it may be necessary to publish without the author's approval.



Excellent visualization in intravenous pyelogram 18 hours after administration of 2½ oz. X-PREP Liquid for preradiographic bowel cleansing. (In the files of the Medical Department of The Purdue Frederick Company.)

To prep the bowel for intravenous pyelography

X-PREP[®] Liquid

(standardized extract of senna fruit)

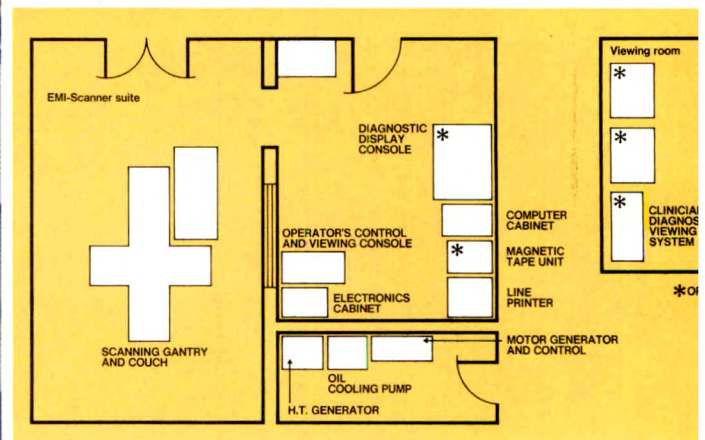
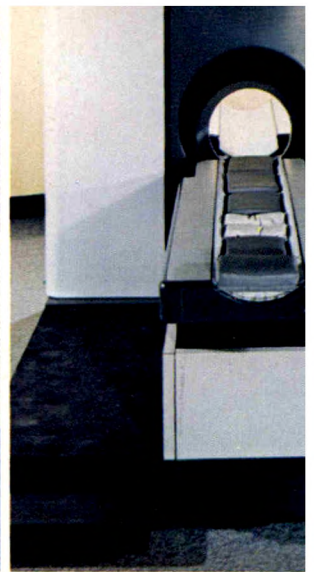
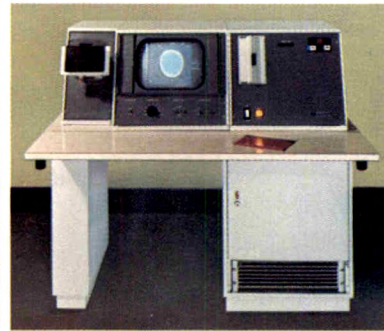
One step • One dose • One bottle

□ X-PREP Liquid is designed specifically for preradiographic bowel cleansing — without enemas, suppositories or overhydration.

□ A single 2½ oz. oral dose is usually all that is required. No residual oil droplets (such as may occur with castor oil).

□ Pleasant taste meets with high patient acceptance. Ease of administration is appreciated by the patient and nursing staff.

**Gray Pharmaceutical Co., Affiliate
The Purdue Frederick Company**



6-213

When you purchase an EMI Scanner you receive The world's savviest installation team

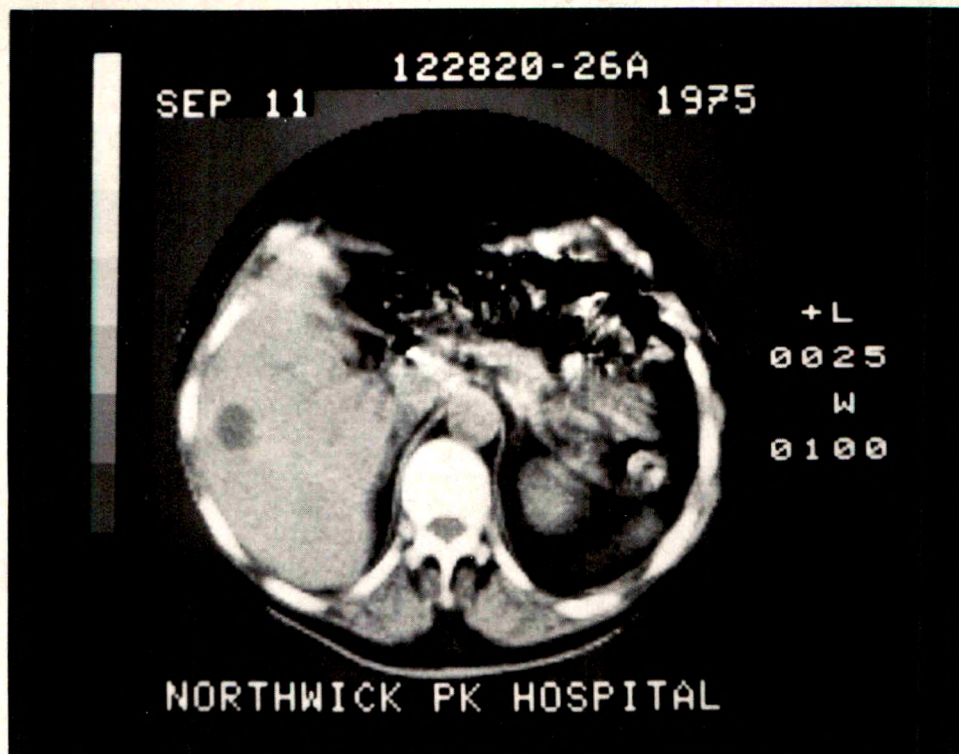
When you purchase either of our EMI-Scanners—the CT1010 Advanced Neuro C.T. System or our CT5005 Advanced General Diagnostic C.T. System, EMI Medical's installation team acts to insure swift, trouble-free installation and start-up. With every scanner purchase we provide a comprehensive Project Planning Guide based on tested concepts of critical path planning. The guide helps establish clear-cut internal procedures, co-ordination and liaison with EMI Medical, and specific checkpoints for the completion of



First in CT installation services

EMI MEDICAL INC

each task. EMI provides continuing assistance for all phases of your EMI-Scanner installation to help insure that the space allotted, the system layout, wiring, shielding, etc. meet desirable operating parameters. After installation, our engineers conduct a thorough final test of your scanner system. Only when you are completely satisfied with your installation, are we. EMI has installed more CT scanner systems than all other manufacturers combined. For more information, call us or write.



EMI-SCAN taken at the level of the 12th thoracic vertebra. The dark area of low absorption is a metastasis from a prostatic carcinoma. This lesion was not suspected until shown on the EMI-SCAN.

6-220

Superior diagnostic information in every EMI-SCAN:

A metastatic lesion at T12

The EMI-Scanner CT5005 Advanced General Diagnostic C.T. System allows accurate visualization of detailed tissue structures that are extremely difficult to investigate with alternative techniques. Based on thoroughly proven EMI technology, this new head and body scanner has also demonstrated improved diagnostic accuracy in areas where current methods have been regarded as satisfactory. The CT5005 employs a rapid scanning cycle to record more than 300,000 X-ray readings per scan. Exceptionally powerful data



**First in CT
imaging,
worldwide**

EMI MEDICAL INC

processing capability ensures that the full potential of the information in the photon beam is realized in the patient's scan pictures. In the high-resolution format, picture elements 0.75 mm x 0.75 mm can be resolved. The diagnostic precision of EMI-SCAN pictures is proving a major benefit in examining conditions such as metastases in organs including the liver, pancreas, and kidneys, and in studies of the skull, retro-sternal area, inferior angles of the lungs, spleen and spinal canal. For information, call us or write.

era of diagnostic advancement. Instead of being limited to a single imaging method, you will take advantage of many techniques, choosing them to meet your specific diagnostic criteria and the condition of your patient.

Searle is helping shape this era of advancement. Over the past decade, guided by your needs, we have developed sophisticated nuclear imaging instruments to a high degree of performance. Now, the knowledge gained during that time is being applied to the creation of instrumentation in the fields of ultrasound and CT scanning.

What Searle developed yesterday in nuclear imaging, the medical community relies on today. And today we are planning significant advances in ultrasonic, CT, and nuclear imaging. Tomorrow is in view.

IMAGING: The Living Art



SEARLE

Searle Radiographics Inc.

Subsidiary of G. D. Searle & Co.

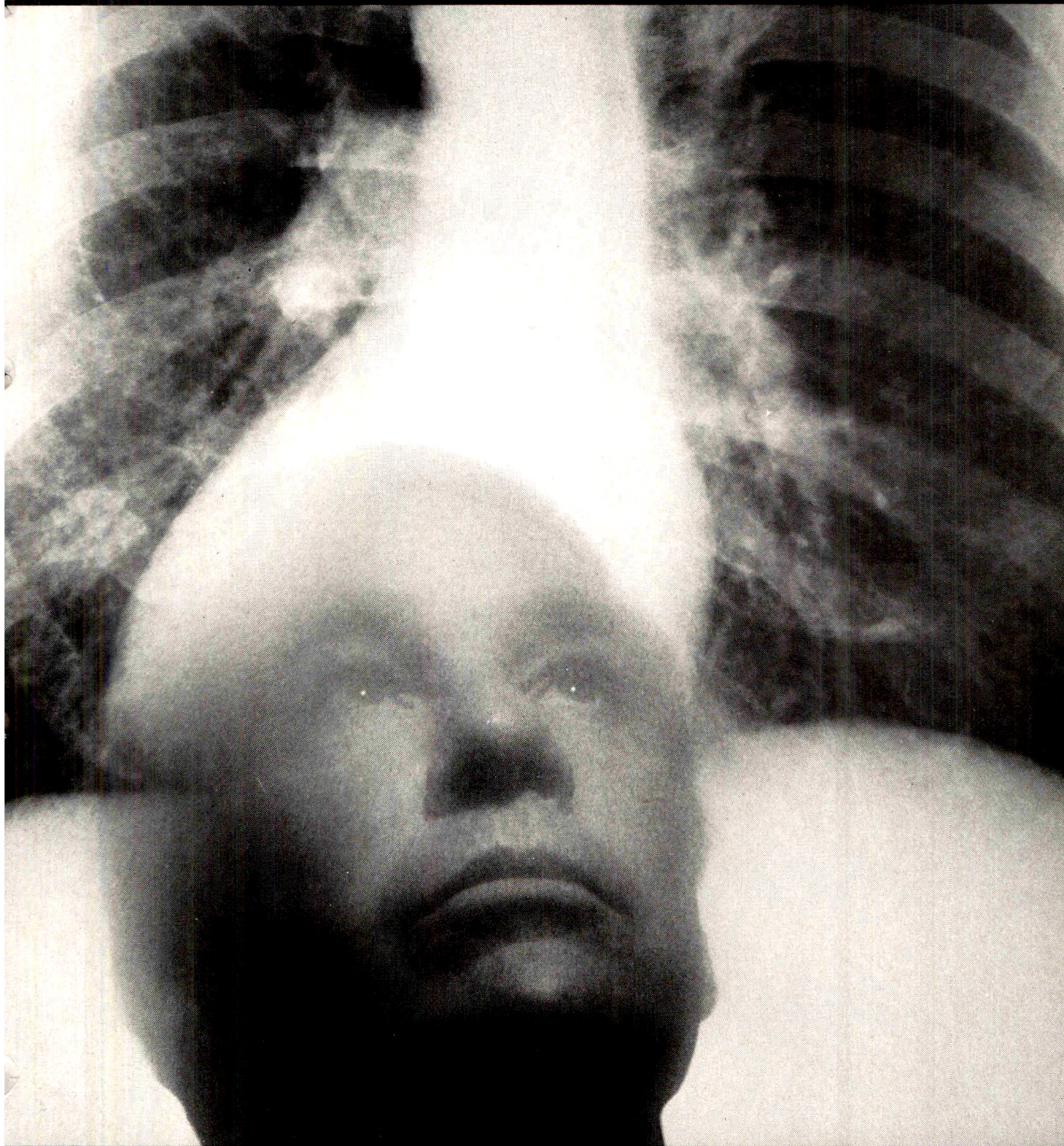
SR-5

**Quality is what
Kodak is all about.**

It goes a long way toward providing consistent imaging results. Quality is the heart of our

products. The ingredient of our services. The extra advantage of the skilled counsel of our technically experienced representatives who can meet your radiographic requirements.

Quality is the Kodak expertise in imaging technology which can be of value to you because diagnostic decisions can sometimes depend on the quality of the diagnostic image.



**When what you want is image quality,
consider Kodak quality.** where can we help you most?

Your concern is Ours is meeting your with Kodak quality.

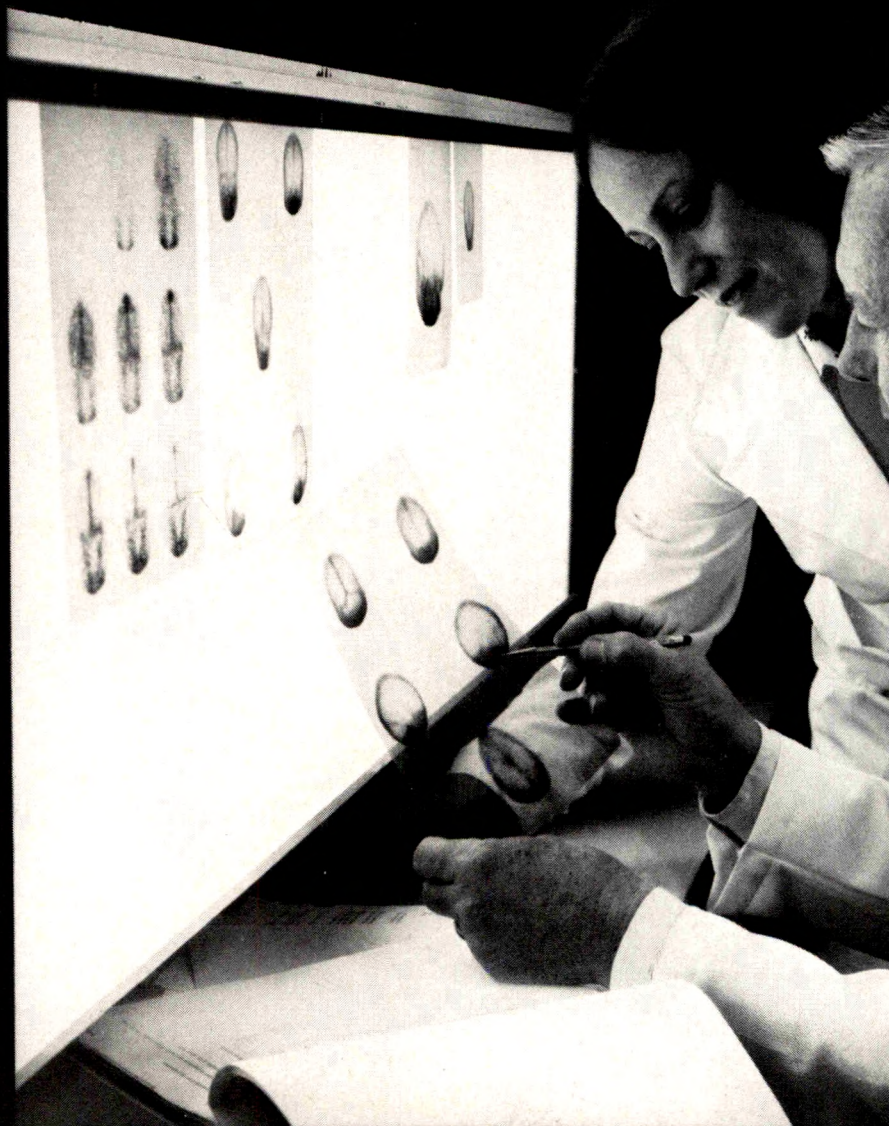
Focus on KODAK Medical X-ray Films.

To meet your varied imaging requirements, Kodak offers a wide range of quality films. Each is designed to consistently provide well-defined diagnostic information on the viewbox — where quality images count.

Films for general radiography. Whether you need a high-contrast film for maximum detail or a wide-latitude film to record variations in tissue densities, Kodak has them. If speed is your concern, use our high-speed films to shorten exposure time. Each of our films provides good transport reliability in automatic film-handling equipment.

Films for special technics.

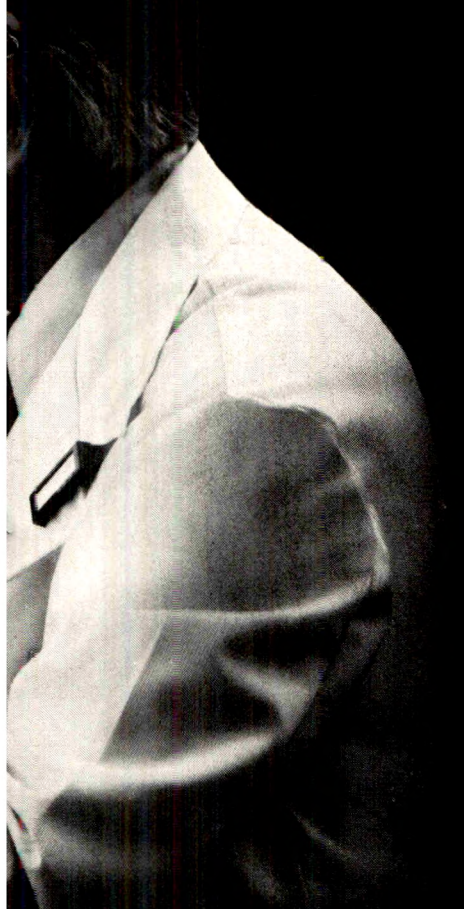
In addition to general radiographic needs, you may have other areas where you require consistent image quality. Here you also have a choice of Kodak films: for special procedures; for subtraction; for therapy localization; for cinefluorography; for spot film radiography; and for cathode-ray tube imaging — thermography, ultrasonography, computerized axial tomography.



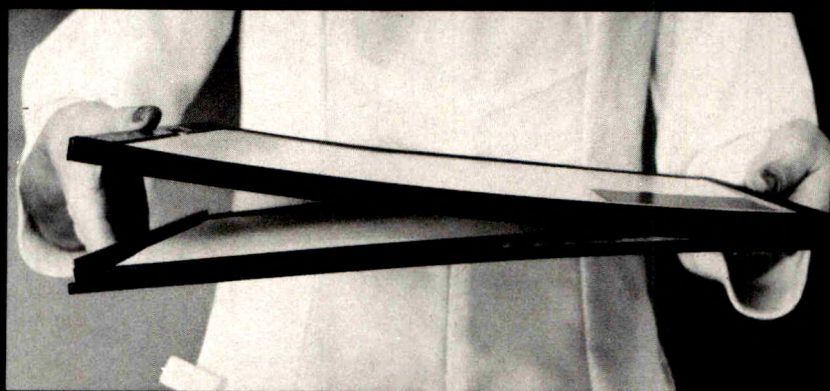
**New Advances
in Imaging Technology.
Products for mammography.** Compared with any current Kodak film and screen combination for mammography, two new products — Kodak Min-R film and Kodak Min-R screen — offer the fastest speed with equal or better image sharpness.

Rare earth imaging products. Research in rare earth phosphors resulted in Kodak Lanex regular screens and Kodak ortho G film. They provide higher speed — so you can shorten exposure time, or reduce kilovoltage, or decrease milliamperage. All of which can help extend your radiographic technic and equipment capabilities.

making a diagnosis. imaging needs...



Films for nuclear medicine. Kodak offers transparency films for single, multiple, or dynamic imaging. These include Kodak film for nuclear medicine SO-179 — ideal for recording images from cathode-ray tube displays. Transparency films resist fading and curling, are easy to store. And they can provide high-quality images through automatic



processing in 90 or 150 seconds.

**Kodak
Efficiency Improvers.
The curved cassette.**

Kodak X-Omatic cassettes have specially designed, curved covers that force out air when closed, creating an intimate screen/film contact for consistently high image quality. Easy to open and close with one hand. Durable — resists damage, either to the cassette or in the screen/film contact.

The positive patient data keeper. The Kodak X-Omatic identification camera records data on the radiograph itself, in full room light. No lead letters or numbers to fall off, less

chances for misidentification. It's an accurate and efficient means of monitoring patient flow.

Automatic processing. When patient load requires rapid access to processed radiographs, Kodak has a 90-second automatic processor you can depend on. If you need a compact processor for emergency or satellite areas, Kodak has a 150-second automatic processor that uses unheated water, cuts back on costs. Both deliver consistent quality radiographs.

**How do you get
all this from Kodak?
Turn the page...**

Having a Kodak TSR who knows your problems gives you a head start on the answers.



What can you expect from your Kodak Technical Sales Representative? More than the name implies.

Your TSR is a professional consultant—highly trained and technically experienced in imaging technology, with a working background in medical radiography, nuclear imaging, photofluorography, cine-fluorography. Here's what the TSR can do:

- Conduct training courses for x-ray department personnel
- Arrange for special courses or group training programs
- Give your staff ready access to comprehensive technical information to help you get the most out of your Kodak films, chemicals, processing equipment
- Provide manuals, product brochures, medical charts, audiovisual presentations, slide lectures, clinical case studies, and a

variety of technical publications on radiography

To get the most out of your Kodak products, get the most out of your TSR. Contact your Kodak representative. Or consult your x-ray products dealer. Or write: Eastman Kodak Company, Department 740-B, Rochester, N.Y. 14650.

**A commitment
to quality.**



Is there an unhappy Amrad Customer?

Seems unhappy customers abound in the x-ray business. But as far as we know, none of them belong to us. In the little over two years we've been in business, we've now shipped over 500 complete units of a superb space-saving 600-MA, 125 KV x-ray room. You know, the one with that super-slick table, plug-in installation and remote generator control.

The one with add-on mammography and tomography capabilities that cost a fraction of any other approach.

And when number 500 went out, we still hadn't heard a whimper. We think a lot of it has to do with our dealer network being so on-their-toes. After all, each of the seventy-five is an independent businessman, too — so they have to be good.

But maybe you should check for yourself. If you ever buy x-ray equipment, send us the coupon below, and we'll send you an unedited list of all the installations we have in our records. Chances are, you'll spot a few colleagues whom you know, and can then find out about this phenomenon in the x-ray business: a manufacturer with no unhappy customers.

Why, you might even want to become a customer yourself!

AMRAD

AMERICAN RADIOLOGIC
SYSTEMS, Inc.

2055 N. Janice Ave.
Melrose Park, Ill. 60160
(312) 865-2600



Why don't you ask around?

To:
C. W. Vatz
AMRAD
2055 N. Janice Ave.
Melrose Park, Ill. 60160

Okay, send me your latest customer list. Your stuff might be worth checking out.

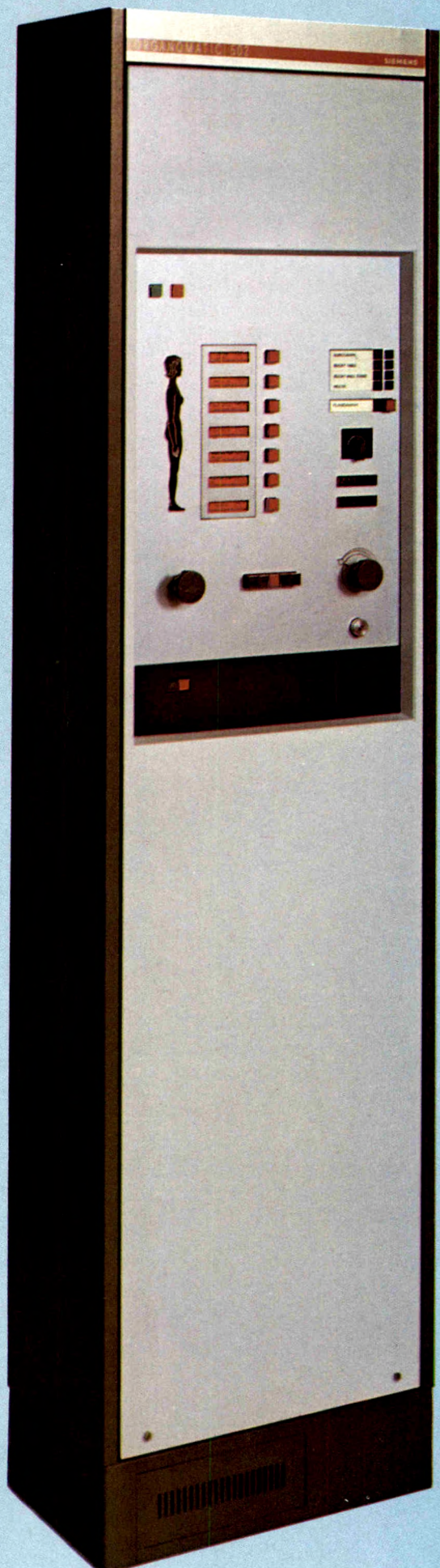
Name _____

Organization _____

Address _____

City _____

State _____ Zip _____



A new series of x-ray generators featuring simple push-button programming: Siemens Organomatic.

Convenience is the idea behind these generators. Any one of 49 preset programs may be selected simply by the turn of the knob and the push of a button.

For ease of identification, push-buttons are organ related.

The proper kV, mAs, mA, focus, screen and tube can be selected with only one button. The need to consult reference tables for desired settings is eliminated. Moreover, through automation, the chances of error and the need for time consuming repeats are substantially reduced.

Selection. Available as a single-phase 600 mA generator (model 502) or a three-phase 500 mA generator (model 506), the Organomatic may be customized to meet specific user needs. All automatic programs can be preset during installation to accommodate any desired combination of kV and mAs settings.

Ease of Service. Solid state circuitry guarantees performance reliability. Circuit board and swing-out rack assembly assures accessibility and ease of maintenance.

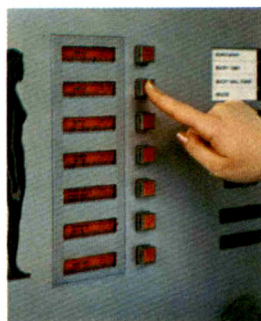
The Organomatic also features an exclusive automatic fault locator / indicator to pinpoint service requirements.

Options. A variety of add-on system features make the Organomatic fully adaptable to specific needs. Among them:

- Automatic exposure timer for correct patient size compensation.
- Planigraphy programming (28 additional programs).
- Fluoroscopy with automatic brightness control.
- Indirect exposure technique with 100 mm cut film camera.
- Over-ride module for free kV and mAs selection.



1 Body region selector.



2 Organ selector buttons.



3 Patient thickness compensation.



4 Exposure release.

Investigate the Siemens Organomatic and ask about convenient lease financing arrangements. For detailed information, contact your Siemens representative, or you may write to: Siemens Corporation, Medical Systems Division, 186 Wood Avenue South, Iselin, N.J. 08830 (201) 494-1000

In Canada: Siemens Canada Limited, P.O. Box 7300, Pointe Claire 730-P.Q.

SIEMENS



Xonics Electron Mammography System

Introducing **XERGTM Mammography by Xonics.**

It's here. It works. It's ready to order.

The mammography system you've been waiting for is here. XERG by Xonics combines everything you want in a mammography system—high resolution, lowest exposure levels, revolutionary new convenience and serviceability—all in one complete system.

Only the XERG Mammography System can deliver high-resolution mammograms (20 line pairs per mil-

limeter) at incident exposure levels of less than 150 mR.

We manufacture the entire system—from micro-focus x-ray tube to the image receptor. And your Xonics/Standard dealer services the entire unit.

Contact your local Xonics/Standard dealer for details, or write us directly for information on ordering the XERG Mammographic System.

Some Xonics/Standard distribution areas are available.
We invite your inquiry.



2495 Pembroke Avenue · Hoffman Estates, IL 60195
Telephone (312) 884-0084

The AECL universal, therapy

TREATMENT PLANNING

system



THERASIM 750

universal simulator—and the

TP-11 computer based treatment planning/programmer.

The preparation of precise treatment prescriptions has become an integral part of modern radiation therapy. The rapid advance in techniques has prompted AECL to develop the Universal Therasim 750 Simulator which, working in concert with the computer controlled (TP-11) Treatment Planning System, provides an unmatched degree of accuracy in the planning of good therapy.

The **THERASIM 750** offers many notable new features including increased isocentric accuracy, longer variable SAD and greater image intensifier X and Y directions.

The **TP-11** offers a comprehensive package of treatment planning programs that permit sophisticated planning in a fraction of the time. Multiple ports, rotations, and irregular fields, with or without filters or

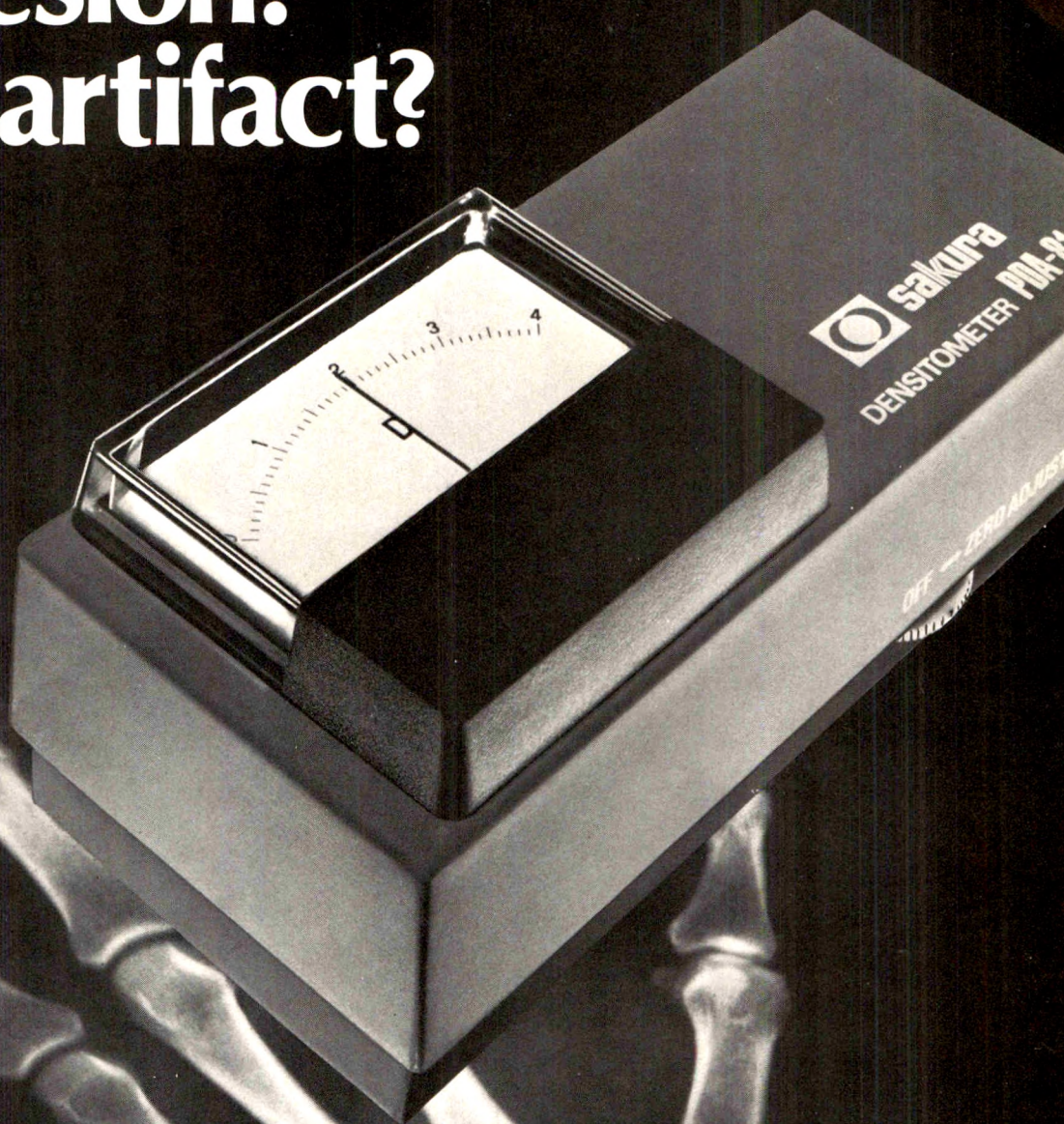
bars, may be calculated singly or combined without limit. Implant distributions may be added to external beams. A concise hard-copy plot is produced, showing the Distribution and Treatment Plan. Utility programs to plot isodoses, design wedge filters, and perform other useful tasks are included.

*For detailed information please write to
Atomic Energy of Canada Limited,
Commercial Products,
P.O. Box 6300, Ottawa, Ontario, Canada. K2A 3W3.
Telephone 613/592-2790. Telex 053-462*



**Atomic Energy
of Canada Limited
Commercial Products**

Is it a lesion? Or an artifact?



Be safe. Be sure. Electronically measure the accuracy and quality of your radiographic exposure and processing. Sakura has the precision densitometer you can rely on.

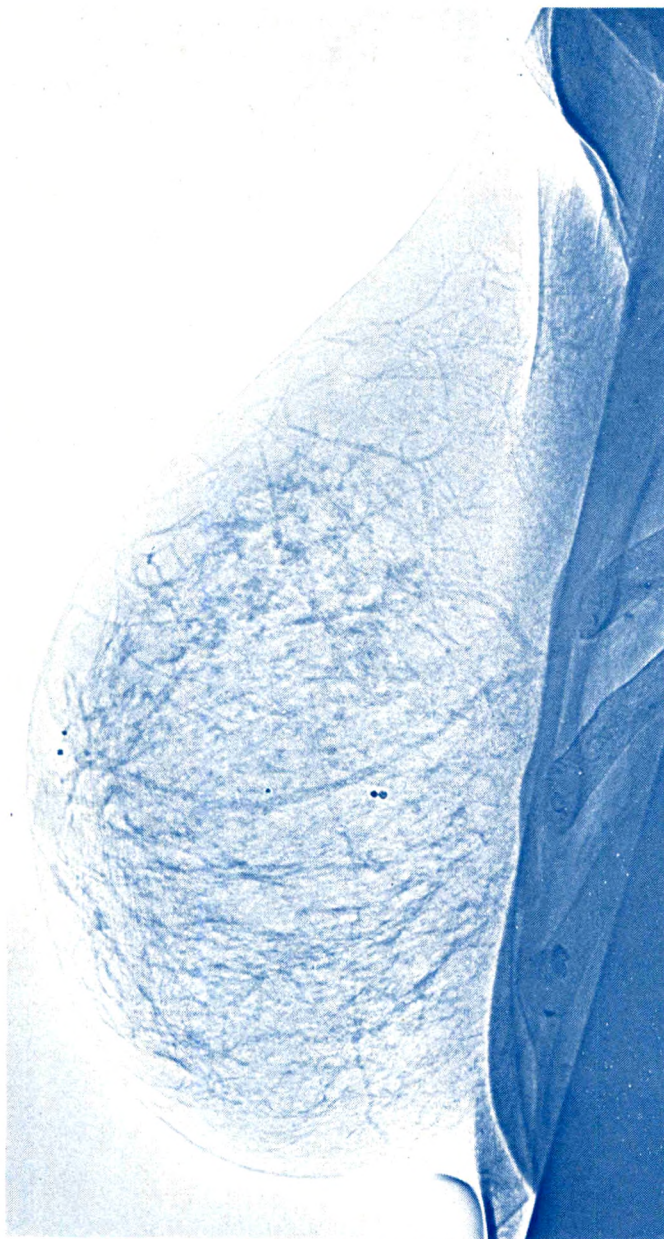
Lightweight and portable, our PDA-81 is conveniently battery powered. Its new, improved silicon photocell gives it an increased density range of 0 to 4.0, with an outstanding accuracy to within $\pm 0.05D$. Yet, there is no carry-over influence from preceding films, and no time lag between readings.

Hand held and pocket sized, PDA-81 lets you take the precision of a bench-top unit into the field, around the hospital – virtually anywhere.

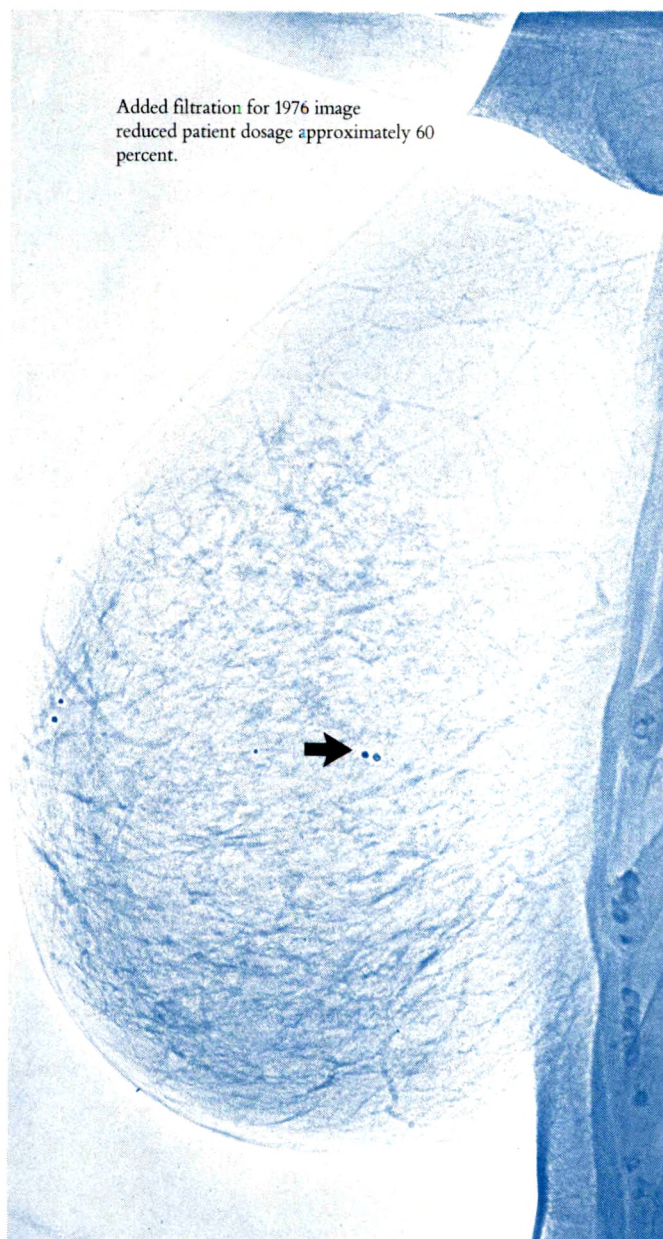
Be safe and sure. Wherever your work takes you. PDA-81, from the leader in radiography systems since 1934: Sakura. Write on your letterhead or call for literature and details:



Sakura Medical Corporation
Radiographic Film and Instrumentation
57 Bushes Lane, Elmwood Park, New Jersey 07407
(201) 794-0800



1972 xeroradiograph. Filtration 0.5 mm aluminum.



1976 xeroradiograph. Filtration 2.0 mm aluminum.

Case history: 63-year-old patient, examined in 1972 because of pain in left breast (right breast previously removed.) Routine follow-up in 1976 revealed occult nonpalpable carcinoma (arrow.) Pathological findings: 3 mm ductal carcinoma with no axillary node involvement. (Images from Gloria Frankl, M.D., Dept. of Diagnostic Radiology, Kaiser Permanente Hospital, Los Angeles, CA 90027.)



3X magnification.

Now you can make Xeroradiography even safer for her.

It turns out to be surprisingly simple.

Carefully controlled laboratory experiments have established that by increasing aluminum filtration, radiation exposure can be greatly reduced without loss of significant information. Clinical work by practicing radiologists confirms these findings.

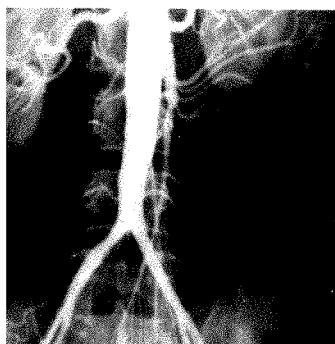
With 2 mm of aluminum the exposure can be as much as 60 percent lower than that required with 0.5 mm, yet the unique xeroradiographic quality is preserved.

For details on how to dramatically reduce mammography dosages with xeroradiography, write to Xeroradiography, Dept. A, P.O. Box 5786, Pasadena, California 91107.

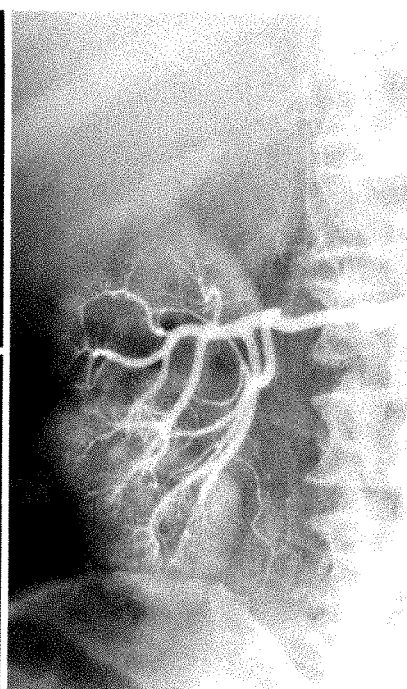
XEROX

the reason is clear™

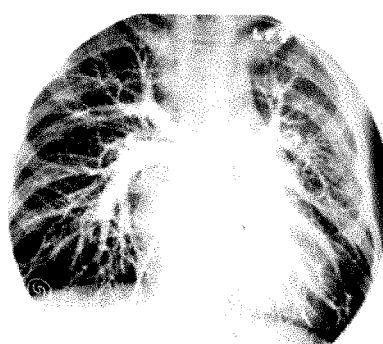
- Excellent image quality
- Rapid visualization of renal pelvis, ureters, and bladder...maximal opacification of renal passages may begin as early as 5 minutes after injection
- 8 indications*



Aortography
Selective coronary
arteriography



Selective renal arteriography



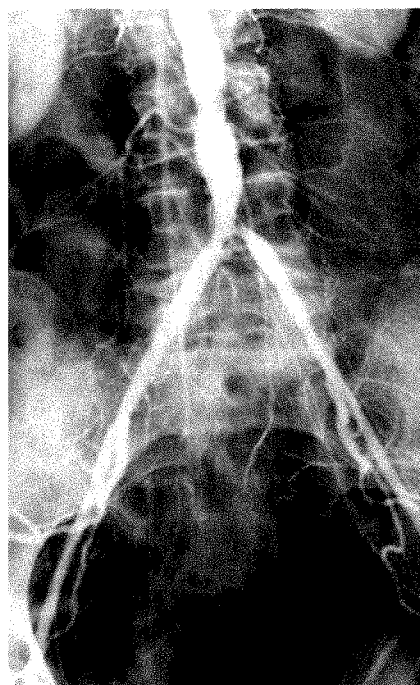
Pediatric angiocardiology
Left ventriculography performed
following coronary arteriography



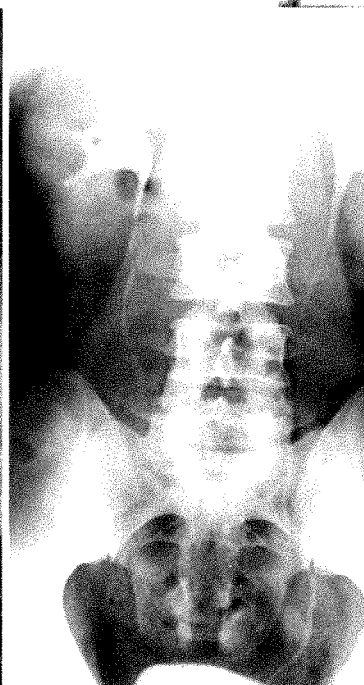
Selective visceral
arteriography

Renografin-76®

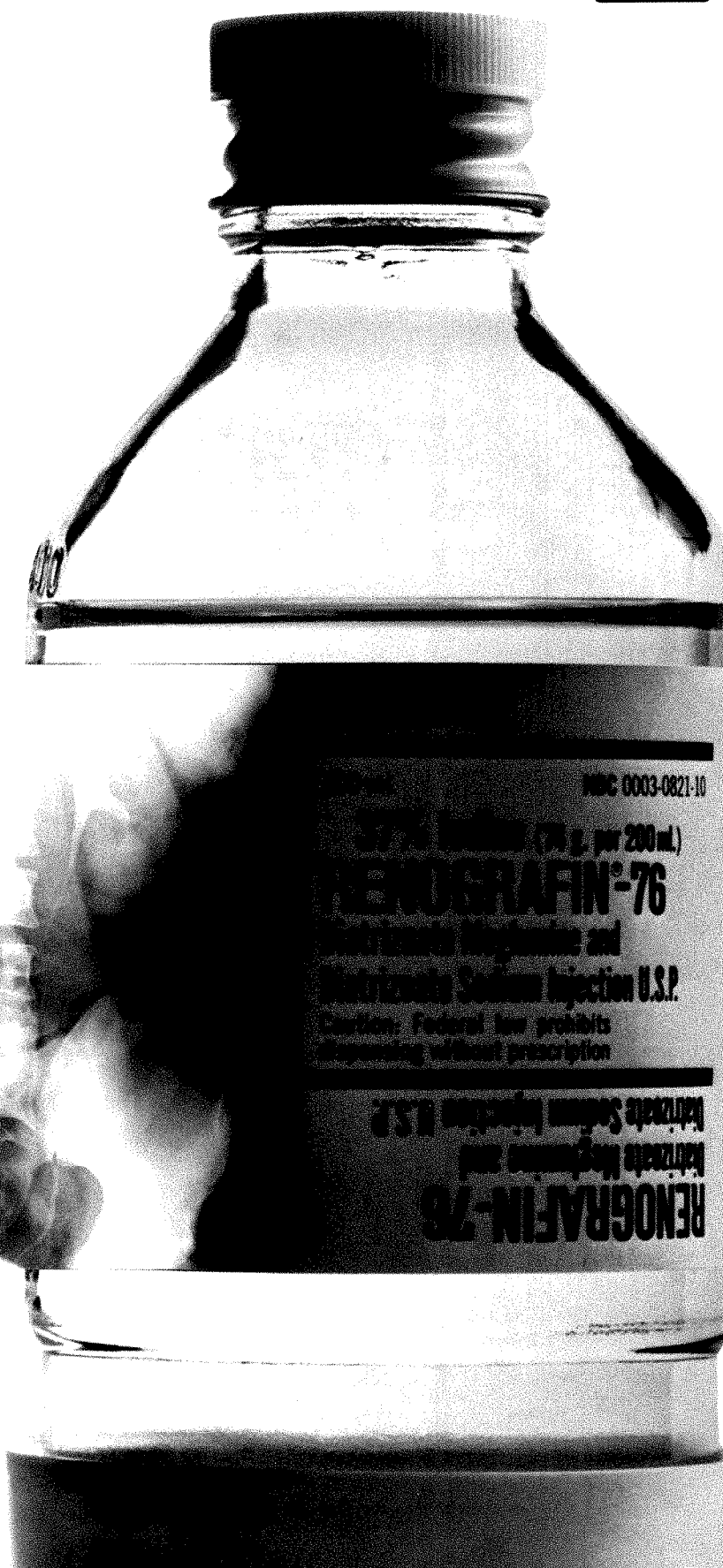
Diatrizoate Meglumine and
Diatrizoate Sodium Injection U.S.P.



Peripheral arteriography



Excretion urography



*For dosage and administration recommendations,
see package insert

Please see following page for brief summary.

RENOGRAFIN-76
Diatrizoate Meglumine and Diatrizoate Sodium Injection U.S.P.

Renografin-76 (Diatrizoate Meglumine and Diatrizoate Sodium Injection U.S.P.) is supplied as a sterile, aqueous solution providing 66% diatrizoate meglumine and 10% diatrizoate sodium with 0.32% sodium citrate as a buffer and 0.04% edetate disodium as a sequestering agent. The solution contains approximately 37% (370 mg./ml.) bound iodine and approximately 4.48 mg. (0.19 mEq.) sodium per ml.

CONTRAINDICATIONS: In patients with a hypersensitivity to salts of diatrizoic acid. Urography contraindicated in patients with anuria.

WARNINGS: A definite risk exists with the use of contrast agents in excretion urography in patients with multiple myeloma. There has been anuria with progressive uremia, renal failure and death. This risk of the procedure in these patients is not a contraindication; however, partial dehydration in preparation for study is not recommended since it may predispose for precipitation of myeloma protein in renal tubules. No therapy, including dialysis, has been successful in reversing this effect. Myeloma should be considered in persons over 40 before undertaking urographic procedures.

In cases of known or suspected pheochromocytoma, if the physician feels that the possible benefits outweigh the considered risks, radiopaque materials should be administered with extreme caution; however, an absolute minimum of material should be injected, the blood pressure should be assessed throughout the procedure, and measures for treating a hypertensive crisis should be available.

Contrast media may promote sickling in homozygous individuals when injected I.V. or intra-arterially. Although a history of sensitivity to iodine *per se* or to other contrast media is not an absolute contraindication, administration of diatrizoate requires extreme caution in such cases. Perform thyroid function tests prior to administration of Renografin-76 (Diatrizoate Meglumine and Diatrizoate Sodium Injection U.S.P.) since iodine-containing contrast agents may alter the test results.

Weigh the inherent risks against necessity for performing *angiocardiology* in cyanotic infants and patients with chronic pulmonary emphysema. In *pediatric angiocardiology*, a dose of 10 to 20 ml. may be particularly hazardous in infants weighing less than 7 kg.; this risk is probably significantly increased if these infants have preexisting right heart "strain," right heart failure, and effectively decreased or obliterated pulmonary vascular beds. Perform *urography* with extreme caution in persons with severe concomitant hepatic and renal disease. Perform *selective coronary arteriography* only in selected patients and those in whom expected benefits outweigh the procedural risk. Perform *selective visceral arteriography* with extreme caution in presence of severe generalized atherosclerosis, specifically with plaques or aneurysms at level of iliac or femoral arteries.

Usage in Pregnancy: Use Renografin-76 (Diatrizoate Meglumine and Diatrizoate Sodium Injection U.S.P.) in pregnant patients only when the physician deems its use essential to the welfare of the patient since safe use during pregnancy has not been established.

PRECAUTIONS: Diagnostic procedures involving use of contrast agents should be performed under the direction of personnel with prerequisite training and a thorough knowledge of the particular procedure. Appropriate facilities should be available for coping with situations which may arise as a result of the procedure and for emergency treatment of severe reactions to the contrast agent itself; competent personnel and emergency facilities should be available for at least 30 to 60 minutes after I.V. administration since delayed reactions have been known to occur. These severe life-threatening reactions suggest hypersensitivity to the contrast agent. A personal or family history of asthma or allergy or a history of a previous reaction to a contrast agent warrants special attention and may predict more accurately than pretesting the likelihood of a reaction although not the type nor severity of the reaction in the individual. The value of any pretest is questionable. The pretest most performed is the slow I.V. injection of 0.5 to 1.0 ml. of the preparation prior to injection of the full dose; however, the absence of a reaction to the test dose does not preclude the possibility of reaction to the full diagnostic dose. Should the test dose produce an untoward response, the necessity for continuing the examination should be re-evaluated. If deemed essential, examination should proceed with all possible caution. In rare instances, reaction to the test dose may be extremely severe; therefore, close observation and facilities for emergency treatment are indicated.

Renal toxicity has been reported in a few patients with liver dysfunction who were given oral cholecystographic agents followed by urographic agents; therefore, if known or suspected hepatic or biliary disorder exists, administration of Renografin-76 (Diatrizoate Meglumine and Diatrizoate Sodium Injection U.S.P.) should be postponed following the ingestion of cholecystographic agents. Consider the functional ability of the kidneys before injecting the contrast agent. Use cautiously in severely debilitated patients and in those with marked hypertension. Bear in mind the possibility of thrombosis when using percutaneous techniques. Since contrast agents may interfere with some chemical determinations made on urine specimens, collect urine before or two or more days after administration of the contrast agent.

In *excretion urography*, adequate visualization may be difficult or impossible in uremic patients or others with severely impaired renal function (see Contraindications). In *aortography* repeated intra-aortic injections may be hazardous; this also applies to *pediatric angiocardiology* particularly in infants weighing less than 7 kg. (see Warnings). In *peripheral arteriography*, hypotension or moderate decreases in blood pressure seem to occur frequently with intra-arterial (brachial) injections; this is transient and usually requires no treatment. Monitor blood pressure during the immediate 10 minutes after injection. It is recommended that *selective coronary arteriography* not be performed for about 4 weeks after diagnosis of myocardial infarction; mandatory prerequisites to this procedure are experienced personnel, ECG monitoring apparatus, and adequate facilities for immediate resuscitation and cardioversion.

ADVERSE REACTIONS: Nausea, vomiting, flushing, or a generalized feeling of warmth are the reactions seen most frequently with intravascular injection. Symptoms which may occur are chills, fever, sweating, headache, dizziness, pallor, weakness, severe retching and choking, wheezing, a rise or fall in blood pressure, facial or conjunctival petechiae, urticaria, pruritus, rash, and other eruptions, edema, cramps, tremors, itching, sneezing, lacrimation, etc. Antihistaminic agents may be of benefit; rarely, such reactions may be severe enough to require discontinuation of dosage. There have been a few reports of a burning or stinging sensation or numbness, of venospasm or venous pain, and of partial collapse of the injected vein. Neutropenia or thrombophlebitis may occur. Severe reactions which may require emergency measures (see Precautions) are a possibility and include cardiovascular reaction characterized by peripheral vasodilatation with hypotension and reflex tachycardia, dyspnea, agitation, confusion, and cyanosis progressing to unconsciousness. An allergic-like reaction ranging from rhinitis or angioneurotic edema to laryngeal or bronchial spasm or anaphylactoid shock may occur. Temporary renal shutdown or other nephropathy may occur.

Adverse reactions as a consequence of *excretion urography* include cardiac arrest, ventricular fibrillation, anaphylaxis with severe asthmatic reaction, and flushing due to generalized vasodilatation. Risks of *aortography* procedures include injury to aorta and neighboring organs, pleural puncture, renal damage (including infarction and acute tubular necrosis with oliguria and anuria), accidental selective filling of right renal artery during translumbar procedure in presence of preexistent renal disease, retroperitoneal hemorrhage from translumbar approach, spinal cord injury and pathology associated with syndrome of transverse myelitis, generalized petechiae, and death following hypotension, arrhythmia, and anaphylactoid reactions. In *pediatric angiocardiology*, arrhythmia and death have occurred. During *peripheral arteriography*, hemorrhage from puncture site, thrombosis of the vessel, and brachial plexus palsy (following axillary artery injection) have occurred. During *selective coronary arteriography* and *selective coronary arteriography with left ventriculography*, transient ECG changes (most patients) transient arrhythmias (infrequent); ventricular fibrillation (from manipulation of catheter or administration of medium); hypotension; chest pain; myocardial infarction; transient elevation of creatinine phosphokinase (occurred in about 30% of patients tested); fatalities have been reported; hemorrhage, thrombosis, pseudoaneurysms at puncture site, dislodgment of arteriosclerotic plaques, dissection of coronary vessels, and transient sinus arrest have occurred due to the procedure. Adverse reactions in *selective renal arteriography* include nausea, vomiting, hypotension, hypertension, and post-arteriographic transient elevations in BUN, serum creatinine and glucose. Complications of *selective visceral arteriography* include hematomas, thrombosis, pseudoaneurysms at injection site, dislodgment of arteriosclerotic plaques; other reactions may include urticaria, hypotension, hypertension, and insignificant changes in renal function and liver chemistry tests.

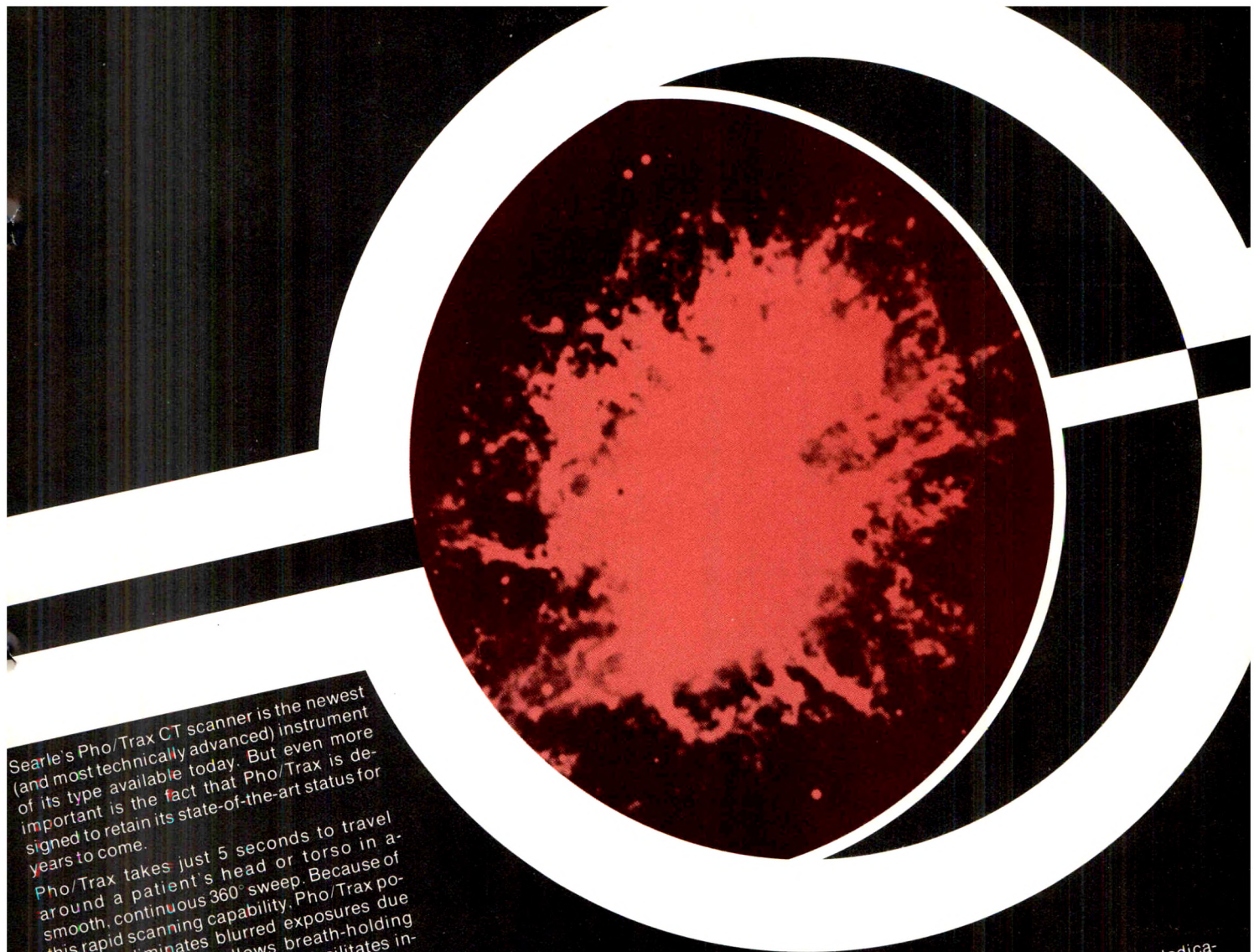
For full prescribing information, consult package insert.

HOW SUPPLIED: Available in 20 ml. and 50 ml. single-dose vials and in 100 ml. and 200 ml. single-dose bottles.

SQUIBB HOSPITAL DIVISION

E. R. Squibb & Sons, Inc.





Searle's Pho/Trax CT scanner is the newest (and most technically advanced) instrument of its type available today. But even more important is the fact that Pho/Trax is designed to retain its state-of-the-art status for years to come.

Pho/Trax takes just 5 seconds to travel around a patient's head or torso in a smooth, continuous 360° sweep. Because of this rapid scanning capability, Pho/Trax potentially eliminates blurred exposures due to patient motion, allows breath-holding even with the severely ill and facilitates infant studies.

Pho/Trax has a 23.5" aperture, which means you can perform torso scans on all but the most obese patients. Evaluation of certain structures in the brain, orbits and abdominal organs may require angled or off-axis views. To help you obtain optimum images in these instances, the Pho/Trax gantry can be tilted in both directions over a 30° range.

VARIABLE SLICE THICKNESS

In scanning small structures such as the optic nerve, a narrower slice thickness can often aid accurate diagnosis. With Pho/Trax, the operator can choose any slice thickness from 3mm to 12mm in 1mm increments. A unique beam-shaping technique controls the x-ray fan, keeping it very close to the slice thickness selected.

VARIABLE SCAN SPEED

For most images, a 5 second scan speed is highly desirable; at this speed, radiation exposure is at a new low while resolution is of a very high order. In circumstances where patient motion is not a problem, and where an exceptional degree of clarity is needed, Pho/Trax lets you select a 10 or 20 second scan speed.

FIELD OF VIEW OPTIMIZATION

Advanced computer technology enables Pho/Trax to use a very high number of picture elements (or "pixels") on the 256 x 256 matrix regardless of the actual size of the area of interest. This is not a simple magnification or "zoom" process, but an algorithmic function which uses 100% of the raw data and does not degrade resolution in any way.

A VARIETY OF IMAGING MODES

Reconstruction time with Pho/Trax is 40 seconds for head and torso scans. There is also a 20-second preview mode which allows the operator to evaluate each scan, with subsequent batch image processing after the study is completed. Typically, 6 12mm brain slices can be reconstructed in 4 minutes, while the next patient is being positioned.

Pho/Trax was developed with the dedication to technical superiority that made Searle the recognized leader for in-vivo and in-vitro radionuclide applications. And as with all Searle instrumentation, Pho/Trax is backed by the industry's largest service organization dedicated to medical imaging devices.

For more information, including sample studies, write Searle CT Systems or call our toll-free "800" number.

CALL 800-323-0221 TOLL-FREE

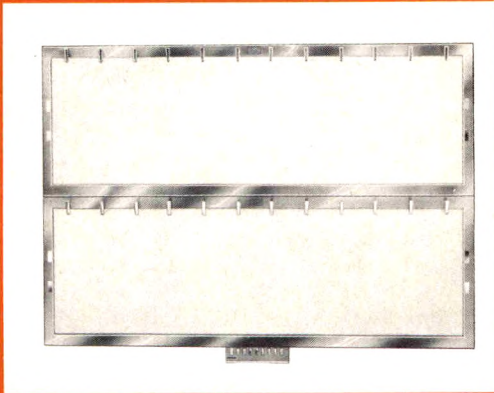
SEARLE

Searle CT Systems
Division of Searle Radiographics, Inc.
4233 North United Parkway
Schiller Park, IL 60176

Designed with the future in mind
Pho/Trax™ CT scanner

Wolf X-Ray

"the illuminator people!"



Singles ■ Panels ■ Mobiles ■
 Angle Vision ■ Explosion-
 Proof ■ Hi-Intensity ■ Spine ■
 Intensi-Spot ■ Fluorescent ■
 Medical ■ Incandescent ■
 Enameled ■ Stainless Steel ■
 Plastic ■ Wall Hanging ■
 Recessed ■ Desk Models ■
 Multiple ■ Specials ■
 Circline ■ Dental.

Whatever your illuminator need, we've got it! Over 235 different sizes and styles, designed for wall installation, desk, or mobile use.

All Wolf illuminators feature a choice of our highly efficient "Roller Clip," or our exclusive "Magic Grip" film retainer that's built right into the frame for positive grip tension. Low voltage leakage is another Wolf feature. And our "Instant Start Lighting" eliminates annoying light delay and flicker... gives you full illumination at the flip of the switch.

The next time you're in need of an illuminator... any kind... think of Wolf. Contact your local Wolf X-Ray Dealer

Wolf X-Ray

Division of IPCO Hospital Supply Corporation
 182-20 Liberty Ave., Jamaica, New York 11412

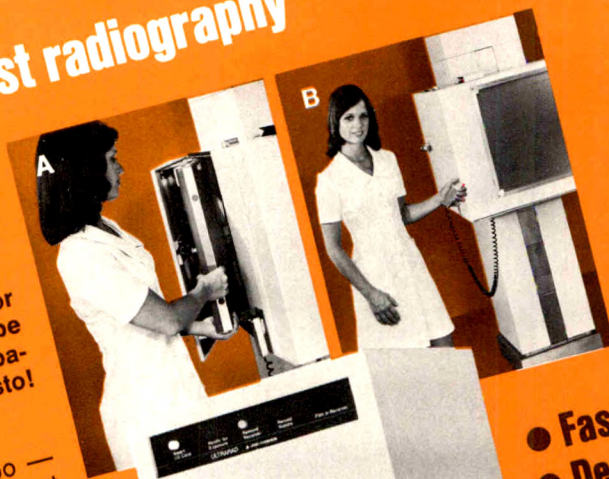
ULTRARAD

for New Efficiency in chest radiography

(A) Instead of handling cumbersome cassettes individually, load a magazine containing up to 75 non-interleaved 14 x 17 inch films in the Ultrarad.

(B) Easy as 1, 2, 3:
1. Position patient (standing, seated or recumbent). 2. Adjust unit and x-ray tube with hand control to accommodate patient's height. 3. Insert ID card — presto! — you are ready for exposure.

There are other Ultrarad features too — quick access to screens and transport area for cleaning — spare magazines furnished — snap-on cassette holder and grid — adaptable to photo-timing. For details, call your x-ray equipment supplier or write for literature.



- Fast
- Dependable
- Compact

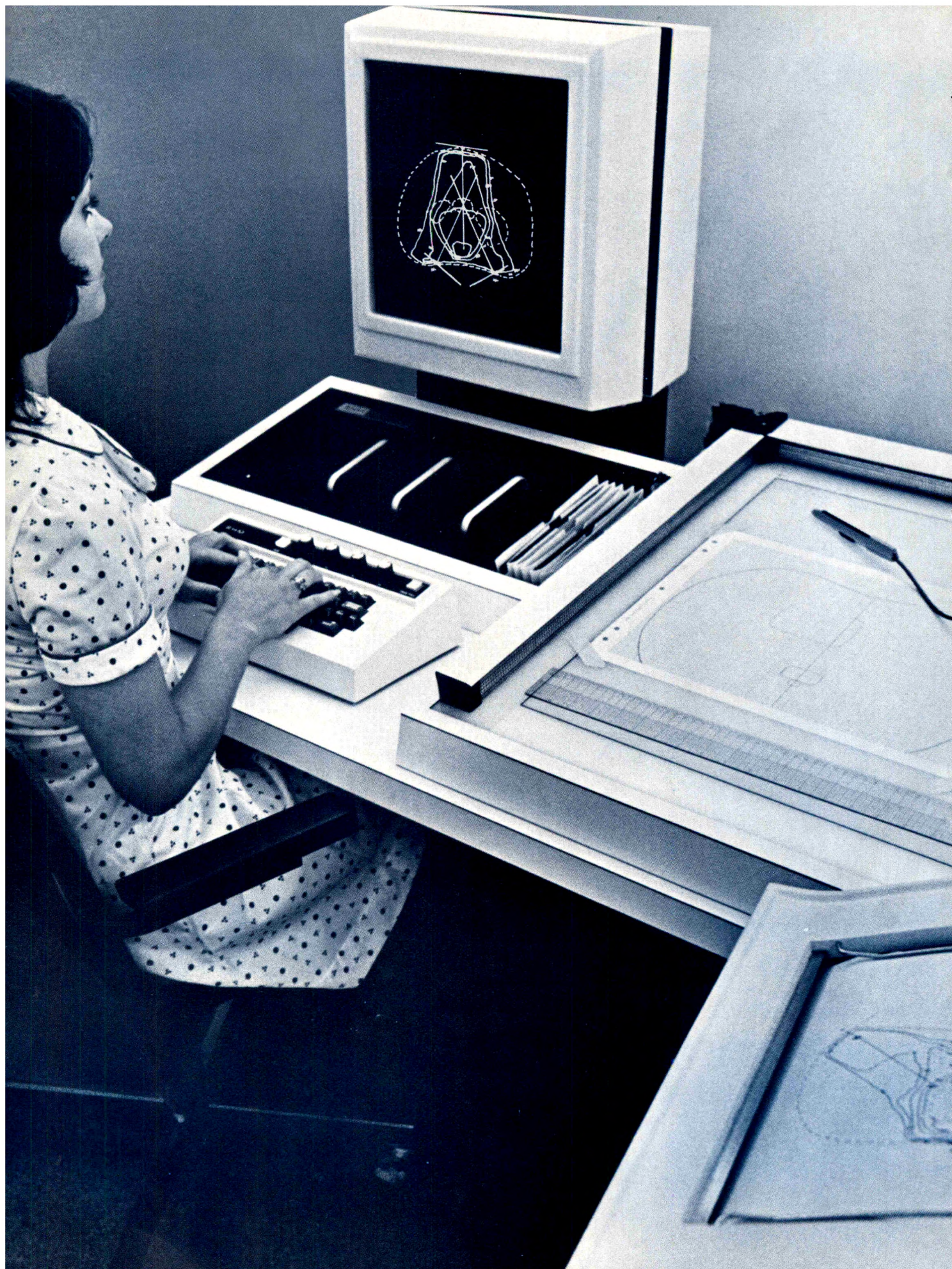


See our New
Automatic Film
Conveyor-to-

Processor at

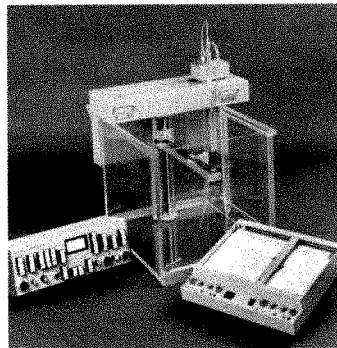
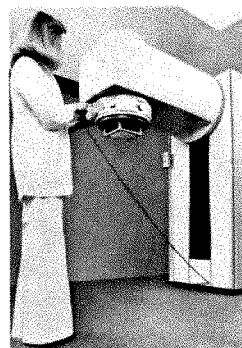
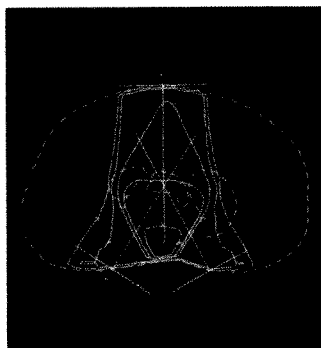
ARRS, Washington, Booths 80 & 81

LIEBEL-FLARSHEIM
SYBRON CORPORATION
111 East Amity Road, Cincinnati, Ohio 45215 U.S.A.



OPTIMIZATION

The optimum therapy treatment plan consists not only of isodose distribution and point doses, but also includes tissue density, heterogeneity and off axis corrections. And the plan evolves to include changes in patient condition and tumor response. □ With the Rad 8 computerized therapy planning system, all these variables are quickly calculated. Multiple port treatment plans, fully optimized and corrected for obliquity, are generated in just a few minutes. Additional corrections and plan updates are made in seconds. And detailed patient records are generated simultaneously. □ Because calculations are completed quickly, patient throughput is increased. And because a level of precision, never before possible, is now instantly available, patient treatment improves. □ Better management and improved patient care. It's the optimum therapy combination. □ SHM Nuclear Corporation, 570 Del Rey, Sunnyvale, CA 94086 (408) 245-3136



The Rad 8 console includes a modern plasma display, floppy disc storage, acoustic pen data entry system. Rad 8 is supported by the profession's most extensive software library. SHM is a total therapy company, offering linear accelerators, isodose plotters and other therapy equipment.

SHM Nuclear Corporation

Clysodrast[®]

(BISACODYL TANNEX)

The safe and certain
barium additive

Helps you
be sure of
what you see



Clysodrast is a unique colonic evacuant. It mixes with barium enemas to give radiologists the only form of tannic acid* available for safe, high-resolution barium enema studies. And a growing body of experimental evidence has shown the diagnostic benefits of Clysodrast added to a barium suspension.^{1,2,3} This combination provides unmatched mucosal visualization for superior roentgenologic diagnoses.

SAFETY YOU CAN COUNT ON

Only tannic acid really prepares the colon and produces the even, thin-film deposition of barium sulfate that a radiologist needs for maximum clarity. Clysodrast combines tannic acid with the contact laxative bisacodyl, for optimum effectiveness. And Clysodrast comes in accurately measured, 2.5 Gm. packets to avoid the danger of accidental overdose.

With Clysodrast, results are consistently safe and uniform, too. No patient has ever suffered hepatic necrosis as a result of Clysodrast being used within the dosage limits indicated in the instructions.^{4,5,6} And it has been used in well over 2 million barium enema procedures since 1970 alone, usually with no more side effects than a water enema produces.^{7,8}

Clysodrast is recommended for double contrast studies with an appropriate form of barium sulfate, such as Barotrast.[®]

It is also indicated for the preparation of patients for radiologic examinations of the colon, sigmoidoscopy and proctologic examinations, when used as directed.

USE CLYSODRAST, FOR SURE

Clysodrast provides radiologists with the assurance of high resolution barium studies no other product can provide. Find out for yourself how Clysodrast can help you see for sure.

Contact your local X-ray supplies dealer.

See summary of prescribing information on adjoining page.

*Bisacodyl tannex

Also see your X-ray supplies dealer for Oratrast,[®] Barotrast[®] and Esophotrast[®]

INDICATIONS: CLYSODRAST (bisacodyl tannex) may be indicated for the preparation of patients for radiologic examinations of the colon, sigmoidoscopy and proctologic examinations.

CONTRAINDICATIONS: CLYSODRAST is contraindicated in patients under the age of 10 because the possibility of absorption of tannic acid has not been adequately studied in this age group to warrant a conclusion of safety. CLYSODRAST is also contraindicated in cases with known or suspected extensive ulcerative lesions of the colon.

WARNING: Usage in Pregnancy. Safe use of CLYSODRAST has not been established with respect to the adverse effects upon fetal development. Therefore, it should not be used in women of child-bearing potential, particularly during early pregnancy, except where, in the judgment of the physician, the potential benefits outweigh the possible hazards.

PRECAUTIONS: Tannic acid, one of the active ingredients of CLYSODRAST, is hepatotoxic if absorbed in sufficient quantity. Deaths have been reported from hepatic damage due to tannic acid used in barium enema examination. Thus, CLYSODRAST should be used with caution in a regimen where multiple enemas are administered. Certain patients, because of age, debility, or underlying disease, require more gentle preparation than the routine castor oil and CLYSODRAST preparation. It is important that the instructions for preparation and administration be followed in detail, and that the recommended dosages not be exceeded.

ADVERSE REACTIONS: The following adverse reactions have been reported: Cramping, weakness, nausea and fainting.

DOSAGE AND ADMINISTRATION: It is important that the entire medical history and condition of the patient be considered in deciding the dosage regimen. Traumatizing procedures, such as repetition of enemas (with or without CLYSODRAST) should be kept at the minimum necessary to achieve the desired result.

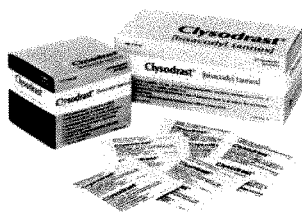
CLEANSING ENEMA: Prepare the cleansing enema by dissolving the contents of one packet (2.5 Gm.) of CLYSODRAST in one liter of lukewarm water and administer.

BARIUM ENEMA: Prepare the barium enema by dissolving the contents of one or not more than two packets (2.5 Gm. or 5.0 Gm.) of CLYSODRAST in one liter of barium suspension. If more than one liter of barium suspension is prepared, it is important that the concentration of CLYSODRAST (bisacodyl tannex) never exceed 0.5 percent (2 packets per liter).

The total dosage of CLYSODRAST for any one complete colonic examination, including the cleansing enema, should not exceed 7.5 Gm. (3 packets). No more than 10 Gm. (4 packets) of CLYSODRAST should be administered to any individual within a 72-hour period.

HOW SUPPLIED: CLYSODRAST is supplied in packets containing 1.5 mg. of 4,4'-(diacetoxydiphenyl)-(pyridyl-2)-methane complexed with 2.5 Gm. of tannic acid, N.F. These packets are supplied in cartons of 25 and 50 packets.

CAUTION: U.S. Federal law prohibits dispensing without prescription.



A Colonic Evacuant
Clysodrast
(bisacodyl tannex)

Barnes-Hind Pharmaceuticals, Inc.
Sunnyvale, California 94086

1. Goldman, L., *Clinical Medicine*, Vol. 28, pg. 28, 1971
2. Hamilton, *American Journal of Roentgenology*, 1946
3. Janower, M. L., *Radiology*, Vol. 85, pg. 887, 1965
4. Burhenne, et al, *American Journal of Roentgenology*, Vol. 96, pg. 510, 1966
5. Lucke, et al, *Canadian Medical Association*, Vol. 89, pg. 1111, 1963
6. McAlister, et al, *Radiology*, Vol. 80, pg. 765, 1963
7. Steinbach, et al, *American Journal of Roentgenology*, Vol. 87, pg. 644, 1962
8. Thomas, *American Journal of Roentgenology*, Vol. 89, pg. 889, 1963

PHYSICIAN AND SONOGRAPHER TRAINING PROGRAM

All aspects of Diagnostic Ultrasound will be covered including how to start and operate an Ultrasound Department. One month physician program with three month and one year sonographer programs for qualified persons. Special arrangements may be considered. Limited number of applicants accepted.

For further information please phone or write:

J. J. CRITTENDEN, M.D.

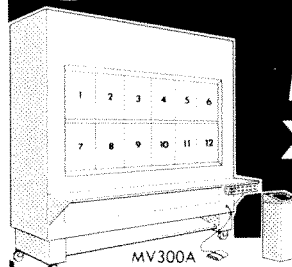
Diagnostic Ultrasound Department

West Florida Hospital and Clinic

8383 North Davis Hwy.,
Pensacola, Florida 32504
904-478-4460 Ext. 174

Radiologists, Doctors

SAVE TIME with S & S MOTORIZED X-RAY VIEWERS



**READ 12 FILMS
Six-over-Six
with the MV300A**

This new Jumbo 6 over 6 300 Film Motorized Viewer is the only Viewer made to read 12-14" x 17" films or smaller film sizes... on 84" wide panels. Individual control of light (bright, normal or off) for each of the 12 films. 50 6 Bank wide plexiglas viewing panels.

The MV200A, a 4 over 4 200 Film Viewer, is also available.

20 to 35% Reductions in reading time reported by Radiologists using S & S Motorized Viewers

Features include: Easier non-glare reading; simple operation, larger capacity, faster action, minimum floor space and lower machine cost per film.

A 50 button MV200C Selector is available for automatic retrieval of desired film.

Both are rugged dependable units. Over 1000 in use!



Accessory Catalog and User List on request.
SOLD BY LOCAL X-RAY DEALERS

87-93 JAY STREET, BROOKLYN N.Y. 11201
Telephone: 212-852-6900

**“It takes three
dual-probe scanners
or two cameras
to handle
the
patient
load
of one
cleon.”**

**“Scan-
dalous!”**



TELEPHONE (617) 444-2494/TELEX 922-552

cleon

CORPORATION ... for maximum patient throughput in whole-body imaging.

SEND FOR THE FACTS:

cleon

CORPORATION
150 Gould Street
Needham, MA 02192

AJR

Yes, I'd like to have the facts about
the Cleon Whole-Body Imager.

NAME _____

DEPARTMENT _____

INSTITUTION _____

ADDRESS _____

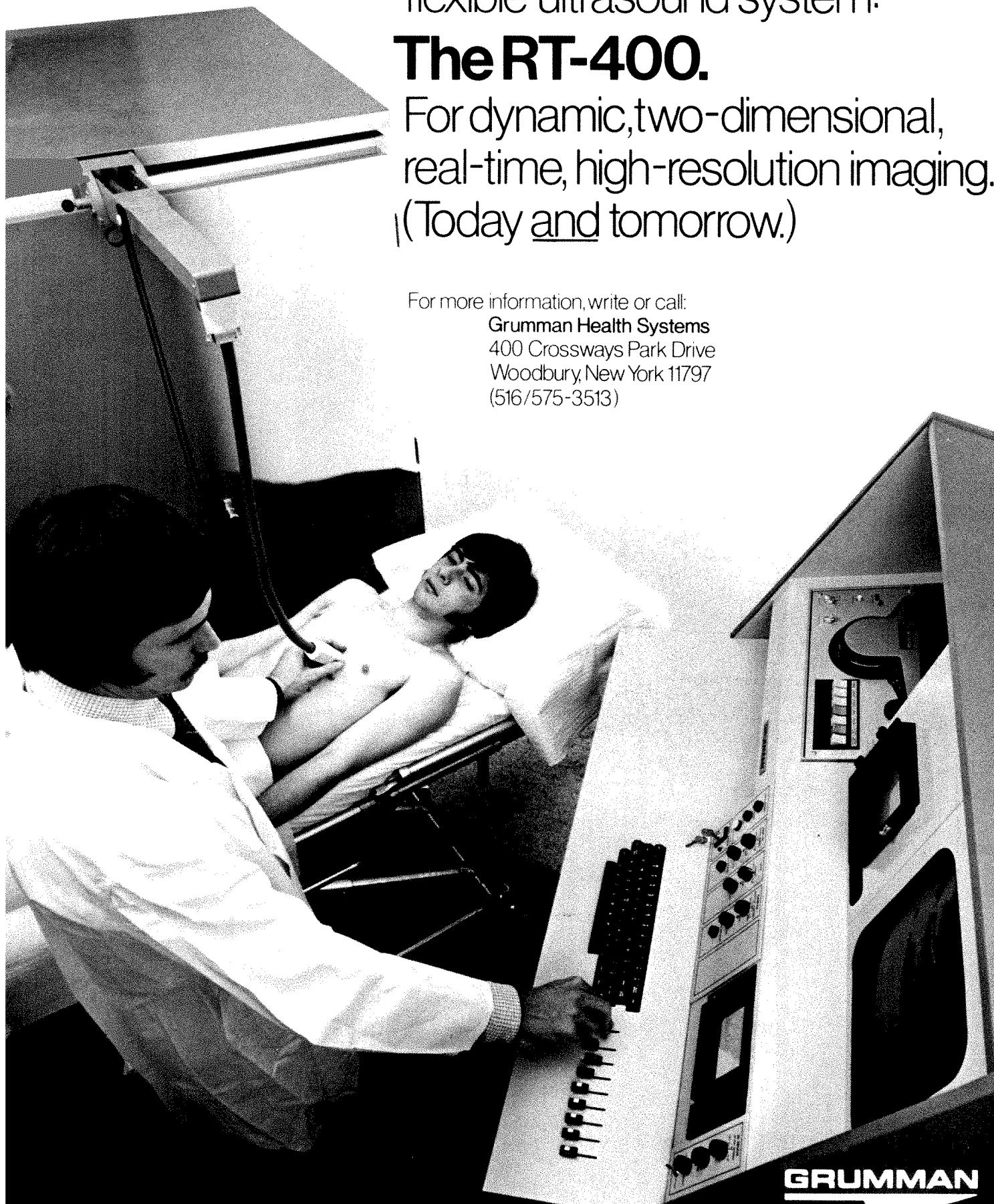
Now the complete,
flexible ultrasound system:

The RT-400.

For dynamic, two-dimensional,
real-time, high-resolution imaging.
(Today and tomorrow.)

For more information, write or call:

Grumman Health Systems
400 Crossways Park Drive
Woodbury, New York 11797
(516/575-3513)



**We want to make
gall bladder studies
more convenient.**

For you. For your patients.



Oragrafin®

Calcium Granules

Ipodate Calcium for Oral Suspension U.S.P.

Oragrafin®

Sodium Capsules

Ipodate Sodium Capsules U.S.P.

SQUIBB®

**contrast
media™**

the
reason
is clear™

Oragrafin(Ipodate) conveniences...

Scheduling flexibility

Diagnostically adequate filling of the gallbladder often takes place within 5 hours or less after ingestion of granules, thereby permitting same-day examinations.

In routine overnight procedures, opacification is attained 10 hours after ingestion of capsules.

Choice of dose forms

Granules or capsules — Rapid absorption of both calcium salt and sodium salt often permits visualization of even poorly functioning gallbladders.

Prepared or unprepared patients

Both salts have been administered to unprepared patients as well as previously prepared patients, with no significant difference in results.

*Please see following page
for brief summary.*



ORAGRAFIN® CALCIUM GRANULES

Ipodate Calcium for Oral Suspension U.S.P.

ORAGRAFIN® SODIUM CAPSULES

Ipodate Sodium Capsules U.S.P.

CONTRAINDICATIONS: Both preparations are contraindicated in patients who are hypersensitive to ipodate salts.

WARNINGS: A history of sensitivity to iodine *per se* or to other iodinated compounds is not an absolute contraindication to the use of these preparations, but calls for extreme caution in administration.

Usage in Pregnancy: The safety of these preparations for use during pregnancy has not been established; therefore, they should be used in pregnant patients only when, in the judgment of the physician, their use is deemed essential to the welfare of the patient.

PRECAUTIONS: Increasing the dosage above that recommended increases the possibility of hypotension. Anuria may result when these preparations are administered to patients with combined renal and hepatic disease or severe renal impairment. Renal toxicity has been reported in a few patients with liver dysfunction who were given oral cholecystographic agents followed by urographic agents. Administration of urographic agents should therefore be postponed in any patient with a known or suspected hepatic or biliary disorder who has recently taken a cholecystographic contrast agent. Gastrointestinal disorders which interfere with absorption and liver disorders which interfere with excretion may result in nonvisualization of the hepatic and biliary ducts and the gallbladder. Contrast agents may interfere with some chemical determinations made on urine specimens; therefore, urine should be collected before administration of the contrast media or two or more days afterwards. Thyroid function tests, if indicated, should be performed prior to the administration of these preparations since iodine-containing contrast agents may alter the results of these tests.

ADVERSE REACTIONS: Mild and transient nausea, vomiting, or diarrhea sometimes occur; the incidence can be reduced by using the calcium granules and restricting the dosage to 3 g. in persons prone to gastrointestinal reactions. Transient headache, dysuria, or abdominal pains may occur.

Hypersensitivity reactions may include urticaria, serum sickness-like reactions (fever, rash, arthralgia), other skin rashes, and rarely anaphylactoid shock. They are more likely to occur in persons with a history of allergy, asthma, hay fever, or urticaria and in those who are known to be hypersensitive to iodine compounds.

Note Concerning Dosage: A total dose of 6 g. (12 capsules or 2 packets of Granules) per 24-hour period should not be exceeded.

For full information, see Package Insert.

HOW SUPPLIED: Oragrafin Calcium Granules (Ipodate Calcium for Oral Suspension U.S.P.) provide 3 g. ipodate calcium per packet; available in boxes of 25 single-dose foil packets. Oragrafin Sodium Capsules (Ipodate Sodium Capsules U.S.P.) provide 0.5 g. ipodate sodium per capsule; available in boxes of 25 vials (each vial contains 6 capsules), in bottles of 100, and in Unimatic® packages of 100.

the reason
is clear™

SQUIBB HOSPITAL DIVISION

E. R. Squibb & Sons, Inc.

©1976 E. R. SQUIBB & SONS, INC. HQ-JU-501



Scintillation Camera Lung Imaging

An Anatomic Atlas and Guide

by CHARLES H. MANDELL, M.D.

The atlas is intended to serve as a guide to radionuclide lung scan anatomy and interpretation. It sets forth basic principles of scan interpretation and illustrates a variety of pathologic entities which may appear in lung scan practice. The use of six views for routine scanning is stressed by use of lung segment models. The model scintiphotos may be used in daily clinical practice as an anatomic guide.

Among the outstanding features of this new work are: first lung scan atlas utilizing gamma camera images; first anatomic models of lung segments specifically illustrating segmental scan architecture in an easily indexed section; use of six views to illustrate normal and pathologic entities, with visual demonstration of frequent superior images utilizing this expanded technique; multiple tables outlining the common range of disease entities producing various specific scan patterns.

1976, 208 pp., illus., \$28.00/£17.10

ISBN: 0-8089-0960-6

Diagnostic Uses of Ultrasound

by BARRY B. GOLDBERG, M.D., MORRIS N. KOTLER, M.D., MARVIN C. ZISKIN, M.D., and ROBERT D. WAXHAM, B.A.

"...an excellent introductory guide to this new and rapidly expanding field."—*Radiology*

Providing a working knowledge of the principles of ultrasound and its applications and limitations—this book focuses on how, in which patients, and to what degree can the ultrasonic techniques now available contribute to effective patient care. Separate chapters deal with the applications of ultrasound to each relevant area of the body and the many illustrations assist the reader in recognizing normal and abnormal ultrasonic recordings for all modalities in current use.

1975, 480 pp., illus., \$30.00/£16.50

ISBN: 0-8089-0879-0

N.B. Postage plus 50¢ handling charge on all orders not accompanied by payment.

Prices are subject to change without notice.



GRUNE & STRATTON

A Subsidiary of

Harcourt Brace Jovanovich, Publishers

111 FIFTH AVE., NEW YORK, N.Y. 10003

24-28 OVAL ROAD, LONDON NW1 7DX

High Dose Urography: Incidence and Relationship to Spontaneous Peripelvic Extravasation

MICHAEL E. BERNARDINO¹ AND BRUCE L. MC CLENNAN¹

A prospective study was undertaken to determine the incidence of spontaneous extravasation of contrast in 82 patients with acute renal colic. The extravasation rate among 37 patients receiving 75 ml of contrast was 8.1%, while the rate among 45 patients receiving either 300 ml of 30% solution by infusion or a 140 ml bolus dose was 24.4%; overall the rate was 17%. Thus the incidence of extravasation was shown to increase with higher doses of contrast media. The primary dose in acute renal colic or other forms of obstructive uropathy should be in the low range (20–25 g I⁻); reinjection after screening can be undertaken if necessary.

Spontaneous peripelvic extravasation of contrast media during intravenous urography for acute renal colic has been considered a rare occurrence [1–5]. In two previous reports the incidence rate was found to be 6.25% and 5%, respectively [6, 7]. However, the amount of contrast administered was not stated. Since the amount of contrast media used routinely today is greater than in past years and infusion urography is the primary urographic procedure at many institutions, we prospectively studied the incidence of spontaneous extravasation during excretory urography for evaluation of ureteral stone disease. We examined the relationship between occurrence of extravasation of contrast media and the dose of contrast media.

Subjects and Methods

Patients with clinical symptoms of acute renal colic were screened using criteria devised by Schwartz et al. [6]. Patients were excluded from the study if they had a recent history of ureteral instrumentation, previous kidney or related surgery, or external trauma. No compression devices were used. Patients meeting the above criteria who were found not to have a calculus on plain films were also excluded, leaving only those with documented stones on initial radiographs. All patients were examined within 12 hr of initial symptoms.

Thirty-seven patients were given 75 ml of 50% Hypaque (21.5 g I⁻), which is our routine dose of contrast (0.5–0.75 ml per pound body weight). The injection time in each case was less than 30 sec. An additional 36 randomly selected patients received 300 ml of 30% Hypaque (42.3 g I⁻) infused over 10–15 min. Nine patients received 140 ml of 50% Hypaque by direct intravenous injection in under 90 sec. The dose of iodine in this group is equal to that in the infusion kit group without the diluting solution. The latter 45 patients constituted the infusion or high dose group. The minimum set of films for each patient, including tomograms, consisted of films immediately postinjection or after half the infusion bottle, at 5 min, 10 min, and 20 min. If needed, delayed films were obtained until the site of obstruction in the ureter was determined.

Results

In the routine dose group, three of 37 patients (8.1%) exhibited peripelvic extravasation. Eight cases of extravasation (22%) occurred among the 36 patients who received the 30% Hypaque infusion (fig. 1). Among the nine patients who received a high bolus dose of 50% Hypaque, three showed extravasation (33%). One of these patients developed a ruptured kidney during the examination *without* peripelvic extravasation of contrast media (fig. 2). The combined infusion and high dose groups exhibited 11 extravasations in 45 cases (24.4%). Overall, the incidence of extravasation was 17% (14 of 82).

Discussion

The incidence of spontaneous extravasation of contrast has been reported to be 6.25% and 5%, respectively [6, 7]. Our overall spontaneous extravasation rate of 17% is strikingly higher. Unfortunately the amount of contrast administered in the two earlier reports is not known; it is possible their patients received far less contrast media than our routine dose group.

Obstruction of a ureter raises intratubular pressure almost equal to the raised intraureteric pressure in rats [8]. Extravasation of contrast material in acute renal colic occurs when there is a rapid rise of intraureteric pressure to as high as 80–100 mm Hg [9, 10]. Our study suggests that the critical high pressures occur more frequently in acute renal colic when higher dosages of contrast are administered during the first 12 hr of symptoms. Contrast media is a potent osmotic diuretic which does not undergo tubular reabsorption in the normal kidney; therefore, it increases both urine flow rate and volume. When the dose of contrast is increased, a critical level is reached at which further additions do not result in higher urine concentrations, but prolonged diuresis is noted [11]. Since contrast media causes kidney swelling and increased subcapsular pressures in normal individuals, prolonged diuresis during high dose urography in obstructive uropathies probably further increases the chance of contrast extravasation [12, 13].

Cook and Bartucz [14] examined the incidence of spontaneous extravasation in 16,574 urograms and found a rate of less than 1%. It is not known how many of these patients received low doses of contrast media. At present, the trend is toward higher doses of contrast for routine intravenous urograms. The commercially available infusion package is a convenient method for administering this con-

Received March 1, 1976; accepted after revision April 27, 1976.

¹ Department of Radiology, George Washington University Medical Center, 901 23d Street N.W., Washington, D.C. 20037. Address reprint requests to B. L. McClennan.



Fig. 1.—Patient with left distal ureteral calculus. *A*, Coned down view of left kidney showing peripelvic extravasation around upper calyx, pelvis, and proximal ureter. *B*, Tomogram taken same time showing extent of peripelvic extravasation to better advantage, especially circumureteric extension.

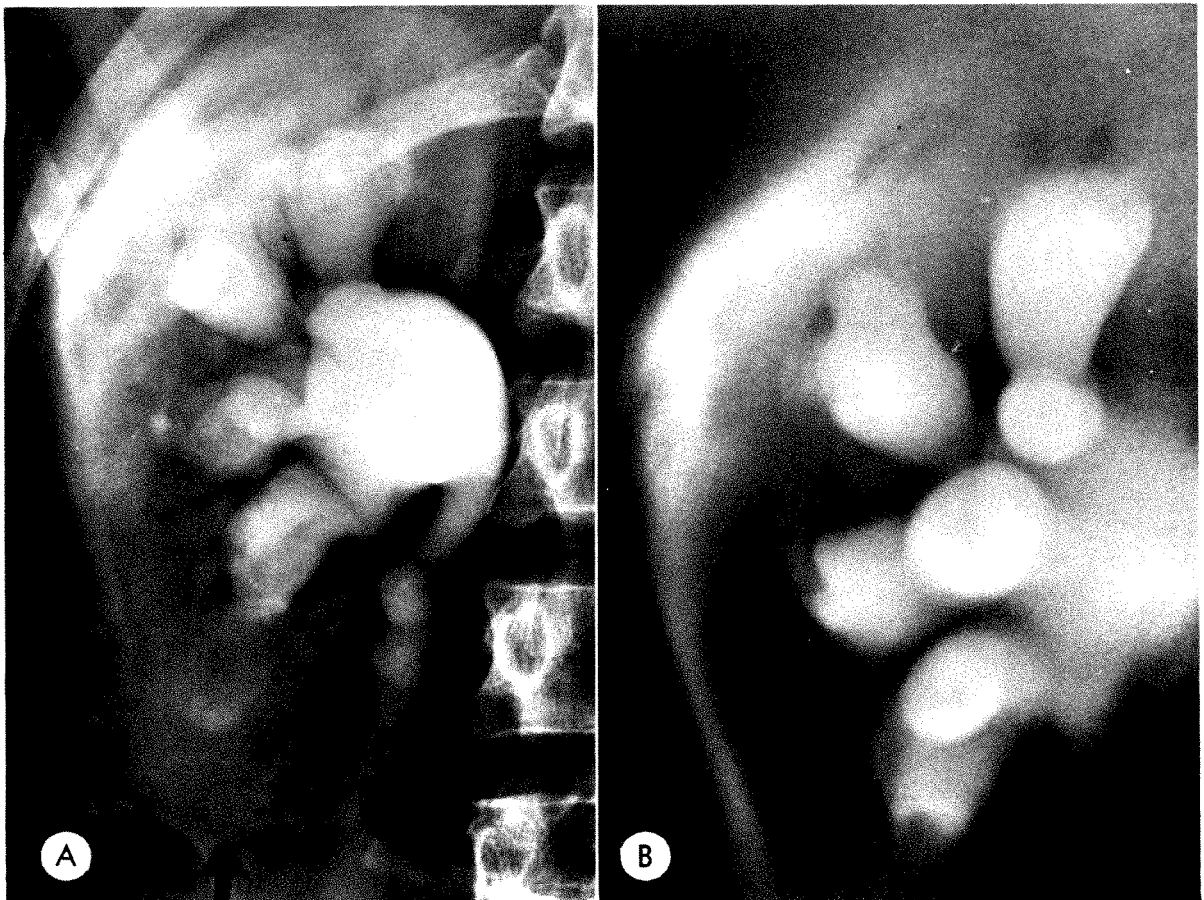


Fig. 2.—Patient with right distal ureteral calculus. *A*, 20 min film from urogram (140 ml Hypaque 50) showing hydronephrosis with extravasation of contrast material out through upper pole calyx with perirenal space outlined by contrast material (*arrows*). No peripelvic extravasation. *B*, Tomogram showing ruptured calyx in upper pole. No peripelvic extravasation.

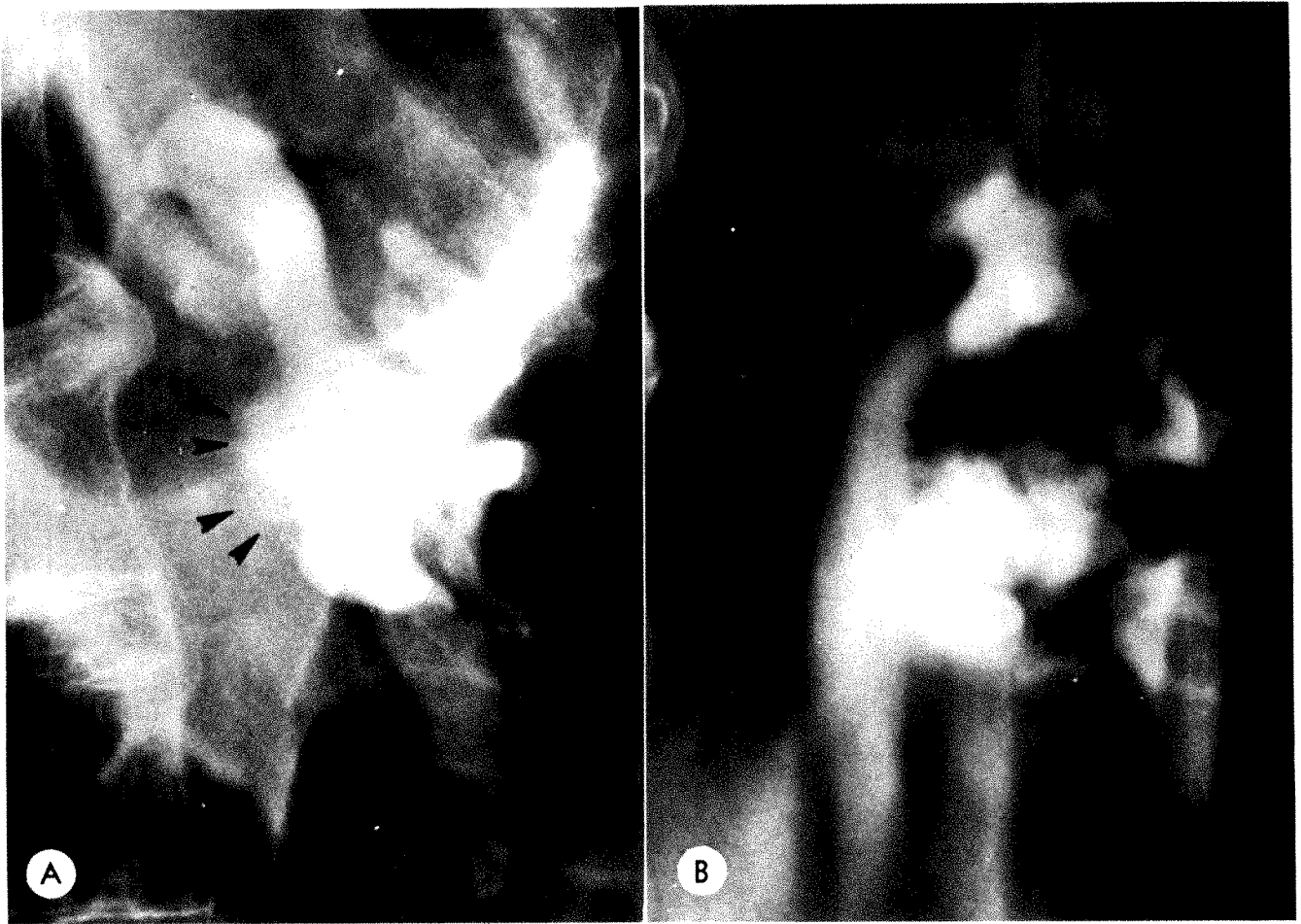


Fig. 3.—Elderly patient with obstructive uropathy due to enlarged prostate. A. Left posterior oblique view from infusion urogram showing peripelvic extravasation posterior to renal pelvis (arrows). B. Tomogram showing "fuzzy" renal pelvis and hilar area secondary to extravasated contrast material.

trast load. With increasing use of the infusion method for evaluation of calculus and other forms of ureteral obstruction (e.g., prostatic enlargement), the incidence of spontaneous peripelvic extravasation can be expected to increase (fig. 3).

Although extravasation usually follows a benign course with occasional low grade fever, peripelvic abscess, pancreatic pseudocyst, and ureteral fibrosis can result [14–16]. None of the patients studied developed any complications secondary to the extravasation.

We recommend a standard dosage in the range of 0.5–0.75 ml per pound body weight of 50%–60% contrast media ($20\text{--}25\text{ g l}^{-1}$) when examining patients with acute renal colic or other obstructive uropathies. Higher dosages of contrast, such as those achieved with infusion sets, increase the incidence of peripelvic extravasation in certain situations and, therefore, the possibility of serious complications. Spontaneous contrast extravasation may not be a problem in the future with the use of nonionic, less osmotically active contrast agents such as Metrizamide.

The fact that our patients were examined early in the course of ureteral obstruction may have affected the number of extravasations. Some institutions do not perform urograms on such an urgent basis.

REFERENCES

1. Bank JP, Basch RI, Cheris DN: Spontaneous rupture of the renal pelvis. *Am J Roentgenol* 98:54–62, 1966
2. Braun WT: Peripelvic extravasation during intravenous urography. *Am J Roentgenol* 98:41–46, 1966
3. Ford WH, Palubinskas AJ: Renal extravasation during excretory urography using abdominal compression. *J Urol* 97:983–986, 1967
4. Ginsberg SA: Spontaneous urinary extravasation in association with renal colic. *J Urol* 94:192–195, 1965
5. Serebro HA, Druskin M, Robbins MA: Spontaneous peripelvic urinary extravasation without kidney rupture. *N Engl J Med* 273:260–262, 1965
6. Schwartz A, Caine M, Hermann G, Bittermann W: Spontaneous renal extravasation during intravenous urography. *Am J Roentgenol* 98:27–40, 1966
7. Olsson O: Frequency of backflow in acute renal colic. *Acta Radiol [Diagn]* 12:469–480, 1972
8. Gottschalk CW, Mylle M: Micropuncture study of pressures in proximal tubules and peritubular capillaries of the rat kidney and their relation to ureteral and renal venous pressures. *Am J Physiol* 185:430, 1956
9. Hinman F: Peripelvic extravasation during intravenous urography, evidence for an additional route for backflow after ureteral obstruction. *J Urol* 85:385–395, 1961
10. Rabinowitz JG, Keller RJ, Wolf BS: Benign peripelvic extra-

- vasation associated with renal colic. *Radiology* 86:220-226, 1966
11. Elkin M: Radiology of the urinary tract: some physiological considerations. *Radiology* 116:259-270, 1975
 12. Dorph S, Øigaard A: Renal distention in response to water-soluble contrast medium and various diuretics. *Scand J Urol Nephrol* 9:114-118, 1975
 13. Lindgren P, Saltzman GF: Increase of subcapsular renal pressure after intravenous iodipamide and other parenteral contrast media. *Acta Radiol [Diagn]* 15:273-279, 1974
 14. Cooke GM, Bartucz JP: Spontaneous extravasation of contrast medium during intravenous urography. *Clin Radiol* 25:87-93, 1974
 15. Harrow BR: Spontaneous urinary extravasation associated with renal colic causing a perinephric abscess. *Am J Roentgenol* 98:47-53, 1966
 16. Pailowski JM: Peripelvic urine granuloma. *Am J Clin Pathol* 34:64-67, 1960

Autonomous Hyperparathyroidism in Patients on Maintenance Home Dialysis

CRAIG A. LEHMAN^{1,2} AND MELVYN H. SCHREIBER¹

Ninety-nine patients with end-stage renal failure treated by maintenance home dialysis whose calcium and phosphorus balance was carefully controlled were studied for radiographic evidence of hyperparathyroidism. A total of 43 showed evidence of hyperparathyroidism despite excellent medical management. In 23 the abnormality was stable and the patients were asymptomatic with regard to the skeleton. The other 20 showed progressive bone disease. Sixteen of these patients were operated upon, and 14 were relieved of their symptoms by parathyroidectomy. Following operation, the radiographic evidence of bone disease halted dramatically, and a decided return toward normal was documented on subsequent films. Thus parathyroidectomy can control the skeletal deterioration and bone pain of hyperparathyroidism in patients who develop this complication. Serial radiographic studies are a reliable indicator of this circumstance.

Introduction

One of the major problems in long term management of the dialysis patient with end-stage renal failure is the occurrence of hyperparathyroidism. In caring for these patients, a serious effort is made to maintain serum phosphorus at near normal levels, since it has been claimed that hyperparathyroidism can usually be prevented if this is accomplished [1, 2]. The incidence of hyperparathyroidism in chronic renal failure is known to be high, Massry et al. [3] reported an incidence of 18%, 70%, and 92% after 1, 2, and more than 2 years of hemodialysis, respectively. Ritz et al. reported phalangeal cortical changes in 57.2%, osteitis fibrosa in as many as 38.5%, vascular calcifications in 34%, cartilage calcification in 21%, and distal clavicle changes in 15.8%. Other investigators have reported similar high percentages [5, 6].

In an effort to gather data on the development and progress of hyperparathyroidism in carefully monitored maintenance dialysis patients with end-stage renal failure, we studied the films and records of 104 patients who were maintained on home dialysis after completing an intensive training program and whose serum chemistry values were fastidiously regulated and documented since the initiation of dialysis. Our goal was to establish the character and natural history of the bone disease in this carefully controlled population.

Materials and Methods

The serial film studies of 104 patients who completed home dialysis training since January 1968 were examined; 99 had a usable series of radiographs on file. Because of our desire to de-

velop criteria which are generally applicable, conventional radiography was employed. Other more sophisticated studies, such as magnification radiography, bone densitometry, microradioscopy, microradiography of biopsy specimens, xeroradiography, and quantitative measurement of certain parameters such as cortical thickness, might have provided finer discrimination but are not apt to be generally available or regularly employed. The films of each patient were examined, and changes were plotted as follows: 0=normal, 1+=questionable, 2+=definite, 3+=severe (fig. 1). Film studies of the chest and hands were available at 3 month intervals.

The criteria used for the radiographic diagnosis of hyperparathyroidism have been described [7-12]. The films were studied for changes of nonspecific demineralization, osteosclerosis, subperiosteal cortical resorption (loss of cortical definition and lacy cortical irregularity, particularly on the radial aspect of the middle phalanges; see fig. 1), cortical thinning and striation (progressive decrease in cortical thickness, usually starting with medullary scalloping, commonly associated with the development of longitudinally oriented radiolucent cortical stripes), vascular calcifications, and other soft tissue calcifications.

The time period covered in each case began with the completion of home dialysis training and continued until the present or until patients were transplanted, died, or transferred to another dialysis program. The average period of evaluation was 36.4 months with a median of 35 months (range, 2-76 months). Films were read by us without advance knowledge of therapy or outcome.

These patients constitute a remarkably well controlled series. Their care was rendered by a medical team with great expertise and long experience in the therapy of patients with chronic renal failure on maintenance home dialysis. Patients underwent overnight dialysis three times a week for a total of 18-30 hr per week. Dialysate calcium was 6 mg/100 ml. Vascular access was either through external arteriovenous shunts or arteriovenous fistulas. Diets were essentially normal except for some restriction of sodium, potassium, and water. Intake of high biologic quality protein was at least 80 g per day.

After the initial training, all patients were followed by weekly analysis of pre- and postdialysis serum calcium and phosphorus determinations. Aluminum hydroxide gel was used to bind dietary phosphate with weekly adjustments of the dosage based on serum phosphorus values. No patient in this series had a calcium-phosphorus product greater than 70. The average values for serum calcium, serum phosphorus, and calcium-phosphorus product were 9.4 (range, 7.9-11.1), 4.7 (range, 2.9-7.1), and 44 mg/100 ml (range, 27-67), respectively. Patients with low serum calcium and normal serum phosphorus values were assumed to have vitamin D resistance and were treated accordingly. None had the typical radiographic changes of hyperparathyroidism.

Patients were selected for subtotal parathyroidectomy on the basis of progressive radiographic abnormalities characteristic of hyperparathyroidism. Parathyroid hormone levels were measured

The views, opinions, and conclusions expressed herein are those of the authors and are not to be understood as those of the U.S. Air Force.

¹ Department of Radiology, University of Texas Medical Branch, Galveston, Texas 77550. Address reprint requests to M. H. Schreiber.

² USAF, MC.

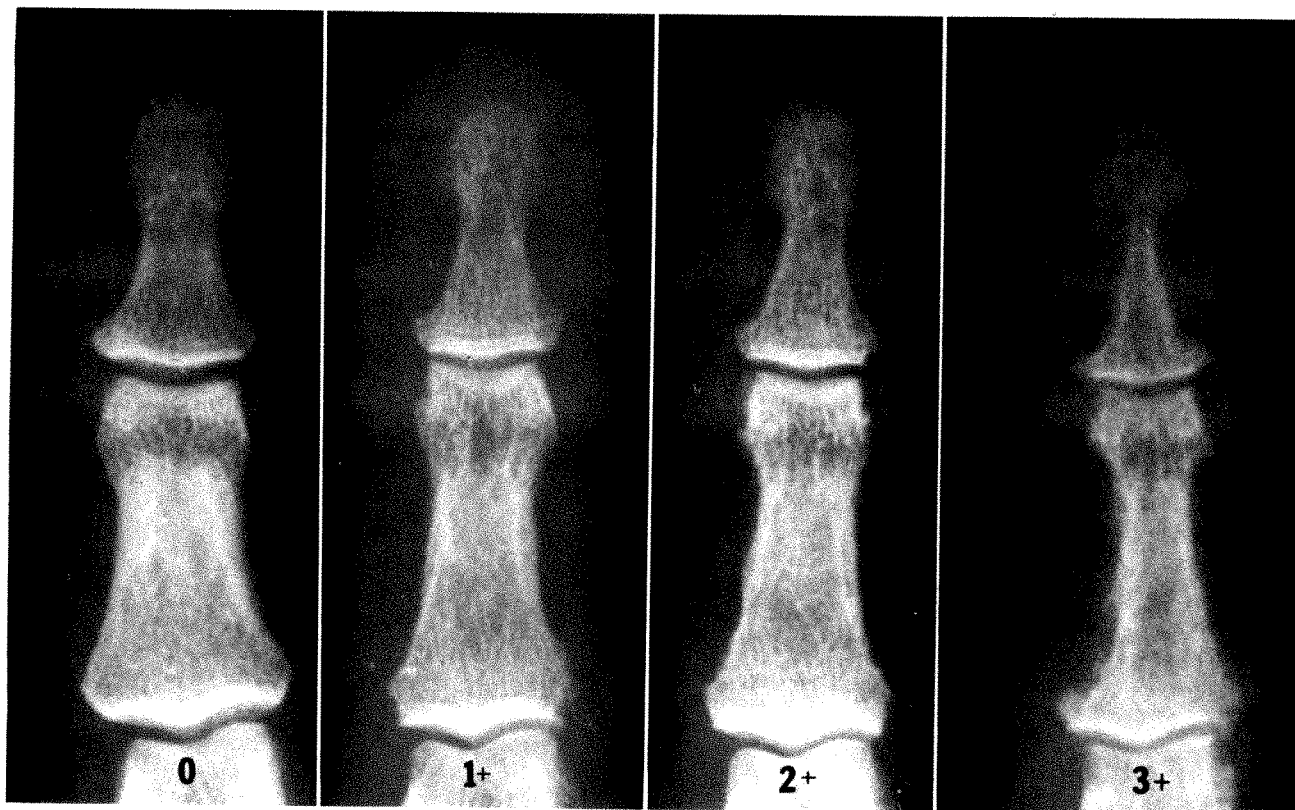


Fig. 1.—Gradations of subperiosteal cortical resorption used to quantitatively assess bone disease. 0 = normal, 1+ = questionable, 2+ = definite, 3+ = severe.

on about half of the patients and were consistently elevated. However, this was not an important criterion in selection for operation. Patients with nonprogressive skeletal changes of hyperparathyroidism also had elevated PTH levels, and there was considerable overlap in these levels between the two groups.

Of the 99 patients whose radiographs were evaluated, 77 remain actively in the study group. Of the 22, 14 died and eight have received transplanted kidneys.

Results

Of the 99 patients evaluated, 48 never demonstrated a bony abnormality radiographically (average time on dialysis, 27.7 months). An additional eight patients showed non-specific bony demineralization only (average time on dialysis, 37.63 months). Forty-three patients showed radiographic evidence of hyperparathyroidism (average time on dialysis, 45.88 months). In 23, the bony abnormality was stable (i.e., showed no tendency toward progression). The remaining 20 patients showed progressive changes of hyperparathyroidism (table 1). In seven of the patients with progressive bony changes, an abrupt halt in this progress was noted, followed by remineralization and in general a pronounced tendency to return toward normal. It was determined later that each of these patients had undergone parathyroidectomy with considerable symptomatic benefit.

Using the single criterion of progressive skeletal changes of hyperparathyroidism, 20 patients from the entire series were selected as potentially benefiting from parathyroidectomy, including the seven referred to above. Judging from the excellent results obtained in those seven, it seemed

likely that the remaining 13 would benefit from parathyroidectomy. Nine of these patients have subsequently had surgery and in eight of them the follow-up period has exceeded 6 months. Because one of these patients developed endometrial carcinoma with widespread metastatic disease to the skeleton, documentation of improvement was possible in only seven. They have shown dramatic improvement in the radiographic appearance of the skeleton.

Generalized skeletal demineralization was the most frequent finding in the 99 patients but was nonspecific and had little discriminatory value (table 2). Soft tissue calcification, chiefly in blood vessels, was found in one-fourth of the patients. Characteristic changes of hyperparathyroidism in the phalanges were found in an equal number.

In table 3, results are analyzed according to year of completion of the training program. After 1 year in the program, the percentage of patients showing no skeletal abnormality was substantially higher after 1969, probably reflecting improvement in patient management. However, the percentage without skeletal abnormality falls each year thereafter, so that by the end of the fourth year the percentages are about the same regardless of the year in which dialysis was begun.

Discussion

Secondary hyperparathyroidism in chronic renal failure is thought to result from diminished renal clearance of phosphate with consequent hyperphosphatemia and depression of serum calcium values. This stimulates the para-

TABLE 1
Incidence of Bone Disease in Patients on
Maintenance Home Dialysis

	No.	%
No evidence of hyperparathyroidism:		
Normal	48	48.5
Nonspecific bony demineralization only	8	8.1
Evidence of hyperparathyroidism:		
Abnormality with improvement	7	7.1
Abnormality with progression	13	13.1
Abnormality, relatively stable	23	23.2
Total	99	...

thyroid glands to excessive function. They ordinarily become hyperplastic and at times adenomatous. Autonomous hyperfunction may occur despite careful control of the serum phosphate, adequate dialysis, and adequate protein intake, and in the absence of vitamin D resistance. In this condition the hyperactive glands may fail to regress functionally even though the stimulus of hyperphosphatemia is removed.

This study shows that autonomous hyperparathyroidism and its radiographically detectable skeletal manifestations may develop in patients with well controlled calcium and phosphorus levels. Indeed, 43% of the patients in this study showed radiographic evidence of hyperparathyroidism; the longer the patient is on dialysis, the more likely bony changes are to develop. Despite continuous successful regulation of serum calcium and phosphate, including prevention of hyperphosphatemia, autonomous parathyroid hyperfunction develops in some patients and cannot be controlled by medical means. It is from this group of patients that candidates for parathyroidectomy are chosen.

The most reliable radiographic indicators of autonomous hyperparathyroidism were the phalanges and soft tissues. Progressive subperiosteal erosion and cortical thinning were the most frequently observed indications of hyperparathyroidism in the skeleton, while calcification of blood vessels, was the most frequent soft tissue abnormality. Distal clavicular erosion, vertebral osteosclerosis, and generalized demineralization of the skeleton were also found but were poor indicators of early disease. The opportunity to detect early radiographic changes of progressive hyperparathyroidism is provided, for the most part, by study of serial films of the hands and chest. Progressive vascular calcification in the aorta or in the small arteries of the hands is a good indicator of advancing disease, as is the development of progressively more florid changes of cortical thinning and striation and subperiosteal resorption in the phalanges.

In all but one of our patients undergoing parathyroidectomy, the progress of bone disease was reversed with the skeleton returning to near normal as judged by radiographic findings. The one exception was the patient with disseminated skeletal metastases from endometrial carcinoma. In no instance was significant improvement in the progressive

TABLE 2
Radiographic Findings

Finding	No (%)
Nonspecific bony demineralization	30 (30.3)
Soft tissue calcification:*	
Blood vessel	19
Cartilage	8
Renal lithiasis	1
Phalangeal alterations:*	
Subperiosteal erosion	22
Cortical thinning	23
Cortical striation	17
Distal clavicle erosion	7 (7.1)
Osteosclerosis	6 (6.1)
Osteoclastoma	3 (3.1)

* Found in 24 patients (24.2%).

TABLE 3
Percentage of Patients with No Skeletal Abnormality

Year Training Completed	No. Years in Program						
	1*	2	3	4	5	6	7
1968	69.2	41.7	33.3	0.0	0.0	14.3	14.3
1969	68.8	66.7	46.2	46.2	30.8	30.8	...
1970	95.0	80.0	52.7	47.0	47.0
1971	88.3	46.7	42.9	42.9
1972	94.2	73.4	50.0
1973+	81.4	81.4

* + 6 months.

radiographic abnormalities of hyperparathyroidism achieved by medical means. Thus radiographic demonstration of progressive bony changes in patients with chronic renal failure who have normal serum calcium and phosphate levels is a reliable indicator of the presence of autonomous hyperparathyroidism and of the probable benefit to be obtained from parathyroidectomy.

Documentation of these progressive changes requires frequent radiographic study; in our patients films of the chest and hands were made at 3 month intervals. Comparison of serial films of the phalanges over a period of time was the most effective means of detecting early signs of hyperparathyroidism. To facilitate comparison, it is important that the same hand be filmed at each 3 month interval and that radiographic technique be standardized.

ACKNOWLEDGMENTS

We are especially indebted to Drs. A. R. Remmers, Jr., and Jay C. Fish for making available their patients and records and for helpful suggestions concerning the manuscript.

REFERENCES

1. Goldsmith RS, Furszyfer J, Johnson WJ, Fournier AE, Arnaud CD: Control of secondary hyperparathyroidism during long-term hemodialysis. *Am J Med* 50: 692-699, 1971
2. Stanbury SW, Lumb GA, Mawer EB: Osteodystrophy develop-

- ing spontaneously in the course of chronic renal failure. *Arch Intern Med* 124:274-281, 1969
3. Massry SG, Coburn JW, Popovtzer MM, Shinaberger JH, Maxwell MH, Kleeman CR: Secondary hyperparathyroidism in chronic renal failure. *Arch Intern Med* 124:431-441, 1969
 4. Ritz E, Krempien B, Mehls O, Malluche H: Skeletal abnormalities in chronic renal insufficiency before and during maintenance hemodialysis. *Kidney Int* 4:116-127, 1973
 5. Johnson C, Graham CB, Curtis FK: Roentgenographic manifestations of chronic renal disease treated by periodic hemodialysis. *Am J Roentgenol* 101:915-926, 1967
 6. Katz AI, Hampers CL, Merrill JP: Secondary hyperparathyroidism and renal osteodystrophy in chronic renal failure. *Medicine* 48:333-374, 1969
 7. Doyle FH: Radiological patterns of bone disease associated with renal glomerular failure in adults. *Br Med Bull* 28:220-224, 1972
 8. Eugenidis N, Olah AJ, Haas HG: Osteosclerosis in hyperparathyroidism. *Radiology* 105:265-275, 1972
 9. Griffiths HJ, Ennis JT, Bailery G: Skeletal changes following renal transplantation. *Radiology* 113:621-626, 1974
 10. Meema HE, Rabinovich S, Meema S, Lloyd GJ, Oreopoulos DG: Improved radiological diagnosis of azotemic osteodystrophy. *Radiology* 102:1-10, 1972
 11. Pugh DG: Subperiosteal resorption of bone: a roentgenologic manifestation of primary hyperparathyroidism and renal osteodystrophy. *Am J Roentgenol* 66:577-586, 1951
 12. Simpson W, Kerr DNS, Hill AVL, Siddiqui JY: Skeletal changes in patients on regular hemodialysis. *Radiology* 107:313-320, 1973

Therapeutic Vascular Occlusion Utilizing Steel Coil Technique: Clinical Applications

SIDNEY WALLACE,¹ CESARE GIANTURCO,¹ JAMES H. ANDERSON,¹ HARVEY M. GOLDSTEIN,¹
L. JOHN DAVIS,² AND ROBERT L. BREE¹

The stainless steel coil has been utilized for permanent intravascular occlusion of the proximal portion of the renal, hepatic, splenic, and internal iliac vessels. This therapeutic approach has been successful in the management of renal arteriovenous fistulas, renal carcinomas, neoplasms of the liver, giant cell tumors of the sacrum, and in hypersplenism. The techniques involved and clinical uses are discussed.

Introduction

The increasing utilization of transcatheter intravascular occlusive therapy for a variety of clinical problems has created the need for safer, more permanent, easily injectable materials. Our experimental studies with a stainless steel coil occluding device have been reported previously [1].

This communication presents our clinical experience with this transcatheter intravascular occluding device in the therapeutic management of 24 patients. The group includes 19 patients with renal carcinomas, two with renal arteriovenous fistulas, one with a hepatic carcinoma, one with hypersplenism associated with histiocytic lymphoma, and one with a giant cell tumor of the sacrum. The technique as well as the present and potential applications are described.

Materials and Methods

Stainless Steel Coil Occluding Device

The Gianturco stainless steel coil occluding device (Cook, Inc., Bloomington, Ind.) is shown in figure 1. The coil is formed from a 2½ inch segment of stainless steel guide wire, 0.036 inches in diameter, from which the central core has been removed. The guide wire segment is preshaped in the form of a helix 3/16 inch in diameter. The length of the segment and the diameter of the coil can be made of various sizes to suit the clinical situation. Four wool strands, each 2 inches long, are attached to the tip of the coil and serve as a nidus for thrombosis. The coil with attached wool strands is straightened and placed in a cartridge made of Teflon tubing. One end of the cartridge is tapered to fit into an enlarged bore stopcock adapter, while the other end of the cartridge is flared for a smooth introduction of the coil (fig. 1A).

Technique

A preshaped no. 7 French thin-walled Teflon catheter with a uniform inner diameter and nontapered tip is introduced percutaneously over a 0.045 inch stainless steel guide wire. The Teflon catheter is utilized because the low coefficient of friction and the relative rigidity it provides supports passage of the coil through the catheter. The low radiopacity of the Teflon necessitates the use of contrast material to enhance its visualization. Selective catheteriza-

tion of the vessel to be occluded is at times facilitated by the use of a catheter deflector. An introducer (fig. 1B) passes the straightened coil through the cartridge and into the Teflon catheter. The coil is first deposited in the distal portion of the catheter by withdrawing the mandril from the introducer (fig. 1C). The coil is then pushed out of the catheter into the vessel lumen by a modified 0.052 inch guide wire which is flexible only in its distal 3¼ inches, (figs. 1D and 1E). When the aorta is tortuous, a standard 0.045 inch guide wire is preferable because its flexibility conforms better to the more acute vascular curves.

As the coil is released into the vessel, it resumes its spiral shape and becomes wedged in place with the steel coil and the wool strands tightly intertwined, forming a plug immediately distal to the catheter tip causing complete obstruction. In approximately 10 min clot forms on the metal and wool and insures more complete vascular occlusion. Usually two coils, but as many as five, have been inserted in a vascular bed to accomplish the occlusion. The use of systemic heparinization for angiography is probably partly responsible for the time required for clot formation, [2].

Illustrative Cases

Renal Vein Occlusion

Case 1. A 60-year-old female patient with known polycystic disease was examined by renal angiography because of uncontrolled persistent hypertension and a bruit over the left flank. Multiple cysts were demonstrated in the right kidney. The origin of the left renal artery was narrowed, presumably secondary to atherosclerosis. An arteriovenous fistula was opacified within the left kidney with a minimal perfusion of the renal parenchyma (fig. 2A). This fistula was considered to have resulted from a needle biopsy 1 year earlier.

In view of the bilateral renal disease and impaired renal function, an alternative to nephrectomy for the arteriovenous fistula seemed advisable. Three days after the arteriogram the intravascular occlusion procedure was performed. The left renal vein was catheterized and the tip of the Teflon catheter was placed into the single fistulous tract. Two coils were placed into the communicating segment (fig. 2B). Repeat left renal arteriography demonstrated that the fistula was occluded with significant improvement in the perfusion through the cystic left kidney (fig. 2C).

Follow-up examination 5 months later revealed no evidence of a bruit, and the patient's hypertension was readily controlled by medication.

Case 2. A 59-year-old female was evaluated because of hematuria and hypertension. She had experienced a similar episode 7 years previously. Intravenous pyelography revealed a filling defect in the collecting system of the upper pole of the left kidney which proved to be a blood clot.

Bilateral selective renal arteriography showed the right renal

Received January 26, 1976; accepted after revision April 20, 1976.

¹ Department of Diagnostic Radiology, University of Texas System Cancer Center, M. D. Anderson Hospital and Tumor Institute, Texas Medical Center, Houston, Texas 77030. Address reprint requests to S. Wallace.

² Department of Radiology, St. Luke's Hospital, Texas Children's Hospital, and the Texas Heart Institute, Texas Medical Center, Houston, Texas 77030.

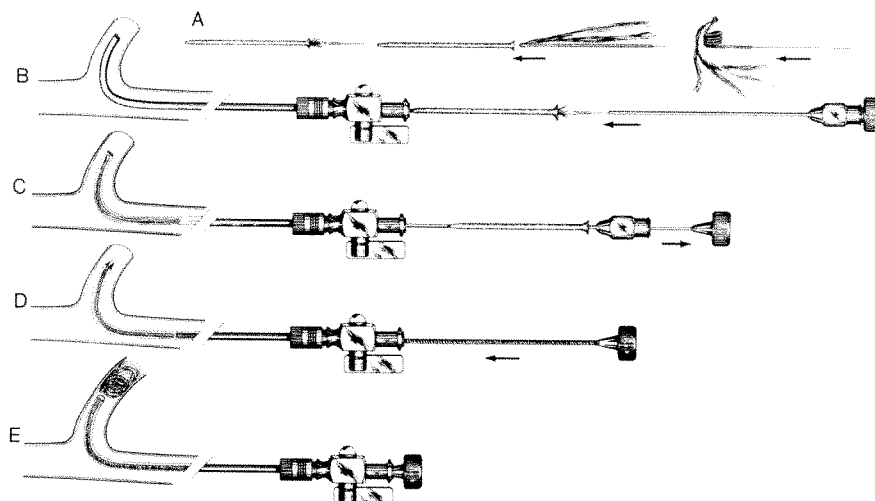


Fig. 1.—Technique. *A*, Straightened stainless steel device. *B*, Introducer passing coil through cartridge into catheter. *C*, Mandril withdrawn from introducer releasing coil into distal portion of catheter. *D*, Modified 0.052 inch guide wire pushing coil through catheter. *E*, Coil deposited in vessel.

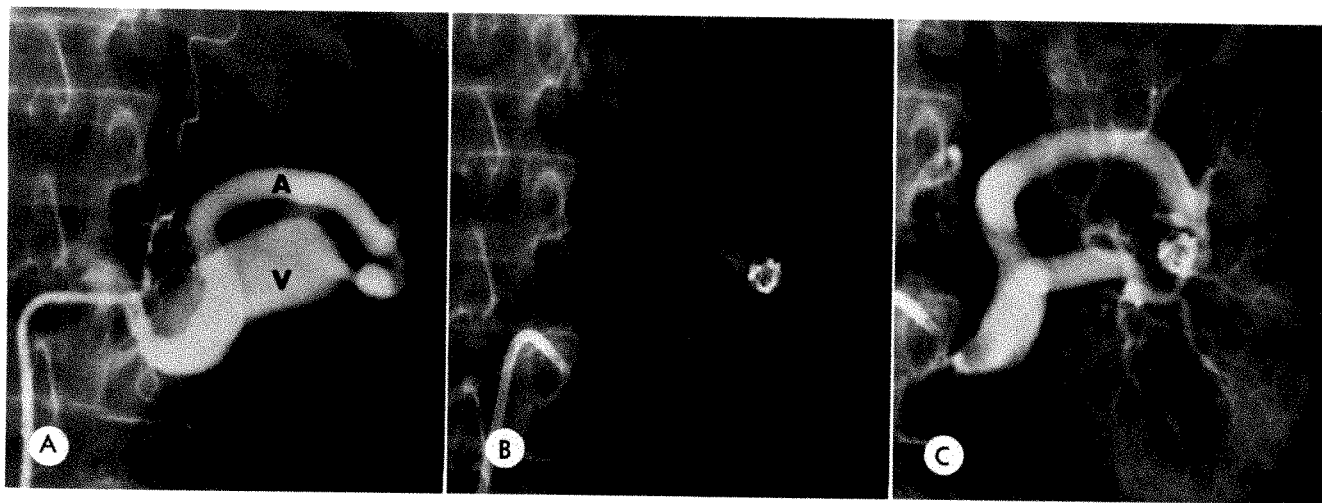


Fig. 2.—Renal vein coil occlusion. Acquired arteriovenous fistula in left kidney (case 1). *A*, Angiogram showing left renal artery stenotic at its takeoff and rapid shunting into renal vein via single fistulous communication (arrow). Minimal perfusion through parenchyma of left kidney. *B*, Fistula occluded via left renal vein by depositing two steel coils into tract. *C*, Repeat left renal arteriography showing improved perfusion of renal parenchyma without evidence of fistulous tract. Later phases demonstrated multiple cysts in kidney as well as in left renal vein.

artery to be involved by medial fibromuscular hyperplasia. An arteriovenous fistula was opacified involving multiple upper pole segments of the ventral branch of the left renal artery with shunting into the renal vein. The fistula was composed of multiple communicating channels.

Two days later intravascular occlusion of the fistula was attempted. Selective catheterization of the ventral branch of the left renal artery was accomplished utilizing a no. 6.5 French nontapered polyethylene catheter with no side holes. The initial attempted occlusion was done using 3 mm segments of straight metallic tubing with 5 mm cotton threads attached [1]. These readily passed through the fistulous tracts to the renal vein. To prevent further pulmonary embolization, occlusion of the major draining branch of the renal vein was undertaken. The right femoral vein was catheterized utilizing a Teflon catheter which was then selectively placed into the branch of the left renal vein draining the arteriovenous fistulas. Two coils were inserted obstructing the peripheral portion of this vein. The feeding segmental arterial branch was then

occluded by the injection of Gelfoam emboli through the arterial catheter. Left renal arteriography following segmental infarction demonstrated the occluded artery and an associated delay in emptying of the remaining renal arterial branches. The patient experienced left flank pain for a few days. There was no change in her labile hypertension and no further hematuria.

Three weeks after the occlusion, an intravenous pyelogram revealed slight delay in function of the left kidney with some reduction in renal size. A left renal arteriogram 3 months later no longer opacified the arteriovenous fistula. The kidney was smaller and still functioning.

Comment on cases 1 and 2. More than 125 renal arteriovenous fistulas have been reported since the initial description by Varela in 1928 [3]. These have been classified as: (1) acquired (secondary to accidental trauma, operations such as nephrectomy, needle biopsy, inflamma-

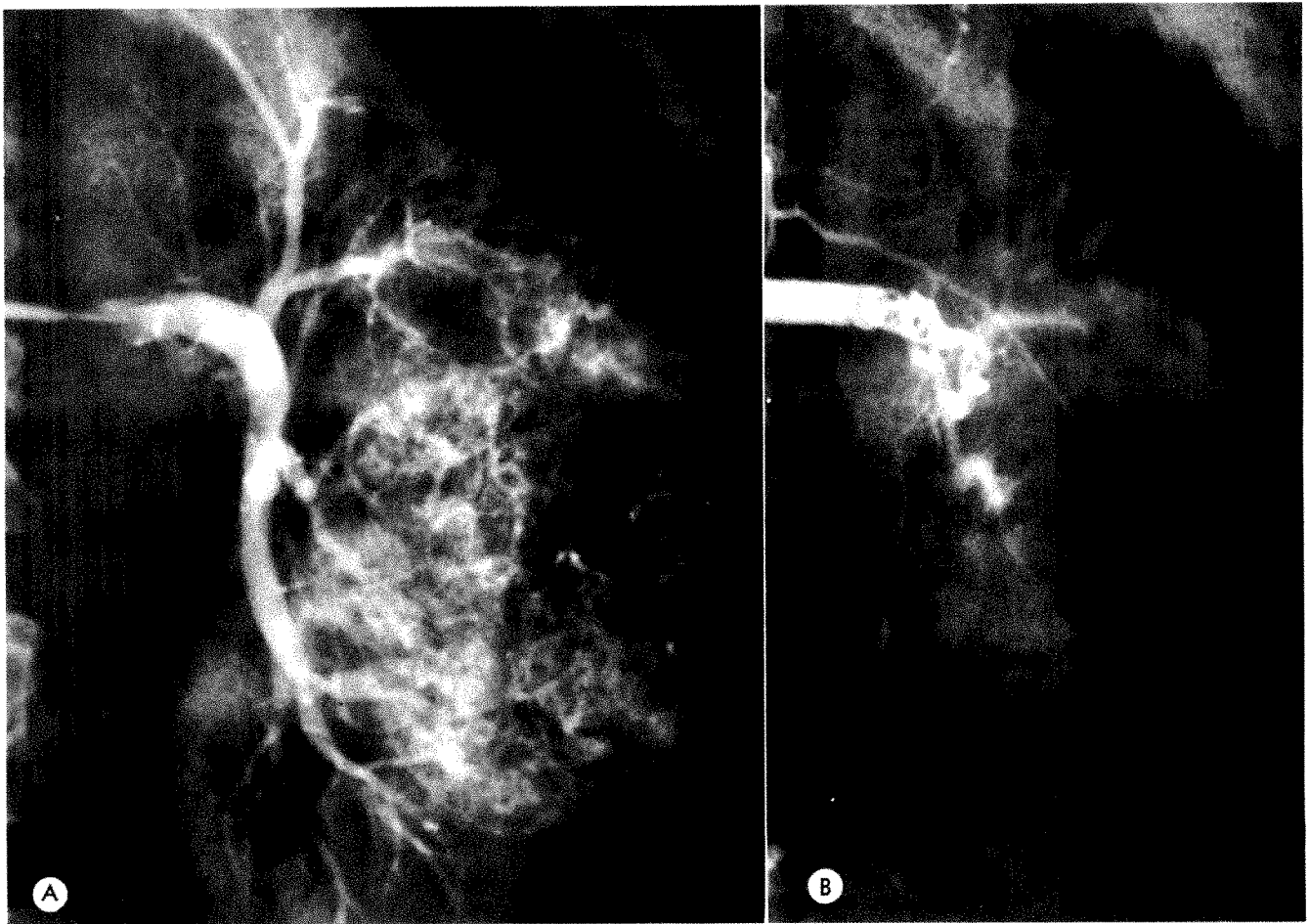


Fig. 3.—Renal artery coil occlusion. Renal carcinoma (case 3). *A*, Left renal arteriogram showing hypervascular hypernephroma. *B*, Renal artery initially embolized with Gelfoam followed by three coils.

tion, rupture of an aneurysm, neoplasm, etc.); (2) congenital or cirroid; and (3) idiopathic [4].

Case 1 illustrates an acquired arteriovenous fistula complicating a renal needle biopsy [5]. This complication has an incidence of 16%. While most of these resolve spontaneously, 4% persist [6]. This variety of arteriovenous fistula is frequently a single intrarenal communicating channel between the artery and the vein. The arteriovenous fistula described in case 2 is of the congenital or cirroid variety which is usually composed of multiple communicating vessels.

Nephrectomy or partial nephrectomy has been the primary treatment for symptomatic arteriovenous fistulas of the kidney. More recently fistulas near the renal hilum have been approached directly by vascular reconstruction with preservation of renal parenchyma [7–9]. Fistulas have also been successfully managed by transcatheter intraarterial embolization using a variety of materials [10, 11]. The potential complications of pulmonary emboli limit its applications.

The value of using a coil to obstruct the venous component of the fistula with salvage of renal parenchyma is illustrated in these two cases. The method was most effective in the presence of a single communication, as in

case 1. In case 2 the venous occlusion was supplemented by arterial embolization because of the multiple fistulous tracts.

Renal Artery Occlusion

Case 3. This 48-year-old female was found to have a mass in the midportion of the left kidney. Arteriography revealed a hypervascular hypernephroma with the opacification of a patent renal vein as well as dilated capsular veins draining the neoplasm (fig. 3).

Two days later, preoperative infarction of the left renal carcinoma was undertaken. The left renal artery was catheterized utilizing a no. 6.5 French polyethylene catheter with an end hole. The catheter was placed as far as possible into the renal artery to minimize reflux. The vascular supply of the neoplasm was initially occluded with Gelfoam emboli. When this was accomplished, the catheter was replaced by a nontapered, end hole, no. 7 French Teflon catheter utilizing a 0.045 inch guide wire in the exchange. The Teflon catheter was placed well into the renal artery. Three coils were necessary to complete the occlusion (fig. 3B).

After the occlusion, the patient experienced pain requiring narcotics, elevated temperature at 101°F, but no hypertension. A nephrectomy was performed 3 days after the infarction. The occlusion of the renal artery created a relatively bloodless operative field. The abnormal veins from the neoplasm as well as renal and capsular veins had collapsed. The plane of cleavage between the neoplasm

and the renal bed also seemed more readily dissected facilitating the surgical procedure.

Case 4. This 65-year-old male was first seen in December 1974 because of multiple nodular lesions in the lung and pleura and lytic areas in the sacrum presumably due to metastases from a carcinoma of the left kidney.

Palliative management included infarction of the hypernephroma utilizing Gelfoam emboli. After occlusion of the left renal artery, the patient experienced left flank pain and fever for 3 days without hypertension. Chemotherapy was instituted consisting of vincristine and hydroxurea.

No histologic confirmation was established of the presumed metastatic foci. The pulmonary and pleural metastases initially decreased in size. Eight months after the renal infarction the pulmonary nodules began to enlarge. Repeat renal arteriography demonstrated a patent left main renal artery supplying the residual tumor and kidney. It was uncertain whether the vascular changes were due to the neoplasm or the previous embolization. The left renal artery was then occluded utilizing two coils.

The presumed metastases in the lung and bone remained stable. In November 1975 a nephrectomy was performed. The left renal artery was found to be completely occluded. The kidney was fibrotic, measuring 3 × 5 cm, with evidence of some residual neoplasm.

Comment on cases 3 and 4. The indications for embolic arterial occlusion of hypernephromas include: (1) preoperative reduction of tumor vascularity to make surgery technically more expedient (case 3); (2) therapeutic reduction of tumor bulk in inoperable cases, either alone or in conjunction with other therapeutic modalities (case 4); (3) palliation of specific symptoms such as pain due to tumor bulk or invasion and bleeding; and (4) as a potential stimulant of immune response, which is still under investigation (case 4).

The side effects of renal tumor infarction consisted of (1) flank pain for an average of 48 hr requiring narcotics for relief; (2) temperature elevation up to 103° F; and (3) moderate gastrointestinal symptoms of nausea, vomiting, and paralytic ileus at times necessitating intravenous fluids to maintain hydration. A transient elevation of diastolic blood pressure occurred in two patients. Complications of renal tumor infarctions included renal failure in two patients, one clearing in 10 days without dialysis. The second patient died, and the histologic examination of the "normal" kidney revealed tubular necrosis without evidence of emboli. It is believed that the amount of contrast material, approximately 100 ml used during the diagnostic and therapeutic procedure, was a contributing factor. Consequently the diagnostic studies and the intravascular therapy are performed on separate days. A third patient expired 6 days after infarction from a renal abscess developing in the infarcted neoplasm.

Of the 38 patients and 42 occlusions of hypernephromas performed at M. D. Anderson Hospital and Tumor Institute [12], 19 have been occluded using Gelfoam emboli in combination with steel coils. Nine of these occlusions were performed preoperatively. Preoperative infarction has been accomplished with Gelfoam alone as long as the surgery follows within a few days, since Gelfoam-occluded vessels usually show some degree of recanalization. However, if

the surgeons feel that a more complete occlusion is desirable, this is readily achieved by the combination of Gelfoam and coils as long as the anatomy and size of the vessels allow selective catheterization with a Teflon catheter. A more complete occlusion also seems preferable for long term palliation, and coils can be employed for this purpose. Chemotherapy usually completes the palliative treatment. The clinical response to this therapeutic approach has recently been summarized [13, 14].

Hepatic Artery Occlusion

Case 5. This 30-year-old female with hepatosplenomegaly and pulmonary metastases was found to have a poorly differentiated carcinoma involving the liver with the largest nodule in the left lateral segment. No primary site was identified, and the possibility of biliary tract origin was considered.

At laparotomy, ligation of the left lateral segmental hepatic artery was performed to devascularize the dominant mass.

Two weeks later percutaneous intravascular occlusive therapy was undertaken to complete the hepatic devascularization. Selective hepatic arteriography opacified the supply to the left lateral segment via intrahepatic collateral circulation from the left medial hepatic artery (fig. 4A). Multiple neoplastic masses were demonstrated throughout the liver. Gelfoam emboli occluded the intrahepatic vasculature. The procedure was completed with the use of a single coil placed in the hepatic artery (fig. 4B).

Comment. The blood supply to primary and secondary neoplasms of the liver is principally by way of the hepatic artery with little contribution from the portal venous system. Hepatic dearterialization as a palliative method of therapy was proposed by Markowitz [15]. This approach can be used alone or in combination with chemotherapy [16–18] to achieve clinical improvement.

Devascularization of the liver has been attempted for the most part by surgical ligation of the hepatic arteries. Case 5 illustrates the difficulties encountered because of collateral circulation. Selective transcatheter intravascular occlusion can be a useful adjunct. Five cases have been treated at M. D. Anderson Hospital by this route using Gelfoam embolization alone. There was a definite decrease in the size of the neoplasm and associated alleviation of symptoms. Although complete occlusion is almost impossible [19], the stainless steel coil can be of considerable assistance.

Splenic Artery Occlusion

Case 6. A 56-year-old male with stage IV histiocytic lymphoma was admitted with extensive and progressive disease including massive splenomegaly, thrombocytopenia of approximately 10,000/mm³, and pneumonia. Chemotherapy had been discontinued primarily because of the thrombocytopenia.

The general condition of the patient contraindicated surgical splenectomy. With no obvious alternative, intravascular splenic artery occlusion was undertaken using Gelfoam to occlude the peripheral splenic arterial bed and two coils for the main splenic artery. Immediately prior to the infarction a platelet transfusion increased the platelet count to 80,000/mm³. Three days post-occlusion the platelet count was 240,000/mm³. Ten days following the infarction a splenic abscess was detected requiring surgical splenectomy. One week after surgery the patient succumbed.

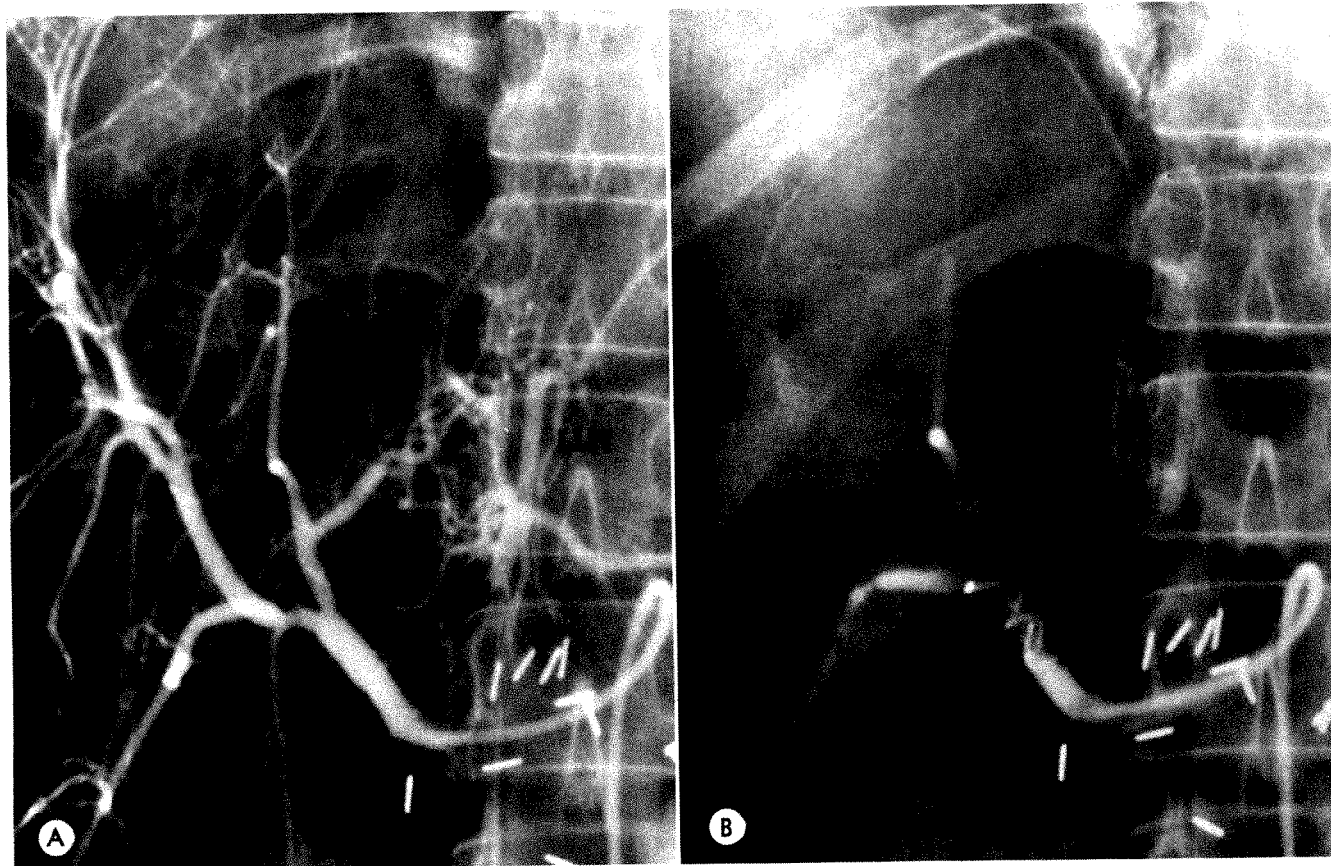


Fig. 4.—Hepatic artery coil occlusion. Carcinoma involving liver (case 5). A, Arteriogram after surgical ligation of left lateral hepatic artery showing intra-hepatic collateral circulation to left lateral segment via left medial segmental branches. LLH = left lateral hepatic artery; LMH = left medial hepatic artery. Multiple neoplastic masses seen throughout liver. B, Hepatic artery occluded initially with Gelfoam followed by single coil.

Autopsy revealed the immediate cause of death was respiratory failure probably due to pulmonary fibrosis secondary to bleomycin toxicity.

Comment. The intravascular occlusive approach to the treatment of hypersplenism is of increasing interest. Maddison [20] described the treatment of hypersplenism in a patient with portal hypertension by the intravascular embolization of autologous blood clot. Chuang and Reuter [21] demonstrated in experimental animals that diminished splenic function resulted from intravascular occlusion of the splenic artery. Anderson et al. [22] have shown that alterations in splenic function could be accomplished for 3–5 weeks by the use of Gelfoam and/or stainless steel coils. Diminished splenic function in a patient with hypersplenism secondary to neoplastic disease allows additional time for chemotherapeutic treatment of the patient's basic disease. The increase in platelets following splenic artery occlusion may decrease the risk of surgical splenectomy.

The occurrence of a splenic abscess in case 6 is a serious complication. The presence of pneumonia in the immunosuppressed patient probably enhanced the possibility of abscess formation in the infarcted spleen. S. R. Reuter and R. Pereiras (personal communications, 1975) each noted a splenic abscess following therapeutic intravascular occlusion of the splenic artery. Splenic abscess was also re-

ported in association with spontaneous splenic infarction in a patient with diabetes [23]. In a study of 20 normal dogs subjected to transcatheter intravascular occlusion of the splenic artery, one animal also developed a splenic abscess with gram-negative bacteria [22].

Internal Iliac Artery Occlusion

Case 7. In 1968 this 45-year-old female was thought to have a simple cyst of the sacrum and was treated by curettage and implantation of bone chips. The patient continued to experience intermittent pain. In October 1974 another biopsy revealed a giant cell tumor which was treated with cobalt 60 therapy.

She was admitted 1 year later because of persistent pain and constipation. On physical examination a pelvic mass originating from the sacrum was palpated. Radiographic examination revealed a large radiolucent lesion of the sacrum. Pelvic arteriography delineated the primary vascular supply to the hypervascular mass in the sacrum originating from the left internal iliac artery (fig. 5A).

In an attempt to provide palliative relief of the persistent pain, intravascular occlusion of the left internal iliac artery was undertaken. This was accomplished by the use of Gelfoam for the peripheral arterial bed and three coils for the proximal occlusion of the left internal iliac artery (fig. 5B). After occlusion the patient had a febrile episode to 103°F for 3 days.

Follow-up examination 2 months after occlusion revealed sclerosis in the margin of the sacral lesion and considerable relief of the pelvic pain.

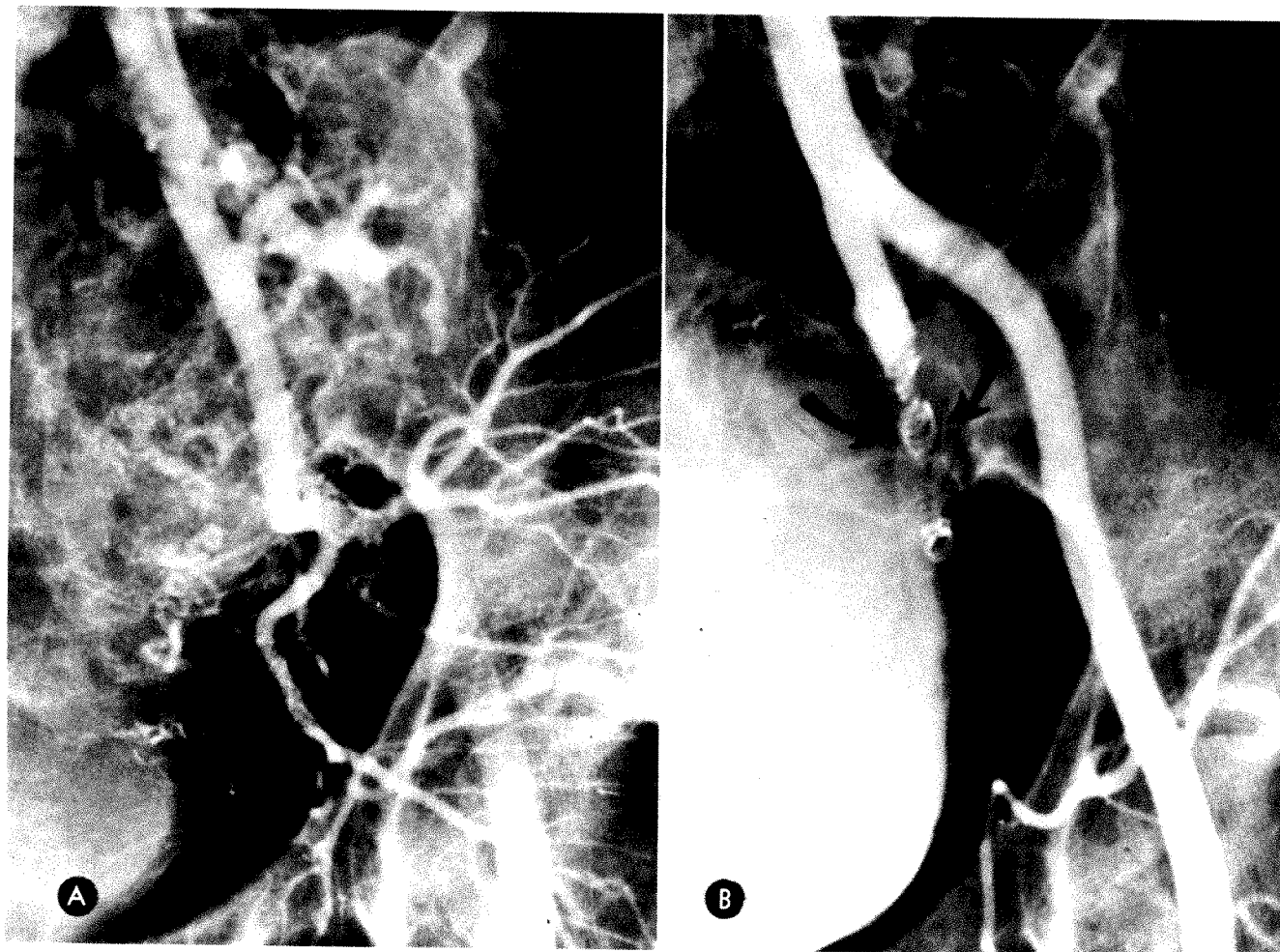


Fig. 5.—Internal iliac artery coil occlusion. Giant cell tumor of the sacrum (case 7). A, Selective left internal iliac arteriogram showing hypervascular sacral mass. B, Internal iliac artery occluded by Gelfoam emboli followed by three coils (arrows).

Comment. Occlusion of the internal iliac artery has been effectively employed to control bleeding from pelvic neoplasms originating in the uterus and bladder [24, 25]. Pre-operative occlusion of the internal iliac artery was of considerable assistance in the removal of an angioliopoma of the buttocks [25]. These intravascular occlusions were accomplished with the use of Gelfoam emboli alone. The addition of coils as in case 7 is more effective when a more permanent occlusion is necessary.

Discussion

Intravascular occlusion has been employed in the therapeutic management of bleeding neoplasms, arteriovenous malformations, and fistulas. The materials used for embolization include: autologous tissue and clot; clot augmented by thrombin, platelets, Amicar, and others; Gelfoam; metallic and Silastic spheres; a variety of silicone preparations; isobutyl 2-cyanoacrylate; and radioactive particles. Occluding devices have also been effective in the more proximal occlusion of larger vessels. These devices include intravascular balloon, Ivalon plugs, and stainless steel coils.

Inflatable balloons of the Fogarty, Wholey-Edwards, and Swan-Ganz varieties have been utilized for temporary occlusion only to be withdrawn after short term application. Serbienko [26] has successfully managed patients with carotid-cavernous fistulas using an intravascular detachable balloon deposited in the fistulous communication. Porstmann et al. [27] has treated a patient with patent ductus arteriosus by the percutaneous intravascular placement of an Ivalon plug.

The stainless steel coil used here is introduced by a no. 7 French Teflon catheter. The Teflon catheter has obvious disadvantages, being relatively less opaque and more rigid than the polyethylene catheter used for angiography. In one patient the rigidity of the modified 0.052 inch guide wire used to push the coil beyond the tip of the catheter caused the catheter to pop out of the renal artery, leaving the coil partially protruding into the aorta. Attempts to replace it in the renal artery failed, and the coil was purposely deposited in the proximal hepatic artery where it caused no significant harm because of adequate collateral circulation through the superior mesenteric artery. For this reason the more flexible standard 0.045 inch guide wire is utilized in patients with tortuous vessels.

ACKNOWLEDGMENTS

We wish to acknowledge Drs. E. C. Price, P. Gerson, and B. P. Griffith for allowing us to participate in the management of cases 1 and 2. We also wish to acknowledge the photographic assistance of Eugene Szwarc and the technical aid of Deborah Wilson and Debra Kruse.

REFERENCES

- Gianturco C, Anderson JH, Wallace S: Mechanical devices for arterial occlusion. *Am J Roentgenol* 124:428-435, 1975
- Wallace S, Medellin H, De Jongh D, Gianturco C: Systemic heparinization for angiography. *Am J Roentgenol* 116:204-209, 1972
- Varela ME: Aneurisma arteriovenoso de los vasos renales y asistolia consecutiva. *Rev Med Latino-Am* 14:3244-3266, 1928
- Boijssen E, Kohler R: Renal arteriovenous fistulae. *Acta Radiol* 57:433-445, 1962
- Meng CH, Ilkin M: Immediate angiographic manifestations of iatrogenic renal injury due to percutaneous needle biopsy. *Radiology* 100:333-341, 1971
- Halpern M: Spontaneous closure of traumatic renal arteriovenous fistula. *Am J Roentgenol* 107:730-736, 1969
- Leiter E, Gribets D, Cohen S: Arteriovenous fistula after percutaneous needle biopsy—surgical repair with preservation of renal function. *N Engl J Med* 287:971-972, 1972
- Tunner WS, Middleton RG, Watson RW, Marshall VF: Repair of an intrarenal arteriovenous fistula with preservation of the kidney. *J Urol* 103:286-289, 1970
- Fry WJ: Surgical considerations in congenital arteriovenous fistula. *Surg Clin North Am* 54:165-174, 1974
- Bookstein JJ, Goldstein HM: Successful management of post-biopsy arteriovenous fistula with selective arterial embolization. *Radiology* 109:535-536, 1973
- Rizk GK, Atallah NK, Bridi GI: Renal arteriovenous fistula treated by catheter embolization. *Br J Radiol* 46:222, 1973
- Goldstein HM, Medellin H, Beydoun MT, Wallace S, Ben-Menachem Y, Bracken RB, Johnson DE: Transcatheter embolization of renal cell carcinoma. *Am J Roentgenol* 123:557-562, 1975
- Bracken RB, Johnson DE, Goldstein HM, Wallace S, Ayala AG: Percutaneous transfemoral renal artery occlusion in patients with renal carcinoma. Preliminary report. *Urology* 6:6-10, 1975
- Johnson DE, Bracken RB, Goldstein HM, Wallace S: Transfemoral renal artery occlusion in patients with renal carcinoma. *Proc Kimbrough Soc* In press, 1976
- Markowitz J: The hepatic artery. *Surg Gynecol Obstet* 95:644, 1952
- Aune S, Schistad G: Carcinoid liver metastases treated with hepatic dearterialization. *Am J Surg* 123:715-717, 1972
- Fortner JG, Mulcare RJ, Solis A, Watson RC, Golbey RB: Treatment of primary and secondary liver cancer by hepatic artery ligation and infusion chemotherapy. *Ann Surg* 178:162-172, 1973
- Larmi TKI, Kärkölä P, Klintrup H-E, Heikkinen E: Treatment of patients with hepatic tumors and jaundice by ligation of the hepatic artery. *Arch Surg* 108:178-183, 1974
- Pettersson H: Arterial collaterals in intrahepatic arterial occlusion. *Acta Radiol* 16:401-406, 1975
- Maddison FE: Embolic therapy of hypersplenism (abstr.). *Invest Radiol* 8:280, 1973
- Chuang VP, Reuter SR: Experimental diminution of splenic function by selective embolization of the splenic artery. *Surg Gynecol Obstet* 140:715-720, 1975
- Anderson JH, Vu Ban A, Burke J, Hester J, Wallace S: Transcatheter splenic artery occlusion. Submitted for publication
- Rittenhouse M, Kruse J, Cruz AB Jr: Pneumoperitoneum associated with splenic infarction and superimposed clostridial infection. *Tex Med* 71:47-50, 1975
- Schwartz PE, Goldstein HM, Wallace S, Rutledge FN: Control of arterial hemorrhage using percutaneous arterial catheter techniques in patients with gynecologic malignancies. *Gynecol Oncol* 3:276-288, 1975
- Bree RB, Goldstein HM, Wallace S: Transcatheter internal iliac artery embolization in the management of pelvic neoplasms. *Surg Gynecol Obstet*. In press
- Serbienko FA: Balloon catheterization and occlusion of major cerebral vessels. *J Neurosurg* 41:125-145, 1974
- Porstmann W, Hieronymi K, Wierny L, Warnke H: Nonsurgical closure of oversized patent ductus arteriosus with pulmonary hypertension: report of a case. *Circulation* 50:376-381, 1974

Embolic Control of Hypertension Caused by Segmental Renal Artery Stenosis

STEWART R. REUTER,¹ PAUL R. POMEROY,² VINCENT P. CHUANG,^{2,3} AND KYUNG J. CHO²

Renovascular hypertension was controlled in a 15-year-old boy by total infarction of the renal parenchyma behind a segmental renal artery stenosis. Two separate embolizations were required to occlude the branches distal to the stenosis. Blood pressure did not return to normal until after the second procedure. This approach may be useful in patients with intrarenal arterial stenoses who would be difficult to approach operatively without sacrificing a significant portion of the kidney.

In recent years investigators have become more aware of the importance of renal artery branch stenoses as a cause of hypertension [1, 2]. Although such segmental stenoses generally accompany a main renal artery stenosis, some occur as isolated findings. In such a patient, operative curability of the hypertension can be determined by assay of the renin activities from upper and lower pole venous samplings [3]. Surgical correction of the lesion—by bypass if the stenosis involves a primary renal artery branch or by dilatation if it involves an interlobar branch—has resulted in cure of the hypertension [4].

In 1974 Goldin et al. [5] reported that total infarction of a single remaining kidney in a patient who had received a cadaver transplant because of rapidly progressive glomerulonephritis markedly decreased the patient's severe hypertension, which was causing problems in her management. Based on that experience, we used segmental infarction to control severe hypertension caused by an isolated stenosis of an interlobar artery in a 15-year-old boy.

Case Report

A 15-year-old black male was first noted to have hypertension in 1969, although treatment was not instituted then. In 1973 his blood pressure at a school physical examination was 166/140 mm Hg, and he was referred to Wayne County General Hospital for evaluation. Physical examination revealed normal vital signs except for a blood pressure of 164/134 mm Hg. He was moderately overweight for his age and height, but there was no clinical evidence of Cushing's syndrome. The remainder of the physical examination was normal. There was no family history of hypertension.

Serum electrolyte and renal function studies were normal. Urine cultures were negative $\times 3$. Thyroid function studies and 24 hr urines for 17-ketosteroids and 17-ketogenic steroids were normal; 24 hr urine collections for VMA and catecholamines were also normal, as were urinary aldosterone levels. An abdominal aortogram showed a normal aorta and main renal arteries; the interlobar arteries were not well visualized.

Antihypertensive treatment was begun during this hospitalization with a diuretic (chlorthalidone, 100 mg/day), but resulting

hyponatremia, hypochloremia, hypokalemia, and mild azotemia necessitated discontinuation. The antihypertensive therapy for the remainder of the hospitalization was Apresoline (25 g q.i.d.) and Ismelin (12.5 mg q.d.). On discharge from the hospital in January 1974 the blood pressure was 150/100 mm Hg.

During the next year his blood pressure remained high (160–170/120–130 mm Hg), but he remained asymptomatic. Additional drugs were added to the regimen.

The lack of control despite a four-drug antihypertensive regimen prompted readmission to the hospital in January 1975 for repeat angiography. This time selective renal angiograms revealed a stenosis of a segmental branch to the upper pole of the left kidney with slight poststenotic dilatation (fig. 1A). Intrarenal, sinusoidal collateral vessels were present. Renal vein renin values were as follows (ng/ml/hr): left renal vein, 3.98; right renal vein, 1.72; high IVC, 1.56; and low IVC, 1.00. A selective sample from the upper pole left renal vein was 30.36 and from the lower pole, 9.84. These values indicate a hemodynamically significant stenosis and probably curable hypertension.

The findings were described to the patient and his family; however, the family wanted to avoid surgery if any alternatives were available. Following a thorough discussion of the possibilities of embolic treatment with both family and the human use committee, the decision was made to infarct the renal parenchyma behind the stenosis.

Just prior to the embolization procedure, the blood pressure was stable in the range of 170–180/130–140 mm Hg. A Cope-Eisenberg coaxial catheter system was introduced into the left renal artery and the coaxial catheter advanced to the stenosis (fig. 1B). Sterile USP barium was then injected through the coaxial catheter until the artery distal to the stenosis was completely filled. The total amount of barium was approximately 0.3 ml. The coaxial catheter was then withdrawn. An angiogram performed through the Cope catheter demonstrated complete occlusion of the stenosed interlobar artery (fig. 1C).

One hour after injection, the blood pressure was 144/100 mm Hg; at hourly intervals readings were 130/94, 124/94, 116/84, 144/100, and 160/100 mm Hg, respectively. During the next week the pressure fluctuated widely, and on several occasions the patient received intramuscular Apresoline. He developed leukocytosis to 13,000 and mild temperature elevation which lasted approximately 4 days. An unanticipated ileus lasted for several days. He was discharged 1 week following the embolization on Aldactazide b.i.d. His blood pressure remained elevated, though lower than pre-embolization levels. At home the patient's blood pressure averaged 145/100 mm Hg initially and gradually increased to 155/105 mm Hg; Inderal (40 mg t.i.d.) was then added to the regimen.

Two months after the embolization the patient was again readmitted for a repeat renal angiogram. The admission blood pressure was 144/100 mm Hg. A repeat arteriogram revealed that

Received March 24, 1976; accepted May 5, 1976.

¹ Department of Radiology, University Hospital, University of Michigan Medical Center, Ann Arbor, Michigan 48109. Present address: Department of Radiology, Martinez Veterans Administration Hospital, Martinez, California 94553. Address reprint requests to S. R. Reuter.

² Department of Radiology, University of Michigan at Wayne County General Hospital, Eloise, Michigan 48132.

³ Present address: Department of Radiology, University of Kentucky Medical Center, Lexington, Kentucky 40506.

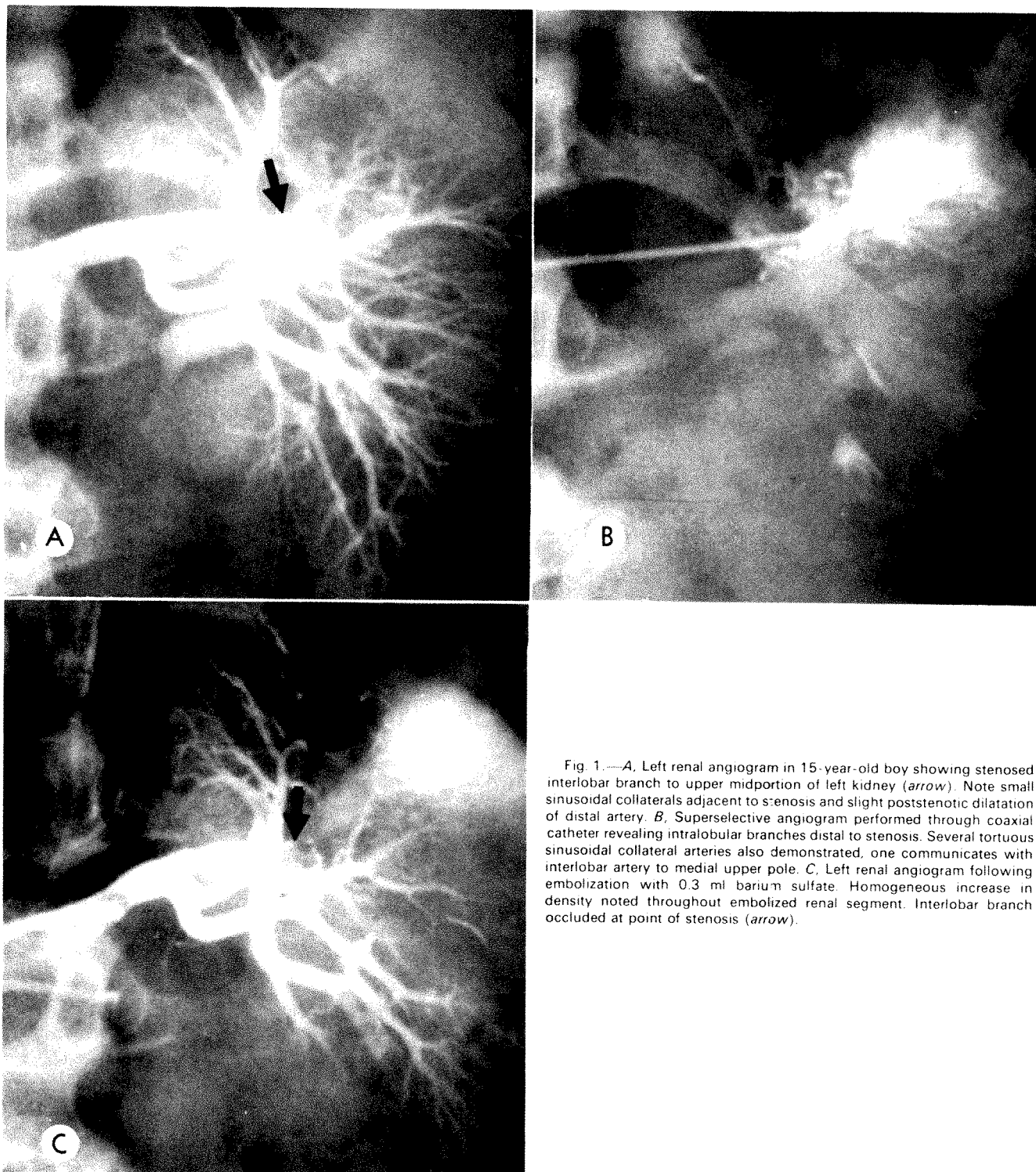


Fig. 1.—A, Left renal angiogram in 15-year-old boy showing stenosed interlobar branch to upper midportion of left kidney (arrow). Note small sinusoidal collaterals adjacent to stenosis and slight poststenotic dilatation of distal artery. B, Superselective angiogram performed through coaxial catheter revealing intralobular branches distal to stenosis. Several tortuous sinusoidal collateral arteries also demonstrated, one communicates with interlobar artery to medial upper pole. C, Left renal angiogram following embolization with 0.3 ml barium sulfate. Homogeneous increase in density noted throughout embolized renal segment. Interlobar branch occluded at point of stenosis (arrow).

the previously embolized stenotic intralobular artery was again patent (fig. 2A). Because of the failure of the barium to effect a complete stenosis, a $2 \times 2 \times 10$ mm piece of Gelfoam was injected into the interlobar branch through a thin-walled red Kifa catheter placed at the stenosis. A repeat angiogram following embolization revealed complete occlusion of the interlobar branch (fig. 2B).

The patient's blood pressure rapidly dropped to 106/70 mm Hg,

and subsequent blood pressure readings taken during his hospitalization fluctuated moderately but were only occasionally above 140/90 mm Hg. He was discharged 1 week later with a stabilized blood pressure of 124/80 mm Hg. For the 6 months following discharge he has been followed in the hypertensive clinic. For the first 3 months he was kept on a diuretic (Aldactazide b.i.d.), but for the last 6 months he has not been on medication. He has remained

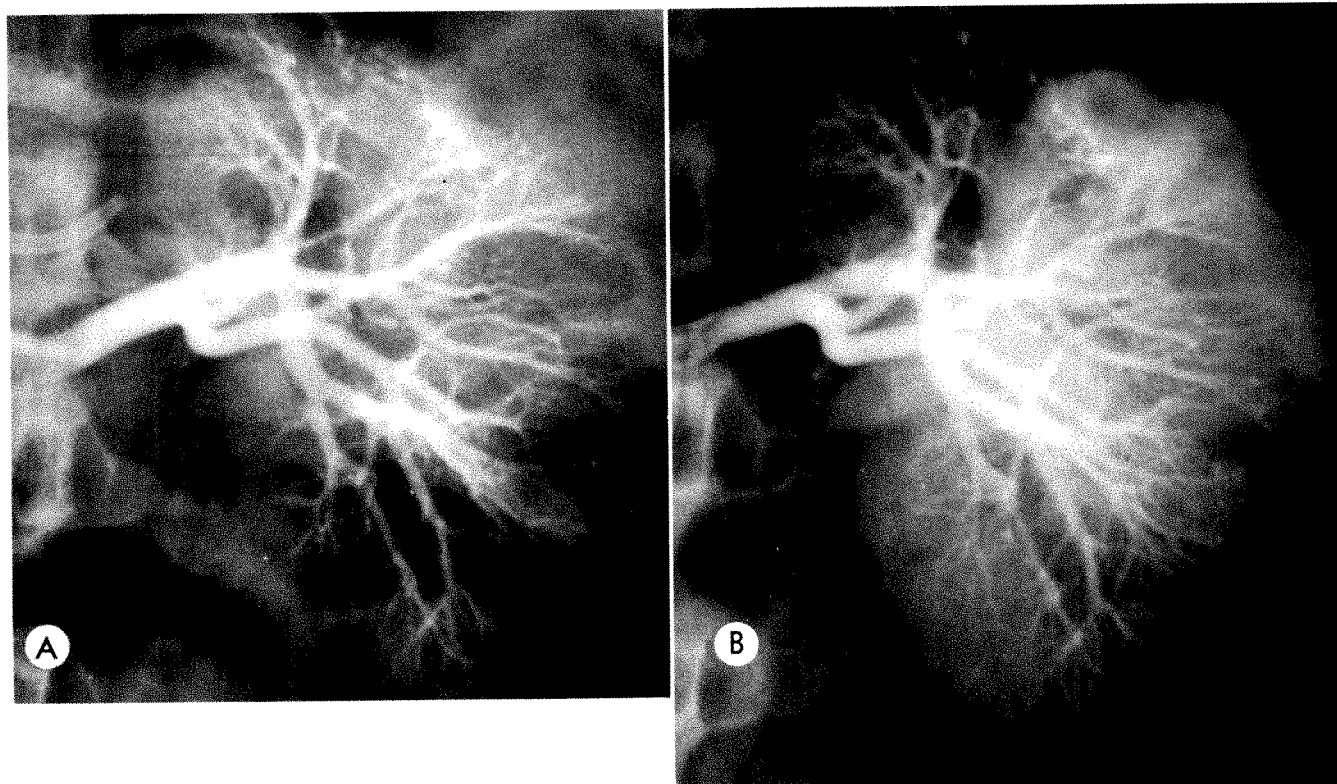


Fig. 2.—A. 2 months after embolization, stenotic interlobar branch again patent. B. After reembolization of stenosed interlobar artery with $2 \times 2 \times 10$ mm piece of Gelfoam, artery again occluded.

normotensive during the 13 months since the repeat embolization.

Discussion

Several studies have shown that although the renin-angiotensin system is activated by a hemodynamically significant stenosis of the renal artery or renal artery branch, complete infarction of a segment of the kidney usually does not produce hypertension [6, 7]. Thus several investigators have embolized interlobar arteries with various embolic materials to control bleeding from arteriovenous fistulas and renal trauma [8]. Although most of these patients have been embolized with autogenous blood clot, which occludes for only a few hours, some have been embolized with materials causing a long-lasting occlusion. To date these patients have not developed hypertension.

Because of the reports of Goldin et al. [5, 9], we elected to use sterile barium with an application similar to theirs. We wanted to use as small an embolic material as possible in order to occlude the interlobular arteries as well as the arcuate and interlobar arteries to the segment. Barium particles are about $1 \mu\text{m}$ in size, and Goldin et al. [9] have demonstrated that they fill these three groups of arteries without passing through the glomeruli.

Failure of the initial embolization is probably related to two factors: (1) since the embolization was segmental, the quantity of barium was limited to avoid spill into other segments, and (2) the barium impacted peripherally with time, allowing the proximal artery to reopen. We have since encountered the same difficulty with barium for segmental

renal artery embolization in experimental animals. Thus we now use materials such as Gelfoam or a combination of Gelfoam and barium.

The drop in blood pressure after the initial embolization suggested that the method was successful at least for a short period. This encouraged us to another attempt at embolization when the reopened interlobar artery was discovered. Gelfoam was selected because it was the longest acting embolic material available to us. It has been shown in animal experiments to remain occlusive from a few weeks to permanently [10]. A permanent occluding agent, such as isobutyl-2-cyanoacrylate [11], probably would have been better.

This case demonstrates that renovascular hypertension due to an isolated, segmental stenosis can be reversed by selective embolization. The method presents an alternative to a major operative procedure such as arterial bypass, arterial dilatation, or partial nephrectomy. Further evaluation of the method is warranted.

REFERENCES

1. Bookstein JJ: Segmental renal artery stenosis in renovascular hypertension. *Radiology* 90:1073-1083, 1968
2. Clayman AS, Bookstein JJ: The role of renal arteriography in pediatric hypertension. *Radiology* 108:107-110, 1973
3. Stockigt JR, Hertz P, Schambelan M, Beglieri EG: Segmental renal vein renin sampling for segmental renal infarction. *Ann Intern Med* 79:67-70, 1973

4. Fry WJ, Brink BE, Thompson NW: New techniques in the treatment of extensive fibromuscular disease involving the renal arteries. *Surgery* 68:959-967, 1970
5. Goldin AR, Naude JH, Thatcher GN: Therapeutic percutaneous renal infarction. *Br J Urol* 46:133-135, 1974
6. Almgard LE, Lunderquist A: Experimental occlusion of the renal circulation in the dog. *Scand J Urol Nephrol* 5:268-272, 1971
7. Chuang VP, Reuter SR, Schmidt RW: Control of experimental renal hemorrhage by embolization with autogenous blood clot. *Radiology* 117:55-68, 1975
8. Chuang VP, Reuter SR, Walter J, Foley WD, Bookstein JJ: Control of renal hemorrhage by selective arterial embolization. *Am J Roentgenol* 125:300-306, 1975
9. Goldin AR, Naude JH, Hickman R: Experimental percutaneous renal infarction. *Br J Urol* 46:127-131, 1974
10. Chuang VP, Reuter SR: Experimental diminution of splenic function by selective embolization of the splenic artery. *Surg Gynecol Obstet* 140:715, 720, 1975
11. Dotter CT, Goldman ML, Rösch J: Instant selective arterial occlusion with isobutyl 2-cyanoacrylate. *Radiology* 114, 227-230, 1975

Aneurysms Secondary to Pancreatitis

ALAN F. WHITE,¹ STANLEY BAUM,² AND SUMALEE BURANASIRI³

In a review of arteriograms of 72 unselected consecutive cases of pancreatitis, seven patients were found to have arterial aneurysms involving branches of the peripancreatic vessels. During the same period, arteriograms of 84 cases of carcinoma of the pancreas were reviewed and no aneurysms of any of these vessels were found.

The demonstration of aneurysms of the peripancreatic arteries in pancreatitis is an important differential feature from carcinoma of the pancreas. Both carcinoma of the pancreas and chronic pancreatitis can cause encasement of the arterial vessels and obstruction of the splenic or the superior mesenteric vein, therefore resulting in a similar angiographic appearance. Thus an aneurysm seen in such a patient is a helpful distinguishing feature. In addition, these aneurysms are an important source of hemorrhage and mortality in pancreatitis.

Introduction

Even with angiography, the differential diagnosis of pancreatitis and tumor can be difficult because both can cause arterial encasement and obstruction of the splenic or superior mesenteric vein [1]. Aneurysms secondary to pancreatitis occur in the peripancreatic arteries. Since aneurysms are not seen in carcinoma of the pancreas, this is a helpful differential feature angiographically.

The pathogenesis of the development of these aneurysms in pancreatitis is actual digestion of the wall of the artery by pancreatic enzymes [2, 3].

We are reporting a series of seven patients to draw attention to the association of aneurysms of peripancreatic arteries and pancreatitis.

Materials and Methods

Using conventional technique, the superior mesenteric artery and the celiac axis were selectively catheterized. When the patient's clinical condition permitted and it was technically possible, subselective arteriograms of the splenic, hepatic, gastroduodenal, or dorsal pancreatic arteries (with or without direct serial magnification) were performed.

The arteriograms of 72 unselected consecutive cases of pancreatitis were reviewed. The diagnosis was established by necropsy, surgery, or long term clinical follow-up in 63 cases; nine cases were lost to follow-up. The arteriograms of 84 cases of carcinoma of the pancreas during the same period were reviewed.

Findings and Discussion

Evaluation of the pancreas remains a perplexing problem in spite of the use of pancreatic scanning, barium studies, and angiography [1, 4, 5]. Many of the arteriographic changes thought to be diagnostic of adenocarcinoma of the pancreas have been reported in pancreatitis and even

in patients subsequently proved at surgery to have a normal pancreas. It is important to differentiate between carcinoma and pancreatitis because the clinical condition of patients with pancreatitis often worsens following biopsy. There is a slightly increased incidence of carcinoma of the pancreas in patients with chronic pancreatitis [6]. To further complicate the differentiation of these two conditions, pancreatitis can occur surrounding a carcinoma of the pancreas.

We wish to draw attention to a finding which is suggestive of pancreatitis, that is, the presence of aneurysms of the arteries in the region of the pancreas. These aneurysms have not been reported in carcinoma of the pancreas. We have studied angiographically 72 patients, 63 of whom were subsequently shown to have pancreatitis by necropsy, surgery, or long term clinical follow-up. We found arterial aneurysms in seven (10%). Clinical details are shown in table 1. These aneurysms are a relatively rare finding but when present suggest that the patient has pancreatitis, not carcinoma of the pancreas. Thus an occasional patient may be spared exploratory surgery.

Occlusion of the splenic vein has been reported both in carcinoma of the pancreas [1] and in pancreatitis [7, 8]. Narrowing of the superior mesenteric vein can likewise be found in pancreatitis [7]. Tumor encasement of arteries

TABLE I
Clinical Data on Patients with Aneurysms

Patient No.	Age (Yr)	Sex	Duration of Pancreatitis (Yr)	Aneurysm Size (cm)	Artery Involved
1.	69	F	10	1.5	Splenic
2.	59	M	*	1.8	Splenic
3.	63	F	5	1.4 2.0	Common hepatic
4.	30	M	4	0.3	Transverse pancreatic
5.	45	M	4	1.0	Transverse pancreatic
6.	60	M	10	2.2 2.4	Celiac axis and splenic
7.	58	M	12	0.3	Transverse pancreatic

Note.—All aneurysms uncalcified except in patient 5
* Patient's previous records not available.

Received January 26, 1976; accepted after revision April 6, 1976.

Presented at the annual meeting of the American Roentgen Ray Society, October 1972.

¹ Department of Radiology, Georgetown University Hospital, 3800 Reservoir Road N.W., Washington, D.C. 20007. Address reprint requests to A. F. White.

² Department of Radiology, Massachusetts General Hospital, Boston, Massachusetts 02114.

³ Department of Radiology, Graduate Hospital, Philadelphia, Pennsylvania 19146.

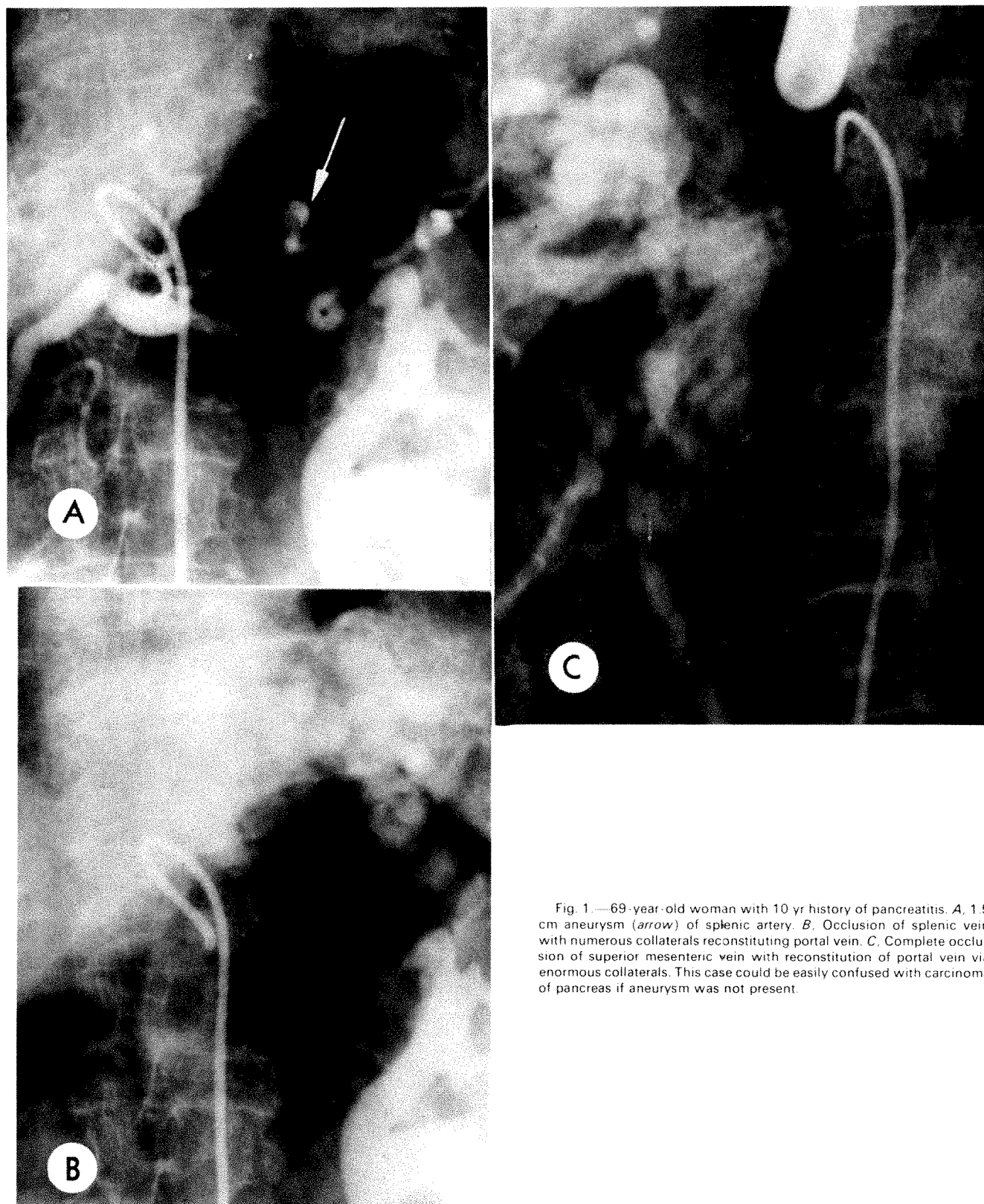


Fig. 1.—69-year-old woman with 10 yr history of pancreatitis. A, 1.5 cm aneurysm (*arrow*) of splenic artery. B, Occlusion of splenic vein with numerous collaterals reconstituting portal vein. C, Complete occlusion of superior mesenteric vein with reconstitution of portal vein via enormous collaterals. This case could be easily confused with carcinoma of pancreas if aneurysm was not present.

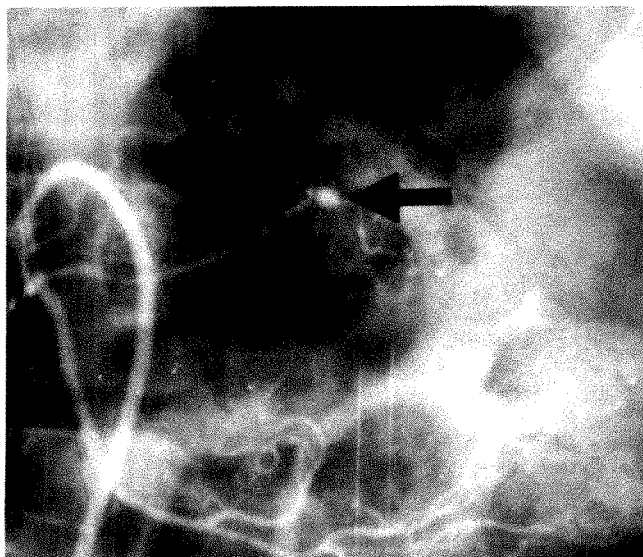


Fig. 2.—30-year-old black male with sickle cell anemia and chronic pancreatitis. Dorsal pancreatic arteriogram showing 3 mm aneurysm (arrow) of transverse pancreatic artery.

artery by the pancreatic enzymes [2, 3]. This has been demonstrated experimentally by inducing pancreatitis in dogs [3]. The most important enzyme in this digestion of the arterial wall is trypsin [3].

Pancreatic enzymes which are released in pancreatitis have also been reported to cause perforation of the colon [12], rupture of the spleen [2], and arterial aneurysms with gastrointestinal bleeding [13].

The present series of cases is reported to draw attention to arterial aneurysms in pancreatitis. In the 84 cases of carcinoma of the pancreas that we studied, there were no arterial aneurysms. Although we have never encountered such a case, a patient could conceivably have an atypical aneurysm of the splenic artery and an unrelated carcinoma of the tail pancreas, with arteriography showing the aneurysm plus splenic vein occlusion. This set of circumstances could lead to an erroneous diagnosis of pancreatitis.

Aneurysms secondary to pancreatitis are an important source of hemorrhage [14] and mortality [15]. Hemorrhage can occur into the parenchyma of the pancreas, the peritoneal cavity [16], or the gastrointestinal tract [14, 15].

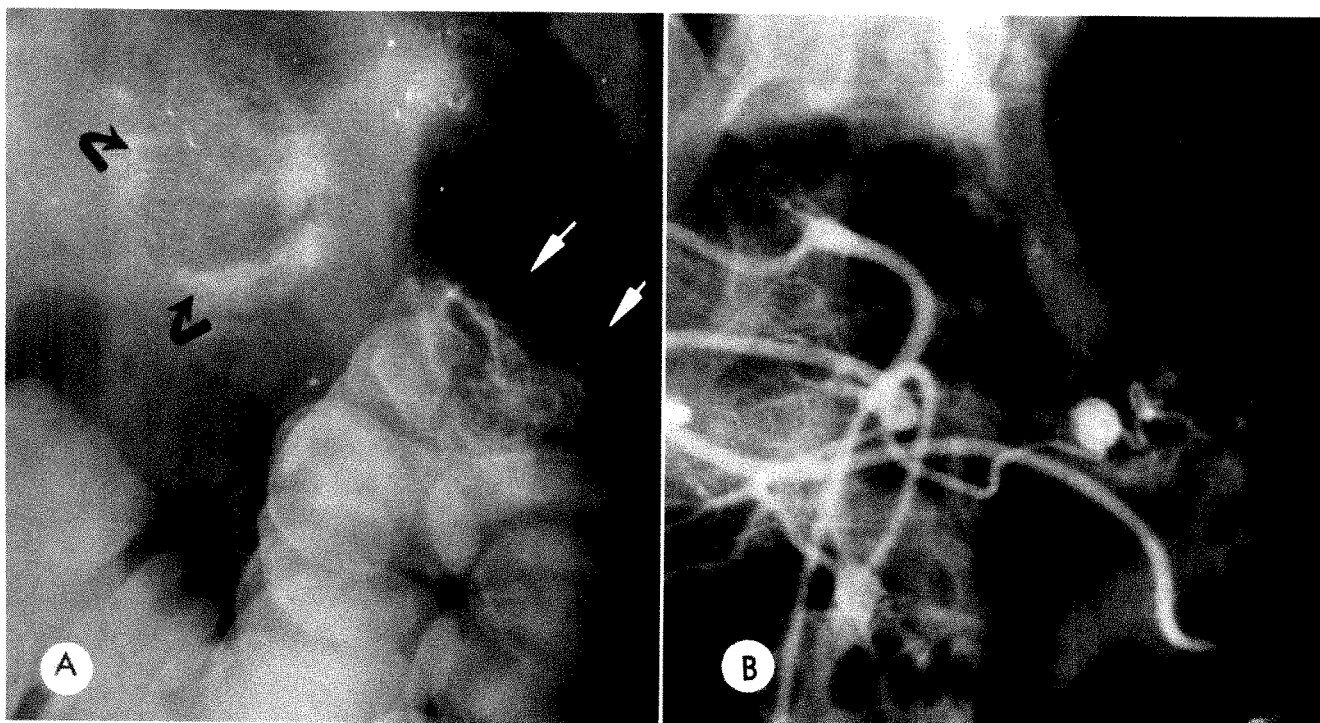


Fig. 3.—45-year-old male with rectal bleeding. A, Barium enema showing 5 cm calcified mass (curved arrows) in left upper quadrant. Irregular lesion (arrows) in colon. B, Dorsal pancreatic artery injection showing aneurysm of transverse pancreatic artery. Large calcified hematoma surrounding this artery and adherent to colon, all secondary to pancreatitis, found at surgery.

has been reported in both pancreatitis [1] and carcinoma [9] of the pancreas. Arterial displacement is also non-specific, indicating only enlargement of the pancreas [5]. Hypervascularity has been reported in pancreatitis [10], carcinoma of the pancreas [4], and even in patients with a normal pancreas [11].

The pathogenesis of aneurysm formation of arteries adjacent to the pancreas is actual digestion of the wall of the

Often the hemorrhage necessitates multiple operations [15], with abscess formation or even death.

REFERENCES

1. Buranasiri S, Baum S: The significance of the venuous phase of celiac and superior mesenteric arteriography in evaluating pancreatic carcinoma. *Radiology* 102:11-20, 1972

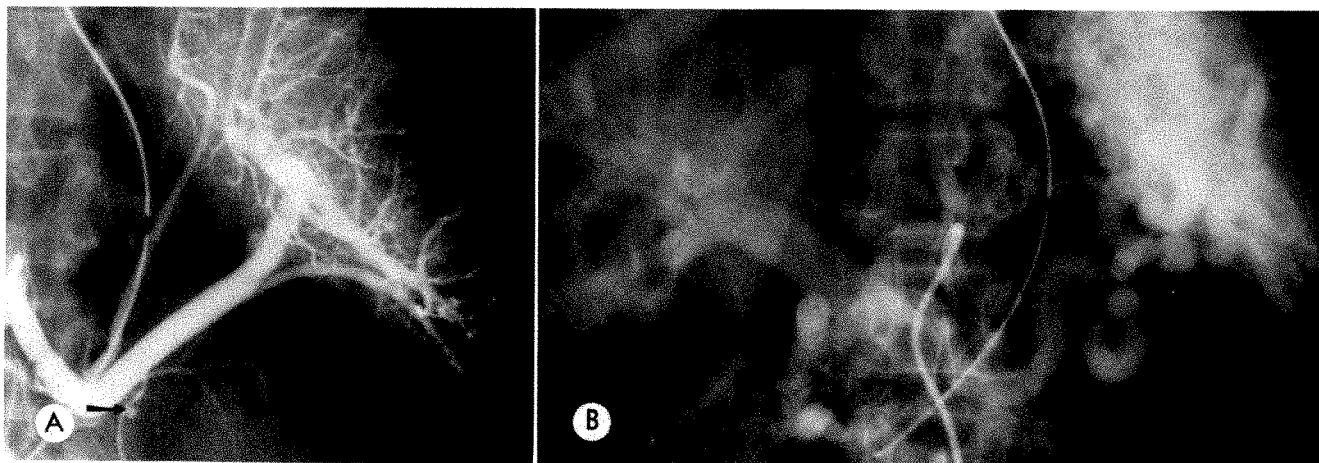


Fig. 4.—Splenic arteriogram of 58-year-old male with long history of pancreatitis. A, Arterial phase showing aneurysm (arrow) of transverse pancreatic artery. B, Venous phase showing occlusion of splenic vein.

2. Castleman B: Case records of the Massachusetts General Hospital—case 46262. *N Engl J Med* 262:1334–1338, 1960
3. Rich A, Duff GL: Experimental and pathological studies on the pathogenesis of acute haemorrhagic pancreatitis. *Bull Johns Hopkins Hosp* 58:212–259, 1936
4. Boijesen E, Efsing HO: Aneurysm of the splenic artery. *Acta Radiol* 8:29–41, 1969
5. Ranniger K, Saldino RM: Arteriographic diagnosis of pancreatic lesions. *Radiology* 86:470–474, 1966
6. Ring EJ, Eaton SB Jr, Ferrucci JT, Short WF: Differential diagnosis of pancreatic calcification. *Am J Roentgenol* 117:446–452, 1973
7. Bookstein J, Reuter S, Martel W: Angiographic evaluation of pancreatic carcinoma. *Radiology* 93:757–764, 1969
8. Reuter SR, Redman HC, Joseph RR: Angiographic findings in pancreatitis. *Am J Roentgenol* 107:56–64, 1969
9. Olsson O: Angiography in the diagnosis of duodenal lesions. *Acta Radiol [Diagn]* (Stockh) 12:49–58, 1972
10. Rösch J, Bret J: Arteriography of the pancreas. *Am J Roentgenol* 94:182–193, 1965
11. Nebesar RA, Pollard JJ: A critical evaluation of selective celiac and superior mesenteric angiography in the diagnosis of pancreatic diseases, particularly malignant tumor: facts and "artefacts." *Radiology* 89:1017–1027, 1967
12. Catanzaro FP, Abiri M, Allegra S: Case report—spontaneous rupture of spleen and pleural effusion complicating pancreatitis. *RI Med J* 51:328–329, 1968
13. Boijesen E, Tylan U: Vascular changes in chronic pancreatitis. *Acta Radiol [Diagn]* (Stockh) 12:34–48, 1972
14. Sandblom P: Gastrointestinal hemorrhage through the pancreatic duct. *Ann Surg* 171:61–66, 1970
15. Boijesen E, Gothlin J, Hallbook T, Sandblom P: Preoperative angiographic diagnosis of bleeding aneurysms of abdominal visceral arteries. *Radiology* 93:781–791, 1969
16. Greenstein A, DeMaio E, Nabseth DC: Acute hemorrhage associated with pancreatic pseudocysts. *Surgery* 69:56–62, 1971

Radiologic and Pathologic Characteristics of the WDHA Syndrome

RICHARD PALMER GOLD,¹ THOMAS J. BLACK,¹ HEIDRUN ROTTERDAM,² AND WILLIAM J. CASARELLA¹

A case of a non-beta islet cell tumor of the pancreas that produced the WDHA (watery diarrhea, hypokalemia, and achlorhydria) syndrome is presented. An enlarged body-tail region of the pancreas is demonstrated on transaxial views; multiple fluid-filled loops of small and large bowel are also noted. The angiography of the tumor is similar to other non-beta islet cell lesions consisting of a large hyper-vascular mass with hypertrophied feeding vessels and a persistent, dense capillary stain. The demonstration of elevated levels of vasoactive intestinal polypeptide in both tumor and plasma and the ultrastructural description of endocrine granules may help to explain the pathophysiology in this case.

Introduction

Hormone-secreting islet cell tumors of the pancreas produce a variety of systemic symptoms. The hypoglycemia of insulin-secreting tumors, the Zollinger-Ellison syndrome of gastrin-secreting lesions, and the diabeticlike and occasional cutaneous manifestations of glucagonoma have all been well described. A fourth syndrome associated with non-beta islet cell lesions is the WDHA or "pancreatic cholera" syndrome. This entity consists of profuse watery diarrhea (WD), severe hypokalemia (H), and hypochlorhydria or histamine-fast achlorhydria (A) and is produced by a pancreatic tumor secreting an as yet unidentified hormone. The possibility that tumors other than pancreatic may secrete this hormone and that vasoactive intestinal polypeptide is responsible has recently been discussed [1].

The hormonally active tumors of the pancreas have recently been recognized as APUDomas [2] or tumors originating from cells derived from the neural crest and whose prime function is the production of polypeptide hormones. The APUD cells share the cytochemical properties of high amine precursor uptake (APU) and high levels of alpha-glycerophosphate dehydrogenase (D). These cells include endocrine cells in the pituitary, pancreatic islets, stomach, duodenum, small intestine, adrenal medulla, lung, urogenital tract, and carotid body.

This paper reports the radiologic and pathologic findings in a WDHA tumor as well as a discussion of the syndrome.

Case Report

A 45-year-old white male was admitted to Columbia-Presbyterian Medical Center in September 1973 for evaluation of 6 months of diarrhea accompanied by a 30 pound weight loss. The diarrhea was watery, nonbloody, and severe enough to have prompted three hospitalizations at other institutions for correction of severe dehydration. Previous evaluations included upper GI series, small intestinal studies, barium enema, proctoscopy, stool cultures and guaiacs, D-xylose excretion, urinary 5-HIAA determinations, and serum gastrin levels; all were reported as normal.

Multiple serum K^+ values measured during this 6-month period were always below 3.0 mg/100 ml. Therapeutic regimens including antibiotics and lactose- and gluten-free diets had no effect. Steroids (prednisone, 20–30 mg daily for 30 months) decreased the frequency of diarrheal stools somewhat.

Physical examination on admission was noncontributory except for diminished skin turgor. Laboratory data included: Ca^{++} , 9.5 mg/100 ml; PO_4 , 3.0; Na^+ , 142; Cl^- , 84; and K^+ , 2.0. Glucose, bacterial agglutinins, folate, and B_{12} levels were normal. A jejunal biopsy was interpreted as normal. Basal gastric acid secretion was 0.12 mg/hr (normal, 1.3 ± 1.6) and histamine-stimulated gastric acid secretion was 5.02 mg/hr (normal, 21.6 ± 13.8). The transaxial view of the pancreas [3] (fig. 1) obtained at the time of upper GI series showed a mass 7 cm in diameter in the body-tail region. Plain films of the abdomen showed large amounts of fluid throughout the large and small intestines (fig. 2).

Abdominal angiography (fig. 3) including selective celiac, splenic, and superior mesenteric artery injections revealed an extremely vascular 8–9 cm mass occupying the entire tail of the pancreas and invading the splenic hilus. Blood supplying the tumor came from an enlarged splenic artery and hypertrophied dorsal pancreatic, pancreatic magna, and inferior polar splenic branches. There were innumerable fine, irregular neovessels with tiny microaneurysms throughout the mass. The tumor stain was intense and persisted 17 sec. The splenic vein was obstructed, resulting in a massive, tortuous collateral network which drained through the coronary and gastropiploic veins. There was no evidence of hyperemia of the gastric wall or of arteriovenous shunting.

At surgery a $7 \times 5 \times 3$ cm tumor was found in the tail of the pancreas with extension to peripancreatic fat, spleen, and anterior surface of the left adrenal gland. The tumor, distal pancreas, and spleen were resected. Microscopic examination showed a tumor composed of trabeculae of large polygonal cells with abundant acidophilic cytoplasm. Each trabeculum was surrounded by prominent thin-walled blood vessels (fig. 4). Special stains for argentaffine granules (characteristic of carcinoids) and alpha and beta granules (characteristic of glucagon- and insulin-producing islet cells, respectively) were negative. Histologic diagnosis was non-beta islet cell carcinoma.

The patient did well postoperatively, but 14 months after his original surgery he noticed easy fatigability and a 7 pound weight loss but no recurrence of altered bowel function. He was admitted for reevaluation. All studies were normal except for iron deficiency anemia with guaiac-positive stools. Barium enema (fig. 5) revealed a 4 cm defect at the anatomic splenic flexure. This was thought to represent either metastasis or direct extension of a recurrent tumor mass and was probably responsible for the gastrointestinal blood loss. Repeat abdominal arteriography showed recurrent tumor in the pancreatic bed and in the base of the mesentery.

In January 1975, a second exploration revealed a $9 \times 7 \times 5$ cm retroperitoneal mass invading portions of stomach, small intestine, descending colon, left kidney, left adrenal gland, and omentum by direct extension. In addition, metastatic tumor was present in mesenteric lymph nodes and the omentum. Microscopic examina-

¹ Department of Radiology, Columbia-Presbyterian Medical Center, 622 West 168th Street, New York, New York 10032. Address reprint requests to R. P. Gold.

² Department of Pathology, Columbia-Presbyterian Medical Center, 622 West 168th Street, New York, New York 10032.

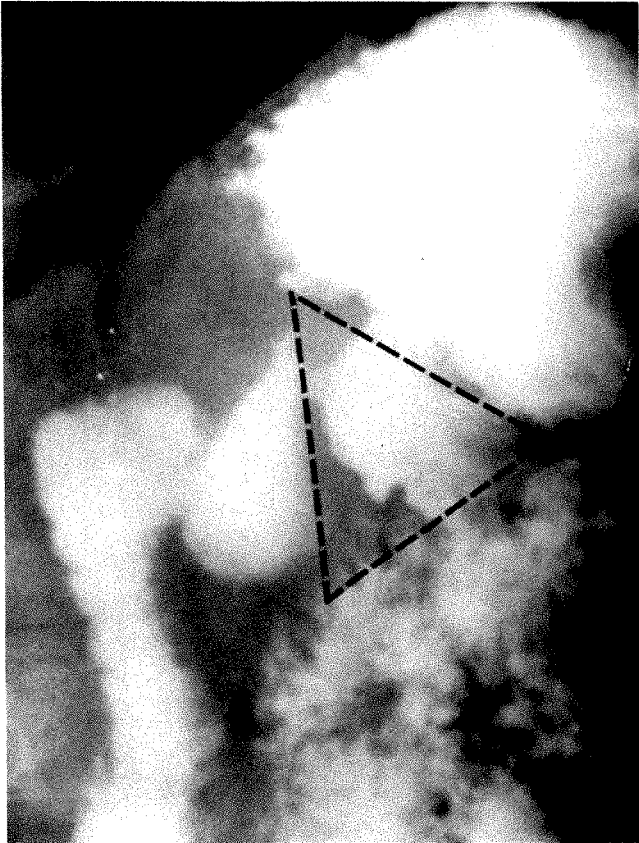


Fig. 1.—Transaxial pancreatic view showing enlargement of body-tail space. Triangular area bounded by posterior wall of stomach; line drawn across top of ligament of Treitz and one parallel to fourth part of the duodenum should not accommodate a circle greater than 3.5 cm in diameter.

tion showed a tumor identical to the previous one (fig. 6). Special stains for identification of argentaffine granules and alpha and beta granules were negative. Histologic diagnosis was recurrent non-beta islet cell carcinoma.

Electron microscopic examination showed closely apposed polygonal tumor cells with abundant cytoplasm containing large numbers of oval and elongated mitochondria, short and slightly distended cisternae of rough- and smooth-surfaced endoplasmic reticulum, few free ribosomes, a prominent Golgi apparatus, and few but distinct endocrine granules (fig. 7). These granules were of uniform size and appearance and were approximately 150 m μ in diameter. They were composed of an electron-dense core surrounded by a narrow clear zone and a thin outer membrane. These features differentiate them from alpha, beta, or delta granules as well as from the enterochromaffine granules of carcinoid tumors.

Snap-frozen tumor tissue and 1 day-postoperative frozen plasma were sent to S. I. Said (University of Texas Southwestern Medical School) who performed radioimmunoassay for vasoactive intestinal polypeptide on the samples. Tumor tissue contained 43 and 72 ng of the polypeptide per gram wet weight at two separate determinations. Plasma contained 3,200 and 4,600 pg/ml at two separate determinations (normal, 0–200 pg/ml).

Discussion

The current case report exemplifies many of the clinical features shared by the documented cases of pancreatic non-beta islet cell tumors that produce the WDHA syndrome

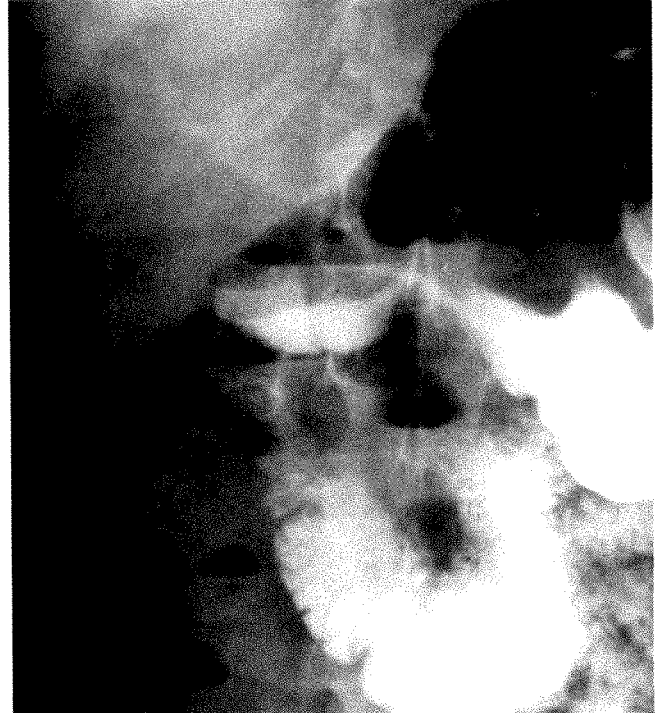


Fig. 2.—Erect view of abdomen after upper GI series showing myriad of air-fluid levels through small bowel and colon. Fluid accumulation due to overproduction stimulated by tumor-elaborated substance.

[4–7]. Unique features of this case include preoperative identification and localization of tumor by angiography, demonstration of a tumor-elaborated secretagogue, and the first instance of ultrastructural characterization of endocrine granules in a vasoactive intestinal polypeptide-producing tumor.

As previously mentioned, the characteristic features of the WDHA syndrome are watery diarrhea, hypokalemia, and achlorhydria associated with a pancreatic islet cell tumor [8, 9]. A common profile would be a middle-aged patient (average age, 47; range, 19–67), usually female (about two-thirds of cases), who presents with recurrent or persistent watery diarrhea of sudden or gradual onset [7]. Multiple hospitalizations are generally required to correct dehydration and electrolyte imbalance during the average 2 yr symptomatic interval prior to diagnosis. Typically the metabolic derangement is refractory even to rigorous intravenous replacement. Acute episodes frequently are accompanied by daily diarrheal fluid losses of as much as 5 liters which contain up to 20 times the daily normal stool content of K⁺.

The metabolic derangement includes hypokalemia secondary to excessive loss in voluminous stools [10] and basal achlorhydria [11, 12], although gastric mucosal biopsies have been normal with normal parietal cell mass [11]. Therefore, suppression of parietal cell function perhaps by a tumor-produced substance probably accounts for the achlorhydria. Metabolic acidosis occasionally is seen during the acute exacerbations and is attributed to excessive HCO₃[−] loss in the diarrheal stools and to renal

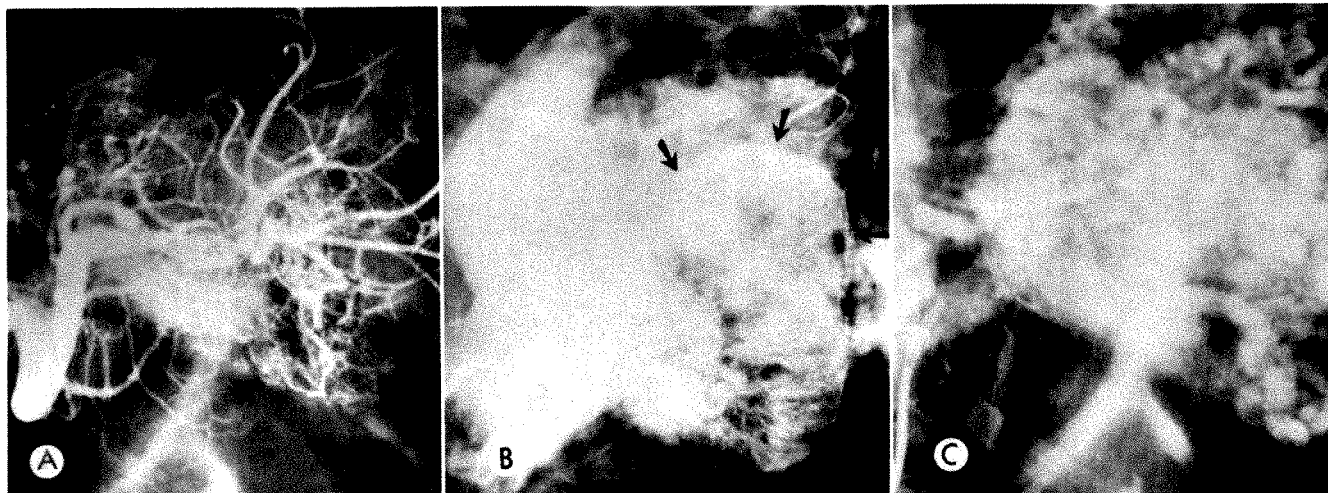


Fig. 3.—Abdominal angiography. *A*, Early arterial phase from selective splenic artery injection illustrating large hypervascular mass occupying entire pancreatic tail and extending to splenic hilus. Tangle of neovascularity and microaneurysms outline size of lesion. *B*, Capillary phase showing dense blush of tumor mass and sharply defined edges. Mass (arrows) in pancreatic tail—splenic hilum region. *C*, Venous phase showing splenic vein obstruction with racemose tangle of collateral veins draining through coronary vein and gastroepiploic veins back to portal system.

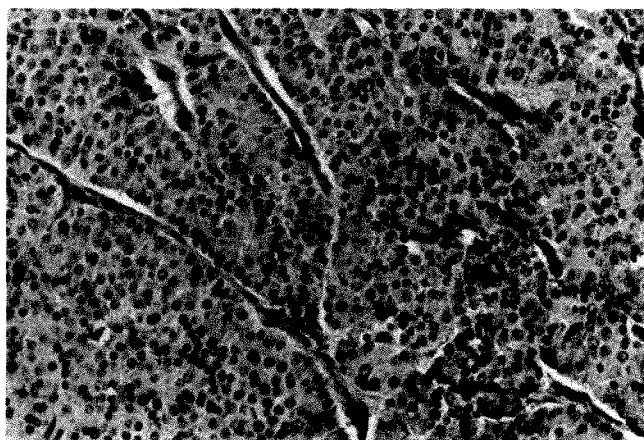


Fig. 4.—Photomicrograph ($\times 240$) of non-beta islet cell tumor. Note endocrine pattern: septa with prominent vessels surround solid nests and cords of tumor cells.

tubular dysfunction secondary to hypokalemia. Less constant features include hypercalcemia [6] and diabetic glucose tolerance tests presumably secondary to hypokalemia [10, 13].

Early demonstration of these tumors by routine radiologic procedures is hindered in about 80% of cases by their location in the body-tail region of the pancreas [13]. The transaxial pancreatic view was helpful in the current case in demonstrating the tumor mass and should be obtained if pancreatic neoplasm is suspected. Other findings are nonspecific and include minimal nonobstructive dilatation of small and large bowel as noted in occasional cases [7] and nonobstructive distension of the gallbladder as documented in about 10% of cases. Both of these features are felt to represent physiological effects of tumor secretagogue.

Although the arteriography of tumors of the islets of Langerhans has been recorded for slightly over a decade [14], only two previous reports of the angiographic demon-

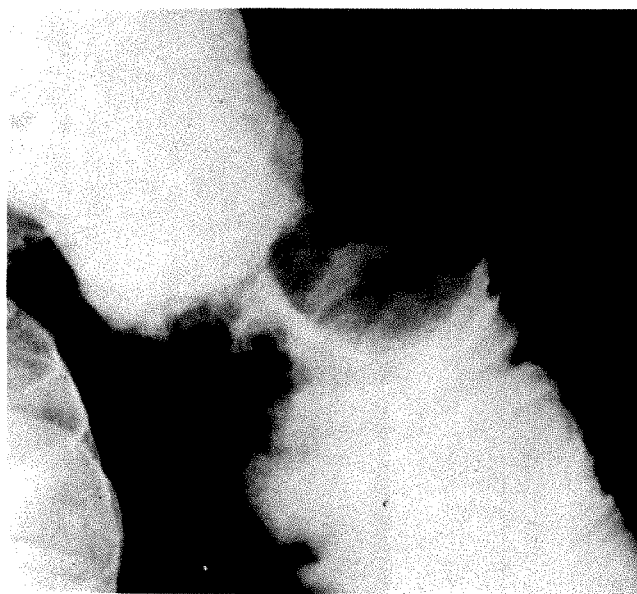


Fig. 5.—Barium enema examination 1½ years after original surgery showing invasion of splenic flexure by recurrent tumor mass.

stration of islet cell tumors that cause the WDHA syndrome have been documented. Comparison of the findings in these and the current case with those in other islet cell tumors illustrates many similarities and some differences.

Most reported series record experience with tumors of beta cell origin largely because of their statistical preponderance. Numerous investigators have claimed insulinoma detection success rates (benign or malignant) ranging from 38% to 100% [15] on the basis of the tendency of these growths to accumulate contrast material in a dense, homogeneous, persistent fashion. Size of lesions discovered by arteriography has ranged from 4 mm to 11 cm [16]. The usual characteristics include: enlarged, tortuous feeding arteries; an early, fine reticular network of normal-appearing

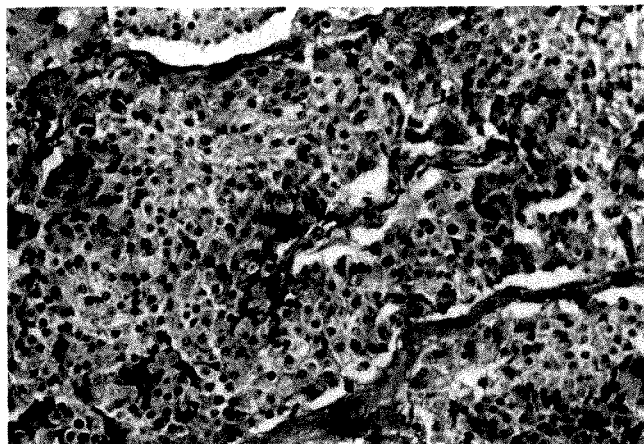


Fig. 6.—Photomicrograph ($\times 240$) of recurrent non-beta islet cell tumor. Note similar appearance to tumor previously resected.

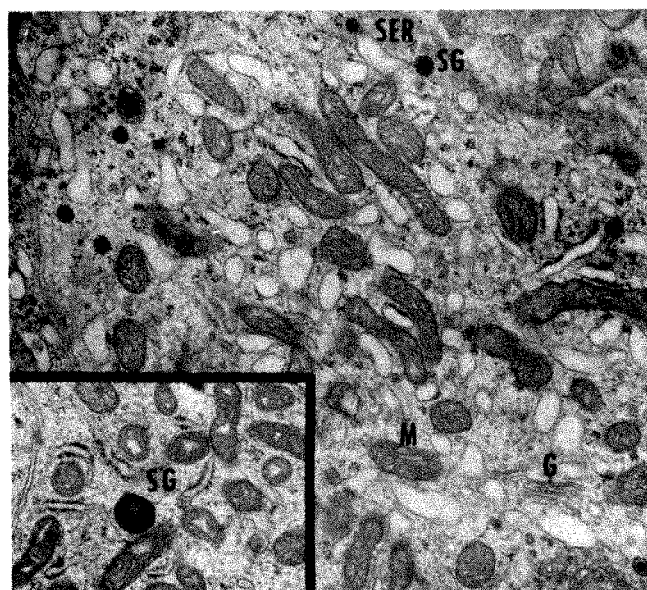


Fig. 7.—Electron micrograph ($\times 22,250$; inset $\times 27,000$) of portion of tumor cell from lesion. Cytoplasm contains numerous mitochondria (M) and prominent Golgi apparatus (G). A few immature secreting granules (SG) seen in close proximity to smooth endoplasmic reticulum (SER). Inset shows mature secretory granule (SG).

arteries; a dense, well defined capillary stain persisting up to 20 sec; and no vascular shunting, encased vessels, or neovasculture.

Considerably less has appeared in the radiologic literature regarding the angiographic findings in gastrin-secreting tumors associated with the Zollinger-Ellison syndrome. Published reports indicate rather large tumor size (2.5–10 cm diameter) at the time of angiographic detection [17, 18]. The description of hypervascular masses with persistent stain and "rich capillary network" is similar to beta cell tumors. No "tumor vessels," encased vessels, or "neo-vessels" have been described in connection with gastrin-producing tumors. Assessment of malignancy has been based on occlusion of the splenic vein and splenic artery branches in one case and vascular metastases in the liver in two others.

Only one alpha cell tumor that produced glucagon has been reported [19]. Angiographic details are scant but a "hypervascular stain" in the tail of the pancreas with liver metastases was described. Both histochemical and electron microscopic analysis revealed the cells to be alpha type, and radioactive immunoassay confirmed high levels of glucagon both in the tumor and serum.

One case of WDHA syndrome from France was described in 1966 [20] in which a 48 g well differentiated islet cell carcinoma was resected from the pancreas. Arteriography revealed hypertrophied hepatic and gastroduodenal arteries, large pancreatic arcades, a hypervascular mass containing neovasculture, pooling of contrast, no early veins, and a "quick-clearing stain." No specific secretagogue was identified. In a case reported in 1972 from Scandinavia [21] a "lemon-sized" highly vascular tumor was described in the head of the pancreas with numerous tortuous vessels and arteriovenous shunting as manifested by "early filling of wide-draining veins." Symptoms of the WDHA syndrome disappeared upon resection. Extract from the mass had a "pancreatic stimulating effect" but no further characterization was noted.

It would seem that the major angiographic difference between the beta and non-beta cell tumors of the pancreas is one related to size. This may in turn be due to the well known delay in diagnosis of the syndromes produced by these non-beta lesions. Large hypervascular masses supplied by dilated, tortuous vessels with a prominent and persistent capillary stain are characteristic. The description of neovasculture and even arteriovenous shunting in these tumors and not in "insulinomas" is also probably related to size.

Hormones implicated in the pathogenesis of the WDHA syndrome include secretin [22], gastrin and glucagon [23], gastric inhibitory peptide [24], and vasoactive intestinal polypeptide [25, 26]. Vasoactive intestinal polypeptide, demonstrated to be present at high levels in the recurrent tumor and at elevated levels in the plasma of our patient, was first isolated from the small intestine of the hog [27]. It is chemically related to secretin and glucagon [27, 28] and exhibits a wide range of biologic actions including vasodilatation (systemic and pulmonary), suppression of gastric secretion, secretinlike stimulation of the pancreas, increased bile flow, relaxation of the gallbladder, stimulation of secretion and motility of the small intestine, relaxation of the large intestine, and increased glycogenolysis.

Vasoactive intestinal polypeptide was recently found in plasma and pancreatic tumors of four patients with the WDHA syndrome, in the plasma and pancreas of one patient with islet cell hyperplasia, and in the plasma and tumor of one patient with a retroperitoneal ganglioneuroblastoma [25].

The biologic actions of vasoactive intestinal polypeptide can explain the presenting symptoms of this patient in 1973. The absence of these symptoms in 1975 when a tumor mass larger than the original one was found is puzzling. It is possible that the recurrent tumor was less differentiated than the original one and partially lost the ability to produce large enough quantities of polypeptide to produce the

WDHA syndrome. Although histologically the degree of differentiation appeared to be the same in both tumors, this hypothesis is supported only by the paucity of endocrine granules seen in the electron microscope. Apparently there was enough polypeptide to produce a positive radio-immunoassay but not enough to cause symptoms, if indeed the polypeptide is etiologic. A comparison of ultra-structure and hormonal content of the original tumor and the recurrent one would have been of great value in understanding the biology of this tumor. Unfortunately, no fresh tissue was saved at the time of the first operation.

The prognosis for our patient is guarded at best. His tumor was biologically malignant from the outset as has been noted in about 50% of islet cell tumors that produce the WDHA syndrome [29]. Of the remaining pancreatic lesions associated with the syndrome, approximately 80% will be adenomas and 20% islet cell hyperplasia [11]. The mean survival following surgical resection of the malignant lesions has been 14 months; most patients have demonstrable metastases at the time of operation.

REFERENCES

1. Said SI, Faloona GR: Elevated plasma and tissue levels of vasoactive intestinal polypeptide in the watery-diarrhea syndrome due to pancreatic, bronchogenic and other tumors. *N Engl J Med* 293:155-160, 1975
2. Pearse AGE: The APUD cell concept and its implications in pathology. *Pathol Annu* 9:27-42, 1974
3. Sorabella PA, Campbell WL, Seaman WB: The axial pancreatic view: a new approach for recognizing enlargement of the body and tail of the pancreas. *Radiology* 111:535-542, 1974
4. Charles B, Cochrane WA: Islet cell tumor of the pancreas with chronic diarrhea and hypokalemia—a recently recognized syndrome. *Can Med Assoc J* 82:579-585, 1960
5. Gjone E, Fretheim B, Nordoy A, Jacobsen CD, Elgjo K: Intractable watery diarrhea, hypokalemia and achlorhydria associated with pancreatic tumor containing gastric secretory inhibitor. *Scand J Gastroenterol* 5:401-408, 1970
6. Kofstad J, Froyshov I, Gjone E, Bix S S: Pancreatic tumor with intractable watery diarrhea, hypokalemia and hypercalcemia: electrolyte balance studies. *Scand J Gastroenterol* 2:246-250, 1967
7. Stoker DJ, Wynn V: Pancreatic islet cell tumor with watery diarrhea and hypokalemia. *Gut* 11:911-920, 1970
8. Hindle W, McBrien DJ, Creamer G: Watery diarrhea and an islet cell tumor. *Gut* 5:359-362, 1964
9. Marks IN, Bank S, Louw JH: Islet cell tumor of the pancreas with reversible watery diarrhea and achlorhydria. *Gastroenterology* 52:695-708, 1967
10. Epiner EA, Beaven DW: Non-specific islet-cell tumor of the pancreas with diarrhea. *Q J Med* 31:447-471, 1962
11. Schein PS, DeLellis RA, Kahn CR, Gorden P, Kraft AR: Islet cell tumors: current concepts and management. *Ann Intern Med* 79:239-257, 1973
12. Matsumoto KK, Peter JB, Schulze RG, Hakim AA, Franck PT: Watery diarrhea and hypokalemia associated with pancreatic islet cell adenoma. *Gastroenterology* 50:231-242, 1966
13. Kraft AR, Tompkins RK, Zollinger RM: Recognition and management of the diarrheal syndrome caused by nonbeta islet cell tumours of the pancreas. *Am J Surg* 119:163-170, 1970
14. Bookstein JJ, Oberman HA: Selective angiography in islet cell tumors of the pancreas. *Radiology* 86:682-685, 1966
15. Robins JM, Bookstein JJ, Oberman HA, Fajans SS: Selective angiography in localizing islet cell tumors of the pancreas. *Radiology* 106:525-528, 1973
16. Kott I, Urca I, Kott E, Garti I: Preoperative localization an insulinoma by angiography. *Isr J Med Sci* 6:655-657, 1970
17. Clemett MD, Park WM: Angiographic demonstration of pancreatic tumors in the Zollinger-Ellison syndrome. *Radiology* 88:32-34, 1967
18. Mortiz M, Kahn P, Callow AD, Levitan R: Unusual clinical and angiographic findings in ZE syndrome. *Ann Intern Med* 71:1133-1140, 1969
19. McGavran MH, Unger RH, Recant L, Polk HC, Kilo C, Levin ME: A glucagon secreting alpha cell carcinoma of the pancreas. *N Engl J Med* 274:1408-1413, 1966
20. Goulon M, Rapin M: WDHA syndrome with a non beta islet cell tumor. *Presse Med* 74:2345-2349, 1966
21. Anderson H, Dotevall G, Fagerberg G, Raotma H, Walan A, Zederfeldt B: Pancreatic tumor with diarrhea, hypokalemia and hypochlorhydria. *Acta Chir Scand* 138:102-107, 1972
22. Zollinger RM, Tompkins RK, Amerson JR, Endahl GL, Kraft AR, Moore FT: Identification of the diarrheogenic hormone associated with non-beta islet cell tumors of the pancreas. *Ann Surg* 168:502-521, 1968
23. Barbexat GO, Grossman MI: Cholera-like diarrhea induced by glucagon plus gastrin. *Lancet* 1:1025-1026, 1971
24. Elias E, Polak JM, Bloom SR, Pearse AGE, Welbourn RB, Booth CC, Kuzio M, Brown JC: Pancreatic cholera due to production of gastric inhibitory polypeptide. *Lancet* 2:791-793, 1972
25. Bloom SR, Polak JM, Pearse AGE: Vasoactive intestinal peptide and watery-diarrhea syndrome. *Lancet* 2:14-16, 1973
26. Schwartz CJ, Kimberg DV, Sheerin HB, Field M, Said SI: Vasoactive intestinal peptide stimulation of adenylate cyclase and active electrolyte secretion in intestinal mucosa. *J Clin Invest* 54:536-544, 1974
27. Said SI, Mutt V: Polypeptide with broad biological activity from small intestine. *Science* 169:1217-1218, 1970
28. Said SI, Mutt V: Isolation from porcine-intestinal wall of a vasoactive octapeptide related to secretin and to glucagon. *Eur J Biochem* 28:199-204, 1972
29. Edmeads JG, Mathews RE, McPhedran NT, Ezrin C: Diarrhea caused by pancreatic islet cell tumours. *Can Med Assoc J* 86:847-851, 1962

Fine Needle Transhepatic Cholangiography: A New Approach to Obstructive Jaundice

JOSEPH T. FERRUCCI, JR.,¹ JACK WITTENBERG, ROBERT A. SARNO, AND JACK R. DREYFUSS

Transhepatic cholangiography performed with a newly introduced fine caliber (0.7 mm OD) "Chiba" needle produces a significantly higher success rate of biliary duct opacification with fewer complications than conventional needle or flexible cannula techniques. Distinct advantages over endoscopic retrograde cholangiography are also apparent, including more frequent bile duct opacification, ease of performance, and lower overall cost. In a group of 50 consecutive patients examined with the fine needle puncture technique, duct opacification was achieved in 92%, including 33 of 33 (100%) of patients with surgically obstructed ducts and 14 of 17 (82%) with normal caliber or narrowed ducts. Fine needle hepatic puncture is recommended as the preferred approach for direct biliary duct opacification in jaundiced patients.

Recent reports indicate that transhepatic cholangiography performed with a newly introduced fine caliber needle (developed at Chiba University, Chiba, Japan) may achieve successful duct opacification with an extremely high degree of frequency and safety [1, 2]. The advantages of the technique over conventional transhepatic cholangiography and endoscopic retrograde cholangiography have already been recognized by clinical hepatologists [2, 3] but have not yet been documented in the radiologic literature. The purpose of this report is to record the favorable results obtained in the initial 50 patients undergoing fine needle transhepatic cholangiography at the Massachusetts General Hospital and to consider the possible implications of this method of biliary duct puncture in the evaluation and management of cholestatic jaundice.

Subjects and Methods

The patient material consists of the first 50 consecutive cases examined by the fine needle technique of percutaneous transhepatic cholangiography in the Department of Radiology at the Massachusetts General Hospital between June 1975 and June 1976. Patients ranged in age from 6 weeks to 83 years. In order to document the technical simplicity of the method, all examinations were performed by radiology residents or fellows under the supervision of attending staff radiologists.

Indications for the procedure included the following: evaluation of obstructive jaundice, 27 cases; incomplete or unsuccessful endoscopic retrograde cholangiograms, 13 cases; and complications of prior biliary-enteric surgical anastomoses in which the anatomic reconstruction precluded the use of endoscopic retrograde cholangiography, 10 cases. Follow-up was obtained on all cases by close monitoring of the clinical course after the examination and review of the intraabdominal findings in all operated cases.

All examinations were performed with the fine caliber needle employed by Okuda et al. [1]. This is a thin-walled flexible steel

needle of very small caliber, 22 gauge (0.5 mm ID, 0.7 mm OD), measuring 15 cm in length. It is available commercially (Cook, Inc., and Becton-Dickenson Co.). The tip is fashioned with a short 30° noncutting bevel, and an inner-fitted stylet is provided. (For purposes of comparison, it should be noted that the conventional 18 gauge flexible Teflon sheath assembly has an outside diameter of 1.3 mm.)

Technique

After confirmation of satisfactory bleeding parameters, the patient is premedicated on arrival in the fluoroscopy suite with 2.5 mg diazepam (Valium) intravenously (Roche). A puncture site is chosen in the eighth or ninth intercostal space in the right midaxillary line on the basis of clinical and fluoroscopic evaluation of hepatic size and configuration. The lateral approach is selected because a longer needle tract is created through the liver substance which promotes tamponade of subsequent bleeding or bile leakage from the interior of the liver.

Following sterile preparation of the puncture site and administration of 1% Xylocaine anesthesia locally, the needle and stylet are introduced in a single rapid thrust during a brief period of end-expiratory apnea. The needle is directed 30° cephalad, is passed in a plane horizontal to the table top slightly above the confluence of the main intrahepatic ducts, and the needle tip is deposited just to the right of the twelfth thoracic vertebral body. The stylet is withdrawn, and a syringe containing contrast material (usually 30% methylglucamine) is attached. Shallow respirations are resumed.

Under fluoroscopic control, the needle is slowly withdrawn in several millimeter increments with intermittent injections of 1.0–2.0 ml of contrast material under fluoroscopic observation. Recognition of the site of contrast material deposition is readily made fluoroscopically: contrast within the hepatic parenchyma persists in an amorphous accumulation; contrast within hepatic venous channels or lymphatics flows rapidly towards the right atrium or shows rapid opacification and clearing of a stellate network of vascular channels; and contrast within bile ducts flows more slowly in a hepatofugal fashion, persisting for prolonged periods in the presence of common duct obstruction.

When dilated ducts are identified, contrast material is judiciously injected in amounts sufficient to establish a diagnosis. No attempt is made to aspirate bile initially, and undue distention of the duct system is carefully avoided. Multiple fluoroscopic and overhead radiographs are then made in various positions. Semierect views are of critical importance in the presence of biliary obstruction to promote

Received February 6, 1976; accepted after revision April 8, 1976.

All authors: Department of Radiology, Massachusetts General Hospital and Harvard Medical School, Boston, Massachusetts 02114.



Fig. 1.—Fine needle cholangiogram in patient with biliary cirrhosis showing diffuse sclerosis of intrahepatic biliary radicles. Needle positioned in duct measuring 3.0 mm in diameter.

TABLE 1
Results of Fine Needle Transhepatic Cholangiography

	No. Patients	Opacification of Ducts	
		No.	%
Dilated	33	33	100
Not dilated	17	14	82
Total	50	46	92

the flow of contrast distally. At the conclusion of the procedure, aspiration of bile and contrast material is attempted for decompression, although this is not always successful. If the ductal system is not punctured on the initial attempt, further passes are made by directing the needle more posteriorly and then more anteriorly up to a maximum of six attempts.

After the procedure, a chest radiograph is obtained to exclude pneumothorax, and the patient is returned to the ward with instructions for monitoring of vital signs and institution of intravenous fluids. If biliary obstruction has been demonstrated, parenteral antibiotics are administered and timely surgical exploration performed.

Results and Discussion

The results in this series are presented in table 1. Duct opacification was successful in 33 of 33 patients (100%) with duct dilatation caused by mechanical obstruction. Of these, 19 patients had neoplastic obstruction, nine had benign strictures, and five had common duct calculi. Patent nondilated ducts of normal or small caliber were opacified in 14 of 17 patients (82%). Of these, six had intrahepatic duct sclerosis of varying etiologies (fig. 1).

TABLE 2
Success Rates of Conventional and Fine Needle Transhepatic Cholangiography

Technique and Reference	Overall		Dilated		Not Dilated	
	No.	%	No.	%	No.	%
Conventional:						
Evans [4]	150/200	75	...	92	...	50
Hines et al. [5]	80/102	78	68/73	93	7/23	30
Fine needle:						
Okuda et al. [1]	268/314	85	95/95	100	54/80	67
Redeker et al. [2]	32/40	80	20/20	100	12/20	60
Present report	46/50	92	33/33	100	14/17	82

TABLE 3
Comparative Features of Direct Cholangiography

Feature	Endoscopic Retrograde Cholangiography	Fine Needle Transhepatic Cholangiography
Success Rate of bile duct opacification (%)	70	90
Time required (min)	90	45
Total cost (\$)	400	100
Operator skill required	Considerable	Modest
Complications:		
Bacteremia (%)	1–2	5–10
Other

It is noteworthy that the 92% overall success rate of duct opacification was achieved by 18 different resident physicians who necessarily were inexperienced with the method, thus attesting to its simplicity and reliability. A mean of three passes per study was required for successful duct entry.

Our results (table 2) confirm and extend the high overall success rate of duct puncture (both dilated and nondilated) using the fine needle technique [1, 2] and clearly exceed the 75%–78% frequency of duct visualization reported using conventional 18–20 gauge needle techniques [4–6]. Remarkably, our results also confirm the 100% success rate of fine needle puncture in the presence of biliary obstruction previously reported by Okuda et al. [1] in 95 patients with malignant bile duct obstruction and by Redeker et al. [2] in 20 patients with biliary tract obstruction of various causes.

The cumulative 100% success rate in 152 patients with mechanical obstruction suggests that failure of opacification excludes a surgical cause of cholestasis with much greater confidence than nonopacification using conventional techniques [4]. In addition, successful puncture of normal or sclerosed ducts in 14 of 17 cases (82%) confirms the 60%–70% success rate of normal duct visualization in prior reports of fine needle puncture [1, 2]. Again, the 30%–50% success rate obtained with large needle methods [4–6] is exceeded by a considerable margin.

Two representative cases of duct opacification in the presence of severe sclerosis of intrahepatic radicles are

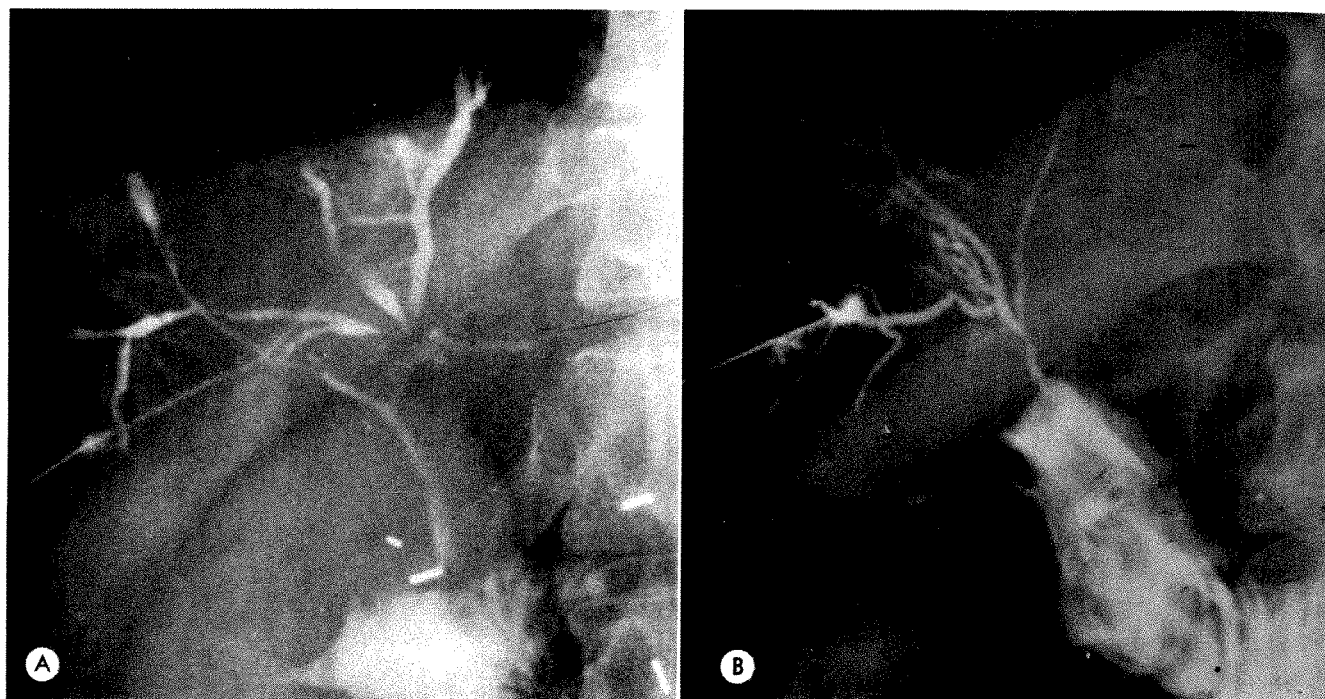


Fig. 2.—Representative examples of successful fine needle puncture of narrowed intrahepatic ducts. A, Sclerosing ascending cholangitis following choledochojunostomy (Whipple procedure). B, Sclerosing ascending cholangitis following hepatojejunostomy. Note small caliber ducts punctured by fine needle.

shown in figure 2. Four patients in the series failed to opacify: two were subsequently shown by intravenous cholangiography to have patent small caliber intrahepatic ducts, a third was a cirrhotic with fatty infiltration on liver biopsy, and the fourth a neonate with complete intrahepatic biliary atresia. Testimony to the clinical acceptance of the method in our institution is given by the accumulation of 50 cases within 12 months after introduction of the fine needle technique. Only six patients were referred for conventional percutaneous transhepatic cholangiography in the preceding 24 months.

Complications occurred in 5 of 50 patients (10.0%). They consisted of one small pneumothorax and four instances of bacteremia with transient fever and hypotension. In these four patients, obstructed bile ducts with complex radiographic abnormalities required generous volumes of contrast material to obtain complete delineation of the anatomy. There was no instance of clinically significant bile leakage or hemorrhage.

A comparable complication rate of 7.9% (no fatalities) was recorded in the 314 cases of Okuda et al. [1]. Again, bacteremia was the most common adverse effect, occurring in 3.5% of cases. Bile leakage and hemorrhage occurred in 1%–2%. While obstructive dilatation of the ducts increases complications of all types, regardless of puncture technique [4], conventional large needle techniques with or without a flexible cannula have generally been more hazardous. Reported complication rates range up to 25% [6] and have frequently required laparotomy for hemorrhage or bile peritonitis.

Because bile cannot be aspirated through the small caliber needle, an injection withdrawal technique must be

used for duct opacification. This explains why bacteremia is the most frequent complication. In the presence of biliary duct obstruction, intraluminal ductal pressures may exceed intrahepatic venous pressure [7]. Further elevation of pressure resulting from introduction of contrast material may create bile-blood fistulae through ductal vascular communications along the needle tract [8]. Since bacterial colonization occurs in up to 50% of cases with common duct obstruction [9], such biliary venous fistulae may result in significant bacterial contamination of the systemic circulation. Hence the introduction of excessive volumes of contrast into an obstructed common bile duct should be assiduously avoided and intravenous antibiotics immediately instituted whenever biliary obstruction is disclosed by this technique.

An additional minor drawback associated with inability to freely aspirate bile through the fine caliber needle is potential misinterpretation of the level of obstruction due to inspissation of thick bile [10]. This occurred in one instance in our series where an impacted distal common duct calculus presented as an obstruction of the contrast column in the mid common duct.

When obstructed ducts are demonstrated by fine needle puncture, prompt operative decompression is carried out to reduce the risk of postprocedure septicemia. The urgency of surgical intervention can be judged from the degree of ductal obstruction. Since the risk of bile leakage is minimized by the small needle tract and the use of an antero-lateral puncture site, immediate postcholangiogram surgery is no longer mandatory unless there is complete bile duct occlusion. With partial obstruction, operation may be performed more electively provided the patient is carefully



Fig. 3.—A and B. Two examples of high grade common bile duct obstruction due to carcinoma of head of pancreas. Cases uneventfully managed by elective laparotomy delayed 6 and 4 days, respectively. No blood or bile detected in abdominal cavity in either case.

monitored and placed under appropriate antibiotic coverage.

In the present series, electively delayed operations (mean 3.5 days) were carried out in 19 patients with biliary duct obstruction. Insignificant amounts of bile staining or clotted blood were seen on the liver surface at surgery. The opportunity to electively schedule the definitive surgical procedure is generally welcomed by the responsible surgeon. Representative examples of high grade common duct obstruction managed by uneventful delayed laparotomy are shown in figure 3.

Alternatively, determinate decompression of dilated ducts with a conventional 18 gauge flexible cannula may be performed using standard percutaneous transhepatic cholangiography techniques [4, 6]. The flexible cannula is readily inserted into a previously opacified biliary radicle under fluoroscopic control and is then externally sutured to the skin, providing therapeutic biliary-cutaneous fistulous drainage of the bile ducts. In some cases this will substantially improve preoperative hepatic function and clotting parameters as well as alleviate subjective complaints of pruritis. In inoperable malignancy, external cannula drainage may provide longer term palliation of obstructive biliary symptoms.

The advantages of fine needle transhepatic cholangiography must be measured in light of competing techniques, particularly endoscopic retrograde cholangiography—a procedure recently in wide use for direct opacification of the biliary tree [11–15] (table 3). Although endoscopic retrograde cholangiography is a reasonably safe procedure with a negligible 1%–2% complication rate [11–15],

exceptional technical proficiency is necessary to consistently produce successful results. Endoscopists possessing the required expertise are often not available in smaller institutions. Even in experienced hands, the maximal rates of bile duct opacification rarely exceed 70% [11–15].

Further, the cannulating fiber optic duodenoscope is a prohibitively expensive instrument. The total dollar cost for perendoscopic retrograde cholangiography at our institution, including the endoscopic, radiologic, and fluoroscopic room charges, exceeds the total charge for fine needle transhepatic cholangiography by 400%. The high puncture rate of dilated ducts, lack of serious complications, and ease of performance confirmed by this study suggest that fine needle transhepatic cholangiography should replace the retrograde technique in jaundiced patients. On the basis of similar considerations and the results of a randomized comparison of the two methods, a similar preference for fine needle transhepatic puncture over the endoscopic approach to cholestatic jaundice has recently been expressed by Elias and co-workers [3]. Experience also suggests that even when nondilated or narrowed ducts are present, the fine needle technique produces a comparable rate of duct visualization with greater ease and lower cost.

Conclusion

Fine needle transhepatic cholangiography provides extremely high rates of ductal opacification with greater ease and a greater margin of safety than conventional transhepatic techniques. Further, despite the recent popularity of endoscopic retrograde cholangiography, direct fine

needle hepatic puncture possesses sufficient advantages that it should be selected for direct cholangiography in jaundiced patients even when both techniques are available.

REFERENCES

1. Okuda K, Tanikawa K, Emura T, Kuratomi S, Urabe K, Sumikoshi T, Kanda Y, Fukuyama Y, Muska H, Mori H, Shimokawa Y, Yakushiji F, Matsuura Y: Nonsurgical percutaneous transhepatic cholangiography: diagnostic significance in medical problems of the liver. *Am J Dig Dis* 19:21-36, 1974
2. Redeker AG, Karvountzis GG, Richman RH, Horisawa M: Percutaneous transhepatic cholangiography: an improved technique. *JAMA* 231:386-387, 1975
3. Elias E, Hamlyn AN, Jain R, Long JA, Summerfield R, Dick R, Sherlock S: A randomized trial of percutaneous transhepatic cholangiography versus endoscopic retrograde cholangiography for bile duct visualization in cholestasis. *Gastroenterology* 69:A-20/820, 1975
4. Evans J: Transhepatic cholangiography, in *Alimentary Tract Roentgenology*, 2d ed, edited by Margulis AR, Burhenne HJ, St. Louis, Mosby, 1973, pp. 1339-1358
5. Hines C, Ferrante WA, Davis WD, Tutton RA: Percutaneous transhepatic cholangiography: experience with 102 procedures. *Am J Dig Dis* 17:868-874, 1972
6. Lang EK: Percutaneous transhepatic cholangiography. *Radiology* 112:283-290, 1974
7. Wechel KL: Percutaneous transhepatic cholangiography: Technique and application. *Acta Chir Scand [Suppl]* 330:1-99, 1967
8. Koch RL, Gorder JL: Bile-blood fistula: a complication of percutaneous transhepatic cholangiography. *Radiology* 93:67-68, 1969
9. Flemma RJ, Schauble JF, Gardner C, Anlyan WG, Capp MP: Percutaneous transhepatic cholangiography in the differential diagnosis of jaundice. *Surg Gynecol Obstet* 116:559-568, 1963
10. Kittredge RD, Baer JW: Percutaneous transhepatic cholangiography: problems in interpretation. *Am J Roentgenol* 125:35-46, 1975
11. Katon RM, Lee TG, Parent JA, Bilbao MK, Smith FW: Endoscopic retrograde cholangiopancreatography (ERCP): experience with 100 cases. *Am J Dig Dis* 19:295-305, 1974
12. Nebel OT, Fornes MF: Endoscopic pancreatocholangiography. *Dig Dis* 18:1042-1050, 1973
13. Robbins AH, Paul RE, Jr, Norton RA, Schimmel EM, Tomas JG, Sugarman HJ: Detection of malignant disease by peroral retrograde pancreatico-biliary ductography. *Am J Roentgenol* 117:432-436, 1973
14. Rohrmann CA, Silvis SE, Vennes JA: Evaluation of the endoscopic pancreatogram. *Radiology* 113:297-304, 1974
15. Bilbao MK, Potter CT, Lee TG, Katon RM: Complications of endoscopic retrograde cholangiopancreatography (ERCP): a study of 10,000 cases. *Gastroenterology* 70:314-320, 1976

Percutaneous Transhepatic Cholangiography with Selective Catheterization of the Common Bile Duct

FLEMMING BURCHARTH¹ AND NIELS NIELBO²

Percutaneous transhepatic cholangiography was performed in 86 patients with jaundice in whom the diagnosis could not be established by conventional means. Selective catheterization of the common bile duct was employed and cholangiograms of high quality were obtained. In cases of obstruction of the biliary passages, the catheter was left indwelling centrally in the biliary passages for external bile drainage. Thus immediate postcholangiogram surgery was not required in these patients.

The procedure was successful in all 60 patients with obstructive jaundice. In 26 patients the possibility of obstruction was ruled out. Complications occurred in four patients but were not exclusively due to the procedure. The incidence of complications may be maintained at an acceptably low level if the technique is meticulously followed.

Routine examinations often fail to reveal the etiology of jaundice. In such cases the diagnosis can be obtained reliably and simply by percutaneous transhepatic cholangiography. Since December 1972 we have carried out 86 procedures using a new technique. Indications for the procedure included: (1) to evaluate obstructive jaundice when other examinations were uninformative (an alternative to exploratory laparotomy); (2) to delineate the anatomy when biliary obstruction was present; and (3) to differentiate between obstructive and nonobstructive jaundice when other examinations failed to do so.

Technique

Percutaneous transhepatic cholangiography is performed using a 27 cm long, smooth polyethylene catheter fitted with a metal mandrin (Wiechel-Stille, 1.00 mm ID/1.45 mm OD; fig. 1). It is introduced under local anesthetic in the right midaxillary line at the level of the twelfth thoracic vertebra. The puncture is carried out under fluoroscopic control with the patient supine. The cannula is inserted horizontally and at a right angle to the sagittal plane to a depth of about 4 cm to the right of the twelfth thoracic vertebra. This point is normally just lateral and cranial to the site of the bifurcation of the common hepatic duct [1, 2].

The metal mandrin is removed; if bile does not appear, the catheter is slowly withdrawn until a bile flow is obtained. If unsuccessful, the procedure is repeated by slightly altering the direction of the cannula without completely withdrawing it from the liver. In case of reflux of bile the contrast medium (60 percent Urografin®) is injected during fluoroscopic control.

When an impression of the biliary tree and the position of the tip of the catheter is obtained, a flexible guidewire

(PE 160) with slightly curved tip is introduced (fig. 1). The guidewire is passed from the punctured peripheral biliary duct into the common bile duct, and the catheter is threaded onto the guidewire, which is subsequently removed. The biliary tree is emptied of bile and filled with contrast.

If a normal biliary tree is demonstrated or if, after five attempts at puncture, the biliary tree has not been demonstrated, the catheter is closed. It is withdrawn several centimeters at a time over a period of 12 hr.

If the cholangiogram demonstrates obstruction of the biliary passages, the catheter is left in the common bile duct to drain bile to a catheter bag. Since the catheter is situated in the common bile duct and further secured with a skin suture, it will not become dislodged from the biliary tree.

If stones were demonstrated, the patient underwent surgery within 24 hr. If stones were not demonstrated, surgery was delayed for several days, allowing time for proper preparation of the patient.

Results

The biliary tree was visualized in 74 of the 86 patients who underwent the procedure; normal bile ducts were demonstrated in 14 of the 74. In all 60 patients suffering from obstruction, the biliary tree and the obstruction were disclosed by the procedure (table 1). Diagnosis was verified at surgery and/or autopsy.

Suspected obstruction was ruled out in 26 patients. Normal bile ducts were demonstrated in 14 patients, and in 12 the biliary tree could not be visualized. The final diagnosis was obtained at surgery or autopsy, by clinical course, or after repeated liver biopsies.

Complications

Four patients had complications after the procedure. Bile leak occurred in one patient with obstructive jaundice after premature withdrawal of the catheter, necessitating immediate surgery. In a cachectic patient who had a large pancreatic cancer with metastases, the catheter was left in place for external drainage. The patient died 23 days later, and the autopsy revealed 4 liters of icteric ascites, possibly related to bile leak.

Two patients had bleeding. Confusion caused one to tear out the catheter soon after the examination. At surgery 24 hr later, 500 ml of blood was found in the peritoneum. The second patient, who had a severe coagulation defect, underwent the examination on an emergency basis

¹ Department of Surgical Gastroenterology, Division S, Gentofte Hospital, University of Copenhagen, DK-2900 Hellerup, Copenhagen, Denmark.

² Department of Radiology, Gentofte Hospital, University of Copenhagen, DK-2900 Hellerup, Copenhagen, Denmark.

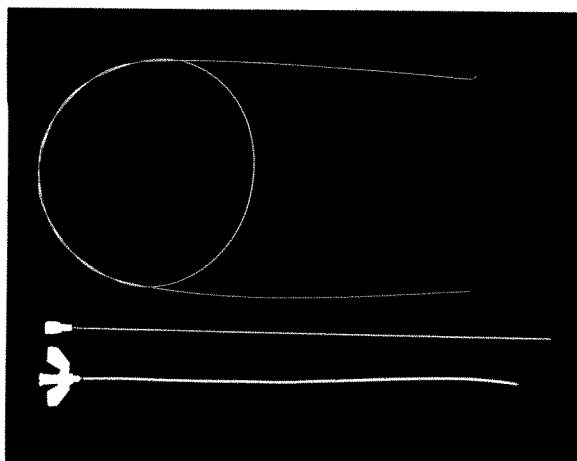


Fig. 1.—Instrument and guidewire used in percutaneous transhepatic cholangiography.

TABLE 1
Results of Percutaneous Transhepatic Cholangiography

	No. Patients	Successful Examinations	
		No.	%
Obstruction	60	60	100
No obstruction	26	14	56
Total	86	74	86

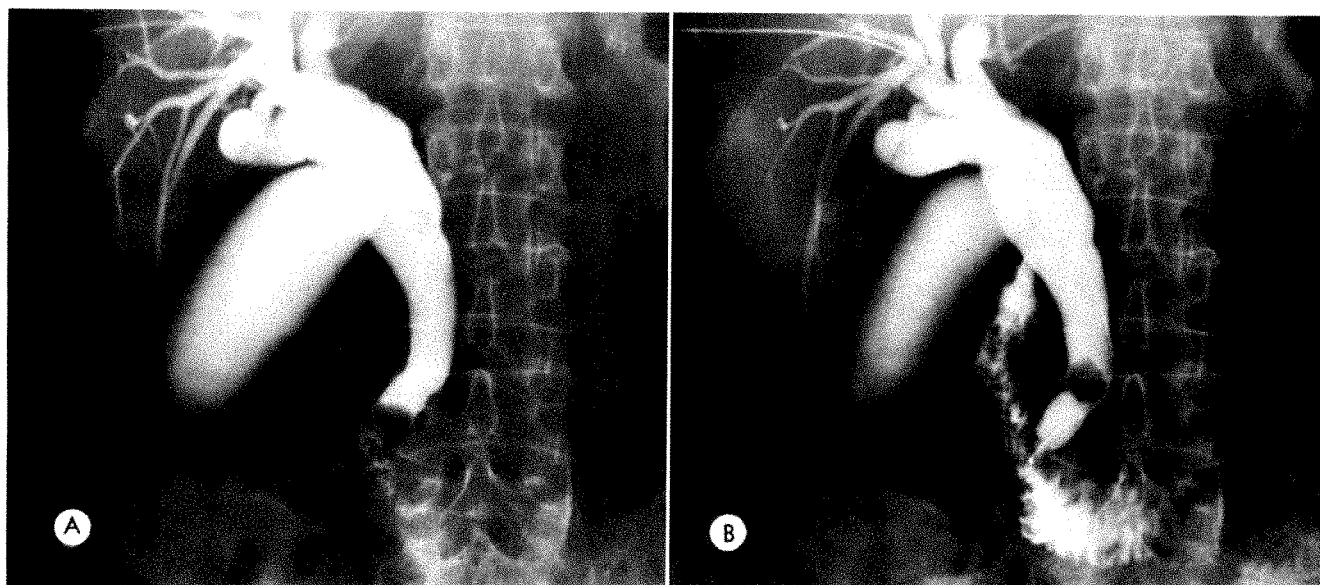


Fig. 2.—A. Distal common bile duct stone with typical stone configuration and moderately dilated biliary tree. B. Passage of catheter beyond stone by guidewire technique. Stone moved upward by guidewire.

because of marked jaundice. The cystic duct was shown to be ligated with the common duct, which had occurred during a total pancreatectomy in which the gallbladder had been used for a biliodigestive anastomosis. The patient died before further surgery; at autopsy 1 liter of blood was found in the peritoneum, possibly caused by the cholangiography.

Discussion

Numerous methods of performing percutaneous transhepatic cholangiography have been described. In nearly all of them a peripheral intrahepatic bile duct is punctured, and, after the contrast injection and x-ray exposures, the puncture instrument is removed. If the biliary passages are obstructed, the patient is operated on immediately after the examination. Our method introduces the catheter from the midaxillary line, thereby avoiding the risk of injury to other

organs. The long puncture canal through the liver substance reduces the risks of bleeding and bile leakage. The chance of entering the bile ducts is also increased since they have greatest extension in the sagittal plane, particularly if dilated [1, 2].

We try to enter a bile duct on the right side of the hilus; in this manner the catheter can be conducted by the guidewire technique to the common duct or close to the obstruction [3]. Consequently good contrast filling of the biliary tree occurs and cholangiograms of high quality are obtained (figs. 2A and 3). It is often possible to move the guidewire and catheter past an obstruction and visualize the biliary tree below the obstruction (figs. 2B and 4). The catheter placed in the common duct is not dislocated from the biliary tree, even if the patient is agitated or coughing.

If successful puncture of a bile duct does not occur on first attempt, the direction of the cannula is altered without

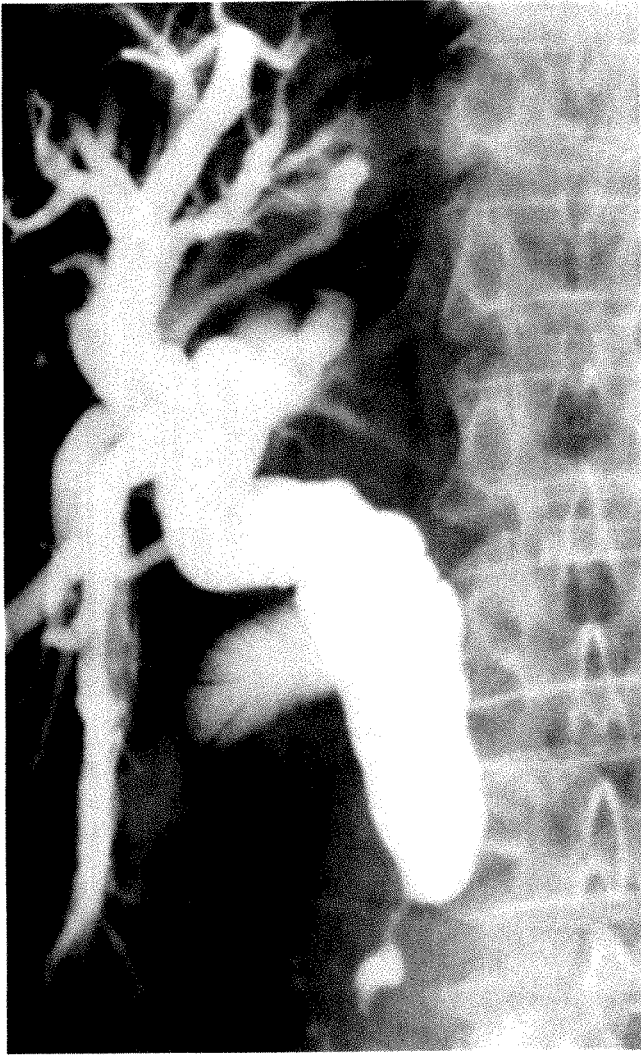


Fig. 3.—Periampullary carcinoma with typical tumor configuration and markedly dilated biliary tree.

completely retracting it from the liver. Thus only one puncture of the liver surface is required.

If presence of an obstruction is established, the catheter is left permanently in the common duct for external bile drainage [3, 4]. The drainage reduces the risk of bile leak, and the patient may be further investigated and prepared for surgery without undue haste [3].

If the biliary tree is normal or if no bile ducts are entered, the catheter is closed and withdrawn gradually over 12 hr. This allows the puncture canal to clot, preventing bleeding and bile leakage.

Most investigators report an 85%–95% success rate using percutaneous transhepatic cholangiography in cases of jaundice caused by extrahepatic obstruction [2]. Using the technique described, our success rate was 100% (i.e., a positive predictive value of 100%; 97½% confidence, 94%–100%) in the case of obstruction.

That percutaneous transhepatic cholangiography is often successful, even in cases where the biliary tree is not

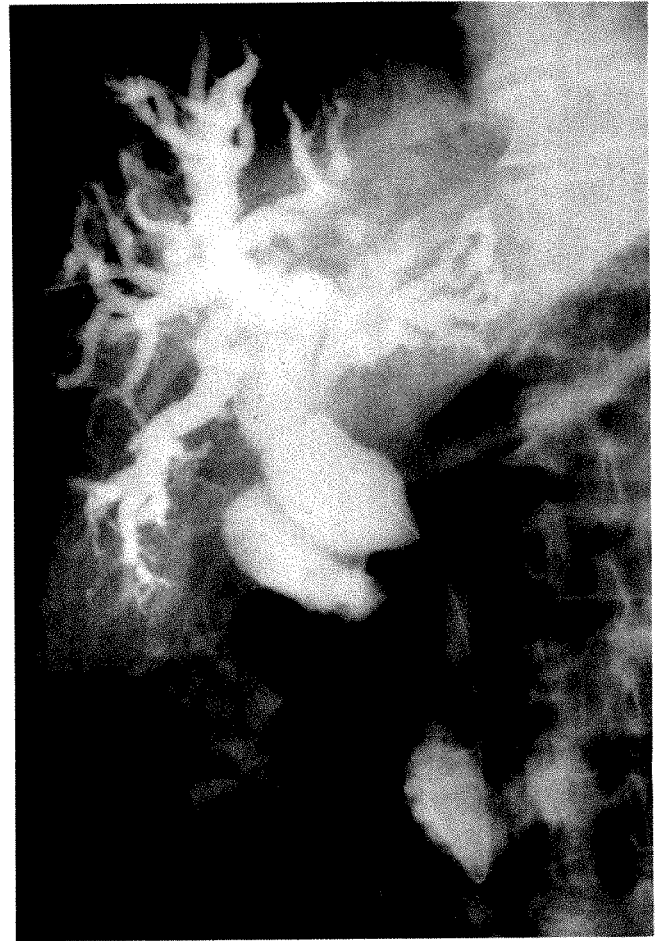


Fig. 4.—Obstruction in middle of common bile duct with typical tumor configuration. Catheter passed through obstruction by guidewire technique demonstrates normal common bile duct and pancreatic duct below obstruction.

dilated, was confirmed in our series [5]. If demonstration of the biliary tree is unsuccessful despite several attempts of puncture, dilatation can virtually be excluded. The negative predictive value was 100% (97½% confidence, 86.8%–100%) in cases of nonobstructive jaundice.

The most serious complications associated with the procedure are bleeding and bile leakage from the liver. In a collective review of 1,629 patients who underwent percutaneous transhepatic cholangiography, complications were found in 5%, with four deaths [6]. Four of our patients had complications (4.6%), but causes were not solely related to the examination. If patients are carefully observed after the examination (e.g., as after liver biopsy), complications may be controlled by surgical intervention [7, 8].

Many investigators routinely administer antibiotics when performing percutaneous transhepatic cholangiography. We only use antibiotics when an existing cholangitis is present since external bile drainage probably prevents it.

REFERENCES

1. Hjortsjö C-H: The topography of the intrahepatic duct systems. *Acta Anat* 11:599–615, 1950

2. Wiechel K-L: Percutaneous transhepatic cholangiography. *Acta Chir Scand [Suppl]* 330:1-99, 1964
3. Marions O, Wiechel K-L: Röntgenologisk ikterusutredning. *Läkartidningen* 70:951-956, 1973
4. Mujahed Z, Evans JA: Percutaneous transhepatic cholangiography. *Radiol Clin North Am* 4:535-545, 1966
5. Okuda K, Tanikawa K, Emura T, Kuratomi S, Urabe K, Sumikoshi T, Kanda Y, Fukuyama Y, Muska H, Mori H, Shimokawa Y, Yakushiji F, Matsuura Y: Nonsurgical, percutaneous transhepatic cholangiography: diagnostic significance in medical problems of the liver. *Am J Dig Dis* 19:21-36, 1974
6. Hines CH, Ferrante WA, Davis WD, Tutton RA: Percutaneous transhepatic cholangiography. *Am J Dig Dis* 17:868-874, 1972
7. Göthlin J, Mansoor M, Tranberg K-G: Combined percutaneous transhepatic cholangiography (PTC) and selective visceral angiography (SVA) in obstructive jaundice. *Am J Roentgenol* 117:419-425, 1973
8. Ham JM, Sorby WA, Colman JVL, Pritchard GR, Yeo BW: Percutaneous transhepatic cholangiography. *Surg Gynecol Obstet* 135:784-786, 1972

Jaundice from Impacted Sediment in a T Tube: Recognition and Treatment

DAVID V. JELASO¹ AND JAN S. HIRSCHFIELD²

Encrustation of bile sediment in the proximal limb of an indwelling T tube may occlude the lumen and cause jaundice. The cholangiographic appearance of this phenomenon is described. Insertion of a torque cable under fluoroscopic control can successfully disimpact the occlusion, restoring patency and relieving the jaundice.

Gratifying palliative results have been reported with biliary stent procedures using elongated T or Y tubes in patients with carcinoma of the proximal bile ducts, when radical resection or biliary-enteric bypass is not possible [1].

Since the primary disease may be slowly progressive locally with late metastases [2], occlusion of the T tube stent by inspissated bile may become a formidable source of morbidity [3]. Various modifications of surgical technique have evolved to avert or delay the need for reexploration to restore biliary drainage [3–5]. The alternative of disimpaction by interventional radiologic techniques has proved successful on several occasions [6–8] and should be attempted before resorting to surgery whenever jaundice from a plugged T tube occurs. Familiarity with the radiologic appearance of the plugged T tube, as illustrated in this case, is important for early accurate diagnosis and initiation of appropriate therapy.

Case Report

A 66-year-old white male was admitted because of progressive jaundice and pruritis of several weeks' duration. He had minimal dyspepsia and bloating but no pain. He had undergone a left colectomy for carcinoma of the sigmoid colon 5 yr earlier; recovery was uneventful. The history was otherwise noncontributory.

Physical examination revealed marked scleral icterus and a soft, flat abdomen with left paramedian scar. The liver was barely palpable in the epigastric region.

Laboratory findings included the following: total bilirubin, 24.4 mg/100 ml; direct bilirubin, 14.6 mg/100 ml; alkaline phosphatase, 1,275 units (normal, 30–85 units); and serum glutamic oxaloacetic transaminase, 135 units (normal, 10–50 units). The upper gastrointestinal series and barium enema were unremarkable. A liver scan was normal. A percutaneous transhepatic cholangiogram (fig. 1) showed a 5.0 cm segment of narrowing in the common hepatic and right main hepatic ducts. The dilated proximal left hepatic duct and a number of tributaries in the left lobe filled through a narrowed, deformed distal segment of the left main hepatic duct.

At laparotomy, an umbilicated necrotic tumor approximately 4.0 × 4.0 cm in diameter was noted in the superoposterior surface of the right lobe of the liver. The liver was otherwise normal, and punch biopsies showed early biliary cirrhosis. The common hepatic duct was not dilated. Curettings from the right hepatic duct showed adenocarcinoma on frozen and paraffin sections. A T tube was inserted across the narrowed segment of common hepatic duct into

the left hepatic duct. The right hepatic duct could not be stented.

A T tube cholangiogram on the ninth postoperative day showed very satisfactory decompression of intrahepatic bile duct radicles by the T tube across the constricted segment. The serum bilirubin returned to normal. The alkaline phosphatase level was 520 units at discharge.

The patient did well for 5 months; during that time he received parenteral 5-fluorouracil chemotherapy. However, the jaundice recurred, with a total bilirubin of 12.3 mg/100 ml. The alkaline phosphatase level was 975 units. A T tube cholangiogram (fig. 24 and



Fig. 1.—Percutaneous transhepatic cholangiogram showing short segments of narrowed proximal common hepatic and right main hepatic ducts constricted by annular tumor mass. Proximal tributaries of right hepatic duct not filled, suggesting catheter tip is within tumor volume. Dilated, deformed left main hepatic duct and tributaries appear with some adjacent caudally extravasated contrast material.

¹ Department of Radiology, Clearwater Community Hospital, Clearwater, Florida 33516. Address reprint requests to D. V. Jelaso.

² Department of Gastroenterology, Clearwater Community Hospital, Clearwater, Florida 33516.

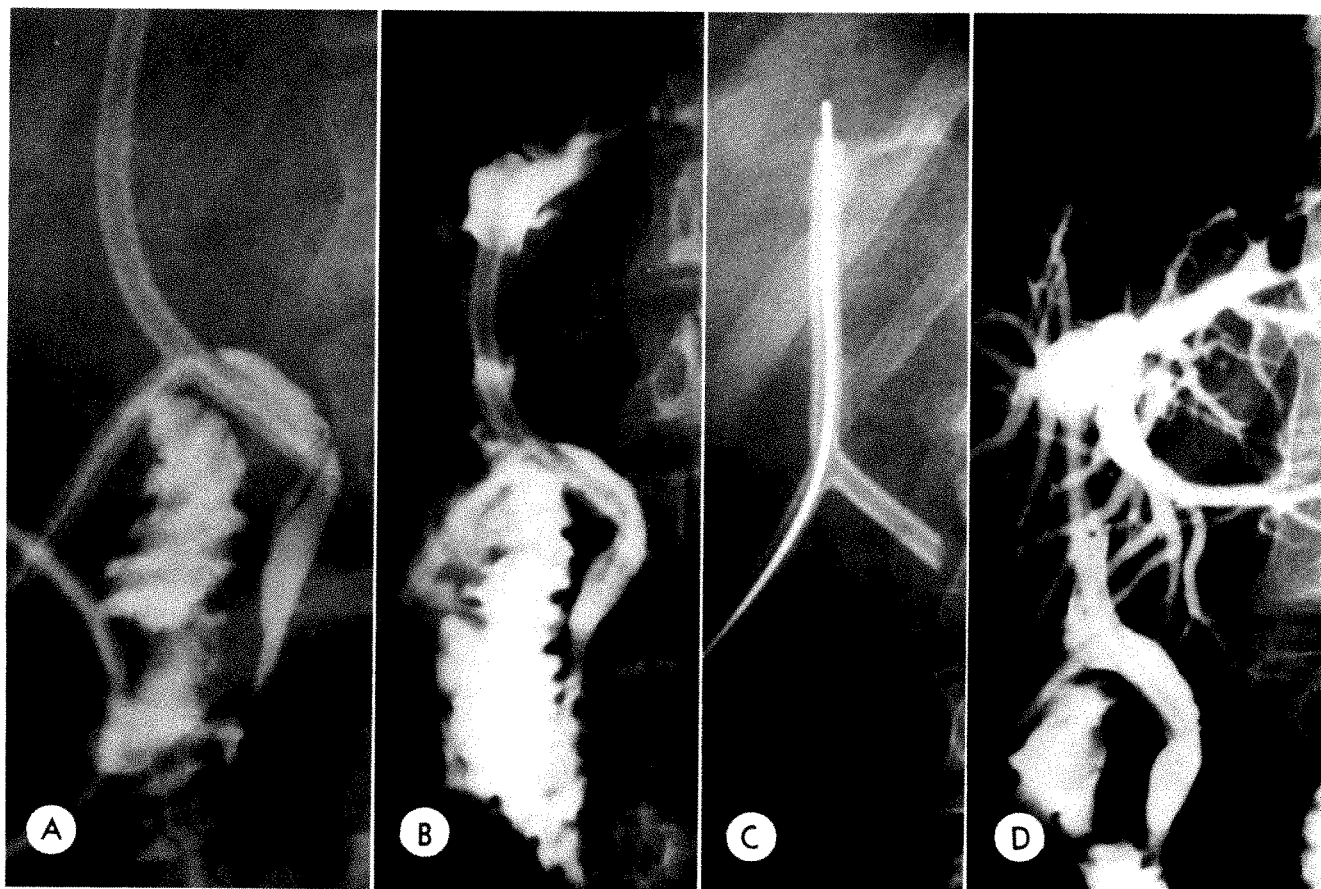


Fig. 2.—T tube cholangiogram 5 months after surgery: jaundice had recurred at this time. *A*, Fluoroscopic spot film early in course of injection showing streaming of contrast material within lumen of T tube distally with spill into duodenum, while plugged proximal limb fails to fill. *B*, Film after further filling showing peritubular proximal flow of contrast material partially outlining intrahepatic bile duct radicles. Note continued absence of contrast material in central core of proximal limb of T tube due to impacted bile sediment. *C*, Film showing insertion of torque cable. *D*, Film showing restored patency of proximal limb of T tube after torque cable disimpaction.

2*B*) showed an occlusion of the central lumen of the proximal limb of the T tube.

Attempts to disimpact this bile sediment plug by irrigation with saline and use of standard and moving core guide wires were unsuccessful. A 1.65 mm Bilbao-Dotter hypotonic duodenography torque cable (Cook, Inc., Bloomington, Ind.) was successfully advanced across the occluded proximal limb of the T tube (fig. 2*C*). Repeated saline irrigations and cable insertions restored patency as shown on a T tube cholangiogram (fig. 2*D*). The patient had a febrile period following the cable manipulation but responded to a course of ampicillin therapy.

Torque cable disimpaction of the plugged T tube was required on several subsequent occasions. These manipulations were separated by prolonged intervals of well being until shortly before the patient's demise, 24 months after the initial admission. Autopsy showed extensive concentric tumor necrosis and microabscesses replacing the right lobe of the liver. The left lobe was spared. There was no remote spread of tumor.

Discussion

The infrequency with which bile duct carcinoma is seen in most radiologic practices may divert the examining radiologist from appropriate emphasis on the T tube cholangiographic study. Blockage of the T tube in this group of cases occurs in the proximal limb as the result of inspissated bile.

Careful fluoroscopic and radiographic scrutiny will reveal an absence of opaque material in the lumen of the proximal limb of the T tube (fig. 2*A*). Peritubular retrograde spill resulting from zealous injection of contrast material may produce opacification of some intrahepatic duct radicles, giving a spurious impression of T tube patency (fig. 2*B*). However, careful attention to the appearance of the central core of the proximal limb of the T tube will show that it remains free of opaque material.

In our case, the proximal limb of the T tube could not be negotiated by standard fixed or movable core guide wires as recommended by Razzaque et al. [7]. The technique of advancing a polyethylene catheter over the guide wire [8] also met with failure due to resistance. Finally, use of the duodenal intubation torque cable imparted with a slight bend near its tip enabled us to achieve sufficient rigidity and torque control to direct the cable through the lumen of the proximal limb of the T tube. Successive saline irrigations and recanalizations by the torque cable were followed by a cholangiogram (fig. 2*D*) which documents disimpaction of the encrustation and restoration of patency of the biliary tree. The 1.65 mm torque cable used here will negotiate T tubes of size 12 French or greater.

The possibility of febrile reaction following this procedure

(as occurred in our patient) should be anticipated. The prophylactic administration of antibiotic, as recommended by Rosch et al. [9] for transjugular cholangiography and Davis et al. [10] for endoscopic retrograde cholangiopancreatography, should probably be adopted whenever cable or catheter T tube manipulation is contemplated.

The nature of the jaundice in patients with carcinoma at the bifurcation of the hepatic ducts may be remarkably elusive, even at the time of laparotomy. In Klatskin's series [11], nine of 13 patients with carcinoma at the bifurcation of the hepatic duct were misdiagnosed at laparotomy. Cholangitis and hepatitis were the most frequent incorrect diagnoses. In the series of Whelton et al. [12], the carcinoma was overlooked at initial laparotomy in 18 of 23 patients. Primary biliary cirrhosis was the most frequent incorrect postoperative diagnosis in this series. Preoperative percutaneous transhepatic cholangiography, endoscopic retrograde cholangiography, or meticulous operative cholangiography is mandatory if correct diagnosis is to be made.

Antecedent primary carcinoma of the colon (as in our patient) was noted in 5% of the patients in the series of Ross et al. [13]. A nonrandom association of bile duct carcinoma in 8% of patients with chronic ulcerative colitis is also reported [13, 14]. This association is approximately as common as the incidence of benign sclerosing cholangitis in chronic ulcerative colitis.

The designation "proximal bile ducts" was offered by Ross et al. [13] to encompass the supraduodenal common bile duct, common hepatic duct, and the right and left hepatic ducts. This group shares a distinctly less favorable prognosis than the group with carcinoma of the distal part of the common bile duct. Warren et al. [2] report a 5 year survival rate of 30% in patients with periampullary carcinoma of the common bile duct. This compares to a 4 year survival rate of 15% in patients with carcinoma of the proximal bile ducts where the histology was favorable [1].

Notwithstanding the poor survival, dramatic relief from pruritis and jaundice may be afforded the majority of patients by simple tube drainage. When such decompression is possible, prolongation of life to an average of 24 months

may be expected compared to a 10 month average survival when the liver is not decompressed [15].

REFERENCES

1. Braasch JW: Carcinoma of the bile duct. *Surg Clin North Am* 53:1217-1227, 1973
2. Warren KW, Mountain JC, Lloyd-Jones W: Malignant tumors of the bile ducts. *Br J Surg* 59:501-505, 1972
3. Terblanche J, Louw JH: U tube drainage in the palliative therapy of carcinoma of the main hepatic duct junction. *Surg Clin North Am* 53:1245-1256, 1973
4. Black HC, Hawk JC Jr, Rambo WM: Long-term intubation of the biliary tract with silastic catheters. *Am Surg* 37:198-202, 1971
5. Praderi RC: Twelve years experience with transhepatic intubation. *Ann Surg* 179:937-940, 1974
6. Margulis AR, Newton TH, Najarian JS: Removal of plug from T tube by fluoroscopically controlled catheter. *Am J Roentgenol* 93:975-977, 1965
7. Razzaque MA, Malhotra C, Wise RE, Whitcomb FF Jr: Treatment of a T tube obstruction by catheterization. *Radiology* 110:739, 1974
8. Short WF, Howard JM, Diven WF: Trans T tube catheterization. Its use in the treatment of postoperative obstruction of the common bile duct. *Arch Surg* 102:136-138, 1971
9. Rosch J, Lakin PC, Ruza A, Antonošić R, Dotter CT: Transjugular approach to liver biopsy and transhepatic cholangiography. *N Engl J Med* 289:227-231, 1973
10. Davis J, Milligan F, Cameron JL: Septic complications following endoscopic retrograde cholangiopancreatography. *Surg Gynecol Obstet* 140:365-367, 1975
11. Klatskin G: Adenocarcinoma of the hepatic duct at its bifurcation within the porta hepatis. *Am J Med* 38:241-256, 1965
12. Whelton MJ, Petrelli M, George P, Young WB, Sherlock S: Carcinoma at the junction of the main hepatic ducts. *Q J Med* 150:211-230, 1969
13. Ross AP, Braasch JW, Warren KW: Carcinoma of the proximal bile ducts. *Surg Gynecol Obstet* 136:923-928, 1973
14. Converse CF, Reagan JW, De Cosse JJ: Ulcerative colitis and carcinoma of the bile ducts. *Am J Surg* 121:39-45, 1971
15. White TT: Carcinoma of the hepatic ducts: review of 11 cases. *Am Surg* 39:445-447, 1973

The Aberrant Gallbladder: Angiographic and Radioisotopic Considerations

VINCENT P. CHUANG¹

There are four types of aberrant gallbladder: (1) intrahepatic, (2) left-sided, (3) transverse, and (4) retrodisplaced. Five cases of the first three types are illustrated. In three of the five patients the aberrant gallbladder produced false positive liver scans which were correctly diagnosed by hepatic angiography; in one it caused the hepatic angiogram to be misinterpreted. The importance of identifying the gallbladder at hepatic angiography by observing the cystic arteries in arterial phase and the gallbladder wall stain in hepatogram phase is stressed.

Although the aberrant gallbladder is a rare congenital anomaly, it is important to both radiologists and surgeons. After the classic review by Gross in 1936 [1], congenital anomalies of the gallbladder have been reported frequently in the surgical literature [2-5]. To date, only incomplete discussions have appeared in the radiological literature [6, 7]. The recognition of an aberrant gallbladder is important to radiologists because it frequently causes a false positive interpretation of the technetium liver scan. An aberrant gallbladder can be localized at hepatic angiography by identification of the cystic artery and the typical gallbladder stain. Failure of an angiographer to recognize this entity may result in misinterpretation of the hepatic angiogram. This paper describes five cases in which an aberrant gallbladder caused diagnostic difficulties.

Classification

There are four types of aberrant gallbladder [1].

Intrahepatic [3]

The gallbladder lies wholly within the substance of the right lobe of the liver and extends from the porta hepatis superolaterally toward the right costophrenic angle (fig. 1A).

Left-sided [2, 7]

The gallbladder lies to the left of the round and falciform ligaments and is partially embedded in the undersurface of the left lobe of the liver. The cystic duct drains to the common duct in the usual manner (fig. 1B).

Transverse [8]

The gallbladder lies in a horizontal position within the transverse fissure and is further posterior than normal (fig. 1C).

Retrodisplaced [5, 6]

The gallbladder courses upward and backward to lie under the inferior and posterior surfaces of the right lobe of the liver (fig. 1D).

An excellent embryological discussion of congenital anomalies of the gallbladder is presented in the classic work of Boyden [9].

The left-sided gallbladder associated with situs inversus represents a separate entity and is not included in this report.

Case Reports

Intrahepatic

Case 1. A 40-year-old man was admitted because of diplococcal pneumonia and severe pulmonary tuberculosis complicated by hydropneumothorax. The abdominal x-ray demonstrated several nodular calcifications in the right upper quadrant. A hepatic angiogram was performed to rule out a primary or secondary hepatic neoplasm. Hepatic angiography revealed tortuous, irregular, and displaced intrahepatic arteries with a nonhomogeneous hepatogram and the suggestion of an 8-9 cm mass at the junction of the right and left lobes (figs. 2A and 2B). The portal vein was normal. The possibility of a calcified hepatoma was suggested in addition to cirrhosis.

An oral cholecystogram revealed an intrahepatic gallbladder extending from the porta hepatis superolaterally with its fundus lying near the right costophrenic angle (fig. 2C). The right upper quadrant calcifications were gallstones, which layered at the fundus of the gallbladder near the right costophrenic angle in the right lateral decubitus projection. Surgery was deferred because of poor pulmonary function. He has been followed for 3 years and there is no clinical evidence of a hepatoma.

In retrospect, a linear density in the hepatogram phase of the

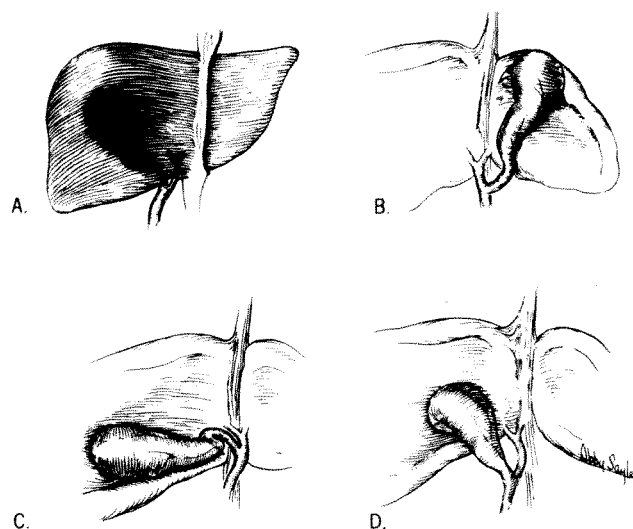


Fig. 1.—Aberrant gallbladders. A, Intrahepatic; B, left-sided; C, transverse; D, retrodisplaced.

Received January 29, 1976; accepted after revision April 6, 1976.

¹ Department of Diagnostic Radiology, University of Kentucky Medical Center, Lexington, Kentucky 40506.

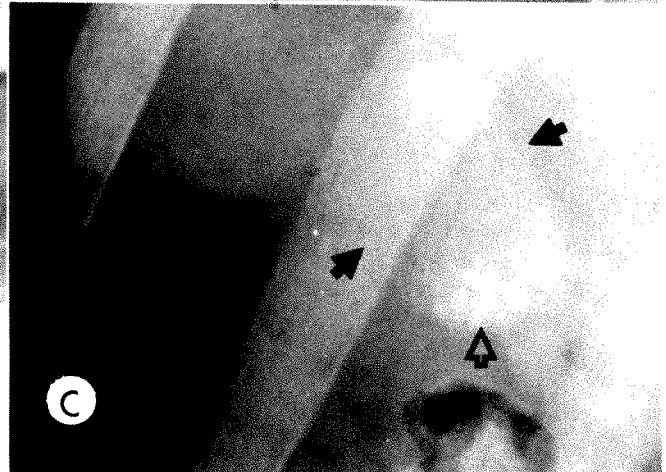
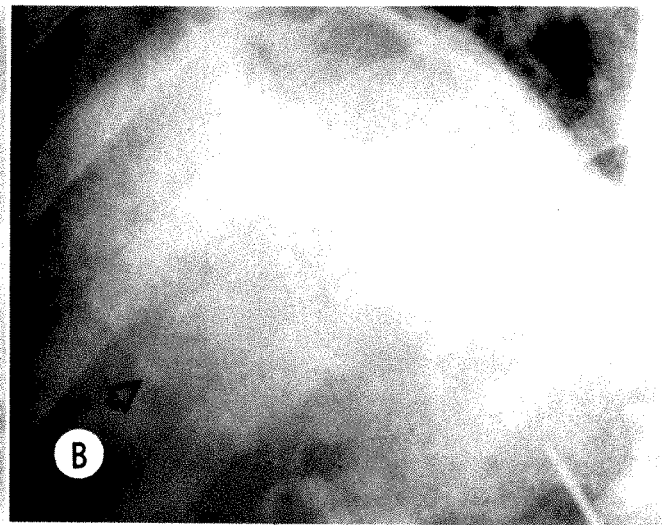
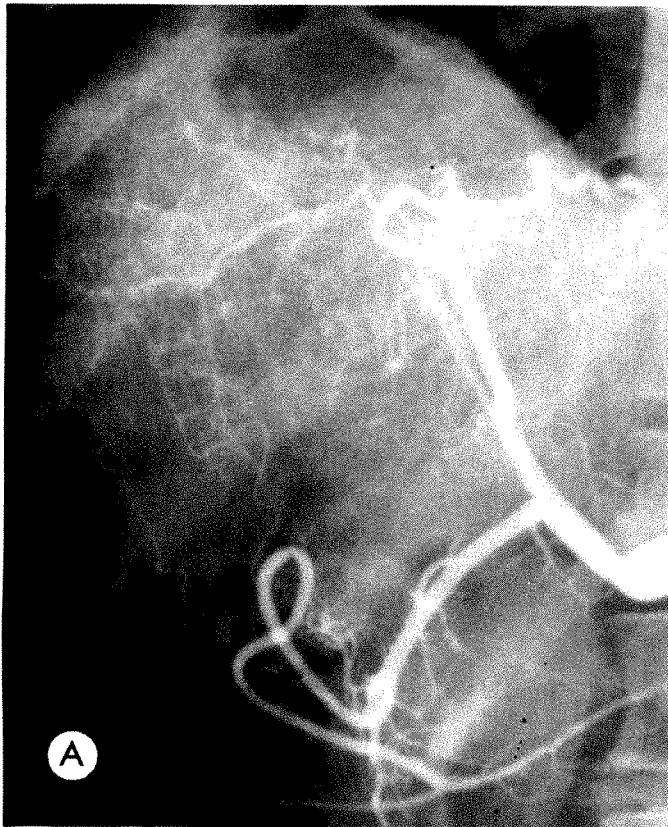


Fig. 2.—Case 1 (intrahepatic). *A*, Arterial phase of selective left hepatic angiogram showing abnormal tortuous and irregular hepatic arteries with suggestion of mass. Cystic artery not seen. *B*, Hepatogram phase showing nonhomogeneity. Border of mass (arrows) probably represents fundus of gallbladder. *C*, Oral cholecystogram showing opacified intrahepatic gallbladder (closed arrows) with several stones (open arrow).

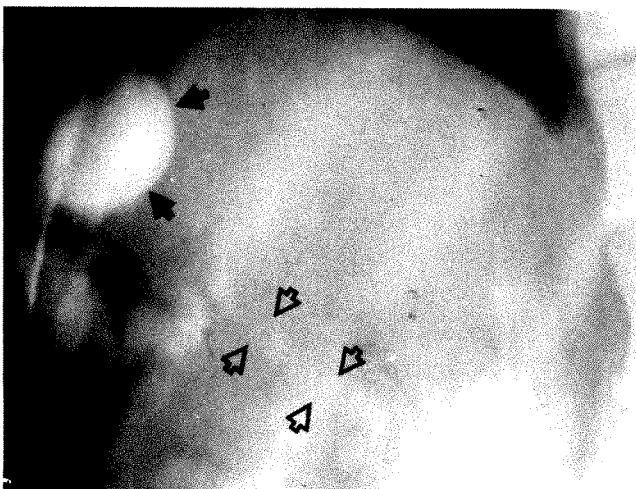


Fig. 3.—Case 2 (intrahepatic). Intravenous cholangiogram in right posterior oblique position showing intrahepatic gallbladder (closed arrows) near right costophrenic angle. Cystic and common ducts (open arrows) demonstrated.

angiogram (fig. 2*B*), originally interpreted as part of the border of the mass, probably represented gallbladder wall.

Case 2. A 51-year-old woman had a history of chronic alcoholism, Laennec's cirrhosis, emphysema, and portal hypertension with

portocaval shunt. She had multiple admissions during the previous 4 years because of recurrent cholecystitis. Two oral cholecystograms with repeat single doses failed to reveal the gallbladder. However, intravenous cholangiograms on two separate occasions demonstrated an intrahepatic gallbladder, cystic duct, and common duct (fig. 3). No biliary calculi were demonstrated.

Despite the diagnosis of acute and chronic cholecystitis, surgery was deferred because of the intrahepatic location of her gallbladder as well as her poor general condition. Her condition improved after medical treatment and she was discharged.

Left-sided (Case 3)

A 58-year-old woman was admitted because of abdominal swelling, general malaise, chronic alcoholism, and jaundice. During hospitalization a technetium liver scan showed a large filling defect in the left lobe of the liver, compatible with a hepatoma (fig. 4*A*). An intravenous cholangiogram failed to show the biliary tree because of elevated bilirubin and alkaline phosphatase. At angiography the hepatic artery branches were dilated with duplication and a corkscrew appearance. The hepatogram was nonhomogeneous. The findings were consistent with severe cirrhosis and focal regeneration (figs. 4*B* and 4*C*).

During the hepatogram phase, a faint stain of the gallbladder wall seen left of the porta hepatis matched well with the area of decreased uptake in the liver scan. This aberrant left-sided gallbladder was thought to have caused the scan defect. A rose bengal liver scan revealed increased uptake in the same area of decreased uptake on

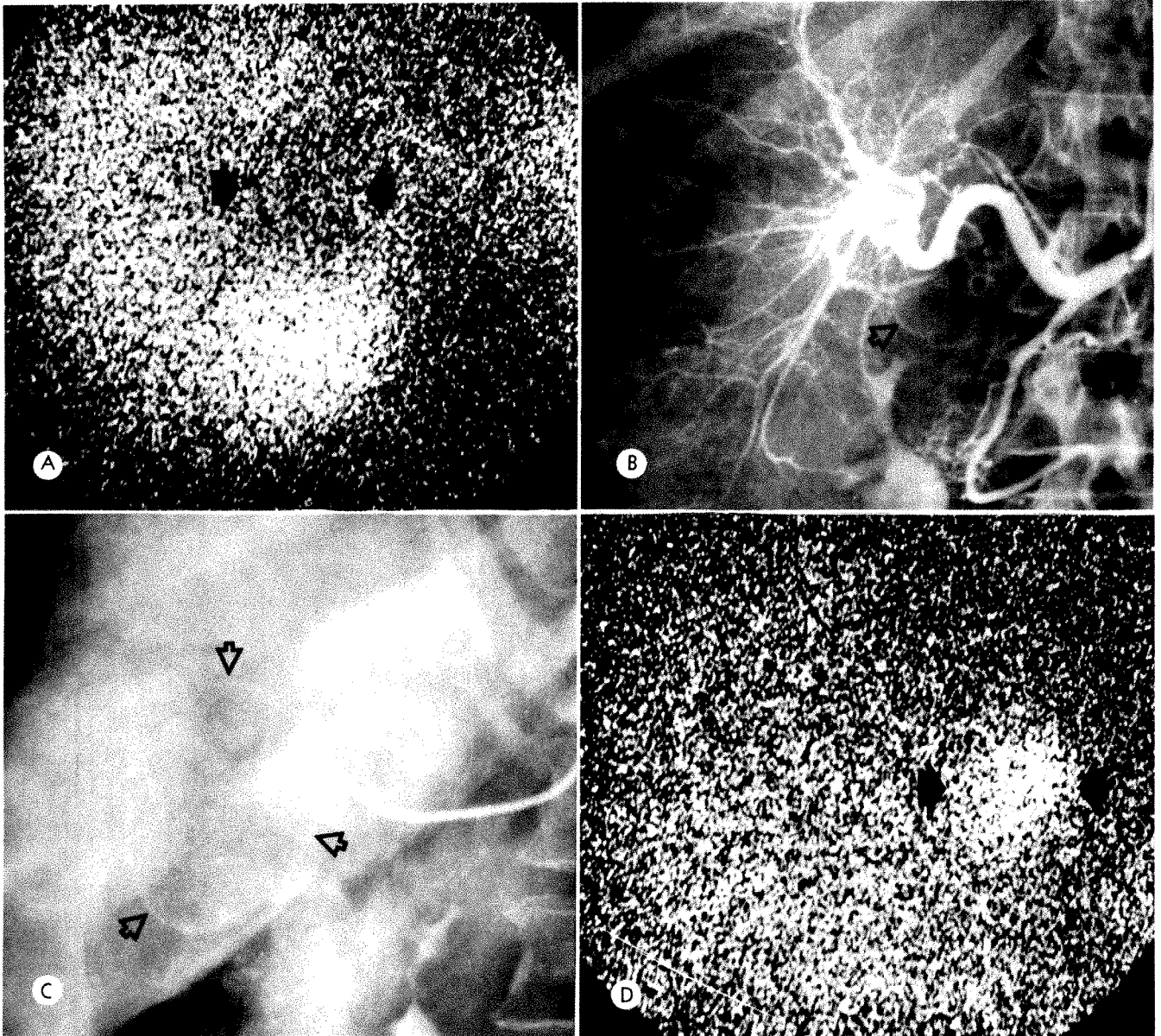


Fig. 4.—Case 3 (left-sided). *A*, Tc-99m liver scan showing large defect in left lobe (arrows). *B*, Arterial phase of celiac angiogram in anteroposterior position. Dilatation, tortuosity, duplication, displacement, and corkscrew appearance of hepatic branches consistent with cirrhosis and focal regeneration. Arrows identify cystic arteries. *C*, Hepatogram phase of common hepatic arteriogram in right posterior oblique position. Dense stain of gallbladder wall (arrows) superimposed on porta hepatis. *D*, Subsequent rose bengal scan showing increased isotopic uptake (arrows) by gallbladder in left lobe of liver.

the technetium scan, thus confirming the diagnosis (fig. 4*D*).

No surgery was performed and the patient died a month later. Autopsy revealed micronodular cirrhosis but no hepatoma. The gallbladder was situated on the undersurface of the left lobe of the liver to the left of the falciform ligament.

Transverse

Case 4. A 39-year-old man was admitted with multiple problems. The physical examination was normal except for a blood pressure of 160/100 mm Hg. An oral cholecystogram was normal (fig. 5*A*). The liver scan revealed a large area of decreased uptake in the inferior right lobe, compatible with hepatoma or perhaps lymphoma (fig. 5*B*).

Hepatic angiography was performed to rule out a hepatoma. The

angiographic findings included: (1) normal hepatic arteries, hepatogram, and portal veins; (2) normal spleen; (3) transverse gallbladder; and (4) no evidence of hepatoma or other neoplasm. The large defect in the liver scan was clearly due to the transverse gallbladder (fig. 5*C*). The patient was discharged without further study of his gallbladder or liver.

Case 5. A 56-year-old woman was admitted for adenocarcinoma of the breast with recurrent malignant pleural effusion. Liver function tests were abnormal. A technetium liver scan showed a defect in the inferior aspect of the right lobe, consistent with metastasis from breast cancer (fig. 6*A*).

Hepatic angiography was performed to position a hepatic artery catheter for arterial infusion chemotherapy. The angiogram revealed a transverse gallbladder encroached upon the right lobe of the

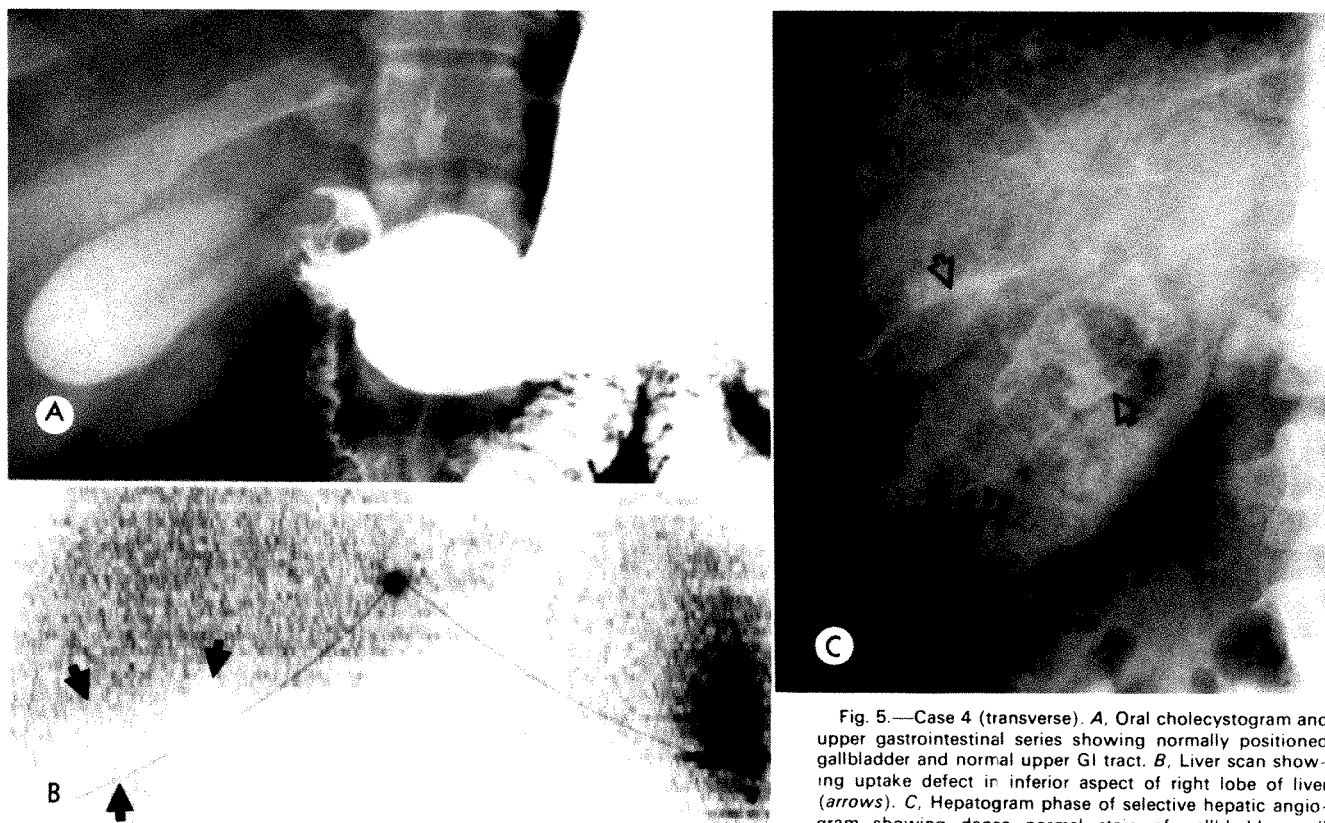


Fig. 5.—Case 4 (transverse). *A*, Oral cholecystogram and upper gastrointestinal series showing normally positioned gallbladder and normal upper GI tract. *B*, Liver scan showing uptake defect in inferior aspect of right lobe of liver (arrows). *C*, Hepatogram phase of selective hepatic angiogram showing dense normal stain of gallbladder wall (arrows) embedded in hepatic parenchyma.

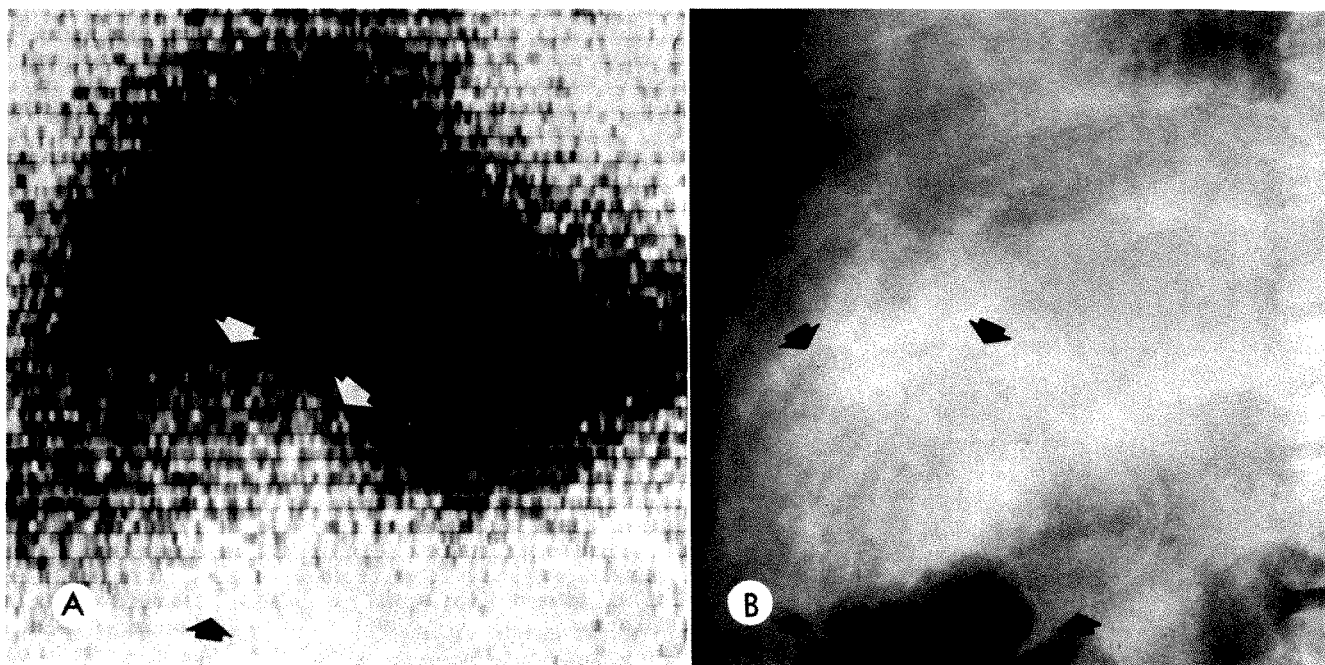


Fig. 6.—Case 5 (transverse). *A*, Technetium liver scan (anteroposterior view) showing large defect in inferior portion of right lobe (arrows), consistent with metastasis. *B*, Venous phase of hepatic angiogram showing typical normal stain of gallbladder wall (arrows) embedded in hepatic parenchyma, causing uptake defect in liver scan. No metastasis present.

liver (fig. 6B), causing the filling defect in the liver scan. Since there was no hepatic metastasis, infusion chemotherapy was terminated.

Discussion

When the gallbladder functions normally, it is readily visualized by oral cholecystography. However, an aberrant gallbladder cannot be detected because of the difficulty of determining its position relative to the liver (case 4). If oral cholecystography and intravenous cholangiography cannot be used because of jaundice, a liver scan is frequently performed to diagnose hepatobiliary disease. As illustrated in cases 3–5, an aberrant gallbladder may result in the false diagnosis of a hepatic mass at technetium liver scan. It is well known that the porta hepatis, as well as a normally located gallbladder, can produce a prominent triangular defect in the inferior border of the liver scan. However, the problem of an aberrant gallbladder producing a defect simulating a liver mass has not been sufficiently stressed.

When a solitary defect is present in a technetium liver scan, the differential diagnosis includes neoplasm, abscess, hematoma, lymphoma, and an aberrant gallbladder. The size and location of the gallbladder in the oral cholecystogram and/or intravenous cholangiogram should be carefully reviewed. If an aberrant gallbladder is suspected, a rose bengal liver scan can reveal its presence and location. However, the combination of decreased uptake on a technetium scan and increased uptake on a rose bengal scan may also be caused by a choledochal cyst, another rare biliary tract anomaly.

Since hepatic angiography is the most accurate method for differentiating hepatic masses, it should be performed on any patient with a focal defect in the liver scan. The gallbladder is frequently localized by hepatic angiography when the cystic arteries are seen in the arterial phase and a typical stain of gallbladder wall in the hepatogram phase. In cases 3–5 the hepatic angiograms allowed the correct diagnosis, thus preventing unnecessary biopsy and surgery. In case 1, the gallbladder was intrahepatic and the contrast accumulation in its wall was misinterpreted at angiography. In case 2, both liver scan and hepatic angiogram were avoided because of the typical intrahepatic gallbladder shown by intravenous cholangiogram.

Bleich et al. [2] reported a case of a left-sided gallbladder which extended across the midline to lie in the left upper

quadrant without situs inversus. If the gallbladder is not visualized at oral cholecystography on a 10 × 12 inch film, Etter [7] suggested that a 14 × 17 inch film of the abdomen should be taken to avoid missing such an anomaly.

An aberrant gallbladder is also important to clinicians because it may produce atypical symptoms in patients with cholecystitis. McGowan et al. [4] reported a patient with cholecystitis in a left-sided gallbladder who had right upper quadrant pain radiating to the left side but not to the shoulder or directly to the back.

The aberrant gallbladder is a challenge for surgeons performing cholecystectomy or other biliary surgery [2, 3, 5, 8]. The anomalous position and the variable degree to which it is embedded in liver parenchyma create technical difficulties. Since an intrahepatic gallbladder can mimic congenital absence of the gallbladder, an operative cholangiogram should be performed during cholecystectomy [3]. Stetten [10] suggested that an intrahepatic gallbladder containing stones should be treated by incision, removal of the stones, and drainage rather than by cholecystectomy.

REFERENCES

1. Gross RE: Congenital anomalies of the gallbladder. A review of 148 cases, with report of a double gallbladder. *Arch Surg* 32: 131–162, 1936
2. Bleich AR, Hamblin DO, Martin D: Left upper quadrant gallbladder. *JAMA* 147: 849–851, 1951
3. Ferris DO, Glazer IM: Congenital absence of gallbladder. *Arch Surg* 91: 359–361, 1965
4. McGowan JM, Nussbaum CC, Burroughs EW: Cholecystitis due to *Giardia lamblia* in a left-sided gallbladder. *Ann Surg* 128: 1032–1037, 1948
5. Rachlin SA: Congenital anomalies of the gallbladder and ducts. *Milit Surg* 109: 20–25, 1951
6. Blanton DE, Bream CA, Mandel SR: Gallbladder ectopia: a review of anomalies of position. *Am J Roentgenol* 121: 396–400, 1974
7. Etter LE: Left-sided gallbladder: necessity for film of the entire abdomen in cholecystography. *Am J Roentgenol* 70: 987–990, 1953
8. Burke J: An anomaly in the position of the gallbladder. *JAMA* 177: 508–509, 1961
9. Boyden EA: The accessory gallbladder: an embryological and comparative study of aberrant biliary vesicles occurring in man and domestic mammals. *Am J Anat* 38: 177–231, 1926
10. Stetten DeW: Cholecystectomy in a case of intrahepatic gallbladder. *Ann Surg* 97: 296–298, 1933

Pathophysiology of Enlargement of the Small Bowel Fold

WILLIAM W. OLMSTED^{1,2} AND DAVID E. REAGIN^{1,3}

Enlargement of the valvulae conniventes is an integral part of the pattern diagnosis of primary small bowel disease causing malabsorption. The pathophysiology underlying enlargement of the fold and the most typical diseases with prominent folds leading to malabsorption are discussed. Differential diagnosis is based on enlargement of the fold and on secondary signs.

In diseases that affect the small bowel diffusely and cause malabsorption, the radiologic differential diagnosis is difficult since the signs of the individual diseases overlap with striking frequency. Simplified schemes of diagnosis based on patterns have been offered [1, 2]. An integral part of any classification is the differential diagnosis of diseases that cause enlargement of the folds (valvulae conniventes, valves of Kerckring, or plicae circulares). Once this specific abnormality is recognized radiologically, diagnosis can be attempted using the secondary signs. A specific diagnosis is difficult; in fact, some investigators feel that specific diagnoses cannot be made [3].

Pathophysiology of Enlargement

Normal valvulae conniventes are crescentic bands of mucosa and submucosa 0.8 cm high and 0.3 mm thick (figs. 1 and 2) [4, 5]. They begin 2–5 cm from the pylorus and reach their greatest height in the duodenum and jejunum. The submucosal connective tissue is firm, giving the folds a degree of permanence. Valvulae conniventes become enlarged when the lamina propria of the villi and/or submucosal space is expanded secondary to edema, infiltration with normal or abnormal cells and/or substances, or dilatation of normally occurring structures (fig. 1) [2, 6, 7].

Lymphoma and Regional Enteritis

Lymphoma and regional enteritis are the most frequent diseases of the small bowel that cause malabsorption associated with thickening of folds (figs. 3 and 4). Enlargement of the folds in both diseases is the result of packing of the lamina propria and submucosa with cells and edema. Atypical reticuloendothelial cell infiltration causes dilated folds and flattened villi in lymphoma (fig. 5); acute and chronic inflammation is the cause in regional enteritis (fig. 6).

Whipple's Disease

The prominent fold is the major radiologic and pathologic finding in Whipple's disease. In a review of the literature

Maizel et al. [8] reported that 87% of cases showed abnormal radiologic findings of the small bowel; in their series of 12 cases, 100% presented with prominent duodenal and jejunal folds (fig. 7). Whipple's disease is distinguished microscopically by the presence of PAS-positive macrophages within the lamina propria of the small bowel wall (fig. 8).

Ultrastructural studies in active cases reveal the presence of diagnostic microorganisms. It is this infiltration (not the villous elongation described by Triano [9]) that causes prominence of the valvulae conniventes. Submucosal lymphatic distention and edema further complicate diagnosis and accentuate thickening [6, 10]. Edema may be secondary to hypoalbuminemia, which has been attributed to increased intestinal loss of protein, decreased hepatic synthesis of protein, and decreased absorption of amino acids [8].

Amyloidosis

Pear [11] stated that the small bowel is radiologically the most sensitive organ in systemic amyloidosis (fig. 9). The signs depend on the degree of infiltration of fibrillary glycoprotein and the anatomic site of involvement. In early amyloidosis, glycoprotein is deposited in the lamina propria and submucosal perivascular spaces (fig. 10) [12]. As the disease progresses, the entire wall may be infiltrated and converted into a rigid tube. Seliger et al. [13] felt that the perivascular deposition of amyloid is the primary cause of

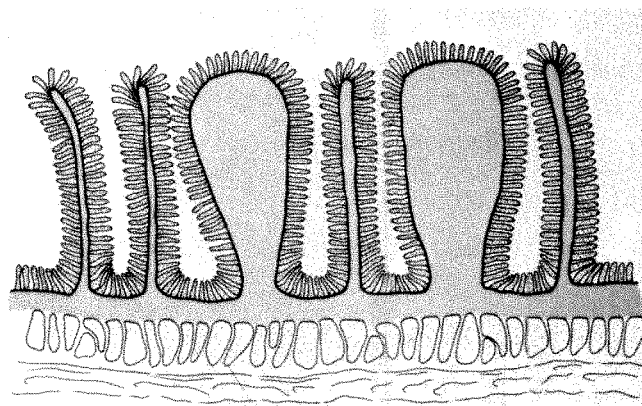


Fig. 1.—Diagram depicting alternating normal and abnormal folds. Thickened folds primarily result from enlargement of submucosal space (gray) and/or lamina propria of villi. (AFIP neg. 75-9694)

Presented at the annual meeting of the American Roentgen Ray Society, Atlanta, Georgia, October 1975.

This work was supported in part by U.S. Public Health Service grant no. CA15413-03 from the National Cancer Institute, Division of Cancer Research Resources and Centers. The opinions or assertions contained herein are the private views of the authors and are not to be construed as official or as reflecting the views of the Departments of the Air Force, Navy, or Defense.

¹ Department of Radiologic Pathology, Division of Gastrointestinal Pathology, Armed Forces Institute of Pathology, Washington, D.C. 20306. Address reprint requests to W. W. Olmsted.

² USAF, MC.

³ MC, USN.

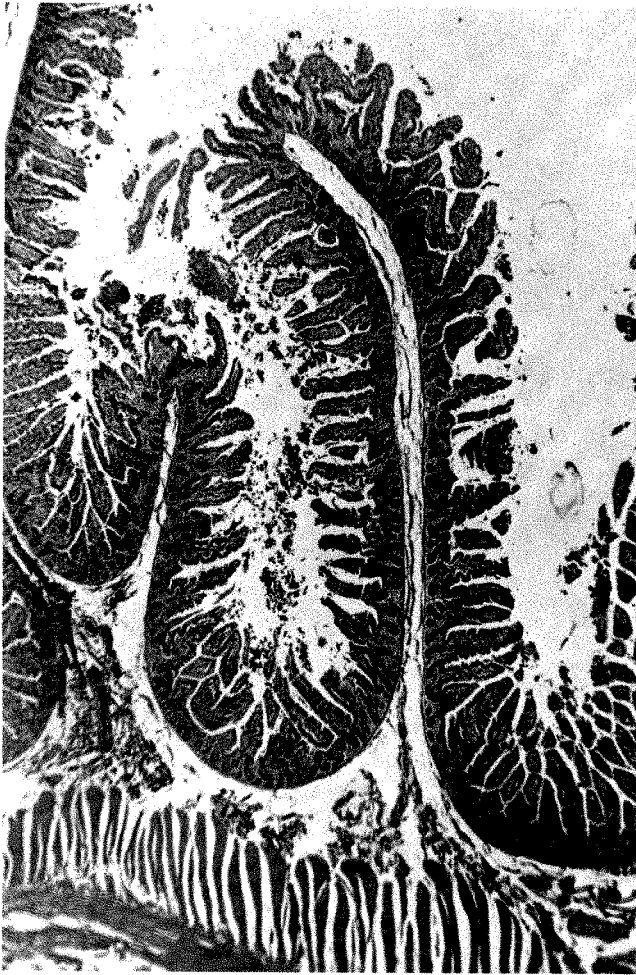


Fig. 2.—Normal villi covering thin submucosa of normal fold. H and E, $\times 14$. (AFIP neg. 75-9688)

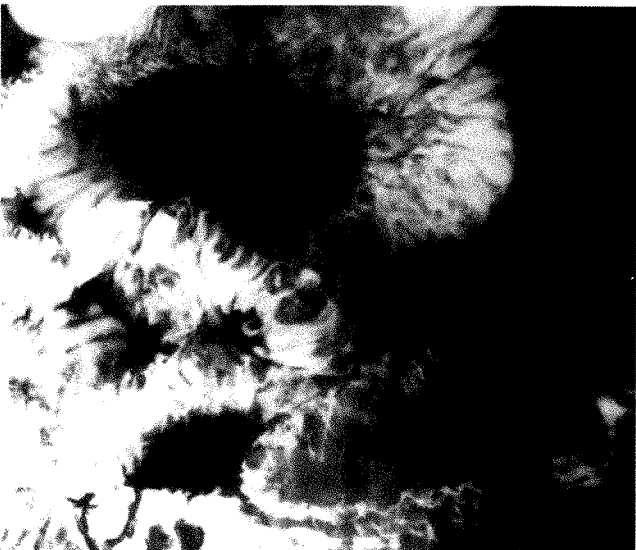


Fig. 3.—Typical presentation of small bowel lymphoma showing thickened and nodular folds. (AFIP neg. 69-11313-1)



Fig. 4.—Thickened folds and nodules caused by regional enteritis. Note associated thickened mesentery causing loops of bowel to spread. (AFIP neg. 68-2236-4)



Fig. 5.—Cellular infiltration of submucosa (immediately under villi) causing thickening of fold in lymphoma. H and E, $\times 10$. (AFIP neg. 75-9689)

thickening of the valvulae conniventes. They hypothesized that amyloid produces vascular blockage that results in ischemia; this produces edema and the resultant thickening.

Actual deposition of amyloid in the lamina propria and submucosa may be an alternate and more reasonable explanation of fold enlargement (fig. 11). Indeed, Pear [11] indicated that both amyloid deposition and edema produced by perivascular amyloid deposits may cause the radiologic signs. With advanced disease and replacement of

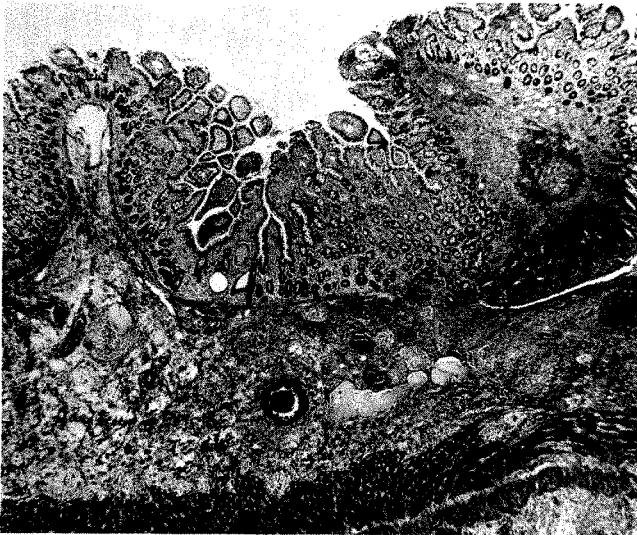


Fig. 6.—Two folds enlarged by inflammation of submucosa in regional enteritis. H and E, $\times 13$. (AFIP neg. 75-7713)

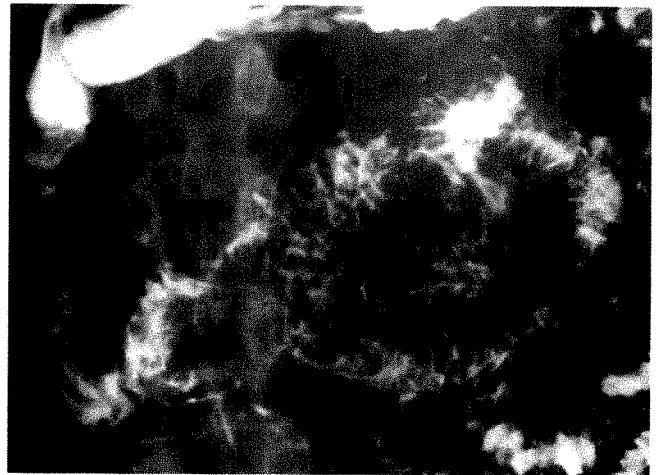


Fig. 7.—Enlargement of folds of proximal small bowel in Whipple's disease. No significant increase in secretions seen. (AFIP neg. 69-11429-1)

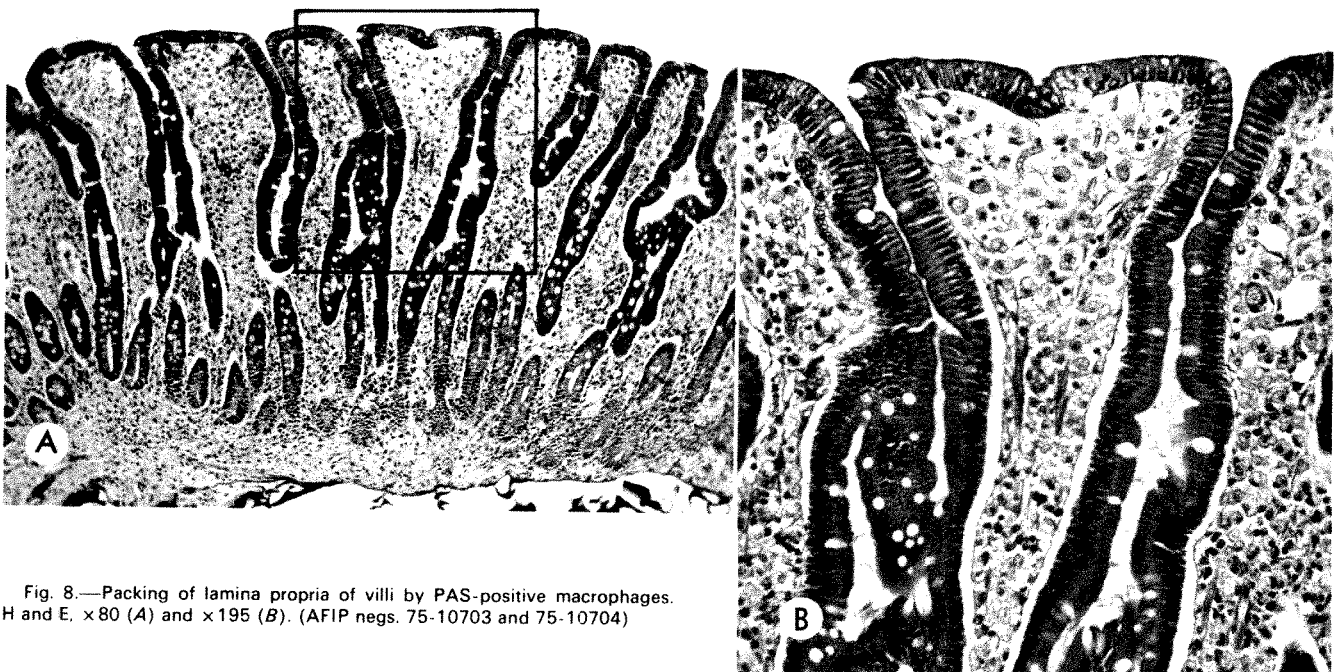


Fig. 8.—Packing of lamina propria of villi by PAS-positive macrophages. H and E, $\times 80$ (A) and $\times 195$ (B). (AFIP negs. 75-10703 and 75-10704)

normal elements of the wall, the small bowel becomes a rigid tube and peristalsis is markedly impaired, resulting in secondary signs of stasis and dilatation.

Lymphangiectasia

In 1961, Waldmann et al. [14] substituted the term intestinal lymphangiectasia for "primary protein-losing gastroenteropathy" based on new histologic data. The striking pathologic abnormality is dilatation of the lymphatics of the lamina propria and submucosa (fig. 12) [15]. Thickening of the fold is the result of dilatation of these structures (fig. 13). Marshak et al. [16] alternately hypothesized that the en-

larged folds are secondary to mucosal and submucosal edema because of hypoproteinemia. Shimkin et al. [17] speculated that there is "a local predilection for interstitial fluid accumulation due to abnormal lymphatic dynamics causing edema of the valvulae."

Nodular Lymphoid Hyperplasia

Nodular thickening of folds is the most prominent feature of nodular lymphoid hyperplasia associated with immunoglobulin deficiencies and infestation by *Giardia lamblia* (fig. 14). Secondary radiologic signs include mild dilatation and hypersecretion. The proximal small bowel is the part



Fig. 9.—Diffusely prominent folds in absence of hypersecretion suggesting amyloidosis of small bowel. (AFIP neg. 69-9700-3)

primarily affected, although the distal jejunum, terminal ileum, and right colon have been involved in some cases [18]. Mechanistically, nodular lymphoid hyperplasia may be a compensatory process for the immunoglobulin deficiency [19]. Microscopically, thickening of the valvulae conniventes is caused by nodular aggregation of lymphoid tissue within the lamina propria of the bowel (fig. 15) [20].

Differential Diagnosis

To proceed logically when presented with increased prominence of the valvulae conniventes in small bowel studies, the examiner must first exclude those diseases or conditions that occur with the greatest frequency and can cause malabsorption: edema (cardiac, hepatic, or renal in origin), regional enteritis, and lymphoma. After they have been excluded, Whipple's disease, amyloidosis, lymphangiectasia, and nodular lymphoid hyperplasia should be the main considerations. An attempt at definitive radiologic diagnosis can then be made by evaluation of secretions, characteristics of the enlarged folds, and their distribution.

Lymphangiectasia and nodular lymphoid hyperplasia cause increased secretions. In lymphangiectasia loss of protein is secondary either to transudation across an intact capillary epithelium when lymphatics are obstructed or to rupture of dilated obstructed lymphatics [14, 17]. Increased secretion in nodular lymphoid hyperplasia is more difficult to explain, but chronic diarrhea is frequently experienced by these patients. Hypersecretion is only occasionally seen

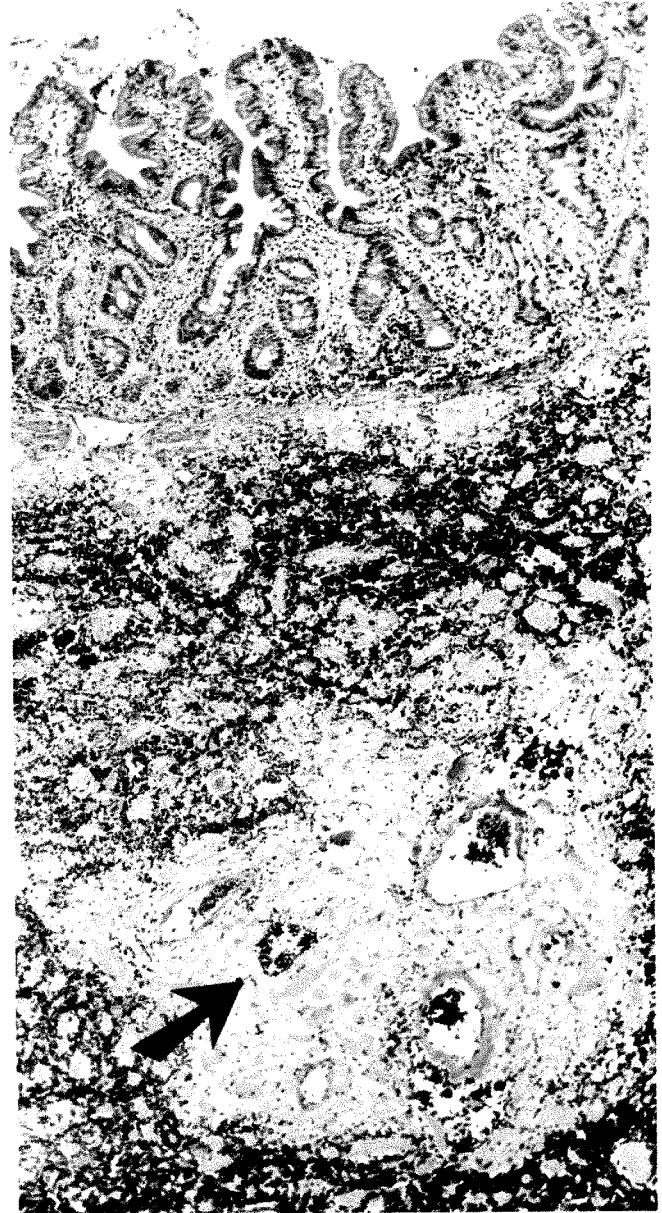


Fig. 10.—Prominent perivascular deposition of amyloid. Note small vessel surrounded by amyloid (arrow). H and E, $\times 50$. (AFIP neg. 75-9694)

in Whipple's disease [21]. Martel and Hodges [10] suggested that unabsorbed fatty acids irritate the bowel causing excessive production of mucus and, therefore, hypersecretion. However, hypersecretion in Whipple's disease is the exception rather than the rule. There should be no increased secretions in amyloidosis.

The character of the fold may be important in the differential diagnosis of these four conditions. In Whipple's disease the folds are generally irregular and somewhat disordered. In amyloidosis and lymphangiectasia they are more regular, while those seen in cases of nodular lymphoid hyperplasia are nodular. Distribution is also important; in Whipple's disease the enlarged folds are located primarily in the duodenum and jejunum. Folds are normally widest

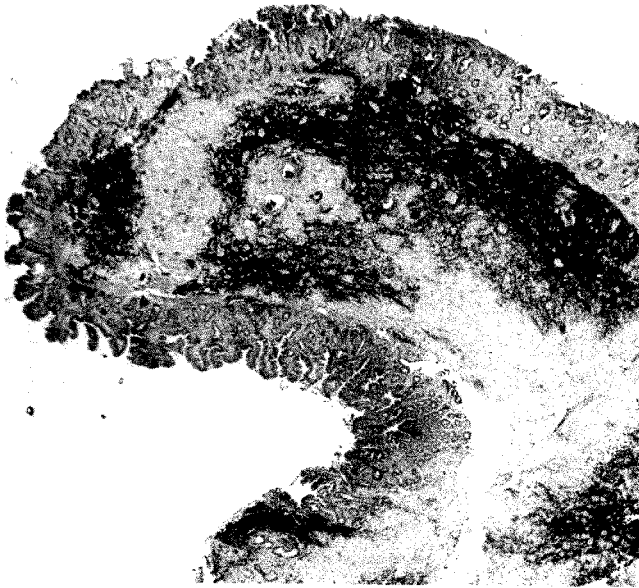


Fig. 11.—Deposition of amyloid and hemorrhage in submucosa causing thickening of fold. H and E, $\times 12$. (AFIP neg. 75-9690)

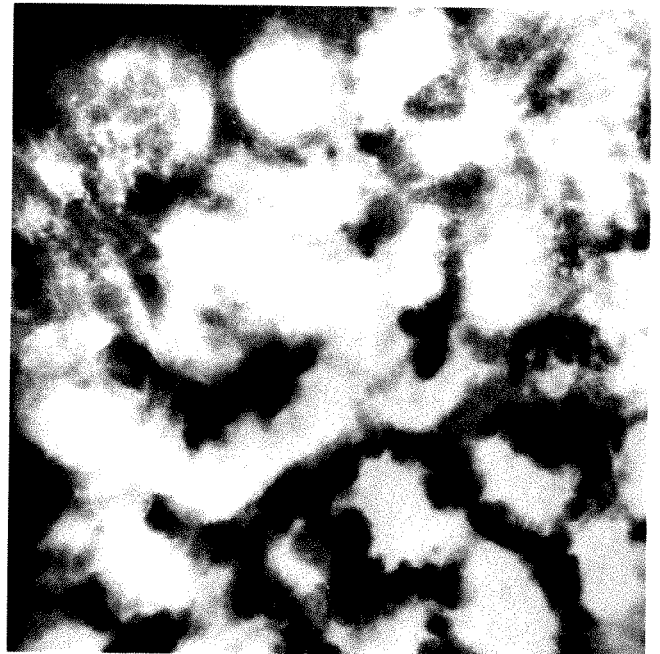


Fig. 13.—Diffusely thickened folds and hypersecretion (haziness of barium column) in lymphangiectasia. (AFIP neg. 75-8843-7)

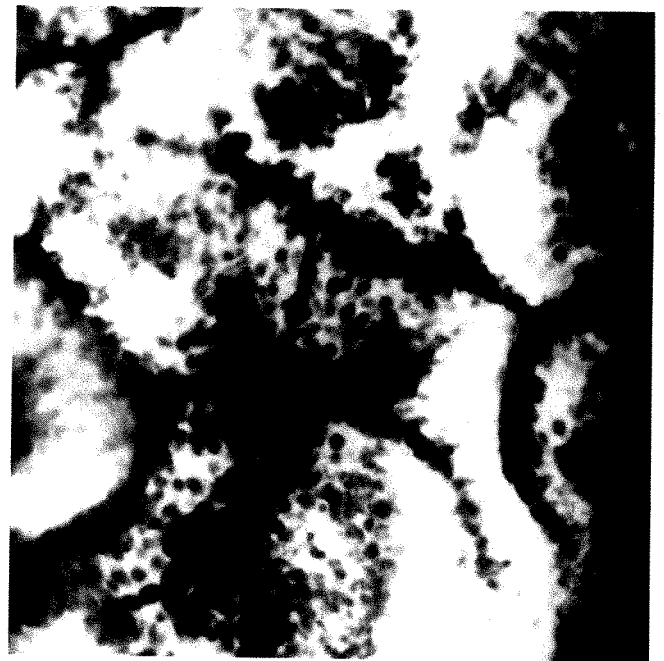


Fig. 14.—Diffuse striking nodularity in nodular lymphoid hyperplasia. (AFIP neg. 72-17035-1)



Fig. 12.—A, Dilated lymphatics in lamina propria of villi contributing to valvular enlargement in lymphangiectasia. H and E, $\times 28$. B, Higher power view showing dilated lymphatics (cell-lined structures in center of field) between normal crypts. H and E, $\times 180$. (AFIP negs. 75-7717 and 75-7721)



Fig. 15.—Lamina propria of villi packed with lymphocytes in nodular lymphoid hyperplasia. H and E, $\times 110$. (AFIP neg. 75-7723)

in this area [10]; therefore it is expected that the greatest thickening of the fold should occur here. Hodgson et al. [18] reported that nodular lymphoid hyperplasia primarily affects the duodenum and jejunum, although other parts of the small intestine may be involved (fig. 14). Thickening of the folds in amyloidosis and lymphangiectasia is generally distributed throughout the entire small bowel, with no predilection for a specific part.

Those diseases that are rare or rarely cause large folds must also be excluded: eosinophilic enteritis [16], mastocytosis [22], infectious mononucleosis [23], and chronic constrictive pericarditis [24]. The latter can cause radiologic and pathologic findings similar to those in intestinal lymphangiectasia.

ACKNOWLEDGMENT

We thank Dr. Elias G. Theros for helpful criticism and advice.

REFERENCES

- Swischuk L, Welsh J: Roentgenographic mucosal patterns in the "malabsorption syndrome": a scheme for diagnosis. *Am J Dig Dis* 13:59-78, 1968
- Tully T, Feinberg S: A roentgenographic classification of diffuse diseases of the small intestine presenting with malabsorption. *Am J Roentgenol* 121:283-290, 1974
- Isbell R, Carlson H, Hoffman H: Roentgenologic-pathologic correlation in malabsorption syndromes. *Am J Roentgenol* 107:158-169, 1969
- Bloom W, Fawcett D: *A Textbook of Histology*, 9th ed. Philadelphia, Saunders, 1968
- Gray H: *Anatomy of the Human Body*, edited by Goss CM, Philadelphia, Lea & Febiger, 1966
- Clemett A, Marshak R: Whipple's disease: roentgen features and differential diagnosis. *Radiol Clin North Am* 7:105-111, 1969
- Pock-Steen O: Roentgenologic changes in protein-losing enteropathy. *Acta Radiol* 4:681-689, 1966
- Maizel H, Ruffin J, Dobbins W: Whipple's disease: a review of 19 patients from one hospital and a review of the literature since 1950. *Medicine* 49:175-205, 1970
- Triano G: Further roentgen observations of the small intestine in Whipple's disease. *Am J Roentgenol* 87:717-720, 1962
- Martel W, Hodges F: The small intestine in Whipple's disease. *Am J Roentgenol* 81:623-636, 1959
- Pear B: Radiographic studies of amyloidosis. *Crit Rev Radiol Sci* 3:425-452, 1972
- Gilat T, Revach M, Sohar E: Deposition of amyloid in the gastrointestinal tract. *Gut* 10:98-104, 1969
- Seliger G, Krassner R, Beranbaum E, Miller F: The spectrum of roentgen appearance in amyloidosis of the small and large bowel: radiologic-pathologic correlation. *Radiology* 100:63-70, 1971
- Waldmann T, Steinfeld J, Dutcher T, Davidson J, Gordon R: The role of the gastrointestinal system in "idiopathic hypoproteinemia." *Gastroenterology* 41:197-207, 1961
- Dobbins W: Electron microscopic study of the intestinal mucosa in intestinal lymphangiectasia. *Gastroenterology* 56:1004-1017, 1966
- Marshak R, Hazzi C, Lindner A, Maklansky D: Small bowel in immunoglobulin deficiency syndromes. *Am J Roentgenol* 122:227-240, 1974
- Shimkin P, Waldmann T, Krugman R: Intestinal lymphangiectasia. *Am J Roentgenol* 110:827-841, 1970
- Hodgson J, Hoffman H, Huizenga K: Roentgenologic features of lymphoid hyperplasia of the small intestine associated with dysgammaglobulinemia. *Radiology* 88:883-888, 1967
- Wolfson J, Goldstein G, Krivit W, Hong R: Lymphoid hyperplasia of the large intestine associated with dysgammaglobulinemia: report of a case. *Am J Roentgenol* 108:610-614, 1970
- Hermans P, Huizenga K, Hoffman H, Brown A, Markowitz H: Dysgammaglobulinemia associated with nodular lymphoid hyperplasia of the small intestine. *Am J Med* 40:78-89, 1966
- Rice R, Roufail W, Reeves R: The roentgen diagnosis of Whipple's disease (intestinal lipodystrophy): with emphasis on improvement following antibiotic therapy. *Radiology* 88:295-301, 1967
- Clemett A, Fishbone G, Levine R, James AE, Janower M: Gastrointestinal lesions in mastocytosis. *Am J Roentgenol* 103:405-412, 1968
- Butler M, Carlton L, DeGreen H, Teplick S, Metz J: Transient malabsorption in infectious mononucleosis: case report. *Am J Roentgenol* 122:241-244, 1974
- Kumpe D, Jaffe R, Waldmann T, Weinstein M: Constrictive pericarditis and protein-losing enteropathy: an imitator of intestinal lymphangiectasia. *Am J Roentgenol* 124:365-373, 1975

Electrical Stimulation for Anal Sphincter Control in Barium Enema Examinations: An Extended Trial

KENNETH CLARK¹ AND DAVID ROWAN²

The routine use in 500 consecutive patients of a barium enema cannula incorporating stimulating electrodes is described. Barium retention was improved by the electrically maintained contraction of the anal sphincter.

The cannula was connected to a battery-powered control unit which provided the stimulus; pulse width was 1 msec and frequency was 20 pulses/sec. The pulse amplitude, adjusted for each patient, was in the range of 5–17 V.

A standard procedure was adopted throughout the trial without the use of colonic relaxants (such as anticholinergic drugs). The barium suspension and water were instilled at body temperature. A comparison with a control series of 200 patients showed a significant reduction in the failure rate from 20% to 4%.

No unpleasant side effects were encountered apart from a tingling sensation in the anal region which was expected. The principal factors contributing to failure were fecal impaction and diverticular disease.

A preliminary study [1] suggested that the use of an enema cannula incorporating electrodes for stimulation of the anorectal sphincters reduced the incidence of failure and barium spillage. The design of the cannula was based on the anal plug electrode developed by Hopkinson and Lightwood [2] for the control of fecal incontinence. An extended trial has now been undertaken and results compared with a control series in which the conventional method was used. Although the basic features have remained the same, certain changes in technique and instrumentation have been made as a result of experience gained.

Materials and Methods

The small stimulator used for the preliminary trial has been discarded because of its vulnerability to barium and water soakage and because it was not sufficiently robust for routine clinical use. A new stimulator (fig. 1), based on a design by Rowan [3] and constructed by the Department of Clinical Physics and Bio-Engineering (Glasgow), consists of a unijunction oscillator and a common emitter output stage (fig. 2). The instrument is capacitive coupled to the patient to avoid electrolytic effects at the electrodes and to protect the patient from possible skin burns if a short circuit fault occurs in transistor TR1. As before, the stimulus consists of rectangular pulses; pulse width was 1 msec and frequency 20 pulses/sec. The pulse amplitude now has a range of 0–17 V and is controlled by a 10-turn potentiometer (VR1). A meter (M1) and a push-button switch (S2) have been incorporated to enable the batteries to be checked before or during examinations.

The two barium cannulae used throughout the trial are shown in figure 3. The newer model is concave in the electrode region, with reduced electrode spacing, which ensures more reliable mucosal contact; this design is in current use.

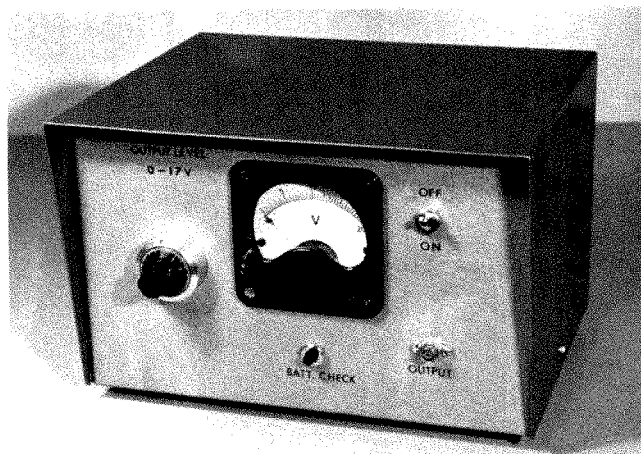


Fig. 1.—Battery-powered stimulator.

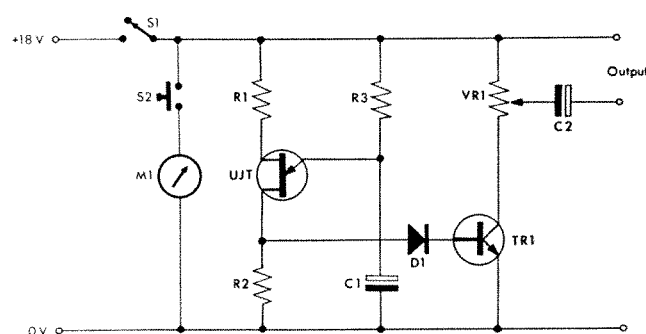


Fig. 2.—Circuit diagram of stimulator. R1, 120 Ω ; R2, 200 Ω ; R3, 2.2 k Ω ; C1 and C2, 10 + 10 F; UJT, 2N2646; D1, 1N914; TR1, 2N3904; VR1, 1 k Ω 10-turn potentiometer; M1, 0–20 V voltmeter; S1, on-off switch; S2, battery test switch.

The examination technique has been reported [1]. After the cannula is connected to the barium delivery tube, it is lubricated with petroleum jelly and inserted into the anal canal. The stimulator is switched on and the voltage increased by rotating the control knob until sphincteric contraction is seen. The voltage is then increased until the patient experiences a slight tingling sensation. In practice the lowest pulse amplitude used was 5 V, with frequent use of the maximum of 17 V in patients with weak sphincters; the average amplitude was 10 V. After anal contraction is seen, it is advisable to wait for approximately 1 min until a stable sphincteric contraction is established. The barium suspension and water, pre-heated to body temperature, is then instilled under fluoroscopic control. No colonic relaxants, such as anticholinergic drugs, are used. At the end of the examination the cannula is washed in Cetavlon and immersed in 1% Chlorhexidine in alcohol.

¹ Department of Radiology, Staffordshire General Infirmary, Stafford ST16 2PA, England.

² Department of Clinical Physics and Bio-Engineering, West of Scotland Health Boards, Glasgow, Scotland.

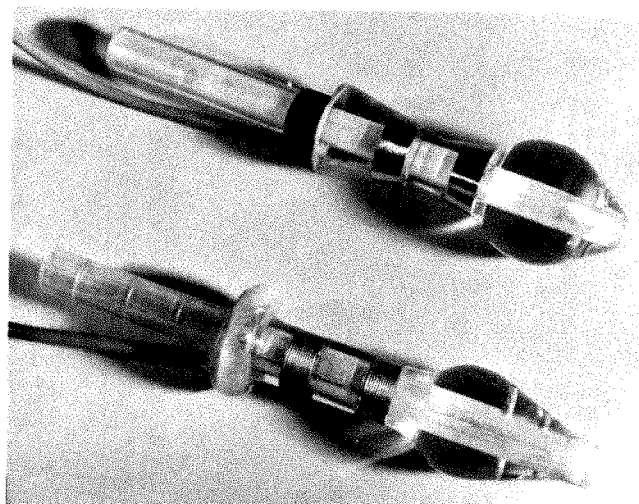


Fig. 3.—Barium cannulae used in trial. *Below*, original design; *above*, improved design (Cardiac Recorders, Ltd., London).

Clinical Trials and Results

The electronic cannula was used in 500 consecutive barium enema examinations conducted by one of us (K. Clark) at two hospitals, Glasgow Royal Infirmary and Staffordshire General Infirmary. As in the first series [1], failure is defined as inability to fill the cecum or to delineate an obstructing agent.

The control series consisted of 200 consecutive examinations, approximately half from each hospital (table 1). Use of two hospitals was considered essential to minimize confounding effects such as age range, social conditions, and technique. The Glasgow series was undertaken earlier without the use of disposable bags and syphonage. At Stafford a syphon technique using disposable equipment was routine.

The results of routine use of the cannula in 500 consecutive cases taken from the two hospitals are given in table 2. The overall failure rate of 4% represents a considerable improvement. An analysis of failures (table 3) shows that the two major contributing factors are fecal impaction and diverticular disease. In the control group, 22% had diverticular disease; in 52% of these cases the examination was unsuccessful. In the trial series the incidence of diverticular disease was 27% with an unsuccessful outcome in 5% of these cases. Our data confirm that failure of barium retention is more common in the elderly (table 3). The two younger patients in the group, aged 23 and 46 years, had complete fecal impaction.

Discussion

The encouraging results obtained in the preliminary trial have been confirmed. The failure rate of 4% at the two hospitals represents a significant improvement over the 20% failure rate in the control series. Results indicate that syphonage has no effect on success rate, although it is known that this technique reduces the incidence of soiling. The marked reduction in failure rate can therefore be attributed to the use of the electronic cannula.

TABLE 1
Conventional Barium Enema Examinations

	Glasgow	Stafford
No. consecutive examinations.....	100	100
Age range (yr).....	18–86	17–89
Average age (yr).....	56	57
No. failures.....	20	19
Failures rate (%).....	20	19

TABLE 2
Barium Enema Examinations with New Cannula

	Glasgow	Stafford
No. consecutive examinations.....	243	257
Age range (yr).....	19–83	12–91
Average age (yr).....	58	56
No. failures.....	9	11
Failure rate (%).....	3.7	4.3

TABLE 3
Analysis of Failures in Trial Series

Age and Cause of Failure	No.
Age (yr):	
Range.....	23–78
Average.....	70
Cause of failure:	
Fecal impaction.....	8
Diverticular disease.....	5
Both impaction and diverticular disease.....	2
No obvious cause.....	5
Total.....	20

Note.—Factors contributing to failure were poor sphincteric activity, hemiplegia, and carcinomatosis.

Unpleasant side effects were not encountered although, as in the first series, a number of patients experienced a prickling sensation as the voltage reached its optimum; this regresses after a few seconds. The strength of anal sphincter contraction produced at higher voltage amplitudes is insufficient for complete anal control in the presence of an obstructing agent such as fecal impaction, diverticular disease, or neoplasm. A dangerous and painful degree of bowel distension is thus avoided.

The equal incidence of failure among males and females suggests that perineal deficiency from childbearing is not a major factor. All these patients had poor sphincteric activity from various causes such as poor cerebral function or general debility. In the control series the examination had to be abandoned in only one patient under the age of 40 years, a very tense girl aged 23. We emphasize that for optimum results the new cannula should be used routinely in the older age group, with selective use in other cases in which sphincteric weakness is suspected.

The new stimulator, which has been in continuous use

for 4 years, proved to be completely reliable. The larger capacity of batteries used has resulted in less frequent renewal. The original cannula was constructed from a single piece of Perspex, while the improved version has a segmental construction. After continuous use with repeated immersion in alcohol and detergent, the segments separated on a few occasions; a satisfactory repair was effected with dental cement. The manufacturers have been informed of this problem.

The marked improvement in the technique resulting

from use of the cannula may encourage other radiologists to adopt this method of examination.

REFERENCES

1. Clark K: Barium enema examination using an electronic technique—a preliminary report. *Br J Radiol* 44:970-972, 1971
2. Hopkinson BR, Lightwood R: Electrical treatment of anal incontinence. *Lancet* 1:297-298, 1966
3. Rowan D: The treatment of impaired bladder function by electronic techniques. *Proc Inst Electron* 11:6-11, 1970

Radiographic Evaluation of Endotracheal Tube Position

LAWRENCE R. GOODMAN,¹ PETER A. CONRARDY,² FAYE LAING,³ AND MORLEY M. SINGER⁴

A malpositioned endotracheal tube is a potential hazard to the intubated patient. Ideally, the tube tip should be 5 ± 2 cm from the carina when the head and neck are in neutral position. In 92 of 100 patients studied, the carina overlay T5, T6, or T7 on portable radiographs. Therefore, even when the carina is not visible, it can be assumed that a tube tip positioned at the level of T3 or T4 is safe. The degree of neck flexion or extension at the time of radiography may be determined by evaluating the position of the mandible relative to the vertebral bodies.

Introduction

Endotracheal intubation may be a life saving procedure. However, a malpositioned endotracheal tube poses a serious threat to the intubated patient. Accidental right mainstem bronchus intubation, seen in as many as 10% of patients, is associated with left-sided atelectasis, right-sided tension pneumothorax, and decreased survival [1]. Conversely, failure to place the tube several centimeters beyond the vocal cords may result in inadvertent extubation, aspiration pneumonia, or laryngeal spasm [1]. Tube malposition is an even greater hazard in infants and children because of their short tracheas [2-4].

Conrardy et al. [5] demonstrated that neck flexion causes a 2 cm descent (range, 0.2-3.1 cm) of the endotracheal tube toward the carina. Similarly, neck extension causes a 2 cm ascent (range, 0.2-5.2 cm) of the tube tip from the carina. They suggested that the ideal distance between the endotracheal tube tip and the carina is 3 ± 2 , 5 ± 2 , and 7 ± 2 cm with the neck flexed, neutral, and extended, respectively.

These recommendations are often difficult to implement because the carina is not visible on every radiograph. In addition, the radiologist does not usually know the position of the patient's neck at the moment the radiograph was taken. The present study was undertaken to solve these problems.

Materials and Methods

Since the vertebral bodies are usually visible on most portable radiographs, even when the carina is not, we studied the location of the carina with respect to the vertebra. In the first 50 males and first 50 females on whom the carina was clearly visible, the position of the carina relative to the vertebra was ascertained. In the few patients where the vertebral bodies were difficult to count, the posterior ribs were counted and followed back to the vertebral bodies. All AP portable radiographs were made at 48 inches, with the central ray perpendicular to the film and the neck in neutral position.

To check the reproducibility of our method with regard to the variation in x-ray projection, 10 additional patients were studied. Each was chosen because his file contained 10 portable films

with both the carina and vertebra visible.

To assess the position of the head and neck at the time of examination, the location of the bottom of the bony mandible relative to the vertebral bodies was tabulated in 30 patients. All were prepositioned by the technologist: 10 in neutral, 10 in flexion, and 10 in extension.

Results

Position of Carina

Data from the 10 patients with 10 radiographs each revealed the carina-vertebral body relationship varied little from film to film (error standard deviation of 0.35 vertebral bodies). Among the 100 patients with single radiographs, the carina was over T6 or the T5-T6 or T6-T7 interspaces in 76 and between T5 and T7 in 92 (figs. 1 and 2). This distribution yielded a mean of T6 and standard deviation (including correction for the error standard deviation) of 0.6 vertebral bodies. Therefore, it can be predicted with greater than 90% confidence that the carina overlies T5, T6, or T7 on the portable radiograph.

No differences were found between the sexes. However, with increasing age the carina projects at a lower level. In the 10 youngest patients, the average carina position was over the T5-T6 interspace; for the 10 oldest, the carina was most often over the T6-T7 interspace.

Position of Mandible

In the neutral position, the mandible projected over C5 or C6 in every patient. The mandible was seen at the T1 level or below in all flexion films and above C3-C4 (or off the film) in all extension films (fig. 1).

Discussion

The radiograph is often the first indicator of endotracheal tube malposition. A routine radiograph should follow every endotracheal intubation because a malpositioned tube may not be detected clinically [2-5]. The following guidelines are recommended for diagnosis of endotracheal tube malposition.

1. With the neck in the neutral position (mandible over C5-C6), the ideal position for the endotracheal tube tip is 5 ± 2 cm from the carina.
2. With the neck flexed (mandible at T1 or below), the tube has descended as far as possible. Thus the ideal position is 3 ± 2 cm from the carina.
3. With the neck extended (mandible above C3-C4 interspace), the tube has undergone maximal ascent. The ideal position is 7 ± 2 cm above the carina.

¹ Department of Radiology, George Washington University Medical Center, 23d Street N.W., Washington, D.C. 20037. Address reprint requests to L. R. Goodman.

² Department of Radiology, Trinity Memorial Hospital, Cudahy, Wisconsin 53110.

³ Department of Radiology, San Francisco General Hospital, San Francisco, California 94110.

⁴ Department of Radiology, Presbyterian Hospital, San Francisco, California 94120.

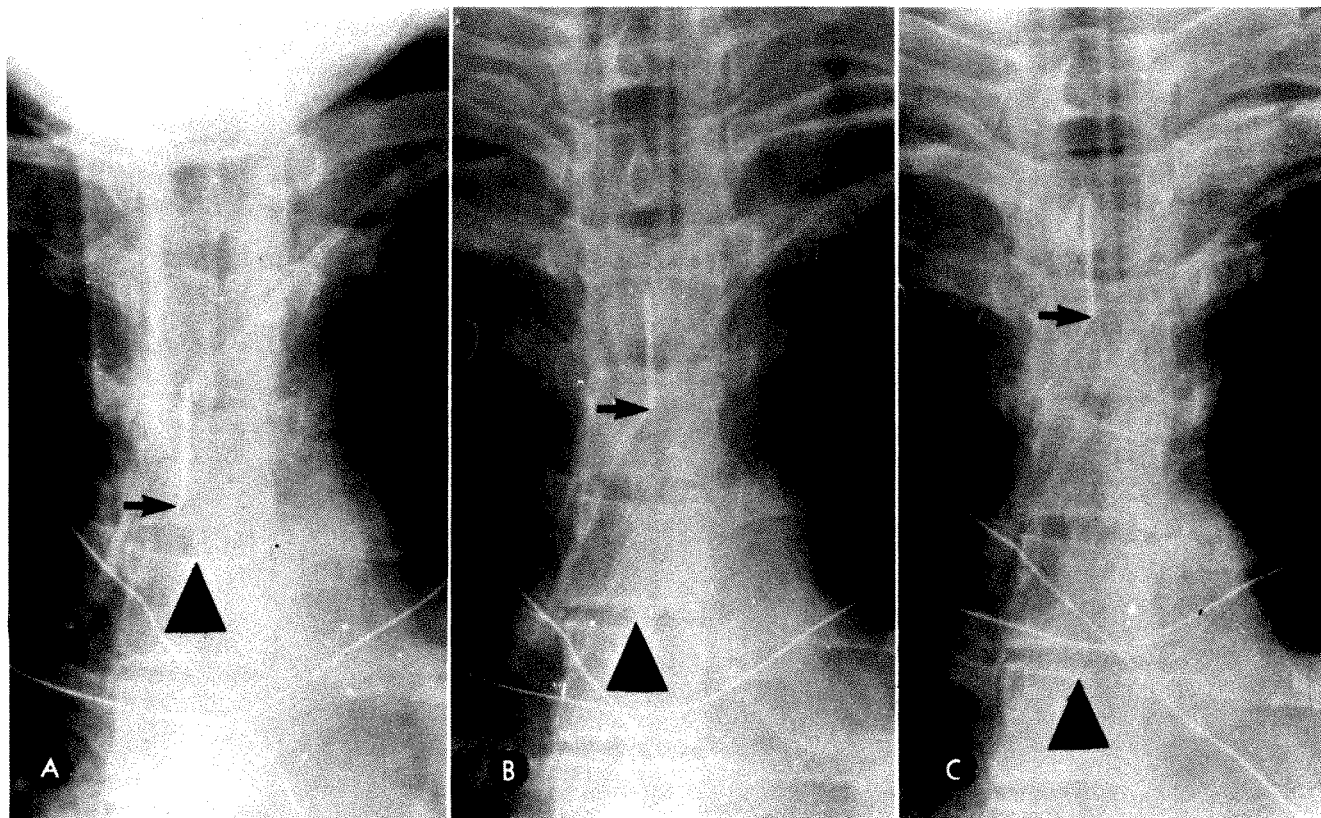


Fig. 1.—A, Neck flexed showing mandible over T1 and carina (arrowhead) at T5–T6 interspace. B, Neck in neutral position. C, Neck extended. Distance from tube tip (arrow) to carina measured 1.1, 4, and 6.5 cm, respectively.

4. Conrardy et al. [5] recommend placement of the endotracheal tube tip in the middle third of the trachea, with the neck in the neutral position. The vocal cords in adults are located at the C5–C6 level, and the carina was found at the $T6 \pm 1$ level in over 90% of the patients in this study. Therefore, when the carina cannot be visualized, ideal positioning of the endotracheal tube tip can be assumed to be at the T2–T4 level with the neck in the neutral position.

5. Tubes may migrate with time due to either the constant weight of the respirator apparatus or manipulation during suctioning [4, 5]. Thus periodic radiographic evaluation is essential.

A comprehensive review of the hazards of endotracheal intubation has been published [7].

ACKNOWLEDGMENT

We thank Mr. Kenneth Weaver for help in preparing this manuscript.

REFERENCES

1. Zwillich CW, Pierson DJ, Creagh CE, Sutton FD, Schatz E, Petty TL: Complications of assisted ventilation. *Am J Med* 57:161–170, 1974
2. Alberti J, Hanafee W, Wilson G, et al: Unsuspected pulmonary collapse during neuroradiologic procedures. *Radiology* 89:316–320, 1967

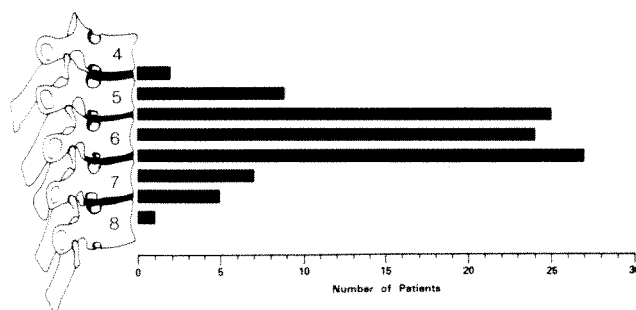


Fig. 2.—Position of carina relative to vertebral bodies on 100 portable chest radiographs.

3. Hamilton W, Stevens W: Malpositioning of endotracheal catheters. *JAMA* 198:1113, 1960
4. Tisi G, Twigg H, Moser K: Collapse of the left lung induced by artificial airway. *Lancet* 1:791–793, 1968
5. Conrardy P, Goodman L, Laing F, Singer M: Alteration of endotracheal tube position—flexion and extension of the neck. *Crit Care Med* 4:8–12, 1976
6. Kuhns LR, Poznanski AK: Endotracheal tube position in the infant. *J Pediatr* 78:991–996, 1971
7. Lewis R, Swerdlow M: Hazards of endotracheal anesthesia. *Br J Anaesth* 36:504–514, 1964

Further Observations on Pulmonary Venous Varix

JACK TWERSKY,¹ DAVID C. LEVIN,^{1,2} NAOMI TWERSKY,¹ AND DAVID H. GORDON¹

Pulmonary venous varix is a well known radiographic entity. Case reports are presented to illustrate the following unusual aspects of this lesion.

1. Hypoplasia of a major pulmonary vein results in increased pulmonary blood flow through the remaining normal ipsilateral pulmonary vein. This may result in variceal enlargement of the normal vein.

2. A pulmonary venous varix may be visualized during angiocardiology but not in a routine chest radiograph. This is most common in children.

3. Elevated pulmonary venous pressure causes dilatation of the central pulmonary veins. Sudden formation of a pulmonary venous varix in a patient with mitral valvular disease may be evidence of a sudden elevation of left atrial pressure.

Pulmonary venous varix, a localized dilatation of a pulmonary vein, is a rare occurrence. Most published reports have dealt with establishing the radiographic diagnosis. We recently observed several aspects of the lesion which have not previously been stressed: (1) a varix caused by anomalous pulmonary venous development; (2) a varix demonstrated by angiocardiology that was not detected on routine chest films; and (3) sudden enlargement of a varix indicating malfunction of a prosthetic mitral valve.

Anomalous Development of Pulmonary Veins

Case 1

N. J. M., a 51-year-old male, was admitted for evaluation of a curvilinear density near the left hilum on a routine chest radiograph (fig. 1). Angiography demonstrated normal pulmonary arteries (fig. 2A). The veins of both upper lobes had an abnormal course and configuration. The curvilinear density was an enlarged single pulmonary vein entering the left atrium (fig. 2B). No other pulmonary vein was present on the left side. Catheterization and angiography of this pulmonary vein via a patent foramen ovale revealed no obstruction at its entrance into the left atrium.

Comment

The normal development of pulmonary veins depends upon (1) development of a pulmonary venous plexus of the primordia of the lungs; (2) development of a common pulmonary vein from the superior wall of the left atrium; and (3) connection of the common pulmonary vein to the pulmonary venous plexus [1]. After the connection occurs, the common pulmonary vein becomes absorbed into the wall of the left atrium [2]. This process results in separate entry of four pulmonary veins into the left atrium. Rarely, stenosis of individual pulmonary veins may occur. The stenosis may be localized, usually at the junction of the vein and the left atrium, or the stenosis may be over a

long segment representing a hypoplastic pulmonary vein. In either form, clinical manifestations are insignificant when the stenosis involves a single vein [3].

We believe that case 1 represents an atresia or hypoplasia of the left inferior pulmonary vein, with passage of the entire left pulmonary venous flow through the single patent superior vein. The increase in flow has caused varicose enlargement of the remaining vein. To our knowledge, only two previous cases of this entity have been described in detail [4, 5]. Both were similar to our case. The patients were asymptomatic, presenting only with an abnormal chest radiograph demonstrating a nodule or curvilinear structure in the left lung. Angiography demonstrated a single left pulmonary vein. In reviewing the literature on pulmonary venous varices, we found two additional cases in which angiography demonstrated drainage of all the pulmonary venous flow from one lung via the varix [6, 7]. These cases, too, may represent atresia or hypoplasia of the ipsilateral pulmonary vein. Therefore, demonstration on plain chest radiographs of any structure thought to be a pulmonary venous varix should suggest the possibility of hypoplasia of an ipsilateral pulmonary vein. The pulmonary venous anatomy should be examined carefully at angiography for this anomaly.

Nondetection on Routine Chest Films

Case 2

B.D., a 14-year-old girl, was admitted to the hospital because of episodes of dizziness. Physical examination was negative except for a systolic and diastolic murmur characteristic of patent ductus arteriosus. A neurologic examination was within normal limits. Chest radiographs revealed cardiomegaly (fig. 3, A and B) but no venous anomaly.

Injection of contrast material into the main pulmonary artery revealed enlargement of the main pulmonary artery and its peripheral branches. During the late phase the pulmonary veins were well visualized with demonstration of a varicose right pulmonary vein attaching normally to the left atrium (fig. 3C). A second injection into the left atrium confirmed the patent ductus arteriosus.

Case 3

S. V., a 2-year-old female, was admitted for cardiac catheterization because of the presence of a cardiac murmur. The patient was first seen at 2 days of age when a diagnosis of esophageal stenosis and tracheoesophageal fistula, type 3B, was made. This was repaired with a satisfactory postoperative course.

The patient was not cyanotic and had no exercise intolerance. A loud systolic murmur was heard best in the left fourth intercostal space.

Chest x-ray revealed general cardiac enlargement (fig. 4A). No

¹ Department of Radiology, Downstate Medical Center, State University of New York, 450 Clarkson Avenue, Brooklyn, New York 11203. Address reprint requests to J. Twersky.

² Present address: Department of Radiology, Peter Bent Brigham Hospital, Boston, Massachusetts 02115.

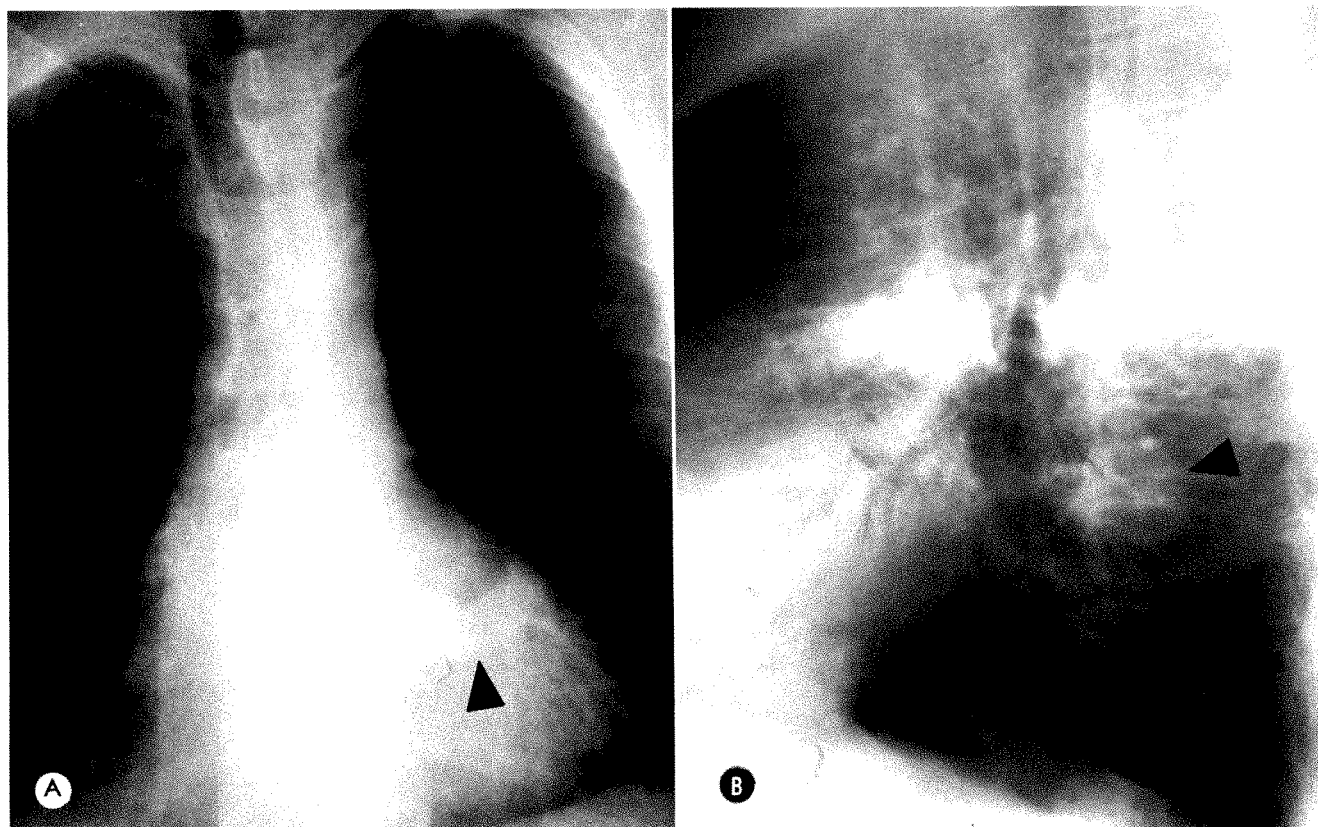


Fig. 1.—Case 1. Chest radiographs showing curvilinear density posterior to left heart (A) with its anterior border adjacent to left atrium (B). Thyroid enlargement accounts for left paratracheal mass.

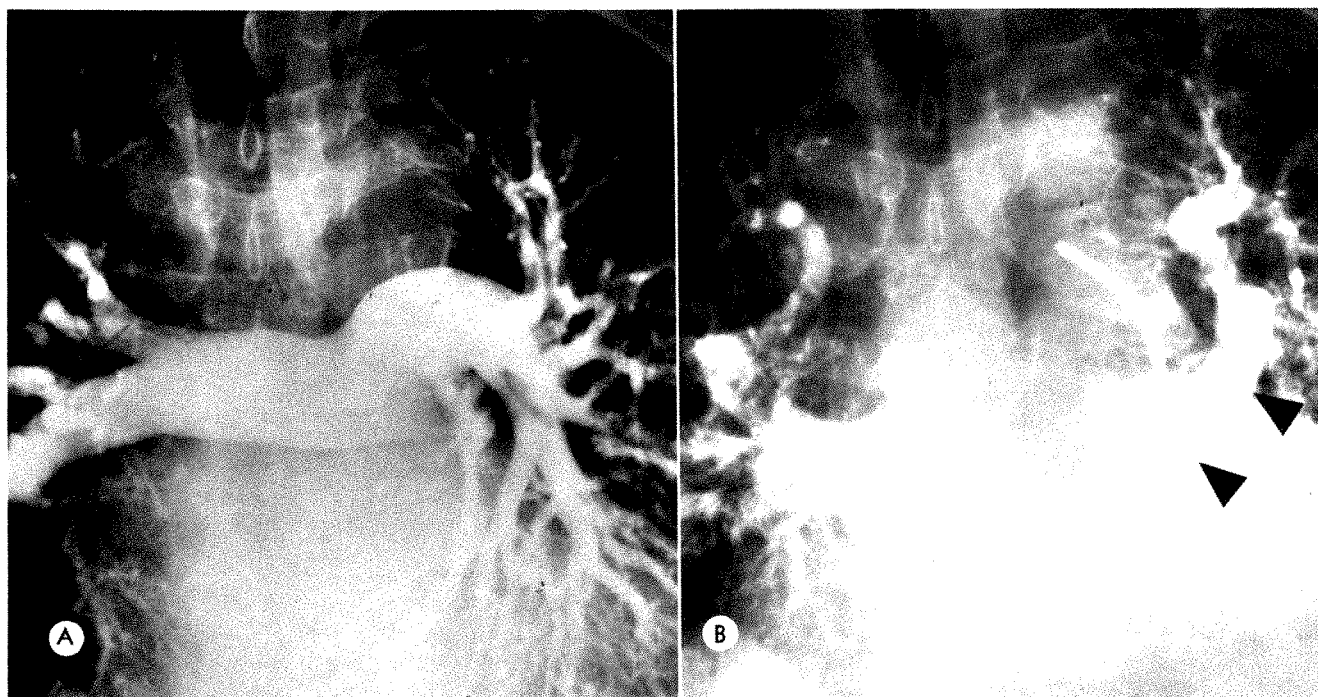


Fig. 2.—Pulmonary angiogram of case 1. A, Normal arterial phase. B, Venous phase revealing tortuous upper lobe veins in both lungs. Large single vein (arrows) drains entire left lung and enters into left atrium.

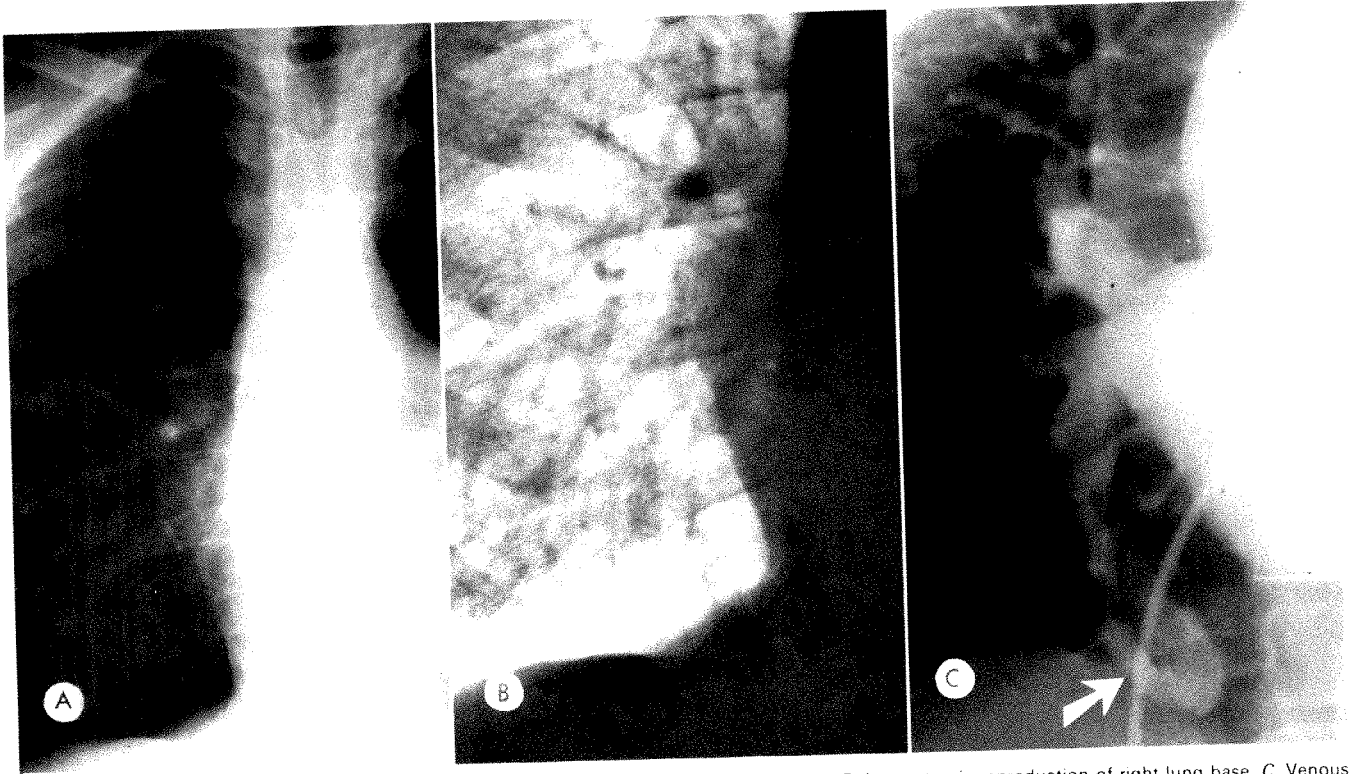


Fig. 3.—Case 2. *A*, Chest radiograph showing no evidence of unusual pulmonary densities. *B*, Log-e-tronic reproduction of right lung base. *C*, Venous phase of pulmonary angiogram of case 2 showing curvilinear varicose vein (arrow) draining medial basal segment of right lower lobe.

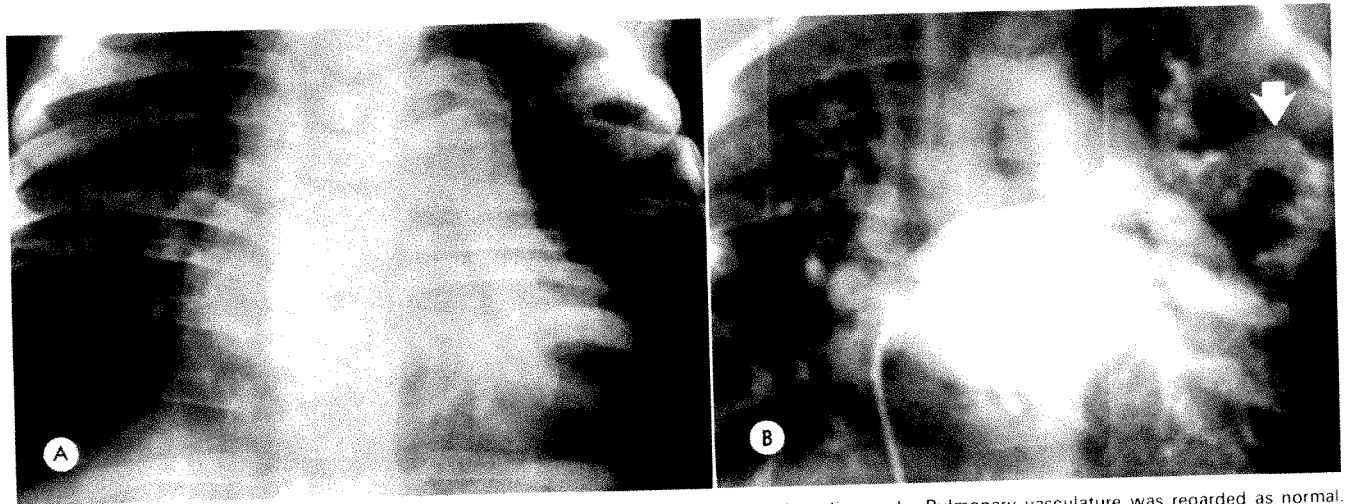


Fig. 4.—Case 3. *A*, Chest radiograph showing multiple rib anomalies and generalized cardiomegaly. Pulmonary vasculature was regarded as normal. *B*, Levophase of right ventricular angiogram demonstrating large varicose pulmonary vein in left midlung field (arrow). Major pulmonary veins all enter left atrium. They are dilated because of large left-to-right shunt.

abnormalities of pulmonary vasculature were suspected. An angiogram revealed a ventricular septal defect with a left to right shunt. A second injection made into the right ventricle revealed a thickened pulmonic valve with poststenotic dilatation of the main pulmonary artery and its branches. During the levophase a varicose pulmonary vein in the left lung was discovered having normal left atrial drainage (fig 4*B*).

Comment on Cases 2 and 3

The etiology of pulmonary venous varix is unknown. Klinck and Hunt [8] suggested that it represents a con-

genital anomaly of pulmonary venous development. In support of this, they described one case in which the varix increased in size over a 1½ year interval.

Three previous cases of pulmonary venous varix in children have been reported [6, 9, 10]. As in our cases, it was seen only on angiography and not on a routine chest radiograph. The association with congenital cardiac lesion [11] in childhood is probably coincidental, the veins being detected during cardiac angiography. In adults, most cases of pulmonary venous varix are isolated radiographic findings.

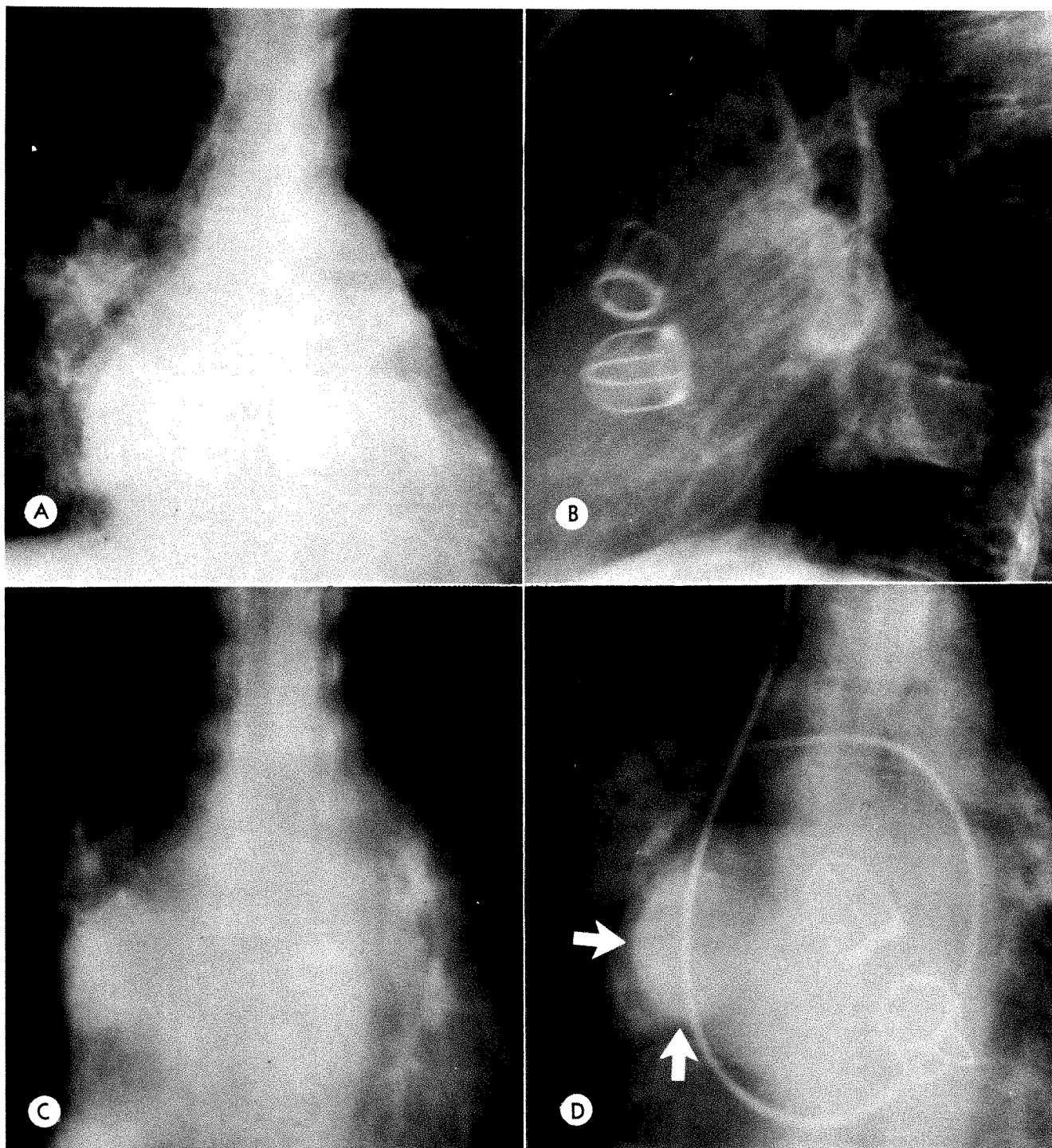


Fig. 5.—Case 4. *A and B*. Chest radiographs showing enlarged heart and dilated pulmonary veins. "Mass" is noted posterior to right side of heart. *C*. *AP* tomogram 2 months later delineating oval-shaped density posterior to right side of heart. *D*. Pulmonary angiogram revealing markedly dilated right upper lobe pulmonary vein at its junction with left atrium (arrows).

Only two cases of pulmonary venous varix unassociated with mitral valvular disease have been followed radiographically for extended periods [11]. These two adult cases, followed 4 and 15 years, respectively, showed no change in the size of the varix. If pulmonary venous varix is a congenital anomaly and present since birth, it probably

enlarges in life, accounting for the fact that most reported cases occur in adults. We hope to follow our two patients into adult life to determine whether enlargement occurs. This is of more than academic interest since two deaths have been reported due to rupture of pulmonary venous varices [8, 12].

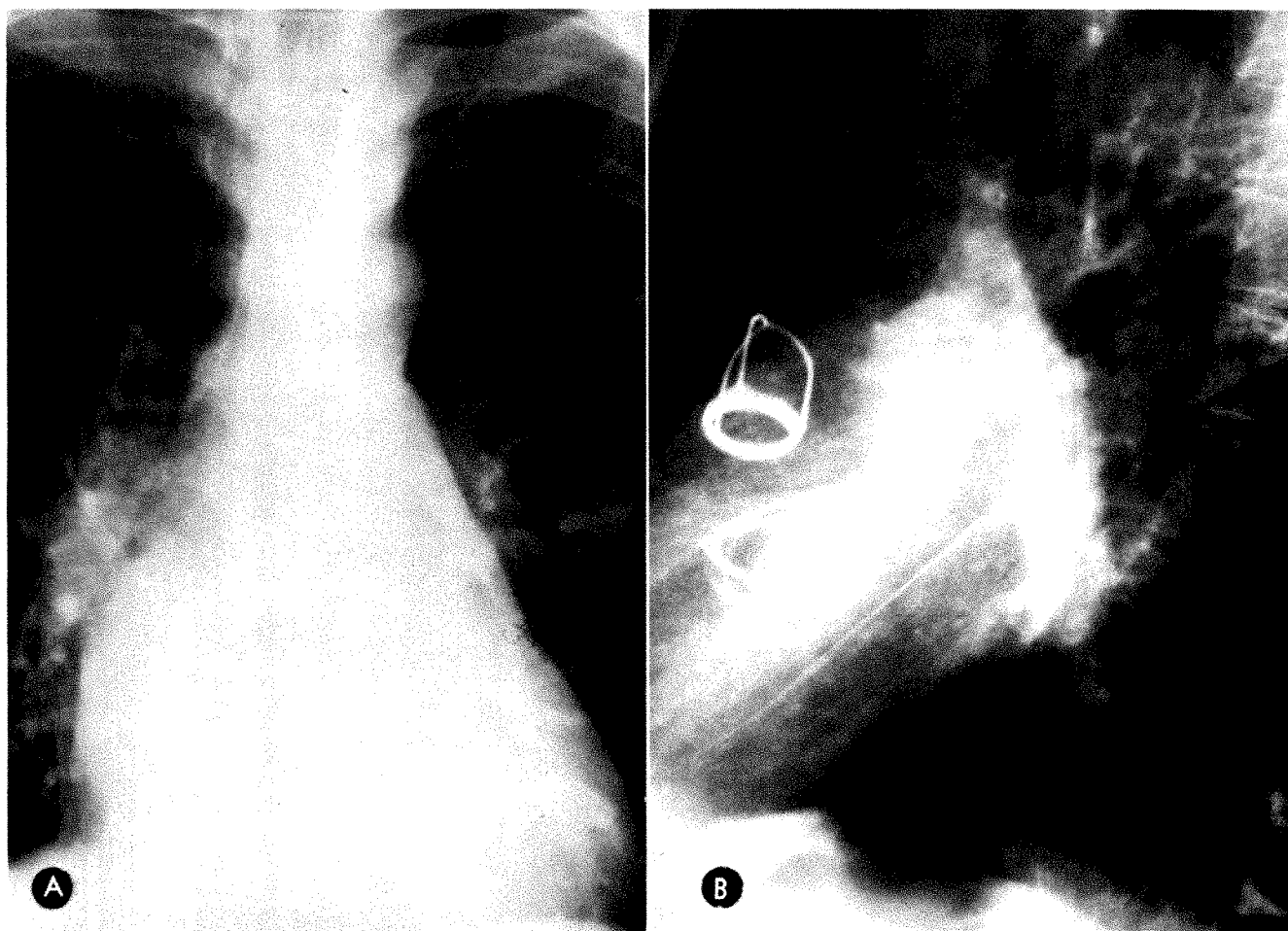


Fig. 6.—Chest films of case 4 after repair of broken suture line. Note considerable decrease in prominence of venous varix.

Malfunction of Prosthetic Mitral Valve

Case 4

R. G., a 34-year-old male, had rheumatic fever when 8 years old. In 1970 he underwent replacement of the aortic and mitral valves. Periodic chest radiographs in early 1971 revealed the typical configuration of a mitral heart with prosthetic aortic and mitral valves. A subsequent radiograph in September 1971 revealed a new 3 cm circular lesion behind the right heart (fig. 5, A and B). This was interpreted as a pulmonary venous varix. In November 1971, the patient presented with cough, blood-tinged sputum, and shortness of breath on moderate exertion. This led to lung tomography (fig. 5C).

Angiography corroborated the diagnosis of a pulmonary venous varix (fig. 5D). Left ventricular end diastolic pressure was 6 mm Hg. Prominent V waves suggested mitral insufficiency. The pulmonary artery pressure was 47/25 mm Hg, and the mean capillary pressure was 28 mm Hg, significantly higher than the previous value of 14 mm Hg immediately after aortic and mitral valve replacement. These findings were interpreted as dysfunction of the mitral valve.

At surgery, a paravalvular leak adjacent to the mitral prosthesis due to a torn suture was found; the suture line was repaired. The postoperative course was uneventful, and a repeat chest radiograph revealed marked decrease in size of the previously noted pulmonary venous varix (fig. 6).

Comment

Most pulmonary venous varices are situated in one of the four main pulmonary veins. Although a focal anatomic abnormality may exist, the localization of the varices in veins of largest diameter can be explained by the law of Laplace, which states that the pressure required to distend a cavity is inversely proportional to the radius of the cavity. Therefore, with equal pressure throughout a vein, enlargement will occur in the part with the largest diameter. With increase in pulmonary venous pressure, dilatation of the central veins occurs. In a study of pulmonary veins in rheumatic heart disease, Ormond and Poznanski [13] found a progressive increase in size of the superior veins as the left atrial pressure increased and an increase in size of the inferior veins up to a maximum at 17 mm Hg left atrial pressure.

Four previously reported cases of pulmonary venous varix [11, 14, 15] have been associated with rheumatic heart disease. Gottesman and Weinstein [15] reported a patient with a pulmonary venous varix in conjunction with worsening of rheumatic mitral stenosis. A mitral commissurotomy led to relief of symptoms, but the varix remained unchanged over a 10 year period. Hipona and

Jamshidi [11] reported progressive enlargement of a pulmonary venous varix in a patient with progressively worsening mitral insufficiency over a 7 year period. Prosthetic replacement of the mitral valve led to a decrease in size of varix.

In our case, the varix may have antedated clinical symptoms of a malfunctioning mitral valve prosthesis, but its enlargement was probably related to the sudden increase in pulmonary venous pressure from leakage around the mitral valve. The dramatic postoperative decrease in size of this varix corroborates the direct relationship between venous pressure and variceal size. Sudden formation of a pulmonary venous varix in a patient with mitral valvular disease should be considered evidence of a sudden elevation of left atrial pressure.

REFERENCES

1. Wagenvoort CA, Heath D, Edwards JE: *The Pathology of the Pulmonary Vasculature*. Springfield, Ill., Thomas, 1964
2. Neill CA: Development of the pulmonary veins. *Pediatrics* 18:880-887, 1956
3. Nakib A, Moller JH, Kanjub VI, Edwards JE: Anomalies of the pulmonary veins. *Am J Cardiol* 20:77-90, 1967
4. Benfield JR, Gots RE, Mills D: Anomalous single left pulmonary vein mimicking a parenchymal nodule. *Chest* 59:101-103, 1971
5. Tretheway DG, Francis GS, MacNeil DJ, Vieweg WVR: Single left pulmonary vein with normal pulmonary venous drainage; a roentgenographic curiosity. *Am J Cardiol* 34:237-239, 1974
6. Bartram C, Strickland B: Pulmonary varices. *Br J Radiol* 44:927-935, 1971
7. Papamichael E, Ikkos D, Alkalais K, Yannacopoulos J: Pulmonary varicosity associated with other congenital abnormalities. *Chest* 62:106-108, 1972
8. Klinck GH, Hunt HD: Pulmonary varix with spontaneous rupture and death. *Arch Pathol* 15:227-237, 1963
9. Steinberg I: Pulmonary varices mistaken for pulmonary and hilar disease. *Am J Roentgenol* 101:947-952, 1967
10. Vengsarkar AS, Kincaid OW, Weidman WH: Selective angiography in diagnosis of varicosity of the pulmonary veins. *Am Heart J* 66:396-398, 1963
11. Hipona FA, Jamshidi A: Observations on the natural history of varicosity of pulmonary veins. *Circulation* 35:471-475, 1967
12. Penet L, Fortelius P: Ruptured aneurysm of a pulmonary vein. *Acta Tuberc Scand* 41:53-55, 1961
13. Ormond RS, Poznanski AK: Pulmonary veins in rheumatic heart disease. *Radiology* 74:552-549, 1960
14. Bryk D, Levin EJ: Pulmonary varicosity. *Radiology* 85:834-837, 1965
15. Gottesman L, Weinstein A: Varicosities of the pulmonary veins. *Dis Chest* 35:322-327, 1959

Pulmonary Metastases from Benign-appearing Smooth Muscle Tumors of the Uterus

DONALD BACHMAN¹ AND MARIANNE WOLFF²

A 42-year-old woman was found to have multiple pulmonary nodules 7 years after hysterectomy for leiomyoma. Thoracotomy revealed multiple well differentiated smooth muscle masses containing epithelial inclusions. This patient is similar to others previously reported as examples of "multiple pulmonary fibroleiomyomatous hamartoma" on the basis of slow-growth, benign-appearing histology, and the presence of epithelial elements. Evidence is presented which suggests that these cases represent metastasis from well differentiated leiomyosarcomas. There is a frequent association with uterine smooth-muscle tumor, cases with equally benign-appearing histology have shown lymph node metastasis, the nonmesenchymal elements have been shown to represent engulfed bits of adjacent pulmonary tissue, and the histologic differentiation of benign from malignant mesenchymal tumors is known to be unreliable in some cases. Unlike more anaplastic leiomyosarcomas, this condition may be associated with few symptoms and prolonged survival despite widespread disease.

The histologic criteria by which benign and malignant smooth muscle tumors are distinguished are not always definitive. In a woman who has had surgical excision of a benign-appearing uterine leiomyoma or is clinically suspected of having a lesion, radiographic detection of pulmonary nodules should suggest the possibility that metastatic spread from the uterine tumor might have occurred. If no infective cause for the lung findings or apparent primary malignant focus is found, thoracotomy may be necessary to establish the diagnosis. The lung metastases may appear as histologically benign as the primary uterine tumor. We have recently seen such a case.

Case Report

A 42-year-old woman was noted to have multiple left pulmonary nodules in March 1973 during preoperative evaluation for a left breast mass. She had undergone total abdominal hysterectomy at this hospital 7 years earlier because of uterine enlargement and brisk intermenstrual bleeding. At operation, the uterus was 10–12 week size and contained several tan intramural masses. No serosal implants were seen, and no extrauterine pathology was noted. On section, the tumors showed partly hyalinized smooth muscle cells in a whorled pattern, consistent with benign leiomyomata. Post-operative follow-up visits for 3 years revealed no symptomatology, and a chest x-ray in July 1966 (not available for reevaluation) was interpreted as being within normal limits.

In March 1973 she was seen because of a gradually enlarging painless left breast mass first noticed by the patient 2 years earlier. She had remained well otherwise except for a mild cough noted 2 weeks before her visit. Admission chest films showed three non-calcified rounded densities in the left lung measuring 1–2 cm in diameter. These were assumed to represent metastases from a

breast lesion (fig. 1). Tomographic sections revealed a total of six noncalcified parenchymal densities, all in the left lung, 0.5–2 cm in diameter. No pleural or bronchial involvement was seen. Intermediate strength tuberculin skin testing was positive; other fungal skin tests were negative. Metastatic evaluation including intravenous urography, upper gastrointestinal series, barium enema, liver scan, and skeletal survey were negative. Breast biopsy revealed a typical fibroadenoma with no evidence of bizarre cells or mitoses.

Because the nature of the lung nodules remained unexplained, a left thoracotomy was performed in May 1973. Five smooth tan-white nodules were found and easily shelled out from the upper and lower lobes. They measured 0.9–1.9 cm in diameter and consisted of well demarcated nonencapsulated masses of tissue in smooth interlacing bundles, suggestive of leiomyomas. Although they appeared bland, they were diagnosed as metastatic leiomyosarcoma on the basis of location and history, reinforced by mild histologic atypia. Three small remaining nodules were visualized on post-operative chest x-rays. Follow-up tomograms over a 2 year period showed slight growth of these masses.

It was elected to reexplore the left chest in January 1975. Six nodules were found in the left upper lobe and were shelled out. Several of these appeared cystic (fig. 2). The patient made an uneventful recovery. Follow-up chest radiographs in August 1975 revealed a 1 cm nodule at the apex of the right lung (fig. 3) which was noncalcified on tomography. The left lung was clear. No change was noted in February 1976 when the patient was last radiographed.

Histologically, the nodules from both thoracotomies appeared similar. They consisted of closely packed bundles of well differentiated smooth muscle cells, with moderate amounts of fibrous and vascular tissue (figs. 4A and 4B). No cartilage or adipose tissue was seen. In each of the nodules, cleftlike spaces lined by cuboidal or ciliated columnar epithelium were noted. Three of the nodules had large epithelial-lined cysts filled with fluid. Enlargement of the cysts may have explained the apparent growth of the lesions removed at the second thoracotomy.

On high power, the nodules were seen to consist of plump, spindle-shaped cells having cigar-shaped nuclei and longitudinal fibrils within the cytoplasm visible on Masson trichrome stain. Rare mitotic figures were observed (less than 10 per 10 high power fields). Electron microscopy demonstrated immature cells dispersed among well differentiated smooth muscle cells, more suggestive of malignancy than the routine sections (fig. 4C).

Discussion

This is an unusual case of metastatic leiomyosarcoma because of the relatively benign course. The histology of the original uterine lesion did not suggest malignancy (a single slide was available for review), and it was largely on the basis of lung metastasis that her disease was differentiated from benign leiomyoma.

¹ Department of Radiology, Columbia-Presbyterian Medical Center, New York, New York 10032.

² Division of Surgical Pathology, Department of Pathology, Columbia-Presbyterian Medical Center, New York, New York 10032.

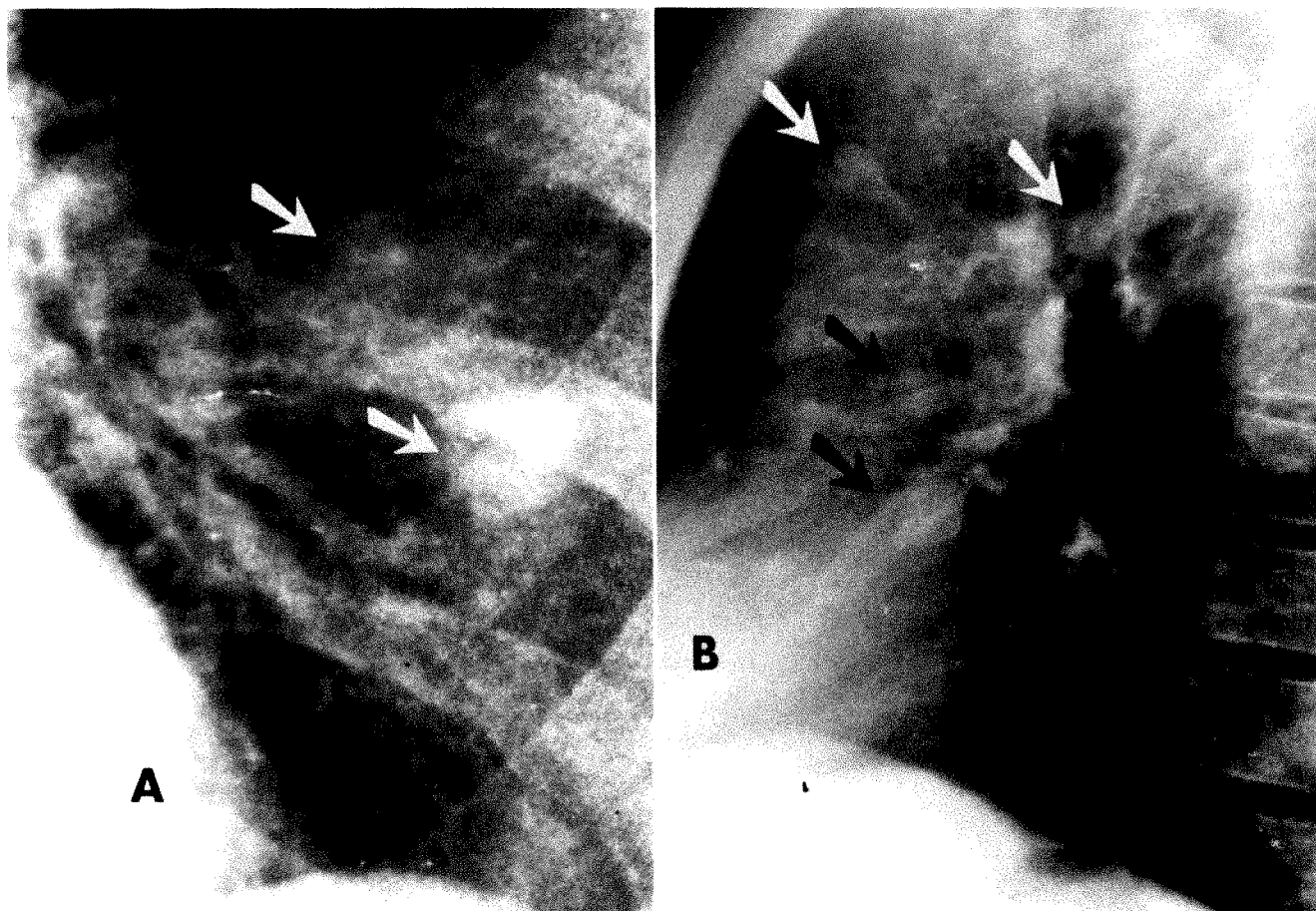


Fig. 1.—Left anterior oblique (*A*) and lateral (*B*) views (March 1973) showing round, noncalcified parenchymal nodules in left lung. Arrows indicate nodules.

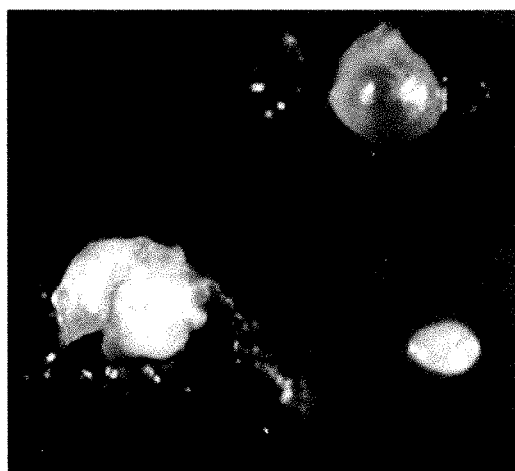


Fig. 2.—Gross specimen of nodules excised at second thoracotomy. Upper nodule is cystic and measured 0.7 cm.



Fig. 3.—Radiograph in August 1975 showing 1 cm nodule at right apex.

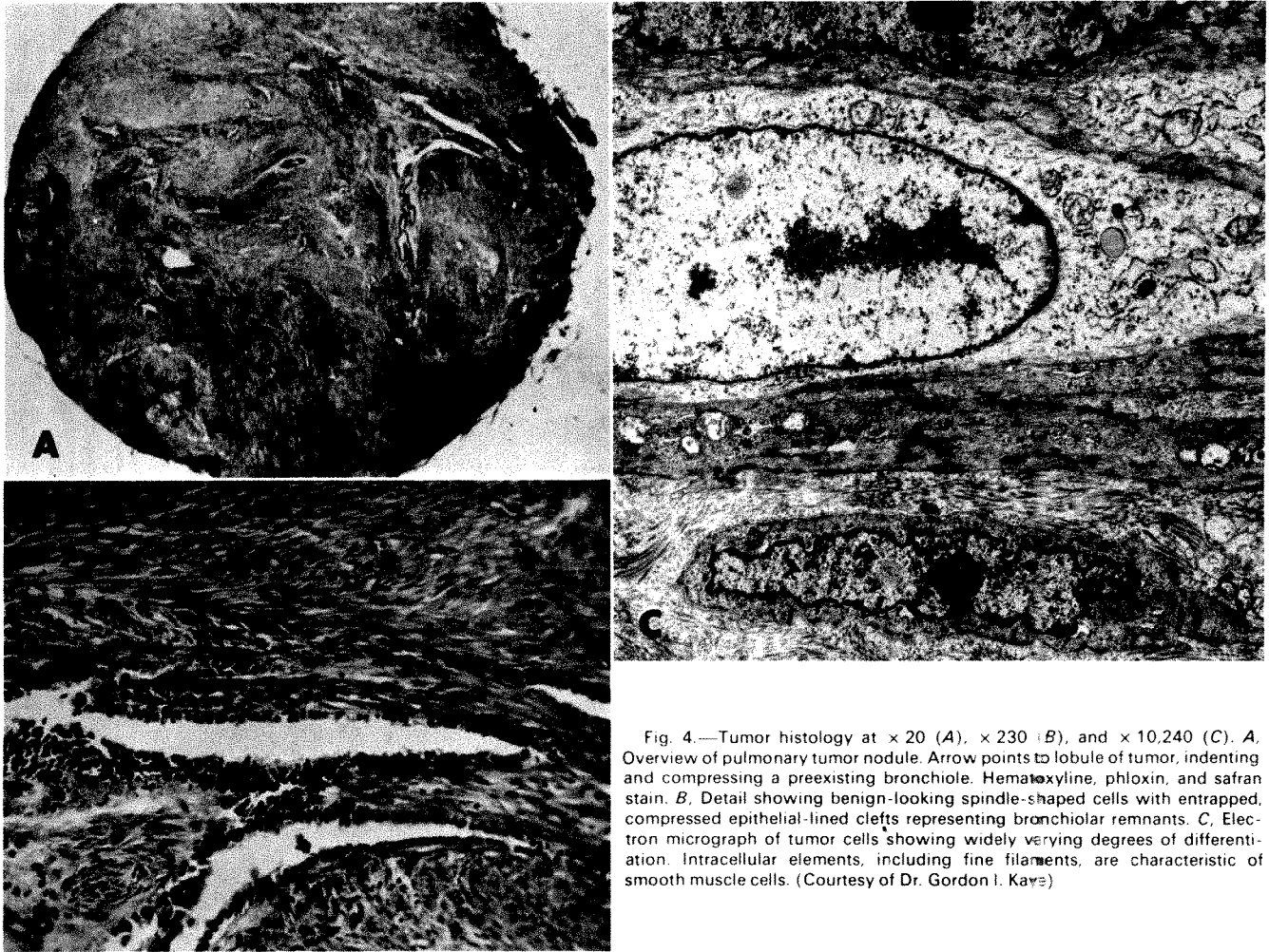


Fig. 4.—Tumor histology at $\times 20$ (A), $\times 230$ (B), and $\times 10,240$ (C). A, Overview of pulmonary tumor nodule. Arrow points to lobule of tumor, indenting and compressing a preexisting bronchiole. Hematoxyline, phloxin, and safran stain. B, Detail showing benign-looking spindle-shaped cells with entrapped, compressed epithelial-lined clefts representing bronchiolar remnants. C, Electron micrograph of tumor cells showing widely varying degrees of differentiation. Intracellular elements, including fine filaments, are characteristic of smooth muscle cells. (Courtesy of Dr. Gordon I. Kavz)

In a review of 105 cases of uterine leiomyosarcoma from the Mayo Clinic, Aaro et al. [1] found that only two patients survived 3 years or more when the disease extended beyond the uterus. They correlated survival with histologic grading (based primarily on a count of the number of mitoses found) and contended that abnormal tumor cells could be found in all cases. In a review of the Armed Forces Institute of Pathology archives, Taylor and Norris [2] reported a median survival of only 10 months for patients with uterine leiomyosarcoma and noted the lungs to be the most common site of extrapelvic spread in autopsied cases. They found no instance of recurrence or metastasis in tumors containing less than 10 mitoses per 10 high power fields and used this to differentiate sarcoma from cellular leiomyoma. They did illustrate one case in which a patient dying of pulmonary metastases had primary and metastatic lesions that looked quite benign except for an elevated mitotic count.

One rare exception to the bleak outlook generally expected was the case reported by McEachern et al. [3]. The patient underwent resection of a pulmonary metastasis 2 years after removal of an anaplastic-appearing uterine leiomyosarcoma; 40 months later she was well without recurrence.

We found 10 reports since 1939 of the so-called benign metastasizing leiomyoma [4–13] (table 1), a term which would best be abandoned in favor of well differentiated leiomyosarcoma. Willis [6] states that the leiomyomas (like osteoclastoma of bone, enchondromas, and slow-growing salivary gland tumors) include "black sheep in innocent families." "On rare occasions tumors of these kinds, though clinically and histologically differing little or not at all from their innocent fellows, surprise us by metastasizing, and their metastasis may present an 'innocent' histological structure" [6, p. 19]. A case is described in which two benign-looking pulmonary metastases were noted in a 46-year-old woman 3 years after hysterectomy for an apparently benign leiomyoma [6, p. 736].

A. Liebow (personal communication 1974) stated that he had collected 17 cases of "leiomyoma of the lung" in females, all who had undergone hysterectomy or myomectomy. Excised lung nodules in these cases looked histologically benign or, in a few cases, showed modest degrees of anaplasia. The clinical progress of the nodules has been variable, with several cases having been followed for prolonged periods. One patient had multiple nodules on a chest radiograph at the time of hysterectomy in 1949 and died of unrelated causes in 1974. Another was noted in

TABLE 1
Cases of Metastases to Lung from Benign-Appearing Uterine Leiomyoma

Reference	Age When Pathology Noted		No. and Location of Lung Nodules	Course
	Lung	Uterine		
Steiner [4].....	36	Postmortem	Many, bilateral	Died after 18 months
Hussy [5].....	42	Postmortem	1 in each	Died during thoracotomy
Willis [6].....	46	44	1 mass in each	Died after 1 year
Ariel and Trinidad [7].....	40	39	4, right	Well with two nodules after 6 years
Konis and Belsky [8].....	36	29	1, right	Well postoperatively; no recurrence
Spiro and McPeak [9].....	41	41	1, left	Well without recurrence after 10 years
Piccaluga and Capelli [10].....	50	Postmortem	Many, bilateral	Died of respiratory insufficiency after 8 years
Lafeyvre et al. [11].....	57	48	Many, bilateral	Died of lung cancer after 25 years
Kaplan et al. [12] (case 2).....	40	37	Many, bilateral	Dyspneic after 7 years; nodules larger
Boyce and Buddhdev [13].....	36	36	Many, bilateral	Died after 4 years

TABLE 2
Cases Termed Multiple Pulmonary Fibroleiomyomatous Hamartoma or Leiomyoma

Reference	Age When Pathology Noted		No. and Location of Lung Nodules	Course
	Lung	Uterine		
Sherman and Malone [22] (case 3) ..	41	41	1, left	Well at 1 year
Glennie et al. [15].....	46	30	Many, bibasilar	Lesions unchanged after 6 years
Laustela [16].....	43	42	6, left	Slow growth for 1 year; well after thoracotomy
Logan et al. [17].....	46	*	2 in each	Well after 2 years
Spotnitz and Hopeman [18].....	42	*	Many, bilateral	Asymptomatic; lung unchanged after 17 months
Inberg et al. [23].....	54	40	1, right	Well at 8 months; lung clear
Sargent et al. [19].....	49	29	2 in each	Well after 6 years; slow growth of remaining nodule
Kaplan et al. [12] (case 1).....	64	34	Many, right	Not given
Sulser and Buhler [20].....	45	32	Many, bilateral	Lived 36 years with extensive lung involvement
Becker et al. [21].....	48	41	Many, bilateral	Well after 8 months
Keers and Smith [24].....	50	†	Many, bilateral	Well with disease after 2 years
Madani et al. [25].....	50	†	8, bilateral	Followed 11 years with slow growth of lesions
Ramchand and Baskerville [26].....	51	‡	2, right	Not given
Clizer and Daughtry [27].....	49	†	3, left	Well after 4 years

* Prior, time not stated.

† No mention.

‡ Adnexal mass, not biopsied.

1962 to have multiple pulmonary nodules 20 years after hysterectomy and still remained in good health 12 years later.

In the cases listed in table 1, the lung lesions were generally found incidentally or in the evaluation of non-specific findings such as dyspnea or dry cough. Lung lesions were found up to 9 years after hysterectomy. The range at the time of detection was 36–64 years.

Radiographic findings included variable numbers of discrete masses, 0.5–7 cm in diameter, appearing round or lobulated. Pleural or bronchial involvement was not observed, and the parenchyma between nodules was normal with the exception of Steiner's [4] case in which obstructive emphysema was noted. Calcifications were not observed. Numerous nodules of varying size covered the lung fields in some cases [4, 10, 11, 13], while others presented with single large masses [8, 9], solitary bilateral nodules [5], and masses confined to one lung [7].

The histology of the pulmonary nodules was strikingly uniform, consisting of well demarcated masses of smooth muscle and connective tissue with few or no observed

mitoses. Engulfed bits of bronchial or alveolar epithelium were commonly noted as clefts or fluid-filled cysts.

The prognosis was excellent when only a few nodules were seen. With florid pulmonary involvement, both rapid decline and long term survival were noted. In one case, a pregnant woman with lung and retroperitoneal lymph node involvement, improvement with regression of metastases after termination of pregnancy was seen, but she relapsed and died of renal failure 4 years later [13]. Survival with no evidence of disease as well as with residual nodules has been seen. Several of the cases had similarly benign-appearing metastases outside the lungs, including retroperitoneal [13] and properitoneal [4], lymph nodes, great vessels of the thorax [5], and invasion of pelvic veins [4, 8, 9].

Differential Diagnosis

The benign histologic appearance and occasional long clinical course in the cases discussed have led to differences in diagnostic interpretation. In eight reported cases [12, 15–21] multiple benign-looking smooth muscle

tumors of lung in women who had undergone removal of uterine "fibroids" were diagnosed as multiple pulmonary "fibroleiomyomatous hamartomas" or as multiple primary pulmonary leiomyomas. These cases are listed in table 2 along with two cases of a single pulmonary smooth muscle tumor found after hysterectomy [22, 23]. These cases were clinically similar to those in table 1, the lesions generally being found incidentally. Multiple lesions were found in one or both lungs in five cases [12, 15, 18, 20, 21] and ranged from one to six in number in the remainder. They were noncalcified, round or lobulated, and measured 0.5–5 cm in diameter. All patients were middle-aged or elderly, with eight of 10 in their forties.

The histology was identical with the first group, consisting of benign-appearing bands of smooth muscle and connective tissue with few or no mitotic figures. Epithelial inclusions or clefts were again seen frequently [12, 18, 20, 21, 23, 26], and no cartilage or calcification was noted. Small foci of adipose tissue were seen in one nodule [17]. In contrast to the previous group, no deaths due to the pulmonary disease were reported. Residual lung nodules after thoracotomy were seen to grow slightly or remain static.

Table 2 includes four additional cases [24–27] with multiple pulmonary leiomyomatous pulmonary nodules in which pelvic pathology or prior surgery is not mentioned. All were middle-aged females. No reported cases of multiple pulmonary leiomyomas or "fibroleiomyomatous hamartomas" were found in males or in patients under the age of 30.

In several of the cases in table 2, the possibility that the lung lesions represented metastases from the uterus was considered but rejected. Glennie and co-workers [15] felt that the 16 year interval between hysterectomy and the discovery of lung lesions in their patient excluded uterine metastases. Kaplan et al. [12] applied similar reasoning in the first of two cases they reported. Laustela [16] and Sulser and Buhler [20] cited the presence of epithelial clefts within the tumor nodules as evidence that these tumors were hamartomas. Sargent, et al. [19] raised the additional objection that in most cases only the lungs were involved. They also cite the lack of apparent anaplasia in the cases they reviewed. Although they considered their case to represent fibroleiomyomatous hamartomas of the lung, A. Liebow (University of California, San Diego) had reviewed it and felt it represented metastatic uterine leiomyosarcoma.

We take exception to the objections cited above and feel that most, if not all, of the cases reported as multiple pulmonary fibroleiomyomatous hamartoma or leiomyoma in fact represent metastases from leiomyosarcoma. In view of the well differentiated histology, a long and indolent course is not surprising and should not exclude metastatic disease. In regard to the epithelial clefts that have been so commonly reported at the periphery of the nodules, the work of Piccaluga and Capelli [10] demonstrated that they were not intrinsic to the tumors. The elegant three-dimensional reconstructions in their paper showed that the masses, growing in a plexiform fashion, isolated and then incorporated bits of the surrounding lung tissue. Cyst formation is readily explained by continued secretion of mucus by the

trapped epithelial elements.

As we previously mentioned, concomitant extrapulmonary metastases have been observed. In addition, benign-appearing metastases from the uterus without lung involvement have been reported in the retroperitoneum by Spiro and McPeak [9] and in the paraaortic lymph nodes by Idelson and Davids [28]. Both of these authors discuss the possible, albeit controversial, relevance of invasion of pelvic venous channels by benign-appearing uterine leiomyomas. A. Liebow (personal communication, 1974) mentioned that he had seen bland-appearing pulmonary metastases in men with well differentiated leiomyosarcoma. A report of similar cases is forthcoming from our institution.

True pulmonary hamartomas are quite unlike the "fibroleiomyomatous" ones described. They are the most common of benign lung tumors. [29]. Cartilage is the most ubiquitous cellular element along with a multiplicity of other tissues [14]. Calcification is common and multiple tumors are an exceptional occurrence, with no more than two nodules in the same patient [30] having been reported in large series. Bragg and Levene [29] emphasized the frequency of a subpleural location and preponderance of male patients, and Gudbjerg's [31] radiologic study of 10 cases noted frequent bronchial involvement.

Less common is the true pulmonary leiomyoma. In the comprehensive reviews by Sweet [32] and Weitzner [33], no acceptable cases of multiple primary tumors were found. The case presented by Castleman and Kibbee [34] of a woman dying with multiple skin and lung leiomyomas is a possible exception, although one of the lung nodules showed frank sarcomatous changes. Unlike the metastatic smooth muscle tumors we have studied, the primary pulmonary leiomyomas often affect men, are seen from the first decade of life, and are frequently intrabronchial in location. These tumors grow by compressing surrounding lung and have not been seen to incorporate epithelial elements. However, Pierce et al. [35] make the valid point that it would be difficult to know whether a solitary pulmonary leiomyoma was primary or metastatic if it were found in a woman with leiomyomatous disease of the uterus.

Pulmonary lymphangiomatosis [36, 37], a rare lesion occurring in young women, is included in the histologic differential diagnosis. It too appears as a proliferation of smooth muscle tissue, but its widespread distribution in the perilymphatic spaces is quite different. The roentgenographic appearance, consisting of interstitial thickening, chylous effusions, and occasional pneumothorax, differs from the cases we have described.

The electron microscopic findings in our case helped reinforce the diagnosis of low grade leiomyosarcoma with metastasis. This approach may be of value in future cases when multiple smooth muscle tumors are found and the light microscopical appearance and mitotic count do not resolve the question of malignancy.

REFERENCES

1. Aaro LA, Symmonds RE, Dockerty MB: Sarcoma of the uterus. *Am J Obstet Gynecol* 94:101–109, 1966

2. Taylor HB, Norris HJ: Mesenchymal tumors of the uterus IV. diagnosis and prognosis of leiomyosarcomas. *Arch Pathol* 82: 40-44, 1966
3. McEachern CG, Gitlin MM, Sullivan RE: Lobectomy for metastatic leiomyosarcoma of the uterus. *JAMA* 174:1734-1735, 1966
4. Steiner PE: Metastasizing fibroleiomyoma of the uterus; report of case and review of literature. *Am J Pathol* 15: 89-109, 1939
5. Hussy P: Malignes Myom. *Zentralbl Gynecol* 64: 1540-1543, 1940
6. Willis RA: *Pathology of Tumors*, 3d ed. London, Butterworths, 1960
7. Ariel IM, Trinidad S: Pulmonary metastasis from a uterine "leiomyoma." *Am J Obstet Gynecol* 94: 110-116, 1966
8. Konis EE, Belsky RD: Metastasizing leiomyoma of the uterus: report of a case. *Obstet Gynecol* 27: 442-446, 1966
9. Spiro RH, McPeak CJ: On the so-called metastasizing leiomyoma. *Cancer* 19: 544-548, 1966
10. Piccaluga A, Capelli A: Fibroleiوماتosi metastizzante dell'utero. *Arch Ital Anat Istologia Patol* 16: 99-104, 1967
11. Lefebvre R, Nawar T, Fortin R, Genest J: Leiomyoma of the uterus with bilateral pulmonary metastasis. *Can Med Assoc J* 105: 501-503, 1971
12. Kaplan C, Katoh A, Mikihiro S, Rogow E, Scott J, Cushing W, Cooper J: Multiple leiomyomas of the lung: benign or malignant. *Am Rev Respir Dis* 108: 656-659, 1973
13. Boyce CR, Buddhdev HN: Pregnancy complicated by metastasizing leiomyoma of the uterus. *Obstet Gynecol* 42: 252-258, 1973
14. Bateson EM, Abbott KE: Mixed tumors of the lung or hamartochondromas. *Clin Radiol* 11: 232-247, 1960
15. Glennie JS, Harvey P, Jewsbury P: Two cases of leiomyosarcoma of the lung. *Thorax* 14: 327-332, 1959
16. Laustela E: Myomatosis of the lung: report of one case. *Acta Chir Scand* 127: 311-313, 1964
17. Logan WD, Rhode FC, Abbott OA, Metzger HD: Multiple pulmonary fibroleiomyomatous hamartoma. *Am Rev Respir Dis* 91: 101-103, 1965
18. Spotnitz M, Hopeman A: Roentgenogram of the month. *Dis Chest* 51: 645-646, 1967
19. Sargent EN, Barnes RA, Schwinn CP: Multiple pulmonary fibroleiomyomatous hamartomas: report of a case and review of the literature. *Am J Roentgenol* 110: 694-700, 1970
20. Sulser H, Buhler H: Multiple leiomyomatose Hamartome der Lunge. *Schweiz Med Wochenschr* 105: 56-60, 1975
21. Becker RM, Vilorio J, Chiu C: Multiple pulmonary leiomyomatous hamartomas in women. *J Thorac Cardiovasc Surg* 71: 631-632, 1976
22. Sherman RS, Malone BH: A roentgen study of muscle tumors primary in the lung. *Radiology* 54: 507-515, 1950
23. Inberg MV, Sutinen S, Tala E: Leiomyoma of the lung and intercostal space. *Scand J Thorac Cardiovasc Surg* 3: 52-58, 1969
24. Keers RY, Smith FA: Case of multiple pulmonary "hamartoma" of unusual type. *Br J Dis Chest* 54: 349-352, 1960
25. Madani MA, Dafee CS, Ross CA: Multiple hamartomata of the lung. *Thorax* 21: 468-472, 1966
26. Ramchand S, Baskerville L: Multiple hamartomas of the lung. *Am Rev Respir Dis* 99: 932-935, 1969
27. Clizer EE, Daughtry DC: Multiple pulmonary tumors of unusual type. *Chest* 67: 501, 1975
28. Idelson M, Davids A: Metastasis of uterine fibroleiomyomata. *Obstet Gynecol* 21: 78-85, 1963
29. Bragg EA, Levene G: Hamartoma of the lung. *Radiology* 54: 227-235, 1950
30. Arrigoni M, Woolner C, Bernatz P, Miller W, Fontana R: Benign tumors of the lung. *J Thorac Cardiovasc Surg* 60: 589-599, 1970
31. Gudbjerg CE: Pulmonary hamartoma. *Am J Roentgenol* 110: 694-700, 1970
32. Sweet RS: Pulmonary leiomyoma. *Am J Roentgenol* 107: 823-826, 1969
33. Weitzner S: Leiomyoma of the lung. *Am Rev Respir Dis* 100: 63-66, 1969
34. Castleman B, Kibbee BU: Case records of Massachusetts General Hospital, case 17-1963. *N Engl J Med* 268: 550-557, 1963
35. Pierce WF, Alznauer RL, Rolle C: Leiomyoma of the lung. *Arch Pathol* 58: 443-448, 1954
36. Silverstein EF, Ellis K, Wolff M, Jaretzki AS III: Pulmonary lymphangiomyomatosis. *Am J Roentgenol* 120: 832-850, 1974
37. Wolff M: Lymphangiomyoma: clinicopathologic study and ultrastructural confirmation of its histogenesis. *Cancer* 31: 988-1007, 1973

Radiology of Knee Joint Replacement

MARTIN I. GELMAN¹ AND HAROLD K. DUNN²

As total knee replacement becomes more successful due to advances in surgery and bioengineering, a greater number of patients will be offered this procedure as a viable alternative to arthrodesis. Radiologic consultation will be sought for evaluation of proper alignment as well as postoperative complications such as loosening, instability, dislocation, limitation of range of motion, fracture, and infection. This evaluation may be accomplished by plain films and arthrography. Radiographic aspects of these features are discussed and illustrated.

The clinical success of total hip replacement has given strong impetus to the development and use of total knee replacement. Because of marked differences in the biomechanics of the two joints, considerably more problems are being encountered in total knee replacement than in total hip replacement. At the present time there are more than 15 types of total knee replacements in clinical use, and undoubtedly many more will be introduced. To function as an integral member of the patient care team, the radiologist must be aware of the characteristics of a satisfactory total knee replacement and of the complications that can occur with it. Thus the biomechanical limitations imposed by the knee joint must be understood. The purpose of this paper is to briefly describe these biomechanical characteristics and to discuss and illustrate some of the prostheses in common use today as well as their more frequent complications.

Biomechanical Aspects of the Knee Joint

The knee should really be considered as a complex of three joints: the patellofemoral articulation and the medial and lateral tibiofemoral articulations. Each of these areas can be a source of pain and limitation of function necessitating both pre- and postoperative evaluation. The patellofemoral articulation is most often forgotten in evaluation of the knee. Very few of the current total knee prostheses replace this articulation, making most "total knee arthroplasties" a misnomer.

The patellofemoral articulation is subject to extremely high loads during everyday activity and can be a source of considerable pain and discomfort. Its function is to increase the lever arm for the quadriceps mechanism in extending the knee. With the knee in the bent position and the patient climbing stairs, the patella is pulled directly back into the femur with a force sufficient to raise the center of gravity of the body about the center of rotation of the knee. Since the center of gravity of the body is on a lever arm that is between four and six times that of the patellar mechanism, the force on the patella is from four to six times the body weight. As the knee is extended and the patient rises on the stairs, the patella with this force on it must glide to its

proximal position when the knee is fully extended.

Arthritic processes unfortunately do not spare this joint, and malalignment of the lines of pull through the patellofemoral articulation can cause the patella and quadriceps mechanism to sublux or dislocate as the knee extends. If the patella has large osteophytes on it or irregularities between its surface and that of the femur, it may hang up or lock in the course of extension, further emphasizing the importance of pre- and postoperative evaluation of this articulation.

The articulation of the femur with the tibia is not a simple hinge joint where all rotation takes place about a fixed center as in a door hinge. Flexion and extension at the tibiofemoral articulation is very complex. In the sagittal plane the center of rotation of the joint moves forward as the knee goes from flexion to extension. In addition, in the coronal plane the tibia externally rotates under the femur as the knee goes into extension. The surface contour and shape of the medial side of the tibiofemoral articulation is far different from that of the lateral side. At the present time design engineers have difficulty describing these complex surface contours; however, even if they could be described, limitations in metallurgical and plastics manufacturing

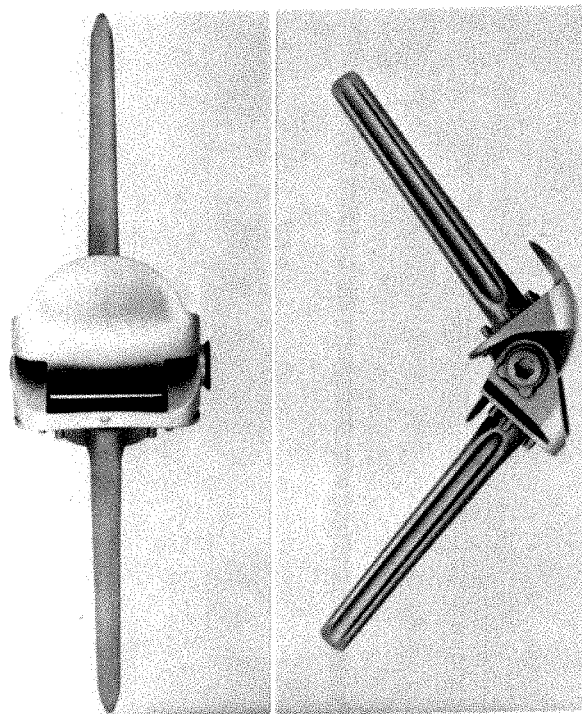


Fig. 1.—Pin hinge prosthesis, Walldius type.

¹ Department of Radiology, University of Utah Medical Center, 50 North Medical Drive, Salt Lake City, Utah 84132.

² Department of Orthopedic Surgery, University of Utah Medical Center, 50 North Medical Drive, Salt Lake City, Utah 84132.

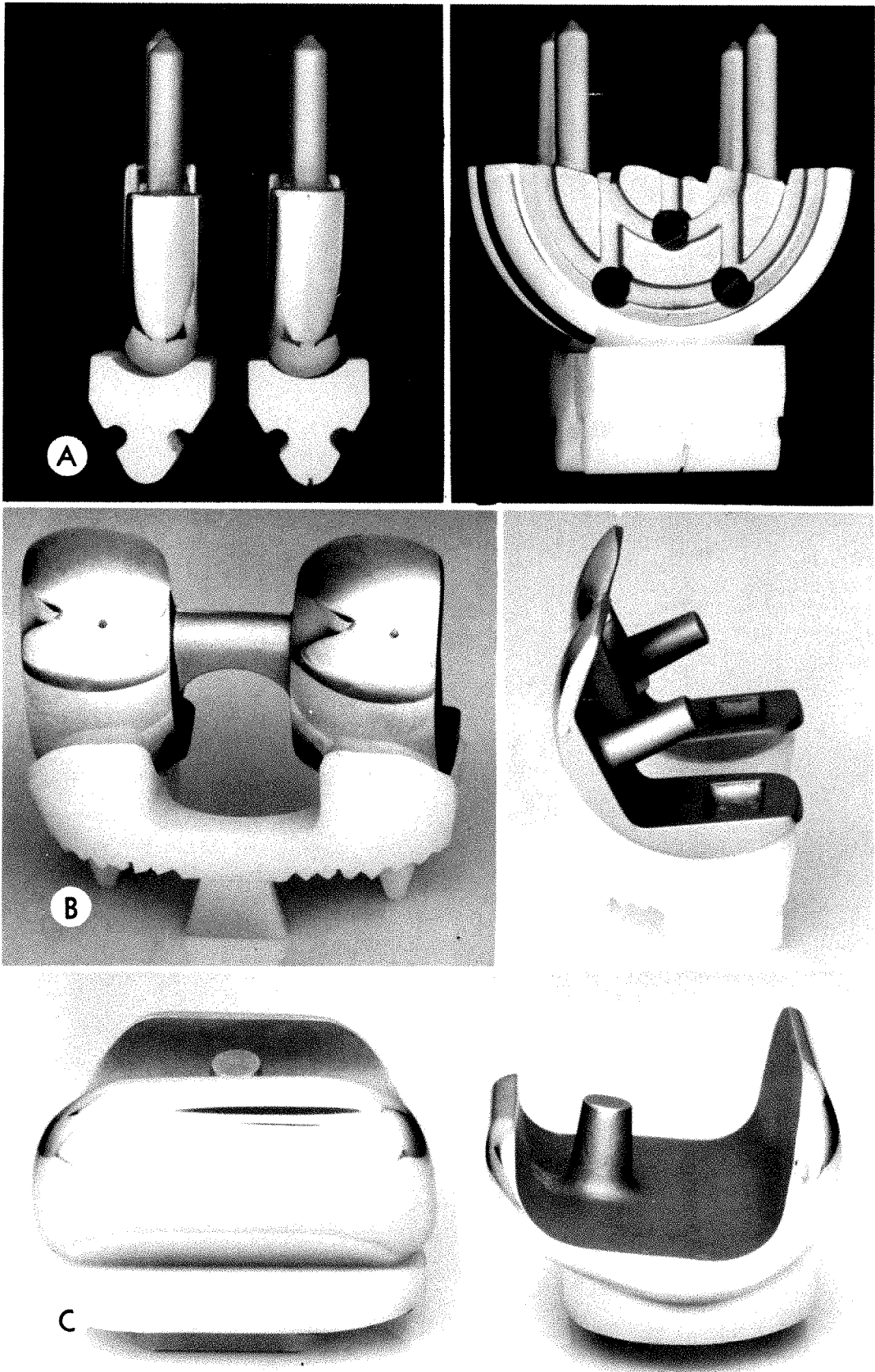


Fig. 2.—Resurfacing prostheses. A, Polycentric; B, geometric; C, Freeman-Swanson.

technology would prevent their exact duplication. For this reason it is currently impossible for any total knee replacement to exactly duplicate the action of the normal human knee.

As the normal knee moves, the articular surfaces glide upon each other and have no tendency to be jammed together. This is not possible in the total knee prosthesis, and consequently some camming and jamming of the surfaces occurs with transmission of high forces to the prosthesis-methacrylate-bone interface. These forces tend to loosen the interface. The amount of force transmitted to the interface rises sharply in heavier patients and especially in those whose activities involve more than walking. Patients who run, climb many stairs rapidly, or carry heavy objects can be expected to overload their prosthesis and have considerable problems at the cement-bone interface.

Because of the complexity of these motions and the limitation of engineering ability to duplicate the surfaces of the knee, the current generation of total knee replacements is for patients with low activity needs. These prostheses at best are for walking and should not be considered for more demanding types of activity.

Many joints (e.g., the hip) have intrinsic stability because of the shape of the joint; this is not true in the knee. Stability in the knee principally comes from the ligaments and capsule that surround it, which are often damaged or destroyed by disease processes. At the present time, satisfactory soft tissue replacements do not exist. In the event

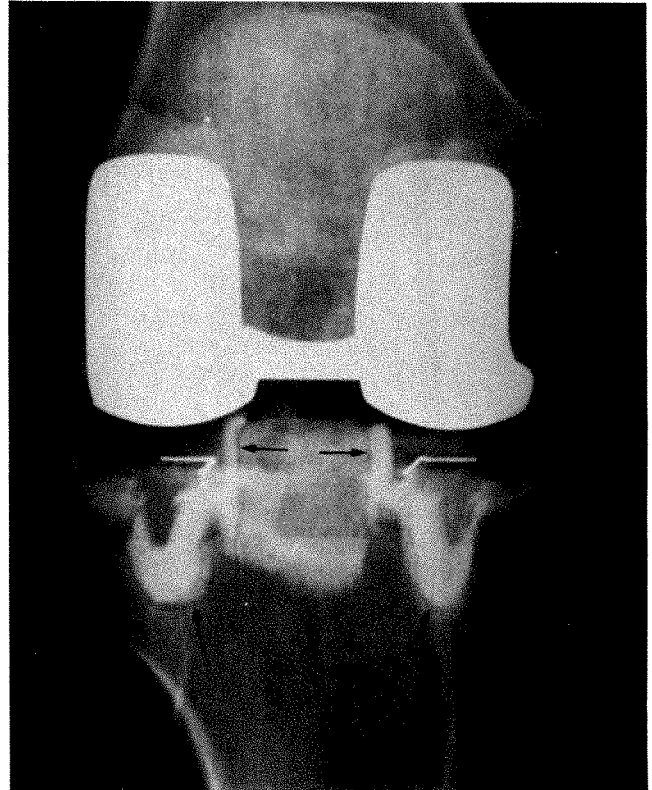


Fig. 3.—Lucent zone (arrows) between bone-methacrylate interface in tibia. May represent fibrous tissue or loosening.

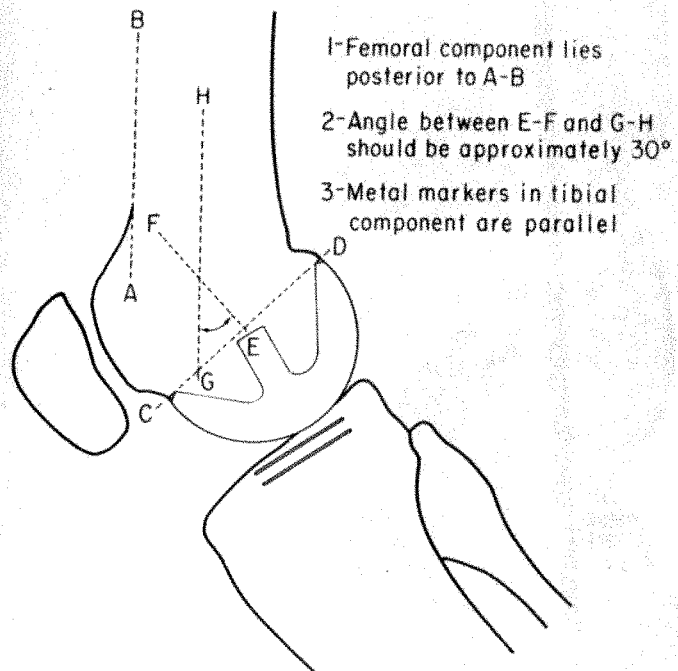
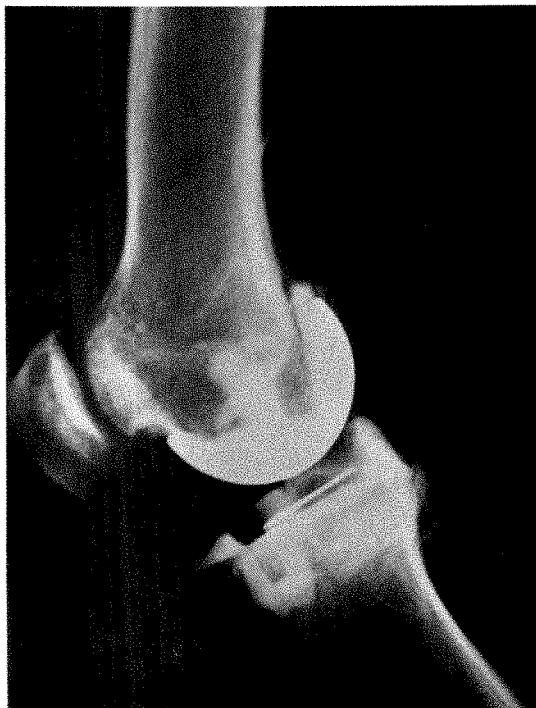


Fig. 4.—Radiograph and corresponding line drawing showing axial relationships of well positioned geometric resurfacing unit. AB=Line parallel to anterior cortex of femoral shaft; CD=line connecting anterior and posterior portion of femoral condylar unit; EF=line perpendicular to CD; GH=line through midaxis of femoral shaft.

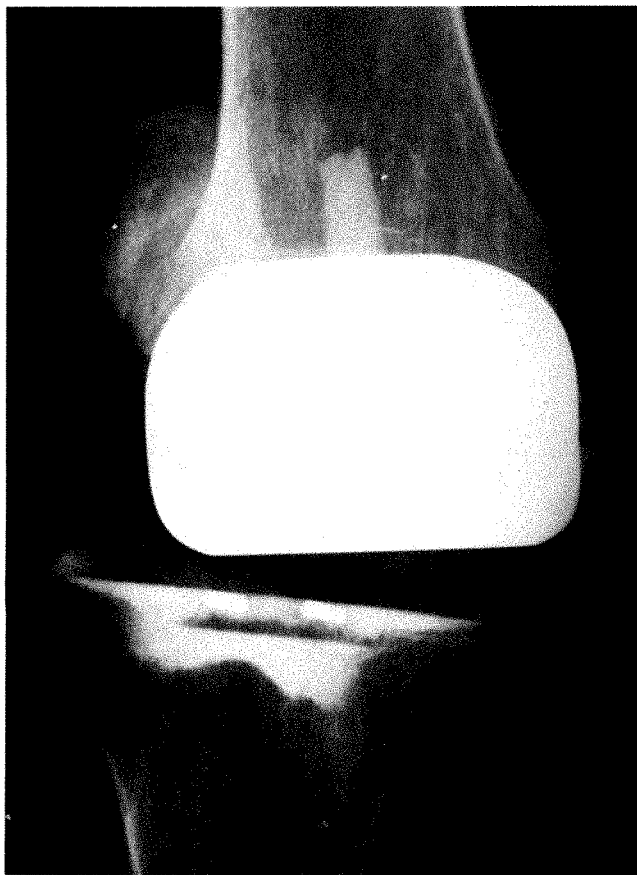


Fig. 5.—Patient with long-standing rheumatoid arthritis. Instability of knee joint uncorrected by Freeman-Swanson total knee replacement. External rotation of foot demonstrates widening of medial joint compartment; dislocation of tibia laterally on femur indicates medial collateral ligament instability.



of severe damage, stability must be accounted for in the design of the prosthesis itself.

Some stability is lent to the knee joint by the strong muscles that work about it, principally the hamstrings and quadriceps. At times even when a ligament complex is destroyed, such as the medial collateral ligament, these muscles will furnish adequate stability. Some stability is also furnished by proper alignment of the surfaces of the femur and tibia. When the patient is in a weight-bearing phase and the surfaces of the femur and tibia are parallel to the ground, there is no varus or valgus stress on the knee. This alignment is very important when evaluating a total knee prosthesis postoperatively.

During walking, the knee is capable of performing its function with a range of motion of only perhaps 40° flexion. Far more motion is needed to carry out other activities of daily living. For example, to get up out of an average-height chair without using one's arms, the knee must be capable of bending sufficiently to allow the foot to be placed under the center of gravity of the body. This requires at least a 90° range of motion. This capability is especially critical in arthritic patients who may have compromised function of

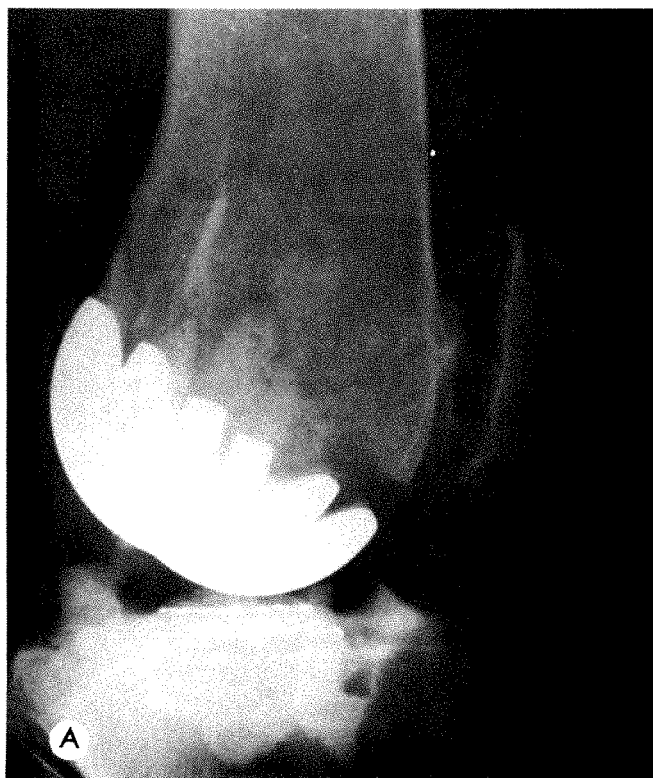


Fig. 6.—Impingement on extension due to inadequate shaving of patellar and femoral osteophytes. A, No impingement while knee in extension. B, Impingement of patella on distal femur during extension following marked flexion of knee.

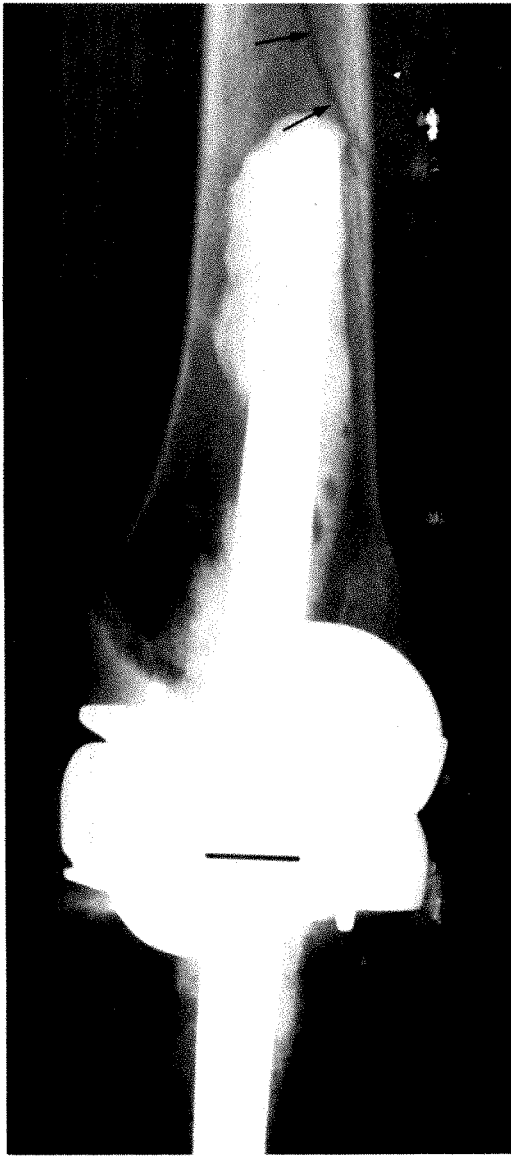


Fig. 7.—Fracture (arrows) of femur just proximal to metal stem which serves as a stress riser in Walldius pin hinge unit. Caused by excess stress.

the upper extremities and be unable to use their arms in assisting themselves. Similarly, at least an 85° range of motion is needed in going up and down stairs for the toes to clear the stair. Thus the mechanical factors interfering with adequate range of motion must be identified and remedied if the knee prosthesis is to function effectively.

Types of Prostheses

Basically, there are two prosthetic designs, the pin hinge and the resurfacing prosthesis. The pin hinge was the first used and is exemplified by the Walldius, Shiers, and Guepar units (fig. 1). It is intrinsically stable since the function of the ligaments is replaced by the metal hinge. However, this rigid linkage and lack of duplication of normal knee motion transmits excessive peak stresses that may loosen the prosthesis or fracture the bone. Currently, use of the hinge prosthesis is reserved for the grossly unstable knee in a

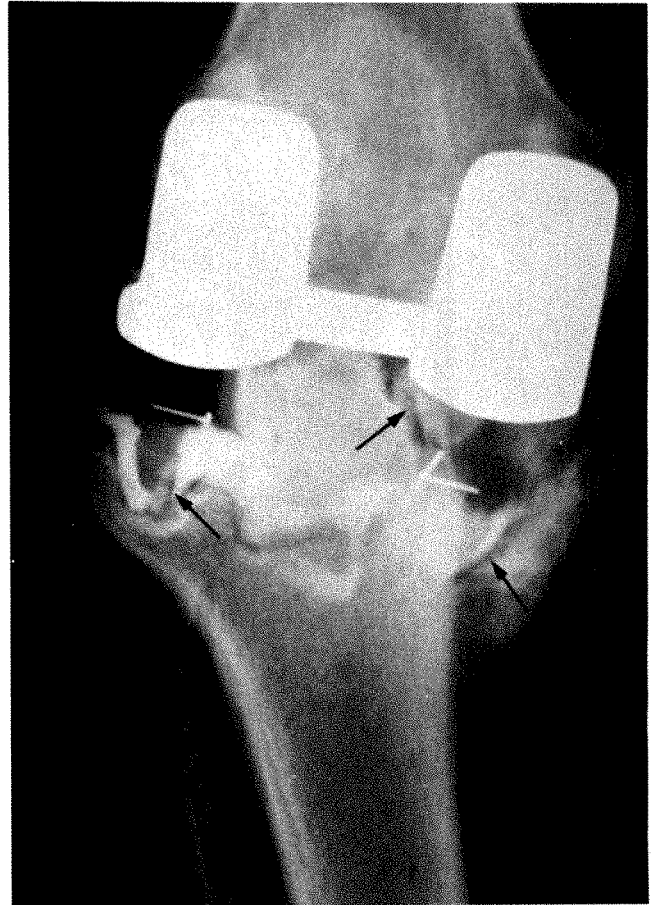


Fig. 8.—Fractures through methacrylate and tibial component (arrows) of geometric prosthesis. Caused by malalignment and unequal stress.

very low demand patient [1, 2].

Resurfacing prostheses (polycentric, geometric, and Freeman-Swanson) constitute the most widely used type (fig. 2). They usually consist of a metal (vitallium or stainless steel) femoral component and a high density polyethylene tibial component. These prostheses are technically more difficult to insert; consequently more alignment problems such as dislocation of the units can be expected [1, 3]. These units are currently being used in patients without gross ligamentous instability in whom conservative treatment or high tibial osteotomy is precluded. They are occasionally used to replace only one side of the tibio-femoral joint.

Radiographic Features

Normal Knee Joint Replacement

The pin hinge is in normal position when the hinge surfaces in the distal femur and proximal tibia are parallel to the resected distal femoral and proximal tibial margins in the supine position and parallel to the ground in the weight-bearing position. A lucent area adjacent to the stem or flange is observed in all prostheses in place more than 5 years. The significance of this lucent area must be correlated with the clinical picture as well as with whether the

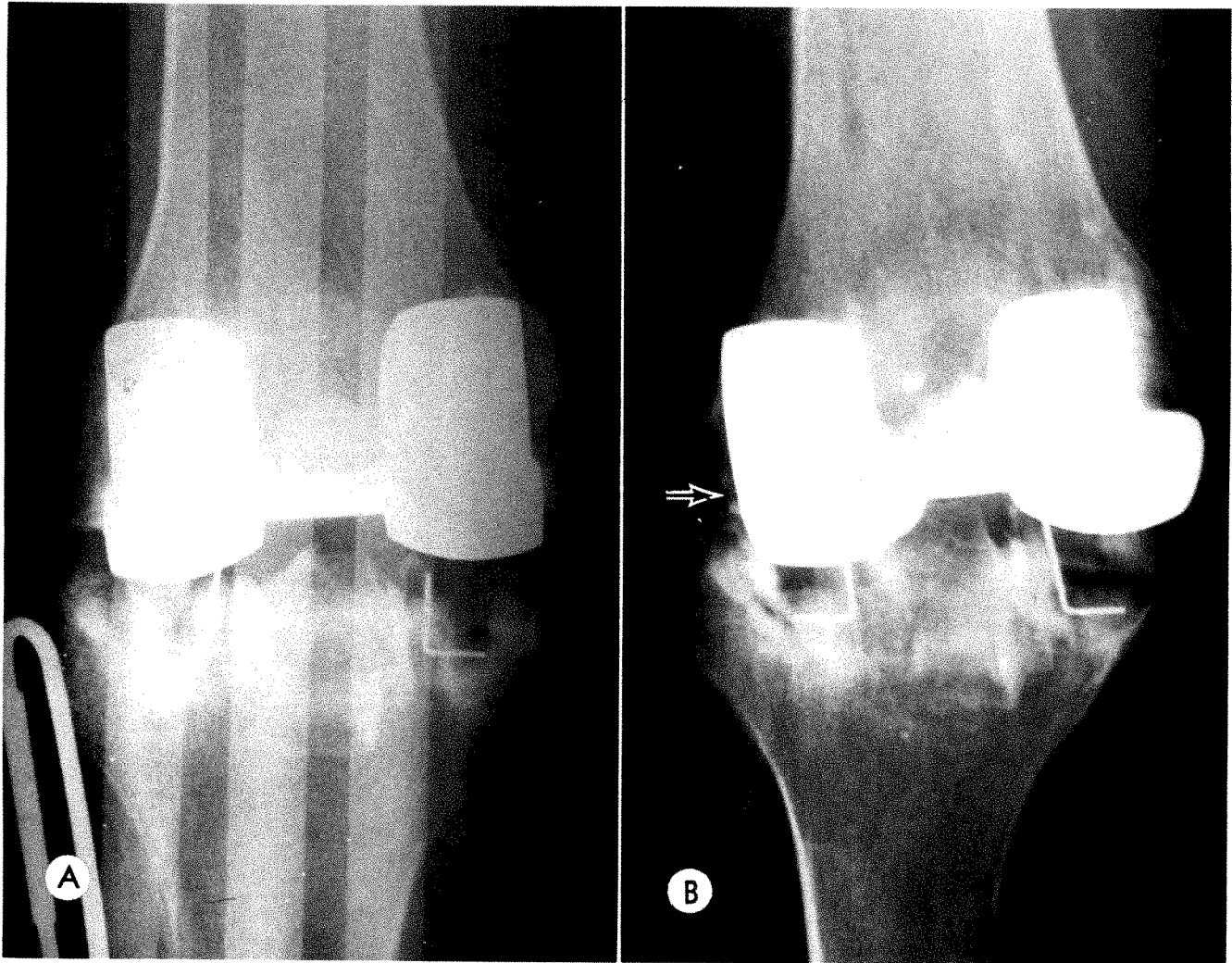


Fig. 9.—Infection. *A*, Early postoperative radiograph showing lateral femoral condyle intact. *B*, Radiograph 2 months later after infection suspected clinically demonstrating bony destruction (arrow). Pus was aspirated from joint space and at surgery femoral component was loose. Femoral and tibial components were removed and subsequent arthrodesis performed.

prosthesis remains parallel to the ground during weight-bearing, since motion may cause bony resorption adjacent to the stem. Partial surgical resection of the posterior aspect of the femoral condyles and shaving of osteophytes from the patella are radiographically evident and are performed to prevent impingement and limitation in range of motion.

The resurfacing units are fixed to the underlying bone by methylmethacrylate, which should completely surround both the femoral and tibial components. A lucent zone between the methylmethacrylate affixing the tibial component and the underlying bone may develop early; however, the significance of this zone with respect to loosening of the component depends upon demonstration by arthrography (fig. 3).

The axial relationship of the resurfacing unit is such that the anterior portion of the femoral component should lie posterior to a line parallel with the anterior cortex of the femoral shaft, so that the articular portion of the prosthesis corresponds to the posterior articular portion of the excised femoral condyles. The axis of the femoral component of the

geometric unit is estimated to be 30° posterior to the axis of the femur; in our experience this measurement is subject to variation [4]. The metal markers in the tibial component should be parallel to each other in the lateral projection (fig. 4). There should be proper axial balance on weight-bearing views without excess varus or valgus [1]. As noted with the metal hinge units, postsurgical changes may be present in the femur, tibia, or patella secondary to removal of osteophytes with a rongeur.

Complications of Knee Joint Replacement

Loosening. Loosening of the stem portion of the hinge prosthesis or of the tibial component of the resurfacing unit may occur. A lucent zone between the bone-methacrylate interface may be a normal development secondary to fibrosis or may represent loosening. Weight-bearing films may demonstrate motion of the loose component, and serial radiographs may show progressive widening of this lucent zone confirming loosening; however, in most cases arthrography is required for confirmation [5].

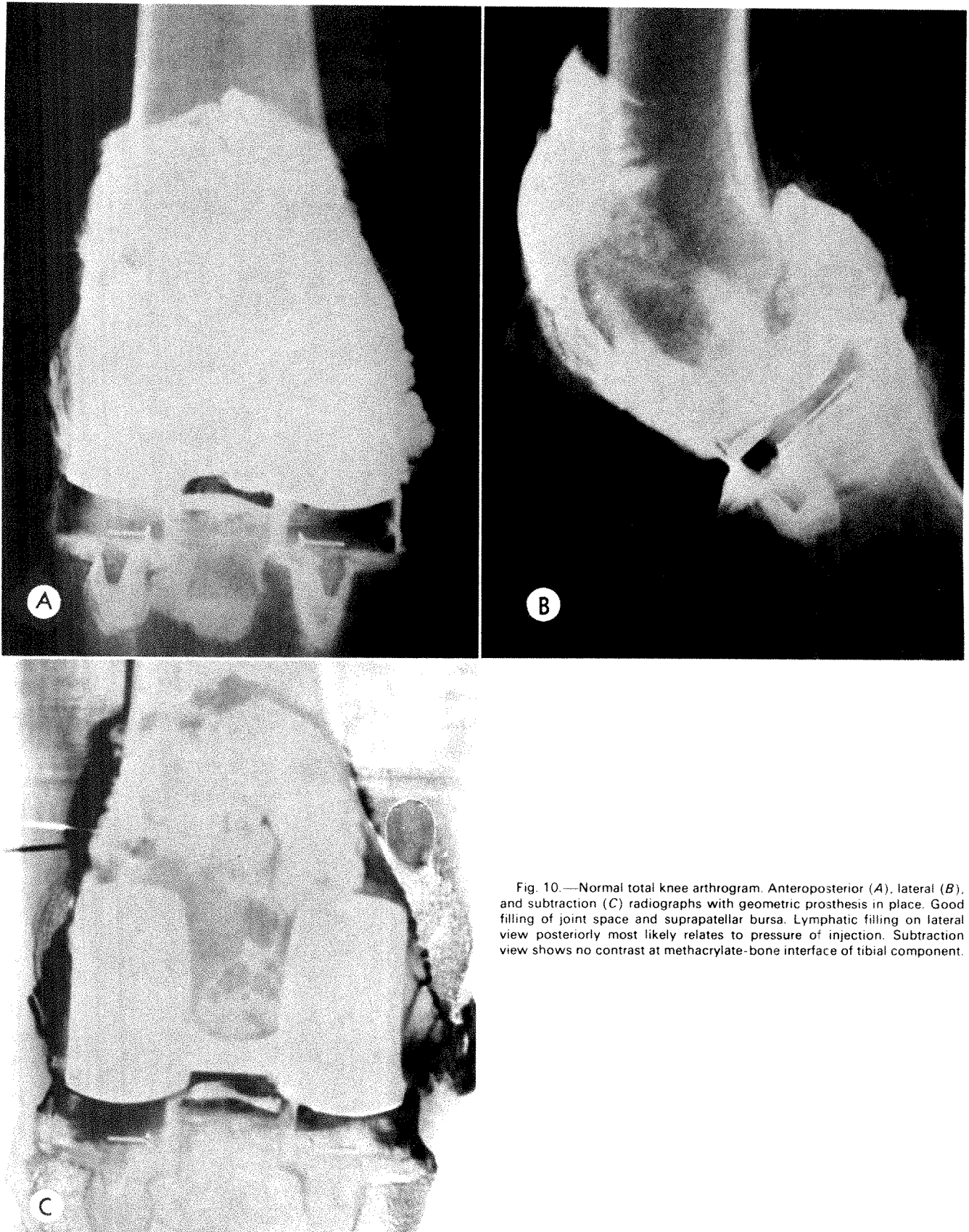


Fig. 10.—Normal total knee arthrogram. Anteroposterior (A), lateral (B), and subtraction (C) radiographs with geometric prosthesis in place. Good filling of joint space and suprapatellar bursa. Lymphatic filling on lateral view posteriorly most likely relates to pressure of injection. Subtraction view shows no contrast at methacrylate-bone interface of tibial component.

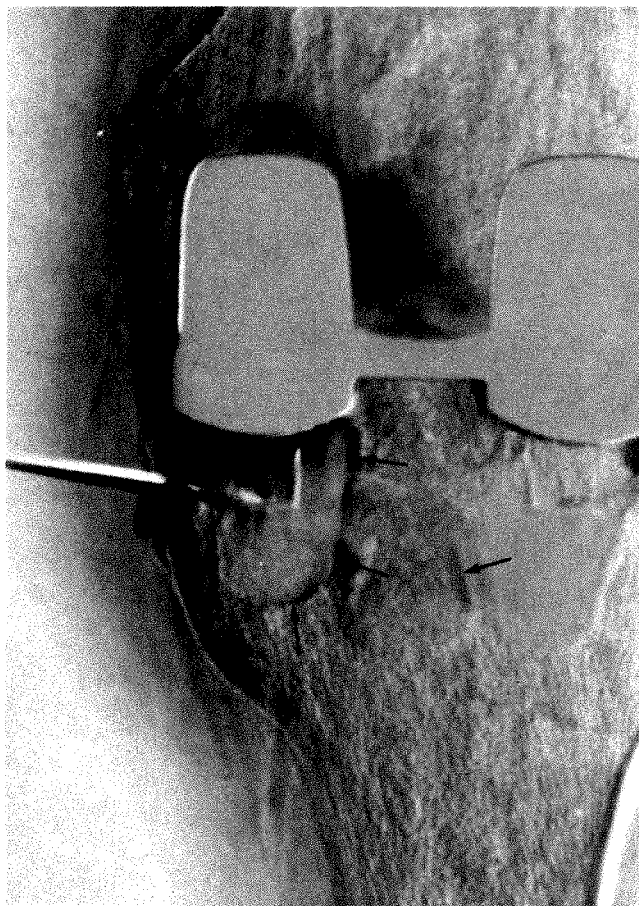


Fig. 11.—Subtraction radiograph demonstrating contrast at methacrylate-bone interface of tibial component indicating loosening (arrows).

Instability. Instability is usually secondary to very lax or absent ligaments. This frequently occurs in rheumatoid arthritis and less frequently in degenerative arthritis. The lax knee usually becomes taut following total knee replacement as muscle strength increases [6]. However, in those cases which do not, the persistent instability may be demonstrated with weight-bearing films or fluoroscopy where stress throws the knee into varus or valgus (fig. 5).

Dislocation. Dislocation may occur when ligamentous laxity is severe. Posterior cruciate ligamentous laxity or absence may allow hyperextension of the knee if the capsule is compromised, whereas collateral ligament insufficiency will allow dislocation of the tibia laterally on the femur. As with instability, dislocation will be considerably reduced or prevented as muscle strength increases postoperatively [6].

Limitation of Range of Motion. Following total knee replacement, range of motion should be at least from 0° full extension to 90° flexion. Inability to extend or flex fully with associated locking sensation may be secondary to bony impingement due to inadequate shaving of patellar or femoral osteophytes (fig. 6). Flexion and extension views will demonstrate this impingement.

Fractures. Fracture may occur at the time of surgery or

postoperatively. Manipulation during surgery may cause fracture due to the marked osteoporosis. The pin hinge prosthesis may cause fractures through the femoral cortex due to excess stress with weight bearing. The stress is transmitted along the metal stem, and the fracture occurs in the bone immediately adjacent to the tip of the stem [7] (fig. 7).

Malalignment of the resurfacing unit may cause fractures of the tibial plateau due to unequal distribution of stress over the tibial surface [8] (fig. 8). Supracondylar fractures may also occur and are most commonly due to the combination of osteoporotic bone and increased activity allowed by the knee prosthesis. Healing usually occurs without necessitating removal of the prosthesis.

Infection. Infection is regarded as the most serious complication since it may necessitate removal of the prosthesis and subsequent arthrodesis (fig. 9). Infection may occur following postoperative hemarthrosis; for this reason suction drains are used in the immediate postoperative period. Another source is chronic infection which may exist in the rheumatoid joint and go undetected prior to joint replacement surgery. The radiographic manifestations of infection include soft tissue swelling and loosening. Arthrography is useful in determining loosening. A sample of the joint fluid should be sent to the laboratory for establishing the presence of infection whenever an arthrogram is done for evaluation of a total knee prosthesis.

Technique for Arthrography of Total Knee Prosthesis

The patient is supine and the lower leg immobilized with sandbags and a clamp. If the patella has not been removed, the needle is advanced under the patella into the patellofemoral joint space in the same manner that a conventional arthrogram is performed. If the patella has been removed, the joint space between the femoral and tibial components is marked laterally on the skin with a felt tip pen under fluoroscopic guidance. The skin is then prepared and draped, and the lateral aspect is locally infiltrated with 1% Xylocaine. A no. 20 gauge needle is advanced into the lateral aspect of the knee joint space, and the position is checked fluoroscopically. A tiny amount of contrast is injected; if flow away from the needle is observed, the intraarticular position is confirmed. A preinjection AP film is obtained at this time for subtraction purposes. At least 15–20 ml of Renografin-76 is injected in order to insure complete filling of the joint space and suprapatellar bursa. With the needle still in place, a second AP projection is made, making sure that the point of entry of the central ray is held constant. The needle is then removed and the knee exercised by passive flexion and extension. AP, lateral, and oblique projections are made in the supine position followed by an AP projection with traction applied to the lower leg. Subtraction radiographs are made when barium-impregnated methylmethacrylate has been used in order to better demonstrate the radioiodinated contrast medium between the bone and the methylmethacrylate (figs. 10 and 11).

ACKNOWLEDGMENTS

We express our appreciation to Mrs. LeVern Jarrad for help in manuscript preparation and to Dr. David G. Bragg for critical review of the manuscript.

REFERENCES

1. Coventry MB, Upshaw JE, Riley LH, Finerman GAM, Turner RH: Geometric total knee arthroplasty. I. Conception, design, indications and surgical technic. *Clin Orthop* 94:171-176, 1973
2. Amstutz HC, Finerman GAM: Knee joint replacement—development and evaluation. *Clin Orthop* 94:24-41, 1973
3. Freeman MAR, Swanson SAV, Todd RC: Total replacement of the knee using the Freeman-Swanson knee prosthesis. *Clin Orthop* 94:153-170, 1973
4. Coventry MB, Finerman GAM, Riley LH, Turner RH, Upshaw JE: A new geometric knee for total knee arthroplasty. *Clin Orthop* 83:157-162, 1972
5. Gilula LA, Staple TW: Radiology of recently developed total knee prostheses. *Radio Clin North Am* 13:57-66, 1975
6. Coventry MB, Upshaw JE, Riley LH, Finerman GAM, Turner RH: Geometric total knee arthroplasty. II. Patient data and complications. *Clin Orthop* 94:177-184, 1973
7. Jackson JP, Elson RA: Evaluation of the Walldius and other prostheses for knee arthroplasty. *Clin Orthop* 94:104-114, 1973
8. Bryan RS, Peterson LFA, Combs JJ Jr: Polycentric knee arthroplasty. A preliminary report of postoperative complications in 450 knees. *Clin Orthop* 94:148-152, 1973

Traumatic Lesions of the Discovertebral Junction in the Lumbar Spine

WILLIAM MARTEL,¹ JOACHIM F. SEEGER, JEFFREY D. WICKS, AND RONALD L. WASHBURN

Lumbar discovertebral abnormalities thought to be due to endogenous or subclinical trauma were evaluated in 22 cases. These consisted of predominantly lytic areas due to intrabody disc herniation in five cases, broad zones of vertebral body sclerosis due to reactive osteitis in 11, and destruction of the vertebral endplates surrounded by diffuse sclerosis in six. Spinal biopsy and negative bacterial cultures were consistent with the diagnosis in eight cases. Follow-up roentgenograms and further clinical evaluation in the remaining 14 showed either no progression or changes consistent with trauma. Only four cases had a history of exogenous trauma.

Intrabody disc herniations usually affected the upper vertebral body with characteristic sparing of the adjacent endplate. The sclerotic lesions tended to occur in the anterior portion of the vertebral body, with the inferior aspect of L4 most frequently involved. These may be confused with osteoblastic metastases, particularly if adjacent disc narrowing is minimal. The lack of progressive vertebral fragmentation helps to distinguish this condition from neuroarthropathy. Lesions characterized by destruction of the vertebral endplates and reactive sclerosis simulate infection; absence of a soft tissue mass and clinical signs of sepsis as well as lack of progression are important differential features.

The radiologic diagnosis of traumatic lesions of the spine is usually not difficult. However, trauma may be endogenous, and a fracture or vertebral deformity may not immediately be obvious. In such cases, radiologic changes at the discovertebral junction can be atypical and easily confused with other conditions. The purpose of this report is to call attention to these lesions and certain characteristic roentgenographic features.

Subjects and Methods

The radiologic and medical records of 45 patients who had lumbar "discovertebral abnormalities" of uncertain etiology at the time of initial radiologic examination were reviewed. These were derived from the files of the Department of Radiology at the University of Michigan, covering a 10 year period (1965-1975). Twenty-three cases were excluded because subsequent evaluation showed them to be nontraumatic in origin (the majority due to infection) or the data or subsequent radiologic or clinical follow-up were inadequate. The remaining 22 cases form the basis of this report. All patients were reevaluated radiologically and clinically over an interval of at least 2 months. Three were recalled at the time of the study for additional roentgenographic examinations.

Biopsy of the disc or adjacent vertebra and bacterial cultures had been obtained in eight of the 22 cases: three were open biopsies and five, percutaneous trochar biopsies under fluoroscopic control. The position of the trochar was verified with frontal and lateral radiographs in each case. The remaining 14 patients were included

because the radiologic appearance of the lesions was similar to those which had been biopsied and follow-up roentgenographic examinations showed either no progression or changes consistent with trauma. Lack of a history of exogenous trauma was not a basis for exclusion. Patients with generalized lumbar degenerative spondylosis were excluded because of the difficulty in distinguishing primary from secondary degenerative changes in such cases.

Results

Radiologic Features

Cases were divided into three groups according to the predominant radiologic appearance of the vertebral body lesion: (1) primarily lytic group, five cases; (2) sclerotic group, 11 cases; and (3) lytic and sclerotic group, six cases. All lesions were in the lumbar spine and involved or were contiguous with a vertebral endplate. A single level was involved in 16 cases and two levels were affected in six (one in the lytic group, four in the sclerotic group, and one in the lytic and sclerotic group). Significant radiologic features are summarized in table 1.

Primarily lytic group. Characteristically, the upper portion of the vertebral body was affected, and the endplate of the adjacent vertebra was spared (figs. 1 and 2). L2 was affected in two cases, L4 in two, and L5 in one. Disc space reduction was moderate in two cases and minimal in three. The anteroposterior diameter of the vertebral body was slightly increased in two cases, and the lytic defect was eccentric with respect to the midsagittal plane in two. None had vertebral malalignment or a vacuum disc phenomenon. Laminograms were available in four cases.

Biopsy showed normal cartilage and bone in two patients; in a third whose roentgenograms had disclosed spondylolysis at L4 prior to the development of the lesion (fig. 2), the biopsy showed minimal reactive inflammation. Infection was thought unlikely in view of the relative acellularity of the biopsy material. Cultures for pathogens were negative in these cases, and radiologic follow-up examination in the remaining two at 2 and 15 months, respectively, showed no significant change.

Sclerotic group. A predilection for the inferior aspect of the body of L4 was conspicuous; characteristically, the adjacent vertebra showed similar, usually less marked sclerosis (figs. 3-6). The sclerosis tended to occur in the anterior portion of the vertebral body, often rather selectively, and was occasionally eccentric with respect to the midsagittal plane. Periosteal bone apposition at the anterior aspect of the body was common but of minimal or moderate degree (fig. 4B). Reduction in disc height, ranging from minimal to severe, occurred in all but one case.

Presented at the annual meeting of the American Roentgen Ray Society, Atlanta, Georgia, October 1975.

¹ All Authors: Department of Radiology, University of Michigan Medical Center, Ann Arbor, Michigan 48104.

TABLE 1
Radiologic Features

Feature	No.
Lytic group (N=5):	
Upper vertebral body affected	5
Adjacent vertebral endplate spared	5
Decreased disc space	5
Increased AP diameter of vertebral body	2
Eccentric defect	2
Vertebral malalignment	0
Vacuum disc phenomenon	0
Laminograms	4
"Negative" biopsy and culture	3
Sclerotic group (N=11):	
Inferior part of L4 affected	9
Adjacent vertebral body affected	8
Anterior localization	6
Periosteal bone apposition	8
Decreased disc space	10
Eccentric sclerosis	2
Vertebral malalignment	3
Vacuum disc phenomenon	4
Laminograms	7
"Negative" biopsy and culture	2
Lytic and sclerotic group (N=6):	
Inferior aspect of L4 affected	3
Adjacent vertebral body affected	5
Anterior localization	3
Periosteal bone apposition	4
Decreased disc space	6
Eccentric lesion	3
Vertebral malalignment	1
Vacuum disc phenomenon	0
Laminograms	4
"Negative" biopsy and culture	3

The sclerosis in the latter regressed virtually completely over a 7 year period (fig. 5). Anteroposterior malalignment was noted in three cases, and a vacuum disc phenomenon occurred in four (figs. 3 and 7B). Laminograms were available in seven cases.

Biopsy of the disc showed reactive granulation tissue; one case contained relatively few inflammatory cells and one had normal fibrocartilage adjacent to dense fibroconnective tissue (fig. 3). Microscopic bone fragments were present in both. Of the remaining nine cases, four were followed for 1–3 years and five for 3 years or more (fig. 6). Only one showed a radiologic change in the appearance of the lesion, consistent with continuous endogenous trauma; this was a male who had bilateral spondylolysis at the level of the lesion (L2) which was followed radiologically for 27 years (fig. 7).

Lytic-sclerotic group. Lesions were similar to those in the sclerotic group in that they frequently occurred at the inferior aspect of L4, tended to involve the anterior portion of the body, often affecting the adjacent vertebra, and were associated with anterior periosteal bone apposition. Disc space reduction was severe in two cases and moderate in four. The lesion was eccentric in three instances, and vertebral malalignment was minimal in one. Laminograms were available in four cases.

Biopsy of the disc and adjacent tissue in three patients showed no evidence of infection; cultures of disc material were negative (figs. 8 and 9). Follow-up radiologic and clinical evaluations in the remaining three cases showed no progression over a period of 4, 6, and 12 months, respectively.

Clinical Features

Significant clinical features in these patients are summarized in table 2. Female predominance was conspicuous in the sclerotic and the lytic-sclerotic groups. While ages varied in the lytic group, all patients in the other two groups were 40 or older. A history of exogenous trauma was significant in three of the five patients in the lytic group but in only one of the 17 patients in the other two groups. Low back pain was frequent, but positive neurologic signs were relatively unusual. Findings were confined to the lower extremities in all but one of four patients who did have such positive signs; this patient also had bladder incontinence. Diabetes mellitus and rheumatoid arthritis were frequently noted in these patients. Only two of the diabetics had peripheral neuropathy, and none had neuropathic joints.

Discussion

Although much of our evidence is indirect, we believe these lesions are traumatic in origin. This is supported by the absence of radiologic change over a significant interval in most cases, the pattern of progression in the few that did show changes, the tendency for these lesions to occur at either one or two levels with no other lesions in the spine, the involvement of characteristic sites, and the consistent absence of a paraspinous mass. The predilection for females over age 40 in the sclerotic and the lytic-sclerotic groups is also an important feature. Although the lesions in this series were in the lumbar spine, they probably also occur at other levels.

Lytic Group

Lesions in the lytic group clearly represent intrabody disc herniations. Experiments have indicated that disruption of the annulus fibrosis by exogenous trauma is usually associated with a fracture of the adjacent vertebral cortex and cartilaginous plate [1, 2]. Points of weakness in the cartilage due to developmental defects [3] may predispose to such intrabody herniations following minimal trauma. The resultant vertebral body defect characteristically shows a sclerotic margin, giving a walled-off effect. This is analogous to the bone formation which occurs in any fracture. However, this effect may be minimal if there is defective osteogenesis, as reflected by osteoporosis; in such cases the lytic defect can be large and atypical. Although the upper part of a vertebral body was affected in all five cases, there was a similar, less extensive lesion in an inferior endplate in one (fig. 1B).

A feature of these lesions not previously emphasized is the tendency to spare the adjacent vertebral endplate. It is as though prolapse of disc tissue, resulting from pressure in the nucleus, takes place at the weakest side of the disc-covertebral junction. With tension in the disc released,

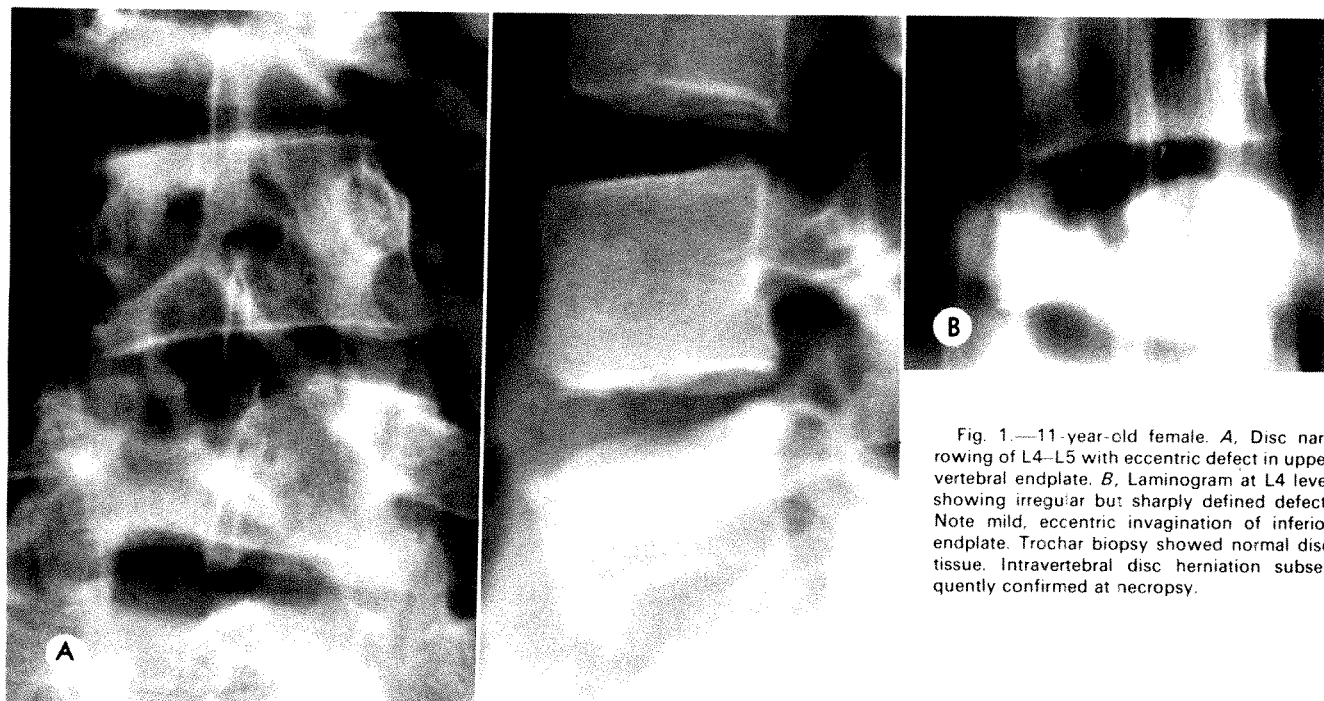


Fig. 1.—11-year-old female. A, Disc narrowing of L4–L5 with eccentric defect in upper vertebral endplate. B, Laminogram at L4 level showing irregular but sharply defined defect. Note mild, eccentric invagination of inferior endplate. Trochar biopsy showed normal disc tissue. Intravertebral disc herniation subsequently confirmed at necropsy.

further extrusion into the adjacent vertebra does not occur. Such sparing of the adjacent endplate appears to be unusual in infections.

As a control measure, we reviewed the roentgenographic appearance of the involved discovertebral junction in 20 cases of proved infection. The causative agents were pyogenic organisms or *M. tuberculosis*. Only in one, a case of tuberculosis, was there similar sparing of the adjacent endplate; however a large paraspinal soft tissue mass and clinical signs of sepsis were present. It is possible that metastatic neoplasm or myeloma may cause vertebral destruction which weakens the vertebral endplate causing secondary intrabody disc herniation, but in our experience such destruction is usually not limited to the endplate. The configuration and sites of vertebral osteolysis usually distinguish these cases.

Sclerotic and Lytic-Sclerotic Groups

The pathogenesis of lesions in these two groups is less clear. Subclinical trauma may cause vertebral endplate fractures which are difficult to detect on routine roentgenograms [4]. These may result in irreversible degenerative changes in the adjacent disc, consisting of thinning and fissure formation in the annulus and fragmentation of the hyaline cartilage [5]. The resultant loss of stability at such a level could cause additional attrition of cartilage, ingrowth of granulation tissue, and reactive osteitis. As the disc is replaced by fibrous tissue, the annulus loses its resilience and ability to withstand compressive rotational forces [3].

In the late stages, direct bony contact between apposing vertebral surfaces, uncushioned by disc substance, also stimulates osteogenesis (figs. 3 and 7B). This is analogous to the sclerosis which occurs in the appendicular joints fol-

lowing destruction of the articular cartilage. Lesions showing both bone destruction and sclerosis may reflect co-existent disc herniation, with granulation tissue developing at the discovertebral junction.

No cases were observed in which a lesion classified as sclerotic converted to a mixed lytic-sclerotic type, or vice versa. However, the number of cases in our series and the period of observation may not be sufficient to exclude such a transition.

The sclerosis was not usually confined to the endplate but involved a rather broad area adjacent to it (figs. 4–6). This feature and the predilection for the anterior portions of the vertebral bodies could be explained by the anterior attachments of the longitudinal ligament and the relationship of the vertebrae to Sharpey's fibers. The latter constitute firm connections between the bony rim, annulus fibrosus, and hyaline cartilage plate. Posttraumatic alterations in the disc, however minimal, could lead to mechanical instability which stresses these fibroosseous attachments. Lumbar lordosis causes the posterolateral portions of the annulus to absorb most of the axial compressive forces [4], and degenerative changes become obvious in these areas as early as the third decade of life [5]. This could cause divergence of the anterior vertebral surfaces (fig. 3) which in turn alters the arrangement of the annular rings.

Vulnerability of the disc to trauma is related to age and lumbar lordosis. Traumatic changes are more common in the lower lumbar discs [6]. This could explain the tendency for lesions in the sclerotic and the lytic-sclerotic groups to occur at L4–L5. Although disc degeneration is most common at L5–S1, Farfan et al. [6] point out that the anatomy of the lumbosacral junction provides a resistance to the

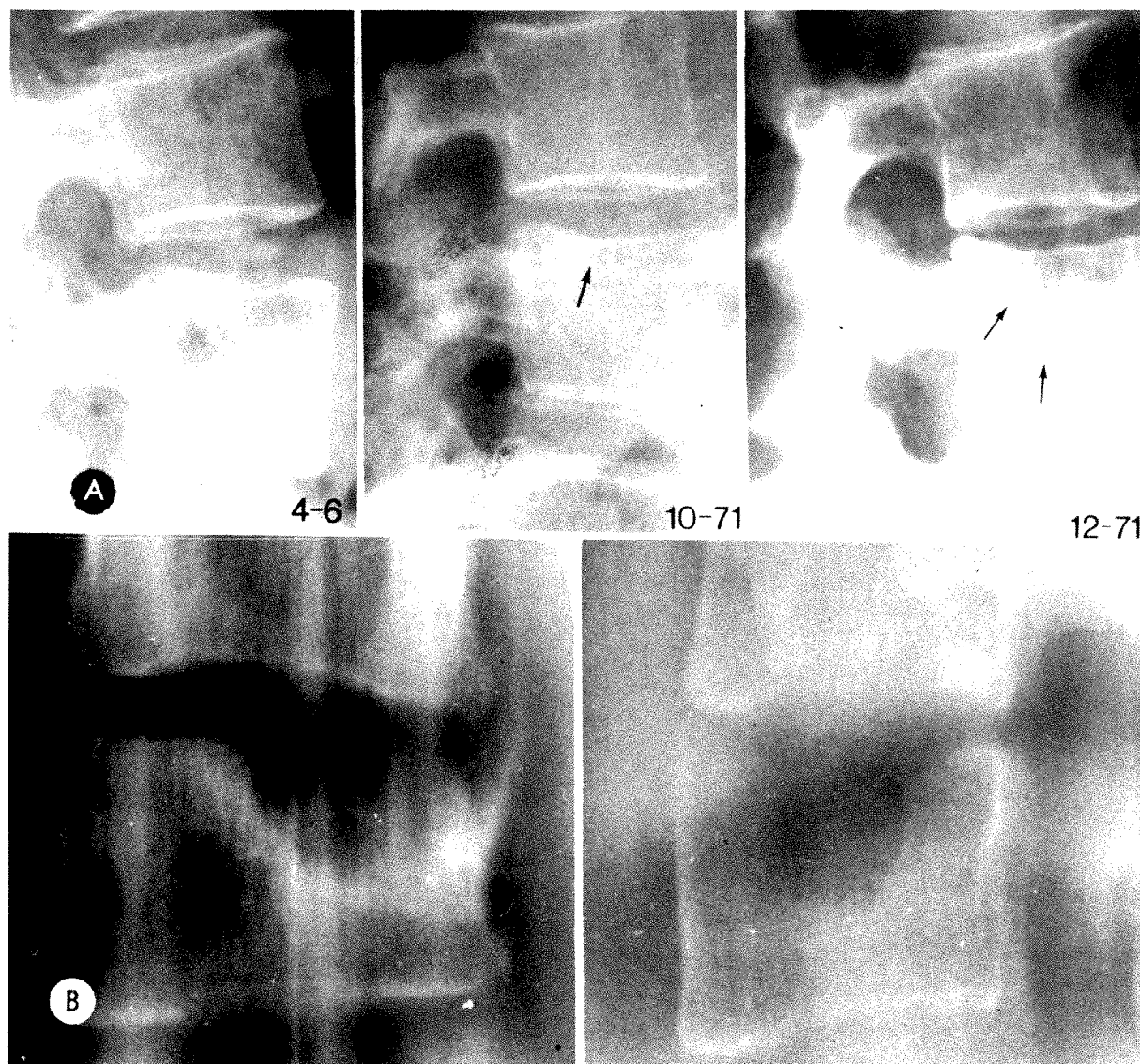


Fig. 2.—49-year-old female with back trauma in September 1971. A, Progressive disc narrowing at L3–L4 with lytic lesion in L4 (arrows). Minimal focal depression of superior endplate seen 1 month after trauma (arrow). Spondylolysis of L4 seen in April 1968 and October 1971 became more obvious in December 1971. B, Laminograms at L4 level (December 1971) showing eccentric lytic defect with slight marginal sclerosis and sparing of adjacent endplate.

effects of torsion at this level. Furthermore, rotational stress may be greatest at L4–L5 since this is usually closer to the “apex of lumbar lordosis” in the upright position.

The sclerotic lesions may be compared to osteitis pubis and osteitis condensans ilii inasmuch as these are thought to be secondary to mechanical stress. These lesions did not coexist in any of our cases. It is significant, however, that all but one of the patients in the sclerotic and the lytic-sclerotic groups were females. There was no clear relationship to pregnancy since four were nulliparous. The disappearance of the sclerosis over a 7 year period in one case (fig. 5) is of interest in that spontaneous resolution in osteitis condensans ilii has recently been noted [7].

Although our hypothesis concerning the etiology of these sclerotic lesions is supported by experimental and postmortem observations [1, 2, 4–6], more conclusive evi-

dence is needed. Ackermann and Schwarz [8] reported a case of idiopathic vertebral sclerosis but were unable to document an abnormality in the two adjacent discs at necropsy; unfortunately, the roentgenograms in this case were not illustrated. They did illustrate a sclerotic lesion of T12 similar to those in our sclerotic group in which microscopic examination showed no evidence of infection or neoplasm. However, they did not comment on the status of the disc.

These lesions may be mistaken for metastases [8] or spinal neuroarthropathy. Feldman et al. [9] recently described acute axial neuroarthropathy in diabetes mellitus as well as tabes dorsalis. Progressive vertebral fragmentation with or without massive bone overgrowth are significant features of this condition. This was not observed in our cases, nor did the lesions in the six diabetics differ from

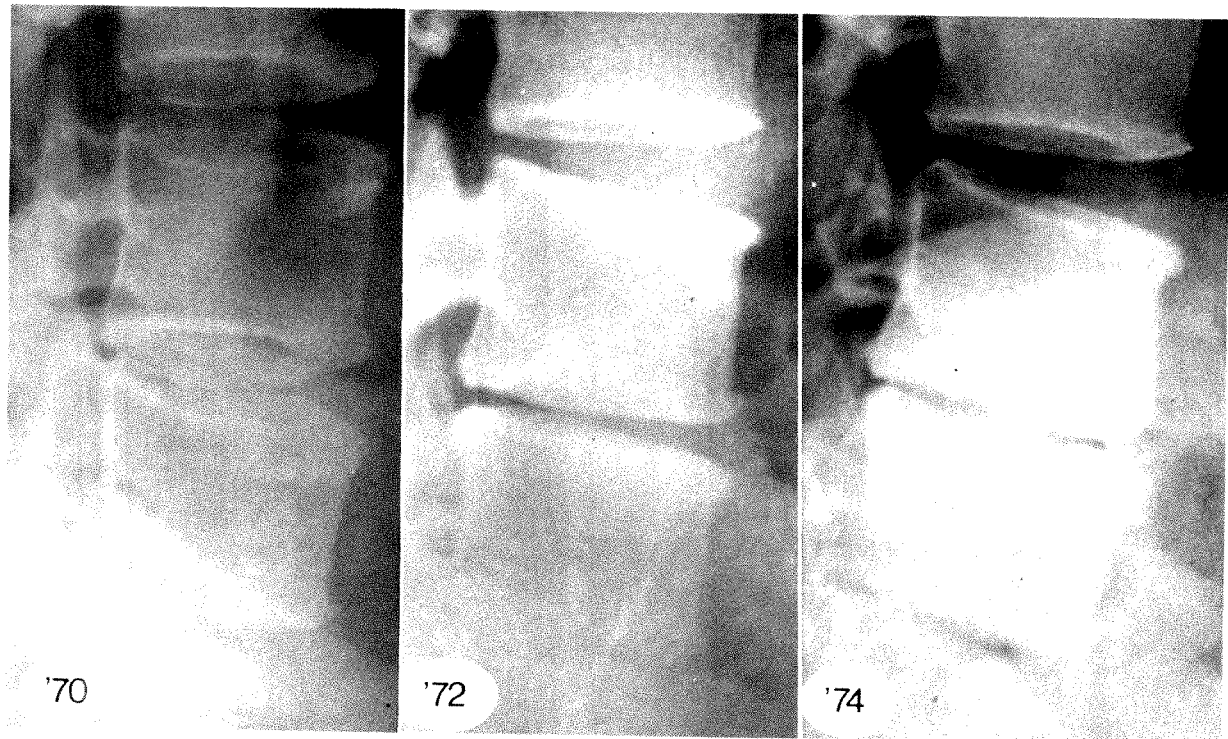


Fig. 3.—40-year-old female with back pain and no history of trauma. Note progressive disc narrowing, vertebral sclerosis and anterior periosteal bone apposition at L4–L5 and L5–S1 with vacuum phenomena at both levels. Biopsy at L4–L5 showed dense fibroconnective tissue with small bone fragments but no granuloma formation.

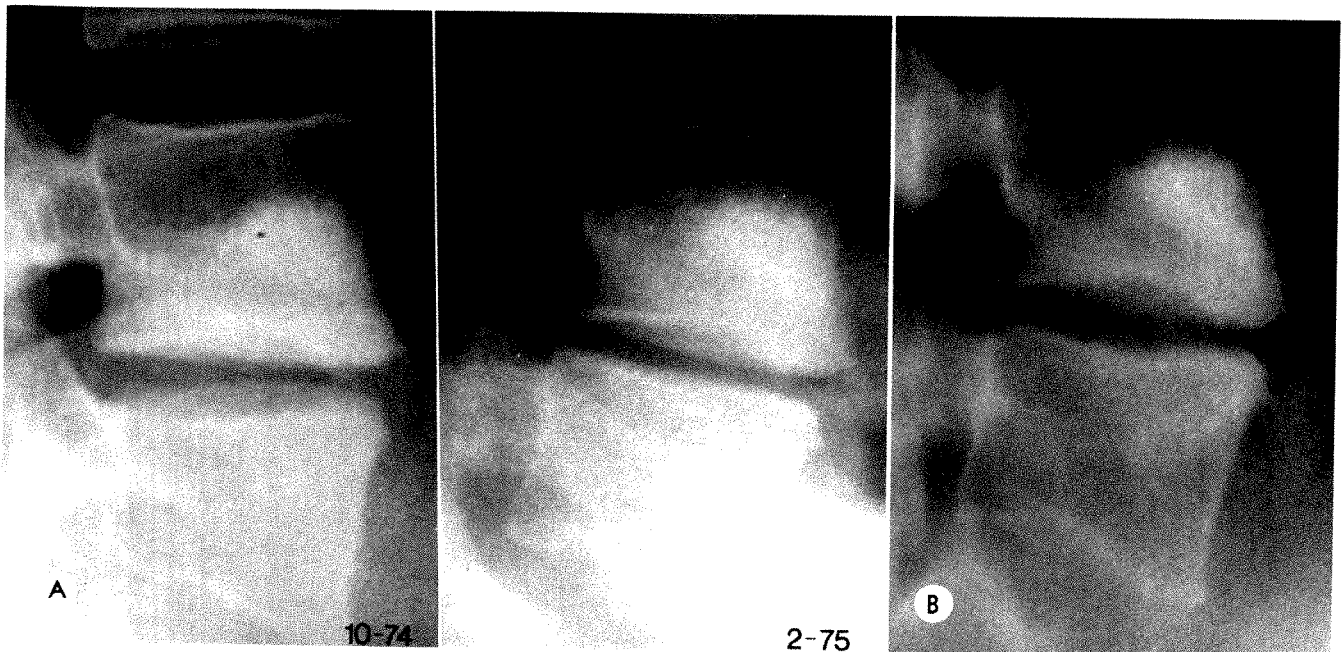


Fig. 4.—40-year-old female with diabetes mellitus. A, Characteristic localization of sclerosis to antero-inferior part of L4 and, to a lesser extent, antero-superior part of L5 with no change. Note anterior periosteal bone apposition and disc narrowing. B, Midline laminogram showing broad zones of sclerosis with no lytic component and periosteal bone apposition.

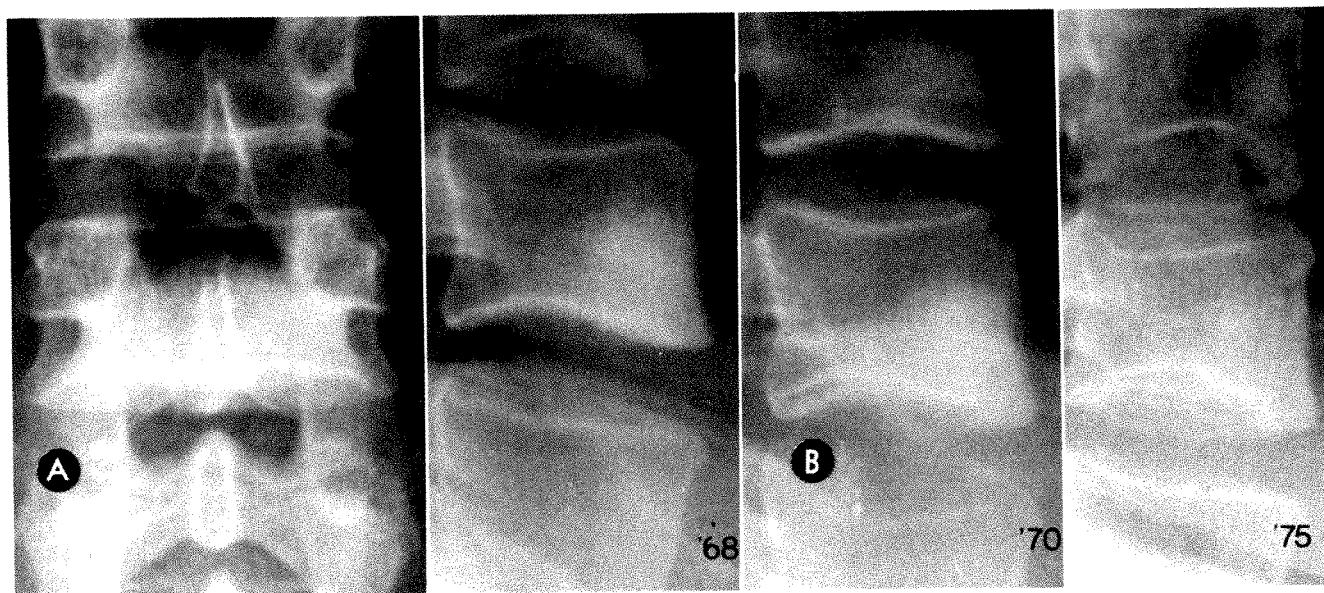


Fig. 5.—43-year-old female with diabetes mellitus. A, 1968 film showing sclerosis of L4 and, to lesser extent, L3 without disc narrowing. B, Gradual regression of sclerosis over this period (confirmed by laminograms).

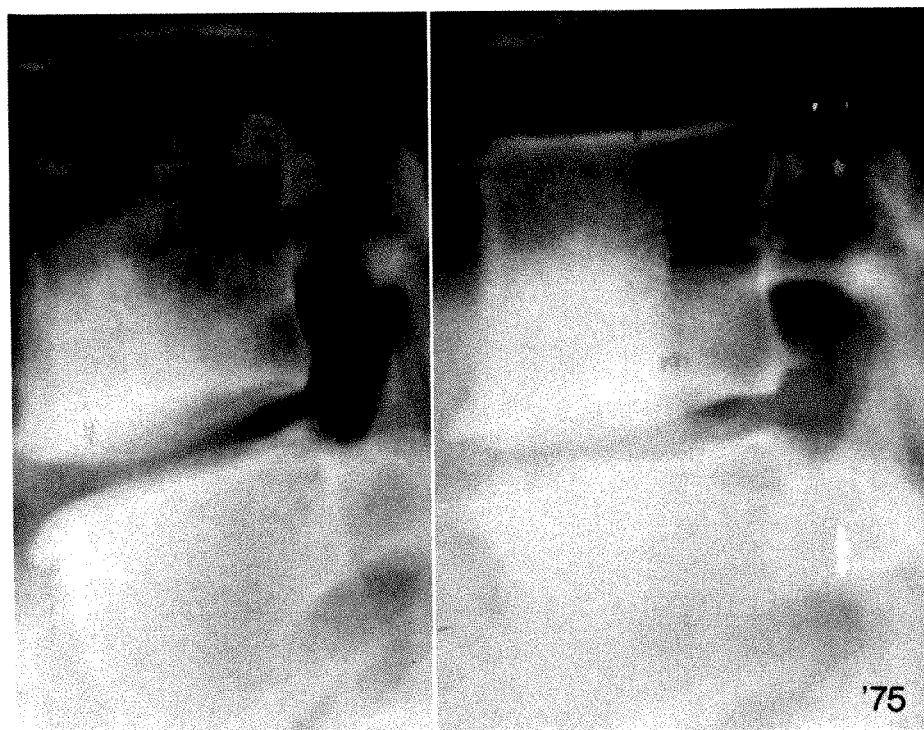


Fig. 6.—46-year-old female with no history of trauma or systemic disease. Sclerosis of L4 and, to a lesser extent, L5 with no significant change over a 3 year interval. Note minimal osteophyte formation and periosteal bone apposition with slight further reduction in disc height over this interval. No other joints affected.

those in the nondiabetics.

The observed association with rheumatoid disease is of equivocal significance because our cases were not randomly selected. Seaman and Wells [10], in discussing destructive lesions of the vertebral bodies in rheumatoid disease (including patients both with ankylosing spondylitis and rheumatoid arthritis), described two females with peripheral rheumatoid arthritis who had destruction of the lumbar vertebral endplates with sclerosis. None of our cases showed rheumatoid granulomata on microscopic

examination. However, rheumatoid involvement of the posterior lumbar joints may cause ligamentous laxity and instability; osteoporosis may make such patients vulnerable to fracture at the discovertebral junction.

Williams et al. [11] termed several cases which were similar to ours "pseudoinfections of the intervertebral disc." These occurred both after disc surgery and in cases in which no surgical procedures were undertaken. They concluded that these were most likely due to low grade infection, despite the fact that clinical evidence of sepsis

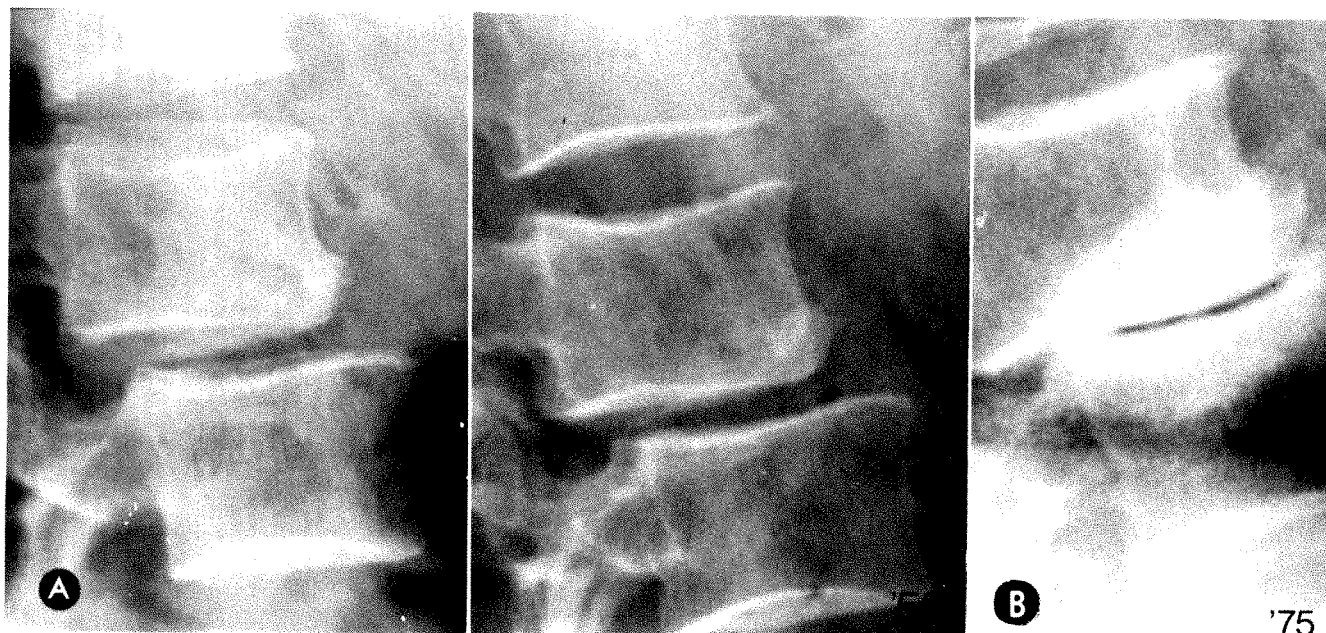


Fig. 7.—30-year-old male with bilateral spondylolysis of L2 in 1948 (confirmed on oblique views). A, Disc narrowing at L2–L3 with minimal osteophyte formation, malalignment, and absence of significant change over 7 year interval. B, 1975 film showing marked disc narrowing with vacuum phenomenon and vertebral sclerosis. Sclerosis is similar to that shown in figs. 4–6.

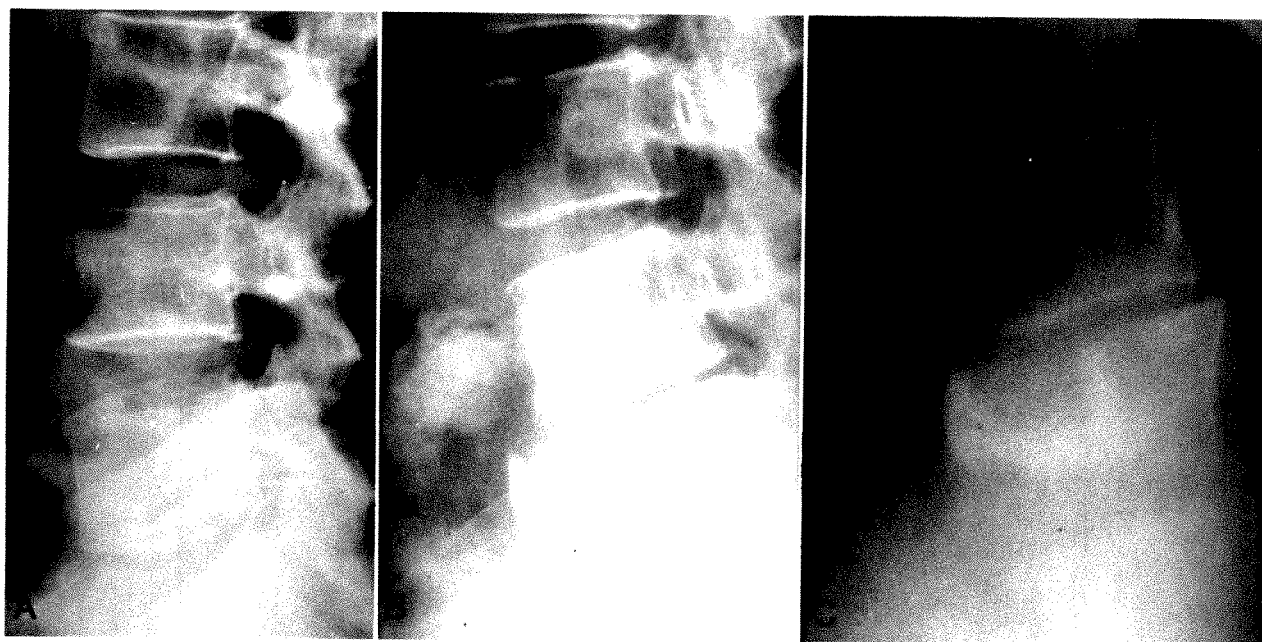


Fig. 8.—47-year-old female with severe rheumatoid arthritis. Lesion in L5 developed between 1957 (A) and 1960 (B). C, Midline laminogram (1960) showing narrowing of L4–L5 disc space and destruction and reactive sclerosis of L5. Note expansion of body of L5, relative sparing of adjacent endplate of L4, and reduced disc at L4–L5. Lesion involved S1 as well. No paraspinous soft tissue mass present. Open biopsy showed extrusion of hyaline and fibrocartilage into bone with reactive fibrosis, granulation tissue, and cartilage metaplasia. There were no rheumatoid lesions; changes were consistent with trauma and intrabody disc herniation.

was lacking and cultures were repeatedly sterile.

Conclusions

The roentgenographic appearance of the lesions in the lytic and sclerotic groups are sufficiently characteristic to warrant conservative management with radiologic re-

evaluation after an appropriate interval. Lesions showing both lytic and sclerotic components could pose a diagnostic problem. The absence of clinical evidence of sepsis or a paraspinous soft tissue mass and the lack of progression should suggest a traumatic rather than infectious etiology. It is important for radiologists to recognize that such lesions

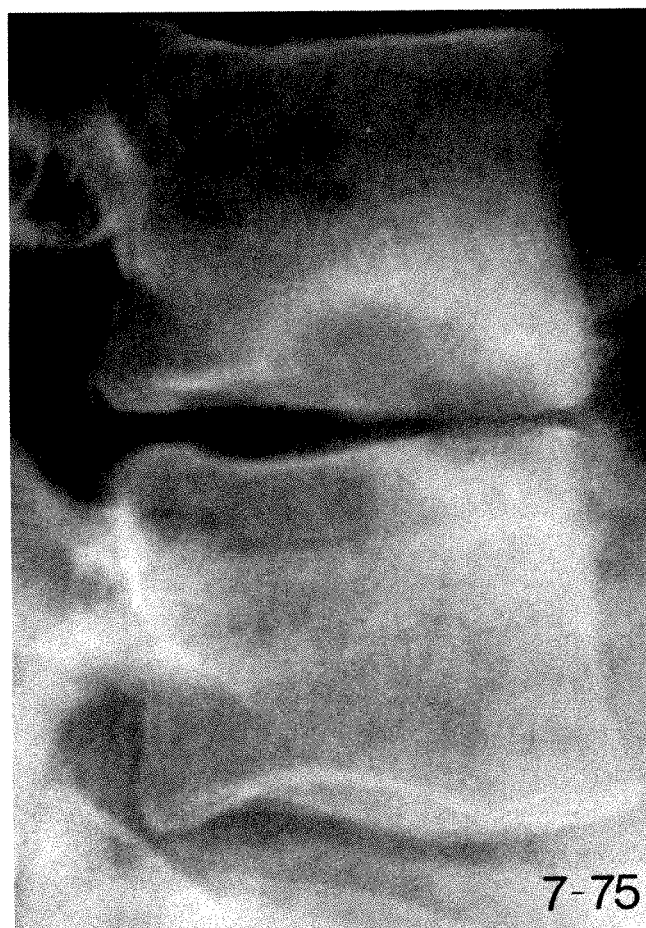


Fig. 9.—45-year-old female with 11 month history of low back pain. Appearance simulates infectious spondylitis, but percutaneous trochar biopsy showed no evidence of inflammation. Cultures of disc material negative.

need not be due to infections, although it may be difficult to exclude this possibility on the basis of a single examination.

REFERENCES

1. Brown T, Hansen RJ, Yorra AJ: Some mechanical tests on the

TABLE 2
Clinical Features

Feature	Group		
	Lytic (N=5)	Sclerotic (N=11)	Lytic and Sclerotic (N=6)
Sex:			
Female	3	10	6
Male	2	1	0
Age:			
<40	3	0	0
40–50	1	8	5
>50	1	3	1
Antecedent trauma	3	1	0
Back pain	4	8	5
Positive neurologic signs	1	3	0
Diabetes mellitus	1	4	1
Rheumatoid arthritis . . .	0	1	2

lumbosacral spine with particular reference to the intervertebral discs. A preliminary report. *J Bone Joint Surg* 39A:1135–1164, 1957

2. Jayson MIV, Herbert CM, Barks JS: Intervertebral discs: nuclear morphology and bursting pressures. *Ann Rheum Dis* 32:308–315, 1973
3. Schmorl G, Junghanns H: *The Human Spine in Health and Disease*. New York, Grune & Stratton, 1971
4. Perey O: Fracture of the vertebral endplate in the lumbar spine: an experimental biochemical investigation. *Acta Orthop Scand [Suppl]* 25:68–78, 1957
5. Ritchie JH, Fahrni WH: Experimental surgery. Age changes in lumbar intervertebral discs. *Can J Surg* 13:65–71, 1970
6. Farfan HF, Huberdeau RM, Dubow HI: Lumbar intervertebral disc degeneration. *J Bone Joint Surg* 54A:492–510, 1972
7. Numaguchi Y: Osteitis condensans ilii, including its resolution. *Radiology* 98:1–8, 1971
8. Ackermann W, Schwarz G: Non-neoplastic sclerosis in vertebral bodies. *Cancer* 11:703–708, 1958
9. Feldman F, Johnson AM, Walter JF: Acute axial neuroarthropathy. *Radiology* 111:1–16, 1974
10. Seaman WB, Wells J: Destructive lesions of the vertebral bodies in rheumatoid disease. *Am J Roentgenol* 86:241–250, 1971
11. Williams JL, Moller GA, O'Rourke TL: Pseudoinfections of the intervertebral disk and adjacent vertebrae? *Am J Roentgenol* 103:611–615, 1968

Congenital Dislocation of the Knee

DAVID H. CARLSON¹ AND JOHN O'CONNOR²

Four cases of congenital dislocation of the knee are presented. The incidence, associated congenital anomalies, presentation, and etiology are discussed with particular attention to the roentgenographic findings.

Congenital dislocation of the knee is a fairly rare congenital anomaly, occurring much less frequently than congenital dislocation of the hip. Its incidence varies from one per 40 [1, 2] to one per 80 [3] hip dislocations. Despite this, congenital knee dislocations have been extensively discussed in the orthopedic literature [1, 2, 4, 5]. In contrast, this entity is virtually unknown in the radiologic literature and scarcely mentioned in the pediatric literature [6-8]. While the general term congenital dislocation is used, a distinction should be made between genu recurvatum and congenital subluxation or dislocation. Genu recurvatum applies only to hyperextension of the knee, while with a dislocation or subluxation there is hyperextension with actual anterior displacement of the tibia [1, 2]. The following four cases demonstrate the presentation, roentgenographic findings, and clinical course.

Case Reports

Case 1

T. L. C., a white newborn female, was delivered by caesarean section at 38 weeks gestation after an uneventful pregnancy. Her 29-year-old mother had four previous caesarean sections with all children alive and well. Her only past clinical illness was surgery for a thyroid nodule. The baby was in vertex presentation before delivery. The left knee was immediately noted to be hyperextended and resistant to flexion. The right leg was normal, and no other anomalies were noted. Roentgenograms showed no evidence of fracture.

Since the knee could be hyperextended almost 60° but showed no evidence of frank dislocation, it was diagnosed a genu recurvatum deformity (fig. 1). Traction was applied to the leg to obtain a vacuum arthrogram which suggested a normal joint space. Since it was possible to gradually flex the leg, more efforts at a traction arthrogram were felt unnecessary. Within a day the knee was manipulated to 60° of flexion and was held in place by a finger splint. One year later, the knee appears normal and the prognosis is felt to be excellent.

Case 2

B. G. T., a black newborn female, was delivered by vertex presentation after a 12 hr labor. Her birth weight was 5 pounds 13 ounces. The 38 week gestation was uneventful. Her 24-year-old mother had an unremarkable medical history, but three of her previous five pregnancies had been breech, and her uterus was bicornius bicollis with a septate vagina. The baby was immediately noted to have a bilateral genu recurvatum deformity.

Roentgenograms in hyperextension showed almost 90° of extension with the tibia displaced anterior to the femur in frank dis-

location (fig. 2). No flexion could be obtained on passive motion. The dislocations were reduced by serial casting, but afterward the patient was lost to follow-up.

Case 3

B. G. K., a black newborn female, was delivered by vertex presentation after a normal full term delivery. Her birth weight was 7 pounds 5 ounces. The mother had three previous unremarkable pregnancies. On physical examination, bilateral genu recurvatum deformities were noted with some subluxation on the left. The right knee was less severely involved and could be flexed actively.

The appearance of the deformity $\frac{1}{2}$ hr after birth is shown in figure 3A; pigmentation was on the dorsal aspect of the knee rather than over the patella. Roentgenograms show a more severe recurvatum deformity on the left side, but the subluxation is not demonstrated (fig. 3B). The knees were easily reduced to 90° of flexion in a cast. Further follow-up was not obtained.

Case 4

C. R., a white newborn female, was the product of a normal vertex delivery. The birth weight was 7 pounds 3 ounces. On ex-

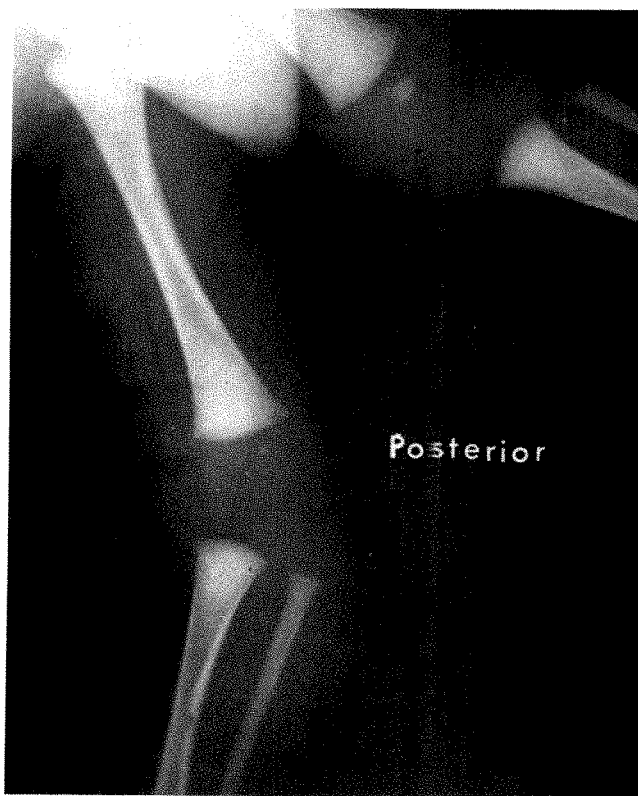


Fig. 1.—Case 1. Lateral views of both knees showing genu recurvatum of right knee with hyperextension. Ossification center on right is hypoplastic.

¹ Department of Radiology, Newton-Wellesley Hospital, Newton Lower Falls, Massachusetts 02162. Address reprint requests to D. H. Carlson.

² Department of Radiology, Boston City Hospital, Boston, Massachusetts 02118.

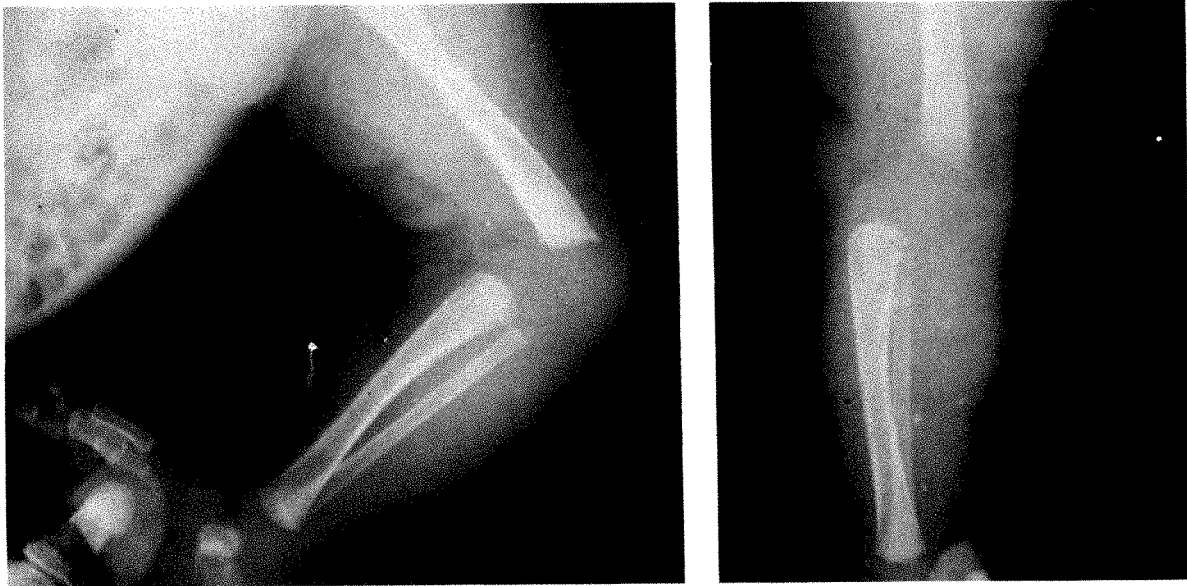


Fig. 2.—Case 2. Lateral views of left knee in hyperextension and neutral position showing frank dislocation.

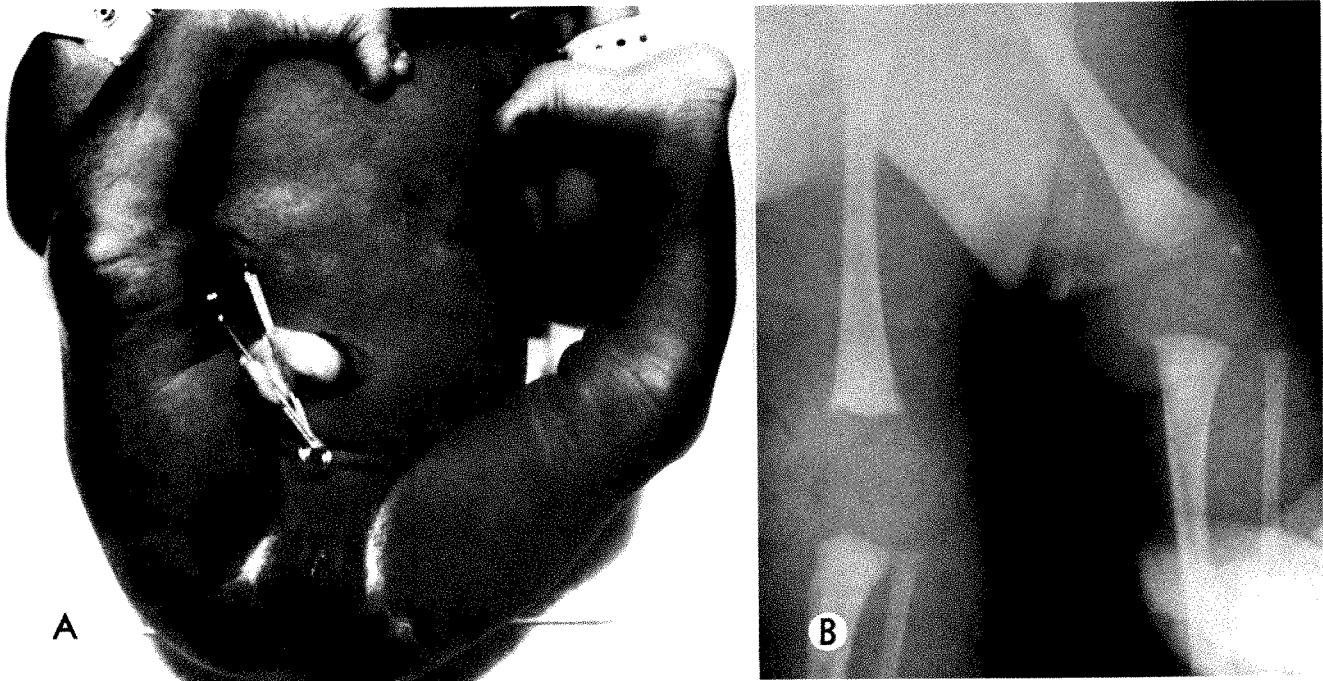


Fig. 3.—Case 3. *A*, Photograph at birth demonstrating bilateral genu recurvatum deformities. *B*, Lateral views of both knees showing bilateral genu recurvatum deformities. Although baby was full term, ossification centers are absent.

amination, the right leg was hyperextended. It could be extended to 40° and flexed to 90° with gross instability laterally. Mild subluxation was noted. The foot was in mild calcaneus position.

Roentgenograms show the characteristic straightening of the affected leg in comparison to the normal degree of varus (fig. 4). The lateral view did not fully demonstrate the degree of hyperextension. The knee was easily reduced, and on roentgenograms obtained 2 years later the knee appeared normal.

Discussion

Associated Congenital Anomalies

The congenital anomalies most frequently associated with congenital dislocation of the knee are congenital dislocation of the hip and congenital anomalies of the feet, such as talipes equinovarus. These have been found in as

high as 45% and 31% of the cases, respectively, in one large series [4]. Patients with brain deformities and myelomeningocele are usually excluded from such surveys since they may develop excessive ligamentous laxity which can simulate congenital dislocation [5].

Patients with arthrogryposis often have congenital dislocations of the knee as well as dislocations of the hip and foot anomalies [1]. In addition, patients with Larsen's syndrome may present with multiple congenital dislocations including the hips, knees, feet, and elbows [9]. These patients may be identified by characteristic facies including prominent forehead and hypertelorism. It is of interest that two cases in a large series of patients with genu recurvatum are obviously afflicted with Larsen's syndrome [5].

Knee dislocations have also been noted in patients with camptodactyly (incurving of the little finger) [10] and in syndromes with associated ligamentous laxity such as Ehlers-Danlos syndrome [11]. Mongolism, cryptorchism, angiomas, facial paralysis, and imperforate anus have been reported in patients with congenital dislocation of the knee [2] but may represent only a chance association. Only one of our patients had a minor foot anomaly (calcanus) which responded well to conservative measures.

In summary patients fall into three categories: (1) sporadic cases of congenital dislocation of the knee, such as our four; (2) patients with multiple dislocations; and (3) those with complete syndromes which predispose to multiple dislocations, such as Larsen's syndrome or arthrogryposis. A review of the cases suggests that patients with dislocated knees alone may have a better prognosis than those with multiple dislocations. While it appears that bilateral cases are usually more severe [2, 5], this impression is not well substantiated.

Incidence

While earlier surveys showed little difference in incidence between the sexes [12], most recent studies show up to twice as many cases in females as males [1, 2, 4, 5]. All four of our patients were female. A marked preponderance of congenital dislocation of the hip in females is also noted [13].

Excluding cases of Larsen's syndrome, it is uncertain whether sporadic cases of congenital dislocation of the knee have a hereditary basis. The case cited most frequently of a mother with a three afflicted children from three different husbands probably represented Larsen's syndrome [14].

Clinical and Radiologic Findings

Diagnosis is readily made by inspection when the involved extremity shows marked asymmetry in posture. With manipulation the limitation of flexion and obvious hyperextension are easily noted. Roentgenograms are valuable in ruling out birth trauma. On the anterior projection the straightening of the affected leg is noted in comparison to the normal varus posture (fig. 4). In lateral projection under manipulation it is easy to quantify the degree of hyperextension and flexion as a means of evaluating improvement.



Fig. 4.—Case 4. AP view demonstrating characteristic straightening of abnormal right knee.

The displacement of the tibia anterior to the femur readily demonstrates the frank dislocation (fig. 2) compared to the simple genu recurvatum (fig. 1). The partial displacement seen with a subluxation demonstrates the intermediate phase. While congenital fusions are rare, an air arthrogram obtained by gentle traction may provide helpful information. Obviously roentgenograms are invaluable in evaluating any problems generated by incomplete or overvigorous manipulation. Finally, prenatal diagnosis of this entity has been reported [15].

Although our four patients were over 36 weeks gestation, the distal femoral ossification centers were absent in three. Two of these were patients with bilateral dislocations (cases 2 and 3). With case 1 the involved knee showed a hypoplastic epiphysis (fig. 1). This is similar to the hypoplasia of the epiphysis seen in congenital dislocation of the hip [13]. To our knowledge this observation has not been made previously with congenital dislocation of the knee even though it has been present on roentgenographic reproductions [2]. In our series and apparently in others, the later development of the ossification centers does not appear to be retarded.

Treatment

The vast majority of patients do extremely well using conservative management with serial casting or traction [1, 4]. All of our cases were reduced using these measures. Difficult cases, particularly neglected dislocations, patients with multiple dislocations, or those with arthrogryposis, often require open reduction [1, 2] and may present real challenges for reconstruction. Surgery is recommended before the age of 2 in complicated cases [1].

Etiology

Numerous theories exist regarding the causes of congenital knee dislocations. A congenital defect in the cruciate ligaments has been suggested by Katz et al. [4] who found hypoplastic cruciates in five patients. This has not been noted by other investigators and may relate to the older age of these patients with resultant adaptive changes [6]. A tendency to a lateral displacement of the patella has been noted [6]. Other experiments with division of ligaments in fetal knees show no single set of ligaments, including the cruciates, to be of prime importance in maintaining stability [5].

Other theories of etiology relate to intrauterine forces such as malposition, increased mechanical pressure, or increased hydraulic pressure being factors in causing deformities of the foot, hip, or knee [2, 8, 12]. Mechanical factors might include oligohydramnios which could result in excessive crowding of the fetal parts. A particularly graphic theory of malposition includes the locking of the extended legs under the chin in a breech presentation with resultant hyperextension of the knees [16]. Some authors feel that breech presentations predispose to this entity [2, 4], but this does not explain all of the cases. None of our patients had oligohydramnios and none were in breech presentation. Finally, it has been shown that adverse environmental influences can produce developmental anomalies indistinguishable from those of genetic origin [17]. Perhaps this avenue of research will be more productive than hypotheses of intrauterine pressure.

ACKNOWLEDGMENTS

We thank Drs. Joseph Kennedy and Forrest Maddix for contributing case material and Dr. Joseph Hanelin for suggestions and review of the manuscript.

REFERENCES

1. Curtis BH, Fisher RL: Congenital hyperextension with anterior subluxation of the knee. *J Bone Joint Surg* 51-A:255-269, 1969
2. Niebauer JJ, King DE: Congenital dislocations of the knee. *J Bone Joint Surg* 42-A:207-225, 1960
3. Kopits, E: Beitrage zur Pathologic und Therapie der angeborenen Kniegelenkssubluxationen. *Arch Orthop Unfallchir* 23:593-609, 1925
4. Katz MP, Grogono BJS, Soper KC: The etiology and treatment of congenital dislocation of the knee. *J Bone Joint Surg* 49-B:112-120, 1967
5. Laurence M: Genu recurvatum congenitum. *J Bone Joint Surg* 49-B:121-134, 1967
6. Abt IA: Pediatrics, vol 5. London, Saunders, 1924
7. Boorstein SW: Congenital backward dislocation of the knee. *Am J Dis Child* 38:107-111, 1929
8. Browne D: Congenital deformities of mechanical origin. *Arch Dis Child* 30:37-41, 1955
9. Larsen LJ, Schottstaedt ER, Bost FC: Multiple congenital dislocations associated with characteristic facial abnormality. *J Pediatr* 37:574-581, 1950
10. Murphy DP: Familial finger contracture and associated familial knee joint subluxation. *JAMA* 86:395-397, 1926
11. Gorlin RJ, Pindborg JJ: *Syndromes of the Head and Neck*. New York, McGraw-Hill, 1964
12. Provenzano RW: Congenital dislocation of the knee: report of a case. *N Engl J Med* 236:360-362, 1947
13. Caffey J: *Pediatric X-Ray Diagnosis*, 5th ed. Chicago, Year Book Medical Publishers, 1961
14. McFarlane AL: A report on four cases of congenital genu recurvatum occurring in one family. *Br J Surg* 34:388-391, 1947
15. McFarland BL: Congenital dislocation of knee. *J Bone Joint Surg* 11:281-285, 1929
16. Shattock SG: Genu recurvatum in a foetus at term. *Trans Pathol Soc London* 42:280-292, 1891
17. Duraiswami PK: Comparison of congenital defects induced in developing chickens by certain teratogenic agents with those caused by insulin. *J Bone Joint Surg* 37-A:277-294, 1955

The Os Incae

ROBERT SHAPIRO¹ AND FRANKLIN ROBINSON²

The os incae is an integral feature of reptilian and various mammalian skulls which demonstrate intramembranous ossification centers behind the parietal bones. In man, the interparietal portion of the occipital squamosa arises in membrane from a single ossific focus. Normally it fuses with the supraoccipital segment of the occipital squamosa. Occasionally there are multiple ossification centers in the interparietal bone which fail to fuse, resulting in one of several varieties of os incae.

Introduction

In 1842 Bellamy [1] described two Peruvian mummy skulls with a transverse suture isolating the superior portion of the occipital squama and assumed that the anomaly was a racial characteristic of the Incas. Two years later, Tschudi [2, 3] confirmed Bellamy's observation in a number of skulls from Peruvian coastal cemeteries and coined the eponym os incae. Geoffroy Saint-Hilaire [4] had reported a similar finding in 1823 under the name os interparietale. The first description of an os incae in man should probably be credited to Bartolomeo Eustachi whose original drawing was reproduced by Albinus in 1744 [5] (fig. 1). Since Bellamy's description, many other authors [6-14] have dealt with the same subject, including Thomas Bartholin who gave the generic term os wormianum to intercalated bones in honor of the Danish anatomist Olaus Wormius. The latter had previously described these bones at some length in a letter to Bartholin [15].

Further studies have shown that this anomaly occurs only in from 5%-23% of Inca skulls [11] and in many other peoples as well. Although a number of terms have been used to describe the same bone (os transversum cranii, os interparietale, os epactale), the popularity of the eponym os incae persists.

Material

In addition to the fetal specimens utilized in studying the embryogenesis of the occipital bone [16], we have examined numerous vertebrate skulls from the collections at the Peabody Museum in New Haven and the Museum of Natural History in New York City.

Comparative Anatomy

The human skull, like that of all vertebrates, is a composite structure consisting of three major components: (1) the dermal or membranous roof; (2) the cartilaginous base; and (3) the visceral palatal complex which gives rise to the upper jaw and roof of the mouth. In cyclostomes (e.g., *Petromyzon marinus*, marine lamprey) and sharklike fishes (e.g., *Squalus acanthias*, spiny dog fish) the primitive brain lies at the base of the skull, protected by a single

piece of cartilage to which the olfactory and otic capsules are attached. With ascending development in primitive vertebrates (e.g., *Necturus maculosus*, mud puppy), membranous bones derived from the bony scales of fishes appear and cover the roof of the cranium. This pattern is repeated in higher vertebrates with variable ossification of the dermal membranous roof.

Mammals are descended from primitive reptilian ancestors. At the mammalian level, dramatic changes in the skull take place. Since the genetic code governing the growth of the chondrocranium is probably inherent in the primitive prechondral mesenchyme, it is not surprising that the human chondrocranium replicates the cartilaginous braincase of the primitive shark in modified form. However, the remarkable cerebral growth in man soon outstrips the capacity of the cartilaginous braincase to contain it. Since the latter covers only the floor and lower back wall of the brain, the new protective roof for the greatly enlarged brain must come from ossified membrane. In addition, the single midline occipital condyle of the reptile is replaced by two condyles and the occipital elements fuse into a single bone.

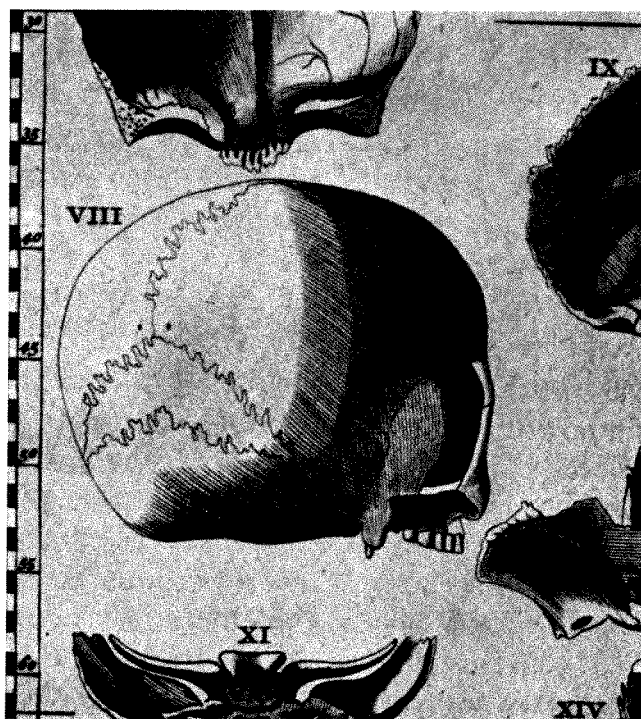


Fig. 1.—Albinus's reproduction of original drawing by Eustachius of an os incae (fig. VIII).

¹ Department of Radiology, Hospital of St. Raphael, Yale University School of Medicine, New Haven, Connecticut 06511.

² Department of Neurosurgery, Hospital of St. Raphael, Yale University School of Medicine, New Haven, Connecticut 06511.



Fig. 2.—Deer skull (*Odocoileus virginianus*) illustrating large interparietal bone (P).



Fig. 3.—Spalteholz preparation of skull of 14-week-old human embryo. Note bipartite os incae below lambda (I). Remainder of interparietal segment is separated from supraoccipital segment by mendosal suture (arrow).

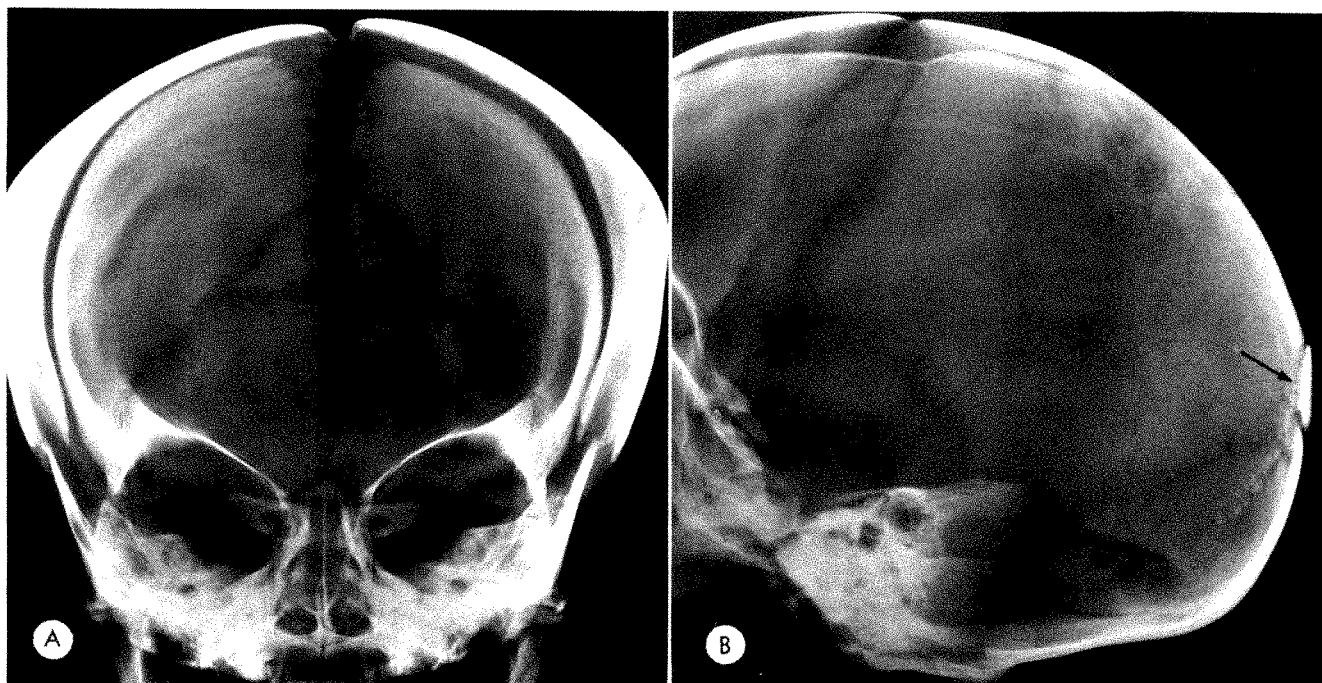


Fig. 4.—Frontal (A) and lateral (B) radiographs of skull of stillborn full term infant demonstrating classical triangular os incae (ip). Note sclerotic appearance in lateral projection (arrow).

The embryology of the occipital bone has been fully discussed [16].

The interparietal bone is an old integrated portion of the reptilian and mammalian skull [17]. In the alligator, some birds, and many mammals (especially marsupials) (fig. 2), intramembranous ossification centers (i.e., postparietal or interparietal bones) are present behind the parietal bones. These centers normally fuse to form a single complex, the interparietal bone, which unites with the supraoccipital segment in man and other mammals. However, in some

species (e.g., *Sirenia*, sea cow), the interparietal bone unites with the parietal bones; in other forms (e.g., *Lepus*, hare), it remains separate. If the interparietal segment in man arises from multiple centers which fail to fuse, its superior portion (os incae) remains separated from the rest of the interparietal bone by a suture (fig. 3).

The most common type of os incae is a single large triangular bone separated from the rest of the interparietal bone by a transverse suture (fig. 4). Less commonly, rhombic or heartshaped forms may be seen. Kadanoff and

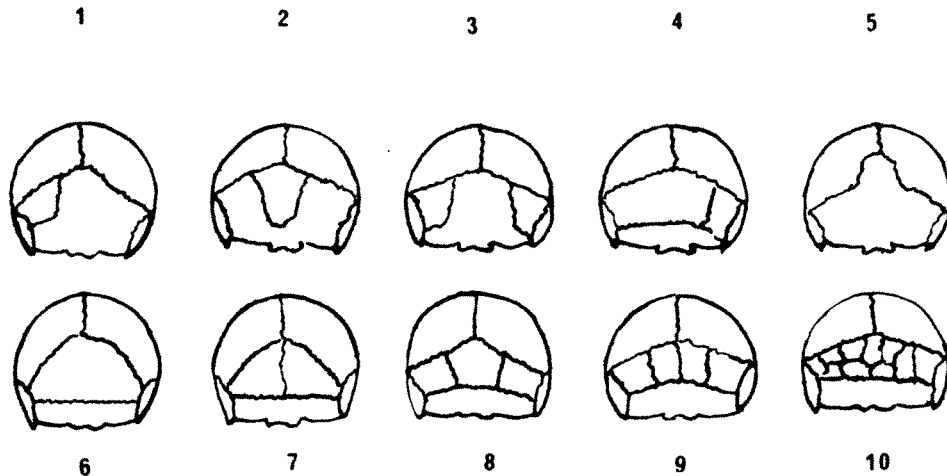


Fig. 5.—Diagrammatic representation of types of os incae in man (modified from [10]). 1, Os incae totum; 2, os incae bipartitum; 3, os incae tripartitum; 4, os incae quadripartitum; 5, os incae multipartitum; 6, os incae laterale; 7, os incae centrale; 8, os incae duplex symmetricum; 9, os incae duplex asymmetricum; 10, pars incoidea squamae occipitalis.

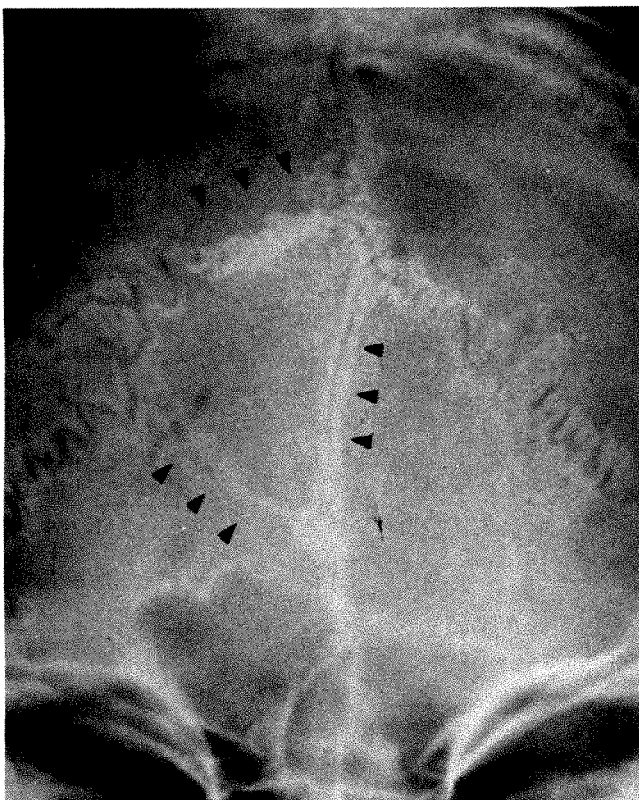


Fig. 6.—Asymmetrical right lateral os incae with sclerotic margins (arrows).

St. Mutafov [10] reviewed 3,522 Bulgarian skulls (fig. 5) and found the classical triangular type in 1.74% of specimens. In the same study, symmetrical bipartite (0.82%) (see fig. 3), tripartite (0.14%), and multipartite (0.14%) examples were noted. Less typical forms (left or right lateral os incae [fig. 6], symmetrical and asymmetrical os incae duplex) occurred in 0.62% of their material.

ACKNOWLEDGMENTS

We are grateful to Dr. John Ostrom of the Peabody Museum of Natural History for his cooperation, to Drs. E. Leon Kier, William

Allen, and Edmund S. Crelin for permitting us to use several dry fetal skulls, to the Yale Medical Historical Library for permission to photograph Tabula XLVI from Albinus's monograph on Eustachius, and to Ferenc A. Gyorgyey of the Yale Medical Historical Library for help in arranging for the aforementioned photograph.

REFERENCES

1. Bellamy CF: Cited in Kadanoff D, St. Mutafov: Os incae bei Bulgaren. *Morphol Jahrb* 105:602–615, 1964
2. Rivero ME Tschudi JJ: *Peruvian Antiquities*, translated from Spanish by Hawkes FL, 1854, pp 38–39, cited in Parker CA: *Wormian Bones*. Chicago, Roberts Press, 1905
3. Tschudi JJ: Über die Ureinwohner von Peru. *Arch Anat Physiol Wiss Med*, 1844, pp 98–109
4. Geoffroy Saint-Hilaire E: Considérations et rapports nouveaux d'ostéologie comparée concernant les animaux. *Mem Museum d'Histoire Naturelle Paris* 10:165, 1823
5. Albinus (Albinus) BS: *Explicatio tabularum anatomicarum*, in *Bartholomaei Eustachii*, edited by Langerak JA, Verbeek JH, Leiden, Netherlands, 1744
6. Aichel O: Über die Entstehung des Incabeins. *Anat Anz* 43:463–469, 1913
7. Debierre C: *Traité élémentaire d'anatomie del homme*, vol 1. Paris, 1890, p 86
8. Broili F: Unpaare Elemente im Schädel von Tetrapoden. *Anat Anz* 49:561–576, 1917
9. Huehne F: Die Herkunft des Os interparietale der Mammalia. *Anat Anz* 42:522–524, 1912
10. Kadanoff D, St. Mutafov: Os incae bei Bulgaren. *Morphol Jahrb* 105:602–615, 1964
11. LeDouble AF: *Traité des variations des os du crâne de l'homme*. Paris, Vigot Frères, 1903
12. Meckel JF: *Beiträge zur vergleichenden Anatomie*, vol 1. Leipzig, 1809, pp 34–64
13. Parker CA: *Wormian Bones*. Chicago, Roberts Press, 1905
14. Wegner RN: Das os interparietale als integrierender Bestandteil der Säuger und Thermomorphenschädel. *Morphol Jahrb* 100:375–419, 1959
15. Wormius O: *Epistolae*. Kopenhagen, 1671
16. Shapiro R, Robinson F: Embryogenesis of the human occipital bone. *Am J Roentgenol* 126:1063–1068, 1976
17. DeBeer GR: *The Development of the Vertebrate Skull*. Oxford, Clarendon Press, 1937

A New Radiographic Technique for Fractures of the Orbit and Maxilla

EDWIN L. LAME¹ AND THOMAS J. REDICK¹

A variant oblique posture of the head is described which eliminates most superimposition in radiographic examination of the orbit and maxilla. The position is simply attained without extraordinary equipment, is comfortable for the patient since there is no pressure on injured parts, and often obviates the need for planigraphy. The following injuries are demonstrated best: displacement at the frontozygomatic suture; deformity of the orbital floor and its distance from the anterior orbital rim; degree of depression of the anterior zygoma, antral wall, and alveolus; and vertical displacement of the zygomatic arch.

Technique

The erect posture at the headstand is preferable (fig. 1). The posteroanterior (PA) oblique is usual, but the anteroposterior (AP) posture may be used if it is more comfortable. In the PA position the affected side is rotated 37° off the cassette holder (unlike an oblique ethmoid position). In figure 1 the right orbit is examined. This produces a record of numerous important structures with minimal interference.

The most frequent undesirable superimposition is that of the zygomatic arch on the orbital floor. When this occurs, a slight lateral tilt of the head to depress the arch toward the ipsilateral shoulder will correct the fault. The arch should be superimposed on the antral air.

Two exposures are made. The lighter (averaging 50 mA, 0.5 sec, 50 kVp) demonstrates the lateral orbital wall (fig. 2) and the darker (averaging 50 mA, 0.5 sec, 65 kVp) the orbital floor and maxilla (fig. 3). The film-screen combination used is Eastman RPS-14 and Radelin midspeed.

Anatomic Variations

The variants which imitate fractures usually are those of the frontozygomatic suture and the nutrient channels at the lateral wall (O. V. Batson, personal communication) (fig. 2).

Since the sloping orbital floor has several depths and carries the infraorbital groove (infraorbital nerve and vessels), it is not unexpected that from one to four cortical layers may be seen normally (fig. 3). Much depends on the angle of incidence of the x-rays.

The anterior wall of the antrum and the alveolus offer no difficulties.

Usage for Specific Fractures

Although the conventional Waters and PA planigrams are used, this new technique has reduced the need for planigrams and has been of great value in the following injuries.

Lateral Wall of Orbit

Injury occurs very commonly at the frontozygomatic suture. There is characteristically displacement of the zygomatic portion by several millimeters medially, posteriorly, or both (figs. 5 and 6), and the deformity may be best demonstrated by this oblique exposure.

Orbital Floor

The deformity is often extremely slight but may be severe. Although most are well demonstrated by the Waters posture and PA planigrams, considerable benefit may be derived from using the oblique method, especially to determine need for surgical repair. Any break in the approximately horizontal cortical lines is strong evidence of fracture, and the degree of deformity (important to the ophthalmologist) is illuminated by the new exposure (figs. 5 and 7). Further, it provides better information than standard anterior views on the distance of the fracture from the anterior orbital cortex.

Anterior Zygoma and Maxillary Antrum, Alveolus and Teeth

Injuries of the anterior eminence of the zygoma and the anterior and lateral aspects of the antral wall of the maxilla are well demonstrated, especially in their AP depression (figs. 5 and 7). The same applies to the maxillary alveolus and teeth, with all images supplied free of superimposition (fig. 5). These injuries are often not demonstrated in conventional views (fig. 8).

Temporozygomatic Arch

The amount of vertical displacement in these injuries is probably best estimated by the present technique. Superimposition of the opposite side of the face is eliminated. Either the orbital soft tissue or the antral air aid in visualization (fig. 9).

Presented at the annual meeting of the American Roentgen Ray Society, Atlanta, Georgia, October 1975.

¹ Radiology Service, Veterans Administration Hospital, Coatesville, Pennsylvania 19320.

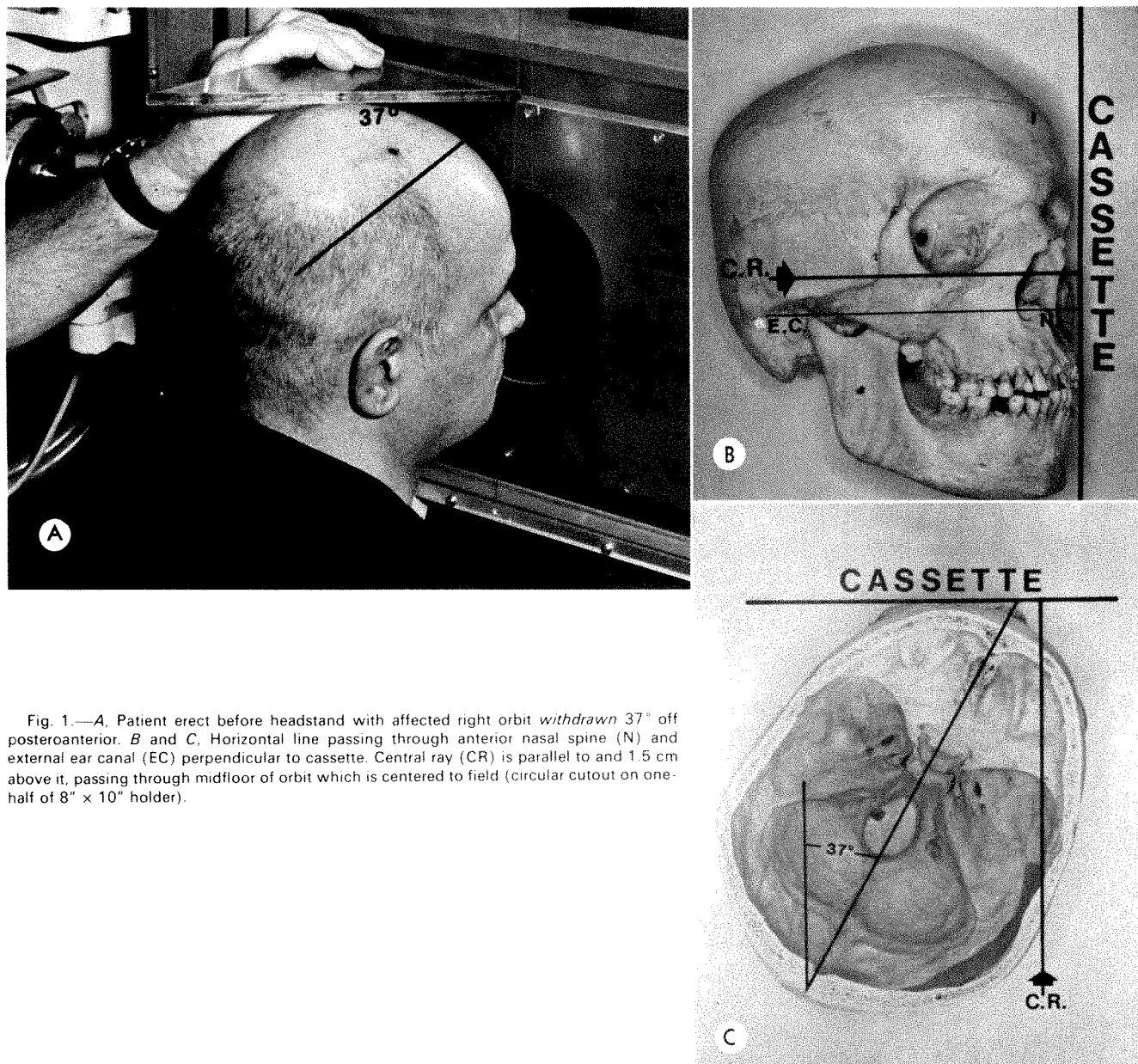


Fig. 1.—A, Patient erect before headstand with affected right orbit *withdrawn* 37° off posteroanterior. B and C, Horizontal line passing through anterior nasal spine (N) and external ear canal (EC) perpendicular to cassette. Central ray (CR) is parallel to and 1.5 cm above it, passing through midfloor of orbit which is centered to field (circular cutout on one-half of 8" × 10" holder).



Fig. 2.—Lighter of two exposures demonstrating lateral orbital wall. Some of many normal variations in living patients are shown. 1, Wide, frequent type of frontozygomatic suture. Uppermost part of sphenozygomatic suture can just be detected descending vertically. 2, Variation mimicking fracture. 3, Oblique combination of fronto- and sphenozygomatic sutures, rarely seen. 4, Very small frontozygomatic suture. 5, Wide nutrient groove forked at lower end. 6, Average normal frontozygomatic suture. 7 and 8, Varieties of nutrient grooves, one (8) without visible frontozygomatic suture.

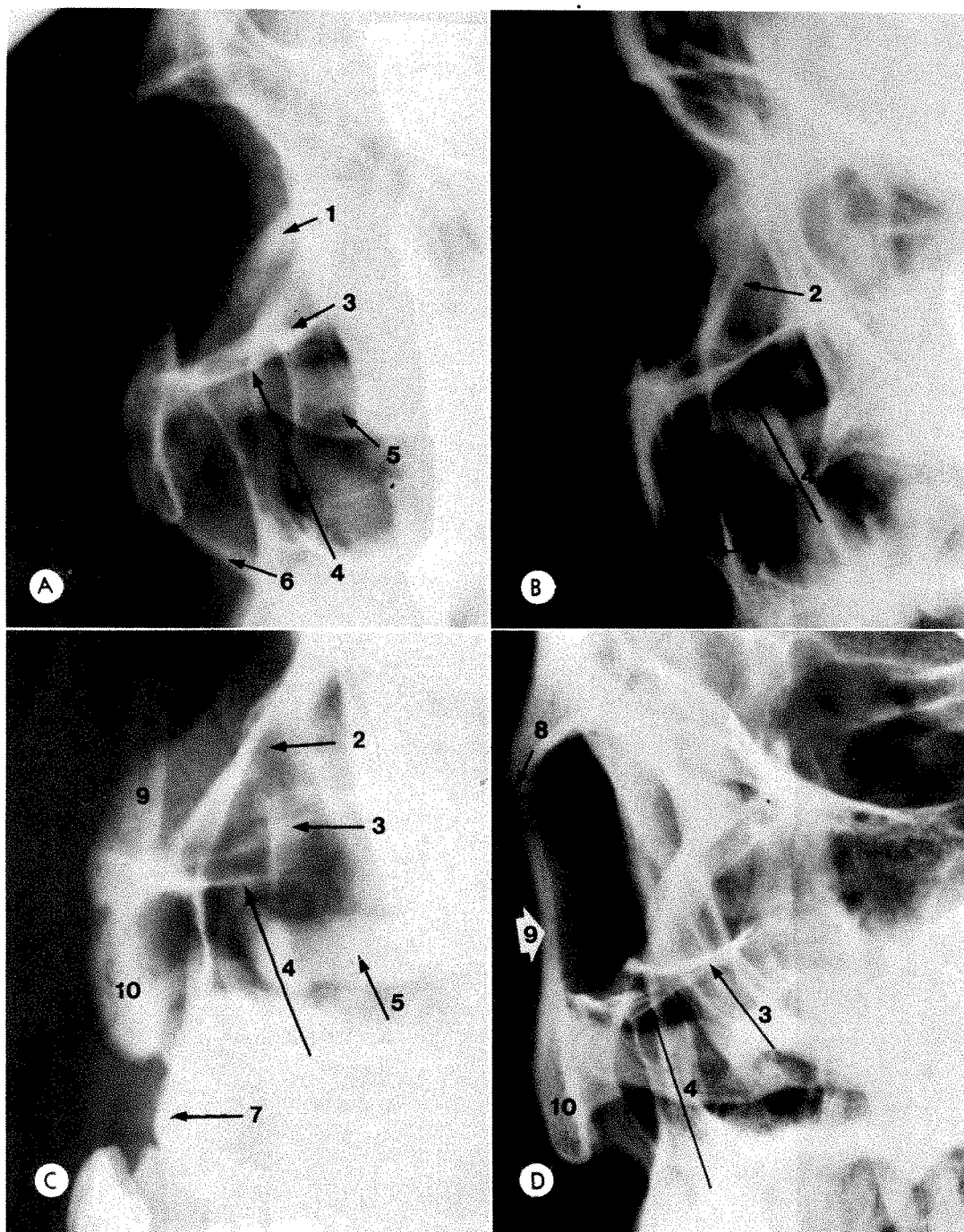


Fig. 3.—Darker of two exposures demonstrating orbital floor and maxilla. *A–C*, Normal variations in living patients. *D*, Dried skull with barium marking medial and lateral orbital floors. 1 = nasal bones; 2 = medial orbital wall; 3 = medial orbital floor; 4 = lateral orbital floor; 5 = temporozygomatic arch; 6 = inferior wall of maxillary antrum; 7 = maxillary alveolus; 8 = fronto-zygomatic suture; 9 = lateral orbital wall; 10 = zygomatic eminence.

Fig. 4.—Anterior cut-away of orbit and antrum. Most common sites of fracture in our series are floor of orbit, inferior wall of antrum, fronto-zygomatic suture, and zygomatic arch. (Adapted with permission from Sobotta J: *Atlas of Human Anatomy*, 6th ed, edited by McMurich, New York, G. E. Stechert, 1928, pp 59–60)

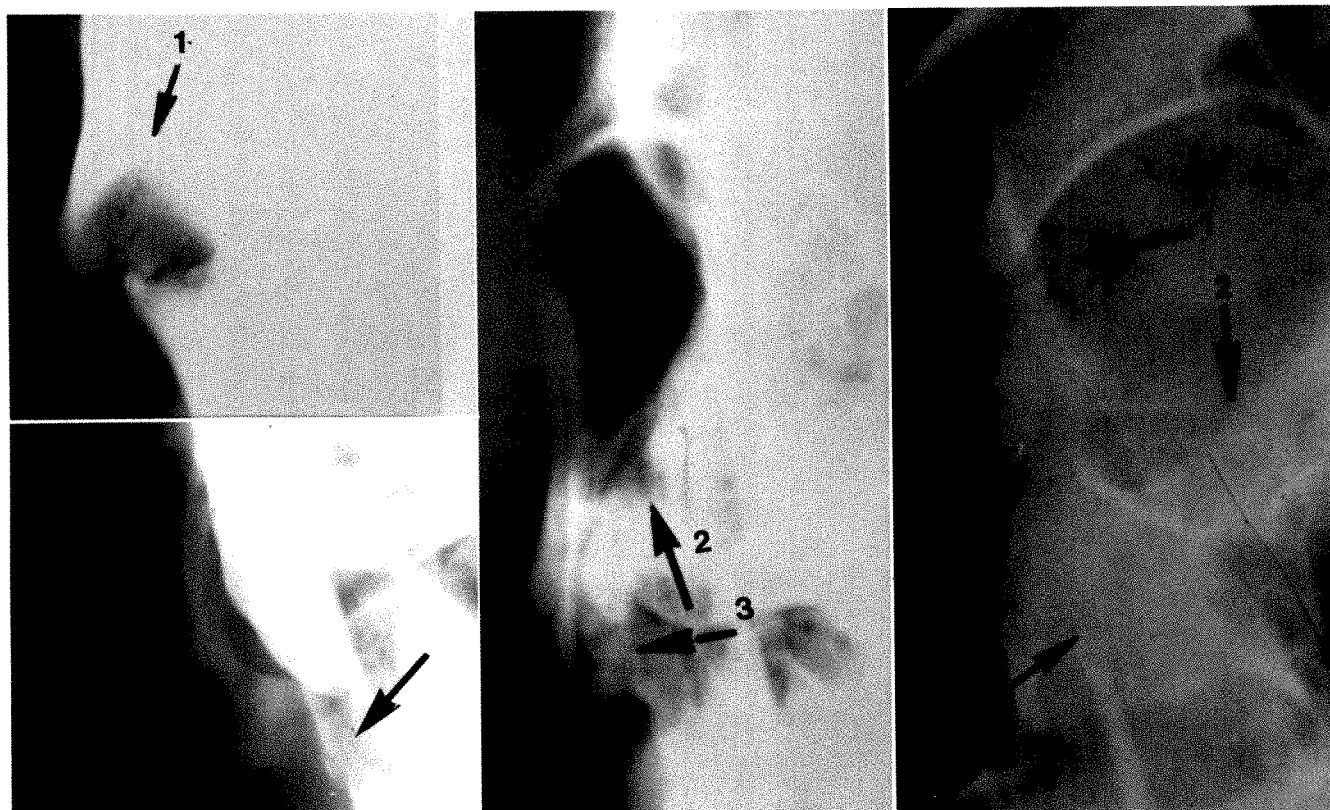
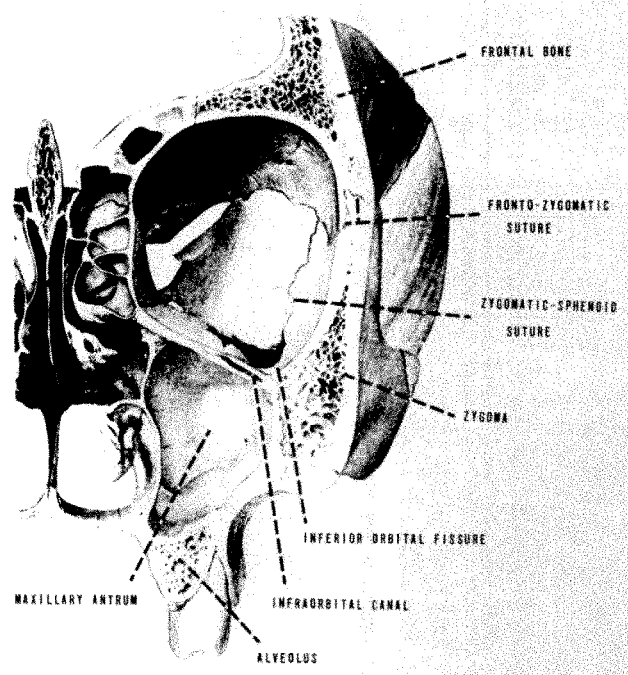


Fig. 5.—Case with four fractures. 1, Frontozygomatic suture with typical medial and posterior displacement of zygoma; 2, orbital floor with blunt depression shown only in the oblique; 3, anterior zygoma completely obscured in Waters view but plain in the oblique; 4, maxillary alveolus seen only in the oblique.

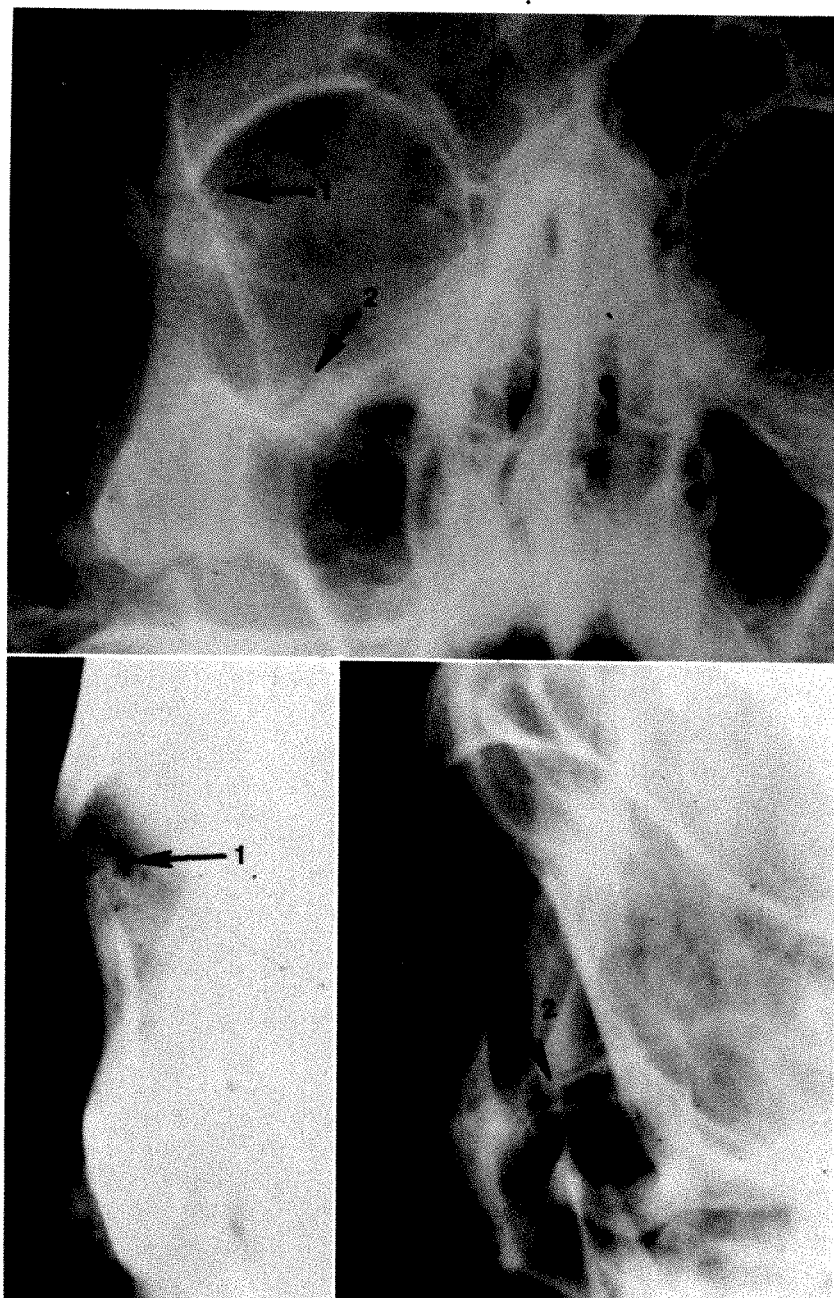


Fig. 6.—Case with two fractures. 1, Frontozygomatic suture with slight medial and posterior displacement of zygoma; 2, floor of orbit having diagonal fracture without depression, confirmed by oblique exposure.

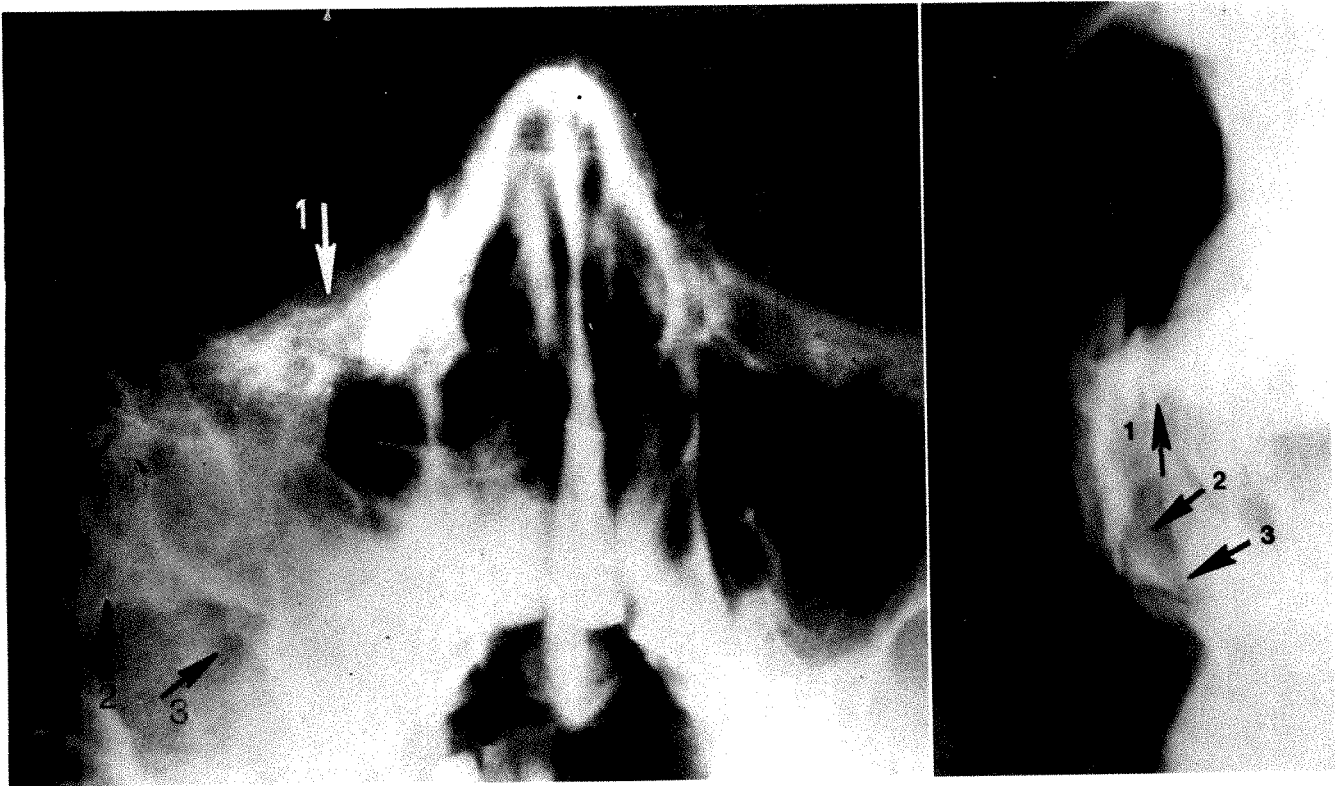


Fig. 7.—Case with three fractures. 1, Floor of orbit with crucial spicule directed vertically, shown only in oblique; 2, anterior zygoma best seen for lack of depression in oblique; 3, inferior wall of antrum. Deformity well seen in both exposures.

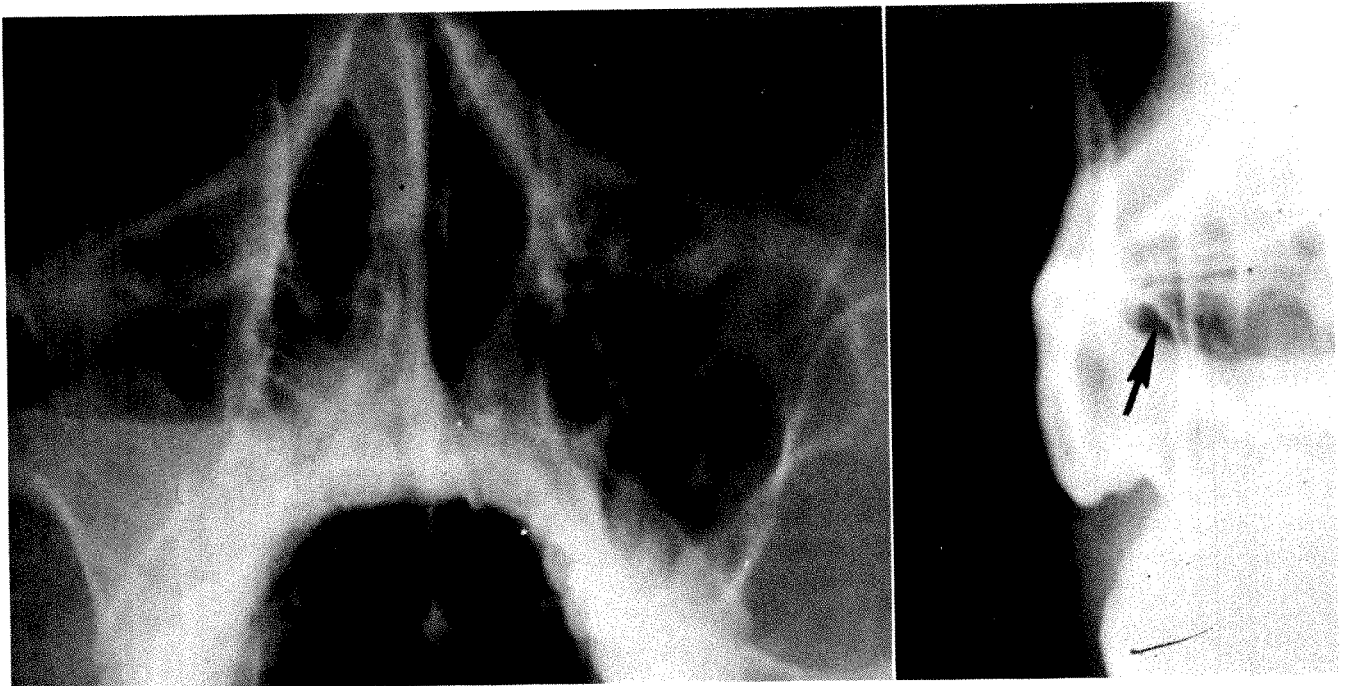


Fig. 8.—Fracture of anterior wall of antrum obscured by effusion but seen in oblique exposure virtually nondisplaced.

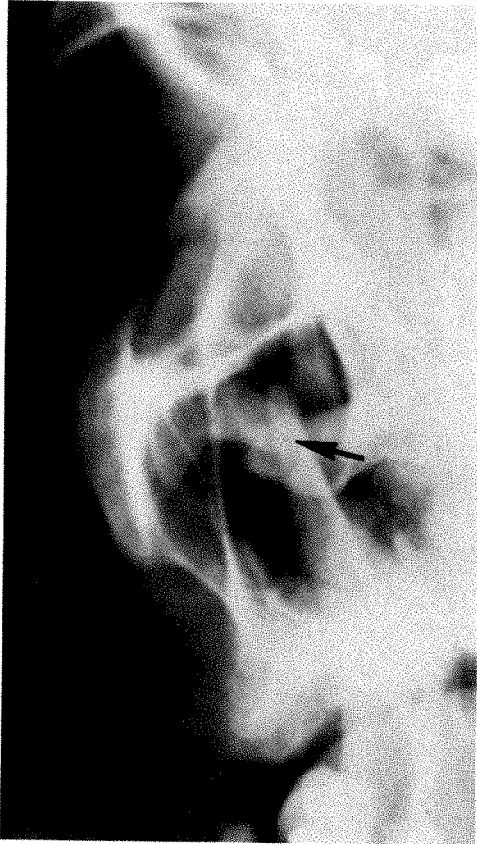


Fig. 9.—Fracture of zygomatic arch with vertical displacement, well seen superimposed on antral air.

Computed Tomography and Brain Scintigraphy in Ischemic Stroke

LEE C. CHIU,¹ LASZLO B. FODOR, STEVEN H. CORNELL, AND JAMES H. CHRISTIE

Radionuclide and computed tomographic (CT) scans were reviewed in 215 patients with ischemic stroke. The findings vary depending on the site of vascular occlusion. In middle cerebral artery occlusion, four distinct patterns may be seen on the scintigrams. The CT scans show little variation in appearance. The tentorial confluence sign is an important finding on scintigrams of patients with occipital infarction; the absence of this sign should suggest another diagnosis. During the first week and after the fourth week following an ischemic stroke, the scintigram is usually negative, whereas the lesion is visible by CT. However, there are a significant number of false negative CT scans; therefore, both examinations are advocated in difficult cases.

Characteristic patterns were seen on radionuclide and computed tomography (CT) scans in 215 patients with ischemic stroke who had both examinations during their hospitalization. The diagnosis of ischemic stroke was confirmed by angiography, autopsy, or long term follow-up. Location of the vascular occlusion determined the appearance of the radionuclide and CT scans.

Location of Occlusion

Middle Cerebral Artery

The middle cerebral artery (MCA) and its branches are the vessels most frequently involved in intracranial ischemic disease [1]. Review of 174 cases revealed the following patterns on ^{99m}Tc-pertechnetate radionuclide scans: (1) normal static scan/abnormal dynamic scan, 18%; (2) static scan with fan-shaped area of uptake, 56%; (3) static scan with crescent-shaped uptake, 21%; and (4) static scan showing multiple areas of uptake, 5%.

In major MCA occlusion the dynamic brain scan may appear either normal or abnormal with decreased, delayed, or increased perfusion depending on the extent of vessel involvement, collateral circulation, and, perhaps, localized metabolic acidosis.

In 31 cases (18%) the static scan was normal, but the anterior dynamic scan revealed decreased perfusion during the early arterial phase followed by a normal venous phase (fig. 1A).

In 98 patients (56%) the static scan demonstrated a fan-shaped pattern seen on the lateral view as a triangular area of increased density corresponding to the sylvian triangle. Increased activity in the MCA distribution could also be seen on the anterior projection (fig. 2A).

The crescent-shaped uptake was present in 36 cases (21%). This is best seen on the AP or PA view as an area of increased uptake parallel to the convex contour of the

skull (fig. 3A). The lateral views are negative or may reveal very faint increased uptake in the temporal region. This pattern is similar to that seen in subdural hematoma.

The multiple focal pattern was present in nine patients (5%) and is best seen on the lateral views (fig. 4A). This pattern is probably the result of multiple occlusions of branches of the MCA. It could also be due to sparing of portions of the brain from ischemia because of adequate collateral circulation.

There were 10% false negative radionuclide scans in comparison with the CT scans. These patients were examined less than 1 week or more than 4 weeks after the insult.

The CT scans demonstrate an area of decreased density in the region supplied by the MCA (figs. 1B, 2B, 3B, and 4B). During the first week after the stroke, the margins are often poorly defined. There may be displacement of the ventricular system secondary to edema (fig. 3B). Later the margins become sharper and the dark central area becomes more homogeneous. In an old infarct with loss of brain substance, there may be dilatation of the ipsilateral ventricle.

There were 14% falsely negative CT scans. Many of these cases were studied with the 80 × 80 matrix which gave scans of inferior quality compared to the 160 × 160 matrix in current use. The quality of many scans was also affected adversely by patient motion. In three instances, there was increased density of the infarct after intravenous injection of contrast material. When this occurs, differentiation from neoplasm is difficult.

Posterior Cerebral Artery

There were 28 patients with occlusion of a posterior cerebral artery. The anterior dynamic radionuclide scan was not helpful unless a vertex scintillation image was used. The static scan was positive in 23 cases (82%). The posterior view typically shows a wedge-shaped area of increased activity adjacent to the midline and extending down to the torcular Herophili and to the medial part of the transverse sinus. The lateral image shows increased activity in the shape of a tapering crescent or triangle which blends in with the normal activity of the posterior sagittal and transverse sinuses (fig. 5A). We call this the tentorial confluence sign. If the abnormally increased uptake is not confluent with the activity of the tentorial region, the possibility of a lesion other than a posterior cerebral artery occlusion should be considered.

The CT scan revealed decreased absorption in the occipital region of 26 patients (93%). If the tentorial confluence sign is absent on the radionuclide scan, CT with

Presented at the annual meeting of the American Roentgen Ray Society, Atlanta, Georgia, October 1975.

¹ All authors: Department of Radiology, University of Iowa Hospitals and Clinics, Iowa City, Iowa 52242.

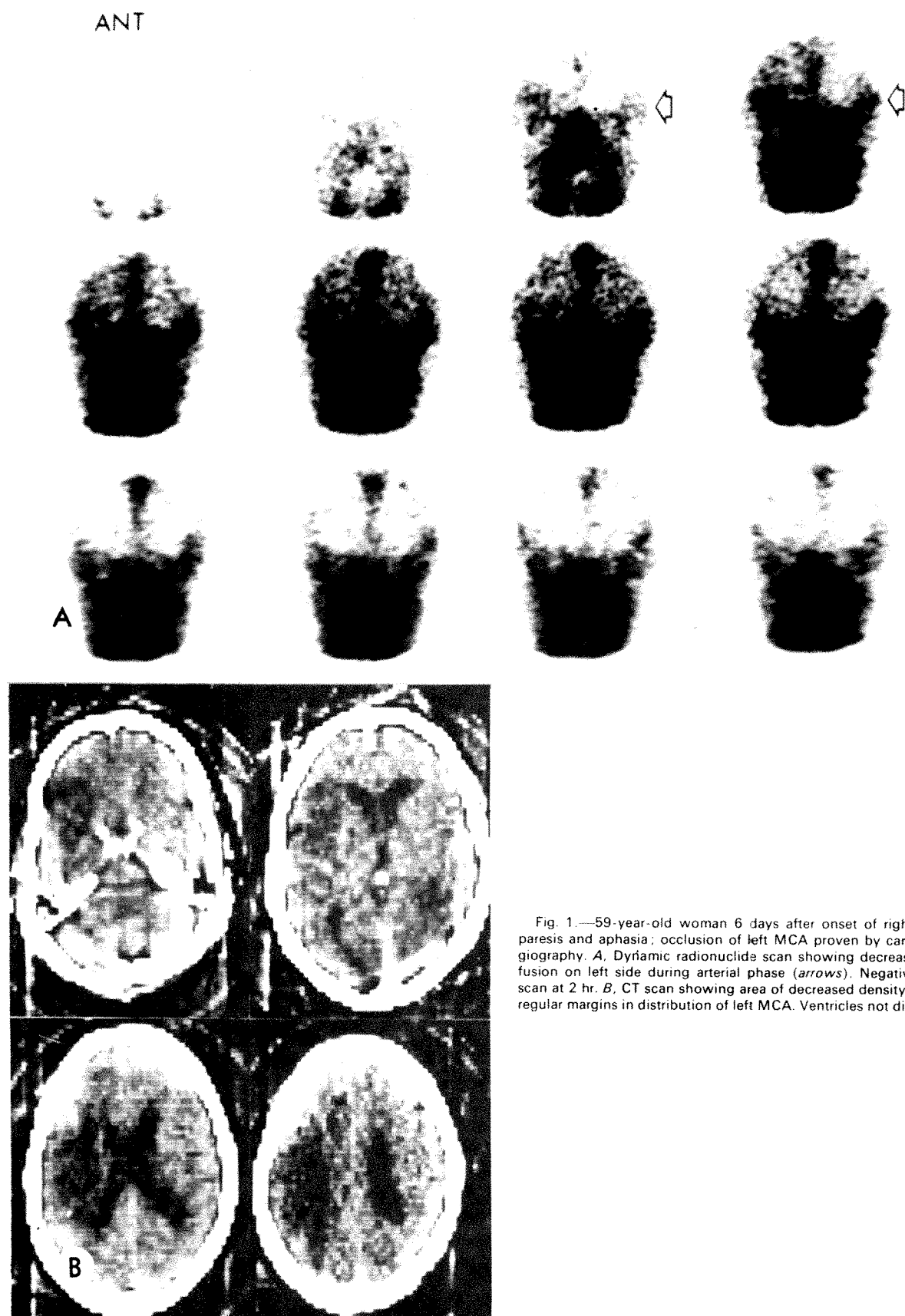


Fig. 1.—59-year-old woman 6 days after onset of right hemiparesis and aphasia; occlusion of left MCA proven by carotid angiography. A, Dynamic radionuclide scan showing decreased perfusion on left side during arterial phase (arrows). Negative static scan at 2 hr. B, CT scan showing area of decreased density with irregular margins in distribution of left MCA. Ventricles not displaced.

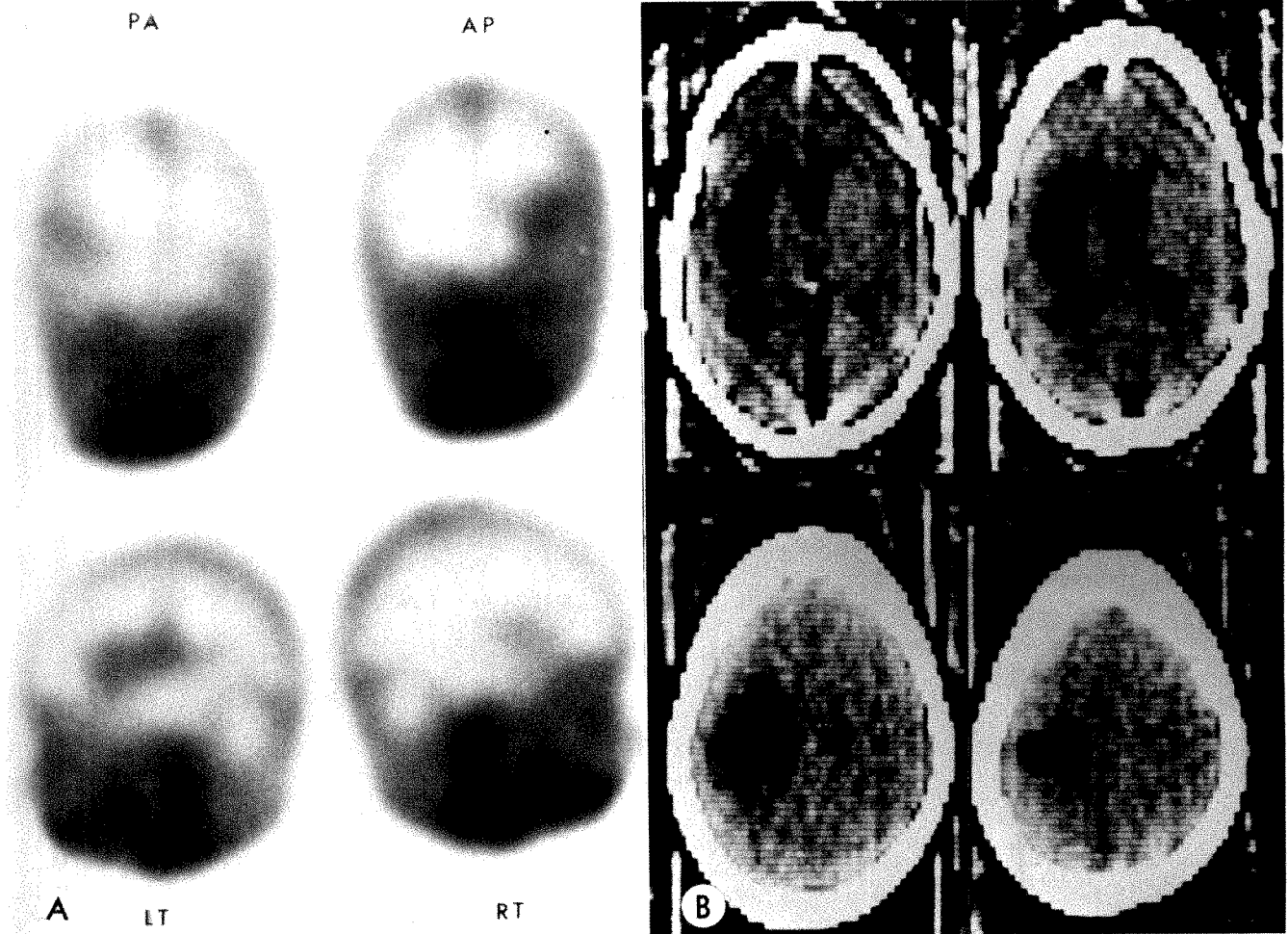


Fig. 2.—48-year-old woman with sudden right hemiplegia 3 weeks after pelvic surgery. Negative dynamic radionuclide scan; 2 months later static scan returned to normal. *A*, Static radionuclide scan showing increased uptake in area supplied by left MCA. Fan-shaped pattern best seen on left lateral projection. *B*, CT scan demonstrating well defined area of decreased density in region supplied by left MCA.

intravenous contrast enhancement can confirm presence of a tumor (fig. 6).

Anterior Cerebral Artery

Only two pure anterior cerebral infarcts were seen in this series, an incidence of approximately 1%. Merritt [1] reported an incidence of 3.6%. Anterior cerebral artery occlusions are difficult to diagnose as they produce the least characteristic abnormalities. In our experience, the dynamic scan has been of no value because of the proximity of the two anterior cerebral arteries. The static scan on anterior projection shows increased uptake in the anterior frontal region adjacent to the midline. On the lateral projection, the increased activity is in the anterior frontal region adjacent to the convexity. However, other lesions in the frontal area may present the same appearance on scintigraphy. The CT scan shows an area of decreased density in the frontal area. The radionuclide and CT scans were positive in both of our patients.

Pathophysiologic Correlation

In the immediate postocclusion period, an ischemic in-

farct shows transient increase in the number of neutrophilic leukocytes [2]. Brain swelling begins within 4–6 hr, and the edema is maximal in 2–5 days [3, 4]. Cerebral anoxia results in swelling of both gray and white matter with vacuole formation [5–7]. The blood-brain barrier breaks down with resultant leakage of plasma proteins into the injured tissue, and neuronal degeneration soon follows. In 14–28 days, repair begins with glial proliferation, macrophage reaction, and eventual fibrogliosis. The end result is cystic degeneration of the area of encephalomalacia or a dense neuroglial scar [2].

These changes correlate roughly with the findings on CT scans. The scans may become positive as early as several hours after stroke, showing an area of decreased density due to brain edema. In the acute stage, the low density area is often patchy with poorly defined margins. At 3–6 days, approximately half of our cases took on a more homogeneous appearance. After 6 days, the involved area remained patchy in about half the cases, whereas in the other half it became more homogeneous. An infarct more than 4 weeks old almost always has well defined borders with a homogeneous center. If there has been

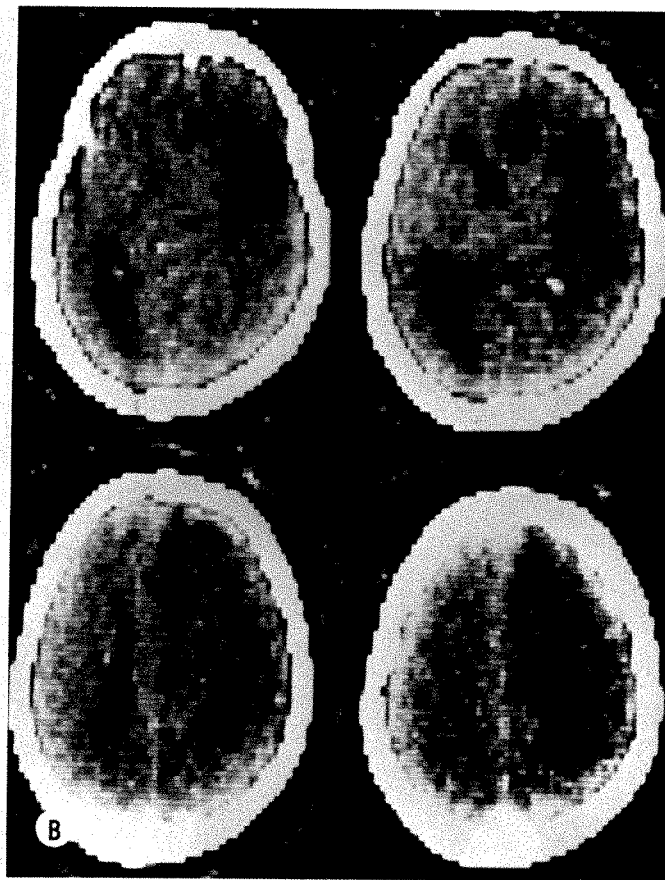
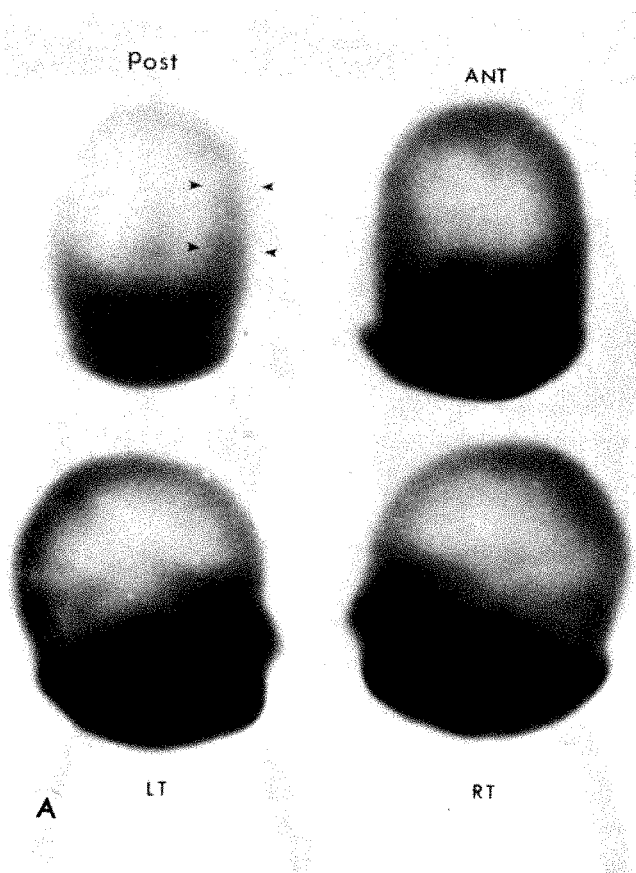


Fig. 3.—72-year-old man 10 days after onset of left-sided seizures and semicoma. Dynamic scan showed decreased perfusion of right hemisphere in arterial phase. A. Static radionuclide scan showing crescent-shaped area of increased uptake on posterior projection parallel to right convexity (arrows). B. CT scan showing large, poorly margined area of decreased density in right hemisphere with some contralateral displacement of ventricular system. At postmortem examination 2 days later, right MCA occluded by thrombus and herniation of uncus and right cingulate gyrus.

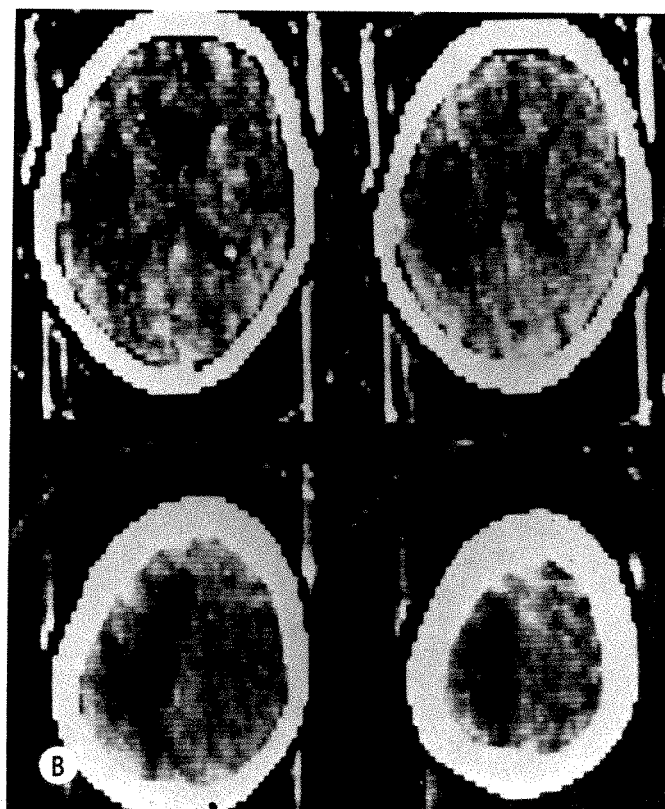
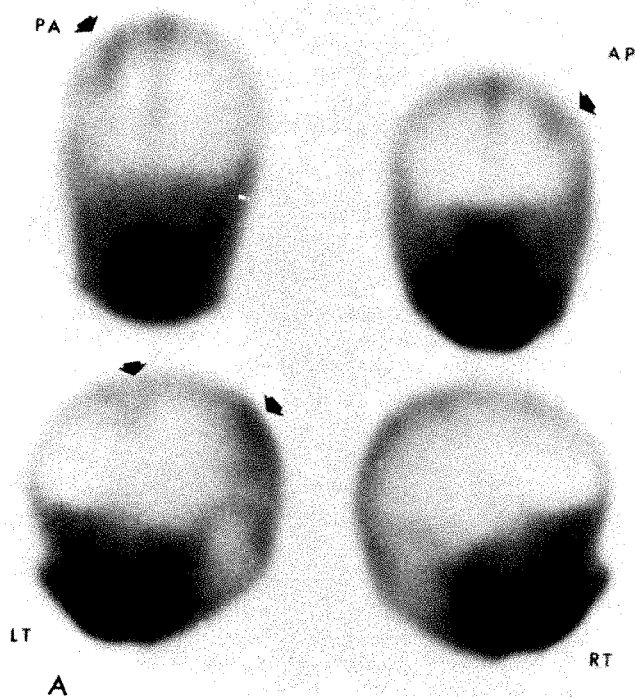


Fig. 4.—66-year-old man 12 days after onset of right hemiparesis. Dynamic radionuclide scan showed decreased perfusion to left hemisphere in early arterial phase; carotid arteriogram demonstrated occlusion of most terminal branches of left MCA. A. Static radionuclide scan showing two areas of increased uptake high in posterior frontal and parietal lobes (arrows). B. CT scan demonstrating dark area along distribution of left MCA.

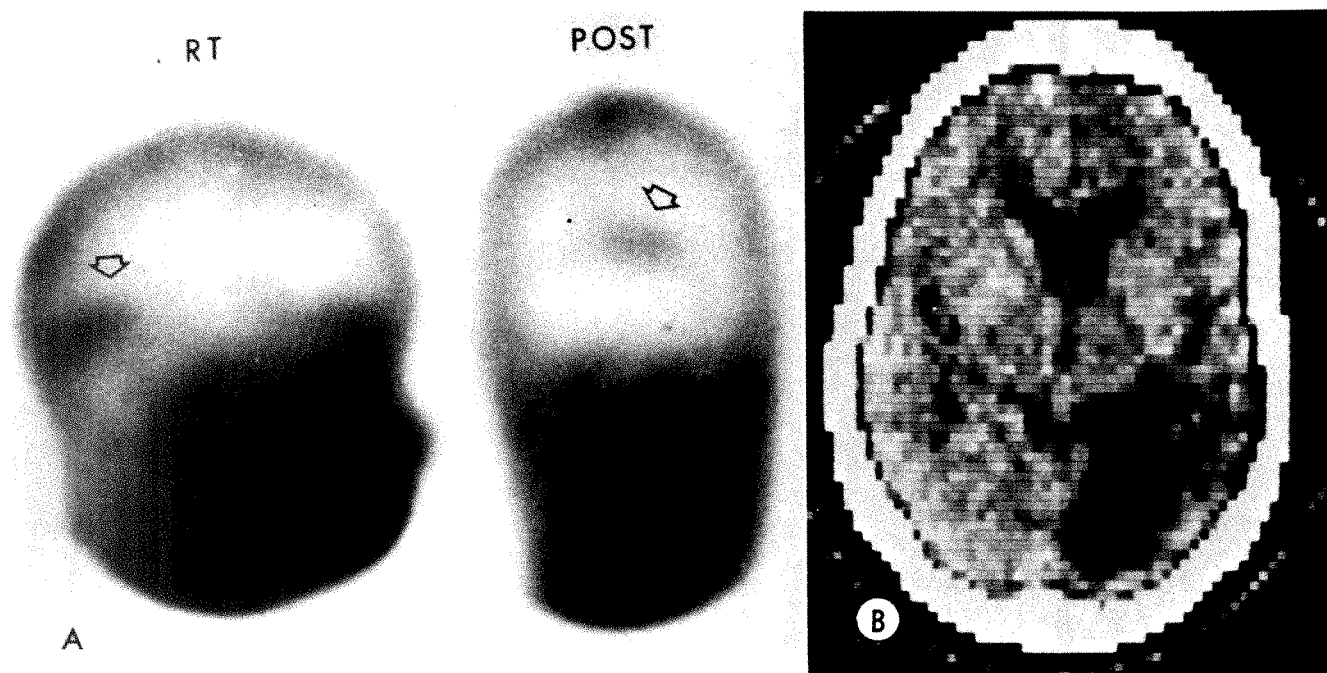


Fig. 5.—54-year-old man with sudden onset of left homonymous hemianopia 12 days before; occlusion of right posterior cerebral artery proved by angiography. *A*, Static radionuclide scan showing area of increased uptake just right of midline on posterior view. On lateral view, wedge-shaped increased uptake extends down to confluence of sinuses and is adjacent to transverse sinus (positive tentorial confluence sign). *B*, CT scan showing sizeable area of decreased density in right occipital lobe.

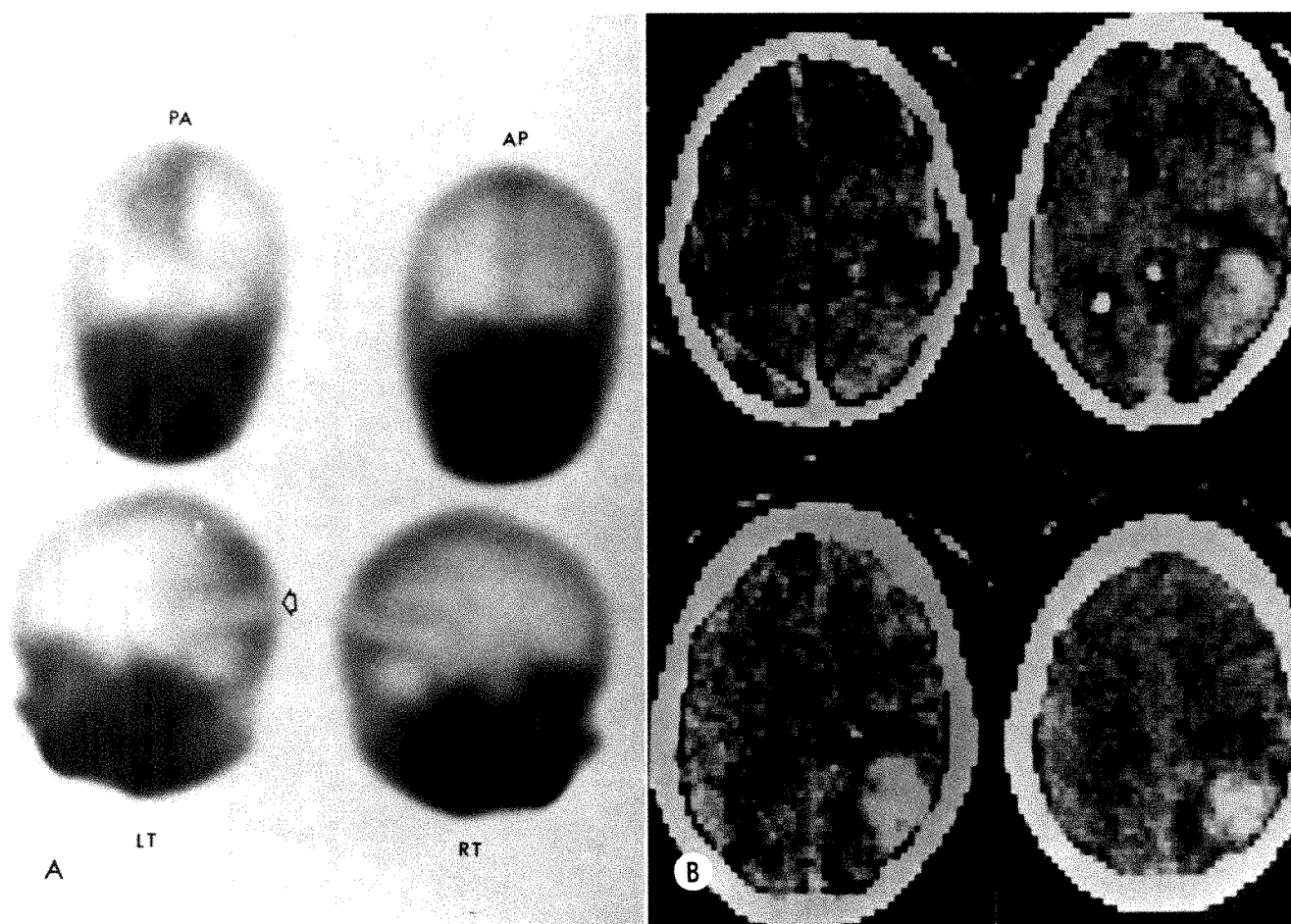


Fig. 6.—56-year-old man with surgically proven glioma. *A*, Static radionuclide scan demonstrating area of increased uptake in right occipital region, separate from tentorium (arrow). Absence of tentorial confluence suggests lesion other than infarct. *B*, CT scan following intravenous infusion of contrast material showing right parietooccipital mass.

significant loss of brain substance, there may be ventricular dilatation and widening of the fissures and sulci [8, 9].

The static radionuclide scans usually become positive within 1–4 weeks after the insult. Complete occlusion of a major vessel may be evident on the dynamic scan very early. The radionuclide scan is usually negative 4 months after the infarction.

Discussion

Clinical differentiation of ischemic stroke, cerebral hemorrhage, hemorrhage into a tumor, or seizure secondary to a tumor can be difficult. The combined use of scintigraphy and CT can help greatly in establishing the correct diagnosis. A fresh intracerebral hemorrhage has a characteristic appearance on the CT scan, as does an acute subdural or epidural hematoma [10]. A tumor generally causes displacement or compression of the ventricular system, but the edema which often accompanies a stroke may also do this. The radionuclide scan should easily differentiate these conditions.

Since the number of false negative radionuclide and CT scans is appreciable, we believe that both tests should be done in doubtful cases. In some patients, cerebral angiography will still be necessary to establish the diagnosis with certainty and to exactly delineate a lesion. As the accuracy of CT scanning improves, fewer patients should need an-

giography, particularly in the acute phase of the disease.

REFERENCES

1. Merrit J: *Textbook of Neurology*, Philadelphia, Lea & Febiger, 1968
2. Adams RD, Sidman RL: *Introduction to Neuropathology*, McGraw Hill Company, 1968
3. Baker HL, Campbell JK, Houser DW, Sheedy PF, Holman CB: Computer assisted tomography of the head: an early evaluation. *Mayo Clin Proc* 49:17–27, 1974
4. Glasgow JL, Currier RD, Goodrich JK, Tutor FT: Brain scans at varied intervals following C.V.A. *J Nucl Med* 6:902–910, 1965
5. O'Brien MD, Waltz AG, Jordan MM: Ischemic cerebral edema and the blood-brain barrier. *Arch Neurol* 30:461–465, 1974
6. Teraura T, Meyer JS, Sakamoto K, Hashi K, Marx P, Sterman-Marinchesu C, Shinmaru S: Hemodynamic and metabolic concomitants of brain swelling and cerebral edema due to experimental cerebral infarction. *J Neurosurg* 36:728–744, 1972
7. West CR, Matsen FA: Effects of experimental ischemia on electrolytes of cortical cerebrospinal fluid and on brain water. *J Neurosurg* 36:687–699, 1972
8. New PFJ, Scott WR, Schnur JA, Davis KR, Taveras JM, Hochberg FH: Computed tomography with the EMI scanner in the diagnosis of primary and metastatic intracranial neoplasms. *Radiology* 114:75–87, 1975
9. Paxton R, Ambrose J: The EMI scanner: a brief review of the first 650 patients. *Br J Radiol* 47:530–565, 1974
10. Messina AV, Chernik NL: Computed tomography: the "resolving" intracerebral hemorrhage. *Radiology* 118:609–613, 1976

Normal Variants and Congenital Anomalies in the Region of the Obelion

GUIDO CURRARINO¹

A number of anatomic bony variants and several congenital anomalies are known to occur at the level of the obelion, that is, in the posterior interparietal region of the head, a short distance in front of the lambda. Among them are: (1) remnants of the embryonic parietal incisura, including parietal fissure, small and large parietal fontanelle, obeliac bones, persistent midline parietal foramen, and small and large parietal foramina; (2) encephalomeningoceles and related defects, including true encephaloceles, herniation of midline intracranial cysts (diencephalic and Dandy Walker cyst), epicranial arachnoid cysts, and scalp defects with ectopic glial tissue; and (3) congenital scalp and skull defects (cutis aplasia congenita). A review of these defects is presented with some illustrative examples not previously reported.

The obelion—probably so named from its resemblance to an obelus or obelisk (\div), a symbol used in ancient manuscripts to mark suspected spurious or superfluous passages or words [1, 2]—has been defined [3] as the region of the skull situated between the two parietal foramina, where the sagittal suture is normally of a more simple type and where its closure usually begins. This generally occurs about 2 cm in front of the lambda in the newborn and 2–5 cm in front of the lambda in adults [4] (fig. 1). The area is of interest since it is the site of a number of anatomic bony variants and several congenital anomalies either limited to the bone or involving the scalp and sometimes the central nervous system as well. These include (1) remnants of the embryonic parietal notch, (2) encephalomeningoceles and variants, and (3) congenital scalp and skull defects. A brief review of these conditions is presented with illustrative examples. (It is of interest to note that true midline dermoid cysts and sinuses, classically located in the midoccipital area, seldom if ever occur in this region.)

Parietal Notch and Derivatives

The parietal bone begins to ossify during the seventh or eighth week of fetal life from a single center according to some authors and from two or more centers which fuse during the fourth month according to others [4–7]. As fetal development progresses, the ossification of the parietal bones radiates in a uniform fashion except for a small area along the sagittal suture slightly in front of the lambda. There a slowing in the spread of ossification results in a notch in the posterosuperior aspect of each bone, causing a widening of the sagittal suture at that level. This notch normally disappears in the fifth fetal month, but vestiges may be observed postnatally in a number of bony defects including the parietal fissure, small and large parietal fon-

tanelle, obeliac bones, persistent midline parietal foramen, and small and large parietal foramina.

Parietal Fissure or Incisura [4, 8, 9]

This is a thin cleft in one or both parietal bones at the obelion which extends outward from the sagittal suture for 1 cm or more. Le Double [8] found it in one of four newborn skulls. The defect is occasionally seen in routine skull roentgenograms where it may simulate a fracture (fig. 2). It probably disappears soon after birth.

Small Parietal Fontanelle [4, 5, 8, 10–14]

This is also referred to as the interparietal, sagittal, accessory, obeliac, or third fontanelle, or the fontanelle of Gerdy.

The defect presents as a round or diamond-shaped widening of the sagittal suture approximately 0.5 cm in size or slightly larger at the level of the obelion (fig. 3). It is usually midline but may indent only one parietal bone: the *unilateral sagittal fontanelle* [8]. It is observed in 5%–6% of newborns and possibly more frequently in infants with Down syndrome [11, 12, 14]. The defect usually disappears during the first 2–3 months of life but sometimes more slowly. How often it leads to small parietal foramina is not known.

Large Parietal Fontanelle

An occasional infant is born with a midline bony defect in the posterior interparietal region which is larger than the usual parietal fontanelle; sometimes it is huge. The larger defects are confluent with the posterior fontanelle and may be accompanied by bulging of the local soft tissues during crying. The anomaly, called here for convenience large parietal fontanelle, probably represents a true anomaly in the ossification of the parietal bone. As in the case of parietal foramina (see below), the differentiation between small and large parietal fontanelle is not clear-cut.

The fate of the defect varies. In most cases, the defect is the precursor of parietal foramina (see below), of varying size, possibly depending on the size of the original bony defect (figs. 4–6). In rare cases the defect may persist as a midline parietal or sagittal foramen (see below). Occasionally it becomes obliterated by a fontanelle bone, also referred to as an *obeliac bone* (fig. 7A), which is probably a type of Wormian bone similar to the "bregmatic bone" sometimes observed in the anterior fontanelle [15]. According to Le Double [8], an obeliac bone is found in about 0.8% of skulls. In some instances, two or more *Wormian bones* appear within the defect (fig. 7B).

¹ Department of Radiology, Children's Medical Center, and University of Texas Southwestern Medical School, Dallas, Texas 75235.

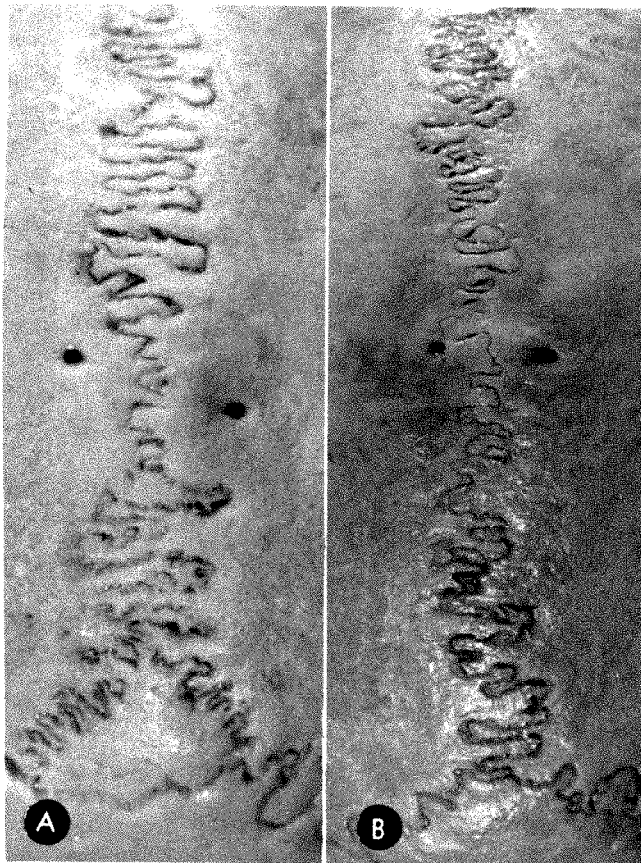


Fig. 1.—Photographs of two adult skulls with small parietal foramina. Metopic suture at level of foramina is of a more simple type than in front or more posteriorly.

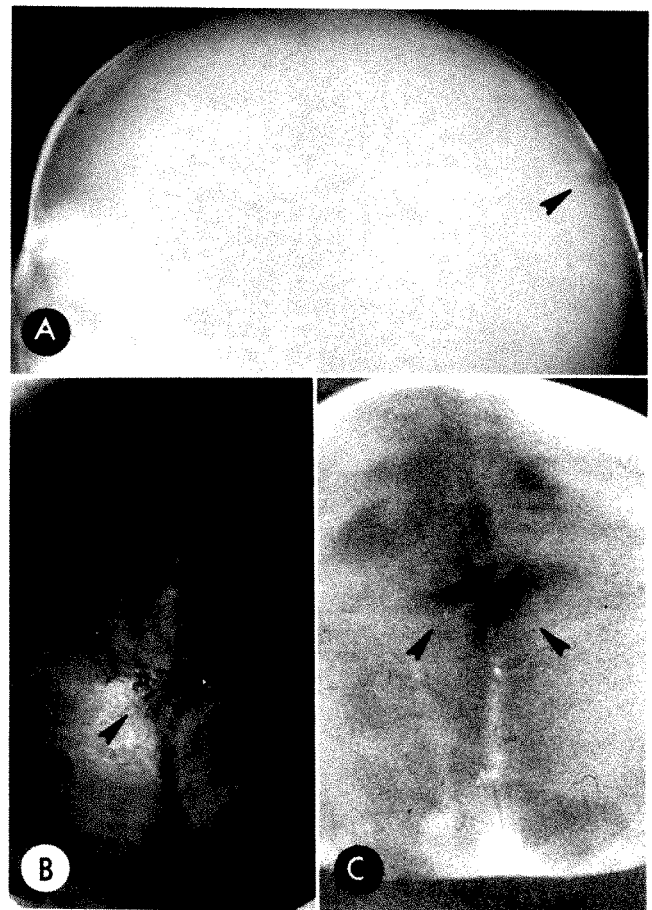


Fig. 3.—Small parietal fontanelle in newborn infant (arrows). *A*, lateral projection during life. *B*, Postmortem photograph of vertex of head with scalp and pericranium removed. Considerable amount of blood oozed from lateral aspects of posterior fontanelle at time of dissection. *C*, Post-mortem roentgenogram of cranial vault.

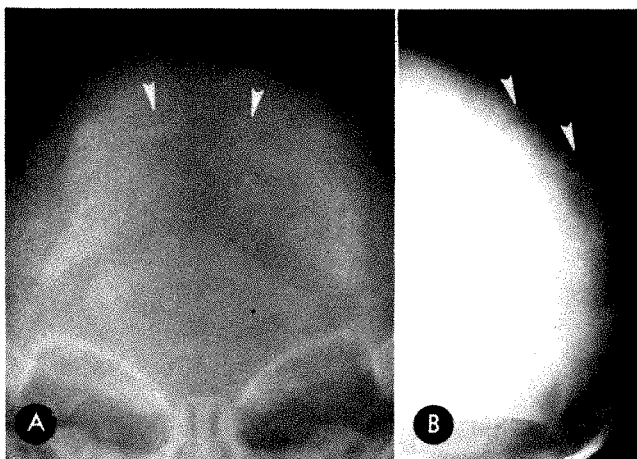


Fig. 2.—Frontal (*A*) and lateral (*B*) roentgenograms of skull of newborn infant with linear defect in posterosuperior aspect of each parietal bone presumably caused by parietal fissure or incisura (arrows).

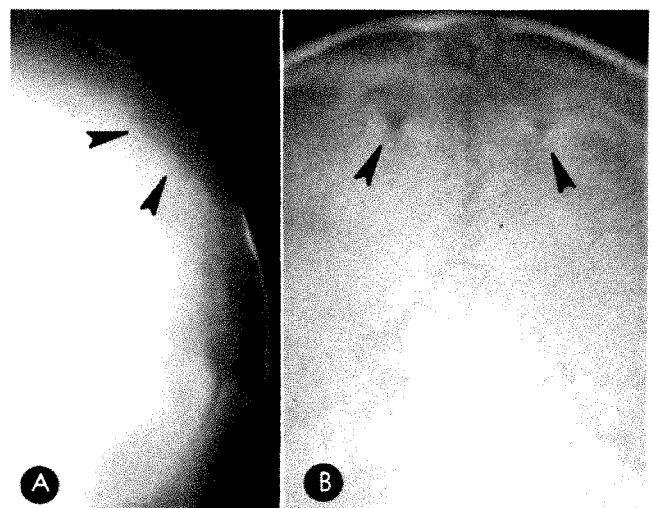


Fig. 4.—*A*, Lateral skull roentgenogram of 2-week-old infant with large parietal fontanelle (arrows). *B*, Frontal view of same patient 9 years later showing only small parietal foramina (arrows).

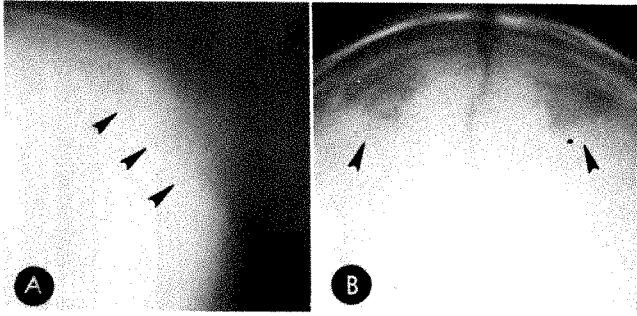


Fig. 5.—A, Lateral skull roentgenogram of 4-week-old infant with large posterior fontanelle and bulging of local soft tissues (arrows). B, Frontal view of same patient 4½ years later showing large parietal foramina (arrows).

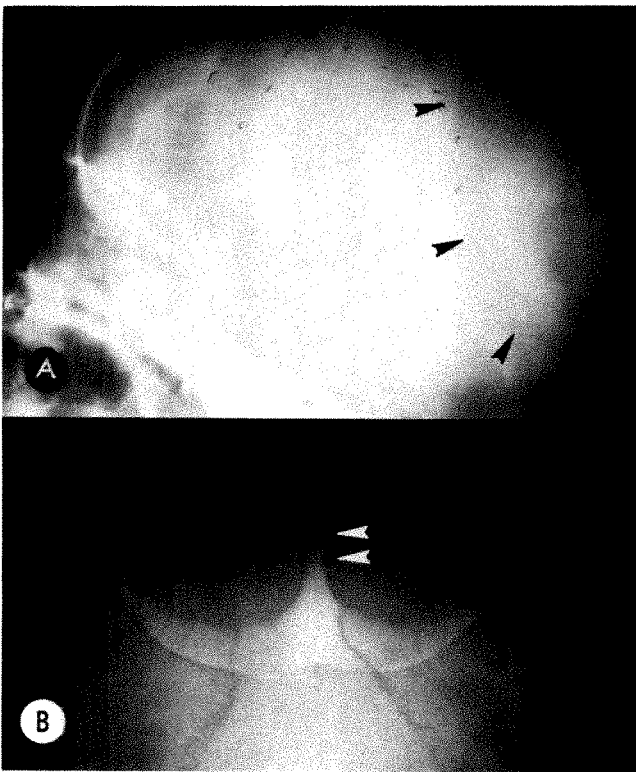


Fig. 6.—A, Lateral skull roentgenogram of newborn infant with large bony defect in posterior interparietal region and bulging of local soft tissues (arrows). At surgery 5 years later to cover defect with stainless steel mesh, galea aponeurotica found to be strongly adherent to defect with many arterial and venous bridging vessels. B, Frontal view of same patient at age 12 years showing very large parietal foramina. No appreciable change in bony defect since surgery except for appearance of strip of bone along sagittal suture (arrows).

Persistent Midline Parietal Foramen

As already noted, a large parietal fontanelle may persist indefinitely as a large midline parietal or sagittal foramen (fig. 8). The anomaly is probably quite rare. A likely instance was reported by Caffey [16] and another by Zarfl [17].

Small Parietal Foramina [4, 6, 8, 18–20]

Also called emissaria parietalia or foramina Santorini, these are two minute round defects about 1 mm in size located at the level of the obelion. There is one on each

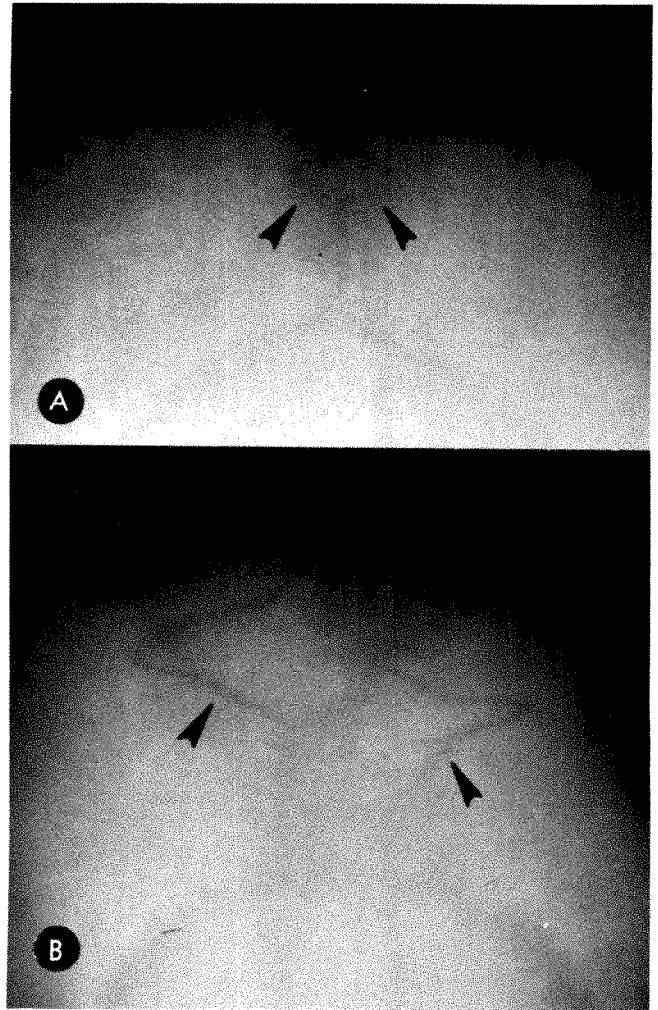


Fig. 7.—A, 7-month-old infant with obelion or posterior fontanelle bone (arrows). B, 8-month-old infant with two large obelion bones (arrows).

parietal bone, usually within 1–2 cm of the sagittal suture but sometimes very close to it (fig. 9). Each foramen transmits an emissary vein, the vein of Santorini, which connects epicranial occipital veins with the superior sagittal sinus and sometimes also a very small artery anastomosing a branch of the occipital with a branch of the middle meningeal artery. These foramina probably represent a persistence of the most lateral aspects of the primitive parietal notch. They are said to occur in 60%–70% of adults and to be unilateral in almost half of the cases.

Small parietal foramina are not easily distinguishable in the newborn and are not always seen in routine skull roentgenograms of children and adults probably because of their small size and the x-ray projection. In frontal skull roentgenograms they sometimes appear like small areas of density of different shapes probably due to the projection of their bony walls rather than to an obliteration of the foramina (fig. 9D). It is not proven that once present they ever close spontaneously.

Large Parietal Foramina [6, 17, 20–32]

Other names include giant parietal foramina, foramina



Fig. 8.—10½-year-old child with large interparietal foramen. Patient reportedly had large "soft spot" at vertex of head in infancy.

parietalia permagna, symmetrical parietal foramina, fenestrae parietales symmetricae, and "Catlin" mark from the name of the family with the anomaly reported by Goldsmith [33]. These are two symmetrical oval or rounded defects located one on each parietal bone, slightly anteriorly to the lambda and near the sagittal suture from which they are separated by a longitudinal strip of bone (figs. 5, 6, and 10). They correspond in location to the small parietal foramina but are much larger, varying from several millimeters to several centimeters in diameter. They are closed by a fibrous membrane which belongs both to the dura and the pericranium [18, 20]. The overlying scalp is normal, but rare cases have been reported in which it was the site of a congenital hairless defect [25, 34].

It seems well established that most, if not all, large parietal foramina are formed postnatally in the following manner. At birth, there is only one midline ossification defect involving both parietal bones (figs. 5 and 6). At times the defect is enormous and involves the entire vertex, simulating that seen in cleidocranial dysostosis (fig. 6A). Between the first and second year of life, small islands of ossification appear within the defect parasagittally. It is sometimes during this phase of development that one or both foramina are still united to the sagittal suture by a cleft or fissure (fig. 10A). Usually in the second or third year this parasagittal ossification becomes complete and the parietal defect becomes clearly double, probably without any further decrease in the size of the defects thereafter.

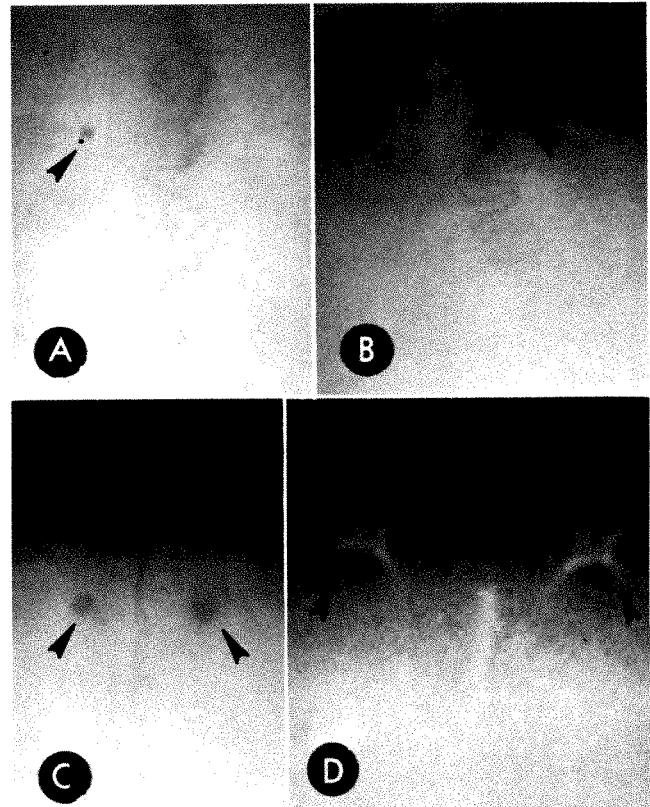


Fig. 9.—Frontal skull roentgenograms of four children aged 2, 5, 2, and 13 years respectively, with small parietal foramina (arrows). *A* and *B*, Unilateral; *C*, bilateral; *D*, bilateral parietal foramina causing starlike densities. Foramina appeared patent in lateral projection.

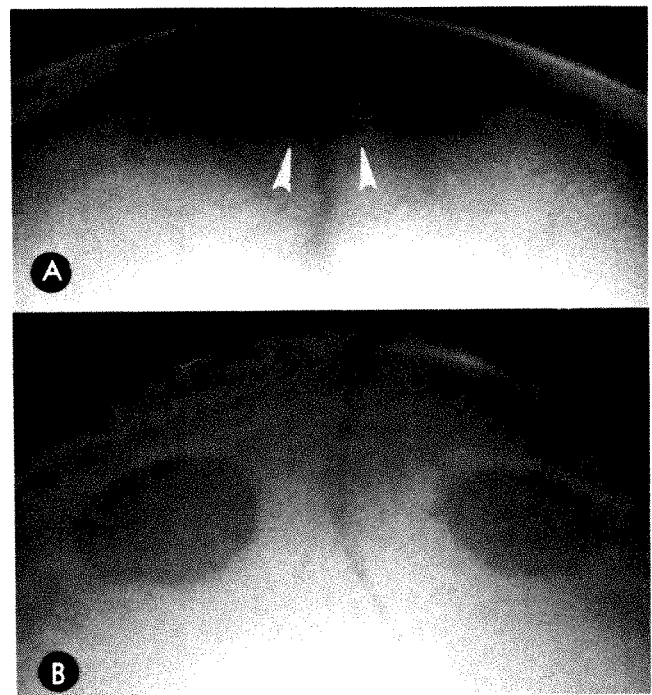


Fig. 10.—Frontal roentgenograms in two children aged 8 months (*A*) and 2½ years (*B*) with large parietal foramina. Foramina still bridged by a non-ossified stripe to sagittal suture in 8-month-old (arrows).

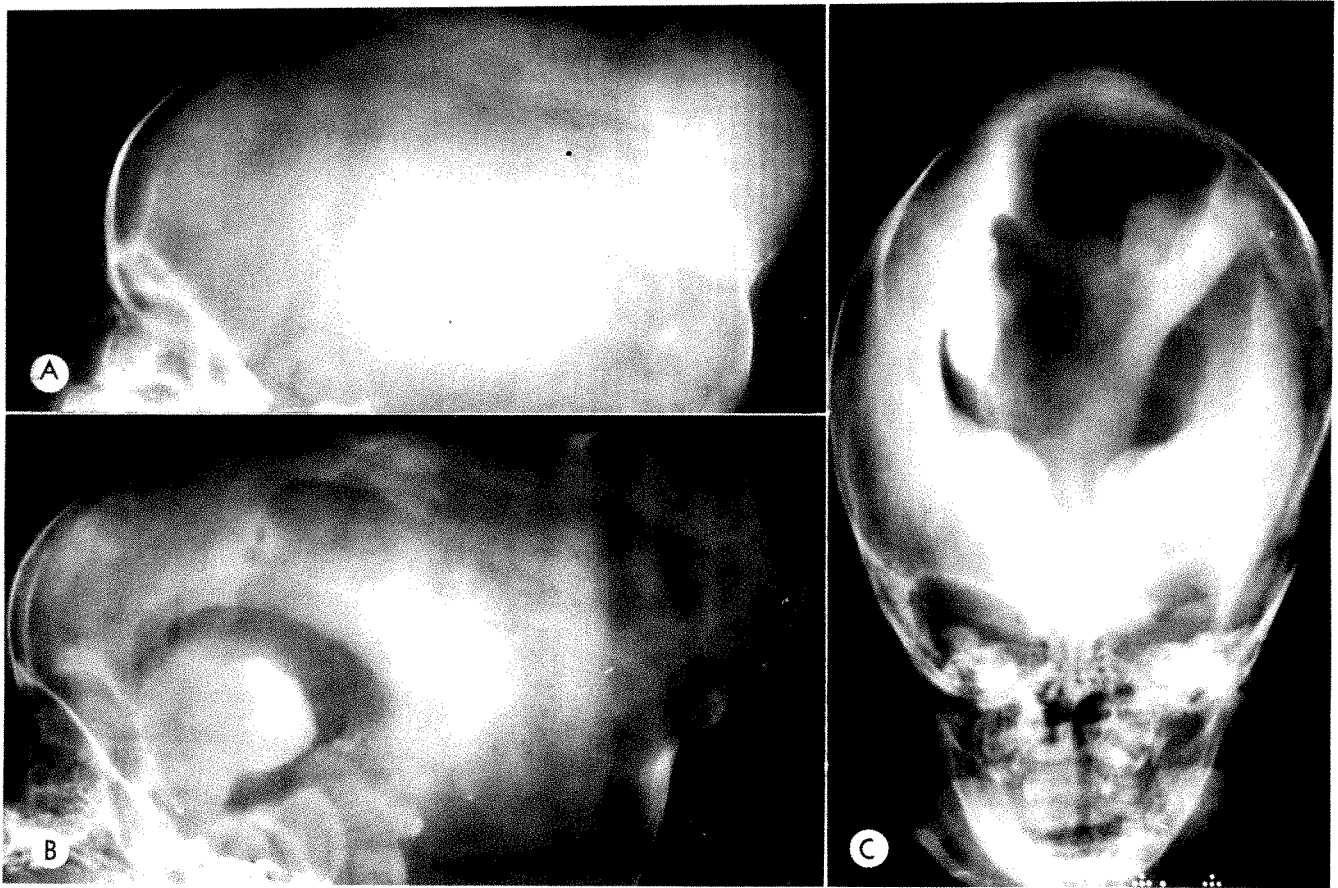


Fig. 11.—Large soft tissue mass in posterior interparietal region due to herniation of third ventricle (dorsal or diencephalic cyst) in newborn with absence of corpus callosum. A, Lateral skull roentgenogram. B and C, Ventriculogram, anterior and frontal projections. (Courtesy of F. N. Silverman)

Large parietal foramina are said to represent an anomaly of ossification of the parietal bone unrelated to small parietal foramina. Their cause is unknown. A familial incidence has been observed in a number of cases with a suggested dominant mode of inheritance. The defect may occur as an isolated lesion or, not uncommonly, in association with other malformations such as turricephaly [25, 35], craniofacial dysostosis [36] and other types of premature craniosynostosis, with asymmetry of the skull, microcephaly, eye and ear defects, mental retardation, convulsions, chest deformities, congenital vertebral anomalies, syndactyly, polydactyly, and many other anomalies [31]. It has also been observed with some frequency in the broad thumb syndrome of Rubenstein and Taybi [37]. Eckstein and Hoare [21] reported the anomaly in association with shortening of the lateral end of the clavicles in a mother and son, without other stigmata of cleidocranial dysostosis.

Encephaloceles and Related Anomalies

The region of the obelion is also the site of a number of uncommon neurocutaneous anomalies which are believed to be closely related developmentally. Some of these are true encephaloceles while others are probably remnants of encephaloceles or meningoceles which became pinched off at the level of the cranial vault during early intrauterine life. The presence of an underlying skull defect similar to a

parietal fontanelle is the rule. These lesions include (1) true encephaloceles and herniations of intracranial midline cysts, (2) epicranial arachnoid cysts, and (3) heterotopic glial tissue.

True Encephaloceles

These occur most often in the occipital and nasofrontal regions and only occasionally in the nasopharynx or at the vertex of the head. Vertex encephaloceles are protrusions through a congenital skull defect of one or both hemispheres, with or without herniations of the ventricular system. As in other types of encephaloceles, the overlying scalp may be defective, meninges may or may not cover the hernia, and microcephaly and other brain deformities often coexist. Vertex encephaloceles are usually located near the anterior fontanelle and only rarely at the obelion. Two possible examples occurring at the obelion have been reported by Müller et al. [38].

Herniation of Midline Intracranial Cysts

A few cases of posterior interparietal "encephaloceles" have been described in which the anomaly was due to herniation of a diencephalic cyst or a Dandy Walker cyst. A *diencephalic cyst*, also called dorsal cyst, is a complicating feature of absence of the corpus callosum. It consists of a gross dilatation and marked upward extension of the third

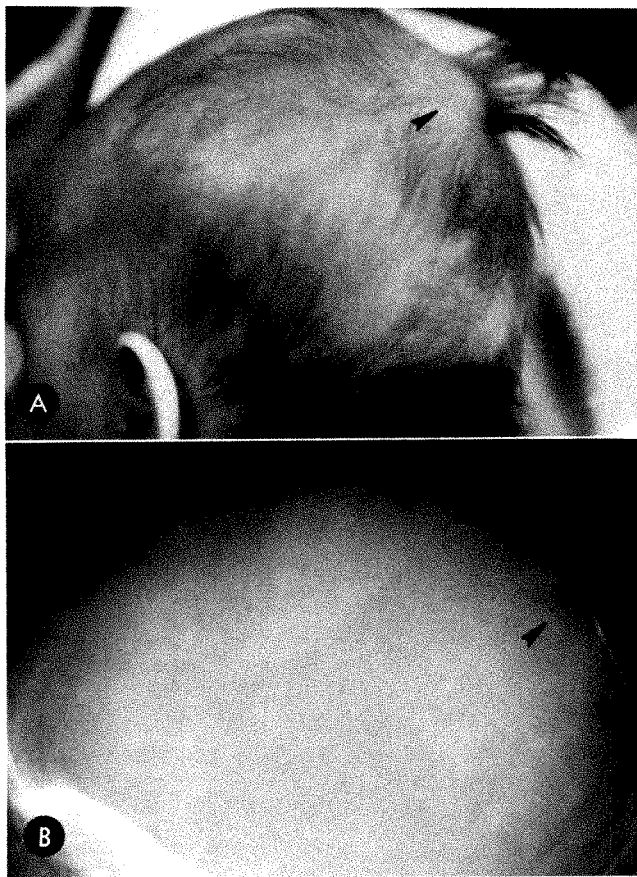


Fig. 12.—A, 2-month-old infant with congenital soft tissue mass in posterior interparietal region, with excessive growth of hair on mass (arrow). B, Lateral roentgenogram of same patient demonstrating underlying skull defect (arrow). A ventriculogram showed absence of the corpus callosum, without hydrocephalus or communication with the epicranial lesion. Diagnosis: epicranial arachnoid cyst.

ventricle between the two lateral ventricles. Brocklehurst [39] reported four cases. In two the cyst herniated through a skull defect at the obelion; in at least one it communicated freely with the surface lesion. A similar case observed by F. N. Silverman is illustrated in figure 11.

A *Dandy Walker cyst* represents a huge dilatation of the fourth ventricle associated with and possibly secondary to a congenital obliteration of the foramina of Luschka and Magendie. The cerebellum is reduced to two nubblings of brain tissue located one on each side of the cyst. The bifurcation of the superior sagittal sinus lies above the lambda, having failed to descend to its normal position in the midoccipital area during fetal life. The other ventricles are dilated. The corpus callosum is sometimes absent. In a case reported by McLaurin [40], the cystic fourth ventricle communicated with a cystic lesion at the vertex of the head just in front of the lambda.

Epicranial Arachnoid Cyst

This is probably the most common congenital mass lesion found at the obelion, a location which appears to be characteristic for the disorder. Typical cases have been reported by McLaurin [40] and by Müller et al. [38]. I have observed

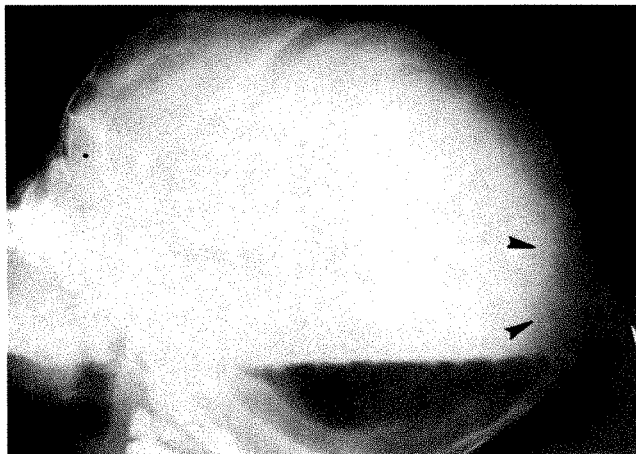


Fig. 13.—Ventriculogram (lateral projection with patient upside down) in newborn with craterlike mass at obelion associated with underlying skull defect (arrows). Nodule composed of glial tissue present in center of crater. Ventriculogram showed massive hydrocephalus but no communication with epicranial lesion.

two additional cases, one which is illustrated in figure 12. The following description is based on these cases plus the histologic observations by B. Landing (personal communication) on the patients reported by McLaurin [40].

The affected infant is born with a firm mass 1 cm or more in diameter located in the posterior interparietal region slightly in front of the lambda. Locally the scalp is intact but hair is usually excessive. A hemangioma on or around the mass may be observed. An underlying skull defect is present probably in all cases. The lesion is composed of arachnoid tissue cells surrounded by a fibrous wall. From this fibrous wall originates a solid or patent fibrous stalk which courses through the skull defect to blend with the dura, without a communication with deeper structures in most, if not all, cases. Epidermoid elements may be present histologically in rare cases. The central nervous system is usually normal, but absence of the corpus callosum has been observed. In a case referred to by McLaurin [40], this was complicated by a dorsal cyst.

Scalp Defect with Ectopic Glial Tissue

Lee and McLaurin [41] reported the case of an otherwise normal 1-year-old child who was born with a circular, hairless scalp lesion about 3 cm in diameter located in the midline of the head slightly anterior to the lambda. The lesion had a dry, flat epitheliumlike surface except for a nodular elevation near its center composed of glial tissue. At surgery this nodule was found to be connected by a stalk to the pericranium, apparently without an underlying skull defect.

I observed a similar case of a newborn with severe hydrocephalus probably caused by aqueductal atresia (fig. 13). Both lateral ventricles appeared to be in contact with the skull at the vertex of the head but did not communicate with the surface lesion. A midline bony defect was present at that level. The surface lesion consisted of a round area of hairless scalp 2 cm in diameter. Its periphery was elevated giving the lesion a craterlike appearance. In the center of the lesion was a nodular elevation composed of glial tissue.

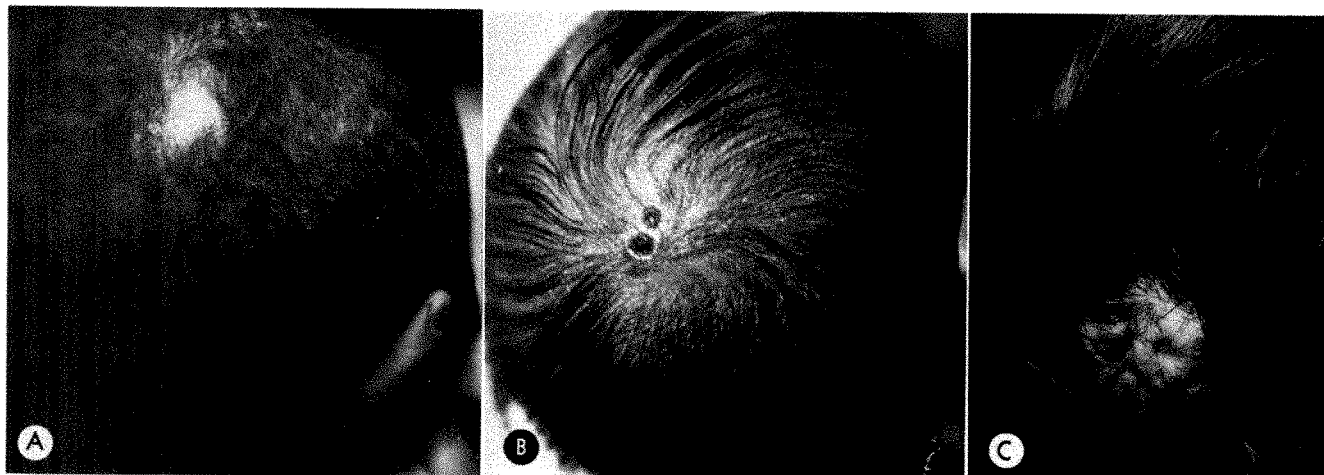


Fig. 14.—Congenital scalp defects at obelion. A, Flat, cicatricial lesion in 1-year-old child. B, Lesion with blister formations in newborn. C, Keloid-type lesion in 1-year-old child.

At surgery the lesion was found to be connected to the dura by a solid fibrous stalk.

Congenital Scalp and Skull Defects

The infant affected by this uncommon anomaly [42–48], also referred to as *cutis aplasia congenita*, is born with a sharply circumscribed area of hairless scalp 1 cm or more in diameter. In the vast majority of cases the defect is located at the vertex of the head just in front of the lambda (fig. 14). Its surface is most often shiny, cicatricial, and flat, but occasionally it is keloid in appearance [49]. In some cases one or more blisters are present, whereas in others there is a superficial ulceration with a serosanguinous exudate or fresh granulation tissue. These fresh lesions heal in a few weeks in a hairless depressed scar. Blister formation, rupture of the blisters, ulceration, and finally scar formation in utero is probably the mode of development of the most common atrophic form observed at birth. The main histologic features include absence of hair follicles, decreased elastic fibers, and an absence of smooth muscles, adipose tissue, subcutaneous glands, and other cutaneous adnexal structures.

According to O'Brien and Drake [46], in 18% of cases there is an underlying defect similar to a sagittal fontanelle without intracranial extension of the lesion. Underlying enlarged parietal foramina have been observed in two patients [25, 34]. The cranial defect is said to heal in a few months. In 5%–10% of cases, there is an area of absent skin in other parts of the body.

Associated malformations have included hydranencephaly, arrhincephaly, hydrocephalus, tracheoesophageal fistula, polycystic kidney, cleft palate, microphthalmia, meningocele, and limb defects. The relatively high frequency of these additional defects may be due to the fact that the lesion occurs in a significant number of patients with trisomy 13–15 [50]. The lesion has also been observed in patients with a deleted short arm of chromosome 4 (46, XX, 4p–) [51] and in Noonan syndrome [52]. Familial cases are on record, and cases occurring in more than 1 generation or in identical twins have been reported [53–57].

The type of inheritance has been interpreted as dominant in some families and as autosomal recessive in others. Only histologic study can distinguish the lesion from the scalp defect with ectopic glial tissue.

REFERENCES

1. Liddell HG, Scott R: *A Greek-English Lexicon*. Oxford, Oxford University Press, 1968
2. *Oxford English Dictionary*, vol VII. Oxford, Oxford University Press, 1933
3. Topinard P: *Anthropology*, translated by Bartley RTH. Philadelphia, Lippincott, 1878
4. Testut L, Latarjet A: *Traité d'Anatomie Humaine*, vol 1. Paris, G. Doin, 1948
5. Anson BJ (ed): *Morris's Anatomy*, 12th ed. New York, McGraw-Hill, 1966
6. O'Rahilly R, Twohig MJ: Foramina parietalia permagna. *Am J Roentgenol* 67:551–561, 1952
7. Shapiro R: Anomalous parietal sutures and the bipartite parietal bone. *Am J Roentgenol* 115:569–577, 1972
8. Le Double A-F: *Traité des variations des os du crâne de l'homme et de leur signification au point de vue de l'anthropologie zoologique*. Paris, Vigot Frères, 1903
9. Paterson AM, Lovegrove FT: Symmetrical perforations of parietal bones: including an account of perforated and distorted cranium from the Liverpool Museum. *J Anat Physiol* 34:228–237, 1900
10. Adair FL, Scammon RE: Observations on the parietal fontanelle in the newborn and in young infants. *Am J Obstet Gynecol* 14:149–159, 1927
11. Chemke J, Robinson A: The third fontanelle. *J Pediatr* 75:617–622, 1969
12. Hoyle CM, Franklin AW: Incidence of the third fontanelle: relation to mongolism. *Lancet* 1:437, 1954
13. Lea A: The sagittal fontanelle. *Lancet* 2:147–148, 1898
14. Tan KL: The third fontanelle. *Acta Paediatr Scand* 60:329–332, 1971
15. Girdany BR, Blank E: Anterior fontanelle bones. *Am J Roentgenol* 95:148–153, 1965
16. Caffey J: *Pediatric X-ray Diagnosis*, 6th ed. Chicago, Yearbook Medical Publishers, 1972
17. Zarfl M: Fenestrae parietales symmetricae. *Z Kinderheilkd* 57:54–66, 1934

18. Boyd GI: The emissary foramina of the cranium in man and the anthropoids. *J Anat* 65:108–121, 1930
19. Boyd GI: Emissary foramina of cranium in primates. *J Anat* 69:113–117, 1934
20. Schmidt-Wittkamp E, Christians H: Die Lückenbildungen der Scheitelbeine: Beobachtungen an 75 Mitgliedern einer Sippe mit gehäuftem Vorkommen von Foramina parietalia permagna. *Fortschr Geb Roentgenstr Nuklearmed* 113:29–38, 1970
21. Eckstein HB, Hoare RD: Congenital parietal "foramina" associated with faulty ossification of the clavicles. *Br J Radiol* 36:220–221, 1963
22. Fein JM, Brinker RA: Evolution and significance of giant parietal foramina: report of five cases in one family. *J Neurosurg* 37:487–492, 1972
23. Hobertsma TJ: Fenestrae parietales symmetricae. *Arch Dis Child* 15:115–120, 1940
24. Hollender L: Enlarged parietal foramina. *Oral Surg* 23:447–453, 1967
25. Lothar K: Familiäres Vorkommen von Foramina parietalia permagna. *Arch Kinderheilkd* 160:156–168, 1959
26. Mücke G-Chr, Poppe W: Fenestrae parietales symmetricae unter phylogenetischem Aspekt. *Fortschr Geb Roentgenstr Nuklearmed* 111:300–303, 1969
27. Murphy J, Gooding CA: Evolution of persistently enlarged parietal foramina. *Radiology* 97:391–392, 1970
28. Pancoast HK, Pendergrass EP, Schagger JP: *The Head and Neck in Roentgen Diagnosis*. Springfield, Ill, Thomas, 1940
29. Pendergrass EP, Pepper OHP: Observations on the process of ossification in the formation of persistent enlarged parietal foramina. *Am J Roentgenol* 41:343–346, 1939
30. Robinson RG: Congenital perforation of the skull in relation to the parietal bone. *J Neurosurg* 19:153–158, 1962
31. Warkany J, Weaver TS: Heredo-familial deviations. II. Enlarged parietal foramina combined with obesity, hypogenitalism, micro-ophthalmos and mental retardation. *Am J Dis Child* 60:1147–1154, 1940
32. Wiedemann HR: Zur Frage der Fenestrae parietales symmetricae (sog. Foramina parietalia permagna). *Monatsschr Kinderheilkd* 105:305–310, 1957
33. Goldsmith WM: The Catlin mark: the inheritance of an unusual opening in the parietal bones. *J Hered* 13:69–71, 1922
34. Wissler: Cited in Lothar K: Familiäres Vorkommen von Foramina parietalia permagna. *Arch Kinderheilkd* 160:156–168, 1959
35. Herrman J, Opitz JM: An unusual form of acrocephalosyndactyly. *Birth Defects: Orig Art Ser* 5(3):39–42, 1969
36. Lehrer HZ, Familant JW: A concordant craniofacial dyostosis with enlarged parietal foramina in twins. *Radiology* 92:127–129, 1969
37. Rubinstein JH: Broad thumb-hallux syndrome, in *Birth Defects: Atlas and Compendium*, edited by Bergsma D, Baltimore, Williams & Wilkins, 1973, pp. 218–219
38. Müller K, Unger R-R, Eckert H, Ditz R: Über parietale Encephalocelen. *Z Kinderheilkd* 105:187–209, 1969
39. Brocklehurst G: Diencephalic cyst. *J Neurosurg* 38:47–51, 1973
40. McLaurin RL: Parietal cephaloceles. *Neurology* 14:764–772, 1964
41. Lee CM, McLaurin RL: Heterotopic brain tissue as an isolated embryonic rest. *J Neurosurg* 12:120–195, 1955
42. Conway H, Johnson G Jr: Congenital absence of scalp and skull. *Ann Surg* 144:1035–1044, 1956
43. Fowler GW, Dumars KW: Cutis aplasia and cerebral malformation. *Pediatrics* 52:861–864, 1972
44. Hunn J McL, Huygens JH, Newman NM: Hereditary scalp and cranial defects. *Med J Aust* 1:219–223, 1969
45. Lynch PJ, Kahn EA: Congenital defects of the scalp: a surgical approach to aplasia cutis congenita. *J Neurosurg* 33:198–202, 1970
46. O'Brien B McC, Drake JE: Congenital defects of the skull and scalp. *Br J Plast Surg* 13:102–109, 1960
47. Pullon DHH: Congenital scalp defects: report of four cases. *NZ Med J* 76:179–182, 1972
48. Scribanu N, Temtamy SA: The syndrome of aplasia cutis congenita with terminal, transverse defects of limbs. *J Pediatr* 87:79–82, 1975
49. Moschella SL: Congenital defects of scalp with keloid formation: cousins show similar defects. *Arch Dermatol* 86:63–64, 1962
50. Magenis E, Hecht F: Chromosome 13 trisomy syndrome, in *Birth Defects: Atlas and Compendium*, edited by Bergsma D, Baltimore, Williams & Wilkins, 1973, pp 251–252
51. Warburton D: Chromosome 4 p syndrome, in *Birth Defects: Atlas and Compendium*, edited by Bergsma D, Baltimore, Williams & Wilkins, 1973, p. 249
52. Summitt RL: Noonan syndrome, in *Birth Defects: Atlas and Compendium*, edited by Bergsma D, Baltimore, Williams & Wilkins, 1973, pp 670–671
53. Cutlip BD, Cryan DM, Vineyard WR: Congenital scalp defects in mother and child. *Am J Dis Child* 113:597–599, 1967
54. Fisher M, Schneider R: Aplasia cutis congenita in three successive generations. *Arch Dermatol* 108:252–253, 1973
55. Hodgman JE, Mathis AW Jr, Levan NE: Congenital scalp defects in twin sisters. *Am J Dis Child* 110:293–296, 1965
56. Johnsonbaugh RE, Light IJ, Sutherland JM: Congenital scalp defects in father and son. *Am J Dis Child* 110:297–298, 1965
57. Keipert JA: Congenital scalp defects in brother and sister. *Med J Aust* 1:866–868, 1972

The Destiny of Brachytherapy in Oncology

BERNARD PIERQUIN¹

TRANSLATED BY J. FRANK WILSON²

At the invitation of the American Radium Society, Pierquin reviews his very large experience with continuous low dose rate irradiation of cancer. The target volume is treated with 6,000–7,000 rad in 3–10 days at a dose rate of 30–100 rad/hr. Preference for continuous low dose rate irradiation is based on the earlier work of Jean Pierquin, Georges Richard, Claudius Regaud, and Ralston Paterson with radium sources. Afterloading techniques with iridium-192 have been substituted allowing safer and more precise placement. An accumulated experience with 5,000 patients over the past 15 years permits conclusions that the techniques are safe, easy, inexpensive, and effective for tumors accessible to direct instrumentation. Dosimetry is based on the Paris system. Standardizing upon a dose of 7,000 rad, Pierquin concludes there is an isoeffect of continuous radiation at low dose rates of 25–100 rad/hr. The differential effect on tumor versus healthy tissue is impressive even when large volumes are irradiated, as in neck adenopathy. Stemming from this experience, three trials have been carried out of low dose rate teletherapy with cobalt-60 sources in oral cavity and oropharynx tumors, delivering 7,000 rad at rates of 90–100 rad/hr. Pierquin hopes for the same very high local control rates (in the order of 95%) achieved by iridium-192 endoradiotherapy of accessible T1, T2, T3, and T4 cancers.

The American Radium Society has asked me to philosophize concerning the destiny of brachytherapy in cancer management. First of all, I hesitate to engage in an extensive biological and clinical review detailing a complete history of curietherapy and opening the vast perspectives of the five continents. Second, a natural preference for concrete considerations has counselled me to limit my inspired reflections. I would, therefore, like to present the experience which I have lived, in the hope that it can be considered representative of a philosophy.

All philosophies have been animated by faith; my personal faith is in the principle of low dose rate irradiation. By this I mean the optimization of therapeutic ratio by distributing in a target volume 6,000–7,000 rad in 3–10 days, at a low dose rate of between 30–100 rad/hr, giving the irradiation continuously or semicontinuously in one or more fractions. This faith is primarily based on my clinical experience as a brachytherapist, where it appeared to me that the differential effect of such irradiation on healthy versus tumor tissue was more important than when similar total doses were given using a fractionated technique at a high dose rate. I posed this simple question: Why is it possible to deliver a dose of more than 6,000 rad at a low dose rate in several days without destroying normal tissue and with a nearly constant assurance of local tumor con-

trol, when with a high dose rate it is necessary to give the same dose over several weeks with multifractionation to avoid the risk of provoking irreparable necroses? Until recently, only the empiricism of clinical observation responded to my question. I intend to comment upon this historical response hoping that radiobiology will shortly provide some clearer confirmation.

The Past

Radium was born into the hands of Pierre and Marie Curie in 1898 at approximately the same time as x-rays to Roentgen. During the next 77 years, curietherapy underwent major development including a period of glory between 1920 and 1950. Among its pioneers were Jean Pierquin and Georges Richard, my father and godfather, respectively, who systematized techniques and doses at the Curie Foundation (Paris) for platinum-encapsulated radium needles and tubes of a type still in use. Aided by the experimental work of Antoine Lacassagne, they demonstrated the biological necessity of filtering the "puree" of radiation from radium to arrest the hard beta and soft gamma components by adding platinum walls 0.5 mm thick so as to treat with only the geometric dispersion of the gamma radiations. Treating cancers of the cervix with correctly filtered radon, my "paternal" defined an optimum time-dose relationship for that epoch which sterilized epidermoid carcinoma without producing necrosis of healthy tissue. This work, realized between 1919 and 1922 under the direction of Claudius Regaud, was a forerunner of the 6,000 rad in 6 days which Ralston Paterson was to systematize at Manchester in the 1930s.

The worldwide use of radium illustrated by the name of this society clinically demonstrated the remarkable curative properties of continuous irradiation at a low dose rate for all carcinomas accessible to methods of plesiocurietherapy or endocurietherapy. Among these were cancers of the skin, upper aerodigestive tracts, and urogenital and anorectal regions; in short, all those which are located either superficially or near body orifices. A cure rate of more than 90% for cutaneous cancers was achieved with good esthetic results, suggesting for the first time an important differential effect.

But all was not rosy for radium. The poor conditions of protection required the curietherapist to use as small a quantity of radioactive material as possible and to operate as quickly as possible. Afterloading was only vaguely envisaged except in the treatment of uterine cancer. As a result, the indications for curietherapy were limited to small

Presented at the annual meeting of the American Radium Society, San Juan, Puerto Rico, May 1975.

¹ Service de Carcinologie Radiothérapique, C. H. U. Henri Mondor, 51 Avenue du Maréchal de Lattre de Tassigny, 94000, Creteil, France.

² Department of Radiology, Medical College of Wisconsin, 8700 West Wisconsin Avenue, Milwaukee, Wisconsin 53226.

target volumes or accessible T1 and T2 tumors. These cancers were relatively curable; thus it was easy to analyze the results of curietherapy and to overlook the differential effect of continuous irradiation at a low dose rate. "You curietherapists only treat the small, easily curable cancers without leaving a tract."

The Present

The birth of artificial radioactivity into the hands of Frederic and Irene Joliot-Curie in 1934 opened the gateway to modern radiation therapy. Whereas teletherapy techniques had been handicapped by the insufficient energy of conventional x-ray therapy, the development of sources of cobalt-60 of massively high activity improved prospects for fractionated teletherapy in the 1950s. The simultaneous development of particle accelerators, such as betatrons and linear accelerators, completed the armamentarium of sources of high energy radiations. With these photon and electron beams, it became possible to distribute at every level in the human body an optimal dose according to optimal protraction. This research opened an effective dialogue with radiobiologists.

Faced with the technical liberation of teletherapy, the role of cancer treatment by brachytherapy, limited to the used radium, was increasingly contested. Simultaneously, well justified protective legislation emerged which was increasingly confining. The example of the Holt Radium Institute of Manchester illustrates this regression of brachytherapy when faced with modern teleradiotherapy. Until the retirement of Ralston Paterson in 1962, that institution used huge quantities of radium. Only 1 year later, the indications for curietherapy, except in gynecology, were drastically suppressed to the sole profit of high dose rate teleradiotherapy. In the 1950s, the disappearance of indications for brachytherapy seemed inevitable unless a substitute for radium could be found.

Above all else, the solution had to assure protection of the operator and his aides, an unachievable goal except through afterloading. Only this principle allowed the therapist to execute a precise placement of his sources while protecting himself and others during the procedure and the dosimetric control. A desirable natural consequence was optimization of the dose-target volume relationship. In addition, inactive guide systems had to be developed for making the application, and radioactive sources, which could be added or substituted later, had to be miniaturized. Steel guide gutters, guide needles, plastic tubes, and hypodermic needles loaded with iridium-192 wires 0.3–0.5 mm in diameter proved the best solution.

Several other radioactive elements were found to meet the requirements of afterloading. Among them were gold-198, cobalt-60, and tantalum-182. Cesium was not available in the 1950s since the nuclear fission industry was hardly born, but it is iridium which has proven to have the best characteristics for afterloading. Henschke and Myers first demonstrated this by systematizing the use of iridium-192 by the plastic tube technique in 1954. I personally applied myself to the task in 1957 aided by the Centre Nucleaire of Saclay. After several attempts to use gold-198

hairpins inserted with guide gutters, in 1960 I systematized, with Daniel Chassagne, the use of iridium-192 wires 0.3 and 0.5 in diameter.

Between 1960 and 1970, I treated more than 3,000 patients at the Institut Gustav Roussy at Villejuif using afterloading techniques. Since 1970, I have continued my work at Hopital Henri Mondor at Creteil, while my former assistant, Daniel Chassagne, has remained on the same track at Villejuif. Several conclusions can be drawn from our accumulated experience which spans more than 15 years and includes 5,000 patients: radioclinical conclusions, on the one hand, and radiobiological conclusions, on the other, leading to the future.

Radioclinical Conclusions

1. Afterloading techniques have proven their efficiency in matters of protection. We perform an average of seven applications per week or 350 per year, usually for sizable target volumes such as breast or uterus requiring as much as 80 mCi of radioactive material each. Yet the dose to our medical personnel has not been measurable on film badges (less than 20 mrem per month).

2. The various techniques of afterloading which I have devised are easy to use and are inexpensive. Simplicity of use must remain an imperative regulation in the development of afterloading. Mechanical "sophistication" in the storing and preparation of the radioactive materials (iridium bank) should also be avoided.

3. Applications should respect the principle of parallel radioactive lines and the dosimetry should be based upon the "Paris system" (formerly called the relational system [1]) and checked by my "point technique" presented at the American Radium Society meeting in 1961 [2].

Whenever possible, the dosimetry should be done manually. Computer calculations can be asked for in particularly complicated cases: for example, a loop with complex topography or for cervicouterine plesiotherapy. The publication of an atlas of isodoses would permit immediate dosimetry by analogy, which would be sufficient in most instances.

4. Indications for brachytherapy are essentially reserved for tumors which are accessible to direct instrumentation; that is, those which are either superficially located or endocavitary yet close to orifices. It is indicated for any T1 or T2 lesion and for a number of T3 and T4 lesions, either as a complete treatment or as a final boost following teletherapy. These indications are summarized in table 1. Representative results are shown in table 2.

Radiobiological Conclusions

Two major conclusions are apparent. One concerns the time factor, the other the differential effect.

Using iridium-192 imposes a significant variation in the total time of irradiation to give an identical tumor dose because of the variations in density of radioactive material to be found in otherwise similar target volumes and because of its relatively short half-life of 74 days. Finding myself in ignorance of this in 1960, I took the risk of simply treating all patients to the same dose of 7,000 rad calculated at the

TABLE I
Brachytherapy: Indications and Techniques

Location	T1	T2	T3	T4
Skin (nose, ear, etc.)	HN(A)	HN, PT(A)	PT, GN(A)	PT, GN(A)
Penis	HN(A)	HN, GN(A)	GN(A)	...
Breast	GN(B)	GN(B)	GN(B)	...
Uterus	PT(mold)	PT(mold)	PT(mold)	...
Vagina	GG, PT(A)	PT(A, B)	PT(A, B)	...
Anus, rectum	GG, PT(A)	GG, PT, GN(A, B)	PT, GN(B)	...
Bladder	PT(A)	PT(A)
Tongue (anterior two-thirds)	GG(A)	GG(A, B)	GG, PT(A, B)	...
Inferior lip	HN(A)	HN, GN(A)	GN(A)	GN(A)
Velum, tonsil	GG(B)	GG(B)	GG, PT(B)	...
Tongue (base) epiglottis	GG, PT(B)	PT(B)	PT(B)	...
Cervical nodes (nonoperable)	...	PT(A, B)

Note.—Techniques: GG = guide gutter; GN = guide needle; HN = hypodermic needle; PT = plastic tube. A = total dose; B = final boost.

TABLE 2
Local Control for Selected Sites Treated by Endoradiotherapy with Iridium-192

Tumor Extent and Site	Years after Treatment				
	1	2	3	4	5+
T1-T2:					
Nose	27/27	12/12	7/7	3/4*	3/3
Ear	18/18	8/8	3/3	2/2	2/2
Lower lip	30/30	19/19	12/12	6/6	3/3
Penis	8/8	4/4	2/2		
Tongue	95/99†	63/67	38/41	28/29	17/18
Total	178/182 (98)	106/110 (96)	62/65 (96)	39/41 (95)	25/26 (96)
T3:					
Nose	15/16*	12/13	9/10	6/7	1/1
Ear	16/17*	11/12	6/7	2/4*	
Lower lip	26/27*	20/21	11/11	7/7	6/6
Penis	14/14	8/8	2/2		
Tongue	51/54†	43/46	35/37*	30/32	24/26
Total	122/128 (95)	94/100 (94)	63/67 (94)	45/50 (90)	31/33 (94)
T4:					
Nose	6/6	5/5	4/4	3/3	2/2
Ear	5/5	5/5	5/5	2/2	2/2
Lower lip	14/15*	11/12	10/11	9/10	5/5
Penis	5/5	2/2	2/2	1/1	
Total	30/31 (97)	23/24 (96)	21/22 (95)	15/16 (93)	9/9 (100)
Overall total	330/341 (96)	223/234 (95)	146/154 (95)	99/107 (93)	65/68 (95)

Note.—Reprinted with permission from Pierquin B, Chassagne D, Cox JD: Toward consistent local control of certain malignant tumors. *Radiology* 99:661-667, 1971. Numbers in parentheses are percentages.

* One case was a recurrence.

† Three cases were recurrences.

‡ Four cases were recurrences.

isodose of reference. I well remember the occasion of the Latin American Congress of Radiology in April 1967 when I walked upon the sands of the beach at Costa Brava with my friend Gordon Stewart, where we had a lively discussion of isodoses of reference and argued the merits of the Manchester system versus my Paris system. Finally, Gordon said to me, "Bernard, you should remain loyal to a fixed dose of 7,000 rad if you want to find a significant answer to the question of the influence of the time factor in brachytherapy." That is what I did, and that is why I can bring

you the answer which we published in 1973 [3]. To summarize, when the tumor dose is 7,000 rad, there is no difference in the rates of recurrence or necrosis if the dose is given in 3-11 days. *There is an isoeffect of continuous irradiation at a low dose rate for rates varying between 25 and 100 rad/hr.*

Hall and Bedford [4] have experimentally shown the same isoeffect in HeLa cells irradiated continuously in vivo at dose rates of less than 100 rad/hr.

This observation was also verified by an inverse demon-

stration at the Netherlands Cancer Institute of Amsterdam in 1974 [5]. When cancers of the tongue were treated with radium according to the Manchester principles, the total dose was usually smallest when the dose rate was greatest. The variations in total dose did not exceed $\pm 10\%$. Recurrences were statistically more frequent when a high dose rate implied a reduction of the total dose to less than 6,000 rad.

The important differential effect of low dose rate irradiation on tumor versus healthy tissue which was apparent using radium in small target volumes has been confirmed in large target volumes implanted with iridium-192. I personally became convinced of this in the course of treating 250 cases of recurrent cervical adenopathies previously treated by one or several series of fractionated external irradiation at a high dose rate to doses of 6,000–10,000 rad. Many had also been subjected to mutilating surgery. These were recurrences in poorly vascularized and oxygenated areas and were inoperable due to extension and fixation in all planes. Often they were entrusted to me to receive brachytherapy as a last resort when a new attempt at fractionated irradiation had met with failure. In most cases the treated volume was large, measuring 10×10 cm and 3–5 cm thick. The total dose was between 6,000 and 7,000 rad. The short term results of this treatment at 3 and 6 months were impressive. There was good regression of the tumor and good recovery of the skin despite its systematic incorporation in the treated volume [6]. I was especially impressed by the slight radioepidermitis which developed compared to the frequent intolerance of similar cutaneous zones when retreated with fractionated photon or electron irradiation. The long term results have been poor, however, because of the regional or general evolution of these malignancies. I exclude ulcerated lymphadenopathies as an indication, but I have accepted all others even when the skin was infiltrated and fixed.

Parallel to this clinical experience, it is appropriate to mention certain experimental radiobiological studies of the oxygen enhancement ratio. Hall et al. [7] have demonstrated an important diminution of this factor for low dose rates compared to high dose rates. The data reveal approximately the same diminution of the oxygen enhancement ratio as when oxygenated and unoxygenated cells are irradiated by neutrons, in particular with the use of californium-252 [8].

The Future

Stemming from the systematic use of iridium-192, my clinical experience led to these fundamental observations: (1) *flexibility of the time factor*, and (2) *enhancement of the differential effect*. This inspired my interest in the revolutionary idea of giving continuous irradiation at a low dose rate, but the same principle remained to be demonstrated using teletherapy.

Technically, the problem was simple. Using a telecobalt apparatus, a low dose rate was obtained by interposing in the beam a sufficient thickness of lead to attenuate the dose rate to the desired level. An alternate solution was to load the unit with a weakly active source of cobalt-60.

For practical reasons, the total dose could not be delivered in a truly continuous manner. I allowed, based on my conclusions, the highest possible dose rate and the longest possible protraction. We ultimately chose a dose rate of around 100 rad/hr and a maximum total protraction of 9–11 days. For a dose of 7,000 rads, I could then reason that by treating 7–8 hr daily, the treatment would be completed in 10 days.

Clinically, I chose to treat advanced tumors of the oral cavity and oropharynx because they can be observed with relative ease as can the surrounding normal tissues.

I started this therapeutic study at Institut Gustav Roussy in early January 1970, delivering radiations through the night with a unit which had its beam attenuated by lead bricks to obtain a dose rate at the center of the target volume of the order of 2 rad/min. A first series of 10 patients quickly confirmed the remarkable effect of this type of irradiation upon the primary tumor and its associated lymph node metastases. The differential effect was also evident in that the skin demonstrated only a mild radioepidermitis followed by good restoration; mucosal reactions remained brisk.

A second series of 27 patients was undertaken at Hôpital Henri Mondor in December 1971, using a cobalt unit containing a small 45 Ci source which permitted us to treat patients during regular work hours. In this series, local recurrences have been rare, but necroses were seen fairly frequently. This is perhaps explained by the fact that most of the tumors were very extensive, poorly oxygenated, and somewhat necrotic from the outset. Several of the less extensive cases (six T3 cases) were apparently cured; only one showed evidence of necrosis [9].

A third series was begun in October 1974 for less advanced lesions to be comparatively studied with a group treated by classical fractionated irradiation. In this series, the total dose of 7,000 rad is given as a split course working with a dose rate of 1.5 rad/min or 90–100 rad/hr. We are giving 3,500 rad in 5–7 days, repeated after a rest interval of 3 weeks. It is too early to report on the results of such treatment, but no true necroses have yet been seen.

The recent studies of Kal [10, 11] using low dose rate teleradiotherapy with either photons or neutrons for rat rhabdomyosarcoma and rat skin have given further evidence of an augmented differential effect with this type of therapy.

In conclusion, the clinical and laboratory research of low dose rate irradiation should be continued on as large a basis as possible in the forthcoming years. It is hoped that when definitive conclusions are drawn, they will confirm the well indicated treatment of accessible lesions with iridium-192 [12] and open new possibilities for the teleradiotherapy of advanced lesions and of tumors at depth.

ACKNOWLEDGMENTS

I would like to thank the numerous collaborators who are associated with this long work, past, present, and future, especially F. Balliet, D. Chassagne, A. Dutreix, G. Mannello, M. Raynal, and I. Turgard.

REFERENCES

1. Pierquin B : Dosimetry : the relational system, in *Proceedings of a Conference on Afterloading in Radiotherapy*, New York City, May 1971, DHEW Publication (FDA) 72-8024, 1971, p 204
2. Pierquin B, Fayos JV : Dosimetry by tomography in interstitial curietherapy : point technique. *Am J Roentgenol* 87 : 585, 1960
3. Pierquin B, Chassagne D, Baillet F, Paine CH : Clinical observations on the time factor in interstitial radiotherapy using iridium-192. *Clin Radiol* 24 : 506, 1973
4. Hall EJ, Bedford JS : Dose rate : its effect on the survival of HeLa cells irradiated with gamma rays. *Radiat Res* 22 : 305, 1964
5. Awwad HK, Burgers JMV, Marcuse HR : The influence of tumor dose specification on the early clinical results of interstitial tongue implants. *Radiology* 110 : 117, 1974
6. Pierquin B, Raventos A, Chassagne D : L'endocuriethérapie des adénopathies cervicales malignes par iridium-192. *J Radiol* 51 : 237, 1970
7. Hall EJ, Bedford JS, Oliver R : Extreme hypoxia : its effect on the survival of mammalian cells irradiated at high and low dose rate. *Br J Radiol* 39 : 302, 1966
8. Hall, EJ, Roizin-Towle LA, Colvett RD : RBE and OER determinations for radium and californium-252. *Radiology* 110 : 699, 1974
9. Pierquin B, Baillet F, Brown C : La téléradiothérapie continue et de faible débit : deuxième rapport. *J Radiol* 55 : 757, 1974
10. Kal HB, Barendsen GW : Effects of continuous low dose rates on a rat rhabdomyosarcoma. *Br J Radiol* 47 : 279, 1972
11. Kal HB, Sissingh HA : Effectiveness of continuous low dose rate gamma irradiation on rat skin. *Br J Radiol* 47 : 673, 1974
12. Pierquin B, Chassagne D, Chahbazian C : *Brachytherapy*. St. Louis, Warren Green. In press, 1975

Laparoscopy and Laparotomy in Staging Hodgkin's and Non-Hodgkin's Lymphoma

U. VERONESI,¹ P. SPINELLI, G. BONADONNA, L. GENNARI, E. BAJETTA, G. BERETTA, G. TANCINI

The use of laparotomy with splenectomy and multiple tissue biopsies has resulted in increasingly accurate staging of Hodgkin's and non-Hodgkin's lymphoma. The data accumulated at the National Cancer Institute of Milan on 550 laparosplenectomies confirm this assumption (table 1). However, this surgical approach is accompanied by a mortality rate of 0.5%–2% according to various reports and by a rather significant morbidity. In addition, late infectious complications can occur, such as *Varicella zoster*. Finally, therapy cannot be started until 2–4 weeks after surgery. For these reasons, it is important to differentiate those patients for whom adequate information on staging may be obtained only by laparosplenectomy and those for whom laparoscopy may be sufficient.

Subjects and Methods

From October 1973 to April 1975 laparoscopy was performed on 175 unselected patients with Hodgkin's and non-Hodgkin's lymphoma.

Clinical diagnostic evaluation included routine hematologic studies and blood chemistry, chest x-ray, skeletal survey, and lower limb lymphography. Liver radionuclide scans were performed in 37 patients and spleen scans in 24. Scans were performed mainly to provide further information for defining the clinical stage.

A posterior iliac crest bone marrow was performed with Jamshidi needle 1–3 days before laparoscopy. Laparoscopy was performed on all patients. The classic staging laparotomy with open iliac crest marrow biopsy was carried out in patients with negative liver histology after laparoscopy (with the exception of two cases) and negative marrow after needle biopsy.

The technique of laparoscopy is as follows. First, determination was made that platelet count, clotting time, prothrombin time, and electrocardiogram were within normal limits. Then, 45 min before the procedure, patients received 10 mg of diazepam. In the operating room 5–20 mg of diazepam and 5–30 mg of pentazocyn were infused intravenously. The pneumoperitoneum was created by injecting 2–3 liters of CO₂ through a Veress needle into the left lower quadrant of the abdomen.

Under local anesthesia, the laparoscopy trocar was inserted 1–2 cm above the umbilicus in the midline. Liver and spleen biopsies were performed with the Trucut needle (Travenol Labs.). If areas appeared abnormal, the liver edge was also biopsied using a Palmer forceps. For liver biopsy, the needle was introduced 2 cm medially to the intercept of the right midclavicular line with the costal margin; for spleen biopsy it was introduced in the left

ninth intercostal space at the intercept with the anterior axillary line.

Only in 12 cases was a single liver biopsy obtained. In the remaining patients, one or more biopsies were performed in each hepatic lobe. One or two splenic biopsies were usually obtained from the medial aspect of the lower pole without use of adrenalin. In the majority of patients the procedure was completed within 20 min.

Results

A list of complications associated with the two procedures is presented in table 2. The most important side effects from peritoneoscopy were four episodes of abdomi-

TABLE 1
Data on Staging Laparotomies

	Hodgkin's Lymphoma	Non-Hodgkin's Lymphoma
No. Cases	347	203
Positive findings (%)		
Spleen	31	27
Liver	6	12
Mesenteric nodes	3	34
Bone marrow	4	28
Lymphography-histology concordance (%)	96	94

Note.—Staging laparotomies performed from September 1970 to March 1975 at the National Cancer Institute of Milan. There were two operative mortalities.

TABLE 2
Complications of Laparoscopy and Laparotomy

Complication	Laparoscopy (N = 175)	Laparotomy (N = 145)
None	170 (97)	96 (66)
Abdominal bleeding from:		
Liver	2	...
Spleen	2	...
Splenic hilus	1
Bronchopneumonia	23 (16)
Bronchopneumonia and pleural effusion	14 (9)
Pleural effusion	4
Left pleural effusion	2 (3)
...	1	1
Pancreatitis	1
Wound infection	2
Intestinal occlusion	1

Note.—Numbers in parentheses are percentages.

Presented at the annual meeting of the American Radium Society, San Juan, Puerto Rico, May 1975.

¹ All authors: Istituto Nazionale Tumori, Milan, Italy.

TABLE 3

Positive Findings in Untreated Cases of Hodgkin's Lymphoma Studied by Laparoscopy Only

	Clinical Stage				Total
	I	II	III	IV	
No. patients	2	2	2	13	19
Positive findings:					
Liver	0	0	1	3	4/19 (21)
Spleen	0	2	2	4	8/17 (47)

Note.—Numbers in parentheses are percentages.

TABLE 4

Positive Findings in Hodgkin's Lymphoma Patients Relapsed after Primary Therapy Studied by Laparoscopy Only

	Clinical Sites of Relapse				Total
	Lymph Nodes	Liver (± Nodes)	Liver and Other Sites	Bone Marrow	
No. patients	3	4	4	1	12
Positive findings:					
Liver	1	1	2	0	4/12 (33)
Spleen	1	1	1	N.D.	3/6 (50)

Note.—Numbers in parentheses are percentages.

TABLE 5

Positive Findings in Untreated Cases of Hodgkin's Lymphoma Studied by Laparoscopy and Laparotomy

	Clinical Stage					Total
	I	II	III	IIIS	IV	
No. patients	18	19	8	1	10	56
Positive findings:						
Laparoscopy* (spleen)	1	1	0	1	1	4/46 (9)
Laparotomy:						
Liver	0	1	0	0	0	1/55 (2)
Spleen	6	4	4	1	4	19/56 (34)

Note.—Numbers in parentheses are percentages.

* All 56 liver biopsies negative.

TABLE 6

Positive Findings in Hodgkin's Lymphoma Patients Relapsed after Primary Therapy Studied by Laparoscopy and Laparotomy

	Clinical Sites of Relapse			Total
	Lymph Nodes	Liver (± Nodes)	Spleen (± Nodes)	
No. patients	13	4	1	18
Positive findings:				
Laparoscopy:				
Liver	1	0	0	1/17 (6)
Spleen	4	1	0	5/16 (31)
Laparotomy:				
Liver	3	1	0	4/18 (22)
Spleen	8	3	1	12/18 (67)

Note.—Numbers in parentheses are percentages.

TABLE 7

Positive Findings in Untreated Cases of Non-Hodgkin's Lymphoma Studied by Laparoscopy Only

	Clinical Stage					Total
	I	II	III	IIIS	IV	
No. patients	9	5	3	1	24	42
Positive findings:						
Liver	1	0	1	1	10	13/42 (31)
Spleen	0	0	1	N.D.	9	10/29 (34)

Note.—Numbers in parentheses are percentages.

TABLE 8

Positive Findings in Untreated Cases of Non-Hodgkin's Lymphoma Studied by Laparoscopy and Laparotomy

	Clinical Stage				Total
	I	II	III	IV	
No. patients	8	8	8	2	26
Positive findings:					
Laparoscopy:					
Liver	0	1	0	0	1 (3.6)
Spleen	1	2	1	0	4/26 (15)
Laparotomy:					
Liver	1*	1	0	1*	3 (11)
Spleen	1	2	2	0	5 (18)

Note.—Numbers in parentheses are percentages.

* Positive in the absence of splenic involvement.

TABLE 9

Summary of Findings by Laparoscopy

	Hodgkin's Lymphoma				Total
	Un-treated	Relapsed after Primary Therapy	Subtotal	Non-Hodgkin's Lymphoma	
No. patients	75	30	105	70	175
Positive findings:					
Liver	4	5	9 (8)	14 (20)	23 (14)
Spleen	12	8	20 (19)	14 (20)	34 (19)

Note.—Numbers in parentheses are percentages.

TABLE 10

Summary of Findings in Patients Studied by Laparoscopy and Laparotomy

	Hodgkin's Lymphoma	Non-Hodgkin's Lymphoma	Total
No. patients	74	28	102
Positive findings:			
Laparoscopy:			
Liver	1 (1)	1 (4)	2 (2)
Spleen	9 (12)	4 (15)	13 (13)
Laparotomy:			
Liver	5 (7)	3 (11)	8 (8)
Spleen	31 (42)	5 (18)	36 (36)

Note.—Numbers in parentheses are percentages.

nal hemorrhage due to bleeding from the liver and spleen. Only one patient with liver hemorrhage required an emergency laparotomy within a few hours of peritoneoscopy. Abdominal bleeding from splenic puncture occurred in two patients with an enormous spleen (3 kg at laparotomy) and was controlled without surgical intervention.

Hodgkin's Lymphoma

A total of 105 patients had Hodgkin's lymphoma; 31 of these were studied without subsequent laparotomy control (19 untreated and 12 relapsed after primary therapy). The results are shown in tables 3 and 4. In the untreated group 21% and 47% showed positive liver and spleen biopsies, respectively. Higher percentages of liver and spleen involvement were found in patients relapsed after primary therapy (table 4).

A total of 74 patients with Hodgkin's lymphoma underwent laparoscopy and laparotomy (56 untreated and 18 relapsed after primary therapy). Results of the two procedures are compared in tables 5 and 6. Among untreated patients, four of 46 spleen biopsies were positive (9%) by laparoscopy, while laparotomy showed the spleen to be involved with disease in 19 patients (34%). Among the 18 patients relapsed after primary therapy, 31% had a positive spleen biopsy at laparoscopy, whereas laparotomy showed positive spleen findings in 12 cases (67%) (table 6).

Non-Hodgkin's Lymphoma

A total of 70 patients had non-Hodgkin's lymphoma; 42 of these were examined only by laparoscopy (table 7). Liver biopsies were positive in 13 cases (31%) and spleen in 10 (34%).

Table 8 shows results for the 26 cases tested by both procedures. The difference in number of positive spleen biopsies is slight (four positive by laparoscopy and five by laparotomy), while two additional cases with positive liver findings were discovered by laparotomy.

Analysis of Data

Table 9 summarizes data on the 175 patients studied by laparotomy. Splenic involvement was detected in approximately 20% of patients with Hodgkin's and non-Hodgkin's lymphoma. Liver involvement was detected in a larger percentage of patients with non-Hodgkin's lymphoma.

Findings on the 102 patients studied by both laparoscopy and laparotomy are shown in table 10. Results of the two procedures correlated well in non-Hodgkin's lymphoma patients (splenic involvement detected in 15% and 18%, respectively). However, a consistent difference was observed in patients with Hodgkin's lymphoma (splenic involvement detected in 12% and 42%, respectively).

Conclusions

Laparoscopy can detect liver and splenic involvement in some patients with Hodgkin's lymphoma, sparing them laparotomy. However, because of the high false negative rate, laparotomy is still required when findings are negative. In patients with non-Hodgkin's lymphoma, laparoscopy has a much lower false negative rate. Thus with further technical improvements, it is likely to replace laparotomy as main staging procedure for patients with non-Hodgkin's lymphoma.

Subtotal Mastectomy and Radiation Therapy in the Definitive Management of Localized Breast Malignancy

PAUL E. WALLNER,¹ LUTHER W. BRADY, JR., JOHN LOUGHEAD, TERUO MATSUMOTO, JOHN ANTONIADES, SRIPRAYOCN PRASASVINICHAJ, JOHN R. GLASSBURN, SUCHA O. ASBELL, AND JEFFREY I. DAMSKER

Between 1961 and 1974, 51 women with primary carcinoma of the breast were treated by external radiation following surgery that was limited to diagnostic biopsy. All patients tolerated therapy well with minimal long term morbidity. While the reported follow-up periods are brief (most patients at risk for less than 3 years), 29 patients remain alive, 25 of whom show no evidence of persistent or recurring disease. These data suggest that local-regional control rates match those obtained following mastectomy. Definitive statements as to local failures and long term survival rates are not yet available.

Introduction

In 1961, radiologists at Hahnemann Medical College and Hospital recognized a need for reevaluation of the role of radiotherapy and its technical application in regard to the management of two categories of patients with primary carcinoma of the breast.

The first group represented those individuals with locally advanced disease. These patients had previously been considered inoperable; when definitive surgery was attempted, wound healing and local control rates were poor, as were long term survival figures. It was felt that radiation therapy techniques utilized up to that time were less than optimal and that a revised approach might offer improved local-regional control rates.

The second group consisted of individuals who had disease apparently limited to small primary breast lesions with or without palpable axillary lymph nodes. This group of patients had traditionally been treated by surgery of varying degrees with or without postoperative external radiation therapy; innumerable published reports existed of long term survival and local-regional control rates. It was hoped that definitive radiation therapy would offer an acceptable alternative to mastectomy for those patients medically unable to undergo surgery or unwilling to sacrifice a breast.

This paper is a retrospective analysis of patients considered to be candidates for definitive radiotherapy following surgical procedures less than simple mastectomy and usually performed solely for diagnosis. All patients were managed by one group of radiation therapists utilizing standard, although evolving techniques.

Patient Population and Treatment Protocol

Between 1961 and 1974, 51 patients, all female, were seen in our department with an established diagnosis of primary carcinoma of the breast and having undergone only

diagnostic surgical procedures. All patients are included in this review.

Ages at the time of diagnosis ranged from 27 to 82 years with the majority of patients in the fifth, sixth, and seventh decades (fig. 1). In nine patients diagnosis was established by needle biopsy, in 14 by incisional biopsy, and in 28 by excisional biopsy.

Clinical staging at the time of diagnosis is shown in figure 2. Retrospectively, all patients were restaged utilizing the UICC TNM system. On this basis, in stage I there were six T1 and 14 T2 lesions. Both stage II patients had T2N1 lesions. As expected, the stage III patients are a heterogeneous group with a majority having large primary lesions and skin or chest wall involvement.

All patients were treated initially by external irradiation. The first two patients in the series were treated with 200 kV X-rays. This was followed by conversion to a 6 MV linear accelerator; 42 patients were treated by this modality. Seven patients were treated initially on cobalt-60 teletherapy devices at two other institutions by members of our department, with dosimetry verified by the Hahnemann physics group.

External irradiation in all cases was directed to the lymph node drainage sites in the internal mammary, lower cervical, supraclavicular, and axillary regions by anterior shaped portals. The intact breast and chest wall were treated by two parallel opposed tangential portals. Dose levels in almost all cases consisted of 5,000 rad in 5–6 weeks or radiobiological equivalents based on the nominal standard dose concept of Ellis.

In the early group, 15 of the patients received no boost dose to the actual tumor bed. Later it was felt that additional local irradiation to the tumor site would be of value, and, depending on the modalities available at the time, boosts of 1,500–3,500 rad were administered. This was carried out utilizing 7 MeV electrons in one patient, 11 MeV electrons in two, cobalt-60 in six, 6 MV in four, interstitial single-plane radium implants in 11, and single-plane iridium-129 implants in 12 (fig. 3). For the past 5 years, interstitial boost therapy has been used almost exclusively, and for the past 3 years the use of iridium implants has predominated.

Iridium wire implantations can be performed in a brief period of time under local anesthesia. The operator has control of both ends of hollow metal trochars so that positioning should always be satisfactory. The procedure is completed by a modified after-loading technique with removal of the trochars and advancement of the iridium seeds

Presented at the annual meeting of the American Radium Society, San Juan, Puerto Rico, May 1975.

¹ All authors: Department of Radiation Therapy and Nuclear Medicine, Hahnemann Medical College and Hospital, 230 North Broad Street, Philadelphia, Pennsylvania 19102. Address reprint requests to P. E. Wallner.

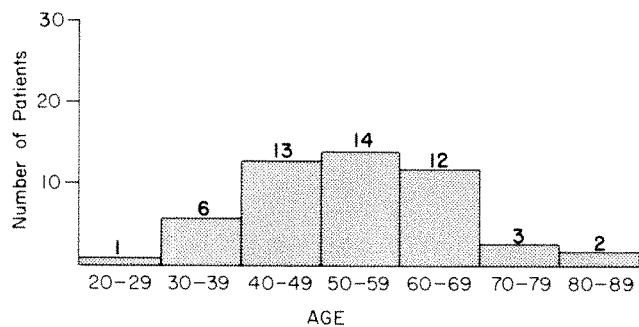


Fig. 1.—Age of patients at time of diagnosis.

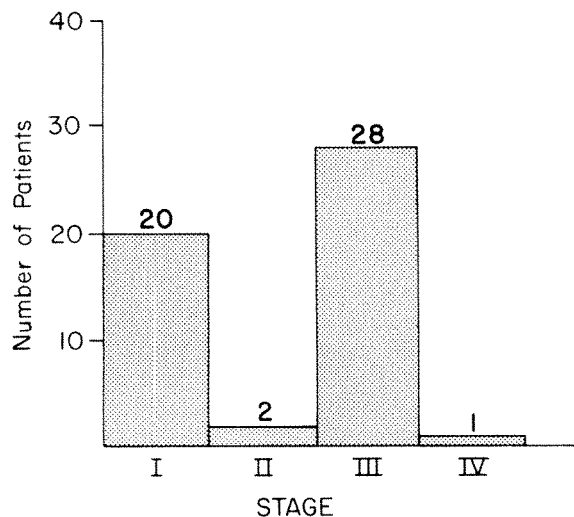


Fig. 2.—Clinical staging at time of diagnosis.

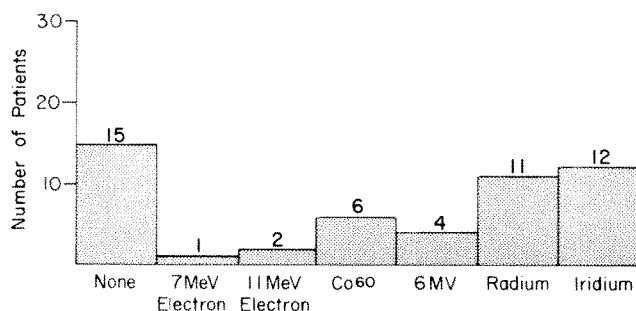


Fig. 3.—Method of boost therapy.

annealed in plastic wire. The implant dosimetry is invariably homogeneous, and dose rates are calculated at a plane 1 cm on either side of the source.

All patients tolerated therapy well. During external irradiation most exhibited a transient mild esophagitis and dry epidermitis, with only four moist skin reactions. In these patients 4 weeks elapsed prior to boost therapy.

Long term morbidity was also minimal. Heavily irradiated mammary tissue tended to become moderately fibrotic with variable amounts of shrinkage. No instances of severe pain or other complications requiring additional surgery were encountered.

TABLE 1
Summary of Patient Status

Status	Living	Dead
No disease present	25	2
Disease present:		
Local	1	6
Regional	3	13
Distant	2	20
Subtotal	4	20
Total	29	22

TABLE 2
Patient Status by Clinical Stage

Stage and Status	Living	Dead
Stage I:		
No disease present	14	1
Disease present:		
Local	1	2
Regional	3
Distant	4
Subtotal	1	4
Total	15	5
Stage II:		
No disease present	1	...
Disease present:		
Local	1
Regional	1
Distant	1
Subtotal	1
Total	1	1
Stage III:		
No disease present	10	1
Disease present:		
Local	3
Regional	3	8
Distant	2	14
Subtotal	3	14
Total	13	15

Note.—One stage IV patient died with regional recurrence and distant metastases.

Results

At the time of analysis, 29 patients were alive and 22 had died (table 1). Of the living patients, 25 had no evidence of persistent or recurrent disease and four were living with disease. There was evidence of local failure within the volume of treatment in one, and two instances of regional and distant disease. Local failures are defined as persistence or recurrence of disease within the treatment fields, regional failures as those within the immediately contiguous areas including chest wall and pleura, and distant metastases as other disseminated areas of disease.

Among the 22 who died, two showed no evidence of malignancy at autopsy; one died of complications secondary to ulcerative colitis and one of medical problems unrelated to her breast malignancy or its treatment. Twenty had evidence of active malignancy (table 1). Of this group,

TABLE 3
Follow-up

Years	No. Patients
0-1	21
1-2	9
2-3	13
3-4	2
4-5	4
5+	2
Total	51

one patient had a concomitant adenocarcinoma of the rectum, Dukes's stage C, treated by anterior resection. It was unclear at the time of her death whether she suffered from dissemination of the rectal or breast malignancy, or both.

Patient status by clinical stage is shown in table 2.

It was felt that the addition interstitial boost therapy to the tumor bed or site of residual induration added significantly to local control rates. A total of 23 patients received radium or iridium implantations. Of this group, there are only three cases of recurrent disease within the treated volume. Each was treated prior to standardization of techniques and dosages. One patient received 2,600 rad in 18 elapsed days to the nodal drainage sites and 3,525 rad in 19 days to the breast. This was followed by a radium needle implant delivering 5,000 rad to a 1 cm plane. The second patient received 4,125 rad in 21 days to the lymph nodes and 5,000 rad in 35 days to the breast followed by 2,800 rad from radium needles. The third patient received 2,000 rad in 14 days to the breast followed by an iridium implant delivering 3,392 rad. Two of these patients were clinical stage III at presentation and one was clinical stage I.

For most patients follow-up periods are brief, with 43 of 51 patients at risk for less than 3 years (table 3). This factor precludes definitive statements as to local failure and long term survival rates.

Discussion

The evaluation of any therapeutic regimen for primary management of localized breast cancer must take several critical factors into account.

One essential variable is local-regional control of disease. Although it has been well documented that local-regional control does not necessarily correlate with survival [1], local recurrences are significant. Chest wall recurrences frequently ulcerate and bleed, supraclavicular metastases often involve the brachial plexus with secondary neurologic symptoms and pain, and axillary masses may cause considerable discomfort.

Extensive data are available to indicate the improvement of local-regional control rates following mastectomy in various clinical situations. Our data and those of others [2-4] tend to suggest that local-regional control rates will be similar if the breast is in place.

A second variable is control of the primary lesion. Despite

a frequent observance of multicentricity of disease within the breast at the time of mastectomy, Baclesse [5] and Guttmann [6] have well documented the ability of external radiotherapy to control locally advanced primary disease and, by inference, early disease. Our data also support this conclusion.

It has been stated that external irradiation, especially to the axilla, can alter local and systemic immunity, thereby enhancing dissemination of disease. Clinical [3-6] and laboratory [7-11] data do not substantiate that claim.

A third and often underestimated variable is the acceptance of a therapeutic regimen by the patient population at risk. There is evidence that fear of mastectomy may cause periods of patient delay, and psychological problems following deforming surgical procedures may provide difficult family situations. Definitive management by combined external and interstitial irradiation has been well accepted by all patients, and the minimal morbidity encountered is well tolerated.

The most significant variable is, of course, long term survival. Any new treatment program must be evaluated against the best available techniques. The present material and that of others using surgical procedures to an extent less than total mastectomy have, unfortunately, not yet withstood the test of time; we must await long term survival figures. In the meantime, we feel the program warrants further investigation with consideration of large scale co-operative studies.

REFERENCES

1. Fisher B, Slack N, Cavanaugh P, Gardner B, Rawdin R: Post-operative radiotherapy in treatment of breast cancer: results of NSABP clinical trial. *Ann Surg* 172:711-732, 1970
2. Fletcher GH: Local results of irradiation in primary management of localized breast cancer. *Cancer* 29:545-551, 1972
3. Peters MV: Wedge resection and irradiation: an effective treatment in early breast cancer. *JAMA* 200:144-145, 1967
4. Prosnitz LR, Goldenberg IS: Radiation therapy as primary treatment for early stage carcinoma of breast. Paper presented at the annual meeting of the American Society of Therapeutic Radiologists, October 1974
5. Baclesse F: Five-year results in 431 breast cancers treated solely by roentgen rays. *Ann Surg* 161:103-104, 1965
6. Guttmann R: Radiotherapy in locally advanced cancer of breast. *Cancer* 20:1046-1050, 1967
7. Crile G, Deodhar SD: Role of preoperative irradiation in prolonging concomitant immunity and preventing metastasis in mice. *Cancer* 27:629-634, 1971
8. Fisher B, Fisher E: Studies concerning regional lymph node in cancer. *Cancer* 29:1496-1501, 1972
9. Markoe AM, Asbell SO, Saluk P, Weidanz W, Brady LW: Effects of acute and fractionated partial body irradiation on circulating immunoglobulin levels in mice. Paper presented at the annual meeting of the American Society of Therapeutic Radiologists, October 1974
10. Perez CA, Stewart CC, Palmer-Hanes LA, Powers WE: Role of regional lymph node in cure of a murine lymphosarcoma. *Cancer* 32:562-572, 1973
11. Nelson AJ, Montague EO: Combinations of surgery and irradiation for cancer of breast. Refresher course, Radiologic Society of North America, 1974

Postoperative Irradiation in the Prevention of Keloids

DAVID S. LEVY,¹ MERLE M. SALTER, AND ROBERT E. ROTH

Low dose superficial x-irradiation to the incisional site after surgical excision of a keloid prevented keloid or hypertrophic scar formation in 31 of 35 patients evaluated (88%). The clinical manifestation of keloids, physiology of wound healing, pathophysiology of keloid formation, and the radiation technique utilized are presented. This study shows that the method is well tolerated, easily administered, and efficient in inhibiting recurrence of keloid or hypertrophic scar formation.

Introduction

Keloids are benign soft tissue tumors which grow beyond the confines of the original wound, whereas hypertrophic scars tend to remain within the wound confines. The keloid or hypertrophic scar tends to occur where there is increased skin tension. Dark-skinned individuals have a greater propensity to form keloid and hypertrophic scars in response to trauma compared to light-complected individuals [1, 2]. Although benign both keloid and hypertrophic scars can produce symptoms of discomfort manifested by pruritis and parasthesia as well as cause cosmetic deformity [3].

Three methods of treatment are currently used to prevent their formation. One is atraumatic excision using meticulous approximation of skin margins with relaxing incisions. This technique has been used by surgeons for many years, although it is often ineffective when used alone [4]. In 1965, Maguire [5] reported the first successful regression of a large keloid using intralesional triamcinolone. Other investigators [5-8] have indicated satisfactory results using triamcinolone injections following central excision of the keloid. Finally, postoperative radiation therapy is an effective method of preventing keloid and hypertrophic scar formation [3, 9, 10].

This paper presents our experience using early postoperative irradiation in the prophylactic treatment of keloids.

Subjects and Methods

A total of 37 patients were treated by surgical excision followed by superficial x-irradiation in an effort to prevent keloid or hypertrophic scar formation. Best results were obtained when treatment was initiated within 24-48 hr after excision of the keloid. The recent incision, including all sutures, plus a 2 mm margin in all directions were enclosed in a lead cutout used to protect all normal tissue beyond the margins. The irradiation was administered using a GE superficial x-ray unit at a subject to screen distance of 35 cm, using 100 kVp and 4 MA with 1 mm thick aluminum inherent filtration. No additional filtration was used.

A time-dose schedule of 300 rad, measured at a depth of 1 mm, was given every other day in five to six fractions over 12-14 days, for a total accumulated dose of 1,500-1,800 rad. The lower dose was given to light-complected individuals; darker-skinned patients received a total dose of 1,800 rad.

A minimum of 6 months elapsed between completion of therapy and initial evaluation. Patients were followed at varying intervals from 6 months to 2 years postirradiation.

Results

Measurements of scar width and thickness were used to evaluate results. A scale ranging from fair-poor to good-excellent was established. On the basis of these criteria, 31 of the 37 evaluable patients scored excellent or good; four patients showed fair or poor results, and two were lost to follow-up.

No undue sequelae were observed. Hyperpigmentation was noted in a few patients. In one individual, depigmentation in the treated area was observed. Although we have never encountered or read of a case of neoplasia resulting from this type of irradiation, it should be considered a remote possibility. Careful shielding of younger patients who have keloid or hypertrophic scars near epiphyseal growth centers or other developing vital structures is mandatory [3].

Discussion

There are three well recognized phases of wound healing [3]. Initially new fibroblasts accumulate in a perivascular nodular pattern around new endothelial buds. Several days later, the number of collagen bundles increases, still arranged in a perivascular pattern. The final phase results in thickening and disarrangement of the collagen bundles with diminution in fibroblasts and blood vessels. If the equilibrium which normally exists between the synthetic and degradative phases of collagen metabolism is somewhat disturbed, the end result is a greater mass of collagen (i.e., keloid or hypertrophic scar).

Radiation is most effective in the early phases of healing. Since developing endothelial vascular buds are extremely radiosensitive, their growth can be retarded. Also, proliferation of new fibroblasts can be decreased by low dosage irradiation, hence decreasing the amount of collagen proliferation and subsequent keloid formation [11].

Time-dose schedules vary widely in prophylactic treatment of keloids, ranging from a single dose to dosage schedules protracted over 4 weeks. Deigert and Allen [3] reported best results with atraumatic excision followed by irradiation within 1-3 days of excision. This was especially true for lesions about the sternum and deltoid region.

The time-dose schedule used in this series has proved to be effective and efficient in the postsurgical prophylactic treatment of keloids. This method of postoperative irradiation is safe, well tolerated, easily administered, and free of undue sequelae.

¹ All authors: Department of Radiation Oncology, University of Alabama in Birmingham, 619 South 19th Street, Birmingham, Alabama 35233.

REFERENCES

1. Cosman B, Crikeliar GF, Ju MC, Gaulin JC, Lattes R: The treatment of keloids. *Plast Reconstr Surg* 27:335, 1961
2. Koonin AJ: Aetiology of keloids: a review of the literature and a new hypothesis. *S Afr Med J* 38:913-916, 1964
3. Deigert FA, Allen KDA: Keloids: reassessment of irradiation therapy. *Rocky Mt Med J* 70:35-37, 1973
4. Ketchum LD, Cohen IK, Masters FW: Hypertrophic scars and keloids—a collective review. *Plast Reconstr Surg* 53:140-154, 1974
5. Maguire HC: Treatment of keloids with triamcinolone acetate injected intralesionally. *JAMA* 192:325-326, 1965
6. Griffith BH: Treatment of keloids with triamcinolone acetate. *Plast Reconstr Surg* 38:202, 1966
7. Ketchum LD, Smith J, Robinson DW, Masters FW: Treatment of hypertrophic scars, keloids, and scar contracture by triamcinolone acetate. *Plast Reconstr Surg* 38:209, 1966
8. Murray RD: Kenalog and the treatment of hypertrophic scars and keloids in negroes and whites. *Plast Reconstr Surg* 31:275-280, 1963
9. Craig RDP, Pearson D: Early post-operative irradiation in the treatment of keloid scars. *Br J Plast Surg* 18:376, 1965
10. Levine W, Gillies H: Radiotherapy in the prophylaxis and treatment of keloid. *Lancet* 1:440, 1942
11. Lever W: *Histopathology of Skin*, 4th ed. Philadelphia, Lippincott, 1967

Parametrial Calcification in Cervical Carcinoma Patients Treated with Radioactive Gold

TONY M. DEETHS^{1,2} AND ROBERT J. STANLEY¹

A unique appearance of soft tissue calcification in the pelvis which may be specific for patients treated with parametrial injection of ¹⁹⁸Au colloid is described. The calcification appears in the area of maximum radiation dose and can appear within 5 years of treatment. It is significant because it occurred in approximately one-half of the cases radiographically reviewed and may be confused with calcification from other etiologies.

Over the last 5 years, a number of patients have been examined in our department who exhibited unusual calcification of the soft tissues of the pelvic region. The unusual location and configuration of the calcifications in these patients and the lack of similarity to commonly described pelvic calcifications prompted further investigation. All of these patients had received parametrial radioactive gold injections for carcinoma of the cervix. To our knowledge, similar findings have not been reported previously.

From 1950 through 1965 over 400 patients were treated at this medical center with injections of colloidal ¹⁹⁸Au into the parametrium. This treatment was performed as an adjunct to surgery and radium therapy in order to treat the lateral parametrium and cervical lymph drainage without significantly increasing the radiation dosage to the bladder and rectum. A brief explanation of the rationale, technique, and dosimetry involved in this treatment is presented in the Appendix. Detailed discussion of the preliminary experiments, dosimetry, efficacy, and complications have been previously reported [1-9].

A 9% incidence of complications directly related to gold therapy has been reported [8]. These include cystitis and periureteritis leading to hydronephrosis, vesico-vaginal fistula, and one case of sciatic neuritis. The patients in our series did not experience different complications, nor was there evidence of a direct correlation between the development of complications and the development of pelvic calcification.

A retrospective film review was carried out to further evaluate the development of calcification in these patients. Of 190 patients surviving for 5 years, 31 had active x-ray films including films of the pelvic region. Of these patients, 17 had soft tissue calcification in the pelvis. With one exception, the calcification occupied the region of the gold injection (fig. 1) and highest radiation dose, coinciding with the region of the hypogastric and iliac nodes. In the one exception, the calcification overlay the obturator foramen on a frontal radiograph, and no calcification was seen in the expected locations. Since one of the complications of the procedure is dissection of the injected material along

the iliac or obturator canals, this is a possible explanation. However, the patient's chart revealed no clinical evidence of this complication. The occurrence of the calcification in these locations must be assumed to be secondary to direct radiation effect.

Kottmeier and Moberger [9] found striking radiation effects within several days of injection. These effects included extravasation of red blood cells, capillary endarteritis, cellular destruction, and focal areas of necrosis. This was followed by reparative changes resulting in a diffuse fibrosis. They also found that a large part of the injected material remained in the parametrial tissue, disposing to the risk of overdosage and damage of normal tissue.

The amount and appearance of the calcification varied somewhat among cases. In the cases with multiple films, a gradual and progressive increase in the amount of calcification was seen (fig. 2). The appearance of the calcification varies from thin and linear to globular and thickened with periosteal involvement (figs. 3-5). Periostitis is not commonly associated with radiation injury, so that this change may be due to causes other than the radiation. The injection technique involved insertion of the needles to the bone; thus some of the injection may have been subperiosteal. Also, the extensive local changes and healing may have induced a reactive periostitis similar to that seen in inflammatory conditions.

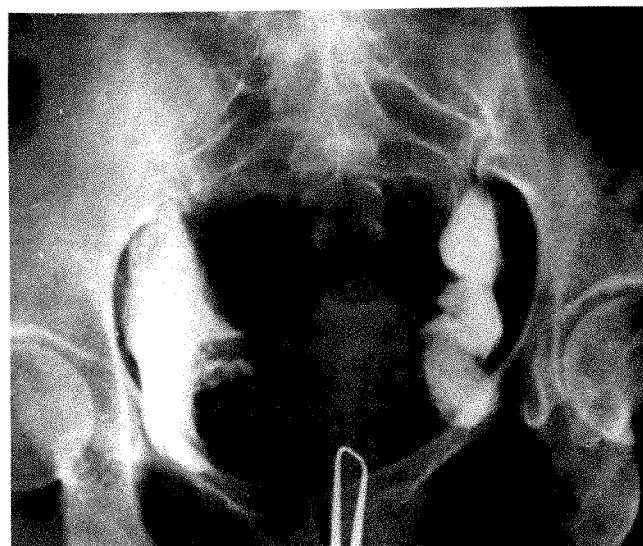


Fig. 1.—Radiograph taken immediately after injection of colloidal gold suspended in 20% diodrast to demonstrate distribution of colloid. (Reprinted with permission from [6])

¹ Mallinckrodt Institute of Radiology, Washington University School of Medicine, 510 South Kingshighway, St. Louis, Missouri 63110. Address reprint requests to R. J. Stanley.

² Present address: Ballas Radiology Group, 777 South New Ballas Road, St. Louis, Missouri 63141.

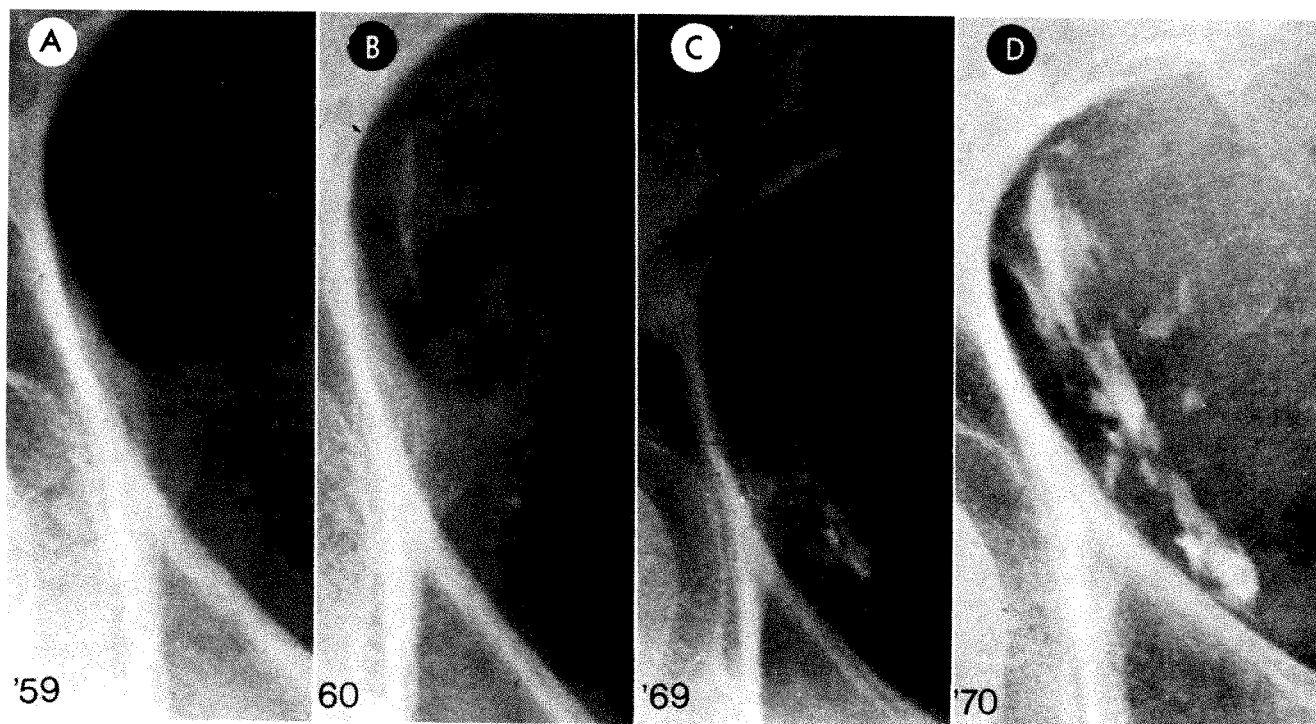


Fig. 2.—Serial radiographs showing progression of calcification over 11-year period.

Most films demonstrating this unusual calcification were obtained 15–20 years after treatment with no interval diagnostic radiographic studies. However, the five cases which showed linear calcification present within 7 years of treatment as well as the several cases demonstrating progressive involvement suggest that the calcification first appears 5–10 years after treatment.

The differential diagnosis of entities causing pelvic calcification is quite extensive; however, in most cases there should be little confusion. Appendiceal calculi and calcified mucocele, enteroliths, gallstones in the bowel, urinary calculi, calcified epiploic appendages, and calcification in a Meckel's diverticulum may all lie in the pelvic region but are usually rounded and not in the same location as the type of calcification under discussion.

While arterial calcification and aneurysmal calcification are usually linear and may be bilateral, they generally follow a course from medial to lateral and do not closely approximate the bony pelvis. Phleboliths in veins often lie along the pelvic wall but are usually discrete and rounded. Calcifications in the genital tract, whether from infection or degeneration, are more medial and of typical configuration. Entities such as leiomyoma, dermoid, teratoma, and lithopedion are clearly different and easily recognized. Parasitic infestation such as cysticercus or bladder wall calcification secondary to schistosomiasis, tuberculosis, or tumor encrustation may cause some confusion; however, the amount of calcification present is usually not very large.

The lesions most difficult to differentiate from calcification secondary to parametrial radiation are bone tumors, lymph nodes calcified secondary to tuberculosis or other

granulomatous disease, cystadenoma or cystadenocarcinoma of the ovary with psammomatous calcification, and old calcified pelvic hematoma. Distinction in these cases can be made on the basis of bilaterality, laminated appearance, the close approximation to the lateral pelvic wall, and the lack of involvement of the region superior to the bladder.

APPENDIX

Rationale for Treatment with ^{198}Au

The rationale for treatment of patients with carcinoma of the cervix with ^{198}Au in conjunction with radiation therapy and surgery was based on several factors. With radium, the cervix and paracervical regions received adequate treatment and the bladder received doses close to tolerance. However, the region of direct spread and lymphatic drainage (i.e., the hypogastric and iliac node groups and the parametrium) did not receive tumoracidal doses. Gold colloid injected in the parametrium had a threefold mode of action: (1) beta radiation of the volume of tissue permeated by the gold, (2) intense beta radiation of the nodes in which the colloid was selectively concentrated, and (3) gamma radiation of a volume of tissue extending beyond the confines of the radioactive gold. It should be noted that except for lymph node concentration of the gold, direct spread through the parametrium did not occur. The volume of tissue occupied by the colloidal gold a few hours after injection did not change over the therapeutic life of the gold.

The radioactive gold was obtained in colloidal form from a commercial source and suspended in a 1% pectin solution in 5% aqueous dextrose at a pH of 7–8. Three sites of injection were selected in each parametrium and 70 mCi, distributed in a volume of 500 cm³ of tissue, gave an average beta ray dose of approximately 10,600 rep. Total gamma ray dose (from radium and ^{198}Au) to the mid-parametrium averaged 5,600 R [3–7]. This mode of therapy was used at this center and elsewhere [8, 9] until 1964 when it was dis-

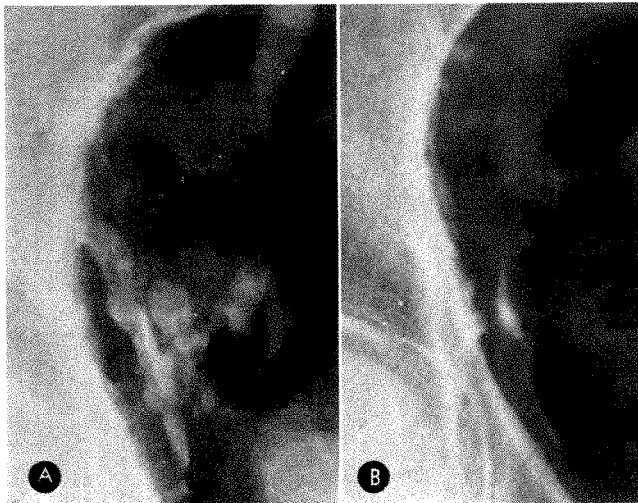


Fig. 3.—Radiographs of two patients showing periosteal thickening. Note globular clumps and relation of calcification to ureters (A).



Fig. 4.—Radiograph showing marked calcification with elevation of bladder floor and bladder diverticulum contiguous with area of calcification.

continued on the basis of the clinical impression of excessive complications and secondarily because of the introduction of super voltage therapy.

REFERENCES

1. Carlin MR: Urological complications following use of radioactive gold for carcinoma of uterine cervix. *J Urol* 78:650-661,

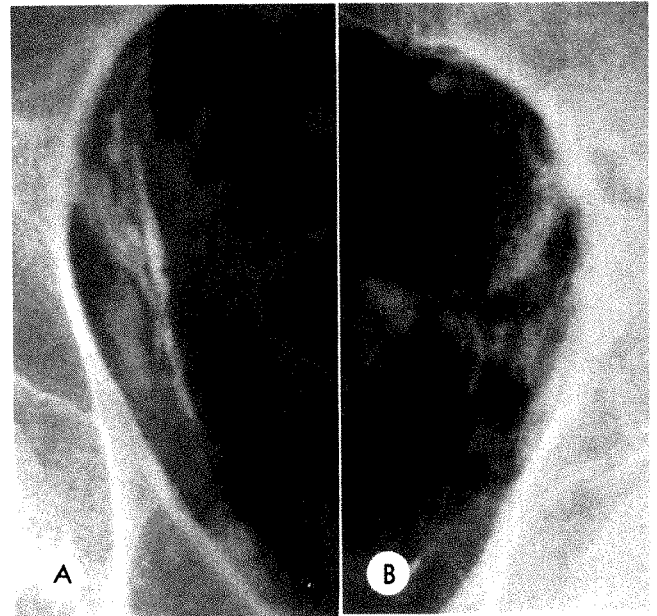


Fig. 5.—Radiographs of one patient showing thin linear calcifications on right (A) and periosteal reaction with globular thickened calcifications on left (B).

1957

2. Kao MS: Paper presented at the district 4 meeting of the American College of Obstetrics and Gynecology, Baltimore, 1974. In preparation
3. Sherman AI, Bonebrake M, Allen WM: The application of radioactive colloidal gold in the treatment of pelvic cancer. *Am J Roentgenol* 66:624-638, 1951
4. Sherman AI, Nolan JF, Allen WM: The experimental application of radioactive colloidal gold in the treatment of pelvic cancer. *Am J Roentgenol* 64:75-85, 1950
5. Sherman AI, Ter-Pogossian M: Lymph-node concentration of radioactive colloidal gold following interstitial injection. *Cancer* 6:1238-1240, 1953
6. Ter-Pogossian M, Sherman AI: Radiation dosimetry in the treatment of carcinoma of the cervix uteri by intraparametrial radioactive gold and radium. *Am J Roentgenol* 74:116-122, 1955
7. Ter-Pogossian M, Sherman AI: Handling of radioactive gold for therapeutic purposes. *Nucleonics* 10:23-27, 1952
8. Baker WS: Further experience with parametrial radiogold as an adjunct to radium therapy in treatment of pelvic lymph nodes in cancer of the cervix. *Am J Obstet Gynecol* 81:797-802, 1961
9. Kottmeier HL, Moberger G: Experience with radioactive colloidal gold as an additional treatment in the radiotherapy of uterine cancer. *Acta Obstet Gynecol Scand* 34:1-29, 1955

Case Reports

Nodular Lymphoid Hyperplasia of the Colon Associated with Dysgammaglobulinemia

ARTHUR A. DE SMET,¹ DAVID G. TUBERGEN,² AND WILLIAM MARTEL¹

A case of dysgammaglobulinemia associated with nodular lymphoid hyperplasia of the colon is reported. The patient had typical immunoglobulin deficiency, diarrhea, recurrent respiratory infections, *Giardia lamblia* in the stool, and lymphoid hyperplasia of the small intestine. His barium enema showed diffuse submucosal nodules. Rectosigmoid biopsy confirmed nodular lymphoid hyperplasia. The similar findings on barium enema in this entity and in lymphosarcoma are stressed.

Dysgammaglobulinemia may be associated with nodular lymphoid hyperplasia of the small bowel in a distinctive clinical entity which includes malabsorption and recurrent respiratory infections. Involvement of the colon by nodular lymphoid hyperplasia has not been emphasized. This report documents a case in which such involvement was striking.

Case Report

A 19-year-old white man was referred to the University of Michigan Medical Center in 1975 because of watery diarrhea for the previous 2 months. After 2 years of intermittent diarrhea, he had developed continuous diarrhea with 8–24 bowel movements per day. This was associated with a 45 pound weight loss and epigastric pain unrelated to meals. He had had eczema since age seven and recurrent respiratory infections with a persistent productive cough for the previous 4 years. There was no family history of immunologic deficiency, but his mother and sister had eczema. He had had a staphylococcal abscess of the face in 1972; at that time serum protein electrophoresis was reported to be normal. Physical examination revealed eczema involving the popliteal fossae, elbows, and left calf. There were firm, palpable lymph nodes in both axillae; the spleen tip was barely palpable.

The following blood tests were normal: serum electrolytes, creatinine, calcium, phosphorous, cholesterol, bilirubin, SGOT, LDH, febrile agglutinins, hepatitis B antigen, LE cell preparation, and antinuclear antibody. He had a mild normocytic, normochromic anemia consistent with chronic infection. The platelet count was normal but there was a mild leukopenia ($3,100\text{--}4,600/\text{mm}^3$) on five specimens with an absolute lymphopenia ($385\text{--}868/\text{mm}^3$). Serum protein electrophoresis revealed the total protein to be 5.8 g/100 ml with 59.8% albumin and 7.2% gammaglobulin fractions. Radial immunodiffusion showed a moderate decrease in IgG (370 mg/100 ml) and a marked decrease in IgA, IgM, and IgD (11, 12.5, and <1.0 mg/100 ml, respectively). The T cell percentage by sheep erythrocyte rosettes was 42% (normal, $68.3\% \pm 7\%$) and the B cells by surface immunofluorescence were at the lower limits of normal.

Skin tests for mumps, dermatophytin, streptokinase-streptodornase, and PPD were negative. The skin test for *Candida* showed

20×25 mm of erythema at 48 hr. In vitro stimulation of the patient's lymphocytes with phytohemagglutinin, concanavallin A, and pokeweed mitogen were normal. Radionuclide imaging of the liver and spleen with $^{99\text{m}}\text{Tc}$ -sulfur colloid confirmed splenomegaly.

Cysts of *Giardia lamblia* were identified in two stool specimens. Sigmoidoscopy revealed multiple submucosal nodules averaging 1–2 mm with normal overlying mucosa. Two separate rectosigmoid biopsies showed many large lymphoid nodules with well defined germinal centers (fig. 1). Plasma cells were absent from the lamina propria.

Radiologic examination of the upper gastrointestinal tract and small bowel showed innumerable regular 1–2 mm filling defects



Fig. 1.—Rectal biopsy showing two large lymphoid nodules in mucosa and submucosa displacing normal colonic glands. Such nodules diffusely present; plasma cells absent from lamina propria. H and E, $\times 105$.

Received March 5, 1976; accepted after revision May 12, 1976.

¹ Department of Radiology, University of Michigan Medical Center, University Hospital, 1401 East Ann Street, Ann Arbor, Michigan 48109. Address reprint requests to W. Martel.

² Departments of Pediatrics and Communicable Diseases, Section of Immunology, University of Michigan Medical Center, Ann Arbor, Michigan 48109.



Fig. 2.—Upper gastrointestinal examination showing innumerable tiny filling defects in jejunum, characteristic of nodular lymphoid hyperplasia. Similar nodules present in duodenum and ileum.

extending from the duodenum to the ileum (fig. 2). There was no hypersecretion, dilatation, ulceration, or distortion of the valvulae. Barium examination of the colon showed diffuse 2–3 mm nodules which were most prominent in the descending and sigmoid portions. Nodularity was particularly striking on the postevacuation film and extended from the cecum to the sigmoid colon (fig. 3). The patient was treated with metronidazole for giardiasis and is currently receiving periodic intravenous plasma with some regression of diarrhea, relief of abdominal pain, and modest weight gain.

Discussion

The association of dysgammaglobulinemia and nodular lymphoid hyperplasia of the small intestine was first recognized by Hermans et al. [1]. Our patient demonstrates the characteristic findings: (1) dysgammaglobulinemia with moderate reduction in IgG and virtual absence of IgA and IgM, (2) susceptibility to sinopulmonary infections, (3) diarrhea, (4) nodular lymphoid hyperplasia of the small intestine, and (5) *Giardia lamblia* in the stools. The small bowel findings of regular, tiny nodules [2] allow the radiologist to make a tentative diagnosis and should suggest the associated immunoglobulin deficiency. Similar findings can be seen in mastocytosis [3], which is readily differentiated clinically. The uniformity of the lesions with normal valvulae and lack of hypersecretion allows differentiation from Whipple's disease, lymphangiectasia, amyloidosis, and lymphoma.

In this entity, involvement of the colon by nodular lymphoid hyperplasia is apparently unusual. Involvement of the rectosigmoid was documented previously by Bird et al. [4] in an adult and by Wolfson et al. [5] in an infant. The differential diagnosis of nodularity of the colon includes the pseudopolyposis of ulcerative colitis, familial polyposis, and lymphosarcoma. Ulcerative colitis and familial polyposis can usually be distinguished on clinical and radiologic grounds.

Patients with hypogammaglobulinemia have approximately an 8% risk of developing a malignancy, usually of the lymphoreticular variety [6]. Lymphoma of the colon may be manifested as a diffuse submucosal nodularity on barium examination. This report emphasizes that nodular lymphoid hyperplasia may involve the colon, giving a similar diffuse pattern. Sigmoidoscopic biopsy and follow-up examinations may be required to distinguish these two conditions. The need for follow-up examination is reinforced by data of Hermans [7]: three of his original nine patients developed gastrointestinal carcinoma, two of the stomach, one of the colon.

This entity is distinct from the normal lymphoid hyperplasia of the colon in children [8]. The childhood condition usually shows characteristic umbilication on barium enema [9]. Histologically the lymphoid nodules are not as well developed, and a normal number of plasma cells are seen

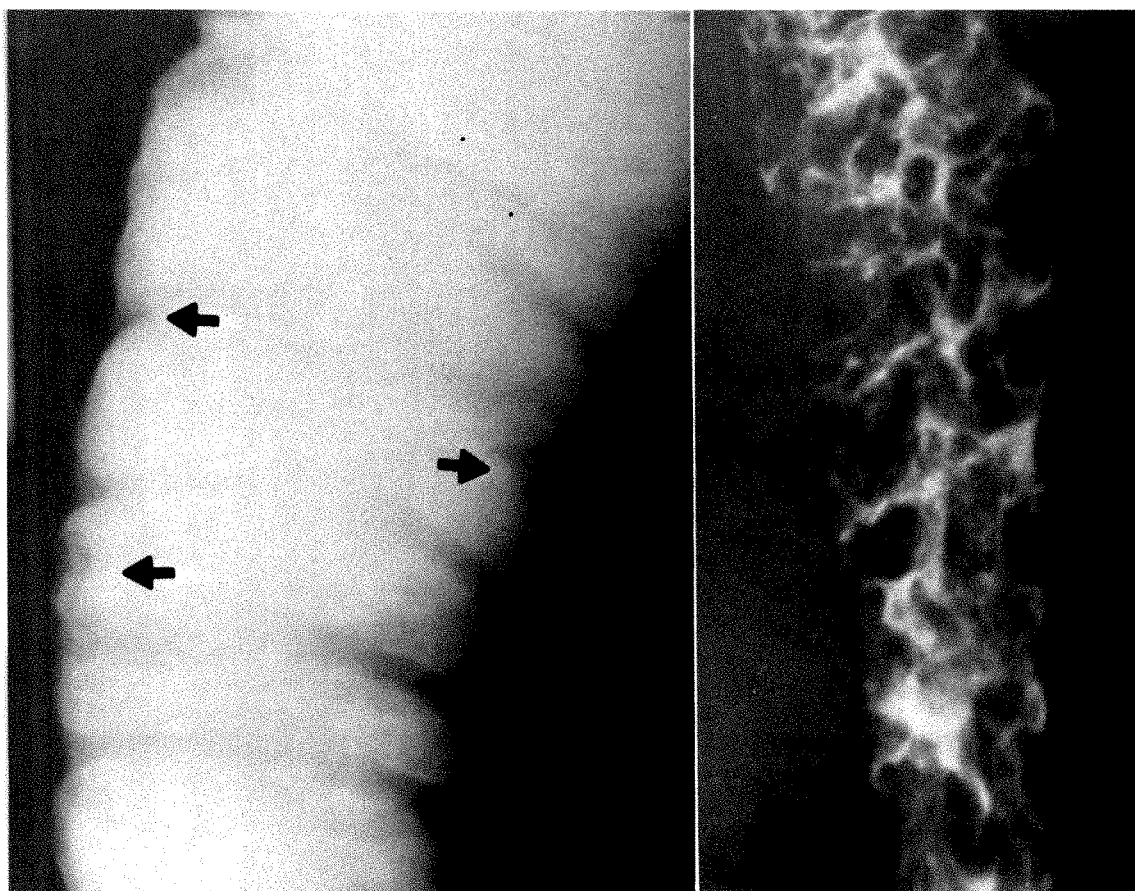


Fig. 3.—Roentgenograms of segment of descending colon before and after evacuation. Small filling defects, faintly seen in filled phase (arrows), are striking on postevacuation film. Such nodules present throughout colon.

in the lamina propria. There is no definite clinical significance to this entity in childhood, although it has been suggested that it may cause rectal bleeding [8].

ACKNOWLEDGMENT

We thank Dr. Murray R. Abell for his assistance in evaluating the pathologic material and providing the photomicrograph.

REFERENCES

1. Hermans PE, Huizenga KA, Hoffman HN, Brown AL, Markowitz H: Dysgammaglobulinemia associated with nodular lymphoid hyperplasia of the small intestine. *Am J Med* 40:78-89, 1966
2. Hodgson JR, Hoffman HN, Huizenga KA: Roentgenologic features of lymphoid hyperplasia of the small intestine associated with dysgammaglobulinemia. *Radiology* 88:883-888, 1967
3. Clemett AR, Fishbone G, Levine RJ, James AE, Janower M: Gastrointestinal lesions in mastocytosis. *Am J Roentgenol* 103:405-412, 1968
4. Bird DC, Jacobs JB, Silbinger M, Wolff SM: Hypogammaglobulinemia with nodular lymphoid hyperplasia of the intestine. *Radiology* 92:643-660, 1969
5. Wolfson JJ, Goldstein G, Krivit W, Hong R: Lymphoid hyperplasia of the large intestine associated with dysgammaglobulinemia. *Am J Roentgenol* 108:610-614, 1970
6. Shackelford GD, McAlister WH: Primary immunodeficiency diseases and malignancy. *Am J Roentgenol* 123:144-153, 1975
7. Hermans PE: Nodular lymphoid hyperplasia of the small intestine and hypogammaglobulinemia: theoretical and practical considerations. *Fed Proc* 26:1606-1611, 1967
8. Franken EA: Lymphoid hyperplasia of the colon. *Radiology* 94:324-334, 1970
9. Capitanio MA, Kirkpatrick JA: Lymphoid hyperplasia of the colon in children. *Radiology* 94:323-327, 1970

Massive Enlargement of the Ileocecal Valve due to Lymphoid Hyperplasia

ALBERT C. SELKE, JR.,¹ JUDA Z. JONA,² AND ROBERT P. BELIN²

Two children with unusual infiltration of the ileocecal valve by lymphoid tissue are described. The large filling defect identified on barium enema may suggest a number of conditions. Operative resection will exclude the possibility of a malignant process and will reduce the chance of recurrent intussusception.

Lymphoid hyperplasia of the small intestine and colon is a well recognized nonmalignant disease, or manifestation of disease, seen primarily in children. The described radiographic and surgical appearances range from multiple small papillary lesions of the intestine to discrete polypoid masses of the terminal ileum and rectum. This paper describes two patients in whom the pathologic process produced massive enlargement of the ileocecal valve.

Case Reports

Case 1

A three-year-old black female was admitted to the University of

Kentucky Medical Center for evaluation of a recent episode of hematochezia. The patient had previously been treated for recurrent urinary tract infections, but the past medical history, family history, and review of systems were otherwise noncontributory. Physical examination revealed no abnormalities. The hematocrit was 26%; all other routine tests, including stools for ova and parasites and bacterial culture, were normal. Barium enema examination revealed a persistent mass approximately 4 cm in diameter arising from the ileocecal valve (fig. 1A).

Following preoperative transfusion, the child was surgically explored. The lesion of the ileocecal valve was easily palpable through the cecal wall, and a limited ileocecal resection was performed (fig. 1B). Pathologic examination revealed submucosal lymphoid hyperplasia of the ileocecal valve. Her postoperative period and subsequent course have been uneventful.

Case 2

A ten-year-old white male was admitted with a 3 day illness characterized by intermittent colicky abdominal pain and watery stools. Two years previously the patient had undergone surgery for

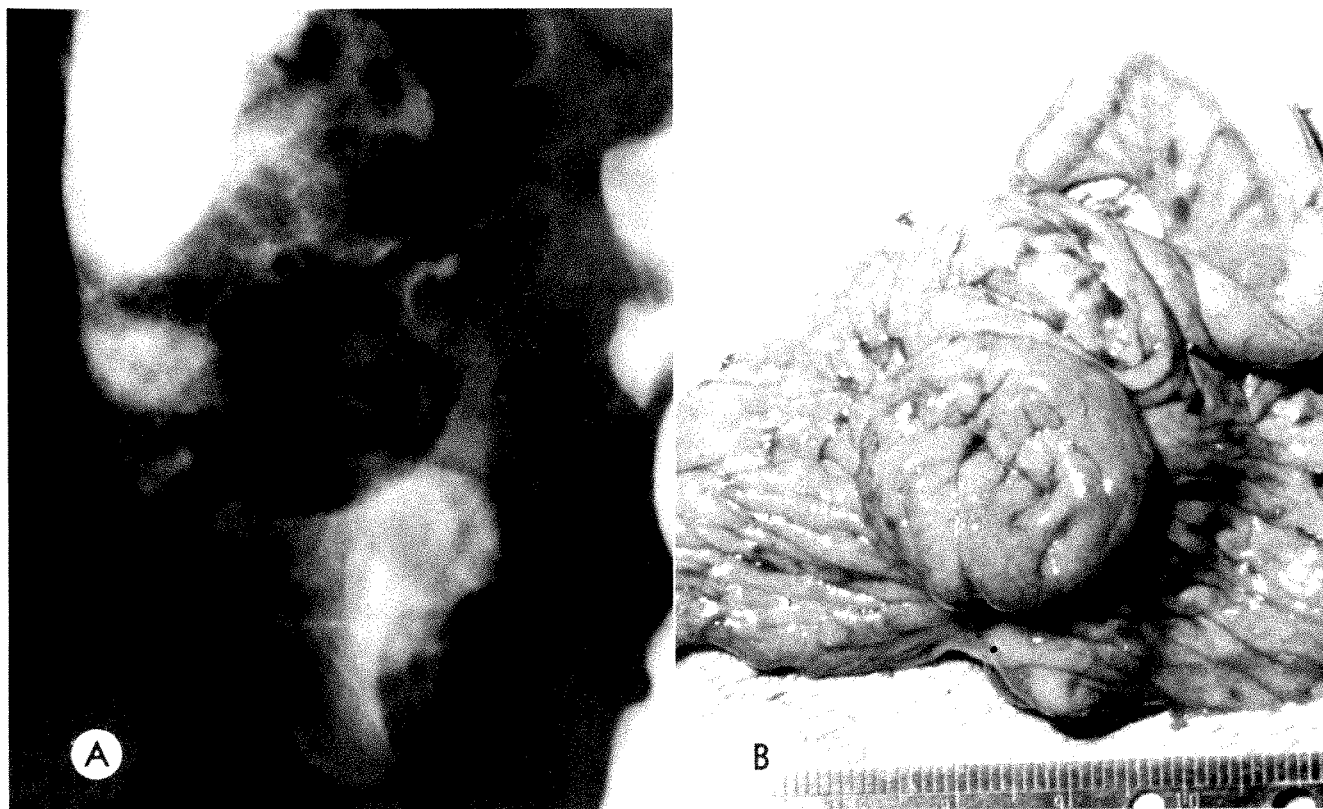


Fig. 1.—Case 1. A. Barium enema demonstrating persistent smooth mass (4 cm) in area of ileocecal valve. B. Resected opened cecum showing mass as marked lymphoid enlargement of ileocecal valve

Received March 16, 1976; accepted after revision May 12, 1976.

¹ Department of Diagnostic Radiology, University of Kentucky Medical Center, Lexington, Kentucky 40506.

² Department of Surgery, Division of Pediatric Surgery, University of Kentucky Medical Center, Lexington, Kentucky 40506.

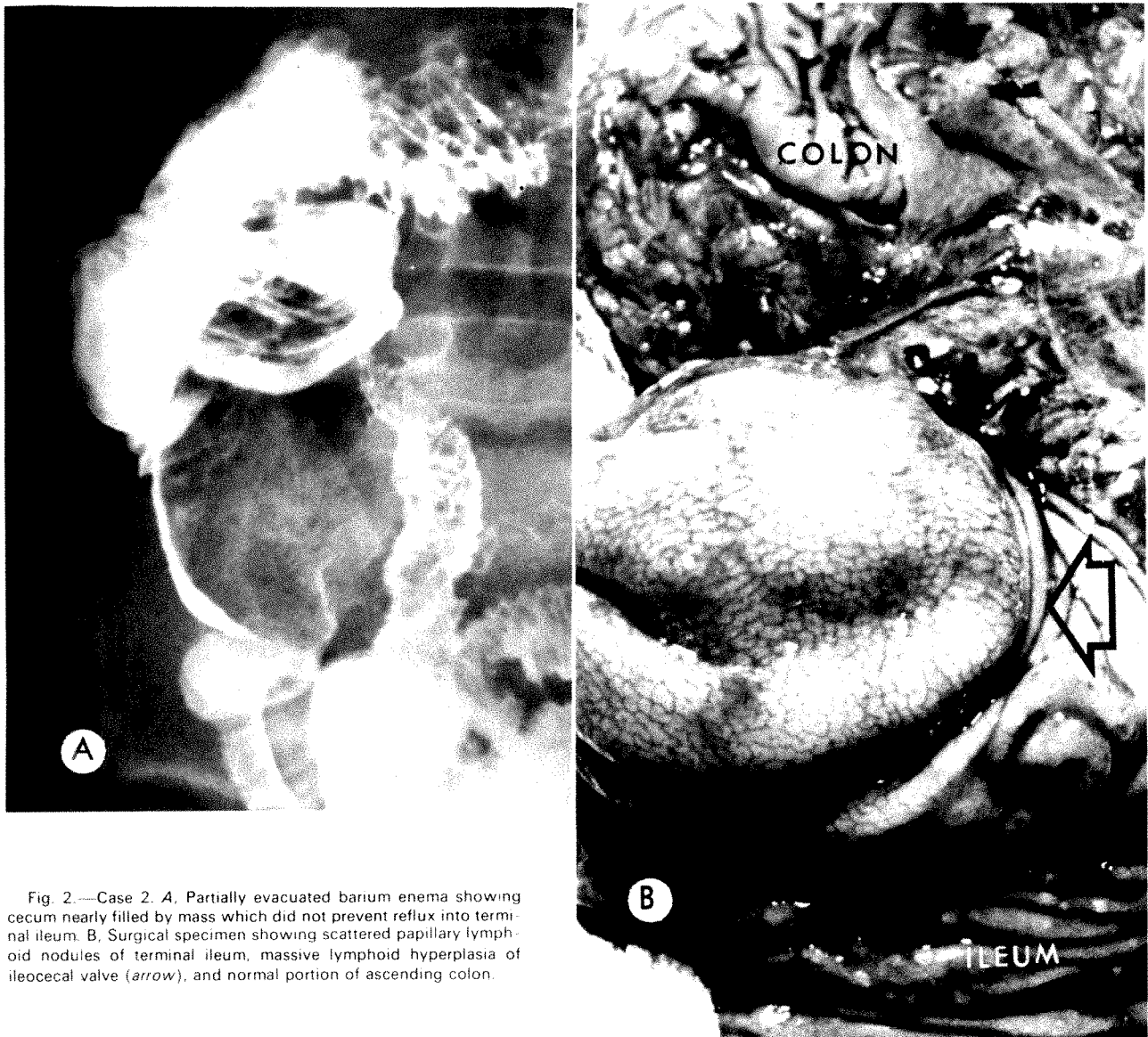


Fig. 2.—Case 2. A, Partially evacuated barium enema showing cecum nearly filled by mass which did not prevent reflux into terminal ileum. B, Surgical specimen showing scattered papillary lymphoid nodules of terminal ileum, massive lymphoid hyperplasia of ileocecal valve (arrow), and normal portion of ascending colon.

suspected appendicitis. The appendix was normal; however, an ileocolic intussusception was present and easily reduced. The patient remained in good health until the current admission.

Physical examination revealed a suggestion of a mass in the right lower quadrant but no other abnormalities. Routine laboratory studies were normal except for a hematocrit of 23%. A barium enema revealed a mass filling the cecum (fig. 2A). Incomplete reduction of an ileocolic intussusception was presumed; however, the demonstrated reflux into the terminal ileum ruled against this impression.

At laparotomy there was no evidence of intussusception, but a large ileocecal valve mass was palpable through the cecal wall. An ileocecal resection was performed (fig. 2B). Whip worms were identified in the enlarged ileocecal valve which microscopically showed submucosal lymphoid hyperplasia. The postoperative course was uncomplicated.

Discussion

Lymphoid hyperplasia of the ileum and colon is a well

known finding in patients with dysgammaglobulinemia who may have concomitant *Giardia* infestation [1, 2]. It has also been seen in patients with ulcerative colitis and regional enteritis. However, the preponderance of reported cases of this entity deal with a benign isolated process of childhood presumed to be a response to nonspecific inflammation.

Colonic involvement is most typically manifested radiographically by small (1–3 mm) papillary lesions with umbilicated centers [3] which may best be demonstrated by air contrast barium enemas [4]. A coalescing polypoid form as large as 1 cm or more in the rectum has been reported [5]. Most of the patients were discovered by examinations prompted by rectal bleeding; however, there is no direct evidence that the bleeding is caused by the lymphoid hyperplasia [3]. The lesions generally undergo spontaneous regression [6]; steroids may accelerate normalcy [7].

Small, scattered lymphoid hyperplasia of the small bowel may indeed be more common than colonic involvement

but, because of the technical and anatomic pitfalls of radiographic evaluation, could easily go undetected. The presence of ileal involvement is frequently identified during operation for suspected appendicitis [8] or after reduction of ileocolic intussusception where the enlarged lymphoid tissue has acted as the leading point [6, 9].

The cases presented here differ from the previously reported variations of this disease in that in both instances we were confronted by a radiographically identifiable mass arising from the ileocecal valve. Conditions that can cause enlargement of the ileocecal valve are edema, lipomatosis, tumor (benign and malignant), herniation of ileal mucosa, and inflammatory lesions due to tuberculosis, amebiasis, typhoid fever, anisakiasis, actinomycosis, regional enteritis, and ulcerative colitis [10–12]. Surgical resection in these children was prompted by major preoperative suspicion of enteric lymphomatous malignancy. Less likely considerations were leiomyoma or leiomyosarcoma, which have been reported in the pediatric population [13, 14]. Since the mass may serve as a leading point for ileocecal-colic intussusception, as in case 2, operative removal is justified to prevent recurrence.

The presence of whip worm infestation in case 2 possibly represents one of many forms of irritation which stimulates this abnormal proliferation of lymphoid tissue.

REFERENCES

1. Reeder MM: RPC of the month from the AFIP. *Radiology* 93: 427–433, 1969
2. Wolfson JJ, Goldstein G, Krivit W, Hong R: Lymphoid hyperplasia of the large intestine associated with dysgammaglobulinemia. *Am J Roentgenol* 108: 610–614, 1970
3. Capitanio MA, Kirkpatrick JA: Lymphoid hyperplasia of the colon in children. *Radiology* 94: 323–327, 1970
4. Franken EA: Lymphoid hyperplasia of the colon. *Radiology* 94: 329–334, 1970
5. Weller MH, Feldman PS: Benign lymphoid polyps of the rectum. *Pediatr Radiol* 3: 209–212, 1975
6. Swartley RN, Stayman JW: Lymphoid hyperplasia of the intestinal tract requiring surgical intervention. *Ann Surg* 155: 238–240, 1962
7. Louw JH: Polypoid lesions of the large bowel in children with particular reference to benign lymphoid polyposis. *J Pediatr Surg* 3: 195–209, 1968
8. Jona JZ, Belin RP, and Burke J: Lymphoid hyperplasia of the bowel and its surgical significance in children. *J Pediatr Surg*. In press, 1976
9. Schenken JR, Kruger RL, Schultz L: Papillary lymphoid hyperplasia of the terminal ileum: an unusual cause of intussusception and gastrointestinal bleeding in childhood. *J Pediatr Surg* 10: 259–265, 1975
10. Berk RN, Davis GB, and Chohassey EB: Lipomatosis of the ileocecal valve. *Am J Roentgenol* 119: 323–328, 1973
11. Berk RN, Lasser EC: *Radiology of The Ileocecal Area*. Philadelphia, Saunders, 1975
12. Calenoff L: Rare ileocecal lesions. *Am J Roentgenol* 110: 343–351, 1970
13. Khanna KK, Chandra RK, Veliath AJ, Kaveramma, Band Upadhyaya, P: Leiomyoma of the cecum. *Am J Dis Child* 116: 676–677, 1968
14. Kriss N: Leiomyosarcoma of the colon in an infant. *Am J Roentgenol* 84: 540–545, 1960

Hepatoscintigraphy, Arteriography, and Ultrasonography in Preoperative Diagnosis of Choledochal Cyst

CHALIW PIYACHON,¹ MAKUMKRONG POSHYACHINDA,¹ AND VISIT DHITAVAT²

A case of choledochal cyst in a 32-year-old female is reported. Information obtained from liver scintigraphy, angiography, and B-mode ultrasonography correlated well and resulted in a correct preoperative diagnosis.

Choledochal cyst, a rare congenital cystic dilatation of the common bile duct, occurs four times as frequently in females as males [1]. Symptoms include a palpable right upper quadrant mass, jaundice, and abdominal pain. The jaundice is usually intermittent and coincides with common bile duct obstruction which leads to enlargement of the mass. In some cases, the choledochal cyst opacifies during oral cholecystography or intravenous cholangiography, and

preoperative diagnosis can be made [1, 2]. Recent reports have indicated the diagnostic value of ¹³¹I rose bengal liver scintigraphy [2, 3], selective celiac arteriography [4], and ultrasonography [5] in the condition. This communication describes a case of choledochal cyst diagnosed on the basis of complementary information obtained from these three studies.

Case Report

A 32-year-old Thai female was hospitalized because of jaundice, abdominal pain, fever, and a mass in the upper abdomen which she had noted for the past 20 days. Past history consisted of a few

Received February 11, 1976; accepted March 24, 1976.

This work was supported in part by a research grant from the China Medical Board.

¹ Department of Radiology, Faculty of Medicine, Chulalongkorn University and Chulalongkorn Hospital, Bangkok, Thailand.

² Department of Surgery, Faculty of Medicine, Chulalongkorn University and Chulalongkorn Hospital, Bangkok, Thailand.

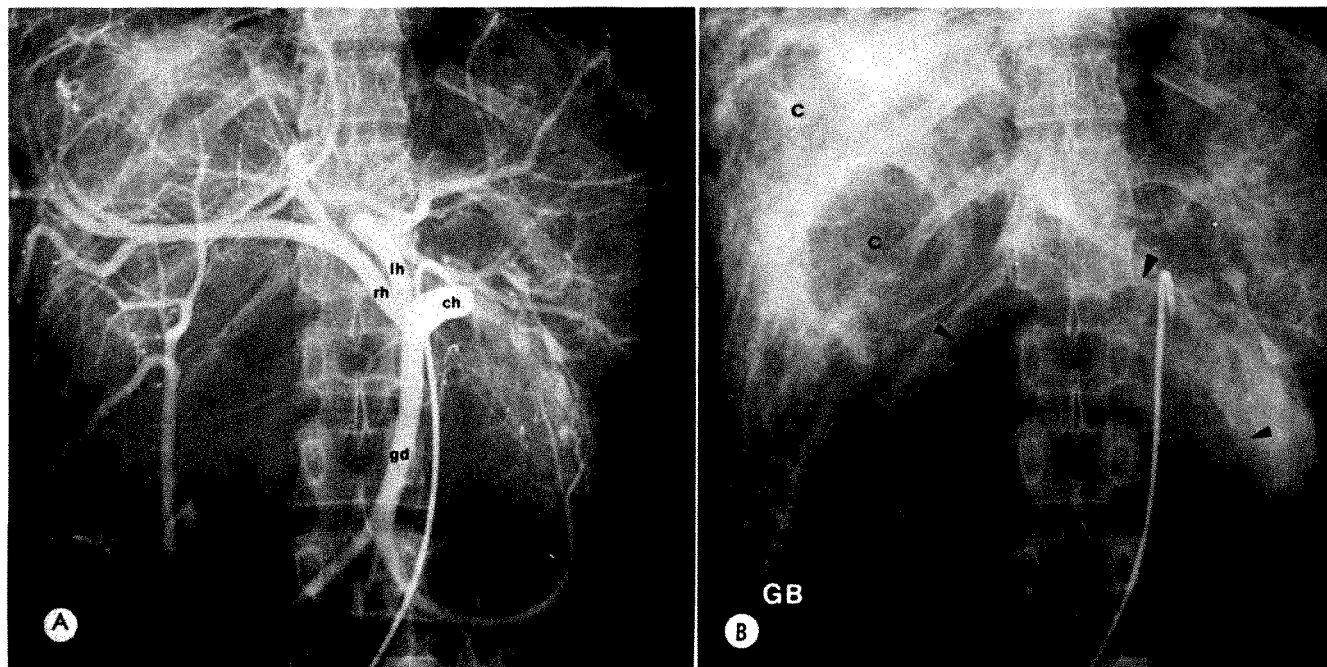


Fig. 1.—Selective hepatic arteriogram. *A*, Arterial phase showing stretching, elongation, and anterior displacement of common hepatic (ch) and gastroduodenal (gd) arteries. Stretching and elevation of right hepatic artery (rh) is also noted. Right and left hepatic branches are draping around space-occupying lesions. ah = accessory hepatic artery; ca = cystic artery. *B*, Parenchymal phase showing multiple lucencies (c) in liver. Large cystic lesion in mid upper abdomen (arrows) is well demonstrated. GB = gallbladder.

episodes of epigastric distress and a sense of fullness. Physical examination revealed a large firm mass in the midportion of the upper abdomen. The liver was slightly enlarged. During her hospital stay the mass was reduced in size and jaundice gradually decreased. Total bilirubin and direct bilirubin were reduced from 20.8 to 2.6 and from 9.4 to 1.5 mg/100 ml, respectively.

Upper gastrointestinal study showed an extrinsic pressure effect on the body of the stomach with displacement to the left and caudad. Barium enema examination demonstrated depression of the hepatic flexure and proximal transverse colon. Liver scintigraphy with colloidal ^{198}Au showed marked enlargement of the liver with a large space-occupying lesion in the anteromedial aspect of the right lobe and another smaller defect in the left lobe. The suspected diagnosis at this stage was malignancy of the pancreas or common bile duct with liver metastasis.

Abdominal aortography and celiac, superior mesenteric, and selective hepatic arteriography showed the mass to be cystic, with anterior displacement, stretching, and elongation of the common hepatic and gastroduodenal arteries. The right hepatic artery was elevated and stretched. The right and left hepatic branches showed a draping effect around the space-occupying lesions in the liver. The cystic artery was a branch of the accessory hepatic artery originating from the gastroduodenal arteries (fig. 1*A*). The parenchymal phase showed multiple lucencies in the liver. A large cyst was noted in the mid upper abdomen, partly outlined by the opacified stomach wall (fig. 1*B*).

Transverse ultrasonic B-mode scanning demonstrated a large cystic lesion extending across the upper abdomen with multiple cystic lesions in the liver. Sagittal ultrasonic B-mode scanning revealed similar findings (fig. 2). Liver scintigraphy with ^{131}I rose bengal showed prompt uptake and good outlining of the liver. A large defect at the junction of the right and left lobes was noted, with multiple small defects in both lobes (fig. 3*A*). Delayed scintigraphy at 24 hr demonstrated accumulation of radioactivity in the area of the previously noted defect (fig. 3*B*).

These findings led to a definite diagnosis of choledochal cyst. At laparotomy, a cystic dilatation of the common bile duct was found, approximately 15 x 20 cm in size, with numerous sand stones impacted in the common hepatic duct. The gallbladder was not dilated. Evacuation of stones and choledochocystojejunostomy (Roux-en-Y) were performed. The patient had an uneventful post-operative course.

Discussion

The diagnosis of choledochal cyst is suggested by clinical data and roentgenologic evidence of displacement of the duodenum and stomach by the cystic mass. A definite pre-operative diagnosis depends upon opacification of the cyst by intravenous cholangiography or oral cholecystography. However, this cannot be always accomplished when jaundice is present. Liver scintigraphy using radioactive rose bengal has proved to be an effective diagnostic tool even when jaundice is severe [3].

Angiographic findings associated with choledochal cyst have been described [4]. The findings in our case are similar but more severe, namely, marked anterior displacement and stretching of the gastroduodenal artery and elevation and stretching of the right hepatic artery. There was no angiographic evidence of malignancy, and the gallbladder was of normal size. Due to marked dilatation of the hepatic ducts secondary to impacted stones, the displacement of hepatic arterial branches and lucencies in the parenchymal phase were markedly prominent.

Findings on B-mode ultrasonography correlated very well with angiographic findings in demonstration of the cyst and dilated hepatic ducts. We believe that demonstration of a sonolucent mass in the epigastrium with small

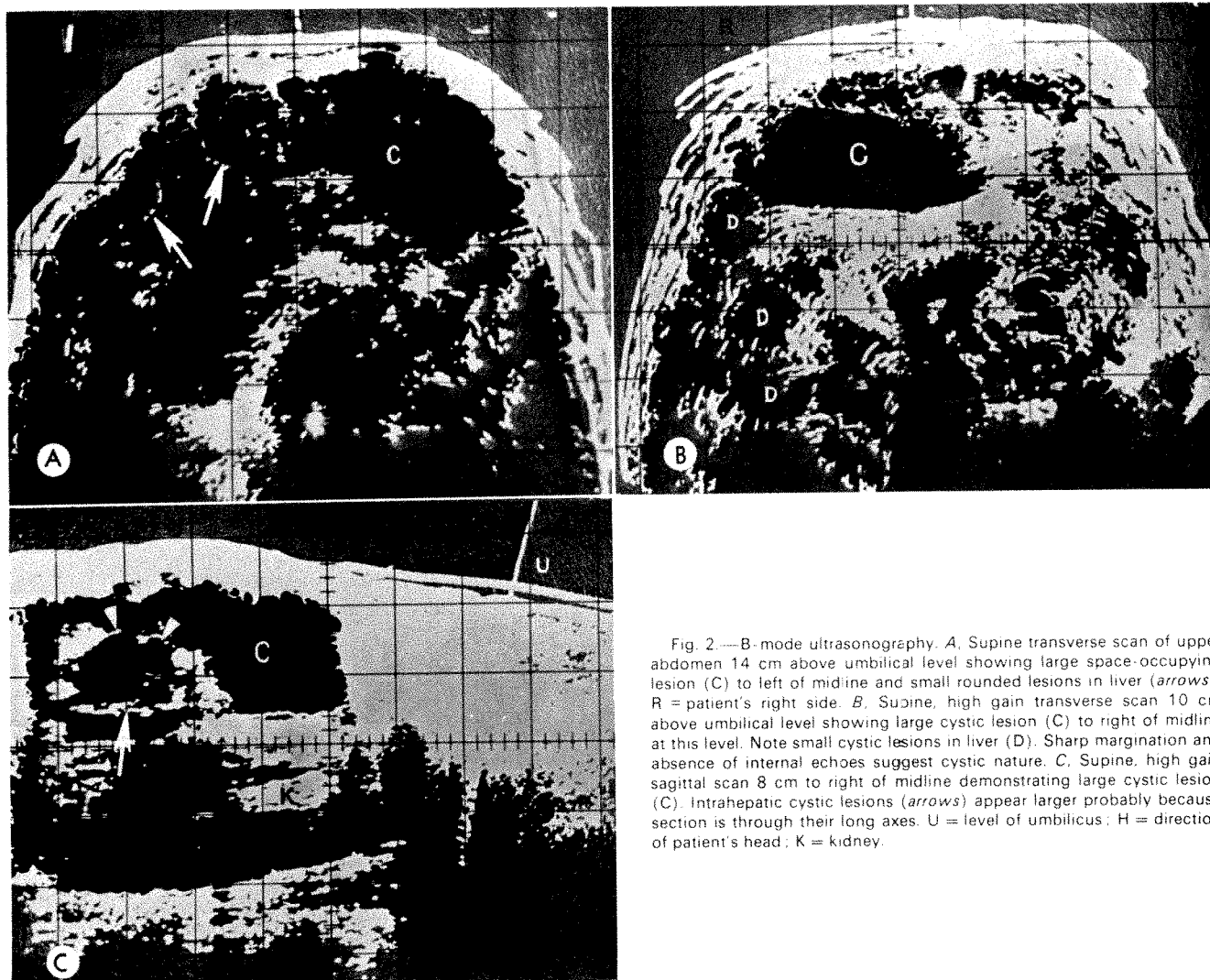


Fig. 2.—B-mode ultrasonography. *A*, Supine transverse scan of upper abdomen 14 cm above umbilical level showing large space-occupying lesion (C) to left of midline and small rounded lesions in liver (arrows). R = patient's right side. *B*, Supine, high gain transverse scan 10 cm above umbilical level showing large cystic lesion (C) to right of midline at this level. Note small cystic lesions in liver (D). Sharp margination and absence of internal echoes suggest cystic nature. *C*, Supine, high gain sagittal scan 8 cm to right of midline demonstrating large cystic lesion (C). Intrahepatic cystic lesions (arrows) appear larger probably because section is through their long axes. U = level of umbilicus; H = direction of patient's head; K = kidney.

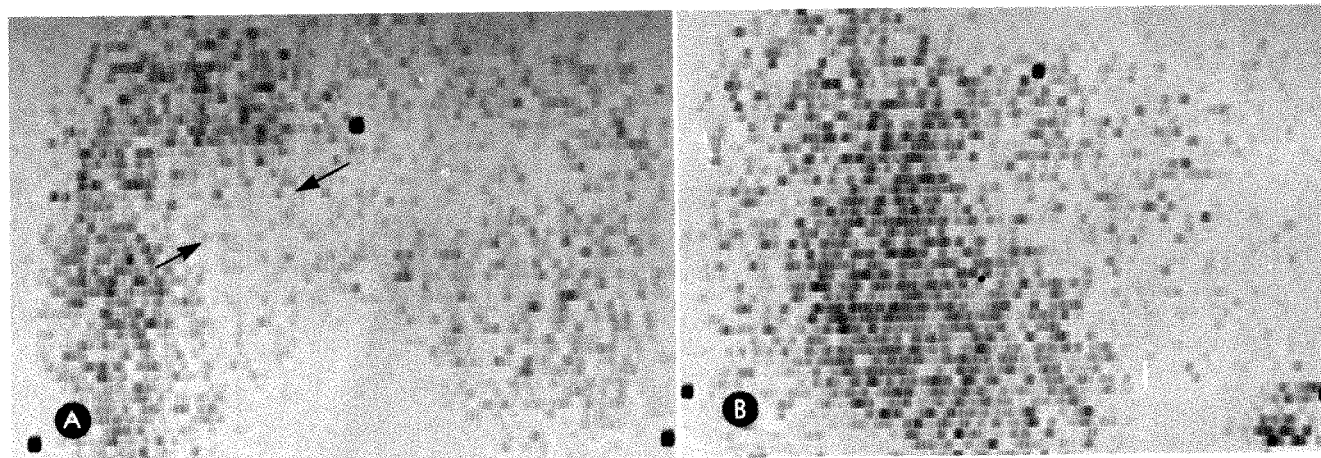


Fig. 3.—Liver scintigraphy with ^{131}I rose bengal. *A*, Immediate scintigram revealing large defect at junction of right and left lobes. *B*, Scintigram at 24 hr showing accumulation of radioactivity in area of previously noted defect, indicative of bile-containing structure.

cystic lesions in the liver is suggestive of the diagnosis. Cystic lesions generally show no internal echoes at a high sensitivity setting and show strong posterior margins [6]. Accumulation of radioactivity in delayed scintigram with the use of ^{131}I rose bengal indicated that the lesion was a bile-containing structure.

Liver scintigraphy with the use of ^{131}I rose bengal, angiography, and B-mode ultrasonography each contribute to the diagnosis of choledochal cyst. Complementary information from these studies is undoubtedly very helpful in arriving at the correct preoperative diagnosis.

REFERENCES

1. Silberman EL, Glassner TS: Roentgen features of congenital cystic dilation of common bile duct: report of two cases. *Radiology* 82:470-475, 1964
2. Williams LE, Fisher JH, Countney RA, Darling DB: Preoperative diagnosis of choledochal cyst by hepatoscintigraphy. *N Engl J Med* 283:85-86, 1970
3. Tada S, Yasukochi H, Shida H, Motegi F, Fukuda A: Choledochal cyst demonstrated by ^{131}I rose bengal scanning: report of a case. *Am J Roentgenol* 116:587-589, 1972
4. Jacobs RP, Palubinskas AJ: Angiographic findings of choledochal cyst. *Br J Radiol* 48:51-52, 1975
5. Gilday DL, Brown R, MacPherson RT: Choledochal cyst, a case diagnosed by radiographic and ultrasonic collaboration. *J Can Assoc Radiol* 20:25-29, 1969
6. Ostrum B, Goldberg B, Isard H: A-mode ultrasound differentiation of soft tissue masses. *Radiology* 88:745-749, 1967

Arachnoid Granulations Simulating Osteolytic Lesions of the Calvarium

RICHARD BRANAN¹ AND CHARLES B. WILSON¹

A case of arachnoid granulations, presenting as circumscribed radiolucent "punched out" lesions located far from the midline, is discussed in relation to radiographically similar processes causing bony defects in the calvaria.

While most benign calvarial markings have characteristic

features that permit their identification and differentiation from pathological conditions, variations present diagnostic problems. The location and position of calvarial defects and the extent to which each table is involved are useful diagnostic criteria, but in some instances either observation or pathological examination is required for confirmation.

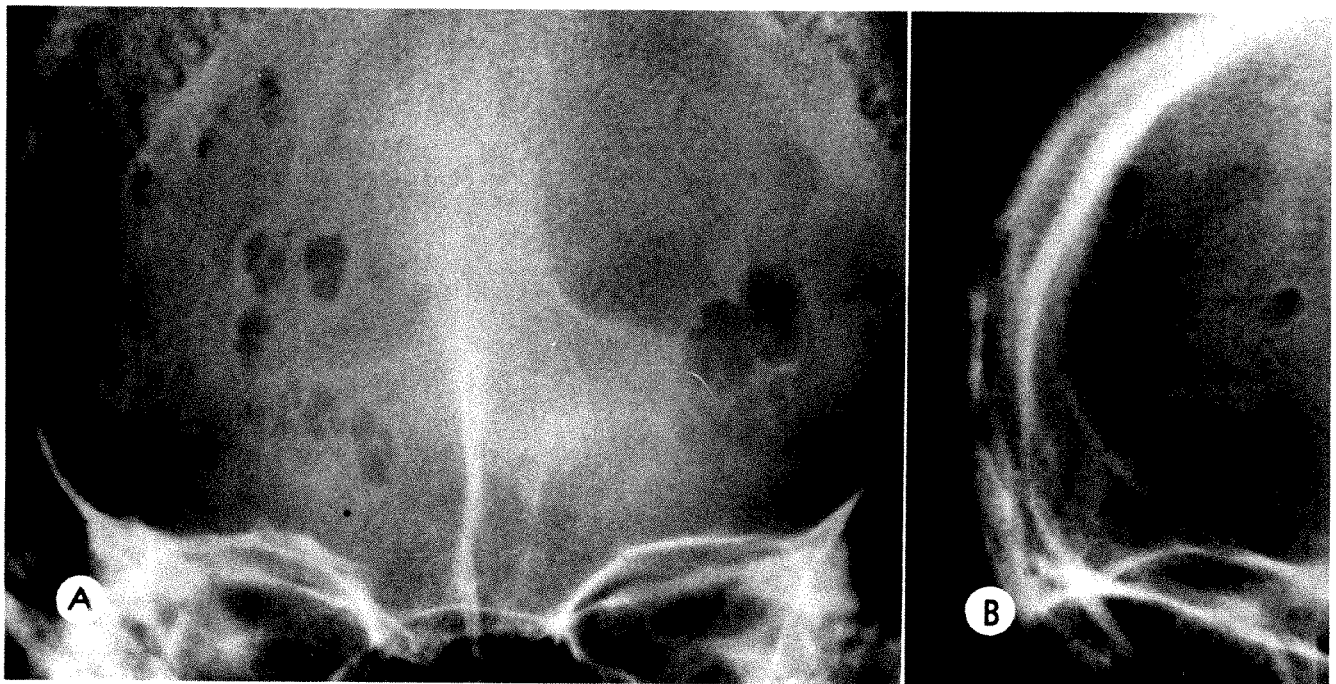


Fig. 1.—AP (A) and left lateral (B) view of skull lesion.

Received March 17, 1976; accepted after revision May 4, 1976.

This work was supported in part by NINDS training grant no. 05593 (R. Branán).

¹ Department of Neurological Surgery, University of California School of Medicine, San Francisco, California 94143. Address reprint requests to C. B. Wilson.

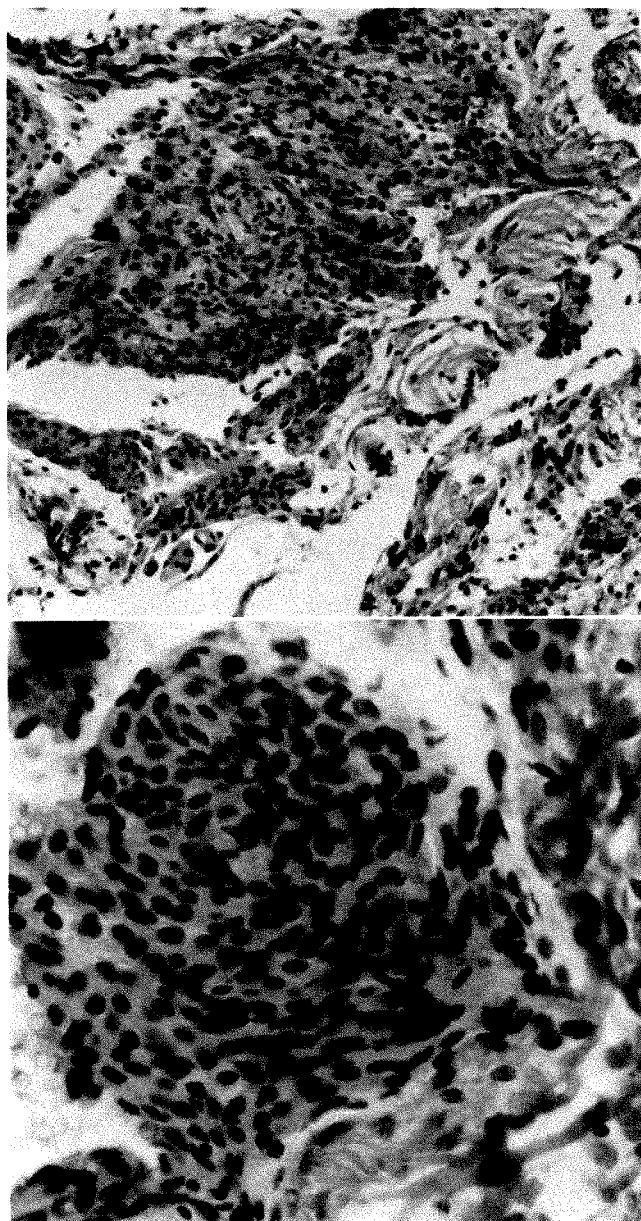


Fig. 2.—Photomicrographs of excised specimen.

Ordinarily the erosions caused by arachnoid granulations are easily differentiated from other markings by virtue of their parasagittal location. At a distance from the midline, they cannot be identified with certainty, particularly if asymmetrical.

The case described presented with multiple frontal defects and an abnormal brain scan. An exceptionally large ectopic arachnoid granulation was found during surgical exploration.

Case Report

The patient, an 18-year-old male, experienced sudden partial loss of vision in March 1973 while riding a motorbike. This progressed rapidly to a right homonymous hemianopsia, followed by severe left occipital headache. The patient also complained of increasing numbness and weakness of the right side of arm, face, and

tongue, with associated slurred speech. His symptoms cleared in 2–3 hr, although his slightly blurred vision and a mild occipital headache persisted and were exacerbated by rapid head movement. He experienced no dizziness, nausea, vomiting, or fever. Past medical history was noncontributory except for a 10 year history of tension-type headache that occurred after heavy exertion. The clinical diagnosis was probable migraine, but a vascular malformation could not be excluded on clinical grounds.

On admission, neurological examination was normal. Skull x-rays disclosed bilateral multiple lytic defects in the frontal region (fig. 1). Brain scan showed increased activity in the left anterior calvarium at the site of the lytic defects. Cerebral angiograms were normal.

On March 30, 1973, the largest lesion was explored; it was approximately 1.5 cm in diameter and located in line with the pupil and midway between the supraorbital rim and hairline. The dark bone over the lesion was immediately identifiable. The thin roof (less than 1 mm thick) was entered to expose underlying tissue that was white and granular. Considerable bleeding was encountered during removal of the specimen.

Microscopic examination revealed fragments of connective tissue continuous with aggregates of typically round to polygonal meningotheelial cells (fig. 2). The clusters of meningotheelial cells were more cellular than normal arachnoid granulations and were interpreted as reactive proliferations. No eosinophilic cells were identified. The clusters were considered to represent arachnoid granulations (S. L. Nielsen, personal communication).

Discussion

Bone erosion and osteolytic activity produce nonspecific markings common to several disease entities and also resemble the markings normally found on the skull. The described case of arachnoid granulations, located far from midline, illustrates the difficulty sometimes encountered in making a precise radiographic diagnosis. Systemic disease and infectious processes can also appear as "punched out" lesions of the calvaria. Malignant processes cannot always be distinguished from benign conditions, and when a definitive diagnosis is in doubt, the lesion should be studied further or explored for pathologic diagnosis.

In addition to arachnoid granulations, a number of normal variants are seen as "punched out" lesions. These include diploic veins and parietal foramina [1, 2]. Developmental abnormalities such as parietal thinning [3], cleidocranial dysostosis, and defects or openings in the calvaria associated with meningocele or encephalocele [4] may also have this appearance. Iatrogenic circumscribed radiolucencies such as burr holes, trephine openings, and craniectomy defects are well known. Lytic lesions of osteomyelitis due to syphilis, yaws, fungal or pyogenic tuberculosis, or other granulomatous infections may be encountered [5]. The histiocytosis group, consisting of Letterer-Siwe disease, xanthoma disseminatum, eosinophilic granuloma, and Hand-Schuller-Christian disease, should be considered.

Radiation necrosis of the skull usually presents as numerous radiolucent "punched out" areas. Tumors of the skull, such as solitary or multiple myeloma, are seen as destructive "punched out" lesions of various sizes, with little evidence of bone regeneration around their peripheries. Conditions beneath the calvaria such as leptomeningeal

cyst, intracerebral cyst, ventricular diverticulum, and tumors of the superficial surface of the brain or dura may cause a circumscribed radiolucent defect in the inner table.

REFERENCES

1. Pendergrass EP, Pepper OHP: Observations on the process of ossification in the formation of persistent enlarged parietal foramina. *Am J Roentgenol* 41:343-346, 1939
2. Pepper OHP, Pendergrass EP: Hereditary occurrence of enlarged parietal foramina; their diagnostic importance. *Am J Roentgenol* 35:1-8, 1936
3. Goldsmith WM: The Catlin mark: the inheritance of an unusual opening in the parietal bones. *J Hered* 13:69-71, 1922
4. McLaurin RL: Parietal cephaloceles. *Neurology* 14:764-772, 1964
5. Rumbaugh CL, Bergeron RT: Infections involving the skull, in *Radiology of the Skull and Brain*. Vol 1: *The Skull*, edited by Newton TH, Potts DG, St. Louis, Mosby, 1971, pp. 721, 735

Unilateral Dysplasia of the Superior Articular Facet of the Axis

R. SALAMA¹ AND S. L. WEISSMAN¹

A case of unilateral dysplasia of the superior articular facet of the axis due to incomplete or delayed ossification is described in a child. This may result in asymmetry of the articular surfaces of the axis in adult life and be a cause of torticollis. To our knowledge, no similar case has been reported.

The upper cervical spine in children may show special features due to incomplete ossification of the atlas and axis, the presence of a secondary ossification center in the dens, and hypermobility due to laxity of the joints. This report describes a case of delayed or incomplete ossification of the axis in a child causing unilateral dysplasia of the supe-

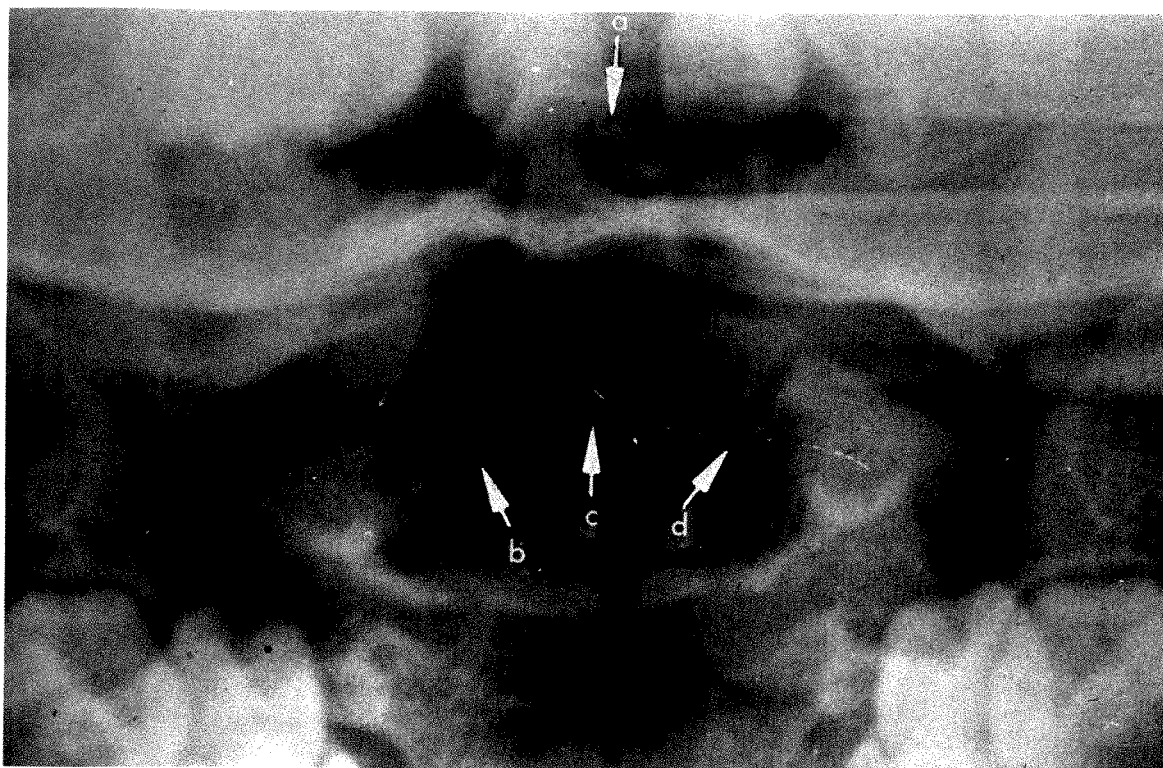


Fig. 1.—Anteroposterior radiograph at C2 level. *a*, Absence of fusion of ossification centers of dens. *b*, Dysplasia of superior articular facet of axis on right side due to incomplete ossification of base of dens and anterior part of center of ossification of neural arch. *c*, Junction of base of dens with ossification center of neural arch on left side continuous with subdentate synchondrosis. "Base of dens" participates in buildup of medial part of articular facet. *d*, Cleft at proximal end of dens with center for tip of dens (ossiculum terminale).

Received January 12, 1976; accepted after revision April 27, 1976.

¹ Department of Orthopaedics and Traumatology, Ichilov Hospital, and Faculty of Medicine, Tel-Aviv University, Tel-Aviv, Israel.

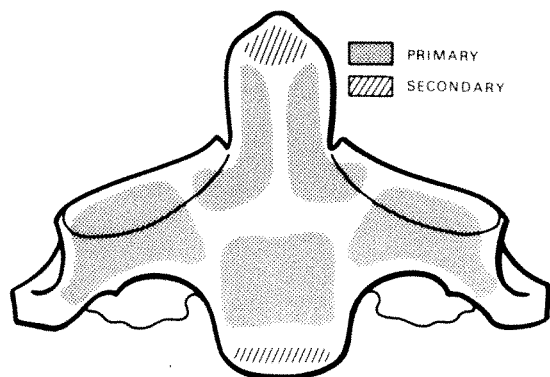


Fig. 2.—Ossification centers of axis.

rior articular facet of the axis which presented as spontaneous torticollis.

Case Report

B. G., a 3½-year-old girl, had pain and stiffness of the neck but no history of trauma. She was referred to the hospital for consultation. Apart from painful limitation of movements of the cervical spine, no other systemic or local clinical findings were noted on examination. Radiographs showed incomplete ossification of the base of the dens and the neural arch on the right side, resulting in unilateral dysplasia of the superior articular facet of the axis (fig. 1, *b*). There was also delayed fusion of the ossification centers of the dens (fig. 1, *a*). Within a week after treatment with a soft collar brace and analgesics, she recovered fully. No other abnormalities were detected on follow-up examinations, and no instability was seen with lateral bending.

Discussion

Ossification of the axis proceeds from seven separate ossification centers [1] (fig. 2). Five are primary centers: one for the centrum, two for the dens, and two for the neural arch. One additional center is for the tip of the odontoid and the other for a thin epiphyseal plate on the undersurface of the body.

Ossification of the dens starts at its base [2]. By the end of the second year, ossification of the neural arch is usually completed [2]. In the present case, unilateral delayed or absent ossification of the "base of the dens" [2], which normally participates in the buildup of the medial parts of the articular facets of the axis (fig. 1, *c*), occurred. This, together with incomplete ossification of the anterior part of the center for the neural arch, resulted in dysplasia of the superior articular facet of the axis on the right side. This dysplasia, which is not necessarily related to child's symptoms, may eventually be the cause of unilateral depression of the superior articular surface of the axis which, although rare, has been described in adults as a cause of torticollis [3]. To our knowledge, this is the first reported case in a child.

The two centers of ossification of the dens fuse at the time of birth. Delay of fusion is anomalous [2] but not rare [3] (fig. 1, *a*).

REFERENCES

1. Johnson TB, Whillis J (eds.): *Gray's Anatomy*, 29th ed. London, Longmans, Green and Co., 1947
2. von Torklus D, Gehle W: *The Upper Cervical Spine*. London, Butterworths, 1972
3. Köhler A, Zimmer EA: *Borderline of the Normal and Early Pathological in Skeletal Roentgenology*, 3d ed. New York, Grune & Stratton, 1968

Arteriographic Findings in Hyperergic Granulomatosis and Vasculitis of a Kidney

GRIGORIOS P. POULIADIS,¹ JOSEF WELLAUER,¹ ROLF STREULI,²
ADRIANO FONTANA,² AND JAKOB BRINER³

A case with a probable diagnosis of a limited form of Wegener's granulomatosis is presented. Arteriography of an involved kidney revealed arterial occlusions and stenoses with infarcted parenchymal regions and a distinct collateral circulation. Compared to the renal changes in other collagenous diseases, the renovasographic findings in this case were more prominent, more centrally located, and of segmental distribution.

Wegener's granulomatosis is a disease characterized by necrotizing granulomatous lesions, generalized angiitis, and glomerulonephritis. Since Klinger's [1] and later Wegener's [2] descriptions, many reports have been published describing more or less similar syndromes [3–6]. Carrington and Liebow [7] reported 16 cases of so-called limited forms of Wegener's granulomatosis with angiitis and granu-

Received December 23, 1975; accepted after revision March 22, 1976.

¹ Department of Radiology, Kantonsspital, University of Zurich, 8091 Zurich, Switzerland. Address reprint requests to G. P. Pouliadis.

² Department of Internal Medicine, Kantonsspital, University of Zurich, 8091 Zurich, Switzerland.

³ Department of Pathology, Kantonsspital, University of Zurich, 8091 Zurich, Switzerland.

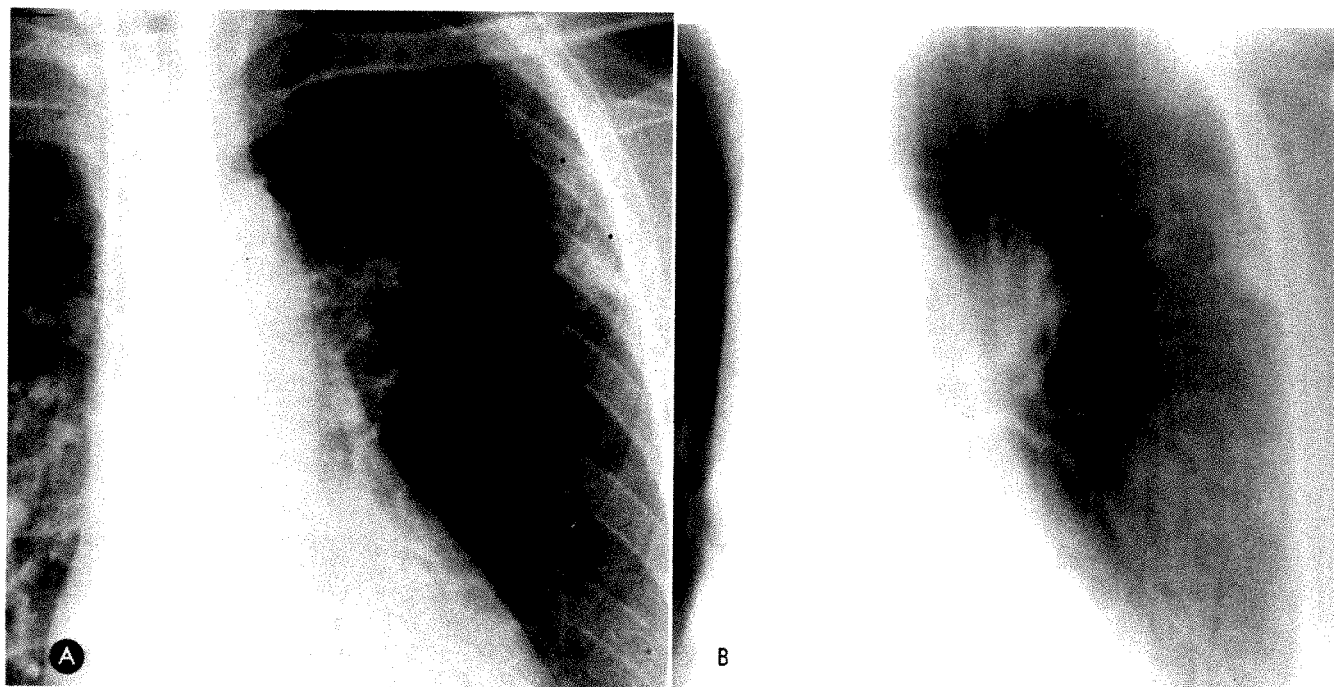


Fig. 1.—A, Posteroanterior film of chest showing left parahilar opacity and peripheral opacity in left upper lung field. No tuberculous scars or calcifications seen. B, Tomogram. Parahilar opacity more likely represents parenchymal consolidation than enlarged lymph node. No cavitation is present.

lomatous lesions but no glomerulitis.

We recently performed a nephroangiography in a case that seemed to be a limited form of angiitis and granulomatosis of Wegener's type. To our knowledge, no reports exist on nephroangiography in this disease.

Case Report

M. I., a 39-year-old white woman, was admitted to our hospital because of diffuse anterior chest and left scapular region pain. She also complained of a slight nonproductive cough, night fever, and loss of 19 kg over the previous year. There was a history of hepatitis, hyperuricemia, and cholelithiasis. On physical examination, the woman was thin and pale but had no abnormality of the lungs or other organs. Her blood pressure was 130/100 mm Hg; pulse rate was 80/min.

Laboratory studies revealed a sedimentation rate of 53 mm in the first hour, a hemoglobin of 11.4 g/100 ml, and a leukocyte count of 7,200 with normal distribution. Serum protein was 8.9 g/100 ml with a hypergammaglobulinemia of 27.1% in the electrophoresis. Serum iron was 65 μ g/100 ml and the total iron binding capacity of the serum was 426 μ g/100 ml.

Uric acid was 4.8 mg/100 ml. The L.E. cell phenomenon and the serologic tests for syphilis were negative. The blood urea nitrogen, creatinine, potassium, calcium, thromboplastin time, alkaline phosphatase, SGOT, and SGPT were all within normal limits.

There was no trace of protein in the urine, but 0–1 leukocytes, and 0–2 fresh erythrocytes were found per high power field. The bone marrow revealed iron-deficiency anemia. No acid-fast stabs could be found in the gastric contents, sputum, bronchial washings, or urine. No malignant cells were found in the sputum or bronchial washings.

A chest x-ray and a subsequent tomographic examination (fig. 1) revealed a poorly defined opacity of homogeneous density in the left parahilar region and a parenchymal consolidation in the periph-

ery of the left upper lung field. No cavitation or calcification was present. Radiologic findings suggested pulmonary tuberculosis or a bronchogenic carcinoma.

The upper and middle calyces of the left kidney were not visualized on the excretory urogram (fig. 2A). Only the lower calyx and part of the pelvis were opacified. There were no calcifications. The kidney was of normal size and had a smooth contour. The right kidney was normal.

A left retrograde pyelogram (fig. 2B) demonstrated obliteration of the upper and middle calyces and an irregular contour of the pelvis. Again the roentgenologic impression was ambivalent; both tuberculosis and malignancy were considered as the most likely diagnoses.

A selective left renal arteriogram (fig. 3) demonstrated irregular stenoses, attenuation, and amputations of the interlobar and arcuate arteries in the middle and lower segments of the kidney. The nephrogram of these areas, distinctly diminished and uneven, suggested infarcts. The clearing of contrast medium from the smaller arteries of these areas was slightly delayed (3 sec). In the region of the renal sinus there were newly formed tortuous vessels, probably representing collateral circulation within the sinus secondary to arterial occlusions and stenoses. The upper pole vessels demonstrated some stretching but were otherwise normal. The renal vein was patent. The roentgenologic diagnosis was transitional cell carcinoma of the renal pelvis. Malignant lymphoma and metastasis were also considered in the differential diagnosis. A left nephrectomy was performed.

Pathologic examination of the specimen (no. 13721/75) revealed a hyperergic granulomatosis and vasculitis (fig. 4). The vasculitis was most prominent in the larger arteries and veins, while the granulomatosis was largely peripelvic. There was no glomerulitis.

The blood pressure after nephrectomy was 210/115 mm Hg. In addition to a primary hypertension, renal hypertension caused by a similar but less prominent process in the right kidney must be con-

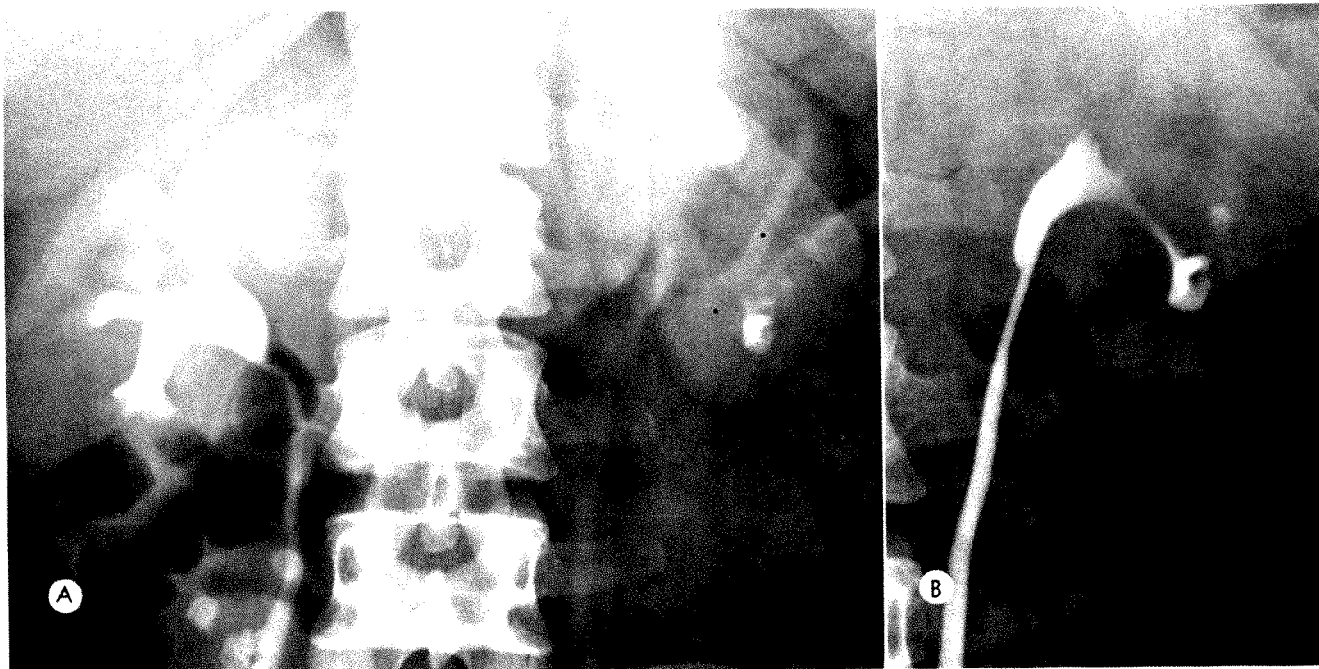


Fig. 2.—A, Intravenous pyelogram (20 min film with compression) showing no opacification of left upper and middle calyces. Left kidney has otherwise normal appearance; normal right kidney. B, Retrograde pyelogram of left kidney showing amputation of upper and middle calyces and irregularity of pelvic contour.

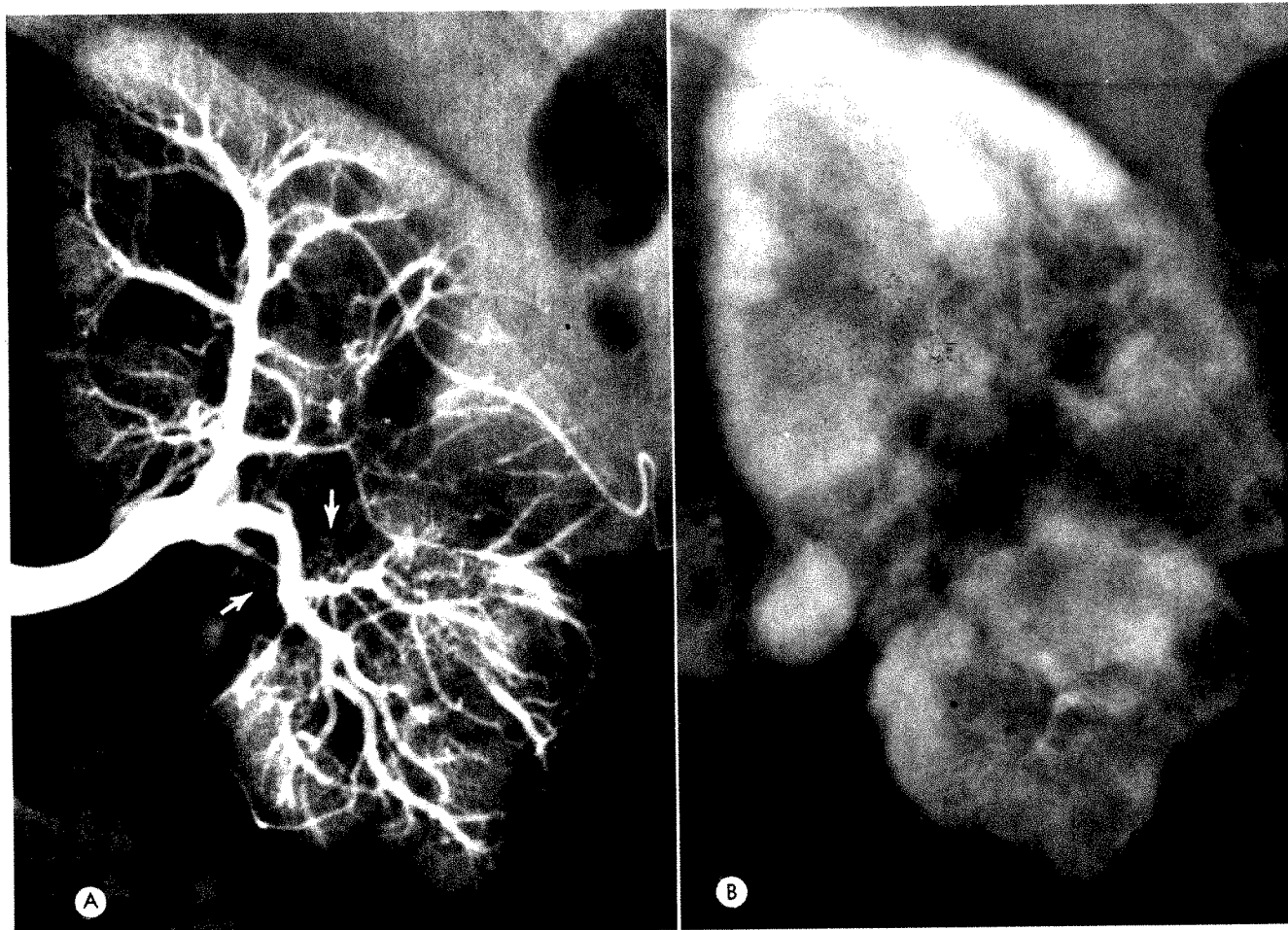


Fig. 3.—Left renal arteriography. A, Late arterial phase showing irregular stenoses with amputations of interlobar and arcuate arteries. Collateral circulation (arrows). Upper pole vessels slightly stretched but otherwise normal. B, Late nephrographic phase showing uneven parenchymal opacification in middle and lower segments with irregular contour; opacified renal vein.

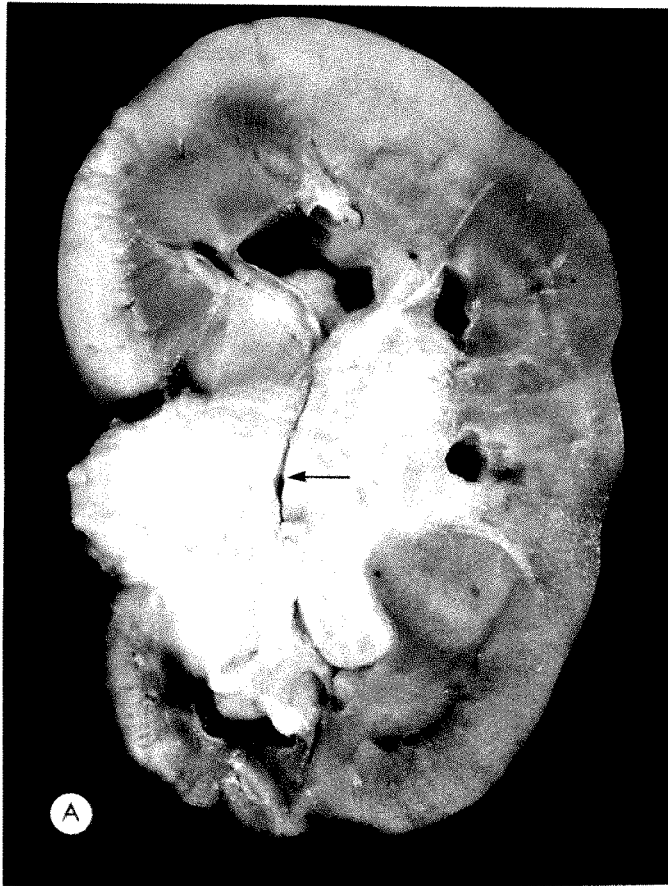
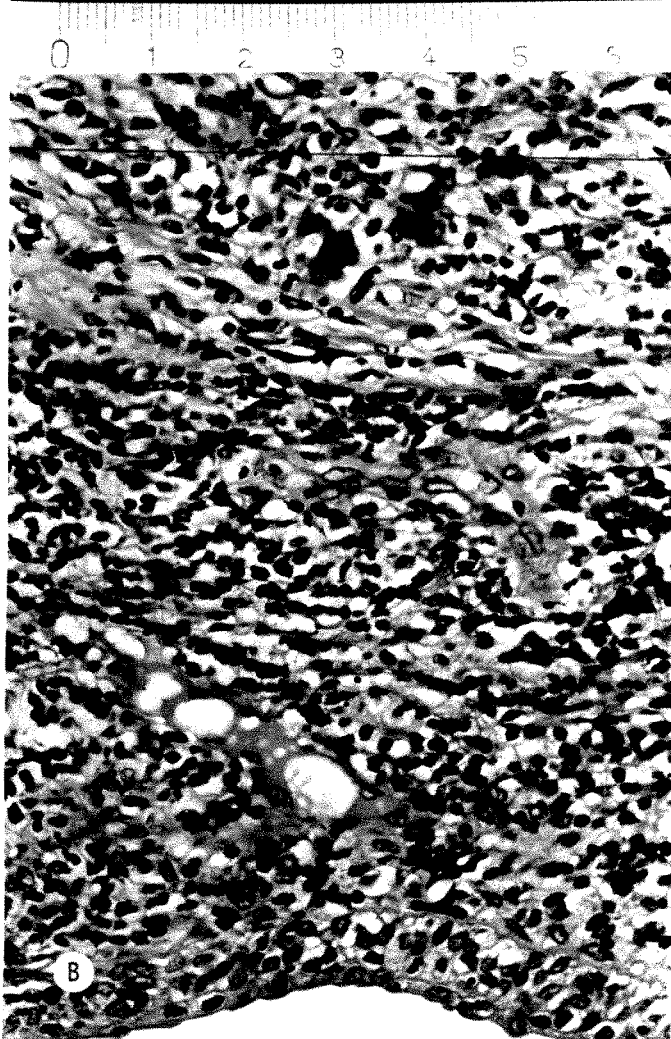


Fig. 4.—A, Gross appearance of sectioned kidney showing granulomatous tissue occupying central portion of pelvis and extending into peripelvic tissue. Renal pelvis reduced to narrow channel (*arrow*). B, Renal granulomatous lesion. In outer region of granuloma (*top*) multinucleated giant cells seen. Granuloma extends beneath epithelium of renal pelvis. H and E, $\times 400$. C, Interlobar artery with almost complete obliteration of lumen by granulomatous tissue. Cellular infiltration of all three layers of vessel. H and E, $\times 40$.



sidered. Unfortunately, no arteriogram of the right kidney was obtained.

A chest x-ray (1 month later) showed no change. A lung biopsy performed under fluoroscopy with a fine needle showed no evidence of malignancy. The diagnosis of tuberculosis or a mycotic infection of the lung is not supported by the available clinical and laboratory data. It seems most likely that the lung pathology is similar, if not identical, to that of the extirpated kidney. The final diagnosis of a limited form of Wegener's granulomatosis seems reasonable.

Discussion

Renovasographic examinations in collagenous disease are relatively sparse. In a case of Wegener's disease reported by Ekelund and Lindholm [8], there was normal renal function and normal renal angiography. In systemic lupus erythematosus there is impaired filling of cortical vessels which are tortuous and attenuated, and the cortico-medullary junction is indistinct [4, 9]. In scleroderma the interlobar and arcuate arteries are irregularly narrowed and tortuous, the circulation time is prolonged, and there is a poor nephrogram [10]. In polyarteritis nodosa the vessels affected most frequently are the arcuate and interlobular arteries. They demonstrate irregularities and stenoses with abrupt terminations. The vascular alterations are distributed uniformly over the whole kidney and the resulting nephrogram is less intense, heterogeneous, and irregularly contoured. Microaneurysm formation is encountered quite often but is not specific for polyarteritis nodosa [9, 11-15].

In comparison, the arteriographic changes in our case are more prominent and centrally located, and there is a segmental distribution with parts of the kidney parenchyma normal. There is also distinct collateral circulation within the renal sinus that has not been described in any of the reported cases of collagenous disease.

The most striking difference between our findings and those in other collagenous diseases seems to be the segmental or focal distribution of the angiographic changes. In our opinion this does not represent simply an early stage of the disease because of the prominence of the alterations already present. The findings cannot be regarded as specific

since even in retrospect it is not possible to differentiate these vascular changes from those encountered in some malignant kidney tumors.

REFERENCES

1. Klinger H: Grenzformen der Periarteritis nodosa. *Frankfurt Z Pathol* 42:455-480, 1931
2. Wegener F: Über generalisierte, septische Gefässerkrankungen. *Verh Dtsch Ges Pathol* 29:202-210, 1936
3. Churg J, Strauss L: Allergic granulomatosis, allergic angiitis, and periarteritis nodosa. *Am J Pathol* 27:277-301, 1951
4. Fienberg R: Pathergic granulomatosis. *Am J Med* 19:829-831, 1955
5. Lansdown FS: Necrosing granuloma of the lung. *Am Rev Respir Dis* 84:422-430, 1961
6. Walton EW: Giant-cell granuloma of the respiratory tract. (Wegener's granulomatosis). *Br Med J* 2:265-270, 1958
7. Carrington CB, Liebow AA: Limited forms of angiitis and granulomatosis of Wegener's type. *Am J Med* 41:497-527, 1966
8. Ekelund L, Lindholm T: Angiography in collagenous disease of the kidney. *Acta Radiol [Diagn]* (Stockh) 15:413-422, 1974
9. Longstreth PL, Korobkin M, Palubinskas AJ: Renal microaneurysms in a patient with systemic lupus erythematosus. *Radiology* 113:65-66, 1974
10. Lester PD, Koehler PR: The renal angiographic changes in scleroderma. *Radiology* 99:517-521, 1971
11. Adamczyk W, Wachowiak A, Dzwonkowski J: Selective renal angiography in the diagnosis of periarteritis nodosa. *Pol Przegl Radiol* 34:644-669, 1970
12. Chudacek Z: Zum Roentgenbild der Periarteritis nodosa der Niere. *Fortschr Geb Roentgenstr Nuklearmed* 105:49-50, 1966
13. Efsen F, Lorenzen U: Nephroangiography in periarteritis nodosa. *Acta Radiol [Diagn]* (Stockh) 7:255-230, 1968
14. Fleming RJ, Stern LZ: Multiple intraparenchymal renal aneurysms in polyarteritis nodosa. *Radiology* 84:100-103, 1965
15. Robins JM, Bookstein JJ: Regressing aneurysms in periarteritis nodosa. *Radiology* 104:39-42, 1972

Interim Report:

Mammographic Exposures at the Breast Cancer Detection Demonstration Project Screening Centers

PETER WOOTTON¹

In the interests of uniformly high radiological physics standards at ACS-NCI Breast Cancer Detection Demonstration Projects, measurements were made at 29 breast cancer screening clinics. These measurements were made throughout the country with equipment calibrated with standards traceable to National Bureau of Standards. Histograms which indicate the frequency distribution of exposures to the surface of a 6 cm breast for various machine/receptor combinations were prepared.

Recently a number of cancer demonstration network projects have been activated by the American Cancer Society and the National Cancer Institute. The Breast Cancer Detection Demonstration Project is one of these. The NCI has also established six regional centers for radiological physics and a coordination program (M. L. Meurk, chm., AAPM Coordination Consultants) to ensure that the radiological physics contribution to the projects is of uniformly high quality.

There are 29 screening clinics participating in the breast cancer detection project. These screening centers use 60 x-ray machines of varied manufacture and employ diverse combinations of exposure parameters, geometry, anodes, filters, and image detectors in order to obtain images of satisfactory diagnostic quality. The six centers for radiological physics made measurements of mammographic radiation exposure on all machines in the 29 screening clinics. Measurements were made for the range of machine settings in clinical use following a measurement protocol developed by the six centers.

The measurements were made with ionization chambers uniquely suited to mammographic measurements. These chambers were specifically designed to have an energy-independent response to within $\pm 1\%$ for x-ray qualities used in mammography (0.3–1.5 mm Al, HVL). All the chambers used in these measurements were calibrated in a facility having standards traceable to the National Bureau of Standards. Each step of the protocol for the measurements was tested; the chambers were compared with one another on mammography equipment prior to measurements at the screening centers to ensure the use of uniform measurement methods throughout the country. The ion chamber measurements were supplemented by measurements using thermoluminescent dosimeters on lucite phantoms at the position of the surface of the breast. This technique is being used for periodic follow-up. "In vivo" measurements are also being offered.

The quality of the clinical beams was evaluated as follows: (1) kilovoltage potential was determined by means of calibrated modified Ardran-Crookes cassettes, and (2) first and second half-value layers were measured using high purity absorbers and the flat response detectors in a jig described in the measurement protocol.

Some qualitative measurements of resolution for structures of various sizes, configurations, and density have also been carried out. However, the optimum phantom for this purpose is still under test and development. The exposure values reported here are based on machine settings which yield images deemed acceptable by the radiologists of the center at which the measurements were made.

Histograms of the number of units employing exposures within an exposure interval versus the median value of that exposure interval expressed in roentgens are shown in figure 1. These histograms summarize the radiation exposure per image for a breast 6 cm thick. Various combinations of image receptors, target material, and filter material are shown.

These data are representative of exposures used up to June 1975. The use of exposures greater than 8 R with a nonscreen film (fig. 1C) has ceased. The center has changed image receptor to a rare-earth screen system and now employs an entirely different technique resulting in an exposure of less than 1 R. Some of the screening centers reported here as using exposures on the order of 6 R with Xerox as the image receptor (fig. 1B) have modified their filtration and technique resulting in exposures on the order of 2 R per image for a 6 cm breast.

A future report will include an analysis of measurements of kilovoltage potential, first and second half-value layers, filtration, exposure at 1 m, target-skin distance, equipment manufacturer, target material, and image receptor. Conclusions regarding correlation of exposure with different types of equipment should not be made until this analysis is available.

Radiologists using procedures which result in exposures above the median quoted in the appropriate histogram should review their techniques with an aim to reducing exposures to the median value or below. Factors that may result in larger exposures than the median are (1) inadequate filtration, (2) inappropriate kilovoltage for the detector used, and (3) less than optimal image processing. Comparisons of dial setting versus measured kilovoltage potential show enough variation that techniques trans-

Submitted on behalf of the regional centers for radiological physics from work conducted for the Division of Cancer Control and Rehabilitation under contracts NO1-CN-45057, NO1-CN-45148, NO1-CN-45152, NO1-CN-45158, NO1-CN-45160, and NO1-CN-45162.

¹ Northwest Center for Radiological Physics, Medical Radiation Physics, RC-08, University of Washington, Seattle, Washington 98195.

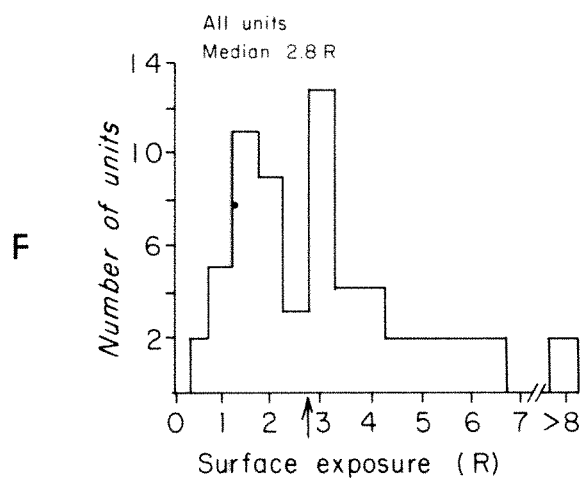
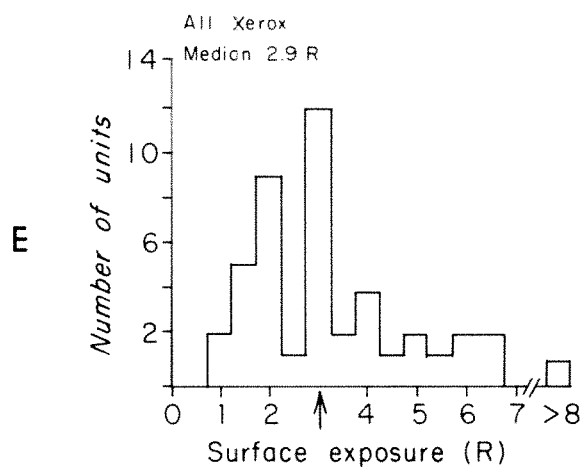
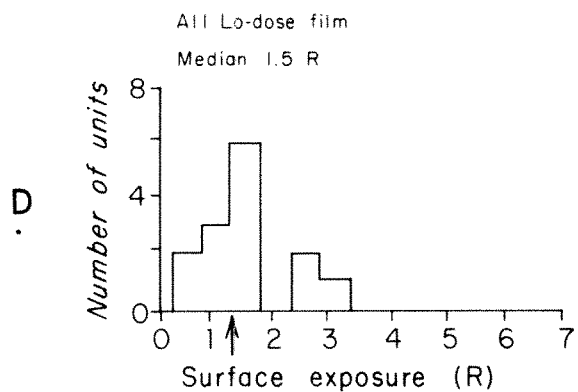
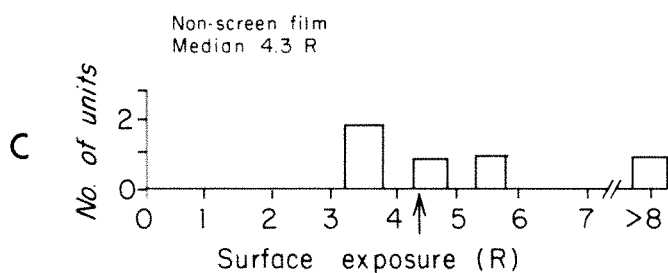
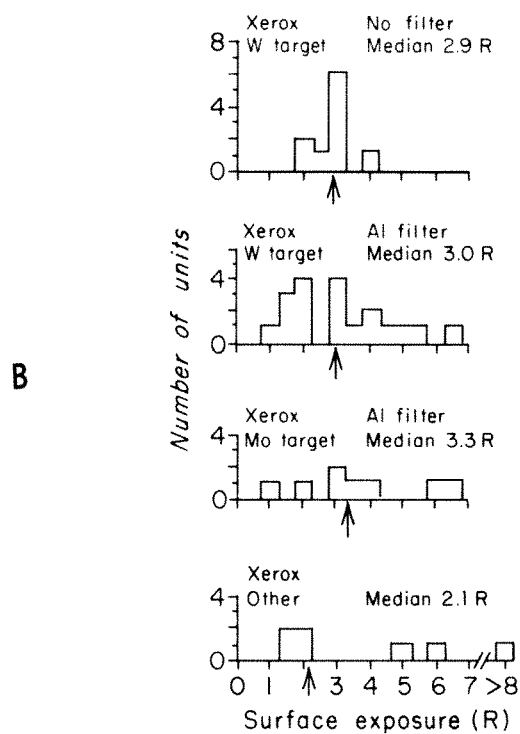
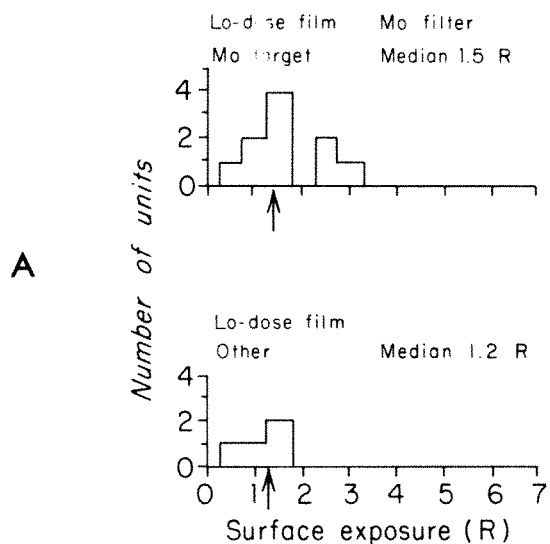


Fig. 1.—Histograms. Arrows indicate medians. •

ferred from one facility to another may not result in the same image quality or radiation exposure to the patient.

Requests for protocol and/or reprints should be directed to the nearest regional center for radiological physics or the coordination program office:

AAPM Coordination Program. L. M. Bates, Suite 307, 6900 Wisconsin Avenue, Chevy Chase, Maryland 20015.

Northeast Center for Radiological Physics. J. S. Laughlin, Memorial Sloan-Kettering Cancer Center, 1275 York Avenue, New York, New York 10021.

Midwest Center for Radiological Physics. P. N.

Shrivastava, Allegheny General Hospital, 320 East North Avenue, Pittsburgh, Pennsylvania 15121.

Midwest Center for Radiological Physics. J. R. Cameron, 1300 University Avenue, Madison, Wisconsin 53706.

Northwest Center for Radiological Physics. P. Wootton, Medical Radiation Physics, RC-08, University of Washington, Seattle, Washington 98195.

Southwest Center for Radiological Physics. W. Hendee, University of Colorado Medical Center, 4200 East Ninth Avenue, Denver, Colorado 80220.

Southern Center for Radiological Physics. R. J. Shalek, M. D. Anderson Hospital, Houston, Texas 77025.

Erratum

In the article "Computed Tomography of the Body: Initial Clinical Trial with the EMI prototype" by Sheedy et al. (127:23-51, 1976), legends and photographs were out of sequence for figures 21, 22, and 24-27. The legends and figures will be reprinted in the October issue.

AJR Bicentennial Issue

Single copies of the special AJR bicentennial issue, devoted entirely to computed tomography, may be ordered for \$3.00 each from Charles C Thomas, Publisher, 301-327 East Lawrence Avenue, Springfield, Illinois 62717. Please enclose payment with orders.

Editorial

Echocardiography: Territorial Imperative?

In August 1975, the Section of Cardiology of the American Academy of Pediatrics asserted in a letter to deans of medical schools that "echocardiography should be supervised, performed and interpreted by physicians skilled in total care of the child with heart disease"; that is, by pediatric cardiologists. In December 1975, the American College of Radiology dissented, in an answering letter to the deans. That letter can be paraphrased as follows: (1) the information used by a pediatric cardiologist does not have to be personally acquired by him; (2) expertise in the use of ultrasonics may be more important than the skills or knowledge of physiologic tests such as catheterization; (3) training programs in pediatric cardiology, in general, are not capable of in-depth training in the physics and instrumentation for ultrasound; and (4) the economics of expensive equipment and the scarcity of qualified technical staff require centralized diagnostic facilities for ultrasound. To a maverick pediatric cardiologist, three of these four arguments are compelling in their logic. The third argument is rapidly diminishing in strength, as instrumentation development makes the operation less complex. At any rate, knowledge of the physical basis for a technique in medicine is not a requirement for its competent application.

Robert Wise, speaking for the ACR, went on to note the contribution of many disciplines to the rapidly developing clinical applications of ultrasound, and urged that we not limit the performance of these procedures to any one specialty group. Rather, the best qualified in each institution should be designated to perform ultrasonic examinations. I find that more fair than the recommendations of my pediatric colleagues, although allowances must be made for new entries into the field. In fairness to the AAP report, it may be more an exhortation to pediatric cardiologists to acquire knowledge and skills in this field than a battle cry against internists and radiologists. It also may have been a generalized response to local experiences of aggression. There is evidence of a power struggle locally and nationally, with strong assertions from some radiologists that ultrasound is *their* territory, by a kind of "manifest destiny." I know of an individual with a master's degree and considerable experience in echocardiography who sought a position in several private hospitals. She was told repeatedly that she would have to go to a junior college to become a radiology technician before she could apply for a technical position in diagnostic ultrasound!

As to who should interpret echocardiography, a definition of the level of interpretation is needed. For the final synthesis of the pediatric patient's workup, the AAP's position, that this should be done by a pediatric cardiologist, seems eminently reasonable, since he will usually have the greatest

experience in congenital heart disease and have the best perspective of the entire spectrum for a given disorder. This perspective is an essential basis for subsequent diagnostic and therapeutic decisions. However, the initial interpretation of an echocardiographic study may reasonably be made by anyone expert in the functional anatomy of the heart, just as angiocardiographic interpretations have been made for many years by radiologists. It should be noted here that most pediatric cardiologists desire to review these angiograms and, on occasion, differ with their radiologic colleagues; particularly about the importance of findings. Not infrequently this duplication has substantial benefit to the patient and, in my opinion, should not be discouraged in the name of health care economics.

The same virtue cannot be found in the duplication of expensive equipment. There is a clear and present need to share the use and maintenance of diagnostic ultrasound equipment and technical staff. Centralization of ultrasonic facilities in radiology departments seems optimal, with access guaranteed to all qualified physicians. The success in avoiding duplication and territorial wars will, of course, depend upon the reasonableness and goodwill of the physicians involved. However, even an excellent central facility should not preclude an investigator from having a separate research laboratory, particularly if he is involved in the development of instrumentation such as sector scans or duplex instruments with transcutaneous Doppler flow and echo.

There is a final bit of heresy I would like to offer. Not only do I accept the idea that pediatric echocardiograms do not have to be performed by pediatric cardiologists, I do not believe that they have to be performed by physicians. Although the expert echocardiographer will undoubtedly wish to personally perform the ultrasonic examination in some or all of his studies, there should be no mandate requiring this. At our institution, most of the studies for both adults and children have been obtained by very talented and dedicated technicians with strong backgrounds in biology, who have learned and grown with this new field. It may be helpful to be present during at least part of the recording of the echo, but not essential, particularly if the key questions about a case have been specified when the study was requested. It is more efficient to let such experienced technicians perform the examination, saving the physician's time for the interpretation of data or for the more dangerous invasive procedures of cardiac catheterizations. The technician brings to his task input from several disciplines and often an intense personal interest in this rapidly evolving technology.

I feel there are strong grounds for centralization of a

facility for ultrasonic diagnosis, and it is reasonable to have echocardiograms performed by the "best qualified," although it would be unwise to exclude interested newcomers with a background in cardiac anatomy and function. The final clinical integration of the echocardiographic data for a child may rightly be the responsibility of a pediatric cardiologist, but the involvement of other specialties in acquiring and interpreting the clinical data seems as acceptable, and even desirable, as in the case of angiocardio-

graphic studies. The resulting cross-fertilization between pediatric and adult cardiology, radiology, and cardiovascular surgeons is and will be as important to echocardiography as I think it has been to angiocardiology, and to children with heart disease.

Warren G. Guntheroth
*Division of Pediatric Cardiology
University of Washington
Seattle, Washington 98195*

A. Justin Williams, 1901–1976

A. Justin Williams died in San Francisco on May 9, 1976, after a long battle with carcinoma of the bladder which he stubbornly fought, working up until a month before he died.

Williams was born July 1, 1901, in Denver, Colorado, the son of Harry and Jenny Williams. His father was a general practitioner. As a child, he went with his father on many house calls and early became imbued with the spirit of practicing medicine.

He received his A.B. degree from Denver University in 1923 and his M.D. from Colorado University Medical School in 1928. He interned at King County Hospital in Seattle in 1928–1929 and was a resident in radiology at the University of Michigan Hospital from 1930 to 1932 and at San Francisco County Hospital on the University of California service in 1932–1933. Following this, he entered practice with Lloyd Bryan (who was part of the team of Ruggles and Bryan in San Francisco for many years). He became a diplomate of the American Board of Radiology in 1935 and was a staff radiologist at a number of San Francisco hospitals, including Childrens, Mt. Zion, the old Dante Hospital, and Franklin Hospital. He was also visiting radiologist at



San Francisco General Hospital. Shortly after Pearl Harbor, he joined the Army. After 3½ years service, he was discharged with the rank of colonel.

Williams was a member of numerous medical societies including the San Francisco Medical Society and San Francisco Radiological Society, both of which he served as president. For many years, he was a delegate to the California Medical Association House of Delegates and a Fellow of the American College of Radiology. He was a member of the AMA, American Roentgen Ray Society, the Radiological Society of North America, the California Academy of Medicine, Fred Jenner Hodges Radiological Society, and the Irwin Memorial Blood Bank of the San Francisco Medical Society. In addition, he was an honorary member of the Rocky Mountain Radiological Society and the Texas Radiological Society.

He was associate clinical professor at the University of California Medical School in San Francisco until his retirement from teaching in 1969. From 1945–1960 he was chief of the Department of Radiology at Franklin Hospital and from 1960–1971, chief of the radiology department at St. Francis Memorial Hospital in San Francisco. He continued an active office practice, and his death came as a shock to his many friends because of his continued activity in spite of his serious illness.

Williams is survived by his wife, Carolyn Helbig Williams, a son, Justin Lowell Williams, of Fresno, California; and a daughter, Lynn Williams Pfeleger, of Ross, California.

Tom M. Fullenlove
San Francisco

Abstracts of Current Literature

Chest

Pseudomesotheliomatous carcinoma of the lung. Harwood TR, Gracey DR, Yokoo H (Northwestern University Medical School, Chicago, Illinois). *Am J Clin Pathol* 65:159, Feb 1976

Six cases of primary lung cancer that closely mimic malignant pleural mesothelioma clinically and anatomically were compared with four cases of proven malignant pleural mesothelioma. Findings on roentgenograms of the chest, clinical history, and gross examination were not helpful in distinguishing between these two neoplasms. The average age of the patients was 57 years and total duration of illness less than 8 months after onset of clinical symptoms. Dyspnea, chest pain, and weight loss were the most common presenting symptoms. All but one were cigarette smokers. Chest x-rays were indicative of either pleural thickening or effusion. Histologically all were classified as adenocarcinomas (five as bronchiolar carcinomas) but in contrast to mesotheliomas, all contained mucin both in the cytoplasm of malignant cells and within the lumina of neoplastic glands. In two of the cases a small subpleural primary focus was demonstrated, suggesting a possible origin of these tumors as a small subpleural neoplasm which becomes widely disseminated via the subpleural lymphatics. It was also postulated that this focus of carcinoma develops beneath a chronically diseased and fibrosed pleura, in a manner similar to scar carcinoma, with ultimate spread across a thickened pleura in a manner similar to malignant mesothelioma.

Louise Wiegenstein
Pathology, U.W.

Cardiovascular

Cross-sectional echocardiography in evaluating patients with discrete subaortic stenosis. Weyman AE, Feigenbaum H, Hurwitz RA, Girod DA, Dillon JD, Chang S (Indiana University School of Medicine, Indianapolis, Indiana 46202). *Am J Cardiol* 37:358-365, March 1976.

Ten patients with discrete subvalvular aortic stenosis were examined using a real time, high resolution mechanical sector scanner. Two patients (Group I) had a thin, discrete subvalvular membrane, five (Group II) had diffuse fibromuscular subvalvular obstruction, and three (Group III) had a residual area of outflow tract obstruction after surgical revision. Patients ranged in age from 5 to 20 years. Left ventricular outflow tract gradients varied from 30-80 mm Hg in Groups I and II, and from 10-52 mm Hg in Group III. Sector scans of the left ventricular outflow tract in both patients with discrete membranous subaortic obstruction (Group I) revealed two well-defined dominant echoes within the outflow tract producing a clearly demarcated area of narrowing. These distinct echoes were separate, but adjacent to the anterior and posterior walls of the left ventricular outflow tract. The dynamic nature of the obstruction was also apparent when viewed throughout the cardiac cycle. In four of five patients with diffuse fibromuscular subvalvular obstruction (Group II), a more generalized area of narrowing was noted. The echoes from the walls of the narrow segment were continuous with those from the walls of the outflow tract proximal and distal to the area of obstruction. In the other patient in this group, there was obvious dynamic outflow tract obstruction between the anterior mitral valve leaflet, and an area of marked septal thickening at the junction of the muscular and membranous septum. In the three patients with residual postoperative outflow tract narrowing (Group III), various patterns of outflow tract obstruction were recognized. Two patients had abnormal echoes along the posterior wall of the outflow tract with obvious narrowing. In the other case,

there was a diffuse area of outflow tract narrowing similar to that seen with Group II lesions.

While left ventricular outflow tract narrowing has been demonstrated with standard M-mode echocardiography, difficulties are frequently encountered because of problems in spatial orientation, and transducer angulation. Real time motion, cross-sectional echocardiography offers an alternative and probably improved method of noninvasive visualization of the left ventricular outflow tract.

Richard B. Jaffe

Gastrointestinal

Near-fatal hemorrhage following gastrografin studies. Gallitano AL, Kondi ES, Phillips E, Ferris E (Boston University Medical Center, Boston, Massachusetts 02118). *Radiology* 118:118:35-36, Jan 1976

The use of upper gastrointestinal studies followed by gastric drainage and observation is recommended for the evaluation and treatment of stomal dysfunction due to edema or gastric atony. Gastrografin though, may be precipitated out and can cause gastrointestinal bleeding if left in the gastric remnant. This agent should be used with proper precautions in the evaluation of postoperative gastric retention.

Author's Abstract

Intrahepatic rupture secondary to duct exploration demonstrated by cholangiography. Goldman SM, Diamond A, Salik JO (Sinai Hospital of Baltimore, Inc., Baltimore, Maryland 21215). *Radiology* 118:13-17, Jan 1976

Seven cases of iatrogenic rupture of the intrahepatic bile ducts were demonstrated on T-tube and/or operative cholangiography. This brings the total of documented case reports to 17. All patients had hepatic duct exploration with either the Fogarty balloon catheter and/or the biliary spoon and/or the biliary forceps and/or Bakeš dilators. These extravasations usually occur from the right hepatic duct. The recognition of this entity is important because potentially serious complications may occur. Most of the previous cases of intrahepatic extravasation ascribed to excessive pressures of injection were probably surgically induced.

Author's Abstract

Hemorrhage from the gastroesophageal junction: a cryptic angiographic diagnosis. Northrop CH, Studley MA, Smith GR (University of Washington, Harborview Medical Center, Seattle, Washington 98104). *Radiology* 117:531-532, Dec 1975

The angiographic localization of gastroesophageal-junction hemorrhage emanating from the left inferior phrenic artery (which originated from the abdominal aorta) is described. The diagnosis was established after conventional selective celiac and left gastric arteriography failed to demonstrate extravasation. The arteriographic evaluation of upper gastrointestinal hemorrhage requires consideration of the variable arterial distribution to the gastroesophageal junction and an awareness of the variable causes of dense opacification (including superimposed adrenal glands) that may mimic extravasation.

Author's Abstract

Postbulbar peptic ulceration of the duodenum. Hines JR, Geurinkre RE, Gordon RT. *Surg Gynecol Obstet* 142:13-15, Jan 1976

The authors experience with 120 patients undergoing surgery for duodenal ulcer disease in a 5 year period yielded 12 (10%) patients with post-bulbar duodenal ulcers. These patients all had

severe ulcer symptoms and responded poorly to medical therapy. Although ulcers in unusual locations should alert the physician to a possible Zollinger-Ellison Syndrome, none of the patients had significantly elevated gastrin levels. Upper GI series in all patients reported duodenal bulb deformity or ulceration, but in none of the reports was a postbulbar ulcer or stenosis mentioned. Retrospective review of the x-rays by the surgical staff suggested the correct diagnosis in six patients. The patients were all treated with vagotomy and pyloroplasty and three patients have had a possible recurrence of the ulcer. A postulated mechanism for the recurrence is the stenosis associated with healing of ulcers in this area. The authors make a very wise plea for inspection of the second portion of the duodenum during operation in all patients with duodenal ulcer since in six patients the abnormal location of the ulcer was unsuspected.

David M. Heimbach
Surgery, U.W.

Genitourinary

Therapeutic bilateral renal infarction in end-stage renal disease. McCarron DA et al. (Tufts New England Medical Center, Boston, Massachusetts 02111). *N Engl J Med* 294:652, March 18, 1976

A 55 year old female with end-stage renal disease secondary to focal sclerosis was undergoing chronic dialysis. To control her continued nephrotic syndrome, the patient underwent bilateral renal infarction via transarterial embolization, employing gelfoam. The patient remained normotensive. Immediate and continued cessation of proteinuria occurred with consequent improvement in serum proteins and nutritional status. Advantages of this technique over surgery include the avoidance of a major surgical procedure in a poor risk patient and consequent earlier hospital discharge. The evaluation of the precise role of this technique requires further clinical experience.

Curtis H. Northrop

Pancreatic pseudocysts presenting as thick-walled renal and perinephric cysts. Lilienfeld RM, Lande A (New York Medical College-Metropolitan Hospital Center, New York City). *J Urol* 115:123-125, Feb 1976

When a thick-walled cyst is seen within or adjacent to the kidney in excretory urography, the differential diagnosis usually includes necrotic hypernephroma, infected renal cyst, renal carbuncle, and perinephric abscess. In addition, however, the authors report that pancreatic pseudocyst can also present as a thick-walled cyst in infusion pyelography with tomography. It is believed that opacification of the wall of the pancreatic pseudocyst is due to two factors. Contrast material will be seen within the proliferating capillaries of the cystic wall itself as well as the adjacent inflammatory tissue. It will also accumulate within the interstitium of the inflamed tissue due to increased permeability of the capillaries. Performance of tomography toward the end of the infusion will permit maximum opacification of the interstitial space. The discussion is illustrated by three case reports, seven radiographs, and one ultrasonogram.

John W. Li

Musculoskeletal

Pyelocancerous backflow: a radiologic finding in renal malignancy. Copeland JS, Schellhammer PF, Devine CJ Jr (Norfolk Medical Center, Norfolk, Virginia) *J Urol* 115:214-215, Feb 1976

Pyelocancerous backflow is found in retrograde pyelography in which there is extravasation of dye into the renal parenchyma in a mottled and irregular pattern. This is believed to indicate the passage of contrast medium from the renal pelvis into a tumor that invades the calyx. This sign can be found in both renal adenocarcinoma and transitional cell carcinoma. The authors also speculate

that the same radiologic finding could be present in any renal destructive lesions such as tuberculosis and renal abscess.

John W. Li

The acute carpal tunnel syndrome: nine case reports. McClain EJ, Wissinger HA (University of Pittsburgh, Pittsburgh, Pennsylvania). *J Trauma* 16:75-78, Jan 1976

This is a report of nine cases of acute onset of median nerve compression within the carpal tunnel of the wrist. The well-known association of this syndrome with wrist trauma was reaffirmed in this study, in that five of the nine cases were traumatic. Hematoma, unrelated to acute trauma was responsible for three cases. The etiology of the bleeding included chronic lymphocytic leukemia, chronic trauma from recurrent distal radio-ulnar dislocation, and giant cell tumor of the tendon sheath. The ninth patient with acute carpal tunnel syndrome had rheumatoid arthritis and developed an acute teno-synovitis. The case histories are briefly summarized and the differential diagnosis is discussed. The importance of prompt surgical decompression is stressed.

Curtis Northrop

The arthropathy of hemochromatosis. Hirsch JH, Killien FC, Troupin RH (University of Washington School of Medicine, Seattle, Washington 98195). *Radiology* 118:591-596, March 1976

Five cases of hemochromatosis arthropathy are presented and the distinctive radiological features of the disease are described. Although the condition is typically degenerative, showing subchondral cyst formation, sclerosis, and thinning of cartilage, its distribution is characteristic. Selective degenerative changes of the second and third metacarpophalangeal joints are striking, particularly in the hands, while abnormalities in the intercarpal joints are variable and the interphalangeal joints are spared. Chondrocalcinosis involving both fibrous and hyaline cartilage is frequently seen as well, particularly in the large joints. The calcification is due to deposition of calcium pyrophosphate crystals, perhaps resulting from iron inhibition of pyrophosphatase.

Author's Abstract

Periostitis and pseudoperiostitis. Forrester DM, Kirkpatrick J (USC-LA Hospital, 1200 North State Street, Los Angeles, California 90033). *Radiology* 118:597-601, March 1976

Stimulation of the periosteal membrane to form new bone may be initiated from within the bone (i.e. osteomyelitis, osseous neoplasm) or from the soft tissues. The latter classically occurs accompanying the inflammatory arthritis of Reiter's syndrome and psoriatic arthritis. Diffuse soft tissue swelling of a finger or toe and fluffy thick periosteal new bone are so characteristic of these two rheumatoid variants that the radiographic findings alone suggest the diagnosis. Occasionally osteoclastic activity is so dramatic that demineralization and cortical tunnelling result in a separation of a margin of cortical bone. Because of its similar appearance to periostitis it has been termed "pseudoperiostitis." It occurs only in conditions of rapid demineralization such as acute immobilization and Sudeck's atrophy. Serial films will document absence of an increase in the diameter of the diaphysis, verifying that no new bone has been laid down along the periphery. In the absence of serial films, the accompanying hallmark of rapid demineralization (moth-eaten appearance of the spongiosa) must be present if one is to attribute the linear paradiaphyseal shadow to pseudoperiostitis rather than periostitis.

D. M. Forrester

The radiology of the subtalar joint with special reference to talo-calcaneal coalition. Beckly DE, Anderson PW, Pedegana LR (Royal Infirmary, Bristol, England). *Clin Radiol* 26:333-341, July 1975

The authors remind us that talo-calcaneal coalition is either bony or fibrocartilaginous fusion between talus and calcaneus and is one of the causes of rigid or spastic flat foot. It may not be diagnosed till near the end of the first decade when minor trauma may initiate

pain and stiffness. There is limitation of motion in the subtalar joint and there may be associated peroneal muscle spasm. Routine films may not show the coalition but the authors describe characteristic secondary signs which should suggest talo-calcaneal coalition and if they are present should lead to further studies.

On a routine lateral film, the posterior and middle subtalar joints are seen; the anterior joint is obscured since it inclines downward and medially although it is usually well seen in the lateral oblique views. There is a brief discussion of anatomical variants in these joints. Rotation of the foot or faulty projection may obscure the middle joint on the lateral film but it may be shown on the axial or heavy-density posteroanterior film. In a fibrous or cartilaginous coalition through the mid joint, there may be a radiolucent zone with poor margins and lack of cortication. Lateral tomograms of this joint must be interpreted with caution because of its obliquity and if taken, they should be in the coronal or lateral oblique plane.

The authors base their study on the findings in 17 patients, including one posterior coalition, three generalized talo-calcaneal fusions and 13 mid joint coalitions; four of which were bilateral making a total of 17 feet with mid joint coalition. Males predominated and the age of presentation was 15.9 years for the mid joint coalitions.

The secondary signs of talo-calcaneal coalition due to restricted motion include:

(1) Bony beak on the dorsal-distal aspect of the talus (found in nine of 17 of mid joint coalitions; in two cases it formed after initial negative films)

(2) Narrowing of the posterior subtalar joint (found in nine of seventeen mid joint coalitions)

(3) Rounded shape of the lateral process of the talus (eight of 17 feet)

(4) Failure to visualize the middle joint on the lateral view (found in all cases of mid joint coalition)

(5) Asymmetry of the anterior subtalar joint in the lateral-oblique view; this may be associated with flattening or concavity of the inferior aspect of the neck of the talus on the affected side (seen in five of eight unilateral cases)

The differential diagnosis includes rheumatoid arthritis where there may be a beak, narrowed posterior joint and rounded lateral process. A talar beak is also seen after trauma, after some surgical procedures and occasionally, valgus flat foot without coalition. The article is well illustrated.

Martha Mottram

Arthrography for the assessment of pain after total hip replacement. Murray WR, Rodrigo JJ. *J Bone Joint Surg* 57A: 1060-1065, Dec 1975

The value of the arthrogram in evaluating pain after total hip replacement is doubtful. Previously when a "positive" arthrogram was demonstrated, loosening was assumed to be the cause of the pain. In this study, one-fifth of 53 asymptomatic hips had arthrographic evidence of loosening. However, the loosening shown by an arthrogram could be confirmed in only seven of 12 patients who were explored operatively. Possibly the dense fibrous tissue and fibrocartilaginous material surrounding total hip prostheses is permeable to contrast agents, thus explaining why contrast material is sometimes seen at the bone-cement interface in patients without any symptoms. Although minor loosening may be asymptomatic, while major loosening may cause symptoms, arthrographic evidence of loosening is not the most reliable criteria to distinguish between the two. The authors recommend that gross loosening be evaluated by push-pull or abduction films as well as fluoroscopy. If a patient shows radiographic evidence of hip arthroplasty loosening, the authors recommend trying conservative therapy first and investigating other causes of pain prior to a high-risk major revision of the total hip replacement

Gerald R. Smith

A unified radiological approach to the detection of skeletal metastases. Mall JC, Bekerman C, Hoffer PB, Gottschalk A (University of Chicago Hospitals and Clinics, Chicago, Illinois 60637). *Radiology* 118:323-328, Feb 1976

Radiographic bone surveys and radionuclide images, the principal methods of detection of skeletal metastases, have traditionally been treated as separate entities. Since their interpretation is related, we attempted to determine the practicability of a unified radiological approach which employs both methods. All consultation requests for "skeletal surveys" or bone scans were reviewed, and an appropriate examination was "tailored" for each patient. During the initial four-month period, 141 patients were examined. Comparison of the final "tailored" examination with the original consultation request indicated that, without radiological guidance, excessive (18%), and inappropriate or inadequate (27%) examinations were ordered in many cases. The unified approach has proven to be feasible and desirable, resulting in a significant reduction of inappropriate examinations.

Author's Abstract

Subchondral resorption of bone in renal osteodystrophy. Resnick D, Niwayama G (Veterans Administration Hospital, San Diego, California 92115). *Radiology* 118:315-321, Feb 1976

In a radiographic-pathologic study of the spine and several axial joints in a cadaver with renal osteodystrophy, subchondral resorption of bone is described as an important mechanism of osseous abnormality. Widening and irregularity of the sacroiliac and sternoclavicular joints and symphysis pubis are related predominantly to trabecular destruction beneath cartilage surfaces, substitutive fibrosis, and new bone formation. Subperiosteal abnormalities at these locations produce juxta-articular erosions. The presence of osteitis fibrosa cystica about multiple Schmorl's nodes within the thoracic vertebral bodies suggests that subchondral resorption beneath the cartilage end-plates of the spine may be associated with disk protrusions and represents one further example of hyperparathyroid joint disease.

Author's Abstract

HL-A W27 in psoriatic arthropathy. Metzger AL, Morris RI, Bluestone R, Terasaki PI (Rodney Bluestone Wadsworth VA Hospital, 691/111J, Wilshire and Sawtelle Boulevards, Los Angeles, California 90073). *Arthritis Rheum* 18:111, March-April 1975

Forty subjects with psoriatic arthritis (PA) underwent HL-A tissue typing. HL-A W27 was significantly increased in psoriatic spondylitis (35%), whereas statistical significance was not reached in patients with peripheral arthritis alone, although W27 was present in a frequency greater than in controls. Psoriatic spondylitis (often asymptomatic) occurred in 57% (23 of 40) of our PA patients. Of interest, psoriatic spondylitis was more often W27 negative than W27 positive; nevertheless, W27-positive and W27-negative spondylitis was clinically and radiographically indistinguishable except that W27-positive disease occurred exclusively in males and the duration of the psoriasis.

Author's Abstract

Nervous System

Cervicovertebral phlebography: pathological results. Thérion J (Département de Neuroradiologie, Service Neurochirurgie, Hôpital Lariboisière, Paris, France). *Radiology* 118:73-81, Jan 1976

Cervical phlebography via the femoral vein approach was done in patients with spinal tumors, cervical radiculopathies, and myelopathies. Tumors originating from or extending into the spinal canal readily compress and obstruct the epidural venous plexus. Because of the lateral position of the epidural veins, the foraminae are deformed when cervical roots are compressed in the intervertebral foramina by spondylosis of the uncinat processes or lateral disk herniation. In congenitally narrow canals without significant spondylotic bars, the epidural veins were not opacified. Nonfilling of veins was also seen when the canal was narrowed by multiple spondylotic bars, the epidural veins were not opacified. Nonfilling of epidural veins opacified but this was interrupted at the affected levels. When a significant spondylotic bar was associated with a narrow canal higher up, filling of the epidural veins at the level of

the bar was completely arrested.

Author's Abstract

Clinical experience with extra-intracranial arterial anastomosis in 65 cases. Gratzl O, Schmiedek P, Spetzler R, Steinhoff H, Marguth F (University of Munich, Munich, West Germany and University of California, San Francisco, California). *J Neurosurg* 44:313-324, March 1976

The authors report their 5-year experience using superficial temporal-middle cerebral artery anastomoses to treat cerebral ischemia. Most of the 65 patients were middle aged men with arteriosclerosis. Cerebral angiography and regional cerebral blood flow measurements using intra-arterial $^{133}\text{Xenon}$ and 16 external detectors were performed to assess extent of disease and surgical result. The best result was obtained when patients were selected on the basis of a focal area of cerebral ischemia on the preoperative regional cerebral blood flow study. Patients with either transient ischemic attacks or stroke with mild neurological deficit showed the most improvement. In this group, 25 of 29 cases were asymptomatic with patent bypass grafts 8-35 months following surgery. In 11, improved regional cerebral blood flow was also demonstrated. Patients with completed strokes and moderate weakness were slightly improved while patients with severe neurological deficits remained unchanged. Operations performed during the acute phase of cerebral ischemia resulted in progressive neurological deterioration in all seven patients despite patent bypass grafts, and five died within the first post-operative month. Attempts to use more than one branch of the superficial temporal artery as a bypass vessel resulted in protracted wound healing and partial scalp necrosis in all three patients. The authors conclude that revascularization has merit in patients selected on the basis of non-acute focal cerebral ischemia.

P. M. Chikos

Recent ischemic brain infarcts at computed tomography: appearances pre- and postcontrast infusion. Yock DH Jr, Marshall WH Jr (Stanford University School of Medicine, Stanford, California 94305). *Radiology* 117:599-608, Dec 1975

Computed tomography (CT) has a high sensitivity for ischemic infarcts. Thirty-seven CT scans of patients with proved or highly suspected infarcts were evaluated. The age of the infarcts ranged from less than 24 hours to 3 months. Infarcts are predominantly low density regions. These areas of low density were characterized visually as well-defined, homogeneous; ill-defined, homogeneous; or irregular, patchy. The age of the infarct could not be determined by its visual characteristics. Differentiation from tumor can be difficult. Eight of the 37 infarcts were associated with "mass effect." Six of these eight were 7 days old or less. Twenty patients had contrast infusion and four of these showed a definite "blush." In several other cases contrast infusion tended to hide the area of infarction.

A. K. Teaford

Adult arteriosclerotic moyamoya. Hinshaw DB, Thompson JR, Hasso AN (Loma Linda University School of Medicine, Loma Linda, California). *Radiology* 118:633-636, March 1976

Progressive idiopathic distal internal carotid artery occlusion in children and young adults associated with the development of bridging channels and tortuous, plethoric intracerebral arterial networks has been termed *moyamoya* or Nishimoto's disease. It is now generally recognized that this unusual angiographic pattern results from collateral supply pathways and is not a primary angiomatous process. The authors describe 2 middleaged patients with intracranial arteriosclerotic occlusive lesions demonstrating secondary collateral patterns angiographically identical to *moyamoya*.

Author's Abstract

Angiographic features of subdural empyema. Kim KS, Weinberg PE, Magidson M. (Northwestern Memorial Hospital, Chicago, Illinois). *Radiology* 118:621-625, March 1976

Subdural empyema, a relatively rare intracranial suppurative disease, is a surgical emergency and requires early diagnosis in order to ensure patient survival. Subdural empyema should be considered with one or a combination of the following in conjunction with an extracerebral collection: (a) an irregular border of the extracerebral collection; (b) a thickened vascular wall of dura; (c) a semilunar avascular zone on the lateral view; (d) spasm of the large arteries at the base of the brain with or without segmental arterial dilatation; (e) multiple peripheral arterial occlusions; and (f) enlargement of the anterior falx artery. Four verified cases are presented.

Author's Abstract

Computed tomography in Graves' ophthalmopathy. Enzmann D, Marshall WH Jr, Rosenthal AR, Kriss JP (Stanford University School of Medicine, Stanford, California 94305). *Radiology* 118:615-620, March 1976

The CT scan with the 160x160 matrix demonstrated both the normal orbital anatomy and the abnormal orbital anatomy of Graves' ophthalmopathy in great detail. In Graves' ophthalmopathy, the cardinal pathologic feature of extraocular muscle enlargement was accurately reflected on the CT scan and was a distinctive, diagnostically reliable finding. Enlargement of the medial and lateral rectus muscles and of the apex of the muscle cone were the most consistent findings. The severity of the CT scan abnormalities correlated well with clinical severity. Because muscle cone abnormality was observed characteristically in those patients with sight loss, we suggest that pressure by the extraocular muscles on the optic nerve may contribute to visual acuity loss in this disease.

Author's Abstract

Participation of the external and internal carotid arteries in the blood supply of acoustic neurinomas. Thérion J, Lasjaunias P. (Department de Radiologie, C.H.U.F., 14000 Caen, France). *Radiology* 118:83-88, Jan 1976

Previously, routine angiographic exploration of the cerebello-pontine angle has been limited to injection of the vertebral system. Opacification of the external carotid system has seemed justified only when there was a possibility of meningioma. Acoustic neurinomas were thought to be supplied only by the vertebral system (internal auditory and subarcuate branches of the anteroinferior cerebellar artery) with vertebral angiograms demonstrating a tumor stain in 20% to 65% of cases. Two cases of acoustic neurinoma with blood supply from the external carotid artery have been reported recently and the authors now report six such cases and suggest a new angiographic protocol for the investigation of masses in the cerebellopontine angle.

To appropriately evaluate the blood supply to the cerebello-pontine angle, the common carotid arteries of 12 cadavers were injected with colored and radiopaque contrast media. A vascular anatomic study of the cerebellopontine angle was then performed after the removal of the nervous structures. The authors define the boundaries of the cerebellopontine angle as the superior petrosal sinus superiorly, the sigmoid sinus posteriorly, and the petrosphenoidal suture medially. The branches of the external carotid arteries which have been found to participate in the blood supply to the area include: (a) the petrosal branches of the middle meningeal; (b) the meningeal branch of the occipital; and (c) the ascending pharyngeal. The internal carotid artery also participates in the blood supply of the region via the lateral artery of the clivus. The clinical material consists of six cases of acoustic neurinoma, evaluated by vertebral, internal carotid and external carotid branch angiography. Injection of the vertebral artery demonstrated a tumor stain in only three cases and, similarly, internal carotid injection showed tumor stain in three cases. However, injection of the internal maxillary and ascending pharyngeal arteries demonstrated tumor stain in all six cases (internal maxillary five cases, and ascending pharyngeal two cases, with one case overlap). Occipital artery injection did not show tumor stain in any instance of these six cases of acoustic neurinoma, although the authors additionally report tumor demonstrated by occipital artery injection and one glomus jugulare tumor and three cases of cerebellopontine angle

meningioma. As a result of their clinical and anatomical evaluation, the authors recommend a new angiographic protocol for the study of the cerebellopontine angle. This protocol should sequentially include: (a) selective vertebral artery injection; (b) selective internal carotid artery injection; and (c) injection into the main stem of the external carotid artery. The radiologist may either discontinue the protocol at this point or proceed to complementary superselective injections into the internal maxillary, middle meningeal, or ascending pharyngeal branches.

E. B. Best

Why do gliomas not metastasize? Alvord EC (University of Washington School of Medicine, Seattle Washington 98125). *Arch Neurol* 33:73-75, Feb 1976

The great rarity of extracranial metastases from gliomas is discussed from the vantage of cytogenetics. Assuming simple exponential growth and average glioma cell 10μ by 10μ in size, 30 generations are necessary to reach the size of 1 cm in diameter. Clinical diagnosis usually occurs at 34 generations when the tumor is 2.5 cm in diameter. Untreated, death occurs at 36 or 37 generations and at 39 generations the tumor would reach the size of one entire cerebral hemisphere. Thus the visible portion of the natural history of gliomas is four or five generations or 10% of its total life history which is about one half the clinical visibility of other cancers. Assuming single cell metastases at surgery and recurrent primary tumor causing death; 20 generations would be necessary to produce a metastasis 4 mm in diameter which would require careful pathologic search for discovery. Either a very early metastasis or repeated surgical interventions would be necessary to allow the 30 generations of growth at which time the metastatic tumor would be 1 cm in diameter and visible at autopsy.

Paul M. Chikos

Positional shift of intraventricular blood clots demonstrated by computed tomography. Vermess M, Di Chiro G, Newby NR, Herdt JR (Bldg 10, Room 6S211, National Institutes of Health, Bethesda, Maryland 20014). *Radiology* 118:341-342, Feb 1976

Computed tomography has greatly improved the radiographic diagnosis of intraventricular hematoma. If one or several of the cerebral ventricles are entirely filled with blood, the scan will demonstrate a cast of the affected ventricle. If clots only fill the ventricles, a definitive diagnosis may be difficult. In these cases a repeat scan in the brow-down position may be diagnostically definitive. A prone scan may demonstrate a gravitational shift in the position of the intraventricular blood clots. Mobility of the ventricular densities indicate their etiology as floating blood clots. A prone scan may also be helpful in other clinical situations in which there is a gravitational shift of intracranial structures according to the position of the head. This method may be useful in the diagnosis of tumoral or other intracranial cavities containing blood or necrotic debris. Information could be obtained about cystic lesions partially filled with low-density substances (such as cholesterol) which produce a layering effect in the cavity according to the specific weight of the different liquids. More important is the demonstration of gravitational change in the position of pedunculated neoplasms, such as small choroid plexus tumors or some colloid cysts of the third ventricle.

J. L. Montgomery

Miscellaneous

Calcification in human breast carcinomas: ultrastructural observations. Ahmed A (University of Manchester, England) *J Pathol* 117:247, Dec 1975

Calcification, a radiologic and histologic feature in certain breast carcinomas where it occurs in fine clusters or microcalcifications, was studied ultrastructurally. Multiple deposits of needle-shaped crystals, intimately associated with electron-dense material, were observed among tumor cells. Electron diffraction and electron probe analyses showed the crystalline material to be hydroxy-

apatite; the electron-dense material is believed to be phospholipid in nature and as in bone, represents the most likely focus of calcification in breast carcinoma. Similar crystalline deposits were found within the cytoplasm of tumor cells, in membrane-bound and partially membrane-bound vesicles. Crystalline deposits were also found in the adjacent stroma although there was no evidence of calcification of stromal collagen or elastic fibers. It was postulated that calcification is the result of an active secretory process by the tumor cells rather than mineralization of necrotic or degenerate tumor cells. The presence of free-lying and partially membrane-bound clusters of crystalline material within the cytoplasm may result from progressive accumulation of crystals in membrane-bound electron-dense vesicles which eventually burst.

Louise Wiegenstein
Pathology, U.W.

Radiological aspects of the basal cell naevus syndrome, in German. Novak D, Bloss W (Priv.-Doz. Dr. med. D. Novak, Radiologische Universitätsklinik 2000 Hamburg 20, Martinistrasse 52, West Germany). *Fortschr Geb Roentgenstr Nuklearmed* 124:11-16, Jan 1976

Based on four cases of their own and 105 cases from the literature, the radiological features of the basal cell naevus syndrome (Gorlin-Goltz syndrome) are described. Ninety-two per cent showed multiple cysts in the mandible and 35% demonstrated additional cysts in the maxilla. Forked, rudimentary and/or synostotic ribs were present in 45%. Lamella-like calcification of the falx was found in 49% and scoliosis of the spine in 32%. The authors' four personal cases also had multiple small cysts in the bones of the hands and forearms. This finding has not been described previously.

Peter F. Winter

Ultrasonics

Echo-tomography, placental thickness and fetal development. Experience with 732 cases. Leroy B, Risse RJ, Franscoli G, Kamkar J, Lefort F. *J Gynecol, Obstet Biol Reprod (Paris)* 4:801-813, 1975

The authors measured the thickness of the placenta on a series of 732 cases from 13 weeks to full-term gestation. Graphs were drawn to represent the normal physiological evolution of the placenta with the progression of pregnancy. The thickness of the placenta as well as the rate of thickening were studied. The authors speculate that intrinsic abnormalities of the fetus could be diagnosed at an earlier stage by serially studying the thickness of the placenta and the rate at which the placenta increases. If the increase occurs at an earlier stage than expected from their graph, abnormality may be suspected.

Catherine Cole-Beuglet

Nuclear Medicine

Comparison of ^{18}F and $^{99\text{m}}\text{Tc}$ polyphosphate in orthopedic bone scintigraphy. Heerfordt J, Visiten L, Bohr H (Hans Bohr, Osteopathology Laboratory, Department of Orthopaedics 2161, Righospitalet, 2100 Copenhagen Ø). *J Nucl Med* 17:98, 1976

$^{99\text{m}}\text{Tc}$ polyphosphate and ^{18}F were compared in 50 patients with a variety of orthopedic diseases. The two agents were also compared experimentally in rabbits in whom degenerative joint changes were induced. In the clinical series, ^{18}F uptake was relatively greater in lesions that were primarily osseous while $^{99\text{m}}\text{Tc}$ polyphosphate uptake was greater in lesions that were primarily synovial. Fractures and sarcomas showed excellent tracer uptake although fluorine appeared superior to $^{99\text{m}}\text{Tc}$ polyphosphate. An unexpected Tc PP accumulation was occasionally seen in an otherwise normal joint. The explanation for this is not clear but may represent subclinical synovitis. Uptake of Tc PP was also seen in mesenchymal soft tissue tumors and this at times could be mistaken for bony abnormalities. After simultaneous administration of both agents, quantitative measurements were performed on specimens of bone

and synovial tissue from diseased joints in human patients and in rabbits. The uptake of ^{99m}Tc PP in synovial tissue was about seven times that of ^{18}F , while their uptake in bone were equal. Overall, no major differences were found between ^{18}F and ^{99m}Tc PP in terms of bone uptake. However, the fact that ^{99m}Tc PP concentrates in abnormal mesenchymal soft tissues must be recognized and considered when interpreting these images.

Thomas G. Rudd

Inadvertent ^{131}I therapy for hyperthyroidism in the first trimester of pregnancy. Stoffer SS, Hamburger JI (Northland Thyroid Laboratory, 20905 Greenfield—Suite 300, Southfield, Michigan 48075). *J Nucl Med* 17:146, 1976

Of 963 physicians surveyed to determine therapeutic attitudes toward, and experience with inadvertent radioiodine therapy for hyperthyroidism during the first trimester of pregnancy, 116 physicians (of 517 responding) reported 237 cases. Therapeutic abortion was advised for 55 patients by 22 physicians. From the 182 remaining pregnancies there were two spontaneous abortions, two still-born, one neonate with biliary atresia, and one with respiratory distress. This complication rate was not greater than might be expected in a similar number of random pregnancies. On the other hand, six infants were hypothyroid (transient for one) and four of these were mentally deficient. Three mothers of hypothyroid infants had received radioiodine therapy in the second trimester. None of the six mothers of hypothyroid infants had had pregnancy tests prior to radioiodine therapy. Survey responses indicate that routine pregnancy testing prior to radioiodine therapy for patients in the child-bearing age is not yet a standard procedure. It should be.

Author's Abstract

Gallium-67 scintigraphy of pulmonary diseases as a complement to radiography. Siemsen JK, Grebe SF, Sargent EN, Wentz D (LAC/USC Medical Center, Los Angeles, California). *Radiology* 118:371–375, Feb 1976

Gallium chest scans of 575 patients were analyzed for their clinical usefulness in conjunction with chest radiographs. The series included patients with pulmonary carcinoma, lymphoma, tuberculosis, sarcoidosis, pneumoconiosis, and interstitial fibrosis. Gallium scintigraphy does not aid in the differential diagnosis of pulmonary diseases but is helpful in determining (a) the degree of activity of a known disease process; (b) treatment response, dosage, and duration; (c) the spatial extent of the disease; and (d) the presence of unsuspected disease foci hidden radiographically in the mediastinum, behind the heart, or in pleural or parenchymal scars.

Author's Abstract

Scintigraphic findings in amebic abscesses of the liver, in German. Buenemann H, Petersen F, Mohr W (Dr. med. H. Buenemann, Allgemeines Krankenhaus St. Georg, Abteilung fuer Nuklearmedizin 2 Hamburg 1, Lohmühlenstrasse 5, West Germany). *Fortschr Geb Roentgenstr Nuklearmed* 124:126–131, Feb 1976

Forty-seven of 52 patients with the clinical diagnosis of an amebic abscess had an abnormal liver scan. A solitary defect was found in 34, and multiple defects in 13. Of these 13 patients, 11 had two lesions and the remaining two patients were found to have three defects. The right lobe of the liver was involved more frequently.

A focal, well-defined area of increased radioactivity in the deshowed rapid diminution in the size of the defects during medical treatment, with the larger lesions exhibiting a more rapid rate of resolution. Complete return to normal during the first 6 months after the institution of therapy occurred in only 17% of the cases.

Peter F. Winter

A comparative study of contrast dacryocystogram and nuclear dacryocystogram. Chaudhuri JK, Saporoff GR, Dolan KD, Chaudhuri TK (Eastern Virginia Medical School and V.A. Center, Hampton, Virginia 23667). *J Nucl Med* 16:605–608, July 1975

The contrast dacryocystogram was compared to the nuclear dacryocystogram to assess the diagnostic accuracy of the tracer procedure. Twenty-one patients with blockage of the lacrimal

drainage apparatus were studied using both procedures. The tracer procedure was performed using 100–200 microcuries of technetium-pertechnetate in distilled saline and a 0.1 cm diameter pin-hole.

Twelve studies demonstrated obstruction of the lacrimal drainage system in both contrast dacryocystography and nuclear dacryocystography. Seven had unilateral obstruction, and five had bilateral obstruction. Five patients underwent surgical repair and a postoperative scan was obtained in this group of patients. Studies on three demonstrated patency of the repair while in two others, no flow was found. These findings correlated well with results of a fluorescein dye test. Two studies were normal on contrast dacryocystography but abnormal on scan. This discrepancy could be explained by the need for lacrimal duct catheterization and manual injection of contrast material with the x-ray procedure; whereas, the scan test relies upon physiologic principle to clear tracer from the eye. Thus, the tracer procedure is better able to demonstrate functional blockage as may occur in abnormal lacrimal pump apparatus or stenosis of the duct where the system irrigates freely but does not permit free passage of tears under normal circumstances. These data suggest that the nuclear procedure is simpler to perform, less traumatic, and may provide better diagnostic ability because it can demonstrate both functional and anatomic blockage.

H. William Strauss

Diagnosis of osteomyelitis in children by combined blood pool and bone imaging. Gilday DL, Eng B, Paul DJ, Paterson J (Hospital for Sick Children, 555 University Avenue, Toronto, Ontario, Canada, M5G 1X8). *Radiology* 117:331–335, Nov 1975

In a child with symptoms of osteomyelitis, the differentiation from pure cellulitis is often difficult, clinically and roentgenographically. By using combined "blood pool" images (made immediately after the injection of Tc-99m methylene diphosphonate) and delayed images (made one to two hours after injection) the authors were able to differentiate osteomyelitis from cellulitis early in the course of the patient's illness.

A focal, well defined area of increased radioactivity in the delayed bone image associated with an identical area of increased activity in the immediate "blood pool" image are characteristic findings of osteomyelitis. The appearance of cellulitis is diffuse increased radioactivity involving soft tissues and bone in both "blood pool" and delayed bone images, due to diffuse soft-tissue hyperemia.

In this prospective study, the authors examined 134 patients suspected of having osteomyelitis. Using the above criteria, the radionuclide findings were correct in 70 of the 71 patients ultimately concluded to have osteomyelitis, in 13 of 13 patients with cellulitis and in eight of the nine patients with septic arthritis. Forty-three normal patients had normal images. The roentgenologic examination was correct in 29 of 66 patients with osteomyelitis and was poorer at differentiating osteomyelitis from cellulitis and septic arthritis.

The authors recommend radionuclide bone imaging as the initial screening procedure which can most readily give the correct diagnosis in the child with symptoms suggesting osteomyelitis, especially early in the disease or if the axial skeleton is involved.

W. R. Carpentier

Therapy of hyperthyroidism with radioactive isotopes of iodine: results in more than 2,000 patients (in German). Glanzmann C, Kaestner F, Horst W (Professor Dr. W. Horst, Univ.-Klinik für Nuklearmedizin und Radiotherapie, Kantonsspital CH-8006 Zürich, Rämistrasse 100, Switzerland). *Klin Wochenschr* 53:669–678, July 1975

The experience in 2,054 patients who were treated with ^{131}I and ^{125}I for hyperthyroidism was reviewed. The greater number was treated with ^{131}I . In small diffuse goiters of less than 60 grams, 6,000 rads were used; in large diffuse goiters, 8,000–10,000 rads were given; in nodular goiters the dose range was between 10,000–12,000 rads; and in autonomous adenomata, 30,000–40,000 rads were administered.

In 86 percent of patients with adenomas and in 75 percent of

patients with diffuse or nodular hyperthyroidism, a single dose was sufficient to control the hyperfunction. Myxedema developed in about twelve percent of all patients as measured after ten years. In the small diffuse goiters 31 percent became myxedematous; in the large diffuse goiters twelve percent, and in nodular goiters six percent became myxedematous. This variation stresses the necessity for calculation of individual doses.

In the past three years, ^{125}I has been administered to patients with small diffuse goiters, and the dose at the interface between the colloid and the cell was 12,000–15,000 rads. Sixty percent of the patients became euthyroid.

Anti-thyroid medication is, for most patients, of only temporary usefulness. Because of the unknown effects of irradiation and anti-thyroid medication on the body tissues and genetic structures, surgical treatment is preferred in young patients. Surgical treatment is likewise preferred in the event of a malignancy and in the presence of a large thyroid with mechanical complications, but, in most of these patients, recurrence after surgery should be treated with radioactive iodine.

E. Frederick Lang

Radiation Oncology

Natural history and survival of inoperable breast cancer treated with radiotherapy and radiotherapy followed by radical mastectomy. Zucali R, Uslenghi C, Kenda R, Bonadonna G (Istituto Nazionale Tumori, Via Venezian, 1–20133, Milan, Italy) *Cancer* 37:1422–1431, 1976

This retrospective study evaluates the time and site of relapse as well as the median survival of 454 consecutive patients with T3–T4 NXM0 breast cancer treated with irradiation from 1968–1972. The first 221 patients received kilovoltage irradiation and the remaining 233 patients were treated with cobalt teletherapy. Chest wall and regional lymph nodes were irradiated in all cases. With orthovoltage irradiation (220kV, 2mm Cu HVL) 4,000–4,500 rads were administered (five fractions a week) to the breast and 3,000 rads to the lymph node-bearing areas respectively for 12 to 16 weeks. Rest periods were at times required in the presence of cutaneous radiation reactions. With cobalt teletherapy 6,000–7,000 rads were given (five fractions a week) to both breast and lymph nodes in 8–9 weeks. Bolus was used for one-third of the treatments.

One hundred thirty-three patients had radical mastectomy with dissection of axillary lymph nodes performed from 5 to 8 months after the initiation of irradiation. Patients selected for mastectomy were usually those achieving a complete clinical remission following irradiation, those with no severe local irradiation reactions and those without regional adenopathy. Sixty-nine percent of the total group of 454 patients were postmenopausal and 72% were primary stage T4. Sixty-seven percent of the patients had involved lymph nodes at the time of diagnosis. Forty-nine percent of the patients relapsed within the first 2 years from the beginning of irradiation. The site of first relapse in 254 patients was within their previously irradiated area in 24% and in distant sites in 68%. Roughly 80% of the relapses occurred within 18 months of initiation of irradiation and the relapse rate appeared independent from the type of irradiation.

In the patients having post irradiation radical mastectomies no residual neoplasm was seen in 25% of the breasts and in 32% of the axillary contents. Both breast and axilla were negative for residual disease in 10% of the patients. The median survival time for the whole series was 2.5 years. The median survival time of patients treated with irradiation only was 2.1 years vs. 3.9 years for those treated with the combined sequential approach. Unfavorable survival was directly related to the presence of regional adenopathy (2.3 years vs. 4 years for N0 patients), supraclavicular fossa adenopathy (1.4 years) and inflammatory carcinoma (1.2 years). The importance of sequentially combining chemotherapy with radiotherapy for patients with primary inoperable breast cancer is discussed. A pilot study involving Adriamycin plus Vincristine preceding radiotherapy is described.

Herbert C. Berry

Acute lymphoblastic leukemia in adults and children. Gee TS, Hagbin M, Dowling MD, Cunningham I, Middleman MP, Clarkson BD (Memorial Sloan-Kettering Cancer Center, 1275 York Avenue, New York City). *Cancer* 37:1256–1264, 1976

The authors review the results of therapy of 23 adult and 75 children patients with acute lymphoblastic leukemia. Similar, intensive, sequential cytotoxic protocols (L 2) were used which included intrathecal methotrexate without cranial or craniospinal irradiation. The incidence of CNS relapse was 27.7% in the adult group and 7.1% in the children. Adults had IT MIX only in the first 2 months of therapy while the children received IT MIX twice weekly during maintenance therapy. The CNS relapse rate in children is felt to be comparable to that in studies using cranial or craniospinal irradiation.

Herbert C. Berry

Effective bone palliation as related to various treatment regimens. Allen KL, Johnson TW, Hibbs GC (Tom Johnson, Group Health Hospital, 200 15th Avenue East, Seattle, Washington 98102). *Cancer* 37:984–987, 1976

The authors retrospectively review the use of irradiation in the palliation of osseous metastases in 110 patients. Excluded were patients who died or were lost to followup within 2 months post treatment and those with pathologic fracture at the site of metastases. All treatments were given with supravoltage equipment and doses were converted into rets. Quantification of pain and narcotic requirements are not recorded. Systemic therapy was received by many patients before, during, and after irradiation. Those patients receiving systemic therapy were scattered equally between the low, medium, and high dosage range groups. Sixty one percent (92/152) of the patients had breast primaries, 19% (29/152) had prostatic primaries, and only 5% (7/152) had lung primaries. Permanent pain relief was obtained in 77%, 78%, and 80% of the low (500–860 rets), medium (980–1,320), and high (1,370–1,710 rets) dosage range groups for 152 fields treated.

Herbert C. Berry

Long-term effects of external radiation on the pituitary and thyroid glands. Zuks Z, Glatstein E, Marsa GW, Bagshaw MA, Kaplan HS (Stanford University School of Medicine, Stanford, California 94305). *Cancer* 37:1152–1161, 1976

The authors describe the incidence of thyroid dysfunction in patients irradiated for lymphoma or carcinoma of the head and neck. Of 235 Hodgkin's disease patients, all of whom had preirradiation lymphangiograms and a dose of from 4,000–5,000 rads, only 85 (36%) were euthyroid. One hundred and three (44%) were compensated hypothyroid, and 47 (20%) were hypothyroid (total thyroid dysfunction 150/235 or 64%). Of 62 non-Hodgkin's lymphoma patients (all had LAG), 36 (58%) had thyroidal dysfunction versus two of 14 (14%) who did not receive neck irradiation. In the control group of head and neck cancer patients (5,000–6,500 rads), 20 of 52 (38%) had thyroid dysfunction. The difference in the incidence of thyroid dysfunction between the lymphoma patients receiving neck irradiation including the thyroid versus head and neck patients is significant ($p < 0.05$).

Herbert C. Berry

Low dose bleomycin and methotrexate in cervical cancer. Conroy JF, Lewis GC, Brady LW, Brodsky I, Kahn SB, Ross D, Nuss R (Hahnemann Medical College and Hospital, Philadelphia, Pennsylvania 19102). *Cancer* 37:660–664, 1976

The authors report their experience in treating disseminated carcinoma of the cervix with a low-dose protracted combination schedule of bleomycin and methotrexate undertaken as a pilot study. Twenty patients received bleomycin, 10 mg/m² weekly and methotrexate, 10 mg/m² every fourth day for recurrent or disseminated carcinoma of the cervix. Fifty percent of the patients experienced no toxicity and bleomycin toxicity did not force discontinuation of that drug. Sixty percent (12/20) of the patients had greater than 50% response with a median remission of 7.5 months. No complete responses occurred.

Herbert C. Berry

The cardiotoxicity of adriamycin and daunomycin in children. Gilladoga AC, Manuel C, Tan C, Wollner N, Sternberg S, Murphy L (Memorial Sloan-Kettering Cancer Center, 1275 York Avenue, New York City 10021). *Cancer* 37:1070-1078, Feb 1976

The authors report on 50 children who received cumulative doses of adriamycin exceeding 500 mg/m². Ages ranged from 8 months to 15 years when adriamycin was first administered. Observation periods were 11-57 months. Eight children also received 1,000-5,000 rads (150-250 rad treatments) to the lungs and/or mediastinum involving the heart before or during adriamycin administration. Of the 42 children who had not received cardiac irradiation, four (9.5%) showed evidence of adriamycin cardiomyopathy; of the eight children receiving cardiac irradiation, four (50%) showed evidence of adriamycin cardiomyopathy ($p=0.02$). Of 60 children receiving daunomycin (age 10 months to 15 years) in cumulative doses over 500 mg/m² followed for 21-87 months, two (3.3%) developed severe cardiomyopathy. None had received incidental irradiation. Maximum cumulative dose recommendations are made.

Herbert C. Berry

Radiological manifestations of radiation-induced injury to the normal upper gastrointestinal tract. Goldstein HM, Robers LF, Fletcher GH, Dodd GD (M. D. Anderson Hospital and Tumor Institute, University of Texas System Cancer Center, Houston, Texas 77025). *Radiology* 117:135-140, Oct 1975

The authors describe their experience with the effects of therapeutic irradiation on the normal esophagus, stomach, and duodenum.

Esophageal manifestations were studied in 30 patients who received 4,500-6,000 rads in six to eight weeks to the mediastinum for bronchogenic, metastatic breast, and testicular carcinoma. The most frequent roentgenologic abnormality was altered esophageal motility. Failure of distal esophageal sphincter relaxation developed in several patients. Stricture occurred in five patients and ulceration in only one case.

Patients who received irradiation to the entire abdominal para-aortic lymph node chain for metastatic cervical carcinoma (121 females) and mixed testicular tumors (52 men) were evaluated for injury to the stomach and duodenum. Doses ranged from 4,000 to 5,000 rads. Frequency of gastric injury could not be determined due to short follow-up of some patients. Five patients developed prepyloric or pyloric ulcers with progressive gastric deformity and four of these failed to heal. Another five patients showed fixed narrowing and deformity of the antropyloric region with little peristaltic ac-

tivity. Few complications occurred in the testicular group, possibly due to some split course administration.

Duodenal manifestations of radiation injury were most prominent in the second portion and varied from large ulcerations to smooth strictures. Again, no significant healing occurred.

Both gastritis and ulceration develop at the 5,000 rad dose level. Pain associated with radiation-induced ulcer is often unrelenting and, despite intense medical management, surgery is often required since healing does not usually occur. Susceptibility to upper gastrointestinal injury resulting from therapeutic irradiation appears to depend on the time-dose relationship and unknown factors of individual sensitivity.

Odis D. Skinner

Radiobiology

Bone marrow scanning with ⁵²Fe. Knospe WH, Rayudu VMS, Cardello M, Friedman AM, Fordham EW (Radiohematology Laboratory, Rush-Presbyterian-St. Lukes Medical Center, 1753 West Congress Parkway, Chicago, Illinois 60612). *Cancer* 37:1432-1442, 1976

The authors have studied 25 patients with malignant lymphoma 0 to 73 months after irradiation by ⁵²Fe bone marrow scanning. Regeneration of the irradiated marrow usually occurred 1 to 2 years after 4,400 rads. Expansion of the erythropoiesis into inactive areas of yellow marrow occurred by 3 months post irradiation and declined after 2 years. This study is felt to be similar to the recent report of Rubin who studied a similar group of irradiated patients using 99 Technetium sulfur colloid.

Herbert C. Berry

The effect of radiation therapy on lymphocyte subpopulations in cancer patients. Raben M, Walach N, Galili U, Schlesinger M (Bowman-Grey School of Medicine, Winston-Salem, North Carolina). *Cancer* 37:1417-1421, 1976

The proportion of T and B lymphocytes in the peripheral blood was determined in patients slated to receive either mediastinal (breast cancer) or pelvic (various pelvic malignancies) irradiation. The level of cells with T cell markers was diminished more than those with B cell markers. Pelvic irradiation resulted in a more rapid reduction without the final relative proportions being greater when compared to the breast cancer patients. Thymic irradiation does not appear to be a requisite for the reduction of T lymphocytes.

Herbert C. Berry

Book Reviews

Radioimmunoassay. Edited by Leonard M. Freeman and M. Donald Blaufox. New York: Grune & Stratton, cloth, 162 pp., 1975. \$14.50

The chapters in this text originally appeared in the April and July, 1975 issues of *Seminars in Nuclear Medicine*. This book is unique among radioimmunoassay texts in that there is considerable discussion of commercial radioimmunoassay kits. The initial chapters are devoted to the basic principles of radioimmunoassay, such as antisera and radioactive substrate production and techniques of separation of assay components as the final step in a RIA system. Also discussed are the direct curve-fitting methods employed to analyze the calibration curves of commercial kits.

The remainder of the book is clinically oriented with an in-depth discussion of different radioimmunoassays with particular emphasis on commercial kits including kit pitfalls. Specific topics discussed are clinical applications of radioimmunoassays of insulin, renin, digoxin, gastrin, carcinoembryonic antigen, growth hormone, thyroid hormones, and principal reproductive steroids and peptide

hormones. The chapters on digoxin and thyroid hormones are particularly well detailed and are of great value to the practicing physician.

The illustrations are excellent and the text is written in a very readable manner.

Because this text examines in some detail the various commercial radioimmunoassay kits, it is especially useful for the nuclear medicine physician or nuclear radiologist or pathologist who is involved in the management of a radioimmunoassay service. This text will also be of value to other physicians because of the excellent discussions of clinical applications of the different radioimmunoassays.

Larry D. Greenfield
City of Hope National Medical Center
Duarte, California

Radiology of the Orbit, vol. 7, Saunders Monographs in Clinical Radiology. By Glyn A. Lloyd. Philadelphia: W. B. Saunders, 216 pp., 1975. \$22.50

Glyn Lloyd's book on orbital radiology is a concise and complete treatise on a subject not previously covered comprehensively. The author is a world authority on the subject and, the material is accurate, appropriate, and up-to-date. In addition to the wealth of information presented, the book's strength lies in its organization which enables the reader to grasp concepts and facts easily. In the first five chapters, the techniques currently used in the roentgenographic examination of the eye are described, beginning with the least invasive and progressing to the most invasive techniques. The internal organization of these chapters is also excellent.

In chapters six through 10 the most common pathologic conditions of the orbit (including unilateral exophthalmos, vascular anomalies, tumors, and pseudotumors, lesions of the head and neck which may affect the orbit, and fractures of the orbit) are discussed. Again, the internal organization of these chapters is excellent starting with techniques to investigate these problems and

ending with pathology. In Chapters 11 and 12, dacryocystography and localization of foreign bodies in the eye are discussed.

There are only a few undesirable features of this text. Arrows would have been helpful on the ultrasound illustrations for the physician uninitiated in orbital ultrasound. Some of the illustrations are photographed with a small field making it difficult to obtain a point of reference. Also, some of the pictures in the initial chapters are annotated with hand-drawn arrows. These complaints are certainly minor and do not detract from the overall value of this well written monograph. Lloyd's book would be appropriate reading for radiologists, neuroradiologists, neurologists, neurosurgeons, head and neck surgeons, and ophthalmologists.

William W. Olmsted
St. Mary's Hospital and Medical Center
San Francisco

Wilms' Tumor. Edited by Carl Pochedly and Dennis Miller. New York: John Wiley & Sons, 239 pp., 1976. \$22.50

This relatively short volume is easily completed in no more than 4 to 5 hr concentrated reading. Its purposes, as stated by the editors, are "to survey in depth the biologic and clinical behavior of Wilms' tumor," and "to provide an up-to-date compendium on the optimal management of this disease for practicing physicians."

The book is divided into 14 chapters, each by a different author. The chapters cover aspects of Wilms' tumor which include historical perspectives, clinical, biochemical, and pathological manifestations of the tumor, diagnostic work-up, and therapeutic management of the patient. Immunologic, genetic, and teratogenic aspects of the tumor are also discussed. Because of the multiple author approach, repetition of material is frequent—at times tedious. (In two separate chapters the identical philosophical quotation from the early literature is used to illustrate a point.) The style of writing and depth of

discussion varies considerably from author to author. The illustrations can only be ranked as fair; some must be classified as poor.

The value of this book does not rest in its discussion of the clinical presentation or workup of the patient with Wilms' tumor, since these portions of the discussion should already be understood by the radiologist who deals with Wilms' tumor with any frequency. The book does provide, however, a ready reference to current treatment modalities for Wilms' tumor and a review of current research particularly in areas of biochemistry, immunology, genetics, teratology, and treatment.

Sandra G. Kirchner
Vanderbilt University Hospital
Nashville, Tennessee

Fundamentals of Abdominal and Pelvic Ultrasonography. By George R. Leopold and W. Michael Asher. Philadelphia: W. B. Saunders Co., 261 pp., 1975. \$21.50

This book is the latest general text on diagnostic ultrasound. In the preface, the authors state that the intent of the book is to describe the technique of scanning and the anatomic interpretation

which they feel has been deficient in other textbooks. They also state they will omit the physics of diagnostic ultrasound and ultrasound machinery because there are other suitable texts which fully

cover these areas.

The first chapter concentrates on ultrasound scanning techniques and other practical areas, such as record keeping, and types of image display. The next seven chapters are devoted to abdominal scanning, which includes: liver, gallbladder, pancreas, spleen, urinary tract, retroperitoneal area, and aorta. Two subsequent chapters are devoted to pelvic ultrasonography and to the gravid uterus. The last two chapters are directed toward gray scale imaging and the clinical applications of abdominal scanning. There is an additional section with 12 color plates of transverse and longitudinal autopsy specimens with accompanying line drawings to display more vividly the normal cross-sectional anatomy seen on an ultrasound examination.

The method used throughout the book is to describe the basic ultrasound technique most useful in each organ or organ system and to supplement this with numerous ultrasound images displaying the normal and pathologic anatomy in each of these areas. One criticism of the book, however, is that the scanning techniques de-

scribed are primarily the techniques used in bistable scanning and the vast majority of the ultrasound images used in the text are bistable pictures. A further criticism of the text is that the orientation of the ultrasound pictures is as if one were viewing the transverse views from above rather than from below. The latter is the format in which most published ultrasound scans are presented. This can be confusing to a beginner in the field of ultrasound. It also is somewhat disappointing to discover the paucity of gray scale imaging when most of the field of ultrasound has converted from the bistable display to the gray scale format.

In general, the text is well written and for the most part the authors have achieved their stated goal of describing the techniques of scanning and the anatomic interpretation of the normal and abnormal anatomy depicted on scans. Aside from these shortcomings, I feel the book would make a useful addition to the ultrasound library of both physician and technician.

Michael S. Shaub
Los Angeles County/USC Medical Center

M-Mode Echocardiographic Techniques and Pattern Recognition. By Sonia Chang. Philadelphia: Lea & Feibiger, 160 pp., 1976. \$7

The author describes this monograph as a "procedure manual," and as such it succeeds rather well. Though the student will have to look elsewhere for the theory, the practical aspects of an echocardiographic examination are described clearly and concisely. The text is richly supplemented by illustrations of excellent quality.

The book begins with a discussion of instrumentation. Although necessarily somewhat limited and oversimplified, this provides a good overview of the operator-controlled variables in echocardiography and serves to introduce the rest of the work.

Subsequent chapters deal with specific areas of examination, covering techniques used in obtaining an adequate tracing and interpretation of the study.

The tone of the work is somewhat uneven, making it difficult to determine the author's intended audience. Some discussion assumes knowledge of the field, while other statements are seemingly directed at the neophyte. One is presumed to know the cardiac events which give rise to the labeled points on a mitral valve tracing, yet the glossary contains definitions of "homogeneous material" and "sound beam." In some places the obvious is overstated. Yet, something far less obvious to a novice such as the apparent projection of a prosthetic valve ball beyond the confines of the cage goes unmentioned.

Chang's practical suggestions on avoiding technical and diagnostic pitfalls are particularly helpful. Her warnings against overreading of aortic cusp separation, left atrial thrombus, and valvular vegetations are especially valuable; perhaps the most important thing to learn is what echocardiography *cannot* do.

The author herself illustrates the difficulty of avoiding such pit-

falls by twice falling into the very traps she describes. Her illustration of mitral valve vegetations is impressive, but I question whether this condition can be reliably diagnosed echocardiographically. "It would be best" as Chang says, "to underread this event." Shortly after describing the illusion of exaggerated motion in condensed-time scanning, Chang illustrates the "exaggerated motion" of the septum in mitral insufficiency. However, when one measures the motion, one finds no difference from the normal.

The book was intended to be read without the distraction of footnotes. This is in general a convenient presentation, and the excellent reference sections at the end of each chapter are quite sufficient for the more inquiring reader. Still, there are a few assertions which should have been supported by annotation.

Also, a few statements, more misleading than erroneous, need to be corrected. The identification of septal thickening as the asymmetrical septal hypertrophy of IHSS seems to minimize the most important element, the asymmetry. Also, the apparent equating of a thin line tracing and a thin valve indicates a tendency to think of the tracing as an anatomic depiction of the cardiac structure. This can lead to very misleading assumptions and should be avoided.

These minor criticisms are not intended to detract from the overall value of this book. This is not a definitive treatise on cardiac ultrasound, and within the limits the author has set herself, she has produced a useful, and very usable, manual of m-mode echocardiography.

Michael Grossman
Newport Beach, California

Fundamentals of Radiology, 2d ed. By Lucy Frank Squire. Cambridge, Mass.: Harvard University Press, 366 pp., 1975. \$17

Lucy Squire has chosen to call this beautiful new edition of her justifiably much-praised textbook for medical students *Fundamentals of Radiology*. The change from roentgenology to radiology was made to be more in keeping with current usage, but it is a little misleading since radiation therapy and nuclear radiology are not discussed, and only x-ray imaging is illustrated and explained.

A few important and noticeable changes mark the production of this new edition. Many of the illustrations have been improved, and some have been discarded. New illustrations have been added, and a little confusing illustrative material has been clarified. The result is a much better book in terms of the illustrations. Even the clarity of reproduction has been improved. The type is cleaner and easier to read, and it is a joy to read a book in which, when the text

refers to an illustration, one finds the picture in question without having to turn the page. The author writes with style and clarity, and while there have been very few changes in the text of this new edition, some portions have been emphasized with italics. Some sections have been revised and improved, particularly those on radiation hazards and on the kidney and gallbladder. An index has been added, preceded by a warning to students not to use the book as a reference work. I quite agree that the index is superfluous; the book should be read from start to finish and not be used as a library in which to investigate the radiologic appearance of some particular entity.

For the most part, the contents of *Fundamentals of Radiology* are not different than found in the first edition. The table of con-

tents shows few headings different from previously published, and even the page numbers are for the most part the same. A large part of the book deals with the chest, and while that may be justified because of the wealth of opportunities found in the thorax to illustrate principles of interpretation, the result is a lopsided presentation with overemphasis on the thorax when the book is viewed as a whole. By mentioning that, the reviewer betrays his own inability to use the book precisely as the author intended, secretly desiring, instead, a volume that covers everything completely.

The colored illustrations in the bone section are the same as those in the first edition, though they seemed sharper in the current edition when compared with an older copy. They are beautiful examples of radiologic-pathologic correlation, and they add considerably to the students' ability to make the mental conversion from radiologic images to their anatomical and pathological equivalents. Also notable are the coronal, sagittal and cross sections of body parts sprinkled throughout the book. They encourage the student to think three dimensionally about the body and are genuine

aids to memory.

But best of all is the humor and wit and intelligence of the author which illuminate every page of this fine book. Boredom has been avoided by the use of familiar examples and arresting challenges, and the tone of the book has been kept light and friendly so the student never feels lectured to or preached at. The reader is made to feel he is a companion in learning with a wise and helpful guide.

The book is best used as required reading for medical students pursuing elective studies in diagnostic radiology, and we have used Squire's first edition for years with our students. It must be supplemented with material designed to teach the student more specific information regarding x-ray contributions to the diagnosis of specific diseases, but it has no parallel when it comes to teaching basic principles of roentgen interpretation and the kind of reasoning required for the unravelling of otherwise mysterious x-ray images.

Melvyn H. Schreiber
Galveston, Texas

Books Received

Receipt of books is acknowledged as a courtesy to the sender. Books that appear of sufficient interest will be reviewed as space permits.

Special Procedures in Chest Radiology. By Stuart S. Sagel. Philadelphia: W. B. Saunders, 219 pp., 137 illustrations, 1976. \$17.50

Tumors of the Kidney, Renal Pelvis, and Ureter. By James L. Bennington and J. Bruce Beckwith. Washington, D.C.: Armed Forces Institute of Pathology, paper, 353 pp., numerous illustrations, 1975. \$6.50

Traité de Radiodiagnostic. Tome XI. Rhumatologie. Articulations. Parties Molles. Edited by Raymond Trial, Maurice Laval-Jeantet, and Marie-Christine Plainfossé. Paris: Masson, 451 pp., 545 figures, 1976. 540 FF

Ultrasonics in Medicine. Edited by E. Kazner, M. de Vlieger, H. R. Müller, and V. R. McCready. Amsterdam and New York: Elsevier Excerpta Medica North-Holland, paper, 360 pp., illustrated, 1975. \$46.50

Radiopharmacy. Edited by Manuel Tubis and Walter Wolf. New York: John Wiley & Sons, 911 pp., 1976. \$44.50

Radiology of the Small Intestine, 2d ed. By Richard H. Marshak and Arthur E. Lindner. Philadelphia: W. B. Saunders, 620 pp., 592 illustrations, 1976. \$37.50

Angiography of Posterior Fossa Tumors. By Samuel M. Wolpert. New York: Grune & Stratton, 196 pp., illustrated, 1976. \$23.50

Chronic Airflow Obstruction in Lung Disease. By William M. Thurlbeck. Philadelphia: W. B. Saunders, 456 pp., 186 illustrations, 1976. \$17

Administration of a Radiology Department. By Murray L.

Janower. Springfield: Charles C Thomas, 59 pp., 1976. \$7.50

Cancer Therapy Abstracts. Edited by Chester M. Southam, George P. Studzinski, George Zinniger, Gordon Schwartz, and Jussi J. Saukkonen. Philadelphia: Franklin Institute Press, 1975, first issue. \$45 for 12 issues

Diagnostic Neuroradiology. Vols. 1 and 2, 2d ed. By Juan M. Taveras and Ernest H. Wood. Baltimore: Williams & Wilkins, 1252 pp., illustrated, 1976. \$79.50 per set

Atlas of Scanning Electron Microscopy in Microbiology. By Zensaku Yoshii, Junichi Tokunaga, Jutaro Tawara. Baltimore: Williams & Wilkins, 233 pp., illustrated, 1976. \$50

Radiotherapy in Modern Clinical Practice. Edited by H. F. Hope-Stone. St. Louis: C. V. Mosby, 358 pp., illustrated, 1976. \$24.50

International Histological Classification of Tumours No. 13: Histological Typing of Female Genital Tract Tumors. By H. E. Poulsen and C. W. Taylor. Geneva: World Health Organization, 89 pp., illustrated, 1975. Sw. fr. 75; with 124 color transparencies, Sw. fr. 200

Parathormone and Calcitonin Radioimmunoassay in Various Medical and Osteoarticular Disorders. By Paul Franchimont and Guy Heynen. Philadelphia: J. B. Lippincott, paper, 134 pp., 6 illustrations, 18 tables, 1976. \$15

Natural Background Radiation in the United States. Report no. 45, Recommendations of the National Council on Radiation Protection and Measurements. Washington, D.C.: National Council on Radiation Protection and Measurements, paper, 163 pp., 1975

Synopsis of Analysis of Roentgen Signs in General Radiology. By Isadore Meschan. Philadelphia: W. B. Saunders, 677 pp., 583 illustrations, 1976. \$26

News

Medical Instrumentation Meeting

The 12th annual meeting and exhibit program of the Association for the Advancement of Medical Instrumentation will be in San Francisco at the Hyatt-Regency Hotel, March 13-17, 1977. Meeting objectives include a review of major developments and trends in medical instrumentation and constructive interaction between all health care professionals. Information is available from AAMI, 1901 North Fort Meyer Drive, Suite 602, Arlington, Virginia 22209.

Pediatric Radiology Postgraduate Course

Pediatric Radiology in the General Hospital is the title of a course to be presented November 4-6 at the Colonnade Hotel in Boston. Sponsored by the Department of Pediatric Radiology of Boston University School of Medicine, the course will be a comprehensive review of the principles of pediatric radiology primarily for general radiologists in community hospitals who do radiologic diagnosis in infants and children. Recent advances in the field will also be covered. Fee is \$175. For additional information contact the Department of Postgraduate Education, Boston University School of Medicine, 80 East Concord Street, Boston, Massachusetts 02118, or telephone 617-247-5602.

CT of Cranium and Body

A seminar course in Computerized Tomography of the Cranium and Body is scheduled for December 9-12 at the Aladdin Hotel, Las Vegas, Nevada. The course is organized by David O. Davis and P. Ruben Koehler of George Washington University and University of Utah, respectively. The course is approved for 20 hours Category I credit. Information is available from D. O. Davis, Radiology Department, George Washington University Hospital, 901 23rd Street, N.W., Washington, D.C. 20037, telephone 202-676-2710.

Radiology of Chest

Radiology of the Chest is the title of a postgraduate course to be held October 27-29 in Mexico City. Fee is \$120 (\$60 for residents) for the session which carries 22 hours Category I credit. For information contact R. Moncada, Department of Radiology, Loyola University Medical Center, 2160 South First Avenue, Maywood, Illinois 60153.

Otology and Oto-Radiology Symposium

The first midwinter Symposium on Frontiers in Otology and Oto-Radiology will take place February 12-19, 1977, in Aspen, Colorado. The American Hearing Research Foundation and Northwestern University are cosponsors. The course carries 32 hours Category I credit. Additional information may be obtained from George E. Shambaugh, Jr., American Hearing Research Foundation, 55 East Washington Street, Suite 2105, Chicago, Illinois 60602.

Stomach and Small Intestine Course

An intensive course on the radiology of the stomach and small intestine will be October 25-29 at the Copley Plaza Hotel, Boston. The course is sponsored by Tufts University School of Medicine.

Faculty includes Robert Paul, Arthur Clemett, Wylie Dodds, Joseph Ferrucci, Jack Wittenberg, and Basil Morson. Each area will be considered from a clinical, endoscopic, radiological, and pathological point of view. Registration fee is \$250. Additional information is available from Emelie S. Born, Box 72, 136 Harrison Avenue, Boston, Massachusetts 02111.

Head Computed Tomography

A 2 day introductory course, Computerized Tomography—Head, will be September 27-28 in Baltimore. The Johns Hopkins Medical Institutions is sponsoring the course for radiologists, neurologists, neurosurgeons, and other physicians with a clinical interest in CT of the head. The program will be devoted to basic principles of equipment operation, normal anatomy, pitfalls in interpretation, plus an evaluation of circulatory, degenerative, inflammatory, posttraumatic, and neoplastic disorders. The course carries 15 hours Category I credit. Fee is \$175 and includes a collection of 100 EMI scans on proven interesting cases. For more information contact Janet B. Hardy, Office of Continuing Education, Room 17, Turner Auditorium, Baltimore, Maryland 21205.

Arthrography Course and Workshop

An arthrography course and workshop is scheduled for December 2-4 at the Hospital for Special Surgery, New York City. Tuition is \$200 for the sessions which carry 16 hours Category I credit. Additional information is available from course director Robert H. Freiburger, Hospital for Special Surgery, 535 East 70th Street, New York 10021.

Body Imaging Conference

The First Annual Body Imaging Conference will be October 9-17 at the Kona Surf Hotel in Kona, Hawaii. Sponsored by the radiology department of West Park Hospital, Canoga Park, California, the conference will provide basic and in-depth comparative and correlative analysis of the indications, limitations, and interpretation of computed tomography, gray scale ultrasonography, and nuclear imaging. Registration fee is \$295 for the conference which is approved for Category I credit. For additional information contact course coordinator Ronald J. Friedman, Department of Radiology, West Park Hospital, 22141 Roscoe Boulevard, Canoga Park 91304.

Computed Tomography: Body and Head

A practical course in computed tomography will be sponsored by the Mallinckrodt Institute of Radiology October 29-31. Leading experts in the field will join faculty of the Mallinckrodt Institute in presenting an up-to-date assessment of the state of the art. Two-thirds of the course will be devoted to the body and one-third to the head. The course will be at the Chase Park Plaza Hotel, St. Louis, Missouri. Inquiries should be directed to Sue Day (314-454-2191).

Stroke Conference

The second National Conference on Cerebrovascular Disease and Cerebral Circulation will be February 25-26, 1977 in Miami, Florida. For more information, write: Administrator, Postgraduate Courses, American Heart Association, 7320 Greenville Avenue, Dallas, Texas 75231.

BRH to Propose X-ray Quality Assurance Recommendations

The Food and Drug Administration's Bureau of Radiological Health (BRH) has issued an Advance Notice of Intent to Propose Recommendations for quality assurance programs in diagnostic x-ray facilities. The goal of the planned recommendations is to encourage health practitioners and others responsible for the operation of diagnostic x-ray facilities to voluntarily establish quality assurance programs.

Interested persons are urged to participate in development of the recommendations by submitting comments and suggestions on the design, components, and implementation of quality assurance programs for various types of facilities. BRH also seeks information on personal experiences with facility-based diagnostic x-ray quality assurance programs. Respondents are asked to refer to the advance notice in the May 7, 1976, *Federal Register* (41FR18863) for the list of questions on which comments are solicited. Copies of the advance notice may be obtained from the Division of Training and Medical Applications (HFX-70), Bureau of Radiological Health, 5600 Fishers Lane, Rockville, Maryland 20852. Comments should be submitted in writing to the Hearing Clerk, Food and Drug Ad-

ministration, Room 4-65, 5600 Fishers Lane, Rockville, Maryland 20852.

Comments received by November 3 will be considered during formation of the recommendations. Proposed recommendations will be published in the *Federal Register* for further comment.

Radium Society Annual Meeting

Abstracts are now being solicited for the 1977 meeting of the American Radium Society which will be in Las Vegas April 24-28. The Scientific Program Committee has selected six major topics: cancer of the breast, cancer of the gastrointestinal tract, head and neck cancer, small round cell tumors of the bone, impact of surgical staging on treatment of gynecologic cancer, and significance of various tests of immunocompetence.

Abstracts should be limited to 250 words and must be submitted no later than November 15 to Luther W. Brady, Hahnemann Medical College and Hospital, 230 North Broad Street, Philadelphia, Pennsylvania 19102. An original and 10 copies are required. Additional information is available from Dr. Brady.

Radiologic Societies

International Societies

Fleischner Society. Secretary, E. Robert Heitzman, State University of New York Upstate Medical Center, Syracuse NY 13210. Annual Meeting: 1977, Town and Country Convention Center, San Diego CA, Feb 27–Mar. 2.

Inter-American College of Radiology. Secretary, Gaston Morillo, Department of Radiology, Jackson Memorial Hospital, 1611 NW 12th Avenue, Miami FL 33136.

International Skeletal Society. Secretary-Treasurer, Jack Edeiken, Radiology Dept. Thomas Jefferson University Hospital, 11th and Walnut Sts, Philadelphia PA 19107.

International Society of Radiology. Hon. Secretary-Treasurer, W. A. Fuchs, Department of Diagnostic Radiology, University Hospital, Inselspital, CH-3010 Bern, Switzerland.

U.S. National Societies

American Association of Physicists in Medicine. Secretary, John Wright, Radiology Department, Geisinger Medical Center, Danville PA 17821.

American Board of Radiology. Secretary, C. Allen Good, Kahler East, Rochester MN 55901.

American College of Radiology. Executive Director, William C. Stronach 20 N. Wacker Drive, Chicago IL 60606.

American Institute of Ultrasound in Medicine. Executive Secretary, Donna LaMaster, PO Box 25065, Oklahoma City OK 73125.

American Nuclear Society. Program Chairman, Ted D. Tarr, U.S. Energy Research and Development Administration, Mail Station A-436 Office of Assistant Administrator for Nuclear Energy, Washington DC 20545.

American Osteopathic College of Radiology. 1976 Program Chairman, Joseph C. Andrews, 13355 East Ten Mile Road, Warren MI 48089. 1977 Program Chairman, George O. Faerber, 1087 Dennison Avenue, Columbus OH 43201. Annual Meeting: Oct 17–21, 1976, New Orleans LA.

American Radium Society. Secretary, Richard H. Jesse, Dept of Surgery, M.D. Anderson Hospital and Tumor Institute, Houston TX 77025. Annual Meeting: Las Vegas, April 24–28.

American Roentgen Ray Society. Secretary, James Franklin Martin, 300 S. Hawthorne Rd., Winston-Salem NC 27103.

American Society of Neuroradiology. Secretary, Arthur E. Rosenbaum, University of Pittsburgh School of Medicine, Pittsburgh PA 15261. Annual Meeting: March 27–April 1, Hamilton Princess Hotel, Bermuda.

American Society of Therapeutic Radiologists. Secretary, Robert W. Edland, 1836 South Ave., LaCrosse WI 54601. Annual Meeting: Oct 13–17, 1976, Hyatt Regency, Atlanta GA.

Association of University Radiologists. Secretary-Treasurer, Gerald T. Scanlon, Milwaukee County Medical Center, Milwaukee, WI 53226. Annual Meeting: April 30–May 4, 1977, Kansas City KA.

Health Physics Society. Executive Secretary, Richard J. Burk, Jr., 4720 Montgomery Lane, Bethesda MD 20014.

North American Society of Cardiac Radiology. Secretary-Treasurer, Erik Carlsson, University of California, San Francisco CA 94143.

Radiation Research Society. Executive Director, Richard J. Burk, Jr., 4720 Montgomery Lane, Bethesda MD 20014.

Radiological Society of North America, Inc. Secretary, Theodore A. Tristan, Fifteenth Floor, One MONY Plaza, Syracuse NY 13202. Annual Meeting: 1976 Nov 14–19; 1977, Nov 27–Dec 2; 1978, Nov 26–Dec 1, all in Chicago IL.

Section on Radiology, American Medical Association. Secretary, Antolin Raventos, Dept of Radiology, School of Medicine, University of California, Davis.

Society of Gastro-Intestinal Radiologists. Secretary-Treasurer, Walter Whitehouse, Dept of Radiology, University of Michigan, Ann Arbor MI 48104.

Society of Nuclear Medicine. President, 475 Park Avenue S, New York NY 10016.

Society for Pediatric Radiology. Secretary-Treasurer, John P. Dorst, 601 N Broadway, Baltimore MD 21205.

The Society of Uroradiology. Secretary-Treasurer, Howard M. Pollack, Dept of Radiology, Episcopal Hospital, Front St at Lehigh Ave, Philadelphia PA 19125.

U.S. State and Local Societies

Alabama

Alabama Academy of Radiology. Secretary-Treasurer, Lawrence E. Fetterman, 1720 Springhill Ave, Suite 201, Mobile AL 36604.

Section of Radiology, National Medical Association. Secretary, Ivy Brooks, Dept of Radiology, Veterans Administration Hospital, PO Box 511, Tuskegee AL 36083.

Southern Radiological Conference. Secretary-Treasurer, J. W. Maxwell, PO Box 2144, Mobile AL 36601. Annual Meeting: Jan 28–30, 1977, Grand Hotel, Point Clear AL 36564.

Alaska

Alaska Radiological Society. Chapter ACR. Secretary-Treasurer, John J. Kottra, 3200 Providence Ave. Anchorage AK 99504.

Arkansas

Arkansas Chapter of ACR. Secretary-Treasurer, Richard Seibold, Jr., Wadley Hospital, Texarkana AR 75501.

Arizona

Arizona Radiological Society. Chapter of ACR. Secretary, Irwin M. Freundlich, 1501 N Campbell Ave, Dept of Radiology, Tucson AZ 85724.

California

California Radiological Society, California Chapter of ACR. Executive Secretary, J. Michael Allen, 1225 8th St, Suite 590, Sacramento CA 95814.

East Bay Radiological Society. Secretary-Treasurer, Richard H. Culhane, 4 Vista del Mar, Orinda CA 74563.

Los Angeles Radiological Society. Secretary, Arthur F. Schanche, 333 N Prairie Ave, Inglewood CA 90301.

Northern California Radiological Society. Secretary, Patrick J. Grinsell, 1207 Fairchild Ct, Woodland CA 95695.

Northern California Radiotherapy Association. Secretary-Treasurer, John D. Earle, Stanford Medical Center, Stanford CA 94305.

Orange County Radiological Society. R. Lawrence Argue, 100 E Valencia Mesa Dr, Fullerton CA 92632.

Radiological Society of Southern California. Secretary-Treasurer, Duane Eugene Blickenstaff, La Jolla Radiology Medical Group, Inc, 7849 Fay Ave, La Jolla CA 92037. Meetings: Oct 1976, Santa Barbara; Dec 1976, Newport; Feb 1977, Palm Springs.

Redwood Empire Radiological Society. Secretary, Hal B. Peterson, 357 Perkins St, Sonoma CA 95476.

San Diego Radiological Society. President, Donald J. Fleischli, 7849 Fay Ave, La Jolla CA 92037.

South Coast Radiological Society Chapter of ACR. Secretary-Treasurer, Brian R. Schnier, Dept of Radiology, Cottage Hospital, Pueblo at Bath, Santa Barbara CA 93105.

Southern California Radiation Therapy Society. Secretary-Treasurer, Jerome Stuhlberg, 514 N Prospect, Redondo Beach CA 90277.

Colorado

Colorado Radiological Society, Chapter of ACR. Secretary, John Pettigrew, 2215 N Cascade, Colorado Springs CO 80907.

Rocky Mountain Radiological Society. Secretary-Treasurer, Lorenz R. Wurtzebach, 4200 E 9th Ave., Denver CO 80220.

Connecticut

Connecticut Valley Radiologic Society. Secretary-Treasurer, Gerald N. LaPierre, 759 Chestnut St, Springfield MA 01107.

Radiological Society of Connecticut, Inc. Secretary, Gerald L. Baker, 85 Jefferson St, Hartford CN 06106.

Delaware

Delaware Chapter of ACR. Secretary, Ekkehard S. Schubert, Wilmington Medical Center, PO Box 1951, Wilmington DE 19899.

District of Columbia

Section on Radiology, Medical Society of the District of Columbia. Secretary-Treasurer, Albert M. Zelna, 21 Masters St, Potomac MD 20854.

Florida

The Florida Radiological Society, Chapter of ACR. Secretary, John T. Johnson, P.O. Box 2075, Sanford FL 32771.

The Florida West Coast Radiological Society, Inc. Secretary-Treasurer, Aaron Longacre, 501 E Buffalo Ave, Tampa FL 33606.

Greater Miami Radiological Society. Secretary, Kenneth D. Keusch, 6201 S.W. 112th St., Miami FL 33156.

North Florida Radiological Society. Secretary, Charles E. Bender, 1430 16th Ave S, Jacksonville Beach FL 32250.

Georgia

Atlanta Radiological Society. Secretary-Treasurer, James H. Larose, Dept of Nuclear Medicine, South Fulton Hospital, East Point GA 30344.

Georgia Radiological Society, Chapter of ACR. Secretary, E. P. Rasmussen, Piedmont Professional Bldg, 35 Collier Rd NW, Atlanta GA 30309.

Hawaii

Hawaii Radiological Society, Chapter of ACR. Secretary-Treasurer, Michael J. McCabe, Straub Clinic and Hospital, Honolulu HI 96813.

Illinois

Chicago Radiological Society, Division of the Illinois Radiological Society, Chapter of ACR. Secretary-Treasurer, Harold J. Lasky, 55 E Washington St, Suite 1735, Chicago IL 60602.

Illinois Radiological Society, Inc., Chapter of ACR. Secretary, Robert D. Dooley, Hinsdale Medical Center, Hinsdale IL 60521.

Indiana

Tri-State Radiological Society. Secretary Thomas Harmon, St. Mary's Hospital, Evansville IN 47750.

Iowa

Iowa Radiological Society, Chapter of ACR. Secretary-Treasurer, Dale L. Roberson, 1948 First Ave NE, Cedar Rapids IA 52402.

Kansas

Kansas Radiological Society, Chapter of ACR. Secretary-Treasurer, Ralph H. Baehr, 310 Medical Arts Bldg, Topeka KA 66604.

Kentucky

Bluegrass Radiological Society. Secretary-Treasurer, James King, 3313 Overbrook Dr, Lexington KY 40504.

Kentucky Chapter of ACR. Secretary-Treasurer, John Hummel, Jr., Kentucky Baptist Hospital, Louisville KY 40204.

Louisiana

Ark-La-Tex Radiological Society. Secretary, Erich K. Lang, Confederate Memorial Medical Center, LSU School of Medicine, Shreveport LA 71101.

Louisiana Radiological Society, Chapter ACR. Secretary-Treasurer, Stover L. Smith, 250 Vincent Ave, Metairie LA 70005.

Section on Radiology, Southern Medical Association. Secretary, Michael Sullivan, 1514 Jefferson Highway, New Orleans LA 70121. Annual Meeting: Nov 7-10, 1976, New Orleans.

Maine

Maine Radiological Society, Chapter of ACR. Secretary-Treasurer, Peter E. Giustra, Dept of Radiology, Penobscot Bay Medical Center, Rockland ME 04841.

Maryland

Maryland Radiological Society, Chapter of ACR. Secretary, David S. O'Brien, Anne Arundel Hospital, Annapolis MD 21401.

Massachusetts

Massachusetts Radiological Society, Chapter of ACR. Secretary, Alan H. Robbins, 150 S. Huntington Ave., Boston MA 02130.

New England Roentgen Ray Society. Secretary, Melvin E. Clouse, 185 Pilgrim Rd, Boston MA 02115.

Pilgrim Rd, Boston MA 02115. Scientific Meetings: Oct 15 and Dec 3, 1976; Feb 18, March 18, April 15, and May 20, 1977; 911 Longwood Towers, Brookline, Mass.

Northeastern Society for Radiation Oncology. Secretary, C. C. Wang, Massachusetts General Hospital, Boston MA 02114.

Michigan

Michigan Radiological Society, Chapter of ACR. Secretary-Treasurer, Francis P. Shea, Bon Secours Hospital, 468 Cadieux, Grosse Pointe MI 48230.

Michigan Society of Therapeutic Radiologists. Secretary-Treasurer, William T. Knapp, St. Mary's Hospital, 830 S Jefferson, Saginaw MI 48601. Annual Meeting: Sept 1976, Ann Arbor.

Minnesota

Minnesota Radiological Society. Secretary-Treasurer, Marvin E. Goldberg, Box 292, Mayo Memorial Health Sciences Center, Minneapolis MN 55455.

Missouri

Greater Kansas City Radiological Society. President-Secretary, Jay I. Rozen, Suite 216, 6400 Prospect, Kansas City MO 64132.

Greater St. Louis Society of Radiologists. Secretary-Treasurer, William B. Hutchinson, 2821 Ballas Rd, St. Louis MO 63131. Annual Meeting: Oct 1976, St. Louis.

Missouri Radiological Society, Chapter of ACR. Secretary-Treasurer, Ronald G. Evens, Mallinckrodt Institute of Radiology, 510 S. Kingshighway, St. Louis MO 63110.

Mississippi

Mississippi Radiological Society, Chapter of ACR. Secretary-Treasurer, James B. Barlow, 514B E Woodrow Wilson, Jackson MS 39216.

Nebraska

Nebraska Chapter of ACR. Secretary-Treasurer, Charles A. Dobry, Dept of Radiology University of Nebraska Medical Center, 42nd at Dewey, Omaha NE 68105.

New Hampshire

New Hampshire Chapter of ACR. Secretary-Treasurer, Edward P. Kane, Claremont General Hospital, Claremont NH 03743.

New Jersey

Radiological Society of New Jersey, Chapter of ACR. Secretary, Fred M. Palace, 2424 Morris Ave, Union NJ 07083.

New Mexico

New Mexico Society of Radiologists, Chapter of ACR. Secretary, W. M. Jordan, 1100 Central Ave SE, Albuquerque NM 87106.

New York

Bronx Radiological Society, New York State, Chapter of ACR. Secretary-Treasurer, Leon J. Corbin, 1369 Rosendale Ave, Bronx NY 10472.

The Brooklyn Radiological Society. Secretary-Treasurer, Ralph Brancaccio, 7901 4th Ave, Brooklyn NY 11209.

Buffalo Radiological Society. Secretary, Jerald P. Kuhn, 9267 Jennings Rd, Eden NY 14057.

Central New York Radiological Society. E. Mark Levinsohn, Radiology Dept, Upstate Medical Center, 750 E Adams St, Syracuse NY 13210.

Kings County Radiological Society. Secretary, Melvin Moore, 7815 Bay Parkway, Brooklyn NY 11214.

Long Island Radiological Society. Secretary, Harry L. Stein, North Shore University Hospital, 300 Community Dr, Manhasset NY 11030.

Mid-Hudson Radiological Society. Secretary-Treasurer, William D. Stiehm, 37 Flower Hill Rd, Poughkeepsie NY 12603.

New York Roentgen Society. Secretary-Treasurer, Thomas C. Benevenuto, 111 E 210th St, Bronx NY 10467.

New York State Chapter of ACR. Secretary-Treasurer, Albert F. Keegan, 6 Secor Dr, Port Washington NY 11050.

Northeastern New York Radiological Society. Secretary, Donald R. Morton, Dept of Radiology, St. Clare's Hospital, Schenectady NY 12304.

Rochester Roentgen Ray Society. Secretary-Treasurer, Robert J.

Bruneau, 1441 East Ave, Rochester NY 14610.

Westchester County Radiological Society. Secretary, Leonard Cutler, 16 Guion Pl, New Rochelle NY 10802.

Nevada

Nevada Radiological Society, Chapter of ACR. Secretary, Charles F. Veverka, Carson Tahoe Hospital, Carson City NV 89701.

North Carolina

Catawba Valley Radiological Society. Secretary, J. N. Owsley, #18 13th Ave. NE, Hickory NC 28601.

North Carolina Chapter of ACR. Secretary-Treasurer, Ernest B. Spangler, Wesley Long Hospital, Greensboro NC 27402. Annual Meeting: Nov 1976, Mid-Pines Club, Southern Pines NC.

North Dakota

North Dakota Radiological Society, Chapter of ACR. Secretary, H. C. Walker Jr., PO Box 624, Devils Lake, ND 58301.

Ohio

Cleveland Radiological Society. Secretary-Treasurer, Charles M. Greenwald, 7007 Powers Blvd, X-ray Department, Parma OH 44129.

Northwestern Ohio Radiological Society. Secretary, Gerald Marsa, 3939 Monroe St, Toledo OH 43606.

Ohio State Radiological Society, Chapter of ACR. Secretary, James Farmer, 3461 Warrensville Center Rd, Cleveland OH 44122.

Oklahoma

Northeastern Oklahoma Radiological Society. Secretary, William L. Lavendusky, 100 Center Plaza Suite, C, Tulsa OK 74119.

Oklahoma State Radiological Society, Chapter of ACR. Secretary, Bob G. Eaton, 2508 Stillmeadow Rd, Edmond OK 73034. Annual Meeting: Oct 1-3, 1976, Shangri-La Lodge on Grand Lake, Afton OK.

Oregon

Oregon State Radiological Society, Chapter of ACR. Secretary-Treasurer, Ray F. Friedman, 3324 SW 44th St, Portland OR 97221.

Pennsylvania

Pennsylvania Radiological Society. Secretary, Joseph A. Marasco, Jr., St. Francis Hospital, Pittsburgh PA 15201.

Philadelphia Roentgen Ray Society. Secretary, Marvin E. Haskin, 230 N Broad St, Philadelphia PA 19102.

Pittsburgh Roentgen Society. Secretary, Klaus M. Bron, Presbyterian-University Hospital, Pittsburgh 15261.

Rhode Island

Radiological Society of Rhode Island, Chapter of ACR. Secretary, Stefan Frater, Rhode Island Hospital, Providence RI 02902.

South Carolina

South Carolina Radiological Society, Chapter of ACR. Secretary, George W. Brunson, 4315 Woodleigh Rd, Columbia SC 29206.

Tennessee

Memphis Roentgen Society. Secretary-Treasurer, D. Randolph Ramey, Baptist Memorial Hospital, 899 Madison Ave., Memphis TN 38140.

Tennessee Radiological Society, Chapter of ACR. Secretary-Treasurer, Jerry W. Grise, Methodist Hospital, 1265 Union Ave, Memphis TN 38104.

Texas

Central Texas Radiology Society. Secretary-Treasurer, E. Jerome Schollar, Scott and White Clinic, Temple TX 76501.

Dallas-Fort Worth Radiological Society. Secretary-Treasurer, William V. Bradshaw, 777 W Rosedale Suite 260, Ft. Worth TX.

Houston Radiological Society. Secretary, Thomas S. Harle, 103 Jesse H. Jones Library Bldg, Texas Medical Center, Houston TX 77030.

Louisiana-Texas Gulf Coast Radiological Society. Secretary-Treasurer, J. Gardiner Bourque, 3155 Stagg Dr, Suite 230 Doctors Bldg, Beaumont TX 77701.

San Antonio Civilian Military Radiological Society. Secretary, Jose Maria Chao, Diagnostic Clinic, San Antonio TX.

Texas Radiological Society, Chapter of ACR. Secretary-Treasurer, Donald N. Dysart, Scott and White Clinic, Temple TX 76501. Annual Meeting: March 17-19, 1977, Fairmont Hotel, Dallas TX.

Vermont

Vermont Radiological Society, Chapter of ACR. Secretary, Peter Dietrich, Medical Center Hospital of Vermont, Burlington VT 05401.

Virginia

Mid-Shenandoah Valley Radiological Society. Secretary, Kenneth L. Dwyer, King's Daughters Hospital, Staunton VA 24401.

Richmond Radiological Society. Secretary, Melvin Vinik, 9504 Carterwood Rd, Richmond VA 23229.

Virginia Chapter of ACR. Secretary-Treasurer, Charles P. Winkler, 3500 Kensington Ave Suite 2-A, Richmond VA 23221.

Washington

Pacific Northwest Radiological Society. Secretary-Treasurer, Kenneth D. Moores, 1118 9th Ave, Seattle WA 98101. Annual Meeting: May 6-8, 1977, Victoria, B.C., Canada.

Washington State Radiological Society, Chapter of ACR. Secretary-Treasurer, Donald J. Hesch, 3216 NE 45th Pl, Seattle WA 98105.

West Virginia

West Virginia Radiological Society, Chapter of ACR. Secretary-Treasurer, Andrew W. Goodwin II, 200 Medical Arts Bldg., Charleston WV 25301.

Wisconsin

Milwaukee Roentgen Ray Society. Vice President, Thomas C. Lipscomb, 1004 N 10th St, Milwaukee WI 53233.

Wisconsin Radiological Society, Chapter of ACR. Secretary-Treasurer, June Unger, Wood VA Hospital, Wood WI 53193.

Wisconsin Society of Therapeutic Radiologists. Secretary, M. Greenberg, Milwaukee County General Hospital, 8700 W Wisconsin Ave, Milwaukee WI 53222.

Wyoming

Wyoming Radiological Society, Chapter of ACR. Secretary, Thomas E. Hettinger, 1609 E 19th St, Cheyenne, WY.

Canada

Canadian Association of Radiologists. Honorary Secretary, C. Germain Beauregard, Suite 806 1440 St. Catherine St W, Montreal, Quebec Canada.

Edmonton and District Radiological Society. Secretary B. Caplan, 12320 103rd Ave, Edmonton, Alberta T5N 0R2, Canada.

Toronto Radiological Society. Secretary, H. Shulman, Sunnybrook Hospital, 2075 Bayview Avenue, Toronto, Ontario, Canada.

Central and South America

Sociedad Chilena de Radiología. Secretary, Manuel Neira, Casilla 13426, Santiago, Chile.

Sociedad Colombiana de Radiología. Secretary-General, Gustavo Sanchez Sanchez, Bogotá, Colombia. Annual Meeting: Feb 1977, Manizales (Caldas) Colombia.

Sociedad de Radiología del Atlantico. Secretary, Raul Fernandez, Calle 40 #41-110, Baranquilla, Colombia. Annual Meeting: Feb 3, 1977, Baranquilla, Colombia.

Sociedad de Radiología, Radiotherapéutica y Medicina Nuclear de Rosario. Secretary-General Marcela Muñoz, Santa Fe 1798, Rosario, Argentina.

Europe

Bavarian-American Radiologic Society. Secretary, Stuart A. O'Byrne, Radiology Service, Stuttgart, West Germany, 5th General Hospital, APO NY 09154.

British Institute of Radiology. Honorary Secretaries, D. H. Trapnell, P. N. T. Wells, 32 Welbeck St, London, W1M/7PG, England.

Čekoslovenská Radiologická Společnost. Secretary, Jaromír Kolář, Radiological Clinic, Parha 2, Unemocnice 2, Czechoslovakia.

Danish Radiological Society. Secretary General, Johannes Praestholm, Radiological Department I, Bispebjerg Hospital, DK-2400, Copenhagen NV

Deutsch Röntgengesellschaft. President, Wolfgang Frik, Dept of Radiology, Techn Univ Aachen, D-5100 Aachen, Goethestrasse 27/29, West Germany.

Faculty of Radiologists. Honorary Secretary, M. Ryan, Faculty of Radiologists, Royal College of Surgeons in Ireland, Stephen's Green, Dublin 2, Ireland.

The Hospital Physicists' Association. Honorary Secretary, R.F. Mould, Westminster Hospital, Physics Department, Page St. Wing, London SW1P 2AR, England.

Norsk Forening for Medicinsk Radiologi. General Secretary, Arnulf Skjennald, Ulleval sykehus, Oslo, Norway.

Nederlandse Vereniging voor Radiologie. Secretary, H.E. Schütte, Department of Radiology, Elizabeth Gasthuis, Haarlem, Netherlands.

Royal College of Radiologists. Secretary, P.D. Thomson, 28 Portland Pl, London, W1N 4DE, England.

Scandinavian Radiological Society. Secretary-General, C-E. Unnérus, Havsvindsv. 5C., 02120 Esbo 12 (Hagalund-Tapiola) Finland.

Schweizerische Gesellschaft für Radiologie und Nuklearmedizin. Société Suisse de Radiologie et de Médecine Nucleaire. Secretary, Gustav A. Schoch, 7 Gellerstrasse, CH-4052 Basel, Switzerland.

Sociedad Española de Radiología y Electrológica Médicas y de Medicina Nuclear. Secretary-General, Pilar Gallar Barberá, Villanueva, Madrid 1, Spain.

Società Italiana di Radiologia Medica e Medicina Nucleare. Administrative Secretary, R. Dall'Acqua, Ospedale Mauriziano, 10128, Torino, Italy. Annual Meeting: Sept 25-28, 1976, XXVII Congresso Nazionale, SIRMN-BARI-Campus Universitario Via Re Daviol, Italy.

Société Européenne de Radiologie Pédiatrique. Secretary, J. Corbaton, Clinica Infantil "La Paz," Av. Generalissimo, 117 Madrid 34, Spain.

Société Française de Radiologie Médicale, Médecine Nucléaire et Electrológica. Secretary-General, J. Sauvegrain, Hôpital des Enfants-Malades, 149 Rue de Sèvres, 75730 Paris Cedex 15, France. Annual Meetings: 1976, Nov 15-18, Centre International de Paris (Porte Maillot); 1977, Nov 15-18, Centre International de Paris.

Société Française de Neuroradiologie. Secretary-General, R. Djindjian, 16, rue de l'Université 75, Paris 7^e, France.

Society of Pediatric Radiology. Secretariat, PO Box 272, S-101 23 Stockholm, Sweden.

Svensk Förening för Medicinsk Radiologi. Secretary, Hans Ringertz, Department of Pediatric Radiology, Karolinska Sjukhuset, S-104 01 Stockholm, Sweden. Annual Meeting: Dec. 1-4, 1976, Stockholm, Sweden.

Africa

Association of Radiologists of West Africa. Honorary Secretary, A. A. Obisen, Department of Radiology, University College Hospital, Ibadan, Nigeria. Annual Meeting: Feb 4-5, 1977, Accra, Ghana.

Radiological Society of South Africa. Secretary, Dr. A. Visser, P.O. Box 8850, Johannesburg, South Africa.

South African International Radiological Congress. Director, Dr. Paul Sneider, P. O. Box 4878, Johannesburg, South Africa. Durban Annual Congress: Oct 1978, International and National Congress.

Near East and Asia

Bengal Radiological Association. Honorary Secretary, B. Chatterji, 262 Rash Behari Ave, Calcutta 700019, India. Annual Meeting: Dec 10, 1976, 3-1 Madan St, Calcutta 700013, India.

Indian Radiological Association. Honorary General Secretary, S. P. Aggarwal, 10-B Kasturba Ghandi Marg, New Delhi 110001, India. Annual Meeting: Jan 1977, Chandigarh, India.

Indonesian Radiological Society. Secretary, Gani Iljas Sasmitaatmadja, Radiology Department, Faculty of Medicine, University of Indonesia, Salemba 6, Jakarta, Indonesia.

Iranian Radiological Society. Secretary Majid Rooholamini, P.O. Box 14-1151

Israel Radiological Society. 50th anniversary, 20th Radiological National Congress: April 27-29, 1977, Haifa, Israel. Congress president, A. Rosenberg, Rambam Government Hospital, Haifa; U.S. information from, I. Horowitz, 881 Lafayette Blvd, Bridgeport CT 06604.

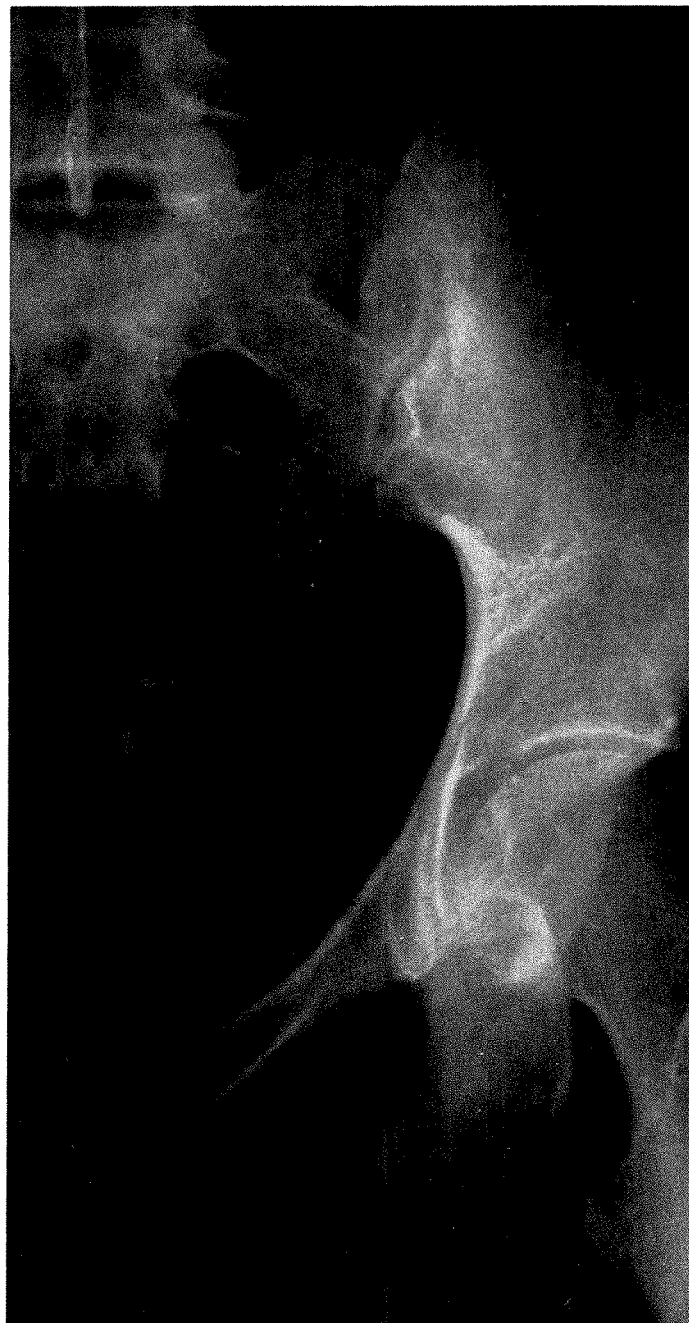
Philippine College of Radiology. Secretary-Treasurer, Antonio Chavez, Box 1284, Commercial Center, Makati, Rizal, D-708, Philippines.

Radiological Society of Thailand. Secretary, Dusdee Prabbasawat, Department of Radiology, Siriraj Hospital Faculty of Medicine, Mahidol University, Bangkok 7, Thailand.

Royal Australasian College of Radiologists. Honorary Secretary, T. P. Loneragan, 45 Macquarie St, Sydney NSW 2000, Australia. Annual Meeting: Oct 10-15, 1976, Jakarta, Indonesia.



Hysterosalpingogram with Salpix Contrast Medium.



24-hour postinjection x-ray of same patient.

now you see it

now you don't

With Salpix as your contrast medium, your gynecologic patient needn't undergo the 24-hour postinjection x-ray usually required with iodized oils. Water-soluble Salpix leaves virtually no irritating radiopaque residue to produce foreign-body reactions, yet it provides the viscosity needed for adequate visualization.

Contraindications: Contraindications to hysterosalpingography include the presence of severe vaginal or cervical infections, existing or recent pelvic infection, marked cervical erosion or endocervicitis, and pregnancy. The procedure is contraindicated during the immediate pre- or post-menstrual phase.

Sensitivity Test: If indicated in the patient's history, an intracutaneous skin test or sublingual absorption observation may be done with 0.1 cc Salpix.

Warning: Not for intravenous use.

© ORTHO PHARMACEUTICAL CORPORATION 1970

CONTRAST MEDIUM
Salpix
TRADEMARK

EACH CC CONTAINS:
sodium acetrizoate 0.53 g and
polyvinylpyrrolidone 0.23 g



ORTHOPHARMACEUTICAL CORPORATION, RUMSON, N.J.

Big ultrasound quality for small ultrasound budgets.

"Expensive" new ultrasound equipment isn't as expensive as you might think. When we streamlined our Echoview® family of ultrasound systems we also streamlined ultrasound economics.

A basic configuration of the Echoview System 80L laminography unit gives you immediate ultrasound capability that can grow as your needs grow. With the addition of a basic Echoview System 80C cardiac unit, your department will possess up-to-the-minute ultrasound capabilities.

And because Echoview

ultrasound is a completely interfaced system of scanning, display and recording capabilities, you needn't worry about a "generation gap" later when you decide to expand your suite.

Picker's comprehensive service program covers installation, maintenance, application assistance from highly trained ultrasonographers, formal training of operators, seminars and symposia and the largest ultrasound emergency service organization of any manufacturer.

Picker offers you total ultrasound capability whenever you need it, today or tomorrow. That's what we mean by

Picker's synergy — the complete interfacing of systems and services for improved diagnostic visualization.

That's why Echoview Systems 80 are the hard-working ultrasound units that are right for the hard-working ultrasound budget.

You may be pleasantly surprised to find out how easy it is to equip your ultrasound department with Picker Echoview systems.

Talk to your Picker representative. Or write Picker Corporation, 12 Clintonville Road, Northford, CT 06472.

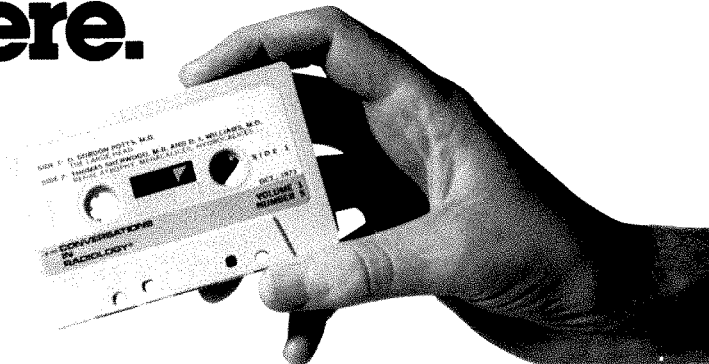


ONE OF THE CIT COMPANIES



Picker's synergy

The post-graduate course you can carry anywhere.



Conversations in Radiology, Volume 4, is now available for subscription

Like the previous Volumes, Volume 4 consists of 8, one-hour audio cassettes plus appropriate reference materials. Each cassette consists of two, 30-minute programs. All tapes are clearly edited to provide focus on new developments or controversial issues, and, review of pertinent topics in the field of radiology.

A portable reference work.

Conversations in Radiology is more than a seminar, it's a valuable reference library which can be reviewed at the physician's leisure... or, utilized as an adjunct to the teaching process.

Meaningful insights.

Conversations in Radiology, Volume 4, will offer the radiologist and allied specialist continuing updates and insights into important areas of subspecialization. Naturally, all tapes are accompanied by a complete reference bibliography plus occasional illustrations.

8, one-hour conversations with leading authorities.

Convenient form.

Your subscription to Conversations in Radiology includes eight sequentially issued audio-cassettes, a convenient bookshelf cassette binder, plus, all appropriate reference materials.

Accredited by the AMA and CMA.

The Conversations in Radiology subscription series is acceptable for 8 credit hours in Category 5 for the Physicians' Recognition Award of the American Medical Association. Each Volume is also acceptable for credit in Category II, Formally Constituted Activities, Section "i," toward the California Medical Association's Certificate in Continuing Medical Education.

Annual subscription: \$74.

Volume 4 of Conversations in Radiology began in April, 1976. Volumes 2 & 3 are still available at \$74 per completed Volume... including binder and reference materials.

Participating Editors:

Pediatric Radiology

Walter Berdon, M.D.
Columbia University

Gastrointestinal Radiology

Joseph Ferrucci, Jr., M.D.
Harvard University
Jack Wittenberg, M.D.
Harvard University

Ultrasound

Barry B. Goldberg, M.D.
Temple University

Bone Radiology

William Martel, M.D.
University of Michigan

Neuroradiology

D. Gordon Potts, M.D.
Cornell University
Irvin I. Kricheff, M.D.
New York University

Angiography

Joseph J. Bookstein, M.D.
Univ. of Calif., San Diego
Helen C. Redman, M.D.
Univ of Calif., San Francisco
Stanford University

Genitourinary Radiology

Lee B. Talner, M.D.
Univ. of Calif., San Diego
Thomas Sherwood, M.B.,
Royal Postgraduate
Medical School
University of London

Chest Radiology

Morris Simon, M.D.
Harvard University

Oncologic Radiology

Ronald Castellino, M.D.
Stanford University

Editors:

Ronald C. Ablow, M.D.
Yale University
Alan J. Davidson, M.D.
Univ. of Calif., San Francisco
Stanford University

Conversations in Radiology

170 9th Street, San Francisco, CA 94103

Gentlemen,
Please enter my subscription to Volume 4, Conversations in Radiology. I understand that for \$74, I will receive eight, one-hour tape cassettes containing 16 half-hour conversations with leading radiologists... plus, a bookshelf binder and appropriate reference materials.

Name _____
Address _____
City _____ State _____ Zip _____

☐ Bill me ☐ Check enclosed
☐ Please send me Volume 3 ☐ Bill me \$74. ☐ Check enclosed.
☐ Please send me Volume 2 ☐ Bill me \$74. ☐ Check enclosed.

**Why don't you stop pushing
your E.R. patients around?**



In the complete new Litton Trauma Room



Once you lift the patient from the ambulance to our Roll-X® Stretcher, you don't have to move or reposition him until he's ready to go to a bed, to surgery or home.

Our equipment does the moving: The Traum-X^{T.M.} Table top parks back to expose the entire Bucky assembly. The radiolucent stretcher glides into place over the Bucky, to achieve optimum radiographic results. The x-ray tube on its overhead conveyor rotates on both a horizontal and a vertical axis, allowing a wide variety of procedures

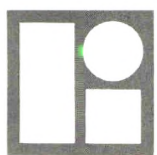
to be performed on the traumatized patient.

A vertical wall Bucky and a powerful Patriot 625 generator with desk-top control unit are standard equipment. Optional generators up to 1600 mA are also available, as is a full line of supplementary equipment—everything from a mobile grid stand to a film processor to a complete monitoring and resuscitation package.

You can have your Trauma Room installed and operating in three weeks after delivery.

Call your Litton Medical Systems Representative today.

everything moves but the patients.



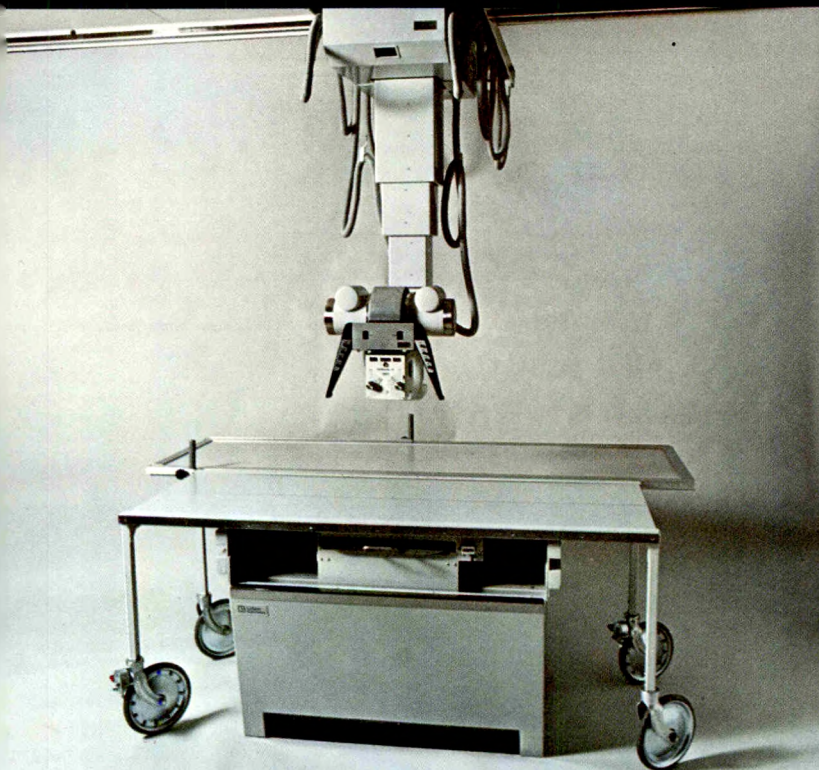
Litton

Medical Systems

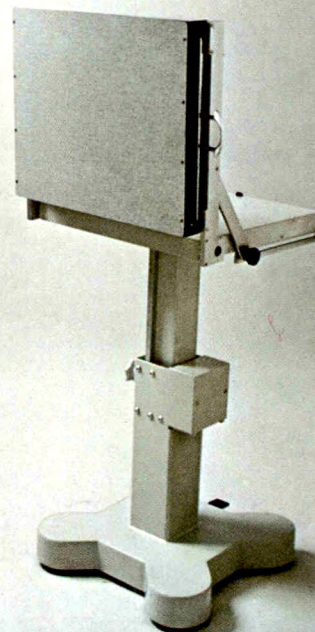
515 E. Touhy Avenue, Des Plaines, Illinois 60018

*Technology, resources, people
committed to mankind's better health.*

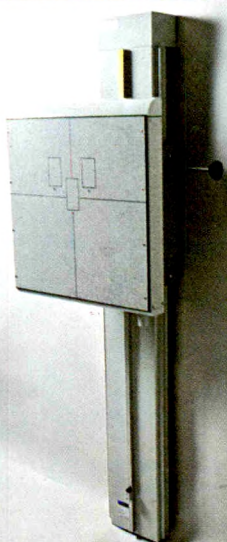
Optimized Litton equipment minimizes patient handling, maximizes care.



Note how the LMS Traum-X Table top is parked back to expose the Bucky assembly, allowing the LMS Roll-X Stretcher to be positioned over it at minimum Bucky-to-patient distance.



The LMS Mobile Pedestal Grid fits beside or below any table, for lateral or decubitus grid radiographs.



The LMS Vertical Bucky permits radiographs in sitting, standing, or recumbent positions.



The LMS Medical Electronics Package is a complete cardiac monitoring and resuscitation system.



The LMS P625 3-phase X-Ray Generator is available as floor unit or with wall-mount control console.



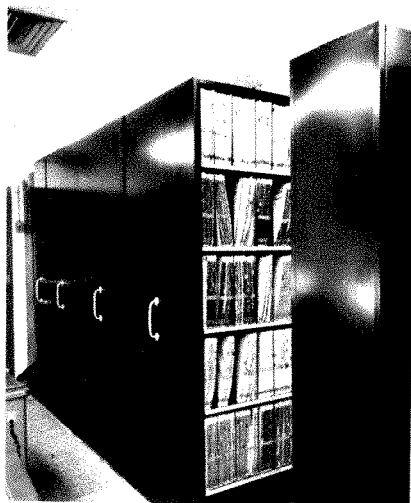
SPACESAVER COMPACT FILING AND STORAGE SYSTEMS

- Spacesaver turns wasted aisles into usable space.
- Manual and electric systems. Adapts to any shelving or files, whether existing or new.
- When system is not being used, it can be rolled together and locked for maximum security.

Other medical applications include

- X-Ray Files
- Pharmacy
- Accounting Records
- Freezer Storage
- Computer Tapes

A typical Spacesaver System can increase storage capacity by an average of 80% in existing floor space.



See us at Booth No. 109
of the American Roentgen-Ray
Society Annual Meeting.



SPACESAVER CORPORATION
1450 JANESVILLE AVE.
FORT ATKINSON, WIS. 53538
414-563-6362 OR 608-868-7550

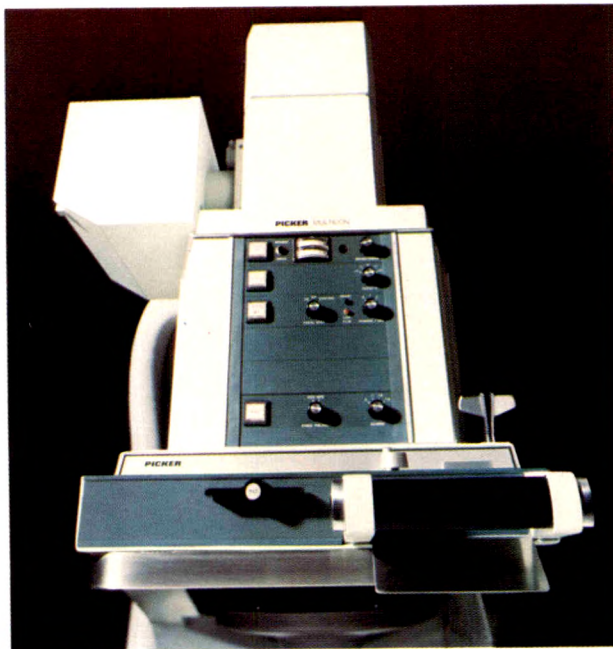


FREE *Illustrated Brochure*

- ☐ I would like more information on the Spacesaver System
- ☐ Have a Spacesaver distributor call

Name _____
Institution _____
Street _____
City _____
State _____ Zip _____

Technology catches up to a good idea. Flushmount.



Integral mounting of the x-ray imaging system has long been recognized as a good idea. Because of recent technological advances, Picker now brings you Flushmount—cassetteless spotfilming of the future.

The mobility and flexibility of Picker's Flushmounted Multicon image intensifier delivers total system reliability, proven results, and eliminates the need of cassettes.

While Picker's Flushmount concept improves the appearance of your radiology

department, more importantly it provides superior patient-film geometry and reduces the overall film handling procedures.

With Flushmount, there is no need to remove and park the imaging system as with heavier imaging system combinations. Changeover from fluoroscopy to radiography and back again is quick and easy.

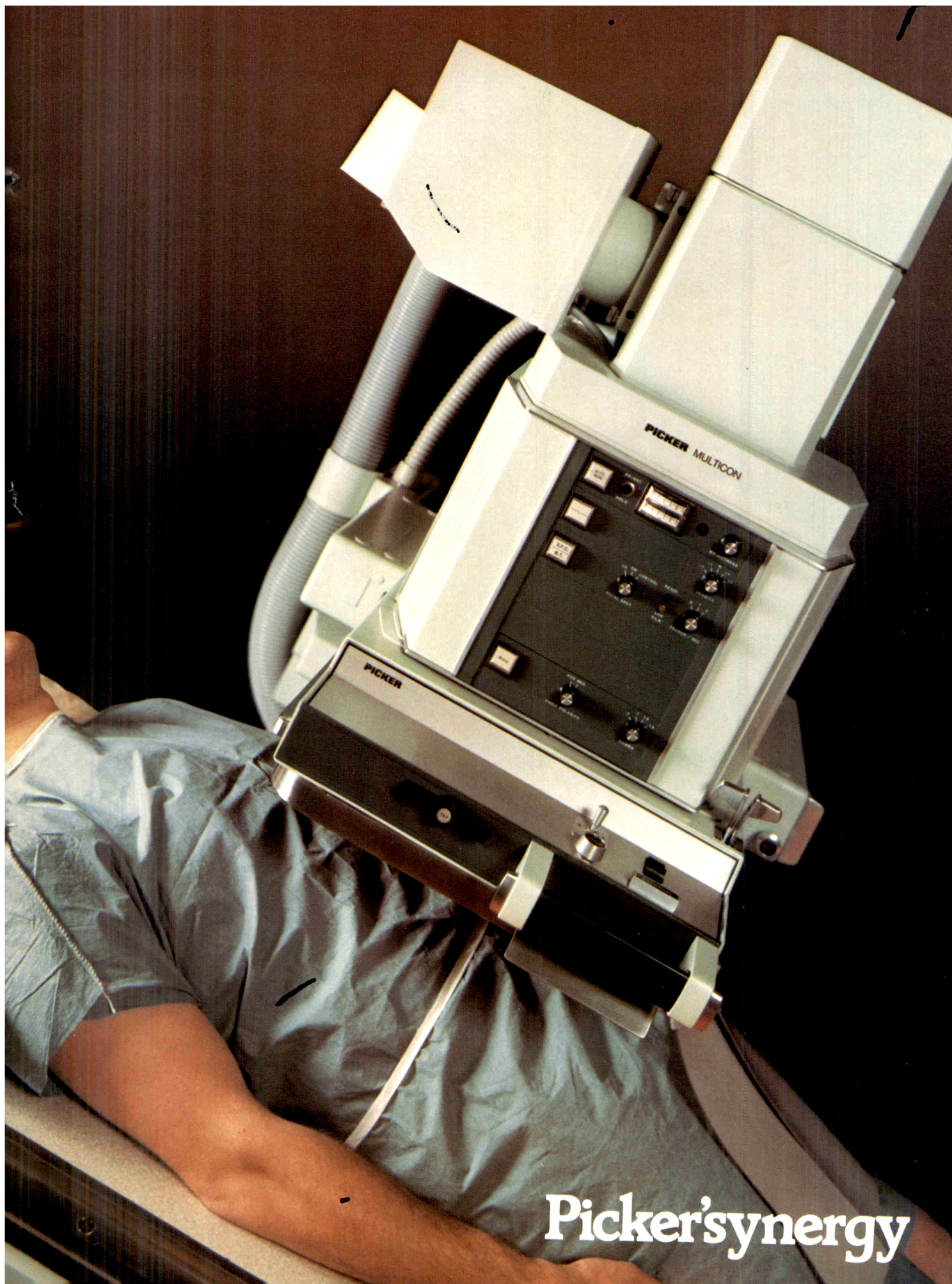
Given Flushmount's reduced mass, "mini-cassetteless" ease of the 100mm film format,

quality results and the field-proven worth of the 90/90 table, Picker today offers the radiologist a hardworking, versatile configuration solid enough to become the backbone of tomorrow's radiology suite.

Flushmount. It's another example of Picker's synergy—the complete interfacing of systems and services for improved diagnostic visualization.

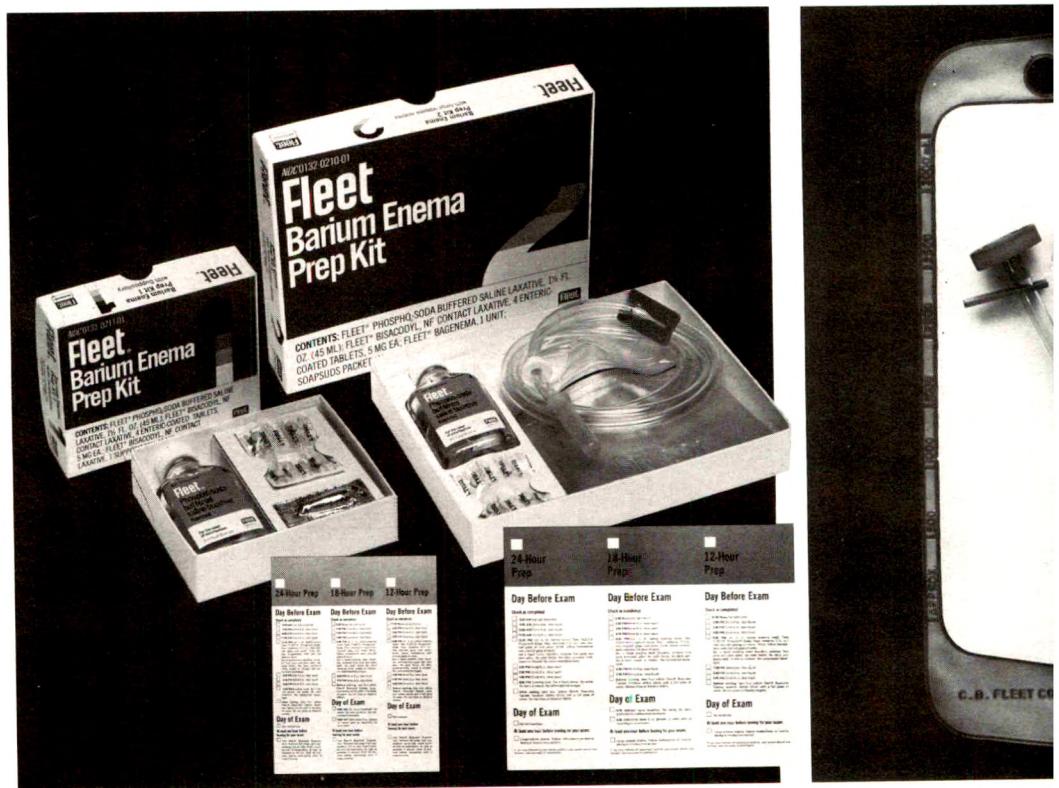
Contact your Picker representative. Or write Picker Corporation, 595 Miner Road, Cleveland, OH 44143.

PICKER®
ONE OF THE C.I.T. COMPANIES



From start to finish, Fleet systematizes

For cleaner colons, clearer x-rays, and fewer retakes.



For preparation,
Fleet Barium Enema
Prep Kits assure
thorough, reliable
colon cleansing by
utilizing a combination
of diet, hydration, and
evacuation.

- Available in two convenient forms with suppository or enema as final step.
- Offering an effective and balanced method of prepping.
- Meeting all criteria for colon preparation as recommended by the American College of Radiology Ad Hoc Committee on Detection of Cancer of the Colon.
- With easy-to-follow instructions.
- With 3 convenient time schedules to fit better into your schedule and your patient's routine.

For the examination

Fleet Barobag offers greater visibility because it contains Ultrasperse™ with a combination of barium sulfate USP (98%) and selected suspending and dispersing agents (2%) for "instantized" mixability.

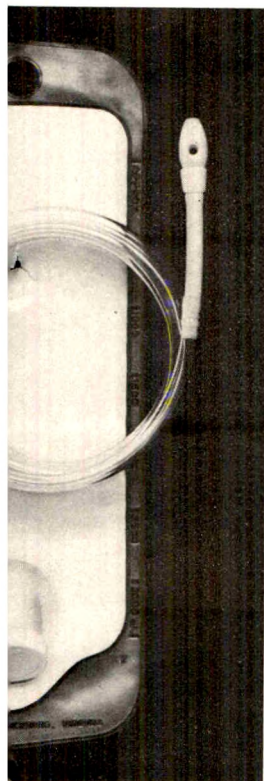
- With excellent suspension stability—up to 2 hours.
- With rapid, free-flow emptying.

barium enema exams...

C. B. Fleet presents a unique three-part system of products that can help you give quality

barium enema exams. It includes Fleet® Barium Enema Prep Kits for colon preparation, Fleet® Barobag for the actual

barium enema examination, and Fleet® Phospho-Soda for aftercare.



leakproof with screw closures for convenience. With angled spout (5") for easier filling and handling. Available with either 12 or 16 oz. Ultrasperse® barium sulfate USP). Also available with retention catheter.

For aftercare,

Fleet Phospho-Soda is gentle and most effective for cleansing the colon of barium and for preventing fecal impaction.

- Works in an hour or overnight, according to dosage, for convenience and flexibility in scheduling.
- Usually produces soft, formed stool with no unusual side effects.
- Promotes natural peristalsis to assure thorough action.

- Buffered for gentleness.
- Easy-to-take.
- Safe for use by patients of all ages, as indicated.

In the final note to *Detection of Colon Lesions* by the American College of Radiology Ad Hoc Committee on Detection of Cancer of the Colon, R. E. Miller states: "Almost every recommendation made is part of urging *quality control* by the radiologist in all aspects of his colon examination."

Fleet's new system of products will answer almost every need you'll encounter in barium enema examinations—from start to finish.

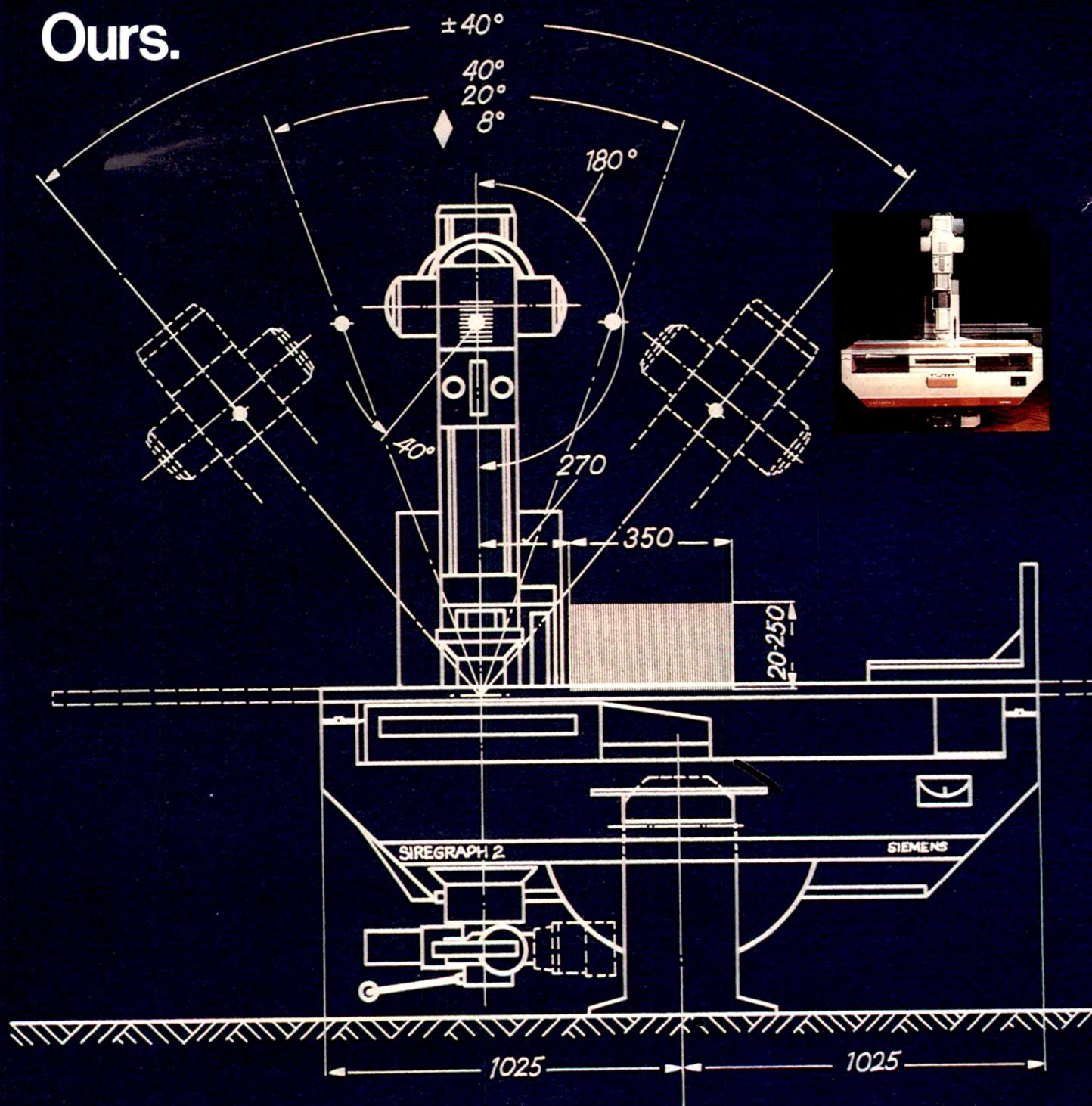
In barium enema exams, quality controls results. And Fleet controls quality.



C.B. FLEET CO., INC.
Lynchburg, Va. 24505

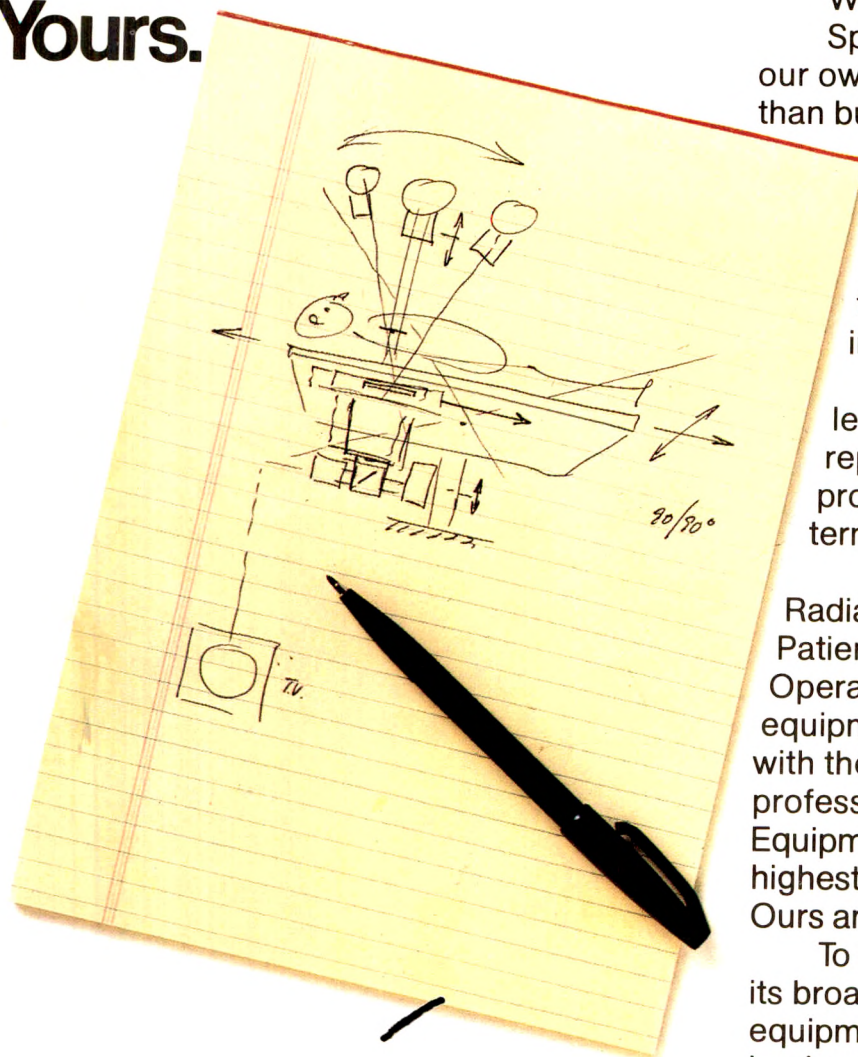
In medical electronics,
every manufacturer aims
at one standard of excellence.

Ours.



**Our excellence
is derived
from one standard.**

Yours.



Siemens became a leader in medical electronics over a century ago by working hand-in-hand with the medical community; we have devoted the same attention to detail in the production of our products as medical professionals exercise in using them.

We still work that way.

Specifically, we emphasize using our own internal components rather than buying outside. This improves quality control and insures that materials work in the system. Also, each production unit is subjected to cumulative testing in the factory as well as in the field.

Siemens customers enjoy less downtime, more reliable and reproducible performance, longer product life and maximum long-term cost-effectiveness.

Whether it be Medical X-ray, Radiation Therapy, Ultrasound, Patient Monitoring, Dental, or Operating and Emergency Room equipment—Siemens products work with the skilled hands of the medical professional—not against them. Equipment that truly meets the highest standards of excellence. Ours and Yours.

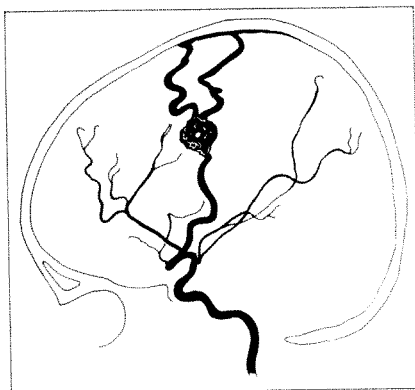
To learn more about Siemens and its broad line of medical systems equipment, planning services, service back-up and lease/purchase options, call or write:

Siemens Corporation
Medical Systems Division
Iselin, New Jersey 08830
(201) 494-1000

SIEMENS

DIAGNOSTIC NEURORADIOLOGY

SECOND EDITION



JUAN M. TAVERAS & ERNEST H. WOOD

The first edition of *Diagnostic Neuroradiology*, issued in 1964 and an instant bestseller, is now regarded as a classic, pioneering text. In their preface to the new second edition, Drs. Taveras and Wood point out that they have greatly expanded the contents because the engineering achievements of the past decade have exceeded the expectations of even the most far-seeing neuroradiologists. They trace the development of solid state circuitry and its application to the computer and television monitoring, discussing their uses today in all fields of diagnostic roentgenology, and especially in the dramatic new field of computed tomography. The accompanying illustrations are profuse.

1976 / 1,384 pages in 2 volumes / 1,200 illustrations / \$79.50

WILLIAMS & WILKINS
428 East Preston Street
Baltimore, Maryland 21202

please type or print

NAME _____

ADDRESS _____

CITY _____ STATE _____ ZIP _____

☐ Check enclosed

☐ Bill me

To order titles on 20-day approval, check selections

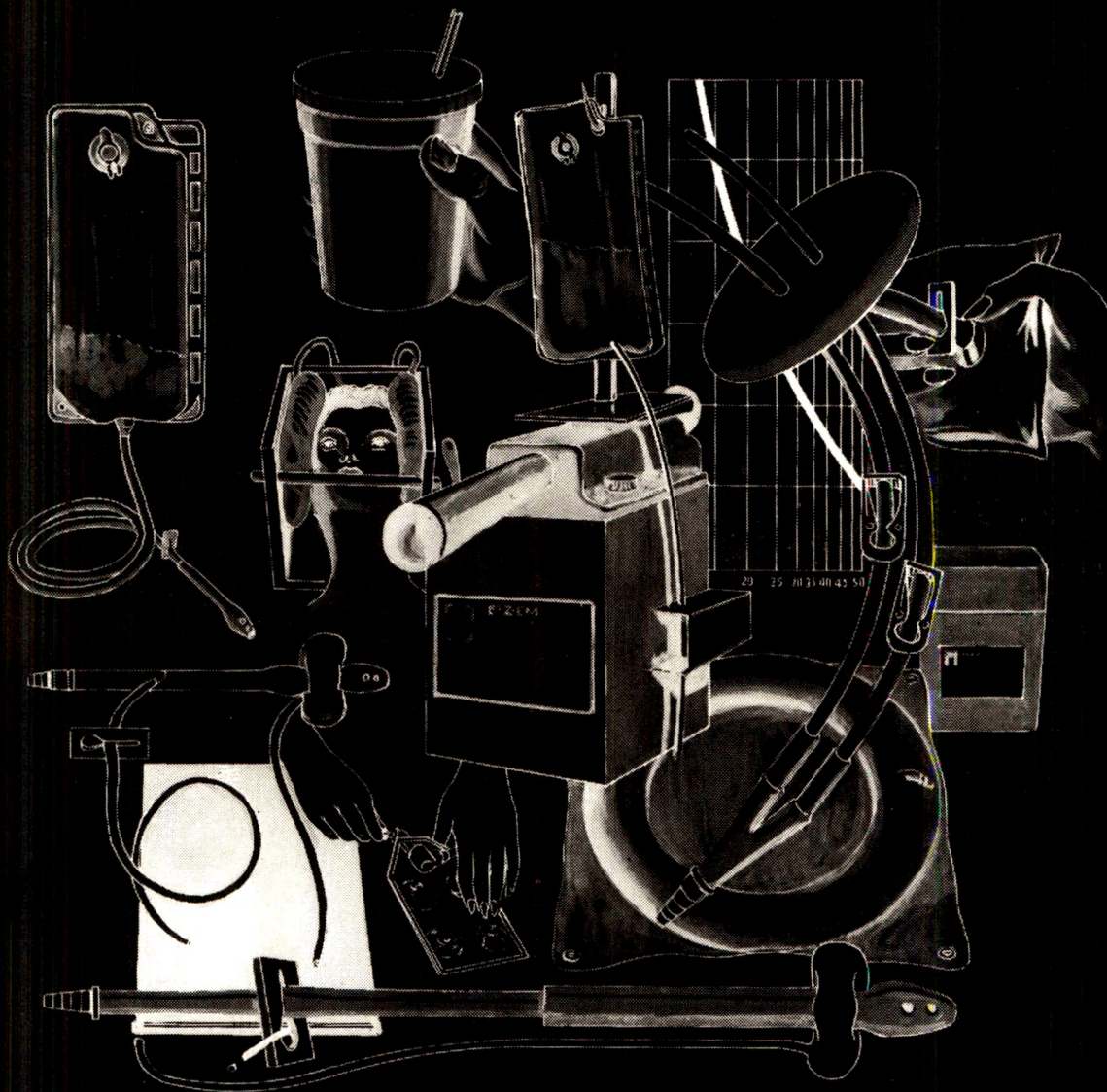
Save postage and handling by enclosing payment with order.

Maryland residents please add 4% sales tax.

☐ Taveras & Wood: *Diagnostic Neuroradiology*
[book #8111-X, \$79.50]

Barium, Barium Systems, and Ancillary Products

**...formulated and designed to meet the realistic
needs of the Modern Radiology Department**



System of your choice

111 SWALM STREET

Westbury, N.Y. 11590 (516) 333-8230

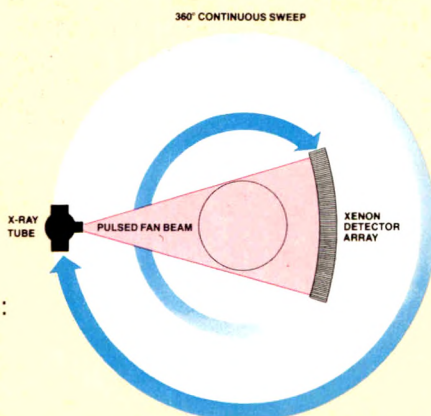
International Affiliates: E-Z-EM Rooster B. V., Infirmieriestraat 6-8, Rotterdam 16, Netherlands

CT/T fast-scanner: the third generation computed tomography system that's versatile, efficient and consistent.

CT/T system: 4.8-second scans, consistently sharp images.

The CT/T total body scanner has established the third generation of computed tomography: GE fast-scan. With this system, one 360° sweep yields the scan information for a full 320 pixel diameter image in just 4.8 seconds.

This unprecedented speed solves the primary problem of slower units: motion unsharpness caused by patients' respiratory motion. First and second generation systems, using an incremental rotate-and-translate principle, take from 18 seconds to 5½ minutes per scan. But the new GE fast-scan unit features a rotating pulsed fan beam with a 320 element xenon detector array. The tube and detectors rotate around the body in one, smooth 360° motion, taking only 4.8 seconds. Most patients can comfortably hold their breath



during the GE fast-scan procedure, with improved resulting image quality.

The CT/T system offers many other diagnostic advantages. Here are just some of the key features:

Versatile viewing capability.

The viewing console allows precise selection of the range of CT numbers displayed. A special feature on the CT/T system is an IDENTIFY button, which causes the CT numbers at the center of the CT range to "blink." This provides rapid identification of picture elements at a selected CT number without changing window widths.

Photographic recording of selected images is provided by a multi-format camera which accommodates three standard film sizes.

Advantages of GE xenon detectors

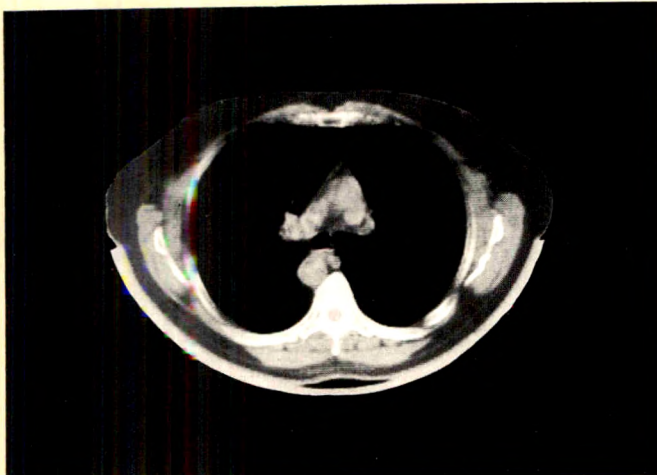
After studying many different detector options for the rotating pulsed fan beam fast-scan system, GE researchers found high-pressure xenon offered numerous advantages over other types of detectors. Here are some of the most important considerations:

Necessary Characteristics. The multi-element xenon detector array possesses the most important requirements for a CT detector: reliability, complete response to x-radiation, and a wide linear dynamic range. Advanced fabricating techniques provide for reliable, consistent detector manufacturing. The detectors are operated in a stable range of voltage and pressure to ensure consistent performance. Unlike vacuum components, impurity contamination is not a problem, and the uniform high pressure of xenon gas within the detector chamber ensures that the response is uniform throughout the detector, and remains so with time. The pulsed mode of operation provides sufficient time for complete response to the incoming x-ray photons. And, the response of the xenon detector is linear over the range of digitization used within the system.

Overall Efficiency. The overall efficiency of the GE rotating fan beam x-ray source and detector system is a product of two main factors: the detection efficiency and the collimation efficiency. The noise

equivalent absorption (NEA) for the xenon detector is about sixty percent that of the best possible scintillator crystal/photomultiplier tube combination. But the collimation efficiency possible with this system is superior to that of any other. Because of this, at least twice as many unscattered x-rays emerging from the patient actually reach the active area of the detector as in other systems. Also, because the scan is carried out through 360° rather than 180°, the reduction in skin dose required for the same integral dose is calculated to be a factor of about 1.6.

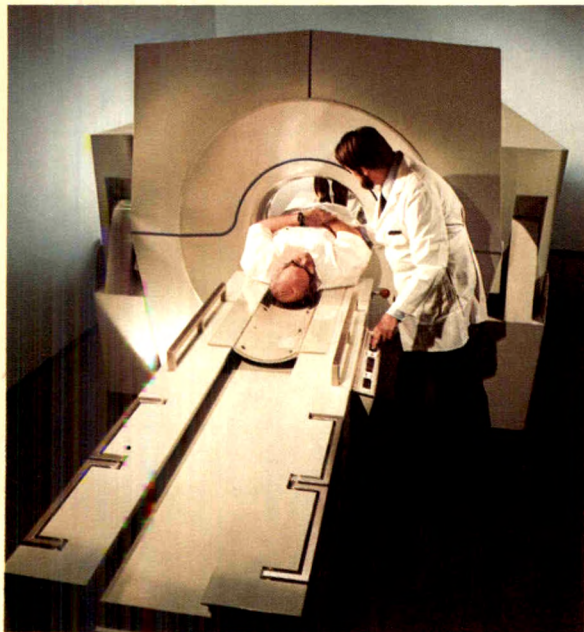
Putting these three factors together (detection efficiency, collimation efficiency and 360° scan) provides an approximate 2X reduction in the skin dose requirement over those systems using a broad x-ray tube focal spot and scintillator crystal/photomultiplier tube detectors. Thus the pulsed fan beam/multi-element xenon detector array provides the design option of keeping the dose low or increasing the dose to improve resolution. There is considerable latitude in changing the system mAs through changes in the pulse, the pulse mA, and the number of pulses. For the typical patient on the CT/T system, it is expected that the skin dose will be approximately 2-4R, although diagnostic quality images have been produced with skin doses substantially under 1R.



Scan of lung area—Level setting is 0; window setting is 200, ranging from +100 to -100. Soft tissue—muscle, heart and subcutaneous fat—is emphasized.



Abdominal scan—Level setting is +27; window setting is 160, ranging from -53 to +107. Scan shows lobulated liver; round tumor near liver; top of right kidney; displaced spleen.



A fast look: fast-scan CT/T system

Scanning speeds—4.8 seconds and 9.6 seconds.

Image reconstruction time—200 seconds.

Matrix dimensions—320 pixel dia. matrix. Each pixel corresponds to a volume element measuring 1.3 mm x 1.3 mm x 10 mm.

Main disc storage—over 200 images.

Archival storage—magnetic tape unit is standard with the system.

Multi-format camera—images may be positioned on film in any order for diagnostic convenience. Film sizes: 8 x 10; 11 x 14; 14 x 17.

Gantry—60 cm opening; 42 cm field of view; $\pm 15^\circ$ gantry angulation; no water bag required.

X-ray tube—Maxiray™ 125.

Generator—3-phase MSI™ 850 II.

Simultaneous reconstruction and viewing.

The display monitor in the viewing console is “refreshed” by a separate high-speed memory, to provide flicker-free images that may be viewed and manipulated without interrupting the computer’s image reconstruction. This dual capability allows faster, more efficient diagnosis and speeds patient flow.

Holds more than 200 images.

The CT/T system’s main memory disc can hold more than 200 images, 320 pixels in diameter. High-speed random access capability of this disc permits image retrieval in a matter of seconds, compared to minutes for tape systems. All computer functions are directed from a “conversational” keyboard/CRT display to simplify operation. A magnetic tape system for archival storage is included with the system.

If you’d like our new brochure with all the facts on the CT/T system, contact your GE representative or write GE Medical Systems, P.O. Box 414, Milwaukee, Wisconsin 53201. We want you to know more about CT/T: the fast-scan total body system backed by General Electric’s corporate commitment to technology, product quality and service.

General Electric Medical Systems,
Milwaukee, Toronto, Madrid.

GE: leading the way in diagnostic imaging.

GENERAL  ELECTRIC

General Electric x-ray systems provide reliable diagnostic imaging—when, where and how you need it.

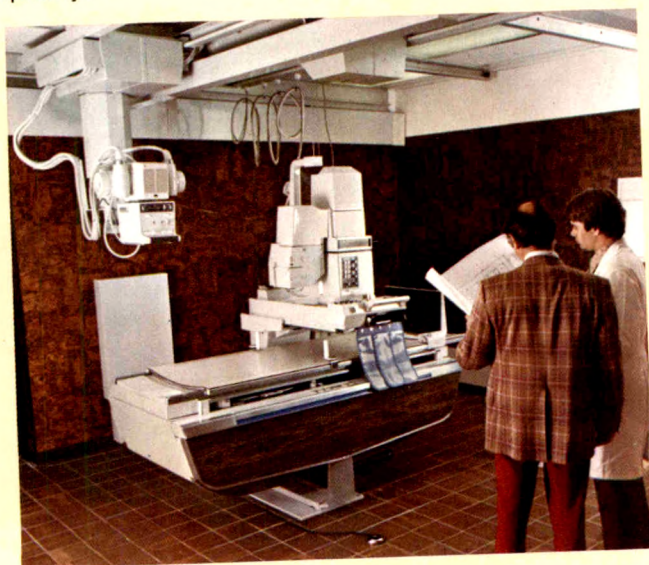
When your patient load depends on basic x-ray systems, make GE your basic source.

For classical R&F: matched components deliver proven performance.

Chances are, your radiographic/fluoroscopic procedures rooms are the mainstays of your radiology department. The performance of those rooms is vital to your overall operation. And unless all components in an R&F room are carefully coordinated, the total system cannot reach its full potential.

That's why General Electric R&F systems are designed and coordinated to maximize the performance of each component. And that performance has been proven, day after day, in radiology departments like yours.

Take the Fluoricon® 300 image system: it delivers high resolution images with maximum diagnostic data. Choose a compact, 6 inch unit or a triple-field 9-6-4½ inch system for the ultimate in image quality.



Monitrol™ diagnostic tables allow exact patient positioning for a wide range of technics. These tables provide smooth, 90°-90° or 90°-15° motor-driven angulation.

Other matched components include: 105 mm photospot camera for high-quality image recording; Maxiray™ x-ray tubes, output-matched to GE generators; and exceptionally stable XT suspension systems.

And now these R&F rooms can be installed through a new time-saving service: GE "pre-staging." Under this plan, your new R&F system is set-up and checked out before it leaves our plant. This "pre-staging" concept allows GE to install a complete new R&F system in your institution in about 3 weeks, minimizing costly downtime.

GE Generators provide precise power, matched for any R&F system. The performance-matched lineup of generators, integrated in all General Electric R&F systems, provides the needed power output for every exposure, every patient. Power capability extends from 300 to 1200 mA . . . the range needed for all valid applications today. Choice of units includes single-phase, 2-pulse for a high percentage of routine R&F applications, including simple GI studies on cooperative patients. Plus 3-phase units for the full range of applications, including those where it's important to have enough power to stop motion. Three-phase MSI generators offer the technic advantages of millisecond interrogation and millisecond exposure termination for consistent phototimed results; MST units feature millisecond termination only. In all cases, available power is useful power for consistent image quality, even with procedures that call for high instantaneous loads and with extended procedure schedules.





XT Suspension system permits exact positioning of the x-ray tube unit with minimum effort; patient on-table or off. Also assures stability of the unit while facilitating a broad range of procedures. Available in outboard or inboard mount for installation convenience and room flexibility.

GE mobile x-ray puts quality imaging on the move.

The **AMX-110™** mobile x-ray unit permits routine radiography, anywhere, with procedure room quality. This cordless, self-propelled system can be moved quickly and easily to any location in the hospital. Ideal as an emergency back-up unit. A gentle push on the thumb-activated switch engages the variable speed power drive. The unit can then be guided with minimum effort, forward or reverse, even over carpeting, thresholds and inclines. When the handle is released, the unit stops automatically. AMX-110 system can be driven nearly a mile and still produce full-power exposures. Three 40 volt nickel cadmium cells store 10,000 mAs at 100 kVp. The system combines a 100 mA rating—equivalent to 150 mA two-pulse conventional generators—and stabilized, low-ripple DC output to 110 kVp. The AMX-110 unit can be recharged to full capacity overnight, or even faster, depending on the stage of discharge. All technic functions are controlled from a conveniently located console.



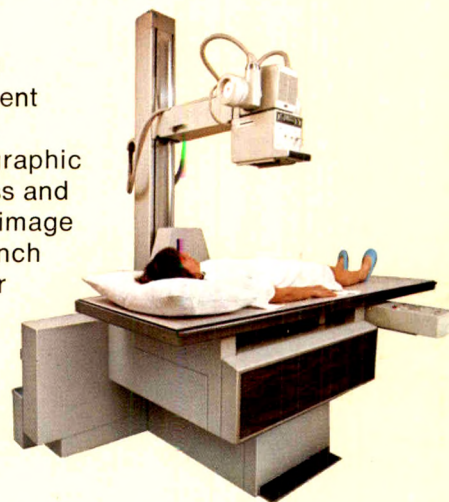
RT Table system: the affordable, all-around room.

Radiography, true linear tomography and zonography ... all these technics can be performed with the moderately priced RT Table system. High quality radiographs are produced with convenient 8 x 10 to 14 x 17 cassettes. A unique motor-driven Bucky raising/lowering unit maintains close tabletop-to-film distances. Cassette size-sensing is automatic. Patient positioning is

precise and effortless. The system's inherent stability yields uniform tomographic plane thickness and resultant high image quality. At 44 inch SID, true linear tomography can be

performed at either 5°, 10°, 20° or 40° angles. Off-table vertical

Bucky and tabletop lateral radiography are facilitated by tube angulation and a rotating column which turns 90° along the longitudinal table axis. The system is available with Quantamat™ ion chamber for classical radiography.



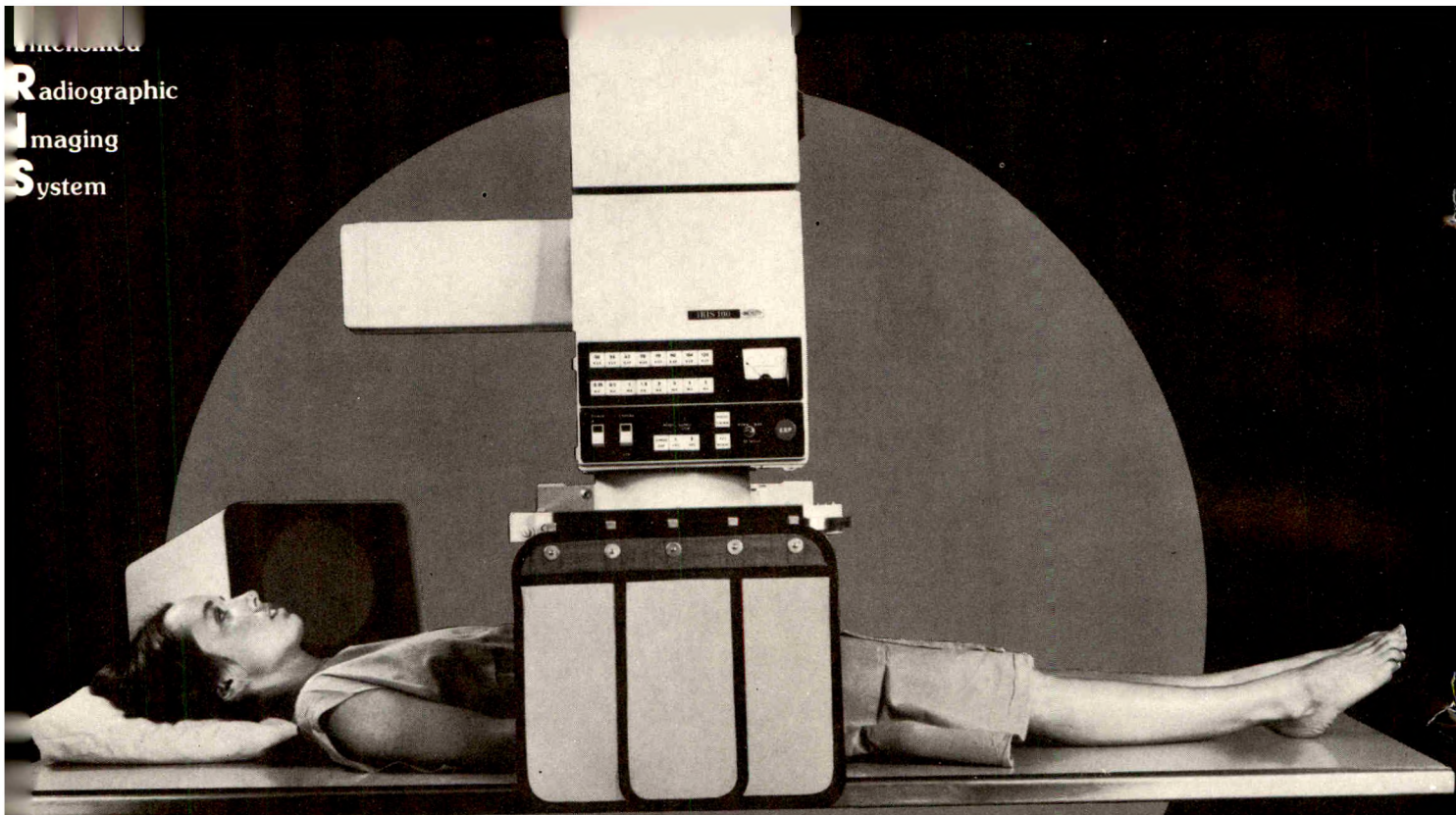
To see how GE basic systems can help you keep pace with patient flow, talk to your General Electric representative.

General Electric Medical Systems,
Milwaukee, Toronto, Madrid.

GE: leading the way in diagnostic imaging.

GENERAL  ELECTRIC

Enhanced
Radiographic
Imaging
System



IRIS 100 adds television fluoroscopy and 100mm spotfilming to your present x-ray room.

Machlett's IRIS 100 system is a sound investment — both for the diagnostician and for the hospital — because it provides the most modern television fluoroscopy/spotfilming capabilities without the need for buying a whole new x-ray room. By improving the radiologist's productivity, moreover, IRIS 100 enables him to apply his much needed skills to a greater patient load.

While its cost is attractive, the real reasons for selecting IRIS 100 for your x-ray room are far more important:

Image Sharpness Machlett's Cesium Iodide Image Intensifier tube with its three focusing grids assures bright, sharp images both on film and on the television screen.

Short F-R-F Time Machlett's "sliding mirror" image distributor lets you quietly shift from fluoroscopy to spot radiography and back to fluoroscopy in *less than one second*.

Rapid Filming The Old Delft "Anodica" camera takes 100mm films singly or sequentially at 1-per-second or 2-per-second rates. Exposures are short enough to freeze peristaltic motion. Phototiming assures uniform film densities.

Human-Engineered Controls Controls are conveniently placed and designed for operation with gloved hands. Warning lights and interlocks eliminate such human errors as exposure without film.

Positive Patient ID The 100mm camera will not operate without the patient identification card in place. Film is identified at the time it is exposed.

For the whole story on IRIS 100, contact your x-ray equipment dealer or



Machlett Laboratories, Incorporated

1063 Hope Street
Stamford, Connecticut 06907
(203) 348-7511

A Raytheon Company

Visit the Machlett exhibit
at the RSNA Show November 14-19

DCA dosimeters measure low energy, diagnostic x-rays ...and let you know now

More examples why DCA is the world leader in direct reading dosimeters.



Low energy Diagnostic x-ray dosimeters

The only low energy dosimeters that measure total integrated gamma- and x-radiations in the 18 to 250 keV range. And they are equally effective for single source or cumulative values. Model 002 (0-200 mR), is for personal monitoring near radiologic equipment. They enable you to determine a radiation exposure, immediately, by direct reading. Models 050 (0-5R) and 099 (0-100R), are laboratory type instruments for monitoring and testing equipment performance.

Calibration accuracy: $\pm 15\%$ @ 30 keV, at midscale.

Electrical leakage: 2% max. per day.

Size: $4\frac{1}{2}$ " long x $\frac{3}{8}$ " diameter max. (11.4 x 1.4 cm).

Weight: $1\frac{1}{4}$ oz. (35.4 g).

Low range and energy The "STRAD" Stray radiation dosimeter

To accurately survey an area for stray (scattered) and low level radiation (0-1mR), depend on the highly sensitive "STRAD". A completely self-contained instrument, including self-charging unit for portable, battery powered operation. Gives direct reading, fast response (100 ms) detection and monitoring of low energies from scale divisions down to .02 mR.

Calibration accuracy: $\pm 15\%$ (radium).

Energy dependence: $\pm 10\%$, 30-100 keV.

Electrical leakage: 2% per hr. max. (above background).

Size: 9" long x 3" diameter (23.8 x 7.6 cm).

Weight: 1 lb. (454 g).

Portable Dosimeter charger model 906

The finest direct reading dosimeter charger available. Accepts any dosimeter and supplies recharging voltages from 100 to 250 Vdc with a single D-cell battery. Automatically recharges when the pressure activated charging contact is depressed by the dosimeter. Internal light source energized at the same time to illuminate dosimeter scale. Solid state, rugged construction for hard day-to-day use.

DCA offers a complete line of direct reading dosimeters for measurements to 600 R. For a complete catalog, write:


dosimeter
CORPORATION
OF AMERICA

6106 Interstate Circle

Elscint: the human side of imaging technology. Because there's more to imaging than hardware.

Elscint, a worldwide leader in imaging technology, seeks the human solution to techno-medical problems. First to recognize the importance of short deadtime in high-count-rate gamma cameras, Elscint perfected and marketed such systems earlier than any other company. Another first by Elscint, digital color and digital gray-scale imaging, has opened new horizons in nuclear diagnoses.

Latest on the list of Elscint firsts is the **Scanex*** Computerized Tomographic Whole Body Scanner. **Scanex** is the only scanner designed to reduce the number of tomographic slices required for a diagnosis. It is also able to generate its uniquely lucid images with a lower radiation dose, and higher patient throughput, than any other scanner.

This high level of developmental output is maintained by a dynamic team of some 100 engineers and scientists who share a deep interest in imaging technology. At Elscint, they are free to work exclusively within this field. The liberty to create allows them to take pride in generating many innovative designs, and in implementing these advances into reliable, human-engineered instruments.

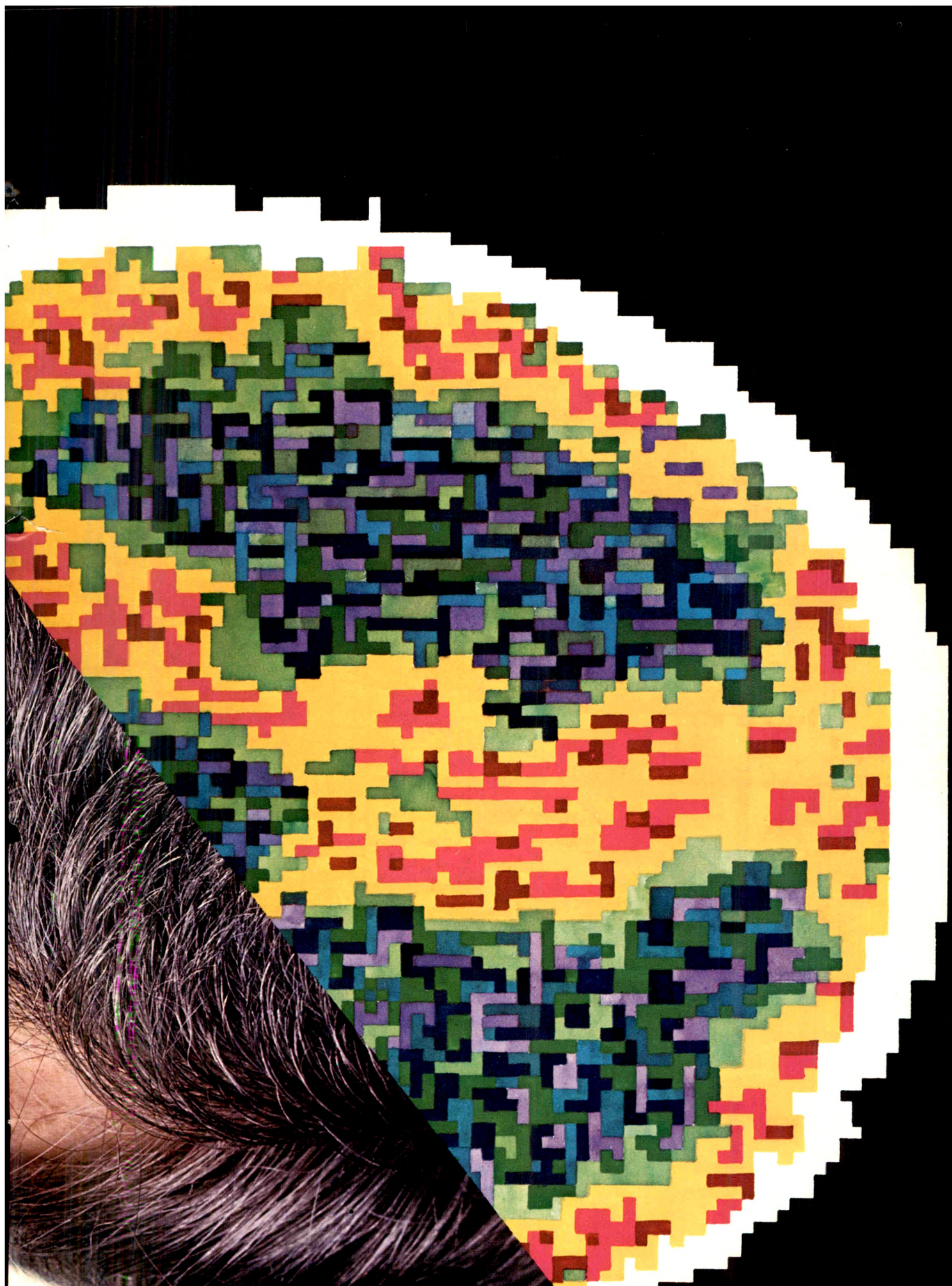
In America, throughout Europe and in Israel, Elscint has the facilities and people to best serve the medical profession. Because Elscint believes there's more to medical technology than hardware. Elscint believes in people. For details, write, indicating your area of major interest to:

*Patents applied for



elscint inc.

138-160 Johnson Avenue, Hackensack, N.J. 07602
Tel: (201) 407-5005



MAGNIFICATION SUBTRACTION

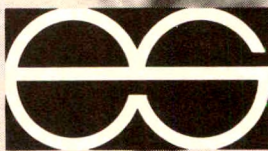
In super-selective angiography

... magnification and subtraction are methods used for better visualization of small vessels.

Full-size, direct angiography is the technique. And Schonander Cutfilm Changers are the instruments.

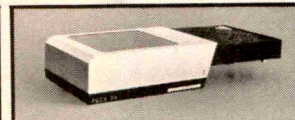
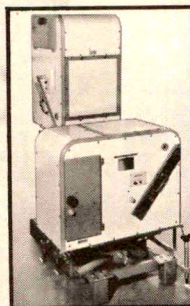
World-wide.

Write for illustrated brochures.



elema-schonander, inc.

699 Lively Boulevard
Elk Grove Village, Illinois 60007
(312) 593-6770



PUCK 20 films/3 exp. per sec./14"X14"/24X30 cm

AOT 30 films/6 exp. per sec./14"X14"/24X30 cm

SCHONANDER CUTFILM CHANGERS—
Precision Instruments for Angiography

**In R/F systems,
consider the finest
remote possibility:**

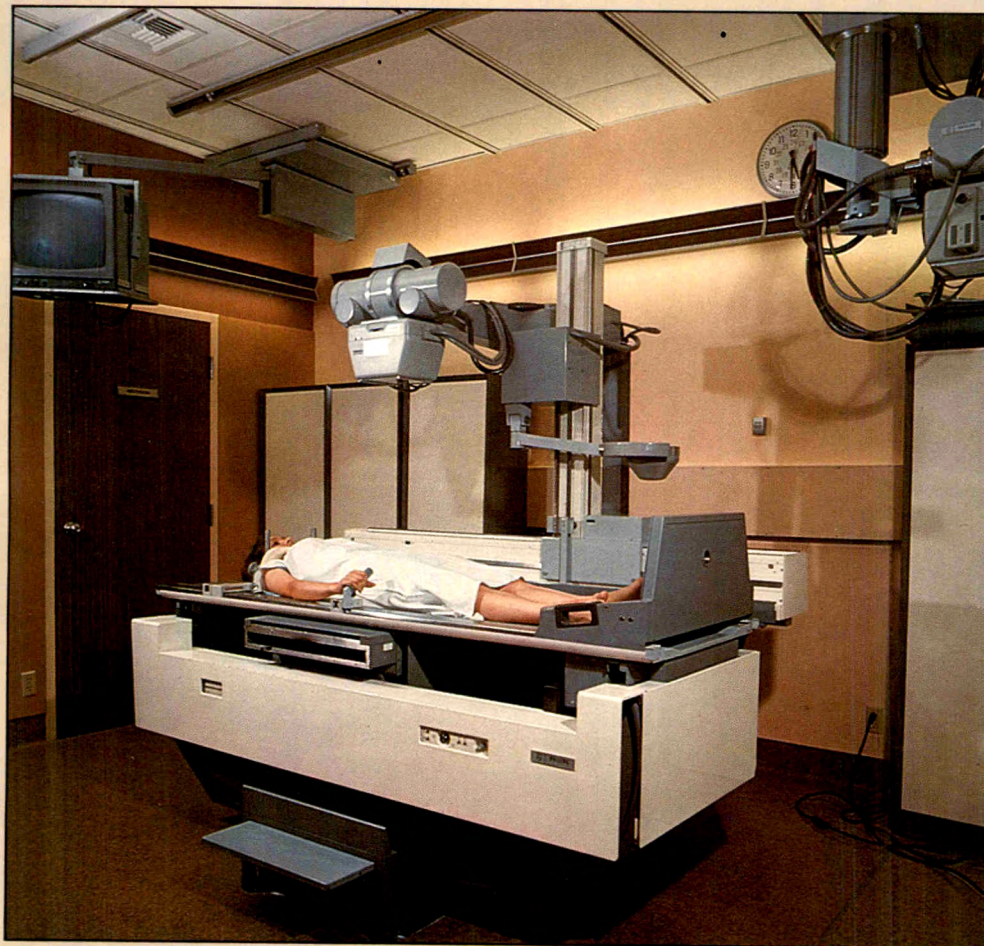
PHILIPS DIAGNOST 100

Philips' remote controlled 90°/90° universal system for routine diagnostics...with facilities for many other applications

Philips offers a complete range of R/F systems. But remote control may well be *your* best choice. First consider the basic reasons:

- ☐ you work in a relaxed, non-radiation area—less fatiguing, less demanding and more efficient
- ☐ less radiation to you and your staff
- ☐ improved efficiency increases the number of patient examinations you can perform
- ☐ the control area can also serve as a conference area for referring or resident physicians.

But Philips Diagnost 100 offers more. *So much more* that it is the one "remote" possibility really worth looking into.



Diagnostic Excellence: Philips' imaging provides consistently outstanding diagnostic results. Excellent visibility, resolution and contrast retention over a large range of patient sizes is a distinct advantage of the 100 . . . and the entire Philips' R/F line.

Philips' modular generators add more valuable benefits to a remote control installation: automatic exposure control, Anatomically Programmed Radiography (APR), isowatt loading for full utilization (and minimum waste) of generator power, and modular design.

Flexibility: The 100's X-ray tube mounting permits maximum use of existing department film changers for special procedures at the head end of the table, as well as for stretcher work. The tubestand is easily adjusted for wall bucky work.

Results: Our users provide the evidence you'll want. For example, one prominent institution equipped with two back-to-back Diagnost 100 rooms, two Philips' modular generators, and one control station, examines an average of 40 patients per morning, using the systems for radiography and tomography in the afternoon. Over 10,000 examinations were performed in 1975!

Remote Control Isn't Your First Choice in R/F Systems, Your First Choice Should Still Be Philips.

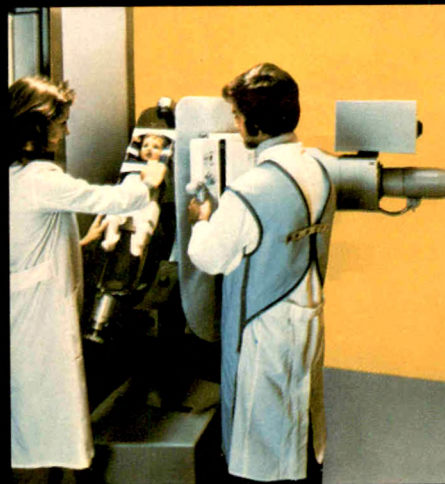
THE 90°/90° UNIVERSAL SYSTEM



The ergonomic answer to general diagnostics, Philips' 90°/90° offers efficient, non-fatiguing operation, thanks to logically arranged controls that adapt the system to your technique—not vice versa. Every film is of the highest image quality. And you have a choice of three extensively automated serial changers (plus Anatomically Programmed Radiography with a Philips' modular generator). One changer includes an automatic film supply system without cassettes.

**ASK FOR
PHILIPS
DIAGNOST 73**

THE 90°/90° PEDIATRIC SYSTEM



The pediatric version of Philips' universal 90°/90° system, this unit features a permanently mounted footstand into which a lightweight C-arm is inserted. The C-arm accepts a comfortable, secure cradle containing the infant. Pre-exam preparation may be done in the cradle. Cradle and C-arm are simply removed for examination of larger children.

**ASK FOR
PHILIPS
DIAGNOST 73-P**

THE 90°/15° SYSTEM



A 90°/15° tilting table with the identical imaging capabilities found on 90°/90° systems.

The spot film device supports a 6" image intensifier with 70mm or 100mm rapid sequence camera (or a 9/5" I.I.) with T.V., all without the encumbrances of an external suspension system.

Rugged, reliable and automated for full efficiency and optimum results, the 90°/15° performs beautifully under the most exacting conditions.

**ASK FOR
PHILIPS
DIAGNOST 1500**

**Philips: a complete range of diagnostic systems
for every need in every discipline**



For additional information, contact your
Philips representative. Or, call or write:

PHILIPS MEDICAL SYSTEMS, INC.

101 Woodport Avenue, Shelton, Conn. 06484

PHILIPS®

Meet Our Back-up Team



Sure. We sell the finest x-ray film and chemistry available... **AGFA-GEVAERT** the world leader in sophisticated imaging technology.

And we sell the finest accessories and supplies, too.

But that's only half of our total customer commitment. The other half is a team of skilled technical professionals, ready and willing to assist you in every way possible... *our back-up team!*

Technical Service

Let's assume that you're having a problem controlling a specific technique. Or that processing parameters are falling short of desired departmental control. Or you're considering a new item of equipment, but aren't sure how it will fit into your overall system.

These, and other technical problems, are a part of the daily routine of our Technical Service Department. They're fully equipped to simulate exact field conditions, analyze results, and advise you on the proper corrective measures.

Whatever your problem or need, this team of professionals, skilled in every aspect of radiography, can be of invaluable service to you.

Automatic Silver Recovery

As part of your back-up team, consider Silver King. This solid state recovery unit works automatically with your processing system recovering as much as 2 ounces of silver every hour.

At today's silver prices, a Silver King unit will more than pay for itself in as little as two month's time.

The attached coupon will bring you full information on the Silver King unit that best fits your needs, as well as information on the services of our entire back-up team.



Processor Service

Just as important to you is the other half of our back-up team... our Processor Service experts.

The program they offer includes a regular schedule of chemistry changes, geared to your needs and processing volume. At the same time, their thorough inspection and preventive maintenance can save you inestimable down-time and repair costs.



Dept. TS
1025 Westchester Ave.
White Plains, N.Y. 10604

A Division of IPCO Hospital Supply Corporation

Please send detailed information on the following:

- ☐ Technical Service
- ☐ Processor Service
- ☐ Silver King 15/28 (High volume automatic processing — nominal recovery of 2 ounces/hour)
- ☐ Silver King Compact (Medium volume automatic processing — nominal recovery of 0.8 ounces/hour)
- ☐ Silver King Manual (Medium volume manual processing — nominal recovery of 0.8 ounces/hour)

Name _____ Title _____

Address _____

City _____

State _____ Zip Code _____

CHARLES · C THOMAS · PUBLISHER

AN ATLAS OF POLYTOME PNEUMOGRAPHY by **Taher El Gammal and Marshall B. Allen, Jr.**, both of *Medical College of Georgia, Augusta*. Assisted by **Paul Dyken**. A large number of studies which supplement the study of normal anatomy of the cerebrospinal fluid pathways and provide comparison for the identification of abnormal structures are presented in this atlas. Concentration is on the findings of polytome pneumography but, where possible and appropriate, correlations are made with angiography, positive contrast ventriculography, and computer assisted tomography. Relative values of these different examinations are also demonstrated. '76, 480 pp. (8 1/2 x 11), 729 il., \$39.50

PANORAMIC DENTAL RADIOGRAPHY by **Lincoln R. Manson-Hing**, *Univ. of Alabama, Birmingham*. Comprehensive material on the subject of panoramic radiography is presented with a great number of illustrations and a minimum of text. Basic technical systems underlying the operating of the various machines are presented in a manner whereby diagnostically meaningful variations between radiographs made by different machines can be easily understood. This volume is unique in featuring the history of pantomography, the basic radiographic systems used, the variety of machines available, radiographic anatomy and artifacts, case presentations, and film processing and viewing. '76, 196 pp. (8 1/2 x 11), 296 il., 6 tables, \$32.50

CORONARY ANGIOGRAPHY (2nd Ptg.) by **Harold A. Baltaxe**, *Cornell Medical College, New York*; **Kurt Amplatz**, *Univ. of Minnesota, Minneapolis*; and **David C. Levin**, *Cornell Medical College, New York*. In addition to describing the gross and radiographic anatomy of the coronary artery tree, this text also deals with the diverse pathologic processes involved. For those organizing a new laboratory devoted to coronary arteriography, there is a section describing equipment and different techniques of catheterization. The chapter on complications lists problems encountered and their order of frequency. Emphasis is placed on visual descriptions. '76, 256 pp., 173 il., \$22.50

ADMINISTRATION OF A RADIOLOGY DEPARTMENT: Hints for Day-to-Day Operation by **Murray L. Janower**, *The St. Vincent Hospital, Worcester, Massachusetts*. To demonstrate that the application of common sense and sound business management principles to a radiology department will result in a marked improvement in its day-to-day operation is the purpose of this volume. Specific attention has been given to the methods used in handling patients, functions of technologists, the establishment of a quality control program, efficient production of radiological reports, methods of film interpretation, darkroom operations and functions of a file room. '76, 72 pp., 8 il., 7 tables, \$7.50

"TRAUMA" AND "NO-TRAUMA" OF THE CERVICAL SPINE edited by **Kenneth R. Kattan**, *Univ. of Cincinnati College of Medicine, Cincinnati, Ohio*. (11 Contributors) All types of trauma of the cervical spine and the diseases that lead to cervical spine trauma are described in this volume. The authors deal not only with trauma, but also with how to differentiate it from other conditions including the normal. The reader will find this to be a complete text on the topic of cervical spine trauma, ranging from the description and excellent illustrations of the anatomy of the cervical spine to the numerous varieties of trauma, their assessment and management. '75, 328 pp., 292 il., \$24.50

HEALTH PROTECTION OF RADIATION WORKERS by **W. Daggett Norwood**, *Hanford Environmental Health Foundation, Richland, Washington*. This volume provides basic facts on ionizing radiation, its measurement and dosimetry; discusses acute, chronic, somatic and genetic effects with emphasis on prevention; outlines radiation protection standards and regulations; and describes methods for maintaining these standards. Diagnosis and treatment of radiation injury from external radiation and/or internally deposited radionuclides are considered for each radioisotope. Medical supervision of radiation workers, radiation accidents, atomic power plants and medicolegal problems are covered. '75, 468 pp., 16 il., 16 tables, \$27.50

Orders with remittance sent by air, postpaid

301-327 East Lawrence Avenue • Springfield • Illinois • 62717

From the very beginning, Pfizer Medical Systems has been aware that growing clinical experience and continuing research would dictate certain refinements and improvements in computerized tomography. Pfizer is determined to be in the forefront of such developments and to make them available as economically as possible.

The first result of this effort is the ACTA-Scanner 0200, which incorporates a more efficient and comfortable patient handling system and an advanced computer system, firmly establishing a modular approach to changing technology. The 0200 user will be able to convert to the 0200FS

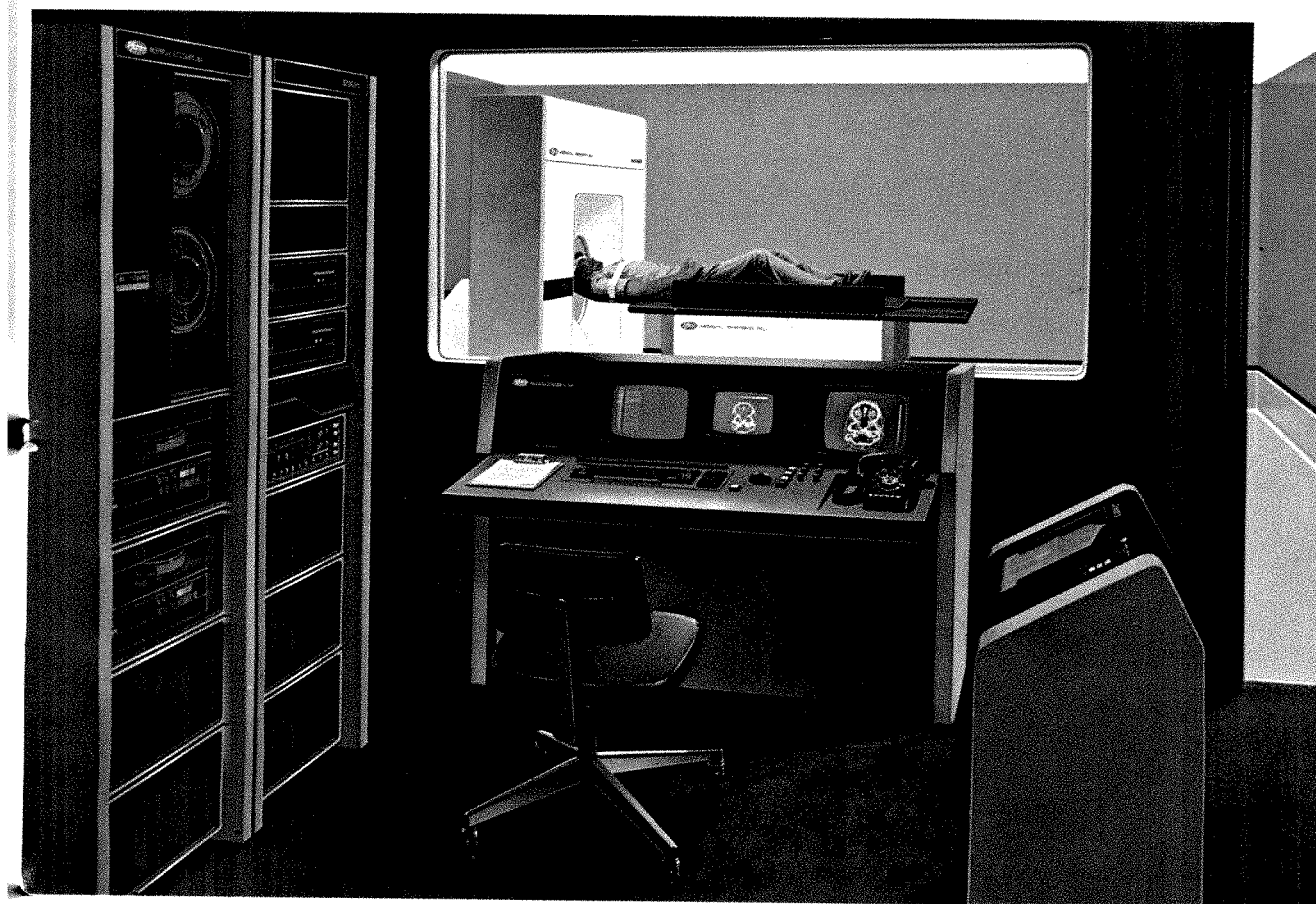
when available. The 0200FS will enable completion and display of a scan in less than 30 seconds. Other operating refinements are described on the next page.

This modularity, of course, will make the advanced features of the 0200FS just as readily available to current as well as prospective users.



MEDICAL SYSTEMS, INC.

A SUBSIDIARY OF PFIZER INC.



Distinguishing Features



MEDICAL SYSTEMS, INC.

A SUBSIDIARY OF PFIZER INC.

ACTA-SCANNER[®]

0200 & 0200FS

Operation and Control Advances (0200FS only)

- Under 30-second scan time minimizes artifacts and increases patient throughput
- Three matrices standard – 160,256,320
- Industry compatible CT numbering system allows universal comparisons
- Advanced computer system
- Light beam guided patient positioning
- Variable scan slice thickness adjustment
- Tilttable gantry ($\pm 20^\circ$) for increased flexibility of scan position
- 22" tunnel diameter to accommodate most patients
- Area of interest analyses

Versatile Patient Record System (0200 & 0200FS)

- *For data storage* – (1) magnetic tape, for low cost mass storage; (2) optional "floppy" disc for easy filing of individual patient scan data
- *For photographic recording* – (1) 105 mm roll or cut film; (2) Polaroid[®] copies; (3) Multiformat Scan Recorder (optional)

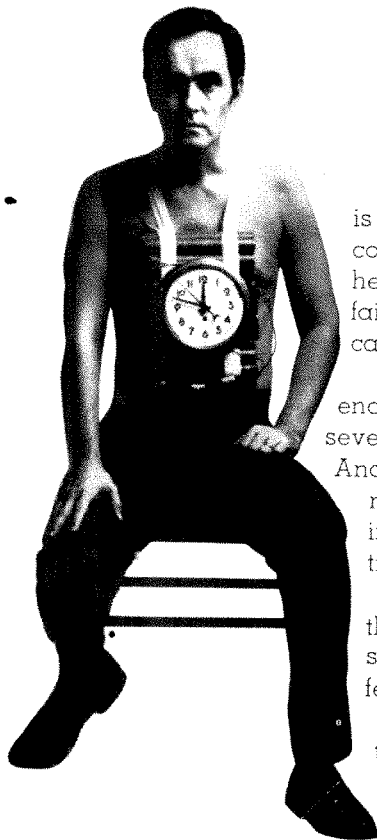
Advanced Patient Handling System (0200 & 0200FS)

- Interchangeable bed modules allow maximum patient throughput
- Bed modules may be rolled to patient rooms, simplifying patient transfers
- Head supports on each bed module allow pre-positioning and immobilization
- Human-engineered for increased patient comfort
- Power mechanism raises bed module and locks it into position
- Movements of bed module are remotely controlled after lock-in

Continuing Features (0100, 0200, 0200FS)

- 320 matrix
- Instant image reconstruction – including 0200FS
- Pfizer commitment to customer service
- 12 month warranty – labor, parts including tube
- Color and black-and-white viewing
- Selective enlargement

ONE-SEVENTH OF YOUR EMPLOYEES MAY BE DYING. HELP SAVE THEIR LIVES.



High Blood Pressure is the country's leading contributor to stroke, heart disease and kidney failure. Any of which can kill.

And, frighteningly enough, one out of every seven of your workers has it. And half of them have no idea they're walking around with this time bomb inside them.

That's because there are usually no symptoms. The victim feels fine.

But all the while, the time bomb is ticking away.

Until, suddenly, it explodes.

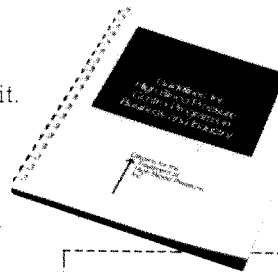
But you can help. By giving your employees a chance to check their blood pressure. It takes only seconds to measure a person's blood pressure. And it's painless. Best of all, your own medical or nursing personnel can do the job, simply.

When a case of High Blood Pressure is detected, the employee is then referred to a doctor for treatment. And treatment is usually as simple as taking a pill every day.

To help you implement this life-saving



program, we have a special kit, "Guidelines for High Blood Pressure Control Programs in Business and Industry." The kit includes complete instructions on screening, publicity, referral, follow-up, education. And more.



Send for your kit today. It may be the best thing you've ever done for your employees. And your company.

A Public Service of
this Magazine &
The Advertising Council



Mail to:

National High Blood Pressure Education Program
120/80, National Institutes of Health
Room 1012—Landow Bldg.
Bethesda, Md. 20014

Please send me _____ copy(ies) of
"Guidelines for High Blood Pressure Control Programs
in Business and Industry."

Name _____

Title _____

Company _____

Address _____

City _____

State _____

Zip _____

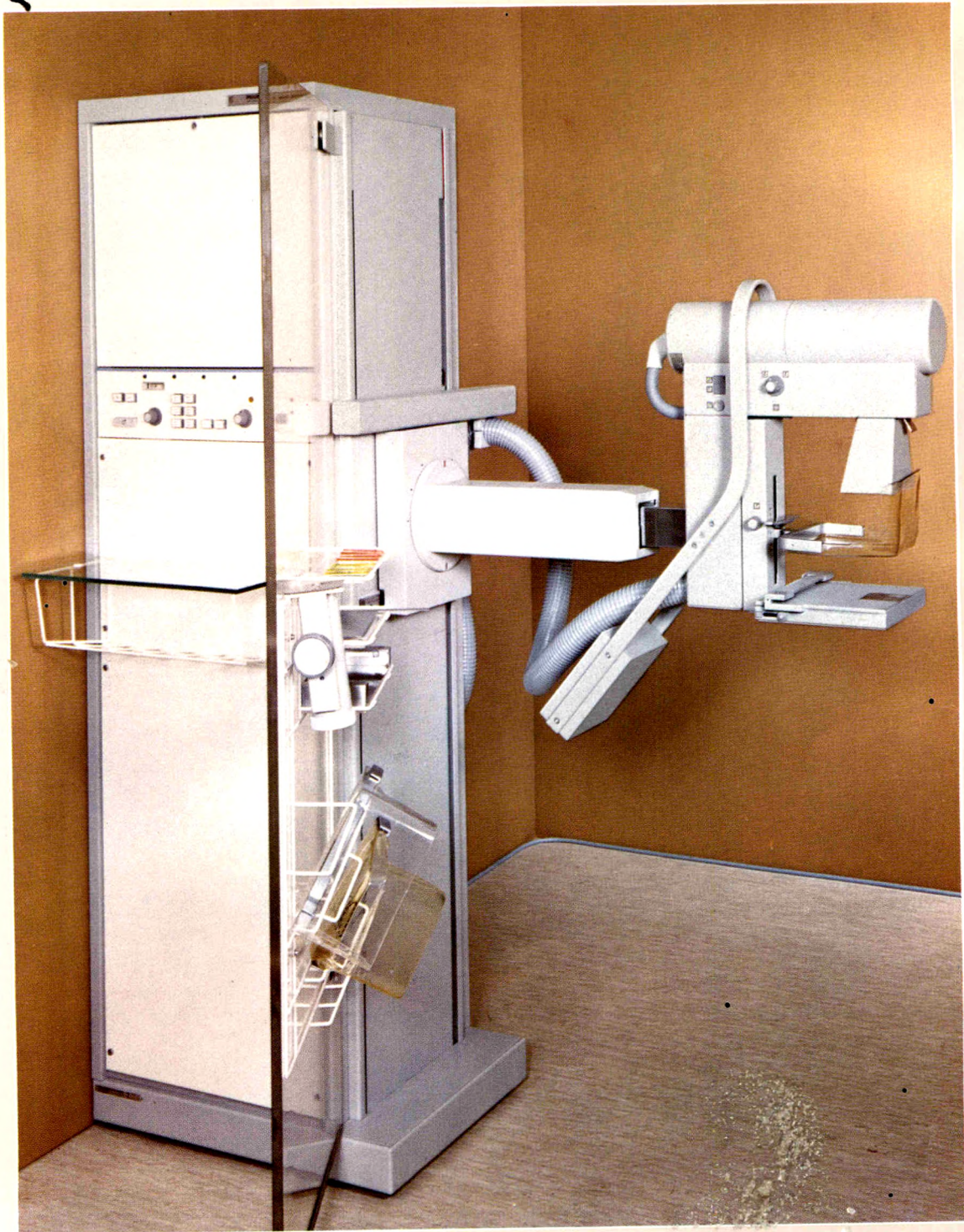


HIGH BLOOD PRESSURE
Treat it...and live.

The National High Blood Pressure Education Program, U.S. Department of Health, Education, and Welfare.

For mammography, take a stand
you can count on:

PHILIPS MAMMO DIAGNOST



Clear detail, the finest contrast and the best possible resolution. All with minimum radiation dose to your patient.

That's what Philips Mammo Diagnost gives you with every film. Whether you use the Mammo Diagnost for radiography or Xeroradiography, you can make your diagnosis with total confidence.

And with convenience. Examinations are easier and faster for you, more comfortable, assuring and relaxing for your patient.

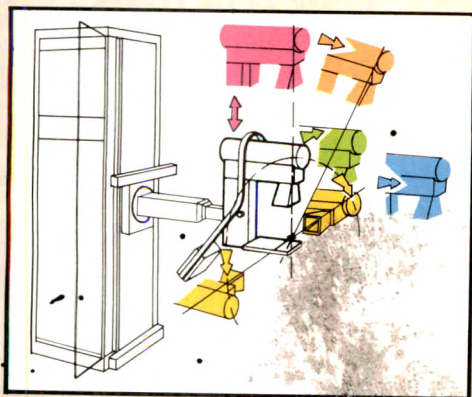
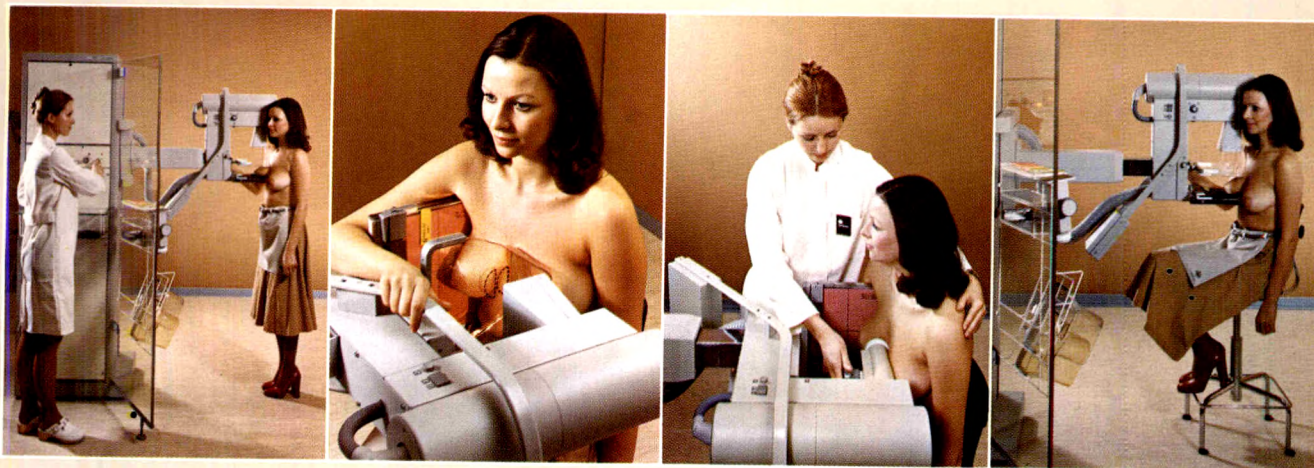
Seated, standing or recumbent patients are examined efficiently, with precise positioning insured by a wide range of tube travel (including caudal angulation).

Self-contained; compact and pre-wired for rapid installation, the Mammo Diagnost also features Automatic Exposure capability, optional water cooling of the X-ray tube, and logically

arranged generator controls for both programmed and manual techniques. Vacuum cassettes and all new low dose films can be used with outstanding results.

For additional information, contact your Philips representative. Or, call or write:

PHILIPS MEDICAL SYSTEMS, INC.
710 Bridgeport Avenue, Shelton, Conn. 06484
Tel. (203) 929-7311



PHILIPS®

INDEX TO ADVERTISERS

AMRAD	xiii
Atomic Energy of Canada	xviii
Barnes-Hind Pharmaceuticals	xxx, xxxi
Cleon Corporation	xxxii
Conversations in Radiology	xl
Dosimeter Corporation of America	lix
Eastman Kodak Company	ix, x, xi, xii
Elema-Schonander, Inc.	lxii
Elscint, Inc.	lx, lxi
EMI Medical, Inc.	vi, vii
E-Z-EM Company	liii
C. B. Fleet	xlvi, xlv
General Electric Company	liv, lv, lvi, lvii
Grumman Health Systems	xxxiii
Grune & Stratton, Inc.	xxxvi
The Liebel-Flarsheim Company	xxvii
Litton Medical Systems	i, xli, xlii, xliii, xlv
Low X-Ray	lxix
Machlett Laboratories	lviii
Ortho Pharmaceutical Corporation	xxxvii
Pfizer Medical Systems	lxxi, lxxii, lxxiii, lxxiv, lxxv, lxxvi
Philips Medical Systems, Inc.	lxiii, lxiv, lxv, lxvi, lxvii, lxviii, lxxviii, lxxix
Picker Corporation	xxxviii, xxxix, xlvi, xlvii
The Purdue Frederick Company	v
Sakura Medical Corporation	xix
Searle Radiographics	viii, xxv
SHM Therapy Systems	xxviii, xxix
Siemens Corporation	ii, xiv, xv, l, li
Spacesaver Corporation	xl
E. R. Squibb & Sons, Inc.	Cover 2, xxii, xxiii, xxiv, xxxiv, xxxv, xxxvi
S & S X-Ray	xxxi
Charles C Thomas • Publisher	lxx
West Florida Hospital and Clinic	xxxii
Williams & Wilkins	Cover 3, lii
Wolf X-Ray	xxvi
Xerox Corporation	xx, xxi
Xonics	xvi, xvii

We try to present an accurate index. Occasionally this may not be possible because of a last-minute change or an omission.

COMPUTED TOMOGRAPHY OF THE BRAIN AND ORBIT:

EMI SCANNING

By Paul F. J. New, M.D., F.A.C.R.,
and William R. Scott, M.D.

1975 / 500 pages / approximately
1,000 illustrations \$41.00

This volume is the first to be published
on EMI Scanning: a thorough and
definitive reference work for
Computed Tomography.



"The introduction of computed tomography must be compared in significance with the introduction of cerebral pneumography, . . . and cerebral angiography, . . . but its importance surpasses those vital contributions to neuroradiological diagnostic methods to the extent that its employment will not result in the morbidity (and still occasional mortality) associated with those traditional methods. An attempt has been made to provide evidence of the value, limitations and present state of the art of computed tomographic scanning in cranial neuroradiological diagnosis. The future is rich with promise . . ."
From the preface

WILLIAMS & WILKINS

428 E. PRESTON STREET
BALTIMORE, MARYLAND 21202

American Journal of Roentgenology

Vol. 127

September 1976

No. 3

DIAGNOSTIC RADIOLOGY

- High Dose Urography: Incidence and Relationship to Spontaneous Peripelvic Extravasation. *M. E. Bernardino and B. L. McClennan* 373
- Autonomous Hyperparathyroidism in Patients on Maintenance Home Dialysis. *C. A. Lehman and M. H. Schreiber* 377
- Therapeutic Vascular Occlusion Utilizing Steel Coil Technique: Clinical Applications. *S. Wallace, C. Gianturco, J. H. Anderson, H. M. Goldstein, L. J. Davis, and R. L. Bree* 381
- Embolio Control of Hypertension Caused by Segmental Renal Artery Stenosis. *S. P. Reuter, P. R. Pomeroy, V. P. Chuang, and K. J. Cho* 389
- Aneurysms Secondary to Pancreatitis. *A. F. White, S. Baum, and S. Buranasiri* 393
- Radiologic and Pathologic Characteristics of the WDHA Syndrome. *R. P. Gold, T. J. Black, H. Rotterdam, and W. J. Casarella* 397
- Fine Needle Transhepatic Cholangiography: A New Approach to Obstructive Jaundice. *J. T. Ferrucci, Jr., J. Wittenberg, R. A. Sarno, and J. R. Dreyfuss* 403
- Percutaneous Transhepatic Cholangiography with Selective Catheterization of the Common Bile Duct. *F. Burcharth and N. Nielbo* 409
- Jaundice from Impacted Sediment in a T Tube: Recognition and Treatment. *D. V. Jelaso and J. S. Hirschfield* 413
- The Aberrant Gallbladder: Angiographic and Radioisotopic Considerations. *V. P. Chuang* 417
- Pathophysiology of Enlargement of the Small Bowel Fold. *W. W. Olmsted and D. E. Reagin* 423
- Electrical Stimulation for Anal Sphincter Control in Barium Enema Examinations: An Extended Trial. *K. Clark and D. Rowan* 429
- Radiographic Evaluation of Endotracheal Tube Position. *L. R. Goodman, P. A. Conrardy, F. Laing, and M. M. Singer* 433
- Further Observations on Pulmonary Venous Varix. *J. Twersky, D. C. Levin, N. Twersky, and D. H. Gordon* 435
- Pulmonary Metastases from Benign-appearing Smooth Muscle Tumors of the Uterus. *D. Bachman and M. Wolff* 441
- Radiology of Knee Joint Replacement. *M. I. Gelman and H. K. Dunn* 447
- Traumatic Lesions of the Discovertebral Junction in the Lumbar Spine. *W. Martel, J. F. Seeger, J. D. Wicks, and R. L. Washburn* 457
- Congenital Dislocation of the Knee. *D. H. Carlson and J. O'Connor* 465
- The Os Incae. *R. Shapiro and F. Robinson* 469
- A New Radiographic Technique for Fractures of the Orbit and Maxilla. *E. L. Lame and T. J. Redick* 473
- Computed Tomography and Brain Scintigraphy in Ischemic Stroke. *L. C. Chiu, L. B. Fodor, S. H. Cornell, and J. H. Christie* 481
- Normal Variants and Congenital Anomalies in the Region of the Obelion. *G. Currarino* 487

RADIATION ONCOLOGY

- The Destiny of Brachytherapy in Oncology. *B. Pierquin*. Translated by J. F. Wilson 495
- Laparoscopy and Laparotomy in Staging Hodgkin's and Non-Hodgkin's Lymphoma. *U. Veronesi, P. Spinelli, G. Bonadonna, L. Gennari, E. Bajetta, G. Beretta, and G. Tancini* 501
- Subtotal Mastectomy and Radiation Therapy in the Definitive Management of Localized Breast Malignancy. *P. E. Wallner, L. W. Brady, Jr., J. Loughhead, T. Matsumoto, J. Antoniadis, S. Prasavinichai, J. R. Glassburn, S. O. Asbell, and J. I. Damsker* 505
- Postoperative Irradiation in the Prevention of Keloids. *D. S. Levy, M. M. Salter, and R. E. Roth* 509
- Parametrial Calcification in Cervical Carcinoma Patients Treated with Radioactive Gold. *T. M. Deeths and R. J. Stanley* 511

CASE REPORTS

- Nodular Lymphoid Hyperplasia of the Colon Associated with Dysgammaglobulinemia. *A. A. DeSmet, D. G. Tubergen, and W. Martel* 515
- Massive Enlargement of the Ileocecal Valve due to Lymphoid Hyperplasia. *A. C. Selke, Jr., J. Z. Jona, and R. P. Belin* 518
- Hepatoscintigraphy, Arteriography, and Ultrasonography in Preoperative Diagnosis of Chole-
dochal Cyst. *C. Piyachon, M. Poshyachinda, and V. Dhitavat* 520
- Arachnoid Granulations Simulating Osteolytic Lesions of the Calvarium. *R. Branan and C. B. Wilson* 523
- Unilateral Dysplasia of the Superior Articular Facet of the Axis. *R. Salama and S. L. Weissman* 525
- Arteriographic Findings in Hyperergic Granulomatosis and Vasculitis of a Kidney. *G. P. Pouliadis, J. Wellauer, R. Streuli, A. Fontana, and J. Briner* 526

RADIATION PHYSICS

- Interim Report: Mammographic Exposures at the Breast Cancer Detection Demonstration Project Screening Centers. *P. Wootton* 531
- Erratum: Sheedy et al. 127:23 51, 1976 533
- Editorial: Echocardiography: Territorial Im-
perative? *W. G. Guntheroth* 534
- A. Justin Williams, 1901-1976 535
- Abstracts of Current Literature 536
- Book Reviews 544
- News 547
- Radiologic Societies 549